THE

LONDON, EDINBURGH AND DUBLIN

# PHILOSOPHICAL MAGAZINE

AND

# JOURNAL OF SCIENCE

CONDUCTED BY

SIR OLIVER JOSEPH LODGE, D.Sc., LL.D., F.R.S.

SIR JOSEPH JOHN THOMSON, O.M., M.A., Sc.D., LL.D., F.R.S.

AND

ALLAN FERGUSON, M.A., D.Sc.

---

> "Nec aranearum sane textus ideo melior quia ex se fila gignunt, nec noster vilior quia ex allenis libamus ut apes."
>
> JUST. LIPS. *Polit.* lib. i. cap. 1. Not.

---

VOL. XXVIII.—SEVENTH SERIES

JULY—DECEMBER 1939

---

LONDON:

TAYLOR & FRANCIS, LTD., RED LION COURT, FLEET STREET, E.C. 4.

*Agents*: WM. DAWSON & SONS, LTD., CANNON HOUSE, PILGRIM STREET, E.C. 4.

“Meditationis est perscrutari occulta; contemplationis est admirari perspicua . . . . Admiratio generat quæstionem, quæstio investigationem, investigatio inventionem.”—*Hugo de S. Victore.*

—— “Cur spirent venti, cur terra dehiscat,
Cur mare turgescat, pelago cur tantus amaror,
Cur caput obscura Phœbus ferrugine condat,
Quid toties diros cogat flagrare cometas,
Quid pariat nubes, veniant cur fulmina cœlo,
Quo micet igne Iris, superos quis conciat orbes
Tam vario motu.”

*J. B. Pinelli ad Mazonium.*

ALERE FLAMMAM.

# CONTENTS OF VOL. XXVIII. (Nos. 186–191)

## (SEVENTH SERIES)

## NUMBER 186—JULY

Page

I. The Ignition of Inflammable Gases by Hot Moving Particles. By STEWART PATERSON, M.A., B.Sc., Metcalfe Research Fellow, Glasgow University ........ 1

II. The Threshold and Equilibrium Curves of Supraconductors. By J. G. DAUNT, Clarendon Laboratory, Oxford ........ 24

III. The Thermal Method of Measuring Losses in Sheet Dielectrics at Radio Frequencies and High Electrical Stresses. By J. T. MACGREGOR-MORRIS, D.Sc.(Eng.), M.I.E.E., and G. L. GRISDALE, Ph.D., B.Sc. ........ 34

IV. Further Observations on the Action of X-rays on the Electrophoretic Mobility of Colloid Particles. By J. A. CROWTHER, M.A., Sc.D., Professor of Physics in the University of Reading, H. LIEBMANN, Ph.D., and R. JONES, B.Sc. ........ 64

V. The Bending of Thick Plates under certain Specified Conditions of Support. By JOHN MORROW, M.Sc., D.Eng., Reader in Engineering, King's College, University of Durham ........ 73

VI. Electron Distribution in Electron-optically Focused Electron Beams. By L. JACOB, M.Sc., A.R.C.Sc.I. ........ 81

VII. The Primary and Secondary Scattering of Sunlight in a Plane-stratified Atmosphere of Uniform Composition. By A. HAMMAD, Ph.D., Department of Mathematics, The Egyptian University, Cairo, and S. CHAPMAN, F.R.S., Imperial College of Science and Technology, London ........ 99

VIII. Ionization by Collisions of Positive Ions. By J. S. TOWNSEND, F.R.S., Wykeham Professor of Physics, Oxford ........ 111

IX. The Arms of a Spiral Nebula. By A. C. BANERJI, Professor of Mathematics, Nizamuddin, and P. L. BHATNAGAR, Research Scholar, Allahabad University ........ 118

X. Notices respecting New Books :—

NICOLAS RASHEVSKY's Mathematical Biophysics ........ 127

Prof. G. STEAD's Notes on Practical Physics ........ 127

Encyclopædia Britannica Book of the Year 1939 ........ 128

## NUMBER 187—AUGUST

Page

XI. The Density and Compressibility of Solid Hydrogen and Deuterium at 4·2° K. By HELEN D. MEGAW ........ 129

XII. Gas Flow in Solids. By R. M. BARRER (Department of Colloid Science), The University, Cambridge ........ 148

XIII. Studies in Photoelectric Photometry. A Photoemissive Cell specially designed for High Precision Measurements. By G. A. BOUTRY and P. GILLOD, Laboratoire d'Essais, Paris ........ 163

XIV. The Influence of the Cathode on the Sparking Potential of Hydrogen. By F. LLEWELLYN JONES, M.A., D.Phil., and J. P. HENDERSON, B.Sc., University College, Swansea ........ 185

XV. The Mechanism of the Spark Discharge in Hydrogen. By F. LLEWELLYN JONES, M.A., D.Phil., University College, Swansea ........ 192

XVI. A Short Wave Generator. By E. W. B. GILL, B.Sc., M.A., Fellow of Merton College, Oxford ........ 203

XVII. A Generalization of the Polynomial $F_n(x)$. By SIMON PASTERNACK ........ 209

XVIII. The Astronomical Consequences of Relativistic Two-Body Problem. By Sir SHAH SULAIMAN, M.A., LL.D., D.Sc., Federal Court, India ........ 227

XIX. On Turbulent Liquid Motion outside a Circular Boundary. By MANOHAR RAY, Lahore, India ........ 231

XX. Optical Activity and Magneto-optical Activity of Crystalline Nickel Sulphate in the Near Ultra-violet. By F. G. SLACK, Ph.D., and PHILIP RUDNICK, Ph.D., Department of Physics, Vanderbilt University. Nashville, Tennessee. (Plate I.) ........ 241

XXI. Two-way Speech by Wireless. By MARIO MARRO, Dr. Ing. ..... 248

XXII. The Surface-Tension and Angle of Contact of Mercury *in vacuo*. By A. E. BATE, M.Sc., Ph.D., F.Inst.P., Northern Polytechnic, London .. 252

XXIII. Notices respecting New Books :—

Mr. R. C. EVANS's Crystal Chemistry ........ 256

## NUMBER 188—SEPTEMBER

XXIV. The Thermodynamic Functions for a Fermi-Dirac Gas. By EDMUND C. STONER, Sc.D., F.R.S., Reader in Physics at the University of Leeds ........ 257

XXV. A Note on Laguerre Polynomials. By W. T. HOWELL ........ 287

XXVI. On the Determination of the Dielectric Constants of Liquids at Radio Frequencies.—Part III. Methyl Alcohol, Water, and Alcohol Water Mixtures : Theoretical. By R. M. DAVIES, D.Sc., and T. TYSSUL JONES, B.Sc., Ph.D., Department of Physics, University College of Wales, Aberystwyth ........ 289

XXVII. On the Determination of the Dielectric Constants of Liquids at Radio Frequencies.—Part IV. Methyl Alcohol, Water, and Alcohol Water Mixtures : Experimental. By T. TYSSUL JONES, B.Sc., Ph.D., and R. M. DAVIES, D.Sc., Department of Physics, University College of Wales, Aberystwyth ........ 307

Page
XXVIII. The Influence of the Cathode on the Sparking Potential of Heavy Hydrogen. By F. Llewellyn Jones, M.A., D.Phil., University College, Swansea ........ 328
XXIX. Harmonic Analysis by the Method of Central Differences. By D. C. Espley, M.Eng., M.I.E.E. (Communication from the Research Staff of the M.O. Valve Company, Limited, at the G.E.C. Research Laboratories, Wembley, England.) ........ 338
XXX. The Permeability of Metal Membranes to Diatomic Gases. By R. M. Barrer ........ 353
XXXI. The Errors in the Numerical Solution of Differential Equations. By F. J. Turton, B.Sc., A.R.C.Sc., City and Guilds College ........ 359
XXXII. A New Form of the Quantum Equation. By M. Fahmy, M.Sc., Egyptian University, Cairo ........ 364
XXXIII. A Mobile Seismic Recording Unit. By F. M. G. Murphy, M.A., and S. T. Cope, Research and Development Department, Marconi Wireless Telegraph Company, Ltd., and J. H. Jones, D.Sc., Chief Geophysicist, Anglo-Iranian Oil Company, Ltd. (Plates II.–IV.) ........ 370
XXXIV. Two Notes on the Numerical Solution of Differential Equations. By F. J. Turton, B.Sc., A.R.C.Sc., City and Guilds College ........ 381
XXXV. Notices respecting New Books :—
Mr. S. Goldstein's Modern Developments in Fluid Dynamics ... 384

## NUMBER 189—OCTOBER

XXXVI. The Electron in Classical General Relativity Theory. By A. Lees, M.Sc., Ph.D., University College, Swansea ........ 385
XXXVII. A Note on the Solution of some Partial Differential Equations in the Finite Domain. By W. T. Howell ........ 396
XXXVIII. Viscosity of Liquids at High Hydrostatic Pressures. By R. B. Dow, A.M., Ph.D., Department of Physics, The Pennsylvania State College, State College, Pa. ........ 403
XXXIX. Quantization under Two Centres of Forces.—Part I. The Hydrogen Molecular Ion. By S. K. Chakravarty, Calcutta (India) ........ 423
XL. The Electrical Double Layer at the Interface of Two Liquids. By E. J. W. Verwey and K. F. Niessen, Natuurkundig Laboratorium der N. V. Philips' Gloeilampenfabrieken, Eindhoven, Holland ........ 435
XLI. The Periodic Flow of Heat in a Hollow Cylinder. By J. H. Awbery, B.A., B.Sc., Physics Department, The National Physical Laboratory, Teddington, Middlesex ........ 447
XLII. The Distortion of a Curved Tube due to Internal Pressure. By W. R. Dean, M.A., Trinity College, Cambridge ........ 452
XLIII. The Latent Heats of Sublimation and Evaporation of certain Substances. By William Hume-Rothery, F.R.S. ........ 465
XLIV. The Magnitude of the Direct Stress in a Beam of Fixed Span. By R. J. Cornish, M.Sc., Assoc.M.Inst.C.E. ........ 481
XLV. Formulæ for Generalized Hypergeometric Functions as Particular Cases of more General Formulæ. By Professor T. M. MacRobert, University of Glasgow ........ 488

Page

XLVI. Some Formulæ for the Product of two Whittaker Functions with Different Arguments. By W. T. Howell ........................ 493

XLVII. Notices respecting New Books :—

Prof. L. F. Bates's Modern Magnetism ........................ 496

Karl K. Darrow's Introduction to Contemporary Physics ...... 496

---

## NUMBER 190—NOVEMBER

XLVIII. X-ray Study of some Meteoric Irons. By Prof. E. A. Owen, M.A., Sc.D., and B. D. Burns, M.Sc., University College of North Wales, Bangor. (Plates V.–VII.) ........................ 497

XLIX. On a Hydraulic Problem involving Discharge into Tidal Water. By A. G. Walker, Ph.D., Department of Pure Mathematics, University of Liverpool, and J. R. Daymond, M.Sc., Department of Civil Engineering, University of Liverpool ........................ 520

L. On the Dielectric Constant of Space containing Electrons. By S. R. Khastgir, D.Sc.(Edin.), Mem.I.R.E., and K. Sirajuddin, M.Sc., Dacca University ........................ 532

LI. The Electric Glow between Carbon Electrodes. By F. H. Newman, D.Sc., F.Inst.P., Professor of Physics, University College, Exeter. (Plate VIII.) ........................ 544

LII. The Magneto-Optical and Natural Dispersions of Isobutyl Butyrate and Ethylene Chloride. By W. J. G. Beynon, B.Sc., Physics Department, University College of Swansea ........................ 548

LIII. The Efficiency of Geiger-Müller Counters. By R. S. Shankland and C. H. Tindal, Case School of Applied Science, Cleveland, Ohio ..... 562

LIV. The Influence of the Free End of a Rod on Heat Transfer. By Max Jakob, Research Foundation of Armour Institute of Technology, Chicago, Illinois ........................ 571

LV. Note on a Problem in the Conduction of Heat. By C. J. Tranter, B.A. ........................ 579

LVI. Note on the Relative Intensity of Spectrum Lines. By F. H. Newman, D.Sc., Professor of Physics, University College, Exeter ........ 584

LVII. Note on the Effective Wave-length to be used in calibrating a disappearing Filament Optical Pyrometer. By F. A. Cunnold, M.A., D.Phil. 588

LVIII. Note on Synchronizing "Clocks" in a Moving System by a Connecting Spindle. By Albert Eagle, B.Sc., A.R.C.Sc., Lecturer in Mathematics in the University of Manchester ........................ 592

LIX. The Effect of Variable Specific Heat of Gases on the Quantities involved in Heat Transmission between Liquids and Gases. By W. J. Walker ........................ 596

LX. Notices respecting New Books :—

Professor E. Geoffrey Cullwick's The Fundamentals of Electro-Magnetism ........................ 600

## NUMBER 191—DECEMBER

Page

LXI. The Magnetic Rotatory Dispersion and the Refractivity of Aqueous Solutions of Nickel Sulphate throughout the Range 5780 Å. to 2482 Å.; especially the Magnetic Rotation in the 3950 Å. Absorption Band. By R. W. Roberts, D.Sc., and S. F. Adams, M.Sc. ............ 601

LXII. Crystal Structure of Cyclohexane at −180° C. By K. Lonsdale and H. Smith, Davy Faraday Laboratory, Royal Institution, London. (Plate IX.) ........ 614

LXIII. Radiation from a Point Charge revolving in a Circular Orbit. By Hillel Poritsky, Ph.D. ........ 617

LXIV. On Transverse Vibrations of Curved Membranes. By C. E. Weatherburn, M.A., D.Sc., Professor of Mathematics in the University of Western Australia ........ 632

LXV. Scattering of Light in Bose-Einstein and Fermi-Dirac Gas. By B. N. Singh, M.Sc., University of Delhi ........ 635

LXVI. Changes in the Internal Resistance of Selenium Barrier-layer Cells caused by Exposure to Light. By Arne Eld Sandström, D.Sc. ... 642

LXVII. Torsional Vibration in Heavy Shafts. By W. A. Tuplin, M.Sc. 649

LXVIII. The Electric Strength of Gases, measured by Corona Discharge. By Emer. Prof. W. N. Thornton, D.Sc., D.Eng. ........ 666

LXIX. A Note on the Viscosity of Gases and Molecular Mean Free Path. By A. E. Schuil, B.Sc. ........ 679

LXX. The Surface Tension of Water and Heavy Water. By A. H. Cockett and Allan Ferguson ........ 685

LXXI. An Alternative Explanation of Relativity Phenomena. By Albert Eagle, B.Sc., A.R.C.Sc., Lecturer in Mathematics in the University of Manchester ........ 694

LXXII. Notices respecting New Books:—

- Prof. T. G. Room's The Geometry of Determinantal Loci ... 702
- Drs. S. S. Stevens and H. Davis's Hearing: Its Psychology and Physiology ........ 703

**Index** ........ 705

## PLATES

I. Illustrative of Drs. F. G. Slack and Philip Rudnick's Paper on Optical Activity and Magneto-optical Activity of Crystalline Nickel Sulphate in the Near Ultra-violet.

II.–IV. Illustrative of Messrs. F. M. G. Murphy, S. T. Cope, and Dr. J. H. Jones's Paper on a Mobile Seismic Recording Unit.

V.–VII. Illustrative of Prof. E. A. Owen and Mr. B. D. Burns's Paper on X-ray Study of some Meteoric Irons.

VIII. Illustrative of Prof. F. H. Newman's Paper on the Electric Glow between Carbon Electrodes.

IX. Illustrative of Mrs. K. Lonsdale and Mr. H. Smith's Paper on the Crystal Structure of Cyclohexane at —180° C.

THE

LONDON, EDINBURGH & DUBLIN

PHILOSOPHICAL MAGAZINE

AND

JOURNAL OF SCIENCE

[SEVENTH SERIES—VOL. 28]

# I. *The Ignition of Inflammable Gases by Hot Moving Particles.*

By Stewart Paterson, M.A., B.Sc., Metcalfe Research Fellow, Glasgow University *.

[Received November 19, 1938.]

## 1. *Introductory.*

That the igniting power of heated solid particles introduced into an inflammable gas will diminish with increasing speed of motion through the gas can be deduced from the observations of several writers †, but no quantitative determinations of the influence of speed seem as yet to have been published.

In view of the practical importance of this matter, especially in connexion with accidents from explosion in mines, as well as its general interest, it was thought desirable to undertake measurements of the effect of speed, which, with theoretical observations upon them, are described in the present paper.

---

* Communicated by Prof. E. Taylor Jones.

† Wüllner and Lehmann, *Ann. Min. Belg.* vi. p. 9 (1886). Couriot and Meunier, *Ann. Min. Belg.* xiii. p. 91 (1908). White and Price, J. Chem. Soc. cxv. pp. 1479, 1501 (1919). Mason and Wheeler, J. Chem. Soc. cxxi. p. 2089 (1922). Burgess and Wheeler, " Safety in Mines Research Board Paper 46," p. 7 (1928); paper 54, p. 10 (1929); paper 62, p. 11 (1930). Coward and Wheeler, S. M. R. B. paper 53, p. 19, 23 ff. (1929). Silver, Phil. Mag. (7) xxiii. p. 641 (1937).

### 2. *Experimental Arrangement.*

The particles used were small platinum and quartz spheres, and the method consisted, briefly, in heating these pellets in a horizontal tube furnace and shooting them by means of compressed air into a vessel containing explosive gas; the speeds were previously determined with a ballistic pendulum.

Fig. 1 illustrates the arrangement finally adopted as most suitable for the purpose of the experiments.

Fig. 1.

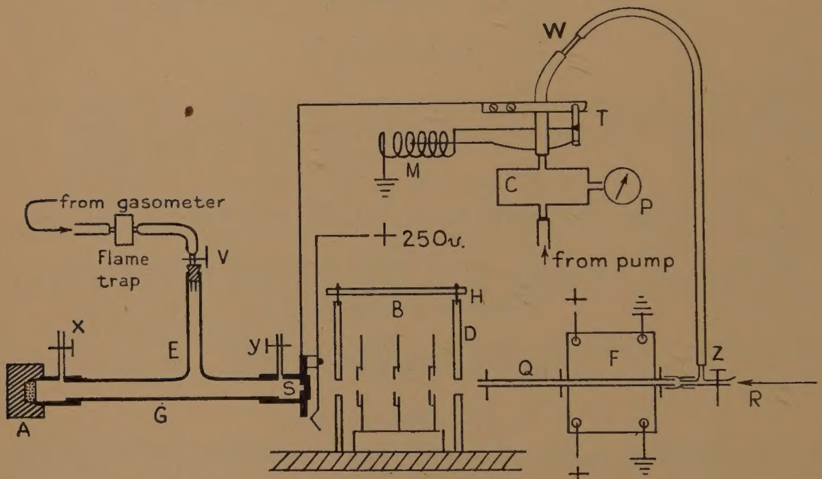

Semi-diagrammatic view of apparatus.

The explosive gas was contained in a horizontal tube G of pyrex glass, 80 cm. long and 4 cm. in diameter. The tube was closed at the end A by a conical cap of wood, which fitted tightly over a conical brass sheath and contained a plug of wet asbestos wool to receive the pellet. The other end bore a brass cap with a circular opening 1 cm. in diameter, which could be closed by the rotary shutter S. The vertical side-tube E served as an indicator of successful ignition by the moving particle: the flame which spread through E could readily be observed, whereas the flame in G, travelling *with* the ball, was much more rapid.

The pellet under examination was heated in a quartz (fused silica) tube Q, clamped within the furnace F. In order to secure a wide range of speed, and accurate aiming, the quartz tube, whose function is to direct and accelerate the pellet, must have a bore very little (usually about 10 per cent.) greater than the diameter of the pellet, and as long a " muzzle " as possible. A glance at the calibration curves of fig. 2 will show the relative importance of this muzzle-distance when higher speeds are required. 2-foot tubes were finally employed, corresponding to a muzzle of about 45 cm. The question of cooling in the muzzle has been considered. (Section 5, p. 10.)

Various metals have been used for the furnace-winding—nichrome, molybdenum, kanthal, and platinum. An efficient and economical furnace was finally constructed on the " cascade " principle due to Harker[*]: its heating element is a platinum-wound alundum tube (12 in. × $\frac{1}{4}$ in.) protected by a wider coaxial " Kanthal A 1 " coil, also mounted on an alundum tube and generously lagged. The furnace consumes about 330 watts at 1300° C. and was used up to that temperature for over 300 hours without injury. It has been taken up to 1500° C.

The quartz tube Q was joined by rubber to a glass " T "-piece, having a tap Z on the horizontal arm. Through this tap the pellet could be introduced into Q and afterwards viewed by an optical (Wanner type) pyrometer, which faced in the direction of the arrow R. Silver[†] has explained that this type of instrument may be used under our conditions. As a check the pyrometer was compared with a standard thermocouple, and found in perfect agreement over the range used (800° C.–1300° C.). Temperatures given below are therefore direct pyrometer readings. The question of how far these readings correspond to the temperature of the pellet *when it enters the explosive mixture* is considered in Section 5, p. 10.

The compressed air was generated in a reservoir C (equipped with a 60 lb./sq. in. gauge P), and released through Q by the tap T. Consistent speeds were obtained only when the rate of release did not vary, and a spring tap was therefore used: it was simply a strip of spring brass bound down across the pressure lead by a rotary switch. This tap reduced the variation in speed at any given pressure to ±1 per cent. A ball-valve W prevented excessive loss of air from C.

For simplicity in operation, the shutter S and tap T were electrically connected, by a device somewhat similar to that used by Silver[‡]. When S had just completely uncovered the entrance to G, it closed a circuit through the solenoid M, and the attraction of M on a soft iron rod was communicated to the switch of T by a slack chain. To eliminate auxiliary switches, the components of T were themselves placed in the solenoid circuit.

---

[*] Harker, Proc. Roy. Soc. (A) lxxvi. p. 235 (1905).

[†] Silver, *loc. cit.* p. 640.

[*] *Loc. cit.* p. 639.

To filter out the pellet from its propelling air, which was found to disturb ballistic measurements and presumably tended to dilute the explosive mixture, as well as being itself capable of producing ignition *, three baffle-plates B were introduced between S and Q. Experience showed that three plates were sufficient, when placed at least 8 cm. apart, the extreme plates being 10 cm. from S and Q respectively. The accurate aiming † permitted the use of such small apertures that the air which passed through B had a scarcely measurable effect on the pendulum. Each plate was furnished with a device which permitted adjustment of the position (and size) of the aperture to compensate for bends developed in Q by the heating. A shield D was erected over the plates in order to trap the ball if it failed to pass through : the gap indicated at H in fig. 1 is necessary, to allow the puff of air an alternative (and wider) exit.

### 3. *Experimental Procedure.*

The pressure gauge on C was first calibrated in terms of speed for a number of convenient muzzles. A ballistic pendulum was used (in place of G), the pellet being caught in a plug of plasticine on the bob and the deflexion recorded by a graduated thread drawn through a smooth hole. Fig. 2 shows a specimen calibration.

As a check this was repeated after each experiment proper. It was done with the furnace cold : variation of speed with temperature is not to be anticipated, in view of the small coefficients of expansion of quartz and platinum.

In ignition experiments the pellet was inserted through tap Z and pushed carefully into the chosen position with a quartz rod. Its temperature and propelling pressure were adjusted to suitable values, and the explosion-vessel filled with gas by displacing the air. Taps X, V, Y, Z were then closed in that order, and S (and thereby T) opened. If an explosion occurred ‡, the condensed water was evaporated from G by a current of air before refilling with gas.

Ignition was recorded by a cross, non-ignition by a circle, on a plane whose coordinates were speed (abscissa) and temperature. When the available ranges of these variables had been covered, the appropriate region of the plane was divided roughly into two parts, one containing crosses only, and corresponding to ignition, the other circles only, corresponding to non-ignition. It was possible to draw a curve separating these regions, and this curve was taken to represent approximately the relation between speed and igniting temperature.

---

* Experiments on the igniting power of hot air are at present in progress.

† The "spread" at A did not exceed 1 cm.; the distance AQ exceeded 1 metre.

‡ There was seldom any ambiguity.

## 4. *Results.*

Coal-gas-air mixtures were used throughout, Silver having shown * that methane-air required inconveniently high temperatures. It is hoped that the observations on coal-gas will apply at least qualitatively

Fig. 2.

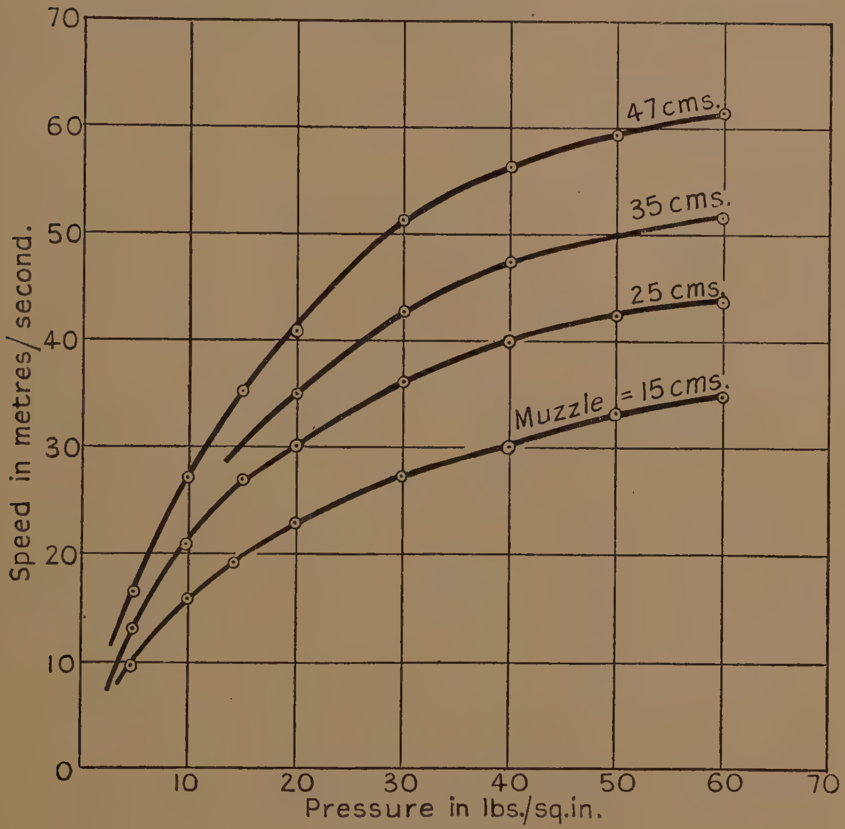

2 mm. platinum.

to other explosive mixtures and in particular to fire-damp. The following analysis of the gas used was kindly supplied by Glasgow Corporation :—

| | $H_2$. | $CH_4$. | CO. | $N_2$. | $CO_2$. | $C_nH_m$. | $O_2$. | Total. |
|---|---|---|---|---|---|---|---|---|
| Per cent. . | 50·1 | 18·8 | 18·4 | 6·5 | 3·4 | 2·3 | 0·5 | 100·0 |

(A). *Platinum Spheres.*—The slope of the characteristic curve was found to decrease as the pellet diameter was increased. For diameters greater than 4 mm. this slope was so small that a temperature range of only some 50° could be covered. As the pyrometer cannot detect differences much less than 10°, the curves were very vague. Our first results apply, therefore, to 3·5 mm. platinum spheres, and are shown in fig. 3.

---

* *Loc. cit.* p. 641.

It is to be understood that the region on the left of any characteristic corresponds to ignition, that on the right to non-ignition. In other words, there is at each temperature a limiting speed, defined by the curve, beyond which ignition is not obtained *. The characteristics are approximately linear, the curve for 9 per cent. coal-gas has a smaller slope than that for 7 per cent., and the " minimum " ignition temperature is about the same for each mixture. The form taken by the curves when both temperature and speed were very high could not be determined, owing to limitations of speed.

Fig. 3.

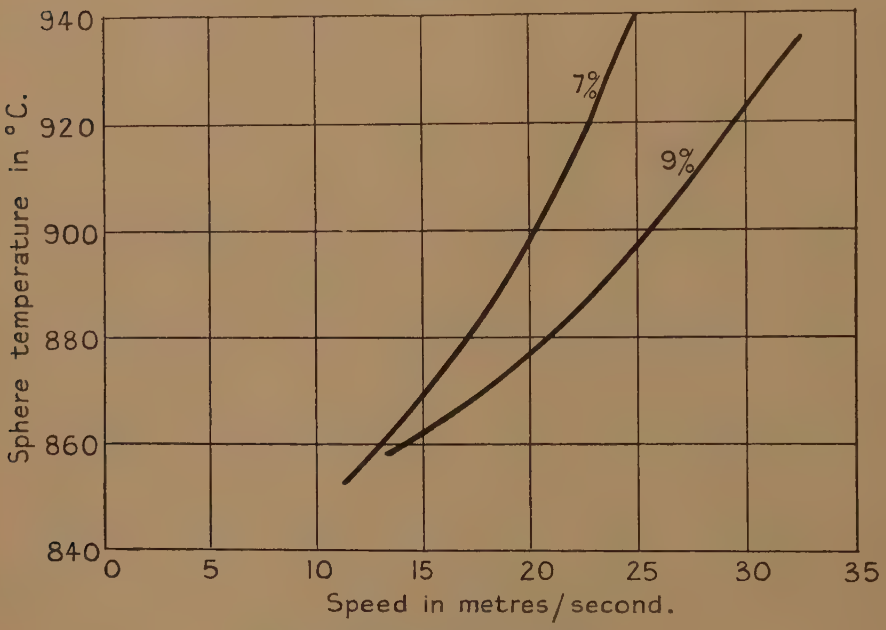

3·5 mm. platinum ; coal-gas-air.

2 mm. platinum spheres were next examined ; this proved to be the most convenient size. We have seen that large spheres give flat and there-

---

* By suitable choice of temperature and speed, ignition can be delayed until the pellet is arrested at the asbestos target, whereupon flame spreads back through G to S. Though this fact is implied in the curves of figs. 3 and 4, it is thought worthy of mention, as a convincing demonstration of the effect of speed upon igniting power.

fore inaccurate characteristics ; in the same way pellets of less than 2 mm. diameter have characteristics which are equally indefinite because they

Fig. 4.

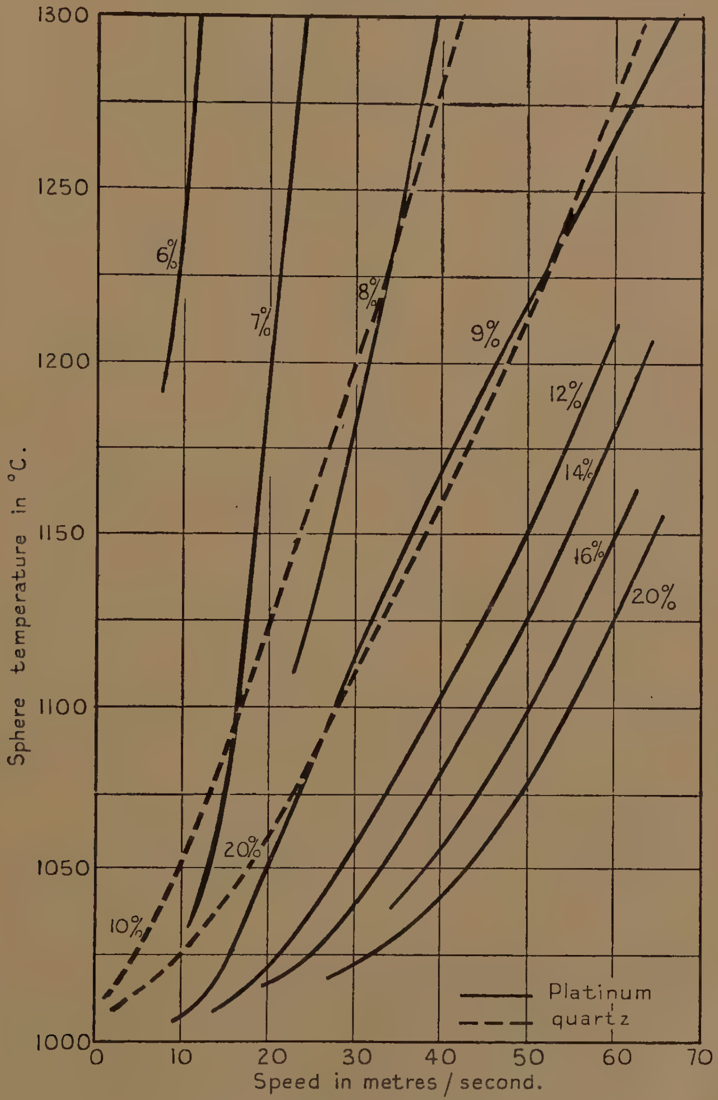

2 mm. spheres: coal-gas-air.

are so steep. The high speeds (over 100 metres/second) available at 60 lb./sq. in. with 1·5 mm. platinum spheres could not, unfortunately, be put to any use. With the 2 mm. pellets, a 9 per cent. mixture was first examined. The characteristic is shown on fig. 4, together with subsequent results for other mixtures. The 9 per cent. characteristic covers the entire available range of speed (0–64 metres/sec.) and over 300° of temperature (980° C.–1310° C.), and summarizes the results of 290 shots.

Similar curves were derived for 6, 7, 8, 12, 14, 16, and 20 per cent. coal-gas : the effect of concentration was found to be very marked (fig. 4). The same features, however, can be noted in fig. 4 as in fig. 3 : the curves are all linear except for an initial " tail "—they all rise from approximately the same minimum temperature, and their slope decreases, as the concentration is raised from the lower limit of inflammability (5–6 per cent.) towards its value for maximum flame-speed (about 20 per cent.).

When the limiting speed (that is, the greatest speed which will permit ignition at a given temperature) is graphed, for any chosen temperature, against percentage gas in mixture, a curve is obtained, which rises as concentration increases, but shows a distinct tendency to flatten out at 16–20 per cent. (fig. 5). This prompts one to enquire whether, for greater concentrations, the curve may descend again. 25, 26, 28, 30, and 32 per cent. mixtures were tried, in order to decide the question. A difficulty was, however, foreseen. When the shutter S is opened, diffusion at once smooths out the discontinuity of concentration, so that every mixture from pure air to the gas in G is to be found in this region. Provided we are using a concentration less than 20 per cent., the above results show that the diluted mixtures are all *less* ignitable, and so any ignition can safely be recorded as an ignition of the gas in G. But if the curves of fig. 5 descend beyond 20 per cent., and if G contains a mixture beyond this strength, then some of the diluted mixtures will be, not less, but *more* ignitable. Hence an explosion may take place under conditions which would not ignite the mixture in G. This explosion will, of course, traverse the (richer) gas in the tube (supposed below the upper limit of inflammability—about 32 per cent.), and unless the flame-speed is low, *i. e.*, the mixture well beyond 20 per cent., it will be difficult to say whether the flame is *accompanying* the pellet or merely *following* it. The turbulence and heating produced by the pellet will evidently exaggerate this difficulty by increasing the normal speed of the flame.

That the curves of fig. 5 do descend again was proved quite clearly by explosions in 28 and 30 per cent. mixtures. These were difficult to ignite *by direct action of the pellet* ; they behaved in much the same way as 7 and 8 per cent. except that, even when a non-ignition was obviously to be recorded, a green flame started at the shutter, as far as could be judged at the moment of passage of the pellet, and floated along the tube in its wake. Counting this as a non-ignition, 30 per cent. could not be ignited at 10 metres/sec. even at 1300° C. 28, 26, and 25 per cent. mixtures behaved very erratically, as indeed the above argument would anticipate. It appeared useless to look for *real* characteristics at these concentrations. One point, however, was tested. If the explosions with these rich mixtures are often due (as there is little doubt) to the diluted gas at the shutter, then the characteristic in which *every* sort of ignition is counted as an " ignition " should coincide with that appropriate to the most ignitable mixture, and so will not be very different from the 20 per cent. curve. This was found approximately true. The curves for " shutter-ignition " in 25, 28, 32 per cent. were all more or less the same, and coincided roughly with that for 20 per cent. ; they seemed to suggest that 21 per cent. might be (slightly) more ignitable than 20 per cent. In fig. 5 the broken lines indicate what is probably the course of the curves above 20 per cent. ; but except near 30 per cent. they are very uncertain.

Fig. 5.

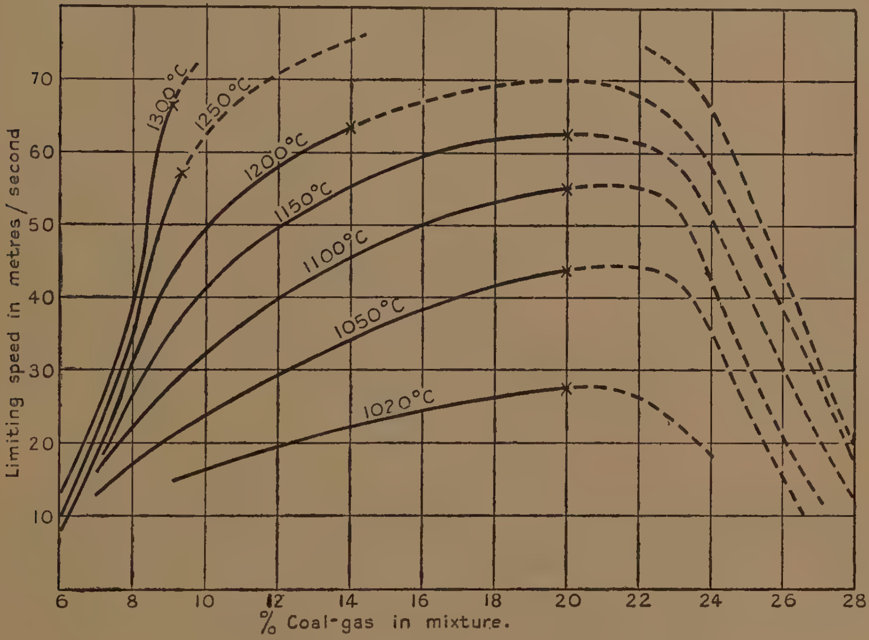

2 mm. platinum: coal-gas-air.

(B) *Quartz Spheres.*—On account of their fragility and irregular shape these have not been used to the same extent as platinum. It was found, however, that good spheres could easily be made in the carbon arc, and results for 2 mm. quartz are shown (by a broken line) in fig. 4. Very high speeds could be commanded, but were of little use, as the characteristics rose much more steeply than in the case of platinum. It will be noticed that the *minimum* ignition temperatures of the two mixtures used coincide, just as was found with platinum ; moreover, what is more interesting, these minimum temperatures are the same for the two substances : this agrees with Silver's * result. At high speeds, however, quartz and platinum show marked differences in behaviour.

### *Note on "Ageing" of Spheres.*

It had been noticed throughout the work with 2 mm. platinum spheres (of which five were used) that the older spheres were always more efficient in igniting than the new. A characteristic was sketched for a new pellet and found approximately parallel to the corresponding curve of fig. 4, but displaced upward, except at the lower end, through about 40°. Similar improvements with platinum wires are on record †. It is thought probable that some connexion exists in the present case between the increased igniting power and the conspicuous surface-changes which took place. Before use the platinum spheres were polished and metallic in appearance. After a few ignitions they took on a milky aspect, as though the surface had been ruffled. Through long use their colour changed to dark grey and finally to a grey-black. The surface looked very rough under a low magnification. (The track on a photographic plate of the "aged" sphere was much brighter than that of a new sphere at the same temperature and speed.)

Sufficient work has not been done with quartz to detect such an improvement if it exists ; but the surface undergoes a rapid change, becoming opaque after a few ignitions.

### 5. *Cooling of Spheres.*

As was pointed out above, the use of baffle-plates requires that the pellet traverse about 40 cm. of air between heating-tube and explosion-vessel. It is obviously important to know whether any considerable cooling takes place in this interval, and, if so, whether it depends on the speed of transit. The question will first be considered theoretically.

The heat-losses from a sphere moving in a fluid are due to :

(*a*) Radiation.

(*b*) Conduction-convection.

(*a*) The radiation loss from a heated surface may be expressed as $<e\sigma AT_s^4$, where $\sigma$ is Stefan's constant ($(5{\cdot}6)10^{-12}$ watt/cm.$^2$.°K.$^4$), A the area and $T_s$ the absolute temperature of the surface, and $e$ a factor depending on the surface and also on $T_s$. The maximum value of $e$ is,

---

* *Loc. cit.* p. 644 ; fig. 3.

† Thornton, Phil. Mag. (6) xxxviii. p. 615 (1919) ; Shepherd and Wheeler, S. M. R. B. paper 36, p. 19 (1927).

of course, 1, when the surface is perfectly black; for polished platinum at 1600° K. International Critical Tables give 0·197 *. We shall probably be safe, therefore, in adopting the value $e=0{\cdot}5$ as an upper limit in our case. The loss per sq. cm. is then $<(2{\cdot}8)10^{-12}(1573)^4$ watts at the upper limit (1573° K.) of our temperature range,

*i. e.*, $$\text{loss/cm.}^2\ \text{sec.} < 4{\cdot}08 \text{ calories.}$$

For a 2 mm. sphere, therefore,

$$\text{loss} \equiv \frac{dH_R}{dt} < 0{\cdot}502 \text{ cals./sec.}$$

The speeds used varied from $10^3$ to $6.10^3$ cm./sec. and the gap was 40 cm., to which must be added a further 30 cm. in the cold muzzle. Thus the time of cooling varied from 0·07 to 0·0117 sec. With the exception of the 6 and 30 per cent. mixtures, however, the minimum speed *at 1573° K.* was over $2.10^3$ cm./sec., and so the time of cooling less than 0·035 sec. Hence the heat-loss ($H_R$) from radiation was always less than 0·0176 cal., and usually *much* less than this.

If, now, the surface temperature $T_s$ be identified with that of the sphere as a whole (see below), a loss of 0·0176 cal. will produce a temperature drop $-\Delta T_s = \frac{0{\cdot}0176}{mc_1}$, $m$ being the mass and $c_1$ the specific heat of the sphere. For a 2 mm. platinum sphere, $m=0{\cdot}093$ gm. As to $c_1$, Landolt-Börnstein † give, for platinum:

$$0\text{–}1000°\text{ C.}: \bar{c_1}=0{\cdot}0377 \text{ cal./gm. °K.}$$
$$0\text{–}1177°\text{ C.}: \bar{c_1}=0{\cdot}0388 \text{ cal./gm. °K.}$$

whence $c_1$ at 1100° C. is approximately 0·045 cal./gm. °K. International Critical Tables ‡ give

$$c_1 = \frac{1}{(4{\cdot}2)(195{\cdot}2)}.[25{\cdot}89+(5{\cdot}23)10^{-3}\theta] \text{ cal./gm. °K.}$$

at Centigrade temperature $\theta$: this expression leads to a value of 0·0386 at 1100° C. Adopting 0·04 as a probable least value in our range, we have, finally,

$$-(\Delta T_s)_R \leq 4°{\cdot}3.$$

(*b*) The loss by conduction–convection is not so readily estimated. In the first place it must be stated that all the results, experimental and theoretical, which we shall use refer to conditions where a *steady* heat-field has been set up; however, the consideration that our pellet emerges from the heating-tube in a sheath of hot air suggests that the estimates of heat-loss on the assumption of steady flow are not likely to be too small.

---

* Vol. v. p. 243.
† *Phys. Chem. Tabellen.*
‡ Vol. v. p. 93.

The only available data on the convective cooling of spheres refer to diameters of the order of 1 cm. and relatively low temperatures and speeds; we have recourse, therefore, to the Similarity Principle, in order to render them applicable. Considerations of similarity show * that the heat-loss per second from a sphere of radius $a$ at temperature $T_s$ (absolute) to a fluid at $T_\infty$, when the state is steady and natural convection relatively small, is

$$\frac{dH_c}{dt}=ak(T_s-T_\infty)\psi(Re,\, St) \quad . \quad . \quad . \quad . \quad . \quad . \quad . \quad (1)$$

$k$ being the thermal conductivity of the fluid, and $\psi(Re, St)$ some unknown function of the Reynolds number ($Re$) and Stanton number ($St$) †. $k$, $Re$, $St$ must be calculated for the appropriate temperature, which is usually taken as $T=\frac{1}{2}(T_s+T_\infty)$ ‡.

Kinetic theory allows us to write $St=$const. for a given gas, and in particular we have $St=1\cdot 35$ § for diatomic gases (*e. g.*, air),

*i. e.*, $k=1\cdot 35\,\mu c_p$, and so (1) becomes

$$\frac{dH_c}{dt}=a\mu c_p(T-T_\infty)\phi(Re) \quad . \quad . \quad . \quad . \quad . \quad . \quad . \quad (2)$$

$\phi$ being some unknown function. Boussinesq, with certain simplifying assumptions, derived $\phi$ theoretically; he gave ||

$$\frac{dH_c}{dt}=4\sqrt{2\pi k\rho c_p V a^3}(T_s-T^{\infty}),$$

*i. e.*,

$$\frac{dH_c}{dt}=[4\sqrt{1\cdot 35\pi}]a\mu c_p(T_s-T_\infty)\sqrt{Re}\cdot$$

which implies that

$$\phi(Re)=8\cdot 26\sqrt{Re.}$$

---

* See Davis, Phil. Mag. (6) xliv. p. 940 (1922).

† $Re\equiv\frac{2Va\rho}{\mu}$; $St\equiv\frac{k}{\mu c_p}$, where $V\equiv$velocity, $\rho\equiv$density, $\mu\equiv$(dynamical) viscosity, and $c_p\equiv$sp. heat (const. press.), of the fluid.

‡ Nusselt, *Zeits. d. Ver. deutsch. Ing.* p. 685 (1917); Davis, Phil. Mag. (6) xli. p. 902 (1921).

§ Eucken, *Phys. Zeits.* xii. p. 1104 (1911); Langmuir, Phys. Rev. xxxiv. p. 404 (1912); Fage and Falkner (Aero. Res. Com. R. and M. no. 1408 (1931)) give $St=1\cdot 30$ as a mean experimental value.

|| *Journ. de Math.* (6) 1, iii. p. 308 (1905), etc. We have written $\rho c_p$ for Boussinesq's "C."

Compan* verified this form of $\phi$ from $Re=2100$ to $Re=8300$, and Mitchell's † results support the same conclusion, though he did not himself accept it, over a range of 1800 to 53,000. Our own values of $Re$ are smaller (190 to 1500), but it is very unlikely that the above form will be departed from *at these values*: in the case of cylinders, the $\sqrt{Re}$-law fails, if it fails at all, only when $Re$ becomes very large ‡. We therefore adopt

$$\frac{dH_c}{dt}=Aa\mu c_p(T_s-T_\infty)\sqrt{Re}, \quad . \quad . \quad . \quad . \quad . \quad . \quad . \quad (3)$$

A being a constant derivable from Compan or Mitchell. It follows that

$$-\left(\frac{dT_s}{dt}\right)_c=\frac{3A}{4\pi}\cdot\frac{\mu c_p}{a^2\rho_1 c_1}\,(T_s-T_\infty)\sqrt{Re},$$

where $\rho_1$, $c_1$ refer to the sphere, at $T_s$,

$$i.\,e., \qquad -\left(\frac{dT_s}{dt}\right)_c=\frac{Bc_p}{\rho_1 c_1}\sqrt{\frac{\mu\rho V}{a^3}}\,.(T_s-T_\infty). \quad . \quad . \quad . \quad (4)$$

For $c_p$, $\mu$, $\rho$ we have adopted the expressions § ($T\equiv$absolute temp.$=\frac{1}{2}(T_s+T_\infty)$)

$$c_p=0\cdot2272(1+0\cdot0002\,T),$$

$$\mu=\frac{(15)10^{-6}T^{3/2}}{124+T},$$

$$\rho=(1\cdot293)10^{-3}\left(\frac{273}{T}\right).$$

Both Mitchell and Compan used copper spheres, and their range of temperature was comparatively low and narrow. Under these conditions, $c_p\sqrt{\mu\rho}$ is almost constant, with a mean value of 0·0001138 at $T=360$. $c_1$ may be taken as 0·1 and $\rho_1$ is 8·93. Inserting Mitchell's values of $\frac{dT_s}{dt}$ ‖, $a$, V, and $T_s-T_\infty$, we find $B\doteq2\cdot72$ (*cf.* Boussinesq: 2·789). The agreement with Boussinesq is striking, but both estimates are almost certainly exaggerated. The theoretical figure refers to conditions of zero viscosity; but the boundary layer must reduce heat-transfer below Boussinesq's value. Indeed a comparison of his expressions ¶ for the loss from cylinders

---

[*] *Ann. de Chim. et de Phys.* xxvi. p. 545 (1902).

[†] Edin. Phil. Trans. xl. p. 47 (1901–4).

[‡] Davis, Phil. Mag. (6) xli. p. 903 (1921).

[§] Langmuir, *loc. cit.* pp. 404–405.

[‖] Uncorrected for radiation, which seems relatively small.

[¶] Boussinesq, *loc. cit.* p. 297.

with the experimental data of King * shows an exaggeration of about 65 per cent. Again, Hughes † has recorded a considerable increase in heat-loss when the sphere is suspended (as in Mitchell's experiments) in a relatively narrow pipe. It seems probable, therefore, that B is less than 2·72 ; but if we adopt that figure, then

$$-\left(\frac{dT_s}{dt}\right)_c = \frac{2{\cdot}72c}{\rho_1 c_1}\sqrt{\frac{\mu\rho V}{a^3}}\,.(T - T_\infty), \quad . \quad . \quad . \quad . \qquad (4')$$

an equation applicable to all cases of spheres in (unbounded) fluids under steady conditions of forced convection. Let us apply (4′) to the 2 mm. platinum spheres. Since the cooling is small, we write $(\varDelta T_s) = \left(\frac{dT_s}{dt}\right)_c \varDelta t$ ; and $\varDelta t = 40/V$ (the *convective* cooling begins only after emergence, *cf.* p. 11). $\frac{T_s - T_\infty}{\sqrt{V}}$ had a max. value $10\sqrt{10}$, and appropriate values of $a$, $\rho$, $\mu$, $c_p$, $c_1$, $\rho_1$, are : $a=0{\cdot}1$, $\rho=(3{\cdot}716)10^{-4}$, $\mu=(4{\cdot}09)10^{-4}$, $c_p=0{\cdot}270$, $c_1=0{\cdot}044$, $\rho_1=21{\cdot}37$.

Hence $$-(\varDelta T_s)_c < 12^\circ{\cdot}2.$$

The maximum radiation drop was 4°·3. These maxima do not really occur together, so that their sum, *i. e.*, 16°·5 is greater than the greatest drop to be expected. In the opinion of the writer it is *considerably* greater.

Compan's results can also be used to evaluate the constant B of (4) : the result is 0·448, which is much smaller than Mitchell's figure. The fact that Compan used a wider pipe may partly account for the difference ; at any rate, the value of our convective drop based on his work would be 2°·0 instead of 12°·2.

It remains to justify the above assumption of uniform temperature throughout the pellet. We make use of Fourier's ‡ well-known solution for symmetrical heat flow in a solid sphere, when the surface loss is proportional to the excess surface temperature $T_s - T_\infty$. It is

$$\frac{T(r,t) - T_\infty}{T_0 - T} = \frac{2pa}{k_1}\sum_{n=1}^{\infty}\left[\frac{\sin\frac{\epsilon_n r}{a}}{\frac{\epsilon_n r}{a}} \cdot \frac{e^{-\frac{k_1}{\rho_1 c_1}\cdot\frac{\epsilon_n^2 t}{a^2}}}{\epsilon_n \operatorname{cosec}\epsilon_n - \cos\epsilon_n}\right],$$

---

* King, Phil. Trans. (A) ccxiv. p. 405 (1914).

† Hughes, Proc. Univ. Durham Phil. Soc. viii. p. 189 (1930).

‡ *Théorie Anal. de la Chaleur*, ch. v.

where $T(r, t)$ is temperature of shell, radius $r$, at time $t$; $T_0$ the (uniform) temperature of sphere when $t=0$; $k_1$ the thermal conductivity of sphere; $p[T(a, t)-T_\infty]$ the heat loss per unit area per second, and $\epsilon_n$ the $n$th+ve real root of the equation

$$\epsilon \cot \epsilon = 1 - \frac{pa}{k_1}.$$

Now $p = p_c + p_R$ (convection and radiation), where

$$p_c \equiv \frac{dH_c/dt}{4\pi a^2(T_s - T_\infty)}$$

$$= 0{\cdot}0003020\sqrt{V} \text{ from (3), (4')},$$

with a maximum value of 0·02340 at $V=6000$; and

$$p_R \equiv \frac{dH_R/dt}{4\pi a^2(T_s - T_\infty)}$$

$$\doteqdot \frac{e\sigma(T_s^4 - T_\infty^4)}{T_s - T_\infty}$$

$$\doteqdot e\sigma T_s^4/(T_s - T_\infty),$$

and while this is not constant we can regard it as being so, with its greatest value, viz., 0·00315 (at $T_s=1573$, $T_\infty=293$)

$$\therefore \quad p \leqq 0{\cdot}0266.$$

As to $k_1$, we have no data for high temperatures, but theoretically $k$ is independent of T for metals. Assuming $k_1=0{\cdot}17$, we have for $\epsilon$ the equation: $\epsilon \cot \epsilon = 1 - 0{\cdot}0157$; the first two roots are: $\epsilon_1 \doteqdot 12° \, 20'$ and $\epsilon_2 \doteqdot 257° \, 39'$. The second term of the series is found to be minute compared with the first, even for $t=0$, $r=0$. Consequently,

$$\frac{T - T_\infty}{T_0 - T_\infty} \doteqdot \frac{2pa}{k_1} \cdot \frac{\sin \frac{\epsilon_1 r}{a}}{\frac{\epsilon_1 r}{a}} \cdot \frac{e^{-\frac{k_1}{\rho_1 c_1} \cdot \frac{\epsilon_1^2}{a^2} t}}{\epsilon_1 \operatorname{cosec} \epsilon_1 - \cos \epsilon_1}.$$

Hence if $T_c$ is the core-temperature

$$\frac{T_c - T_\infty}{T_s - T_\infty} = \frac{\epsilon_1}{\sin \epsilon_1} \doteqdot \frac{100}{99{\cdot}3}.$$

There is thus, in our experiments with 2 mm. platinum spheres (and *a fortiori* with larger sizes) never more, and generally much less, than 1 per cent. drop in surface-temperature as compared with core-temperature.

The above analysis suggests that the cooling during flight is not of such a magnitude as to vitiate our experimental results. In particular it may be observed that the effect increases with decrease of speed, so that the slower ball is, if anything, *cooler* than the faster ball. There is, therefore, no question of the effect of speed upon ignition being due to cooling.

The theory has been tested in three ways :—

(1) Calorimetric measurements were made by shooting the ball into a small brass vessel, placed beyond the baffles, and connected to a thermocouple. No difference in heat-loss could be detected between a 15 metre/sec. and a 30 metre/sec. ball after traversing the same stretch of air (the apparatus was accurate to $\frac{1}{2}$ per cent.).

(2) Ignition curves were derived in the usual way with the mouth of the heating tube removed to 64 cm. instead of 40 cm. from the explosion tube. The curves coincided with those formerly obtained at 40 cm. This indicates that the heat-loss at 40 cm. was of such a magnitude that (assuming it to be proportional to the distance traversed) an increase of 50 per cent. was unobservable. The original heat-loss, itself, may therefore be taken as negligible.

(3) Direct photographic record was made of the temperature of the pellet surface during flight, by shooting it across the field of a wide angle lens. A series of tracks, on one plate, corresponding to the same speed of flight (indicated by curvature), but different temperatures, allowed the cooling to be estimated. Differences of 20° produced a noticeable change in intensity, and it could be said with conviction that no such cooling occurred.

## 6. *Theoretical.*

The factors which may be supposed to affect the ignition of a gas by a hot moving surface are so many, and in some cases so obscure, that a complete theory is probably out of the question. To begin with, the hydrodynamical problem of fluid flow round a sphere, except in the ideal case of zero viscosity and subcritical speeds, is exceedingly complex. It is true that viscosity-effects in gases are small at a distance from solid surfaces ; but they become important in the boundary layer adjoining these surfaces, and it is precisely with such a layer that we are concerned ; moreover, the speeds employed have often been above the critical limit for stream-line flow ; in other words, ignition spreads through a turbulent wake, and the conditions of continued propagation may be thereby complicated. When the hydrodynamical equations are taken in conjunction with the equations of heat transfer, they present a problem which cannot in general be solved exactly. Its solution, however, would be of doubtful value for our purpose, as we may expect the conditions of fluid-flow and heat-transfer to be modified if not transfigured by the chemical reaction. This reaction in turn is far from simple, when initiated, as in our case, by an incandescent surface. How far the ignition is purely thermal and how far it depends on adsorption at the surface we do not know.

The following theory is a " thermal " one, developed along the lines followed by Silver *, *i. e.*, on the assumption that extinction is due to over-rapid loss of heat to the unburnt gas. The process of ignition is considered to occur in the viscous boundary layer surrounding the sphere : we therefore regard the sphere as at rest in, and at the same temperature as, the immediately adjoining gas, but losing heat at a rate dependent (as indicated in section 5 above) on its real velocity through the distant gas, and proportional to its temperature excess over that gas. This implies a surface temperature gradient which is similarly proportional; and we further assume with Silver, though this may perhaps be questioned, that the same gradient persists for a small, but finite distance out into the gas, *i. e.*, that $\frac{\partial^2 T}{\partial n^2}=0$ at the surface, $n$ being a normal vector.

Let us assume the rate of heat-transfer (total) to be given by equation (3) of section 5, *i. e.*, by

$$\frac{dH}{dt}=Aa\mu c_p(T_s-T_\infty)\sqrt{Re}$$

$$=\frac{A}{1\cdot35}ak(T_s-T_\infty)\sqrt{\frac{2aV\rho}{\mu}}\,\dagger.$$

We assume also spherical symmetry, and therefore adopt a uniform surface gradient $\frac{\partial T}{\partial n}$ given by :

$$-4\pi a^2k\frac{\partial T}{\partial n}=\frac{A}{1\cdot35}ak(T_s-T_\infty)\sqrt{\frac{2aV\rho}{\mu}},$$

whence
$$\frac{\partial T}{\partial n}=-C(T_s-T_\infty)\sqrt{\frac{V\rho}{a\mu}}\,\ddagger,$$

in which $C=\frac{A\sqrt{2}}{(1\cdot35)4\pi}$ is a numerical constant with a probable value of about 0·6 (Boussinesq : 0·8358). This gradient is assumed to hold throughout a shell of thickness $\delta$. The rate of *loss* of heat from this shell is therefore

---

* *Loc. cit.* p. 649.

† See page 12.

‡ It is interesting to note that essentially the same expression for $\frac{\partial T}{\partial n}$ is obtained by assuming the temperature to fall uniformly from $T_s$ to $T_\infty$ in the thickness of the boundary layer; for this thickness is of the order of $\sqrt{\frac{a\mu}{V\rho}}$ (see Prandtl, *Handbuch der Experimentalphysik*, iv. 1, p. 36).

$$4\pi(a+\delta)^2 Ck\sqrt{\frac{V\rho}{a\mu}}(T_s-T_\infty)-4\pi a^2 Ck\sqrt{\frac{V\rho}{a\mu}}(T_s-T_\infty)$$

*i. e.*,

$$8\pi Ck\delta(T_s-T_\infty)\sqrt{\frac{V\rho a}{\mu}},$$

which must be equated to the rate of development of heat through reaction in order to define a critical condition for flame. This heat of reaction is, in Silver's notation, $\int_a^{a+\delta} 4\pi x^2\beta Q e^{-A/RT(x)}dx$, where $T(x)$ by our assumption is $=T_s-C(T_s-T_\infty)\sqrt{\frac{V\rho}{a\mu}}(x-a)$. In order that the variable part may be relatively small and the integral reduce to $4\pi a^2\delta\beta Q e^{-A/RT_s}$, we require $\delta C\sqrt{\frac{V\rho}{\mu a}}$ small: in other words, $\delta$ must be small compared with the thickness of the boundary layer ($C \simeq 1$), which is otherwise evident. Equating these heats,

$$8\pi Ck\sqrt{\rho/\mu}(T_s-T_\infty)V^{1/2}=\beta Q a^{3/2}e^{-A/RT_s} \quad . \quad . \quad . \quad . \quad . \quad (1)$$

In this equation, $k\sqrt{\rho/\mu}$ will vary little with temperature in our range $[\frac{1}{2}(T_s+T_\infty)=783 \text{ to } 933]$ for any one explosive mixture: for air the variation is only between $(14{\cdot}38)10^{-5}$ and $(14{\cdot}27)10^{-5}$; it will vary to a greater extent with the mixture strength, but still not enough to vitiate our (chiefly qualitative) applications of (1). Again, Q is a characteristic of the reaction, which we suppose the same in each case. Hence $\frac{8\pi kC\sqrt{\rho/\mu}}{Q}$ will be regarded as a single constant D. In the resultant equation, viz.,

$$D(T_s-T_\infty)V^{1/2}=\beta a^{3/2}e^{-A/RT_s}, \quad . \quad . \quad . \quad . \quad . \quad . \quad . \quad (2)$$

$\beta$ depends only on the concentration (for a given reaction), A is regarded as constant, and R is the gas-constant per gram-molecule.

### *Comparison with Experiments (on Coal-Gas).*

(*a*) If the mixture ($\beta$) and V, $T_\infty$ are kept constant, (2) gives

$$a^{3/2} \propto (T_s-T_\infty)e^{A/RT_s}.$$

We suggest, therefore, that $\log\left(\frac{T_s-T_\infty}{a^{3/2}}\right)$ will vary linearly with $1/T_s$

and that the "gradient" will be $-\frac{A}{R}$. Inserting Silver's results, we find that this is true, except that, as with Silver's own expression $\log\left(\frac{T_s - T_\infty}{a}\right)$, the gradient seems more nearly $-\frac{2A}{R}$. But the value of A is uncertain.

(*b*) If $T_s$, $T_\infty$, and $a$ are constant, and the mixture ($\beta$) variable, then

$$V \propto \beta^2.$$

$\beta$ consists of two factors, the constant C of the integrated van't Hoff isochore $w = Ce^{-A/RT}$ and a factor $f$ which depends on the concentration of the mixture. While $f$ is unknown unless the kinetics of the reaction are completely specified, it may be taken as varying from zero at a 0 per cent. mixture through a maximum to zero at a 100 per cent. mixture. Since, therefore, $V \propto f^2$ we have qualitative agreement with our experimental curves of fig. 5.

(*c*) Keep $\beta$, $a$, $T_\infty$ constant, as in the principal series of explosions. Then

$$V \propto \frac{1}{(T_s - T_\infty)^2} e^{-2A/RT_s};$$

writing

$$\frac{RT_s}{2A} \equiv \theta, \quad \frac{RT_\infty}{2A} \equiv \theta_\infty, \quad \text{we}$$

have

$$V \propto \frac{1}{(\theta - \theta_\infty)^2} e^{-1/\theta}.$$

Now

$$\frac{\theta_\infty}{\theta} = \frac{T_\infty}{T_s} \doteqdot \frac{3}{13} \quad \text{when} \quad T_s = 1300$$

$$\text{and} \quad \doteqdot \frac{3}{16} \quad \text{when} \quad T_s = 1600.$$

$\therefore \frac{\theta_\infty}{\theta}$ varies only a little, and we may write $V \propto \frac{1}{\theta^2} e^{-1/\theta} \equiv v$ (say). When $v$ is plotted against $\theta$, it gives a curve of the well-known frequency shape, which is linear (approx.), with $\frac{d\theta}{dv}$ positive, between $\theta = 0{\cdot}1$ and $\theta = 0{\cdot}4$, *i. e.*, between

$$T_s = \frac{2A}{10R} \quad \text{and} \quad T_s = \frac{8A}{10R}.$$

If we take A as 10,000 * and R as 2, the limits become : $T_s=1000$ °K. and $T_s=4000$ °K. These include our range of temperature. The theory therefore accounts for the linear form and the direction of the characteristics in figs. 3 and 4 ; it must be pointed out, however, that the value of A here assumed, while probably sound, is not that suggested by paragraph (*a*) above.

As to the *slopes* of the characteristics, they can be obtained from our theory in terms of the current coordinates V and $T_s$ ; for evidently

$$\frac{dV}{dT_s}=\frac{2V}{T_s}\left\{\frac{A}{RT_s}-1-\frac{T_\infty}{T_s}\right\}$$

$$\doteqdot\frac{2V}{T_s}\left\{\frac{4700}{T_s}-1\right\}$$

Fig. 6.

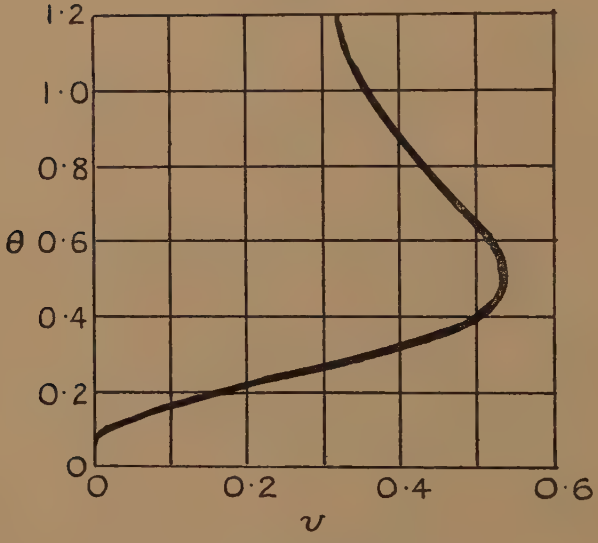

Graph of $v=\frac{1}{\theta^2}e^{-1/\theta}$.

on the present assumption. The slopes have been calculated from this expression for the points on the curves of fig. 4 where $T_s=1423$ (except 6 per cent.). They are all of the same order of magnitude as those displayed in fig. 4 ; in most cases the discrepancy is small, but in some it amounts to as much as ±50 per cent. No systematic variation is apparent. The same remarks apply to fig. 3.

---

* *Cf.* Silver, *loc. cit.* p. 652.

(*d*) $\beta$, $T_s$, $T_\infty$ constant. Then

$$V \propto a^3.$$

This relation is difficult to test, for unless the diameters of our spheres are very nearly equal there is no temperature at which points are known for *both* characteristics. For example, the 2 mm. platinum curves begin at about 1000° C., and those for 3·5 mm. platinum, owing to limitations of speed, have not been extended above 930° C. By extrapolation we have estimated the limiting speed for a 3·5 mm. sphere at 1020° C. in 7 per cent. coal-gas-air to be about 35 metres per second. The observed value for a 2 mm. sphere is 10 metres per second. These figures suggest rather $V \propto a^2$ than $V \propto a^3$.

(*e*) Our theory makes no provision for the nature of the surface, nor the material of the sphere. It is therefore probably unable to explain the difference in behaviour of quartz and platinum, and the "ageing" of the platinum spheres.

(*f*) Finally, keeping $\beta$, V, and $a$ constant, let us examine the effect on $T_s$ of varying $T_\infty$. From (2),

$$\frac{\partial T_s}{\partial T_\infty} = \frac{1}{1 - \frac{A}{RT_s^2}(T_s - T_\infty)}.$$

If $\frac{A}{R} = 5000$, as before, $T_s = 1300$, $T_\infty = 300$, then $\frac{\partial T_s}{\partial T_\infty} \doteqdot -\frac{1}{2}$. Thus $T_\infty$, $T_s$ should have variations of the same order, but in opposite directions. The explosive mixture was heated to above 200° C. in the hope of detecting this effect, but $(T_s)_{\text{min.}}$ for the 2 mm. platinum spheres did not change by an observable amount from its value when $T_\infty$ was the normal room-temperature (20° C.). The question calls for more detailed examination.

In conclusion we may say that, while the above theory accounts for most of the prominent features of ignition by hot particles, it leaves a good deal to be desired in other respects. Improvement is perhaps to be expected when the mechanism of heat-exchange and reaction at the surface are more precisely known, and the temperature distribution around a moving sphere has been completely analysed in the light of contemporary knowledge of boundary layers and turbulent flow. The fact that speed has such a pronounced influence upon ignition precludes any purely surface theory of the effect: the mechanism of transference (whether "thermal" or "chain") must play a part. But the conditions at the surface, though not the only factors, are, in the writer's opinion, of prime importance.

## 7. *Summary.*

(1) A survey of the literature of ignition by hot surfaces suggests that the speed of relative motion of gas and surface is a factor determining whether ignition takes place ; it is further surmised that increase of speed results in decrease of igniting power.

(2) An apparatus for examining the effect of speed when the surface is that of a small sphere is then described in detail.

(3) The results obtained with this apparatus are given. They apply to coal-gas-air and may be summarized as follows :—

(*a*) There is a minimum ignition temperature, for a given size of sphere, below which ignition has not been obtained. This temperature appears independent of the richness of the mixture, of the " age " of the sphere, and of its material, as far as this has been varied (quartz and platinum). It is well above the ignition temperatures by the more usual sources of ignition.

(*b*) For temperatures above this minimum, ignition is regularly observed, provided that the speed does not exceed a critical value. When this value is exceeded ignition does not take place.

(*c*) This critical speed is a function of the temperature : it increases as the temperature is increased, according to a roughly linear relation.

(*d*) The slope of the temperature-critical speed characteristic decreases (*i. e.*, the critical speed for any given temperature increases) as the richness of the mixture is increased from its value at the lower explosive limit. The slope reaches a minimum value at a concentration somewhat in excess of that corresponding to maximum flame-speed ; and subsequently increases as the mixture-strength is further raised towards its upper explosive limit.

(*e*) The characteristics for fused silica (" quartz ") spheres rise more steeply than those for platinum spheres of the same size, but the minimum ignition temperature is the same as before, and shows the same constancy with varying mixture-strength.

(*f*) The platinum spheres are found to improve their igniting power with use.

(*g*) The initial temperature of the mixture appears to have no effect (over a range of 200° C.) on the *minimum* igniting temperature of a platinum sphere (2 mm.).

(4) The question of cooling suffered by the spheres before entry into the mixture is examined theoretically and experimentally. The effect is concluded to be negligible in the present experiments.

(5) A theory is given which explains qualitatively the main features of the work ; the points mentioned in (3) (*e*), (*f*), (*g*), above do not find

an explanation in this theory, which is of an excessively simple nature. Suggestions for improvement are made.

The experiments were conducted in the Research Laboratories of the Natural Philosophy Department at Glasgow University, under the supervision of Professor E. Taylor Jones, and I am glad to have this opportunity of expressing my indebtedness to him for constant help and encouragement. I wish also to thank Imperial Chemical Industries, Ltd., who suggested the problem, for permission to publish, and for a personal grant. To Dr. G. Green I am obliged for many valuable references.

# II. *The Threshold and Equilibrium Curves of Supraconductors.*

By J. G. DAUNT, Clarendon Laboratory, Oxford *.

[Received December 23, 1938.]

THE experiments reported in this paper were carried out to investigate the agreement between the critical magnetic fields required to disturb supraconductivity at different temperatures, as found (1) by resistance measurements and (2) by determination of the induction for a number of pure supraconductive substances. In a previous publication $^{(1)}$, the critical field at which an infinitely long pure supraconducting specimen changes *reversibly* from zero to normal induction has been termed the "equilibrium" field, in contra-distinction to the more well-known term of threshold field which we will now reserve for those critical fields at which the electrical resistance disappears. Very considerable differences between threshold and equilibrium values have already been observed by Mendelssohn and Moore$^{(2)}$ on tantalum. As it was, however, not clear to what extent these differences had been caused by chemical and physical impurities, it was necessary to extend the experiments to metals in which these difficulties could be avoided.

The equilibrium fields are by definition those which must be used in any evaluation of the thermodynamic properties of the supraconducting substance (*e. g.*, the difference in entropy and difference in specific heat between the normal and the supraconductive states, etc.). And it was the purpose of the experiments described below to test with what degree of accuracy the threshold fields could be used for such similar evaluations. It is well known that it is possible for supraconducting bodies in which the induction is different from zero to show at the same time zero resistance (*cf.* $^{(2)}$), and it cannot be predicted on theoretical grounds alone that the equilibrium and threshold values will be identical †‡.

---

* Communicated by Dr. K. Mendelssohn.

† In transverse fields the situation is even more complex, the fields at which the induction first becomes finite and those at which the resistance first differs from zero showing at times marked differences. See *e. g.*, de Haas, Voogd and Jonker, *Physica*, i. p. 281 (1934); A. D. Misener, Proc. Roy. Soc. A, clxvi. p. 43 (1938); and Mann, Grayson-Smith and Wilhelm, Phys. Rev. liv. p. 754 (1938).

‡ The fundamental equation of F. and H. London (Proc. Roy. Soc. A, clix. p. 71 (1935) treats the "ideal" case in which threshold and equilibrium field coincide.

### *Experimental Arrangements.*

The supraconductive substances tested were tin, mercury, and lead. The tin and lead were the purest obtainable, as supplied by Messrs. Adam Hilger (H–S tin, Lab. no. 10,000, purity 99·996 per cent.; H–S lead, Lab. no. 8334, purity 99·999 per cent.). The purest mercury supplied by Messrs. Hopkin and Williams was employed and redistilled before using. All these substances had been previously used in the determination of their equilibrium values and were found to be very pure indeed(1).

Fig. 1.

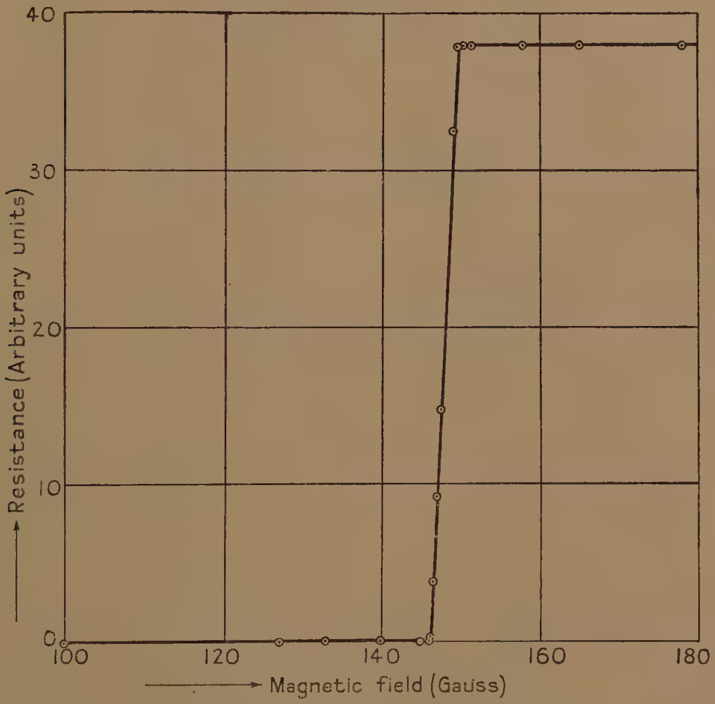

Resistance transition curve of tin at 2.54° K.

The resistance threshold values were measured for these substances by employing the shielding effect of the persistent currents in a supraconductive surface to small A.C. magnetic fields, as an indication of the existence of zero resistance in the specimen. The method has been described in detail in a previous publication(3). The specimens were in the form of long hollow cylinders of length 10 cm., diameter 1 cm., and of wall thickness 1 mm., and the disturbance of supraconductivity was measured in a longitudinal magnetic field (the demagnetizing factor being in this case negligible). The magnetic field was homogeneous to within 0·5 per cent. throughout the whole volume occupied by the specimen. The transitions from zero to normal resistance and *vice versa* were measured at constant temperature by increasing or decreasing the applied magnetic field, and were found to be very sharp (except for lead, as will be described later) and quite reversible, as is shown by a typical case for tin given in fig. 1. The slight finite interval of transition, from 146·0 gauss to 149·6 gauss, is due to the technique of the A.C. method

TABLE I.

Threshold Values of Tin, Mercury, and Lead.

| Tin. | | Mercury. | | Lead. | |
|---|---|---|---|---|---|
| Temp. °K. | Field. Gauss. | Temp. °K. | Field. Gauss. | Temp. °K. | Field. Gauss. |
| 3·443 | 38·5 | 3·880 | 52·7 | 7·22 | 0 |
| 3·325 | 53·5 | 3·746 | 77·9 | 6·98 | 50·5 |
| 3·014 | 94·6 | 3·586 | 104·7 | 6·80 | 98·0 |
| 3·002 | 95·0 | 3·482 | 122·9 | 6·74 | 101·5 |
| 2·290 | 104·7 | 3·284 | 156·0 | 6·52 | 148 |
| 2·702 | 131·6 | 3·136 | 179·7 | 6·50 | 150 |
| 2·640 | 139·1 | 2·954 | 208·0 | 6·28 | 196 |
| 2·537 | 147·8 | 2·784 | 229·3 | 6·22 | 204 |
| 2·255 | 177·6 | 2·604 | 256·8 | 6·13 | 225 |
| 2·237 | 181·6 | 2·432 | 278·5 | 6·08 | 230 |
| 2·117 | 195·0 | 1·535 | 364·8 | 5·94 | 256 |
| 2·073 | 199·0 | | | 5·81 | 279 |
| 1·59 | 240·6 | | | 5·43 | 336 |
| | | | | 5·18 | 383 |
| | | | | 4·96 | 425 |
| | | | | 4·76 | 455 |
| | | | | 4·69 | 466 |
| | | | | 4·58 | 485 |
| | | | | 4·37 | 517 |
| | | | | 4·23 | 547 |
| | | | | 3·65 | 627 |
| | | | | 3·47 | 649 |
| | | | | 3·26 | 674 |
| | | | | 2·92 | 710 |
| | | | | 2·65 | 738 |
| | | | | 2·32 | 762 |
| | | | | 2·06 | 781 |
| | | | | 1·53 | 810 |

employed, and is exactly equal to twice the amplitude of the applied A.C. field. The exact threshold value therefore is given by the middle of this interval of transition, *i. e.*, 147·8 gauss at 2·54° K.

Fig. 2.

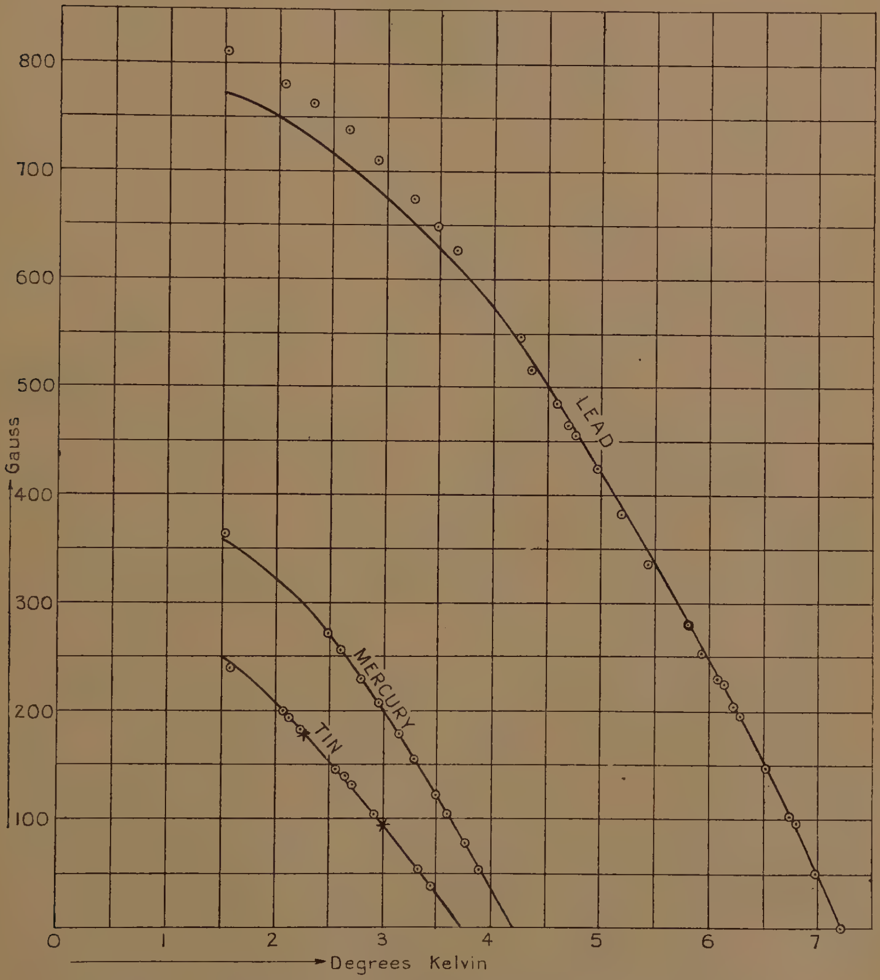

The full curves give the equilibrium values and the points marked with a circle the threshold values measured.

All the measurements both above and below 4·2° K. were made in small helium cryostats, which have already been fully described by Mendelssohn and the author⁽⁴⁾.

### *Results.*

The threshold values obtained for tin, mercury, and lead are given in Table I., and are plotted in fig. 2. The accuracy to which the magnetic field could be measured was less than 0·5 per cent., and the accuracy of temperature measurement below 4·2° K. was within 0·003° K. by the use of a special device⁽⁵⁾. The temperatures above 4·2° K. were measured by a helium gas thermometer which, after the necessary corrections had been made, gave an accuracy to within 0·03° K.

The equilibrium curves⁽¹⁾ of these substances are also plotted in fig. 2 for comparison.

### *Discussion.*

It will be seen from fig. 2 that for tin the agreement found between the resistance threshold values measured in this way and the equilibrium values is well within experimental error, as has been pointed out already by de Haas and Miss Engelkes ⁽⁶⁾ for this substance. Indeed, in two experiments with the tin hollow cylinder, the disturbance of supraconductivity was observed by the A.C. resistance method and by simultaneously measuring the induction of the *same* specimen directly. The latter measurements were effected by having a small flip coil which could be moved relative to the specimen in the usual way⁽⁵⁾. In these experiments the agreement between the resistance threshold values and the magnetic equilibrium values was striking, the induction becoming normal at exactly the same field strength at which the resistance was restored to that of the normal state *. The points obtained in this way are marked with a star in fig. 2.

For mercury also over the whole temperature range measured (1·5° K. to the transition point), the threshold and the equilibrium values were, within experimental error, the same, except perhaps for the lowest point at 1·535° K., where the threshold value seems to be slightly higher than equilibrium curve.

For lead, however, as is shown in fig. 2, there is a most noteworthy difference between the threshold and the equilibrium values †. At high temperatures (above 4·2° K.) the two methods do not show a marked difference, but as the temperature is lowered the differences becomes steadily greater, the resistance values in all cases being above the magnetic values. At 1·5° K. the difference is as much as 40 gauss, *i. e.*, 5·2 per cent.

---

* This has also been done by de Haas and Miss Engelkes ⁽⁶⁾ at one temperature with a different method, yielding the same result.

† The equilibrium values of lead below 4·2° K. measured by Schubnikow and collaborators, *Phys. Zeit. Sowjetunion*, x. p. 165 (1936), lie in between the equilibrium and the threshold values given here, which may be due to the slight hysteresis that occurs in magnetic measurements⁽¹⁾.

In order to understand the possible mechanism of the transition which causes these results, it is interesting to compare the actual resistance transition curves for tin (given in fig. 1) and for lead (see fig. 3). It will be seen from fig. 1 that the resistance of the tin specimen increases suddenly when the threshold field is reached (the finite small interval of transition, as has been explained earlier, being due to the special technique of the A.C. method), and that after normal resistance has been attained, a further increase of the magnetic field produces no further increase of resistance. For lead, however, as is shown in fig. 3, the resistance does not rise immediately at the threshold field to a value

Fig. 3.

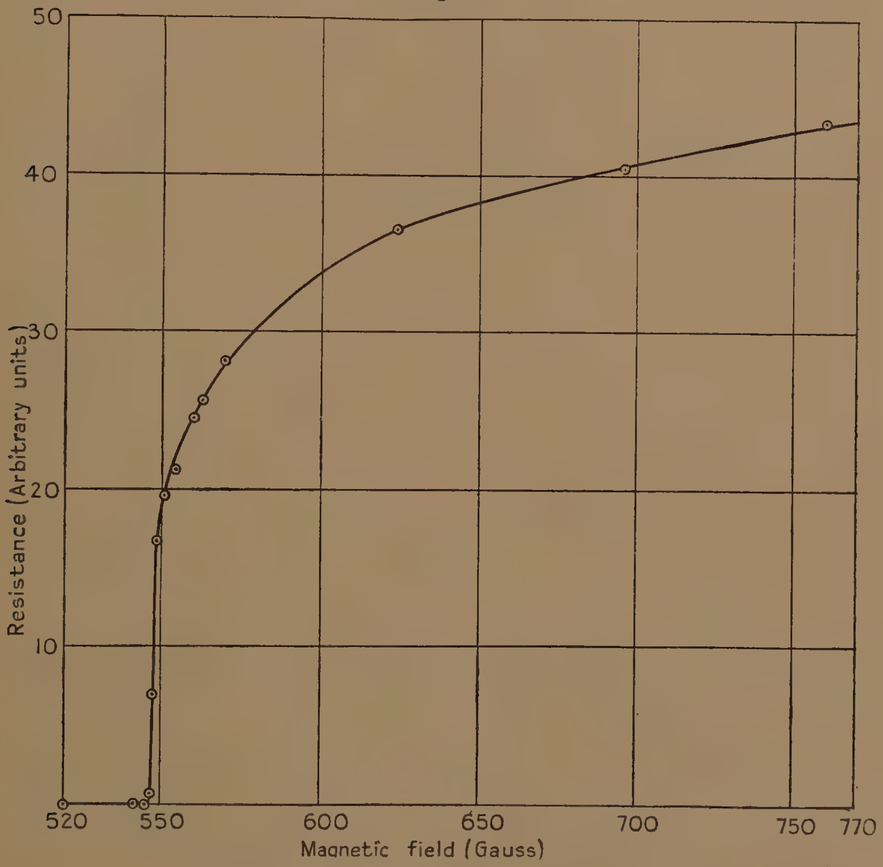

Resistance transition curves of lead at 4·23° K.

which remains constant when the field is increased further, but continues to rise gradually as the field is raised above the threshold value *. On decreasing the field little or no hysteresis is observed.

At the temperature 4·23° K. at which the curve of fig. 3 was measured, the resistance was still increasing with increase of magnetic field at one-and-a-half times the threshold field strength. In order to check the slight possibility that this behaviour might be due to the technique employed, direct measurements of the resistance of wires drawn from the same Hilger lead were made at the same temperatures. It was found that exactly similar transition curves were obtained, showing that the method employed in measuring the resistance gave correct results.

Further, it was found that these transition curves for lead only showed this broadening in high magnetic fields, *i. e.*, at temperatures well below the transition point (7·2° K.). Similar curves taken at higher temperatures showed a growing similarity to the ideal transition curve of tin as the temperature was raised.

It might be suggested at first that this steady increase of the resistance of lead with increasing magnetic field *above* the threshold value is simply due to the normal "magneto-resistance" effect, observed also in non-supraconductors. This seems improbable, however, first because one would expect the resistance in this case to increase with the square of the magnetic field, as observed for example in the case of tin(7), a relationship which is not shown by these experiments on lead ; and secondly, it seems unlikely, owing to a consideration put forward by Mendelssohn and Pontius(8) with regard to the determination of the heat resistance of lead in a magnetic field. They found the heat resistance of lead to *decrease* even after the threshold value of the magnetic field is exceeded, and pointed out that this decrease of the heat resistance in increasing magnetic fields and the increase of the electrical resistance under the same conditions are evidently due to a common cause. It thus appears that the gradual decrease of the thermal resistance, and coupled with it the increase of the electrical resistance above the threshold value, are connected with the phenomenon of supra-conductivity, and not with the ordinary magneto-resistance effect, as the latter should result in an

---

* A similar transition was observed in Voogd, 'Dissertation,' Leiden, p. 71 (1931), in measurements of the resistance of a lead wire. He ascribed this broadening of the transition to deformations in crystal structure of the wire, which may have been caused by drawing . As, however, the same properties are observed in our experiments on cast bulk lead, and by Pontius (13) on carefully annealed lead wires, this explanation cannot hold. Owing to this broadening of the transition of lead in a magnetic field, it must be pointed out that the threshold values given in Table I. and fig. 2 are the values of the field at which the first sudden increase of resistance occurred.

*increase* both of the heat and the electrical resistance, as has been shown by de Haas and Bremmer⁽⁷⁾, and by Grueneisen and Giellessen ⁽⁹⁾.

It seems also impossible to ascribe the anomalous behaviour of lead to impurities, as the lead contained less than 0·001 per cent. of other metals and showed practically no " frozen-in " magnetic moment in the magnetic induction experiments⁽¹⁾. It is further evident that, as quite generally the addition of impurities increases both the thermal and electrical resistivity of a metal, the same arguments, which have been applied against the explanation of the effect by the ordinary action of a magnetic field, are also valid against impurities.

The disagreement between the threshold and the equilibrium values, as well as the broadening of the transition curve in lead of high purity, seems to indicate that we have to deal in this case with a somewhat gradual change between the supra-conductive and the normal state, which cannot be accounted for by chemical or physical impurities of the substance alone.

The evidence collected so far on the occurrence of supra-conductivity in pure metals indicates that all the properties of the substance change very abruptly at the transition from one state into the other (with the possible exception of the thermo-electric properties⁽¹⁰⁾). In fact, such transitions seem to be completely discontinuous (*cf.* ⁽⁵⁾), showing no evidence of a preparation for the change from one state to the other until the actual transition value of temperature * or magnetic field is reached. However, here in the case of extremely pure lead the transition in high magnetic fields shows a gradual dying out of some of the supraconductive properties (electrical and heat resistance) in increasing magnetic fields; and also shows in decreasing the magnetic field from values far above the threshold value a preparation for the supraconductive state by a gradual decrease in the electrical resistance. It is possible that at high fields, in which the difference in free energy between the supraconductive and the normal state is comparatively great, there is a greater possibility of the supraconductive parts of the body to split up into small regions, which would have a lower free energy than the bulk material. (The threshold fields for lead are approximately three times as high as those for tin.) These small regions would possess far higher threshold values than the bulk material ⁽¹¹⁾, and hence not lose their supraconductive properties until fields well above the normal threshold field of the bulk material are exceeded. And similarly, it may be supposed that on decreasing the field again small supraconductive regions begin to appear, long before the bulk of the specimen becomes supraconductive, on account of the lower free energy of such an arrangement. Such a behaviour is already well known to occur in supraconductive alloys⁽¹²⁾, all of which have very much higher threshold fields than pure supraconductors; and it is interesting to note that those pure supraconductors which have very steep threshold curves (*e. g.*, tantalum, niobium, etc.) show a very great tendency to behave in high magnetic fields like an alloy⁽¹⁾ ⁽²⁾.

---

* Keesom and van Laer, *Physica*, iv. p. 487 (1937), find evidence of a broadening of the transition of a pure tin ellipsoidal (solid) specimen in passing into the normal state from calorimetric measurements, and have suggested that at the end of the transition very fine needles remain in the supraconductive state which do not pass into the normal state until a field higher than the threshold field is applied.

Pontius⁽¹³⁾ has shown that the threshold value of very pure lead can be increased if specimens of small size are employed *; and it would be interesting to see whether in other metals, which show ordinarily a very abrupt transition, the transition would also be broadened as the threshold field increases with decreasing size of the specimen.

This splitting up into small regions of supraconductive material would explain the changes in electrical and heat resistance in high magnetic fields, and yet would have little effect on the induction owing to the extremely small volume of such regions, as is indeed the case. That it should have some effect on the induction method of measuring the equilibrium values, however, is suggested by the slight hysteresis which is observed⁽¹⁾.

Such a description of an actual existence of supraconductive "needles" surrounded by normal metal is, of course, a very crude one, and the phenomena described in this paper might perhaps be interpreted by considering this intermediate state as being of a more homogeneous structure. The outcome of our experiments seems to indicate, however, without doubt, that the transition between the supraconductive and the normal state loses its abrupt character and proceeds in a more gradual way the higher the magnetic field is in which this transition takes place.

In conclusion I should like to thank Dr. K. Mendelssohn for many helpful discussions.

## *Summary.*

The threshold values of tin, mercury, and lead were found from measurements of their resistance.

The threshold values were found to agree well with previously measured equilibrium values for tin and mercury, although there was a marked difference in the case of lead.

---

* This result has recently been confirmed by experiments of Shalnikow, 'Nature,' cxlii. p. 74 (1938), and of Appleyard and Misener, 'Nature,' cxlii. p. 474 (1938).

It was observed that the change to zero resistance in lead becomes more gradual as the temperature is decreased, and it is thought probable that quite generally the transition region between the supraconductive and the normal metal loses its abrupt character in high magnetic fields.

### *References.*

(1) J. G. Daunt and K. Mendelssohn, Proc. Roy. Soc. A, clx. p. 127 (1937).
(2) K. Mendelssohn and Miss J. R. Moore, Phil. Mag. (7) xxi. p. 532 (1936).
(3) J. G. Daunt, Phil. Mag. (7) xxiv. p. 361 (1937).
(4) J. G. Daunt and K. Mendelssohn, Proc. Phys. Soc. l. p. 525 (1938).
(5) K. Mendelssohn, Proc. Roy. Soc. A, clv. p. 558 (1936).
(6) W. J. de Haas and Miss A. D. Engelkes, *Physica*, iv. p. 325 (1937).
(7) W. J. de Haas and H. Bremmer, *Leid. Comm.* 214*d* (1931); and *cf.* C. J. Milner, Proc. Roy. Soc. A, clx. p. 207 (1937).
(8) K. Mendelssohn and R. B. Pontius, Phil. Mag. (7) xxiv. p. 777 (1937).
(9) E. Grueneisen and J. Gielessen, *Ann. Phys.* xxvi. p. 449 (1936).
(10) W. H. Keesom and C. J. Mattijs, *Physica*, v. p. 1 (1938).
(11) See, *e. g.*, C. J. Gorter, *Physica*, ii. p. 449 (1935); H. London, Proc. Roy. Soc. A, clii. p. 650 (1935); M. von Laue, *Ann. Phys.* xxxii. p. 71 (1938).
(12) See, *e. g.*, W. J. de Haas and J. Voogd, *Leid. Comm.* 214 *b* (1931); K. Mendelssohn and Miss J. R. Moore, 'Nature,' cxxxv. p. 826 (1935); J. N. Rjabinin and L. W. Schubnikow, *Phys. Zeits. Sowjetunion.* vii. p. 122 (1935).
(13) R. B. Pontius, Phil. Mag. (7) xxiv. p. 787 (1937).

# III. *The Thermal Method of Measuring Losses in Sheet Dielectrics at Radio Frequencies and High Electrical Stresses* *.

By J. T. MacGregor-Morris, D.Sc.(Eng.), M.I.E.E.,
and G. L. Grisdale, Ph.D., B.Sc. †.

[Received March 30, 1939.]

## Summary.

The measurement of dielectric losses by the calorimetric estimation of the heat produced in a specimen of dielectric when it is subjected to an alternating stress is discussed theoretically The factors affecting the accuracy of the method are examined; the method is obviously best suited for conditions under which appreciable heat is developed, *i. e.*, when there is a high voltage stress of high frequency.

Apparatus is described with which measurements of dielectric losses may be measured by a transient thermal method. Results are given for several of the materials tested.

## Contents.

Page
I. Introduction .................................... 35
II. Theory of Method ............................ 35
    Fundamental Principles ....................... 35
    Determination of Heat produced ............. 36
        (*a*) The Steady State Method ............... 36
        (*b*) The Transient Method .................. 37
    Examination of Temperature-rise Curve ........ 39
        Initial Transient Condition .................. 43
III. Experimental Methods ........................ 47
    Review of Previous Work ..................... 47
    Conclusions regarding Electrode Design ....... 50
    Electrodes in Vacuum ........................ 51
        Cooling of Electrodes ....................... 54
    Experimental Method used .................... 55
    Accuracy of Measurements ................... 56
    Auxiliary Apparatus .......................... 57
IV. Results ........................................ 58
V. Conclusions .................................... 61
    Acknowledgments ............................ 63
    Bibliography .................................. 63

---

* Abstract of a thesis by G. L. Grisdale approved for the degree of Doctor of Philosophy in the University of London.

† Communicated by the Authors.

## I. INTRODUCTION.

THE better-known methods of determining dielectric losses may be termed "electrical methods," for they all involve purely electrical means of finding the electrical constants of a given piece of dielectric. These include bridge, substitution, wattmeter, and oscillographic methods; an account of the work done in this field was given some years ago by Hartshorn (1). The conductivity or specific loss of a dielectric may also be measured by a calorimetric measurement of the heat produced in the dielectric, the only assumption being that all the energy supplied electrically appears as heat in the dielectric. The method is only suitable for high frequency and high stress measurements, for only in these circumstances do the losses result in a measurable temperature rise. In addition, the purely electrical methods have not, to the authors' knowledge, been applied at high stresses and high frequencies.

## II. THEORY OF METHOD.

### *Fundamental Principles.*

This paper deals solely with sheet dielectrics, since a disk cut from a sheet is the most convenient form of test specimen.

Such a specimen of dielectric has a capacity given by

$$C=\frac{\epsilon A}{4\pi s\times 9\times 10^{11}}\text{ farads} \quad . \quad . \quad . \quad . \quad . \quad . \quad . \quad (1)$$

and an equivalent parallel resistance

$$R=\frac{s}{\sigma A}\text{ ohms,} \quad . \quad . \quad . \quad . \quad . \quad . \quad . \quad . \quad (2)$$

where A is the area in square cm., $s$ is the thickness in cm., $\epsilon$ and $\sigma$ are the dielectric constant or permittivity and the conductivity of the dielectric at the frequency of the applied voltage. When the power factor of the condenser formed by the dielectric specimen is very small, as it is in the case of all practical insulating materials, it may be assumed that the power factor is equal to the tangent of the loss angle, so that

$$\text{Power Factor}=\tan\delta=\frac{2\sigma\times 9\times 10^{11}}{\epsilon f}, \quad . \quad . \quad . \quad . \quad . \quad (3)$$

where $f$ is the frequency in cycles per second.

The power loss in the dielectric when subjected to a sinusoidal voltage of R.M.S. value E is

$$W=\frac{E^2\sigma A}{s}=\frac{E^2Af\times\epsilon.\tan\delta}{2s\times 9\times 10^{11}}\text{ watts.} \quad . \quad . \quad . \quad . \quad . \quad (4)$$

Therefore

$$\epsilon . \tan \delta = \frac{Ws \times 1{\cdot}8 \times 10^{12}}{E^2 A f} . \quad \ldots \ldots \quad (5)$$

If the loss in a given piece of sheet dielectric can be accurately measured the product of the power factor and dielectric constant may be determined. These two factors can be separated if the current flowing into the dielectric can be measured, for

$$\text{Power Factor} = \frac{W}{E . I} . \quad \ldots \ldots \quad (6)$$

The accuracy of the determination of the specific loss depends upon the accuracy of a number of measurements, amongst which is the measurement of the heat produced in the dielectric.

### *Determination of Heat produced.*

The sample of dielectric whose power losses are to be determined is placed in an electrode system, which is constructed mainly of materials of high thermal conductivity. One electrode contains a heater winding, so that a known D.C. wattage may be dissipated in the electrode system. By this means the thermal capacity of the electrodes may be found. Assuming that at any instant the temperature is the same at all parts of the electrode system, *i. e.*, that the thermal resistances of the electrodes and specimen are negligibly small, the temperature varies according to the relation

$$W = m . \frac{d\theta}{dt} + f(\theta - \theta_0) , \quad \ldots \ldots \quad (7)$$

where $\theta$ = the temperature of the electrode system,

$m$ = the thermal capacity of the electrode system,

W = the power loss in the electrodes.

The function $f(\theta - \theta_0)$ represents the power loss from the system by cooling, this loss being a function of the difference between the temperature of the electrodes $\theta$ and the temperature of the surroundings $\theta_0$, to which the electrodes lose heat by conduction, convection, and radiation.

When the heat is produced by losses in the dielectric material these losses may be determined in either of two ways.

(*a*) *The Steady State Method.*—If the quantity of heat produced is reasonably small the temperature may reach a constant steady value within the normal working range of the apparatus, and all the heat produced will then be lost in cooling. Under these conditions $W = f(\theta - \theta_0)$. The cooling function may be found by making similar steady state observations with a known input to the heater.

(*b*) *The Transient Method.*—The loss may be determined by making observations of the temperature before the electrodes reach a steady state condition. It can be seen from equation (7) that the loss may be found from observations of $\frac{d\theta}{dt}$ if $m$ and $f(\theta-\theta_0)$ are known. The method of finding the cooling function by steady state determinations is tedious; the cooling may be found by heating the electrodes to a high temperature and allowing them to cool freely, taking a temperature-time graph. Under these conditions $W=0$, and the temperature varies according to

Fig. 1.

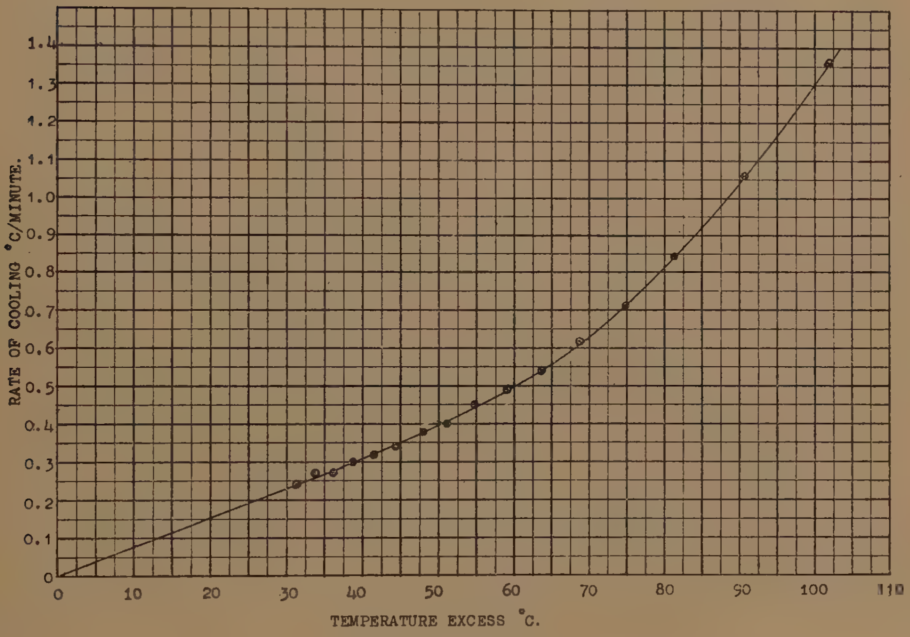

Cooling correction.

$$\frac{d\theta}{dt}=-\frac{f(\theta-\theta_0)}{m}.$$

Thus, by drawing tangents to the cooling curve, $\frac{f(\theta-\theta_0)}{m}$ may be plotted as a function of $\theta-\theta_0$.

Having determined the cooling function we are now in a position to find the thermal capacity of the electrode system. A temperature rise curve is taken with a constant input to the heater, the equation of temperature rise being, from (7),

$$\frac{W}{m}=\frac{d\theta}{dt}+\frac{f(\theta-\theta_0)}{m}. \qquad (8)$$

W is accurately measurable, $\frac{d\theta}{dt}$ is obtained by drawing tangents to the temperature rise graph, and the cooling function has already been found experimentally and plotted for a range of values of $(\theta-\theta_0)$ so that the thermal capacity $m$ may be calculated.

Fig. 2.

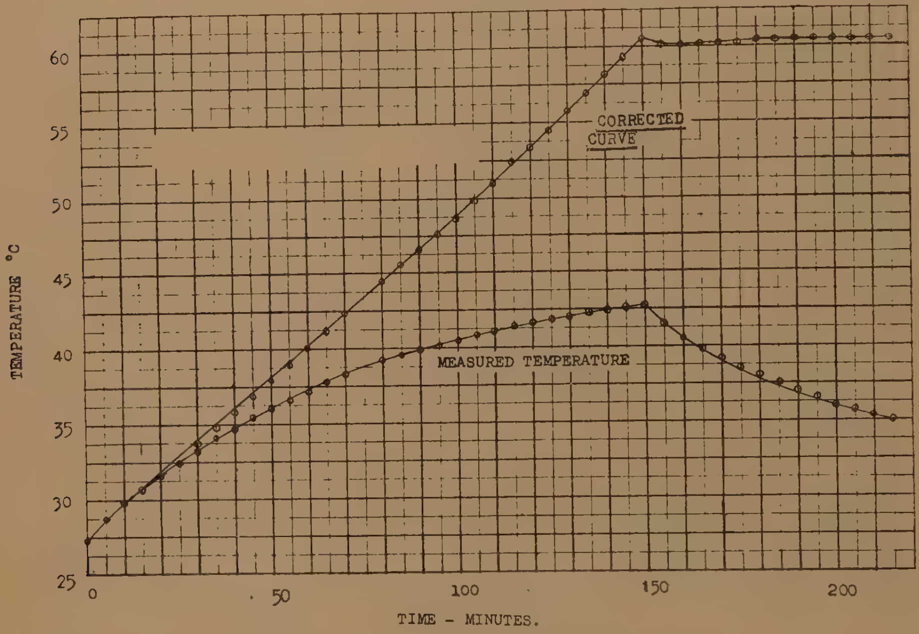

Temperature-rise curve using D.C. heater.

It must be observed that the cooling function as plotted varies inversely as $m$, so that if $m$ is changed a correction must be applied to the cooling function. Such a change occurs when a specimen of different thermal capacity is inserted in the electrodes. The cooling correction for one set of electrodes is shown in fig. 1.

It is now possible to determine the magnitude of the loss in the electrodes from temperature observations, using equation (8). The high frequency loss in the dielectric can thus be measured. Figs. 2 and 3 show temperature-rise curves for constant heater input and high frequency loss respectively. The lower curve in each case shows the actual temperature/time variation, the upper curve being obtained after correcting each reading for cooling. It can be seen that the corrected curve for D.C. heating is a straight line, whereas that for H.F. loss is curved up to the point of switching off the input. The D.C. input remained constant, but the high frequency loss became smaller as temperature increased. In most of the temperature-rise curves the high frequency voltage applied to the electrodes was kept constant, a decreasing loss in the dielectric indicating that the specific loss of the dielectric decreases with temperature, and *vice versa.* In practice the corrected cooling curve is not drawn for each test, the quicker method of drawing tangents to the measured temperature-rise curve and correcting for cooling being used as already indicated.

Fig. 3.

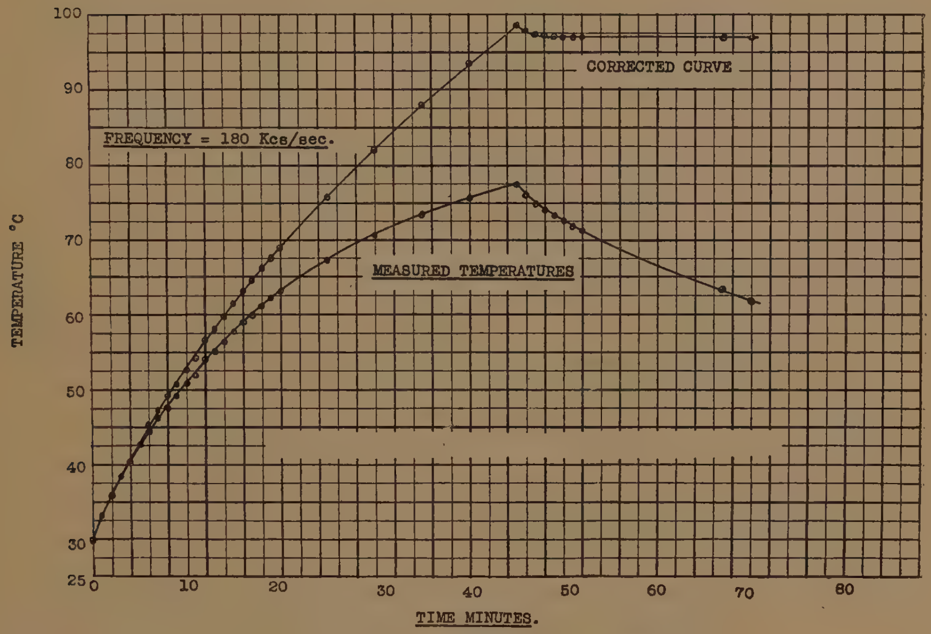

Temperature-rise curve for H.F. heating.

### *Examination of Temperature-rise Curve.*

It has been assumed that all parts of the electrode system are at the same temperature—that is, that the electrode system has no thermal resistance. Since this is not true, and heat has to be transferred from the locality in which it is produced to the rest of the electrode system, thermal gradients must exist in the system. It will be shown that the simple theory of the temperature rise method as presented may be used in calculations so long as certain precautions are taken in the construction of the electrode system and in the evaluation of results.

The following symbols will be used throughout this section :—

$\theta$=the temperature in °C. at any point in the dielectric.
$\theta_1$= ,, ,, ,, ,, at the lower electrode.
$\theta_2$= ,, ,, ,, ,, at the upper electrode.
$\theta_0$= ,, ,, ,, ,, of the surroundings, which is also assumed to be the ambient temperature of electrodes.
$s$=the thickness of the dielectric in cm.
A=the area of the dielectric in square cm.
$x$=the distance of a point along the axis of the dielectric, measured in the direction lower electrode to upper electrode.
K=the thermal conductivity of the dielectric in watts . cm$^{-1}$ . °C$^{-1}$.
$\lambda$=the specific heat of the dielectric in watts . seconds . °C$^{-1}$ . grams$^{-1}$.
$\rho$=the density of the dielectric in grams . cm$^{-3}$.
$\sigma$=the electrical conductivity of the dielectric at high frequency in mhos per cm. cube.
$m_1$=the thermal capacity of the lower electrode in watts . seconds . °C$^{-1}$.
$m_2$=the thermal capacity of the upper electrode in watts . seconds . °C$^{-1}$.
$m_3$=the thermal capacity of the dielectric specimen.
W=the input to the heater or the total high frequency loss in the dielectric in watts.
R=the thermal resistance represented by the cooling in °C. watts$^{-1}$.
E=voltage applied to dielectric.
$M=m_1+m_2+m_3$.

It will be assumed that the dielectric specimen constitutes the only substance in the system which possesses thermal resistance, the thermal conductance of the electrodes being comparatively large. The surfaces of the disk of dielectric are therefore isothermal surfaces, and as the disk is thin it will be assumed that there is no loss of heat from the edge of the disk. Thus the isothermal surfaces inside the dielectric will be parallel to the surfaces. Under these conditions the temperature inside the dielectric is given by

$$\frac{\partial\theta}{\partial t}=\frac{K}{\rho\lambda}\cdot\frac{\partial^2\theta}{\partial x^2}+\frac{E^2\sigma}{\rho\lambda s^2}. \quad \ldots\ldots\ldots \quad (9)$$

If the distance $x$ is measured from the middle of the dielectric the boundaries of the dielectric are $x=-\frac{s}{2}$ and $x=+\frac{s}{2}$.

A solution of equation (9) is

$$\theta = Ct + Dx^2 + Fx + G + \sum_{n=1}^{n=\infty} [A_n e^{(-a^2\alpha^2{}_n t)} \cos \alpha_n x + B_n e^{(-a^2\alpha_n{}^2 t)} \sin \alpha_n x], \qquad (10)$$

in which $a^2 = \frac{K}{\rho\lambda}$.

This solution satisfies equation (9) whatever the value of $\alpha_n$. The values of the constants will be determined by the initial and boundary conditions.

Equation (9) is a general equation which applies for the heater case as well as for high frequency loss. In the former case the second term of the right-hand side of equation (9) is zero, since E is zero. The boundary conditions are, however, different in the two cases. If the cooling is neglected the boundary conditions are :

(1) Heater Loss Conditions.

$$\text{At } x = -\frac{s}{2}, \quad W - m_1 . \frac{\partial\theta}{\partial t} = -KA\frac{\partial\theta}{\partial x}. \quad . \quad . \quad . \quad . \quad (11)$$

$$\text{At } x = +\frac{s}{2}, \quad m_2 . \frac{\partial\theta}{\partial t} = -KA\frac{\partial\theta}{\partial x}. \quad . \quad . \quad . \quad . \quad (12)$$

(2) High Frequency Loss Conditions.

$$\text{At } x = -\frac{s}{2}, \quad m_1 . \frac{\partial\theta}{\partial t} = -KA\frac{\partial\theta}{\partial x}. \quad . \quad . \quad . \quad . \quad . \quad (13)$$

$$\text{At } x = +\frac{s}{2}, \quad m_2 . \frac{\partial\theta}{\partial t} = -KA\frac{\partial\theta}{\partial x}. \quad . \quad . \quad . \quad . \quad . \quad (14)$$

The initial condition that when $t=0$, $\theta=\theta_0$ applies in both cases.

It will be observed that the general solution of the temperature equation (9) consists of two parts, the second of which is a transient term which ultimately becomes negligible. It is important to know the magnitude of this transient term, for it introduces errors in the determination of the heat produced in the electrode system. The evaluation of this transient term is difficult to solve rigidly, and a useful practical approximation is given later.

The first part of equation (10) indicates the distribution of temperature after the transient term has become very small, and if there is no cooling. Under these conditions the temperature would continue to rise at a steady rate, and a constant distribution of temperature would be set up in the dielectric. This approximates to the practical state of affairs when the temperature excess between the electrodes and surroundings is small, and therefore little cooling takes place. By applying the initial and boundary conditions the first part of equation (10) may be evaluated. It is found that for heater loss conditions

$$\theta=\frac{W}{M}t+\frac{Wm_3}{2KAMs}x^2-\frac{W(2m_2+m_3)}{2KAM}x+\theta_0$$
$$-\frac{Ws}{24KAM^2}[m_3^2+9m_1m_3-3m_2m_3+12m_1m_2-12m_2^2], \quad . \quad (15)$$

and for high frequency dielectric loss

$$\theta=\frac{W}{M}t-\frac{W(m_1+m_2)}{2KAMs}x^2+\frac{W(m_1-m_2)}{2KAM}x+\theta_0$$
$$+\frac{Ws}{24KAM^2}[9m_1^2+9m_2^2-6m_1m_2+m_1m_3+m_2m_3]. \quad . \quad . \quad (16)$$

Fig. 4.

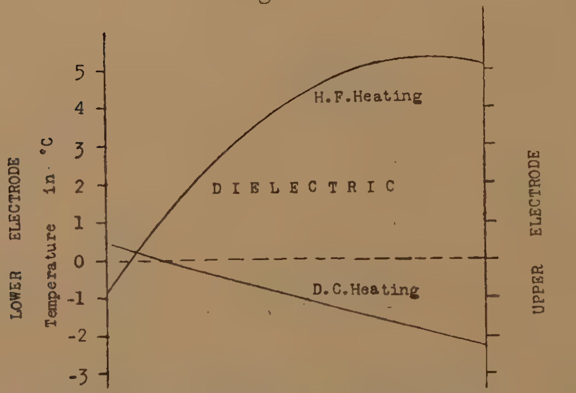

Distribution of temperature through the electrodes after a steady state of temperature rise has set in.

Thickness of dielectric = 0·1 cm.
Loss in electrodes = 1 watt.

In the electrodes used in the vacuum method the constants of the electrodes were :—$m_1=110$ watts . secs . °C$^{-1}$, $m_2=19$ watts . secs . °C$^{-1}$. A specimen of 10 square cm. area was used, and assuming this to be Mycalex 0·1 cm. thick and having 1/K=175° C. watts$^{-1}$ . cm., $m_3=1{\cdot}6$ watts . secs . °C$^{-1}$., the following distribution of temperature is found :—

Heater Loss Conditions.

$$\theta=\theta_0+W(0{\cdot}0077t+1{\cdot}07x^2-2{\cdot}66x-0{\cdot}095).$$

High Frequency Heating.

$$\theta=\theta_0+W(0{\cdot}0077t-86{\cdot}4x^2+6{\cdot}08x+0{\cdot}426).$$

These equations have been plotted in fig. 4 for an input of 1 watt.

When the heating is due to the loss in the heater in the lower electrodes the temperature falls almost linearly towards the upper electrode; this is due to the fact that the thermal capacity of the dielectric layer is small compared to the thermal capacity of the upper electrode. When the loss in the dielectric causes the heating the temperature reaches a maximum value inside the dielectric. This is apparent from the fact that heat must flow out from both faces of the dielectric to the electrodes, and the temperature gradient must be positive looking into the dielectric from each side.

### *Initial Transient Condition.*

As all parts of the electrodes and dielectric are initially at the same temperature there can be no conduction of heat at the instant of switching on. Immediately after switching on a high frequency voltage the loss, which is uniformly distributed through the dielectric, produces a temperature gradient in the dielectric, so that heat may subsequently be transferred to the electrodes. Since the thermal capacity of the dielectric is so small compared with the thermal capacity of the electrodes the time taken to set up this thermal gradient is very small and contributes very little to the initial transient effect. Because both electrodes are initially at the same temperature and their thermal capacities are large the initial temperature gradient in the dielectric must be almost symmetrical about the centre of the dielectric, the surfaces remaining at the ambient temperature until the gradient is set up. When the electrode system has reached a steady state of temperature rise more heat must be transferred to the larger electrode than to the smaller, so that the maximum temperature must be nearer to the smaller electrode, as shown in fig. 4. It is this change from one form of temperature distribution to the final one which causes the major transient.

The dielectric thermal capacity must be taken into account when considering the total thermal capacity of the electrode system, for this directly influences the steady rate of rise of temperature, but when the distribution of temperature in the dielectric is being considered the actual value of $m_3$ is not of great importance, being comparatively small. Let us consider, then, that the thermal capacity of the dielectric is equally divided and that half of this thermal capacity is concentrated on each electrode surface—in other words, the thermal capacities of the electrodes will be considered to be $(m_1+\frac{1}{2}m_3)$ and $(m_2+\frac{1}{2}m_3)$. The total thermal capacity therefore remains as before $M=m_1+m_2+m_3$.

Under these conditions the rates of change of temperature for the electrodes becomes for the lower electrode $m_1$, which contains the heater,

$$\frac{d\theta_1}{dt}=\frac{W}{M}\left[1+\frac{(m_2+\frac{1}{2}m_3)}{(m_1+\frac{1}{2}m_3)}\cdot e^{-\beta t}\right] \text{ for heater loss conditions, .} \quad (17)$$

$$\frac{d\theta_1}{dt}=\frac{W}{M}\left[1-\frac{(m_1-m_2)}{2(m_1+\frac{1}{2}m_3)}\,.\,e^{-\beta t}\right] \text{ for high frequency loss, } . \quad (18)$$

and for the upper electrode $m_2$

$$\frac{d\theta_2}{dt}=\frac{W}{M}(1-e^{-\beta t}) \text{ for heater loss conditions, } . \; . \; . \; . \; . \quad (19)$$

$$\frac{d\theta_2}{dt}=\frac{W}{M}\left[1+\frac{(m_1-m_2)}{2(m_2+\frac{1}{2}m_3)}\,.\,e^{-\beta t}\right] \text{ for high frequency loss, } . \quad (20)$$

Fig. 5.

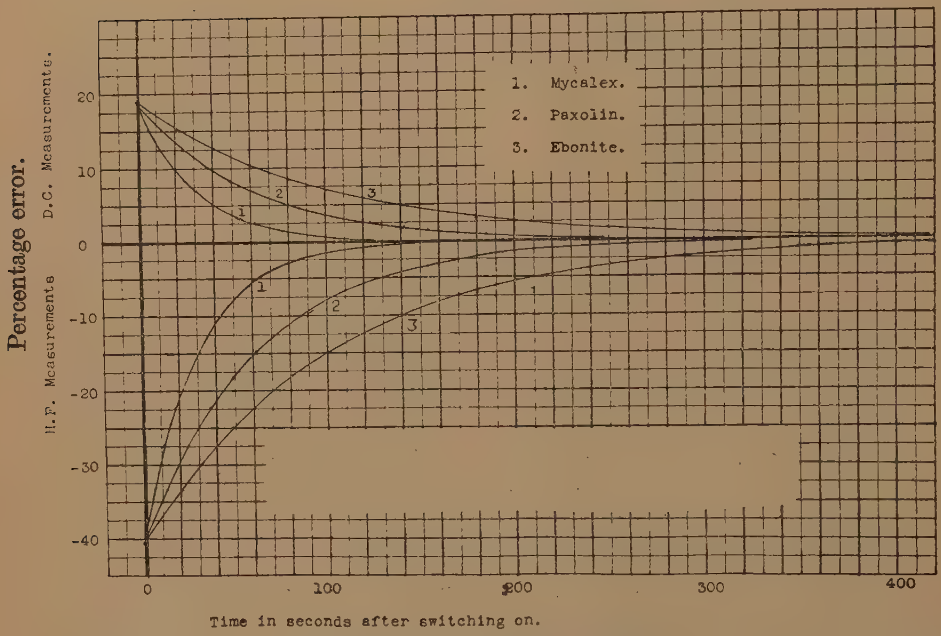

Errors in the calculation of results due
to initial temperature transient.

Thickness of specimen $=0{\cdot}1$ cm.

where
$$\beta=\frac{M}{(m_1+\frac{1}{2}m_3)(m_2+\frac{1}{2}m_3)\dfrac{s}{KA}}.$$

The heater is assumed to be inside the lower electrode $m_1$, the temperature of this electrode being measured in all the experiments. Equations (17) and (19) show that when the heater is used the rate of rise of temperature of the lower electrode is initially greater than that of the upper electrode, as would be expected. Equations (18) and (20) show that if the electrodes have equal thermal capacities the transient terms become zero (for high frequency loss heating) and the temperatures of both electrodes increase at the same rate.

Fig. 6.

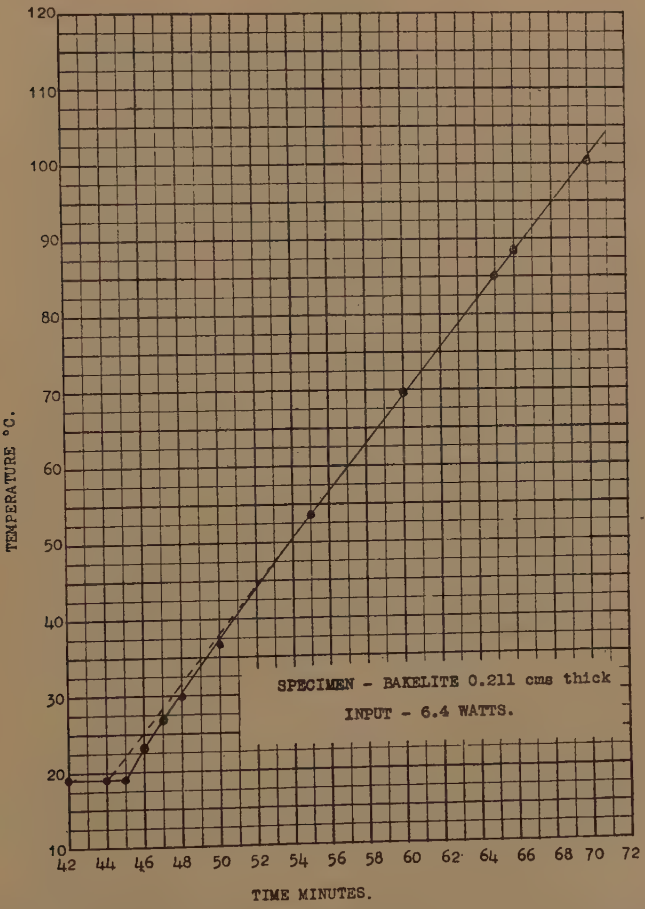

Corrected D.C. temperature-rise curve, showing initial transient period.

It can be seen that although the transient term may be reduced to zero for high frequency heating by making the electrodes of equal thermal capacities, the transient only vanishes for electrode heater loss if the electrode $m_2$ is made infinitely small. The time constant of the transient term is $\beta$, and this can be made large by having one electrode larger than the other. These considerations indicate, therefore, that the electrode containing the heater should have a larger thermal capacity than the other electrode. The dimensions of the electrodes used have already been given, and the value of the transient parts of equations (17) and (18), expressed as a percentage of the constant term, are shown in fig. 5. These values have been calculated for specimens of three insulating materials

Fig. 7

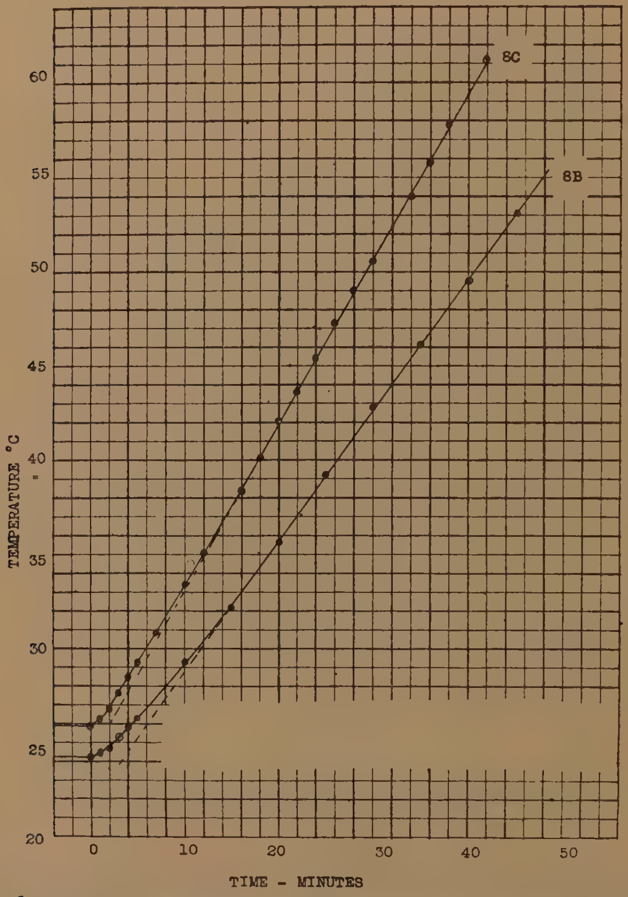

High frequency temperature-rise curves after correction for cooling.

0·1 cm. thick. In the worst case of ebonite (having the lowest thermal conductivity of the three) the error would not exceed 1 per cent. after seven minutes. For thicker specimens the time would be correspondingly longer. These curves indicate the time that must elapse after switching-on before the temperature rise can be said to give an accurate indication of the wattage loss in the electrode system. Some temperature-rise curves for a thick specimen of dielectric are shown in figs. 6 and 7. The initial temperature rise can be seen to be rapid for heater loss and slow for dielectric loss heating.

## III. EXPERIMENTAL METHODS.

### *Review of Previous Work.*

Various modifications of the calorimetric method have been used by previous workers for the estimation of dielectric losses in solid insulating materials. Rosa and Smith⁽²⁾ (1899) made measurements by a continuous flow method at power frequencies; Granier ⁽³⁾ (1923) also used a steady state method; Owen ⁽⁴⁾ (1929) developed a differential calorimeter method, balancing a high frequency dielectric loss on one side against a heater loss on the other. Race and Leonard ⁽⁵⁾ (1936) used the transient calorimetry method with samples of dielectric in the form of cylinders 1½ to 2 inches long. In order to distribute the measured direct current loss in a similar manner to the high frequency dielectric loss a specimen of dielectric was coated with a conducting layer, in which the measured loss was produced. The loss was switched on for exactly two minutes, after which a thermo-junction was pressed into contact with the side of the rod of dielectric, and temperature readings were taken whilst the dielectric cooled. By extrapolating back the cooling curve the temperature at the end of the heating run could be found, and the loss thereby estimated. The discussion of temperature distributions in thin sheets of dielectric in the first part of this paper has shown that some time must elapse befor the dielectric surfaces begin to take up a steady rate of temperature rise. Race and Leonard used rods ½ inch in diameter, taking readings after only two minutes from switching-on, so that a considerable error might be expected due to radial temperature gradients.

At Queen Mary College a thorough investigation of thermal methods has been made. Preliminary measurements beginning in 1928 by F. D. Bolt and W. Lethersich indicated that a transient method would have important advantages over the steady state methods, the chief consideration being the shorter time taken by transient methods. A. Kobler designed and used the electrode system shown in fig. 8. Two samples of dielectric (S) were used in this apparatus, there being one central electrode and two outer electrodes. The three electrodes (KLOP) were of the same area, each consisting of a central electrode of 10 sq. cm. area and surrounded by guard-rings of 20 sq. cm. area. The inner electrode (O) and its guard-ring (P) contained heater windings. Thermo-junctions were soldered to various parts of the apparatus. The electrodes were mounted in a wooden stand (A), and were centred by means of thin paxolin holders (Q) which ran on the brass rods (E). Pressure was applied to the electrodes through the paxolin blocks (F, G) and three ebonite spacers (H) at each end. The outer electrodes (K) and their guard-rings (L) were supported by paxolin rings (M), which transmitted the pressure to the electrodes. The annular gap between the electrodes and their guard-rings was 1 mm. wide, and the electrodes and guard-rings were ground flat together. The guard-rings were surrounded by paxolin rings (N) which prevented the formation of edge corona. The thermo-junction leads from the central inner electrode had to be brought out through its guard-ring; the insulation of the fine wires was thin cellulose acetate sheet. Kobler mounted his electrodes in a large box containing

Fig. 8.

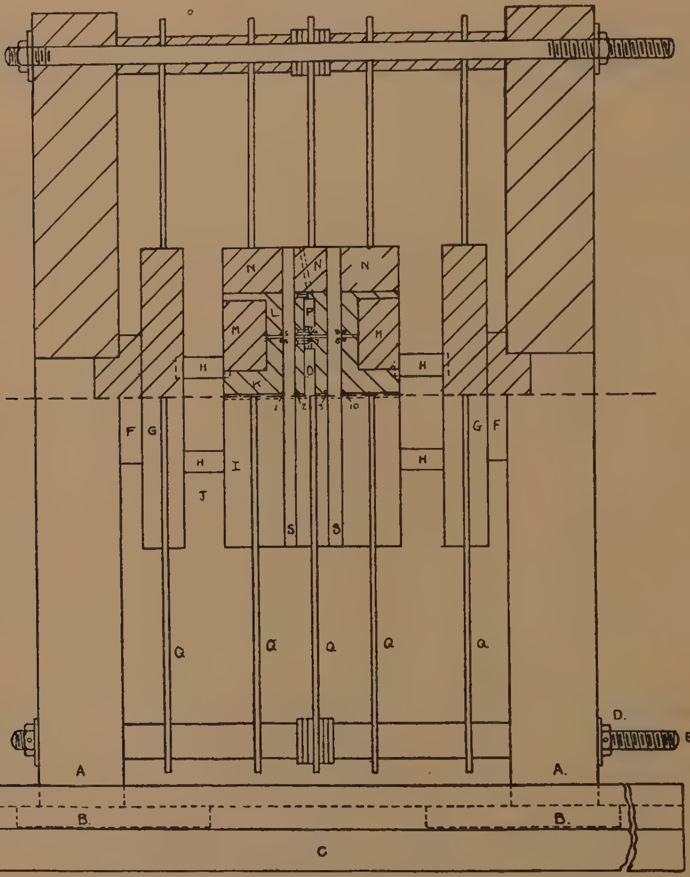

Section through apparatus designed by Kobler.

an air-cooling metal tube system in which water circulated. Cooling was by convection, and took place only from the outer electrodes, the temperature of the inner electrode guard-ring being controlled by means of its heater, so that no heat was lost radially from the central electrode.

The high frequency voltage was applied between the middle electrode and the two outer electrodes, which were earthed. The heater circuits and thermocouples on the central electrode were therefore at high potential, and had to be adequately insulated. The effective area of dielectric tested was the 10 sq. cm. inside the guard-rings. It was assumed that the same amount of material in the electrodes was heated, whether the heating was due to losses in the portion of the dielectric under test or loss in the central electrode due to the heater embedded in it—in other words, the isothermal lines were identical in both cases.

Kobler came to the conclusion that his apparatus was easier to handle than previous electrode systems, due to the smaller number of adjustments to be made. Modification of the apparatus of Kobler was made by the present authors, for it is undesirable to have to make adjustments to circuits at high frequency potential. Kobler had measured the temperature of the outer electrodes, from which cooling was taking place; this had the advantage that an accurate cooling correction could be applied, since the temperature of the cooling surface was known. Calculation showed, however, that the temperature of the inner electrode differed so little from that of the outer electrodes that a sufficiently accurate cooling correction could be applied if only the former temperature were known The high frequency voltage was therefore applied to the outer electrodes, the central electrode being earthed. In this way all the thermocouples and the heaters were at earth potential, as shown in fig. 9. The temperature of the inner central electrode was measured, the two thermocouples on each side of the annular gap being used differentially, the current in the guard-ring heater being adjusted so that there was no temperature difference across this gap. The outer electrode guard-rings were used only electrostatically, so that the current into the desired portion of the dielectric was measured. The electrodes were enclosed in a copper thermostat, a fan being used to obtain better constancy of the temperature.

The thermal capacity of the apparatus was obtained by temperature rise curves, an input of 0·2 to 1·8 watts being dissipated in the central electrode heater. Cooling corrections were applied as indicated in Section II. Similar temperature rise curves were obtained for high frequency heating, and the specific loss calculated. The curves of figs. 2 and 3 were obtained with this apparatus.

The value of the effective thermal capacity of the electrodes was found to vary according to the input wattage, the thermal capacity decreasing with the wattage. This was due to the fact that the temperature of certain parts of the electrode system, particularly thermally insulated sections and the insulating material itself, lagged behind the temperature of the electrodes. This effect made it necessary to correct for the variation in thermal capacity according to the input used.

Fig. 9.

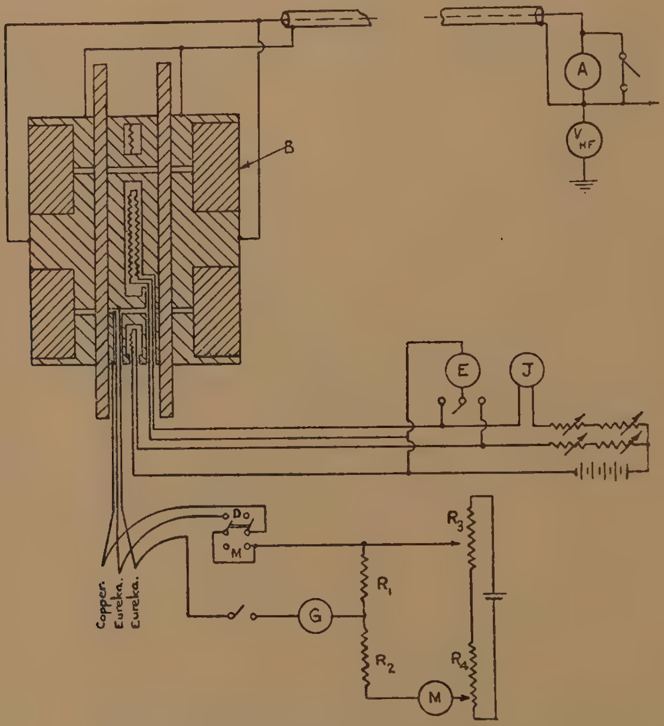

General circuit arrangement.

### *Conclusions regarding Electrode Design.*

(*a*) The presence of large masses of thermal insulating material results in a variation of the effective thermal capacity with the input ; this effective thermal capacity may depend upon the location in which the loss is taking place, *i. e.*, in the heater winding for the calibration loss or in the dielectric for the high frequency loss. The thermal insulation also leads to errors in the cooling correction, but with the electrodes described this effect is very small.

(*b*) The use of three electrodes, each consisting of a central electrode and guard-ring, makes it difficult to ensure an even contact over the surface of the dielectric. It is well known that contact errors play an important part in loss measurements, particularly if the specific loss is low.

(*c*) The use of two samples and extensive guard-rings puts a large capacity load on the high frequency generator. This militates against the production of high stresses by the use of thinner dielectrics and also encourages the generation of harmonics.

(*d*) The cooling from the electrode system is large, so that measurements cannot be made on low loss materials by the transient method, the temperature rise being too small.

(*e*) The actual electrodes are so enclosed by guard-rings that if any corona occurs at the electrode it cannot be detected until the apparatus is dismantled.

With these limitations the apparatus designed by Kobler is capable of yielding results which may be said to be properties of the material tested. Previous work has involved the use of electrodes which do not produce a uniform stress throughout the sample tested; such systems can yield only comparative results between different dielectrics. The separation of the components of the loss, permittivity, and power factor is possible providing a large range of instruments is available for the measurement of the current into the tested portion of the dielectric.

### *Electrodes in Vacuum.*

An electrode system has been developed the design of which was based upon theoretical considerations and the experience gained with previous arrangements. The apparatus has been simplified as far as possible, and the range of the method has been extended so that low loss dielectrics may be tested. It was considered necessary:

(*a*) To reduce the cooling of the electrodes.

(*b*) To make the thermal capacity of the electrodes small, so that a small loss would cause a measurable rise of temperature.

(*c*) That the electrodes should be free of corona.

(*d*) That the dielectric should have a small area, so that the capacity should be low, enabling high stresses to be used.

Granier (3), in 1923, used a vacuum flask in order to reduce the cooling from the electrodes; his electrodes were of cylindrical form, with which only comparative results could be obtained. A large vacuum flask would be required to accommodate flat electrodes, and under these conditions it was found experimentally that the cooling would not be greatly reduced due to the flask.

The electrodes themselves were therefore mounted in an evacuated enclosure, the pressure around the electrodes being low enough to provide electrical as well as thermal insulation. The apparatus had to be easily demountable, so that dielectric specimens could be quickly changed. Details of the electrode system are shown in figs. 10 and 11.

Fig. 10.

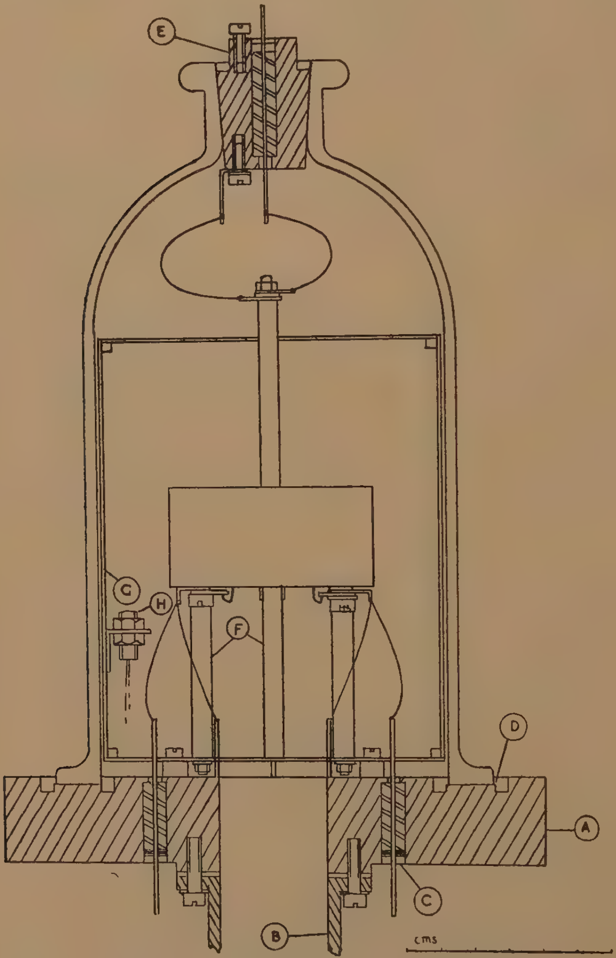

Electrodes mounted in bell-jar.

The vacuum chamber consisted of a glass bell-jar standing on a steel base plate (A), there being a ground grease-joint (D) between them. The top neck of the bell-jar carried a ground steel bushing (E) which formed the high voltage connexions to the electrodes. Inside the bell-jar was a rhodium-plated copper can (G) which restricted the cooling from the electrodes; the base of the can was screwed to the base plate (A), the sides and top being demountable. The metal electrodes were supported by three glass tubes (F), the connexions to the heater, thermo-junctions and lower electrodes being brought through the steel base plate through glass capillaries (C), which were sealed on the outside with vacuum wax. The enclosure was evacuated by the pumping equipment, the top of the final pump being shown at (B).

Fig. 11.

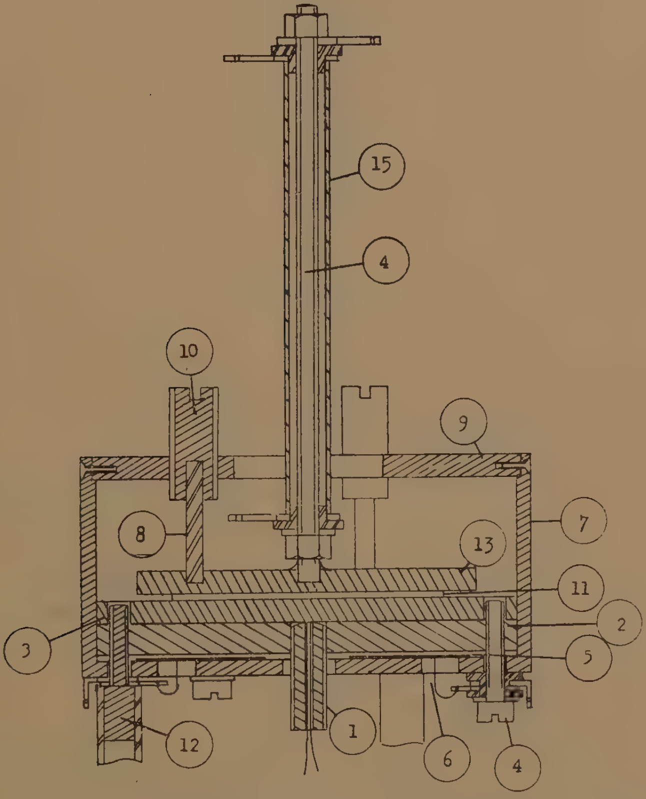

Electrodes for use with vacuum method.

Fig. 11 shows a section through the electrode system. A single disk of dielectric material (11) is clamped between the earthed electrode (3) and the high voltage electrode (13). The electrodes were almost completely surrounded by an aluminium cup (7) and annular top plate (9).

A flat heater winding (5) was tightly clamped between the heater cover plate (2) and the outer shell (7). The actual lower electrode (3) was made of brass, and rested on top of the copper heater cover plate (2), the surfaces in contact being ground flat to reduce the thermal resistance. By this construction the electrode surface could easily be removed for regrinding. The temperature of the electrode was measured with the thermo-junction (1), which screwed into the heater cover plate and pressed against the back of the electrode itself. The electrodes were supported by three glass tubes which fit over aluminium spigots (12).

The top electrode (13) rested on the dielectric (11), and was clamped on to it by the three quartz rods (8) and aluminium adjusting screws (10). The connexion to the top electrode was made through the brass rod (4), which was surrounded by an insulated brass tube (15). This tube acted as an electrostatic guard, so as to reduce the capacity of the central rod to earth; the arrangement was used in the same way as the shielded cable in fig. 9.

It can be seen that the area of the electrodes was greater than the area of the dielectric. Thus the stress in the dielectric was uniform, electrical guard-rings being unnecessary. This construction was made possible because the electrodes operated *in vacuo*; under these conditions no steps needed to be taken to prevent corona. The only insulation in the apparatus consisted of the dielectric itself and the three quartz spacers (8). It was found experimentally that there was no loss in the spacers.

Aluminium was used for the outer casing of the electrode system to reduce the loss of heat by radiation. Several surfaces were tested. The thermal capacities of the electrodes have already been given. The geometrical form of the electrodes is such that thermal gradients in the electrodes are reduced to a small value. The insulation between the heater, wound with flat nichrome strip, and the metal surfaces clamping it consisted of thin mica sheets.

### *Cooling of Electrodes.*

Since the electrodes were operating *in vacuo* the only means by which heat could be lost from them was by radiation and by conduction along the supports and wire leads.

The combined conductance of the three glass supporting tubes was calculated to be $5 \times 10^{-4}$ watts per °C. The leads through the steel base plate were of 20 S.W.G. wire, about one inch projecting inside the bell-jar, where thinner wires completed the connexions to the lower electrode. There were six such wires; the current leads to the heater were completed with 36 S.W.G. copper; there were two 40 S.W.G. copper wires from the ends of the heater, so that its voltage could be accurately measured; lastly, the two thermocouple wires were 40 S.W.G.

copper and eureka. The wires to the top electrode from the top of the bell-jar were 36 S.W.G. copper. The combined thermal conductivities of these wires was $8\times10^{-4}$ watts per °C., and with the glass supports the total conductance was $1{\cdot}5\times10^{-3}$ watts per °C. As the input to the electrodes was never less than 0·2 watt the conductance cooling was not serious for small temperature excesses.

If higher frequencies or higher stresses were to be used the diameter of the wires carrying the high frequency current would have to be increased. The increased cooling would, however, be offset by the increased losses in the dielectric. Under these conditions a new cooling curve would have to be taken.

Cooling by radiation was found to be more serious than the conduction loss. Silvering the inside of the bell-jar was first tried, and reduced cooling by 15 per cent., but the coating of silver was easily damaged in use. A copper shielding can was therefore constructed to almost completely surround the electrodes. The inside of the can was rhodium-plated, this being resistive to the effects of mercury vapour should any diffuse up from the pumps. The shielding can also served as an ambient temperature from which an accurate cooling correction could be calculated ; its temperature was measured by means of a thermocouple mounted on a bracket on the inside of the can.

It was found by experiment that an aluminium outer surface for the electrodes resulted in a lower cooling than was obtained with four other materials tested. Dueval (6) has given the cooling characteristics of a number of materials.

### *Experimental Method used.*

For every new specimen of dielectric used the thermal capacity of the electrode system had to be measured, since the thermal capacity of the specimen is included in the total thermal capacity. Tests on a specimen of dielectric therefore consisted of one temperature rise experiment with a measured heater input and a similar experiment at each high frequency at which the specific loss was required.

The input to the heater for the calibration of the electrodes was kept constant at about 2 watts for some 40 minutes. Sometimes a cooling curve was taken to check the cooling correction, but this was always found to be unchanged. The rate of rise of temperature was taken at several points on the temperature-rise curve, each point being corrected for cooling. From these figures the thermal capacity was calculated, a mean value being taken. Readings were ignored during the initial transient period indicated by fig. 5.

High frequency voltages of the order of 500 to 3000 were applied to the dielectric, and similar temperature rise observations were taken. After correction for cooling the loss in the dielectric was calculated and its specific loss was found. The current into the electrodes was measured, and thus the electrode capacity could be calculated. The capacity of the electrodes for various spacings had been found previously, and the permittivity of the dielectric could therefore be calculated.

### *Accuracy of Measurements.*

The calorimetric accuracy has been discussed. A certain time was allowed to elapse after switching on for the transient temperature rise effect to become small. The actual temperature measurements were made to an accuracy of ±0·1 °C., the limit being set by the thermocouple arrangement and the potentiometer.

A correction was applied for the losses in the thin leads; the power dissipated in the leads was partly transferred to the electrodes and partly lost outside. It was found that half the loss could be assumed to be transferred to the electrodes, the other half being lost. The loss when the heater was used was easy to calculate. When the current was of high frequency the variation of the resistance of the leads with frequency had to be taken into account.

The high frequency generator was designed to give an output as far as possible free of harmonics. It has been calculated that to give an error of 1 per cent. in the loss measurement a second harmonic content of 7 per cent. would have to be present. This corresponds to a damping of 25 per cent. in the output circuit; as this damping was always less than 1 per cent. the effect of harmonics in the high frequency voltage could be neglected.

A large amount of work has been carried out by A. Kobler and others(7) on the effects of different contacts upon the loss in the electrodes. The contact material introduces series capacity and resistance to the dielectric sample. For power frequency work a layer of graphite is deposited on the dielectric. This causes a series resistance to the specimen, and at high frequencies the contact loss is greatly increased due to the increased current. For high frequency work a layer of grease between the electrodes and the dielectric has been found to lead to consistent results; so long as the grease has a power factor of the same order as the dielectric the additional loss is negligible. In the present experiments the grease was a vacuum grease, Apiezon M. The use of oil immersion was considered, but the presence of oil led to breakdown of the evacuated space when high frequency voltage was applied to it. The grease was used in quantities just sufficient to cover the area of the dielectric; a small lump of grease was deposited on each side of the dielectric, and the electrodes were clamped on to it. The electrodes were usually heated to about 60° C. with the heater in order to soften the grease before the clamping screws were finally tightened up. So long as the calibration with the heater was carried out before a high frequency test there was no trouble due to breakdown of the evacuated volume.

Fig. 12.

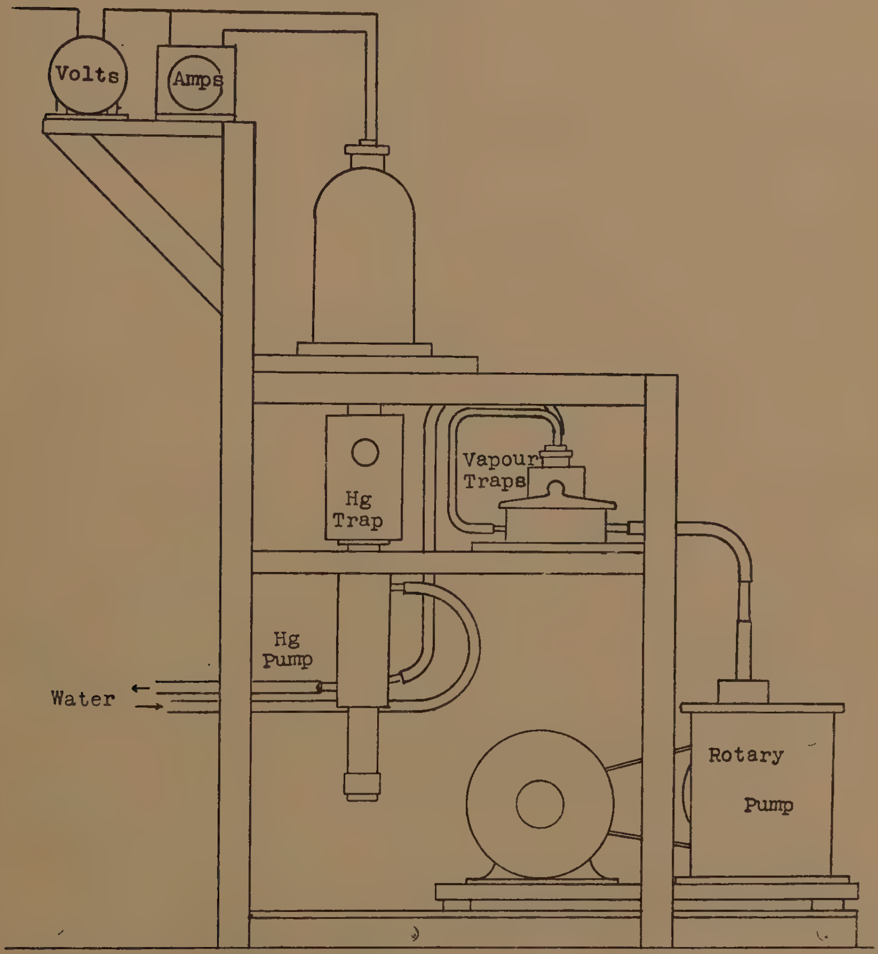

Arrangement of apparatus on wooden stand.

### *Auxiliary Apparatus.*

The arrangement of the pumping system is shown in fig. 12. The mercury vapour trap was bolted under the steel base plate by means of a ground flange fitting. The trap was filled with solid carbon dioxide and ether. Immediately beneath the trap was the Kaye III diffusion pump.

Traps for mercury and water vapour were inserted between the mercury vapour pump and the two stage backing pump.

The high frequency generator covered a frequency range of 100 Kc./s. to 3 Mc./s. This was covered in six ranges by means of plug-in coils. The generator had three stages—oscillator, neutralized buffer amplifier, and final power amplifier. The equipment followed normal transmitter practice as far as the output circuit. The output required in this case was the maximum voltage consistent with a low percentage of harmonics, the question of the power output being of little importance. This can best be attained by making the damping of the output circuit as low as possible. The coils were therefore made large, and of low loss design.

Fig. 13.

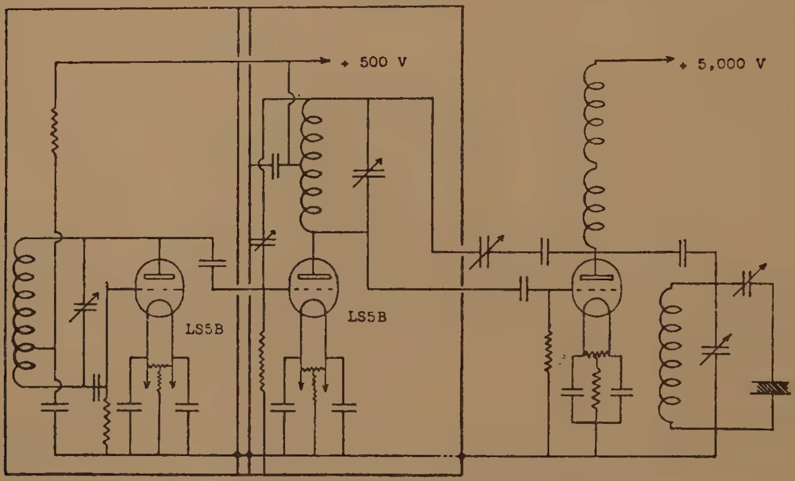

High frequency generator circuit diagram.

The output circuit was choke coupled to the output valve, so that the output circuit could have one end earthed. The circuit of the generator is shown in fig. 13. The power supplies were of orthodox design.

Thermo-junction voltages and the heater current and voltage were measured with a potentiometer and high-grade meters. The heater current was supplied from a 10-volt battery. Thermocouples were individually calibrated from mercury thermometers, the accuracy being ±0·1° C.

As can be seen from equation (5) the high frequency voltage is squared in the expression for the loss. It is therefore important that this measurement should be accurate. It was considered that the direct reading electrostatic voltmeter offered the best type of instrument for this purpose. Several of the instruments available for low frequency work were tried at radio frequencies, but numerous difficulties were encountered with these instruments :

(*a*) Due to increasing losses at higher frequencies the insulation becomes overheated. In one case the bakelite back of one instrument blistered after one hour's run with 1500 volts at 2 mc./s.

(*b*) High frequency corona takes place at a much lower voltage than at power frequencies; also, the power involved in high frequency corona is great, and in some cases the edge of the vane has melted without a complete breakdown having taken place.

(*c*) To reduce corona and the possibility of breakdown the spacing of the vanes has to be increased to at least double the spacing for a power frequency instrument of the same voltage rating. The spring therefore has to be very light, and at high frequency its inductance must be taken into account. This error in the final instrument used for the present work amounted to 0·2 per cent. at 10 mc./s. This neglects the effect of the capacity of the spring, which would minimize the effect.

(*d*) The spring must be capable of carrying the vane current. The terminal capacity of the instrument was 5·2 pF. With 3000 volts at 10 mc./s. applied the total current was 1 ampere, of which about 150 milliamperes was estimated to pass through the spring.

(*e*) The jewel bearings are often mounted on insulated metal strips whose capacity to the high voltage electrodes was found to produce a discharge across the jewel to the spindle. The design of the movement was changed so that the mounting of the jewel could be earthed.

The instrument used was based upon the dwarf voltmeter of Messrs. Everett Edgcumbe and Co., who made the alterations indicated by the experiments. The voltmeter has been fully described elsewhere (8).

## IV. RESULTS.

Specimens were turned from sheet dielectric. The diameter was 3·6 cm., giving an area of 10 sq. cm., and the thickness usually of the order 0·1 cm. The specimens were not conditioned in any way before insertion in the apparatus, but they were usually taken through a temperature cycle up to 80° C. during the heater calibration test. The maximum temperature to which the dielectric was subjected naturally depended upon its thermal properties.

The results of tests upon cellulose acetate, made with Kobler's electrodes, are shown in fig. 14, and for Mycalex in fig. 15, the latter being made with the vacuum electrodes. These curves show the variation of losses with frequency at various temperatures. The tests on cellulose acetate indicate that at the frequencies used the specific loss decreases with increasing temperature. This is contrary to the results obtained at power frequencies (9), and the fact that the graphs cross shows that this reversal might take place in the lower radio frequency region. In the case of Mycalex the loss increases with frequency.

Fig. 16 compares the losses in three substances at 1 Mc./s. In the case of the bakelite the loss reaches a maximum value at about 60° C. The losses in trolitul do not appear to vary greatly with temperature over the limited range used. This substance softens at 60° C.

Fig. 14.

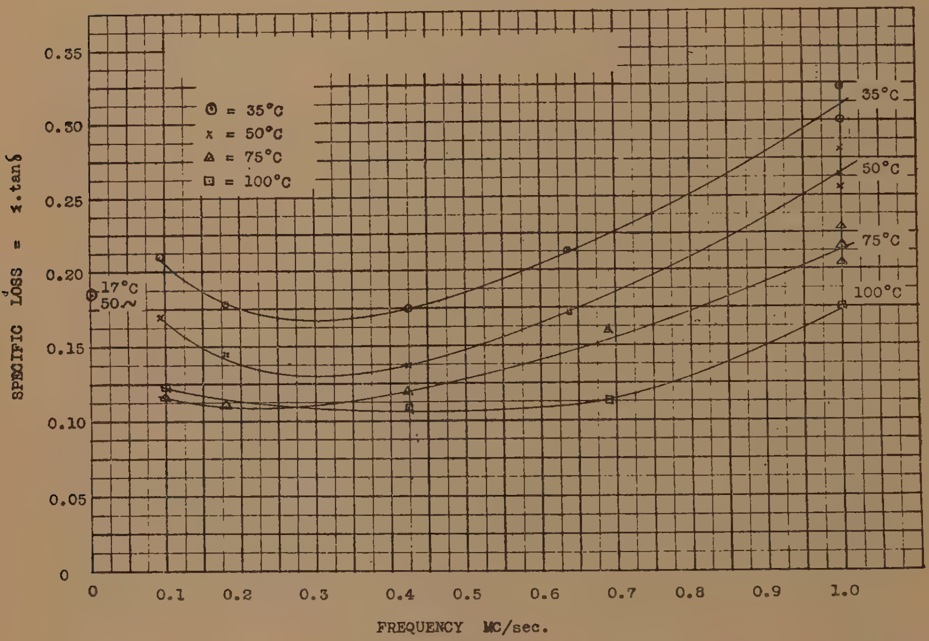

Losses in cellulose-acetate.

Both cellulose acetate and Mycalex appear to have a minimum specific loss in the radio frequency range. Baldwin (5) has observed the same results for quartz, but Bairsto (10) states that for most substances the loss reaches a maximum at a certain frequency. Bairsto does not mention the use of any contact medium, and results at Queen Mary College have shown that bad contact between the electrodes and the dielectric may lead to errors up to 50 per cent. in the loss measurements. Hartshorn (1), in a review of the results of work up to 1926, states that most of these results do not indicate any great change of loss with frequency over the frequency range covered in the present work. The variations observed by the present authors are not large, and certainly do not compare with the variations reported by Bairsto.

The losses at audio frequencies agree with absorption theories (1), the power loss obeying the law

$$W = Af^m,$$

where $W$ = the specific loss in the dielectric,

$f$ = the frequency.

Fig. 15.

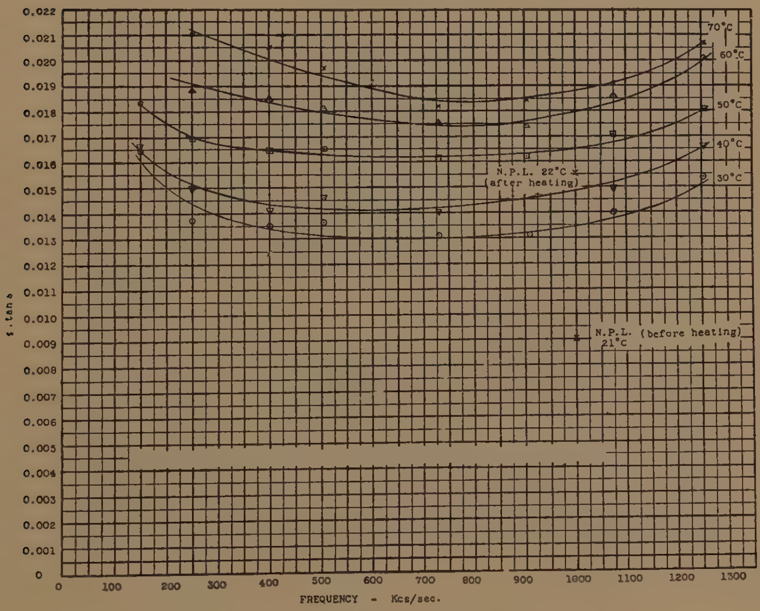

Losses in Mycalex.

A and $m$ are constants of the material, $m$ being slightly less than 1. The losses at radio frequencies certainly do not obey such a law.

## V. Conclusions.

Losses may be measured by the thermal method at high stresses of the same order as those found in practice. The apparatus has so far been used at stresses up to 50 kilovolts per centimetre. In certain cases the permittivity and power factor can be separately obtained, although with less accuracy than their product.

The thermal resistance between different points on the same electrode must be small, and the heater must be in intimate contact with the electrode in which it is housed. The thermal and electrical capacity of the electrode system should be small. The use of guard-rings means that high frequency energy is being used outside the area tested, and with materials of low power this causes the harmonic content of the high frequency generator output to increase.

Fig. 16.

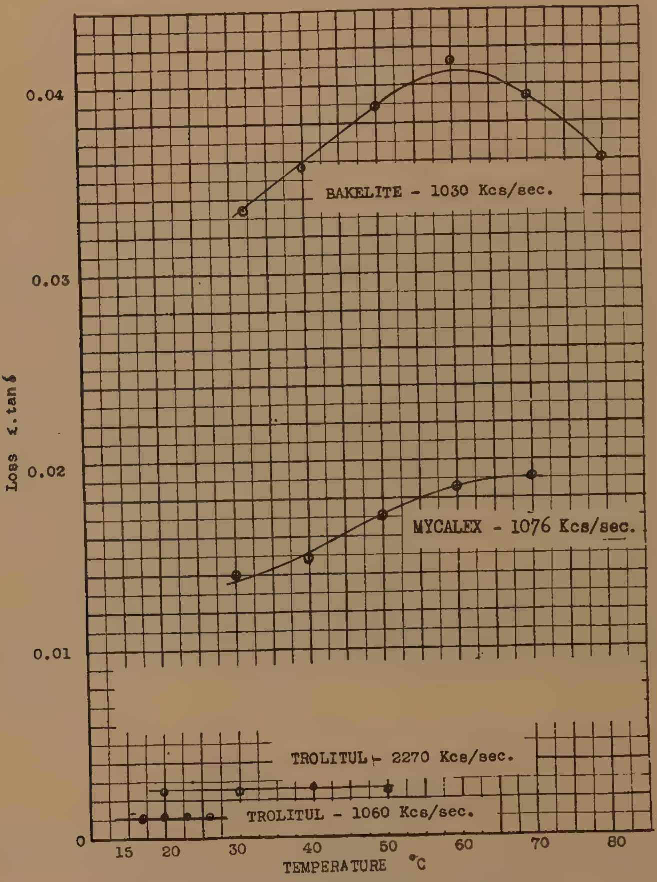

Losses in Mycalex, Bakelite, and Trolitul, showing variation with temperature.

Certain precautions are necessary in order to obtain accurate thermal measurements. The specimens must be thin in order that the initial temperature transient shall be small, and temperature observations must not be taken until this transient has reached a negligibly small quantity. The error due to the transient may be calculated if the thermal constants of the electrode system and dielectric are known.

If there are large masses of insulating material in the electrode system errors occur in the cooling correction and the effective thermal capacity of the apparatus varies. This error is eliminated by the use of vacuum insulation.

The use of the vacuum method does not greatly increase the operating difficulties, since the electrode system can be considerably simplified and there are fewer adjustments to be made. The vacuum apparatus can be evacuated in 15 minutes; to change a sample and clean the electrodes takes 30 to 45 minutes. A test at any one frequency takes 30 to 120 minutes according to the loss.

Summarizing, the work has shown that a loss of between 0·5 and 10 watts may be accurately measured by the transient calorimetry method. The method is preferable to the steady state method because it takes less time and because it provides a means of obtaining the losses over a range of temperatures by means of a single experiment. This is important, particularly at high frequencies, since many failures follow a condition of thermal instability. The thermal method provides a means of comparing the thermal stability of different insulating materials under working conditions.

## *Acknowledgments.*

The work described in this paper formed part of the programme of the British Electrical and Allied Industries Research Association, to whom thanks are due for permission to publish the results of the research. Thanks are also due to the authorities of Queen Mary College (University of London) for the facilities afforded in the Electrical Engineering Department of the College; to Mr. F. E. J. Ockenden for his help in the development of a suitable high frequency voltmeter, and to Mr. A. Kobler for permission to publish details of his work.

## *Bibliography.*

(1) L. Hartshorn, J. I. E. E. lxiv. p. 1152.
(2) Rosa and Smith, Phys. Rev. viii. p. 79.
(3) Granier, Bull. de la Societé Française des Electriciens, iii. p. 333 (1923).
(4) Owen, Phys. Rev. xxxiv. 2, p. 1035 (1929).
(5) Race and Leonard, ' Electrical Engineering,' lv. p. 1347 (Dec. 1936).
(6) Dueval, ' Refrigerating Engineering,' p. 223 (October 1930).
(7) Hartshorn, Ward, Sharpe, and O'Kane, J. I. E. E. lxxv. p. 730.
(8) Ockenden, J. Sc. I. xiv. p. 406.
(9) Whitehead and Nethercot, Proc. Phys. Soc. xlvii. p. 974 (1935).
(10) Bairsto, Proc. Roy. Soc. cxvi. p. 363 (1919).

# IV. *Further Observations on the Action of X-rays on the Electrophoretic Mobility of Colloid Particles.*

By J. A. Crowther, M.A., Sc.D., Professor of Physics in the
University of Reading, H. Liebmann, Ph.D.,
and R. Jones, B.Sc.*

[Received February 14, 1939.]

In previous communications from this laboratory it has been recorded that the electrokinetic potential, $\zeta$, of colloidal particles undergoes rhythmic variations with steadily increasing doses of X- and $\gamma$-radiation. The effect has been demonstrated with colloidal solutions of ferric hydroxide (1), and suspensions of graphite (2), (3), positive and negative carbon (2), and quartz, and more recently with gold sols (4). The existence of the effect in gold sols is of particular interest, because it is possible to prepare uniform sols with particles of different size. This affords a possibility of determining how the effect varies with the diameter of the particles in the sol and obtaining further information on an interesting and at present inexplicable phenomenon.

A series of gold sols of varying particle size was prepared by Zsigmondy's method, using the technique described by Westgren (5). This consists, in brief, in the reduction of a gold chloride solution with phosphorus, giving a "seed" sol of very small particle size. If small quantities of this sol are brought into a dilute gold chloride solution and hydrogen peroxide is added as reducing agent, the gold is deposited on the gold nuclei already present and the mass of the particles is thus increased. The process can be repeated until the particles attain the required dimensions. The number of particles was found by counting in the ultramicroscope, and the gold content was determined by titration with potassium cyanide, a method described by Pennycuik and Woolcock (6). The average mass of a particle is thus obtained. The "radius" $a$, quoted in the tables, is the radius of a sphere having the same mass as one of the particles. Conditions were so adjusted during preparation that the electrolyte content was roughly the same in all sols used for the experiments.

The methods employed for exposing the sol to radiation and measuring the electrophoretic mobilities have been fully described in previous communications. The radiation used in the present series of experiments was obtained from a demountable X-ray tube with a palladium anticathode, excited at 60 K.V. peak voltage, filtered with 0·05 mm. of silver, in order to reduce the amount of softer radiation. In all five different sols have been investigated, the particle radius ranging from $1{\cdot}74\times10^{-6}$ to $6{\cdot}15\times10^{-6}$ cm. This represents the full range available for the experiment. Smaller particles are difficult to see under the ultramicroscope, while larger ones sediment too rapidly. The results obtained for these sols are represented graphically in fig. 1. The abscissæ give the doses measured in rontgen, the ordinates the corresponding change in mobility of the particles. The measurements are all reduced to a standard temperature of 17°. The complete data for all the sols are collected in Table I.

---

* Communicated by J. A. Crowther, M.A., Sc.D.

Fig. 1.

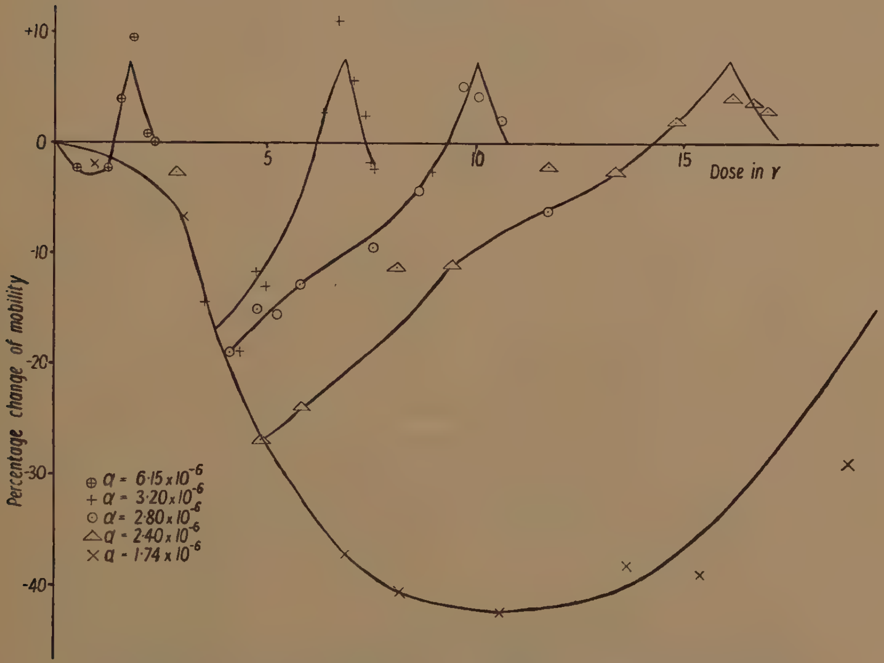

Relation between mobility and dosage for a series of gold sols.

It will be seen from the graph that the curves relating the electrophoretic mobility with the dosage are essentially similar to those obtained with other sols. The only striking point of difference is that, whereas for the other sols the initial portion of the curves shows a rise in mobility, for gold the mobility of the particles shows a decrease after exposure to small doses of radiation. It is at once apparent from the data that the phenomenon is very markedly affected by the size of the particles in the sol. The total percentage change from maximum to minimum produced by the radiation in the mobility of the particles increases regularly from 10 per cent. in the case of the largest particles to as much as 45 per cent. in the case of the smallest particles. The magnitude of the change is, in fact, roughly inversely proportional to the radius of the particle. The dose required to take the particle through its cycle also increases as the size of the particle diminishes, varying from 1·8 *r* for coarsest sol to 28 *r* for the finest.

It may be assumed that the effect of the radiation is to produce some change in the net charge of the colloidal particle and the ion atmosphere around it. The resultant change in potential produced by a given change in charge will be inversely proportional to the electrical capacity of the system, and will thus be the greater as the radius of the particle is decreased. A complete theory of the field round a particle suspended in an electrolyte solution is complicated, and from the mobility data we cannot yet draw any definite conclusions as to the $\zeta$ potential of the moving particles, especially in the case where the particles are electrical conductors. As a first approximation, however, one can regard the $\zeta$ potential as existing between the plates of a spherical condenser. The radial distance of the plates is given by the magnitude $1/\kappa$ of the Debye-Hueckel theory. Calculated from the electrolyte content of the sols used in our experiments it should be of the order of $10^{-5}$ cm. Adopting this simplified representation of the system the charge $q$ on the particle can be expressed by

TABLE I.

| $a \times 10^6$. | $u_0 \times 10^4$. | $D_{min.}$ | $D_{max.}$ | $u_{min.}/u_0$ per cent. | $u_{max.}/u_0$ per cent. |
|---|---|---|---|---|---|
| 1·74 | 2·21 | 9·5*r* | 28·3*r* | 42·5 | 7·5 |
| 2·40 | 2·32 | 5·1 | 16·0 | 26·5 | 7·5 |
| 2·80 | 2·36 | 4·8 | 9·8 | 20·0 | 7·5 |
| 3·20 | 2·27 | 4·2 | 6·7 | 15·5 | 7·5 |
| 6·15 | 2·44 | 1·2 | 1·8 | 2·2 | 7·5 |

$D_{min.}$=Dose required to produce first minimum.
$D_{max.}$=Dose required to produce first maximum.
$u_{min.}$=Minimum mobility. $u_{max.}$=maximum mobility.

$$q = Ka(\alpha+\delta)\,\zeta/\delta,$$

where $a$ is the radius of the particle If we further assume the validity of the Helmholtz equation

$$u=\frac{K\zeta}{4\pi\eta},$$

where K is the dielectric constant of the medium and $\eta$ its viscosity, we can write

$$q=4\pi\eta a(a+\delta)u/\delta \quad . \quad . \quad . \quad . \quad . \quad . \quad . \quad . \quad (1)$$

Fig. 2.

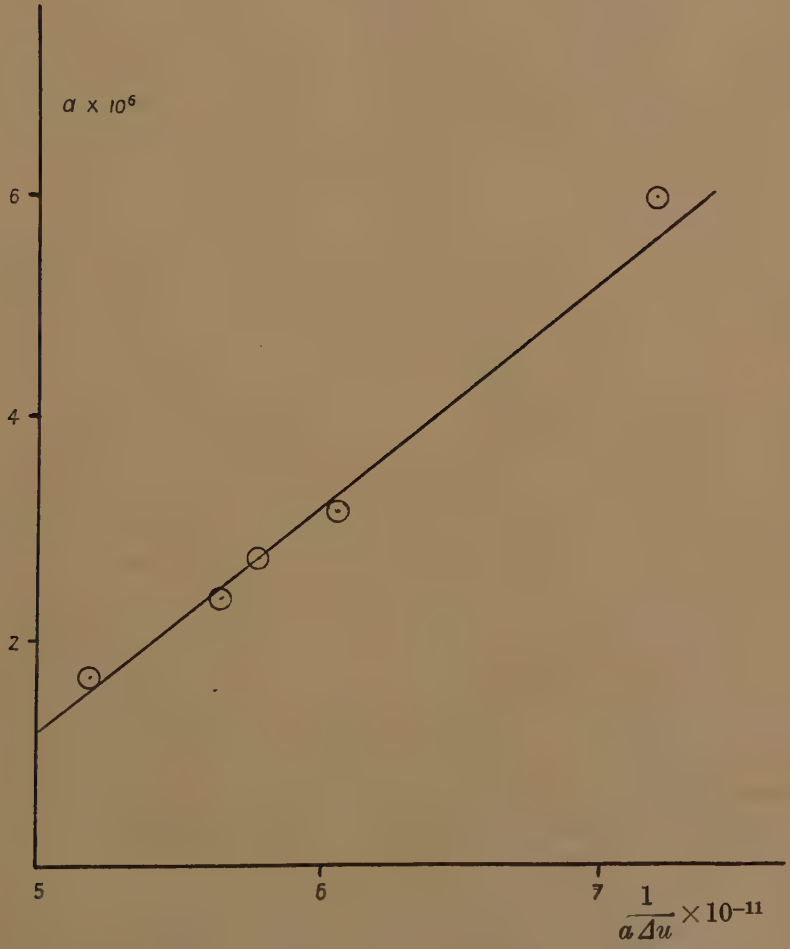

Relation between particle radius, $a$, and change in mobility, $\Delta u$.

In Table II. the second column gives the maximum change in mobility, $\Delta u$, produced by irradiation of particles of radius $a$ recorded in the first column. The third column gives the corresponding values of the product $a\Delta u$. If the reciprocal of this product, which varies slowly with the radius, is plotted against the corresponding radius, a linear graph is obtained which does not pass through the origin (fig. 2). Experimentally, then, the relation between $a$ and $\Delta u$ is of the form

$$a(a+\delta)\,\Delta u=\text{constant}.$$

The value of $\delta$ so deduced from the data, $8\times10^{-6}$ cm., is of the order of magnitude to be expected from the ionic concentration in the sols.

Comparing this result with equation (1), it appears that the charge taken up or lost by irradiated particles in passing from a minimum to a maximum is independent of the size of the particle. In other words, particles under the action of X-radiation can gain or lose a charge the maximum value of which is independent of the particle size. On the simplified theory its magnitude can be calculated by substitution in the formula, and has a value of about $20\,e$, where $e$ is the electronic charge.

TABLE II.

| $a\times10^6$. | $u\times10^4$. | $a\Delta u\times10^{10}$. | $a(a+8\times10^{-6})\ \Delta u\times10^{15}$. |
|---|---|---|---|
| 1·74 | 1·09 | 1·90 | 18·5 |
| 2·40 | 0·78 | 1·87 | 19·4 |
| 2·80 | 0·64 | 1·80 | 19·4 |
| 3·20 | 0·51 | 1·63 | 18·3 |
| 6·15 | 0·22 | 1·36 | 19·1 |

$\Delta u$=Difference between maximum and minimum value of electrophoretic velocity.

If it is accepted that the charge which can be added or removed from the particle by irradiation is independent of the radius, it is natural to expect that the dose required to effect the change will be greater for the smaller particle, as on almost any hypothesis a small particle would be a less effective collector than a large one. The exact relation between the dose and the particle size, however, remains a matter for speculation. While the maximum change in mobility can be measured with reasonable accuracy, the exact doses corresponding to the maxima and minima of the curves cannot be fixed with the same precision, and the dose values recorded in Table I. may be in error in some cases by as much as 10 per cent. It is possible to find more than one empirical relation between dosage and particle size which will fit the data to this degree of accuracy.

Fig. 3.

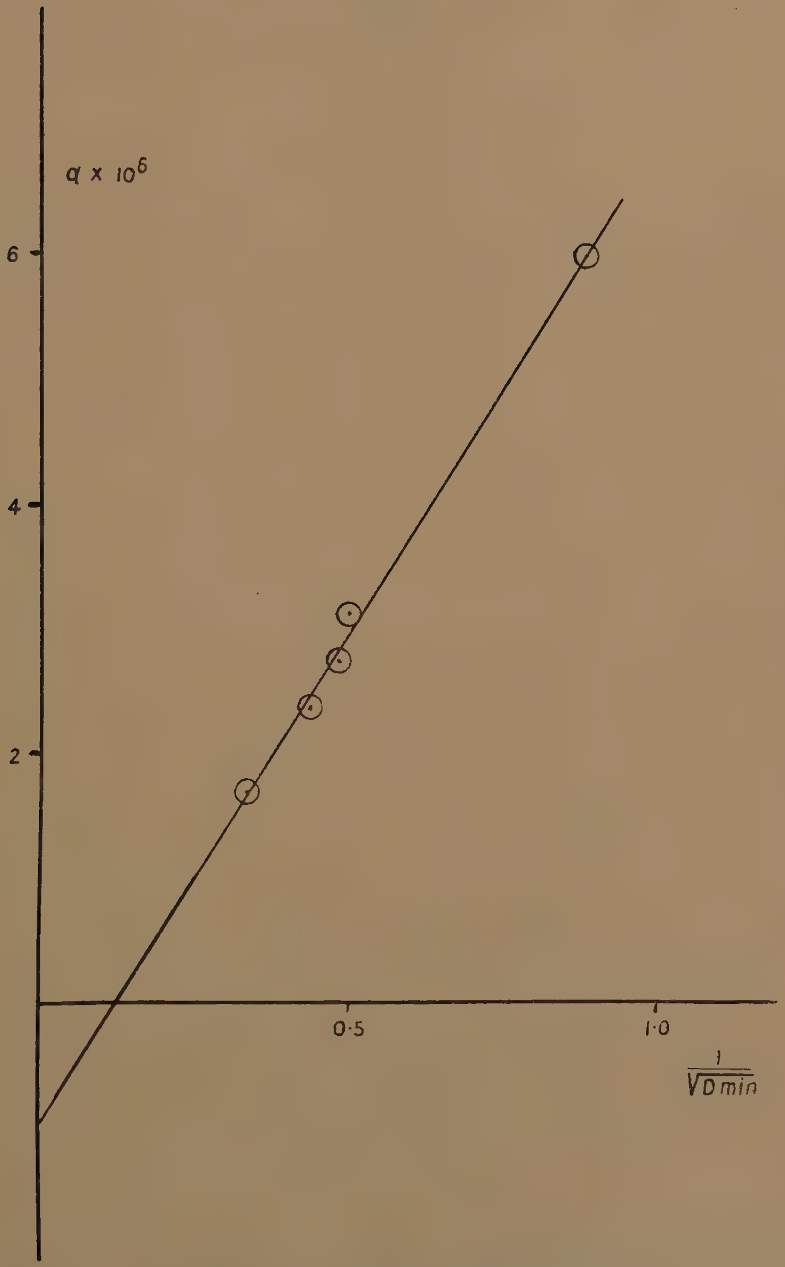

Relation between particle radius and dosage.

An inspection of the collected results shows that the dose, $D_{\text{min.}}$, required to reduce the mobility of the sol to its minimum value varies roughly as the inverse square of the particle radius. The graph showing the particle radius plotted against $1/\sqrt{D_{\text{min.}}}$, fig. 3, is reasonably linear, indicating a relation of the form

$$(a+z)^2 \times D_{\text{min.}} = \text{constant},$$

with a value for $z$ of the order of $8 \times 10^{-7}$ cm. It is tempting to regard $(a+z)$ as the radius of a " target area " through which some projectile, corpuscular or electromagnetic, must pass in order to discharge the colloid particle, where $z$ may perhaps be the shell of solvent adhering to the particle. Photoelectrons ejected by the absorption of the X-radiation in the sol suggest themselves as possible bullets. Calculation, however, shows that the total number of photoelectrons produced per gram of sol during the irradiation is less than the number of colloid particles present, while the probability that a given photoelectron will hit a target of the area suggested is only of the order of 0·3 per cent.

A study of the dosage curves (fig. 1) for the series of sols suggests that the relation between particle size and dosage is different for the descending and ascending portions of the curves. The descending curve is approximately common to particles of all sizes, while the slopes of the ascending portions become gentler as the particle size diminishes. The dose required to change the mobility of the sol from a minimum to a maximum certainly varies more rapidly than the inverse square of the particle radius, but the data are not sufficiently accurate to discriminate with certainty between the various possible experimental relationships.

The dose required to produce a given change in the mobility of the gold sol varies rapidly with the temperature at which the irradiation is carried out. Thus the gold sol with particles of radius $2{\cdot}8 \times 10^{-6}$ cm., which at room-temperature (17° C.) was brought to its first maximum by a dose of $9{\cdot}8\,r$, required only $5{\cdot}5\,r$ to produce the same effect if the irradiation was carried out at a temperature of 65°.

A similar effect was observed for the graphite sols, as recorded in a previous communication. A further analysis of the results for graphite has now been made. It has been found that, if the logarithm of the dose required to bring about a given change in the mobility of the sol is plotted against the reciprocal of the absolute temperature at which the irradiation is carried out, the points lie on a straight line to a very considerable degree of accuracy. This is shown in fig. 4. The circles refer to the doses required at different temperatures to produce the first maximum in the mobility curves, the crosses to the doses producing the second maximum. The two sets of observations are adjusted to agree at 17°, the mid-point in the graph. We thus arrive at the interesting result that the dose required to produce a given change in the sol can be represented with some precision by a relation of the form

$$D = A\epsilon^{b/\theta},$$

Fig. 4.

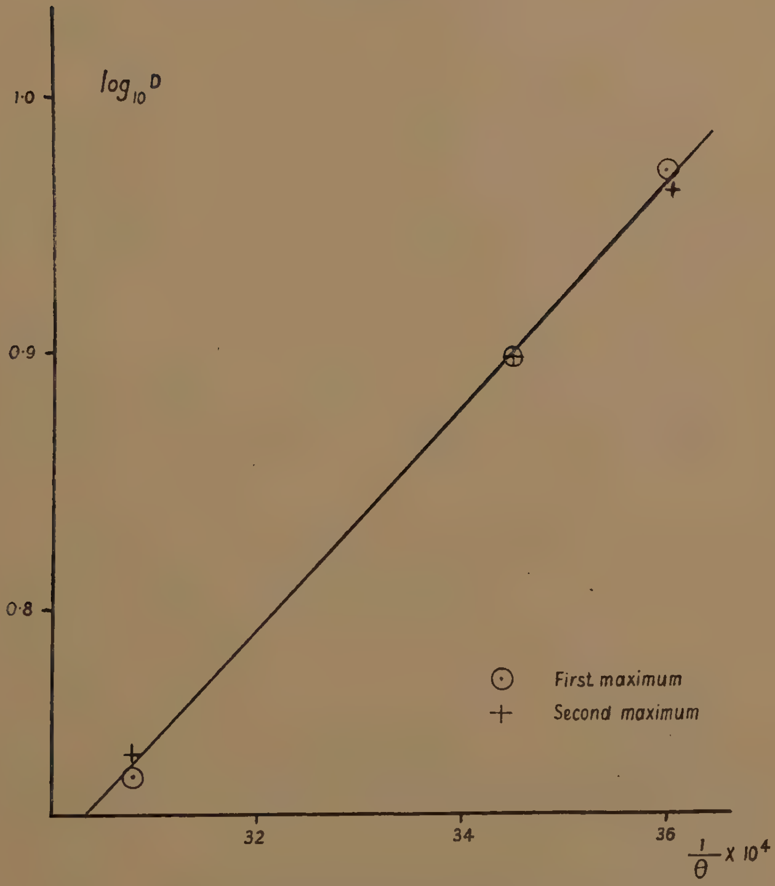

Temperature effect for a graphite sol.

where $b$ has the value $1{\cdot}04 \times 10^6$. Owing to the rapid variation of the exponential factor, a relation of the type

$$D = A\theta^n\epsilon^{b/\theta},$$

where $n$ has any value not greater than $\pm 2$ gives an equally satisfactory fit with, of course, a somewhat different value for $b$.

If we take the natural course of putting $b = w/k$ where $k$ is Boltzmann's constant, the value $w$ for graphite is 0·09 electron volt. For gold sols the magnitudes are somewhat higher, $w$ having a value of 0·11 $e$V.

### *Summary.*

The rhythmical variations in the electrophoretic mobility of colloidal particles under the influence of X-radiation have been studied in a series of gold sols of varying particle sizes. Both the maximum change in mobility and the dose necessary to produce the change increase markedly with diminution in particle size.

The change in mobility produced by the radiation varies from 10 per cent. for the largest particles to 50 per cent. for the smallest particles. It is shown that the results are consistent with the hypothesis that the magnitude of the charge gained or lost by the particle during irradiation is independent of its size. The dose required to reduce the mobility of the particles to a minimum is proportional to $(a+z)^{-2}$, where $a$ is the radius and $z$ a constant of about $8\times10^{-7}$ cm.

The dose D required to produce a given change in the mobility of the colloidal particles is related to the absolute temperature $\theta$ at which the irradiation takes place by an equation of the form $D=A\epsilon^{w/k\theta}$, where $k$ is Boltzmann's constant and $w$ has a value 0·09 $e$V for graphite and 0·11$e$V for gold.

The work recorded in this paper has been made possible by a grant from the British Empire Cancer Campaign, to whom we would express our grateful thanks. One of us (R. J.) acknowledges with thanks the assistance of a training grant from the Department of Scientific and Industrial Research.

### *References.*

(1) Crowther, Liebmann, and Mill, Brit. Journal of Radiology, ix. (new series), p. 631 (1936).
(2) Crowther, Liebmann, and Lane, Phil. Mag. ser. 7, xxiv. p. 654 (1937).
(3) Crowther, Liebmann, and Jones, Phil. Mag. ser. 7, xxvi. p. 120 (1938).
(4) Crowther, 'Nature,' cxlii. p. 569 (1938).
(5) Westgren, *Z. anorg. Chem.* xciii. p. 151 (1915).
(6) Pennycuik and Woolcock, 'Australian Journal of Experimental Biology,' xv. p. 423 (1937).

The University of Reading.
February 9, 1939.

# V. *The Bending of Thick Plates under certain Specified Conditions of Support.*

By John Morrow, M.Sc., D.Eng., Reader in Engineering, King's College, University of Durham *.

[Received October 24, 1938.]

In discussing the problem of the thick rectangular plate under uniform transverse load and with clamped edges, it is usually assumed that in the unstressed state the middle surface of the plate is plane and the support is such that, in the strained state, the edges of the middle surface remain in the same plane. The pressure of the plate on its support is not uniform, but is greatest at the middles of the edges, and is negative at and near the corners †.

In the problem now considered, whilst the four corners of the middle surface remain in the original plane, the supports are shaped to permit a slight bending of the plate at the edges in such a way that the linear intensity of pressure on its support is uniform along each edge of the rectangle.

Apart from the theoretical interest which attaches to an "exact" solution of this kind, the results should be of value in connexion with the difficulty sometimes experienced in maintaining gas-tight joints and in showing to what extent the state of stress in the plate is affected by slight bending of the edges. They also throw some light on the behaviour of thick plates in general.

The case examined is that of a plate of uniform thickness supported and clamped in such manner that one-quarter of the total load is borne at each edge. Let the origin and the axes of $x$ and $y$ be in the middle plane of the unstrained plate, which will be regarded as horizontal, the upper and lower surfaces being given by $z=\pm h$, and the edges by $x=\pm a$ and by $y=\pm b$.

Writing $X_x$, $Y_y$, $Z_z$ and $Y_z$, $Z_x$, $X_y$ for the components of stress and $u$, $v$, $w$ for the components of displacement ‡, the conditions to be satisfied

---

* Communicated by Prof. A. E. H. Love, M.A., D.Sc., F.R.S.

† A solution of this problem, involving series, has been given by J. Vint, Proc. London Math. Soc. series 2, xli. part 2 (1936).

See also "Stresses in rectangular Plates clamped at their Edges and loaded with a uniformly distributed Pressure," by C. E. Inglis, 'Transactions of the Institution of Naval Architects,' 1925.

‡ The notation throughout is that used in 'The Mathematical Theory of Elasticity,' by A. E. H. Love. (Cambridge University Press, 1927.)

at the edges are taken to be (1) that, at $x=\pm a$, $\int Z_x\,dz$ is to be constant and (2), at $y=\pm b$, $\int Z_y\,dz$ is to be constant.

The shear components $Z_x$ and $Z_y$ must vanish at $z=\pm h$, and we investigate the circumstances in which $Z_x$ is not a function of $y$ and $Z_y$ is not a function of $x$; in which case, for any constant value of $z$, $Z_x$ must vary as $x$ and $Z_y$ as $y$. The simplest forms for these stress components are then

$$Z_x=A(h^2-z^2)x, \qquad Z_y=A(h^2-z^2)y, \quad . \quad . \quad . \quad . \quad . \quad (1)$$

in which the constant A must be evaluated so that the sum of the integrals of $Z_x$ on the edge-faces $x=\pm a$ and of $Z_y$ on the faces $y=\pm b$ must together equal the total pressure on the upper surface.

Hence if $p$ be the intensity of the uniform normal pressure on the upper surface the total load is $4pab$, and

$$\int_{-b}^{+b}\int_{-h}^{+h} A(h^2-z^2)a\,dy\,dz=pab, \quad . \quad . \quad . \quad . \quad . \quad . \quad (2)$$

so that, when one-quarter of the load is carried by the vertical shear on each edge,

$$A=\frac{3}{8}\frac{p}{h^3}.$$

In the absence of body forces and acceleration the stress equation for equilibrium parallel to O$z$ gives

$$\frac{\partial Z_z}{\partial z}=-\left(\frac{\partial Z_x}{\partial x}+\frac{\partial Z_y}{\partial y}\right)=-2A(h^2-z^2), \quad . \quad . \quad . \quad . \quad (3)$$

and since $Z_z$ is to vanish at $z=-h$ and is not to be a function of $x$ or $y$ at $z=+h$, and since, moreover, its integral over the upper surface is to be $-4pab$, it is given by

$$Z_z=-2A\left(\frac{2}{3}h^3+h^2z-\frac{z^3}{3}\right), \quad . \quad . \quad . \quad . \quad . \quad . \quad . \quad (4)$$

in which A has the value already attributed to it. The expressions given above for $Z_x$, $Z_y$, and $Z_z$ are the same as those adopted in Love's treatise under the heading "Plate bent by pressure uniform over a face"*; but, in his further treatment, stress components $X_y$ and $Y_x$ are introduced which necessitate horizontal components of tangential stress at the edges. With the stress system so far described it is possible, however, for $X_y$ and $Y_x$ to be zero throughout; we therefore here assume this to be the case, and we seek for a solution of the displacement equations of equilibrium consistent with all the above conditions. These equations can be written in the form

$$(\lambda+\mu)\left(\frac{\partial}{\partial x},\ \frac{\partial}{\partial y},\ \frac{\partial}{\partial z}\right)\Delta+\mu\nabla^2(u,v,w)=0.$$

---

* *Loc. cit.* pp. 477–479.

The solution which accords with the stress components already determined is

$$\left.\begin{aligned}
u&=\frac{\mathrm{A}x}{\mathrm{E}}\left[\frac{1-\sigma^2}{3}x^2z-(1+\sigma)(2-\sigma)\frac{z^3}{3}+2\sigma h^2\left(\frac{2}{3}h+z\right)\right]\\
&\quad+\frac{1}{\mathrm{E}}\left[\mathrm{C}_1xy-\frac{\mathrm{C}_2}{2}(\sigma x^2+y^2-\sigma z^2)+(\mathrm{B}_1-\sigma\mathrm{B}_2)zx+(\alpha_1-\sigma\alpha_2)x\right]+u_1,\\
v&=\frac{\mathrm{A}y}{\mathrm{E}}\left[\frac{1-\sigma^2}{3}y^2z-(1+\sigma)(2-\sigma)\frac{z^3}{3}+2\sigma h^2\left(\frac{2}{3}h+z\right)\right]\\
&\quad+\frac{1}{\mathrm{E}}\left[\mathrm{C}_2xy-\frac{\mathrm{C}_1}{2}(x^2+\sigma y^2-\sigma z^2)+(\mathrm{B}_2-\sigma\mathrm{B}_1)yz+(\alpha_2-\sigma\alpha_1)y\right]+v_1,\\
w&=\frac{\mathrm{A}z}{\mathrm{E}}\left[\frac{(1+\sigma)^2}{6}z^3-h^2z-\frac{\sigma}{2}(1+\sigma)(x^2+y^2)z-\frac{4}{3}h^3\right]\\
&\qquad-\frac{\sigma z}{\mathrm{E}}\left[\mathrm{C}_2x+\mathrm{C}_1y+\frac{\mathrm{B}_1+\mathrm{B}_2}{2}z+\alpha_1+\alpha_2\right]+w_0,
\end{aligned}\right\} \quad . \quad (5)$$

in which $w_0$, the normal displacement of the middle plane, is given by

$$\begin{aligned}
w_0=\frac{1}{\mathrm{E}}\Bigg[&-\frac{1-\sigma^2}{12}\mathrm{A}(x^4+y^4)+\mathrm{A}h^2(x^2+y^2)\\
&-(\mathrm{B}_1-\sigma\mathrm{B}_2)\frac{x^2}{2}-(\mathrm{B}_2-\sigma\mathrm{B}_1)\frac{y^2}{2}\Bigg]+w_1 \quad . \quad . \quad . \quad (6)
\end{aligned}$$

and $u_1$, $v_1$, $w_1$ represent the translation and small rotation possible in a rigid body,

$$u_1=\gamma_1-\beta_3y+\beta_1z,\qquad v_1=\gamma_2-\beta_2z+\beta_3x,\qquad w_1=\gamma_3-\beta_1x+\beta_2y.$$

$\mathrm{B}_1$, $\mathrm{C}_1$, $\mathrm{B}_2$, $\mathrm{C}_2$, $\alpha_1$ and $\alpha_2$ are arbitrary constants.

The components of strain are then

$$\left.\begin{aligned}
e_{xx}&=\frac{\mathrm{A}}{\mathrm{E}}\left[(1-\sigma^2)x^2z-(1+\sigma)(2-\sigma)\frac{z^3}{3}+2\sigma h^2\left(z+\frac{2}{3}h\right)\right]\\
&\qquad+\frac{1}{\mathrm{E}}[\mathrm{C}_1y-\sigma\mathrm{C}_2x+(\mathrm{B}_1-\sigma\mathrm{B}_2)z+\alpha_1-\sigma\alpha_2],\\
e_{yy}&=\frac{\mathrm{A}}{\mathrm{E}}\left[(1-\sigma^2)y^2z-(1+\sigma)(2-\sigma)\frac{z^3}{3}+2\sigma h^2\left(z+\frac{2}{3}h\right)\right]\\
&\qquad+\frac{1}{\mathrm{E}}[\mathrm{C}_2x-\sigma\mathrm{C}_1y+(\mathrm{B}_2-\sigma\mathrm{B}_1)z+\alpha_2-\sigma\alpha_1],\\
e_{zz}&=\frac{\mathrm{A}}{\mathrm{E}}\left[\frac{2}{3}(1+\sigma)^2z^3-2h^2z-\sigma(1+\sigma)(x^2+y^2)z-\frac{4}{3}h^3\right]\\
&\qquad-\frac{\sigma}{\mathrm{E}}[\mathrm{C}_2x+\mathrm{C}_1y+(\mathrm{B}_1+\mathrm{B}_2)z+\alpha_1+\alpha_2],\\
e_{yz}&=\frac{2(1+\sigma)}{\mathrm{E}}\mathrm{A}(h^2-z^2)y,\quad e_{zx}=\frac{2(1+\sigma)}{\mathrm{E}}\mathrm{A}(h^2-z^2)x,\quad e_{xy}=0.
\end{aligned}\right\} \quad . \quad (7)$$

$$\Delta=\frac{1-2\sigma}{\mathrm{E}}\mathrm{A}\left[-\frac{2}{3}(1+\sigma)z^3+(1+\sigma)(x^2+y^2)z-2h^2\left(z+\frac{2}{3}h\right)\right]$$
$$+\frac{1-2\sigma}{\mathrm{E}}[\mathrm{C}_2x+\mathrm{C}_1y+(\mathrm{B}_1+\mathrm{B}_2)z+\alpha_1+\alpha_2]\quad . \quad (8)$$

The stress components corresponding with the above are

$$\left.\begin{aligned}
\mathrm{X}_x&=\mathrm{A}z\left(x^2+\sigma y^2-\frac{2+\sigma}{3}z^2\right)+\mathrm{C}_1y+\mathrm{B}_1z+\alpha_1,\\
\mathrm{Y}_y&=\mathrm{A}z\left(\sigma x^2+y^2-\frac{2+\sigma}{3}z^2\right)+\mathrm{C}_2x+\mathrm{B}_2z+\alpha_2,\\
\mathrm{Z}_z&=2\mathrm{A}\left(\frac{1}{3}z^3-h^2z-\frac{2}{3}h^3\right),\\
\mathrm{Y}_z&=\mathrm{A}(h^2-z^2)y,\quad \mathrm{Z}_x=\mathrm{A}(h^2-z^2)x,\quad \mathrm{X}_y=0,
\end{aligned}\right\}\quad . \; . \; . \quad (9)$$

and it may be verified without difficulty that these satisfy the equations of equilibrium in the absence of body force and acceleration.

### *Symmetry.*

In the particular problem under consideration, the origin being at the middle point of the unstrained plate, considerations of symmetry show that, when $x=y=0$, $u$ and $v$ must vanish for all values of $z$. Hence, for the rectangular plate,

$$\gamma_1=\gamma_2=\beta_1=\beta_2=\mathrm{C}_1=\mathrm{C}_2=0.\quad . \; . \; . \; . \; . \; . \quad (10)$$

Also, at the origin, $\frac{\partial u}{\partial y}$ and $\frac{\partial v}{\partial x}$ must vanish ; $\therefore\ \beta_3=0$.

### *Conditions at Clamped Edges.*

Since $\frac{\partial w_0}{\partial x}$ must vanish at $x=a$, and $\frac{\partial w_0}{\partial y}$ must vanish at $y=b$, we have

$$\left.\begin{aligned}
\mathrm{B}_1&=\mathrm{A}\left(\frac{2}{1-\sigma}h^2-\frac{a^2+\sigma b^2}{3}\right),\\
\mathrm{B}_2&=\mathrm{A}\left(\frac{2}{1-\sigma}h^2-\frac{\sigma a^2+b^2}{3}\right),
\end{aligned}\right\}\quad . \; . \; . \; . \; . \; . \; . \quad (11)$$

and since, at the edges, $u$ and $v$ are to be zero when $z=0$,

$$\alpha_1=\alpha_2=-\frac{1}{2}\frac{\sigma}{1-\sigma}p.\quad . \; . \; . \; . \; . \; . \; . \; . \quad (12)$$

The profile of the support at the edges being arranged so that the height of the points on the middle surface at each of the four corners is unchanged when the pressure $p$ is applied, $w_0$ must vanish at $x^2=a^2$, $y^2=b^2$. This gives, for the deflexion of the middle surface at the origin,

$$\gamma_3=-\frac{1}{12}\frac{1-\sigma^2}{\mathrm{E}}\mathrm{A}(a^4+b^4),\quad . \; . \; . \; . \; . \; . \; . \quad (13)$$

and, remembering that $A=\frac{3}{8}\frac{p}{h^3}$, all the constants in the solution have been determined.

*Solution when Edges are Clamped.*

The displacement is now given by

$$\left.\begin{aligned}
u&=\frac{3}{8}\frac{1+\sigma}{E}\frac{p}{h^3}xz\left[\frac{1-\sigma}{3}(x^2-a^2)-\frac{2-\sigma}{3}z^2+2h^2\right],\\
v&=\frac{3}{8}\frac{1+\sigma}{E}\frac{p}{h^3}yz\left[\frac{1-\sigma}{3}(y^2-b^2)-\frac{2-\sigma}{3}z^2+2h^2\right],\\
w&=\frac{3}{8}\frac{1+\sigma}{E}\frac{p}{h^3}z\left[\frac{1+\sigma}{6}z^3-\frac{1}{1-\sigma}h^2z\right.\\
&\qquad\left.-\frac{\sigma}{2}\left(x^2+y^2-\frac{a^2+b^2}{3}\right)z-\frac{4}{3}\frac{1-2\sigma}{1-\sigma}h^3\right]+w_0,
\end{aligned}\right\}\quad . \quad . \quad . \quad (14)$$

the vertical displacement of the middle plane being

$$w_0=-\frac{1-\sigma^2}{32E}\frac{p}{h^3}[(a^2-x^2)^2+(b^2-y^2)^2] \quad . \quad . \quad . \quad . \quad . \quad (15)$$

The state of strain becomes

$$\left.\begin{aligned}
e_{xx}&=\frac{3}{8}\frac{1+\sigma}{E}\frac{pz}{h^3}\left[(1-\sigma)x^2-\frac{2-\sigma}{3}z^2+2h^2-\frac{1-\sigma}{3}a^2\right],\\
e_{yy}&=\frac{3}{8}\frac{1+\sigma}{E}\frac{pz}{h^3}\left[(1-\sigma)y^2-\frac{2-\sigma}{3}z^2+2h^2-\frac{1-\sigma}{3}b^2\right],\\
e_{zz}&=\frac{3}{8}\frac{1+\sigma}{E}\frac{p}{h^3}\left[\frac{2}{3}(1+\sigma)z^3-\frac{2}{1-\sigma}h^2z\right.\\
&\qquad\left.-\sigma\left(x^2+y^2-\frac{a^2+b^2}{3}\right)z-\frac{4}{3}\frac{1-2\sigma}{1-\sigma}h^3\right],\\
e_{yz}&=\frac{3}{4}\frac{(1+\sigma)}{E}\frac{p}{h^3}(h^2-z^2)y,\quad e_{zx}=\frac{3}{4}\frac{1+\sigma}{E}\frac{p}{h^3}(h^2-z^2)x,\quad e_{xy}=0,
\end{aligned}\right\}\quad . \quad (16)$$

and the dilatation

$$\Delta=\frac{3}{8}\frac{(1+\sigma)(1-2\sigma)}{E}\frac{p}{h^3}\left[-\frac{2}{3}z^3+\left(x^2+y^2+\frac{2h^2}{1-\sigma}-\frac{a^2+b^2}{3}\right)z-\frac{4}{3}\frac{h^3}{1-\sigma}\right] . \quad (17)$$

The stress components are

$$\left.\begin{aligned}
X_x&=\frac{3}{8}\frac{p}{h^3}\left[-\frac{2+\sigma}{3}z^3+\left(x^2+\sigma y^2+\frac{2h^2}{1-\sigma}-\frac{a^2+\sigma b^2}{3}\right)z-\frac{4}{3}\frac{\sigma}{1-\sigma}h^3\right],\\
Y_y&=\frac{3}{8}\frac{p}{h^3}\left[-\frac{2+\sigma}{3}z^3+\left(\sigma x^2+y^2+\frac{2h^2}{1-\sigma}-\frac{b^2+\sigma a^2}{3}\right)z-\frac{4}{3}\frac{\sigma}{1-\sigma}h^3\right],\\
Z_z&=\frac{3}{4}\frac{p}{h^3}\left(\frac{z^3}{3}-h^2z-\frac{2}{3}h^3\right),\\
Y_z&=\frac{3}{8}\frac{p}{h^3}(h^2-z^2)y,\quad Z_x=\frac{3}{8}\frac{p}{h^3}(h^2-z^2)x,\quad X_y=0.
\end{aligned}\right\}\quad . \quad (18)$$

The profiles of the supports, in order that the shearing force on each edge may be uniform, are such as to allow the following values of $w_0$:

$$\left.\begin{array}{lll} \text{At} & x=\pm a \text{ and } z=0, & w_0=-\dfrac{1-\sigma^2}{32\mathrm{E}}\dfrac{p}{h^3}(b^2-y^2)^2. \\ \text{At} & y=\pm b \text{ and } z=0, & w_0=-\dfrac{1-\sigma^2}{32\mathrm{E}}\dfrac{p}{h^3}(a^2-x^2)^2. \end{array}\right\} \quad . \quad . \quad . \quad (19)$$

The middle points of the edges at $x=\pm a$ are depressed

$$\frac{1-\sigma^2}{32\mathrm{E}}\frac{p}{h^3}b^4$$

and those of the edges at $y=\pm b$ are depressed

$$\frac{1-\sigma^2}{32\mathrm{E}}\frac{p}{h^3}a^4$$

below the level of the corners at $z=0$.

It is noteworthy that the vertical displacement, or deflexion, at the origin is equal to the sum of the depressions of the middle points of two adjacent sides; and that the deflexion of the middle plane is the sum of two deflexions, each of which, taken separately, is the deflexion into a cylindrical surface of which the corresponding edge of the middle plane is the profile.

### *Solution when Expansion of the Middle Plane is permitted.*

The conditions given for a clamped edge require the imposition of a small compressive force normal to the edge-faces of the plate in order to prevent expansion of the middle plane.

If the plate be free from any resultant horizontal traction on its edges at $x=\pm a$ and at $y=\pm b$, the only stress tending to expand the middle plane will be due to the vertical compressive stress caused by the surface load, $p$. This stress varies in intensity from $p$ at the upper surface, $z=h$, to zero at the lower surface, $z=-h$; and, although its variation is not uniform, its value at the middle plane is $\frac{1}{2}p$. This causes a small uniform strain, parallel to each of the directions O$x$ and O$y$, in the middle plane, of amount $\dfrac{\sigma p}{2\mathrm{E}}$. Instead of applying constraint we now consider the solution when this small expansion is allowed to occur.

The conditions $u=v=0$ at a clamped edge are now replaced by the proviso that each edge is to be free from all resultant traction except the vertical shear necessary to support the surface load $p$. This requires that, at $x=\pm a, \iint \mathrm{X}_x dy\, dz=0$, and hence $\alpha_1=0$, and at $x=\pm b, \iint \mathrm{Y}_y dx\, dz=0$, and hence $\alpha_2=0$. These replace the expression for $\alpha_1$ and $\alpha_2$ in the previous solution; the other coefficients being unchanged.

The displacement is now expressed by

$$\left.\begin{aligned}
u&=\frac{3}{8}\frac{1+\sigma}{\mathrm{E}}\frac{p}{h^3}x\left[\frac{1-\sigma}{3}(x^2-a^2)z-(2-\sigma)\frac{z^3}{3}+2h^2z+\frac{4}{3}\frac{\sigma}{1+\sigma}h^3\right],\\
v&=\frac{3}{8}\frac{1+\sigma}{\mathrm{E}}\frac{p}{h^3}y\left[\frac{1-\sigma}{3}(y^2-b^2)z-(2-\sigma)\frac{z^3}{3}+2h^2z+\frac{4}{3}\frac{\sigma}{1+\sigma}h^3\right],\\
w&=\frac{3}{8}\frac{1+\sigma}{\mathrm{E}}\frac{p}{h^3}z\left[\frac{1+\sigma}{6}z^3-\frac{1}{1-\sigma}h^2z\right.\\
&\qquad\left.-\frac{\sigma}{2}\left(x^2+y^2-\frac{a^2+b^2}{3}\right)z-\frac{4}{3}\frac{h^3}{(1+\sigma)}\right]+w_0,
\end{aligned}\right\}. \quad (20)$$

the vertical displacement of the middle plane being, as before,

$$w_0=-\frac{1-\sigma^2}{32\mathrm{E}}\frac{p}{h^3}[(a^2-x^2)^2+(b^2-y^2)^2], \quad .\ .\ .\ .\ . \quad (21)$$

it follows that the profiles of the supports are the same as in the previous case.

The state of strain becomes

$$\left.\begin{aligned}
e_{xx}&=\frac{3}{8}\frac{1+\sigma}{\mathrm{E}}\frac{p}{h^3}\left[(1-\sigma)x^2z+\left(2h^2-\frac{1-\sigma}{3}a^2\right)z-\frac{2-\sigma}{3}z^3+\frac{4}{3}\frac{\sigma}{1+\sigma}h^3\right],\\
e_{yy}&=\frac{3}{8}\frac{1+\sigma}{\mathrm{E}}\frac{p}{h^3}\left[(1-\sigma)y^2z+\left(2h^2-\frac{1-\sigma}{3}b^2\right)z-\frac{2-\sigma}{3}z^3+\frac{4}{3}\frac{\sigma}{1+\sigma}h^3\right],\\
e_{zz}&=\frac{3}{8}\frac{1+\sigma}{\mathrm{E}}\frac{p}{h^3}\left[\frac{2}{3}(1+\sigma)z^3-\sigma\left(x^2+y^2-\frac{a^2+b^2}{3}\right)z\right.\\
&\qquad\left.-\frac{2}{1-\sigma}h^2z-\frac{4}{3(1+\sigma)}h^3\right],\\
e_{yz}&=\frac{3}{4}\frac{1+\sigma}{\mathrm{E}}\frac{p}{h^3}(h^2-z^2)y,\quad e_{zx}=\frac{3}{4}\frac{1+\sigma}{\mathrm{E}}\frac{p}{h^3}(h^2-z^2)x,\quad e_{xy}=0,
\end{aligned}\right\}. \quad (22)$$

and the components of stress are

$$\left.\begin{aligned}
\mathrm{X}_x&=\frac{3}{8}\frac{p}{h^3}z\left(x^2+\sigma y^2-\frac{2+\sigma}{3}z^2+\frac{2}{1-\sigma}h^2-\frac{a^2+\sigma b^2}{3}\right),\\
\mathrm{Y}_y&=\frac{3}{8}\frac{p}{h^3}z\left(\sigma x^2+y^2-\frac{2+\sigma}{3}z^2+\frac{2}{1-\sigma}h^2-\frac{\sigma a^2+b^2}{3}\right),\\
\mathrm{Z}_z&=\frac{3}{4}\frac{p}{h^3}\left(\frac{z^3}{3}-h^2z-\frac{2}{3}h^3\right),\\
\mathrm{Y}_z&=\frac{3}{8}\frac{p}{h^3}(h^2-z^2)y,\quad \mathrm{Z}_x=\frac{3}{8}\frac{p}{h^3}(h^2-z^2)x,\quad \mathrm{X}_y=0.
\end{aligned}\right\}. \quad (23)$$

The stress components $\mathrm{X}_x$ and $\mathrm{Y}_y$ have their highest positive and negative values at the upper and lower surfaces of the four corners of the plate, at which points $\mathrm{X}_x$, $\mathrm{Y}_y$, and $\mathrm{Z}_z$ are principal stresses.

For a steel plate in the form of a square of 100 cm. side and 20 cm. thick, the greatest values of $X_x$ and $Y_y$ under a load, $p$, of 40 atmospheres would be about $3{\cdot}5 \times 10^8$ dynes per sq. cm., corresponding to about one-twelfth of the breaking stress in a simple tensile test of ordinary mild steel. The depression of the supports at the middle of each edge would be about 0·0035 cm. The linear intensity of the supporting force would be constant, and the same at all four edges.

### *Uniqueness of the Solutions.*

In either case, whether expansion of the middle plane is permitted or not, no external force is applied to the surface at $z=-h$, and the pressure $p$ is the only force on the surface $z=h$. Hence if the tractions applied to the edges are in accordance with equations (18) in the one case, or with equations (23) in the other, the solutions are exact and unique.

For any other distribution of the tractions at the edges, giving the same stress resultants and couples, the expressions for the displacements and for the components of stress and strain are sufficiently approximate at all points of the plate which are not close to the edge.

# VI. *Electron Distribution in Electron-optically Focused Electron Beams.*

By L. Jacob, M.Sc., A.R.C.Sc.I. *

(Communication from the Staff of the Research Laboratories of The General Electric Company, Limited, Wembley, England.)

[Received March 9, 1939.]

## Summary.

1. A method is described for obtaining the electron distribution in a focused beam. The image size is obtained from this under a certain convention which is described.

2. The electron distribution follows a Gaussian law.

3. The image size decreases with decreasing modulation and with increase in first accelerator voltage.

4. A variation of 5 per cent. in focus voltage can increase the image size in the ratio of 2/1.

5. Variation in cathode temperature in the range (900–1075) °C. causes little change in image size over three-fourths of the modulation range.

6. The peak current density in the image is about 50 ma./cm.$^2$. This is one-eighth the theoretical value deduced from Langmuir's formula.

7. The slit width (used in the method) introduces an error of some 10 per cent. at the lowest modulation, where ratio $\frac{\text{spot width}}{\text{slit width}} \doteqdot 5$.

## *Introduction.*

One of the major problems in design of electron-optical focusing systems is the production of a lens field with minimum aberrations. Before work can proceed on these lines it is necessary to have knowledge of the electron structure of the image produced by the field. The electron structure and distribution are further of paramount importance in connexion with scanning systems in television, since the fine structure of the television images as well as the filter characteristics and width of the frequency band depend on them. The present investigation directs attention to an experimental method developed to study the fine structure of the electron image produced by the focusing field.

---

* Communicated by C. C. Paterson.

It is an entirely objective method which gives knowledge of the electron distribution in the image as well as its size under different conditions; these can be recorded visually in an auxiliary cathode-ray tube.

The results apply strictly to the electron image, but work on parallel lines goes to show that with homogeneous fluorescent screens the light distribution can be interpreted in terms of the electron distribution without serious error.

## *Description of Apparatus.*

The work was carried out in a demountable cathode-ray tube shown in fig. 1. This consisted of (*a*) the main bulb, which was flanged at one end and had a Faraday cage sealed into the tubular projection at the other end, (*b*) the "head," which supported the system and also had a ground flange. The use of low pressure Apeizon N grease between the flanges allowed the vacuum of $10^{-5}$ mm. Hg. to be maintained by a three-stage mercury diffusion pump. The electron optical system is shown in fig. 2. It consisted of an oxide-coated cathode C, a modulator electrode M which controlled the intensity of the electron beam produced

Fig. 1 (*a*).

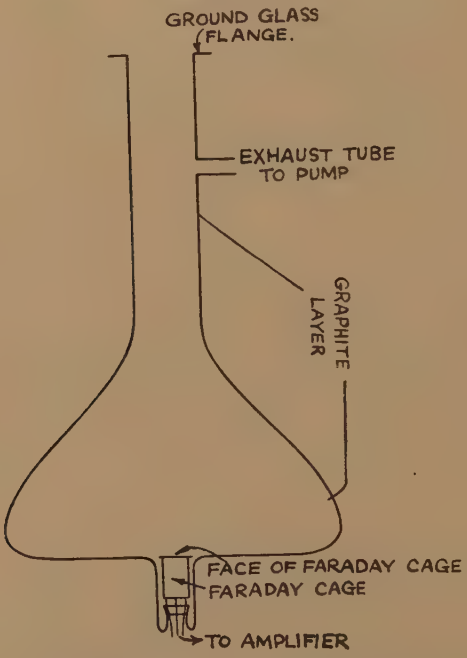

Demountable tube: main bulb.

by the first lens system :—cathode-modulator-accelerator $A_1$. This beam entered the main lens as a diverging beam, and after electrostatic focusing by the main lens $A_2$ $A_3$, passed between two pairs of deflecting plates $Px$, $Py$ mutually at right angles, as a converging beam to the screen or face of the Faraday cage.

Fig. 1 (*b*).

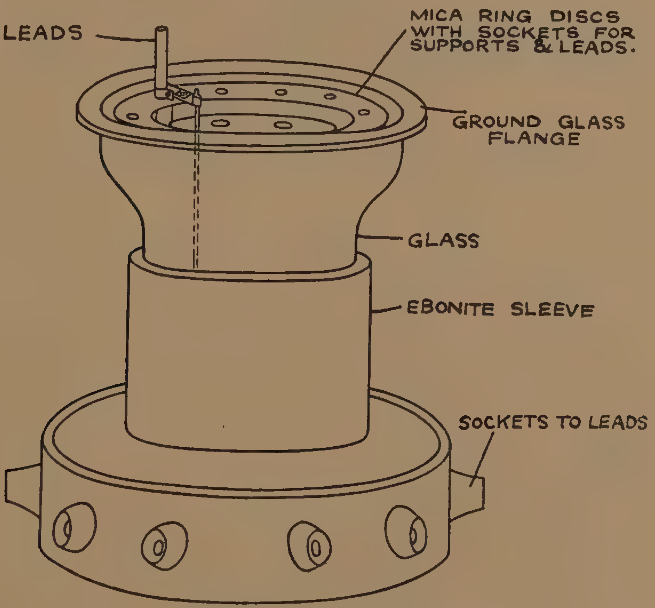
LEADS
MICA RING DISCS WITH SOCKETS FOR SUPPORTS & LEADS.
GROUND GLASS FLANGE
GLASS
EBONITE SLEEVE
SOCKETS TO LEADS

Demountable tube " head."

Fig. 2.

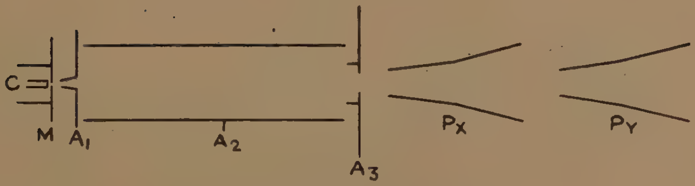
C
M
A1
A2
A3
PX
PY

Electron optical system.

Figs. 3 (*a*) and 3 (*b*) show the Faraday cages, both the earlier and later ones used. In the case of fig. 3 (*a*) the spot was moved across a circular hole of 0·19 mm. diameter at the centre of the flat face, and the electron distribution across various " chords " separated a known distance apart could be obtained. The distribution across a diameter was obtained by integration of these curves. This method was very slow. To expedite the work the use of 0·2 mm. slits was tried in place of the original hole since the integration is automatically performed by the slit.

The face of the later Faraday cages thus contained two accurately cut slits 0·2 mm. wide and 7 mm. long. These are at right angles but do not cross; they act as resolving slits for obtaining the electron distribution across two diameters at right angles.

Fig. 3 (*a*).

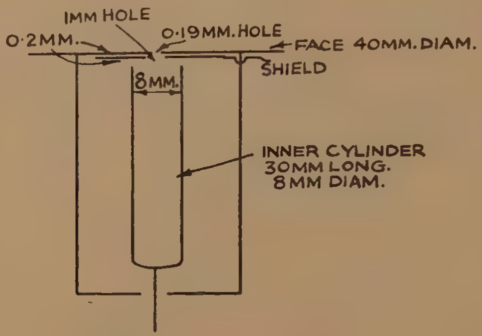
1MM HOLE
0·2MM.
0·19MM. HOLE
FACE 40MM. DIAM.
SHIELD
8MM.
INNER CYLINDER
30MM LONG.
8 MM DIAM.

Early Faraday cage.

Fig. 3 (*b*).

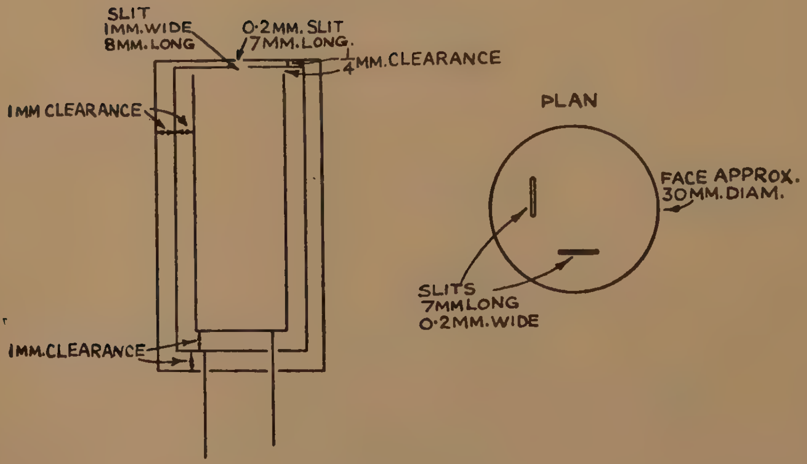
SLIT
1MM. WIDE
8MM. LONG
0·2MM. SLIT
7MM. LONG.
$\frac{1}{4}$MM. CLEARANCE
1MM CLEARANCE
PLAN
FACE APPROX.
30MM. DIAM.
SLITS
7MM LONG
0·2MM. WIDE
1MM. CLEARANCE

Later Faraday cage.

As used, the front face was thinly sprayed with willemite to show up the position of the spot image. Two fine lines also at right angles were engraved on this face at known distances from the edges to define the length of the fluorescent line trace.

The middle box was kept at a negative potential of about 100 volts with respect to the outer box, to prevent secondary electrons entering the collector.

A further development was to make the distribution visible as a trace on a second oscillograph. To do this, the spot was deflected across the slit fifty times per second by introducing a small alternating voltage across the required deflecting plates.

This caused the spot to trace out a line at right angles to whatever slit was being used. The Faraday cage thus receives a series of unidirectional current impulses which are amplified and applied to one pair of plates of the auxiliary oscillograph, the other pair being fed from the same sinusoidal supply. The resultant trace is a magnified picture of the electron distribution in the spot image across a diameter, and is calibrated in terms of the 8 mm. length of the fluorescent line on the Faraday face. This calibration was checked on occasions with a valve voltmeter and from a knowledge of the sensitivity of the deflectors used. The amplifier calibration showed that up to an input of 1·1 volts, corresponding to a deflexion of 40 mm., the deflexion follows a linear law.

Fig. 4.

ELECTRON DISTRIBUTION: COMPLETE CIRCUIT

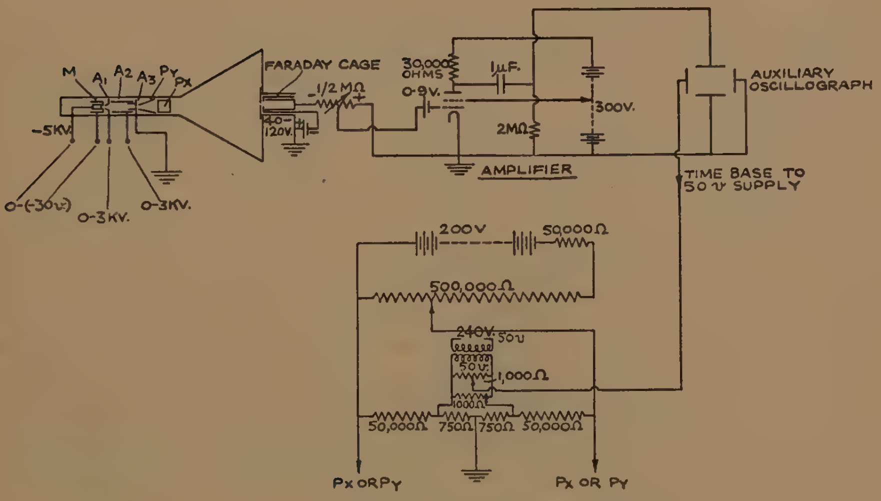
M
$A_1$
$A_2$
$A_3$
PY
PX
-5KV
0-(-30V)
0-3KV.
0-3KV.
FARADAY CAGE
1/2 MΩ
40-120V.
30,000 OHMS
0-9V.
1μF.
2MΩ
300V.
AMPLIFIER
AUXILIARY OSCILLOGRAPH
TIME BASE TO 50 ~ SUPPLY
200V
50,000Ω
500,000Ω
240V
50~
50V.
1,000Ω
1000Ω
50,000Ω
750Ω
750Ω
50,000Ω
PX OR PY
PX OR PY

SHIFT AND SUPERPOSITION CIRCUIT.

In all the work on electron distributions the maximum peak amplitude of the trace was kept at 30 mm. at all modulation voltages. This was done by varying the resistance in series with the collecting cylinder and greatly facilitated measurements on the curves, since the ratio of any two ordinates is constant no matter by what factor they are each multiplied. The complete circuit is shown in fig. 4.

### *Experimental Details.*

As the tube could not be baked out great care was necessary to ensure that the vacuum was at least $10^{-5}$ mm. Hg. before lighting the oxide coated cathode. The latter is formed by flashing at 6 volts for two to three minutes (50 per cent. overload) until the carbonates are decomposed into the oxides, and then a potential of 10–20 volts is placed on the modulator electrode M for about half an hour during which the emission gradually crept up to 15–20 ma. Having formed the cathode in this way, the $A_1$, $A_2$, $A_3$ voltages were applied to the system. The $A_3$ voltage was kept fixed at 5 kv. throughout the whole series of experiments. The $A_1$ voltage determines the cut-off point of the beam—that is to say, at what modulator voltage negative to the cathode the electron beam is suppressed. The $A_2$ voltage in this case controls the focusing action on the beam, and was carefully adjusted so that the spot, when viewed through a neutral filter of density 1000, appeared to be in best visual focus. To avoid physiological and psychological differences the same observer was employed throughout the series of experiments. It should be pointed out that this " best visual focus " did not coincide with the best electrical focus as revealed by the oscillograph.

It was essential to keep the voltages on the $A_2$ and $A_3$ electrodes constant to well within 1 per cent. at any time, since the ratio of these two voltages defines the cardinal points of the main lens. To this end " bleeder " resistances from 3–60 megohms were shunted across the outputs from the H.T. units used, with delicate microammeters in series. The output voltage was kept constant by fine control on the primary side of each unit—a variation of 5/1000 could thus be detected and corrected for on both the $A_2$ and $A_3$ units ; both these were well within the 2 per cent. variation which caused distortion of the traces.

A further point that arose during the work was the effect of sparkover in the tube on the distributions. This took place at irregular intervals usually where a high $A_1$ voltage was being used, and led to three separate effects connected with surface changes on the cathode :

1. Permanent deformation of the trace, independent of time of pumping, making the peak flat-topped and broadening the curve.
2. Temporary deformation, which disappears after five to ten minutes' pumping.
3. No deformation, but permanent improvement in cathode emission.

This was the rarest of all three types. It should be mentioned that these effects were not accompanied by any appreciable change in beam current.

The trace is, as a rule, a symmetrical curve of the same shape and form as the normal probability curve. It has a tail portion on each side and rises to a maximum in the middle corresponding to the centre of the spot.

The effects on the distribution of varying the focus voltage $A_2$, the modulator voltage M, the accelerating voltage $A_1$, and the temperature of the cathode were separately investigated.

### *Electron Distribution and Spot Size.*

The electron distribution trace is influenced to a marked degree by the state of the cathode. For any one set up a repetition accuracy of 15 per cent. could be obtained, but there was a wide spread in results for different cathodes which necessitated a statistical analysis of results. An examination of hundreds of curves brings out their Gaussian character, as shown in fig. 5. In many cases the width as measured from tail to tail was 1·5–2·0 times the true Gaussian width ; this may be caused by lens aberrations.

Fig. 5.

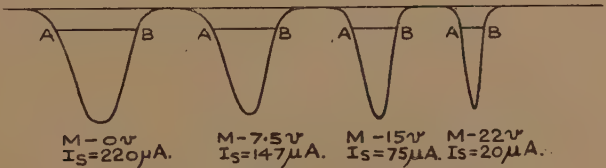

Electron distribution traces.

$A_1$ 1350 v. BO—30 v. $A_3$ 5 kv. ; aperture 4 mm. $A_3$/screen 400 mm. Barrel length 45 mm. AB=index of effective spot width.

The Gaussian property was proved by measuring the heights $y$ of the ordinates for various values of $x$, the distance from the peak ordinate, and finding the standard deviation $\sigma$ from these, as follows :—

| $x$. | $x^2$. | $y$. | $x^2y$. |
|---|---|---|---|
| 0 | 0 | 30 | 0 |
| 2 | 4 | 18 | 72 |
| 4 | 16 | 8 | 128 |
| 6 | 36 | 5 | 180 |
| 8 | 64 | 3·5 | 224 |
| 10 | 100 | 2·0 | 200 |
| | | 66·5 | 804 |

$$\text{Mean square } \frac{804}{66{\cdot}5} \doteqdot 12 \;\therefore\; \sigma = \sqrt{12} \doteqdot 3{\cdot}5.$$

The ordinates of points whose abscissæ were 0·5 $\sigma$, $\sigma$, 1·3 $\sigma$ were next read off the curve, and gave 26·4, 18, 12·9 mm. respectively. Reference to the probability tables confirmed that these were the values to be expected for the above values of $\sigma$.

It must be pointed out that not all the curves were Gaussian. The following abnormal types were met with, and are shown in fig. 6 :— (*a*) regular peak, but sharp points of inflexion in tail, (*b*) flat-topped or humpy peaks, (*c*) steep-sided conical peaks. All these types appear to be associated with high current beams, and it was possible to transform them to the perfectly normal form by adjustment to the focus voltage. This has been done experimentally for certain families of curves where the best electrical focus conditions were specially looked for, but will not be discussed here.

To check that the total current to the screen was the integral of the curve representing the electron distribution the auxiliary oscillograph deflexion was calibrated in terms of current. The total area of the distribution curve was found by counting the squares, and the unit of current was obtained taking into account the slit width. A good check was obtained in this way.

Fig. 6.

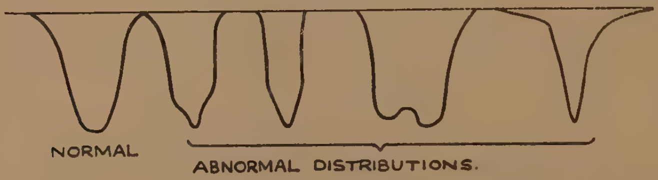

Coming next to the question of spot width, the difficulty introduced by the tail portions is overcome by the following arbitrary convention for the "effective spot width." A line is drawn parallel to the base at a height from it which is 1/5th the peak ordinate. The distance between the points in which this line meets the curves on both sides is defined as "the effective spot width." Fig. 7 makes this clear. For a true probability distribution the areas (*a*) and (*b*) together total about 1/15th the total area of the curve, so that this represents the total light flux fringing due to the superpositions of two line scans in an actual television picture. Wheeler and Loughren * have shown that an ideal spot necessary to produce equal "widths of confusion" in both directions should have a $\cos^2$ distribution whose effective width defined in the above sense is 0·59 of the base. This closely agrees with our convention, since in our case the effective spot width is 0·6 times the length of base.

* P. I. R. E. xxvi. p. 540 (1938).

## EXPERIMENTAL RESULTS.

### *Variation of Spot Size with Modulation and* $A_1$ *Voltage.*

The variables affecting the image size are object size and object distance, and both these are uniquely determined by the first lens combination—cathode, modulator, $A_1$, geometry and voltage.

For any fixed geometry and $A_1$ voltage, the object being imaged should vary in size and position as the power of this lens combination is altered by variation of modulator voltage. Alternatively for any fixed modulator voltage a variation in $A_1$ volts should produce a similar effect. Fig. 8 shows how the image size varies with modulator volts for a fixed $A_1$ volts, and also the family of curves obtained at different $A_1$ voltages. They all show the " swelling spot " characteristic.

Fig. 7.

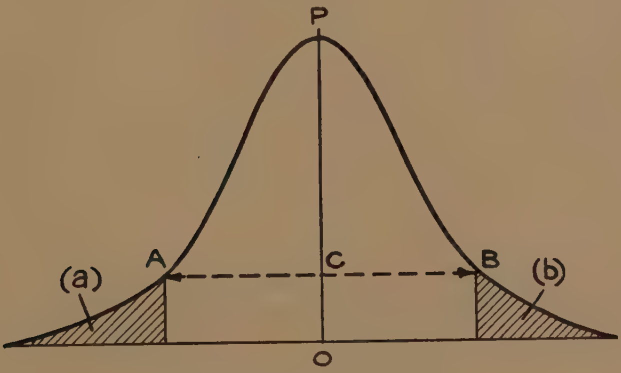

Spot width convention.

OC=1/5 OP. Areas (*a*)+(*b*) 1/15 total area.
AB=" effective spot width."

The dotted curve shows the effect of the $A_1$ volts by itself at 30 volts above the cut-off point on the modulation characteristic. Notice that the spot decreases in size with increase in $A_1$ volts.

Increased modulation gives both bigger beam currents $I_B$ and larger image sizes S, but the ratio $I_{B/S^2}$ increases with increasing $V_M$. This ratio also increases with increasing $A_1$ volts.

### *Variation of Spot Size with Focus Voltage.*

Observations previously taken showed that the best visual focus did not coincide with the best electrical focus, and the actual variation in spot characteristics with small increments and decrements starting from the "best visual" focus voltage was determined to elucidate this point.

Fig. 9 shows the results. The curious kinks on some curves occur at 100 volts below the best visual focus. Here the spot enlarges with *decreased* modulation, an entirely reverse effect to that normally obtained.

Fig. 8.

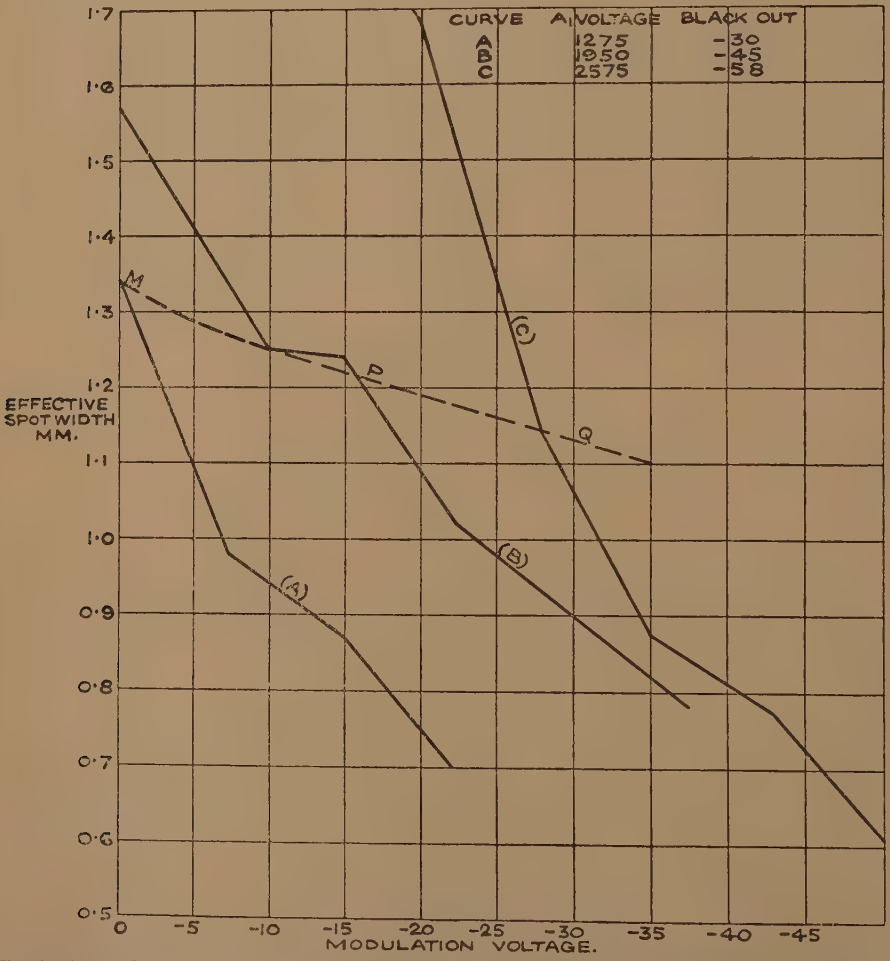

Variation of spot width with modulation and with first accelerator voltage $A_1$.

The curves are plotted in a different way in fig. 10, and show that the best electrical focus is some 70 volts below the best visual focus for this family. The latter is on the same ordinate for each curve, a fortuitous coincidence, not generally met with in practice.

A departure of some 50 volts on either side of this gives an increase in spot size in the ratio of 2/1 or higher. In the majority of cases the

Fig. 9.

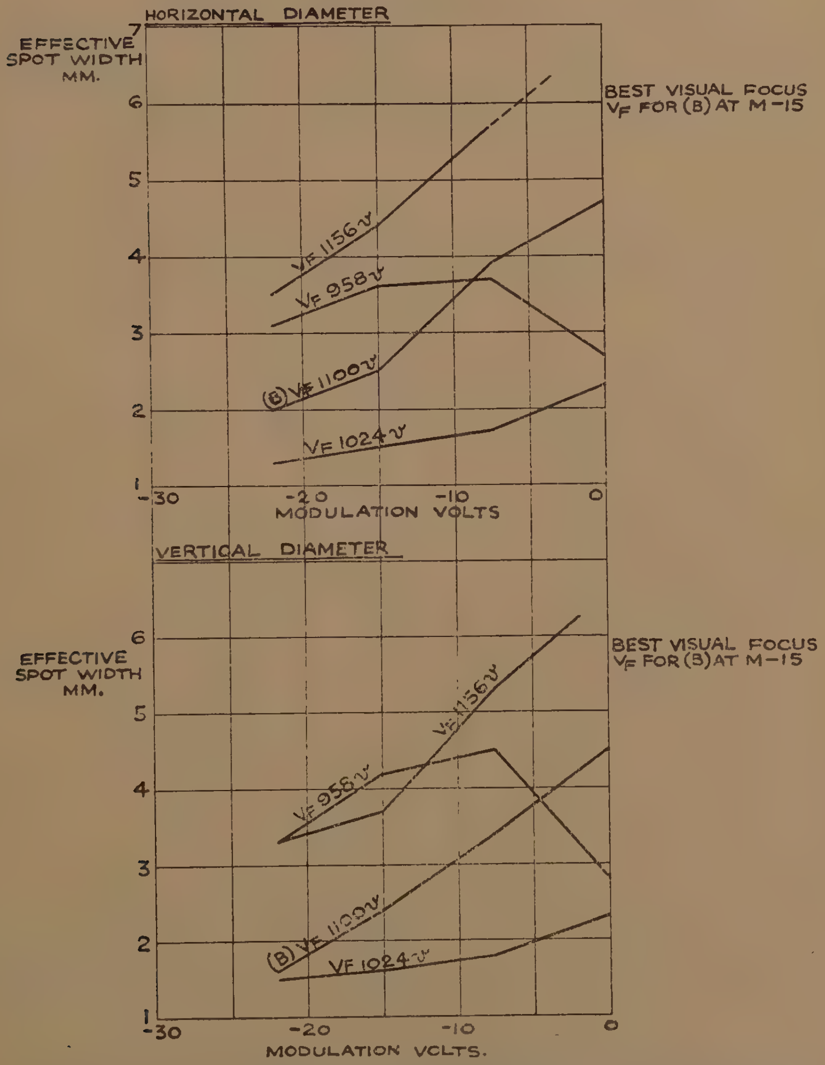

Variation of spot width with modulation, also showing the effect of variation in focus voltage.

minimum spot size (and with it the focus voltage at which it is produced) does not occur at the same value of the focus voltage for each point on the modulation characteristic, so that there is always a certain defocusing effect present under normal conditions.

### *Effect of Cathode Temperature.*

The variations imposed on the triode portion—cathode, modulator, $A_1$, as well as variations in size of emitting cathode area determine the position and size of the crossover. The latter is thus affected by the cathode temperature, and a study of image size with temperature in the range (910–1075° C.) was undertaken. It is essential to keep the geometry of cathode, modulator, $A_1$ system constant throughout. This was done by adjusting the cathode modulator separation at each temperature (by mounting the cathode on an extensible metal bellows worked by an external screw arrangement), so that the cut-off point of the beam was —30 volts.

Fig. 10.

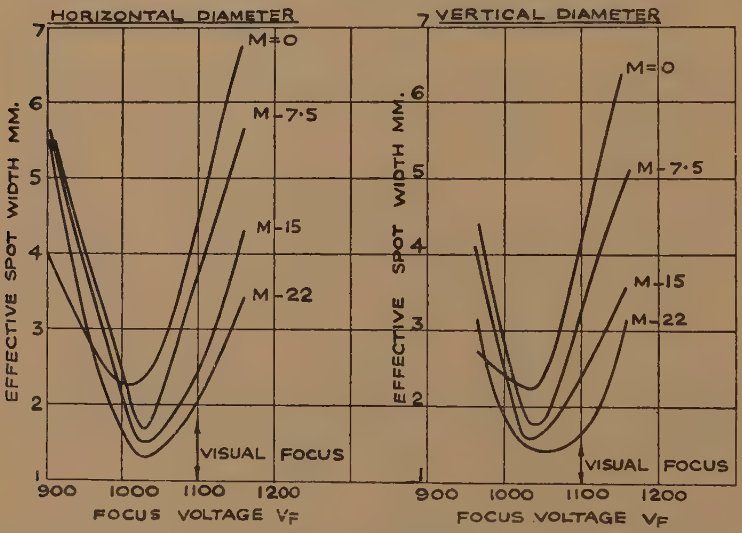

Variation of spot width with focus voltage for various values of modulation voltage.

The curves of fig. 11 show that the spot size is independent of temperature over 3/4 of the modulation range. A reasonable inference from this is that the size of the crossover must be constant and independent of temperature within the range investigated. The only change introduced by raising the temperature is to increase the current into the beam up to the point where it is space-charge limited.

The first lens combination thus produces an image of the cathode source of definite size for all temperatures, and is independent of the crossover current density.

### *Current Density in the Image.*

The effective spot size, as deduced from the distribution curves, enables the average effective current density to be calculated.

In order to arrive at the peak current density it is important to realize that the resolving slit has to analyse a three-dimensional beam having a circular base and a Gaussian envelope. Further, the section of the beam by the slit also has a Gaussian distribution along the slit, so that as a first approximation we require the ratio of peak to effective height for a solid Gaussian distribution. This is obtained as follows :—

Fig. 11.

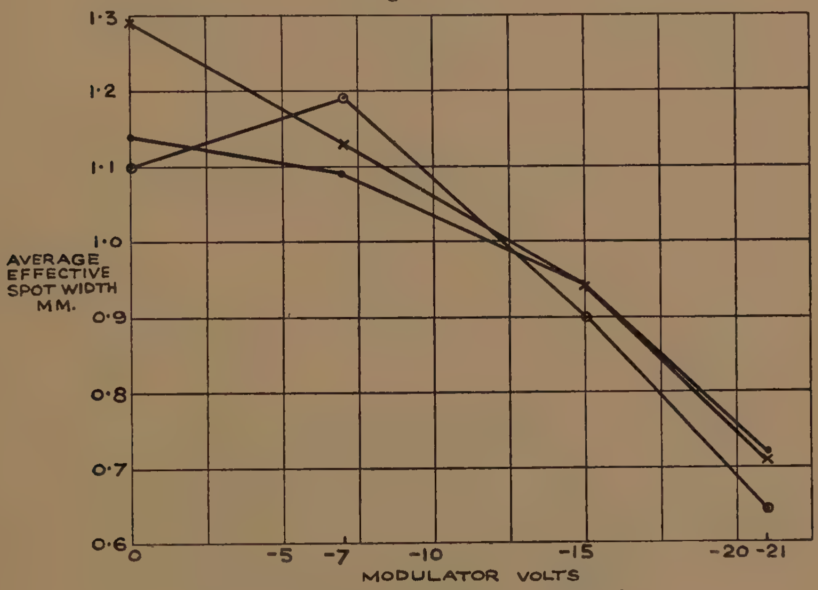

Effect of cathode temperature on spot size.

× cathode at 1075° C.
● „ „ 1000° C.
⊙ „ „ 910° C.

Let $y=e^{-x^2}$ be the equation to the envelope ; then the total volume V of the solid Gaussian distribution can be obtained by treating it as a solid of revolution.

$$\therefore \quad V=\int_0^\infty \pi x^2\,dy=\pi\int_0^\infty -2x^3e^{-x^2}\,dx.$$

Integrating by parts,

$$V=\pi[(x^2e^{-x^2})_0^\infty-\int e^{-x^2}.\,2x\,dx]=\pi[(x^2e^{-x^2})_0^\infty+1]=\pi.$$

This is the volume when $y_0=1$ at $x=0$. Under our convention of measurement $y=0{\cdot}2$ $\therefore$ log $0{\cdot}2=-x^2$.

$$\text{Effective Area}=\pi x^2=-\pi\log_e(0{\cdot}2).$$

$$\therefore\quad \text{Effective height}=\frac{1}{-\log_e(0{\cdot}2)}=\frac{1}{1{\cdot}61};$$

hence $\dfrac{\text{peak}}{\text{effective height}}=1{\cdot}6$, so that the peak current density is about 1·6 times the effective current density.

The following table is for a representative case :—

| Mod. volts. | Ave. effect spot size (mm.). | Current $I_B$ in spot ($\mu$a.). | Ave. effect curr. density (ma./cm.$^2$). | Peak current density (ma./cm.$^2$). |
|---|---|---|---|---|
| 0 ..... | 0·94 | 190 | 29 | 47 |
| − 7·5 ..... | 0·94 | 123 | 19 | 31 |
| −15 ...... | 0·84 | 59 | 11 | 18 |

The curves in fig. 12 show the variation of peak current density with modulation. The relation is nearly linear, and for a 30 volt cut-off the peak is about 50 ma./cm.$^2$. The decrease with modulation implies that the current is falling faster than the spot width. Law * has shown that at the crossover the current density at any point $r$ from the axis is

$$J_0=\frac{I_B}{\pi}\,a\mathrm{E}e^{-a\mathrm{E}r^2},$$

where E=accelerating voltage and $a$ is a constant for any given set up. The form of the distribution is here Gaussian, which is expected from the initial assumption of a Maxwellian distribution for the electrons emitted by the cathode. No attempt has been made here to follow this through and calculate the crossover size, because of uncertainties introduced by the aberrations of the preliminary focusing field as well as by the space-charge.

The calculations are further complicated by the effect of modulation, which varies the current and angle of the incident beam.

---

* P. I. R. E. xxv. p. 954 (1937).

Further work by Langmuir*, assuming an ideal focusing field, has led to an expression for the maximum current density $J_i$ obtainable in a focused beam in terms of that at the cathode $J_c$ and the half angle $\phi$ of the beam converging on the image;

$$J_i = J_c \left[\frac{Ee}{kT} + 1\right] \sin^2 \phi.$$

In our case $E = 5000$ volts, $T = 1200°$ K., $\sin \phi = 0{\cdot}05$; hence $J_i = 1{\cdot}2\,J_c$.

Fig. 12.

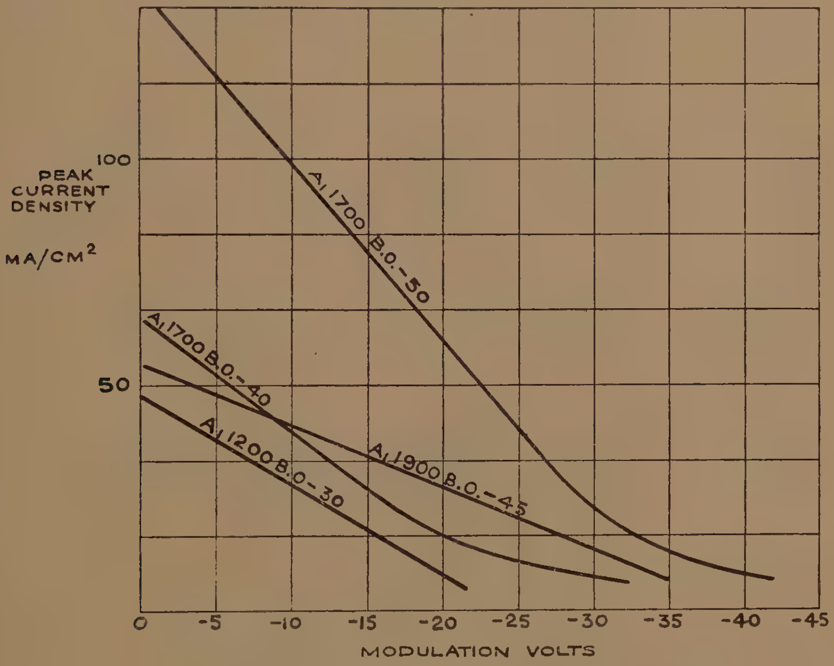

Variation of peak current density with modulation.

The value of $J_c$ can, to a first approximation, be found from the cathode current at $M = 0$, and the area of the hole in the modulator M. The peak cathode current thus works out at about 350 ma./cm.$^2$

$$\therefore \quad J_i = 420 \text{ ma./cm.}^2.$$

The measured value of $J_i$ was only about 50 ma./cm.$^2$, hence the aberrations are responsible for cutting down the maximum current density in the focused spot to about one-eighth of its theoretical value, since the space-charge correction involved in this case is negligible.

---

* P. I. R. E. xxv. p. 977 (1937).

### *Effect of Slit Width.*

It is clear that the slit width in relation to the spot width determines its faithfulness as an analyser, and with the 0·2 mm. slit in use corrections have to be applied when the spot width is some four times the slit width at the lowest modulations.

It is interesting to take a simple case—a circular spot of 2 mm. diameter with uniform distribution in the first instance. The height of any ordinate recorded in the distribution would then be $2w\sqrt{r^2-x^2}$, where $w$=slit width, $r$=radius of spot, $x$=distance of slit centre to spot centre. The current I into the slit at any point $a$ along a diameter is then given by

$$\mathrm{I}=2\int_{x=a-w/2}^{x=a+w/2}\sqrt{r^2-x^2}\,dx=\left[r^2\sin^{-1}\frac{x}{r}+x\sqrt{r^2-x^2}\right]_{a-w/2}^{a+w/2},$$

and it can be shown that the error in the ordinate recorded for a point at 0·8 mm. from the centre (thus, in the tail) is only about 1 per cent. for the 0·2 mm. slit. In the case of a two-dimensional non-uniform distribution such as that given by the probability curve which corresponds with the distribution traces previously described, the tail effect can be simply calculated at $x=1{\cdot}8\,\sigma$ ($\sigma$=standard deviation), since this value of the abscissa corresponds to the $y$ of the point which, with our convention, is 1/5th the peak ordinate.

It is possible from the following considerations to make a comparison between the ordinates at any fixed $x$ for different slits.

Let $\mathrm{I}_1$=current into slit (1) at $x=0$.
,, $\iota_1$= ,, ,, (1) ,, $x=x_1$.
,, $\mathrm{I}_2$= ,, ,, (2) ,, $x=0$.
,, $\iota_2$= ,, ,, (2) ,, $x=x_1$.

Since we are working at constant amplitude $\mathrm{I}_1\mathrm{R}_1=\mathrm{I}_2\mathrm{R}_2$, where $\mathrm{R}_1$ and $\mathrm{R}_2$ are the input resistances.

Now

$$\frac{\text{ordinate at } x=x_1 \text{ with slit (1)}}{\text{ordinate at } x=x_1 \text{ with slit (2)}}=\frac{\iota_1\mathrm{R}_1}{\iota_2\mathrm{R}_2}=\frac{\iota_1}{\iota_2}\times\frac{\mathrm{I}_2}{\mathrm{I}_1}$$

$$=\frac{\text{current at } x=x_1 \text{ with slit (1)}}{\text{current at } x=x_1 \text{ with slit (2)}}\times\frac{\text{current at } x=0 \text{ with slit (2)}}{\text{current at } x=0 \text{ with slit (1)}}.$$

Considering half the curve only, $\sigma=\frac{1}{3}$ new base; hence $x=0{\cdot}6$ base. The areas of overlap with the slit at this point at which our measurements are made in the case of two slits with a width ratio of 4/1 are then as follows :—

| $x$. | 0·2 slit. | 0·05 mm. slit. |
|---|---|---|
| 0 | 0·5738 of total area. | 0·1465 of total area. |
| 0·6 | 0·0496 of total area. | 0·0112 of total area. |

Hence

$$\frac{\text{ordinate at } x=0\cdot6\, b \text{ with } 0\cdot2 \text{ mm. slit}}{\text{ordinate at } x=0\cdot6\, b \text{ with } 0\cdot05 \text{ mm. slit}}$$

$$=\frac{0\cdot0496}{0\cdot0112}\times\frac{0\cdot1465}{0\cdot5738}=1\cdot13.$$

Fig. 13.

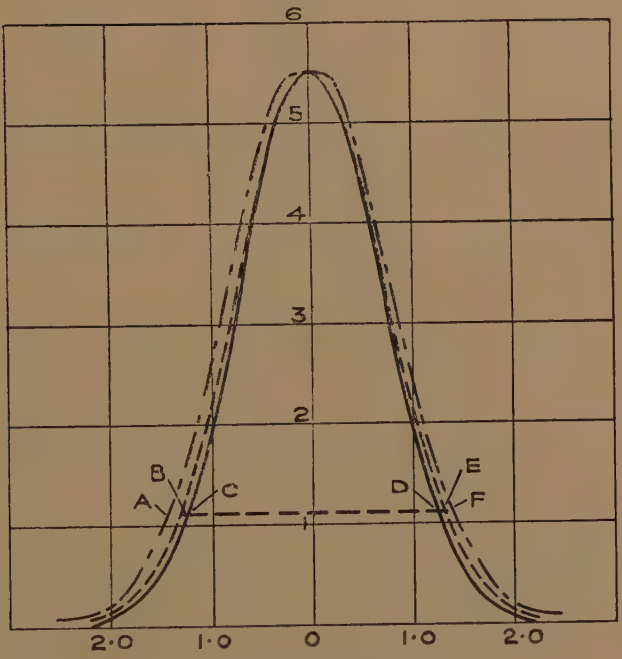

Effect of slit width.

——— theoretical.
– – – 0·2 mm. slit.
—-—- 0·4 mm. slit.
BE=measured spot width.
CD=actual spot width.

Error is $\frac{2\text{DE}}{\text{CD}}$ =4 per cent. (for 0·2 mm. slit).

Here the wider slit tends to enhance the tail ordinate by some 10 per cent., so that the spot size measurements on such a distribution would be high by some 3 per cent. This was checked on an actual trace, and is made clear in fig. 13, which is purely diagrammatic.

The errors deduced on the basis of the true probability curve are on the high side, as the following rigid calculation applied to a representative set of distribution curves shows.

Actually the problem is to find how the experimental curve would be modified if an infinitely narrow slit had been used. Runge* has given an expression in terms of finite differences for the case where there are two slits. I am indebted to Mr. J. W. Ryde of these laboratories for the corresponding expression for one slit which is needed here. It is

$$\phi(x)=F_0-\frac{1}{2^2\underline{|3}}\,\Delta^2F_{-1}+\frac{9}{2^4\underline{|5}}\cdot\Delta^4F_{-2}-\frac{225}{2^6\underline{|7}}\cdot\Delta^6\,F_{-3}+\ldots$$

Here $\phi(x)$=true ordinate.

$F_0$=ordinate on curve at measuring point (6 mm.).
$F_{-1}$= ,, ,, ,, one slit width in negative direction.
$F_{-2}$= ,, ,, ,, two slit widths ,, ,,
$F_{+1}$= ,, ,, ,, one slit width in positive direction.
$\Delta^2F_{-1}=F_1-2F_0+F_{-1}$.
$\Delta^4F_{-2}=F_2-4F_1+6F_0-4F_{-1}+F_{-2}$.

| | M=0. | M=−7·5. | M.=−15. | M=−22. |
|---|---|---|---|---|
| $F_{-1}$ ....... | 12 | 13 | 15 | 25 |
| $F_{-2}$ ....... | 19 | 20 | 22 | 30 |
| $F_{+1}$ ....... | 3 | 3 | 0 | 3 |
| $F_{+2}$ ....... | 0 | 1·5 | 1·5 | 0 |
| $\phi(x)$ ....... | $6-\frac{19}{128}$ | $6-\frac{19}{96}$ | $6-\frac{54}{240}$ | $6-\frac{85}{96}$ |
| % error .... | 2·5 | 3·3 | 3·7 | 15 |

It is thus seen that the results confirm the previous calculations; it is not until the lowest modulation point is reached that any serious error is involved in the spot width measurements. As a first approximation the error involved in the measurement of the spot width is of the same order as the error in the height of the ordinate, so that over three-quarters of the modulation range the measurements give a result for the spot width which is in excess of the true value on our convention by less than 5 per cent.

---

* *Zeits. f. Math. u. Phys.* xlii. p. 205 (1897).

# VII. *The Primary and Secondary Scattering of Sunlight in a Plane-stratified Atmosphere of Uniform Composition* *.

By A. Hammad, Ph.D. †, Department of Mathematics,
The Egyptian University, Cairo,
and
S. Chapman, F.R.S., Imperial College of Science
and Technology, London.

[Received March 2, 1939.]

## *Introduction.*

1. In this paper we consider a part of the difficult and complex problem of the illumination of the ground and the atmosphere by sunlight. A general analysis and formulation of this problem has been given by us elsewhere ‡. In this paper we consider only the primary and secondary scattering of the sunlight, in a plane-stratified atmosphere of uniform composition, and for wave-lengths for which transformations of energy from or to other wave-lengths, by absorption and re-emission, can be neglected. Consequently we are able to restrict our attention, throughout, to a monochromatic constituent of the light, between the wave-lengths $\lambda$ and $\lambda+d\lambda$. We do not consider the refraction or the polarization of the light.

Our problem is thus a very restricted form, and part, of the actual problem of atmospheric illumination; but our treatment is exact. In particular, we take full account of the Rayleigh law of scattering §, so that our results differ from the important but approximate earlier treatment of this subject by L. V. King ||.

## *Notation and Definitions.*

2. Let $h$ denote height above the ground, and $\rho$ the air-density at that height. Then M, the total mass of air in a vertical column of unit cross-sectional area, is given by

$$M=\int_0^\infty \rho\, dh.$$

---

* Communicated by the Authors.

† Part of this paper was included in a Ph.D. thesis of the University of London.

‡ 'La Météorologie,' to be published.

§ Rayleigh, Phil. Mag. xli. pp. 107, 274, 447 (1871); xii. p. 81 (1881); Collected Works, i. pp. 87, 104, 518.

|| L. V. King, Phil. Trans. A, ccxii. pp. 375–433 (1913).

The absorption and scattering of the light by the air are taken to depend only on the *mass* of gas traversed, without regard to the *distance*. Hence it is convenient to specify the height of any point P in the atmosphere in terms of the fraction of the total mass that lies above or below P. This procedure, which was adopted by King, has the advantage that formulæ expressed in such terms can at a late stage be applied to any height-distribution of mass.

The fraction of the mass *below* the height of P will be denoted by $m$, and the fraction *above* this height will be denoted by $\overline{m}$ (with a bar *above* the symbol $m$); we shall refer to $m$ as giving the *level* of P, and to $\overline{m}$ as giving its *depth* in the atmosphere; the level $m$ increases upwards, and the depth $\overline{m}$ increases downwards. Clearly

$$m=\int_0^h \rho\, dh/\mathrm{M}, \quad \overline{m}=\int_h^\infty \rho\, dh/\mathrm{M},$$

$$m+\overline{m}=1, \quad \rho\, dh=\mathrm{M}\, dm=-\mathrm{M}\, d\overline{m}.$$

At the ground $m=0$, $\overline{m}=1$; at the top of the atmosphere $m=1$ and $\overline{m}=0$.

3. The absorption and scattering coefficients of the air, per unit mass for light of wave-length $\lambda$, will be denoted by $\alpha(\lambda)$ and $\sigma(\lambda)$. We also write

$$a(\lambda)=\alpha(\lambda)\mathrm{M}, \quad s(\lambda)=\sigma(\lambda)\mathrm{M}, \quad c(\lambda)=a(\lambda)+s(\lambda);$$

$a(\lambda)$ and $s(\lambda)$ are called the coefficients of total absorption and total scattering of the atmosphere for vertically incident light of wave-length $\lambda$, and $c(\lambda)$ is the corresponding coefficient of *extinction*.

Since in this paper we consider only a single monochromatic constituent of the light (§1), we usually omit the reference to $\lambda$ in $\alpha(\lambda)$, . . . ., and write simply $\alpha$, $\sigma$, $a$, $s$, $c$.

4. The zenith angle of the sun will be denoted by $z$. Relative to the vertical, and the vertical half-plane through the sun, any other direction may be specified by its polar angles $\theta$ and $\phi$, or by the unit vector $\mathbf{k}$ in that direction; similarly, the direction $\theta'$, $\phi'$ may be specified by the unit vector $\mathbf{k}'$. The unit vector directed towards the sun will be denoted by $\mathbf{s}$; its polar angles are $z$, 0.

The angles between $\mathbf{s}$ and $\mathbf{k}$, and $\mathbf{s}$ and $\mathbf{k}'$, will be denoted by $\psi$ and $\psi'$ respectively, and $\chi$ will denote the angle between $\mathbf{k}$ and $\mathbf{k}'$; hence

$$\begin{aligned}\cos\psi &=\cos z\cos\theta+\sin z\sin\theta\cos\phi,\\ \cos\psi' &=\cos z\cos\theta'+\sin z\sin\theta'\cos\phi',\\ \cos\chi &=\cos\theta\cos\theta'+\sin\theta\sin\theta'\cos(\phi-\phi').\end{aligned}$$

5. A small solid angle around the direction $\mathbf{k}$ will be denoted by $d\mathbf{k}$; similarly for $d\mathbf{k}'$ and $d\mathbf{s}$; thus, in integrals, $d\mathbf{k}$ may be regarded as a convenient abbreviation for $\sin\theta\, d\theta\, d\phi$.

A cone of small solid angle $d\mathbf{k}$ about the direction $\mathbf{k}$ will be called the cone $\mathbf{k}$, $d\mathbf{k}$, or, if its vertex is at P, the cone P ; $\mathbf{k}$, $d\mathbf{k}$.

6. The symbols $c \sec z$, $c \sec \theta$, $c \sec \theta'$ occur often in our formulæ, and it is convenient to write

$$Z = c \sec z, \quad \Theta = c \sec \theta, \quad \Theta' = c \sec \theta'.$$

Clearly $Z = \Theta$ if $z = \theta$, and $Z - \Theta$ always has the same sign as $z - \theta$.

7. Let

$$R(\lambda, h, z, \mathbf{k})\, d\lambda\, dS\, d\mathbf{k}$$

denote the rate of flow of energy of radiation of wave-length $\lambda$ to $\lambda + d\lambda$, received from directions lying within the small cone $\mathbf{k}$, $d\mathbf{k}$, across a small plane element of area $dS$ normal to $\mathbf{k}$ and situated at the height $h$, when the sun's zenith angle is $z$ ; then $R(\lambda, h, z, \mathbf{k})$ is called the *intensity* of such received radiation at this height.

When the height $h$ is specified by the level $m$ or the depth $m$, these symbols may replace $h$ in this function R (and likewise in other functions of $h$). The wave-length $\lambda$ will often be omitted from the symbol for R, and the other variables also will often not be specifically indicated.

The intensity R is made up of contributions from the direct sunlight, from scattered light of all orders of scattering, and from light returned to the atmosphere from the ground. The contributions due to the direct sunlight, and to the primary and secondary scattered sunlight, which alone are considered in this paper, will be distinguished by the respective suffixes 0, 1, and 2.

8. The direct sunlight comes from directions confined within a small cone $\mathbf{s}$, $d\mathbf{s}$, where $d\mathbf{s}$ denotes the solid angle subtended by the sun at the earth. We write

$$R_0(\lambda, \infty, z, \mathbf{s})\, d\mathbf{s} = I_\infty(\lambda),$$

so that $I_\infty(\lambda)$, usually here written $I_\infty$, denotes the solar radiant energy of the wave-lengths $\lambda$ to $\lambda + d\lambda$, which is received per unit time on a unit area normal to $\mathbf{s}$, outside the earth's atmosphere ($h = \infty$). For directions $\mathbf{k}$ outside the cone $\mathbf{s}$, $d\mathbf{s}$, $R_0(\mathbf{k}) = 0$ for all values of $\lambda$, $h$, and $z$.

We also write

$$R_0(\lambda, h, z, \mathbf{s})\, d\mathbf{s} = I(\lambda, h),$$

so that $I(\lambda, h)$, usually here written I, denotes the intensity of the monochromatic constituent $\lambda$ to $\lambda + d\lambda$ of the solar beam at the height $h$.

9. The rate of emission f radiant energy of wave-lengths $\lambda$ to $\lambda + d\lambda$, in directions lying within the cone $\mathbf{k}$, $d\mathbf{k}$, per unit *mass* per unit time, by air at the height $h$, when the sun's zenith angle is $z$, will be denoted by $E(\lambda, h, z, \mathbf{k})\, d\lambda\, d\mathbf{k}$ ; the parts of E due to primary, secondary, . . . . scattered sunlight will be distinguished by the suffixes 1, 2, . . . .

### *The Attenuation of the Direct Sunlight.*

10. When a beam of light of intensity $\mathrm{I}\,d\lambda$, such as the direct solar beam, passes through a small volume of air, $dv$, of mass $\rho\,dv$, it loses energy at the rate $(\alpha+\sigma)\rho\mathrm{I}\,d\lambda\,dv$; the rate of loss per unit mass of air is $(\alpha+\sigma)\mathrm{I}\,d\lambda$. Of this energy abstracted from the beam, part is re-emitted, as energy of primary scattered sunlight, at the rate $\sigma\mathrm{I}\,d\lambda$ per unit mass per unit time.

If the element $dv$ is that part of the region traversed by a pencil of the incident radiation, of normal cross-section $d\mathrm{S}$, which is intercepted between the heights $h$ and $h+dh$, then $dv=\sec z\,d\mathrm{S}\,dh$, so that the rate of loss of energy in this volume is

$$(\alpha+\sigma)\rho\,\mathrm{I}\sec z\,d\mathrm{S}\,dh\,d\lambda.$$

This reduces the rate of flow of energy along the pencil, from $(\mathrm{I}-d\mathrm{I})\,d\mathrm{S}\,d\lambda$ at the upper height to $\mathrm{I}\,d\mathrm{S}\,d\lambda$ at the lower. Hence

$$d\mathrm{I}\,d\mathrm{S}\,d\lambda=(\alpha+\sigma)\rho\mathrm{I}\sec z\,d\mathrm{S}\,dh\,d\lambda$$

or

$$d\mathrm{I}=(\alpha+\sigma)\rho\mathrm{I}\sec z\,dh=-(a+s)\mathrm{I}\sec z\,d\bar{m}$$
$$=-\mathrm{I}c\sec z\,d\bar{m}=-\mathrm{ZI}\,d\bar{m},$$

by §§ 2, 3, 6. Hence, since $\mathrm{I}=\mathrm{I}_\infty$ when $\bar{m}=0$ (at the top of the atmosphere),

$$\mathrm{I}=\mathrm{I}_\infty e^{-\mathrm{Z}\bar{m}}=\mathrm{I}_\infty e^{-z(1-m)}.$$

### *The Emission of Primary Scattered Sunlight.*

11. Radiant energy (of wave-length $\lambda$ to $\lambda+d\lambda$) is "emitted" by primary scattering, in all directions, by the air at the height $h$, at the rate $\sigma\mathrm{I}\,d\lambda$ or $\sigma\mathrm{I}_\infty e^{-\mathrm{Z}\bar{m}}\,d\lambda$ per unit mass per unit time (§ 10).

Rayleigh showed that the intensity of the light scattered in directions lying with the cone $\mathbf{k}$, $d\mathbf{k}$, from incident radiation in the direction $\mathbf{k}'$, is proportional to $(1+\cos^2\chi)\,d\mathbf{k}$, where $\chi$ (§ 4) is the angle between $\mathbf{k}$ and $\mathbf{k}'$. Since

$$\int(1+\cos^2\chi)\,d\mathbf{k}=\frac{16}{3}\pi \quad . \quad . \quad . \quad . \quad . \quad . \quad . \quad . \quad (1)$$

(where the integration is over all directions $\mathbf{k}$), it follows that the actual fraction of the light emitted by this scattering, within the cone $\mathbf{k}$, $d\mathbf{k}$, is $\dfrac{3}{16\pi}(1+\cos^2\chi)\,d\mathbf{k}$. This is the same for the directions $\pm\mathbf{k}$.

In the case of the primary scattering of sunlight, $\mathbf{k}=\mathbf{s}$, so that $\chi=\psi$ (§ 4). Hence the intensity of the primary scattered sunlight ($\lambda$ to $\lambda+d\lambda$) emitted per unit mass of air at the height $h$, within the cone $\mathbf{k}$, $d\mathbf{k}$, is given by

$$\mathrm{E}_1(\lambda, h, z, \mathbf{k})\,d\lambda\,d\mathbf{k}, \quad . \quad . \quad . \quad . \quad . \quad . \quad . \quad . \quad (2)$$

where

$$E_1 = \frac{3\sigma}{16\pi} I_\infty (1+\cos^2 \psi) e^{-Z\overline{m}} \quad . \quad . \quad . \quad . \quad . \quad . \quad . \quad (3)$$

### *The Reception of Primary Scattered Sunlight.*

12. The primary scattered light ($\lambda$ to $\lambda + d\lambda$) *received* at (or crossing) a small surface-element $dS$ (normal to $\mathbf{k}$, at the height $h$), and coming *from* directions lying within the cones $\mathbf{k}$, $d\mathbf{k}$, is emitted (scattered) by the air which lies within the cones P; $\mathbf{k}$, $d\mathbf{k}$, where P is any point on $dS$. It is denoted (§ 7) by $R_1(\lambda, h, z, \mathbf{k})\, d\lambda\, dS\, d\mathbf{k}$.

Let $dv'$ be a volume-element of air, of density $\rho'$, at the height $h'$, that contributes to this light; let its distance from $dS$ be $r$, in the direction $\mathbf{k}$, so that $h' = h + r\cos\theta$. Then $dS$ subtends a solid angle $dS/r^2$ at $dv'$, so that the light from $dv'$ that crosses $dS$ travels in directions lying within a cone of this small solid angle, around the direction $-\mathbf{k}$. The rate of emission from $dv'$ (which contains a mass of air $\rho' dv'$), within this solid angle, is $E_1(\lambda, h', z, -\mathbf{k})\, d\lambda (dS/r^2) \rho' dv'$. As in § 9 for the incident sunlight, so also for this light, travelling in the direction $-\mathbf{k}$, at the zenith angle $\pi - \theta$, the intensity on reaching $dS$ is reduced by absorption and secondary scattering, so that only a fraction $e^{-c(\overline{m} \sim \overline{m}')\sec\theta}$ or $e^{-\Theta(m \sim \overline{m}')}$ reaches $dS$ (see §§ 3, 6). To obtain the total light ($\lambda$ to $\lambda + d\lambda$) crossing or reaching $dS$, within the cones P; $\mathbf{k}$, $d\mathbf{k}$, the expression

$$e^{-\Theta(\overline{m} \sim \overline{m}')} E_1(\lambda, h', z, -\mathbf{k}) d\lambda (dS/r^2) \rho'\, dv'$$

must be summed over all the contributory elements $dv'$. Those elements whose distance from $dS$ lies between $r$ and $r + dr$ together make up a length $dr$ of the cones P; $\mathbf{k}$, $d\mathbf{k}$, and their combined volume is $r^2\, dr\, d\mathbf{k}$. Hence these elements contribute to $R_1\, d\lambda\, dS\, d\mathbf{k}$ an amount

$$\rho' e^{-\Theta(\overline{m} \sim \overline{m}')} E_1(\lambda, h', z, \mathbf{k})\, d\lambda (dS/r^2) r^2\, dr\, d\mathbf{k}$$

(where we have replaced the $-\mathbf{k}$ in $E_1$ by $\mathbf{k}$, because, as mentioned in §10, the rates of scattering in the directions $\pm\mathbf{k}$ are equal). Hence, by integrating from $r = 0$ to $r = \infty$, we find that

$$R_1(\lambda, h, z, \mathbf{k}) = \int_0^\infty e^{-\Theta(\overline{m} \sim \overline{m}')} E_1(\lambda, h', z, \mathbf{k}) \rho'\, dr.$$

Since $r = (h' - h)\sec\theta$, $\rho' dr = \rho' \sec\theta\, dh' = M\sec\theta \mid dm' \mid = M\sec\theta \mid d\overline{m}' \mid$, where $\mid \quad \mid$ indicates that the positive numerical magnitude is to be taken; this is necessary here because $r^2\, dr\, d\mathbf{k}$ represents an essentially positive volume.

Hence, now taking $m$ as the variable in $R_1$ and $E_1$, and remembering that $m \sim m' = \overline{m} \sim \overline{m}'$, we have

$$R_1(\lambda, m, z, \mathbf{k}) = M.\sec\theta \int_m e^{-\Theta(m \sim m')} E_1(\lambda, m', z, \mathbf{k}) \mid dm' \mid, \quad . \quad . \quad (1)$$

where the unspecified upper limit of integration is $m=0$ (the ground) if **k** is downward (corresponding to upward travelling light), or $m=1$ (the top of the atmosphere) if **k** is upward (corresponding to downward travelling light).

Since, by § 11,

$$\mathrm{E}_1(\lambda, m', z, \mathbf{k}) = \frac{3\sigma}{16\pi} \mathrm{I}_\infty (1+\cos^2 \psi) e^{-\mathrm{Z}\overline{m}},$$

where $\overline{m}=1-m$, by integration of (1) we obtain the formulæ :

$$\mathrm{R}u_1(\lambda, m, z, \mathbf{k}) = f(\lambda, z, \mathbf{k}) e^{-\mathrm{Z}} \frac{e^{\mathrm{Z}m} - e^{-\Theta m}}{\mathrm{Z}+\Theta}, \quad . \quad . \quad . \quad . \quad . \quad (2)$$

$$\mathrm{R}d_1(\lambda, m, z, \mathbf{k}) = f(\lambda, z, \mathbf{k}) \frac{e^{-\Theta \overline{m}} - e^{-\mathrm{Z}\overline{m}}}{\mathrm{Z}-\Theta}, \quad . \quad . \quad . \quad . \quad . \quad (3)$$

where

$$f(\lambda, z, \mathbf{k}) = \frac{3s}{16\pi c} \mathrm{I}_\infty(\lambda) \Theta (1+\cos^2 \psi). \quad . \quad . \quad . \quad . \quad . \quad . \quad (4)$$

Here $\mathrm{R}u_1$ and $\mathrm{R}d_1$ refer respectively to the reception of upgoing light (**k** downward) and downgoing light (**k** upward).

When $\theta = z$, the last factor in the expression for $\mathrm{R}d_1$ takes the form 0/0 ; it must then be replaced by $-de^{-\mathrm{Z}\overline{m}}/d\mathrm{Z}$, that is, by $\overline{m}e^{-\mathrm{Z}\overline{m}}$.

### *The Emission of Secondary Scattered Sunlight.*

13. The air at any height $h$ receives primary scattered light from all directions $\mathbf{k}'$, and all such light is scattered in all directions. The light $\lambda$ to $\lambda + d\lambda$ emitted by secondary scattering per unit mass of air at height $h$, in directions lying within the cone $\mathbf{k}$, $d\mathbf{k}$, is $\mathrm{E}_2 \, d\lambda \, d\mathbf{k}$ (§ 9) ; the contribution to this, made by the primary scattered sunlight coming from directions lying within the cone $\mathbf{k}'$, $d\mathbf{k}'$, may be calculated as in § 11. We were there concerned with the scattering of direct sunlight coming only from directions lying within a cone $\mathbf{s}$, $d\mathbf{s}$, so that now $\mathrm{R}_1 \, d\lambda \, d\mathbf{k}'$ must be substituted for $\mathrm{R}_0 \, d\lambda \, d\mathbf{s}$, which there was written $\mathrm{I} \, d\lambda$ (§ 8), equal to $\mathrm{I}_\infty e^{-\mathrm{Z}\overline{m}} d\lambda$. Hence in place of § 11 (2, 3) we now have

$$\frac{3\sigma}{16\pi} (1+\cos^2 \chi) \mathrm{R}_1(\lambda, h, z, \mathbf{k}') \, d\lambda \, d\mathbf{k}' \, d\mathbf{k}$$

as representing the contribution made to $\mathrm{E}_2 \, d\lambda \, d\mathbf{k}$ by the primary scattered light received from the directions $\mathbf{k}'$, $d\mathbf{k}'$ ; $\chi$, the angle between $\mathbf{k}$ and $\mathbf{k}'$ (§ 4), here replaces the angle $\psi$ of § 11. By summing this expression over all directions $\mathbf{k}'$, $d\mathbf{k}'$, we obtain $\mathrm{E}_2(\lambda, h, z, \mathbf{k}) d\lambda \, d\mathbf{k}$. Hence

$$\mathrm{E}_2(\lambda, h, z, \mathbf{k}) = \frac{3\sigma}{16\pi} \int (1+\cos^2 \chi) \mathrm{R}_1(\lambda, h, z, \mathbf{k}') \, d\mathbf{k}',$$

where the integration extends over all directions of $\mathbf{k}'$, except at the ground and at the top of the atmosphere, where it extends only over one hemisphere.

In this equation we substitute for $R_1$ from §12 (1) (but changing $\mathbf{k}$ to $\mathbf{k}'$, $\theta$ to $\theta'$, $\Theta$ to $\Theta'$ in that formula), afterwards inserting the value of $E_1$; we also write $\sin\theta'\, d\theta' d\phi'$ in place of $d\mathbf{k}'$; thus we find that

$$E_2(\lambda, h, z, \mathbf{k}) = \frac{9\sigma s}{256\pi^2} I_\infty \int_0^{2\pi}\int_0^{\frac{1}{2}\pi}\int_0^1 e^{-Z\overline{m}' - \Theta'(m \sim m')}(1+\cos^2\psi')(1+\cos^2\chi)\sec\theta' \sin\theta' dm' d\theta' d\phi'.$$

Here the integration with respect to $\phi'$ only affects the factors $(1+\cos^2\psi')(1+\cos^2\chi)$; it is easily shown that

$$\frac{1}{\pi}\int_0^{2\pi}(1+\cos^2\psi')(1+\cos^2\chi)\,d\phi' = A_0(z, \mathbf{k}) + A_1(z, \mathbf{k})\cos^2\theta' + A_2(z, \mathbf{k})\cos^4\theta'$$

where

$$A_s\ (z, \mathbf{k}) = \sum_{r=0,\,1,\,2} A_{s,r}(z, \theta)\cos r\phi,$$
$$A_{0,0}(z, \theta) = 2(1+\tfrac{1}{2}\sin^2 z)(1+\tfrac{1}{2}\sin^2\theta),$$
$$A_{1,0}(z, \theta) = 4 - 2\sin^2 z - 2\sin^2\theta - 3\sin^2 z\sin^2\theta,$$
$$A_{2,0}(z, \theta) = 2(1-\tfrac{3}{2}\sin^2 z)(1-\tfrac{3}{2}\sin^2\theta),$$
$$A_{0,1}(z, \theta) = 0,$$
$$A_{1,1}(z, \theta) = \sin 2z \sin 2\theta = -A_{2,1}(z, \theta),$$
$$A_{0,2}(z, \theta) = \tfrac{1}{4}\sin^2 z\sin^2\theta = A_{2,2}(z, \theta)$$
$$A_{1,2}(z, \theta) = -\tfrac{1}{2}\sin^2 z\sin^2\theta.$$

The further integrations, with respect to $\theta'$ and $m'$, lead to the result:

$$E_2(\lambda, h, z, \mathbf{k}) = \frac{9\sigma s}{256\pi} I_\infty\{A_0(z, \mathbf{k})L_1(c, z, m) + A_1(z, \mathbf{k})L_3(c, z, m) + A_2\ (z, \mathbf{k})L_5(c, z, m)\},$$

or, alternatively,

$$E_2(\lambda, h, z, \mathbf{k}) = \frac{9\sigma s}{256\pi} I_\infty\{F_0(c, z, \theta, m) + F_1(c, z, \theta, m)\cos\phi + F_2(c, z, \theta, m)\cos 2\phi\},$$

where

$$F_r = A_{0,r}(z, \theta)L_1(c, z, m) + A_{1,r}(z, \theta)L_3(c, z, m) + A_{2,r}(z, \theta)L_5\ (c, z, m)$$

for $r=0, 1, 2$; and

$$L_n(c, z, m) = \frac{1}{c}e^{-\overline{Z}}\ \{Ek_n(cm, -\sec z) + Ek_n(c\overline{m}, \sec z)\},$$
$$Ek_n(\tau, b) = \int_0^{\tau} e^{bt}\, Ej_n(t)\,dt,$$
$$Ej_n(t) = \int_1^{\infty} e^{-tx}x^{-n}\, dx.$$

### *The Reception of Secondary Scattered Sunlight.*

14. The calculation of the secondary scattered sunlight received at any level, in terms of the secondary emitted sunlight, is precisely similar to the corresponding "primary" calculation of § 12. The result is obtainable from § 12 (1) by changing the suffix 1 into 2; hence we obtain, after integration, the two forms for $R_2$, analogous to § 12 (2, 3),

$$\mathrm{R}u_2(\lambda, m, z, \mathbf{k})=\frac{9s^2}{256\pi}\mathrm{I}_\infty \sec\theta\,\{\mathrm{A}_0(z, \mathbf{k})\,\mathrm{L}u_1(c, z, m, \theta)$$

$$+\mathrm{A}_1(z, \mathbf{k})\,\mathrm{L}u_3(c, z, m, \theta)+\mathrm{A}_2(z, \mathbf{k})\,\mathrm{L}u_5(c, z, m, \theta)\},$$

$$\mathrm{R}d_2(\lambda, m, z, \mathbf{k})=\frac{9s^2}{256\pi}\mathrm{I}_\infty \sec\theta\,\{\mathrm{A}_0(z, \mathbf{k})\mathrm{L}d_1(c, z, m, \theta)$$

$$+\mathrm{A}_1(z, \mathbf{k})\mathrm{L}d_3(c, z, m, \theta)+\mathrm{A}_2(z, \mathbf{k})\mathrm{L}d_5(c, z, m, \theta)\},$$

where

$$\mathrm{L}u_n(c, z, m, \theta)=e^{-\Theta m}\int_0^m e^{\Theta m'}\,\mathrm{L}_n(c, z, m')dm',$$

$$\mathrm{L}d_n(c, z, m, \theta)=e^{-\Theta\bar{m}}\int_0^{\bar{m}} e^{\Theta\bar{m}'}\,\mathrm{L}_n(c, z, m')d\bar{m}'.$$

Here $\mathrm{R}u_2$ and $\mathrm{R}d_2$ refer respectively to the upgoing (**k** downward) and downgoing (**k** upward) secondary scattered sunlight.

### *The Integrals $\mathrm{E}j_n$.*

15. In the integral $\mathrm{E}j_n(t)$ of § 13, we are concerned with positive integral values of $n$, and positive or zero values of $t$; the integral is then real and positive, and convergent except when $n=1$, $t=0$. When $n>1$,

$$\mathrm{E}j_n(0)=\int_1 x^{-n}\,dx=\frac{1}{n-1}.$$

Clearly $\mathrm{E}j_n\,(t)$ decreases as $t$ increases; in fact,

$$\frac{d\mathrm{E}j_n(t)}{dt}=-\mathrm{E}j_{n-1}(t),\quad n>1,$$

$$\frac{d\mathrm{E}j_1(t)}{dt}=-\frac{e^{-t}}{t}.$$

Moreover, $\mathrm{E}j_n(t)$ decreases as $n$ increases. Integration by parts gives the recurrence relation

$$(n-1)\,\mathrm{E}j_n(t)=e^{-t}-t\mathrm{E}j_{n-1}(t),\quad n>1,$$

which enables $\mathrm{E}j_n$ to be calculated if we know $\mathrm{E}j_1$. Now

$$\mathrm{E}j_1(t)=\int_1^\infty e^{-tx}x^{-1}\,dx=\int^\infty e^{-x}x^{-1}\,dx=-\mathrm{E}i(-t),$$

where E$i$ denotes the exponential integral which has been tabulated by Glaisher *. The function E$i$ $(-t)$ is finite when $t$ is positive, provided that the principal value of the integral (near the origin) is taken; it may be expressed in the form (valid for all positive and negative values of $t$)

$$\mathrm{E}i(-t)=\tfrac{1}{2}\log t^2+\mathrm{B}(t),$$

where

$$\mathrm{B}(t)=\gamma+\sum_{s=1}(-1)^s\frac{t^s}{s\,!\,s}$$

and $\gamma$ denotes Euler's constant 0·5772.

Clearly $\mathrm{B}(t)\to\gamma$ as $t\to 0$; also, if $t$ is positive,

$$\mathrm{E}i(-t)-\log t=\mathrm{B}(t),$$
$$\mathrm{E}i(t)-\log t=\mathrm{B}(-t).$$

### *The Integrals* E$k_n(t)$.

16. In the case of the integrals

$$\mathrm{E}k_n(\tau,b)=\int_0^\tau e^{bt}\mathrm{E}j_n(t)\,dt,$$

we are concerned with the following values of $n$, $\tau$, and $b$; $n$ is a positive integer, $0<\tau<c$, and $b=\pm\sec z$, so that $|b|>1$. The integral is clearly positive when $\tau>0$, and

$$\mathrm{E}k_n(0,b)=0\,;$$

also E$k_n$ decreases as $n$ increases, and increases with $\tau$; when $b$ is positive, E$k_n$ increases with $b$; when $b$ is negative, E$k_n$ decreases as $b$ increases numerically.

An integration by parts gives the recurrence relation

$$b\,\mathrm{E}k_n(\tau,b)=e^{b\tau}\mathrm{E}j_n(\tau)-\frac{1}{n-1}+\mathrm{E}k_{n-1}(\tau,b),$$

from which E$k_n$ can be determined if we know E$k_1$; the latter was discussed by King (*loc. cit.* p. 387 (54)).

If $\tau>\tau'>0$, an integration by parts shows that, whatever the sign of $b$,

$$\int_{\tau'}^{\tau}e^{bt}\mathrm{E}j_1(t)\,dt=\frac{1}{b}\{\mathrm{E}i(b\tau-\tau)-e^{b\tau}\mathrm{E}i(-\tau)$$
$$-\mathrm{E}i(b\tau'-\tau')+e^{b\tau'}\mathrm{E}i(-\tau')\}\,;$$

when $\tau'\to 0$, this becomes

$$\mathrm{E}k_1(\tau,b)=\frac{1}{b}\{e^{b\tau}\mathrm{E}j(\tau)+\log\tau+\mathrm{B}(\tau-b\tau)\},$$

---

* J. W. L. Glaisher, Phil. Trans. Roy. Soc. A, c. p. 367 (1878); see also J. B. Dale, 'Mathematical Tables,' p. 85.

where, as is necessary, the same argument has been taken for log $(1-b)$ in the two expressions in which it occurs.

### *The Functions* $\mathrm{L}_n(c, z, m)$.

17. From the definition of $\mathrm{L}_n$ it may readily be shown that it decreases as either $n$, or $z$, or $c$, increases; its variation with $m$, however, is not monotonic, and it has a maximum at some value $m > \frac{1}{2}$; for

$$\frac{\partial \mathrm{L}_n}{\partial \bar{m}} = -\frac{\partial \mathrm{L}_n}{\partial m} = \mathrm{E}j_n(\bar{m}) - \mathrm{Z}\,\mathrm{L}_n - e^{-\mathrm{Z}}\mathrm{E}j_n(cm).$$

From this formula it is easy to show, using the mean value theorem, that at the top of the atmosphere

$$\left(\frac{\partial \mathrm{L}_n}{\partial \bar{m}}\right)_{\bar{m}=0} = \{\mathrm{E}j_n(0) - \mathrm{E}j_n(c')\} + e^{-\mathrm{Z}}\{\mathrm{E}j_n(c') - \mathrm{E}j_n(c)\},$$

where $0 < c' < c$, so that $\partial \mathrm{L}_n / \partial m$ is positive there, that is to say, $\mathrm{L}_n$ there increases downwards.

Similarly, at the ground,

$$\left(\frac{\partial \mathrm{L}_n}{\partial m}\right)_{m=0} = \mathrm{E}j_n(c'') - \mathrm{E}j_n(c) + e^{-\mathrm{Z}}\{\mathrm{E}j_n(0) - \mathrm{E}j_n(c'')\},$$

where $0 < c'' < c$, so that $\partial \mathrm{L}_n / \partial m$ is positive, that is, $\mathrm{L}_n$ increases upwards, at the ground. Moreover, at $m = 1/2$, $\mathrm{L}_n$ is still increasing upwards, because it is easy to show that there

$$\frac{1}{2} e^{\frac{1}{2}\mathrm{Z}} \left(\frac{\partial \mathrm{L}_n}{\partial m}\right)_{m=\frac{1}{2}} = (\sinh \tfrac{1}{2}\mathrm{Z})\{\mathrm{E}j_n(c''') - \mathrm{E}j_n(\tfrac{1}{2}c)\},$$

(where $0 < c''' < \frac{1}{2}c$), which is positive. It is also easy to prove that $\mathrm{L}_n$ is greater at the top of the atmosphere than at the ground.

The functions $\mathrm{L}_n$ are connected by the recurrence relation

$$\begin{aligned} \mathrm{Z}^2\mathrm{L}_n(c, z, m) = {} & \mathrm{Z}\,\mathrm{E}j_n(c\bar{m}) + c\,\mathrm{E}j_{n-1}(c\bar{m}) - \mathrm{Z}e^{-\mathrm{Z}}\mathrm{E}j_n(c, m) \\ & + ce^{-\mathrm{Z}}\mathrm{E}j_{n-1}(cm) - 2ce^{-\mathrm{Z}\bar{m}}/(n-2) + c^2\mathrm{L}_{n-2}(c, z, m), \end{aligned}$$

and for $\mathrm{L}_1$ we have the formula

$$\begin{aligned} \mathrm{Z}e^{\mathrm{Z}\bar{m}}\mathrm{L}_1(c, z, m) = {} & \log\{(\mathrm{Z}+c)/(\mathrm{Z}-c)\} + \mathrm{E}i\{(\mathrm{Z}-c)\bar{m}\} \\ & - \mathrm{E}i\{-(\mathrm{Z}+c)m\} + e^{\mathrm{Z}\bar{m}}\mathrm{E}j_1(c\bar{m}) - e^{-\mathrm{Z}m}\mathrm{E}j_1(cm). \end{aligned}$$

### *The Integrals* $\mathrm{L}u_n(c, z, m, \theta)$ *and* $\mathrm{L}d_n(c, z, m, \theta)$.

18. The integrals $\mathrm{L}u_n$ and $\mathrm{L}d_n$ are expressible in terms of the functions $\mathrm{E}j$ and $\mathrm{E}i$; the formulæ are as follows :—

$$\begin{aligned} \mathrm{Z}(\mathrm{Z}+\Theta)e^{-\Theta m}\mathrm{L}u_1 = {} & e^{-(\mathrm{Z}+\Theta)\bar{m}}\left\{\mathrm{E}j_1(\mathrm{Z}m+cm) + \mathrm{E}i(\mathrm{Z}\bar{m}-c\bar{m})\right. \\ & \left. + \log\frac{\sec z+1}{\sec z-1}\right\} + e^{-(\mathrm{Z}+\Theta)}\left\{\mathrm{E}i(\Theta m-cm) - \mathrm{E}i(\mathrm{Z}-c)\right. \end{aligned}$$

$$\left.-\log\frac{\sec\theta-1}{\sec z-1}\right\}+\mathrm{E}i(-\Theta-c)-\mathrm{E}i(-\Theta\bar{m}-c\bar{m})+(\mathrm{Z}/\Theta+1)\mathrm{Q}u,$$

where

$$\mathrm{Q}u=e^{-\Theta\bar{m}}\mathrm{E}j_1(c\bar{m})-e^{-\Theta}\mathrm{E}j_1(c)-e^{-\mathrm{Z}-\Theta\bar{m}}\mathrm{E}j_1(cm)-\mathrm{E}i(-\Theta-c)$$
$$+\mathrm{E}i(-\Theta\bar{m}-c\bar{m})-e^{-\mathrm{Z}(+\Theta)}\{\mathrm{E}i(\Theta m-cm)-\log(\sec\theta-1)\};$$

also

$$\mathrm{Z}\Theta e^{-\Theta\bar{m}}\mathrm{L}u_3=c^2(\Theta/\mathrm{Z})e^{-\Theta\bar{m}}\mathrm{L}u_1+lu_3+(\cos z-\cos\theta)(lu_2-\cos\theta\,\mathrm{Q}u)$$
$$-2c\Theta(e^{-(\mathrm{Z}+\Theta)\bar{m}}-e^{-\mathrm{Z}-\Theta})/(\mathrm{Z}^2+\Theta\mathrm{Z}),$$

and

$$\mathrm{Z}\Theta e^{-\Theta\bar{m}}\mathrm{L}u_5=c^2(\Theta/\mathrm{Z})e^{-\Theta\bar{m}}\mathrm{L}u_3+lu_5+(\cos z-\cos\theta)(lu_4$$
$$-lu_3\cos\theta+lu_2\cos^2\theta-\cos^3\theta\mathrm{Q}u)$$
$$-\frac{2}{3}c\Theta(e^{-(\mathrm{Z}+\Theta)\bar{m}}-e^{-\mathrm{Z}-\Theta})/(\mathrm{Z}^2+\Theta\mathrm{Z}),$$

where

$$lu_n=e^{-\Theta\bar{m}}\mathrm{E}j_n(c\bar{m})-e^{-\Theta}\mathrm{E}j_n(c)+(-1)^n e^{-\mathrm{Z}-\Theta\bar{m}}\mathrm{E}j_n(cm)-(-1)^n\frac{1}{n-1}e^{-\mathrm{Z}-\Theta};$$

similarly,

$$\mathrm{Z}(\mathrm{Z}-\Theta)e^{\Theta\bar{m}}\mathrm{L}d_1=\mathrm{E}j_1(\mathrm{Z}+c)-e^{-(\mathrm{Z}-\Theta)\bar{m}}\{\mathrm{E}j_1(\mathrm{Z}m+cm)+\mathrm{E}i(\mathrm{Z}\bar{m}-c\bar{m})\}$$
$$+(1-e^{-(\mathrm{Z}-\Theta)\bar{m}})\log\frac{\sec z+1}{\sec z-1}$$
$$+\mathrm{E}i(\Theta\bar{m}-c\bar{m})-\log\frac{\sec\theta-1}{\sec z-1}+e^{\Theta-\mathrm{Z}}\{\mathrm{E}i(-\Theta-c)-\mathrm{E}i(-\Theta m-cm)\}$$
$$+(\mathrm{Z}/\Theta-1)\mathrm{Q}d,$$

where

$$\mathrm{Q}d=e^{\Theta\bar{m}}\mathrm{E}j_1(c\bar{m})-e^{-\mathrm{Z}+\Theta\bar{m}}\mathrm{E}j_1(cm)+e^{-\mathrm{Z}}\mathrm{E}j_1(c)$$
$$+\mathrm{E}i(\Theta\bar{m}-cm)-\log(\sec\theta-1)-e^{\Theta-\mathrm{Z}}\{\mathrm{E}i(-\Theta m-cm)-\mathrm{E}i(-\Theta-c)\};$$

also

$$\mathrm{Z}\Theta e^{\Theta\bar{m}}\mathrm{L}d_3=c^2(\Theta/\mathrm{Z})e^{\Theta\bar{m}}\mathrm{L}d_1+ld_3+(\cos z+\cos\theta)(ld_2+\cos\theta\,\mathrm{Q}d)$$
$$-2c\Theta(1-e^{(\Theta-\mathrm{Z})\bar{m}})/(\mathrm{Z}^2-\Theta\mathrm{Z})$$

and

$$\mathrm{Z}\Theta e^{\Theta\bar{m}}\mathrm{L}d_5=c^2(\Theta/\mathrm{Z})e^{\Theta\bar{m}}\mathrm{L}d_3+ld_5$$
$$+(\cos z+\cos\theta)(ld_4+ld_3\cos\theta+ld_2\cos^2\theta+\cos^3\theta\mathrm{Q}d)$$
$$-\frac{2}{3}c\Theta(1-e^{(\Theta-\mathrm{Z})\bar{m}})/(\mathrm{Z}^2-\Theta\mathrm{Z}),$$

where

$$ld_n=e^{\Theta\bar{m}}\mathrm{E}j_n(cm)-\frac{1}{n-1}-(-1)^n e^{-\mathrm{Z}}\mathrm{E}j_n(c)+(-1)^n e^{-\mathrm{Z}+\Theta\bar{m}}\mathrm{E}j_n(cm).$$

The integrals L$u$ are associated with the upgoing, and L$d$ with the downgoing, radiation; the former will therefore be expected to vanish at the ground and the latter at the top of the atmosphere. It is not difficult to verify this, though some formal difficulties are encountered connected with $Ej_1(0)$ and $Ei(0)$; but these difficulties may be overcome by taking the limit of the expressions involving these functions, when $\bar{m}\to 1$ or $m\to 0$.

### *Further Treatment of the Problem.*

19. The preceding analysis completes the exact formal solution of the restricted problem defined in § 1; but in order that the solution may be of use in connexion with actual observations of scattered sunlight it is necessary to evaluate the formulæ for $R_1$ and $R_2$ numerically, and also to state in general terms the nature of the results. The formulæ for $R_1$ are simple and easily evaluated; those for $R_2$, when expressed exactly (as in §§ 14–18) in terms of functions that may be considered as known or easily tabulated (such as E$i$ or E$j$), are immensely more complicated; nevertheless, with sufficient labour they can be evaluated numerically. They indicate clearly, however, that an exact analytical formulation of $R_3$, the intensity of the tertiary scattered sunlight, will involve expressions so lengthy and elaborate as practically to preclude their numerical evaluation and discussion.

Further progress towards a complete solution of the problem of scattered sunlight can, however, be made, taking account of all orders of scattering, but ignoring, for the present, the illumination of the atmosphere by light scattered or reflected at the ground. We hope to show, in a later paper, that the elaborate exact formulæ for $R_2$ can be replaced by much simpler expressions, whose numerical values agree with those of $R_2$ within assigned close limits. These simpler expressions are of value in the numerical discussion of $R_2$ itself, and still more because they facilitate the calculation of the scattered light of higher orders, $R_3$, $R_4$, . . . ., still taking account (as is very desirable) of Rayleigh's law of scattering at each stage.

# VIII. *Ionization by Collisions of Positive Ions.*

By J. S. Townsend, F.R.S., Wykeham Professor of Physics, Oxford *.

[Received May 12, 1939.]

1. The theory of ionization by the collisions of electrons and positive ions with molecules of a gas which I gave many years ago provides a consistent explanation not only of photo-electric currents, but also an explanation of the conductivity of gases in various forms of discharges. But from time to time alternative theories have been proposed by physicists, who have formed the opinion that molecules of a gas are not ionized by positive ions in discharges between parallel plates when the pressure of the gas is much greater than that at which the sparking potential is a minimum. The defect of these theories is that they cannot be reconciled with the properties of photo-electric currents in a uniform field and with the properties of corona discharges.

The opinions which have been expressed on the hypothesis that positive ions effect ionization are summarized as follows by Wheatcroft in his treatise on 'Gaseous Electrical Conductors.'

The principal evidence in support of the hypothesis that molecules are ionized by the collisions of positive ions is based on the fact that a discharge is obtained from a positively charged point to a plate even when the electric force in the neighbourhood of the plate is extremely small, which can hardly be explained by alternative hypotheses. And the principal objection is that, all direct experiments, as well as all modern knowledge of atomic processes, lead to the conclusion that positive ions cannot effect ionization of molecules of a gas at the low values of $Z/p$ which occur in a uniform electric field ($Z$ being the electric force and $p$ the pressure of the gas).

2. With regard to these objections, it may be noted that there are several modern theories of electrical discharges, and there is much divergence of opinion as to what modern knowledge of atomic processes may mean.

But it may be seen that the hypothesis that positive ions effect ionization of molecules of gases is not inconsistent with any well-established physical principle.

---

* Communicated by the Author.

The number of positive ions which may acquire sufficient energy to ionize molecules in discharges diminishes rapidly as the pressure of the gas is increased, but that is not a reason for supposing that none of the positive ions effects ionization of molecules or that the small number which may ionize molecules is not sufficient to maintain a discharge in air at atmospheric pressure in the space between parallel plates at one centimetre apart.

The experiments on which the theory of ionization by collision is based show that the effect of the positive ions also diminishes as the pressure is increased, and it may be seen that the number of molecules which are ionized in air at atmospheric pressure is probably much less than the number of free paths in which ions may acquire sufficient energy to ionize molecules.

The most conclusive results, however, which may be deduced from the experiments on the conductivity of air at high pressures in the space between parallel plates and in corona discharges, without making any calculations depending on the lengths of free paths of ions, is that the modern theories do not provide a consistent explanation of the properties of the discharges.

3. Assuming that the conductivity of air depends principally on the ionization of molecules by collisions of electrons and positive ions, the coefficients of ionization may be deduced from measurements of photo-electric currents between parallel plates. It has been found that if a number $n_0$ of electrons be set free by the action of ultra-violet light from the negative electrode, the number $n$ that arrive at the positive electrode depends on the electric force Z and the distance $z$ between the plates. With a constant electric force the number $n$ is given in terms of the distance $z$ by the equation

$$n=n_0(\alpha-\beta)\epsilon^{(\alpha-\beta)z}/(\alpha-\beta\epsilon^{(\alpha-\beta)z}),$$

where $\alpha$ is the coefficient of ionization by electrons and $\beta$ the coefficient of ionization by the positive ions. The coefficients $\alpha$ and $\beta$ may be expressed in terms of Z and $p$ by equations of the form $\alpha/p=f(\mathrm{Z}/p)$ and $\beta/p=\phi(\mathrm{Z}/p)$.

The denominator in the equation for $n$ diminishes as $z$ increases, and becomes zero for the distance S between the plates given by the equation $\alpha/\beta=\epsilon^{(\alpha-\beta)\mathrm{S}}$. At this point a continuous current or a discharge is obtained when the potential V between the plates is $\mathrm{Z}\times\mathrm{S}$. In air and many other gases $\beta$ is small compared with $\alpha$, and in order to determine $\beta$ for the smaller values of $\mathrm{Z}/p$ it is convenient to determine $\alpha$ from the experiments on photo-electric currents and $\beta$ from the equation $\beta=\alpha\epsilon^{-\alpha\mathrm{S}}$.

The value of $\beta$ for a discharge in air at atmospheric pressure between parallel plates one centimetre apart may thus be obtained from the values of $\alpha$ and V given by Wheatcroft (*loc. cit.* p. 144). In this case V is 33,000 volts and $\alpha$ is 19·8, so that $\beta$ is $19 \cdot 8\, \epsilon^{-19 \cdot 8}$.

Since $\beta$ is the number of molecules ionized by a positive ion in moving a distance of one centimetre in the direction of the force, this number should be less than the number of collisions ($c$) in which the ion has sufficient energy to ionize a molecule.

4. The number $c$ depends on the energy $V_0$ of a positive ion, before a collision, which is just sufficient to ionize a molecule, and the distribution of the energies of the electrons about the mean.

The minimum energy required to ionize a molecule may be taken to be the ionizing potential of an electron, which for air is 15 volts, so that the energy $V_0$ of a positive ion is 30 volts, since the mass of the ion is equal to that of the molecules and the momentum of the ion before a collision is equal to the sum of the momentums of the ion and the molecule after the collision.

There are no measurements of mean energy of agitation, or of the mean free paths of ions moving with energies of about 20 volts on which the distribution of the energies depends. It is necessary, therefore, to consider the possible values of the free paths of ions as deduced from the theory of viscosity. In this theory the mean free path is inversely proportional to the section, $\pi\sigma^2$, of the sphere which is supposed to represent a molecule, and it has been shown by Jeans* from ordinary mechanical considerations that the size of the spheres must be supposed to decrease as the velocity of the molecule increases.

This is in accordance with the experiments on the viscosity of air at temperatures from 0° C. to 1216° C., which show that the cross-section $\pi\sigma^2$ diminishes as the temperature increases.

It has thus been found that in air at constant density the mean free path of a molecule is proportional to $T^{(n-\frac{1}{2})}$, T being the absolute temperature and $n$ a constant which for air is 0·76. If it be assumed that the expression for the mean free path deduced from the viscosity applies to much larger energies, the mean free path of molecules moving with energies of about 20 volts would be about 5·2 times the mean free path $l_0$ at 0° C. But there is also in increase in the mean free path of an ion in the proportion $\sqrt{2} : 1$ when the ion is moving in air at ordinary temperatures. Since the kinetic energy of the ion is much greater than that of the molecules, the mean free path of an ion moving with the energy of 20° volts in air at 0° C. is therefore about $7 \cdot 3 \times l_0$.

The mean free path of a molecule in air at atmospheric pressure and 0° C. is $9 \cdot 6 \times 10^{-6}$ cm., and the mean free path $l$ of an ion in a discharge may be taken to be $7 \times 10^{-6}$ cm.

---

* Jeans, 'Dynamical Theory of Gases,' p. 255, 1904 edition.

5. In the discharge between parallel plates at a distance apart of one centimetre, where the electric force is 33,000 volts per centimetre, the energy acquired by an ion in moving the distance of the mean free path in the direction of the force is 2·3 volts, and the number C of free paths of an ion in moving a distance of one centimetre in the direction of the force is 14,300.

The number of free paths $c$ exceeding the length $x$ is $C\epsilon^{-x/l}$, and if the energy of an ion at the beginning of a free path be very small it moves in the direction of the force Z and acquires the energy $Z \times x$ in a free path of length $x$.

The number $c$ of free paths in which ions acquire energies greater than $V_0$ is $C\epsilon^{-V_0/lZ}$, and in the discharge through air at atmospheric pressure the number of free paths in which a positive ion acquires energies greater than 30 volts is $14{,}300 \times \epsilon^{-13}$, which exceeds the number ionized ($\beta$) by the factor $6 \times 10^5$.

The ionization of the gas which is indicated by the coefficient $\beta$ in the equation $\beta = \alpha\epsilon^{-\alpha S}$ may therefore be attributed to ionization of molecules by the collisions of positive ions on the hypothesis that a molecule is ionized in a small proportion of the total number of collisions of ions with energies greater than 30 volts.

It has already been shown that a consistent explanation of currents between wires and co-axial cylinders is obtained on this hypothesis *.

6. But the photo-electric currents in a gas between parallel plates may also be explained on the hypothesis that the increase in the currents in a uniform field with the distance between the plates is due to the ionization of molecules of the gas by collisions of electrons, and a secondary emission of electrons from the negative electrode caused by the impacts of positive ions or by radiation from the gas or by metastable atoms coming into contact with the electrode. In all these cases the number $n_2$ of electrons in the secondary emission is proportional to the number $n_1$ of positive ions generated in the gas, and in this theory the ratio $\gamma$ of the number $n_2$ to $n_1$ is the same as the ratio $\beta/\alpha$ in the equation $\beta = \alpha\epsilon^{-\alpha S}$, when $\beta$ is small compared with $\alpha$.

The experiments on discharges through air at different pressures show that $\gamma$ decreases with the ratio $Z/p$ and becomes very small in discharges where the ratio is less than 40.

Thus in the discharge through air at 3·4 millimetre pressure between plates one centimetre apart the ratio $Z/p$ is 175 and the ratio $\beta/\alpha$ is $8{\cdot}2 \times 10^{-4}$, and in air at atmospheric pressure the ratio $Z/p$ is 43·4 and $\beta/\alpha$ is $2{\cdot}4 \times 10^{-9}$.

7. There is, therefore, a very large decrease in the secondary emission from the negative electrode when $Z/p$ is reduced from the value 175 to

---

* Phil. Mag. (6) xxvii. p. 789 (1914), and (6) xxviii. p. 85 (1914).

43·4, and the change in the secondary emission indicated by the change in the value of $\gamma$ from $8{\cdot}2\times10^{-4}$ to $2{\cdot}4\times10^{-9}$ must therefore be attributed to the change in the value of $Z/p$ at the negative electrode.

This change in the coefficient $\gamma$ with the value of $Z/p$ shows that in the discharges from a positively charged wire to a coaxial cylinder the emission from the surface of the cylinder becomes indefinitely small as the radius of the cylinder is increased. And if the conductivity between the wire and the cylinder depended on the emission from the negative electrode it would be necessary, in order to maintain a discharge, to have a large increase in the electric force in the space near the wire, when the radius of the cylinder is increased. Since there is no increase in the force near the wire it becomes impossible to reconcile this theory of the conductivity with the properties of the discharges between wires and cylinders.

The modern explanation, which is supposed to overcome this difficulty in explaining the discharges from wires to cylinders, is that the secondary emission is a photo-electric effect of radiation emitted by the recombination of positive ions with electrons from the electrode, so that the emission does not change to any large extent with the value of $Z/p$ at the electrode, regardless of the fact that in order to explain the conductivity between parallel plates it is necessary to suppose that the emission is reduced in the proportion of $8{\cdot}2\times10^{-4}$ to $2{\cdot}4\times10^{-9}$ when $Z/p$ is reduced from 175 to 43·4. It may be mentioned that in the experiments * on corona discharges, which were quoted as showing that molecules of the gas are ionized in the space near the wire, the value of $Z/p$ at the surface of the cylinder was much less than 40, and the coefficient of emission $\gamma$ much less than $10^{-9}$.

8. It should be noticed that the preceding calculation of inequalities in the energies of positive ions only indicates the order of the number of ions that may ionize molecules, as it cannot be supposed that an exact value of the mean free path of an ion moving with the energy of 10 or 20 volts may be deduced from measurements of the viscosity at different temperatures. As in the case of electrons, there may be large changes in the free paths of positive ions due to changes in the energy of the ions. It is necessary therefore in some cases to rely on the results of experiments on the conductivity of gases in order to form an estimate of the mean free paths of the ions. The experiments which have been made with hydrogen and helium are of interest from this point of view,

It is well known that in gases at low pressures, less than the pressure corresponding to the minimum sparking potential, the discharge between parallel plates is maintained to some extent by secondary emission from the cathode, and in these discharges the ionization indicated by the

---

* 'Electricity in Gases,' p. 369, and also Phil. Mag. [6] xxviii. p. 83 (1914).

coefficient $\beta$ in the equation $\beta=\alpha\epsilon^{-\alpha S}$, is due partly to secondary emission $\gamma_1$ from the negative electrode and partly to the ionization $\beta_1$ of molecules by the collisions of positive ions.

In order to investigate these actions of positive ions in discharges where $Z/p$ is of the same order as in the discharge when the sparking potential between parallel plates is a minimum, an experiment was arranged to separate the two effects. The experiments showed definitely that in hydrogen and in helium molecules were ionized by positive ions and electrons were set free from the negative electrode by impacts of positive ions.

In hydrogen* the coefficient of ionization $\beta_1$ and the coefficient of emission $\gamma_1$ were too small to be measured when Z was less than 70. When $Z/p$ was 185, $\beta_1/p$ was ·034.

The ionization potential of hydrogen (for electron collisions) is 13·4 volts, the mean free path of a molecule in the gas at one millimetre pressure and 0° C. is $1{\cdot}4\times10^{-2}$ cm., and the mean free path of an ion moving with the energy of 20 volts is $7\times10^{-2}$ cm. (allowing for the decrease in the molecular section, $\pi\sigma^2$, as explained in the calculation of the mean free path of an ion in air).

Under these conditions the number of ions that acquire energies greater than 26·8 volts in moving one centimetre under the action of a force of 185 volts per centimetre is 1·8, which is much greater than the coefficient $\beta_1$ (·034).

These results are therefore consistent with the hypothesis that the ionization represented by the coefficient $\beta_1$ is effected by the collision of positive ions with molecules.

In helium † the coefficients $\beta_1$ and $\gamma_1$ were too small to be measured when $Z/p$ was less than 14, and when $Z/p$ was 44, $\beta_1/p$ was ·03. The ionization potential of helium for electron collisions is 25 volts, and the mean free path of an ion moving with the energy of 40 volts in the gas at five millimetre pressure is ·022 cm.

In this case the number of ions that acquire energies greater than 50 volts in moving one centimetre under the action of a force of 220 volts per centimetre is $2\times10^{-3}$, which is much less than the value of $\beta_1$ (·15).

In order to reconcile this method of calculating the number $c$ with the hypothesis that atoms of helium are ionized by the collisions of positive ions moving with energies greater than 50 volts it is necessary to assume that the mean free path of an ion moving with energies of the order of 40 volts in helium at five millimetre pressure is about ·06 cm.

---

* J. S. Townsend and F. Ll. Jones, Phil. Mag. xv. p. 282 (Feb. 1933).

† J. S. Townsend and G. D. Yarnold, Phil. Mag. xviii. p. 594 (Oct. 1934).

But the number $C\epsilon^{-V_0/lZ}$ is a lower limit to the number of collisions in which the energies of the ions exceed the value $V_0$, as it is assumed that at the beginning of a free path the energy of an ion is zero. For a more accurate estimate of this number it would be necessary to take into consideration the fact that there are large inequalities in the amounts of energy lost by ions in collisions with molecules, and at the beginning of some free paths the ions have energies of several volts.

Also, since it has been shown that electrons lose much less energy in collisions with atoms of monatomic gases than with molecules of diatomic gases, and according to the kinetic theory of gases the monatomic gases are spherically symmetrical, it must be supposed that ions lose less energy in collisions with atoms of monatomic gases than with molecules of diatomic gases.

According to this theory, therefore, the fact that the value of $\beta$ in the discharges in pure as well as in impure helium are much greater than in discharges in hydrogen or in air may be attributed partly to the smaller losses of energy of ions in collisions with atoms of helium and partly to the longer free paths of the ions in helium.

# IX. *The Arms of a Spiral Nebula.*

By A. C. Banerji, Professor of Mathematics, Nizamuddin, and
P. L. Bhatnagar, Research Scholar, Allahabad University *.

[Received September 20, 1938.]

The shape of the spiral nebula raises great difficulties, and several theories have been suggested to explain the formation of spiral arms.

Jeans⁽¹⁾ has worked out the case of a rotating compressible mass and obtained a series of configurations with increasing rates of rotation. He supposes that as soon as the ellipsoidal nebula becomes unstable, when the rate of rotation has sufficiently increased, matter will be thrown out in the equatorial plane along the spiral arms. Jeans's theory rules out the possibility of star clouds existing in the ellipsoidal nebula, which is assumed to be gaseous in nature. This is not verified by observation, and the observed spectra of ellipsoidal nebulæ cannot be explained by Jeans's theory about their composition.

Bok⁽²⁾ has applied Jeans's theory to Roche's compressible model of a massive point nucleus surrounded by an atmosphere of negligible total mass. He also assumed that this configuration is rotating with uniform angular velocity about the minor axis. This is rather hypothetical, as it is inconceivable that almost all the mass of a nebula will be concentrated in a massive point nucleus.

Brown⁽³⁾ has assumed that originally every spiral nebula was a highly flattened homogeneous ellipsoid of revolution. Later on minor variations in the uniform density were caused by the perturbations due to rather close encounters with passing galaxies. These perturbations ultimately lead to the formation of the spiral arms. Brown also concludes that after each encounter the spiral arms gradually coil up and the nebula ultimately reverts to its original shape. According to him the spiral formation is a periodic phenomenon. The main objection to Brown's theory is that he assumes uniform density throughout the galaxy.

Vogt⁽⁴⁾ has assumed that most of the mass of a spiral nebula is concentrated in the nucleus. In addition to the force of attraction he also introduces a force of repulsion proportional to the distance from the centre of the nucleus. The chief defect in Vogt's theory is his assumption of the force of repulsion. He does not explain the cause of its existence.

Lindblad⁽⁵⁾ has worked out the case of a small condensed nucleus

---

* Communicated by the Authors.

which is surrounded by a rotating spheroidal structure of uniform density from which spiral arms emanate. But if the diffuse matter in the spheroidal structure obeys ordinary gas laws, then it does not seem justifiable to assume that it is of uniform density. In a recent paper Lindblad has assumed that " the stellar system may be divided formally into a number of sub-systems of approximately the same extension in the galactic plane, but with different degree of flattening towards the plane and different speed of rotation at the same distance from the axis."

It need hardly be mentioned that no satisfactory theory about the formation of the spiral arms can be established until and unless we get a more thorough knowledge of the constitution of galaxies.

Recent investigations by Plaskett and Pearce(6) about our local galaxy tend to show that " the whole galactic system is immersed in a gaseous substratum consisting of atoms of various elements . . . . The separate atoms while obeying ordinary gas laws, participate in a rotational movement around a distant central mass in galactic longitude 325°. " The observed rotational acceleration seems to be the same as for the stars, so that the atoms are not subjected to any appreciable radiation pressure from the central mass."

The above conclusions have led the authors to work out in this paper the case of a rotating spheroidal central mass of finite dimensions and of uniform density surrounded by a spheroidal structure of rotating compressible gas of variable density. The authors have investigated the condition necessary for the formation of spiral arms. The size of the central mass is taken to be small compared to that of the outer boundary of gaseous structure.

Instead of assuming a uniform density(7) in the compressible gaseous configuration it is more reasonable to take

$$\rho=\rho_0 e^{\frac{\phi}{c}+\frac{\omega^2 r^2}{2c}},$$

where $\phi$ is the gravitational potential and $c=\frac{\mathrm{RT}}{\mu}$, where R is the universal gas constant and has the value $8{\cdot}26\times10^7$. $\mu$ is the molecular weight in terms of hydrogen and T is the absolute temperature. Accepting Eddington's value we can take temperature of interstellar gaseous matter to be about $10^{4°}$ absolute.

Generally the rotational velocity of the nebulæ is very small, and $c$ is of the order $10^{10}$ cm. per sec. Considering the nebulæ for which $\frac{\omega^2 a^2}{2c}$, where $a$ is the equatorial radius of the spheroidal boundary, has a very small value, we find that the density can, without any appreciable error, be taken to be $\rho=\rho_0 e^{\frac{\phi}{c}}$, since $e^{\frac{\omega^2c^2}{2c}}=1$ approx. In a second paper, we hope to discuss the case for which $\frac{\omega^2a^2}{2c}$ is not small.

As the gravitational forces form a system of conservative forces so we readily see that the surfaces of equal density are similar spheroids, and it is clear, without any detailed analysis, that the density at a point which is at a sufficient distance from the centre of the system varies as the square of the equatorial radius of the similar spheroid passing through it.

Let $a$ be the equatorial radius of the outer boundary of the gaseous configuration, $k_0a$ the equatorial radius of the spheroidal boundary of the central mass, and $ka$ the equatorial radius of the similar spheroid passing through the point in the gaseous configuration at which density $\rho$ is required.

If $k_0a$ is of sufficient magnitude, although $k_0$ is small we can, without serious error$^{(8)}$, take

$$\rho=\frac{k_0{}^2}{k^2}\rho_0, \text{ where } 1 \geqslant k \geqslant k_0 \text{ and}$$

$\rho_0$ is the uniform density of the central mass.

Plaskett and Pearce$^{(6)}$ have also come to the conclusion that "so far as the observational material is concerned, there are no outstanding difficulties in the acceptance of the view that the space in our stellar system is pervaded by very diffuse matter . . . . and ionized by the general radiation of the stars." The authors have also investigated the effect of ionization on the formation of spiral arms.

At a point in the interior of the ionized material the potential of the electric field due to separation of changes$^{(9)}$ is found to be a constant multiple of the gravitational potential, but at an external point the above potential is found to be negligible.

We shall now investigate the path of a particle or a small amount of matter which may have been ejected, due to a slight perturbation, from the equatorial plane of the galactic structure which we have assumed. The intensity of attraction at an external point in the equatorial plane may be taken as $f=f_1+f_2$, where $f_1$ is the force of attraction at the external point in the equatorial plane due to the inner homogeneous spheroid of density $\rho_0$ and equatorial radius $k_0a$, and $f_2$ is the attraction at the same point, of the gaseous spheroidal shell having $a$ and $k_0a$ as the two bounding equatorial radii.

We have$^{(10)}$

$$f_1=\frac{2\pi\rho_0(1-e^2)^{\frac{1}{2}}}{e^3}r\left[-\frac{k_0ae}{r}\sqrt{1-\frac{k_0{}^2a^2e^2}{r^2}}+\sin^{-1}\frac{k_0ae}{r}\right];$$

and we have to calculate $f_2$.

The potential of an oblate homogeneous spheroid of equatorial radius $ka$ and eccentricity $e$ at an external point is(11) .

$$V=\frac{4}{3}\frac{\pi k^3a^3(1-e^2)^{\frac{1}{2}}}{r}\rho\left[1-\frac{3}{3}\cdot\frac{P_2}{5}\cdot\left(\frac{ae}{r}\right)^2k^2+\frac{3}{5}\cdot\frac{P_4}{7}\cdot\left(\frac{ae}{r}\right)^4k^4-\ldots\right.$$
$$\left.\ldots.+\frac{(-1)^n.3.P_{2n}}{(2n+1)(2n+3)}\left(\frac{ae}{r}\right)^{2n}k^{2n}+\ldots\right],$$

where $e<1$ and $k<1$ and $P_2, P_4$ etc. are Legendre's coefficients. Now the potential due to the spheroidal shell of matter having bounding equatorial radii as $ka$ and $(k+dk)a$ is given by

$$V'=\frac{dV}{dk}.dk=\frac{4}{3}\cdot\frac{\pi a^3(1-e^2)^{\frac{1}{2}}k^2\rho}{r}\left[3-\frac{3\cdot5}{3\cdot5}.P_2\left(\frac{ae}{r}\right)^2k^2\right.$$
$$\left.+\frac{3}{5}\cdot\frac{P_4}{7}\cdot\frac{7}{1}\cdot\left(\frac{ae}{r}\right)^4k^4-\ldots+\frac{(-1)^n.3.(2n+3)}{(2n+1)(2n+3)}.P_{2n}.\left(\frac{ae}{r}\right)^{2n}k^{2n}\ldots\right].$$

Now putting

$$\rho=\rho_0\left(\frac{k_0^2}{k^2}\right),$$

and then integrating, we get the potential $V_2$ at an external point of the gaseous spheroidal shell

$$V_2=\frac{4}{3}\cdot\frac{\pi a^3\rho_0(1-e^2)^{\frac{1}{2}}k_0^2}{r}\int_{k_0}^{1}\left[3-\frac{3}{3}\cdot\left(\frac{ae}{r}\right)^2k^2P_2+\frac{3}{5}\left(\frac{ae}{r}\right)^4k^4P_4-\ldots\right.$$
$$\left.+(-1)^n.\frac{3}{2n+1}\cdot\left(\frac{ae}{r}\right)^{2n}k^{2n}P_{2n}+\ldots.\right]$$
$$=\frac{4}{3}\cdot\frac{\pi a^3\rho_0(1-e^2)^{\frac{1}{2}}k_0^2}{r}\left[3(1-k_0)-\frac{3}{9}\cdot\left(\frac{ae}{r}\right)^2(1-k_0^3)P_2\right.$$
$$\left.+\frac{3}{25}\left(\frac{ae}{r}\right)^4(1-k_0^5)P_4-\ldots+(-1)^n.\frac{3}{(2n+1)^2}\left(\frac{ae}{r}\right)^{2n}(1-k_0^{2n+1})P_{2n}+\ldots\right].$$

In the equatorial plane we have to find out the value of $-\frac{dV_2}{dr}$ to get the attraction $f_2$. We also note(12) that, when $\theta=\frac{\pi}{2}$,

$$P_2=-\frac{1}{2},\ P_4=\frac{3}{8},\ P_6=-\frac{5}{16};\ldots P_{2n}=(-1)^n.\frac{1.3\ldots(2n-1)}{2.4\ldots 2n}.$$

Therefore

$$f_2=\frac{4}{3}.\pi a^3\rho_0k_0^2(1-e^2)^{\frac{1}{2}}\left[\frac{3(1-k_0)}{r^2}+\frac{1}{2}(1-k_0^3)\frac{a^2e^2}{r4}\right.$$
$$+\frac{9}{40}.(1-k_0^5).\frac{a^4e^4}{r^6}+\ldots+\frac{3.1.3\ldots(2n-1)\cdot}{(2n+1).2.4\ldots 2n}$$
$$\left.\times(1-k_0^{2n+1})\frac{a^{2n}e^{2n}}{r^{2n+2}}+\ldots\right].$$

Now

$$f_1 = \frac{2\pi\rho_0(1-e^2)^{\frac{1}{2}}}{e^3} . r\left[\sin^{-1}\frac{k_0ae}{r} - \frac{k_0ae}{r}\sqrt{1-\frac{k_0^2a^2e^2}{r^2}}\right].$$

By expanding the expression in the brackets we get

$$f_1 = 2\pi\rho_0a^3k_0^3(1-e^2)^{\frac{1}{2}}\left[\frac{2}{3}\cdot\frac{1}{r^2} + \frac{1}{5}\cdot\frac{a^2k_0^2e^2}{r^4} + \frac{3}{28}\cdot\frac{a^4k_0^4e^4}{r^6} + \ldots \right.$$
$$\left. + \frac{1.3\ldots(2n-1)}{2\cdot4\ldots2n}\cdot\frac{2}{2n+3}\cdot\frac{a^{2n}k_0^{2n}e^{2n}}{r^{2n+2}} + \ldots\right].$$

Therefore the total force of attraction measured positively towards the centre is

$$f = f_1 + f_2$$
$$= \frac{4}{3}.\pi a^3\rho_0(1-e^2)^{\frac{1}{2}}k_0^2\left[\frac{(3-2k_0)}{r^2} + \frac{a^2e^2}{r^4}\cdot\frac{(5-2k_0^3)}{10} + \frac{a^4e^4}{r^6}\cdot\frac{(63-18k_0^5)}{280}\right.$$
$$\left. + \ldots + \frac{a^{2n}e^{2n}}{r^{2n+2}}\cdot\frac{1.3\ldots(2n-1)}{2\cdot4\ldots2n}\cdot\frac{3(2n+3-2k_0^{2n+1})}{(2n+1)(2n+3)} + \ldots\right].$$

As $r<a$ and $e<1$, the series is convergent. By keeping up to terms containing $e^{2n}$, we get

$$f = \frac{A_0}{r^2} + \frac{A_1}{r^4} + \ldots + \frac{A_n}{r^{2n+2}},$$

where

$$A_0 = \frac{4}{3}\pi a^3\rho_0(1-e^2)^{\frac{1}{2}}k_0^2(3-2k_0) = \frac{4}{3}.\pi a^3\rho_0k_0^2(1-e^2)^{\frac{1}{2}}.\alpha_0,$$

$$A_1 = \frac{4}{3}.\pi a^5\rho_0(1-e^2)^{\frac{1}{2}}k_0^2e^2.\frac{(5-2k_0^3)}{10} = \frac{4}{3}\pi a^5\rho_0k_0^2e^2(1-e^2)^{\frac{1}{2}}.\alpha_1,$$

. . . . . . . . . . . . . . . . . . . . . . . . . . . . . . . . . . . . . . . . . . . .

$$A_n = \frac{4}{3}\pi a^{2n+3}\rho_0(1-e^2)^{\frac{1}{2}}k_0^2e^{2n}.\frac{1.3\ldots(2n-1)}{2.4\ldots2n}\cdot\frac{3.\{2n+3-2k_0^{2n+1}\}}{(2n+1)(2n+3)}$$
$$= \frac{4}{3}\pi a^{2n+3}\rho_0k_0^2e^{2n}.(1-e^2)^{\frac{1}{2}}.\alpha^n,$$

where

$$\alpha_0 = 3-2k_0,$$
$$\alpha_1 = \frac{5-2k_0^3}{10},$$

. . . . . . . .

$$\alpha_n = \frac{1.3\ldots(2n-1)}{2.4\ldots2n}\cdot\frac{3.\{2n+3-2k_0^{2n+1}\}}{(2n+1)(2n+3)}.$$

The equation of the orbit of an external particle which has been just ejected in the equatorial plane is

$$\frac{d^2u}{d\theta^2} + u = \frac{f}{h^2u^2} = \frac{1}{h^2}(A_0 + A_1u^2 + A_2u^4 + \ldots + A_nu^{2n}) \text{ where } u = \frac{1}{r}.$$

The effect of some such disturbing factor as tidal action will be to cause a slight perturbation, but this will leave $h$ unchanged, and we can therefore take $h^2=a^2\omega$, $\omega$ being the angular velocity. Therefore

$$\left(\frac{du}{d\theta}\right)^2+u^2=\frac{2}{h^2}\left[\mathrm{A}_0u+\frac{\mathrm{A}_1}{3}u^3+\ldots+\frac{\mathrm{A}_n}{2n+1}\,.\,u^{2n+1}\right]+\mathrm{E},$$

where E is the constant of integration. We can get the value of E by noticing that when $u=u_0=\frac{1}{a}$, the orbit is circular and $\frac{du}{d\theta}=0$.

Substituting the value of E and taking the square root we get

$$\frac{du}{d\theta}=\pm\sqrt{\frac{2}{h^2}\left(\mathrm{A}_0u+\frac{\mathrm{A}_1}{3}u^3+\ldots+\frac{\mathrm{A}_n}{2n+1}u^{2n+1}\right)-u^2+u_0^{\,2}-\frac{2}{h^2}\left(\mathrm{A}_0u_0+\frac{\mathrm{A}_1}{3}u_0^{\,3}+\ldots+\frac{\mathrm{A}_n}{2n+1}u_0^{\,2n+1}\right)}.$$

We have, therefore,

$$\frac{dr}{d\theta}=\pm r^2\sqrt{\begin{array}{l}\frac{2}{h^2}\cdot\frac{4}{3}\pi a^3\rho_0k_0^{\,2}\left[\frac{\alpha_0}{r}+\frac{\alpha_1}{3}\cdot\frac{a^2e^2}{r^3}+\ldots+\frac{\alpha_na^{2n}e^{2n}}{(2n+1)r^{2n+1}}\right](1-e^2)^{\frac{1}{2}}\\ -\frac{1}{r^2}+\frac{1}{a^2}-\frac{2}{h^2}\cdot\frac{4}{3}\pi a^3\rho_0k_0^{\,2}\left[\frac{\alpha_0}{a}+\frac{\alpha_1e^2}{3a}+\ldots+\frac{\alpha_ne^{2n}}{(2n+1)a}\right](1-e^2)^{\frac{1}{2}}.\end{array}}$$

Now for a spiral form, $\frac{dr}{d\theta}$ must be real, finite, continuous, and of the same sign, as $r$ changes with $\theta$. It is therefore necessary that the expression under the root sign must be positive for all values of $r>a$. In order that the spiral form may be possible we get, after substituting $a^2\omega$ for $h$, for all values of $r>a$,

$$\frac{1}{a^2}-\frac{1}{r^2}>\frac{2}{a^4\omega^2}\cdot\frac{4}{3}\cdot\pi a^3\rho_0k_0^{\,2}\left[\alpha_0\left(\frac{1}{a}-\frac{1}{r}\right)+\frac{\alpha_1e^2}{3}\left(\frac{1}{a}-\frac{a^2}{r^3}\right)+\ldots\right.$$
$$\left.+\ldots+\frac{\alpha_ne^{2n}}{2n+1}\left(\frac{1}{a}-\frac{a^{2n}}{r^{2n+1}}\right)\right](1-e^2)^{\frac{1}{2}}.$$

On slight reduction we have

$$\frac{r+a}{r}>\frac{8}{3}\cdot\frac{\pi\rho_0k_0^{\,2}}{\omega^2}\left[\alpha_0+\frac{\alpha_1e^2}{3}\left(1+\frac{a}{r}+\frac{a^2}{r^2}\right)+\ldots+\ldots\right.$$
$$\left.+\frac{\alpha_ne^{2n}}{2n+1}\left(1+\frac{a}{r}+\frac{a^2}{r^2}+\ldots+\frac{a^{2n}}{r^{2n}}\right)\right](1-e^2)^{\frac{1}{2}}.$$

The condition for the spiral formation is all the more satisfied if

$$\frac{r+a}{r}>\frac{8}{3}\frac{\pi\rho_0k_0^{\,2}}{\omega^2}[\alpha_0+\alpha_1e^2+\ldots+\alpha_ne^{2n}](1-e^2)^{\frac{1}{2}}.$$

This is all the more satisfied if

$$\frac{r+a}{r} > 1 > \frac{8}{3} \cdot \frac{\pi \rho_0 k_0{}^2}{\omega^2} [\alpha_0 + \alpha_1 e^2 + \ldots + \alpha_n e^{2n}](1-e^2)^{\frac{1}{2}},$$

or

$$\frac{\omega^2}{2\pi\rho_0} > \frac{4}{3} k_0{}^2 (1-e^2)^{\frac{1}{2}} [\alpha_0 + \alpha_1 e^2 + \ldots . + \alpha_n e^{2n}].$$

If this condition is satisfied then the two values of $\frac{dr}{d\theta}$, which are opposite in sign but equal in magnitude, show that two spiral arms may emanate as a result of slight perturbation from two diametrically opposite points in the equatorial plane.

We shall now consider briefly the effect of ionization on the formation of spiral arms. Eddington⁽⁹⁾ has shown that at an internal point the resultant mechanical force on every particle whether ion or electron is the same, *i. e.*, $\mu \frac{\partial \phi}{\partial r}$, where $\phi$ is the gravitational potential and $\mu$ is the mean molecular weight. He points out that although " in ionized material the electrons are far lighter than the ions and tend to rise at the top, yet the separation is almost stopped before it has begun, because the minutest inequality creates a large electrostatic field which stops any further diffusion." He has calculated that there is hardly a deficiency of one electron in every million tons of matter, so the assumption that there is no appreciable separation of the charges is thus verified. After ionization we can therefore take without any appreciable error each molecule to be more or less a rigid doublet formed of masses M (mass of the ion) and $m$ (mass of the electron) We can take the mechanical force on each of the three masses to be $\mu \frac{\partial \phi}{\partial r}$, so the intensity of the mechanical force on the rigid frame of the doublet acting at its centre of gravity is

$$\frac{2\mu}{\mathrm{M}+m} \cdot \frac{d\phi}{dr}.$$

If the atomic number is Z, then $\mu = \frac{\mathrm{M}+\mathrm{Z}m}{\mathrm{Z}+1}$. We find that the factor $\frac{2\mu}{\mathrm{M}+m} < 1$ if $\mathrm{Z} > 1$, which is always so except in case of hydrogen. Thus ionization reduces the gravitational force. It can be readily seen without any detailed analysis that the electrical force on a charged particle or a doublet situated at an external point is negligible, so the resultant mechanical force on the particle in the doublet is merely the gravitational force.

When the spiral arms⁽¹³⁾ are fairly thin the decrease of size and mass of our galactic structures may be neglected. In this case the spiral arm, more or less, represents the actual orbit of a particle on the arm.

Ionization will not have any effect in altering the magnitude of the mechanical force acting on this particle. The force acting on it will be purely gravitational.

When the spiral arms(13) are heavy the decrease of mass of the spheroidal structure due to the formation of the arms must be taken into account. Consequently the equatorial radius decreases and the central nucleus also decreases in size as $k_0a$ decreases. The arm can no longer represent exactly the orbit of one of its particles. Due to decrease of mass of the spheroidal body, gravitational force decreases with increasing development of the arms, and the true orbit is likely to be wider in the outer regions. So the arms rather open out. In the case of heavy arms the effect of ionization will have to be taken into account as the ionized particles are no longer isolated. We have seen that, due to ionization, gravitational force is further reduced, and its effect is to open the arms still more.

Neglecting powers of $k_0$ higher than the second, we find that our condition for formation of spiral arms becomes

$$\frac{\omega^2}{2\pi\rho_0} > \frac{4}{3}k_0{}^2(1-e^2)^{\frac{1}{2}}\left[3+\frac{1}{2}e^2+\ \ ..+\frac{3.1.3\ldots(2n-1)}{2.4\ldots2n(2n+1)}e^{2n}\right].$$

Plaskett(14) says "It has been convincingly demonstrated that galaxy is a single dynamical unit rotating in its own plane with angular velocity decreasing with distance from the centre, like the planets round the sun, thus indicating a great condensation of matter towards the centre of the system." If $\omega$ was constant, on account of the enormous size of the galaxy, the quantity $\frac{\omega^2a^2}{2c}$ may be large and $\rho$ will be very great in the periphery of our galaxy, and instability will ensue. If $\omega$ decreases with the distance from the centre of the nucleus it may be very small at the periphery, and in that case $\frac{\omega^2a^2}{2c}$ will be small and we may take $e^{\frac{\omega^2a^2}{2c}}$ to be approximately equal to unity. With this assumption the condition for the formation of the spiral arms will remain the same for our galactic system also.

Now we shall calculate the upper limit for $k_0$ in case of our galaxy and Andromeda nebula, neglecting the effect of ionization.

*Our Galactic System* :

Equatorial diameter $=30{,}000$ parsecs ;
Polar diameter $=6000$ parsecs ;
Period of rotation $=2{\cdot}3\times10^8$ years ;
$\rho_0=10^{-25}$ gm./cm.$^2$ (say).

Then

$$1-e^2=\frac{1}{25} \quad \text{and so} \quad e^2=\frac{24}{25}.$$

We find that for the spiral formation $k_0$ should not be greater than $\frac{1}{900}$. So we see that the equatorial diameter of the central nucleus cannot be greater than 35 parsecs. If $\rho_0$ has the greater value than what has been assumed, the size of the central nucleus will be still smaller.

*For Andromeda Nebula* :

Equatorial diameter of the outer spheroid = 20,000 parsecs ;
Polar diameter = 1000 parsecs ;
Period of rotation = 16,000,000 years ;

$$\rho_0=10^{-25} \text{ gm./cm.}^3 \text{ (say)}.$$

Then

$$1-e^2=\frac{1}{400} \quad \text{and so} \quad e^2=\frac{399}{400}.$$

We find that for the spiral formation $k_0$ should not be greater than $\frac{1}{32}$. In this case the equatorial diameter of the central nucleus cannot be greater than 600 parsecs. Also if $\rho_0$ has a greater value than what has been assumed, the size of the central nucleus would become smaller.

## *References.*

(1) Jeans, ' Astronomy and Cosmogony,' chap. xiii. (1929).
(2) Bok, ' Yerkes Observatory Notes ' (1936).
(3) Brown, Obs. li. p. 277 (1928).
(4) Vogt, *Astron. Nachtr.* ccxlii. p. 181 (1931) ; ccxlv. p. 281 (1932).
(5) Lindblad, *Stockholms Observatoriums Annales*, Band 12, no. 4 (1936).
(6) Plaskett and Pearce, ' Dominion Astrophysical Observatory,' vol. v. no. 3, pp. 173–174 (1933).
(7) Jeans, ' Dynamical Theory of Gases,' 353 pp. (1916).
(8) Jeans, ' Astronomy and Cosmogony,' 250 pp. (1929) ; and Darwin, Phil. Trans. clxxx. A (1889).
(9) Eddington, ' Internal Constitution of Stars,' 273 pp. (1926).
(10) Jeans, ' Astronomy and Cosmogony,' 257 pp. (1929).
(11) Routh, ' Statics,' vol. ii. pp. 153–154 (1908).
(12) Jeans, ' Electricity and Magnetism,' pp. 217–219 (1927).
(13) Lindblad, *Stockholms Observatoriums Annales*, Band 12, no. 4 (1936), pp. 47–48.
(14) Plaskett, ' The Dominion Astrophysical Observatory,' vol. v. no. 4, 327 pp. (1936).

## X. *Notices respecting New Books.*

*Mathematical Biophysics.* By Nicolas Rashevsky. [Pp. xviii+340.] (University of Chicago Press, 1938.)

In this interesting and important volume Professor Rashevsky gives a connected account of attempts to find what may be described as a physico-mathematical basis for biology by methods analogous to those employed so successfully in the development of physical theory. Just as the kinetic theory of matter was built up by considering the behaviour of an assemblage of highly over-simplified "atoms," so the attempt is being made to elucidate the main features of biological behaviour by postulating a highly simplified biological unit or structure and studying its physical and chemical reactions to its environment. The subjects dealt with include respiration, cell-division, irritability, conditioned reflexes, gestalt-phenomena, and inhibition.

Much of the work included in the volume is due to Professor Rashevsky himself, and members of his school; but the contributions of other authors are not ignored. There is, for example, a fair account of A. V. Hill's theory of excitation. Much—perhaps most—of the work is of a very preliminary character, and some of the suggestions made may not stand a more exacting scrutiny. This is only to be expected in a subject so new and so complex.

To an author who renders us the great service of producing a connected account of a very rapidly growing subject much may be forgiven; and Professor Rashevsky seems so conscious of the possible imperfections of his book as to disarm criticism. In fact, however, considering that most of the work described has been published within the last three of four years, and some of it while the manuscript was actually being written, the imperfections are amazingly slight. The inclusion of considerable mathematical detail, which makes the book in places rather dull reading to the physicist, is intended to smooth the path of the biological reader. Physicists and mathematicians who feel that their subjects have an important part to play in the development of biology will find the book of great interest, both for its outlines of what has already been done and its suggestions for future advances. J. A. Crowther.

*Notes on Practical Physics.* By Prof. G. Stead. [Pp. 74.] (London: Taylor and Francis, Ltd., 1939. Price 3*s*.)

Professor Stead's unassuming little book will be welcomed alike by teachers and by students of elementary physics. It contains clear and concise directions for carrying out some fifty-six experiments of intermediate standard. The experiments cover the different branches of physics usually studied in an intermediate course, and include half-a-dozen well-selected exercises on purely mechanical problems. The descriptions, brief as they are, are amply sufficient to enable a student to carry out the experiments unaided, and practically all the descriptions are illustrated by simple line-cuts. Considerable use is made of graphical methods,—a feature of the book which might well be extended in future editions. A most useful appendix contains statements of forty-eight revision experiments.

There is much to commend, and little to criticize, but it would improve the accuracy of the experiment on the latent heat of steam if the water-trap were omitted, and in the experiment on the electro-chemical equivalent of copper it would be well to emphasize the fact that it is the current-density, rather than the current, which is the important factor.

The book should have a wide sale and may be warmly commended. The usefulness of the book would be considerably increased if, without increasing the price, a few tables, and an introduction giving some general hints to the students, could be added.

A. F.

*Encyclopædia Britannica Book of the Year* 1939. [Pp. xvi—760.] (London: Encyclopædia Britannica Co., Ltd., 1939. Price 45*s*. net.)

The Encyclopædia Britannica Book of the year for 1939 is the second of the yearly volumes which has been issued and, like its predecessor for 1938, it may fairly be classed among the indispensables. No library which aims at completeness, especially in the matter of reference books, can afford to be without this temperate and objective guide to the events and developments that have occurred in the year 1938. Science, Literature, Politics, Religion, Education, Sport, Art, Crime . . . very little has been left untouched in this authoritative and comprehensive survey. The articles are sufficiently detailed to enable an intelligent reader to see the events or developments in their proper perspective, and in many instances where the accounts are necessarily brief or elementary in character, references are provided to current literature from which more details may be gleaned than is possible in a single limited article.

A striking feature of the volume is what may be termed its " fine-grainedness." It would be a serious error to assume that its articles deal solely with topics classified under broad and general titles. The seeker for information concerning gastric carcinoma, the flight of funds, Jamaica production of ginger, the reduction of dust in mines, diet in hot climates, housing, the cost of living, the fur trade, corneal grafting, Wicken Fen, Sir John Simon and Shirley Temple, will find, and will find easily, authoritative information on these and on thousands of other topics. The phrase " find easily " is to be emphasized, for the indexing, a matter of primary importance in a work of this character, is most complete, detailed and intelligently conceived and carried out,

The scientific articles, as far as the reviewer has tested them, are accurate, clear, concise and helpful alike to the layman and to the specialized student.

The book is well illustrated, is admirably produced, and should be assured of a wide circulation.

---

[*The Editors do not hold themselves responsible for the views expressed by their correspondents.*]

# XI. *The Density and Compressibility of Solid Hydrogen and Deuterium at* 4·2° *K.*

By HELEN D. MEGAW *.

[Received May 15, 1939.]

## *Introduction.*

THE study of the properties of condensed hydrogen is of particular interest, since the existence of the two isotopes gives us for comparison two systems which differ widely in their zero-point energy, because of their different masses, but are otherwise identical and have the same binding forces. As Bennewitz and Simon have pointed out (1), the effect of the zero-point energy on the properties becomes very great for condensed substances of low boiling-point. For instance, in helium (15), (2) the zero-point energy makes up the greater part of the lattice energy, and is decisive in determining its structure; it may be calculated that its volume would be about one-sixth of that actually observed if there were no zero-point energy. In hydrogen it may be roughly estimated that half the lattice energy is zero-point energy.

Investigation of many of the properties of condensed hydrogen and deuterium have been made by Clusius and Bartholomé (3). Among other things they have measured the heat of melting and evaporation of deuterium, its specific heat at constant pressure, and the molar volume and compressibility of the liquid; and hence they have calculated the heat of sublimation at absolute zero and the molar volume of the solid at the triple point. They have compared their results with the corresponding values for hydrogen (4), and shown qualitatively how the differences are to be attributed to the difference in zero-point energy. Bartholomé (5) has also measured directly the specific heat at constant volume of solid hydrogen and deuterium, and hence estimated the thermal expansion and the molar volume at absolute zero.

For the theoretical treatment a more direct knowledge of the molar volumes at absolute zero is necessary, and an experimental determination of these quantities, and also of the compressibilities, was desirable. For this purpose the present work was undertaken (a preliminary report of which has already been given (6)). The densities of hydrogen and deuterium have been measured at the boiling-point of helium, 4·2° K., over a pressure-range of 100 atmospheres. The molar volumes at this temperature probably differ negligibly from those at absolute zero, which are the values of primary interest for the theoretical treatment; the same is true of the compressibilities. The theoretical conclusions which can be deduced from a knowledge of these quantities will be discussed later, after the account of the experimental work.

---

* Communicated by the Author.

A pycnometer method was chosen for the work, methods using a cylinder and piston being rejected as presenting too great experimental difficulties at the low temperatures *. In the method selected, a vessel of known volume containing a measured mass of the solid is filled with a liquid of known density whose mass is also measured. The only substance available for a filling liquid at this temperature is liquid helium, which has a very large compressibility—a compressibility, as the experiment showed, about ten times that of solid hydrogen itself. This inevitably means that the method cannot be one of high accuracy. In practice, however, when suitable precautions were taken, the results obtained were sufficiently accurate to be of interest.

## *Experimental Method.*

In outline the method was as follows. A small vessel of known volume was attached to a helium liquefier; it was nearly filled with condensed hydrogen or deuterium, and when this was solid completely filled with liquid helium at a known pressure. The lead by which the gases entered the vessel was of capillary tubing, so that corrections for its volume should be as small as possible. The masses of helium and hydrogen were determined by measuring their pressure, volume and temperature as gases in an external system, and from the known density of the liquid helium the density of the solid hydrogen at the pressure applied to the pycnometer was found.

The hydrogen used in the experiments was taken from the ordinary supply of electrolytic hydrogen for the helium liquefaction process. It was cleaned by charcoal immersed in liquid air, and further purified by condensation in the liquefier just before use. The deuterium was prepared by electrolysis of $D_2O$ of 99·8 per cent. purity (for the gift of which my thanks are due to Professor Polanyi); the electrolyte was $K_2SO_4$, and traces of oxygen were removed with a red-hot platinum spiral. The final purification was made by condensation in a vessel surrounded with liquid hydrogen.

The production of the low temperatures followed the technique introduced by Simon (7). The liquid helium is produced in the apparatus itself, by the expansion of the gas from temperatures attainable with liquid hydrogen. The apparatus is shown in fig. 1 (where only the part where the low temperatures are produced is drawn to scale). The liquefier consists of a helium chamber B soldered to a hydrogen chamber E, both enclosed in a space J containing helium gas at a low pressure (" exchange gas ") to give thermal contact between the liquefier and the surrounding bath of liquid hydrogen. The chamber B is filled with

---

* A method using thin metal bellows might, however, be practicable.

Fig. 1.

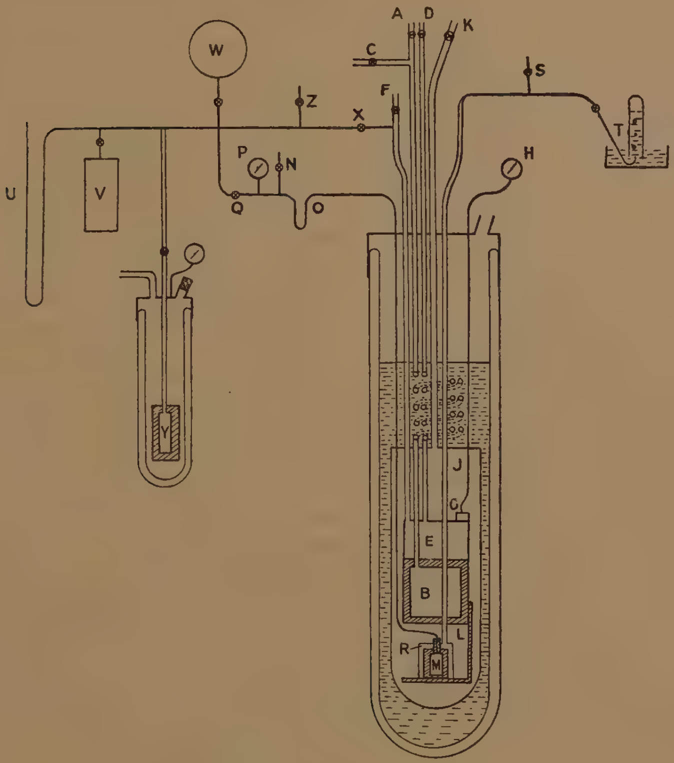

Diagram of apparatus.

A, helium inlet to liquefier ; B, helium chamber of liquefier ; C, helium expansion valve ; D, hydrogen inlet to liquefier ; E, hydrogen chamber of liquefier ; F, connexion to backing pump ; G, H, gas thermometer ; J, vacuum space ; K, connexion to diffusion pump ; L, bracket ; M, pycnometer ; N, helium inlet to pycnometer ; O, U-tube immersed in liquid air ; P, small Bourdon-type manometer ; Q, fine adjustment tap ; R, jacket containing liquid helium ; S, connexion to helium supply ; T, outlet from jacket R ; U, mercury manometer ; V, helium container of known volume ; W, hydrogen or deuterium container of known volume ; X, connexion for filling W with hydrogen ; Y, cleaner for deuterium ; Z, connexion to diffusion pump.

helium gas at about 120 atmospheres pressure, and hydrogen gas is led into E, where it condenses, till the chamber is full. The liquefier is then thermally insulated by removing the exchange gas, and the hydrogen is pumped off from E, so that it boils under reduced pressure and cools the whole liquifier and the helium contained in it to about 10 or 11° K. The helium is then allowed to expand by opening the tap C; it cools in so doing, and finally liquefies in B. This is the standard apparatus, to which is added that part needed for the particular experiment.

The pycnometer was made of thick-walled copper with a hard-soldered lid, its volume being about 4 c.c. It rested on a copper bracket soldered to the liquefier, and was connected to the rest of the apparatus by a capillary tube. Through this it was filled with gaseous hydrogen, which condensed when the liquefier was between 20° K. and 14° K. (with deuterium, at 20° K.) until it was about three-quarters full. In practice this part of the experiment gave some difficulty; the condensation was slow, owing to the length of the capillary, and the hydrogen or deuterium tended to condense in the tube and block it when solidification occurred. To prevent this as far as possible, the capillary was not in direct thermal contact with the liquefier, and the pycnometer was arranged so that the cooling was from the bottom.

When the temperature had been reduced below the triple point and the hydrogen or deuterium was solid the pycnometer was connected to the high pressure helium supply. To prevent blockage of the capillary by small traces of impurities in the helium, it was passed through a charcoal and liquid air cleaner just before entering the pycnometer system through the tap N (fig. 1), and then through a U-tube O, of very small volume, also immersed in liquid air, to remove any possible traces of tap-grease. When the temperature of the liquefier had reached the helium boiling-point the vessel became filled with liquid helium at a pressure which could be adjusted as desired (generally about 100 atmospheres), and which was read on a small Bourdon-type manometer, filled with oil in order to keep the dead volumes small. The inlet tap N was then closed.

The temperature of the pycnometer during these measurements was controlled by a jacket R containing liquid helium; it was filled during the expansion, after which it was closed and connected to a tube T leading under water, where the evaporating helium could be observed as it bubbled out.

At the beginning of the experiment the pycnometer was full of liquid helium at 4·2° K. and 100 atmospheres pressure. Successive amounts of helium were allowed to escape from it through the outlet tap Q into the external system, where they were measured. This system consisted of a metal cylinder and glass leads of known volume, and a mercury manometer on which the pressure was read. For each pycnometer pressure the amount of helium which had come out up to that point was measured.

The helium in the pycnometer cools itself by its own expansion (8) during the measurements, and if it is allowed to escape too rapidly the thermal equilibrium with the liquefier is not maintained. Then the liquid in the surrounding jacket is cooled, and its rate of evaporation is observed to decrease. Readings of the pressure in the pycnometer were only taken after a time interval when the evaporation had again become normal. The jacket, in fact, acts both as a thermostat and as a vapour-pressure thermometer for the pycnometer, and thus errors due to the rapid variation of the density of liquid helium with temperature are eliminated.

To obtain the reading for a pressure of about 1 atmosphere in the pycnometer the mercury manometer had to be used, as the Bourdon manometer was useless for low pressures. For this purpose the large vessel V was closed at such a point that the final pressure in the glass leads and manometer was about 85 or 90 cm. Thus the pycnometer, which was in equilibrium with the leads, was at more than atmospheric pressure, and remained full of liquid.

Then the temperature was allowed to rise, and the remaining helium measured in V; this was the helium which had filled the pycnometer with liquid at a pressure of 1 atmosphere. It evaporated while the liquefier was at 7–10° K., at which temperature the vapour pressure of the hydrogen was completely negligible. Then V was closed. In the experiments with deuterium the remaining helium was pumped out of the pycnometer, to leave the deuterium pure for further use; with hydrogen, where fresh material was used each time, this precaution was unnecessary, and a correction was simply made in the calculation for the amount remaining.

Exchange gas was introduced into J, and the pycnometer was connected to a flask W of known volume into which the hydrogen or deuterium was allowed to evaporate as the temperature rose, and its pressure and temperature were measured.

## *Calculation, Corrections, and Errors.*

If $m_{\mathrm{H}}$ and $m_{\mathrm{He}}$ are the measured masses of solid hydrogen and liquid helium respectively, $\rho_{\mathrm{He}}$ the density of the helium, and $v$ the volume of the pycnometer, the density of the hydrogen is given by

$$\rho_{\mathrm{H}}=\frac{m_{\mathrm{H}}}{v-\dfrac{m_{\mathrm{He}}}{\rho_{\mathrm{He}}}};$$

$m_{\mathrm{He}}$ is found by subtracting the mass of helium gas in the outer parts of the apparatus at the given pycnometer pressure from the total mass of helium when all has evaporated. The measurements made, and the errors involved, in the determination of the various quantities are discussed in what follows.

*Pycnometer Volume.*—This was determined by weighing empty and full of water, acetone and $CCl_4$ being used as a check. The volume at room temperature was 4·095±·010 cm.$^3$.

The correction for thermal expansion, using the values for copper given in the International Critical Tables, is ·034±·001 cm.$^3$, and the volume at 4·2° K. is therefore 4·061±·010 cm.$^3$. The correction for change of volume with pressure for 100 kg./cm.$^2$ was calculated and found to be ·002 cm.$^3$, which is so small that even large uncertainties in the formula used to arrive at it cannot cause a serious error.

The assumption is made that the liquid helium fills the pycnometer exactly to its neck, above which the whole capillary is filled with gas. At the higher pressures this will not be exactly true, but since the area of the capillary is small (diameter 0·7 mm.) and the density of the gas at high pressures not widely different from that of the liquid the error is small and may be neglected.

*Density of Helium.*—The density of helium has been measured by Keesom (9) at pressures up to 35 kg./cm.$^2$. For the present experiment it was necessary to know it up to 100 kg./cm.$^2$. It was measured in a preliminary experiment with the same apparatus, in which the pycnometer was filled entirely with helium. The results agree with Keesom's within the estimated limits of error over the pressure range that they have in common. They are shown in Table I. and graphically in Fig. 2. The agreement with Keesom's figures is evidence that there is no large undetected error in the method *.

---

* The compressibility of helium, calculated from this experiment, is given in the following table (where the value for 1 kg./cm.$^2$ is calculated from Keesom's results, and is only approximate) :—

| Pressure in kg./cm.$^2$. | Compressibility in cm.$^2$/kg. × $10^4$. |
|---|---|
| 20 | 63 |
| 50 | 29 |
| 100 | 13 |
| Average from 1–100 | 48 |

### Table I.

Density of Liquid Helium at 4·2° K.

| Pressure, kg./cm.$^2$. | Density, gm./cm.$^3$. |
|---|---|
| 20 | $\cdot164_1 \pm \cdot001$ |
| 35 | $\cdot176_8$ |
| 50 | $\cdot185_8$ |
| 70 | $\cdot195_4$ |
| 86 | $\cdot201_0$ |
| 101 | $\cdot206_4 \pm \cdot002$ |

Fig. 2.

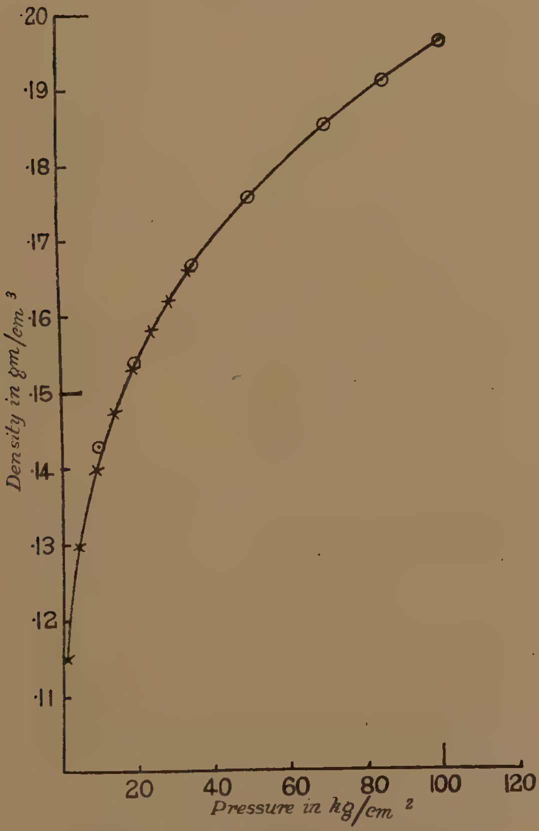

Density of liquid helium at 4·2° K.
Circles show results of present experiment.
Crosses show Keesom's values.

*Amount of Helium.*—The apparatus used in measuring this was made up of a high pressure system and a low pressure system, and the volume, pressure and temperature of all parts of it had to be found.

The low pressure system consisted of a metal cylinder V, of known volume, immersed in a water-bath at room temperature, of which the temperature was read on a mercury thermometer; and the glass connecting tubes and mercury manometer, of small volume, measured by comparison with V and assumed to be at room temperature.

The high pressure system included the pycnometer itself, the capillary tube leading to it, the U-tube O immersed in liquid oxygen, and the manometer and leads at room temperature. These volumes were all small. The pressure was measured on a Bourdon type manometer, which was subsequently calibrated, and which read correct to 1 kg./cm.$^2$.

For the temperature of the capillary lead it was assumed that between liquid air and liquid hydrogen, and again between liquid hydrogen and the pycnometer at 4·2° K., there was a uniform temperature gradient. The uncertainty of this assumption, and the possibility that the capillary tube might not always have been in thermal equilibrium when the readings were taken, have been recognized in estimating the limits of error.

There is a small correction, easily applied, for the mass of gaseous helium remaining in the pycnometer when the liquid has evaporated and the hydrogen is still solid.

*Amount of Hydrogen or Deuterium.*—A flask of known volume was used; the pressure was measured on the mercury manometer, and the temperature on a mercury thermometer.

### *Accuracy of Results.*

The errors may be summarized in two groups, variable and systematic. The variable errors, which differ from one point to the next on the curve, arise from the readings of the pressures; they affect the density by about 0·2 per cent. The systematic errors, which apply to the whole curve, include the errors in the volumes and temperatures of the parts at room temperature, and in the pressure of the hydrogen or deuterium, which are all of the same order of magnitude; they also include the errors in the volume and temperature of the capillary and the effective volume of the U-tube, which become important at the higher pressures, where they can be larger than the other errors. The errors arising from the density of the liquid helium are also systematic, and may be large at high pressures. The systematic error in the hydrogen density may amount to 0·5–0·7 per cent. at 100 atmospheres.

Besides these possible errors of measurement errors due to solution of helium in the hydrogen must also be considered, but these are probably negligible. With respect to this, it may be noted :

(i.) That the helium was not introduced into the pycnometer till the hydrogen was solid, and therefore less likely to dissolve it.

(ii.) That the amount of hydrogen coming out of the pycnometer after the experiment was the same, within the errors of measurement, as that put in, and therefore did not contain any appreciable amount of helium, implying that the solution, if any, was reversible.

(iii.) That if a small quantity of helium is dissolved, and is measured as hydrogen instead of helium, there is no error as long as the volumes of the two are additive ; and as it is improbable that large deviations from additivity occur solution can thus only result in errors of the second order of magnitude.

The effect of variations in the ortho-para ratio must also be considered. For this no special precautions were taken ; but since the hydrogen was always purified by passing it over charcoal at liquid oxygen temperature, the ratio should be that appropriate to this temperature, and therefore always the same ; and the agreement between the different experiments indicates either that this was true or else that the difference between the molar volumes is negligible. The latter is probably true in any case ; Clusius and Bartholomé (3) have estimated that the difference in molar volume between the two pure substances is 0·07 cm.$^3$, giving an extreme difference of densities of 0·3 per cent., which is less than the errors of measurement in the present experiment.

## *Results.*

The results obtained are shown in fig. 3, *a* and *b*, where the hydrogen and deuterium densities are plotted against pressure. Each curve represents the results of one experiment only, to allow the individual points to be shown clearly.

The densities and molar volumes at 4·2° K. and a pressure of 1 kg./cm.$^2$ are recorded in Table II. These figures are taken from the mean of three experiments.

The value ·0890±·0004 for the density of solid hydrogen is to be compared with the figure ·088 at 2° K. found by Keesom, de Smedt and Mooy (10) by an X-ray method ; the difference lies within their experimental error of 1½ per cent.

The compressibilities are found from the slope of the curves in fig. 3, *a* and *b*. They have been calculated for pressures of 1 kg./cm.$^2$ and 100 kg./cm.$^2$, though the latter must only be considered as a very rough

Fig. 3.

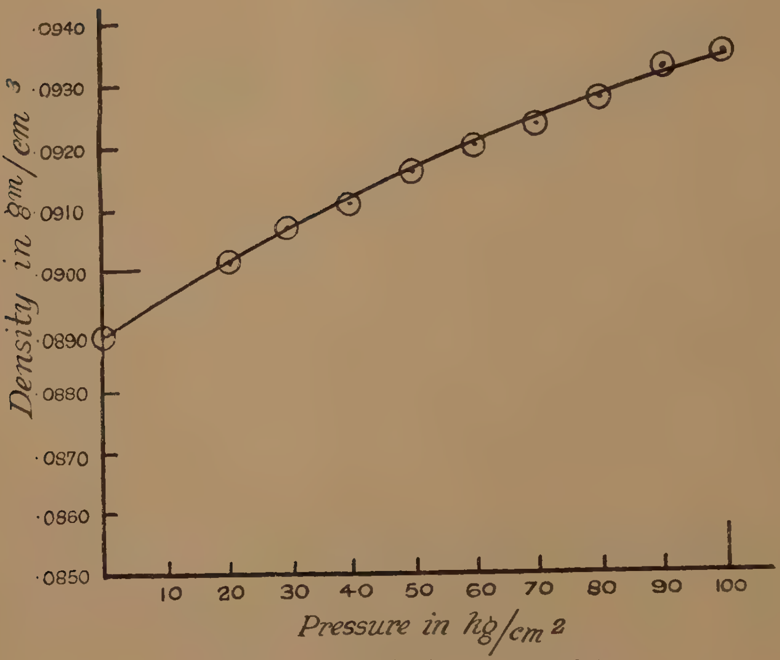

(*a*) Density of solid hydrogen at 4·2° K.

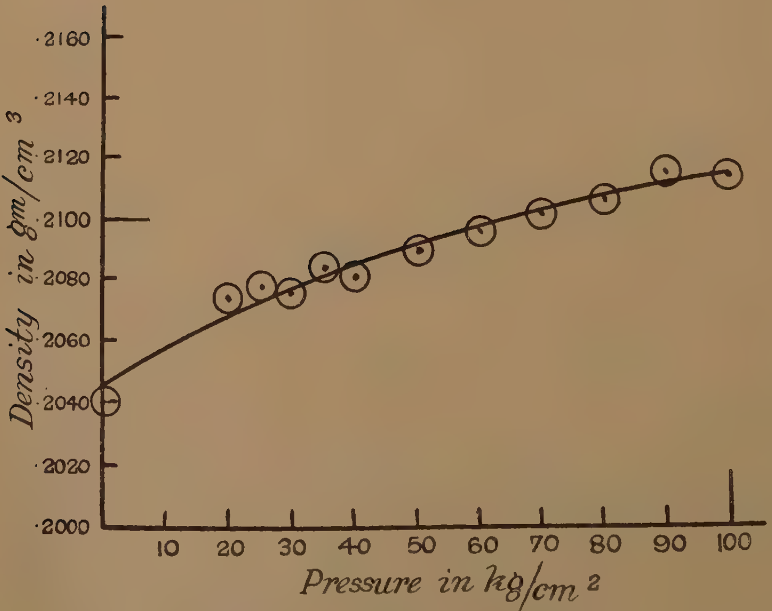

(*b*) Density of solid deuterium at 4·2° K.

estimate, because of the larger experimental error. The mean compressibility over the whole pressure range is also given, with the others, in Table II.

TABLE II.

Density, Molar Volume, and Compressibility of Hydrogen and Deuterium at 4·2° K.

| | Hydrogen. | Deuterium. |
|---|---|---|
| Density (gm./cm.$^3$) at 0 kg./cm.$^2$ pressure | ·0890±·0004 | ·2059±·0010 |
| Molar volume (cm.$^3$) at 0 kg./cm.$^2$ pressure | 22·65±·1 | 19·56±·1 |
| Compressibility (cm.$^2$/kg.) at 0 kg./cm.$^2$ pressure | $(6{\cdot}8 \pm 1{\cdot}5) \times 10^{-4}$ | $(4{\cdot}5 \pm 2) \times 10^{-4}$ |
| Compressibility (cm.$^2$/kg.) at 100 kg./cm.$^2$ pressure | $3{\cdot}2 \times 10^{-4}$ | $2{\cdot}1 \times 10^{-4}$ |
| Compressibility (cm.$^2$/kg.), average for range 0–100 kg./cm.$^2$ | $(5{\cdot}0 \pm 0{\cdot}5) \times 10^{-4}$ | $(3{\cdot}3 \pm 0{\cdot}7) \times 10^{-4}$ |

It is of interest to compare these compressibilities with that of liquid helium at the same temperature, which has an average value, over the range 1–100 kg./cm.$^2$, of $48 \times 10^{-4}$ cm.$^2$/kg., about ten times as great as that of hydrogen.

The only values for hydrogen and deuterium with which the present experimental results can be compared are the calculated values of Bartholomé (5), which have appeared since our note to 'Nature' was published. His values, calculated from a different set of measurements, while necessarily very rough, are of interest at least for their order of magnitude. From the measured value of $\frac{dv}{dp}$ for the liquid, and the calculated change in $\frac{dv}{dp}$ at the transition to the solid, he finds $\frac{dv}{dp}$ for solid hydrogen and deuterium to be 0·014±·006 and 0·006±·006 respectively. These are to be compared with the present experimental values of 0·016±·003, 0·009±·004. The agreement is satisfactory, though strictly the experimental values refer to 4·2° K. while the calculated values refer to the triple point. Similarly from the measured value of $\frac{dv}{dT}$ for the liquid and the calculated change in $\frac{dv}{dT}$ at the transition he finds $\frac{dv}{dT}$ for the solid at the melting-point to be 0·05±·09, −0·08±·12, for hydrogen and deuterium respectively. From the difference between the specific heats at constant pressure and at constant volume (a method whose validity is discussed in more detail later) he obtains values for the expansion coefficient which give $\frac{dv}{dT}$ as

0·12±·04, 0·08±·04. Taking both these methods into consideration, he chooses 0·12±·04, 0·04±·02 as the best values of $\frac{dv}{dT}$ at the triple point. The molar volumes at the triple point are known (3) (see Table III.). Then, assuming that the expansion coefficient is proportional to the cube of the absolute temperature, he calculates the molar volumes at absolute zero, and finds them to be 22·90±·1, 20·3±·1, as compared with the present experimental values at 4·2° K. of 22·65±·1, 19·56±·1. The discrepancy for deuterium is large. This method of calculating the expansion coefficient at different temperatures, however, is probably not to be relied on, for reasons which will be discussed later.

Table III.

Molar Volume and Expansion Coefficients of Hydrogen and Deuterium.

| | Hydrogen. | Deuterium. |
|---|---|---|
| Molar volume (cm.³) at 4·2° K. ................ | 22·65 | 19·56 |
| Molar volume (cm.³) at triple point (3).......... | 23·31 | 20·48 |
| Expansion (cm.³) up to triple point, $\Delta v$ ........ | ·66 | ·92 |
| Percentage change in volume, $\frac{\Delta v}{v}\times 10^2$ ....... | 2·9 | 4·7 |
| Calculated volume (cm.³) at 0° K. .............. | 22·57 | 19·49 |
| Volume expansion coefficient at 11° K., calculated from experimental $C_p-C_v$ ............. | $\cdot 51\times 10^{-2}$ | $\cdot 37\times 10^{-2}$ |
| Volume expansion coefficient at 4·2° K., calculated from $C_v-(C_v)_{v_T}$ ..................... | $\cdot 24\times 10^{-2}$ | $\cdot 17\times 10^{-2}$ |

### *Discussion.*

In what follows an attempt is made to apply Grüneisen's theory (11) to solid hydrogen, and it will be seen that a consistent picture cannot be obtained. Since, however, a recognition of the discrepancies is a necessary step in overcoming them, it is important to consider the application of the theory in detail.

It is supposed that the crystal of solid hydrogen may be considered as an isotropic lattice with a single characteristic frequency. Actually the crystal structure (10) is not cubic, but hexagonal close-packed; but physically the difference between these structures is small. It is known (12), (13) that the frequencies of a lattice must in reality be represented by a continuous spectrum; in general the only practicable treatment is that of Debye, which assumes a single maximum frequency, and a corresponding characteristic temperature $\theta$. It is doubtful whether, considering the large zero-point energies, this simple theory may justifiably be applied to solid hydrogen, but it will be of interest to make the attempt and see what consequences follow.

The ortho-para equilibrium is not concerned in the questions which are to be discussed. It has been shown already that the values of the densities are not appreciably altered. The ortho-para transition of course affects the specific heat by the internal transitions due to degeneration of the ortho term, but this is not a molecular vibration but another degree of freedom, and so can be neglected for our discussion. In what follows "specific heat" will be used to mean that part only which is due to molecular vibrations.

The Debye theory applies to the specific heat at constant volume; but the specific heats at constant pressure were the first to be measured 3), (4), and were found to fit satisfactorily on to a Debye curve with $\theta$ equal to 91° K. for hydrogen and 89° K. for deuterium. The quantities needed in order to calculate $C_p - C_v$ were then unknown, and the correction was thought to be small. It can now be calculated, however, that it is very large; and meanwhile Bartholomé and Eucken (5), (14) have proved the same fact directly by measuring $C_v$ experimentally. They find that $C_v$ also follows a Debye curve for both hydrogen and deuterium, the $\theta$'s being 105° and 97° respectively. These $\theta$'s refer to the volume at 11° K. and saturation pressure (practically zero pressure), the volume having been enclosed under those conditions.

At this point it is necessary to make clear to what $C_v$ refers. Normally if $C_p$ is measured $C_v$ can be calculated by means of the thermodynamic formula

$$C_p - C_v = \frac{(3\alpha)^2 T v}{K}, \quad . \quad . \quad . \quad . \quad . \quad . \quad . \quad . \quad . \quad (1)$$

where K is the compressibility, $\alpha$ the linear coefficient of thermal expansion, and $v$ the volume at 0° K., all these being known. These $C_v$'s, however, calculated in this way from the $C_p$ curve, do not refer all to the same volume, but each to the volume the substance will take up at the particular temperature if the pressure is kept constant. We shall denote them by $(C_v)_{v_T}$. Hence the $C_v$—T correlation determined in this way cannot be directly compared with theory, for example with the Debye theory, for it deals with a substance which is kept at constant volume throughout. These specific heats, referring to the volume occupied at 0° K., we shall call $(C_v)_{v_0}$. In most cases $(C_v)_{v_T}$ does not differ very much from $(C_v)_{v_0}$, but in the present case, as we shall see, the differences are appreciable. This consideration also affects $\theta$; thus $(\theta)_{v_{11}}$, deduced from measurements of $(C_v)_{v_{11}}$, will be less than $(\theta)_{v_0}$, which is derived from $(C_v)$ . The difference is given by

$$\frac{\delta\theta}{\theta} = -\gamma\frac{\delta v}{v} = -\gamma\int_0^T 3\alpha . dT, \quad . \quad . \quad . \quad . \quad . \quad . \quad (2)$$

where, by definition,

$$\gamma=-\frac{d\log\theta}{d\log v}, \quad . \quad . \quad . \quad . \quad . \quad . \quad . \quad . \quad . \quad . \quad (3)$$

which is assumed to be a constant. When $\gamma$ and $\alpha$ are known $\delta\theta$ may be calculated.

It is now possible to make calculations using the experimentally determined facts.

A comparison of the $\theta$-values for hydrogen and deuterium may be used to find $\gamma$. Theoretically if both had the same molar volume their $\theta$'s should be in the ratio $\sqrt{2}:1$. Suppose that deuterium is made to expand until its molar volume equals that of hydrogen at the same temperature, its characteristic temperature meanwhile changing from $\theta_D$ to $\theta'_D$. Then

$$\gamma_D=-\frac{\delta\log\theta}{\delta\log v}=\frac{\log\theta_D-\log\theta'_D}{\log v_H-\log v_D}=\frac{\log\theta_D-\log\theta_H+\frac{1}{2}\log 2}{\log v_H-\log v_D}.$$

For $\theta_H=105°$, $\theta_D=97°$, this gives $\gamma_D$ equal to 1·8. The same value is obtained for $\gamma_H$ (as is implied in the assumptions of the method). Since $\gamma$ is about 2 for most simple crystals this seems a reasonable result.

It will be noticed that in this calculation we have used the $(\theta)_{v_{11}}$'s. Actually it makes little difference what temperature the $\theta$'s are referred to in calculating $\gamma$, as the ratio of the pair remains nearly constant, and hence $\gamma$ is unaffected. The $(\theta)_{v_0}$'s at 11° K. may be calculated from equation (2), by substituting the value of $\gamma$ and deducing $3\alpha\,.\,dT$ from the total change of volume up to the triple point on the assumption that $\alpha$ is linear with T, which will be justified later; they are found in this way to be 108°, 101° respectively.

Using this value of $\gamma$, the part of the compressibility arising from the zero-point energy may be calculated. It has been shown by Simon(15) that there is a pressure $p^{(\circ)}$ due to the zero-point energy,

$$p^{(\circ)}=\frac{9}{8}R\gamma\frac{\theta}{v},$$

which in turn gives rise to a compressibility $K^{(\circ)}$,

$$K^{(\circ)}=\frac{v}{\frac{9}{8}R\theta\gamma(\gamma+1)},$$

if $\gamma$ is taken as constant. When this is evaluated, taking $\theta$ as $(\theta)_{v_0}$, and putting $\gamma$ equal to 1·8, $K^{(\circ)}$ is found to be $4{\cdot}5\times10^{-4}$ for hydrogen and $4{\cdot}2\times10^{-4}$ for deuterium. This is of the same order of magnitude as the experimentally determined compressibility, and strongly suggests that the greater part of the whole compressibility is attributable to the zero-point energy.

There are no measurements of the thermal expansion coefficients of solid hydrogen and deuterium at different temperatures, though the total thermal expansions from 4·2° K. to the triple points are known * (Table III.). It is usual to assume the truth of Grüneisen's law, that the expansion coefficient is proportional to the specific heat,

$$3\alpha=\gamma\frac{C_v K}{v}, \quad . \quad . \quad . \quad . \quad . \quad . \quad . \quad . \quad . \quad . \quad (4)$$

$\gamma$ being constant. Then since $C_v$ follows a Debye curve, $\alpha$ should be proportional to $T^3$ at low temperatures. Now it can easily be shown that this is in direct disagreement with the experimental results, for if both $C_v$ and $C_p$ follow Debye curves, as the experiments indicate, $\alpha$ must be roughly proportional to T instead of to $T^3$ as the theory assumes. To prove this, neglecting for the moment the difference between $(C_v)_{v_T}$ and $(C_v)_{v_0}$, and taking K as constant †, we have

$$C_p-C_v \propto \alpha^2 T,$$

and, at low temperatures where the approximation holds,

$$C_p \propto T^3, \quad C_v \propto T^3.$$

Hence $$\alpha^2 T \propto T^3,$$

or $$\alpha \propto T.$$

It has been assumed that the Debye curve represents the $C_p$ and $C_v$ values down to the lowest temperatures; actually, of course, this is an extrapolation from experiment. $C_v$ has been measured down to 11° K., $C_p$ for deuterium has been measured down to 10° and begins to show departure from the curve below 11°, but $C_p$ for hydrogen follows it down to 4° K., below which temperature the ortho-para change makes the values uncertain.

If the errors introduced by putting $(C_v)_{v_0}$ equal to $(C_v)_{v_T}$ and substituting a $T^3$ law for the Debye function are considered, both corrections are found to have the effect of making $\alpha$ increase more slowly at higher temperatures, *i. e.*, the curve of $\alpha$ against T will be concave to the T-axis. If $\alpha$ is proportional to T then, according to (4), $\gamma$ is not constant but inversely proportional to $T^2$.

It is possible to carry out the calculation of $\alpha$ from the experimental values of $C_v$ and $C_p$:

$$(3\alpha)^2=\frac{(C_p-C_v)K}{vT}. \quad . \quad . \quad . \quad . \quad . \quad . \quad . \quad . \quad (5)$$

---

* These, however, are the differences of quantities determined in two quite separate experiments, using completely different methods, and are therefore liable to have a large percentage error.

† If K is assumed not to be constant, in an attempt to evade the difficulty, then in order that Grüneisen's law may hold K must be proportional to $T^4$, which is very improbable.

This formula strictly refers to $(C_v)_{v_T}$, while the experimental results give $(C_v)_{v_{11}}$, but the difference may be neglected for a first approximation; its effect will be discussed in the next paragraph. A set of values for $3\alpha$ is obtained, and these are plotted against T in fig. 4, *a* and *b* (curve I). This calculation does not use the experimental value of $\triangle v$, the total change in volume between 4·2° K. and the triple point, which may therefore be used to check its validity. From the curves, $\triangle v=4\cdot3\times10^{-2}$ for hydrogen and $4\cdot9\times10^{-2}$ for deuterium, as compared with the experimental values of $2\cdot9\times10^{-2}$, $4\cdot7\times10^{2}$ respectively. This is reasonably good agreement.

It does not seen justified, however, to neglect $(C_v)_{v_T}-(C_v)_{v_{11}}$, and an attempt may be made to take it into account. For calculating the correction, if $C_v$ is proportional to $\left(\frac{T}{\theta}\right)^3$, since $\gamma$ is $-\frac{d\log\theta}{d\log v}$,

$$(C_v)_{v_T}-(C_v)_{v_{11}}=3(C_v)_{v_{11}}\gamma\frac{v_T-v_{11}}{v_{11}}$$

$$=3(C_v)_{v_{11}}\gamma\sum_{0}^{T}3\alpha.\delta T. \quad . \quad . \quad . \quad . \quad . \quad (6)$$

A corrected formula can be used to take into account departure from the $T^3$ law. $\gamma$ is assumed to be 1·8, as found above. When T is 11° K. the correction is zero, and $3\alpha_{11}$ has the value already found. Taking $\alpha$ as constant from 11° to 12°, $(C_v)_{v_{12}}$ can then be calculated from (6). This, substituted in (5), gives $3\alpha_{12}$, and so in turn $(C_v)_{v_T}$ can be found for each value of T up to 14° K. The same method can be applied to temperatures below 11°, $(C_v)_{v_T}$ here being less than $(C_v)_{v_{11}}$. When this correction is carried out the curves of $3\alpha$ plotted against T are as shown in fig. 4, *a* and *b*, curve II. It will be seen that the values are only slightly higher than in the uncorrected curves up to 11° K., above which they reach a maximum and then decrease. Whether this decrease is real may be questioned, because at these temperatures the values of $C_p-C_v$ thus calculated are fairly sensitive to variation in $\gamma$, which has here been taken as constant. Below 11° the course of the curves shows that the correction is in any case small at these temperatures. Each curve is in this region nearly a straight line, with a slight concavity to the T-axis; the values of $\triangle v$ calculated from them are almost identical with those from the uncorrected curves. The values of $3\alpha$ at 4·2° and 11°, thus found, are given in Table III.

One consequence of this must be noted. If $\alpha$ varies roughly as T, and not as $T^3$ as has hitherto been assumed, it can no longer be said that the molar volume at 4·2° K. is equal to that at the absolute zero. The graph in fig. 4 allows us to calculate the latter. Taking the uncorrected curves, we obtain for hydrogen

$$\frac{[\Delta v]_0^{4\cdot 2}}{[\Delta v]_{4\cdot 2}^{14}} = \frac{\cdot 49}{4\cdot 32} = \cdot 11,$$

Fig. 4.

Thermal expansion calculated from $C_p - C_v$.

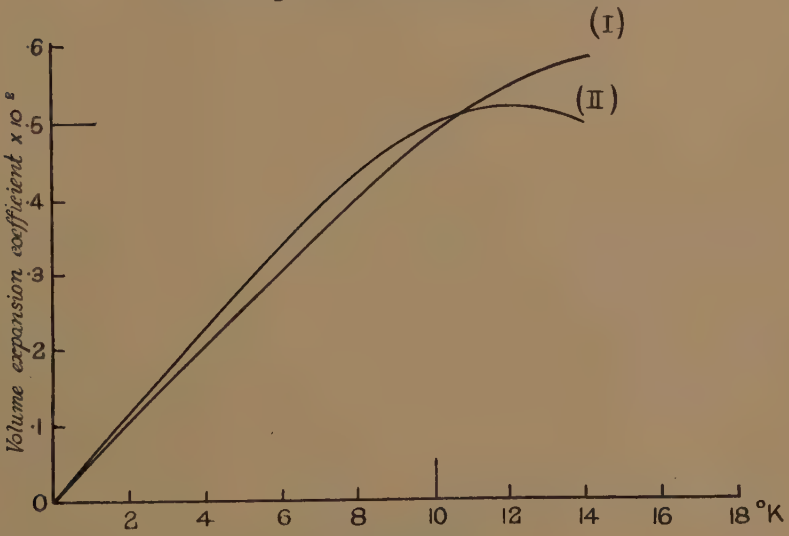

(*a*) Hydrogen.

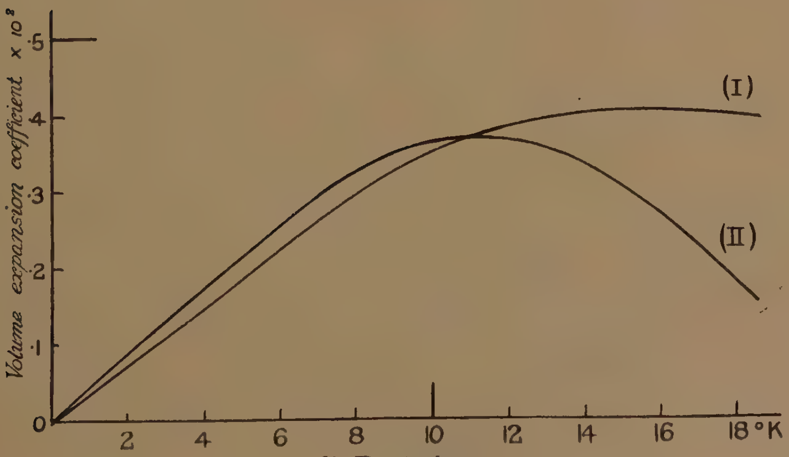

(*b*) Deuterium.

(I) Uncorrected curve.
(II) Corrected curve.

$$\therefore \qquad [\Delta v]_0^{4\cdot 2} = \cdot 66 \times \cdot 11 = \cdot 08 \text{ cm.}^3,$$

$$\therefore \qquad v_0 = 22\cdot 65 - \cdot 08 = 22\cdot 57 \text{ cm.}^3;$$

and for deuterium

$$\frac{[\Delta v]_0^{4\cdot 2}}{[\Delta v]_{4\cdot 2}^{18\cdot 65}} = \frac{\cdot 34}{4\cdot 26} = \cdot 08,$$

$$\therefore \qquad [\Delta v]_0^{4\cdot 2} = \cdot 92 \times \cdot 08 = \cdot 07 \text{ cm.}^3,$$

$$\therefore \qquad v_0 = 19\cdot 56 - \cdot 07 = 19\cdot 49 \text{ cm.}^3$$

These corrections are of the same order of magnitude as the experimental error.

It follows directly from the experimental data, then, that the variation of the expansion coefficient with temperature is not that usually postulated by theory. Grüneisen's law, with a single constant $\gamma$, cannot be used to express it. This explains the discrepancies which are found when an attempt is made to calculate $C_v$ from the curve for $C_p$, introducing the experimental values of K and $v$ into the ordinary thermodynamic formulæ (1) and (4), which are used alternately to find $C_v$ by a series of successive approximations. It will be clear from what has gone before that this calculated $C_v$ cannot follow a Debye curve, and is thus in contradiction to experiment.

There are two possible explanations: either the experimental results for the specific heats are inaccurate or the ordinary theory cannot be applied to this case. For hydrogen the $C_p$ measurements go down to about 3° or 4° K., below which they cannot be relied on owing to ortho-hydrogen present as impurity. For deuterium measurements have been made down to 10·4°; below 11° they departed somewhat from the Debye curve, with $\theta$ rather less than 89°. The measurements of $C_v$ have been made down to 11°. It does not seem likely that an explanation of the difficulty is to be found here. The conclusion which must be drawn is that the ordinary treatment cannot be applied to a substance of high zero-point energy. It is possible that treatment on the lines of London's theory of helium (2) might account satisfactorily for it, or perhaps a combination of this with the ordinary theory; but in any case it is obvious that the treatment will be difficult.

From the experimental point of view it would be of very great interest to have direct measurements of the expansion coefficients at different temperatures. The X-ray method of measuring the change in lattice spacing seems the most promising for this purpose. It would also be desirable that exact determinations of the specific heats should be carried out down to liquid helium temperature.

## *Acknowledgments.*

I am very greatly indebted to Professor F. Simon for suggesting this work and for his advice and helpful criticism throughout its course. My thanks are also due to Professor F. A. Lindemann for his kind permission to work in the Clarendon Laboratory, Oxford ; to Girton College, Cambridge, for the Research Fellowship which made the work possible ; and to Dr. N. Kurti for his constant and valuable help throughout the experiments.

The work described in this paper was carried out in 1935–6, but its publication has been delayed owing to the intervention of other work.

## *Summary.*

Direct experimental determinations have been made of the density of solid hydrogen and deuterium at 4·2° K. and pressures up to 100 atmospheres, and the compressibilities have been calculated. These results have been used to discuss the relations between the specific heats at constant pressure and constant volume and the expansion coefficients from the standpoint of Grüneisen's law and the Debye theory. It is shown that the usual treatment fails to give consistent results, the failure being attributed to the large part played by zero-point energy, which is not taken into consideration in the ordinary theory.

## *References.*

(1) Bennewitz and Simon, *Z. Physik.* xvi. p. 183 (1923).
(2) F. London, Proc. Roy. Soc. A, cliii. p. 576 (1936).
(3) Clusius and Bartholomé, *Z. Phys. Chem.* B, xxx. p. 237 (1935).
(4) Simon and Lange, *Z. Physik*, xv. p. 307 (1923).
(5) Bartholomé, *Z. Phys. Chem.* B, xxxiii. p. 387 (1936).
(6) Megaw and Simon, 'Nature,' cxxxviii. p. 244 (1936).
(7) See, for instance, *Actes du VII Congrès International du Froid*, i, p. 367 (1936) ; and Proc. Phys. Soc. xlvii. p. 678 (1935).
(8) Kaischew, Dissertation, Breslau, 1932.
(9) W. H. Keesom and A. P. Keesom, 'Physica,' i. p. 128 (1933).
(10) Keesom, de Smedt and Mooy, Proc. Acad. Amsterdam, xxxiii. p. 814 (1930)
(11) See, for instance, *Handbuch der Physik*, vol. x. Berlin, 1926.
(12) Born, 'Atomtheorie des Festen Zustandes,' 1923.
(13) Blackman, Proc. Roy. Soc. A, cxlviii. p. 365 (1935).
(14) Bartholomé and Eucken, *Z. Elektrochem.* xlii. p. 547 (1936).
(15) Simon, 'Nature,' cxxxiii. p. 529 (1934).

# XII. *Gas Flow in Solids.*

By R. M. Barrer
(Department of Colloid Science), The University, Cambridge *.

[Received May 15, 1939.]

The permeability (P) and the diffusion constant (D) are the most characteristic quantities measured in the study of gas flow in solids. They are given by the equations

$$P=-D\frac{\partial c}{\partial x},$$

$$\frac{\partial c}{\partial t}=D\frac{\partial^2 c}{\partial x^2}.$$

Solids for which no surface reactions are involved in the flow processes follow the various solutions of the diffusion equation, such as those given below for diffusion into and through a plate of thickness $l$ :

$$P=D\frac{c_1-c_2}{l} \text{ (in the steady state),} \quad . \quad . \quad . \quad . \quad . \quad (1)$$

where $c_1$ and $c_2$ are the concentrations at $x=0$, $x=l$, and $c_0$ is the initial concentration in the solid. Also

$$c=c_1+(c_2-c_1)\frac{x}{l}+\frac{2}{\pi}\sum_{n=1}^{\infty}\frac{c_2\cos n\pi-c_1}{n}\sin\frac{n\pi x}{l}e^{-\frac{Dn^2\pi^2t}{l^2}}$$
$$+\frac{4c_0}{\pi}\sum_{m=0}^{\infty}\frac{1}{(2m+1)}\sin\frac{(2m+1)\pi x}{l}e^{-\frac{D(2m+1)^2\pi^2t}{l}}, \quad . \quad . \quad . \quad (2)$$

where $c$ denotes the concentration in the solid at a point $x$ and a time $t$. Also $\phi$, the quantity sorbed at time $t$, when $c_1=c_2$ is given by

$$\phi=c_1l-(c_0-c_1)\frac{4l}{\pi^2}\sum_{m=0}^{\infty}\frac{1}{(2m+1)^2}e^{-\frac{D(2m+1)^2\pi^2t}{l^2}} \quad . \quad . \quad . \quad . \quad (3)$$

When gas flows through the plate, and the steady state of flow is not established, the curve of $c$ against $t$ on the outgoing side of the plate (here taken as $x=l$) approaches asymptotically a line whose intercept (1) on the axis at $t=0$ is

$$L=\frac{l^2}{6D}\frac{1}{(c_1-c_2)}[c_1+2c_2-3c_0]. \quad . \quad . \quad . \quad . \quad . \quad . \quad (4)$$

---

* Communicated by Eric K. Rideal.

From equations such as (2) one may measure D in two ways :—

(*a*) from $c$ as a function of $x$ at a given $t$.

(*b*) from $c$ as a function of $t$ at a given $x$.

When three processes occur, solution at the surface, desorption into the surface, and diffusion within the solid, one has still in equations similar to (1), (2), (3), and (4), if they could be derived, sufficient relations to allow each velocity constant to be calculated. The diffusion problem may be more complex if one has an adsorbed layer in equilibrium with a gas phase, and a dissolved phase simultaneously, for here five constants are involved. By measuring the adsorption at the surface a new relation between the velocity constants may be found, and in principle one has then enough equations to determine the five constants. Usually one aims at conducting the experiment so that some processes are so much faster than others as not to be in any way rate controlling.

J. S. Wang (2), treating the problem of gas flow in metals, introduced two further surface processes so that seven constants are involved. Like the three and five constant problems, this has not been solved for non-stationary states of flow. Wang's equation for the steady state contains seven constants, none of which can be explicitly evaluated.

The object of the present paper is to solve the three-constant problem, and also for special circumstances the five-constant problem. The methods used are those employed in solving the equation for combined heat flow and radiation. This is a two-constant problem which may, however, be adapted to the present more complex systems. The general solution can be obtained as the sum of two superposed solutions for more restricted cases.

## *Formulation of the Problem.*

Across a slab of the solid of thickness $l$, bounded by the planes $x=0$ and $x=l$, the initial state is as illustrated in fig. 1 *a*.

There are gas phase concentrations $v_3$ and $v_4$, and surface concentrations $v_1$ and $v_2$. Inside the solid there is an initial distribution $v=f(x)$. The following processes may occur :—

(1) Gas to sorption layer. Velocity constant $k_3$.

(2) Sorption layer to gas. Velocity constant $k_4$.

(3) Sorption layer to solid (through the planes $x=0$, $x=l$). Velocity constant $k_1$.

(4) Solid to sorption layer (through the planes $x=0$, $x=l$). Velocity constant $k_2$.

(5) Diffusion within the solid, between $x=0$, $x=l$, for which

$$\frac{\partial u}{\partial t}=\mathrm{D}\frac{\partial^2 u}{\partial x^2}.$$

The two additional processes suggested by Wang (2) for gas flow in metals are:

(6) A gas molecule dissociates as it strikes the surface, one atom remaining on the surface and the other atom entering the solid. Velocity constant $k_5$.

(7) A gas atom in the metal enters the surface, combines with another atom and evaporates as a molecule. Velocity constant $k_6$.

The distribution expressed in fig. 1 (*a*) may be divided into the two distributions of fig. 1 (*b*) and (*c*). Fig. 1 (*c*) represents the distribution for the steady state of flow, and fig. 1 (*b*) represents a non-stationary state of flow in which the concentrations at the boundaries $x=0$ and $x=l$ are so nearly zero that the process (3) may be neglected. The distribution of fig. 1 (*b*) tends to preclude several mechanisms of flow. Process (7) involves a surface concentration. The processes (1) to (5) are possible only when $k_4$ is $\geqslant k_2$, because otherwise a surface concentration could build up at $x=0$ and $x=l$. With this proviso, however, fig. 1 (*b*) and (*c*) give distributions suitable for solving the problem.

Fig. 1.

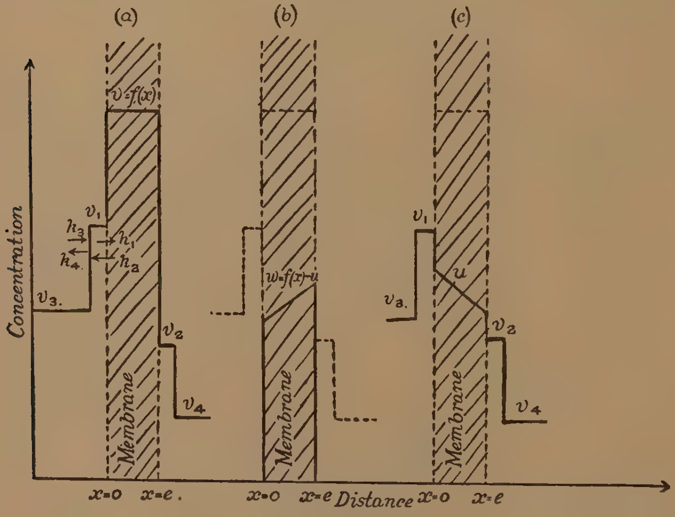

Concentration distribution.

(*a*) Initial distribution.
(*b*) and (*c*) Distributions used in solving for initial distribution.

The solutions to be given treat two main problems :

I. Adsorption equilibrium is rapidly established compared with absorption processes across the interfaces $x=0$ and $x=l$. Processes (6) and (7) are not considered.

II. Absorption does not occur from an adsorbed layer, but molecules enter and leave the solid directly from gas phase to solid, or *vice versa*. This problem is a special case of the first problem, and will be considered after solving the first.

In both I. and II. the molecular states are supposed to be the same in the gas phase and in the solid.

### PROBLEM I.

#### (A) *Solution for the Non-Stationary State of Flow* (fig. 1 (*b*)) (*solution for w*).

From fig. 1 (*b*) one may write the equation of flow and the boundary conditions as follows :

$$\frac{dw}{dt}=\mathrm{D}\frac{d^2w}{dt^2}\,(0<x<l). \quad . \quad . \quad . \quad . \quad . \quad . \quad . \quad (5)$$

At $x=0$

$$\frac{-dw}{dt}+\frac{k_2}{\mathrm{D}}w=0. \quad . \quad . \quad . \quad . \quad . \quad . \quad . \quad . \quad (6)$$

At $x=l$

$$\frac{dw}{dt}+\frac{k_2}{\mathrm{D}}w=0. \quad . \quad . \quad . \quad . \quad . \quad . \quad . \quad . \quad (7)$$

At $t=0$

$$w=f(x)-u=w_0. \quad . \quad . \quad . \quad . \quad . \quad . \quad . \quad . \quad (8)$$

The expression $e^{-\mathrm{D}\alpha^2t}$ ($\mathrm{A}.\cos\alpha x+\mathrm{B}\sin\alpha x$) satisfies (22). It also satisfies (23) and (24) if

$$-\alpha\mathrm{B}+\frac{k_2}{\mathrm{D}}.\mathrm{A}=0$$

$$\alpha(\mathrm{B}\cos\alpha l-\mathrm{A}\sin\alpha l)+\frac{k_2}{\mathrm{D}}(\mathrm{B}\sin\alpha l+\mathrm{A}\cos\alpha l)=0. \quad . \quad . \quad . \quad (9)$$

From (9) one obtains

$$\left.\begin{aligned} \mathrm{A}&=\frac{\alpha\mathrm{D}}{k_2}.\mathrm{B},\\ \tan\alpha l&=\frac{2\alpha\frac{k_2}{\mathrm{D}}}{\alpha^2-\left(\frac{k_2}{\mathrm{D}}\right)^2}.\end{aligned}\right\} \quad . \quad . \quad . \quad . \quad . \quad . \quad (10)$$

Thus the problem takes the same form as the flow of heat in a plate of thickness $l$ with radiation at the ends into an enclosure at zero temperature. A solution of this problem has been given elsewhere $^{(3)}$, so that the details need not be considered here. Writing $h$ for $\frac{k_2}{\mathrm{D}}$, the solution becomes

$$w=2\sum_{1}^{\infty}e^{-\mathrm{D}\alpha_n^2t}\frac{\alpha_n\cos\alpha_nx+h\sin\alpha_nx}{(\alpha_n^2+h^2)+2h}\int_0^l(f(x)-u)(\alpha_n\cos\alpha_nx+h\sin\alpha_nx)dx, \quad . \quad . \quad . \quad (11)$$

where $\alpha_n$ is the $n$th positive root of $\tan\alpha l=\frac{2\alpha h}{(\alpha^2-h^2)}$.

Should the value of $v=f(x)$ at $t=0$ (fig. 1 ($a$)) be $v=v_0$, then inspection of fig. 1 ($b$) shows that

$$w_0=f(x)-w=v_0-u_0+(u_0-u_l)\frac{x}{l}, \quad . \quad . \quad . \quad . \quad . \quad . \quad (12)$$

where $u_0$ denotes the value of $u$ at $x=0$, and $u_l$ is the value of $u$ at $x=l$. One may now obtain the unevaluated integral of the general solution (11). If

$$\mathrm{I}=\int_0^l(f(x)-u)(\alpha_n.\cos\alpha_nx+h.\sin\alpha_nx)dx,$$

with the value of $w_0$ given by (12) one may integrate directly, obtaining

$$\mathrm{I}=(v_0-u_0)\left[\sin\alpha_nl\frac{\alpha_n^2+h^2}{2\alpha_n^2}+\frac{h}{\alpha_n}\right]+(u_0-u_l)\left[\sin\alpha_nl\frac{(\alpha_n^2+h^2)}{2\alpha_n^2}\left(1+\frac{1}{lh}\right)-\frac{1}{l\alpha_n}\right]=\frac{k_2}{\mathrm{D}\alpha_n}\{2(v_0-u_0)+(u_0-u_l)\}. \quad (13)$$

(B) *Solution for the Steady State of* fig. 1 ($c$).

($a$) There are two sets of equations to be obtained. The first set gives the relations between the surface concentrations ($v_1$, $v_2$) and the concentrations ($u_0$, $u_l$) at a point just inside the solid, and in the gas phase respectively ($v_3$, $v_4$). The first set of equations is thus

$$\text{At } x=0,\ 0=k_3v_3\left(1-\frac{v_1}{v_s}\right)+k_2u_0\left(1-\frac{v_1}{v_s}\right)-k_4v_1-k_1v_1\left(1-\frac{u_0}{u_s}\right). \quad . \quad . \quad (14)$$

$$\text{At } x=l,\ 0=k_3v_4\left(1-\frac{v_2}{v_s}\right)+k_2u_l\left(1-\frac{v_2}{v_s}\right)-k_4v_2-k_1v_2\left(1-\frac{u_l}{u_s}\right). \quad . \quad . \quad (15)$$

(where $v_s$, $u_s$ denote saturation concentrations on the surface and in the solid respectively), so that

$$v_1=\frac{k_3v_3+k_2u_0}{k_3\frac{v_3}{v_s}+k_2\frac{u_0}{v_s}+k_4+\left(1-\frac{u_0}{u_s}\right)k_1}. \quad . \quad . \quad . \quad . \quad (16)$$

$$v_2=\frac{k_3v_4+k_2u_l}{k_3\frac{v_4}{v_s}+k_2\frac{u_l}{v_s}+k_4+\left(1-\frac{u_l}{u_s}\right)k_1}\quad . \quad . \quad . \quad . \quad . \qquad (17)$$

For the conditions when the solutions of equations (11) and (13) may be applied, *i. e.*, when sorption-desorption equilibrium between gas and adsorbed phase is very rapidly established, one has

$$v_1=\frac{k_3v_3}{\frac{k_3v_3}{v_s}+k_4}\quad . \quad . \quad . \quad . \quad . \quad . \quad . \quad . \quad . \qquad (18)$$

$$v_2=\frac{k_3v_4}{\frac{k_3v_4}{v_s}+k_4}\quad . \quad . \quad . \quad . \quad . \quad . \quad . \quad . \quad . \qquad (19)$$

(*b*) One may now formulate the second set of equations for the transfer of adsorbed and dissolved gas across the interfaces at $x=0$, $x=l$ and its diffusion in the solid in the steady state of flow. These equations are

$$\frac{d^2u}{dx^2}=0 \quad (0<x<l) \quad . \quad . \quad . \quad . \quad . \quad . \quad . \quad . \qquad (20)$$

$$\text{At } x=0,\quad \mathrm{D}\frac{du}{dx}-k_2u_0\left(1-\frac{v_1}{v_s}\right)+k_1v_1\left(1-\frac{u_0}{u_s}\right)=0. \quad . \quad . \qquad (21)$$

$$\text{At } x=l,\quad -\mathrm{D}\frac{du}{dx}-k_2u_l\left(1-\frac{v_2}{v_s}\right)+k_1v_2\left(1-\frac{u_l}{u_s}\right)=0. \quad . \quad . \qquad (22)$$

The equation $u=\mathrm{A}x+\mathrm{B}$ satisfies (20). It will also satisfy (21) and (22) if

$$\mathrm{DA}-k_2\mathrm{B}\left(1-\frac{v_1}{v_s}\right)+k_1v_1\left(1-\frac{\mathrm{B}}{u_s}\right)=0, \quad . \quad . \quad . \quad . \qquad (23)$$

$$-\mathrm{DA}-k_2(\mathrm{A}l+\mathrm{B})\left(1-\frac{v_2}{v_s}\right)+k_1v_2\left(1-\frac{\mathrm{A}l+\mathrm{B}}{u_s}\right)=0. \quad . \quad . \qquad (24)$$

If one writes $\beta_1=1-\frac{v_1}{v_s}$, $\beta_2=\left(1-\frac{v_2}{v_s}\right)$ one finds on solving (23) and (24)

$$\mathrm{A}=\frac{k_1k_2v_2\beta_1-k_1k_2v_1\beta_2}{\left(k_2\beta_1+\frac{k_1v_1}{u_s}\right)\left(\mathrm{D}+k_2\beta_2+\frac{k_1v_2}{u_s}\right)+\mathrm{D}\left(k_2\beta_2+k_1\frac{v_2}{u_s}\right)}\quad . \quad . \qquad (25)$$

$$\mathrm{B}=\frac{\mathrm{D}k_1v_2+k_1v_1\left(\mathrm{D}+k_2l\beta_2+\frac{k_1v_2l}{u_s}\right)}{\left(k_2\beta_1+\frac{k_1v_1}{u_s}\right)\left(\mathrm{D}+k_2l\beta_2+\frac{k_1v_2l}{u_s}\right)+\mathrm{D}\left(k_2\beta_2+k_1\frac{v_2}{u_s}\right)}\quad . \quad . \qquad (26)$$

The complete expressions (25) and (26) assume more simple form when special conditions apply, most of which are, from a practical viewpoint, very important :

(1) The pressure on the ingoing side is very high so that $\beta_1=0$.

$$A=\frac{-k_1k_2v_1\beta_2}{\frac{k_1v_1}{u_s}\left(D+k_2l\beta_2+\frac{k_1v_2l}{u_s}\right)+Dk_2\beta_2+\frac{k_1v_2\cdot}{u_s}} \quad . \quad . \quad . \quad (27)$$

$$B=\frac{Dk_1v_2+k_1v_1\left(D+k_2\beta_2+\frac{k_2v_2l}{u_s}\right)}{k_1\frac{v_1}{u_s}\left(D+k_2\beta_2+\frac{k_1v_1l}{u_s}\right)+D\left(\frac{k_1v_2}{u_s}\right)+Dk_2\beta_2}, \quad . \quad . \quad (28)$$

while $u=Ax+B$.

(2) If the pressure on the outgoing side of the membrane is very low, and that on the ingoing side is very high, one has $\beta_2=1$, $\beta_1=0$ ; $v_1=v_s$, $v_2=0$. Then

$$A=\frac{-k_1k_2v_s}{D\left(\frac{k_1v_s}{u_s}+k_2\right)+\frac{k_1k_2v_sl}{u_s}}, \quad . \quad . \quad . \quad . \quad . \quad . \quad . \quad (29)$$

$$B=\frac{k_1v_s(D+k_2l)}{k_1\frac{v_s}{u_s}(D+k_2l)+Dk_2}, \quad . \quad . \quad . \quad . \quad . \quad . \quad . \quad (30)$$

where $u=Ax+B$.

(3) If the pressures on both the ingoing and the outgoing sides are sufficiently low, or the temperature sufficiently high, one may write $\beta_1=\beta_2=1$. Also $v_1$, $v_2 \ll v_s$, and if $v_s$ and $u_s$ are of the same order, $v_1$, $v_2 \ll u_s$. This case is most frequently encountered experimentally. One then has

$$A=\frac{k_1(v_2-v_1)}{2D+k_2l}, \quad . \quad . \quad . \quad . \quad . \quad . \quad . \quad . \quad . \quad . \quad (31)$$

$$B=\frac{Dk_1v_2+k_1v_1(D+k_2l)}{k_2(2D+k_2l)}, \quad . \quad . \quad . \quad . \quad . \quad . \quad . \quad (32)$$

where $u=Ax+B$.

### *The Permeabilities in the Steady State.*

The permeability P is defined by

$$P=-D\frac{du}{dx}=-DA,$$

and is thus defined by equation (25) multiplied by $-\mathrm{D}$ for the general case. In the special cases (1), (2), and (3) of the preceding section, the permeability is defined by equations (27), (29), and (31) respectively, each multiplied by $-\mathrm{D}$.

It is important to show how the permeability differs from that which would be found for the analogous diffusion system where $k_1=k_2=\infty$, *i. e.*, where the two processes of penetration from the surface into the solid, and desorption from it into the surface, may be neglected, and a one constant problem $\frac{\partial v}{\partial t}=\mathrm{D}\frac{\partial^2 v}{\partial x^2}$ is to be solved (equations (1) to (4)). The comparison is readily made for cases (2) and (3). Case (2) gives the following expressions:—

(*a*) If $k_1, k_2 \gg \mathrm{D}$,

$$\mathrm{P}_a=\frac{\mathrm{D}.u_s}{l} \quad \ldots\ldots\ldots\ldots \quad (33)$$

(*b*) If $k_1=k_2=\mathrm{D}$,

$$\mathrm{P}_b=\frac{\mathrm{D}.v_s}{\frac{v_s}{u_s}(1+l)+1} \quad \ldots\ldots\ldots\ldots \quad (34)$$

(*c*) If $k_1, k_2 \ll \mathrm{D}$,

$$\mathrm{P}_c=\frac{k_1.k_2.v_s}{k_1\left(\frac{v_s}{u_s}+k_2\right)} \quad \ldots\ldots\ldots\ldots \quad (35)$$

The ratio

$$\frac{\mathrm{P}_a}{\mathrm{P}_b}=\frac{1+l}{l}+\frac{1}{l}\frac{u_s}{v_s} \quad \ldots\ldots\ldots\ldots \quad (36)$$

becomes $\frac{\mathrm{P}_a}{\mathrm{P}_b}=11+10.\frac{u_s}{v_s}$ when $l=0{\cdot}1$ cm., *i. e.*, for a membrane 1 mm. thick. Even if $\frac{u_s}{v_s}\ll 1$, the effect of the surface processes $k_1$, $k_2$ has been to reduce the permeability 11-fold. Since as a rule $\frac{u_s}{v_s}$ will not be negligible, it can be seen how great the influence of the surface processes may be.

Case (3) of the preceding section, when A and B are given by (31) and (32), is also interesting. One now finds

(*d*) If $k_1, k_2 \gg \mathrm{D}$,

$$\mathrm{P}_d=\mathrm{D}.\frac{k_1}{k_2}\left(\frac{v_1-v_2}{l}\right)=\frac{\mathrm{D}(u_0-u_l)}{l} \quad \ldots\ldots\ldots\ldots \quad (37)$$

(*e*) When $k_1=k_2=\mathrm{D}$,

$$\mathrm{P}_e=\frac{\mathrm{D}.(v_1-v_2)}{2+l} \quad \ldots\ldots\ldots\ldots \quad (38)$$

(*f*) When $k_1$, $k_2 \ll D$,

$$P_f = \frac{k_1}{2}(v_1 - v_2), \quad . \quad . \quad . \quad . \quad . \quad . \quad . \quad . \quad . \quad . \qquad (39)$$

so that the rate of flow of gas through the wall is independent of its thickness, and is a function only of $k_1$ and $v_1$, $v_2$.

The permeabilities expressed by (37), (38), and (39) may be compared with that obtained for a simple diffusion process, *i. e.*, $P = \frac{D(v_1 - v_2)}{l}$. From equation (38), for example, one finds

$$\frac{P_e}{P} = \frac{l}{2+l},$$

and if $l \sim 0{\cdot}1$ cm., this ratio is $\frac{1}{21}$. If $l \sim 0{\cdot}01$ cm., the ratio is $\frac{1}{201}$. The expression serves to show how sensitive is the permeability to the surface processes. Even if $k_1 = k_2 = 20$ D, and $l = 0{\cdot}1$ cm., $\frac{P_e}{P} = \frac{1}{2}$.

The equations (34) and (37) show that to reduce the effects of phase boundary processes it will be necessary to increase the thickness of the membrane. The effect of increasing the thickness is, however, not proportional to the thickness.

### *Phase Boundary Concentration Discontinuities.*

In the general case, the phase boundary discontinuities in concentration between the sorption layer and the solid are given by

$$\text{At } x=0, \quad v_1 - u_0 = v_1 - B, \quad . \quad . \quad . \quad . \quad . \quad . \quad . \quad . \qquad (40)$$

$$\text{At } x=l, \quad u_l - v_2 = Al + B - v_2, \quad . \quad . \quad . \quad . \quad . \quad . \quad . \qquad (41)$$

and one has simply to substitute the values of A and B given by equations (25) and (26) to evaluate them. To show the type of discontinuity encountered, it will be sufficient to give the discontinuity for the conditions of equations (29) and (30) and of (31) and (32) of the preceding section.

In the first case, when the pressure on the in-going side is the saturation pressure, and that on the out-going side is very low, so that $\beta_2 = 1$, $\beta_1 = 0$; $v_1 = v_s$, $v_2 = 0$, the discontinuities are

$$\text{At } x=0, \quad v_1 - u_0 = v_1 - \frac{k_1 v_s(D + k_2 l)}{k_1 \frac{v_s}{u_s}(D + k_2 l) + Dk_2}. \quad . \quad . \quad . \quad . \qquad (42)$$

$$\text{At } x=l,\quad u_l-v_2=\frac{k_1v_s(\mathrm{D}+k_2l)}{\mathrm{D}\left(k_1\frac{v_s}{u_s}+k_2\right)\frac{+k_1k_2v_sl}{u_s}}-\frac{k_1k_2v_sl}{k_1\frac{v_s}{u_s}(\mathrm{D}+k_2l)+\mathrm{D}k_2}. \qquad (43)$$

When $k_1=k_2=\mathrm{D}$ one has $\frac{v_s}{u_s}=1$, and so

$$\frac{u_l-v_2}{v_1-v_2}=\frac{v_1-u_0}{v_1-v_2}=\frac{\text{Discontinuity at } x=0 \text{ or } l}{\text{Total concentration Drop}}=\frac{1}{(2+l)},$$

so that if $l$ is small (*e. g.*, 0·1 cm.) the sum of the concentration discontinuities is very nearly the total concentration drop across the membrane. The diffusion gradient is only $\frac{l}{2+l}$ of its value $\frac{v_s}{l}$ when there are no phase boundary processes.

In the second case, when the pressures on the in-going and out-going sides are both small, $\beta_2=\beta_1=1$; $v_1$, $v_2$, $\ll v_s$ or $u_s$, and the discontinuities are

$$\text{At } x=0,\quad (v_1-u_0)=v_1-\frac{+\mathrm{D}k_1v_2+k_1v_1(\mathrm{D}+k_2l)}{k_2(2\mathrm{D}+k_2l)}. \qquad (44)$$

$$\text{At } x=l,\quad (u_l-v_2)=\frac{k_1k_2(v_2-v_1)+\mathrm{D}k_1v_2+k_1v_1(\mathrm{D}+k_2l)-v_2}{k_2(2\mathrm{D}+k_2l)}. \qquad (45)$$

When $k_1=k_2=\mathrm{D}$ one has, as before,

$$\frac{u_l-v_2}{v_1-v_2}=\frac{v_1-u_0}{v_1-v_2}=\frac{\text{Discontinuity at } x=0 \text{ or } l}{\text{Total concentration Drop}}=\frac{1}{2+l}.$$

### (C) *The Complete Solution for* fig. 1 *a*.

The complete solution of the problem may now be given for the flow of gas into and through a solid, when two phase boundary reactions occur, with a simultaneous diffusion within the solid. The solution is the sum of the solutions in (A) (equation (11)) and (B) ($u=\mathrm{A}x+\mathrm{B}$ when A is given by equation (25) and B by equation (26)):

$$v=u+w=\frac{(k_1k_2v_2\beta_1-k_1k_2v_1\beta_2)x+\mathrm{D}k_1v_2+k_1v_1\left(\mathrm{D}+k_2l\beta_2+\frac{k_1v_2l}{u_s}\right)}{\left(k_2\beta_1+\frac{k_1v_1}{u_s}\right)\left(\mathrm{D}+k_2l\beta_2+\frac{k_1v_2l}{u_s}\right)+\mathrm{D}\left(k_2\beta_2+k_1\frac{v_2}{u_s}\right)}$$
$$+2\sum_1^{\infty}e^{-\mathrm{D}\alpha_n^2t}\frac{\alpha_n\cos\alpha_nx+h\sin\alpha_nx}{(\alpha_n^2+h^2)l+2h}\int_0^l(f(x)-u)(\alpha_n\cos\alpha_nx$$
$$+h\sin\alpha_nx)dx, \qquad (46)$$

where $\alpha_n$ is the $n$th positive root of $\tan\alpha l=\frac{2\alpha h}{\alpha^2-h^2}$ and $h=\frac{k_2}{\mathrm{D}}$.

### *Specific cases of Equation* (46).

From its general form, equation (46) may be reduced to more simple forms for various cases.

When the pressure on the in-going side is very high, so that $v_1=v_s$, the saturation concentration and the pressure on the in-going side are very low, so that $v_2$ may be neglected compared with $v_1$, and also when the initial concentration $f(x)$ throughout the solid is constant at $v_0$, equation (46) becomes

$$v=u+w=\frac{-k_1k_2v_sx}{\mathrm{D}\left(k_1\frac{v_s}{u_s}+k_2\right)+k_1k_2\frac{v_s}{u_s}l}+\frac{k_1v_s(\mathrm{D}+k_2l)}{k_1\frac{v_s}{u_s}(\mathrm{D}+k_2l)+\mathrm{D}k_2}+2\sum_1^\infty e^{-\mathrm{D}\alpha_n{}^2t}$$

$$\times\frac{\alpha_n\cos\alpha_nx+h\sin\alpha_nx}{(\alpha_n{}^2+h^2)l+2h}\mathrm{I}, \quad . \quad (47)$$

where

$$\mathrm{I}=\frac{k_2}{\mathrm{D}\alpha_n}[2(v_0-u_0)+u_0-u_l)]. \quad . \quad . \quad . \quad . \quad . \quad . \quad (13)$$

If the pressures on the in-going and out-going sides are both small, so that $\beta_1=\beta_2=1$, and if $v_1$, $v_2 \ll u_s$, the equation for $v$ is

$$v=u+w=\frac{k_1v_1}{k_2}-\frac{(v_1-v_2)(k_1k_2x+\mathrm{D}k_1)}{k_2(2\mathrm{D}+k_2l)}+2\sum_1^\infty e^{-\mathrm{D}\alpha_n{}^2t}$$

$$\times\frac{\alpha_n\cos\alpha_nx+h\sin\alpha_nx}{(\alpha_n{}^2+h^2)l+2h}\mathrm{I}. \quad . \quad (48)$$

### *The Quantity Sorbed at any Given Time.*

To find the quantity of gas $\phi$ in unit area of the membrane at any time $t$ one has to integrate (47) or (48) from 0 to $l$, thus obtaining for the conditions giving (47) and (48) respectively the following equations:

$$\phi=\frac{-k_1k_2v_sl^2}{2\left\{\mathrm{D}\left(k_1\frac{v_s}{u_s}+k_2\right)+k_1k_2\frac{v_s}{u_s}l\right\}}+\frac{k_1v_s(\mathrm{D}+k_2l)l}{k_1\frac{v_s}{u_s}(\mathrm{D}+k_2l)+\mathrm{D}k_2}+2\sum_1^\infty e^{-\mathrm{D}\alpha_n{}^2t}$$

$$\times\frac{2h}{\alpha_n\{(\alpha_n{}^2+h^2)l+2h\}}\mathrm{I}. \quad . \quad (49)$$

$$\phi=\frac{k_1}{k_2}v_1l-\frac{\left(v_1-v_2)(k_1k_2\frac{l^2}{2}+\mathrm{D}k_1l\right)}{k_2(2\mathrm{D}+k_2l)}+2\sum_1^\infty e^{-\mathrm{D}\alpha_n{}^2t}\frac{2h}{\alpha_n\{(\alpha_n{}^2+h^2)l+h2\}}\mathrm{I}. \quad (50)$$

When $v_1=v_2$, equation (50) becomes

$$\phi=\frac{k_1}{k_2}v_1l+2\sum_1^\infty e^{-\mathrm{D}\alpha_n{}^2t}\frac{2h}{\alpha_n\{(\alpha_n{}^2+h^2)l+2h\}}\mathrm{I}_1. \quad . \quad . \quad . \quad (51)$$

In the case of equation (51), when $v_0=f(x)=0$, the equation (51) for $I_1$ simplifies to

$$I_1=\frac{-2v_1k_1}{D.\alpha_n}. \quad . \quad . \quad . \quad . \quad . \quad . \quad . \quad (13\,a)$$

The quantity which has diffused into or out of the membrane, per unit area, is given by

$$\phi_0-\phi=(v_0l-\phi), \quad . \quad . \quad . \quad . \quad . \quad . \quad . \quad . \quad (52)$$

where $\phi$ is given for the different cases by equation (49), (50), and (51).

*Flow of Gas through a Plate in the Non-Stationary State.*

The quantity of gas leaving the plate per unit of time at the face $x=l$ is

$$P=-D\left(\frac{du}{dx}\right)_{x=l}-D\left(\frac{dw}{dx}\right)_{x=l},$$

which gives for the boundary conditions, corresponding respectively to (47) and (48), the rate of flow through the plate

$$P=\frac{D.k_1k_2.v_s}{D\left(k_1\frac{v_s}{u_s}+k_2\right)+k_1k_2\frac{v_s}{u_s}l}+2D\sum_1^\infty e^{-D\alpha_n^2t}\frac{\alpha_nh}{(\alpha_n^2+h^2)+2h}I. \quad . \quad (53)$$

$$P=\frac{Dk_1(v_1-v_2)}{(2D+k_2l)}+2D\sum_1^\infty e^{-D\alpha_n^2t}\frac{\alpha_nh}{(\alpha_n^2+h^2)l+2h}I, \quad . \quad . \quad . \quad . \quad . \quad (54)$$

where I is defined by equation (13).

The total number of moles of gas N which have entered the gas phase at the face $x=l$ in time $t$ is given by $N=\int_0^tP.dt$. For the system represented by (54), for example, one finds

$$N=\frac{k_1D(v_1-v_2)t}{2D+k_2l}+2\sum_1^\infty\frac{1}{\alpha_n}(1-e^{-D\alpha_n^2t})\frac{h}{(\alpha_n^2+h^2)l+2h}I. \quad . \quad (55)$$

As $t$ tends to infinity, the curve obtained when N is plotted against $t$ tends to the line

$$\frac{k_1D.(v_1-v_2)t}{2D+k_2l}+2\sum_1^\infty\frac{1}{\alpha_n}\frac{h}{(\alpha_n^2+h^2)l+2h}I, \quad . \quad . \quad . \quad . \quad (56)$$

which may be written as

$$\frac{k_1D(v_1-v_2)}{2D+k_2l.}\left(t+\frac{2D+k_2l}{k_1D.(v_1-v_2)}2\sum_1^\infty\frac{h}{\alpha_n[(\alpha_n^2+h^2)l+2h]}I\right), \quad . \quad (57)$$

so that the intercept L which this curve makes on the axis of $t$ at $t=0$ is

$$L=-\frac{2D+k_2l}{Dk_1(v_1-v_2)}\sum_1^\infty\frac{2h}{\alpha_n[(\alpha_n^2+h^2)l+2h]}I. \quad . \quad . \quad . \quad . \quad (58)$$

Similarly equation (53) gives for the intercept L

$$\mathrm{L}=-\frac{\mathrm{D}\left(k_1\frac{v_s}{u_s}+k_2\right)+k_1k_2\frac{v_s}{u_s}l}{\mathrm{D}k_1k_2v_s}\sum_1^{\infty}\frac{2h}{\alpha_n[(\alpha_n{}^2+h^2+2h]}\mathrm{I}. \quad . \quad . \quad (59)$$

The most important case arises when $v_0=f(x)$, the initial concentration in the solid, is zero; and where $v_2$ is very small compared with $v_1$. I, as given by equation (13), now simplifies to

$$\mathrm{I}_2=-\frac{v_1k_1}{\alpha_n\mathrm{D}} \quad . \quad . \quad . \quad . \quad . \quad . \quad . \quad . \quad . \quad . \quad (13\,b)$$

and from (58) one finds

$$\mathrm{L}=-\frac{2\mathrm{D}+k_2l}{\mathrm{D}.k_1v_1}\sum_1^{\infty}\frac{2h}{\alpha_n[(\alpha_n{}^2+h^2)l+2h]}\mathrm{I}_2. \quad . \quad . \quad . \quad . \quad . \quad (60)$$

Equations (13 *b*) and (60) show that the concentration vanishes from the expression for L, and so L is a constant dependent only upon $k_1$, $k_2$, D, and $l$. Equation (59) may be treated analogously.

Some special cases of equation (60) arise and may be briefly considered:

(1) $k_1=k_2=\mathrm{D}$; $v=f(x)$ is 0 at $t=0$; $v_2\sim 0$. Here the three processes occur with equal velocity constants, the membrane is initially free from gas, and the pressure on the out-going side is very small. One now has

$$\mathrm{L}=\frac{2+l}{\mathrm{D}}\sum_1^{\infty}\frac{2}{\alpha_n{}^2[(\alpha_n{}^2+1)l+2]}, \quad . \quad . \quad . \quad . \quad . \quad . \quad . \quad (61)$$

where $\alpha_n$ denotes the $n$th$+ve$ root of $\tan\alpha=\frac{2\alpha}{\alpha^2-1}$.

(2) $k_1$, $k_2\ll\mathrm{D}$; $v=f(x)$ is 0 at $t=0$; $v_2\sim 0$. Here the permeation rate is controlled by the phase boundary reactions only; $h=\frac{k_2}{\mathrm{D}}\sim 0$, and thus $\alpha_n$ is the $n$th positive root of $\tan\alpha=\frac{2h}{\alpha}\sim 0$. Thus $\alpha_n=\frac{n\pi}{l}$, and the expression for L becomes

$$\mathrm{L}=\frac{4}{\mathrm{D}}\sum_1^{\infty}\frac{hl^4}{(n\pi)^4}=\frac{360l^4}{\mathrm{D}}h. \quad . \quad . \quad . \quad . \quad . \quad . \quad . \quad . \quad (62)$$

The right-hand side of this equation is very small, since $h\rightarrow 0$, and so one sees that there is no appreciable time lag in setting up the stationary state of flow in a system where phase boundary processes control the permeation rate.

(3) $k_1$, $k_2\gg\mathrm{D}$; $v=f(x)$ is zero at $t=0$; $v_2\sim 0$. Here the diffusion velocity alone governs the permeation rate, and $\alpha_n$ is the $n$th positive root of $\tan\alpha l=\frac{2\alpha h}{\alpha^2-h^2}$. Since $h=\frac{k_2}{\mathrm{D}}$ is very great, initially $\alpha_n=\frac{n\pi}{l}$. $n$, however, becomes infinitely great, so that $\alpha_n$ also becomes infinitely

great. As $n$ increases the function $\frac{2\alpha h}{\alpha^2-h^2}$ is seen to start at zero when $n=0$, to approach the value $-\infty$ when $n \gg h$, and to return from $+\infty$ to 0 when $h \ll n \leqslant \infty$. Therefore as $n \rightarrow \infty$, the roots are again $\frac{n\pi}{l}$; but at some unknown intermediate value of $n$ the roots are $\frac{(2m+1)}{2}\frac{\pi}{l}$, where $m$ is an integer. Thus the function $\frac{2\alpha h}{\alpha^2-h^2}$, where $h$ is large, consists of two hyperbolas, and the summation in the expression for L,

$$\mathrm{L}=\frac{1}{\mathrm{D}}\sum_{1}^{\infty}\frac{2h^2}{\alpha_n^2[(\alpha_n^2+h^2)]} \quad . \quad . \quad . \quad . \quad . \quad . \quad . \quad . \quad (63)$$

cannot be made. However, the correct value * for L is obtainable from equation (4) putting $c_2=0$, $c_0=0$, and is

$$\mathrm{L}=\frac{l^2}{6\mathrm{D}} \quad . \quad . \quad . \quad . \quad . \quad . \quad . \quad . \quad . \quad . \quad (4\,a)$$

Fig. 2.

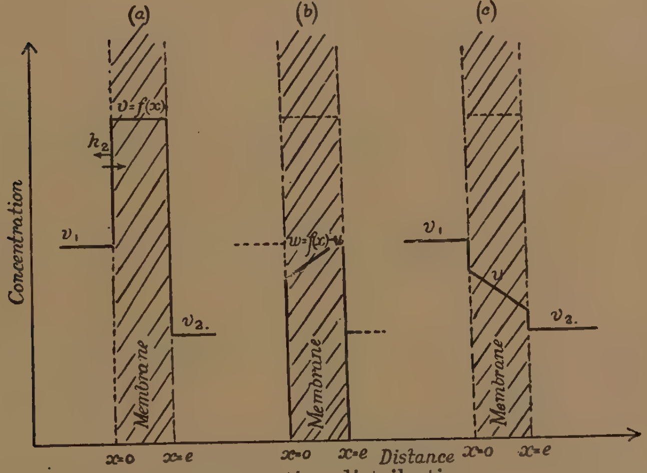

Concentration distribution.

(*a*) Initial distribution.
(*b*) and (*c*) Distribution used in solving for initial distribution.

### Problem II.

When the molecules pass directly from gas phase to solid and *vice versa*, the distributions corresponding to figs. 1 (*a*), 1 (*b*), and 1 (*c*) become those in figs. 2 (*a*), 2 (*b*), and 2 (*c*) respectively, the adsorption layer, if not too concentrated, being inert.

---

* This allows the indefinite series $\sum_{n=1}^{\infty}\frac{2h^2}{\alpha_n^2[\alpha_n^2+h^2]}$, where $h$ is large and where $\alpha_n$ is a root of $\tan \alpha l=\frac{2\alpha h}{\alpha^2-h^2}$ to be summed. One finds from (63) and (4 *a*) that $\sum\frac{2h^2}{\alpha_n^2[\alpha_n^2+h^2]}=\frac{l^2}{6}$.

The solution for the non-stationary state is that given by equation (11) as before.

The solution for the stationary state is to be obtained from the equations

$$\frac{d^2u}{dx^2}=0.$$

$$\mathrm{D}.\frac{du}{dx}-k_2u_0+k_1v_1\left(1-\frac{u_0}{u_s}\right)=0.$$

$$-\mathrm{D}.\frac{du}{dx}-k_2u+k_1v_2\left(1-\frac{u_l}{u_s}\right)=0.$$

The solution of this problem is $u=\mathrm{A}x+\mathrm{B}$, where A and B are got from equations (25) and (26) by writing $\beta_1=\beta_2=0$. Thus the problem appears as a special case of the previous one and need not be considered further.

### *Summary.*

Solutions of the diffusion equation $\frac{\partial c}{\partial t}=\mathrm{D}\frac{\partial^2 c}{\partial x^2}$ are known for

(1) The concentration as a function of distance and time.
(2) The quantity of gas adsorbed or desorbed at a given time.
(3) The permeability in the steady state.
(4) The permeability in the non-stationary state of flow.
(5) The intercept which the curve pressure against time (*i. e.*, the permeability curve in the non-stationary state) makes on the axis of time.

These quantities all afford methods of measuring D. The present paper investigates the problem of gas flow by diffusion in combination with phase boundary processes corresponding to transfer from a gas phase or an adsorbed layer into the solid, and transfer from the solid into an adsorbed layer or into a gas phase. Solutions corresponding to each case (1) to (5) have been obtained, and are given for the general as well as for special cases. The results show that there can be an unexpectedly large influence of these surface processes upon properties such as permeability, and a very big concentration discontinuity at the surfaces.

Sufficient different types of equation are given for the evaluation of all three of the velocity constants involved.

### *References.*

(1) R. M. Barrer, Trans. Far. Soc. (1939) xxxv. p. 628.
(2) J. S. Wang, Proc. Camb. Phil. Soc. p. 657 (1936).
(3) Carswell, ‘ Conduction of Heat,’ Macmillan, p. 74 (1921).

## XIII. *Studies in Photoelectric Photometry.*
## *A Photoemissive Cell specially designed for High Precision Measurements.*

By G. A. Boutry and P. Gillod.
Laboratoire d'Essais, Paris *.

[Received May 24, 1939.]

### § 1. *Introduction.*

It has been evident for some time that the electric response of commercial photoemissive cells † was not strictly proportional to the amount of light incident on the cell cathode. Generally speaking, a departure from proportionality of the order of 1 per cent. often appears when the illumination of the cathode is increased from 1 to 10 ‡. The examination of the cell shape, design, and method of preparation will not always enable the observer to form any conclusion as to whether the cell response is or is not " proportional "—even the sign of the departure from proportionality being imprevisible. In fact, we are to-day, as regards the making and use of photoemissive cells, in very much the same position as physicists were, when, some fifteen years ago, they wanted thermionic triodes capable of giving fair performance in short-wave work. This particular difficulty was easily solved in time by a patient study of the design of the valves. The opinion of the present writers being that a similar process applied to photoelectric cells would yield similar results, their first study carried along these lines is recorded here.

### § 2. *Causes of an Imperfectly Proportional Response.*

We have no reason to doubt the fundamental law of photoelectricity, which stipulates strict proportionality between the number of light quanta incident on a photoemissive cathode and the number of photoelectrons released, *i. e.*, the electric charge which may appear in the circuit. If, in spite of this, the law of proportionality does not hold for most photoemissive cells, the design of the cell and the way it is used must yield the explanation.

---

* Communicated by the Authors.

† For the meaning of symbols and denominations used in this paper see G. A. Boutry, 'Photoelectricity' (Phys. Soc. Progress Reports, vol. iii. 1936).

‡ Preston and McDermott, Proc. Phys. Soc. xlvi. p. 256 (1934).

Most photoemissive cells now in use may be described as follows: a cathode of silvered glass (part of the wall of the cell) or metal, coated with the photosensitive deposit and of any shape (spherical, cylindrical, plane, v-shaped . . .); an anode generally of very small surface (wire, rod, spiral, grid . . .), generally coated with the same deposit; the distance anode-cathode varies within large limits; the shape and size of the bulb may be anything. During the last ten years we have used in our laboratory more than fifty cells of really strikingly different design and shape; an easy construction seems very often to have been the only guide.

(1) There is evidently no reason, in such cells, why all the electrons liberated by the light incident on the cathode should fall on the anode, except when very high p.d.'s are used. In fact, "saturation" occurs only for p.d.'s ranging from 25 to 200 volts, according to type (the theoretical saturation p.d., it will be remembered, should be equal to the Volta p.d. between cathode and anode, never more than 4 volts and generally much less). Now, the vacuum in the cell is never perfect, so that ionization by collision will occur in the residual atmosphere, under the influence of these high electrical fields. Such ionization will give a response curve $i=f(\phi)$, such as that of fig. 1.

Fig. 1.

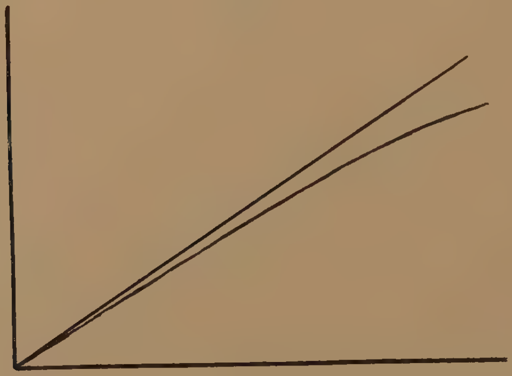

(2) In most photoemissive cells, the anode surface being very small, it follows that, as soon as the number of photoelectrons liberated by light ceases to be negligible, a space-charge is built-up, the concentration of which may be important in the neighbourhood of the anode. This, again, growing with the luminous flux used, will alter the response of the cell, the effect being in opposition with tha of the above factor; the response curve, in that case, would be like that given in fig. 2.

(3) Both these influences will co-exist in most photocells, so that a balance may sometimes be obtained. It is clear that the laws followed by the two phenomena being different, a perfect compensation will normally exist only for one or a few points of the response curve, which will assume some such shape as that represented in fig. 3. As a matter of fact, numerous measurements have shown us that such types of response are quite often met with in practice.

Fig. 2.

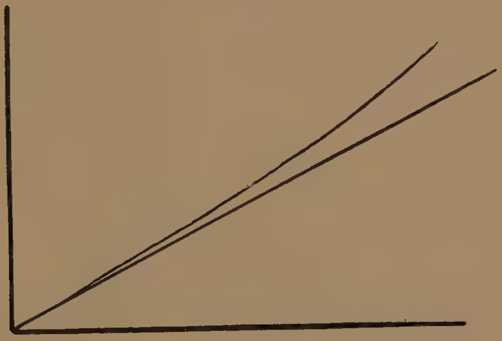

Fig. 3.

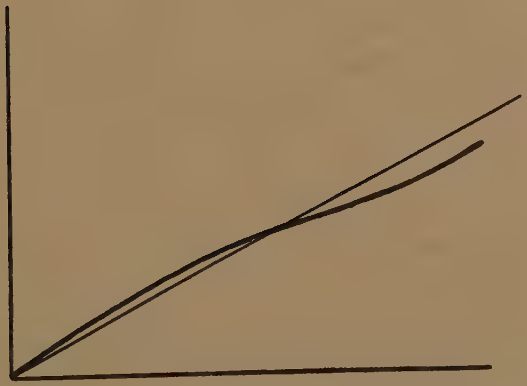

(4) The influence of surface charges on the walls of the cell should also be considered; this may be twofold. It is a well-known fact that, owing to the high vapour tension of the alkaline metals, the walls of any photoelectric cell become coated, on the inside, with a thin transparent metallic film. This may not be continuous, and in any case its electrical resistance is extremely high. The cell being submitted to relatively high tension, the walls will gather slowly charges which may shift and

dissipate equally slowly ; one of the disturbing results is that the properties of a given cell may fluctuate, particularly at the beginning of a series of measurements ; this is an effect entirely different from the " ageing " produced by the evolution with time of the cathodic photoemissive layer.

Another effect of this metallic coating of the walls of the cell will be an increase of the " dark " current. Again the response curve of the cell may be affected ; as soon as light is turned on the cathode it is also diffused on the walls of the cell, creating a new distribution of surface charges, and altering the apparent " dark-resistance."

All this explains why a photoemissive cell giving an accurately proportional response over a large register of luminous flux variation is seldom met with : such a cell seems to be the product of chance rather than purpose.

It will be seen, however, that most of the causes of non-proportionality roughly described in the present section would disappear or become greatly reduced in importance if two principal conditions were satisfied : (*a*) the photoelectronic paths should not be distorted by any exterior influence such as that of stray charges on the walls of the cell ; (*b*) the p.d. necessary to reach saturation should be made as small as possible. It is clear that each of these two conditions is related to the other : condition (*a*) will be satisfied by using electric screening, while condition (*b*) involves using an anode working after the fashion of a Faraday cylinder—which comes to practically the same thing. It is also evident that each of these main conditions involves many secondary consequences : for instance, it is not necessary to stipulate that the density of disturbing space charges should be reduced as much as possible : the fulfilment of condition (*b*) is only possible if that is so.

## § 3. *Design of a Cell giving Proportional Response.*

Cells were made and used more than thirty years ago which fulfilled moderately well the above conditions ; their only drawback was, and is, that it is not possible to get a large photoelectric yield from them ; we allude to cells of the type known as central cathode cells, with which many determinations of the energy distribution of photoelectrons have been carried out. In these cells, the anode is a sphere made of an electrically conducting material which completely surrounds a point-like cathode (fig. 4), two small holes being provided, one for the admission of light, and one for the exit of the cathode lead. The results given by such cells are classical ; saturation is obtained for a p.d. difference very close to the theoretical value, on condition that the illumination be small enough not to create an appreciable space charge in the vicinity of the small cathode. This practically forbids such a design in modern technique.

Moreover, the large anode generally gives an important "negative" current which reduces the sensitivity *.

Now, conditions (*a*) and (*b*) would also hold in a cell having infinite parallel plane electrodes ; it is not impossible to build cells working nearly in the same way as this ideal type : finite plane parallel electrodes with guard-rings will meet the case. But a cell built in such a way must have at least one transparent electrode for the admission of light. It is a cell of such a type that will now be described † (fig. 5).

Fig. 4.

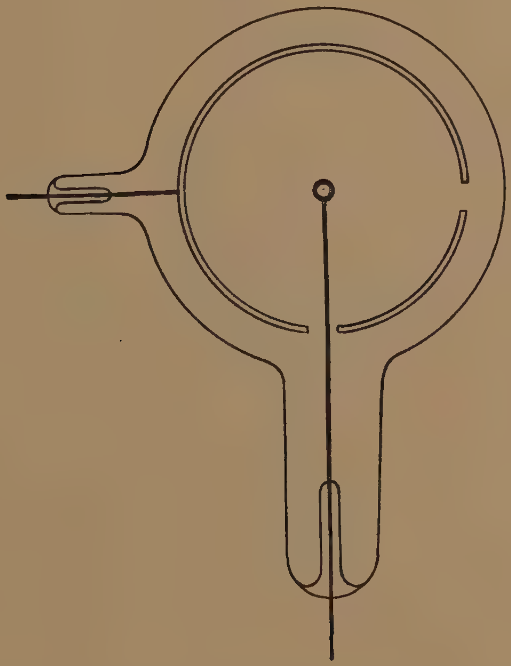

The cathode C is a disk, cut in a plane sheet of silver and surrounded by a guard-ring R, cut into the same material, whose width is approximately equal to the diameter of the cathode. Both these electrodes, during the making of the cell, were oxidized and coated with a thin layer of cæsium. The cathode and guard-ring leads are insulated from

---

[*] Hughes and du Bridge, 'Photoelectric Phenomena,' pp. 115–120 : New York, 1932. Boutry, 'Les Phénomènes Photoélectriques et leurs Applications,' i. pp. 47–49 : Paris, 1936.

[†] The first cell of this type, imagined by one of the authors (G. A. B.) in 1934, was only built in 1936, with the very able help of M. P. Cherdakoff ; numerous technical difficulties explain this delay.

each other and from the anode lead. Precautions were taken in the making of the cell to have this insulation as good as possible. It will be seen from fig. 5 that the electric path along the walls of the cell connecting any one of the three electrodes to the others is quite long; moreover, the tube D containing the cathode lead could be heated to

Fig. 5.

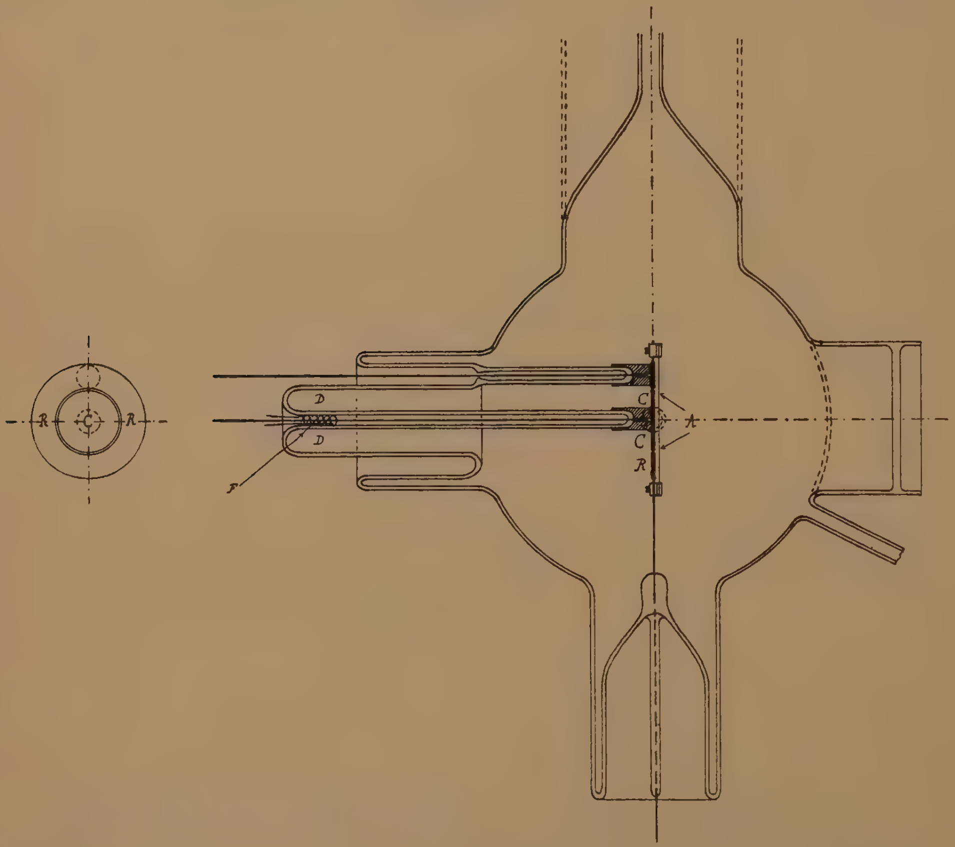

250° with a small electric coil F without danger to the cell. Such a precaution, however, seems superfluous.

The design of the anode A is somewhat complicated, and is shown in detail in fig. 6. It is not a metallic plate, but a grid of parallel vertical tungsten wires of very small diameter ($18\,\mu$). The distance separating each wire from its neighbour varies with the cells from 0·25 to 1 mm. These wires are held at the top and bottom by two nickel bars insulated from each other: this arrangement permits the heating of the wires by passing a current through them; the purpose of this will be examined in section 6. Anode and cathode were mounted parallel to each other, the distance between them being about 2 mm.

The bulb of the cell may have any dimension or shape; for ease of preparation and security, the bulbs used were large pyrex balls of about 12 cm. diameter. A plane glass window would be a useful adjunct.

The above description speaks for itself. At a small distance from the wires, the electric field between anode and cathode has the same distribution as between infinite plane parallel electrodes, provided the guard-ring and the cathode are kept at the same potential. Again, if the guard-ring and the *anode* are kept at the same potential, the cell should behave as if its cathode was completely surrounded by its anode (Faraday cylinder type). In both cases saturation should be obtained near the theoretical Volta contact potential difference, and proportionality of response for the cathodic current should hold over large intervals, *whether the guard-ring be illuminated or not*: one sees that such a cell may be tried and used in many ways. The sensitivity should be of the same order as that of commercial vacuum cells now in use; an additional advantage being that no perfect vacuum should be necessary, as no ionization by collision can occur.

Fig. 6.

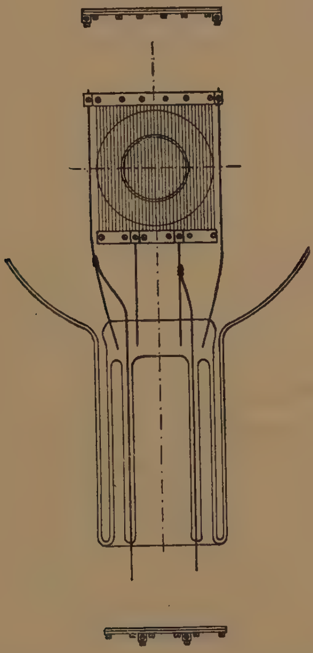

The only drawback to this encouraging theoretical picture is that the anode is not really a plate; though its apparent surface, as regards potential distribution in the field, is the same as that of the cathode and guard-ring, this does not hold near the wires, where the space charge is not negligible and still causes local distortion of the field; this effect will be investigated in section 6.

## § 4. *Testing the Cells.*

When testing a cell for proportional response, many methods may be—have been—employed. These fall into two classes: in the first, the luminous flux, originally $\phi$, is adjusted, by means of neutral filters or wedges, polarizers, etc. . . . to a lower value, $K\phi$ or $\phi^n$, the factors K and $n$ being accurately known from previous calibration; in the second, two or more fluxes, $\phi_1$, $\phi_2$, . . . $\phi_n$, unknown, fall first one after the other on the cell; after which, the sums $\phi_1+\phi_2$, $\phi_1+\phi_2+\phi_3$ . . . are turned on, and the responses measured. No calibration is needed in the last case; it is only necessary that $\phi_1$, $\phi_2$ . . . $\phi_n$ remain constant throughout the test. Preston & McDermott * and Fleury † have used methods of this kind.

Fig. 7.

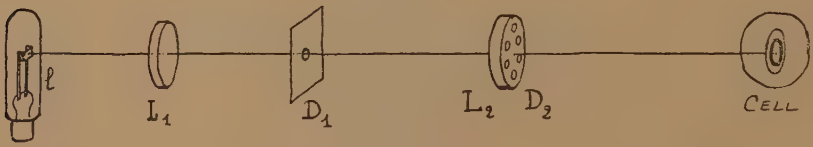

The method here described belongs to the same class: the source of light was a tungsten ribbon lamp fed by a large battery. Tension and intensity were permanently controlled with a potentiometer and kept constant throughout a series of measurements, the variation being less than 1 part in 50,000. The rate of cooling of the lamp was kept as constant as possible (protecting funnels, doors and windows blocked, movement of operators avoided in the room, etc. . . .). One hour after the lighting of the lamp, its emission was thus kept constant with an accuracy of at least 1 part into 10,000.

The adding device is shown on fig. 7. The lens $L_1$ gives a good image of the central part of the ribbon covering the hole bored in diaphragm $D_1$. The lens $L_2$ gives in the plane of the cell's cathode a circular image of $D_1$, uniformly illuminated and of variable size ($l$, $L_1$ and $D_1$; $L_2$ are mounted on two slides on a photometer bench). A diaphragm $D_2$, in which circular holes of nearly equal areas are bored, is kept in front of lens $L_2$, whose components are well enough corrected to give no sensible displacement of image, however situated the holes used are. The quantity of light passing through hole No. 1, $\phi$, being taken as unity, the quantity of light issuing from holes Nos. 2, 3, . . . $n$, $\phi_2$, $\phi_3$, . . . $\phi_n$ can be written $1+\epsilon_2$, $1+\epsilon_3$, . . . $1+\epsilon_n$, where $\epsilon_2$, $\epsilon_3$, . . . $\epsilon_n$ are small enough for a direct comparison of $\phi_1$, $\phi_2$, . . . $\phi_n$ by means of the cell to be legitimate, even if the response of the cell used be not strictly proportional; if $\epsilon_2$, $\epsilon_3$ . . . $\epsilon_n$ are of the first order, the errors involved will be of the second. The relative values of $\phi_1$, $\phi_2$, . . . $\phi_n$ being thus determined, the sum $\phi_1+\phi_2$, $\phi_1+\phi_2+\phi_3$ . . . , $\phi_1+\phi_2$ . . .$+\phi_n$ are then measured and compared to their theoretical values.

---

* Preston and McDermott, *loc. cit. supra.*

† Fleury, *Comptes Rendus*, cxcix. p. 195 (1934).

There are obvious limitations to the number of holes; but, if a monochromatic light filter is used, or if there is no objection to a change in the spectral distribution of the light used (that is to say, if the cell shows no departure from proportionality specifically dependent on the colour of the light used) the range of measurements can be increased by adjusting the intensity of the source $l$: after a set of measurements, $\phi_1$, $\phi_1+\phi_2$ . . . , $\Sigma=\phi_1+\phi_2+$. . .$\phi_n$ having been measured, the current feeding the lamp is adjusted till the quantity of light passing through the first hole $\phi'_1=\Sigma$. In this step by step way, measurements have been made for values of the luminous flux ranging from 1 to 30 arbitrary units. As well as can be estimated without any absolute measurements, the range 0·002 to 0·06 lumen has thus been covered.

The photoelectric currents were measured with a potentiometer, a Lindemann electrometer being employed as null indicator (fig. 8). The circuit is very nearly that described in 1932 by P. Fleury *.

The current to be measured, $i$, flows through the high resistance $\rho$ and thence to earth through part of the potentiometric coils $r$, $r'$. Through the constant resistance $r+r'$ also flows a constant current $j$; the photocurrent $i$ always has a negligible value as compared to $j$, which is of the order of a few milliampères, that is to say about $10^5\,i$.

The electrometer needle can be electrically connected either to the earth T or to point K (cathode) through the key L; let us suppose that there is no deflexion when this is done: this means that the coils $r$ have been so adjusted that the fall of potential $rj$ exactly compensates that, $\rho i$, due to the photocurrent flowing in $\rho$; then

$$i=j\,.\,\frac{r}{\rho}\,.$$

It will be seen that throughout the work, the cell can be kept under a constant p.d. $v_0$ given by battery $B_1$, whatever the values of $\rho$ and $i$ may be: a very troublesome correction is thus avoided.

---

* Fleury, *Revue d'Optique*, xi. p. 385 (1932).

For the measurement of $j$, a standard cell E and a third position of the key L are provided; when the key is shifted to M, and the potentiometric coils adjusted in such a way ($r_m$, $r'_m$) that there is no deflexion of the needle, then

$$r_m \cdot j = e,$$

where $e$ is the known e.m.f. of the Weston standard cell.

During the measurements, the guard-ring R was also kept at a constant potential, either that of the earth or that of the cell's anode. It will be seen from fig. 8 that only the current flowing to the cathode was measured. In other sets of measurements, however, both current flowing to the guard-ring and to the cathode were measured. *No tension on the cell greater than 4 volts was used.*

Fig. 8.

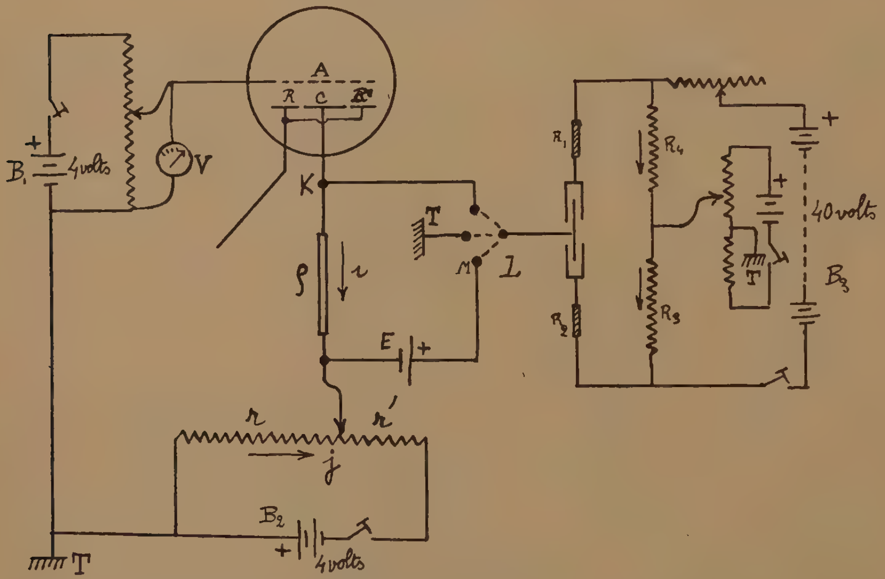

The potentials of the electrometer quadrants were adjusted through a potentiometric arrangement $R_3R_4$. The whole apparatus was properly screened and in the insulation fused silica was used throughout. Very stable results and comfortable operation were thus obtained. The limit of sensitivity of the apparatus was somewhat below $10^{-12}$ amp. The general accuracy of one set of measurements was seldom worse than 1 in 1000, as will be seen below.

## § 5. *Results: Response of the Cells to Light.*

Measurements were carried on from June, 1937, to June, 1938, on a series of six cells of the same type; sets made in which the light used was filtered through a Corning monochromatic red glass (No. 246); in other sets the total radiation of the lamp was used. Some examples of the results obtained are given here.

Cell No. 11.—" Red " Light.

| Flux. | Photocurrents measured. | Flux. | Photocurrents. | |
|---|---|---|---|---|
| | | | Measured. | Computed, admitting proportional response. |
| $\phi_1$ | 438 | $\phi_1+\phi_2$ | 883 | 884 |
| $\phi_2$ | 446 | $\phi_1+\phi_2+\phi_3$ | 1331 | 1333 |
| $\phi_3$ | 449 | $\phi_1+\phi_2+\phi_3+\phi_4$ | 1748 | 1749 |
| $\phi_4$ | 416 | | | |

Cell No. 13.—" White " Light.

| Flux. | Photocurrents measured. | Flux. | Photocurrents. | |
|---|---|---|---|---|
| | | | Measured. | Computed, admitting proportional response. |
| $\phi_1$ | $166_2$ | | | |
| $\phi_2$ | $169_4$ | $\phi_1+\phi_2=\Sigma_1$ | $335_5$ | $335_6$ |
| $\phi_3$ | $182_4$ | $\phi_1+\phi_2+\phi_3=\Sigma_2$ | $519_0$ | $518_5$ |
| $\phi_4$ | $179_0$ | $\phi_1+\phi_2+\phi_3+\phi_4=\Sigma_3$ | $698_0$ | $697_5$ |
| $\Sigma_2=\phi_5$ | $519_5$ | | | |
| $\phi_6$ | $560_5$ | $\phi_5+\phi_6=\Sigma_4$ | $1080_5$ | $1080_0$ |
| $\Sigma_4=\phi_7$ | $1080_5$ | | | |
| $\phi_8$ | 1154 | $\phi_7+\phi_8=\Sigma_5$ | $2239_5$ | $2234_5$ |
| $\Sigma_5=\phi_9$ | 2239 | | | |
| $\phi_{10}$ | 2038 | $\phi_9+\phi_{10}$ | 4277 | 4277 |

Cell No. 14.—“ White ” Light.

| Flux. | Photocurrents measured. | Flux. | Photocurrents. | |
|---|---|---|---|---|
| | | | Measured. | Computed, admitting proportional response. |
| $\phi_1$ | $285_0$ | | | |
| $\phi_2$ | $276_0$ | $\phi_3+\phi_4$ | $601_0$ | $601_5$ |
| $\phi_3$ | $300_5$ | $\phi_2+\phi_3+\phi_4=\Sigma$ | $875_5$ | $877_5$ |
| $\phi_4$ | $301_0$ | $\phi_1+\phi_2+\phi_3+\phi_4$ | $1164_5$ | $1162_5$ |
| $\Sigma=\phi_5$ | $875_5$ | | | |
| $\phi_6$ | $812_0$ | $\phi_5+\phi_6$ | $1687_0$ | $1687_5$ |

Other numerical examples would be tedious. The results can be summed up very simply : with none of the cells could any systematic departure from proportionality of response greater than the incertitude involved by measurement be found. This holds whether the guard-ring was illuminated or not, and whether its potential was that of the anode or that of the cathode, the only condition to be fulfilled being evidently that the distribution of light and electric conditions should remain the same during one complete set of measurements.

None of the cells, during all the time they were in use, gave any dark-current that could be detected. Heating the cathode stem proved unnecessary. This, of course, is due to the extremely low values of the potential differences used on the cells. Partly for the same reason, and partly because of the screening, no “ fatigue ” and no “ shift ” were seen during the measurements, the photocurrent keeping very constant indeed, in spite of the fact that caesium layers are generally of poor stability.

## § 6. *Results.—Space-charge, Negative Currents and the Shape of the Current.—Potential Characteristics.*

From the fact that the law of proportionality holds for these cells whether the guard-ring is illuminated or not, and whether the guard-ring is connected to the anode or to the cathode, one should not imply that the properties of the cells are the same in all these cases. On the contrary, the shape of the characteristic curves $1=f(V)$ is largely dependent upon these conditions.

1. *Space Charge.*—Let us begin with the simplest case: the whole surface of the cathode and guard-ring is uniformly illuminated and both these electrodes are earthed or connected to one terminal of the battery (fig. 8). Some of the response curves for constant illumination $i=f(V)$ obtained in this case are given on fig. 9, which shows immediately that, as foretold, the cell yields a photocurrent even for retarding potentials, and saturation is obtained for a very small accelerating potential difference, in the present case about 1 volt. This value has no connexion with the theoretical Volta potential difference between tungsten and caesium: in the three cells to which fig. 9 is related, anode and cathode had both been coated with a caesium layer; the Volta potential difference between the surfaces thus obtained, much smaller than that between Tu and Cs, could not be foretold, and is probably slightly different from one cell to another. This difficulty prevented a systematic investigation of the influence of the geometrical characteristics of the cells on their properties; six cells had been built with different values of the distances between anode and cathode and of the distances between the anode wires. Unhappily, the variations adopted were too small, and the effect produced was of the same order of magnitude as that due to the shift in Volta potential difference from one cell to another, so that, apart from

Fig. 9.

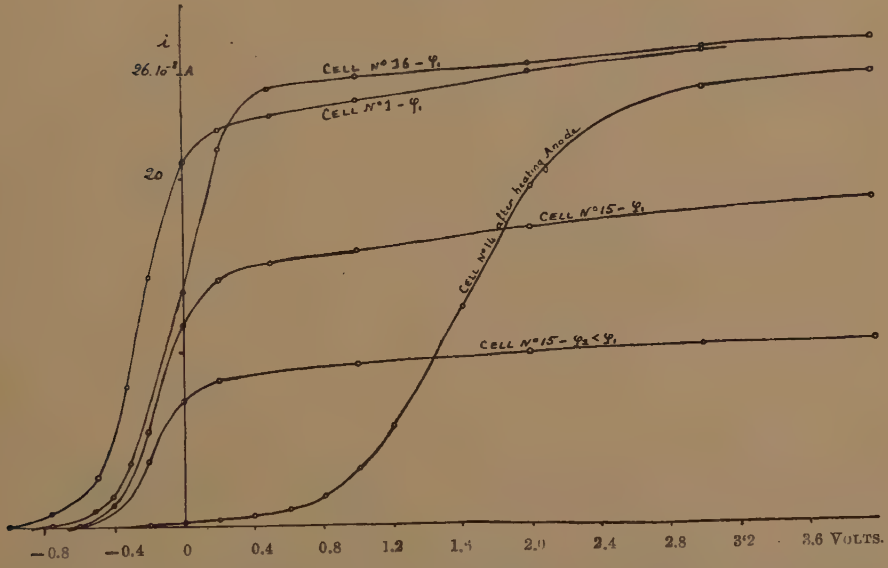

the fact that the greater the number of the anode wire the smaller the saturation potential difference, no very clear results were obtained.

Heating the anode wires before using the cells evaporated the caesium layer and greatly increased the saturation potential, as appears also in fig. 9: the anode of cell 14 in this figure had been heated just before measuring the response curve $i=f(\mathrm{V})$ shown on this figure, and the saturation potential difference became of the order of 4 volts, which is reasonably near the value of the Volta potential difference between tungsten and caesium (3±0·6 volt). Fig. 9 shows further that no complete saturation really occurs. The response curve $i=f(\mathrm{V})$ is never quite flat; nor is it quite straight; on a smaller scale, we meet here the same defect as in commercial cells. The cause also is the same: the space charge, though greatly reduced, is not negligible.

To study this further, the problem of potential distribution between plane-parallel electrodes, when the cathode is emitting electrons, has been investigated. Langmuir's classical calculation is of little aid here as the working hypotheses used in it do not hold in the present case: the initial energy of the photoelectrons is very far from being negligible, and is, as a matter of fact, of the same order of magnitude as the accelerating potential difference used; the value of the electric field on or near the cathode, too, cannot be taken as 0. Using only Poisson's condition and the kinetic energy theorem,

$$\frac{d^2\mathrm{V}}{dx^2}=\frac{4\pi j}{v},$$

$$v^2-v_0^2=-\frac{2e}{m}\mathrm{V}$$

(where V is the accelerating potential difference, $x$ the distance of the electrodes, $j$ the current per square centimeter, $v$ the speed of the photoelectrons at point $x$, and $v_0$ their initial speed for $x=0$), the position of the equipotential surfaces in the space between anode and cathode was calculated. The following equation was obtained:

$$\left[\mathrm{K}-\frac{2m}{e}4\pi j\sqrt{v_0^2-\frac{2e}{m}\mathrm{V}}\right]^{\frac{1}{2}}\cdot\left\{\frac{1}{6}\left[\mathrm{K}-\frac{2m}{e}4\pi j\sqrt{v_0^2-\frac{2e}{m}\mathrm{V}}\right]+\mathrm{L}\right\}$$
$$+\mathrm{M}=\pm\frac{m}{e}(4\pi j)^2x,$$

in which K, L, M, are constants, determined by the limiting conditions

cathode: $\mathrm{V}=0 \quad \frac{d^2\mathrm{V}}{dx^2}=4\pi\frac{j}{v_0},$

anode: $\mathrm{V}=\mathrm{V}m$ *,

their numerical values in specified conditions being easily computed.

---

* For details, see appendix (p. 182).

From this equation, it was ascertained that, for initial energies ranging from 0 to 4 volts, and for saturation currents not greater than $10^{-7}$ amp./cm.$^2$, the distortion of the field was just detectable, the displacement of equipotential surfaces never being greater than 0·5 per cent. But it must be remembered that the anode is not really a plane surface, and that the total projected surface of the wires that compose it is of the order of 1/100 of the surface of the cathode. As K in the working conditions of the cell is always great compared with

Fig. 10.

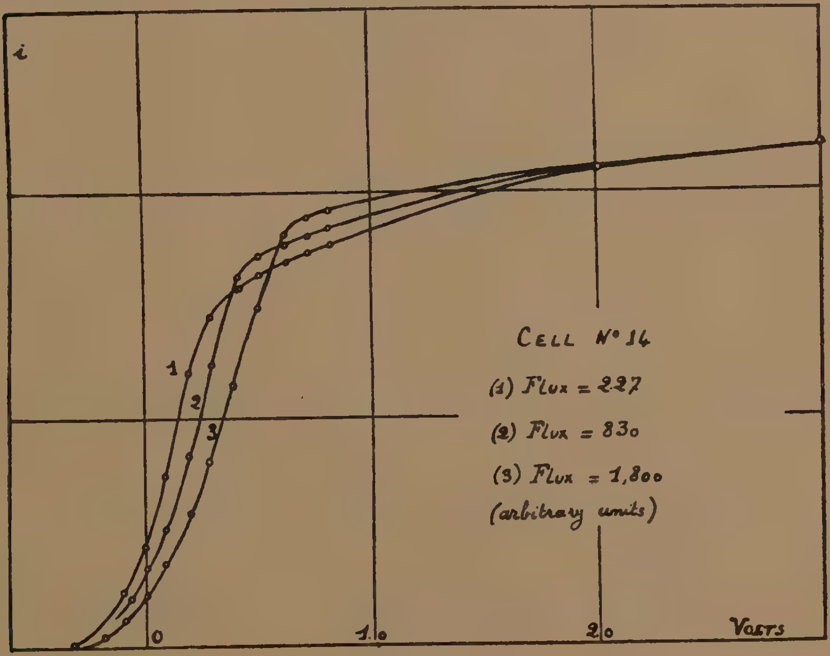

$$\frac{2m}{e}4\pi j\sqrt{v_0{}^2-\frac{2e}{m}\mathrm{V}},$$

the distortion of the field is not multiplied by 100, but in the neighbourhood of the anode it ceases to be negligible, so that measurable retardations of saturation should occur even when $j<10^{-7}$ amp. The best way to show this is, having drawn curves $i=f(\mathrm{V})$ for increasing illuminations of the cell cathode, to compute from these results the first derivative

$$\frac{di}{d\mathrm{V}}=e\frac{d\mathrm{N}}{d\mathrm{V}}.$$

If there is no space-charge retardation effect, $\frac{dN}{dV}$ is the normal energy distribution function of the photoelectrons, and the curves

$$\frac{di}{dV}=f(V)$$

should all coincide. If, on the other hand, the preceding remarks hold true, a shift of these curves with growing illumination should appear, the apparent initial energy of the photoelectrons growing less when their number increases.

Fig. 11.

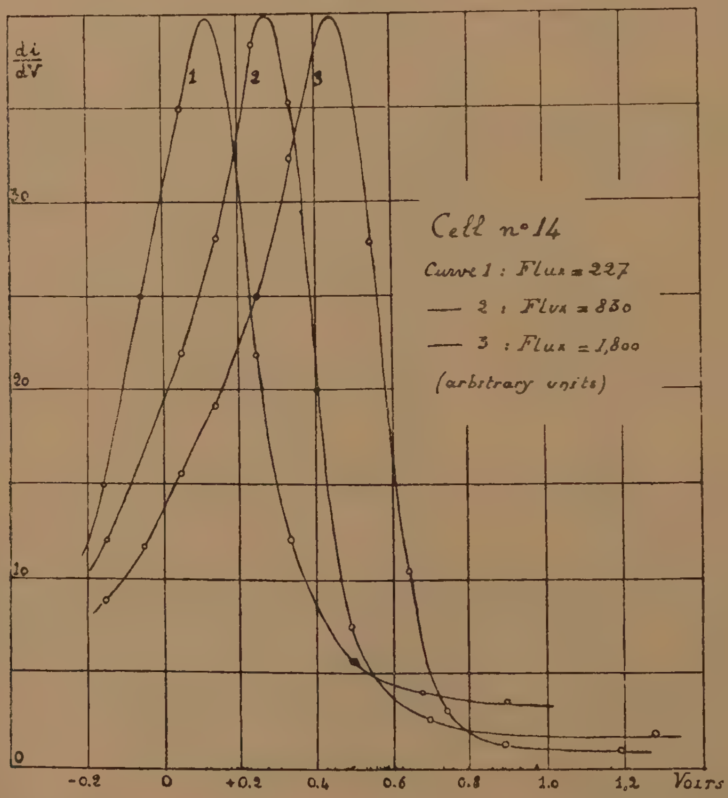

This is actually the case. From the reduced characteristic curves $i=f(V)$ of fig. 10, the curves $\frac{di}{dV}=f(V)$ have been computed (cell No. 14 before heating; fig. 11). The shift in the peak of the curves is here greater than 0·3 volt; the largest current measured in this experiment was $5 \cdot 10^{-8}$ amp.: as previously stated, this proved that even in these cells distortion of the field is not absent. Though its effect on the response of the cell to light is not detectable, its influence is felt on the curves $\frac{di}{dV}=f(V)$. Incidentally, this shows with what care experiments on the determination of the energy distribution function of photoelectrons must be conducted, to avoid errors due to this effect.

2. *Negative Currents.*—Fig. 9, giving the shape of the curves $i=f(V)$ for uniform illumination of the whole sensitive surface, is not complete.

Fig. 12.

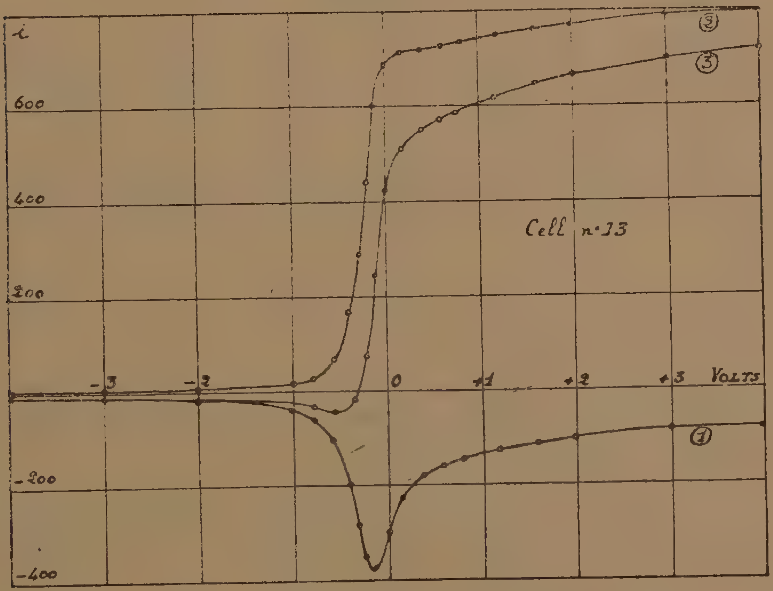

When increasing negative potential differences are applied to the cell, the current-voltage curves cross the horizontal axis and "tail off," a negative current being measurable even for a retarding potential difference of 4 volts. Curve No. 3 on fig. 12 shows this effect, measured on cell No. 13. These negative currents have two origins: (*a*) one part, $i_1$ is yielded by the anode, when this bears a caesium layer: it is always less than 1 per cent. of the total; (*b*) the rest, $i_2$, comes from the illuminated guard-ring, whose photoelectrons may fall on the adjoining cathode *.

---

* Naturally, electrons coming from the cathode also fall on the guard-ring in comparable numbers. It will be remembered that only the cathodic current is measured and plotted.

When the field $h$ has the direction given in fig. 13, the path of a photo-electron liberated on the surface of the guard-ring may be such as the dotted parabola on fig. 13 ; in that case, the electrons fall on the cathode at a distance $x$ from its starting-point,

$$x=\frac{m}{e}\frac{v^2}{h}\sin^2\alpha.$$

As long as the retarding field $h$ has large values, the value of $x$ remains very small, so that few electrons coming from the guard-ring may fall on the cathode. When $h$ decreases, $x$ increases ; so does the negative current. This should reach a maximum when $x$ takes values of the order of magnitude of the cathode diameter ; from now on, the negative current should diminish and become negligible as soon as the sign of $h$ changes, that is to say, when saturation occurs : the variations of the number of electrons released on the guard-ring and falling on the cathode should vary with the potential difference in the manner illustrated by fig. 14.

Fig. 13.

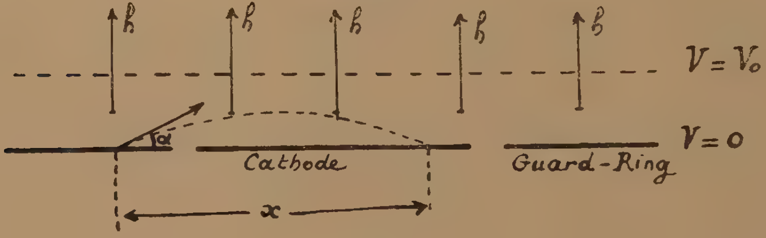

Fig. 14.

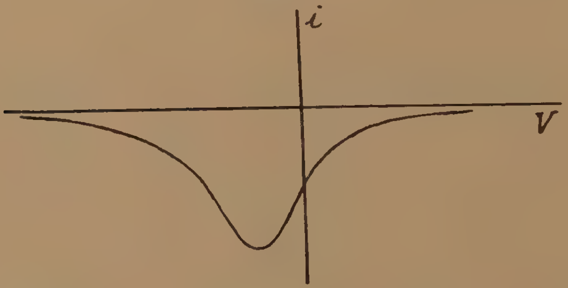

Now, such a phenomenon can be isolated and studied alone in a very simple way : by using a suitably shaped diaphragm, the light falling on the cathode may be intercepted, and the guard-ring alone illuminated ; curve I on fig. 13 gives a representation of the cathodic current measured in this case. It will be easily seen that, for increasing positive potentials, this current decreases much more slowly than in fig. 14; the curve is not symmetrical; we have been unable to demonstrate the reason for this fact, which has been found in all the cells *.

Anyhow, further proof of the origin of this negative current can be obtained by measuring the cathodic current obtained when the cathode alone is illuminated. Curve II on fig. 13 is then obtained. If the small anodic component $i_1$ be excepted (in all cases $i_1$ is always too small to be seen on fig. 13), the negative tail of the current potential characteristic has entirely disappeared. The apparent sensitivity is increased. Moreover, the algebric sum of the currents given by the cathode in case I and II for each value of the potential difference, when plotted, fall on curve III with an approximation of 1 in 1000, that of the whole set of measurements. This, though not a proof that no ejected electron is lost or multiplied may be considered as indirect evidence that the cell response to illumination is linear. Needless to say, most of these illuminating phenomena disappear when the guard-ring is electrically connected to the anode. It has been already stated that, in that case also, the response of the cell to illumination was linear, a fact which the reader will probably think now to be self-evident.

## § 7. *Conclusion.*

The cells whose properties have been described in the present paper were made for a practical purpose: that of finding solutions at the same time simpler and more accurate to the problems of photoelectric photometry and spectrophotometry. The writers hope that, with these cells, it will always be found possible to use the simple direct method of measurement, thus avoiding the complications involved in the null or equal deviation methods. It is expected that a registering spectrophotometer, now being built in the Laboratoire d'Essais, will give an example of such simplification.

Attention must also be drawn to the fact that the cells may be used either with the whole available light concentrated upon a part of the cathode or with constant illumination over the whole surface of cathode and guard-ring; in the first case, the luminous flux is measured; in the second, the brightness of a source may be directly determined. It will be seen at once that in many cases this possibility may be useful. As an

---

[*] A possible reason for that is found in the fact that between guard-ring and cathode (both kept at the same potential), there exists a circular region, due to the finite thickness of the electrodes, bounded by an emitting surface of no negligible area, and where the electric field is practically 0, whatever value is given to the anode potential.

example, it is possible to build with such a cell a direct reading optical pyrometer giving high precision.

Owing to the low tensions they employ, the cells are much easier to use than most commercial photoemissive cells. For the same reason, their "noise-level" when used with an amplifier is extremely small, so that—though the designer had not thought of this application—the talking-film industries might find them of use.

The first cells were exceedingly difficult to make: everything was built in a metrological laboratory, without proper equipment. There is no reason now why they could not be made cheap and of small size, particularly if one realizes that the present laboratory design could be greatly simplified without sacrificing any of its qualities. For instance, cells have recently been built in this Laboratory, designed as shown in fig. 15: the anode is a Faraday cylinder A, at the bottom of which is the photosensitive cathode C; the light comes in through a plane glass window P. The properties of such cells, now under investigation, are substantially the same: low saturation potential (*circa* 0·1 volt), strict linearity of response to light, space-charge much smaller than was the case with the first model, so that after saturation, the current-potential characteristics are quite straight and horizontal up to the first excitation potential of the residual gas in the cell. Many other designs giving similar results can be conceived.

Fig. 15.

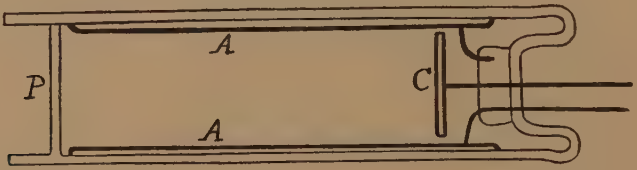

### Appendix.

*The Electric Field between two Plane-Parallel Electrodes, Electrons being present.*

As the calculation may be found useful for the study of other problems in electronics, it is given here in full (notations, p. 176).

Starting from the fundamental conditions:

$$\mathrm{I}\begin{cases}\dfrac{d^2V}{dx^2}=\dfrac{4\pi j}{v}, & \ldots\ldots\ldots \quad (1)\\[2ex] v^2-v_0{}^2=-\dfrac{2e}{m}V, & \ldots\ldots\ldots \quad (2)\end{cases}$$

and

$$\mathrm{II}\left\{\begin{array}{ll}\dfrac{d^2V}{dx^2}=4\pi\dfrac{j}{v}, & \qquad (1)\\[2ex] mv\dfrac{dv}{dx}=-e\dfrac{dV}{dx}, & \qquad (2')\end{array}\right.$$

one finds

$$\frac{d^2V}{dx^2}=4\pi j\frac{1}{\sqrt{v_0^2-\frac{2e}{m}V}}, \qquad (3)$$

and

$$(4\pi j)^2\frac{m}{e}\left(\frac{d^3V}{dx^3}\right)-\left(\frac{d^2V}{dx^2}\right)^3.\frac{dV}{dx}=0, \qquad (4)$$

eq. (3) is easily integrated by substituting $p$ for $\frac{dV}{dx}$, the resultant equation being

$$\left(\frac{dV}{dx}\right)^2=-\frac{2m}{e}(4\pi j)\sqrt{v_0^2-\frac{2e}{m}V}+K, \qquad (5)$$

eq. (4), by substituting, $h=\frac{dV}{dx}$ and $q=\frac{dh}{dx}$, gives, by two successive integrations, the equation

$$\frac{1}{6}\left(\frac{dV}{dx}\right)^3+L\frac{dV}{dx}+M=-(4\pi j)^2\frac{m}{e}x. \qquad (6)$$

Eliminating $\frac{dV}{dx}$ between these two equations, one finds the equation given, p. 176 :

$$\left[K-\frac{2m}{e}.4\pi j.\sqrt{v_0^2-\frac{2e}{m}V}\right]^{\frac{1}{2}}\left\{\frac{1}{6}\left[K-\frac{2m}{e}.4\pi j\sqrt{v_0^2-\frac{2e}{m}V}\right]+L\right\}+$$
$$+M=\pm\frac{m}{e}[4\pi j]^2x. \qquad (7)$$

Only one relation between constants K, L, M can be computed by an easy algebric method. On the cathode, we have

$$\frac{d^2V}{dx^2}=4\pi\frac{j}{v_0}; \qquad (8)$$

from equation (II.) it can be shown that

$$\frac{d^2V}{dx^2}=\frac{-[4\pi j]^2\frac{m}{e}}{\frac{1}{2}\left(\frac{dV}{dx}\right)^2+L}; \qquad (9)$$

eliminating $\left(\frac{dV}{dx}\right)$ between equations (5) and (9) we find

$$K=-2L. \qquad (10)$$

In the case of $v_0=0$, one more relation can be found by making $x=V=0$; in equation (7), we find

$$M=\frac{1}{3}K^{\frac{3}{2}}.$$

In all cases K is to be calculated numerically for stated values of $j$, $x_0$ (distance of electrodes) and $V_0$. The actual calculation of the location of equipotential surfaces, though not difficult, is slow: the coefficient of $x$ being small, the first member of the equation, which is a sum of three terms all of the same order of magnitude, must be known to within many places of decimals (9 at least for $j=10^{-6}$ amp. and $x=2$ mm.). In contradistinction with the classical hypothesis, the electric field near the cathode is not found to be null.

# XIV. *The Influence of the Cathode on the Sparking Potential of Hydrogen.*

By F. Llewellyn Jones, M.A., D.Phil., and J. P. Henderson, B.Sc., University College, Swansea *.

[Received February 14, 1939.]

## 1. *Introduction.*

The development of a complete theory of the spark discharge in gases has been handicapped by the lack of reliable data concerning the influence of the material of the cathode on the sparking potential. However, measurements with neon †, argon ‡. and mercury vapour § have supplied evidence of the dependence of the sparking potential of the monatomic gases on the material of the cathode. On the other hand, older data indicate that the sparking potential of the commoner gases is independent of the cathode material, and that their minimum sparking potential is a property of the gas only ‖.

The experiments described in this paper were carried out with hydrogen, in order to investigate whether the sparking potential of a simple diatomic gas depends on the electrode material. In a diatomic gas it is possible that there is less restriction on the energies of the positive ions, because the process of electron exchange is not so effective in limiting the energies of the ions as it is in a monatomic gas. To test the effect of the cathode, the sparking potential was measured for six different cathodes throughout the range of gas pressures from 1 to 520 mm. of mercury.

## 2. *Description of the Apparatus.*

The type of discharge-tube used and the general experimental procedure were similar to those described in a previous paper on mercury vapour ¶. Three tubes were constructed in which the pairs of electrodes were parallel disks of: (i.) commercial aluminium and slightly oxidized Staybrite steel, (ii.) nickel and pure aluminium, (iii.) clean Staybrite steel and copper. The edges of the electrodes were rounded to avoid sharp points, and they were held about 3·5 mm. apart. The exact distances were measured by means of a cathetometer. The ratio between the diameter of the electrodes and their distance apart was about 12, so that the electric field between them was sensibly uniform. Before assembly the electrodes were highly polished, and, together with the tungsten wires for the seals, they were thoroughly de-gassed at a high temperature (750° C. for Fe, Ni, and Cu) in a vacuum furnace. When the Pyrex glass discharge-tubes were complete, they were maintained at 400° C. for some days and continuously evacuated. The diffusion of mercury vapour from the McLeod gauge and the diffusion pump into the gas system or the discharge-tubes was prevented by a liquid-air trap, and the tubes were further isolated from all taps by another liquid-air trap, which prevented the diffusion of vapours from the vacuum-grease taps into the tubes. This particular trap was immersed in liquid air throughout the course of the measurements, so that the possibility of contamination of the gas and the discharge-tubes was remote. All three tubes were open to one another, as shown in fig. 1, so that the gas in each tube was in the same state of purity.

---

* Communicated by the Authors.

† G. Holst and E. Oosterhuis, *Vers. Kon. Akad. Wet. Am.* xxiv. p. 849 (1920).

‡ S. P. McCallum and L. Klatzow, Phil. Mag. xvii. p. 291 (1934); F. M. Penning and C. C. Addink, 'Physica,' i. p. 1007 (1934); R. Schöfer, *Zeits. f. Phys.* cx. p. 21 (1938).

§ F. Llewellyn Jones and W. R. Galloway, Proc. Phys. Soc. l. p. 207 (1938).

‖ J. J. and G. P. Thomson, 'Conduction of Electricity through Gases,' 3rd edit. ii. pp. 476–487, Cambridge University Press (1933).

¶ F. Llewellyn Jones and R. Galloway, *loc. cit.*

Fig. 1.

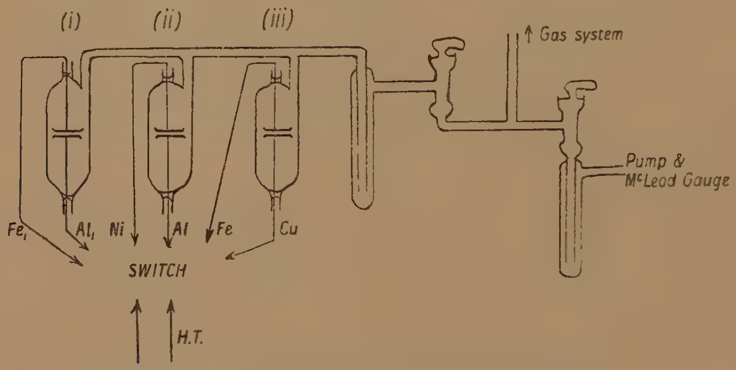

The arrangement of the discharge-tubes.

The hydrogen was prepared by the electrolysis of barium hydrate, and after drying over phosphorus pentoxide the gas was admitted to the discharge-tubes through heated palladium, and, finally, through the tube cooled by liquid air. The potential was applied to the electrodes through a resistance of 16 $M\Omega$, and the sparking potential was taken as the potential which would then just maintain a current through the gas, as this was found to be simpler than using an electrometer, which gave the same results. A suitably designed switch, mounted on ebonite to ensure good insulation, could reverse the polarity and rapidly apply the high tension to any tube as desired

Fig. 2.

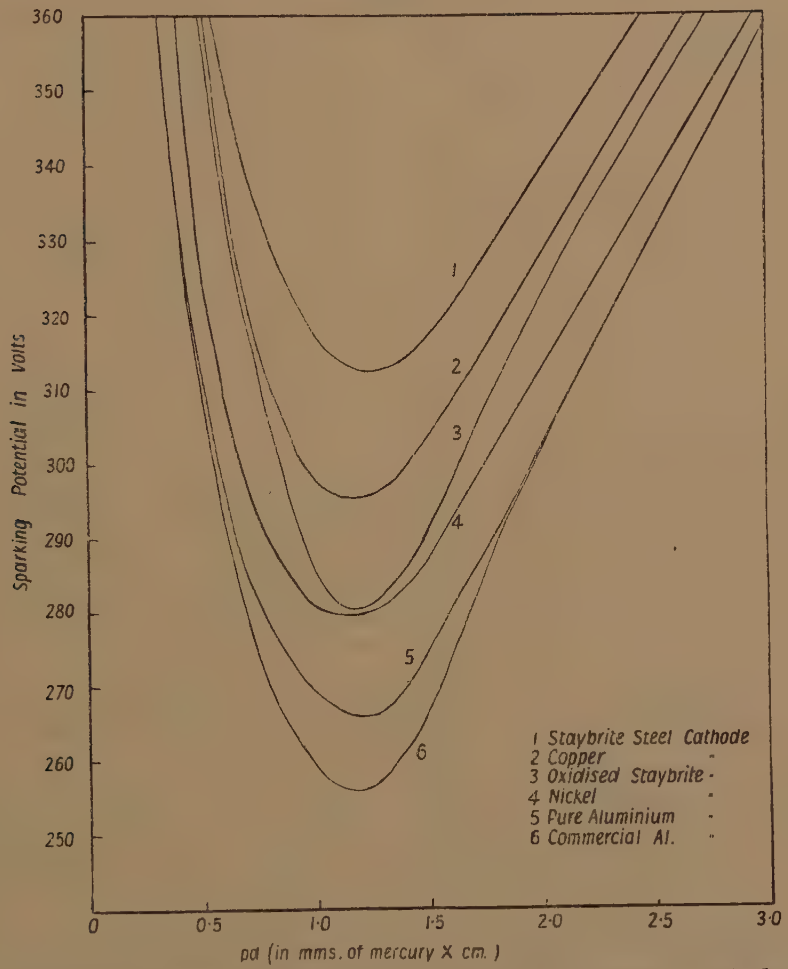

The minimum sparking potential of hydrogen with different cathodes.

## 3. *Experimental Results.*

### *The Minimum Sparking Potential.*

The range of pressures near those corresponding to the minimum sparking potential were investigated when each of the six electrodes was in turn used as the cathode, and the results are given in fig. 2. The spark parameter is $\rho d$, where $\rho$ is the density of the gas expressed as its pressure at 15° C. It can be seen from fig. 1 that the potentials are definitely a function of the cathode material, and the minimum values obtained with the different surfaces are given in the following table :—

| Cathode. | Minimum sparking potential in volts at $Z/\rho=230$. |
|---|---|
| Commercial aluminium | 256 |
| Pure aluminium | 266·5 |
| Nickel | 279·6 |
| Oxidized Staybrite steel | 280 |
| Copper | 295 |
| Clean Staybrite steel | 312·5 |

Since these values are independent of any error made in estimating $\rho d$, they enable a direct comparison of the sparking potentials for the different cathodes to be made easily. Except in the case of the nickel cathode, which has the highest work function, the minimum sparking potential increases with the work function of the cathode surface ; and it is lowered by the presence of impurities in the cathode material or by the oxidation of the surface.

These results can only be interpreted on the assumption that secondary emission of electrons from the cathode plays an important part in the mechanism of the spark, at least for most electrodes. It follows that slight oxidation of the surface, or the presence of small impurities in the metal, considerably increases the secondary emission from the cathode. This is in accordance with the results of direct experiments on secondary emission ; for it is well established that the secondary emission of electrons due to the impact of positive ions *, and also to the incidence of ultraviolet light, is profoundly influenced by the state of the surface of the cathode. Moreover, Farnsworth † found that the exposure of a nickel target to hydrogen after de-gassing considerably increased its secondary emission under electron impact, and it is possible that some similar effect is responsible for the anomalous position of nickel in the table.

---

* F. M. Penning, *Verh. Kon. Akad. Wet. Amst.* xxxiii. p. 941 (1930).

† H. E. Farnsworth, Phys. Rev. xx. p. 358 (1922).

*The Complete Sparking Curves.*

Early measurements * of the sparking potential of diatomic gases at pressures of the order of atmospheric have indicated that the sparking potential was completely independent of the cathode material, and in order to verify this conclusion the sparking potential of hydrogen was measured for the six cathodes at pressures up to 520 mm. of mercury. The procedure was to measure the change in sparking potential in each tube on reversing the potential, because small errors in estimating *pd* are of great importance at high pressures, and this makes it difficult to

Fig. 3.

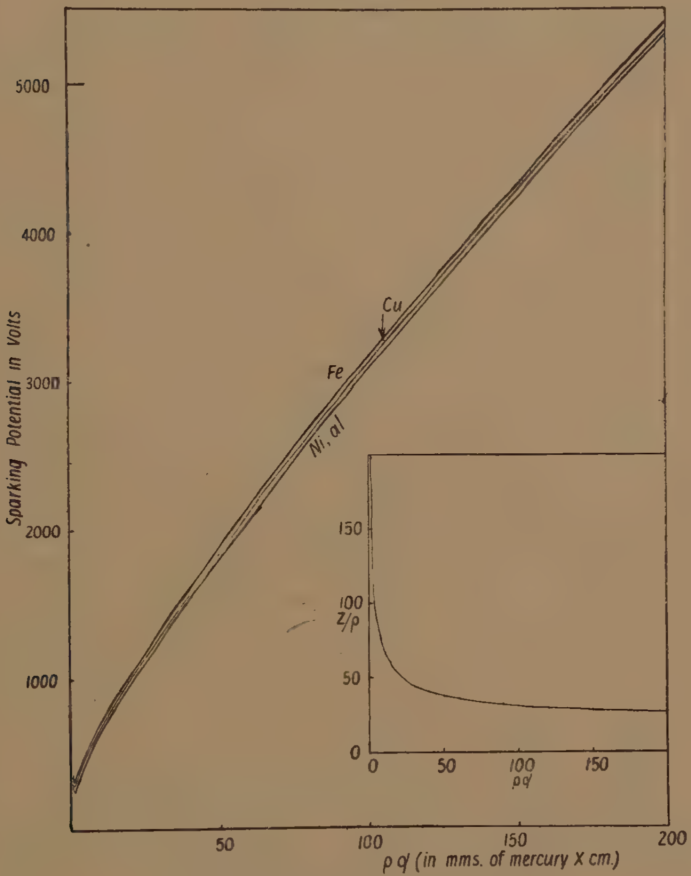

The sparking potential of hydrogen.

---

* ‘Conduction of Electricity through Gases,’ p. 475.

compare, with any great accuracy, the values of the sparking potentials obtained with different tubes. With each tube the change in the potential was found to increase slightly as $\rho d$ increased from about 10 to 200, but the average difference over the full pressure range was slightly less than the difference between the minimum sparking potentials. For example, with tube (i.), the average difference between the sparking potentials for the cathodes of commercial aluminium and slightly oxidized Staybrite steel was 24·6 volts, while the difference between the minima was 25·6 volts. Consequently, while the fractional change in the minimum sparking potentials was 10 per cent. at the highest pressure, when $\rho d$ was 200, the change in sparking potential was less than 0·5 per cent. A similar result was obtained with tube (ii.), but with tube (iii.) the difference slowly increased with the pressure. Hence it would appear that, at pressures greater than atmospheric, the change in sparking potential would become small enough to fall within the experimental error, and the sparking potential would then appear to be completely independent of the cathode material, at least for the commoner metals.

The complete sparking curves are given in fig. 3. The curves obtained with tube (i.) lie so near those obtained with tube (ii.) that they could not be drawn separately. The curve for a nickel cathode is in good agreement with that given recently by Schöfer *. It can be seen that the ratio $Z/\rho$ falls rapidly from about 230, at the minimum sparking potential, to 27 at the highest pressure when $\rho d$ was 200, and it is highly probable that the limiting value of $Z/\rho$ is not less than 25.

In conclusion we wish to express our best thanks to Prof. E. J. Evans for extending to us the facilities of his laboratory and for his kind interest.

## *Summary.*

The sparking potential of hydrogen between parallel electrodes, previously de-gassed at a high temperature, was measured throughout a range of gas pressures from 1 to 520 mm. for six different cathodes of the following metals: clean and slightly oxidized Staybrite steel, pure and commercial aluminium, nickel, and copper. Marked dependence of the sparking potential on the cathode material was found, especially at the minimum values. These were 266·5, 280, 295, and 312·5 volts for Al, Ni, Cu, and Fe respectively. The change in sparking potential due to a change of cathode at any given pressure was practically constant throughout the pressure range; consequently, at 520 mm. the fractional change in potential was very small. This change was about 10 per cent. at the minimum sparking potential, but less than 0·5 per cent. at 520 mm.

---

* *Loc. cit.*

Hence it was concluded that, at pressures greater than atmospheric, the material of the cathode would appear to have a negligible effect on the sparking potential of hydrogen.

*Note added in Proof.*—Since the above was written, sparking potential curves for hydrogen with platinum and sodium cathodes have been given in a recent paper by Ehrenkranz (*Phys. Rev.* lv. p. 219 (1939)), who obtained results in general agreement with ours. However, Ehrenkranz considered that her values were lowered, possibly by the effects of small traces of impurities. This view is confirmed by the fact that, when $pd$ is less than 50, her values of the sparking potential with a platinum cathode are actually lower by about 5 per cent. than those given above in fig. 3 for a Staybrite steel cathode ; although for higher values of $pd$ the two curves are identical. This fact suggests a slight contamination of the platinum cathode.

Further, it may be pointed out that the values of the minimum sparking potentials given in fig. 2 are those corresponding to conditions of equilibrium between the cathodes and the gas, for if the potentials are measured immediately after the admission of the gas to the discharge-tubes which have been kept evacuated for some time previously, then the minimum sparking potentials for all six electrodes are raised by about 15 volts, with a corresponding increase in $pd$, so that the ratio $Z/p$ remains at 230. The values measured in this way for the Fe, Cu, and Al cathodes are 329, 319, and 278. The effect is most pronounced in the neighbourhood of the minima, for at greater values of $pd$ the sparking potentials are the same as those given above.

Swansea.
13th February, 1939.

# XV. *The Mechanism of the Spark Discharge in Hydrogen.*

By F. Llewellyn Jones, M.A., D. Phil.,
University College, Swansea *.

Received February 27, 1939.]

## I. *The Sparking Potential and Cathode Processes.*

The observed † changes in the sparking potential of hydrogen due to changes in the cathode material can be readily interpreted on the Townsend theory of the spark discharge. Let V be the sparking potential defined as that potential which, independent of the current, will maintain a current however small. If $\alpha$ is the coefficient of ionization by electrons, the condition for the passage of a spark between parallel electrodes at a distance $d$ apart is ‡

$$0=1-\delta/\alpha\,.\,(e^{\alpha d}-1), \qquad \qquad (1)$$

where

$$\alpha=pf(\mathrm{Z}/p)=pf(\mathrm{V}/pd)=pf(x).$$

The factor $\delta$ depends on the mechanism of the secondary inonization process, and if this consists simply of the secondary emission of electrons from the cathode as a result of the impact of positive ions, then $\delta$ can be written as $\alpha\gamma$, where $\gamma$ is the average number of electrons which leave the cathode on account of the impact of each positive ion. Alternatively, if the electron emission is entirely due to the photo-electric effect of the radiation excited by the collisions of electrons with the molecules of the gas, then $\delta\,.\,dx$ is the number of electrons set free from the cathode by the photons excited by each electron in traversing 1 cm. in the direction of the electric field. It is highly probable, however, that in general $\delta$ does not represent any one single process, but a combination of secondary processes.

Putting $\delta/\alpha=y$, and differentiating equation (1), it follows that

$$\begin{aligned} d\mathrm{V} &= -dy/\{y(1+y)f'(\mathrm{V}/pd)\} \\ &= -dy/\{yf'(x)\}, \qquad \qquad (2) \end{aligned}$$

since $y$ is small, and $(1+y)$ is then approximately equal to 1.

---

* Communicated by the Author.

† F. Llewellyn Jones and J. P. Henderson, Phil. Mag. xxviii. p. 185 (1939).

‡ J. S. E. Townsend, Phil. Mag. xlv. p. 444 (1923).

Thus the change in V due to a change in $\delta/\alpha$ depends on $Z/p$, so that $dV$ is a constant when $Z/p$ is constant. Now it is a characteristic of all discharges in gases that $Z/p$ becomes very nearly constant for high gas pressures, and in hydrogen $Z/p$ only falls from 32 to 28 when $pd$ is increased from 90 to 200, and for still higher pressures it is highly probable that $Z/p$ never falls below 25. Consequently, the sparking potential curves for the different cathodes should be nearly parallel at high pressures, and the curves obtained experimentally show this to be the case. In order to calculate the value of $dV$ corresponding to any fractional change in $(\delta/\alpha)$, it is necessary to know the form of the function which expresses $\alpha/p$ in terms of $Z/p$. An empirical formula for $\alpha/p$ has been given by Townsend *, which is in good agreement with the experimental determinations of Ayres † and others ‡, throughout the range of $Z/p$ from 30 to 400, which was the range covered in the measurements of the sparking potential. The values of $\alpha/p$ and of $f'(x)$ are given in fig. 1, where

Fig. 1.

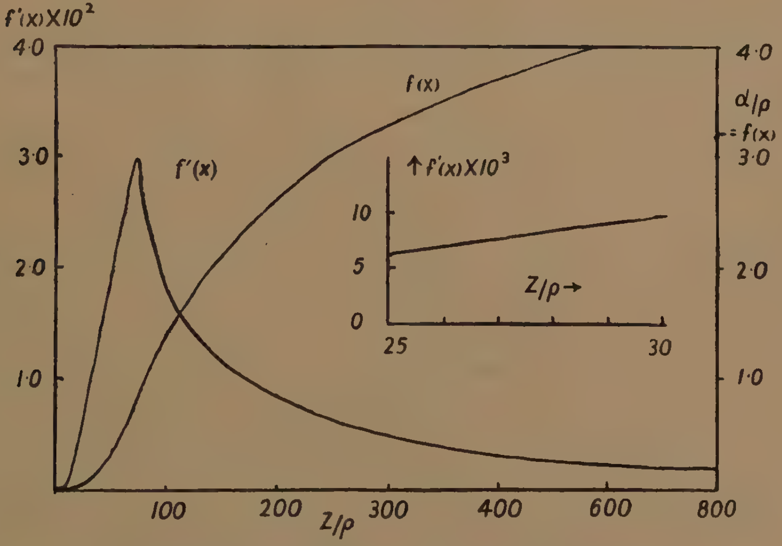

Graphs of the functions $\alpha/p=f(Z/p)$ and $y=f'(x)$.

$$\alpha/p=Ae^{-B/x},$$

and A and B are constants respectively equal to 5 and 130.

---

* J. S. E. Townsend, 'Ionization by Collision,' p. 25, Constable (1910).

† T. L. R. Ayres, Phil. Mag. xlv. p. 353 (1923).

‡ A. v. Engel and M. Steenbeck, *Electrische Gasentladung*, Bd. i. p. 106, Springer, Berlin (1932).

It can be seen from fig. 1 that $f'(x)$ has the same value when $Z/\rho$ is about 27 ($\rho d=200$) as when $Z/\rho$ is 210, which corresponds to the minimum sparking potential. Consequently, if the same process of secondary emission is operative, and $dy/y$ is constant, then $dV$ should have the same value at the high pressures as at the minimum sparking potential. This was confirmed experimentally with two pairs of electrodes, for which $Z/\rho$ was about 210 to 220 at the minimum sparking potential; these pairs were the oxidized Staybrite steel—commercial aluminium pair, and the pure aluminium-nickel pair. Further, $f'(x)$ exhibits a sharp maximum at $Z/\rho=75$, where its value is six times that at $Z/\rho=25$, or at $Z/\rho=300$. Consequently, $dV$ should be least when $Z/\rho=75$, which corresponds to values of $\rho d$ of about 5 or 6. Actually, it was found that the sparking potential curves did tend to converge within the range $10>\rho d>5$ and afterwards to diverge, but the effect was not very pronounced. It was most noticeable in the case of the aluminium-nickel pair of electrodes, for which $dV$ was zero for values of $\rho d$ between 4 and 6.

The fractional change in V is given by the equation

$$dV/V=-dy/\{yVf'(x)\}. \qquad (3)$$

For high values of $\rho d$ the ratio $Z/\rho$ is practically constant at about 25, and fig. 1 shows that $f'(x)$ varies very little in this region, as it only falls from $9{\cdot}5\times10^{-3}$ to $6{\cdot}5\times10^{-3}$ when $Z/\rho$ falls from 30 to the limiting value of 25, which is only reached at extremely high pressures. Thus $dV/V$ is nearly inversely proportional to V; and it follows that, if $dy/y$ is not too great, the fractional change in the sparking potential due to a change of cathode becomes small enough to fall within the experimental error. This accounts for the fact that, at high pressures ($\rho d>90$), the sparking potential curves of hydrogen for the different cathodes: Al, Ni, commercial Al, and oxidized Staybrite steel, were practically indistinguishable, although the difference between them and the curves for the clean Staybrite steel and copper cathodes was still noticeable. Hence it follows that the change $(y_{Fe}-y_{Al})/y_{Al}$ must be much greater than the change $(y_{Ni}-y_{Al})/y_{Al}$. There is some evidence, which will be discussed below, that at the higher pressures the photo-electric effect at the cathode is of importance, and a comparison of the magnitudes of this effect on aluminium and iron cathodes has been made by Wallraff and Horst *. This comparison can serve as a guide to the relative values of the factor $y$ for the two cathodes of Staybrite steel and aluminium. The photo-electric emission from iron due to the radiation from a spark in air was found to be about 1/3 to 1/4 of that from aluminium. Hence

---

* A. Wallraff and B. Horst, *Arch. f. Electrotechnik*, xxxi. p. 790 (1937).

if at high pressures the photo-electric effect at the cathode due to the radiation from the gas is of fundamental importance in the mechanism of the spark, then $dy/y$ would still be large enough to ensure an appreciable difference in the sparking potential for the change from an aluminium to a steel cathode.

The fact that an increase of gas pressure reduces the influence of the cathode on the sparking potential in hydrogen can be generalized for those gases for which a similar function expresses $\alpha/p$ in terms of $Z/p$. From an analysis of the electrical properties of nitrogen, Loeb * concluded that its sparking potential should be completely independent of the cathode material at atmospheric pressure, in spite of the fundamental importance of the cathode process. Consequently, the early measurements † which showed that the sparking potential of the commoner gases at atmospheric pressure was independent of the cathode material, cannot be regarded as evidence of the absence of any cathode process in the secondary ionization, since equation 3 shows that the principal factor which determines the effect of any cathode process on the sparking potential is $f'(x)$. This consideration is quite apart from the fact that the sparking potential is probably only characteristic of the cathode if it has been de-gassed. Hence it is seen that the Townsend theory is capable of explaining the general dependence of the sparking potential on the cathode material, and the above considerations are independent of the exact nature of the processes represented by the coefficient $(\delta/\alpha)$, provided that it does vary with the cathode material.

## 2. *The Coefficient* $(\delta/\alpha)$ *for Hydrogen.*

By substituting the values of $\alpha/p$ given by Ayres and others, and the values of V and $pd$ obtained from the sparking potential curves, the coefficient $\delta/\alpha$ can be calculated from equation (1), and the values thus obtained for the various cathodes are given in fig. 2.

When the ratio $Z/p$ is less than about 50 it is not easy to obtain exact values of $\delta/\alpha$ by measurement of the sparking potential, owing to the large variation of the potential with the distance between the plates; and possible inaccuracies in the published values of $\alpha/p$ are then extremely important. However, there is little doubt that $\delta/\alpha$ in hydrogen varies with $Z/p$, and that large increases in $\delta/\alpha$ occur when $Z/p$ is increased above 125. When $Z/p$ exceeds 600, the curves appear to bend over to approach a value of about 0·13; but when $Z/p$ is greater than 400, $pd$ is less than that corresponding to the minimum sparking potential, so that the values of $\delta/\alpha$ are then not highly reliable, owing to possible non-uniformity in the electric field.

---

* L. B. Loeb, Rev. Mod. Phys. viii. p. 267 (1936).

† J. J. and G. P. Thomson, 'Conduction of Electricity through Gases,' 3rd ed., vol. ii. p. 476, Cam. Univ. Press (1933).

However, the curves have the same general shape as that given for nitrogen by Posin *, rather than that given by Bowls †, provided that there are no significant errors in the published values of $\alpha/p$. The sharp increase in the value of $\delta/\alpha$ when $Z/p$ exceeds 150 was observed in nitrogen by both Posin and Bowls.

Fig. 2.

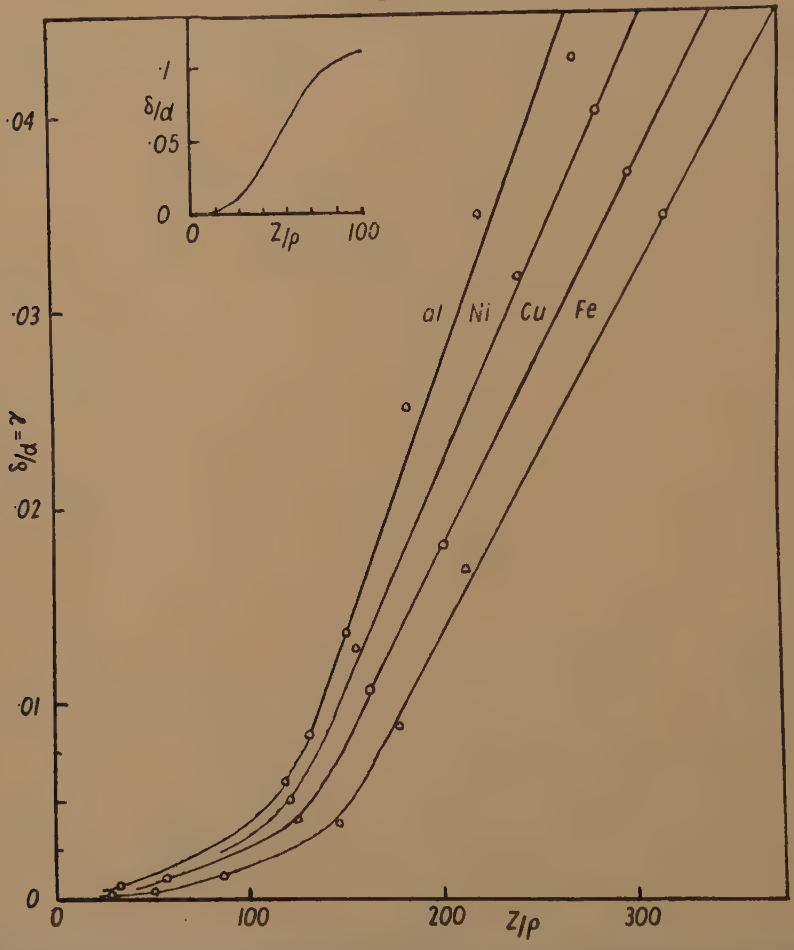

The variation of $\delta/\alpha$ with $Z/p$ for Al, Ni, Cu, and Fe cathodes in contact with hydrogen, obtained from measurement of the sparking potential.

---

* D. Q. Posin, Phys. Rev. l. p. 650 (1936).

† W. E. Bowls, Phys. Rev. liii. p. 293 (1938).

The values of $\delta/\alpha$ for the lower values of $Z/\rho$ are very important in the theory of the discharge, and they are given in the following table for the copper cathode.

| $\rho d$ | 210 | 180 | 150 | 120 | 90 | 60 | 45 | 30 | 15 |
|---|---|---|---|---|---|---|---|---|---|
| $Z/\rho$ | 26·6 | 27·5 | 28·5 | 30 | 31·9 | 35·4 | 38·5 | 43·7 | 55·7 |
| $\alpha/\rho \times 10^{-2}$ | 4·5 | 5·35 | 6·25 | 7·2 | 9·25 | 13·35 | 17·2 | 24·25 | 49·6 |
| $\delta/\alpha \times 10^{-6}$ | 0·73 | 0·65 | 0·82 | 1·2 | 2·0 | 3·0 | 4·5 | 6·0 | 7·8 |

It can be seen that $\delta/\alpha$ is increased ten times when $Z/\rho$ is only doubled, but there appears to be a slight tendency for $\delta/\alpha$ to increase with the pressure at the lowest values of $Z/\rho$. Moreover, if the above values of $\alpha/\rho$ are too high at the lower values of $Z/\rho$, then the tendency of $\delta/\alpha$ to increase with the pressure would be accentuated.

### 3. *The Variation of* $(\delta/\alpha)$ *with* $Z/\rho$.

The variation of $(\delta/\alpha)$ with $Z/\rho$, and with the electrode material, affords general evidence upon which to assess the relative importance of the three secondary processes of ionization. Consider first the photo-electric effect at the cathode; the quantity of radiation emitted per second by the current in the gas depends on the mean energy of the electrons, on their energy distribution function, on the excitation function of the gas molecules, and on the number of collisions made per second by the electrons with the molecules of the gas. The way in which these quantities determine the variation of the intensity of the radiation emitted with the pressure of the gas in a discharge has been discussed previously *.

The mean energy and the distribution function, which depend on the variation of the mean free path with velocity and the collisional losses, are determined by the ratio $Z/\rho$. Since this ratio is very nearly constant in a gas discharge at high pressures, the number of exciting collisions per second must be nearly proportional to the pressure of the gas. The radiation emitted from a corona discharge at high pressures in hydrogen has been measured by Christoph †, who found that the quantity of radiation emitted per second was directly proportional to the pressure, thus confirming the above conclusion. Now, with any reasonable distribution function and a low mean energy, the number of electrons with energies exceeding the excitation energy of the molecules is

* F. Llewellyn Jones, Proc. Phys. Soc. xlviii. p. 513 (1936).

† W. Christoph, *Ann. der Phys.* xxx. p. 446 (1937).

enormously greater than the number which have energies exceeding the ionization potential. This is especially the case in hydrogen, particularly if the distribution there is no broader than that given by Maxwell's formula *. Further, the change in $Z/\rho$ from 55 to 27 produces a decrease in the mean energy of agitation of the electrons from 6 v. to 3·6 v. † ; and the corresponding proportional decrease in the number of electrons with energies exceeding an excitation energy of, say, 12 v., is less than the proportional decrease in the number of electrons with energies exceeding the ionization potential of the gas. The factor $\delta$ is proportional to the number of exciting collisions, while $\alpha$ is proportional to the number of ionizing collisions, therefore the ratio $\delta/\alpha$ should increase with the pressure at high pressures. This conclusion has been previously pointed out by Townsend and McCallum ‡ in a discussion of the photo-electric effect in neon. Thus an increase in the factor $(\delta/\alpha)$ with the pressure, *i. e.*, as $Z/\rho$ diminishes, may be taken as evidence of the predominating influence of the photo-electric effect at the cathode. A full discussion of the variation of $(\delta/\alpha)$ with $Z/\rho$ for high values of $Z/\rho$ has been given by Loeb §, when $(\delta/\alpha)$ represents a photo-electric effect.

In considering the action of the positive ions on the cathode it may be assumed, as shown by direct experiments, that the secondary emission coefficient, $\gamma$, increases with the velocity of the ions. Hence if the velocity of the ions increases with $Z/\rho$, then $\gamma$ must also increase: and if the energy of the ions is maintained constant in spite of increases in $Z/\rho$, then $\gamma$ remains independent of $Z/\rho$, and this is found to be generally the case with the monatomic gases.

Thirdly, ionization by collision by positive ions will occur when the ions attain high energies, and this will result in large increases in $\delta$ $(=\beta)$, and probably in $\delta/\alpha$, *i. e.*, in $\beta/\alpha$, also at very high values of $Z/\rho$.

## 4. *The Second Townsend Coefficient.*

The marked variation of the sparking potential of hydrogen with the material of the cathode, and the fact that the experimental results are readily accounted for by equation (2), prove that the coefficient $(\delta/\alpha)$ must, in part at least, represent a cathode process. Nevertheless, in order to account for the observed variation of the sparking potential with the material of the cathode, it is not essential that the factor $(\delta/\alpha)$ should represent cathode processes only, to the entire exclusion of any ionization by collision in the gas. It is, however, possible to calculate from the curves in fig. 2 the minimum proportion of the total secondary ionization which must be effected by cathode processes.

---

* R. W. Lunt and C. A. Meek, Proc. Roy. Soc. A, clvii. p. 146 (1936).

† J. S. E. Townsend, 'Motion of Electrons in Gases,' p. 33. Clarendon Press.

‡ J. S. E. Townsend and S. P. McCallum, Phil. Mag. vi. p. 857 (1928).

§ *Loc. cit.*

Let the coefficient $\delta$ be composed of two parts: one part $\beta$ which represents the ionization by collision by positive ions, and another part $\delta'$ which represents the total effect of the two cathode processes. The values of $(\delta/\alpha)$ given in fig. 2 are likely to be most accurate for values of $Z/\rho$ near those which correspond to the minimum sparking potential: and the values, when $Z/\rho$ is 200, are 0·026 for the aluminium cathode and 0·013 for the steel cathode. Hence for aluminium, at $Z/\rho=200$,

$$(\delta/\alpha)_1=\beta/\alpha+(\delta'/\alpha)_1=0{\cdot}026,$$

and for Staybrite steel at the same value of $Z/\rho$,

$$(\delta/\alpha)_2=\beta/\alpha+(\delta'/\alpha)_2=0{\cdot}013,$$

because $\beta/\alpha$ must be the same in both cases.

Hence

$$(\delta'/\alpha)_1-(\delta'/\alpha)_2=\beta/\alpha+(\delta'/\alpha)_2.$$

Thus, in the extreme case of no secondary emission from the steel cathode,

$$(\delta'/\alpha)_2=0, \quad \text{and} \quad \beta/\alpha=(\delta'/\alpha)_1,$$

which means that with aluminium the emission of electrons from the cathode must contribute at least 50 per cent. of all the secondary ionization. For nickel and copper, the corresponding minimum fractions of the total secondary ionization which must be cathode processes are 41 and 28 per cent. respectively, on the assumption, of course, that there is no electron emission from a steel cathode. The existence of any secondary emission from the iron cathode, which Penning * found to be of the order of 5 per cent. with neon ions, would raise the proportions for the other cathodes. For example, if the secondary emission from steel is 1/3 that from aluminium, as Christoph found for photo-electric emission, then the proportion for that metal would be 66 per cent., while if the secondary emission from steel is one-half that from aluminium, then all the secondary ionization with the aluminium cathode must be due to the emission of electrons from the cathode.

It now remains to estimate the relative importance in hydrogen of the two mechanisms by which electrons can be liberated from the cathode. It can be seen from the curves in fig. 2 and the table (p. 197) that, as $Z/\rho$ increases from 27 to 300, *i. e.*, by a factor of 12, $(\delta/\alpha)$ is increased from $0{\cdot}7\ 10^{-4}$ to $3{\cdot}5\ 10^{-2}$, *i. e.*, by a factor of 500. However, within the range of $Z/\rho$ from 300 to 100, the corresponding decrease of $(\delta/\alpha)$ is linear, but this linear change is not continued for values of $Z/\rho$ below 100. Hence it is reasonable to consider separately the two sections of the $(\delta/\alpha)$,

---

* F. M. Penning, *Proc. Kon. Akad. Wetens Amst.* xxxiii. p. 841 (1930).

$Z/p$ curve, first the region when $Z/p > 100$, and second that when $Z/p < 100$; for, as the shape of the curves suggests, it is not unlikely that the two sections represent different processes of secondary emission. Considering first the case when $Z/p$ exceeds 100, it can be shown from the results of former experiments on the action of positive ions in hydrogen, that the secondary ionization can be almost entirely accounted for by the action of positive ions and not by the effect of radiation from the gas. The total ionization $(\beta/\alpha+\gamma)$ produced by positive ions moving through hydrogen up to a copper cathode has been measured *, and the previously published values of $(\beta/\alpha+\gamma)$ are given in the following table for comparison with the values of $(\delta/\alpha)$ deduced from the sparking potential with a copper cathode. Further, the copper cathodes used in both sets of experiments had been treated in similar ways.

| $Z/p$ | 154 | 186 | 230 | 277 | 412 |
|---|---|---|---|---|---|
| $(\beta/\alpha+\gamma)$ | 0·008 | 0·015 | 0·022 | 0·033 | 0·053 |
| $(\delta/\alpha)$ | 0·009 | 0·015 | 0·024 | 0·034 | 0·065 |

The factor $(\beta/\alpha+\gamma)$ was obtained by measuring the total number of electrons produced by the positive ions, and it is quite independent of any further estimates of the relative values of $\beta/\alpha$ and $\gamma$.

Hence it must be concluded that the effect of radiation from the gas is small compared with the effect of the positive ions when $Z/p$ exceeds 150. The estimates of the relative values of $\beta/\alpha$ and of $\gamma$, made as a result of previous experiments, are not incompatible with the relative proportions deduced above from the change in sparking potential with change of cathode material, on the assumption that there is no secondary emission from a steel cathode. As, however, this assumption is highly doubtful, it would appear that the relative values of $\beta/\alpha$ and of $\gamma$, previously given, require modification; in any case an error of 30 per cent. in those values is possible. As $Z/p$ increases from, say 150 to 300, the values of $Z/p$ are great enough to produce large changes in the mean energy of agitation of the positive ions, especially if they are in the atomic form; but an increase in $Z/p$ from 27 to 55 is not likely to produce large changes in the energies of the ions. However, the table in section 2 shows that $(\delta/\alpha)$ increases by a factor of 10 when $Z/p$ increases from 27 to 55, so that it follows that this increase cannot be due to a correspondingly large increase in the mean energy of the ions. Also, if when $Z/p < 50$, the

---

* J. E. E. Townsend and F. Llewellyn Jones, Phil. Mag. xv. p. 288 (1933).

factor ($\delta/\alpha$) represents only the action of positive ions, then the efficiency with which they liberate electrons from the cathode must be a hundred times lower than their efficiency when $Z/\rho$ exceeds 150. Now there are two processes which can contribute to the reduction in the efficiency of secondary emission, and these are (i.) the formation of ionic clusters *, and (ii.) the backward scattering of the electrons towards the cathode which removes them from the current. Little is known about the action of an ion cluster in liberating electrons from a cathode, except that its efficiency is lower than that of a simple ion, owing to its lower potential energy.

The backward scattering of electrons has been investigated by Young and Bradbury †, who expressed in terms of $Z/\rho$ the ratio of the actual current which leaves the cathode to the saturation value of the current. It can be shown from their formula that the increase of $Z/\rho$ from 27 to 56 can produce at most a 50 per cent. increase in the current which leaves the cathode. However, the considerations in section 3 indicate that it is not easy to account for the increase in ($\delta/\alpha$) with $Z/\rho$, in this range of low ionic energies, on the basis of a photo-electric effect alone, so that ($\delta/\alpha$) must be attributed mainly to the action of positive ions on the cathode. Now it is significant to note here that recent measurements ‡ of mobility of $H_2^+$ in hydrogen show that, when $Z/\rho < 20$, the mobility is independent of $Z/\rho$, but that when $Z/\rho$ exceeds 20 the mobility increases almost linearly with $Z/\rho$. Further, this increase corresponds to an increase in mean energy of the positive ions above that of thermal agitation of the gas molecules. An approximate estimate of the mean energy of drift of the positive ions from the mobility values shows that the change of $Z/\rho$ from 27 to 56 increases the mean energy of the ions about $2\frac{1}{2}$ times. If it is probable that the secondary emission from the cathode is proportional to the energy of the ions, then the combined effects of this increase in energy and the diminution of the backward scattering to the cathode can account for an increase in $\gamma$ of about 4 to 5, as $Z/\rho$ increases from 27 to 56. On the other hand, if the secondary emission from the cathode is proportional to the velocity of the incident positive ions, instead of to their energy, then the total increase in $\gamma$, as $Z/p$ increases from 25 to 56, is about 9 or 10, which is just the increase required by the experimental results.

For still higher pressures, when $Z/\rho < 27$, the values of $\gamma$ appear no longer to decrease, and may possibly show an increase. As the energy

---

* J. J. and G. P. Thomson, 'Conduction of Electricity through Gases,' 3rd ed. ii. p. 520.

† L. A. Young and N. E. Bradbury, Phys. Rev. xliii. p. 34 (1933).

‡ A. M. Tyndall, 'Mobility of Positive Ions in Gases,' p. 70. Cambridge Physical Tracts (1938).

of the positive ions is still decreasing slightly, it follows that the effects of radiation from the gas must now predominate, and this conclusion is confirmed by the considerations of section 3. This conclusion is also in agreement with that deduced from experiments with monatomic gases *.

## 5. *Summary.*

In this paper the general dependence of the sparking potential of hydrogen on the material of the cathode was interpreted on the Townsend theory, and it was found that the experimental results could be readily accounted for. The second Townsend coefficient, $\gamma(=\beta/\alpha)$, was evaluated for four different cathodes, and in all cases $\gamma$ was found to be a function of $Z/\rho$. The variation of $\gamma$ with $Z/\rho$ was discussed in relation to the mechanism of the spark discharge, and it was concluded that over a large range of pressures, when $28<Z/\rho<300$, the secondary ionization was produced mainly by the action of the positive ions, and that the influence of radiation from the gas only predominated at the highest pressures, when $Z/\rho<28$.

The dependence of the sparking potential on the cathode material proves that part, at least, of the total secondary ionization must be attributed to the emission of electrons from the cathode; and the minimum proportions of the total secondary ionization which must be attributed to the emission of electrons, in order to account for the observed dependence of the sparking potential on the cathode material, were calculated for cathodes of Al, Ni, Cu, and Fe.

Swansea.
24th February, 1939.

---

* A. A. Kruithof and F. M. Penning, *Physica*, v. no. 3, p. 203 (1938).

# XVI. *A Short Wave Generator.*

By E. W. B. GILL, B.Sc., M.A., Fellow of Merton College, Oxford *.

[Received May 24, 1939.]

(1) THERE are a few types of valve generator which for a particular applied voltage exhibit a decided preference for oscillating on a particular wave-length or set of wave-lengths. The best known of these are (i.) the Barkhausen oscillations produced by a triode valve when the grid is at a positive potential to the filament and the anode at approximately the same as the filament; and (ii.) the split anode magnetron, where the cylindrical anode is divided into two equal halves by cuts parallel to the filament, the anodes are at a positive potential to the filament and a magnetic field is applied parallel to the filament.

In both these cases the periodic time of the the wave-lengths most strongly regenerated bears some relation to the transit times of the electrons across the valve; which results in the possibility of the production of extremely short waves. Thus a magnetron can produce very strong oscillations of about 40 cms. wave-length, and the Barkhausen produces wave-lengths of the same order but much more weakly.

The actual working of the split anode magnetron appears to depend on "negative resistance." When the anode sectors are oscillating in potential the electron stream, from the filament, reaching the one momentarily at negative potential is greater than that to the other, which is at that instant positive.

There is no such simple explanation of the Barkhausen oscillation, where the action is more complicated.

The generator to be described uses the circuit potential arrangements of the Barkhausen oscillator, but its mode of action appears to resemble that of the split anode magnetron.

(2) The valve used was of the split anode type modified by having two single thin grid wires equidistant from and parallel to the filament, one on each side; the filament, grid wires and gaps between the anodes being all in one plane. The radius of the anode cylinders was 5 mm. and the grid wires were about 1 mm. from the filament.

---

* Communicated by Prof. Townsend, F.R.S.

The leads to the anodes came separately out of the top of the valve, and a Lecher wire system was attached to these, the Lecher wires being shorted by a sliding plate enabling the wave-lengths of the oscillatory circuit, which comprised the two anodes and the wires up to the plate, to be altered. (A plate is better than the more usual sliding bar as it reduces end effects.)

A point on the plate, symmetrical with regard to the Lecher wires, will be a potential node of the oscillations, and a lead was taken from it back to the filament. This lead included a microammeter to detect any current to the anodes. The grid was put at a positive potential of some 20 to 40 volts above the filament.

The potentials of the electrodes are thus identical with the Barkhausen arrangement. No magnetic field was applied.

(3) With this arrangement, if the filament is heated the equality of potential of anode and filament results in general in the current reaching the anodes from the filament being inappreciable (all the electrons from the filament ultimately reaching the grid), but it was found, if the slider plate was moved along, that a region of the Lecher wires would be reached where the microammeter showed an anode current.

This anode current is a sign that oscillations are occurring ; one proof of oscillations being that, if an absorption wave-meter consisting of a second Lecher wire system with slider be brought near, at the appropriate tuning this anode current disappears.

The oscillations are extremely weak, a relative estimate of their strength being given by the magnitude of the anode current, though their strength is not necessarily proportional to this current.

For a given filament heating and fixed grid potential, there is thus a small range of wave-lengths which can be maintained and one wave-length, for which the anode microammeter reads highest, which is maintained most efficiently. It is this wave-length to which attention will be directed in what follows.

It was found that this optimum wave-length depended on two factors—the potential of the grid wires and the emission from the filament. Or, in other words, for a fixed grid voltage any wave-length in a certain range can be produced most efficiently by adjusting the emission. In this way the following table was obtained, showing the emission required for best oscillations on various wave-lengths when the grid wires were at 30·5 volts positive to filament.

The third column gives some idea of the relative strengths of the oscillations, and it will be seen that 30·5 volts on the grid can maintain any wave-lengths between about 1 and 3 metres, but the wave-length it maintains best is about 160 cm.

TABLE.

| λ in cm. | Emission in milliamp. | Anode current in microamp. |
|---|---|---|
| 294 | ·76 | 5·0 |
| 271 | ·81 | 9·8 |
| 249 | ·96 | 15·4 |
| 228 | 1·20 | 20·2 |
| 207 | 1·46 | 30·0 |
| 183 | 1·70 | 39·2 |
| 158 | 2·10 | 42·4 |
| 131 | 2·50 | 27·0 |

Fig. 1 gives the relative strengths of oscillations as measured by the anode current (ordinates) for different wave-lengths (abscissæ). The curves are plotted for the fixed grid voltages 40, 30·5, 22·1, and 18·1.

Fig. 1.

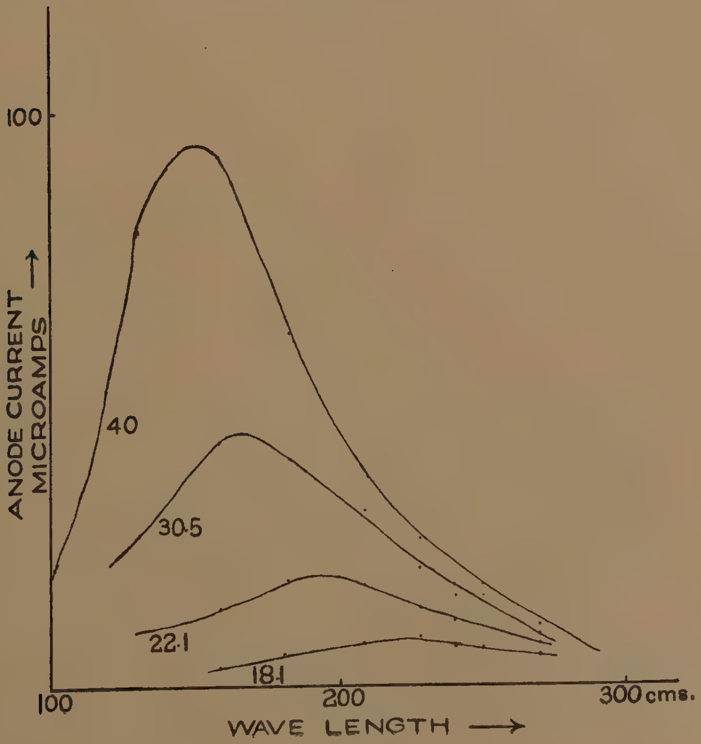

These curves show that :—

(*a*) Any grid voltage will generate a range of short waves, and that an increase in grid voltage extends the range of wave-lengths in both directions.

(*b*) The wave-length at which a valve produces its best oscillation gets shorter as the grid voltage is increased.

(*c*) The higher the grid voltage the stronger the oscillation on any wave-length.

It is not necessary to tabulate for fig. 1 the actual emissions corresponding to different points of the curves ; all that need be said is that as the voltage is increased the emission has to be increased to get the best result on any wave-length.

It is this last fact which, in practice, prevents ultra-short wave-lengths being used. With the grid at 40, the peak of the curve representing a wave-length of about 150 cm. required an emission of 3·2 milliamp., and the thin grid wires are bombarded with this current (less the tiny anode current) dropping through 40 volts. A much shorter wave-length would require both higher voltages and higher emissions, and the bombardment would be likely to prove disastrous to the grid wires.

It was not possible to generate longer wave-lengths by this method, for if the wave-length was much increased by moving the slider far down the wires, oscillations commenced not on the fundamental but on an harmonic which lay in the range of fig. 1.

(4) The following explanation is based on a negative resistance effect similar to that operating in a split anode magnetron. It is necessary to explain first how an oscillation is maintained at all, and second why a particular wave-length is especially favoured.

An electron which leaves the filament in the direction of an anode gap and just misses the appropriate grid wire will follow a lobe-like path, the sharper end of the lobe being near the filament, the grid wire in the middle of the lobe, and the broader end of the lobe near the anode gap. There will be a similar but oppositely traversed lobe-like path for an electron which passes the other side of the grid wire.

If now one anode segment is slightly positive and the other slightly negative, the effect on an electron following one of these paths will be to bring it nearer to or even onto the more negative anode segment, while the effect on the other electron path will be to bend it still further away from the more positive anode segment.

Hence, if the anode segments become alternately positive and negative, there will be a negative resistance effect, and oscillations will be set up in a suitably attached circuit.

If the first time an electron path is bent in this manner the electron does not reach the negative anode segment, it continues close by the filament and reaches the other gap. If, by this time, the oscillation has made one complete cycle—*i. e.*, the anode which was negative last time is again negative—there will be a further bending of the path, and this action continues cumulatively until the momentarily negative anode is finally reached by the electron in question. There is thus an enhanced negative resistance effect which is most effective for the wave-length determined by the transit time from one gap to the other, passing the filament on the way, and if the Lecher wires are tuned to this wave-length, the oscillations will be stronger than if they are tuned to any other.

If all the electrons followed the same paths, this transit time would be the same for all, but since they miss the grid by different distances, the times are different. The potential outside the grid wires drops very rapidly with distance, and as this potential gives a measure of the maximum velocity of the electron, it follows that an electron which passes by the grid at some distance moves a good deal slower than one which passes close. There is thus a whole range of electron speeds, and a corresponding range of transit times.

There is, however, a further point to be considered. The electron paths will be bent where they pass the grid wires, those nearest (the fastest electrons) being bent most. The electrons which contribute to the oscillatory action are those which pass close to the anode gap, and these will be the ones which do not pass too close to the grid wires, *i. e.*, the slower ones. Thus the wave-length most strongly generated is a good deal longer than would be expected from calculations based on the assumption that the speed of all the electrons is the same and determined by the grid wire potential. A variety of electrons pass the gap at different distances and with different transit times, the slower ones passing closest.

Electrons are thus available for regenerating various wave-lengths, and the complication is due to the fact that although those passing the gap most closely are the most efficient, the effect of those passing further away may be enhanced by the number moving with the same velocity being larger. It is difficult to say which layer of electrons will have the preponderating effect, but certainly all the fastest ones will have been so much deflected as to be quite inoperative. It seems likely, however, that with large emissions, the mutual repulsion of the dense electron streams on both sides of the grid wires would tend to reduce the bending at the grid, and faster electrons would pass nearer the gap than for small emissions. This would explain the experimental fact that for a fixed grid voltage an increase in emission reduces the wave-length.

The average speed of the electrons depends of course on the grid voltage, so that, other things being equal, an increase of grid voltage would be expected to reduce the wave-length, which is also in accordance with fig. 1.

The complexity of electron motion with a single grid wire appears to render any exact mathematical calculation quite impossible.

I should like to thank Mr. Moullin for reading and criticising this paper, and Professor Townsend in whose laboratory the experiments were conducted.

# XVII. *A Generalization of the Polynomial* $F_n(x)$.

By Simon Pasternack*.

[Received September 14, 1938.]

## 1. *Introduction.*

Prof. H. Bateman (1) has discussed the polynomial $F_n(x)$, which satisfies the operational equation

$$F_n(D)\operatorname{sech} x = \operatorname{sech} x P_n(\tanh x),$$

where D denotes the operator $d/dx$ and $P_n(x)$ is the Legendre polynomial. An interesting generalization of this polynomial is the polynomial $F_n^m(x)$, which satisfies the operational equation

$$F_n^m(D)\operatorname{sech}^{m+1} x = \operatorname{sech}^{m+1} x P_n(\tanh x),$$

where $n$ is a positive integer or zero, and $m$ is any real or complex number except $-1$. The case $m=1$ has been discussed briefly by H. Bateman(2). In this article some of the properties of the polynomial $F_n^m(x)$ will be developed, together with the extension to the case of non-integral $n$.

A physical application of these polynomials is found in the computation of the mean values of $r^s$ for electronic orbits in hydrogen-like atoms(3). It has been shown that

$$\begin{aligned}\overline{r^{-q-2}} &= \frac{(2l-q)\,!}{(2l+q+1)\,!}\left(\frac{2Z}{na_0}\right)^{2q+1}\overline{r^{q-1}},\\ &= \frac{(-1)^q}{2n}\frac{(2l-q)\,!}{(2l+1)\,!}\left(\frac{2Z}{na_0}\right)^{q+2} F_q{}^{2l+1}(2n),\end{aligned}$$

where $n$ is the total quantum number, $l$ is the azimuthal quantum number, Z is the effective atomic number of the atom, and $a_0$ is the Bohr atomic unit. Equations (4.1) and (4.2) then provide simple formulæ for these mean values.

These polynomials also furnish a solution for the problem of the forced vibrations of a rotating string of weights. This problem will be discussed in section 12 of the paper.

---

* Communicated by Prof. H. Bateman.

## 2. *The Generating Function.*

We define $F_n^m(z)$ by means of the generating function

$$(1-t)^{-1}F\left(\tfrac{1}{2},\ \tfrac{1}{2}+\tfrac{1}{2}m+\tfrac{1}{2}z\ ;\ 1+m\ ;\ \frac{-4t}{(1-t)^2}\right)=\sum_{n=0}^{\infty} t^n F_n^m(z), \quad . \quad (2.1)$$

where $F(a,\ b\ ;\ c\ ;\ x)$ is the hypergeometric series, and $|t|<3-\sqrt{8}$. From this definition it follows readily, by expansion of the hypergeometric series in powers of $t$, that

$$\begin{aligned} F_n^m(z) &= \sum_{r=0}^{n} \frac{(-n)_r(n+1)_r(\frac{1}{2}+\frac{1}{2}m+\frac{1}{2}z)_r}{r\,!\ r\,!\ (m+1)_r} \\ &= F\begin{bmatrix} -n,\ n+1,\ \frac{1}{2}+\frac{1}{2}m+\frac{1}{2}z \\ 1,\ m+1 \end{bmatrix}, \quad . \quad . \quad . \quad . \quad (2.2) \end{aligned}$$

where $F\begin{bmatrix} a,\ b,\ c \\ e,\ f \end{bmatrix}={}_3F_2(a,\ b,\ c\ ;\ e, f\ ;\ 1)$ is the generalized hypergeometric series with unit argument. We are here using the notation

$$(a)_r=a(a+1)(a+2)\ldots(a+r-1).$$

When the series is written backwards, it becomes

$$F_n^m(z)=(-1)^n\frac{(2n!)\ (\frac{1}{2}+\frac{1}{2}m+\frac{1}{2}z)_n}{n\,!\ n\,!\quad (m+1)_n}F\begin{bmatrix} -n,\ -n,\ -m-n \\ -2n,\ \frac{1}{2}-\frac{1}{2}m-\frac{1}{2}z-n \end{bmatrix}. \quad (2.3)$$

From the series (2.2) it is evident that

$$\lim_{N\to\infty} F_n^N(Nz)=F(-n,\ n+1\ ;\ 1\ ;\ \tfrac{1}{2}+\tfrac{1}{2}z)=(-1)^n P_n(z), \quad . \quad (2.4)$$

and also that

$$F_n^{z-1}(z)=P_n(-1)=(-1)^n. \quad . \quad . \quad . \quad . \quad . \quad (2.5)$$

By use of the well-known relation

$$F(a,\ b+1\ ;\ c\ ;\ z)-F(a,\ b\ ;\ c\ ;\ z)=\frac{az}{c}F(a+1,\ b+1\ ;\ c+1\ ;\ z),$$

together with the generating function (2.1), we obtain the formula

$$\begin{aligned} &\sum_{n=0}^{\infty}\{F_n^m(z-2)-F_n^m(z)\}t^n \\ &\qquad =\frac{2t}{(m+1)(1-t)^3}F\left(\tfrac{3}{2},\ \tfrac{1}{2}+\tfrac{1}{2}m+\tfrac{1}{2}z\ ;\ m+2\ ;\ \frac{-4t}{(1-t)^2}\right). \quad (2.6) \end{aligned}$$

Expansion in powers of $t$ then leads to the relation

$$F_n^m(z-2)-F_n^m(z)=\frac{n(n+1)}{m+1}F\begin{bmatrix} -n+1,\ n+2,\ \frac{1}{2}+\frac{1}{2}m+\frac{1}{2}z \\ 2,\ m+2 \end{bmatrix}. \quad (2.7)$$

$F_n^m(0)$ can be evaluated from (2.2) by means of a formula due to Whipple (4) :

$$F\begin{bmatrix} a,\ b,\ c \\ \frac{1}{2}(a+b+1),\ 2c \end{bmatrix}=\frac{\Gamma(\frac{1}{2})\,\Gamma(\frac{1}{2}+c)\,\Gamma(\frac{1}{2}+\frac{1}{2}a+\frac{1}{2}b)\,\Gamma(\frac{1}{2}-\frac{1}{2}a-\frac{1}{2}b+c)}{\Gamma(\frac{1}{2}+\frac{1}{2}a)\,\Gamma(\frac{1}{2}+\frac{1}{2}b)\,\Gamma(\frac{1}{2}-\frac{1}{2}a+c)\,\Gamma(\frac{1}{2}-\frac{1}{2}b+c)},$$

provided that $c$ is not a negative integer. This yields the result that, if $m$ is not a negative integer,

$$\mathrm{F}_n^m(0)=\frac{\Gamma(\frac{1}{2})\,\Gamma(\frac{1}{2}m+1)\,\Gamma(\frac{1}{2}m+\frac{1}{2})}{\Gamma(\frac{1}{2}-\frac{1}{2}n)\,\Gamma(1+\frac{1}{2}n)\,\Gamma(\frac{1}{2}m+1+\frac{1}{2}n)\,\Gamma(\frac{1}{2}m+\frac{1}{2}-\frac{1}{2}n)}. \quad . \quad (2.8)$$

Thus, if $n$ is an odd integer, $\mathrm{F}_n^m(0)$ vanishes.

## 3. *The Operational Equations.*

If D denotes the operator $d/dx$, then

$$(\mathrm{D}+m+2r-1)(\mathrm{D}+m+2r-3)\ldots(\mathrm{D}+m+1)\operatorname{sech}^{m+1}x$$
$$=(m+1)_r \operatorname{sech}^{m+1}x(1-\tanh x)^r.$$

Hence

$$\mathrm{F}_n^m(\mathrm{D})\operatorname{sech}^{m+1}x=\sum_{r=0}^{n}\frac{(-n)_r(n+1)_r}{r!\;r!\;(m+1)_r}(m+1)_r \operatorname{sech}^{m+1}x(\tfrac{1}{2}-\tfrac{1}{2}\tanh x)^r$$
$$=\operatorname{sech}^{m+1}x\mathrm{F}(-n,\,n+1\,;\;1\,;\;\tfrac{1}{2}-\tfrac{1}{2}\tanh x).$$

Consequently,

$$\mathrm{F}_n^m(\mathrm{D})\operatorname{sech}^{m+1}x=\operatorname{sech}^{m+1}x\mathrm{P}_n(\tanh x). \quad . \quad . \quad . \quad . \quad (3.1)$$

The substitution of $x-\frac{1}{2}\pi i$ for $x$ then yields the equation

$$\mathrm{F}_n^m(\mathrm{D})\operatorname{csch}^{m+1}x=\operatorname{csch}^{m+1}x\mathrm{P}_n(\coth x). \quad . \quad . \quad . \quad . \quad (3.2)$$

Another operational equation satisfied by $\mathrm{F}_n^m(x)$ is

$$\mathrm{F}_n^m(\mathrm{D}-m)\operatorname{sech}x=\Gamma(m+1)e^{mx}\operatorname{sech}x\mathrm{P}_n^{-m}(\tanh x), \quad . \quad . \quad (3.3)$$

where $\mathrm{P}_n^m(x)$ is Ferrer's associated Legendre polynomial of the first kind. To prove this, we note that

$$(\mathrm{D}+2r-1)(\mathrm{D}+2r-3)\ldots(\mathrm{D}+1)\operatorname{sech}x=r\,!\operatorname{sech}x\,(1-\tanh x)^r.$$

Hence

$$\mathrm{F}^n(\mathrm{D}-m)\operatorname{sech}x=\operatorname{sech}x\sum_{r=0}^{n}\frac{(-n)_r(n+1)_r}{r!\,(m+1)_r}(\tfrac{1}{2}-\tfrac{1}{2}\tanh x)$$
$$=\operatorname{sech}x\mathrm{F}(-n,\,n+1\,;\,m+1\,;\,\tfrac{1}{2}-\tfrac{1}{2}\tanh x)$$
$$=\operatorname{sech}x\,\Gamma(m+1)e^{mx}\mathrm{P}_n^{-m}(\tanh x).$$

The substitution of $x-\frac{1}{2}\pi i$ for $x$ then gives

$$\mathrm{F}_n^m(\mathrm{D}-m)\operatorname{csch}x=\Gamma(m+1)e^{mx-\frac{1}{2}m\pi i}\operatorname{csch}x\mathrm{P}_n^{-m}(\coth x). \quad . \quad (3.4)$$

### 4. *Further Formulæ.*

Two useful formulæ for $F_n^m(x)$ are the following :

$$F_{2n}^m(z)=F\left[\begin{matrix}-n,\ n+\tfrac{1}{2},\ \tfrac{1}{2}m+\tfrac{1}{2}+\tfrac{1}{2}z,\ \tfrac{1}{2}m+\tfrac{1}{2}-\tfrac{1}{2}z\\ 1,\ \tfrac{1}{2}m+\tfrac{1}{2},\ \tfrac{1}{2}m+1\end{matrix}\right],$$

$$=1-\binom{n}{1}\frac{2n+1}{(m+1)(m+2)}\,\frac{[(m+1)^2-z^2]}{2}$$

$$+\binom{n}{2}\frac{(2n+1)(2n+3)}{(m+1)(m+2)(m+3)(m+4)}\,\frac{[(m+1)^2-z^2][(m+3)^2-z^2]}{2\,.\,4}$$

$$+\ldots \quad . \quad . \quad (4.1)$$

$$F_{2n+1}^m(z)=-\frac{z}{m+1}\,F\left[\begin{matrix}-n,\ n+\tfrac{3}{2},\ \tfrac{1}{2}m+\tfrac{1}{2}+\tfrac{1}{2}z,\ \tfrac{1}{2}m+\tfrac{1}{2}-\tfrac{1}{2}z\\ 1,\ \tfrac{1}{2}m+1,\ \tfrac{1}{2}m+\tfrac{3}{2}\end{matrix}\right],$$

$$=-\frac{z}{m+1}\left\{1-\binom{n}{1}\frac{2n+3}{(m+2)(m+3)}\,\frac{[(m+1)^2-z^2]}{2}\right.$$

$$+\binom{n}{2}\frac{(2n+3)(2n+5)}{(m+2)(m+3)(m+4)(m+5)}\,\frac{[(m+1)^2-z^2][(m+3)^2-z^2]}{2\,.\,4}$$

$$\left.+\ldots\right\} \quad . \quad . \quad . \quad (4.2)$$

To prove equation (4.1), we note that

$$[(m+2r-1)^2-D^2][(m+2r-3)^2-D^2]\ldots[(m+1)^2-D^2]\operatorname{sech}^{m+1}x$$
$$=(m+1)_{2r}\operatorname{sech}^{m+2r+1}x.$$

Therefore

$(a)$ $(\tfrac{1}{2}m+\tfrac{1}{2}+\tfrac{1}{2}D)_r(\tfrac{1}{2}m+\tfrac{1}{2}-\tfrac{1}{2}D)_r\operatorname{sech}^{m+1}x=(\tfrac{1}{2}m+\tfrac{1}{2})_r(\tfrac{1}{2}m+1)_r\operatorname{sech}^{m+2r+1}x.$

Also

$$P_{2n}(\tanh x)=F(-n,\ n+\tfrac{1}{2}\ ;\ 1\ ;\ \operatorname{sech}^2 x).$$

Hence, from equation (3.1),

$$F_{2n}^m(D)\operatorname{sech}^{m+1}x=\sum_{r=0}^{n}\frac{(-n)_r(n+\frac{1}{2})_r}{r!\,r!}\operatorname{sech}^{m+2r+1}x.$$

The use of formula $(a)$ for $\operatorname{sech}^{m+2r+1}x$ then leads immediately to equation (4.1).

Similarly, equation (4.2) follows from the fact that

$$-D[(m+2r-1)^2-D^2][(m+2r-3)^2-D^2]\ldots[(m+1)^2-D^2]\operatorname{sech}^{m+1}x$$
$$=(m+1)_{2r+1}\operatorname{sech}^{m+2r+1}x\tanh x,$$

together with the formula

$$P_{2n+1}(\tanh x)=\tanh x\,F(-n,\ n+\tfrac{3}{2}\ ;\ 1\ ;\ \operatorname{sech}^2 x).$$

Equations (4.1) and (4.2) show that

$$F_n^m(-z)=(-1)^n F_n^m(z). \quad . \quad . \quad . \quad . \quad . \quad . \quad . \quad (4.3)$$

This relation could be used to modify some of the preceding formulæ.

A number of interesting results follow from the application to equations (4.1) and (4.2) of a formula of Whipple's ⁽⁵⁾ :

$$F\begin{bmatrix}a,\ b,\ c,\ -n\\ u,\ v,\ w\end{bmatrix}=\frac{(v-c)_n(w-c)_n}{(v)_n(w)_n}F\begin{bmatrix}u-a,\ u-b,\ c,\ -n\\ u,\ 1-v+c-n,\ 1-w+c-n\end{bmatrix},$$

if $u+v+w-a-b-c+n=1$. We get

$$F_{2n}^m(z)=\frac{(2n)\,!}{(m+1)_{2n}}\binom{z}{2n}F\begin{bmatrix}-n,\ \tfrac12-n,\ \tfrac12z+\tfrac12+\tfrac12m,\ \tfrac12z+\tfrac12-\tfrac12m\\ 1,\ \tfrac12z+\tfrac12-n,\ \tfrac12z+1-n\end{bmatrix},$$

$$F_{2n+1}^m(z)=\frac{-(2n+1)\,!}{(m+1)_{2n+1}}\binom{z}{2n+1}F\begin{bmatrix}-n,\ -\tfrac12-n,\ \tfrac12z+\tfrac12+\tfrac12m,\ \tfrac12z+\tfrac12-\tfrac12m\\ 1,\ \tfrac12z-n,\ \tfrac12z+\tfrac12-n\end{bmatrix}.$$

We can combine both of these equations into one :

$$F_n^m(z)=(-1)^n\frac{n\,!}{(m+1)_n}\binom{z}{n}F\begin{bmatrix}-\tfrac12n,\ \tfrac12-\tfrac12n,\ \tfrac12z+\tfrac12+\tfrac12m,\ \tfrac12z+\tfrac12-\tfrac12m\\ 1,\ \tfrac12z+\tfrac12-\tfrac12n,\ \tfrac12z+1-\tfrac12n\end{bmatrix}. \tag{4.4}$$

This result leads to another generating function for $F_n^m(z)$. For

$$\sum_{n=0}^{\infty}\binom{n+m}{n}F_n^m(z)t^n=\sum_{n=0}^{\infty}\sum_{r=0}^{r\leqslant\frac12n}(-1)^n\binom{z}{n-2r}\frac{(\tfrac12z+\tfrac12+\tfrac12m)_r(\tfrac12z+\tfrac12-\tfrac12m)_r}{r\,!\,r\,!}t^n.$$

Changing the order of summation, and putting $s=n-2r$, we see at once that

$$\sum_{n=0}^{\infty}\binom{n+m}{n}F_n^m(z)t^n=(1-t)^zF(\tfrac12z+\tfrac12+\tfrac12m,\ \tfrac12z+\tfrac12-\tfrac12m\ ;\ 1\ ;\ t^2). \tag{4.5}$$

Equation (4.4) also shows that, if $m$ is not an integer,

$$F_n^{-m}(z)=\frac{(1+m)_n}{(1-m)_n}F_n^m(z). \quad .\ .\ .\ .\ .\ .\ . \tag{4.6}$$

## 5. *Recurrence Relations.*

A number of recurrence relations exist for the function $F_n^m(z)$ :

$$(n+1)(n+m+1)F_{n+1}^m(z)+(2n+1)zF_n^m(z)-n(n-m)F_{n-1}^m(z)=0. \ . \tag{5.1}$$

$$\begin{aligned}4n(n+1)F_n^m(z)&=[(z+1)^2-m^2][F_n^m(z+2)-F_n^m(z)]\\&\quad+[(z-1)^2-m^2][F_n^m(z-2)-F_n^m(z)].\end{aligned} \tag{5.2}$$

$$(z^2-m^2)F_n^m(z-1)=(z^2-m^2+2n^2-2nz)F_n^m(z+1)+2n(n-m)F_{n-1}^m(z+1). \quad .\ .\ . \tag{5.3}$$

$$(z^2-m^2)F_{n-1}^m(z-1)=(z^2-m^2+2n^2+2nz)F_{n-1}^m(z+1)+2n(n-m)F_n^m(z+1). \quad .\ .\ . \tag{5.4}$$

$$(z^2-m^2)F_n^m(z+1)=(z^2-m^2+2n^2+2nz)F_n^m(z-1)-2n(n-m)F_{n-1}^m(z-1). \quad .\ .\ . \tag{5.5}$$

$$(z^2-m^2)F_{n-1}^m(z+1)=(z^2-m^2+2n^2-2nz)F_{n-1}^m(z-1)-2n(n-m)F_n^m(z-1). \quad .\ .\ . \tag{5.6}$$

The first of these relations can be derived by differentiation of the operational equation (3.1) and use of the well-known relations

$$(x^2-1)\frac{d}{dx}\mathrm{P}_n(x)=nx\mathrm{P}_n(x)-n\mathrm{P}_{n-1}(x),$$

$$(2n+1)x\mathrm{P}_n(x)=(n+1)\mathrm{P}_{n+1}(x)+n\mathrm{P}_{n-1}(x).$$

To prove (5.2) we make use of equation (2.7). Let

$$\begin{aligned}\mathrm{A}\equiv{}&[(z-1)^2-m^2][\mathrm{F}_n^m(z-2)-\mathrm{F}_n^m(z)]+[(z+1)^2-m^2][\mathrm{F}_n^m(z+2)-\mathrm{F}_n^m(z)]\\ ={}&\frac{n(n+1)}{m+1}\sum_{r=0}^{n}\frac{(-n+1)_r(n+2)_r}{(r+1)!\,r!\,(m+2)_r}\left(\frac{z+m+1}{2}\right)_r\\ &\qquad\{(z-1-m)(z-1+m)-(z+1-m)(z+m+2r+1)\}.\end{aligned}$$

But

$$\begin{aligned}&(z-1-m)(z-1+m)-(z+1-m)(z+m+2r+1)\\ &\qquad=4(r+1)(r+m+1)-4(r+2)\left(\frac{z+m+2r+1}{2}\right).\end{aligned}$$

Therefore

$$\begin{aligned}\mathrm{A}=4n(n+1)\Bigg\{&\sum_{r=0}^{n}\frac{(-n+1)_r(n+2)_r}{r!\,r!\,(m+1)_r}\left(\frac{z+m+1}{2}\right)_r\\ &-\sum_{r=0}^{n-1}\frac{(-n+1)_r\,(n+2)_r\,(r+2)}{(r+1)!\,r!\,(m+1)_{r+1}}\left(\frac{z+m+1}{2}\right)_{r+1}\Bigg\}.\end{aligned}$$

Collecting coefficients of $\left(\frac{z+m+1}{2}\right)_r$, we find that this expression reduces to $4n(n+1)\mathrm{F}_n^m(z)$.

To prove (5.3) we proceed similarly.

$$\begin{aligned}z^2-m^2=4&\left(\frac{z+m+2r+2}{2}\right)\left(\frac{z+m+2r+4}{2}\right)\\ &-4(m+2r+3)\left(\frac{z+m+2r+2}{2}\right)+4(r+1)(m+r+1).\end{aligned}$$

Let

$$\begin{aligned}\mathrm{B}\equiv{}&(z^2-m^2)[\mathrm{F}_n^m(z-1)-\mathrm{F}_n^m(z+1)]+2n(z-n)\mathrm{F}_n^m(z-1)-2n(n-m)\mathrm{F}_{n-1}^m(z-1)\\ ={}&\frac{4n(n+1)}{(m+1)}\sum_{r=0}^{n}\frac{(-n+1)_r(n+2)_r}{r!\,(r+1)!\,(m+2)_r}\left(\frac{z+m+2}{2}\right)_r\Bigg\{\left(\frac{z+m+2r+2}{2}\right)\\ &\left(\frac{z+m+2r+4}{2}\right)-(m+2r+3)\left(\frac{z+m+2r+2}{2}\right)+(r+1)(m+r+1)\Bigg\}\\ &+4n\sum_{r=0}^{n}\frac{(-n)_r(n+1)_r}{r!\,r!\,(m+1)_r}\left(\frac{z+m+2}{2}\right)_r\left\{\frac{z+m+2r+2}{2}-\frac{n+m+2r+2}{2}\right\}\\ &+2n(m-n)\sum_{r=0}^{n-1}\frac{(-n+1)_r(n)_r}{r!\,r!\,(m+1)_r}\left(\frac{z+m+2}{2}\right)_r\end{aligned}$$

By collecting coefficients of $\left(\frac{z+m+2}{2}\right)_r$ it can be readily verified that this expression reduces to zero.

Equation (5.4) may be derived by combining (5.1) and (5.3), and then replacing $n$ by $n-1$. To get equations (5.5) and (5.6), $z$ is replaced by $-z$ in (5.3) and (5.4); and equation (4.3) is used.

Equation (5.1) can also be proved in a manner similar to that used in the proofs of equations (5.2) and (5.3), by the collection and simplification of the coefficients of $(\frac{1}{2}z+\frac{1}{2}m+\frac{1}{2})_r$.

## 6. *Sign and Inequality for $F^m_n$ $(z)$.*

From the recurrence relation (5.1),

$$(n+1)(n+m+1)F^m_{n+1}(z)=-(2n+1)zF^m_n(z)+n(n-m)F^m_{u-1}(z).$$

But

$$F^m_0(z)=1. \quad F^m_1(z)=-\frac{z}{m+1}.$$

Hence it follows by induction, for $n \geqq m > -1$, that, if $z$ is negative, then $F^m_n(z)$ is positive for all values of $n$; whereas if $z$ is positive, then $F^m_n(z)$ is positive for even values of $n$ and is negative for odd values of $n$.

Also, by induction, it follows from the relation (5.1) that, for $|z| \leqq 1$, $m \geqq 0$,

$$|F^m_n(z)| \leqq 1. \quad \ldots \ldots \ldots \quad (6.1)$$

This inequality also holds for $0 > m > -1$, $|z| < m+1$.

By successive application of the recurrence relations (5.5) and (5.3), it is then possible to derive inequalities for the cases $1 \leqq z \leqq 3$, $3 \leqq z \leqq 5$, ...

## 7. *Definite Integrals for $F^m_n(z)$.*

There is a well-known integral for the hypergeometric series,

$$B(\beta, \gamma-\beta)F(\alpha, \beta\,;\gamma\,;x)=\int_0^1 u^{\beta-1}(1-u)^{\gamma-\beta-1}(1-xu)^{-\alpha}\,du,$$

in which $B(a, b)$ is the Beta function, and $|x|<1$. From this integral it follows at once that, for $|t|<3-\sqrt{8}$,

$$B(\tfrac{1}{2}m+\tfrac{1}{2}+\tfrac{1}{2}z, \tfrac{1}{2}m+\tfrac{1}{2}-\tfrac{1}{2}z)\frac{1}{(1-t)}F\left(\tfrac{1}{2}, \tfrac{1}{2}m+\tfrac{1}{2}+\tfrac{1}{2}z\,;m+1\,;\frac{-4t}{(1-t)^2}\right)$$
$$=\int_0^1 u^{\frac{1}{2}m-\frac{1}{2}+\frac{1}{2}z}(1-u)^{\frac{1}{2}m-\frac{1}{2}-\frac{1}{2}z}\{(1-t)^2+4tu\}^{-\frac{1}{2}}du.$$

By equating coefficients of $t^n$, we obtain

$$B(\tfrac{1}{2}m+\tfrac{1}{2}+\tfrac{1}{2}z, \tfrac{1}{2}m+\tfrac{1}{2}-\tfrac{1}{2}z)F^m_n(z)=\int_0^1 u^{\frac{1}{2}m-\frac{1}{2}+\frac{1}{2}z}(1-u)^{\frac{1}{2}m-\frac{1}{2}-\frac{1}{2}z}P_n(1-2u)\,du, \quad \ldots, \quad (7.1)$$

in which $|\mathrm{R}(z)|<\mathrm{R}(m)+1$, and hence $\mathrm{R}(m)>-1$. If we put

$$1-2u=t=\tanh x,$$

we get

$$\mathrm{B}(\tfrac{1}{2}m+\tfrac{1}{2}+\tfrac{1}{2}z,\ \tfrac{1}{2}m+\tfrac{1}{2}-\tfrac{1}{2}z)\mathrm{F}_n^m(z)=2^{-m}\int_{-1}^{1}\left(\frac{1-t}{1+t}\right)^{\frac{1}{2}z}(1-t^2)^{\frac{1}{2}m-\frac{1}{2}}\mathrm{P}_n(t)\,dt, \quad (7.2)$$

$$\mathrm{B}(\tfrac{1}{2}m+\tfrac{1}{2}+\tfrac{1}{2}iz,\ \tfrac{1}{2}m+\tfrac{1}{2}-\tfrac{1}{2}iz)\mathrm{F}_n^m(iz)$$
$$=2^{-m}\int_{-\infty}^{\infty}e^{-ixz}\operatorname{sech}^{m+1}x\,\mathrm{P}_n(\tanh x)\,dx. \quad . \quad (7.3)$$

Inverting this integral by Fourier's Theorem, we obtain the formula

$$\operatorname{sech}^{m+1}x\ \mathrm{P}_n(\tanh x)$$
$$=\frac{2^m}{2\pi}\int_{-\infty}^{\infty}e^{ixz}\mathrm{B}(\tfrac{1}{2}m+\tfrac{1}{2}+\tfrac{1}{2}iz,\quad \tfrac{1}{2}m+\tfrac{1}{2}-\tfrac{1}{2}iz)\mathrm{F}_n^m(iz)\,dz. \quad (7.4)$$

The above equations reduce to those of H. Bateman in the case $m=1$.

Another definite integral can be obtained from the formula

$$\operatorname{sech} x=\tfrac{1}{2}\int_{-\infty}^{\infty}e^{ixz}\operatorname{sech}(\tfrac{1}{2}\pi z)\,dz.$$

Operating on both sides with $\mathrm{F}_n^m(\mathrm{D}-m)$, and using (3.3), we have

$$\Gamma(m+1)e^{mx}\operatorname{sech} x\,\mathrm{P}_n^{-m}(\tanh x)=\tfrac{1}{2}\int_{-\infty}^{\infty}e^{ixz}\mathrm{F}_n^m(iz-m)\operatorname{sech}(\tfrac{1}{2}\pi z)\,dz. \quad (7.5)$$

Inverting the integral by Fourier's Theorem, we get

$$\mathrm{F}_n^m(iz-m)\operatorname{sech}(\tfrac{1}{2}\pi z)=\frac{1}{\pi}\Gamma(m+1)\int_{-\infty}^{\infty}e^{(m-iz)x}\operatorname{sech} x\,\mathrm{P}_n^{-m}(\tanh x)\,dx. \quad (7.6)$$

Still another definite integral can be obtained from equation (2.2), by making use of Cauchy's integral

$$\frac{1}{r\,!}(\tfrac{1}{2}z+\tfrac{1}{2}m+\tfrac{1}{2})_r=\frac{2}{\pi}\int_0^{\frac{\pi}{2}}(2\cos\theta)^{r+\frac{1}{2}z+\frac{1}{2}m-\frac{1}{2}}\cos\{(r+\tfrac{1}{2}-\tfrac{1}{2}m-\tfrac{1}{2}z)\theta\}\,d\theta,$$

where $\mathrm{R}(m+z)>-1$. We find that, if $z+m$ is real,

$$\mathrm{F}_n^m(z)=\frac{2}{\pi}\mathrm{R}\int_0^{\frac{\pi}{2}}(2\cos\theta e^{-i\theta})^{\frac{1}{2}z+\frac{1}{2}m-\frac{1}{2}}\sum_{r=0}^{n}\frac{(-n)_r(n+1)_r}{r\,!\,(m+1)_r}(2\cos\theta e^{i\theta})^r\,d\theta$$
$$=\frac{2}{\pi}\mathrm{R}\int_0^{\frac{\pi}{2}}(1+e^{-2i\theta})^{\frac{1}{2}z+\frac{1}{2}m-\frac{1}{2}}\mathrm{F}(-n,\ n+1;\ m+1;\ 1+e^{2i\theta})\,d\theta.$$

But

$$\mathrm{P}_n^{-m}(-1-2e^{2i\theta})=\frac{1}{\Gamma(m+1)}(1+e^{-2i\theta})^{\frac{1}{2}m}\mathrm{F}(-n,\ n+1;\ m+1;\ 1+e^{2i\theta}).$$

Therefore, putting $\phi=2\theta$, we have

$$\mathrm{F}_n^m(z)=\frac{1}{\pi}\,\Gamma(m+1)\mathrm{R}\int_0^{\pi}(1+e^{-i\phi})^{\frac{1}{2}z-\frac{1}{2}}\mathrm{P}_n^{-m}(-1-2e^{i\phi})\,d\phi, \quad . \quad (7.7)$$

where $z$ and $m$ are real, and $z>-m-1$. If we define $(1-e^{-i\varphi})^{\frac{1}{2}z-\frac{1}{2}}$ appropriately, we can write

$$\mathrm{F}_n^m(z)=\frac{1}{2\pi}\,\Gamma(m+1)\int_0^{2\pi}(1+e^{-i\phi})^{\frac{1}{2}z-\frac{1}{2}}\mathrm{P}_n^{-m}(-1-2e^{i\phi})\,d\phi. \quad . \quad (7.8)$$

## 8. *Some Expansions.*

*a*. If $r$ is a positive integer, it follows from (2.2) that

$$\mathrm{F}_n^m(-2r-m-1)=\sum_{s=0}\binom{r}{s}\frac{(-1)^s(-n)_s(n+1)_s}{s!\,(m+1)_s}.$$

But this sum is the coefficient of $x^r$ in $(1+x)^r\mathrm{F}(-n,\,n+1\,;\;m+1\,;\;-x)$, and

$$\mathrm{F}(-n,\,n+1\,;\;m+1\,;\;-x)=\Gamma(m+1)(1+x)^{\frac{1}{2}m}x^{-\frac{1}{2}m}\mathrm{P}_n^{-m}(1+2x).$$

Therefore

$$\mathrm{F}_n^m(-2m-r-1)=\frac{\Gamma(m+1)}{r!}\left\{\frac{d^r}{dx^r}[(1+x)^{r+\frac{1}{2}m}x^{-\frac{1}{2}m}\mathrm{P}_n^{-m}(1+2x)]\right\}_{x=0}. \quad (8.1)$$

If we now apply Lagrange's Expansion, in the form

$$f'(\zeta)\frac{d\zeta}{dt}=\sum_{r=0}^{\infty}\frac{t^r}{r!}\left\{\frac{d^r}{dx^r}[\{\phi(x)\}^{r+1}f'(x)]\right\}_{x=0},$$

we get the result that, for $|t|<1$,

$$t^{-\frac{1}{2}m}(1-t)^{-1}\mathrm{P}_n^{-m}\left(\frac{1+t}{1-t}\right)=\frac{1}{\Gamma(m+1)}\sum_{r=0}^{\infty}t^r\mathrm{F}_n^m(-2r-m-1). \quad . \quad (8.2)$$

*b*. There is an expansion for $\mathrm{P}_p(x)\mathrm{P}_q(x)$ in a series of Legendre polynomials :

$$\mathrm{P}_p(x)\mathrm{P}_q(x)=\sum_{r=0}^{p}a_r\mathrm{P}_{p+q-2r}(x),$$

where

$$a_r=\frac{(\frac{1}{2})_r(\frac{1}{2})_{p-r}(\frac{1}{2})_{q-r}(p+q-r)!}{r!\,(p-r)!\,(q-r)!\,(\frac{1}{2})_{p+q-r}}\,\frac{2p+2q-4r+1}{2p+2q-2r+1},$$

and $p\leqq q$. If we multiply this series by

$$\left(\frac{1-x}{1+x}\right)^{\frac{1}{2}}(1-x^2)^{\frac{1}{2}m-\frac{1}{2}}$$

and integrate from $-1$ to $1$, we get

$$\int_{-1}^{1} \mathrm{P}_p(x)\mathrm{P}_q(x)\left(\frac{1-x}{1+x}\right)^{\frac{1}{2}z}(1-x^2)^{\frac{1}{2}m-\frac{1}{2}}\,dx$$

$$=2^{-m}\mathrm{B}(\tfrac{1}{2}m+\tfrac{1}{2}+\tfrac{1}{2}z,\ \tfrac{1}{2}m+\tfrac{1}{2}-\tfrac{1}{2}z)\sum_{r=0}^{p} a_r\mathrm{F}^m_{p+q-2r}(z). \qquad (8.3)$$

A similar result can be deduced from the expansion for $\mathrm{P}_p(x)\mathrm{Q}_q(x)$.

*c*. When $r$ is a positive integer, there is an expansion

$$(1-x)^r=\sum_{n=0}^{r}\frac{(-1)^n(2n+1)r\,!\,r\,!\,2^r}{(r-n)\,!\,(r+n+1)\,!}\mathrm{P}_n(x).$$

Putting $x$ equal to $1-2y$, multiplying by $y^{\frac{1}{2}m-\frac{1}{2}+\frac{1}{2}z}(1-y)^{\frac{1}{2}m-\frac{1}{2}-\frac{1}{2}z}$ and integrating from 0 to 1, we see from equation (7.1) that, if $|\mathrm{R}(z)|<\mathrm{R}(m)+1$,

$$2^r\mathrm{B}(\tfrac{1}{2}m+\tfrac{1}{2}+\tfrac{1}{2}z+r,\ \tfrac{1}{2}m+\tfrac{1}{2}-\tfrac{1}{2}z)$$

$$=\sum_{n=0}^{r}\frac{(-1)^n(2n+1)r\,!\,r\,!}{(r-n)\,!\,(r+n+1)\,!}\mathrm{B}(\tfrac{1}{2}m+\tfrac{1}{2}+\tfrac{1}{2}z,\ \tfrac{1}{2}m+\tfrac{1}{2}-\tfrac{1}{2}z)\mathrm{F}^m_n(z).$$

On simplifying this result, we get

$$(z+m+1)(z+m+3)\ldots(z+m+2r-1)$$

$$=r\,!\,r\,!(m+1)_r2^r\sum_{n=0}^{r}\frac{(-1)^n(2n+1)}{(r-n)\,!\,(r+n+1)\,!}\mathrm{F}^m_n(z). \qquad (8.4)$$

*d*. When $|\mathrm{R}(z)|<\mathrm{R}(m)+1$, then, from (7.1),

$$\sum_{n=0}^{\infty}(2n+1)\mathrm{Q}_n(u)\mathrm{F}^m_n(z)\mathrm{B}(\tfrac{1}{2}m+\tfrac{1}{2}+\tfrac{1}{2}z,\ \tfrac{1}{2}m+\tfrac{1}{2}-\tfrac{1}{2}z)$$

$$=\sum_{n=0}^{\infty}(2n+1)\mathrm{Q}_n(u)\int_0^1 t^{\frac{1}{2}m-\frac{1}{2}+\frac{1}{2}z}(1-t)^{\frac{1}{2}m-\frac{1}{2}-\frac{1}{2}z}\mathrm{P}_n(1-2t)\,dt,$$

$$=\int_0^1 t^{\frac{1}{2}m-\frac{1}{2}+\frac{1}{2}z}(1-t)^{\frac{1}{2}m-\frac{1}{2}-\frac{1}{2}z}(u-1+2t)^{-1}\,dt,$$

by Heine's expansion. This latter integral is evaluated by Heine (6) to be

$$\mathrm{B}(\tfrac{1}{2}m+\tfrac{1}{2}+\tfrac{1}{2}z,\ \tfrac{1}{2}m+\tfrac{1}{2}-\tfrac{1}{2}z)\left(\frac{u+1}{u-1}\right)\ \mathrm{F}\left(1,\ \tfrac{1}{2}m+\tfrac{1}{2}+\tfrac{1}{2}z\ ;\ m+1\ ;\ \frac{2}{1-u}\right).$$

Hence we have the expansion

$$(u-1)^{-1}\mathrm{F}\left(\tfrac{1}{2}m+\tfrac{1}{2}+\tfrac{1}{2}z,\ 1;\ m+1;\ \frac{2}{1-u}\right)=\sum_{n=0}^{\infty}(2n+1)\mathrm{Q}_n(u)\mathrm{F}^m_n(z). \qquad (8.5)$$

Differentiation $m$ times with respect to $u$ and substitution of $-2k-1$ for $z$ then leads to the formula

$$(u+1)^k(u-1)^{-k-1}=\sum_{n=0}^{\infty}(2n+1)\mathrm{F}^m_n(-2k-1)\mathrm{Q}^m_n(u). \quad .\ .\ (8.6)$$

*e*. There is a well-known expansion

$$\mathrm{P}_q^k(w)=\frac{(q+k)!}{k!\,(q-k)!}\left(\frac{1-w}{1+w}\right)^{\frac{1}{2}k}\left(\frac{w+1}{2}\right)^q\mathrm{F}\left(-q,\ k-q;\ k+1;\ \frac{w-1}{w+1}\right),$$

where $q\geqq k$. Hence

$$(1+s^2)^{-p}\mathrm{P}_q^k\left(\frac{1-s^2}{1+s^2}\right)=\frac{(q+k)!}{k!\,(q-k)!}\,s^k(1+s^2)^{-p-q}\mathrm{F}(-q,\ k-q;\ k+1;\ -s^2)$$

$$=\frac{(q+k)!}{k!\,(q-k)!}s^k\sum_{m=0}^{\infty}\binom{-q-p}{m}\mathrm{F}\left[\begin{matrix}k-q,\ -q,\ -m\\ k+1,\ -q\ -p-m+1\end{matrix}\right]s^{2m}.$$

If we then use the formula ⁽⁷⁾

$$\mathrm{F}\left[\begin{matrix}a,\ b,\ -m\\ e,\ f\end{matrix}\right]=(-1)^m\frac{\Gamma(f)\,\Gamma(1+b-f)}{\Gamma(f+m)\,\Gamma(1+b-f-m)}\mathrm{F}\left[\begin{matrix}e-a,\ b,\ c\\ e,\ 1-f+b+c\end{matrix}\right],$$

we obtain the expansion

$$(1+s^2)^{-p}\mathrm{P}_q^k\left(\frac{1-s^2}{1+s^2}\right)$$

$$=\frac{(q+k)!}{k!\,(q-k)!}s^k\sum_{m=0}^{\infty}\binom{-p}{m}\mathrm{F}\left[\begin{matrix}-q,\ q+1,\ -m\\ k+1,\ p\end{matrix}\right]s^{2m}. \qquad (8.7)$$

The case $k=0$ has been derived by H. Bateman ⁽⁸⁾, viz.,

$$(1+s^2)^{-p}\mathrm{P}_q\left(\frac{1-s^2}{1+s^2}\right)=\sum_{m=0}^{\infty}\binom{-p}{m}\mathrm{F}_q^{p-1}(-2m-p)s^{2m}. \qquad (8.8)$$

The case $p=1$ yields the result

$$(1+s^2)^{-1}\mathrm{P}_q^k\left(\frac{1-s^2}{1+s^2}\right)=\frac{(q+k)!}{k!\,(q-k)!}s^k\sum_{m=0}^{\infty}(-1)^m\mathrm{F}_q^k(-2m-k-1)s^{2m}. \qquad (8.9)$$

## 9. *Power Series for $F_n^m(z)$.*

To determine the power series for $\mathrm{F}_n^m(z)$, we shall need the value of the integral

$$\mathrm{C}_p^q=\int_{-\infty}^{\infty}x^p\,\mathrm{sech}^{m+1}x\tanh^q x\,dx.$$

An integration by parts yields the reduction formula

$$(p+1)\mathrm{C}_q^p=(q+m+1)\mathrm{C}_{p+1}^{q+1}-q\mathrm{C}_{p+1}^{q-1}.$$

We also have

$$\mathrm{C}_{2p+1}^0=\mathrm{C}_{2p}^{2q+1}=\mathrm{C}_{2p+1}^{2q}=0.$$

$$(m+1)\mathrm{C}_p^1=p\mathrm{C}_{p-1}^0.$$

$$(m+q)\mathrm{C}_0^q=(q-1)\mathrm{C}_0^{q-2}.$$

Also

$$\mathrm{C}_{2p}^0=2^{m+2}\int_0^{\infty}\frac{x^{2p}e^{-(m+1)x}}{(1+e^{\ 2x})^{m+1}}dx.$$

Expanding the denominator in powers of $e^{-x}$, and carrying out the integration, we obtain

$$C^0_{2p}=2^{m+2}\sum_{r=0}^{\infty}(-1)^r\frac{(m+1)_r}{r!}\frac{(2p)!}{(2r+m+1)^{2p+1}}.$$

From the reduction formula we find that

$$\frac{(m+1)_q C^q_p}{p!}=\sum_{s=0}^{s\leqslant\frac{1}{2}q}N^{(s)}_q\frac{C^0_{p-q+2s}}{(p-q+2s)!},$$

where

$$N^{(0)}_q=1.\quad q(m+q)N^{(s)}_{q-1}=N^{(s+1)}_{q+1}-N^{(s+1)}_q.$$

Here $C^0_{p-q+2s}$ is to be taken as zero if $p-q+2s<0$.

We thus see that

$$N^{(1)}_b=\sum_{r=1}^{q-1}r^2+m\sum_{r=1}^{q-1}r,$$

$$N^{(2)}_q=(q-1)(q+m-1)\sum_{r=1}^{q-3}r^2+(q-2)(q+m-2)\sum_{r=1}^{q-4}r^2+\ldots+m\sum_{r=1}^{q-3}r+m\sum_{r=1}^{q-4}r+\ldots,$$

and so on. Now

$$P_n(z)=\sum_q\frac{(-1)^{\frac{1}{2}n-\frac{1}{2}q}(n+q)!}{2^n(\frac{1}{2}n+\frac{1}{2}q)!\,(\frac{1}{2}n-\frac{1}{2}q)!\,q!},$$

where $n-q$ is zero or an even integer. Hence, from (7.5),

$$\begin{aligned}&2^m B(\tfrac{1}{2}m+\tfrac{1}{2}+\tfrac{1}{2}iz,\ \tfrac{1}{2}m+\tfrac{1}{2}-\tfrac{1}{2}iz)F^m_n(iz)\\&\qquad=\sum_{p=0}^{\infty}\sum_q\frac{(-iz)^p(-1)^{\frac{1}{2}n-\frac{1}{2}q}(n+q)!}{p!\,2^n q!\,(\frac{1}{2}n-\frac{1}{2}q)!\,(\frac{1}{2}n+\frac{1}{2}q)!}C^q_p\\&\qquad=\sum_{p=0}^{\infty}\sum_q\sum_{s=0}^{s\leqslant\frac{1}{2}q}\frac{(-iz)^p(-1)^{\frac{1}{2}n-\frac{1}{2}q}(n+q)!\,N^{(s)}_q C^0_{p-q+2s}}{2^n q!\,(m+1)_q(\frac{1}{2}n-\frac{1}{2}q)!\,(\frac{1}{2}n+\frac{1}{2}q)!\,(p-q+2s)!}.\end{aligned}$$

But, from (7.5), if we put $n$ equal to zero and use the fact that $C^0_{2r+1}$ vanishes, we get

$$2^m B(\tfrac{1}{2}m+\tfrac{1}{2}+\tfrac{1}{2}iz,\ \tfrac{1}{2}m+\tfrac{1}{2}-\tfrac{1}{2}iz)=\sum_{r=0}^{\infty}\frac{(-iz)^{2r}C^0_{2r}}{(2r)!}.$$

Hence, if in our triple sum we sum first over $p$, keeping in mind that $C^0_{p-q+2s}$ vanishes unless $p-q+2s$ is an even integer, we see that

$$F^m_n(iz)=\sum_{q\geqslant 2s}\sum_{s=0}\frac{(-1)^{\frac{1}{2}n-\frac{1}{2}q}(n+q)!\,(-iz)^{q-2s}N^{(s)}_q}{2^n q!\,(m+1)_q(\frac{1}{2}n-\frac{1}{2}q)!\,(\frac{1}{2}n+\frac{1}{2}q)!},$$

where $n-q$ is zero or an even integer. Replacing $iz$ by $x$ and $q-2s$ by $q$, we then obtain

$$F^m_n(x)=\sum_q\sum_s\frac{(-1)^{\frac{1}{2}n+\frac{1}{2}q}(n+q+2s)!\,N^{(s)}_{q+2s}}{2^n(q+2s)!\,(m+1)_{q+2s}(\frac{1}{2}n-\frac{1}{2}q-s)!\,(\frac{1}{2}n+\frac{1}{2}q+s)!}x^q,$$

where $n-q$ is zero or an even integer, and $s$ ranges from 0 to $\frac{1}{2}(n-q)$.

### 10. *Integral of a Product.*

Let

$$G_n^m(iz) \equiv 2^m B(\tfrac{1}{2}m+\tfrac{1}{2}+\tfrac{1}{2}iz,\ \tfrac{1}{2}m+\tfrac{1}{2}-\tfrac{1}{2}iz) F_n^m(iz), \quad . \quad . \quad (10.1)$$

$$J_{n,\,p}^m \equiv \int_{-\infty}^{\infty} G_n^m(iz) G_p^m(-iz)\, dz. \quad . \quad . \quad . \quad . \quad . \quad . \quad . \quad . \quad (10.2)$$

From equations (7.3) and (7.4) we have

$$G_n^m(iz) = \int_{-\infty}^{\infty} e^{-ixz} \operatorname{sech}^{m+1} x P_n(\tanh x)\, dx, \quad . \quad . \quad . \quad (10.3)$$

$$\operatorname{sech}^{m+1} x P_n(\tanh x) = \frac{1}{2\pi}\int_{-\infty}^{\infty} e^{ixz} G_n^m(iz)\, dz. \quad . \quad . \quad . \quad (10.4)$$

Hence

$$J_{n,\,p}^m = \int_{-\infty}^{\infty} dz \int_{-\infty}^{\infty} e^{izt} G_n^m(iz) \operatorname{sech}^{m+1} t P_p(\tanh t)\, dt.$$

It is permissible to change the order of integration. Equation (10.4) then gives

$$J_{n,\,p}^m = 2\pi \int_{-\infty}^{\infty} \operatorname{sech}^{2m+2} t P_n(\tanh t) P_p(\tanh t)\, dt.$$

Replacing $\tanh t$ by $x$, we get

$$J_{n,\,p}^m = 2\pi \int_{-1}^{1} (1-x^2)^m P_n(x) P_p(x)\, dx. \quad . \quad . \quad . \quad . \quad (10.5)$$

Now it is evident from the properties of the Legendre polynomial that this integral vanishes if $n+p$ is odd, or if $m$ is an integer and $|n-p|>2m$. If $m=0$, then⁽⁹⁾

$$J_{n,\,p}^0 = (-1)^n \frac{4\pi}{2n+1}, \text{ if } n=p, \quad . \quad . \quad . \quad . \quad . \quad (10.6)$$

$$=0 \text{ otherwise.}$$

We can evaluate the integral in the general case by use of the expansions

$$P_{2n}(x) = F(n+\tfrac{1}{2}, -n\,;\, 1\,;\, 1-x^2),$$

$$P_{2n+1}(x) = xF(n+\tfrac{3}{2}, -n\,;\, 1\,;\, 1-x^2),$$

and the integral

$$\int_{-1}^{1} (1-x^2)^q dx = B(q+1, \tfrac{1}{2}).$$

We get, for example,

$$J_{2r,\,2s}^m = 2\pi \sum_h \sum_k \frac{(r+\frac{1}{2})_h(-r)_h}{h!\ h!} \frac{(s+\frac{1}{2})_k(-s)_k}{k!\ k!} B(m+h+k+1, \tfrac{1}{2}).$$

But

$$B(m+h+k+1, \tfrac{1}{2}) = B(m+1, \tfrac{1}{2}) \frac{(m+1)_h(m+h+1)_k}{(m+\frac{3}{2})_h(m+h+\frac{3}{2})_k}.$$

Therefore

$$J^{m}_{2r,\,2s}=2\pi B(m+1,\tfrac{1}{2})\,\sum_{h}\frac{(r+\frac{1}{2})_{h}(-r)_{k}(m+1)_{h}}{h!\,h!\,(m+\frac{3}{2})_{h}}F\left[\begin{matrix}s+\frac{1}{2},\ m+h+1,\ -s\\ m+h+\frac{3}{2},\ 1\end{matrix}\right]. \quad . \quad . \quad . \quad (10.7)$$

The hypergeometric series can be summed by a theorem of Saalschutz (10):

$$F\left[\begin{matrix}a,\ b,\ -n\\ c,\ 1+a+b-c-n\end{matrix}\right]=\frac{(c-a)_{n}(c-b)_{n}}{(c)_{n}(c-a-b)_{n}}.$$

If we then write the series (10.7) backwards, it becomes

$$J^{m}_{2r,\,2s}=\frac{2\pi B(m+1,\ \frac{1}{2})(-1)^{r+s}(m+1)_{r}(\frac{1}{2}+r)_{r}(\frac{1}{2})_{s}(m+1+r-s)_{s}}{r!\,s!\,(m+\frac{3}{2})_{r+s}}$$
$$\times F\left[\begin{matrix}-r,\ -m-r+s,\ -m-r-s-\frac{1}{2},\ -r\\ -m-r,\ \frac{1}{2}-2r,\ -m-r\end{matrix}\right].$$

By applying the formula of Whipple, which we used in § 4, we finally get

$$J^{m}_{2r,\,2s}=2\pi B(m+1,\ s+r+\tfrac{1}{2})\frac{(-m-r)_{s}(-m-s)_{r}}{r!\,s!}$$
$$\times F\left[\begin{matrix}-r,\ -s,\ -m,\ -m-r-s-\frac{1}{2}\\ -m-r,\ -m-s,\ \frac{1}{2}-r-s\end{matrix}\right]. \quad (10.8)$$

In a similar manner we can derive the formula

$$J^{m}_{2r+1,\,2s+1}=2\pi B(m+1,\ s+r+\tfrac{3}{2})\,\frac{(-m-r)_{s}(-m-s)_{r}}{r!\,s!}$$
$$\times F\left[\begin{matrix}-r,\ -s,\ -m,\ -m-r-s-\frac{3}{2}\\ -m-r,\ -m-s,\ -\frac{1}{2}-r-s\end{matrix}\right]. \quad (10.9)$$

These formulæ are valid for $m>-1$. If $m=0$ they reduce to (10.6).

## 11. *Generalization to Non-Integral Values of n.*

G. N. Shabde(11) defines $F_{n}(z)$ for all values of $n$ by means of the integral expression

$$F_{n}(z)\sec(\tfrac{1}{2}\pi z)=\frac{1}{\pi}\int_{0}^{1}u^{\frac{1}{2}-\frac{1}{2}z}(1-u)^{-\frac{1}{2}-\frac{1}{2}z}P_{n}(1-2u)\,du,$$

where $P_{n}(x)$ is the general Legendre polynomial, and $|z|<1$. We can here use equation (7.1) to make a similar generalization :

$$B(\tfrac{1}{2}m+\tfrac{1}{2}+\tfrac{1}{2}z,\ \tfrac{1}{2}m+\tfrac{1}{2}-\tfrac{1}{2}z)F^{m}_{n}(z)$$
$$=\int_{0}^{1}u^{\frac{1}{2}m-\frac{1}{2}+\frac{1}{2}z}(1-u)^{\frac{1}{2}m-\frac{1}{2}-\frac{1}{2}z}P_{n}(1-2u)\,du$$
$$=2\ ^{m}\int_{1}^{-1}\left(\frac{1-t}{1+t}\right)^{\frac{1}{2}z}(1-t^{2})^{\frac{1}{2}m-\frac{1}{2}}P_{n}(t)\,dt, \quad (11.1)$$

where $|R(z)|<R(m)+1$.

The convergence of this integral in the given range of values of $z$ can be readily shown. For in the interval $u=0$ to $u=1-\epsilon$, $P_n(1-2u)$ converges absolutely and uniformly. Near $u=1$,

$$P_n(1-2u)=\log(1-u)\,f(u)+g(u),$$

where $f(u)$ and $g(u)$ are analytic at $u=1$. The integral involving $\log(1-u)$ is seen to converge by an integration by parts; and the other integral obviously converges.

Now

$$P_n(1-2u)=F(-n, n+1;\ 1;\ u).$$

Hence, if we multiply this series by $u^{\frac{1}{2}m-\frac{1}{2}+\frac{1}{2}z}(1-u)^{\frac{1}{2}m-\frac{1}{2}-\frac{1}{2}z}$ and integrate term by term, we get

$$F_n^m(z)=F\left[\begin{matrix}-n,\ n+1,\ \frac{1}{2}m+\frac{1}{2}+\frac{1}{2}z\\ 1,\ m+1\end{matrix}\right]. \quad . \quad . \quad . \quad . \qquad (11.2)$$

The term by term integration is permissible (12).

It is then easy to verify that many of the relations proved for integral values of $n$ hold also for non-integral $n$. Among these are equations (2.6), (2.7), (5.1), (7.5), and (7.6).

We can obtain an expansion for $F_n^m(x)$ similar to Dougall's expansion:

$$P_n(x)=\frac{\sin n\pi}{\pi}\sum_{p=0}^{\infty}(-1)^p\left(\frac{1}{n-p}-\frac{1}{n+p+1}\right)P_p(x).$$

Multiplying this series by $1+x$ and using the well-known relation

$$(2p+1)xP_p(x)=(p+1)P_{p+1}(x)+pP_{p-1}(x),$$

we get

$$(1+x)\,P_n(x)=\frac{\sin n\pi}{\pi}\sum_{p=0}^{\infty}a_pP_p(x),$$

where $a_p=0(p^{-2})$. Since also $|P_p(x)|\leqq 1$, the series converges uniformly and absolutely; so that we can multiply it by $(1-x)^{\frac{1}{2}m-\frac{1}{2}+\frac{1}{2}z}(1+x)^{\frac{1}{2}m-\frac{3}{2}-\frac{1}{2}z}$ and integrate from $-1$ to 1. We thus get

$$F_n^m(z)=\frac{\sin n\pi}{\pi}\sum_{p=0}^{\infty}(-1)^p\left(\frac{1}{n-p}-\frac{1}{n+p+1}\right)F_p^m(z), \quad . \quad . \qquad (11.3)$$

where $|R(z+1)|<R(m)$.

### 12. *Modes of Vibration of a Rotating String of Weights* (13).

Let us consider the rotation about one end of a weightless inextensible string, on which are strung N equal weights at equal intervals $l$. Let the weight at distance $nl$ from the fixed end be numbered $n$. We shall neglect the effect of gravity. Let the axis of rotation be taken as the $z$ axis, the direction of dynamic equilibrium of the string as the $x$ axis, and the direction perpendicular to these two as the $y$ axis. Then the equations of motion of the weights in this moving system of coordinates are

$$m\ddot{z}_n=\mathrm{T}_n\left(\frac{z_{n+1}-z_n}{l}\right)-\mathrm{T}_{n-1}\left(\frac{z_n-z_{n-1}}{l}\right), \quad . \quad . \quad . \quad . \quad . \quad . \quad (12.1)$$

$$m(\ddot{x}_n-2\omega\dot{y}_n-\omega^2x_n)=\mathrm{T}_n-\mathrm{T}_{n-1}, \quad . \quad . \quad . \quad . \quad . \quad . \quad . \quad . \quad . \quad (12.2)$$

$$m(\ddot{y}_n+2\omega\dot{x}_n-\omega^2y_n)=\mathrm{T}_n\left(\frac{y_{n+1}-y_n}{l}\right)-\mathrm{T}_{n-1}\left(\frac{y_n-y_{n-1}}{l}\right), \quad (12.3)$$

where $\mathrm{T}_n$ is the tension of the section of the string joining the weights numbered $n$ and $n+1$, $m$ is the mass of each weight, $\omega$ is the angular velocity of rotation, and the dots denote derivatives with respect to time.

We assume that, to a first approximation,

$$\ddot{x}_n=0, \quad \omega\dot{y}_n=0, \quad \omega\dot{x}_n=0, \quad x_n=nl. \quad . \quad . \quad . \quad . \quad (12.4)$$

Then, from (12.2), by summation over $n$, we get

$$\mathrm{T}_n-\mathrm{T}_0=-\tfrac{1}{2}m\omega^2ln(n+1).$$

But $\mathrm{T}_\mathrm{N}=0$. Hence

$$\mathrm{T}_0=\tfrac{1}{2}m\omega^2l\mathrm{N}(\mathrm{N}+1),$$

and

$$\mathrm{T}_n=\tfrac{1}{2}m\omega^2l\{\mathrm{N}(\mathrm{N}+1)-n(n+1)\}. \quad . \quad . \quad . \quad . \quad (12.5)$$

Equations (12.1) and (12.3) then become

$$\ddot{z}_n=\tfrac{1}{2}\omega^2\{(\mathrm{N}+\tfrac{1}{2})^2-(n+\tfrac{1}{2})^2\}(z_{n+1}-z_n)-\tfrac{1}{2}\omega^2\{(\mathrm{N}+\tfrac{1}{2})^2-(n-\tfrac{1}{2})^2\}(z_n-z_{n-1}), \quad . \quad . \quad . \quad (12.6)$$

$$y_n-\omega^2y_n=\tfrac{1}{2}\omega^2\{(\mathrm{N}+\tfrac{1}{2})^2-(n+\tfrac{1}{2})^2\}(y_{n+1}-y_n) \\ -\tfrac{1}{2}\omega^2\{(\mathrm{N}+\tfrac{1}{2})^2-(n-\tfrac{1}{2})^2\}(y_n-y_{n-1}). \quad . \quad (12.7)$$

To find the normal modes of vibration, we put

$$z_n=\mathrm{A}e^{ipt}\mathrm{Z}_n, \quad y_n=\mathrm{B}e^{iqt}\mathrm{Y}_n, \quad . \quad . \quad . \quad . \quad . \quad . \quad (12.8)$$

where it is understood that the real parts of the complex expressions are to be taken. Equations (12.6) and (12.7) then become

$$2p^2\omega^{-2}\mathrm{Z}_n=\{(n+\tfrac{1}{2})^2-(\mathrm{N}+\tfrac{1}{2})^2\}(\mathrm{Z}_{n+1}-\mathrm{Z}_n)+\{(n-\tfrac{1}{2})^2-(\mathrm{N}+\tfrac{1}{2})^2\}(\mathrm{Z}_{n-1}-\mathrm{Z}_n), \quad . \quad . \quad . \quad (12.9)$$

$$(2q^2\omega^{-2}+2)\mathrm{Y}_n=\{(n+\tfrac{1}{2})^2-(\mathrm{N}+\tfrac{1}{2})^2\}(\mathrm{Y}_{n+1}-\mathrm{Y}_n)+\{(n-\tfrac{1}{2})^2 \\ -(\mathrm{N}+\tfrac{1}{2})^2\}(\mathrm{Y}_{n-1}-\mathrm{Y}_n). \quad . \quad (12.10)$$

Comparison of these equations with relation (5.2) then leads to the result

$$\mathrm{Z}_n=\mathrm{F}_r^{2\mathrm{N}+1}(2n), \quad \mathrm{Y}_n=\mathrm{F}_r^{2\mathrm{N}+1}(2n), \quad . \quad . \quad . \quad . \quad . \quad (12.11)$$

where $r$ and $s$ satisfy the equations

$$r(r+1)=2p^2\omega^{-2}, \quad s(s+1)=2q^2\omega^{-2}+2. \quad . \quad . \quad . \quad . \quad (12.12)$$

By the application of Gauss's test for convergence it is seen that the series for $F_r^{2N+1}(2n)$ diverges if $n$ is put equal to N and $r$ is not an integer. Hence, in order that the vibrations at the moving end of the string remain finite, the series must terminate. That is, $r$ and $s$ must be integers.

Integral values of $r$ greater than 2N may be discarded. For, from equation (4.4), we have

$$Z_n=\frac{r!\,(-2n)_r}{(2N+2)_r}F\left[\begin{matrix}-\frac{1}{2}r,\ \frac{1}{2}-\frac{1}{2}r,\ n+1+N,\ n-N\\ 1,\ n+\frac{1}{2}-\frac{1}{2}r,\ n+1-\frac{1}{2}r\end{matrix}\right].$$

The hypergeometric series terminates before any zeroes appear in the denominator, and the term $(-2n)_r$ consequently makes $Z_n$ vanish for all values of $n$ from zero to N. The same argument applies to $s$.

If we then impose the boundary condition that the end $n=0$ is fixed, we see from (2.8) that $r$ and $s$ must be odd integers. Replacing $r$ and $s$ by $2r+1$ and $2s+1$ respectively, we have, finally,

$$z_n=\sum_{r=0}^{N-1}(A_r\cos p_rt+B_r\sin p_rt)\,F_{2r+1}^{2N+1}(2n), \quad . \ . \ . \quad (12.13)$$

$$y_n=\sum_{s=0}^{N+1}(C_s\cos q_st+D_s\sin q_st)F_{2s+1}^{2N+1}(2n), \quad . \ . \ . \quad (12.14)$$

where the allowable frequencies of vibration are given by

$$p_r^2\omega^{-2}=(r+1)(2r+1),\quad q_s^2\omega^{-2}=s(2s+3). \quad . \ . \ . \quad (12.15)$$

The constants $A_r$, $B_r$, $C_s$, and $D_s$ are adjusted to fit the initial conditions.

If we let the separation of the masses approach zero, the above solutions reduce to the solutions for the rotation of a continuous string$^{(14)}$. Thus, if we put

$$nl=x,\quad Nl=L,\quad m=\rho l, \quad . \ . \ . \ . \ . \quad (12.16)$$

we get

$$Z_n=F_{2r+1}^{2N+1}\left(2N\frac{x}{L}\right),\quad Y_n=F_{2r+1}^{2N+1}\left(2N\frac{x}{L}\right).$$

But, by equation (2.4),

$$\lim_{N\to\infty}F_{2r+1}^{2N+1}\left(2N\frac{x}{L}\right)=-P_{2r+1}\left(\frac{x}{L}\right).$$

Hence, if we let $N\to\infty$, $l\to0$, and $m\to0$, in such a way that equations (12.15) remain satisfied, we get the well-known solutions for the case of a continuous string :

$$Z=P_{2r+1}\left(\frac{x}{L}\right),\quad Y=P_{2s+1}\left(\frac{x}{L}\right), \quad . \ . \ . \ . \quad (12.17)$$

where $r$ and $s$ satisfy (12.15). The tension $T_0$ is seen from (12.5) to approach the value $\frac{1}{2}\rho\omega^2l^2$.

## *Conclusion.*

I wish to express my thanks to Dr. H. Bateman for many helpful suggestions during the preparation of this paper.

## *References.*

(1) H. Bateman, Tôkohu Math. Journ. xxxvii. p. 23 (1933).
(2) H. Bateman, Annals of Math. xxxv. p. 767 (1934).
(3) S. Pasternack, Proc. Nat. Acad. Sci. xxiii. p. 91 (1937).
(4) F. J. W. Whipple, Proc. Lond. Math. Soc. (2) xxiii. p. 104 (1925).
(5) F. J. W. Whipple, Proc. Lond. Math. Soc. (2) xxv. p. 525 (1926).
(6) H. E. Heine, ‘Handbuch der Kugelfunktionen,’ Bd. 2, p. 22 (1881).
(7) W. N. Bailey, ‘Generalized Hypergeometric Series’ (Cambridge Tract, no. 32), p. 22.
(8) H. Bateman, Duke Math. Journ. iv. p. 39 (1938).
(9) H. Bateman, Proc. Nat. Acad. Sci. xx. p. 63 (1934).
(10) W. N. Bailey, ‘Generliazed Hypergeometric Series’ (Cambridge Tract, no. 32), p. 9.
(11) G. N. Shabde, Proc. Benares Math. Soc. xvi. p. 5 (1934).
(12) T. J. I'A. Bromwich, ‘An Introduction to the Theory of Infinite Series,’ p. 497 (1926).
(13) This problem, and its connexion with the polynomial $F_n^m(x)$, were suggested in class by Dr. H. Bateman.
(14) P. M. Morse, ‘Vibration and Sound,’ p. 82 (McGraw-Hill, 1936). A. C. Stevenson, Phil. Mag. (7) xxiv. p. 293 (1937).

California Institute of Technology.

# XVIII. *The Astronomical Consequences of Relativistic Two-Body Problem.*

By Sir SHAH SULAIMAN, M.A., LL.D., D.Sc., Federal Court, India*.

[Received January 15, 1939.]

1. PROF. TULLIO LEVI-CIVITA has considered the two-body problem in the 'American Journal of Mathematics' (lix. pp. 225–34, April 1937). He has taken " the *absolute* motion of the centres of mass of a double star," supposed that " everything has been reduced to ordinary space . . . with reference to some *fixed* or Galilean frame," " employed the classical integrals of energy and *areas*," and bringing " *relative* motion also under the Lagrangian scheme " has " applied the Lagrangian operator to the Newtonian constant of energy, regarding it a genuine constant of energy to a first approximation " (pp. 225–227). Treating the relativistic effects as first-order perturbations, and applying Newtonian principles, he has found that for two bodies of comparable masses the trajectory may be considered to be that of a *central* force with the potential function for relative motion (p. 229) as

$$\frac{\mathrm{P}}{r}+\frac{\mathrm{Q}}{r^2}+\frac{\mathrm{R}}{r^3},$$

where
$$\mathrm{P}=\frac{f(m_0+m_1)}{c^2},$$

$$\mathrm{Q}=3\left\{1-\frac{1}{2}\cdot\frac{m_0m_1}{(m_0+m_1)^2}\right\}\frac{f^2(m_0+m_1)^2}{c^4},$$

and
$$\mathrm{R}=\frac{1}{2}\cdot\frac{m_0m_1}{(m_0+m_1)^2}\cdot\frac{\mathrm{C}^2c^2}{f^2(m_0+m_1)^2}\cdot\frac{f^3(m_0+m_1)^3}{c^6},$$

in which $\frac{f(m_0+m_1)}{c^2}$ is the total gravitational mass, $m_0$ and $m_1$ are the two masses, $ct$ is taken as the independent variable, $c$ being the velocity of light and C double the areal velocity, while $r$ is the distance $\mathrm{P}_0\mathrm{P}_1$ between the two masses.

He has concluded that the first term represents the Newtonian attraction and the other two (both of the second order) are the relativistic perturbations consisting of central attractions varying as the inverse cube and the inverse fourth power of the distance respectively. He has inferred that by putting one of the masses equal to zero one gets

---

* Communicated by the Author.

$$\frac{3f^2(m_0+m_1)^2}{c^4}\cdot\frac{1}{r^2}$$

for the perturbative function of Einstein's one-centre problem (p. 229). Following the ordinary method of Newtonian dynamics, which necessarily involves the relation $r^2\frac{d\theta}{dt}=C$, he has deduced the angular precession (per revolution) of the periastron in the case of a double star as

$$\sigma=\frac{6\pi f^2(m_0+m_1)^2}{c^2C^2},$$

which is the same as the precession for an infinitesimal planet moving about a central mass possessing the total mass of the binary system. He has also concluded that in *absolute* motion there is a net acceleration of the common centre of gravity.

2. It is submitted that the extra terms do not really represent the Einsteinian perturbation.

From Levi-Civita's potential function the acceleration is obtained by differentiation as

$$-\frac{P}{r^2}-\frac{2Q}{r^3}-\frac{3R}{r^4}.$$

For an infinitesimal planet ($m_1=0$) we get

$$-\frac{P}{r^2}-\frac{2Q}{r^3}\text{ only,}\quad\text{with } m_1=0.$$

We take

$$\frac{1}{c^2}\frac{d^2r}{dt^2}-\frac{1}{c^2}.r\left(\frac{d\theta}{dt}\right)^2=-\frac{P}{r^2}-\frac{2Q}{r^3},$$

and substitute $r=\frac{1}{u}$, and therefore

$$\frac{d^2r}{dt^2}=-C^2u^2\frac{d^2u}{d\theta^2},$$

where C stands for $r^2\frac{d\theta}{dt}$. This is perfectly legitimate for the transformation, because Levi-Civita's function has been deduced with the help of the classical integral of areas, holds for a trajectory of a central force, and the advance of the periastron has also been deduced by the ordinary dynamical method involving that relation. Accordingly

$$-C^2u^2\frac{d^2u}{d\theta^2}-u^3C^2=-Pc^2u^2-2Qc^2u^3,$$

or
$$\frac{d^2u}{d\theta^2}+u=\frac{Pc^2}{C^2}+\frac{2Qc^2}{C^2}.u.$$

This is not at all identical with Einstein's equation, in which the last term contains $u^2$ and not $u$.

Putting
$$\sqrt{1-\frac{2Qc^2}{C^2}}=k\,;\ kC=C' \ \text{ and } \ k\theta=\theta'$$

the equation becomes
$$\frac{d^2u}{d\theta'^2}+u=\frac{Pc^2}{C'^2},$$

which has the Newtonian and not the Einsteinian form, and for which the solution is
$$u=\frac{Pc^2}{k^2C^2}+A\cos(k\theta+B),$$

where A and B are constants.

3. On Newtonian principles, as adopted by Levi-Civita, no value for the spectral shift of light from the Sun can be obtained. And even the value for the deflexion of light from a star past the sun obtained from Levi-Civita's formula does not tally with Einstein's value.

If $R_0$ be the perpendicular distance from the centre of the Sun on an asymptote and $\psi$ the angle between the radius vector and this perpendicular, then the deflexion
$$\epsilon=\frac{1}{c^2R_0}\int_{-\frac{\pi}{2}}^{\frac{\pi}{2}}\left[-\frac{Pc^2}{r^2}-\frac{2Qc^2}{r^3}\right]r^2\cos\psi\,d\psi,$$

where
$$r\cos\psi=R_0.$$

Hence
$$\epsilon=-\frac{1}{R_0}\left(2P+\frac{\pi Q}{R_0}\right)$$
$$=-\frac{2fm_0}{c^2R_0}\left(1+\frac{3\pi fm_0}{c^2R_0}\right),$$

which is equal to the Newtonian value nearly, and not to Einstein's, because the second term is too small.

4. Unlike the principal corrective force in Relativity, Levi-Civita's corrective force is central and also differs in magnitude and sign. In Relativity, where
$$r^2\frac{d\theta}{dt}=C\left(1-\frac{2fm_0}{c^2r}\right)\text{nearly},$$

the principal corrective radial force is $\frac{2f^2m_0^2}{c^2r^3}$ (see Eddington's

'Relativity,' par. 44, page 97; also Chazy's 'Relativité,' vol. i. p. 101). But Levi-Civita's corrective force, when the function is reduced to one-body problem, is $-\frac{6f^2{m_0}^2}{c^2r^3}$ nearly. It is this larger magnitude of different sign which enables him to deduce by ordinary dynamics the correct value for the advance of the perihelion.

As $\gamma^3$ in the additional relativistic contribution has a factor $\frac{m_0m_1}{(m_0+m_1)^2}$, this term necessarily vanishes when the function is reduced to a one-body problem, and so the difficulty remains the same even if the more approximate value of the force-function is considered.

5. It was shown by me in the 'Proceedings of the National Academy of Sciences, India' (vi. p. 280, August 1936), that by regarding the extra term in Einstein's form of the orbital equation as being due to a perturbative force the acceleration of $P_1$ relative to $P_0$ is

$$-\frac{f(m_0+m_1)}{r^2}-\frac{3f(m_0+m_1)C^2}{c^2}\cdot\frac{1}{r^4}.$$

This for the one-centre problem retransforms exactly into Einstein's differential equation

$$\frac{d^2u}{d\theta^2}+u=\frac{fm_0}{C^2}+\frac{3fm_0}{c^2}.u^2.$$

The first term of the acceleration does not produce any advance of the periastron; but from the well-known formula the second term gives

$$d\varpi=\left\{\frac{3f(m_0+m_1)}{c^2}\cdot\frac{1}{r^4}\right\}\cdot\frac{C}{f(m_0+m_1)}\cdot\frac{\cos\theta}{e}dt.$$

We take

$$\frac{1}{r^2}=\frac{f^2(m_0+m_1)^2}{C^2}(1+e\cos\theta)^2 \quad\text{and}\quad dt=\frac{r^2\,d\theta}{C}.$$

Hence for one complete revolution

$$\begin{aligned}\varpi&=\frac{3f^2(m_0+m_1)^2}{C^2c^2.e}\cdot\int_0^{2\pi}(1+e\cos\theta)^2\cos\theta\,d\theta\\&=\frac{6\pi f^2(m_0+m_1)^2}{C^2c^2}.\end{aligned}$$

This is exactly the same as Levi-Civita's value. The deflexion of light tallies with Freundlich's observation.

This law, of course, gives no net acceleration of the common centre of gravity.

# XIX. *On Turbulent Liquid Motion outside a Circular Boundary.*

By Manohar Ray, Lahore, India *.

[Received September 29, 1938.]

## 1. *Introduction.*

There are at present two theories of turbulent liquid motion. One is due to Prandtl⁽¹⁾, who assumes a transport of momentum without suffering a change for a length within the turbulent layer, and the second is the one due to Taylor⁽²⁾, who proceeds on the idea that the vorticity is transported in that manner. Both theories enable us to obtain a velocity distribution in the turbulent layer over a plate, the calculations of the vorticity transport theory agreeing, however, very satisfactorily with some experimental data. Goldstein⁽³⁾ has given a neat shape to the equation of Taylor's general turbulent theory in three dimensions, which makes the problem of turbulent motion somewhat handier as regards analytical treatment. Up to now the turbulence problems which have been found amenable to mathematical treatment are those of a uniform stream over a plane plate⁽⁴⁾, of wake behind an obstacle⁽⁵⁾, and of two-dimensional and axially symmetric jets⁽⁶⁾. The object of the present paper is to obtain solutions of Goldstein's equations in the neighbourhood of a circular boundary and information regarding turbulence therefrom. The starting point has been the general equations of Taylor as given by Goldstein⁽³⁾. They have been transformed into a form suitable for treatment near any curved wall. Though these equations become somewhat simpler for a circular boundary, an exact solution has not been found possible. To get an insight into the problem, a solution has been constructed by successive approximation which ultimately gives the velocity profile in the turbulent layer near the boundary, though the approximation may not be sufficient to reach the transition layer between turbulence and stream-line motion. As usual, the solution has been adjusted to give on the wall an infinitely large normal derivative of the velocity parallel to the wall, an artificial attempt to reach the turbulent layer immediately from the wall. This process necessarily ignores the viscous layer near the wall. As in such a layer the above normal derivative is finite, vanishing at the point of separation of the boundary layer, our solution cannot be expected to give any information regarding this viscous layer very near the boundary. An important feature of our solution is the retrograde velocity in the turbulent layer parallel to the wall. The velocity profile curve shows how this retrograde velocity gradually changes into a direct one, after which the stream-line motion is established.

---

* Communicated by the Author.

## 2. *Field Equations in Curvilinear Coordinates.*

In the generalized vorticity transport theory we still suppose that fluid element has at some time the average vorticity of its surroundings, but, instead of supposing it to be displaced a distance $l$ parallel to the $y$-axis, we let it undergo a vector displacement L where L has components $L_1$, $L_2$, $L_3$. Let V be the vector mean velocity with components $(u, v, w)$; V′ the vector eddy velocity with components $(u', v', \omega')$; $\widehat{\omega}$ the mean vorticity with components $(\xi, \eta, \zeta)$; $\widehat{\omega}'$ the eddy vorticity with components $(\xi', \eta', \zeta)$; F the external force acting on the fluid per unit mass, $p$ the mean pressure, and $\rho$ the density of the fluid. Then

$$\widehat{\ }=\text{curl } V, \quad \widehat{\omega}'=\text{curl } V'. \qquad (1)$$

The fluid is taken to be incompressible with $\rho$ constant and the mean motion to be steady. The vector equation of the mean motion is

$$\text{grad } \tfrac{1}{2}V^2-V\times\widehat{\omega}=F-\text{grad}\left(\frac{p}{\rho}+\frac{1}{2}\overline{V'^2}\right)+\overline{V'\times\widehat{\omega}'}. \qquad (2)$$

Goldstein in a paper (3) has shown that $\widehat{\omega}'$ can be expressed in terms of $\widehat{\omega}$ in a vector form, namely,

$$\widehat{\omega}'=\text{curl } L\times\widehat{\omega}, \qquad (3)$$

and that the equation of continuity, when the second order terms are neglected, can be written as

$$\text{div } L=0, \ i.\,e., \ \Delta L=0. \qquad (4)$$

The above equations being all in vector forms, we can write down the equations of motion in any orthogonal coordinates.

For motion outside an infinite cylinder the motion is evidently two-dimensional, and $\widehat{\omega}$ has only one component $\zeta$. We choose as the $x$-coordinate the length of the arc of the cross-section of the cylinder, the $y$-coordinate the normal to the section. If P be any point $(x, y)$, then the elementary area at P is the area bounded by the elementary length $dx$, of the curve through P parallel to the cross-section and the element $dy$ of the normal.

If $r(x)$ be the radius of curvature, then evidently

$$\frac{dx_1}{dx}=\frac{r+y}{r}. \qquad (5)$$

If $(u, v)$ be the component of the vector V, then its divergence $\varDelta$ is obtained by applying Green's theorem to the elementary volume of unit height, where base is the area enclosed by $dx_1$ and $dy$ and is given by

$$\varDelta\, dx_1 dy = \frac{\partial}{\partial x_1}(u\,dy)\,dx_1 + \frac{\partial}{\partial y}(v\,dx_1)\,dy$$

or using (5), we get

$$\varDelta = \frac{r}{r+y}\frac{\partial u}{\partial x} + \frac{\partial v}{\partial y} + \frac{v}{r+y} \quad . \; . \; . \; . \; . \; . \; . \; . \quad (6)$$

Again $\zeta$, the curl of the vector V, can also be easily found by applying Stokes's theorem to the same elementary area, and is given by

$$\zeta\, dx_1 dy = -\frac{\partial}{\partial y}(u\,dx_1)\,dy + \frac{\partial}{\partial x_1}(v\,dy)\,dx_1,$$

Fig. 1.

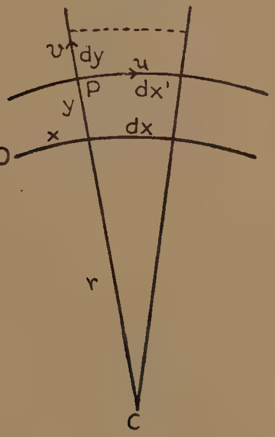

or by using (5) again, we get

$$\zeta = \frac{r}{r+y}\frac{\partial v}{\partial x} - \frac{\partial u}{\partial y} - \frac{u}{r+y} \quad . \; . \; . \; . \; . \; . \; . \; . \quad (7)$$

Next to find $\widehat{\omega}'$ from equation (3), we notice first that the vector $\mathrm{L}\times\widehat{\omega}$, *i. e.*, $\mathrm{L}\times\zeta$ in our case, has two components, $\mathrm{L}_2\zeta$ and $-\mathrm{L}_1\zeta$, in the directions of $x$ and $y$, so that

$$\zeta' = \mathrm{curl}\ \mathrm{L}\times\zeta = \frac{r}{r+y}\frac{\partial}{\partial x}(-\mathrm{L}_1\zeta) - \frac{\partial}{\partial y}(\mathrm{L}_2\zeta) - \frac{\mathrm{L}_2\zeta}{r+y}.$$

Now since

$$\varDelta \mathrm{L} = 0,\ i.\ e., \frac{r}{r+y}\frac{\partial \mathrm{L}_1}{\partial x} + \frac{\partial \mathrm{L}_2}{\partial y} + \frac{\mathrm{L}_2}{r+y} = 0, \quad . \; . \; . \; . \quad (8)$$

the above expression for $\zeta'$ reduces to

$$\zeta'=-\frac{r}{r+y}L_1\frac{\partial\zeta}{\partial x}-L_2\frac{\partial\zeta}{\partial y}. \quad . \quad . \quad . \quad . \quad . \quad . \quad . \qquad (9)$$

We are now in a position to determine the term $\overline{V'\times\bar{\omega}'}=\overline{V'\times\zeta'}$ on the right-hand side of equation (2). Its $x$-component is

$$\overline{v'\zeta'}=-\overline{L_1v'}\frac{r}{r+y}\frac{\partial\zeta}{\partial x}-\overline{L_2v'}\frac{\partial\zeta}{\partial y},$$

from (9).

Using (7), the $x$-component of $\overline{V'\times\zeta'}=$

$$-\overline{L_1v'}\left\{\left(\frac{r}{r+y}\right)^2\frac{\partial^2v}{\partial x^2}+\frac{r}{(r+y)^2}\frac{\partial v}{\partial x}\frac{dr}{dx}-\frac{r^2}{(r+y)^3}\frac{\partial v}{\partial x}\frac{dr}{dx}-\frac{r}{r+y}\frac{\partial^2u}{\partial x\partial y}\right.$$
$$\left.-\frac{r}{(r+y)^2}\frac{\partial u}{\partial x}+\frac{r}{(r+y)^3}u\frac{dr}{dx}\right\}$$
$$-\overline{L_2v'}\left\{\frac{r}{r+y}\frac{\partial^2v}{\partial x\partial y}-\frac{r}{(r+y)^2}\frac{\partial v}{\partial x}-\frac{\partial^2u}{\partial y^2}-\frac{1}{r+y}\frac{\partial u}{\partial y}+\frac{u}{(r+y)^2}\right\} \quad . \quad . \qquad (10)$$

To simplify the above expression (10), we make the usual assumption that $\frac{\partial u}{\partial x}$, $\frac{\partial v}{\partial x}$, $\frac{\partial v}{\partial y}$ are small compared with $\frac{\partial u}{\partial y}$, then it becomes

$$-\overline{L_1v'}\frac{r}{(r+y)^3}u\frac{dr}{dx}+\overline{L_2v'}\left\{\frac{\partial^2u}{\partial y^2}+\frac{1}{r+y}\frac{\partial u}{\partial y}-\frac{u}{(r+y)^2}\right\}. \quad . \qquad (11)$$

We can now write down the equation of motion (2). We assume that the derivative of $\left(\frac{p}{\rho}+\frac{1}{2}\overline{V'^2}\right)$ may be neglected to a first approximation, and then, when the fluid is free from body forces, the $x$-equation is

$$\frac{\partial}{\partial x_1}\frac{1}{2}(u^2+v^2)-v\zeta=\overline{v'\zeta'}, \quad . \quad . \quad . \quad . \quad . \quad . \quad . \qquad (12)$$

or using (5), (7), and (11), we get

$$\frac{r}{r+y}u\frac{\partial u}{\partial x}+v\frac{\partial u}{\partial y}$$
$$+\frac{uv}{r+y}=-\overline{L_1v'}\frac{r}{(r+y)^3}u\frac{dr}{dx}+\overline{L_2v'}\left(\frac{\partial^2u}{\partial y^2}+\frac{1}{r+y}\frac{\partial u}{\partial y}-\frac{u}{(r+y)^2}\right). \qquad (13)$$

Similarly, the $y$-equation of motion can be written as

$$\frac{r}{r+y}u\frac{\partial v}{\partial x}+v\frac{\partial v}{\partial y}-\frac{u^2}{r+y}$$
$$=\overline{L_1u'}\frac{r}{(r+y)^3}u\frac{dr}{dx}-\overline{L_2u'}\left(\frac{\partial^2u}{\partial y^2}+\frac{1}{r+y}\frac{\partial u}{\partial y}-\frac{u}{(r+y)^2.}\right). \quad . \quad . \quad . \quad . \qquad (14)$$

Equations (13) and (14) are the field equations in the turbulent layer. They have to be combined with the equation of continuity. We note that if the $x$-axis be straight, the above equation (13) gives the usual two-dimensional equation for the vorticity transport theory, namely,

$$u\frac{\partial u}{\partial x}+v\frac{\partial u}{\partial y}=lv'\frac{\partial^2 u}{\partial y^2}. \quad . \quad . \quad . \quad . \quad . \quad . \quad . \quad . \quad (15)$$

Applying the above results to the case of an infinite circular cylinder of radius $r$, we get the following equations. First, the $x$-equation of motion is

$$\frac{r}{r+y}u\frac{\partial u}{\partial x}+v\frac{\partial u}{\partial y.}+\frac{uv}{r+y}=\overline{\mathrm{L}_2v'}\left(\frac{\partial^2 u}{\partial y^2}+\frac{1}{r+y}\frac{\partial u}{\partial y}-\frac{u}{(r+y^2)}\right); \quad (16)$$

further, we have the equation of continuity, namely,

$$\frac{r}{r+y}\frac{\partial u}{\partial x}+\frac{\partial v}{\partial y}+\frac{v}{r+y}=0, \textit{ i. e.}, \frac{\partial u}{\partial x}+\frac{\partial}{\partial y}\left(\frac{r+y}{r}v\right)=0. \quad . \quad . \quad (17)$$

We shall see later that the second equation of motion does not give anything new.

Making the usual assumption of Prandtl for the mixture length, we put

$$\overline{\mathrm{L}_2v'}=-l^2\frac{\partial u}{\partial y}, \quad . \quad . \quad . \quad . \quad . \quad . \quad . \quad . \quad (18)$$

so that the equation (16) becomes

$$\frac{r}{r+y}u\frac{\partial u}{\partial x}+v\frac{\partial u}{\partial y}+\frac{uv}{r+y}=-l^2\frac{\partial u}{\partial y}\left(\frac{\partial^2 u}{\partial y^2}+\frac{1}{r+y}\frac{\partial u}{\partial y}-\frac{u}{(r+y)^2}\right) \quad (19)$$

### 3. *Solution of the Equations for a Circular Boundary.*

We shall now attempt to find the solution of the equations (19) and (17) for the turbulent motion set up by a stream past a fixed infinite circular cylinder. An exact solution has not been possible, but to get some idea about the nature of turbulence outside the cylinder a solution has been constructed in successive stages by approximation. First it is assumed that the region of turbulence is small compared with the dimension of the cylinder, which justifies our restriction to the case where $y/r$ is small ($y/r \ll 1$). Equations (19) and (17) will now be simplified to

$$u\frac{\partial u}{\partial x}+v\frac{\partial u}{\partial y}+\frac{uv}{r}=-l^2\frac{\partial u}{\partial y}\left(\frac{\partial^2 u}{\partial y^2}+\frac{1}{r}\frac{\partial u}{\partial y}-\frac{u}{r^2}\right) \quad . \quad . \quad . \quad (20)$$

and

$$\frac{\partial u}{\partial x}+\frac{\partial v}{\partial y}=0. \quad . \quad . \quad . \quad . \quad . \quad . \quad . \quad . \quad (21)$$

We shall later justify our approximation of the solutions obtained herefrom.

Equation (21) is satisfied by

$$\left.\begin{aligned} u &= \frac{\partial\psi}{\partial y}, \\ v &= -\frac{\partial\psi}{\partial x}. \end{aligned}\right\} \tag{22}$$

Hence, putting

$$u = 2\mathrm{U} f(\eta) \sin\frac{x}{r}, \tag{23}$$

where

$$\eta = y/r, \tag{24}$$

and $f(\eta)$ is an unknown function of $\eta$, we get

$$\psi = 2\mathrm{U}\sin\frac{x}{r}\int f(\eta)\,dy = 2r\mathrm{U}\sin\frac{x}{r}\int f(\eta)\,d\eta = 2r\mathrm{U}\sin\frac{x}{r}\,\mathrm{F}(\eta),$$

where

$$\mathrm{F}(\eta) = \int f(\eta)\,d\eta.$$

Hence from (21) we get

$$\left.\begin{aligned} u &= 2\mathrm{UF}'(\eta)\sin\frac{x}{r}, \\ v &= -2\mathrm{UF}(\eta)\cos\frac{x}{r}. \end{aligned}\right\} \tag{25}$$

To solve equation (20), with these values of $u$ and $v$, we put for $l$

$$l^2 = y^2 f_1(\eta)\cot\frac{x}{r}, \tag{26}$$

where $f_1(\eta)$ is another unknown function of $\eta$, which we shall choose suitably. The points $x=0$ and $x/r=\pi$ are outside the region considered.

Using equations (25) and (26) in (20) we get

$$\mathrm{F}'^2 - \mathrm{FF}'' - \mathrm{FF}' = -\eta^2 f_1(\eta)\mathrm{F}''(\mathrm{F}''' + \mathrm{F}'' - \mathrm{F}'), \tag{27}$$

where the dashes denote differentiation with respect to $\eta$, as the equation which will ultimately give us the velocity distribution in the turbulent layer.

The conditions to be satisfied on the circular boundary are $\dfrac{\partial u}{\partial y} = \infty$ and $v=0$, *i. e.*, $\mathrm{F}'' = \infty$ and $\mathrm{F}=0$ for $\eta=0$. $u$, consequently $\mathrm{F}'$, may be, however, finite, or negatively infinite, as is generally the case in the problem of the plate. To find a solution of the equation (27) which will give the necessary fit on the circular boundary, we have to choose the function $f_1(\eta)$ suitably, as is going to be done presently.

We now start a first approximation calculation by taking the first term on each side of the equality (27) to be dominant, and put

$$\mathrm{F}'^2 = -\eta^2 f_1(\eta)\mathrm{F}''\mathrm{F}'''. \tag{28}$$

This step will be justified in detail subsequently.

In choosing now the form of $f_1(\eta)$ we note that equation (28) will be satisfied subject to the condition at the boundary, if we put

$$f_1(\eta)=\eta(\log\eta)^2. \qquad \ldots\ldots\ldots \qquad (29)$$

This gives the equation

$$F'^2=-\eta^3(\log\eta)^2F''F'''. \qquad \ldots\ldots\ldots \qquad (30)$$

A suitable solution of this equation is

$$F'=A\log\eta, \qquad \ldots\ldots\ldots \qquad (31)$$

where A is a constant.

We note here that with the above value (29) for $f_1(\eta)$, $l$ tends to zero on the boundary of the cylinder, as should be the case, and, further, the terms neglected in equation (27) in our approximation are really of lower order than those retained.

Equation (27) in consideration of (29) now has the form

$$F'^2+\eta^3(\log\eta)^2F''F'''=FF''+FF'-\eta^3(\log\eta)^2F''(F''-F'), \quad . \quad (32)$$

the first approximation solution of which is given by (31).

We now proceed to the second approximation by putting

$$F'=A\log\eta+B, \qquad \ldots\ldots\ldots \qquad (33)$$

where B is a constant. Substituting this in (32), we get

$$A^2(\log\eta)^2+B^2+2AB\log\eta-A^2(\log\eta)^2=A^2(\log\eta-1)+AB+\eta$$

$$\{A(\log\eta-1)+B\}(A\log\eta+B)-A\eta^2(\log\eta)^2(A/\eta-A\log\eta-B).$$

Equating the coefficients of the terms of the highest order, namely, log $\eta$ for both sides, we obtain

$$B=A/2.$$

Our next approximation would be

$$F'=A(\log\eta+\tfrac{1}{2})+\frac{c}{\log\eta},$$

the value of C being found by a similar process. This process may be repeated and subsequent higher approximation terms may be added to F′, but it has one disadvantage. The second and third terms on the right-hand side of (32) do not really contribute anything in this calculation. This is due to the terms being associated with a factor $\eta$, which for small values of $\eta$ is of lower order than $1/(\log\eta)$. The solution found is thus expected to be valid only close to the boundary. The validity of this approximation will, however, be subsequently justified by calculating the relative contribution of the terms of the equation. Pursuing the approximations further we obtain the following solution:

$$\left.\begin{aligned}
\mathrm{F}' &= \mathrm{A}\left\{\log\eta+\cdot5-\frac{\cdot1875}{\log\eta}+\frac{\cdot0937}{(\log\eta)^2}-\frac{\cdot1289}{(\log\eta)^3}\right.\\
&\qquad\left.+\frac{\cdot1839}{(\log\eta)^4}-\frac{\cdot4665}{(\log\eta)^5}+\frac{\cdot9952}{(\log\eta)^6}\right\},\\
&\text{which gives}\\
\mathrm{F} &= \mathrm{A}\eta\left\{\log\eta-\cdot5-\frac{\cdot1875}{\log\eta}-\frac{\cdot0937}{(\log\eta)^2}-\frac{\cdot3164}{(\log\eta)^3}\right.\\
&\qquad\left.-\frac{\cdot7652}{(\log\eta)^4}-\frac{3\cdot5274}{(\log\eta)^5}-\frac{16\cdot4857}{(\log\eta)^6}\right\}.
\end{aligned}\right\} \quad . \quad . \quad (34)$$

Equation (25) now gives the velocities thus:

$$\begin{aligned}
u=2\mathrm{AU}&\left\{\log\eta+\cdot5-\frac{\cdot1875}{\log\eta}+\frac{\cdot0937}{(\log\eta)^2}-\frac{\cdot1289}{(\log\eta)^3}\right.\\
&\left.+\frac{\cdot1839}{(\log\eta)^4}-\frac{\cdot4665}{(\log\eta)^5}+\frac{\cdot9952}{(\log\eta)^6}\right\}\sin\frac{x}{r}. \quad . \quad . \quad . \quad (35)
\end{aligned}$$

$$\begin{aligned}
v=-2\mathrm{AU}\,\eta&\left\{\log\eta-\cdot5-\frac{\cdot1875}{\log\eta}-\frac{\cdot0937}{(\log\eta)^2}-\frac{\cdot3164}{(\log\eta)^3}\right.\\
&\left.-\frac{\cdot7652}{(\log\eta)^4}-\frac{3\cdot5274}{(\log\eta)^5}-\frac{16\cdot4857}{(\log\eta)^6}\right\}\cos x/r. \quad . \quad . \quad . \quad (36)
\end{aligned}$$

With the help of these solutions (35) and (36) we can now justify that equations (20) and (21) are correct approximation of equations (19) and (17). The highest order of the terms neglected in (19) is contributed by $\frac{y}{r}u\frac{\partial u}{\partial x}$, which itself is of the order $\eta\mathrm{F}'^2$, *i. e.*, of the order $\eta(\log\eta)^2$. This is evidently small compared with the terms retained, which are at least of the order of $\log\eta$. Similarly, in deriving equation (21) from equation (17), the terms neglected are $v$ and $y\frac{\partial v}{\partial y}$, which are of the order $\eta\log\eta$, and this is again small compared to the other terms retained in our approximations.

## 4. *Results.*

The velocity distribution as given by (35) and (36) will be true for points near the surface of the cylinder and can be made more and more accurate by calculating more and more terms on the right-hand sides of (35) and (36). Of course this statement is true only for points close to the cylinder. The constant A remains here undetermined and is to be found experimentally by observing the velocity at a definite point in the turbulent region near the boundary. Apart from this magnification factor A and the periodic factors, the profiles of $u$ and $v$ can be represented by plotting the functions F′/A and F/A as given by (34).

Table I. gives the values of the functions corresponding to different values of $\eta$ and fig. 2 (p. 240) gives the corresponding profiles of $u$ and $v$. The error of the table increases as we go down, *i. e.*, move away from the wall. For this reason higher approximations had to be worked out for the reliability of the figures near the bottom of the table. But our expectation of the reliability does not go much beyond the value of $\eta = \cdot 2$. A justification of our approximation will be found in Table II., which gives the numerical values of the terms of equation (32) (calculated up to the order $1/(\log \eta)^6$).

TABLE I.

| $\eta$. | $u/(2\mathrm{AU} \sin x/r)$. | $v/(2\mathrm{AU} \cos x/r)$. |
|---|---|---|
| 0 | $-\infty$ | 0 |
| ·05 | −2·4123 | ·1724 |
| ·1 | −1·6717 | ·2795 |
| ·15 | −1·2088 | ·3821 |
| ·2 | − ·7979 | ·538 |
| ·25 | − ·3728 | ·8753 |
| ·3 | ·1891 | 1·7445 |

TABLE II.

| | $F'^2$. | $\eta^3(\log \eta)^2 F''F'''$. | $FF''$. | $FF'$. | $-\eta^3(\log \eta)^2 F''^2$. | $\eta^3(\log \eta)^2 F'F''$. |
|---|---|---|---|---|---|---|
| $\eta = \cdot 1$ . | 2·7946 | −6·0504 | −2·9953 | +·4672 | −·6312 | −·0966 |
| $\eta = \cdot 2$ . | ·6366 | −3·0264 | −3·7036 | +·4292 | −·982 | −·1138 |

It is to be noted that $u$ is negative for a small region round the cylinder. This retrograde motion slowly diminishes outwards till the general streamline motion is reached. $v$ will be zero on the surface of the cylinder and will gradually increase outwards.

As has been stated before, we do not expect from the above solution any information about the effect of viscosity in the boundary layer or the point of separation.

We now examine the second equation of motion (14). For a circular cylinder it becomes

$$\frac{r}{r+y} u \frac{\partial v}{\partial x} + v \frac{\partial v}{\partial y} - \frac{u^2}{r+y} = -\overline{\mathrm{L}_2 u'} \left( \frac{\partial^2 u}{\partial y^2} + \frac{1}{r+y} \frac{\partial u}{\partial y} - \frac{u}{(r+y)^2} \right) \quad . \quad (37)$$

For our approximation we see at once, by comparing (37) with (16), that $\overline{\mathrm{L}_2 u'}$ is of the same order as $\overline{\mathrm{L}_2 v'}$.

Fig. 2.

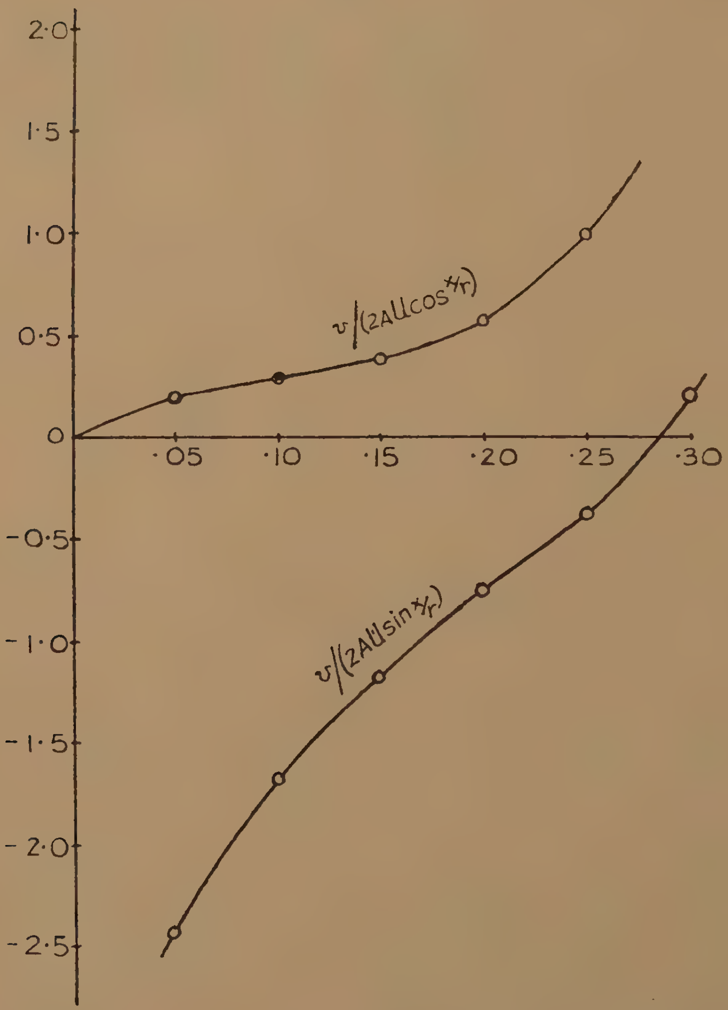

In conclusion, I wish to express my thanks to Prof. N. R. Sen, of the Calcutta University, for his kind help in this work.

*References.*

(1) Prantdl, Z. A. M. M. v. p. 136 (1925).
(2) Taylor, Proc. Roy. Soc. A, cxxxv. p. 685 (1932).
(3) Goldstein, Proc. Camb. Phil. Soc. xxxi. (1935).
(4) Howarth, Proc. Roy. Soc. A, cliv. (1936).
(5) Goldstein, Proc. Camb. Phil. Soc. xxxiv. (1938).
(6) Howarth, Proc. Camb. Phil. Soc. xxxiv. (1938).

Forman Christian College,
Lahore, India.

# XX. *Optical Activity and Magneto-optical Activity of Crystalline Nickel Sulphate in the Near Ultra-violet.*

By F. G. Slack, Ph.D., and Philip Rudnick, Ph.D., Department of Physics, Vanderbilt University, Nashville, Tennessee *.

[Received September 29, 1938.]

[Plate I.]

Recently reports have been made on the optical activity⁽¹⁾ and on the magneto-optical activity⁽²⁾ of crystalline nickel sulphate in the visible region. These measurements have now been extended to wave-lengths below the absorption band of the crystal which occurs at 3850 Å. Also an improved technique in making photographic measurements has resulted in somewhat different and better data for the optical activity at both ends of the visual region near the absorption bands.

## *Experimental Method and Results.*

Crystals of the α-hexahydrate of nickel sulphate cut along the cleavage plane (001) were used. This plane lies perpendicular to the optic axis, along which the beam of polarized light traverses the crystal.

The general method and procedure have been described in the articles⁽¹⁾, ⁽²⁾ referred to. For measurement in the ultra-violet a carbon arc was used as a light source, and a Hilger E–31 quartz spectrograph replaced the glass prism instrument used in the visible region. It was found possible to use the Lippich polarimeter with Nicol prisms and glass lenses to obtain measurements over a range of about one hundred Ångstroms below the violet absorption band. Thus the method of Fizeau and Foucault⁽³⁾ was used, improved by the addition of a section of levorotatory quartz, 7·92 mm. thick, cut perpendicular to its optic axis and inserted to increase the rotatory dispersion. A further improvement in technique, referred to above, was made by the comparison of right- and left-hand crystals. First a photograph was made with a right-hand crystal and with the polarimeter analyser set to give extinction for a desired wave-length (as computed from the known rotatory dispersion of quartz and an approximate value for the crystal, as determined from previous photographs). Then a left-hand crystal was substituted and the analyser rotated by an amount equivalent to the total estimated rotation for the two crystals at the wave-length in question. In case this estimated rotation was exactly correct, the extinction point in the second photograph would lie at the same wave-length as in the previous exposure, and thus in the same position on the plate. By several trials these two extinction points could be made to fall in almost identical positions, leaving only small corrections to the analyser settings to be made from plate measurements(4). This method eliminates possible errors in allowing for quartz rotation, and enables extinction point positions to be compared in practically identical spectra. This is important near absorption bands, where unequal densities on the two sides of the extinction point tend to falsify its position. The same procedure was used for the magnetic rotatory power measurements, except that instead of changing crystals it was necessary simply to reverse the field current and rotate the analyser by double the estimated magnetic rotation between exposures. To prevent excessive heating by the magnet current, exposures were made by five minute intervals on and off. Temperatures were measured and, from observations made with the quartz plate alone, corrections were made for change in its activity with temperature. The distances of the extinction points from lines of adjacent comparison spectra were measured by a micrometer microscope. The observations were also checked by a micro-projector, which afforded a very rapid comparison of the spectra.

---

* Communicated by the Authors.

The new data for the optical activity in the ultra-violet indicated a departure from the curve(1) made to fit the earlier data for the visible region. Therefore, a check on points near the ends of the visible spectrum was made with some care and by comparison of the right and left crystals. Also thinner crystals were used so that more light was available, and appropriate filters were inserted in the light path to eliminate over-exposure and fogging of the plate by light in regions of the spectrum not under observation. Fig. 1 (Pl. I.), a reproduction of our plate 34, shows the extinction points for left (*a*) and right (*b*) rotating crystals, each of thickness 0·74 mm. The analyser was rotated 2·94° between the two exposures. The average position of the extinction points is at 6285 Å., and the point in exposure (*a*) is displaced ·09 mm. to the long wave-length side of that in (*b*), indicating a rotation by both crystals ·65° greater than the analyser displacement. Thus a value 2·43° per mm. results from this photograph. The comparison spectra are from a hydrogen Geissler tube and show Hα clearly. Fig. 2 (Pl. I.) shows the spectrum of the Pointolite lamp, taken through one of these crystals to indicate the position and extent of the absorption band whose centre is at 3850 Å. The mercury comparison spectum serves to locate wave-lengths.

Fig. 3 shows the natural optical rotatory power for the $\alpha-NiSO_4.6H_2O$ throughout the range from 3400 Å. to 6550 Å. The experimental points are indicated on the plot and the sources of the data are indicated by the symbols used. The smooth and dotted curves are computed, as will be explained later. As already mentioned, the data presented here are not quite in agreement with those previously given(1) at the extremities of the previous curve. However, re-measurement of the original plates and a more rigorous interpolation of the quartz rotatory dispersion data, which must be carefully evaluated when using the single crystal method, bring these data into approximate agreement with the new data from right- and left-hand crystals. New sets of photographs at 6500 Å. consistently gave a rotatory power lower than at 6300 Å. This result is a little surprising, but seems as well established as our other measurements. The position of this point and the necessity of ascribing the general characteristics of the main portion of the curve to an unusual infra-red absorption band call for further observation in the infra-red, and this work is contemplated in the near future.

Fig. 3.

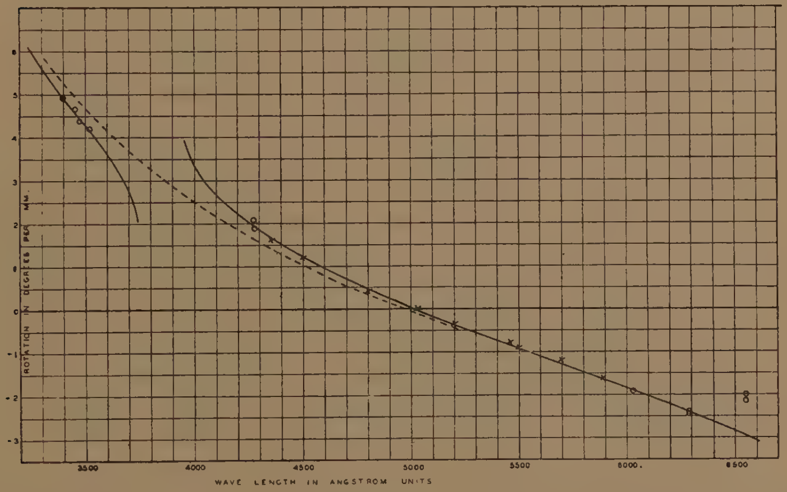

Natural rotatory power of $\alpha$—$NiSO_4.6H_2O$. Circles are data from new photographs; crosses are visual data by Underwood, Slack, and Nelson. Smooth and dotted curves plotted respectively from three and two terms of equation (2).

Fig. 4 shows the magneto-optical rotatory power for the nickel sulphate crystal. All data on this plot, with the exception of the single point at 3470 Å., are taken from the previous paper of Slack, Lageman and Underwood (2). This point was determined as the mean of several photographs, but the individual values were not precise enough to indicate the slope of the curve in this region and are therefore averaged. The addition of this short wave-length point results in the extension of the curve through the violet absorption band, and verifies the previous indication that this absorption frequency has little or no effect on the magnetic rotatory power of the crystal.

## *Analytical Representation of Data.*

### (a) *Natural Rotatory Power.*

We have tried to represent the experimental curve of fig. 3 by means of a relation of the accepted type (5), equation (1), containing

$$\alpha(\lambda)=\Sigma_i \frac{A_i}{\lambda^2-\lambda_i^2} \qquad \ldots\ldots\ldots \quad (1)$$

Fig. 4.

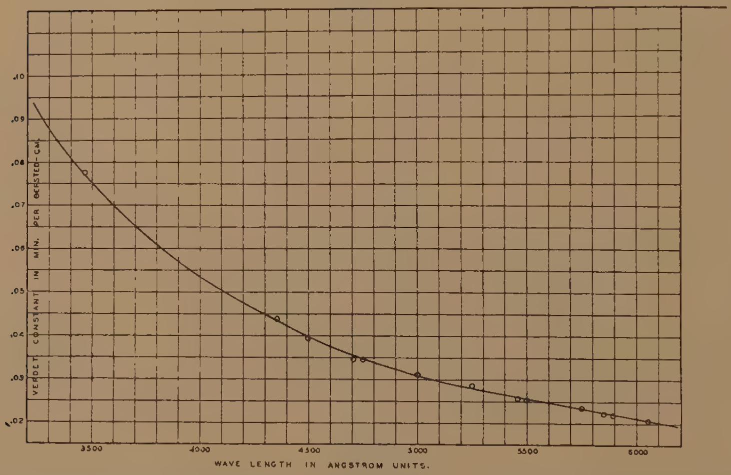

Magnetic rotatory power of $\alpha$—$NiSO_4.6H_2O$. Point at 3470 Å. from new photographs; others from visual data by Slack, Lageman, and Underwood. Smooth curve from equation (5).

only two terms in the right member, with only partial success. The experimental point at 6550 Å. is not correctly reproduced, and in the violet region the curve obtained invariably is a little too steep, so that it must be either too high at 3500 Å. or too low at 4300 Å. With these exceptions the data can be quite well represented by two terms, having critical wave-lengths in the far ultra-violet, and in the infra-red, respectively. For data of the present precision, one wave-length may be placed anywhere below 2000 Å. with the other in a corresponding position between 8000 Å. and 9500 Å.; the shape of the curve in the visible region is rather insensitive to changes in these constants⁽⁶⁾. The best two-term representation does not differ greatly from the first two terms in the right member of equation (2),

$$\alpha=\frac{\cdot 718}{\lambda^2-\cdot 0244}+\frac{1\cdot 834}{\lambda^2-\cdot 8156}+\frac{\cdot 0104}{\lambda^2-\cdot 1482}. \quad . \quad . \quad . \quad . \qquad (2)$$

Equation (2), which is plotted with a solid line in fig. 3, is an adequate representation of all the data except the point at 6550 Å. $\lambda$ is to be expressed in microns, and $\alpha$ in degrees per mm. The first two terms, with critical wave-lengths at 1560 Å. and 9030 Å., supply the major part of the rotatory power. The small third term, with critical wave-length 3850 Å., the observed position of most intense absorption in the near ultra-violet, has been made no larger than necessary to complete the fit with the experimental data in the violet region. Its effect is to supply a small positive contribution to the rotatory power around 4300 Å. and a similar negative one around 3500 Å. This is indicated in fig. 3 by the dotted curve, which represents only the first two terms of equation (2). A formal alternative for getting the same result is to assign a more remote value to the critical wave-length in the far ultra-violet, but nothing short of an inadmissible negative value of the $\lambda_i^2$ will give a change of the necessary amount. We therefore find the third term in equation (2) necessary.

In general, the vanishing of rotatory power at one wave-length, such as occurs in this crystal, may arise through the cancellation of terms in equation (1) having numerators of opposite sign, and critical wave-lengths lying on the same side of the null point; this is the most usual case. The second possibility is that the cancelling terms may have numerators of the same sign, but critical frequencies on opposite sides of the null point. The representation of equation (2) falls unmistakably in the latter category. Direct algebraic analysis shows that no *two* partial rotations with critical wave-lengths in the far ultra-violet can even crudely represent the data, the formal requirement being again bands which are too "remote," *i. e.*, having negative values of $\lambda_i^2$. The possibility has also been considered that the contributions of three or more far ultra-violet bands may combine to produce the main features of the experimental curve. If, in equation (1), all the $\lambda_i$ are smaller than $\lambda$, the right member may be expanded as a power series in $\left(\frac{1}{\lambda^2}\right)$.

$$\alpha=\frac{1}{\lambda^2}\sum_i A_i+\frac{1}{\lambda^4}\sum_i A_i\lambda_i^2+\frac{1}{\lambda^6}\sum_i A_i\lambda_i^4+,\text{ etc.} \quad . \quad . \quad . \quad . \qquad (3)$$

In this series the coefficients of higher powers of $\left(\frac{1}{\lambda^2}\right)$ will in general tend toward smaller values, although in special cases any of the earlier may be smaller than those which immediately follow. The experimental values have been examined as a function of $\left(\frac{1}{\lambda^2}\right)$, with the conclusion that a power series representation, if possible, must have such prominent third and fourth degree terms as to indicate that the data can be represented in this manner only as very small differences between large and almost completely cancelling partial rotations. We therefore choose the representation given in equation (2) as being more straightforward, even though the assignment of a principal critical wave-length in the infra-red region is quite unusual.

From the position of our experimental point at 6550 Å., a fourth partial rotation can be inferred, which is not included in equation (2), both because its presence is indicated experimentally at only one wave-length, and because there is at present no basis for separating its contribution from that of the infra-red term already present in equation (2). In fact, this latter term may well represent the composite effect of two critical wave-lengths both considerably shorter than 9030 Å., with rotational strengths of opposite sign.

(*b*) *Magnetic Rotatory Power.*

Following the procedure of Slack, Lageman and Underwood⁽²⁾, the magnetic rotatory dispersion data may be represented by an equation of the Drude type with a single effective absorption wave-length $\lambda_1$. The lack of data on the refractive index of the nickel sulphate crystal for short wave-lengths limits the precision of this calculation. The value $n_{(3470)}=1{\cdot}538$, determined by extrapolation of the data of Topsöe and Christiansen as given by Mellor⁽⁷⁾, was used in the calculation. The resulting Ketteler-Helmholtz equation for the refractive index is

$$n_\lambda^2-1=b_0+\frac{b_1}{\lambda^2-\lambda_1^2}=1{\cdot}2461+\frac{{\cdot}012126}{\lambda^2-({\cdot}135)^2}, \quad . \quad . \quad . \quad . \quad . \quad (4)$$

and the magnetic rotatory dispersion may be represented by the equation :

$$n_\lambda\delta_\lambda=\frac{k\lambda^2}{[\lambda^2-\lambda_1^2]^2}=\frac{{\cdot}01025\lambda^2}{[\lambda^2-({\cdot}135)^2]^2}. \quad . \quad . \quad . \quad . \quad . \quad (5)$$

The smooth curve of fig. 4 is plotted from this equation and is seen to fit the experimental points reasonably well throughout. The critical absorption wave-length (1350 Å.) is somewhat higher than that indicated by the previous data alone, but is more nearly consistent with the absorption region required by the natural (rotatory) dispersion data.

## *References.*

(1) N. Underwood, F. G. Slack, and E. B. Nelson, Phys. Rev. liv. p. 355 (1938).
(2) F. G. Slack, R. T. Lageman, and N. Underwood, Phys. Rev. liv. p. 358 (1938).

(3) T. M. Lowry, 'Optical Rotatory Power' (Longmans, Green and Co., 1935), p. 199.

(4) The relation between wave-length and rotatory power of quartz is very similar to the relation between wave-length and measured positions of lines on a spectrographic plate. As a result the relation between quartz rotation and plate position is very nearly linear over considerable spectral ranges. Once this relation has been determined with care, it affords a very convenient and accurate means of determining the change in rotation by the quartz plate corresponding to a small measured displacement of an extinction point in a spectrum, and eliminates the difficulty of accurate routine interpolation on dispersion curves.

(5) See for example E. U. Condon, Rev. Mod. Phys. ix. p. 432 (1937).

(6) The four constants, $\lambda_1$, $\lambda_2$, $A_1$, and $A_2$, in a two-term equation were computed from the following experimental data :—

(1) The wave-length of vanishing rotatory power, $\lambda_0$.

(2) The slope $\frac{d\alpha}{d\lambda}$ at $\lambda=\lambda_0$, denoted by $s$.

(3, 4) The values $\alpha'$ and $\alpha''$ of rotatory power at respective wave-lengths $\lambda'$ and $\lambda''$, so chosen that

$$\lambda_0^2-\lambda'^2=\lambda''^2-\lambda_0^2=\Delta.$$

The algebraic relationships involved are simple enough to be convenient not only for numerical computation, but also for studying by inspection the dependence of $\lambda_1$ and $\lambda_2$ on the assumed values of $\alpha$. Let :

$$a=\lambda_0^2-\lambda_1^2, \qquad b=\lambda_0^2-\lambda_2^2,$$

$$\delta=-\frac{4\lambda_0}{s\Delta}, \qquad M=\frac{\left(\frac{1}{\alpha'}+\frac{1}{\alpha''}\right)^2}{2\delta\left(\frac{1}{\alpha'}-\frac{1}{\alpha''}-\delta\right)}-1,$$

Then :

$$\frac{a}{b}=M\pm\sqrt{M^2-1},$$

$$a=-\left(1+\frac{a}{b}\right)\frac{\Delta\delta}{\left(\frac{1}{\alpha'}+\frac{1}{\alpha''}\right)},$$

$$\frac{A_1}{a}=-\frac{A_2}{b}=\alpha'\left[\left(1-\frac{\Delta}{a}\right)^{-1}-\left(1-\frac{\Delta}{b}\right)^{-1}\right]^{-1}=\alpha''\left[\left(1+\frac{\Delta}{a}\right)^{-1}-1+\frac{\Delta}{b}\Bigr)^{-1}\right]^{-1}.$$

(7) J. W. Mellor, 'A Comprehensive Treatise on Inorganic and Theoretical Chemistry,' vol. xv. p. 459.

# XXI. *Two-way Speech by Wireless.*

By Mario Marro, Dr. Ing.*

[Received November 28, 1938.]

Following-up my experimental research on the persistence of hearing † and the possibility of transmitting voice and music at regular intervals of time, by equal alternations of transmission and rest, I found several transmission frequencies at which the voice can be transmitted satisfactorily. The results of these experiments are shown below ‡ :—

| Number of interruptions per sec. | Observed results. |
|---|---|
| 10 to 25 | Voice is altered ; badly understood. |
| 25 to 50<br>125 to 170 | Voice is less altered ; and becomes intelligible. |
| 210 to 270 | Voice is much altered ; badly understood. |
| 290 to 300 | Voice is better reproduced ; one can understand what is pronounced. |
| 400 to 1500 | Voice much altered ; words incomprehensible. |
| 2000 to 2500 | From 2000 interruptions upwards, speech is clearly and perfectly heard. |

In order to interrupt the telephonic circuit carrying the voice a great number of times per second, instead of the commutator shown in my preceding communication I used the circuit of fig. 1. A tube, I, acts as diode. Its grid is submitted to positive and negative voltages alternately. Thus, when it is positive, the microphone current is allowed to pass into the listening line L. On the contrary, when it is negative no current flows into the line. The oscillating tube O gives the alternating voltage to the grid of tube I. The frequency of this oscillation is controlled by the variable condenser C. The frequency of the oscillation of tube O is also heard because tube I has a non-linear characteristic.

From experimental observations it appears that in the case of some low frequencies there are zones, doubtless related to the constituent frequencies of speech, in which the periodical interruptions do not greatly alter the voice and allow it to pass in a comprehensible form. Above 2000 interruptions per second speech is perfectly heard.

---

* Communicated by the Author.

† "On the Persistence of the Sensation of Speech," Phil. Mag. xxii. p. 847 (1936).

‡ "Two-way Speech by Wireless," 'The Electrician,' cxviii. no. 3057, p. 5 (1937).

Starting from the said observations I devised a radiotelephony system which permits simultaneous transmission and reception, employing the same wave-length at each end, with a single antenna. The layout comprises an auxiliary valve oscillator, with a frequency of about 8000 c.p.s., for example, which acts by alternating voltages on the screen grid or on the suppressor grid of the oscillating tube of the transmitting end, and on the screen grid or on the suppressor grid of the detector valve at the receiving end.

Fig. 1.

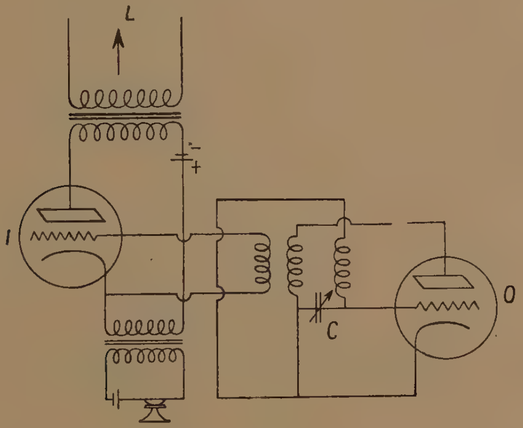

In this way transmission will occur at intervals of $\frac{1}{16,000}$ sec., spaced at second intervals of equal duration, during which the receiver will come into action.

If sufficiently high commutation frequencies are used synchronism and isochronism are not necessary between the two stations, which would be difficult to obtain. But we suppose that the low frequency oscillation of one station is a little different from that of the other station ; it is sufficient that the frequency of the resulting beats to be, for instance, 2000 c.p.s., in order to allow the voice to be transmitted with full intelligibility. On the other hand, it is not desirable to increase too much the commutation frequency in order not to enlarge the transmitted band ; this one would undoubtedly be accepted by short-wave communications.

In the diagram (fig. 2) O represents the oscillating valve and circuit of the transmission end ; Q represents the modulating valve ; R represents the detecting valve and circuit at the receiving end; P the low frequency amplifier valve; N represents the auxiliary oscillating valve; T is the telephone line connected with the radio set. We can suppose the switch S at the position *b*, *b*, that is, allowing the apparatus to receive and transmit simultaneously.

Fig. 2.

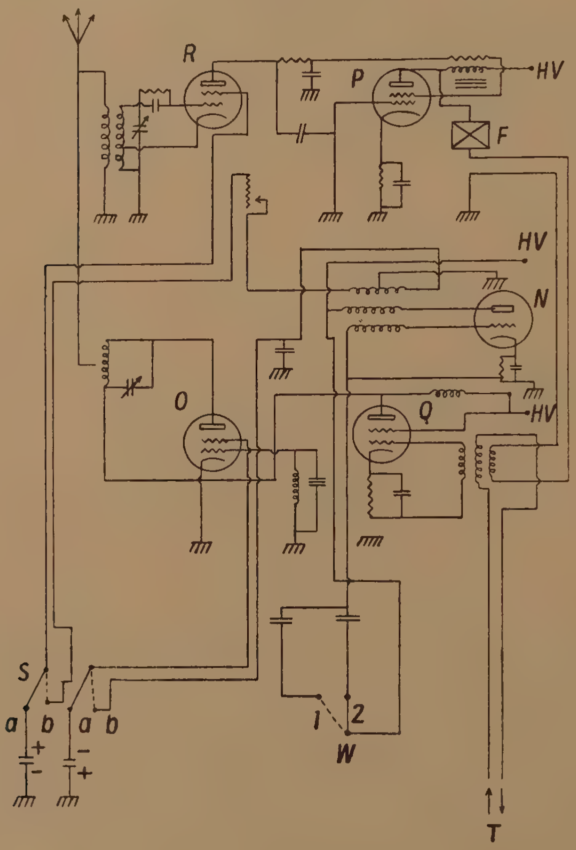

At the instant when the screen grid of valve O becomes positive the screen grid of valve R becomes negative, or *vice versa*. In this way during the time intervals when valve O oscillates in transmission, valve R will not be able to detect. When valve O does not oscillate because its screen grid is negative and the apparatus cannot act as transmitter, valve R will enter into action as detector, and, consequently, the apparatus will act as receiver.

It is necessary to use a band-pass filter F in order to avoid the whistle provoked by the beating between the commutation frequencies of the two communicating stations. I used a band-pass filter allowing a frequency-range from 300 to 2800 c.p.s.

It could be objected that the station power must be increased because of the fact that power transmission occurs during a part of time only. This is not true if we consider that during transmission intervals the power is the same as if it were transmitted in a steady manner. Because persistence of the sensation of hearing and shortness of interruption times the voice is heard with about the same loudness.

The radiotelephony system with which I experimented is very suitable for naval communications, particularly for communications between warships. It may also prove of great service to the air force.

The apparatus is ordinarily at reception, with switch S at the position *a*, *a*. By this arrangement the screen grid of the detecting tube is positive. The screen grid of the oscillating tube O is negative, in order not to disturb reception. When the station is called, the operator leads switch S into *b*, *b* position. Thus screen grid of tube R and screen grid of tube O will be submitted to the alternating voltages of oscillator N. The apparatus is now able to receive and transmit simultaneously with the calling station.

As I said, it is advisable that the commutation frequency of one station be different from that of the other station. The calling station, for instance, will operate with 8000 c.p.s. The switch W will be in position 1, thus connecting a condenser giving the desired frequency of 8000 c.p.s. in the oscillating circuit. At the called station the switch W will be placed at position 2, thus connecting a condenser for the 12,000 c.p.s. frequency.

When conversation is finished, the called station will put switch S in position *a*, *a*, in order to be in readiness for another call. Also the calling station will put itself in the condition to be called in its turn.

It is evident that the electric circuit represented in the diagram is merely one possible arrangement. The principle of the persistence of hearing and that of the auxiliary modulation may be applied to any wireless set.

I have carried out some tests employing a single antenna and a wavelength of exactly 100 metres. The voice heard was perfectly intelligible; the tone was very little altered.

Via Indipendenza, 59,
Bologna, Italy.

# XXII. *The Surface-Tension and Angle of Contact of Mercury* in vacuo.

By A. E. Bate, M.Sc., Ph.D., F.Inst.P.,
Northern Polytechnic, London *.

[Received February 28, 1939.]

## *Introduction.*

A well-known firm † provided the writer with doubly distilled mercury in a clean glass tube. It had been boiled in the tube which afterwards was evacuated and sealed. The surface of the mercury was unexpectedly found to be plane when the axis of the tube was vertical. This indicated that either the surface-tension was zero, or that the angle of contact between the mercury and glass was 90°. The latter was readily verified by tilting the tube, for the vertical section of the surface of the mercury was S-shaped, as shown in the first diagram. At each point of contact the angle was 90°, the higher part of the surface being concave, and the lower convex.

The portion of the surface which was near the axis of the tube was plane, and is marked P in the elevation and PP in the cross-section ; the line of contact with the glass is dotted.

Increased tilting caused the mercury to advance along the tube at the bottom, and to recede at the top, the line PP acting as an axis about which the surface appeared to rotate. The tube, which had been specially selected for uniformity of wall and diameter, was about 10 cm. long and 0·9 cm. internal diameter. It was almost exactly half-full of mercury, so that when the axis was horizontal the meniscus again was plane. Rotation of the horizontal tube about the axis caused the surface to incline toward the direction of rotation, but it became horizontal when the movement ceased.

The determination of the value of the surface-tension in vacuo presented some difficulty. The capillary method, in which the mercury is poured into a U-tube composed of a capillary tube and a wide tube, at once suggests itself, as the air could easily be removed, but as the angle of contact is 90° the levels in both tubes would be the same, thus rendering the method useless.

The sessile drop method appeared to present a solution, but this involves complications both in forming the drop and in observing it.

---

* Communicated by the Author.

† Messrs. Negretti and Zambra, London.

Finally, however, the result was obtained by direct observation of the mercury in the tube.

## *Theory.*

When the tube was tilted at a small angle $\alpha$, the mercury surface appeared as in fig. 1. Consider the lower portion as shown in fig. 2.

Let T be the surface-tension; then, for a very narrow strip of surface of width $\delta s$ perpendicular to the drawing, the forces due to surface-tension in a direction parallel to the plane of the paper are as shown. The resultant of the horizontal forces is $T(1-\sin\alpha)\,\delta s$ to the left, and this balances the horizontal component of the hydrostatic pressure on the strip, due to the mercury above the level of the point of contact Q; the height is marked $h$. This pressure has a mean value of $hg\rho/2$, so that the total horizontal thrust on the strip is $(h^2g\rho/2)\delta s$, where $g$ is the gravitational acceleration, and $\rho$ is the density of mercury.

Fig. 1.

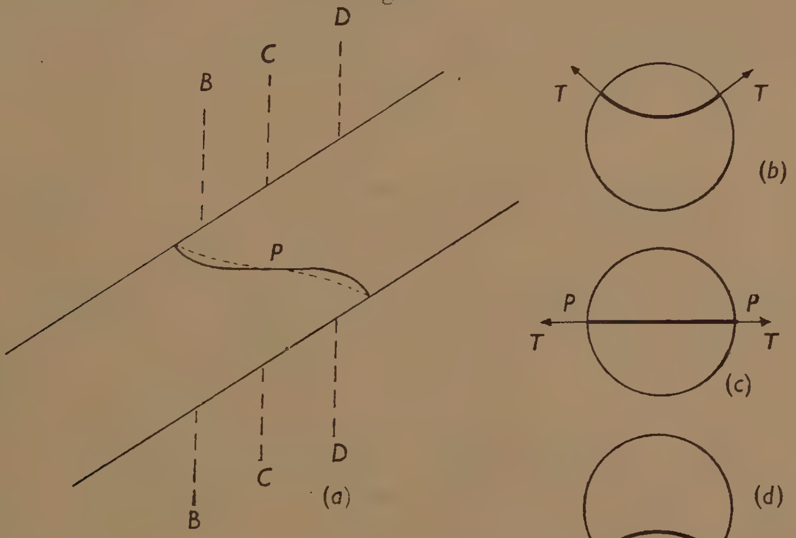

Elevations. Sections.

Thus

$$T(1-\sin\alpha)\delta s=(h^2g\rho/2)\delta s,$$

or

$$T=h^2g\rho/[2(1-\sin\alpha)].$$

This expression makes it appear that, when the tube is horizontal, *i. e.*, $\alpha=0$, T could be determined by direct measurement of $h$; in fact, the formula would then be that for the sessile drop above the horizontal plane of maximum area. Two factors, however, prevent this; first, the mercury rises at the end of the tube when the axis is horizontal; secondly, if the tube is less than half full, the height of the surface is diminished, due to the downward components of the surface-tension, as shown in fig. 1 (*c*) unless a very wide tube is used.

Even then, the level is below the axis of the tube, and this is a likely source of error in the measurement of *h*, due to refraction.

Actually, the fact that the angle of contact is 90° solved the problem. Referring to fig. 1, it will be seen that the point P is at the centre of the tube, and therefore, when P is viewed horizontally, the incidence is normal to the glass tube. Further, as the surface is plane here, the surface-tension at the sides of the tube acts horizontally, and the pressure beneath the surface of the mercury is equal to that above it. Thus, the surface in the vicinity is to be regarded as a free surface.

Fig. 2.

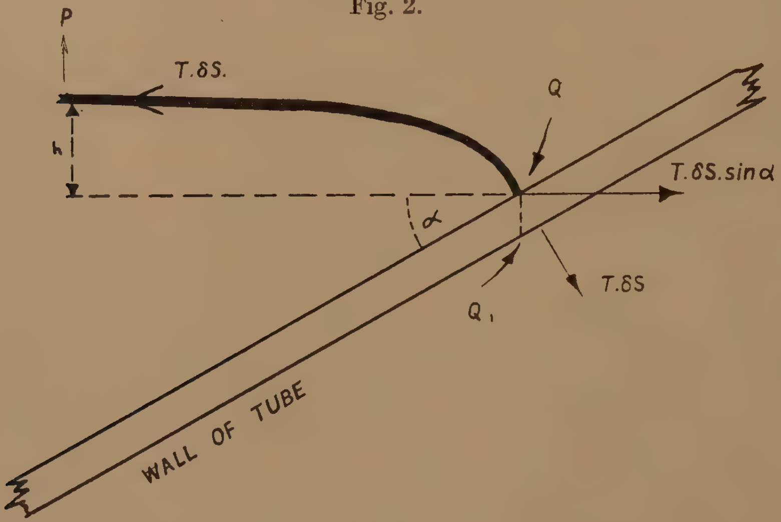

*Apparatus.*

The glass tube was placed with its axis horizontal in a hollow metal cylinder fitted with four screws at each end. These screws were equally spaced round the cylinder, and were directed inwards to hold the tube and enable its position to be adjusted so that it was coaxial with the cylinder. The cylinder was hinged at one end to a heavy base, and was fitted with a screw at the other by which it could be tilted. The angle of tilt was indicated to the nearest minute by a vernier fixed to the cylinder, which moved over a protractor attached to the base. Portions of the cylinder at the middle were cut away to allow the glass tube and mercury to be seen. The base was provided with levelling screws.

A microscope, fitted with vertical and horizontal cross-wires, and which could be made to travel horizontally and vertically over scales reading to 0·01 mm., completed the apparatus.

### *Procedure.*

The tube was tilted through a small angle and the point P (fig. 2) was viewed through the microscope, which was adjusted until the cross-wires coincided with it. The vertical scale was read, and the microscope was moved horizontally until the vertical cross-wire coincided with the point Q ; it was then lowered until the horizontal cross-wires met the *outer* edge of the tube at $Q_1$, immediately beneath Q. The height through which the microscope was lowered was thus obtained, and will be referred to as $h+t$, $t$ being the *vertical* thickness of the wall of the glass, QQ. It was necessary to measure to $Q_1$, as refraction prevents trustworthy observation of Q in a direction parallel to the axis of the tube.

### *Results.*

Three sets of readings were taken, the values being :

| | | | |
|---|---|---|---|
| Angle of tilt, $\alpha$ .......... | 4° | 3° | 2° |
| $h+t$ ..................... | 0·431 | 0·435 | 0·439 mm. |

At 1° tilt, the mercury surface at Q (fig. 2) was hidden by the cylinder ; from the run of the figures, $h+t$ would become ·447 mm. when $\alpha=0$. For this value of $\alpha$, $t$ becomes equal to the thickness of the glass. This was measured directly by cutting the tube, and found to be 0·176 cm. ; this gives $h=·271$ for $\alpha=0$.

The expression derived above becomes $T=h^2g\rho/2$ for $\alpha=0$, and the surface-tension of mercury in vacuo is therefore 490 dynes per cm. (at 20° C.), the angle of contact with glass being 90°.

This value of T compares well with that of Bosworth (Faraday Soc. Trans. xxxiv. p. 1501 (1938)), who obtained 484 dynes per cm. at 20° C. for a mercury–air surface, and for mercury–$CO_2$ about 1 per cent. less.

When the tube was cut and the air entered, the mercury meniscus became slightly convex, the contact-angle being about 100° ; two days later this had increased to about 135°, with a marked tendency to adhere to the tube. This tendency diminished after a further period of two days.

The author wishes to acknowledge the assistance of Mr. V. Hinkley, Lecture Demonstrator, and Mr. G. Chambers, Instrument-maker, of this Department, during the design and construction of the apparatus.

### ABSTRACT.

Clean dry mercury, which partly filled an evacuated and sealed tube, was found to have an angle of contact of 90° with the side of the tube, and a surface-tension of 490 dynes per cm. The method of obtaining this value is described.

## XXIII. *Notices respecting New Books.*

*Crystal Chemistry.* By R. C. Evans. [Pp. 388+xi.] (Cambridge University Press. Price 18*s*. net.)

This is a welcome addition to the literature dealing with the results of crystal analysis; it covers ground not adequately treated elsewhere, certainly in English, and does not overlap appreciably with books dealing with other aspects of modern crystallography. The author avoids the two main pitfalls awaiting the writer on this subject; he does not introduce the subject by giving a wholly unnecessary review of methods of crystal analysis, nor does he reduce the subject to a dull catalogue of structural types and numerical details. The subject is tackled from the standpoint of the four main types of interatomic force: ionic, homopolar, metallic, and van der Waals. Following a short account of the main features of these types of force the author proceeds to discuss the physical and chemical properties of solids under the headings metallic elements, alloy systems, homopolar compounds, ionic compounds (subdivided under four headings), and molecular compounds. In describing the structures from the standpoint of the binding forces, the author makes extensive use of the terms homodesmic, heterodesmic, isodesmic, anisodesmic, mesodesmic, which are largely unknown outside the ranks of Cambridge crystallographers. Admittedly the terms are defined in the book, and they will probably be useful to chemical crystallographers, but as the book will very probably be read by a much wider circle of readers the introduction of new technical terms is unfortunate, and the reviewer feels reluctant to admit their necessity.

The style of the book is good. The exposition is clear and concise, the figures adequate, the tables of numerical data sufficient for the purpose they serve, and the price reasonable. There is a three-page bibliography, twelve pages of references, and a subject-index; the omission of the usual name-index is partly covered by the alphabetical list of references.

G. W. B.

---

[*The Editors do not hold themselves responsible for the views expressed by their correspondents.*]

Fig. 1.

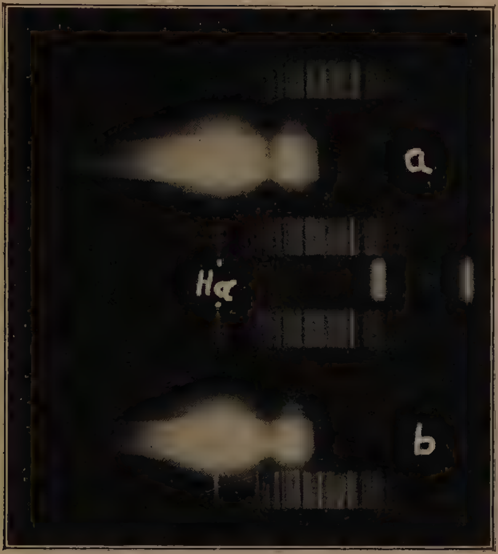

Taken with (*a*) left- and (*b*) right-hand crystals of $\alpha$—$NiSO_4.6H_2O$, showing extinction points near 6285 Å. Comparison spectrum, hydrogen Geissler tube.

Fig. 2.

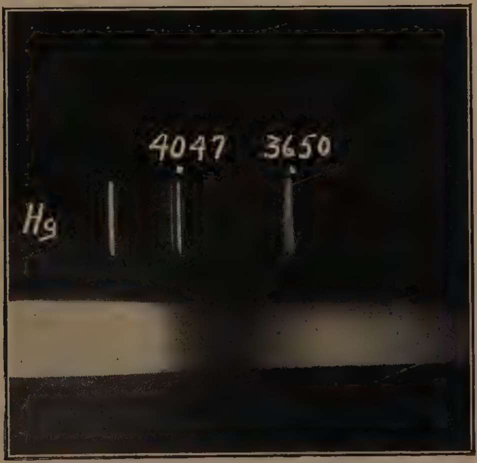

Spectrum showing absorption by $\alpha$—$NiSO_4.6H_2O$ around 3850 Å. Comparison spectrum, mercury arc.

# XXIV. *The Thermodynamic Functions for a Fermi-Dirac Gas.*

By Edmund C. Stoner, Sc.D., F.R.S.,
Reader in Physics at the University of Leeds *.

[Received June 16, 1939.]

## 1. *Introduction.*

The results of a statistical mechanical treatment of any material system are generally most usefully presented by means of expressions for the more familiar thermodynamic functions for the system, as functions of appropriate variables, and in forms such that numerical calculations may be made without undue difficulty. Once this has been done, use may be made of the various thermodynamic relations in the derivation of theoretical values for quantities which are convenient for direct experimental determination. In this paper the thermodynamic functions for an ideal Fermi-Dirac gas will be considered. Particular expressions for some of these functions, appropriate when either the quasi-classical " high temperature " limit or the completely degenerate " low temperature " limit is approached, have frequently been given. A much more complete treatment is now possible through the evaluation of the basic Fermi-Dirac integrals associated with a standard energy distribution of states (McDougall and Stoner, 1938). Since the basic integrals can now be regarded as known functions, general expressions involving them become satisfactory from a numerical as well as from a formal standpoint. Further, accurate numerical determinations of the values of the various thermodynamic functions can be made for the whole temperature range.

Tables, such as are given in this paper, of the numerical values of the various thermodynamic functions for a Fermi-Dirac gas, effectively covering a wide range of temperature, have a direct practical utility in connexion with electrons in metals, provided that the form of the distribution of states approximates to that for free electrons, and also in connexion with stellar material in a highly ionized state. For ordinary gases the numerical tables are of limited utility, for whether the gases are subject to Fermi-Dirac or Bose-Einstein statistics, the conditions are usually such that the approximations provided by the quasi-classical limiting forms are adequate. Even here, however, it is of considerable interest to examine the character of the temperature variation of the thermodynamic functions in the low temperature range, for the quasi-classical approximations necessarily give no indication of the behaviour as the low temperature limit is approached. Such an examination, moreover, is not without value in clearing up the confusion which is frequently felt about thermodynamic functions, particularly in connexion with such questions as those relating to the bearing of Nernst's heat theorem.

---

* Communicated by the Author.

The temperature variation of the internal energy, E, has previously been treated with reasonable numerical completeness for the whole temperature range, the calculations having an immediate practical bearing in connexion with electronic specific heat (Stoner, 1938 *a*). Owing to the simple relation between the energy and the product of the pressure and volume, the determination of the entropy, S, as a function of temperature, is then sufficient to enable the other usual functions, the Helmholtz free energy, F, the total heat, H, and the Gibbs free energy, G, to be obtained.

In order to show clearly the significance of the functions which are considered, and also to simplify the utilization of the expressions and numerical results here given in connexion with the diverse formulations of the statistical scheme, a brief survey of the essential thermodynamic relations is first given, and a derivation of the statistical formulæ is outlined. Expressions for the thermodynamic functions are then obtained in forms involving directly or indirectly the basic integrals which have been evaluated. Series representations are given for the thermodynamic functions which are appropriate when the conditions approximate to those for the quasi-classical high temperature limit, or the completely degenerate low temperature limit. Where appropriate, numerical values are given for the coefficients in these series to facilitate numerical computations. Numerical tables are provided to cover the intermediate range with adequate accuracy for most practical applications. Finally, a brief discussion is given of the relations between the Fermi-Dirac and Maxwell-Boltzmann functions, and some of the points arising in their application are considered.

## 2. *Thermodynamic Functions.*

In this section a summary is given of the defining equations of the more useful thermodynamic functions, and some of the relations between them are indicated, with a view to showing clearly the status of the functions. One of the questions discussed is that of the completeness of the information about a system conveyed by expressions for these functions in terms of different variables. Reference may be made to a Progress Report by Awbery (1938) for a good general survey, and to Guggenheim's 'Modern Thermodynamics' (1933) for a fuller treatment of the properties of the basic functions. The symbols recommended in the Report of the Joint Committee of the Chemical, Faraday and Physical Societies (1937) are adopted as far as possible, though the second preferences E and F for internal energy and Helmholtz free energy are used rather than the first preferences U and A.

For a given system, the internal energy, E, may be defined, apart from an additive constant depending on the chosen standard state of reference from which energy is to be measured, by the equation

$$\delta \mathrm{E}=\delta q+\delta w, \quad \quad (2.1)$$

where $\delta q$ is the heat entering the system, $\delta w$ the work done on the system by its surroundings ; or, in the differential form for a limiting process,

$$d\mathrm{E}=dq+dw. \quad \quad (2.2)$$

The work term may be written

$$dw=-\Sigma \mathrm{X}_i\, dx_i, \quad \quad (2.3)$$

where $\mathrm{X}_i$, $x_i$ represent a generalized force and the corresponding co-ordinate, this reducing, when the only forces to which the system is subjected are those arising from a uniform pressure, to

$$dw=-\mathrm{P}d\mathrm{V}, \quad \quad (2.4)$$

where P, V are the pressure and volume.

The function, E, defined by (2.2), is referred to as internal or intrinsic energy, and also as total energy. This last designation is equally appropriate when the work term is of the type (2.4), but when there are forces due to external fields, so that the energy is in part mutual potential energy of the particular system under consideration and other systems, it may be convenient to use the terms internal and total energy to distinguish different energy functions which may usefully be defined for the particular system (*cf.* Stoner, 1935, 1937). Although mention of this possible distinction is not strictly relevant to the present paper, which is concerned exclusively with functions associated with a work term of the type (2.4), it is relevant to the consideration of systems in electric and magnetic fields, to which some of the most important applications of Fermi-Dirac statistics are made.

The equation (2.2) is an expression of the first law of thermodynamics. It is to be noted that changes in E are determinable very directly from experiment through the measurement of heat and work. The second law may be expressed by the equation

$$dq \leq \mathrm{T}d\mathrm{S}, \quad \quad (2.5)$$

where T is the absolute temperature, S the entropy, and the equality sign applies to reversible changes. The equation for reversible changes provides a definition of the entropy function, S, again apart from an additive constant. The equation also provides a means of obtaining an absolute temperature scale.

For reversible changes in a system of constant composition, where the work term is given by (2.3), the basic equation (2.1) becomes

$$dE = TdS - PdV.$$

To incorporate the effect of changes of composition a further term is necessary, the more general equation being

$$dE = TdS - PdV + \Sigma \mu_i dn_i, \qquad \ldots\ldots\ldots \qquad (2.6)$$

where $n_i$ is the number of units of quantity of the chemical species $i$, and

$$\mu_i = (\partial E / \partial n_i)_{s,\,v,\,n_j}$$

is the chemical potential of the species $i$, referred to the chosen unit of quantity.

The formal relations between the four usual thermodynamic functions, the internal energy, E, the total heat, H, the Helmholtz free energy, F, and the Gibbs free energy, G, are shown by the following equations :

$$\begin{array}{lll}
E, & dE = TdS - PdV\,; \quad \ldots\ldots & (2.7) \\
H = E + PV, & dH = TdS + VdP\,; \quad \ldots\ldots & (2.8) \\
F = E - TS, & dF = -SdT - PdV\,; \quad \ldots & (2.9) \\
G = F + PV, & dG = -SdT + VdP. \quad \ldots & (2.10)
\end{array}$$

The equations on the right are given in the form applicable to systems of fixed content. The more general forms are obtained by adding $\mu_i dn_i$ to the right-hand side of each, as in (2.6). By integration of (2.6), and use of (2.10), the result obtained, for a system containing a single chemical species, is

$$G = \mu n. \qquad \ldots\ldots\ldots\ldots \qquad (2.11)$$

If a molecular point of view is introduced, the unit of quantity may be chosen as the molecule, and $n$ is then the number of molecules in the system. Thus, the molecular chemical potential is equal to the Gibbs free energy per molecule. It will be shown below that a basic parameter in the statistical treatment is closely related to this molecular chemical potential.

From the equations (2.7) to (2.10) the various reciprocity relations may be at once obtained, and also the important Gibbs-Helmholtz relations :

$$E = -T^2 \frac{\partial}{\partial T} \left( \frac{F}{T} \right), \qquad \ldots\ldots\ldots \qquad (2.12)$$

$$H = -T^2 \frac{\partial}{\partial T^2} \left( \frac{G}{T} \right). \qquad \ldots\ldots\ldots \qquad (2.13)$$

It is unnecessary to consider these and other relations in detail or to discuss the part played by the functions in the treatment of equilibria under different conditions, but it is perhaps desirable to comment on the relation between the functions and experimentally determinable quantities, and also on the forms of expression for the functions which are practically convenient.

Differences in the values of E and H for two states are experimentally determinable from measurements on the heat and work input in changing from one state to the other. Reversibility of the change is not essential to the determination of the difference of energy in the two states, but if the change is irreversible difficulties arise in the precise specification of the states. It is sufficient here to consider only reversible changes. Measurements of the specific heat at constant volume, $C_V$, over a range of temperature, serve to give E (at constant volume) as a function of T, and similarly measurements of $C_P$ give H (at constant pressure) owing to the relations

$$C_V=(\partial E/\partial T)_V, \quad C_P=(\partial H/\partial T)_P. \quad . \quad . \quad . \quad (2.14)$$

Further experiments are necessary to determine the dependence of E on V, or of H on P, which may be of a somewhat elaborate character (*e. g.*, the porous plug experiment). The final result is that experimental expressions for E and H may be obtained in the forms

$$E=E(T, V)\,; \quad H=H(T, P). \quad . \quad . \quad . \quad . \quad . \quad (2.15)$$

Much of the " awkwardness " of thermodynamic functions seems to arise from just this circumstance, that the experimentally convenient variable T in the expressions for E and H differs from the theoretically appropriate variable S (see equations 2.7, 2.8). The fundamental equations (using " fundamental " in the Gibbs sense) are of the form

$$E=E(S, V)\,; \quad H=H(S, P), \quad . \quad . \quad . \quad . \quad . \quad (2.16)$$

and from these it would be possible to derive equations of the type (2.15); unique relations of the type (2.16) cannot, however, be derived from those of (2.15). A discussion of this question was given by Gibbs (1875). Since relations involving S explicitly would be inconvenient, the usual procedure is to develop as fundamental equations those for F or G in the forms

$$F=F(T, V)\,; \quad G=G(T, P). \quad . \quad . \quad . \quad . \quad . \quad . \quad (2.17)$$

By integration of the equations

$$(\partial S/\partial T)_V=C_V/T, \quad (\partial S/\partial T)_P=C_P/T, \quad . \quad . \quad . \quad . \quad (2.18)$$

and equations involving V and P as variables, expressions for S may be obtained. These necessarily include an additive constant, $S_0$, referring to the (indeterminate) entropy in some chosen standard state. They may be used in conjunction with (2.15) in the construction of expressions for F and G in the fundamental form (2.17). These expressions include additive terms, essentially indeterminate, of the type $TS_0$ as well as $E_0$, where $S_0$, $E_0$ refer to the entropy and internal energy in the chosen standard state. Either of the equations (2.17) so obtained is fundamental in the sense that other functions may be derived from it. Thus, from F(T, V), from (2.9), S and P may be found, and the other functions, E, H, and G may be built up. In considering a single component, single phase system, the constants $E_0$ and $S_0$ may be assigned arbitrarily to the chosen standard state without affecting any experimentally significant conclusions which can be drawn from a thermodynamic treatment. Except for strictly independent systems, however, energy and entropy differences between chosen standard states are determinate, and may be physically significant in particular problems. This must be borne in mind in any assignment of constants; the constants assigned must be consistent with any relevant and in principle determinable energy and entropy differences.

One of the main purposes of this discussion has been to show how complete information about a thermodynamic system can be embodied in an expression for one or other of the four thermodynamic functions E, H, F, G, provided that the expression is in terms of appropriate variables—the variables indicated by (2.7) to (2.10). Thus a knowledge of the dependence of E on T and V provides important information about the properties of the system, but the information is necessarily incomplete. The information becomes complete if a knowledge of the dependence of S on T and V is also available. Complete information is provided by a knowledge of the dependence of F on T and V, and of the possible fundamental equations, that involving these relations is often the one which is most readily developed.

## 3. *Derivation of Statistical Formulæ.*

The derivation of the basic formulæ of Fermi-Dirac statistics is outlined in this section, partly for completeness, and partly to show clearly the relation between the general formulæ and those for the particular distribution of states subsequently considered. For further details reference may be made to accounts of Nordheim (1934), whose presentation is closely followed in the first part of the section, or of Wilson (1936), or, for treatments from a more fundamental quantum mechanical standpoint, to the treatises of Fowler (1936) and Tolman (1938).

It is required to find the most probable energy distribution of a system of $n$ similar particles, which are not individually distinguishable or localized, and which are subject to the Fermi-Dirac condition that there can be not more than one particle in a given quantum state. The particles are regarded as independent in the sense that the state of the system as a whole can be treated as derivable from the states for the individual particles. Instead of considering the distribution over individual quantum energy states, it is convenient to consider the distribution over small energy ranges 1, 2 . . $s$ . . . , the mean energy for the small range $s$ being denoted by $\epsilon_s$, and the number of distinct quantum states in the range by $a_s$. The condition of the system is specified by the numbers $n_1, n_2 \dots n_s \dots$ of particles in the ranges 1, 2 . . $s$ . . Since there cannot be more than one particle in each individual state, the number of arrangements of $n_s$ particles among $a_s$ states is the number of ways of selecting $n_s$ from $a_s$, that is

$$\frac{a_s\,!}{n_s\,!\,(a_s-n_s)\,!}.$$

Since the particles are indistinguishable, $n_s$ can be chosen from $n$ in only one way, and the total number of distinct arrangements (complexions) corresponding to the condition specified by $n_1, n_2 \dots n_s \dots$ is

$$W=\Pi\frac{a_s\,!}{n_s\,!\,(a_s-n_s)\,!}. \qquad (3.1)$$

(The number of " complexions " corresponds to the number of independent wave functions for the system as a whole.) The most probable distribution is obtained by making W, or more conveniently, log W, a maximum, subject to the subsidiary conditions, imposed by fixed values of the total number of particles and the total energy,

$$\Sigma n_s=n, \qquad (3.2)$$

$$\Sigma n_s\epsilon_s=E. \qquad (3.3)$$

These conditions give, for a variation in the numbers $n_s$,

$$\delta \log W=0, \qquad (3.4)$$

$$\Sigma\delta n_s=0, \qquad (3.5)$$

$$\Sigma\epsilon_s\delta n_s=0. \qquad (3.6)$$

By using undetermined multipliers, $\alpha$ and $\beta$ for the second and third of these equations, the equations combine to give

$$\delta \log W-\alpha\Sigma\delta n_s-\beta\Sigma\epsilon_s\delta n_s=0. \qquad (3.7)$$

Using the adequate approximation $\log n\,!=n\log n-n$ provided by Stirling's theorem,

$$\log W=\Sigma\left\{n_s\log\left(\frac{a_s}{n_s}-1\right)-a_s\log\left(1-\frac{n_s}{a_s}\right)\right\}, \qquad (3.8)$$

and

$$\delta \log W=\Sigma\log\left(\frac{a_s}{n_s}-1\right)\delta n_s.$$

Substituting in (3.7), the distribution expression is obtained in the form

$$n_s = a_s/(e^{\alpha+\beta\epsilon_s}+1). \qquad (3.9)$$

Substitution of (3.9) in (3.2) and (3.3) gives implicit equations for $\alpha$ and $\beta$ in terms of $n$ and E. Substituting for $(a_s/n_s)$ in (3.8), the value of W corresponding to the most probable distribution, which will be denoted by $W_e$, the subscript connoting the equilibrium state, is given by

$$\log W_e = \Sigma\{n_s(\alpha+\beta\epsilon_s)+a_s \log(1+e^{-\alpha-\beta\epsilon_s})\}. \qquad (3.10)$$

The connexion with thermodynamics may be made by considering the statistical expression for the change of energy of the system in the form

$$\delta E = \Sigma\epsilon_s\delta n_s + \Sigma n_s\delta\epsilon_s. \qquad (3.11)$$

The first and second terms on the right may be shown to be identifiable with the heat and work terms $\delta q$ and $\delta w$ of (2.1). For passage through a series of equilibrium states (*i. e.*, for reversible changes) from (3.10), using (3.9),

$$\delta \log W_e = \beta\Sigma\epsilon_s\delta n_s. \qquad (3.12)$$

Under the same conditions,

$$\delta q = \Sigma\epsilon_s\delta n_s = T\delta S, \qquad (3.13)$$

giving, with (3.12),

$$T\delta S = \frac{1}{\beta}\,\delta \log W_e. \qquad (3.14)$$

The relation (3.14) is satisfied by

$$\beta = 1/kT, \qquad (3.15)$$

$$S = k \log W_e + S_0, \qquad (3.16)$$

where $k$ is a constant identifiable with Boltzmann's constant when temperature is measured on the absolute scale. The constant $S_0$ may be regarded as such that $S_0/k$ gives the logarithm of the number of microscopic states (complexions) for the system when $W_e=1$, that is, of states additional to those explicitly considered in the treatment. It is usually permissible to put $S_0=0$, provided that there is adequate reason to assume that such additional states are irrelevant to the physical situation under consideration. This assumption will be made in the further treatment. The equation (3.16) gives a statistical interpretation of entropy which is in strict accordance with the thermodynamic definition. It is to be noted that $W_e$ refers to an equilibrium state. A procedure sometimes followed is to use the equation

$$S = k \log W \qquad (3.17)$$

without, or with, an additive constant $S_0$, as a statistical definition of entropy, applicable to non-equilibrium as well as to equilibrium states.

This may be convenient, and it seems unobjectionable provided that the distinction is borne in mind between the entropy of the purely statistical definition (3.17) and the entropy of thermodynamics, interpreted by (3.16).

It is convenient to introduce a symbol for the sum over states in (3.10) by writing

$$Z=\Sigma a_s \log\left(1+e^{-\alpha-\beta\epsilon_s}\right). \quad . \quad . \quad . \quad . \quad . \quad . \quad . \qquad (3.18)$$

This function plays a part similar to that of the partition functions of classical statistics, and extensive use is sometimes made of it in applications, with little reference to the usual thermodynamic functions. (A function $\Omega$ which has sometimes been used is related by Z by $\Omega=-k\mathrm{TZ}$.) This procedure has the disadvantage of obscuring the treatment by inessential complications, owing to the unusual appearance of relations, whose equivalents, as thermodynamic relations, are relatively familiar. It seems preferable, for most purposes, to utilize the function Z mainly as a convenient intermediary in building up the more usual functions. The function Z has the easily verified properties

$$n=-\partial Z/\partial\alpha, \quad . \quad . \quad . \quad . \quad . \quad . \quad . \quad . \quad . \qquad (3.19)$$

$$X_i=k\mathrm{T}\,\partial Z/\partial x_i, \quad . \quad . \quad . \quad . \quad . \quad . \quad . \quad . \qquad (3.20)$$

where $X_i$, $x_i$ have the same significance as in (2.3), and in particular,

$$P=k\mathrm{T}\,\partial Z/\partial V. \quad . \quad . \quad . \quad . \quad . \quad . \quad . \quad . \quad . \qquad (3.21)$$

By the use of equations (9), (10), (15), (16), and (18) of this section, the following expressions for thermodynamic functions are readily obtained :

$$S/k=n\alpha+E/k\mathrm{T}+Z\,; \quad . \quad . \quad . \quad . \quad . \quad . \quad . \qquad (3.22)$$

$$F=-k\mathrm{T}(n\alpha+Z). \quad . \quad . \quad . \quad . \quad . \quad . \quad . \qquad (3.23)$$

The sum over states Z is a function of $\alpha$ and $\beta$ (or of T, by (3.15)) and also, for the type of system under consideration in this paper, of V, being linear in this variable (see next section). The operation $V(\partial/\partial V)$ on Z then reproduces Z, and making use of this and of (3.19), the simple relation between the Gibbs free energy, G, and the statistical parameter $\alpha$ may be obtained as follows :

$$\left.\begin{aligned} G&=F+PV=F-V(\partial F/\partial V)_T\\ &=-k\mathrm{T}(\alpha n+Z)+k\mathrm{TV}\left\{n\frac{\partial\alpha}{\partial V}+\frac{\partial Z}{\partial\alpha}\frac{\partial\alpha}{\partial V}+\frac{\partial Z}{\partial V}\right\}\\ &=-nk\mathrm{T}\alpha. \end{aligned}\right\} \quad . \quad . \qquad (3.24)$$

The parameter $\alpha$ is, therefore, simply related to the chemical potential per particle, for, using (2.11),

$$\mu=-k\mathrm{T}\alpha. \quad . \quad . \quad . \quad . \quad . \quad . \quad . \quad . \qquad (3.25)$$

This result may also be derived from (3.23) by using the relation $\mu=(\partial F/\partial n)_{T,V}$. By applying the Gibbs-Helmholtz relations (2.12), (2.13), to (3.23) and (3.24), expressions for E and H may be obtained in a form which is useful when the treatment is based on the use of the function Z.

The formulæ obtained in this section are not specific to any particular energy distribution of states. They are not all completely general, as the effect of external fields has not been explicitly considered. The necessary extensions could, however, be developed without difficulty. In practical applications a particular energy distribution of states has necessarily to be considered. Formulæ applicable to a basic type of distribution are developed in the next section.

## 4. *Thermodynamic Functions for a Fermi-Dirac Gas in Terms of Basic Integrals.*

For the quasi-continuous distribution of states characteristic of a system of particles in a finite volume, when the number and density of particles is large, the sums in the formulæ of § 3 may justifiably and conveniently be replaced by integrals. Denoting the number of states per unit energy range by $\nu(\epsilon)$, the number of states and the number of particles in a small energy range $\delta\epsilon$, previously denoted by $a_s$ and $n_s$, are expressed by

$$a_s=\nu(\epsilon)\delta\epsilon, \quad n_s=(dn/d\epsilon)\delta\epsilon, \quad . \quad . \quad . \quad . \quad . \quad . \quad . \quad (4.1)$$

$\nu(\epsilon)$ and $dn/d\epsilon$ having the values appropriate to $\epsilon=\epsilon_s$. It seems appropriate in the sequel to use N in place of $n$ for the total number of particles, to convey that this is the number associated with the volume, V, energy, E, etc. The distribution expression (3.9) then takes the form

$$dN/d\epsilon=\nu(\epsilon)/(e^{\alpha+\epsilon/kT}+1), \quad . \quad . \quad . \quad . \quad . \quad . \quad . \quad (4.2)$$

and the sum over states (3.18) is transformed into an integral,

$$Z=\int_0^\infty \nu(\epsilon)\log\{1+e^{-\alpha-\epsilon/kT}\}d\epsilon. \quad . \quad . \quad . \quad . \quad . \quad . \quad . \quad (4.3)$$

For the type of system considered, the usual treatment gives as the number of particle states in the momentum range $p$ to $p+dp$

$$4\pi(g/h^3)Vp^2dp,$$

where $g$ is the statistical weight of a given momentum state, that is the number of distinct particle states associated with a given value of $p$. (For electrons, $g=2$, corresponding to the two spin directions.) If the energy is purely kinetic,

$$\epsilon=p^2/2m, \quad . \quad . \quad . \quad . \quad . \quad . \quad . \quad . \quad . \quad . \quad (4.4)$$

giving

$$\nu(\epsilon)=2\pi(g/h^3)V(2m)^{3/2}\epsilon^{1/2}. \quad . \quad . \quad . \quad . \quad . \quad (4.5)$$

It may be noted here that a distribution of states in which the energy density of states is proportional to the square root of the energy is not exclusively characteristic of the energy relation (4.4), which holds when the energy is purely kinetic, though it is this which is to be primarily considered here. Many of the expressions to be given, however, will be in such a form as to be applicable to a wider range of physical situations than those covered by the particular coefficient of (4.5).

When Fermi-Dirac statistics is applicable, in the lowest energy state of the system there will be one particle in each of the lowest particle energy states. The maximum particle energy, under these conditions, will be denoted by $\epsilon_0$, the energy corresponding to the top of the Fermi distribution at absolute zero. The number of particles is thus equal to the number of states up to $\epsilon_0$:

$$\mathrm{N}=2\pi(g/h^3)\mathrm{V}(2m)^{3/2}\int_0^{\epsilon_0}\epsilon^{1/2}d\epsilon, \quad . \quad . \quad . \quad . \quad . \quad (4.6)$$

giving

$$\epsilon_0=\frac{h^2}{2m}\left(\frac{3\mathrm{N}}{4\pi g\mathrm{V}}\right)^{2/3}. \quad . \quad . \quad . \quad . \quad . \quad . \quad . \quad . \quad (4.7)$$

It is often convenient to use $\epsilon_0$ as an abbreviation for the expression of the right. The expression (4.5) for the distribution of states then becomes

$$\nu(\epsilon)=\tfrac{3}{2}\mathrm{N}(\epsilon^{1/2}/\epsilon_0^{3/2}). \quad . \quad . \quad . \quad . \quad . \quad . \quad . \quad . \quad (4.8)$$

It is to be noted that, for given N, $\mathrm{V}\epsilon_0^{3/2}$ is a constant. The distribution expression (4.2) may be written

$$\frac{d\mathrm{N}}{d\epsilon}=\frac{\tfrac{3}{2}\mathrm{N}(\epsilon^{1/2}/\epsilon_0^{3/2})}{e^{\alpha+\epsilon\mathrm{T}/k}+1}. \quad . \quad . \quad . \quad . \quad . \quad . \quad . \quad . \quad (4.9)$$

Writing

$$x=\epsilon/k\mathrm{T}, \quad . \quad . \quad . \quad . \quad . \quad . \quad . \quad . \quad . \quad . \quad (4.10)$$

$$\eta=-\alpha, \quad . \quad . \quad . \quad . \quad . \quad . \quad . \quad . \quad . \quad . \quad (4.11)$$

integration of (4.9) gives

$$\begin{aligned}\mathrm{N}&=\frac{3}{2}\mathrm{N}\left(\frac{k\mathrm{T}}{\epsilon_0}\right)^{3/2}\int_0^{\infty}\frac{x^{1/2}dx}{e^{x-\eta}+1},\\ &=\frac{3}{2}\mathrm{N}\left(\frac{k\mathrm{T}}{\epsilon_0}\right)^{3/2}\mathrm{F}_{1/2}(\eta). \quad . \quad . \quad . \quad . \quad . \quad . \quad . \quad (4.12)\end{aligned}$$

The retention of N on both sides in (4.12) is unnecessary, but it serves to keep clear the physical content of the equation. Using (4.9), (4.10), and (4.11), a corresponding expression for the total energy, E, may be obtained:

$$\begin{aligned}\mathrm{E}&=\int_0^{\infty}\epsilon\frac{d\mathrm{N}}{d\epsilon}d\epsilon=\frac{3}{2}\mathrm{N}\left(\frac{k\mathrm{T}}{\epsilon_0}\right)^{3/2}k\mathrm{T}\int_0^{\infty}\frac{x^{3/2}dx}{e^{x-\eta}+1},\\ &=\frac{3}{2}\mathrm{N}k\mathrm{T}\left(\frac{k\mathrm{T}}{\epsilon_0}\right)^{3/2}\mathrm{F}_{3/2}(\eta)\,; \quad . \quad . \quad . \quad . \quad . \quad . \quad . \quad . \quad (4.13)\end{aligned}$$

$$\mathrm{E}/\mathrm{N}k\mathrm{T}=\mathrm{F}_{3/2}(\eta)/\mathrm{F}_{1/2}(\eta). \quad . \quad . \quad . \quad . \quad . \quad . \quad (4.14)$$

For the functions $F_{1/2}(\eta)$, $F_{3/2}(\eta)$, which are members of the class

$$F_k(\eta)=\int_0^\infty \frac{x^k dx}{e^{x-\eta}+1}, \quad . \quad . \quad . \quad . \quad . \quad . \quad . \quad (4.15)$$

representations are obtainable in the form of convergent series for the range $\eta<0$ (corresponding, approximately, to $kT/\epsilon_0>1$), and in the form of asymptotic series expansions, first given by Sommerfeld, for the range $\eta \gg 1$ (corresponding to $\epsilon_0/kT \gg 1$). Numerical tables of $F_{3/2}(\eta)$, $F_{1/2}(\eta)$, and also of the derivatives $F'_{1/2}(\eta)$, $F''_{1/2}(\eta)$, and $F'''_{1/2}(\eta)$ covering the range $-4{\cdot}0 \leqslant \eta \leqslant +20{\cdot}0$, at intervals of $0{\cdot}1$ in $\eta$, have been given by McDougall and Stoner (1938), who also discuss the series representations and the general properties of the functions. Among these general properties, one of the most important is the recurrence relation,

$$\frac{d}{d\eta}F_k(\eta)=F'_k(\eta)=kF_{k-1}(\eta),$$

giving, in particular,

$$\frac{d}{d\eta}F_{3/2}(\eta)=F'_{3/2}(\eta)=\tfrac{3}{2}F_{1/2}(\eta). \quad . \quad . \quad . \quad . \quad . \quad . \quad (4.16)$$

In view of the fact that $F_{3/2}(\eta)$ and $F_{1/2}(\eta)$ and its derivatives are now "known" functions, it becomes appropriate to express the various thermodynamic functions, as well as functions developed in the course of the statistical treatment, as far as possible in terms of them. Owing to their frequent occurrence it will often be convenient, in the sequel, to omit the argument $\eta$, and to write

$$F_k=F_k(\eta),\ F'_k=\frac{d}{d\eta}F_k(\eta),\ \text{etc.}$$

For a proper understanding of the procedure in dealing with thermodynamic functions, a clear appreciation is necessary of the variables involved in equations such as (4.12), (4.13), (4.14). The basic equation leading to the expression of $\eta$ and the relevant $F_k(\eta)$ in terms of the usual thermodynamic variables is (4.12), $\epsilon_0$ being given by (4.7) :

$$F_{1/2}(\eta)=\frac{2}{3}\left(\frac{\epsilon_0}{kT}\right)^{3/2}=\frac{1}{2\pi g}\cdot\frac{h^3}{(2mk)^{3/2}}\cdot\frac{N}{VT^{3/2}}. \quad . \quad . \quad (4.17)$$

This provides an implicit equation for $\eta$ in the form

$$\eta=\eta(\epsilon_0/kT)=\eta(N,\ T,\ V). \quad . \quad . \quad . \quad . \quad . \quad . \quad . \quad (4.18)$$

Convenient expressions, giving $\eta$ as an explicit function of N, T, V, are obtainable only for $\eta<0$ and $\eta \gg 1$. The generally applicable method for the determination of $\eta$, given N, T, V, is to use (4.17) to calculate $\epsilon_0/kT$ and hence $F_{1/2}(\eta)$, and then to find $\eta$ by inverse interpolation in the $\eta$, $F_{1/2}(\eta)$ tables. From (4.18) it follows that E, in (4.14), is in the form

$$E=E(N,\ T,\ V). \quad . \quad . \quad . \quad . \quad . \quad . \quad . \quad . \quad (4.19)$$

Owing to the manner in which N, T, and V enter into the functional relations, it is generally convenient to obtain the various thermodynamic functions, in suitably reduced form, as functions of $k\mathrm{T}/\epsilon_0$, this resulting in a considerable abbreviation in the presentation of essential results. Thus, from (4.14), either $\mathrm{E}/\mathrm{N}\epsilon_0$ or $\mathrm{E}/\mathrm{N}k\mathrm{T}$ may be treated in this way. In a previous paper (Stoner, 1938*a*) numerical tables of $\mathrm{E}/\mathrm{N}\epsilon_0$ as a function of $k\mathrm{T}/\epsilon_0$ have been given. Owing to the form (4.19) for E, as shown by the discussion in § 2, these tables do not provide complete information about the thermodynamic properties of the system, for which further information, such as is provided by a knowledge of the entropy, S, as S(N, T, V) is needed. For the derivation of suitable expressions for S, as well as for the other thermodynamic functions, it is convenient to obtain first an expression for the sum over states, Z, in terms of the known functions $\mathrm{F}_k(\eta)$.

Substituting for $\nu(\epsilon)$ from (4.8) in the expression (4.3) for the sum over states, Z, and using (4.10), (4.11), and (4.15),

$$\mathrm{Z}=\frac{3}{2}\mathrm{N}\left(\frac{k\mathrm{T}}{\epsilon_0}\right)^{3/2}\int_0^\infty x^{1/2}\log\,(1+e)^{\eta-x}\,dx.$$

By partial integration,

$$\int_0^\infty=\left|\tfrac{2}{3}x^{3/2}\log\,(1+e)^{\eta-x}\right|_0^\infty+\int_0^\infty\frac{\tfrac{2}{3}x^{3/2}e^{\eta-x}}{1+e^{\eta-x}}\,dx,$$

so that, since the integrated part is zero at both limits,

$$\mathrm{Z}=\mathrm{N}\left(\frac{k\mathrm{T}}{\epsilon_0}\right)^{3/2}\mathrm{F}_{3/2}(\eta)=\tfrac{2}{3}\mathrm{N}\mathrm{F}_{3/2}(\eta)/\mathrm{F}_{1/2}(\eta). \quad . \quad . \quad . \quad (4.20)$$

An expression for the entropy, S, follows from (3.22), using (4.14) :

$$\left.\begin{aligned}\mathrm{S}/\mathrm{N}k&=\alpha+\mathrm{E}/\mathrm{N}k\mathrm{T}+\mathrm{Z}/\mathrm{N},\\&=\tfrac{5}{3}(\mathrm{F}_{3/2}/\mathrm{F}_{1/2})-\eta.\end{aligned}\right\} \quad . \quad . \quad . \quad . \quad . \quad . \quad (4.21)$$

For the Helmholtz free energy, F, using (2.9), (4.14), and (4.22), or more directly from (3.23) and (4.22),

$$\mathrm{F}/\mathrm{N}k\mathrm{T}=\eta-\tfrac{2}{3}(\mathrm{F}_{3/2}/\mathrm{F}_{1/2}). \quad . \quad . \quad . \quad . \quad . \quad . \quad (4.22)$$

In view of (4.19) and (4.20) this equation for F is in the fundamental form, and expressions for all the other thermodynamic functions may be derived from it. When the energy is purely kinetic the pressure will be two-thirds of the total energy density, as may be shown by simple considerations, such as by an application of the virial method. To illustrate the manipulation of the Fermi-Dirac functions, this result will be derived here from the relation between pressure and free energy. From (2.9) and (4.22),

$$\frac{\mathrm{P}}{\mathrm{N}k\mathrm{T}}=-\frac{1}{\mathrm{N}k\mathrm{T}}\left(\frac{\partial\mathrm{F}}{\partial\mathrm{V}}\right)_{\mathrm{T}}=-\frac{\partial\eta}{\partial\mathrm{V}}+\frac{2}{3}\cdot\frac{1}{\mathrm{F}_{1/2}^2}\left\{\mathrm{F}_{1/2}\frac{\partial\mathrm{F}_{3/2}}{\partial\mathrm{V}}-\mathrm{F}_{3/2}\frac{\partial\mathrm{F}_{1/2}}{\partial\mathrm{V}}\right\},$$

Using (4.16) and (4.17),

$$\frac{\mathrm{P}}{\mathrm{N}k\mathrm{T}}=-\frac{\partial\eta}{\partial\mathrm{V}}+\frac{2}{3}\cdot\frac{1}{\mathrm{F}_{1/2}^{2}}\cdot\frac{3}{2}\mathrm{F}_{1/2}^{2}\frac{\partial\eta}{\partial\mathrm{V}}+\frac{2}{3}\cdot\frac{1}{\mathrm{F}_{1/2}^{2}}\cdot\frac{\mathrm{F}_{3/2}\,.\,\mathrm{F}_{1/2}}{\mathrm{V}},$$

giving

$$\mathrm{PV}=\tfrac{2}{3}\mathrm{N}k\mathrm{T}(\mathrm{F}_{3/2}/\mathrm{F}_{1/2})=\tfrac{2}{3}\mathrm{E}. \quad \ldots\ldots \quad (4.23)$$

Expressions for the total heat, H, and the Gibbs free energy, G, may now at once be obtained, using (2.8), (4.14), (4.23), and (2.10), (4.22), (4.23), respectively :

$$\mathrm{H}/\mathrm{N}k\mathrm{T}=(\mathrm{E}+\mathrm{PV})/\mathrm{N}k\mathrm{T}=\tfrac{5}{3}(\mathrm{F}_{3/2}/\mathrm{F}_{1/2}), \quad \ldots\ldots \quad (4.24)$$

$$\mathrm{G}/\mathrm{N}k\mathrm{T}=(\mathrm{F}+\mathrm{PV})/\mathrm{N}k\mathrm{T}=\eta. \quad \ldots\ldots \quad (4.25)$$

Neither of the relations (4.24), (4.25) is in the fundamental form, since H is effectively expressed in terms of T and V rather than of S and P, and G in terms of T and V rather than of T and P. Although it would be possible, in principle, to obtain formal expressions for E, H, and G in terms of variables appropriate to the fundamental relations, these expressions would be extremely cumbersome (except in the limiting cases), and little useful purpose would be served by considering them in detail in view of the fact that all the essential thermodynamic relations are implicit in (4.22), which gives an expression in fundamental form for the Helmholtz free energy, F.

The formulæ obtained in this section are sufficient for a complete numerical treatment of the thermodynamic functions of a Fermi-Dirac gas, for which results adequate for most purposes are given in the Tables of § 7. The essential characteristics of the functions are, however, made more clear by the explicit expressions which can be obtained for them when the quasi-classical and completely degenerate limits are approached. These expressions will be considered in the next two sections.

## 5. *Series Expansions for Low Temperatures*, $k\mathrm{T}/\epsilon_0 \ll 1$.

The series expansions appropriate for low temperatures are derived from the asymptotic series expansions for the functions $\mathrm{F}_k(\eta)$ for $\eta \gg 1$. These series have been fully discussed previously (McDougall and Stoner, 1938), and it is sufficient to give here the leading terms in the series for $k=1/2$, $k=3/2$.

$\underline{\eta \gg 1.}$

$$\mathrm{F}_{1/2}(\eta)=\frac{2}{3}\eta^{3/2}\left\{1+\frac{\pi^2}{8}\eta^{-2}+\frac{7\pi^4}{640}\eta^{-4}\ldots.\right\}; \quad \ldots \quad (5.1)$$

$$\mathrm{F}_{3/2}(\eta=\frac{2}{5}\eta^{5/2}\left\{1+\frac{5\pi^2}{8}\eta^{-2}-\frac{7\pi^4}{384}\eta^{-4}\ldots.\right\}. \quad \ldots \quad (5.2)$$

The most generally useful approximations are obtained by the retention of terms corresponding to those included in the above expressions. The following abbreviations, the first from (4.7), will be used :

$$\epsilon_0=\frac{h^2}{2m}\left(\frac{3\mathrm{N}}{4\pi g\mathrm{V}}\right)^{2/3} ; \quad . \; . \; . \; . \; . \; . \; . \; . \quad (5.3)$$

$$k\mathrm{T}/\epsilon_0=\mathrm{T}/\theta_{\mathrm{F}}=\tau. \quad . \; . \; , \; . \; . \; . \; . \; . \; . \; . \quad (5.4)$$

Here $\theta_{\mathrm{F}}$ (sometimes loosely referred to as the " degeneracy temperature ") is a Fermi-Dirac characteristic temperature (playing a part analogous to that of $\theta_{\mathrm{D}}$ in the Debye theory of specific heats) and $\tau$ a " reduced " temperature. From (4.17) and (5.4),

$$\mathrm{F}_{1/2}(\eta)=\tfrac{2}{3}(\epsilon_0/k\mathrm{T})^{3/2}=\tfrac{2}{3}\tau^{-3/2}. \quad . \; . \; . \; . \; . \; . \; . \quad (5.5)$$

Using this, the inverse series for $\eta$ from (5.1) takes the form

$$\eta=\frac{1}{\tau}\left\{1-\frac{\pi^2}{12}\tau^2-\frac{\pi^4}{80}\tau^4\ldots\right\}. \quad . \; . \; . \; . \; . \; . \quad (5.6)$$

By manipulation of the expressions (5.1), (5.2), and (5.6), series expressions may be obtained for the various thermodynamic functions in the low temperature range from the formulæ in § 4. These expressions are collected below. In this range it is convenient to consider the expressions for energy in the reduced form obtained by division by $\mathrm{N}\epsilon_0$ rather than by $\mathrm{N}k\mathrm{T}$.

$$\underline{\tau=(k\mathrm{T}/\epsilon_0)=(2mk\mathrm{T}/h^2)(4\pi g\mathrm{V}/3\mathrm{N})^{2/3}\leqslant 1.}$$

$$\mathrm{E}/\mathrm{N}\epsilon_0=(3/5)\ \{1+(5\pi^2/12)\tau^2-(\pi^4/16)\tau^4\} ; \quad . \; . \; . \quad (5.7)$$

$$\mathrm{H}/\mathrm{N}\epsilon_0=\{1+(5\pi^2/12)\tau^2-(\pi^4/16)\tau^4\} ; \quad . \; . \; . \quad (5.8)$$

$$\mathrm{F}/\mathrm{N}\epsilon_0=(3/5)\ \{1-(5\pi^2/12)\tau^2+(\pi^4/48)\tau^4\} ; \quad . \; . \; . \quad (5.9)$$

$$\mathrm{G}/\mathrm{N}\epsilon_0=\{1-(\pi^2/12)\tau^2-(\pi^4/80)\tau^4\} ; \quad . \; . \; . \quad (5.10)$$

$$\mathrm{PV}/\mathrm{N}\epsilon_0=(2/5)\ \{1+(5\pi^2/12)\tau^2-(\pi^4/16)\tau^4\} ; \quad . \; . \; . \quad (5.11)$$

$$\mathrm{S}/\mathrm{N}k=(\pi^2/2)\tau-(\pi^4/20)\tau^3 ; \quad . \; . \; . \; . \; . \; . \; . \; . \; . \; . \quad (5.12)$$

$$\mathrm{TS}/\mathrm{N}\epsilon_0=(\pi^2/2)\tau^2-(\pi^4/20)\tau^4. \quad . \; . \; . \; . \; . \; . \; . \; . \; . \quad (5.13)$$

The thermodynamic functions are here all expressed effectively as functions of N, T, V. Of the four functions E, H, F, G, it is only F which is expressed in fundamental form. The Gibbs-Helmholtz relation (2.12) between E and F is readily verified, but the verification of the relation between H and G is more troublesome owing to the fact that in (2.13) the partial differentiation is to be carried out with respect to P constant. In view of its fundamental form, it is perhaps desirable to give an explicit expression for F in terms of N, T, V. It is sufficient to give the series as far as the term in $T^2$:

$$F=\frac{3}{5}\left(\frac{h^2}{2m}\right)\left(\frac{3}{4\pi g}\right)^{2/3}N\left(\frac{N}{V}\right)^{2/3}\left[1-\frac{5\pi^2}{12}\right.$$
$$\left.\times\left\{\left(\frac{2mk}{h^2}\right)\left(\frac{4\pi g}{3}\right)^{2/3}\right\}^2\left\{T\left(\frac{V}{N}\right)^{2/3}\right\}^2+\ldots\right]. \quad . \quad (5.14)$$

By differentiation, using $P=-\partial F/\partial V$, or from (5.11), an expression for P is obtained:

$$P=\frac{2}{5}\left(\frac{h^2}{2m}\right)\left(\frac{3}{4\pi g}\right)^{2/3}\left(\frac{N}{V}\right)^{5/3}\left[1+\frac{5\pi^2}{12}\right.$$
$$\left.\times\left\{\left(\frac{2mk}{h^2}\right)\left(\frac{4\pi g}{3}\right)^{2/3}\right\}^2\left\{T\left(\frac{V}{N}\right)^{2/3}\right\}^2-\ldots\right]. \quad . \quad (5.15)$$

This expression gives one form of the equation of state of a Fermi-Dirac gas at low temperatures. (Extensive use has been made of the approximation provided by the first term of the series in the theoretical treatment of the pressure density relations in highly ionized stellar material.) By inversion of the series an expression for V as V(N, T, P) may be obtained, and substitution in (5.10) will then give G in the fundamental G(N, T, P) form. By suitable manipulation of the various series, E and H may also be obtained in the forms E(N, S, V) and H(N, S, P). It is unnecessary to give the expressions *in extenso*, as they can be readily derived, if required, and they provide no further information about the system than is contained in (5.14).

The numerical coefficients in the series (5.7) to (5.13) can be obtained from the following values:—

$$\pi^2/12=0{\cdot}822\ 467, \qquad \pi^4/80=1{\cdot}217\ 614.$$

Numerical values for factors involving physical constants will be given in § 7. The accuracy obtainable by the use of these low temperature asymptotic series has been fully considered previously in connexion with the series (5.7) for E (Stoner, 1938 *a*). With the three term series, the error is within 0·005 per cent. up to $\tau=0{\cdot}1$, 0·2 per cent. up to $\tau=0{\cdot}2$, and 1 per cent. up to $\tau=0{\cdot}3$. The uncertainties with the other series will be of the same order. In view of the high accuracy obtainable from the series expansions for small values of $\tau$, and their convenience, it is clearly advantageous to make numerical calculations by means of them rather than by the use of the Fermi-Dirac function tables in this range.

## 6. *Series Expansions for High Temperatures*, $kT/\epsilon_0>1$.

The series expansions appropriate for high temperatures are derived from the series expansions for the functions $F_k(\eta)$ for $\eta<0$,

$$F_k(\eta)=\Gamma(k+1)\sum_{r=1}^{\infty}(-)^{r-1}\frac{e^{r\eta}}{r^{k+1}}, \quad . \quad . \quad . \quad . \quad . \quad (6.1)$$

the particular expansions required here being

$$\mathrm{F}_{1/2}(\eta=\frac{\sqrt{\pi}}{2}e^{\eta}\left\{1-\frac{e^{\eta}}{2^{3/2}}+\frac{e^{2\eta}}{3^{3/2}}-\ldots\right\}, \quad . \quad . \quad . \quad (6.2)$$

$$\mathrm{F}_{3/2}(\eta)=\frac{3\sqrt{\pi}}{4}e^{\eta}\left\{1-\frac{e^{\eta}}{2^{5/2}}+\frac{e^{2\eta}}{3^{3/2}}-\ldots\right\}, \quad . \quad . \quad (6.3)$$

The range $\eta<0$ corresponds approximately to $k\mathrm{T}/\epsilon_0=\tau>1$ (more accurately, $\tau>0{\cdot}988\ 734$). Using (5.3), (5.4) and (5.5), the inverse series to (6.2) may be written (*cf.* Stoner, 1938 *c*)

$$e^{\eta}=\frac{4}{3\sqrt{\pi}}\left(\frac{1}{\tau}\right)^{3/2}(1+\mathrm{A}), \quad . \quad . \quad . \quad . \quad . \quad . \quad . \quad (6.4)$$

where

$$\mathrm{A}=\sum_{r=1}^{\infty}a^{r}\left(\frac{1}{\tau}\right)^{3/2},$$

with the following values for the coefficients :—

$$\frac{4}{3\sqrt{\pi}}=0{\cdot}752\ 253,\ a_1=\frac{4}{3\sqrt{\pi}}\times\frac{\sqrt{2}}{4}=0{\cdot}265\ 962,$$

$$a_2=\left(\frac{4}{3\sqrt{\pi}}\right)^2\times\left(\frac{1}{4}-\frac{\sqrt{3}}{9}\right)=0{\cdot}032\ 567,$$

$$a_3=\left(\frac{4}{3\sqrt{\pi}}\right)^3\times\left(\frac{1}{8}+\frac{5\sqrt{2}}{32}-\frac{5\sqrt{6}}{36}\right)=0{\cdot}002\ 454.$$

Expressions for $\eta$ are also required. From (6.4),

$$\eta=\log\frac{4}{3\sqrt{\pi}}\left(\frac{1}{\tau}\right)^{3/2}+\log(1+\mathrm{A}), \quad . \quad . \quad . \quad . \quad . \quad (6.5)$$

and for the range $\tau>1$, a series representation may be obtained for the second term :

$$\log(1+\mathrm{A})=\mathrm{A}'=\sum_{r=1}^{\infty}a_r'\left(\frac{1}{\tau}\right)^{3r/2}, \quad . \quad . \quad . \quad . \quad . \quad . \quad (6.6)$$

where the coefficients of the leading terms have the following values :

$$a_1'=\left(\frac{4}{3\sqrt{\pi}}\right)\times\frac{\sqrt{2}}{4} \qquad =+0{\cdot}265\ 962,$$

$$a_2'=\left(\frac{4}{3\sqrt{\pi}}\right)^2\times\left(\frac{3}{16}-\frac{\sqrt{3}}{9}\right) \qquad =-0{\cdot}002\ 801,$$

$$a_3'=\left(\frac{4}{3\sqrt{\pi}}\right)^3\times\left(\frac{1}{8}+\frac{5\sqrt{2}}{48}-\frac{\sqrt{6}}{9}\right) \qquad =+0{\cdot}000\ 063.$$

The series expansion for $F_{3/2}(\eta)/F_{1/2}(\eta)$, as a function of $\tau$, which is required in the expressions for the thermodynamic functions, may be written

$$\left.\begin{aligned} &F_{3/2}(\eta)/F_{1/2}(\eta)=\tfrac{3}{2}(1+B), \\ \text{where}\qquad &B=\sum_{r=1}^{\infty} b_r\left(\frac{1}{\tau}\right)^{3r/2} \end{aligned}\right\} \quad . \; . \; . \; . \; . \; . \quad (6.7)$$

with the following values for the coefficients :—

$$b_1=\left(\frac{4}{3\sqrt{\pi}}\right)\times\frac{\sqrt{2}}{8} \qquad =\frac{1}{2}a_1'=+0{\cdot}132\ 981,$$

$$b_2=\left(\frac{4}{3\sqrt{\pi}}\right)^2\times\left(\frac{1}{8}-\frac{2\sqrt{3}}{27}\right) \qquad =\frac{2}{3}a_2'=-0{\cdot}001\ 867,$$

$$b_3=\left(\frac{4}{3\sqrt{\pi}}\right)^2\times\left(\frac{3}{32}+\frac{5\sqrt{2}}{64}-\frac{\sqrt{6}}{12}\right)=\frac{3}{4}a_3'=+0{\cdot}000\ 047.$$

By the use of (6.5), (6.6) and (6.7), series expressions may be obtained for the various thermodynamic functions from the formulæ of § 4. These are collected below. In this range it is appropriate to consider the expressions for energy in the reduced form obtained by division by $NkT$.

$$\underline{\tau=kT/\epsilon_0=(2mkT/h^2)(4\pi gV/3N)^{2/3}>1.}$$

$$E/NkT=(3/2)(1+B), \quad . \; . \; . \; . \; . \; . \; . \; . \; . \; . \; . \; . \quad (6.8)$$

$$H/NkT=(5/2)(1+B), \quad . \; . \; . \; . \; . \; . \; . \; . \; . \; . \; . \; . \quad (6.9)$$

$$F/NkT=\log\frac{4}{3\sqrt{\pi}}\left(\frac{1}{\tau}\right)^{3/2}-(1-A'+B), \quad . \; . \; . \; . \; . \; . \quad (6.10)$$

$$G/NkT=\log\left(\frac{4}{3\sqrt{\pi}}\right)\left(\frac{1}{\tau}\right)^{3/2}+A', \quad . \; . \; . \; . \; . \; . \; . \; . \quad (6.11)$$

$$PV/NkT=(1+B), \quad . \; . \; . \; . \; . \; . \; . \; . \; . \; . \; . \; . \quad (6.12)$$

$$S/Nk=(5/2)\left(1+B-\frac{2}{5}A'\right)-\log\left(\frac{4}{3\sqrt{\pi}}\right)\left(\frac{1}{\tau}\right)^{3/2} . \; . \; . \quad (6.13)$$

The quasi-classical limiting forms are readily obtained from the above expressions by proceeding to the limit $A'\to 0$, $B\to 0$. This limit is referred to as " quasi "-classical because, although the expressions (6.8), (6.9) and (6.12) for E, H, and PV then agree with those obtained using classical (Maxwell-Boltzmann) statistics, the remaining expressions differ by terms corresponding to the term $\log N!=N\log N-N$ in the classical expression for $S/k$, arising from the assumption of distinguishability of the particles.

In view of its fundamental form, an expression for F as a function of N, T, V is given below. Only the first term indicating the deviation from the quasi-classical form is given, as further terms can readily be obtained, if required, from the preceding expressions:

$$\mathrm{F}=\mathrm{N}k\mathrm{T}\left[\left\{\log \mathrm{N}-\log \mathrm{V}-\frac{3}{2}\log \mathrm{T}-1-\log\frac{g(2\pi\, mk)^{3/2}}{h^3}\right\}\right.$$
$$\left.+\frac{\sqrt{2}}{8}\left\{\frac{h^3}{g(2\pi mk)^{3/2}}\left(\frac{\mathrm{N}}{\mathrm{VT}^{3/2}}\right)\right\}\cdot\;\cdot\;\cdot\;\cdot\;\right]\cdot\;\cdot\;\cdot \qquad (6.14)$$

From (6.14), expressions for all the other thermodynamic functions may be obtained by application of the usual thermodynamic relations. Thus, expressions for E, S, and P are obtained by application of the Gibbs-Helmholtz relation (2.12), and by partial differentiation with respect to T and V respectively (see (2.9)). This procedure simply reproduces expressions which are directly obtainable from (6.8)–(6.13), but it illustrates clearly the manner in which all the thermodynamic properties of the system are embodied in the expression for F in suitable form.

The use and accuracy of high temperature series representations have been previously considered in connexion with the series (6.8) for E (Stoner, 1938 *a*). For $\tau>1$, the series converge rapidly and are then reasonably convenient for numerical computation. For $\tau$ greater than about 1·5 more accurate results can, in fact, be obtained from the series than by use of the Fermi-Dirac integral tables. The series may, moreover, be used in practice even for $\tau<1$, and, if terms are included up to that involving $b_3$ (see 6.7), the accuracy in the value of E is within 0·1 per cent. for $\tau\geqslant 0{\cdot}3$. The numerical characteristics of the series A′ are clearly similar to those of B. Owing to the fact that both the series A′ (6.6) and B (6.7) involved in the expressions (6.8)–(6.13) are alternating, limits of error may readily be obtained, and these are reasonably narrow, except for the smallest values of $\tau$. Although the series can be used to give reasonably accurate results over a wide range, they are clearly inconvenient except for $\tau$ greater than about 1·5, where they may be applied in a similar manner to that of the low temperature series for $\tau$ less than about 0·1. For the whole of the intermediate range the use of the Fermi-Dirac integral tables is both more accurate and more convenient. Numerical results obtained by means of these tables are given in the next section.

## 7. *Numerical Tables.*

The series expressions for the thermodynamic functions of the last two sections are appropriate, in principle, for $k\mathrm{T}\epsilon_0=\tau\ll 1$, and $\tau>1$. The previous numerical study of the temperature variation of energy (Stoner, 1938 *a*) shows that the series expressions could be used in practice to obtain values correct to within 0·01 per cent. for $\tau \leqslant 0{\cdot}2$, and $\tau \geqslant 0{\cdot}5$. For the intermediate range, however, the series expressions are unsatisfactory, as the limits of error obtained by the use of the series alone are uncertain, and the actual errors (as shown by empirical test) may be large. Moreover, except for large and small values of $\tau$ (say $\tau > 1{\cdot}5$, and $\tau < 0{\cdot}1$), the use of the series for numerical purposes is inconvenient, owing to the number of terms which it is necessary to sum to obtain numerically accurate results. By the use of the tables of Fermi-Dirac integrals (McDougall and Stoner, 1938), and the expressions for the thermodynamic functions in § 4, accurate numerical values for these functions may be obtained for the whole range covered by the tables (the range of the tables, $-4{\cdot}0 \leqslant \eta \leqslant +20{\cdot}0$, corresponds to the range $11{\cdot}95519 \geqslant \tau \geqslant 0{\cdot}04990$). Outside this range, accurate values may easily be obtained from the series expressions.

It is appropriate to tabulate the suitably reduced values of the various functions with the reduced temperature $\tau = kT/\epsilon_0$ as argument. For a given value of $\tau$, $F_{1/2}(\eta)$ is first found from (4.12). The value of $\eta$ is obtained by inverse interpolation in the $\eta$, $F_{1/2}(\eta)$ table. The value of $F_{3/2}(\eta)$ is then found by direct interpolation in the $\eta$, $F_{3/2}(\eta)$ table. Knowing the corresponding values of $kT/\epsilon_0$, $\eta$, $F_{1/2}(\eta)$, and $F_{3/2}(\eta)$, the reduced value of the energy as $E/NkT$ or $E/N\epsilon_0$ may be obtained from (4.21), and similarly the reduced values of F, H, G from (4.22), (4.24) and (4.25) respectively. The entropy, S, is obtained in the reduced forms $S/Nk$ or $TS/N\epsilon_0$, using (4.21). The methods for direct and inverse interpolation appropriate for use with the Fermi-Dirac tables have been described in previous papers, and the accuracy attainable has been discussed, so that further consideration here is unnecessary. The five decimal place values in the tables are rounded from values in which the uncertainty should not exceed 2 units in the sixth place.

In Table I the values of the thermodynamic functions, G, E, F and S, suitably reduced, are tabulated at intervals of 0·05 in $\tau (= kT/\epsilon_0)$ for the range $0{\cdot}0 \leqslant \tau \leqslant 2{\cdot}0$. The table is divided into two parts. In the first, Table I *a*, covering the range $0{\cdot}0 \leqslant \tau \leqslant 1{\cdot}0$, the reduced values of G, E, F tabulated are those obtained by division by $N\epsilon_0$; in the second, Table I *b*, covering the range $1{\cdot}0 \leqslant \tau \leqslant 2{\cdot}0$, those obtained by division by $NkT$. The transformation from one reduced form to the other is readily effected by division or multiplication by $\tau$. The choice of different reduced values for the $\tau \leqslant 1$ and $\tau \geqslant 1$ ranges has the advantage of showing clearly the character of the temperature variation of the functions, and large numbers are avoided. That functions such as $G/NkT$ approach a limiting variation as $1/\tau$ as $\tau$ decreases renders them inappropriate for tabulation in the lower part of the range, while for the higher part of the range the tabulated values of $E/NkT$, in particular, show more clearly the approach to the quasi-classical limiting ratio than would values of $E/N\epsilon_0$. In connexion with the Fermi-Dirac integral tables, however, it is values of $\eta$ which are required, and these are given by $G/NkT$. Thus Table I*b* gives values of $\eta$ directly, but the $G/N\epsilon_0$ values of Table I*a* must be divided

### TABLE I.

### Thermodynamic Functions for a Fermi-Dirac Gas as Functions of the Reduced Temperature.

In the first line in each part of the table are shown the functions tabulated, and in the second the corresponding thermodynamic quantities.

$\tau \quad = kT/\epsilon_0 = T/\theta_F$ ;

$\epsilon_0 \quad = \frac{h^2}{2m}\left(\frac{3N}{4\pi g V}\right)^{2/3}$ ; $F_k(\eta) = \int_0^\infty \frac{x^k dx}{e^{x-\eta}+1}$ ;

$F_{1/2} = F_{1/2}(\eta) = \frac{2}{3}\tau^{-3/2}$ ; $F_{3/2} = F_{3/2}(\eta)$ ;

G, Gibbs free energy ; E, internal energy ; F, Helmholtz free energy ; S, entropy.

I*a*.—$0{\cdot}0 \leqslant \tau \leqslant 1{\cdot}0$.

| $\tau$.<br>$kT/\epsilon_0$. | $\tau\eta$.<br>$G/N\epsilon_0$. | $\tau(F_{3/2}/F_{1/2})$.<br>$E/N\epsilon_0$. | $\tau(\eta - \frac{2}{3}F_{3/2}/F_{1/2})$.<br>$F/N\epsilon_0$. | $\frac{5}{3}F_{3/2}/F_{1/2} - \eta$.<br>$S/Nk$. |
|---|---|---|---|---|
| 0·00 | 1·00000 | 0·60000 | 0·60000 | 0·00000 |
| 0·05 | 0·99794 | 0·60615 | 0·59384 | 0·24612 |
| 0·10 | 0·99164 | 0·62428 | 0·57545 | 0·48831 |
| 0·15 | 0·98073 | 0·65336 | 0·54516 | 0·72132 |
| 0·20 | 0·96458 | 0·69152 | 0·50357 | 0·93975 |
| 0·25 | 0·94262 | 0·73671 | 0·45147 | 1·14095 |
| 0·30 | 0·91458 | 0·78724 | 0·38976 | 1·32493 |
| 0·35 | 0·88045 | 0·84181 | 0·31925 | 1·49303 |
| 0·40 | 0·84035 | 0·89949 | 0·24069 | 1·64699 |
| 0·45 | 0·79449 | 0·95960 | 0·15475 | 1·78854 |
| 0·50 | 0·74311 | 1·02164 | 0·06202 | 1·91925 |
| 0·55 | 0·68649 | 1·08525 | −0·03701 | 2·04048 |
| 0·60 | 0·62487 | 1·15014 | −0·14189 | 2·15338 |
| 0·65 | 0·55850 | 1·21609 | −0·25223 | 2·25895 |
| 0·70 | 0·48761 | 1·28294 | −0·36768 | 2·35802 |
| 0·75 | 0·41242 | 1·35054 | −0·48793 | 2·45130 |
| 0·80 | 0·33314 | 1·41879 | −0·61272 | 2·53939 |
| 0·85 | 0·24994 | 1·48760 | −0·74180 | 2·62282 |
| 0·90 | 0·16300 | 1·55690 | −0·87493 | 2·70204 |
| 0·95 | 0·07248 | 1·62663 | −1·01194 | 2·77744 |
| 1·00 | −0·02146 | 1·69674 | −1·15262 | 2·84936 |

TABLE I. (*cont.*).

I *b*.—$1{\cdot}0 \leqslant \tau \leqslant 2{\cdot}0$.

| $\tau$.<br>$kT/\epsilon_0$. | $\eta$.<br>$G/NkT$. | $(F_{3/2}/F_{1/2})$.<br>$E/NkT$. | $(\eta - \frac{2}{3}F_{3/2}/F_{1/2})$.<br>$F/NkT$. | $\frac{5}{3}F_{3/2}/F_{1/2} - \eta$.<br>$S/Nk$. |
|---|---|---|---|---|
| 1·00 | —0·02146 | 1·69674 | —1·15262 | 2·84936 |
| 1·05 | —0·11305 | 1·68303 | —1·23507 | 2·91810 |
| 1·10 | —0·19918 | 1·67084 | —1·31307 | 2·98391 |
| 1·15 | —0·28047 | 1·65994 | —1·38710 | 3·04704 |
| 1·20 | —0·35743 | 1·65015 | —1·45754 | 3·10769 |
| 1·25 | —0·43050 | 1·64132 | —1·52472 | 3·16604 |
| 1·30 | —0·50005 | 1·63332 | —1·58893 | 3·22225 |
| 1·35 | —0·56640 | 1·62605 | —1·65044 | 3·27648 |
| 1·40 | —0·62984 | 1·61941 | —1·70945 | 3·32886 |
| 1·45 | —0·69061 | 1·61334 | —1·76617 | 3·37951 |
| 1·50 | —0·74893 | 1·60776 | —1·82077 | 3·42853 |
| 1·55 | —0·80499 | 1·60262 | —1·87340 | 3·47603 |
| 1·60 | —0·85895 | 1·59788 | —1·92421 | 3·52209 |
| 1·65 | —0·91098 | 1·59350 | —1·97331 | 3·56681 |
| 1·70 | —0·96120 | 1·58943 | —2·02082 | 3·61025 |
| 1·75 | —1·00974 | 1·58565 | —2·06684 | 3·65248 |
| 1·80 | —1·05671 | 1·58212 | —2·11146 | 3·69358 |
| 1·85 | —1·10220 | 1·57883 | —2·15476 | 3·73359 |
| 1·90 | —1·14632 | 1·57576 | —2·19682 | 3·77258 |
| 1·95 | —1·18913 | 1·57288 | —2·23772 | 3·81060 |
| 2·00 | —1·23072 | 1·57018 | —2·27750 | 3·84768 |

by $\tau$. The character of the temperature variation of the entropy, S, which as $\tau$ decreases approaches a limiting variation as $\tau$, is such that it seems better to tabulate $S/Nk$ in both parts of the table. In Table I *b* the tabulation of $TS/N\epsilon_0$ would perhaps be preferable on the ground of strict consistency, but $TS/N\epsilon_0$ may be readily obtained if required either from $(E-F)/N\epsilon_0$ or from $S/Nk$ by multiplication by $\tau$.

It is unnecessary to tabulate values for the total heat, H, or the product PV, since these are given simply by $\frac{5}{3}E$ and $\frac{2}{3}E$ respectively (see (4.23) and (4.24)). A numerical value for the sum over states Z is also readily obtained, since $Z/N$ is equal to $\frac{2}{3}E/NkT$ (see (4.20)). It may be noted that tables given previously for electronic specific heat, spin paramagnetism and ferromagnetism (Stoner, 1938 *a*, *b*, *c*, 1939), supplement those given here for the basic functions.

In the first line of the tables the functions tabulated are given in terms of $\eta$, $F_{1/2}(\eta)$, $F_{3/2}(\eta)$, and $\tau$ ($\tau$ and $F_{1/2}(\eta)$ being related by (5.5)). In the second line the thermodynamic significance of the functions for a Fermi-Dirac gas is indicated.

*Physical Constants and Conversion Factors.*—For a system of particles having an energy distribution of states of the standard form considered, suitably reduced forms of the various thermodynamic functions can all be expressed as unique functions of the reduced temperature $kT/\epsilon_0$. To convert the numerical results for, say, $E/N\epsilon_0$ as a function of $kT/\epsilon_0$, into results for E as a function of T, with suitable units for E, requires the determination of the conversion factors appropriate for the particular particles under consideration. This has been discussed previously (Stoner, 1938 *a*, *b*) in connexion with electrons, for which the numerical factors then obtained are included below, factors for atoms being given in addition. A list of the adopted values of the physical constants was given in the previous paper, which may be consulted for a discussion of the uncertainties in the values of conversion factors—the probable error may be greater than 1 part in 1000—arising from uncertainties in the values of the constants. (Values adopted include $h=6{\cdot}610\times10^{-27}$ erg. sec.; electronic mass, $m_0=9{\cdot}105\times10^{-28}$ gm.; Avogadro's number, $N_A=6{\cdot}027_5\times10^{23}$ mole$^{-1}$.) The expression involved is (4.7) for $\epsilon_0$:

$$\epsilon_0=\frac{h^2}{2m}\left(\frac{3N}{4\pi gV}\right)^{2/3}. \quad . \quad . \quad . \quad . \quad . \quad . \quad . \quad . \quad . \quad (7.1)$$

(*a*) *Atoms.* For a Fermi-Dirac gas, of density $\rho$, atomic weight A, statistical weight factor $g$, the Fermi energy $\epsilon_0$, and the corresponding degeneracy temperature, $\theta_F$, such that $\epsilon_0=k\theta_F$, and $\tau=T/\theta_F$, are given by

$$\epsilon_0/3{\cdot}616\times10^{-14}=\theta_F/2{\cdot}622\times10^2=(\rho/g)^{2/3}A^{-5/3}, \quad . \quad . \quad (7.2)$$

where $\epsilon_0$ is expressed in ergs. For the corresponding Fermi energy per gram atom, $N_A\epsilon_0$,

$$\frac{N_A\epsilon_0}{(\rho/g)^{2/3}A^{-5/3}}=2{\cdot}179\times10^{10}\text{ erg.}=5{\cdot}208\times10^2\text{ cal.} \quad . \quad . \quad (7.3)$$

(*b*) *Electrons.* For free electrons ($g=2$), the Fermi energy expressed in ergs, $\epsilon_0$, electron volts, $V_0$, and as a corresponding temperature, $\theta_F$, is given by

$$\epsilon_0/5{\cdot}817\times10^{-27}=V_0/3{\cdot}633\times10^{-15}=\theta_F/4{\cdot}217\times10^{-11}$$
$$=(N/V)^{2/3}. \quad . \quad . \quad . \quad . \quad . \quad . \quad . \quad . \quad . \quad . \quad . \quad (7.4)$$

For free electrons to the number $q$ per atom in a metal of density $\rho$, atomic weight A,

$$\epsilon_0/4{\cdot}150\times10^{-11}=V_0/2{\cdot}592\times10=\theta_F/3{\cdot}009\times10^5$$
$$=q\rho A^{-2/3}. \quad . \quad . \quad . \quad . \quad . \quad . \quad . \quad . \quad . \quad . \quad . \quad . \quad (7.5)$$

The energy per gram atom corresponding to $\epsilon_0$ is equal to $N_A q\epsilon_0$, numerical values being given by

$$\frac{N_A q\epsilon_0}{q^2\rho A^{-2/3}}=2\cdot503\times10^{13}\text{ erg}=5\cdot977\times10^5\text{ cal.} \quad . \quad . \quad . \quad (7.6)$$

A brief account will be given in the next section of the conditions under which the numerical results for different parts of the $\tau$ range (such as those in Table I for $0\cdot0\leqslant\tau\leqslant2\cdot0$) are practically relevant.

## 8. *Survey of Results and Discussion.*

*Graphical Representations.*—The general character of the temperature variation of the various thermodynamic functions is most readily appreciated with the aid of graphical representations. The curves of fig. 1 show the temperature variation of the internal energy, E, total heat, H, Helmholtz free energy, F, and Gibbs free energy, G. Reduced values

Fig. 1.

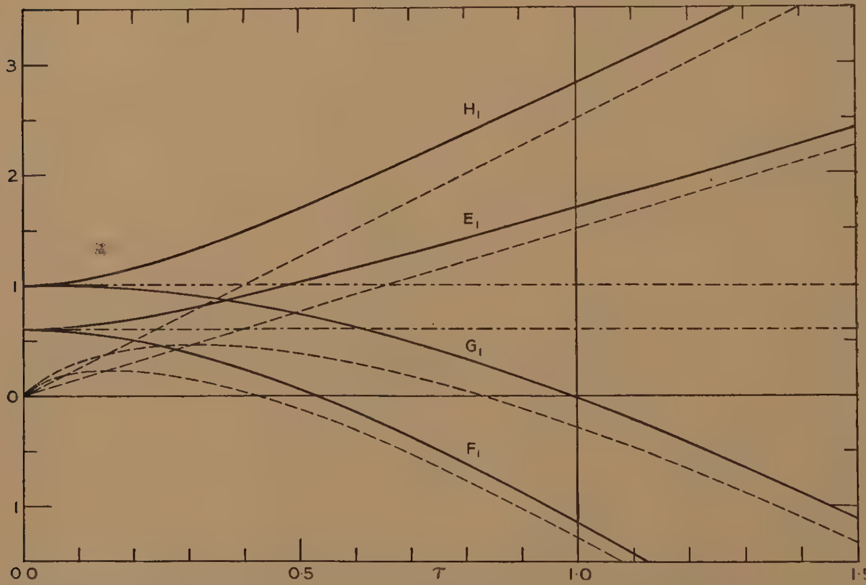

Temperature variation of the thermodynamic functions internal energy, E, total heat, H, Helmholtz free energy, F, and Gibbs free energy, G.

Reduced values of the functions, $E_1$, $H_1$, $F_1$, $G_1$, obtained by division of E, H, F, G by $N\epsilon_0$ are plotted against the reduced temperature $\tau=kT/\epsilon_0$. Thus,

$$E_1=E/N\epsilon_0=\bar{\epsilon}/\epsilon_0,$$

and similarly for the other functions. The broken lines correspond to the limiting expressions for $\epsilon_0/kT\rightarrow0$ (quasi-classical limit), the dot-dash lines to those for $kT/\epsilon_0\rightarrow0$ (Fermi-Dirac limit).

obtained by division by $N\epsilon_0$ are plotted against the reduced temperature $\tau = kT/\epsilon_0$. Thus $E_1 = E/N\epsilon_0 = \bar{\epsilon}/\epsilon_0$, where $\bar{\epsilon}$ is the mean energy per particle, and similarly for the other functions. Curves corresponding to the use of the limiting low and high temperature forms of expression are also shown. (See § 4 and § 5.) In connexion with the quasi-classical limiting curves, the parameter $\epsilon_0$ can hardly be regarded as retaining its significance as the maximum particle energy at absolute zero, but simply as an abbreviation for the expression (4.7), involving $(N/V)^{2/3}$. It may be noticed that the limiting curves for E and H, which are linear ($E = \frac{3}{2}NkT$, $H = \frac{5}{2}NkT$) do not involve $\epsilon_0$, and correspond to strict classical statistics.

The temperature variation of the entropy is not conveniently shown in fig. 1 as it would lead to confusion in the diagram. In fig. 2 the entropy S, in the reduced forms $S/Nk$ and $TS/N\epsilon_0$, is plotted against the reduced temperature $\tau = kT/\epsilon_0$. Values corresponding to the use of the limiting expressions are indicated as in fig. 1. The character of the temperature variation of the entropy is perhaps most clearly brought out by the reduced form $S/Nk$. The reduced entropy $TS/N\epsilon_0$ is such that it is equal to the difference between $E_1$ and $F_1$ and between $H_1$ and $G_1$ of fig. 1.

Fig. 2.

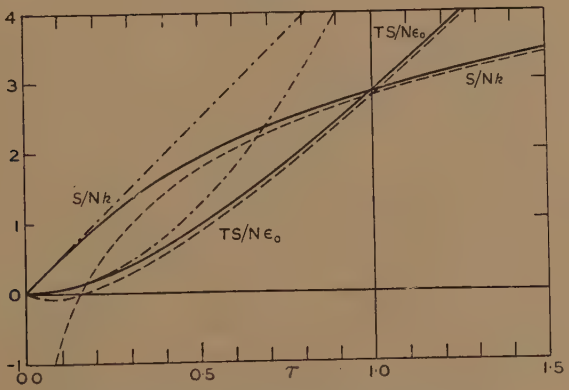

Temperature variation of entropy, S.

Reduced values of the entropy, $S/Nk$ and $TS/N\epsilon_0$ are plotted against the reduced temperature, $\tau = kT/\epsilon_0$. Values given by the limiting expressions are indicated in the same way as in fig. 1.

To show more clearly the manner of approach to values given by the quasi-classical limiting expressions for F, G, and S as well as for E and H, the reduced functions are plotted in fig. 3 with a logarithmic scale for the reduced temperature $\tau$. With this scale, the limiting expressions give linear relations, as is apparent from (6.8) at (6.13).

The curves of fig. 1 have the same general form as those suggested by

Nernst many years ago as being applicable to pure solid or liquid substances. The Nernst heat theorem has the effect of supplementing the thermodynamic relation F→E for T→0 by $(\partial F/\partial T)\rightarrow(\partial E/\partial T)$ for T→0, and this leads to a temperature variation of the functions E and F in the low temperature region similar to that of the figure. That S→0 as T→0 (fig. 2) corresponds to the equivalent alternative statement of the heat theorem. It is of interest that the low temperature characteristics postulated by Nernst, and within limits successfully utilized in connexion with pure crystalline solids, find their ideal exemplification in the Fermi-Dirac gas.

Fig. 3.

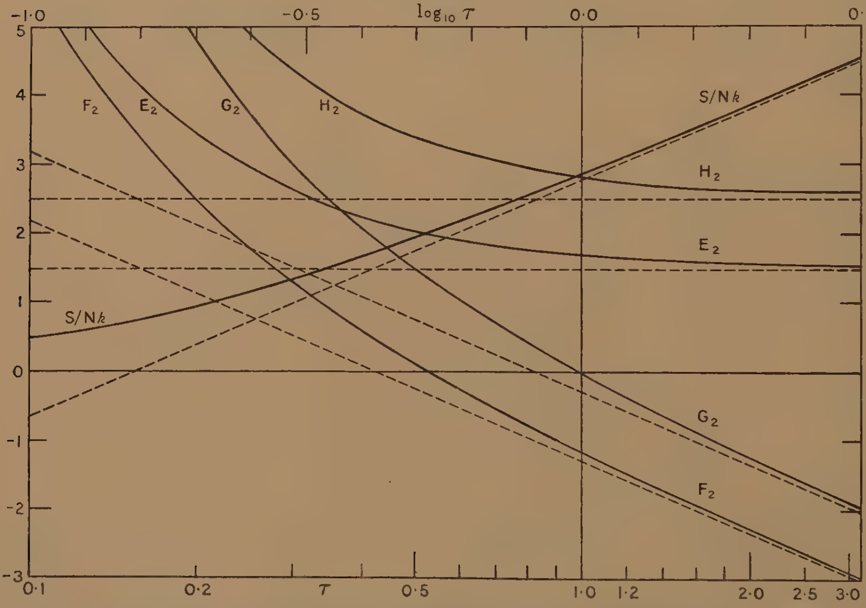

Curves showing the approach of the values of the thermodynamic functions to the values given by the quasi-classical limiting expressions.

The reduced values $E_2$, $H_2$, $F_2$, $G_2$ are obtained by division of E, H, F, G by N*k*T. Thus,

$$E_2=E/NkT=\bar{\epsilon}/kT,$$

and similarly for the other functions. A logarithmic scale is used for the reduced temperature $\tau=kT/\epsilon_0$, as shown by the upper scale. The values of $\tau$ are indicated by the lower scale. Values given by the quasi-classical limiting expressions are shown by the broken lines.

The crossing over of the quasi-classical F and E (and also G and H) curves in fig. 1 is associated with the large negative values of S/N*k* indicated for low temperatures (or, strictly, low reduced temperatures) by the quasi-classical expression (see figs. 2 and 3). Using this expression, the value of $\tau$ at which S/N$k$ becomes zero is given by (*cf.* (6.13)).

$$\log_e\tau=\frac{2}{3}\left(\log_e\frac{4}{3\sqrt{\pi}}-\frac{5}{2}\right],$$

corresponding to

$$\tau=kT/\epsilon_0=0{\cdot}156\ 225.$$

The formal appearance of a negative entropy has no physical significance. It simply brings out, primarily, the invalidity of the quasi-classical expression, even as a rough approximation to the Fermi-Dirac (or Bose-Einstein) expressions for small values of $\tau$, *i. e.*, small values of $T(V/N)^{2/3}$. Apart from this, however, it should be borne in mind that the limiting expression (6.13) for S/N$k$ does not correspond strictly to the quantized form of classical statistics (for distinguishable or localized particles). To obtain the correct expression it is necessary to add $(1/N)\log N!$ ($\sim\log N-1$). This would result in an enormous diminution in the value of $\tau$ required, formally, to make S/N$k$ zero. The conditions, however, would then be such as to render invalid the usual replacements of summations by integrations, and the use of the Stirling approximation for factorials. (A similar difficulty encountered in connexion with Bose-Einstein statistics has been considered in detail by London, 1938.) With the convention adopted in this paper (§ 3) Fermi-Dirac, Bose-Einstein and the quantized form of Maxwell-Boltzmann statistics all give $S/Nk\rightarrow0$ for $T\rightarrow0$. From a mathematical point of view, the treatment of the lowest temperature range is much simpler with Fermi-Dirac statistics than with the other two forms, owing to the fact that the number of relevant particle states remains comparable with the number of particles, and the replacement of summations by integrations remains justifiable.

*Applications.* (*a*) *Atoms.*—It is clear from (7.2) that for atomic gases of the N.T.P. density (with $\rho/A$ equal to about $5\times10^{-5}$) the degeneracy temperature, $\theta_F$, even for small atomic weights, would be of the order 0·1° K, and that over the range in which such densities can occur for a gaseous phase deviations from classical characteristics would be quite inappreciable. Moreover, for actual gases, the conditions of density necessary for the appearance of appreciable deviations would be such as to result in much larger deviations for other reasons. (For densities of the order unity, such as occur for liquids, $\theta_F$ for $A=1$ would be of the order 200° K., but it is doubtful whether any liquid is of the kind to which applications of Fermi-Dirac statistics could usefully be made.)

The above considerations show that, in the treatment of vapour pressures over liquids and solids, it will in practice be justifiable, *a fortiori*, to make use of the quasi-classical expressions for the gaseous phase. Even at the lowest attainable temperatures, owing to the low density of the gas-phase, the reduced temperature $\tau$ for the gas will be so high that the classical expressions will be applicable. According to the usual treatment in deriving an expression for the vapour pressure constant, it is essential for equilibrium that G for the gas-phase should not be positive. On the reduced temperature scale, G becomes positive at approximately $\tau=1$ (see fig. 1), and the above remarks imply that the range $\tau<1$ is not involved, in practice, in vapour pressure considerations. The academic exercise of tracing the precise course of the equilibrium with the ultimate approach to absolute zero will not be undertaken.

(*b*) *Electrons.*—The most extensive and significant field of application of Fermi-Dirac statistics is in connexion with free or quasi-free electrons constituting what may be called an electron gas. The numerical factors required in the treatment of the ideal electron gas are provided by equations (7.4) to (7.6). The nearest approach to the ideal is probably to be found in stellar material. For highly ionized high density material in stars of the wide dwarf type ($\rho\sim10^5$, $A/q\sim2$) it is apparent from (7.4) that the degeneracy temperature $\theta_F$ is extremely high (of the order $10^9$), and conditions are approached in which the limiting Fermi-Dirac expressions form close approximations, if account is taken of relativistic modifications. There is now a fairly extensive literature dealing with the problem of equilibrium of dense stars, usually treated by using the relativistic or non-relativistic expressions for the completely degenerate Fermi-Dirac gas. In view of the decrease of density outwards in stars a more complete treatment of this problem would involve the use of Fermi-Dirac results, such as are given in this paper, for the complete range of reduced temperature. Attention has perhaps been particularly directed to white dwarf stars, owing to the complete failure of classical statistics in connexion with them. Fermi-Dirac statistics will, however, lead to significant modifications in the treatment of the internal constitution of stars generally (except possibly for stars of low central density), and will probably play an increasing part in theoretical astrophysics.

The free electron treatment is usefully applicable, as a fair approximation, in considering the electronic properties of such metals as those in the first column of the periodic table. For metals generally the value of $(q\rho/A)^{2/3}$ ranges from about 0·06 to 0·3, and the value of $\theta_F$ (*i. e.*, the value of T for which $\tau=1$) for free electrons would range from about $1{\cdot}8\times10^4$ to $9\times10^5$. The "experimental" temperature range would then be effectively covered by the range $\tau<0{\cdot}2$, and for most purposes the series expressions of § 5 would give numerical results of adequate accuracy. For many metals, however, although the unfilled electronic energy bands may differ greatly from those for free electrons, the form of the bands, over a relevant energy range, may be of approximately the same form, the number of states varying as the square root of the energy measured from an appropriate zero. If this relation is satisfied, the whole of the present numerical results can be utilized, retaining $\epsilon_0$ as giving the energy width of the occupied (or unoccupied) part of the band at absolute zero, but not as being directly calculable, using (7.2) or (7.3), from the electronic density in the metal. In particular cases the effective value of $\epsilon_0$ may then be of the order of a tenth of a volt, and the degeneracy temperature of the order of 1000°, so that the experimental temperature range may correspond to practically the whole of the range covered by the numerical tables in this paper. It is of interest to note that the experimental temperature range for which accurate theoretical values are most desirable (for example, the range including the Curie temperatures of the ferromagnetic metals) often corresponds to that for which the Fermi-Dirac series representations are inadequate. A Fermi-Dirac treatment of collective electron specific heat, spin paramagnetism, and ferromagnetism for electrons in bands of the standard form has been given in a series of papers (Stoner, 1938 *a*, *b*, *c*, 1939), and preliminary considerations have shown that the general character of the experimental results is in close agreement with that indicated by the theoretical treatment. Exact agreement would not be expected, for it is known that the actual form of the electronic bands in metals often differs widely from the standard form for which the detailed calculations have been made. None the less, it seems very desirable that detailed consideration should be given to the standard form of band in order that a basic set of theoretical results should be available against which experimental results may be considered. In a sense it may be said that divergencies between the two are of even greater physical interest than concordances. The position is almost precisely similar to that in connexion with the Debye theory of specific heats, where the basic calculations are made for a particular distribution of vibrational states from which the actual distribution may differ widely.

The form of the energy distribution of states here considered is of fundamental interest, since it is only for this form that the results given by Fermi-Dirac statistics pass over, in the limit, to those of classical statistics. Moreover, the results have a very wide range of direct or indirect practical utility. It is for these reasons that it has seemed desirable to develop in some detail in this paper the general scheme of statistical-thermodynamical relations, and to provide reasonably complete and precise numerical tables for the basic thermodynamic functions.

I have pleasure in thanking the Government Grants Committee of the Royal Society for the loan of a Brunsviga calculating machine.

## *Summary.*

A detailed account is given of the thermodynamical-statistical relations for a perfect Fermi-Dirac gas. The properties of the main thermodynamic

functions are summarized, with particular reference to the convenience and appropriateness of different sets of variables in terms of which they can be expressed. The derivation of the essential statistical formulæ for a system of particles subject to Fermi-Dirac statistics is outlined. The formulæ are then specialized for the particular energy distribution of states characteristic of a perfect gas (with the energy density of states proportional to the square root of the energy). Expressions are obtained for the thermodynamic functions energy, E, total heat, H, Helmholtz free energy, F, Gibbs free energy, G, and entropy, S, in terms of the basic Fermi-Dirac integrals, $\mathrm{F}_{1/2}(\eta)$ and $\mathrm{F}_{3/2}(\eta)$, which have previously been evaluated. Suitably reduced forms of these functions, such as $\mathrm{E}/\mathrm{N}k\mathrm{T}$ or $\mathrm{E}/\mathrm{N}\epsilon_0$, are unique functions of a reduced temperature $\tau=k\mathrm{T}/\epsilon_0$, where $\epsilon_0$ is the Fermi zero energy (the maximum particle energy at absolute zero) proportional, for a system of free particles, to $(1/m)(\mathrm{N}/\mathrm{V})^{2/3}$, where $m$ is the particle mass, V the volume of the system. Numerical tables are given of reduced forms of E, F, G, and S for the range $0{\cdot}0 \leqslant \tau \leqslant 2{\cdot}0$, at intervals of 0·05 in $\tau$, with numerical factors for converting from the $\tau$ to the T scale for atoms and electrons. Series representations are also developed which are applicable for $\tau \rightarrow 0$ (approach to the Fermi-Dirac limit) and $\tau > 1$ (approach to the quasi-classical limit), and convenient for numerical calculations for $\tau \leqslant 0{\cdot}1$ and $\tau \geqslant 1{\cdot}5$. The general character of the temperature variation of the various thermodynamic functions is shown in three figures, and the behaviour at low temperatures is discussed in relation to Nernst's heat theorem, and to the range of validity of the quasi-classical approximations. The various physical fields of application of the theoretical results are indicated.

## *References.*

Awbery, J. H., 'Reports on Progress in Physics,' iv. p. 103 (1938).
Fowler, R. H., 'Statistical Mechanics' (Cambridge, 1936).
Gibbs, J. W., Trans. Connecticut Acad. iii. p. 108 (1875) or 'Collected Works,' i. p. 88 (New York, Longmans, 1928).
Guggenheim, E. A., 'Modern Thermodynamics' (Methuen, 1933).
London, F., Phys. Rev. liv. p. 947 (1938).
McDougall, J., and Stoner, E. C., Phil. Trans. Roy. Soc. ccxxxvii. p. 67 (1938).
Nordheim, L., 'Müller-Pouillets Lehrbuch der Physik,' IV. iv. p. 237 (Braunschweig, 1934).
Stoner, E. C., Phil. Mag. xix. p. 565 (1935); xxiii. p. 833 (1937); xxv. p. 899 1938); Proc. Leeds Phil. Soc. iii. p. 403 (1938); Proc. Roy. Soc. clxv. p. 372 (1938); clxix. p. 339 (1939).
Tolman, R. C., 'The Principles of Statistical Mechanics' (Oxford, 1938).
Wilson, A. H., 'The Theory of Metals,' p. 244 (Cambridge, 1936).

Physics Department,
University of Leeds.
June 1939.

## XXV. *A Note on Laguerre Polynomials.*

By W. T. HOWELL *.

[Received February 9, 1939.]

THE well-known result

$$\int_0^\infty J_\nu(at)t^{\mu-1}\exp(-p^2t^2)\,dt=\frac{\Gamma\left(\frac{1}{2}\mu+\frac{1}{2}\nu\right)\left(\frac{1}{2}\frac{a}{p}\right)^\nu}{2\Gamma(\nu+1)p^\mu}\exp\left(-\frac{a^2}{4p^2}\right)$$
$$\times{}_1F_1\left\{\frac{1}{2}\nu-\frac{1}{2}\mu+1\,;\ \nu+1\,;\ \frac{a^2}{4p^2}\right\};\quad R(\mu+\nu)>0,$$

with the definition

$$\frac{\Gamma(n+\alpha+1)}{\Gamma(n+1)\Gamma(\alpha+1)}{}_1F_1(-n\,;\ \alpha+1\,;\ x)=L_n^\alpha(x)$$

enables us to write

$$J_\alpha(2\sqrt{ax})\,(ax)^{n+\frac{\alpha}{2}}\supset\Gamma(n+1)\left(\frac{a}{p}\right)^{n+\alpha}e^{-\frac{a}{p}}L_n^\alpha\left(\frac{a}{p}\right)\quad .\quad .\quad .\quad (1)$$

Where the symbol $\supset$ implies that $f(x)$ and $\phi(p)$ satisfy a relation of the form

$$p\int_0^\infty e^{-px}f(x)\,dx=\phi(p).$$

Since by Borel's theorem

$$\frac{\phi(p)\psi(p)}{p}\subset\int_0^x f(\xi)\,g(x-\xi)d\xi,$$

we have at once

$$\Gamma(n+1)\,\Gamma(m+1)a^{n+\alpha}p^{-(n+m+2\alpha+1)}L_n^\alpha\left(\frac{a}{p}\right)L_m^\alpha\left(\frac{1}{p}\right)e^{-\frac{1}{p}(1+a)}$$
$$\subset\int_0^x(a\xi)^{n+\frac{\alpha}{2}}(x-\xi)^{m+\frac{\alpha}{2}}J_\alpha(2\sqrt{a\xi})\,J_\alpha(2\sqrt{x-\xi})\,d\xi$$
$$=2\int_0^{\frac{\pi}{2}}a^{n+\frac{\alpha}{2}}\sin^{2n+\alpha+1}\theta\,\cos^{2m+\alpha+1}\theta\,x^{n+m+\alpha+1}J_\alpha(2\sin\theta\sqrt{ax})$$
$$\times J_\alpha(2\cos\theta\sqrt{x})\,d\theta.\quad (2)$$

---

* Communicated by the Author.

Using the formula *

$$\int_0^\infty \exp(-px)\,J_\nu(a\sqrt{x})J_\nu(b\sqrt{x})\,x^{\frac{\mu}{2}-1}\,dx$$

$$=\frac{\Gamma(\nu+\frac{1}{2}\mu)}{\pi p^{\frac{\mu}{2}}\Gamma(2\nu+1)}\left(\frac{ab}{p}\right)^\nu\int_0^\pi \exp\left(\frac{\varpi^2}{4p}\right){}_1F_1\left(1-\frac{\mu}{2};\ \nu+1;\ \frac{\varpi^2}{4p}\right)\sin^{2\nu}\phi\quad\phi.$$

where $$\varpi^2=a^2+b^2-2ab\cos\phi,$$
we obtain

$$\Gamma(n+1)\Gamma(m+1)e^{-\frac{1}{p}(a+1)}L_n^\alpha\left(\frac{a}{p}\right)L_m^\alpha\left(\frac{1}{p}\right)\frac{\Gamma(2\alpha+1)}{\Gamma(n+m+2\alpha+2)}$$

$$=\frac{2}{\pi}\int_0^{\frac{\pi}{2}}\int_0^\pi \sin^{2n+2\alpha+1}\theta\cos^{2m+2\alpha+1}\theta\,.\exp\left(-4p\right)$$

$$\times{}_1F_1\left(-n-m-\alpha-1;\ \alpha+1;\ \frac{\varpi^2}{4p}\right)\sin^{2\alpha}\phi\,d\phi\,d\theta,$$

where $$\varpi^2=a\sin^2\theta+\cos^2\theta-2\sin\theta\cos\theta\cos\phi\sqrt{a}.$$

We may now replace $\frac{a}{p}$ by $x$, and $\frac{1}{p}$ by $y$, so that

$$\frac{\Gamma(2\alpha+1)\Gamma(n+1)\Gamma(m+1)}{\Gamma(n+m+\alpha+2)\Gamma(\alpha+1)}e^{-(x+y)}L_n^\alpha(x)L_m^\alpha(y)\,2^{-2\alpha}$$

$$=\frac{2}{\pi}\int_0^{\frac{\pi}{2}}\int_0^\pi \sin^{2n+2\alpha+1}\theta\cos^{2m+2\alpha+1}\theta\,.\exp(-E)L_{n+m+\alpha+1}^\alpha(E)\sin^{2\alpha}\phi\,d\phi\,d\theta,\qquad\ldots\quad(3)$$

where $$E=x\sin^2\theta+y\cos^2\theta-2\sqrt{xy}\sin\theta\cos\theta\cos\phi.$$

If we use the formula †

$$J_\mu(Xz)J_\nu(xz)=\frac{X^\mu x^\nu}{\pi}\int_{-\frac{\pi}{2}}^{\frac{\pi}{2}}e^{\iota(\mu-\nu)\phi}\left(\frac{\lambda_1}{\lambda_2}\right)^{\mu+\nu}J_{\mu+\nu}(z\lambda_1\lambda_2)\,d\phi,$$

where $\lambda_1=+\sqrt{(e^{\iota\phi}+e^{-i\phi})}$; $\lambda_2=(X^2e^{-\iota\phi}+x^2e^{i\phi})^{\frac{1}{2}}$; $R(\mu+\nu)>0$,
in (2) we get

$$\frac{\Gamma(n+1)\Gamma(m+1)}{\Gamma(n+m+2)}e^{-(x+y)}L_n^\alpha(x)L_m^\alpha(y)$$

$$=\frac{2^{2\alpha+1}}{\pi}\int_0^{\frac{\pi}{2}}\int_{-\frac{\pi}{2}}^{\frac{\pi}{2}}\sin^{2n+2\alpha+1}\theta\cos^{2m+2\alpha+1}\theta\exp(-F)L_{n+m+1}^{2\alpha}(F)\cos^{2\alpha}\phi\,d\phi\,d\theta,$$

where $$F=2\cos\phi(x\sin^2\theta e^{\iota\phi}+y\cos^2\theta e^{-i\phi}).\qquad\ldots\quad(4)$$

The author is obliged to D. S. R., Admiralty, for permission to publish this note.

---

* Watson, 'Theory of Bessel Functions,' equation (13.31).

† Dixon and Ferrar, "Integrals for the Product of Two Bessel Functions," equation (7.22), Q. J. M. vol. iv. (1933).

# XXVI. *On the Determination of the Dielectric Constants of Liquids at Radio Frequencies.*—Part III. *Methyl Alcohol, Water, and Alcohol Water Mixtures : Theoretical.*

By R. M. Davies, D.Sc., and T. Tyssul Jones, B.Sc., Ph.D.,
Department of Physics, University College of Wales, Aberystwyth *.

[Received January 13, 1939.]

Contents.

| | | Page |
|---|---|---|
| I. | Introduction | 289 |
| II. | Detection of Resonance | 291 |
| III. | The Effect of Lead Inductance | 296 |
| IV. | References | 304 |
| | Appendix | 304 |

## I. *Introduction.*

The work described in the present paper is a continuation of that described in two previous communications⁽¹⁾,⁽²⁾ from this Laboratory on the measurement of dielectric constants (d.c.). The aim of the work as a whole has been to supplement the standard work of Hartshorn and Oliver⁽³⁾ on the determination of the d.c. of benzene by determining with an accuracy of one or two parts in a thousand, the d.c's. of a number of liquids which are chemically stable and which can be purified fairly easily. These liquids can then be regarded as secondary standards to supplement benzene (the primary standard) for purposes such as calibrating condensers for the measurement of d.c's. and dipole moments. The first paper⁽¹⁾ of the present series (hereafter quoted as I.) gave an account of the measurement of the d.c. of carbon tetrachloride and chloroform, benzene being used as a standard. The second paper⁽²⁾ (hereafter quoted as II.) dealt with the measurement of the d.c. of chlorobenzene and ethylene dichloride, carbon tetrachloride being used as a standard. These two papers thus dealt with liquids of d.c. varying from about 2·2 to about 10·4 ; in the present paper the range of d.c. is extended by the use of methyl alcohol, water, and various methyl alcohol-water mixtures, thus covering a range of d.c. from about 34 to about 81.

The method used in the present work is essentially the same as that described in I. and II. ; the method is a comparison method, employing a resonant circuit at radio frequencies. Omitting the apparatus used to detect resonance, the main features of the method and apparatus are shown in fig. 1, in which O represents the output coil of the radio frequency oscillator V.O. described in I., p. 11; D represents the coupling coil of the resonant circuit, D and O being enclosed in a screening box which is shown dotted in fig. 1. M represents the main coil of the resonant circuit, $C_1$ the variable condenser system, and C the d.c. condenser, which can be switched into or out of circuit by means of the key K. The screening arrangements are similar to those described in I. The experimental data necessary for the evaluation of d.c's. are the values of the capacitance of $C_1$, with and without C in circuit; in the standardization experiments C is filled first with air and then with the standardizing liquid; later, similar data are obtained when C is filled with air and then with the liquid under investigation.

---

* Communicated by Prof. E. J. Williams, F.R.S.

Fig. 1.

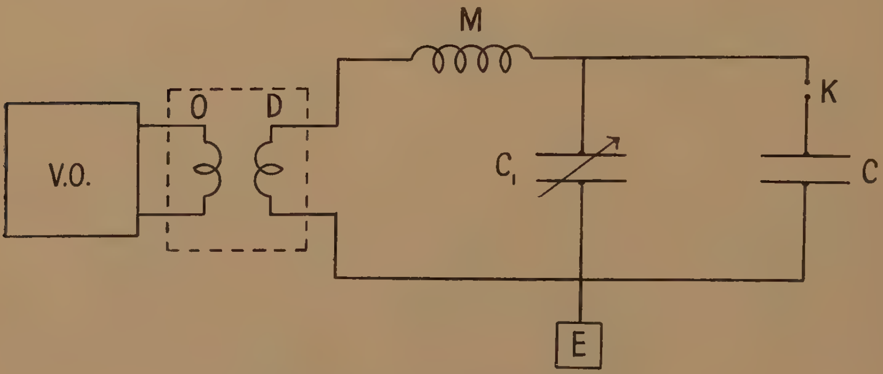

Arrangement of experimental circuit.

In the present work chlorobenzene has been used for standardization purposes on account of its stability and ease of purification; its d.c. has been assumed to have the values found in II., namely, 5·714 at 20° C. and 5·626 at 25° C.

As before, two different types of d.c. condenser have been used—a cylindrical and a parallel plate condenser; in order to keep the capacitance of the variable condenser system within reasonable limits when determining the d.c. of water, it becomes necessary to make the replaceable air capacitance of the d.c. condensers much less than before. This has been accomplished by constructing condensers of different dimensions, the designs remaining unchanged. For each condenser the key K of fig. 1 consisted of a simple plug switch of rigid construction, mounted directly on the condenser lid. The total capacitance of the parallel plate condenser was about 27 $\mu\mu$F., the replaceable air capacitance being about 19·5 $\mu\mu$F. ; the total capacitance of the cylindrical condenser was about 23 $\mu\mu$F., its replaceable air capacitance amounting to approximately 18·5 $\mu\mu$F.

In the work described in I. and II. the liquids were of very low electrical conductivity compared with the liquids used in the present work ; this implies that the equivalent shunt resistance of a d.c. condenser could previously be considered as infinite, whereas it must now be regarded as finite. This fact necessitates reconsideration of some experimental details and also of some points in connexion with the theory of the method. We shall first discuss the detection of resonance and then proceed to consider the effects of the leads in the various parts of the circuit.

## II. *Detection of Resonance.*

With liquids of low conductivity it is justifiable to use a vacuo-junction and galvanometer system, connected in series in the resonant circuit, to indicate resonance (I., p. 6). With liquids of higher conductivity this arrangement involves troublesome corrections, which are, however, avoided if resonance is detected by a high-impedance voltage measuring instrument, *e. g.*, a valve voltmeter, connected in parallel with the capacitance or inductance in the resonant circuit(4). The necessary theory has been given by Jezewski(5) and by Hartshorn and Ward(6), who consider the case of a resonant circuit such as that shown in fig. 2, consisting of a coil of inductance $L_0$, resistance $R_0$, together with a condenser of effective capacitance $C_0$ and equivalent shunt resistance R. Comparing figs. 1 and 2, it is seen that the coil $R_0$, $L_0$ of fig. 2 includes

Fig. 2.

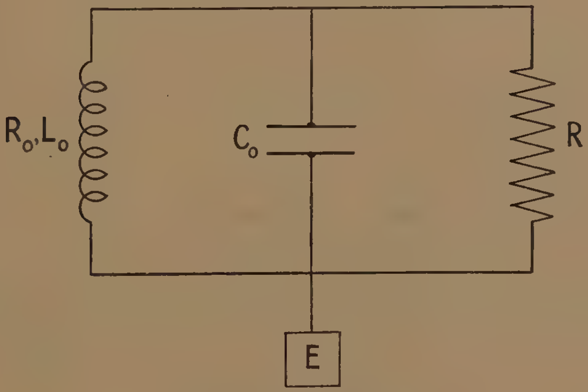

Resonant circuit.

the coupling coil D and the main coil M of fig. 1, together with their leads; the capacitance $C_0$ of fig. 2 includes the capacitances $C_1$ and C of fig. 1, together with various lead capacitances. Turning to the resistance R, when the d.c. condenser is out of circuit or is in circuit, filled with air or standardizing liquid, R can be considered as infinite, but when the d.c. condenser is in circuit and is filled with the liquids now under investigation, R must be considered as finite.

If the pulsatance $(=2\pi \times \text{frequency})$ is $\omega$ it is shown that the p.d. V across $C_0$ of fig. 2 has a maximum or resonant value $V_r$ when $C_0$ is equal to $C_r$ which is given by the equation

$$C_r = \frac{L_0}{R_0^2+\omega^2 L_0^2} . \qquad \qquad (2.1)$$

$C_r$ is thus independent of the value of the shunt resistance R and all corrections due to the finiteness of the value of R are avoided.

Further, it can be shown(6) that if $C_a$ and $C_b$ be two different values of $C_0$ ($C_a<C_r$, $C_b>C_r$) giving equal values of V, *i. e.*, equal deflexions in the valve voltmeter, then $C_r=\frac{1}{2}(C_a+C_b)$. As in the case discussed in I. (p. 9), an indirect determination of $C_r$ in this way is more accurate than a direct determination carried out by finding the value of $C_0$, which gives maximum V.

For these reasons the voltage method of detecting resonance was adopted in the present work, the value of $C_r$ being determined by the equal deflexion method.

Considering the effect of the shunt resistance R in the circuit of fig. 2, it can be shown that when R becomes finite, both the sharpness of tuning of the circuit and the resonance value of the p.d. across $C_0$ will decrease.

In order to discuss the question of sharpness of tuning, consider the resonance curve obtained by plotting the valve-voltmeter deflexion, *d*, say, as ordinate against the capacitance $C_0$ of fig. 2 as abscissa; let $d_r$ be the deflexion at resonance. Since the voltmeter is a square-law instrument, *d* will be proportional to $V^2$; consider a deflexion *d* such that $d=d_r/q$. Let $C_a$ and $C_b$ be the two values of $C_0$($C_a<C_r$, $C_b>C_r$) which give the deflexion *d* and let $\Delta C=C_b-C_a$; $\Delta C$ is thus the width of the resonance curve for a deflexion *d*. Then, as shown by Hartshorn and Ward (*loc. cit.*, equation (6)),

$$\Delta C = \frac{2\sqrt{q-1}}{\omega}\left\{\frac{R_0}{R_0^2+\omega^2 L_0^2}+\frac{1}{R}\right\} . \qquad \qquad (2.2)$$

For given values of $q$, R, $R_0$, and $L_0$, it is clear that $\Delta C$ increases when $\omega$ decreases, and it is therefore advantageous from the present standpoint to use as high a frequency as possible. It is also seen that the smaller the value of R, *i. e.*, the higher the conductivity of the liquid, the flatter the tuning. It is interesting to compare the widths of the resonance curves, at given values of $q$ and $\omega$ with the d.c. condenser filled first with air and then with water. Under these circumstances, let $\Delta C_a$ be the value of $\Delta C$ when the d.c. condenser is filled with air ($R=\infty$) and $\Delta C_w$ its value with water ($R\neq\infty$). It follows from equation (2.2) that

$$\frac{\Delta C_w}{\Delta C_a}=1+\frac{R_0^2+\omega^2L_0^2}{RR_0}. \qquad (2.3)$$

In the present experiments $R_0\doteqdot 2{\cdot}5$ ohm, $L_0\doteqdot 50\,\mu$H., $\omega\doteqdot 4{\cdot}2\times10^6$, giving $\omega L_0\doteqdot 210$, so that $R_0^2$ can be neglected in comparison with $\omega^2L_0^2$. To evaluate R we may use the well-known result for the resistance R of a condenser of capacitance C when filled with liquid of d.c. $\epsilon$ and conductivity $\kappa$. If C be expressed in farads, R in ohms, $\kappa$ in ohm$^{-1}$ . cm.$^{-1}$, then

$$R=8{\cdot}84\times10^{-14}\epsilon/\kappa C.$$

For the purpose of illustration we may take the case of the parallel plate condenser filled with water, with $C\doteqdot 1600\,\mu\mu$F., $\kappa\doteqdot 10^{-6}$ ohm$^{-1}$.cm.$^{-1}$, $\epsilon\doteqdot 80$, giving $R\doteqdot 4400$ ohm. Using these values, it is found from equation (2.3) that $\Delta C_w$ is approximately five times $\Delta C_a$.

Considering next the effect of the finite value of R on the p.d., $V_r$, developed across the condenser system at resonance, we may use an equation given by Jezewski for the circuit of fig. 2. If $E_0$ be the e.m.f. induced in the resonant circuit, then

$$V_r=\frac{E_0}{\dfrac{\sqrt{R_0^2+\omega^2L_0^2}}{R}+\dfrac{R_0}{\sqrt{R_0^2+\omega^2L_0^2}}}. \qquad (2.4)$$

If $V_{r1}$ be the value of the resonance p.d. when R is infinite, $V_{r2}$ its value when R is finite, then, neglecting $R_0^2$ in comparison with $\omega^2L_0^2$ as before, it is easy to show that

$$\frac{V_{r1}}{V_{r2}}=1+\frac{\omega^2L_0^2}{RR_0}. \qquad (2.5)$$

To the present degree of accuracy the right-hand sides of equations (2.3) and (2.5) are identical, and thus, for the parallel plate condenser filled with water, the ratio of $V_{r1}$ to $V_{r2}$ is about 5, the ratio of the corresponding voltmeter deflexions being about twenty-five.

This effect gives rise to a serious experimental difficulty since, in the course of the experiments, it is necessary to find resonance settings, first with the d.c. condenser out of circuit ($R=\infty$) and then, immediately after, with the d.c. condenser, filled with water, in circuit ($R\neq\infty$).

Some method of overcoming this difficulty is necessary. One method would be to alter the coupling between the oscillator and the resonant circuit when taking the two resonance settings; as will be seen from fig. 1, this would imply altering the position of the coupling coil within its screening box; in turn, this would change the "stray" capacitance in the circuit, whereas it is essential that this capacitance should remain constant.

Another possible method would be to use an insensitive galvanometer in the anode circuit of the valve voltmeter when taking the setting without d.c. condenser, and substituting a more sensitive instrument when taking the setting with the d.c. condenser in circuit. In practice this method is unsuccessful, since the rectified anode current is small in one case and large in the other; consequently, when taking a series of alternate readings in quick succession, the anode dissipation of the valve is continually being altered and the voltmeter is unsteady.

Fig. 3.

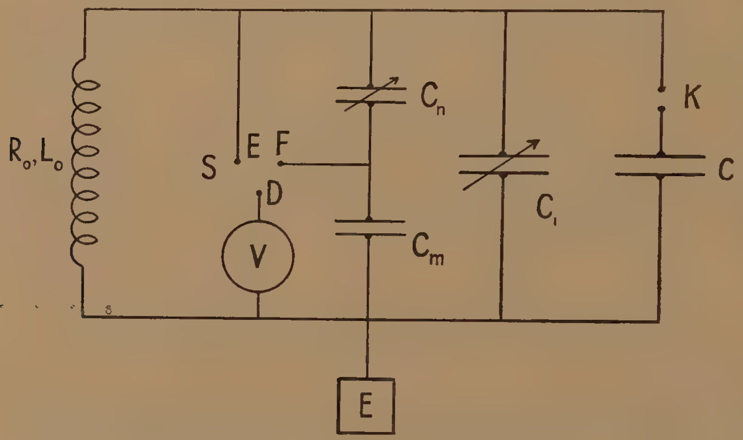

The capacitance potential divider.

The method finally adopted can be illustrated by means of fig. 3, which has been lettered to correspond with figs. 1 and 2, C representing the d.c. condenser, K its switch, and $C_1$ the variable condenser system. Two condensers, $C_m$ and $C_n$, are connected in series across $C_1$, forming a capacitance potential divider; $C_m$ is a fixed mica condenser whose capacitance is approximately 100 $\mu\mu$F., whilst $C_n$ is a variable air condenser whose capacitance can be varied between 5 and 35 $\mu\mu$F. By connecting the points D and E of the two-way switch S, the full p.d. developed across the resonant circuit is applied between the terminals of the valve voltmeter V; when the points D and F are connected together, the fraction $C_n/(C_m+C_n+C_v)$ of the full p.d. is applied to the valve voltmeter, $C_v$ being the capacitance of the latter. Thus, with a given liquid in C, if D and F are connected together when C is out of circuit, and if D and E are connected together when C is in circuit, the voltmeter deflexions can be made approximately equal by varying $C_n$. When working with a liquid of different conductivity, the equivalent shunt resistance of C will be different; in this case, the deflexions can again be equalized by varying $C_n$.

Since V is connected across $C_m$ in one case, whilst it is connected across $C_m$ and $C_n$ in series in the other, the condition for resonance will be different in the two cases.

Consider first the voltmeter connected across $C_m$, C being out of circuit. Let $C_{v1}$ be the capacitance of the valve voltmeter together with the appropriate portion of the switch S; let $C_f$ be the fixed "stray" capacitance in the circuit and C′ the capacitance of the lead from the insulated terminal of $C_1$ to the switch K. Then it can be shown (*vide* Appendix) that the p.d. across $C_m$ will be a maximum when $C_1$ has the value $C_{1a}$ given by the equation

$$C_f+C_{1a}+C'+\frac{C_n(C_m+C_{v1})}{C_m+C_n+C_{v1}}=\frac{L_0}{R_0^2+\omega^2L_0^2}. \quad . \quad . \quad . \quad (2.6)$$

Next consider the voltmeter connected across $C_m$ and $C_n$, C being in circuit. The condition for maximum p. d. between the voltmeter terminals can be derived from equation (2.1), and if $C_{1b}$ is the value of the variable condenser capacitance and $C_{v2}$ the joint capacitance of the voltmeter and the appropriate portion of S, then

$$C_f+C_{1b}+C'+C+C_{v2}+\frac{C_mC_n}{C_m+C_n}=\frac{L_0}{R_0^2+\omega^2L_0^2}. \quad . \quad . \quad (2.7)$$

It should be noticed that $C_{v1}$ and $C_{v2}$ are not necessarily equal since the bridge of the switch S is moved inside its earthed screen in going from one position to the other.

If

$$\Delta=C_{v2}+\frac{C_mC_n}{C_m+C_n}-\frac{(C_m+C_{v1})C_n}{C_m+C_n+C_{v1}}, \quad . \quad . \quad . \quad . \quad . \quad . \quad (2.8)$$

then it follows, from equations (2.6) and (2.7), that

$$C=C_{1a}-C_{1b}-\Delta. \quad . \quad . \quad . \quad . \quad . \quad . \quad . \quad . \quad (2.9)$$

Thus C is determined not only by $C_{1a}$ and $C_{1b}$, but also by $C_{v1}$, $C_{v2}$, $C_m$, and $C_n$; $\Delta$, which is a positive quantity, may be regarded as a correction to the apparent capacitance, $C_{1a}-C_{1b}$, of C.

The present procedure thus involves the determination of $\Delta$ as well as the two settings of the variable condenser system. The simplest method of determining $\Delta$ is to make C zero, which gives $\Delta=C_{1c}-C_{1d}$ where $C_{1c}$ and $C_{1d}$ are the variable condenser capacitances at resonance, corresponding respectively to the connexions D to F and D to E of S. In the actual experiments the value of $\Delta$ was determined immediately after each experimental run by this method; the key K was left open and resonance obtained for the two positions of the switch S, a sensitive Tinsley galvanometer being used in the valve voltmeter for the connexion D to F and a Unipivot instrument for the connexion D to E. As regards the statement made above as to the unsteadiness of the valve voltmeter when used with two indicating instruments of different sensitivities, it should be pointed out that this is of little importance in determining $\Delta$, since only moderate accuracy is required on account of the smallness of $\Delta$ in comparison with $C_{1a}-C_{1b}$. With water, for example, $C_{1a}-C_{1b}\doteqdot 1550\,\mu\mu\text{F}$. for the parallel plate condenser, whilst $\Delta=20\,\mu\mu\text{F}$.; it is easy to determine $\Delta$ within less than $0{\cdot}2\,\mu\mu\text{F}$., which gives ample accuracy.

In conjunction with the equal deflexion method the procedure which has just been described enabled resonance settings to be determined with excellent precision; experimental conditions were most unfavourable when water was used in the d.c. condenser, and even under these conditions independent determinations of C gave results which never differed from each other by more than 0·03 per cent.; the precision of the mean was a good deal better than this, since some fifteen or twenty independent determinations were usually made.

## III. *The Effect of Lead Inductance.*

It is well known that the effective or apparent value of a circuit component can differ from its true value on account of the leads which are used to connect the component to the remainder of the circuit. With a condenser the important factor is the inductance of the leads, since their capacitance can usually be eliminated. The inductance of the leads always causes the effective capacitance of a condenser to be greater than its true value, the magnitude of the effect increasing with increasing frequency. In order to minimize the effect it is therefore necessary to use comparatively low frequencies; on the other hand, it has already been seen that it is advisable to use comparatively high frequencies in order to obtain sharp tuning. In practice this means that the frequency used in an experiment must be a compromise and that the lead inductance correction must be taken into consideration. Preliminary experiments showed that in the worst case (water) the lowest frequency which gave sufficiently sharp tuning was of the order of 680 kc./sec. ($\lambda=440$ m.), and frequencies of this order were used throughout the experiments.

The effect of lead inductance is complicated by the fact that the liquids investigated had comparatively high conductivity, and it is thus necessary to consider the general case of leads of inductance $L'$ and capacitance $C'$, terminated by a condenser of capacitance C, whose equivalent shunt resistance is R. If $\omega$ be the pulsatance and if $C_s$ and $R_s$ be the effective capacitance and shunt resistance of the arrangement (measured from the input terminals of the leads), then it can be shown⁽⁷⁾ that

$$\left.\begin{aligned} C_s &= \frac{(C+C')(1-\omega^2L'C)-\dfrac{L'}{R^2}}{(1-\omega^2L'C)^2+\dfrac{\omega^2L'^2}{R^2}}, \\ R_s &= R(1-\omega^2L'C)^2+\frac{\omega^2L'^2}{R^2}. \end{aligned}\right\} \quad . \quad . \quad . \quad . \quad . \quad . \quad (3.1)$$

Since the voltage method of detecting resonance does not involve the shunt resistance, it is unnecessary to consider $R_s$ in detail. In connexion with $C_s$, we shall first estimate the importance of the terms involving R; it will be sufficient to consider the worst case—water. With the parallel plate condenser, $C \doteqdot 1600\,\mu\mu F.$, $R \doteqdot 4400$ ohm, $L'=3\times10^{-7}$ H., $C'=10\,\mu\mu F.$, $\omega=4{\cdot}2\times10^6$. Considering the numerator, $(C+C')(1-\omega^2L'C) \doteqdot 1{\cdot}6\times10^{-9}$, which is large in comparison with $L'/R^2 \doteqdot 1{\cdot}5\times10^{-14}$. In the denominator, $\omega^2L'^2/R^2 \doteqdot 8{\cdot}2\times10^{-8}$, which is small in comparison with $(1-\omega^2L'C)^2$, which is of the order of 0·98. Thus, even in the worst case, the terms in question have a negligible effect and equation (3.1) reduces to the well-known equation

$$C_s=(C+C')/(1-\omega^2L'C) \quad . \quad . \quad . \quad . \quad . \quad . \quad . \quad (3.2)$$

to a sufficient degree of accuracy.

The leads used were sufficiently short to allow terms of the form $\omega^2L'C'$ to be neglected in comparison with unity and to allow the distributed characteristics to be replaced by lumped characteristics (*vide* ref. ⁽⁷⁾, p. 79); when this is done the circuit of fig. 1 is equivalent to that shown in fig. 4, in which A and B represent the terminals of the valve voltmeter V. The portion of the circuit to the left of AB represents those parts of the circuit which remain unaltered during an experiment; these parts are equivalent to a coil of inductance $L_0$, resistance $R_0$, shunted by the fixed capacitance $C_f$. The coil $L_0$, $R_0$ comprises the main coil of the resonant circuit, the coupling coil, and also the inductance of the various leads in this part of the circuit; the capacitance $C_f$ is composed of capacitances such as the lead capacitances, the self-capacitances of the coils, and the valve-voltmeter capacitance. The portion of the circuit to the right of AB consists of the variable condenser system of capacitance $C_1$ and the d.c. condenser of capacitance C, the latter being switched into or out of circuit by means of the switch K. The leads from AB to the terminals D, E, of $C_1$ are assumed to have inductance $L_1'$ and capacitance $C_1'$, whilst the leads from D and E to the d.c. condenser are supposed to have capacitance $C'$ and inductance $L'$. In order to agree with the notation used in I. and II., we shall assume $L'$ to be the inductance from D to the point where it is attached to the insulated plate of the d.c. condenser (*i. e.*, the lower end of C in fig. 1 of II. and of H in fig. 2 of II.); on the other hand, C′ will be regarded as the capacitance from D to the key K, the capacitance from K onwards being therefore included in C (*cf.* I., p. 5). As we have already shown, it is unnecessary to consider the shunt resistance of C when discussing resonance conditions.

When the circuit is adjusted to resonance, first with K open and then with K closed, it follows from equation (2.1) that the total capacity between the terminals of the valve voltmeter will remain constant, and therefore that the capacitance to the right of AB will remain constant.

Let $C_{1a}$ be the value of the variable condenser capacitance when K is open and $C_{1b}$ its value when K is closed.

Fig. 4.

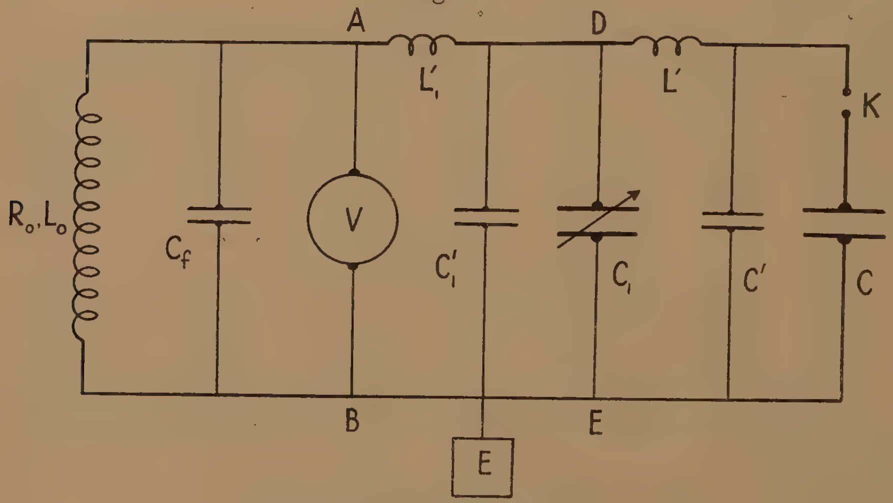

The effect of lead inductances.

First let us neglect the lead inductances, but take into account the lead capacitances; then

$$C_{1a}+C_1'+C'=C_{1b}+C_1'+C'+C,$$

giving

$$C_{1a}-C_{1b}=C. \quad \ldots \ldots \ldots \quad (3.3)$$

Next let us allow for the inductance L′ of the leads from D and E to C, but neglect for the moment the inductance $L_1'$ of the leads from A and B to D and E; using equation (3.2) to find the effective capacitance of C with its leads, we have

$$\begin{aligned} C_{1a}+C_1'+C' &= C_{1b}+C_1'+(C+C')/(1-\omega^2L'C) \\ &= C_{1b}+C_1'+(C+C')(1+\omega^2L'C), \end{aligned}$$

since the maximum value assumed by $\omega^2 L'C$ is 0·009, and we may therefore neglect squares and higher powers.

Usually $C'$ is small in comparison with C and $C_{1b}$, so that $C'(1+\omega^2 L'C)$ may be equated to $C'$ with sufficient accuracy. With these simplifications we obtain the equation commonly employed, namely,

$$C=(C_{1a}-C_{1b})(1-\omega^2 L'C). \quad . \quad . \quad . \quad . \quad . \quad . \quad . \qquad (3.4)$$

It is not immediately obvious that the use of this equation is justified, since we have neglected the lead inductance $L_1'$. When both $L'$ and $L_1'$ are taken into consideration, the effective capacitance to the right of AB, with K open, is

$$C'+(C_{1a}+C_1')/(1-\omega^2 L_1' C_{1a}). \quad . \quad . \quad . \quad . \quad . \quad . \qquad (3.5)$$

When K is closed, the effective capacitance to the right of DE is

$$(C+C')/(1-\omega^2 L'C),$$

and this is in parallel with the capacitance $(C_{1b}+C_1')$, the whole being in series with the inductance $L_1'$. If we neglect the terms $\omega^2 L_1' C_1'$ and $\omega^2 L'C'$, it follows that the effective capacitance to the right of AB, with K closed, is

$$\frac{C_{1b}+C_1'+(C+C')/(1-\omega^2 L'C)}{1-\omega^2 L_1'(C+C_{1b})}. \quad . \quad . \quad . \quad . \quad . \quad . \qquad (3.6)$$

If we assume $\omega^2 L_1'(C+C_{1b})$ and similar terms to be small, and if we neglect the products of these terms with $C_1'$ and $C'$, equating (3.5) and (3.6), we obtain

$$C=\frac{C_{1a}[1+\omega^2 L_1' C_{1a}]-C_{1b}[1+\omega^2 L_1'(C_0+C_{1b})]}{1+\omega^2[L'C+L_1'(C+C_{db})]}. \quad . \quad . \quad . \qquad (3.7)$$

In the small correction term $\omega^2 L_1'(C+C_{1b})$ it is legitimate to assume that the approximate equation (3.3) holds and write $C+C_{1b}=C_{1a}$; equation (3.7) then reduces to

$$C=(C_{1a}-C_{1b})(1-\omega^2 L'C),$$

which justifies the use of equation (3.4).

We now turn to consider the effect of the lead inductance $L_1'$ on the capacitance of the variable condenser system $C_1$, since it is known that lead inductance may cause the slope, *i. e.*, the capacitance per degree rotation, of a linear-law condenser to vary with scale reading (*cf.* reference (7), p. 90). In the present work the variable condenser system consisted of three condensers in parallel—a small Sullivan variable condenser, a large Sullivan variable condenser, and a third variable condenser which was kept constant during a particular d.c. measurement and which was used as a loading condenser to bring the total capacitance in the circuit to a suitable value. The small Sullivan condenser gave a capacitance change of 1·45 $\mu\mu$F. per degree rotation and a useful range of 80 to 260 $\mu\mu$F., whilst the large Sullivan condenser had a nominal slope of 7 $\mu\mu$F. per degree rotation with a useful range of 100 to 1200 $\mu\mu$F. A d.c. measurement by the present method is a relative measurement and the capacitance unit may have any convenient value; as in I. and II., the unit adopted here is the mean value of the capacitance per degree rotation of the small Sullivan condenser. It is interesting to know whether the slope of the small Sullivan condenser will be affected by the lead inductance under the conditions prevailing in the present work.

In this connexion, we use equation (6.3) of reference (7), namely,

$$b_s = b/[1-\omega^2 L'(a+b\theta)]^2, \quad \ldots \ldots \quad (3.8)$$

where $b$ is the slope when the lead inductance is negligibly small, $b_s$ the slope when the leads have inductance L′, $\theta$ the condenser scale reading, and $a$ the capacitance corresponding to zero scale reading, In the apparatus used $\omega$ was of the order of $4{\cdot}2\times10^6$, $b$ of the order of 1·45 $\mu\mu$F. per degree rotation, whilst $(a+b\theta)$ was about 260 $\mu\mu$F. at the highest setting used; L′ was calculated to be about $8\times10^{-8}$ H., and $\omega^2 L'(a+b\theta)$ about $3{\cdot}7\times10^{-4}$, giving $b/b_s=1{\cdot}0007$, which is considerably less than the intrinsic error of the condenser. In any event, the variation due to the leads is eliminated for any particular frequency by calibrating by the usual step-by-step method, maintaining the frequency constant and placing the calibrating condenser between the points A and B of fig. 4; in the present work it is possible to maintain the frequency constant during calibration by compensating an increase of capacitance in the small condenser by a decrease of capacitance in the large condenser, and *vice versa*.

It follows, in the same way, that the effective slope of the large Sullivan condenser will be affected both by the inductance of the leads from A, B to the terminals of the small condenser, and also by the inductance of the leads between the terminals of the large and small variable condensers; since the maximum capacitance of this condenser is about 1200 $\mu\mu$F., the lead effect will become important. In this connexion it has to be remembered that it becomes necessary to calibrate the large condenser in terms of the small, and, in order to lighten this work, the large condenser is used only as a semi-variable condenser, changes in its capacitance being made only between suitably-placed scale readings. Owing to lead effects, the number of degrees on the small condenser which correspond to a given interval on the large will vary with wave-length. The effect was eliminated in the present work by keeping the wave-length constant during the actual d.c. determination and during the subsequent condenser calibration; with the condenser system used here this procedure is made possible by the provision of the loading condenser, which is manipulated so as to maintain the total circuit capacitance constant.

We turn next to consider the effect of the leads to the d.c. condenser; this effect is likely to be appreciable, since the capacitance of the d.c. condenser will vary from about 20 $\mu\mu$F. (when the d.c. condenser contains air) to about 1600 $\mu\mu$F. (when the d.c. condenser is filled with water).

Consider the d.c. condenser filled first with air and then with the standardizing liquid of d.c. $\epsilon_s$. When the d.c. condenser is filled with air, let the capacitance of the variable condenser system at resonance, without and with the d.c. condenser in circuit, be $C_{1a}$ and $C_{1b}$ respectively. Assuming that the appropriate calibration corrections have been applied to the readings of the variable condensers, in the way described above, the effects of the inductance of the leads from A, B, to D, E (fig. 4) are accounted for. Hence, if $C_{as}$ be the true capacitance of the d.c. condenser, measured from the key K onwards, when filled with air, from equation (3.4),

$$C_{as}/(1-\omega_s^2L'C_{as})=C_{1a}-C_{1b}=D_{as} \text{ (say)}, \quad . \quad . \quad . \quad (3.9)$$

where $\omega_s$ is the pulsatance and L′ is the inductance of the leads from the variable condenser system to the d.c. condenser, as defined above.

For $C_{as}$ we have (I., p. 5) that

$$C_{as}=C_{ra}+C_d+C_k, \quad . \quad . \quad . \quad . \quad . \quad . \quad . \quad (3.10)$$

where

$C_{ra}$=the "replaceable" air capacitance of the condenser;

$C_d$=the capacitance of the condenser due to the solid dielectric used to separate the insulated and earthed plates;

$C_k$=the capacitance of the lead, measured from the key K (fig. 4) to the point where the lead will enter the liquid when the d.c. condenser will contain liquid.

When the d.c. condenser is filled with standardizing liquid, let the capacitance of the variable condenser system at resonance without and with the d.c. condenser in circuit be $C_{1c}$ and $C_{1d}$ respectively. Since the determination of these settings is carried out within a short time of the determination of $C_{1a}$ and $C_{1b}$, we may take the pulsatance as $\omega_s$. If $C_s$ be the true capacitance of the d.c. condenser, measured from the key K onwards,

$$C_s/(1-\omega_s^2L'C_s)=C_{1c}-C_{1d}=D_s \text{ (say)} \quad . \quad . \quad . \quad . \quad (3.11)$$

and

$$C_s=\epsilon_sC_{ra}+C_d+C_k. \quad . \quad . \quad . \quad . \quad . \quad . \quad . \quad (3.12)$$

As before, we may neglect squares and higher powers of terms involving $\omega_s^2L'$ as a factor; we thus obtain, from equations (3.9) and (3.10),

$$D_{as}=C_{ra}+C_d+C_k+\omega_s^2L'C_{as}^2=\frac{C_{as}}{1-\omega_s^2L'C_{as}}, \quad . \quad . \quad (3.13)$$

and from equations (3.11) and (3.12)

$$D_s=\epsilon_s C_{ra}+C_d+C_k+\omega_s^2 L' C_s^2=\frac{C_s}{1-\omega_s^2 L' C_s}, \quad . \quad . \quad . \quad (3.14)$$

whence

$$D_s-D_{as}=(\epsilon_s-1)C_{ra}+\omega_s^2 L'(C_s^2-C_{as}^2). \quad . \quad . \quad . \quad (3.15)$$

From equations (3.12) and (3.10)

$$C_s-C_{as}=(\epsilon_s-1)C_{ra},$$

and from equations (3.13) and (3.14)

$$C_s+C_{as}=D_s(1-\omega_s^2 L' C_s)+D_{as}(1-\omega_s^2 L' C_{as}).$$

Multiplying these two expressions we obtain the value of $(C_s^2-C_{as}^2)$, and since this quantity is involved only in a small correction term, we may take the coefficients of $D_s$ and $D_{as}$ in the expression for $(C_s+C_{as})$ as unity. This gives

$$(C_s^2-C_{as}^2)=(\epsilon_s-1)C_{ra}(D_{as}+D_s) \quad . \quad . \quad . \quad . \quad . \quad (3.16)$$

In conjunction with equation (3.15) this equation gives

$$C_{ra}=\frac{D_s-D_{as}}{\epsilon_s-1}[1-\omega_s^2 L'(D_{as}+D_s)]. \quad . \quad . \quad . \quad . \quad (3.17)$$

which enables $C_{ra}$ to be determined from experimentally observed quantities.

If the lead-correction be neglected, the apparent value $C'_{ra}$ of the replaceable air capacitance is

$$C'_{ra}=\frac{D_s-D_{as}}{\epsilon_s-1}, \quad . \quad . \quad . \quad . \quad . \quad . \quad . \quad . \quad (3.18)$$

and the relation between the real and apparent values of the replaceable air capacitance is

$$C_{ra}=C'_{ra}[1-\omega_s^2 L'(D_{as}+D_s)]. \quad . \quad . \quad . \quad . \quad . \quad (3.19)$$

In calculating experimental results it is often convenient to evaluate $C'_{ra}$ first from equation (3.18); $C_{ra}$ can then be calculated using equation (3.19).

Consider next the d.c. condenser filled with a liquid of unknown d.c. $\epsilon$; the pulsatance in this experiment will not necessarily be the same as that in the standardization experiment, and so let the pulsatance now be $\omega$.

Let $D_{au}$ be the difference between the capacitances of the variable condenser system without and with the d.c. condenser filled with air; let $D_u$ be the corresponding difference without and with the d.c. condenser filled with the liquid of unknown d.c.

Proceeding as before, we find an equation similar to equation (3.17), namely,

$$\epsilon-1=\frac{D_u-D_{au}}{C_{ra}}[1-\omega^2 L'(D_{au}+D_u)], \quad . \quad . \quad . \quad . \quad (3.20)$$

which, since $C_{ra}$ is now known, enables $\epsilon$ to be determined. This procedure has been used in the present work in the calculation of the d.c. of methyl alcohol, since a number of different frequencies were used in the standardization experiments, and also with the alcohol.

If it happens that the frequency used with the unknown liquid is the same as that used for standardization, *i. e.*, that $\omega_s=\omega$, the correction under discussion is simplified. Dividing equation (3.20) by equation (3.17), and remembering that $D_{au} \doteqdot D_{as}$ and that these two quantities can therefore be equated in the correction term involving $\omega^2 L'$, we obtain

$$\epsilon-1=\frac{(\epsilon_s-1)(D_u-D_{au})}{D_s-D_{as}}\cdot[1-\omega^2 L'(D_u-D_s)]. \quad . \quad . \quad (3.21)$$

The value of the d.c. of the liquid, calculated without taking the effect of lead inductance into consideration, may be termed the apparent d.c., $\epsilon'$ say. Then from equation (3.21)

$$\epsilon'-1=\frac{(\epsilon_s-1)(D_u-D_{au})}{D_s-D_{as}}=\frac{D_u-D_{au}}{C'_{ra}}, \quad . \quad . \quad . \quad . \quad . \quad (3.22)$$

which, when combined with equation (3.12), gives

$$\epsilon=\epsilon'-\omega^2 L'(\epsilon'-1)(D_u-D_s). \quad . \quad . \quad . \quad . \quad . \quad . \quad (3.23)$$

From equation (3.14) and the corresponding equation for $D_u$, in the correction term in equation (3.23), we may write

$$D_u-D_s=(\epsilon-\epsilon_s)C_{ra}=(\epsilon'-\epsilon_s)C'_{ra} \quad . \quad . \quad . \quad . \quad . \quad . \quad (3.24)$$

without appreciable error. From equations (3.23) and (3.24)

$$\epsilon=\epsilon'-\omega^2 L' C'_{ra}(\epsilon'-\epsilon_s)(\epsilon'-1). \quad . \quad . \quad . \quad . \quad . \quad . \quad (3.25)$$

In the present work equations (3.22) and (3.25) have been used for calculating the d.c's. of water and the alcohol-water mixtures, since, with one exception, all readings were taken at the same frequency.

As to the order of magnitude of the correction term, this is a maximum for the parallel plate condenser filled with water; at about 20° C., $\epsilon' \doteqdot 81{\cdot}0$, $\epsilon_s \doteqdot 5{\cdot}7$; $\omega \doteqdot 4{\cdot}2\times10^6$; $L' \doteqdot 3\times10^{-7}$ H.; $C'_{ra} \doteqdot 19{\cdot}6\ \mu\mu$F., giving $\omega^2 L' C'_{ra}(\epsilon'-\epsilon_s)(\epsilon'-1) \doteqdot 0{\cdot}62$. In this case the correction is very important, amounting to about 0·75 per cent. of the value of the d.c.

In order to evaluate the lead inductance $L'$ for applying this correction, a small size, " wireless " mica condenser, $C_m$, whose capacitance was about 1400 $\mu\mu$F. was used. The leads used to connect $C_m$ in circuit were made as short as possible, so that their inductance could be neglected and, when possible, the position of $C_m$ was kept fixed. It has been seen that $L'$ consists of the inductance of the lead from the insulated terminal of the small variable condenser to the insulated terminal of the d.c. condenser, and, in addition, the lead from the condenser terminal to its insulated plate. In order to include the latter, replicas of the condenser lids, cases, and insulated leads were made for both d.c. condensers ; in each instance the bottom of the case was left open so that $C_m$ could be inserted or taken out of circuit at the lower end of the lead.

To evaluate L′, the lead capacitance C′ was first evaluated by finding the variable condenser settings at resonance, first with the lead in circuit, and then with the lead disconnected at the variable condenser terminal.

The lead was then disconnected and the value of $C_m$ found by finding the variable condenser settings at resonance, first with $C_m$ connected at the variable condenser terminal, and then with $C_m$ disconnected.

Finally, with the lead connected, $C_m$ was connected at the lower end of the lead as described above, and from the resonance settings of the variable condenser system with this arrangement and with $C_m$ disconnected it is possible to find the effective capacitance of $C_m$ together with its leads, *i. e.*, the quantity $(C_m+C')/(1-\omega^2 L'C_m)$. Then, knowing $\omega$, it becomes possible to evaluate L′. For both condensers experiments were carried out with two values of $\omega$ which were used in the d.c. experiments, namely, $4{\cdot}76_5$ and $4{\cdot}22_1\times10^6$. For the parallel plate condenser leads the values of L′ so determined were $2{\cdot}95$ and $3{\cdot}11\times10^{-7}$ H, and for the cylindrical condenser leads, $2{\cdot}36$ and $2{\cdot}50\times10^{-7}$ H. The discrepancy between the two individual results for L′ does not lead to a very large error in the final value of the d.c., since L′ is only involved in a correction term. For example, with the parallel plate condenser filled with water, using the data given above, the correction term in equation (3.25) amounts to 0·61 if L′ is $2{\cdot}95\times10^{-7}$ H. and to 0·64 if L′ be $3{\cdot}11\times10^{-7}$ H. ; in the final value of $\epsilon$ this corresponds to a discrepancy of about 0·04 per cent. For the calculation of the correction the mean values of L′ were used, namely, 3·03 and $2{\cdot}43\times10^{-7}$ H. for the parallel plate and cylindrical condensers respectively.

## IV. *References.*

(1) Davies, Phil. Mag. xxi. p. 1 (1936).
(2) Davies, Phil. Mag. xxi. p. 1008 (1936).
(3) Hartshorn and Oliver, Proc. Roy. Soc. cxxiii. p. 664 (1929).
(4) Lattey and Gattey, Phil. Mag. vii. p. 985 (1929).
(5) Jezewski, *Zeit. für Phys.* xliii. p. 442 (1927) and xlviii. p. 123 (1928).
(6) Hartshorn and Ward, J. I. E. E. lxxix. p. 597 (1936).
(7) Davies, Phil. Mag. xx. p. 75 (1935).

---

## APPENDIX.

### *The Calculation of the Resonance Condition with the Capacitance Potential Divider.*

When the valve voltmeter is connected across $C_m$ of fig. 3, the circuit becomes equivalent to that shown in fig. 5, in which the main and coupling coils of the resonant circuit are represented by the coil $R_0$, $L_0$. $C_m$ and

$C_n$ are the condensers which constitute the capacitance potentiometer, $C_{v1}$ represents the capacitance of the valve voltmeter, and $C_t$ the capacitance of the remainder of the circuit. In the notation used in connexion with fig. 3, $C_t$ is the sum of the fixed "stray" capacitance $C_f$, the variable condenser capacitance $C_{1a}$, and the lead capacitance $C'$.

Let the instantaneous values of the currents in the various branches of the resonant circuit be $i$, $i_1$, $i_2$, $i_3$, and $i_4$, as indicated in the diagram; let $e$ be the instantaneous value of the e.m.f. induced into the circuit and $v$ the p.d. between the terminals of the valve voltmeter, *i. e.*, between the points Q and R.

Fig. 5.

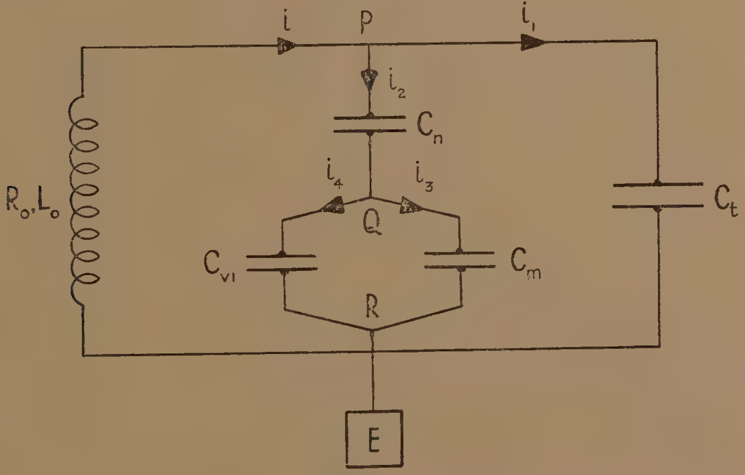

Let $C_p$ be the total capacitance between P and R through Q, *i. e.*, the capacitance of $C_n$ in series with $C_m$ and $C_n$ in parallel; then

$$C_p = C_n(C_m + C_{v1})/(C_m + C_n + C_{v1}). \quad . \quad . \quad . \quad . \quad . \quad (A.\ 1)$$

Considering the main current $i$, we have

$$i = \frac{e}{R_0 + j\omega L_0 + \dfrac{1}{j\omega(C_t + C_p)}}, \quad . \quad . \quad . \quad . \quad . \quad (A.\ 2)$$

where $j$ is the imaginary, $\sqrt{-1}$.

For the currents in the various branches we find

$$\frac{i_1}{j\omega C_t} = \frac{i_2}{j\omega C_p}; \quad v = \frac{i_3}{j\omega C_m} = \frac{i_4}{j\omega C_{v1}},$$

$$i_2 = i_3 + i_4 = j\omega v(C_m + C_{v1}),$$

giving, finally,

$$i = i_1 + i_2 = j\omega v(C_m + C_{v1})(C_t + C_p)/C_p. \quad . \quad . \quad . \quad . \quad (A.\ 3)$$

Eliminating $i$ from equations (A. 2) and (A. 3), we find that

$$\frac{v}{e}=\frac{C_p}{C_m+C_{v_1}}\cdot\frac{1}{[1-\omega^2L_0(C_t+C_p)]+j\omega R_0(C_t+C_p)}\quad . \; . \; . \quad (\mathrm{A.}\ 4)$$

If E and V are the virtual values of the e.m.f. induced in the resonant circuit and of the p.d. across the valve voltmeter respectively,

$$V=\frac{C_p}{C_m+C_{v_1}}\cdot\frac{E}{\sqrt{\{[1-\omega^2L_0(C_t+C_p)]^2+\omega^2R_0{}^2(C_t+C_p)^2\}}}\quad . \; . \quad (\mathrm{A.}\ 5)$$

Under experimental conditions all quantities on the right-hand side of this equation remain constant with the exception of $C_t$, which is varied until V is a maximum. If we write

$$F=[1-\omega^2L_0(C_t+C_p)]^2+\omega^2R_0{}^2(C_t+C_p)^2,\quad . \; . \; . \; . \quad (\mathrm{A.}\ 6)$$

then V will be a maximum when F is a minimum. Differentiating F with respect to $C_t$ and equating to zero, we find that F is a minimum when $C_t$ has the value $C_{tr}$ given by

$$C_{tr}=\frac{L_0}{R_0{}^2+\omega^2L_0{}^2}-C_p,\quad . \; . \; . \; . \; . \; . \; . \quad (\mathrm{A.}\ 7)$$

and substituting from equation (A. 1), we find

$$C_{tr}+\frac{C_n(C_m+C_{v_1})}{C_m+C_n+C_{v_1}}=\frac{L_0}{R_0{}^2+\omega^2L_0{}^2},\quad . \; . \; . \; . \; . \quad (\mathrm{A.}\ 8)$$

from which equation (2.6) follows immediately.

# XXVII. *On the Determination of the Dielectric Constants of Liquids at Radio Frequencies.*—Part IV. *Methyl Alcohol, Water, and Alcohol Water Mixtures: Experimental.*

By T. Tyssul Jones, B.Sc., Ph.D., and R. M. Davies, D.Sc.,
Department of Physics, University College of Wales, Aberystwyth *.

[Received January 13, 1939.]

Contents.

Page
I. Introduction .............................. 307
II. Purification of Materials .................... 308
III. Experimental Results...................... 309
IV. Discussion of the Results and comparison with the results of previous investigations........ 322
V. References .............................. 327

## I. *Introduction.*

The first two papers of the present series ⁽¹⁾,⁽²⁾ (hereafter quoted as I. and II. respectively) have dealt with the measurement of the dielectric constant (d.c.) of carbon tetrachloride, chloroform, chlorobenzene, and ethylene dichloride, benzene being used as a standard. These papers describe an experimental procedure which has been found to give results of excellent accuracy, and, in the main, the experimental work described in the present paper is similar to that previously described. On account of the comparatively high conductivity of the liquids used here, certain modifications of the original procedure become necessary, and these have been discussed at length in Part III ⁽³⁾ (hereafter quoted as III.) of the series. It is thus only necessary, in the present paper, to discuss points in which the experimental work differs specifically from that described in I. and II.

In the previous work the refractive index (R.I.) of the liquids was determined by a Zeiss Pulfrich refractometer in order to obtain a check on their purity. The same procedure was adopted here for the standardizing liquid (chlorobenzene), but it was decided that density determinations would serve the purpose better in the case of methyl alcohol and the alcohol water mixtures, since the R.I.'s of water and methyl alcohol at 20° C. (1·333 and 1·329 for sodium light respectively) are so close together. In addition, the densities of various alcohol-water mixtures are accurately known (4), and it is therefore possible to deduce the concentration of any given solution from its density. The determination of density was carried out at approximately 20° C. by the method of Hartley and Barratt (5), using two different glass pyknometers in conjunction with tares whose volumes are approximately equal to those of the corresponding pyknometers. The temperature of the thermostat in which the pyknometers were brought to temperature equilibrium was 20·14° C., and it became necessary to reduce the experimental results to 20·00° C., the density of water at 4° C. being taken as unity. For this purpose the relation

---

* Communicated by Prof. E. J. Williams, F.R.S.

$$\delta_{20}=\delta_{20\cdot14}(1+0\cdot14\ \alpha)$$

was used, $\delta_{20\cdot14}$ and $\delta_{20}$ being the densities of a given liquid at 20·14 and 20·00° C. (both referred to water at 4° C.), whilst $\alpha$ is the coefficient of cubical expansion of the liquid. For pure water, $\alpha=2\cdot3\times10^{-4}$ and for pure methyl alcohol $\alpha=11\cdot9\times10^{-4}$ (quoted in Landolt-Börnstein). The correction in question is very small, in fact it amounts to 14 $\alpha$ per cent., and its maximum value (for alcohol) is only 0·015 per cent. This fact was used in evaluating $\alpha$ for the alcohol-water mixtures, since no data could be found in the literature for the coefficient of expansion of these mixtures; it is clearly justifiable to interpolate between the two values given for the pure substances, assuming a linear relationship between $\alpha$ and concentration.

Little need be said about the d.c. condensers; both condensers were constructed of brass, the parallel plate condenser being chromium-plated and the cylindrical condenser tinned. The condensers were longer than those described in II., thus allowing a greater depth of immersion in the thermostat. In the previous work it was extremely important to prevent access of water to the substances investigated, and thus a stream of dry air was passed through the condensers during an experimental run. This procedure was adopted in the present work for the chlorobenzene standardization and for the determination of the d.c. of the alcohol; the procedure is unnecessary with water, and it was decided to discontinue it also with the alcohol water mixtures, since the dry air stream might cause differential evaporation of the alcohol and water with a consequent change in the concentration of the solutions. In these cases evaporation was minimized by closing the condenser inlet tubes.

## II. *Purification of Materials.*

### (i.) *Chlorobenzene.*

Altogether ten samples were used, most of these being purified following the general plan given in II. All ten samples were finally distilled over calcium turnings a little before they were required for use. Three samples (nos. 2, 6, and 7), from a supply obtained from Messrs. Hopkin & Williams, labelled " Pure Chlorobenzene," were used without preliminary washing with acid, alkali, and water ; these samples were given only a preliminary drying overnight over phosphorus pentoxide and then distilled over calcium turnings.

### (ii.) *Methyl Alcohol.*

Seven samples were used for the determination of the d.c. of the pure liquid, while four main samples were used to synthesize the alcohol-water mixtures. The starting material in each case was methyl alcohol of A.R. grade, free from acetone, supplied by James Burrough, Ltd. ; this was first fractionated in two-quart lots over metallic calcium for about ten hours, using a fractionating column about 1·5 metres long ; it was then distilled and kept in air-tight bottles. Except for the first three samples, the liquid was also given a further preliminary drying by dissolving in it some Kahlbaum sodium that had been washed in a little of the stock alcohol ; this was then fractionated for about an hour and then distilled slowly. When a sample was required for an experiment, a sufficient quantity of the partly-purified liquid was further distilled over calcium in an all-pyrex Quickfit and Quartz apparatus fitted with a " bubble " fractionating column 30 cm. long.

### (iii.) *Water.*

Four samples were used for the determination of the d.c. of pure water and four samples were prepared from which to synthesize the mixtures. Tap-water was used as the starting material ; this was distilled and then redistilled in the Quickfit and Quartz apparatus and kept in well-stoppered glass bottles. This material was given a final distillation before use.

### (iv.) *Alcohol-Water Mixtures.*

The various mixtures were synthesized by weight, a weight pipette being used ; in all cases precautions were taken to avoid loss by evaporation etc.

## III. *Experimental Results.*

D.c.'s were measured at two temperatures in the neighbourhood of 20° and 25° C. The temperature of the liquid in a condenser differed slightly from the thermostat temperature, and the appropriate correction, determined by experiment, was applied in order to evaluate the exact liquid temperature. All temperatures were measured with thermometers which had been compared with a thermometer calibrated at the N.P.L.

(i.) *Calibration.*

During the course of the work some ten calibration experiments were carried out at each temperature; different samples of chlorobenzene, purified as described in the preceding section, were used, and the values found in II. for the d.c. were adopted, namely, $\epsilon_{20}=5{\cdot}714$, $\epsilon_{25}=5{\cdot}626$ and $\frac{d\epsilon}{d\theta}=-1{\cdot}74_4\times10^{-2}$. In the course of the experiments a small alteration had to be made in the volume of liquid used in the d.c. condensers, and for this reason the calibration with samples nos. 1–7 differs slightly from that with samples nos. 8–10. Calling the calibration with samples 1–7 the A value and the calibration with samples nos. 8–10 the B value, the A value applies to all the alcohol experiments except the last, for which the B value is applicable. For water and the alcohol water mixtures the B value is to be used throughout.

The A calibration experiments and the alcohol experiments were carried out at three different frequencies, and it is thus necessary to calculate the lead inductance correction separately for each result, as shown in III. In the notation of this paper we call $D_{as}$ the difference of the variable condenser capacitance with and without the d.c. condenser filled with air, and $D_s$ the corresponding difference when the d.c. condenser is filled with standardizing liquid of d.c. $\epsilon_s$. If $\omega_s$ be the pulsatance, $L'$ the inductance of the leads, $C_{ra}$ the replaceable air capacitance of the d.c. condenser and $C'_{ra}$ the apparent replaceable air capacitance, *i. e.*, the value uncorrected for lead inductance, then from equations (3.18) and (3.19) of III.,

$$\left.\begin{aligned} C'_{ra}&=(D_s-D_{as})/(\epsilon_s-1),\\ C_{ra}&=C'_{ra}(1-c),\\ \text{where}\quad c&=\omega_s^2L'(D_{as}+D_s).\end{aligned}\right\}\quad\ldots\ldots\quad(3.1)$$

In the following results, $C_{ra}$ and $C'_{ra}$ are expressed in terms of the mean capacitance per degree rotation of the small variable condenser, and for this purpose $D_s$ and $D_{as}$ are in the same units. For the calculation of $c$ it is necessary to express $D_s$ and $D_{as}$ in terms of the farad as unit, and the slope of the condenser calibration curve ($1{\cdot}45\ \mu\mu$F. per degree) is used as a conversion factor for this purpose.

The results obtained in the A calibrations are summarized in Tables I. (*a*) and I. (*b*), the former relating to the cylindrical d.c. condenser and the latter to the parallel plate d.c. condenser. In the column headed $\omega_s$, (i.) implies that $\omega_s$ is $3{\cdot}732\times10^6$, (ii.) that $\omega_s$ is $4{\cdot}221\times10^6$, and (iii.) that $\omega_s$ is $4{\cdot}765\times10^6$. For the cylindrical condenser, the values of $c$ corresponding to these frequencies are 4·3, 5·4, and $7{\cdot}0\times10^{-4}$ respectively,

### TABLE I. (*a*).

### Cylindrical Condenser: A calibrations.

| Sample no. | $\omega_s$. | Temp. (° C.). | $D_s - D_{as}$. | $C'_{ra}$. | $C_{ra}$. |
|---|---|---|---|---|---|
| 1........ | ii. | 20·14<br>24·88 | 60·55<br>59·52 | $12{\cdot}85_3$<br>$12{\cdot}86_0$ | $12{\cdot}84_6$<br>$12{\cdot}85_3$ |
| 2........ | iii. | 20·14<br>24·88 | 60·54<br>59·48 | $12{\cdot}85_1$<br>$12{\cdot}85_1$ | $12{\cdot}84_2$<br>$12{\cdot}84_2$ |
| 3........ | iii. | 20·14<br>24·88 | 60·48<br>59·45 | $12{\cdot}83_8$<br>$12{\cdot}84_5$ | $12{\cdot}82_9$<br>$12{\cdot}83_6$ |
| 4........ | ii. | 20·14<br>24·88 | 60·53<br>59·49 | $12{\cdot}84_9$<br>$12{\cdot}85_5$ | $12{\cdot}84_2$<br>$12{\cdot}84_8$ |
| 5........ | i. | 20·35<br>24·88 | 60·52<br>59·50 | $12{\cdot}85_7$<br>$12{\cdot}85_6$ | $12{\cdot}85_2$<br>$12{\cdot}85_1$ |
| 7........ | ii. | 20·14<br>24·88 | 60·55<br>59·48 | $12{\cdot}85_3$<br>$12{\cdot}85_2$ | $12{\cdot}84_6$<br>$12{\cdot}84_5$ |

### TABLE I. (*b*).

### Parallel Plate Condenser: A Calibrations.

| Sample no. | $\omega_s$. | Temp. (° C.). | $D_s - D_{as}$. | $C'_{ra}$. | $C_{ra}$. |
|---|---|---|---|---|---|
| 2........ | iii. | 20·14<br>24·89 | 63·44<br>62·32 | $13{\cdot}46_6$<br>$13{\cdot}46_6$ | $13{\cdot}45_4$<br>$13{\cdot}45_4$ |
| 3........ | iii. | 20·14<br>24·89 | 63·41<br>62·33 | $13{\cdot}46_0$<br>$13{\cdot}46_8$ | $13{\cdot}44_8$<br>$13{\cdot}45_6$ |
| 4........ | ii. | 20·14<br>24·89 | 63·48<br>62·38 | $13{\cdot}47_4$<br>$13{\cdot}47_9$ | $13{\cdot}46_4$<br>$13{\cdot}46_9$ |
| 5........ | i. | 20·35<br>24·89 | 63·36<br>62·30 | $13{\cdot}46_0$<br>$13{\cdot}46_1$ | $13{\cdot}45_2$<br>$13{\cdot}45_3$ |
| 6........ | i. | 20·14<br>24·89 | 63·41<br>62·29 | $13{\cdot}46_0$<br>$13{\cdot}45_9$ | $13{\cdot}45_2$<br>$13{\cdot}45_1$ |
| 7........ | ii. | 20·14<br>24·89 | 63·39<br>62·28 | $13{\cdot}45_6$<br>$13{\cdot}45_5$ | $13{\cdot}44_6$<br>$13{\cdot}44_5$ |

The individual results are seen to be in excellent agreement, and for the cylindrical condenser the mean values are found to be:

(i.) At approximately 20° C., $C_{ra} = 12{\cdot}84_2$.
(ii.) At approximately 25° C., $C_{ra} = 12{\cdot}84_6$.

For the parallel plate condenser the mean values are:

(i.) At approximately 20° C., $C_{ra} = 13{\cdot}45_3$.
(ii.) At approximtaely 25° C., $C_{ra} = 13{\cdot}45_4$.

L′ being 0·243 μH. (*vide* III.) ; for the parallel plate condenser they are 5·6, 7·1, and $9{\cdot}1\times10^{-4}$ respectively, L′ being 0·303 μH.

Turning next to the B calibrations, the results obtained with the cylindrical condenser are given in Table II. (*a*), and those with the parallel plate condenser in Table II. (*b*). These experiments, together with the corresponding d.c. experiments, were carried out at the same pulsatance ($4{\cdot}221\times10^6$), and the simplified calculation described in III. can thus be used ; for this reason it is only necessary to calculate the apparent replaceable air capacitance, using equation (3.1).

TABLE II. (*a*).

Cylindrical Condenser : B calibrations.

| Sample no. | Temp. (° C.). | $D_s - D_{as}$. | $C'_{ra}$. |
|---|---|---|---|
| 8.......... | 20·14 | 60·40 | $12{\cdot}82_2$ |
| | 24·88 | 59·37 | $12{\cdot}82_7$ |
| 9.......... | 20·14 | 60·41 | $12{\cdot}82_3$ |
| | 24·78 | 59·39 | $12{\cdot}82_8$ |
| 10.......... | 20·14 | 60·39 | $12{\cdot}82_0$ |
| | 24·88 | 59·35 | $12{\cdot}82_3$ |

TABLE II. (*b*).

Parallel Plate Condenser : B Calibrations.

| Sample no. | Temp. | $D_s - D_{as}$. | $C'_{ra}$. |
|---|---|---|---|
| 8.......... | 20·14 | 63·26 | $13{\cdot}42_9$ |
| | 24·89 | 62·17 | $13{\cdot}43_3$ |
| 9.......... | 20·14 | 63·29 | $13{\cdot}43_5$ |
| | 24·78 | 62·21 | $13{\cdot}43_8$ |
| 10.......... | 20·14 | 63·25 | $13{\cdot}42_6$ |
| | 24·89 | 62·16 | $13{\cdot}43_0$ |

The mean values of these results for the cylindrical condenser are :

(i.) At approximately 20° C., $C'_{ra}=12{\cdot}82_2$.

(ii.) At approximately 25° C., $C'_{ra}=12{\cdot}82_6$.

For the parallel plate condenser the mean values are :

(i.) At approximately 20° C., $C'_{ra}=13{\cdot}43_0$.

(ii.) At approximately 25° C., $C'_{ra}=13{\cdot}43_4$.

The R.I., $n_{20}$, of the various samples for sodium light at 20° C. is given in Table III., the reduction to 20° C. being carried out using the temperature coefficient ($10{\cdot}51\times10^{-3}$) used in II.

TABLE III.

| Sample no... | 1 | 2 | 3 | 4 |
|---|---|---|---|---|
| $n_{20}$ .... | 1·52337 | 1·52336 | 1·52339 | 1·52339 |
| Sample no... | 5 | 6 | 7 | 8 |
| $n_{20}$ .... | 1·52349 | 1·52345 | 1·52341 | 1·52329 |
| Sample no... | 9 | 10 | | |
| $n_{20}$ .... | 1·52323 | 1·52323. | | |

The mean value of $n_{20}$ is $1{\cdot}5233_6$, which differs from the value found in II. by less than 0·1 per cent.

(ii.) *Methyl Alcohol.*

The results obtained with pure methyl alcohol, purified as described in the preceding section, are shown in Tables IV. (*a*) and IV. (*b*), the former relating to the cylindrical condenser and the latter to the parallel plate condenser. Calibration A applies to the results obtained with samples nos. 1–6 and calibration B to sample no. 7. Three different pulsatances were used in the experiments with samples nos. 1–6, and in Tables IV. (*a*) and IV. (*b*), the symbols (i.), (ii.), and (iii.) in the column headed $\omega$ signify the same values of the pulsatance as they do in Tables I. (*a*) and I. (*b*). Since different frequencies are involved, it is necessary to use equation (3.20) of III. in calculating the value of the d.c. If $D_{au}$ be the difference of the variable condenser capacitancies, with and without the d.c. condenser filled with air, and if $D_u$ be the corresponding difference when the d.c. condenser is filled with the liquid of unknown d.c. $\epsilon$, then

$$\left.\begin{aligned}\epsilon&=1+(D_u-D_{au})(1-d)/C_{ra},\\ \text{where}\qquad d&=\omega^2L'(D_u+D_{au}).\end{aligned}\right\}\quad . \quad . \quad . \quad . \quad . \quad (3.2)$$

The value of $(D_u+D_{au})$ differs for different temperatures, and it is necessary to take this into account in the present case. At about 20° C., for the cylindrical condenser, the values of $d$ corresponding to pulsatances (i.), (ii.), and (iii.) are 2·20, 2·82, and $3{\cdot}58\times10^{-3}$, and at the same temperature, for the parallel plate condenser, they are 2·86, 3·66, and $4{\cdot}65\times10^{-3}$. At about 25° C., for the cylindrical condenser, we find $d$ equal to 2·14, 2·74, and $3{\cdot}50\times10^{-3}$ for pulsatances (i.), (ii.), and (iii.), and for the parallel plate condenser, for these pulsatances, $d$ is 2·78, 3·51, and $4{\cdot}52 \times 10^{-3}$ respectively.

In connexion with sample no. 7, the same frequency has been used in the calibration experiment and in the d.c. experiment; in this case it is simpler to calculate $\epsilon$ by means of equations (3.22) and (3.25) of III. If $\epsilon'$ be the apparent d.c., *i. e.*, the value obtained without allowing for lead inductance, then it follows from equation (3.22) that

$$\epsilon' = 1 + (D_u - D_{au})/C'_{ra}, \quad \ldots\ldots\ldots \tag{3.3}$$

TABLE IV. ($a$).

Cylindrical Condenser: Methyl Alcohol.

| Sample no. | $\omega$. | Temp. °( C.). | $D_u - D_{au}$. | $\epsilon_t$. | $\epsilon_{20}$. | $\epsilon_{25}$. |
|---|---|---|---|---|---|---|
| 1...... | iii. | 20·5 | 418·88 | $33{\cdot}49_9$ | $33{\cdot}59_7$ | |
| | | 24·93 | 407·47 | $32{\cdot}60_9$ | | $32{\cdot}59_5$ |
| 2...... | iii. | 20·14 | 419·36 | $33{\cdot}53_6$ | $33{\cdot}56_4$ | |
| | | 24·93 | 406·83 | $32{\cdot}55_9$ | | $32{\cdot}54_5$ |
| 3...... | ii. | 20·14 | 419·40 | $33{\cdot}56_4$ | $33{\cdot}59_2$ | |
| | | 24·90 | 407·71 | $32{\cdot}65_1$ | | $32{\cdot}63_1$ |
| 4...... | ii. | 20·14 | 419·16 | $33{\cdot}54_5$ | $33{\cdot}57_3$ | |
| | | 24·90 | 407·53 | $32{\cdot}63_7$ | | $32{\cdot}61_7$ |
| 5...... | i. | 20·14 | 419·26 | $33{\cdot}57_3$ | $33{\cdot}60_1$ | |
| | | 24·90 | 407·40 | $32{\cdot}64_6$ | | $32{\cdot}62_6$ |
| 6...... | i. | 20·14 | 419·21 | $33{\cdot}56_9$ | $33{\cdot}59_7$ | |
| | | 24·88 | 407·37 | $32{\cdot}64_4$ | | $32{\cdot}62_0$ |
| 7...... | ii. | 20·14 | 418·79 | $33{\cdot}58_8$ | $33{\cdot}61_5$ | |
| | | 24·86 | 407·05 | $32{\cdot}66_6$ | | $32{\cdot}63_8$ |

In $\epsilon_{20}$ the maximum discrepancy is about 0·15 per cent. and in $\epsilon_{25}$ about 0·3 per cent.; the mean values and temperature coefficient are found to be

$$\epsilon_{20} = 33{\cdot}59_1\,;\ \epsilon_{25} = 32{\cdot}61_0\,;\ \frac{d\epsilon}{d\theta} = -0{\cdot}196_4.$$

where $C'_{ra}$ is the apparent replaceable air capacitance of the d.c. condenser as defined in connexion with equation (3.1) of the present paper. The true value of the d.c. is then calculated by means of equation (3.25) of III., namely,

$$\left.\begin{aligned} \epsilon &= \epsilon' - e, \\ \text{where} \qquad e &= \omega^2 L' C'_{ra}(\epsilon' - \epsilon_s)(\epsilon' - 1). \end{aligned}\right\} \quad \ldots\ldots \tag{3.4}$$

For the cylindrical condenser $e = 0{\cdot}074$ at 20° C. and 0·070 at 25° C., whilst for the parallel plate condenser the value of $e$ is 0·095 at 20° C. and 0·090 at 25° C.

In Tables IV. (*a*) and (*b*) the column headed $\epsilon_t$ gives the values of the d.c.'s at the temperatures stated in column 3; from the two values corresponding to a given sample, the values of the d.c.'s at 20° C. and 25° C. are calculated by extrapolation, using the mean temperature coefficient given by all the samples, and are given in the columns headed $\epsilon_{20}$ and $\epsilon_{25}$.

TABLE IV. (*b*).

Parallel Plate Condenser : Methyl Alcohol.

| Sample no. | $\omega$. | Temp. (° C.). | $D_u - D_{au}$. | $\epsilon_t$. | $\epsilon_{20}$. | $\epsilon_{25}$. |
|---|---|---|---|---|---|---|
| 1...... | iii. | 20·5 | 437·99 | $33{\cdot}40_6$ | $33{\cdot}50_2$ | |
| | | 24·94 | 426·92 | $32{\cdot}58_9$ | | $32{\cdot}57_7$ |
| 2...... | iii. | 20·14 | 439·60 | $33{\cdot}52_5$ | $33{\cdot}55_2$ | |
| | | 24·94 | 426·58 | $32{\cdot}56_3$ | | $32{\cdot}55_1$ |
| 3...... | ii. | 20·14 | 439·50 | $33{\cdot}54_9$ | $33{\cdot}57_6$ | |
| | | 24·89 | 427·12 | $32{\cdot}63_6$ | | $32{\cdot}61_5$ |
| 4...... | ii. | 20·14 | 439·43 | $33{\cdot}54_4$ | $33{\cdot}57_1$ | |
| | | 24·89 | 427·15 | $32{\cdot}63_8$ | | $32{\cdot}61_7$ |
| 5...... | i. | 20·14 | 439·29 | $33{\cdot}56_1$ | $33{\cdot}58_8$ | |
| | | 24·89 | 427·03 | $32{\cdot}65_1$ | | $32{\cdot}63_0$ |
| 6...... | i. | 20·14 | 439·41 | $33{\cdot}57_0$ | $33{\cdot}59_7$ | |
| | | 24·89 | 426·78 | $32{\cdot}63_2$ | | $32{\cdot}61_2$ |
| 7...... | ii. | 20·14 | 439·07 | $33{\cdot}59_9$ | $33{\cdot}62_6$ | |
| | | 24·87 | 426·69 | $32{\cdot}67_3$ | | $32{\cdot}64_8$ |

In each case the maximum discrepancy is about 0·3 per cent., and the mean values and temperature coefficients are found to be

$$\epsilon_{20} = 33{\cdot}57_3\,;\quad \epsilon_{25} = 32{\cdot}60_7\,;\quad \frac{d\epsilon}{d\theta} = -0{\cdot}193_2.$$

The discrepancy between the mean values found by the cylindrical and parallel plate condensers is seen to be less than one in a thousand, and taking the mean of these results, the final results for the d.c.'s at the two standard temperatures are

$$\underline{\epsilon_{20} = 33{\cdot}58\,;\quad \epsilon_{25} = 32{\cdot}61,}$$

whilst the mean temperature coefficient is

$$\underline{\frac{d\epsilon}{d\theta} = -0{\cdot}194_6.}$$

The density of three samples of the alcohol was measured, the values obtained for the density at 20° C., referred to water at 4° C., being

$$0{\cdot}79130, \qquad 0{\cdot}79146, \qquad 0{\cdot}79124,$$

giving a mean value of

$$0{\cdot}7913_3,$$

which agrees with the value ($0{\cdot}7913_2$) calculated from the formula given as the "best" value in the 'International Critical Tables' (I.C.T.), vol. iii. p. 27.

(iii.) *Water.*

Tables V. (*a*) and V. (*b*) give the results obtained with pure water; the results given in Table V. (*a*) are those obtained with the cylindrical condenser, whilst those in Table V. (*b*) were obtained with the parallel plate condenser. Calibration B applies to all these results; the values of $\epsilon$ have been calculated using equations (3.3) and (3.4) of the present paper, the values of the lead-correction term $e$ being

TABLE V. (*a*).

Cylindrical Condenser: Water.

$\omega=4{\cdot}221\times10^6$.

| Sample no. | Temp. (° C.). | $D_u-D_{au}$. | $\epsilon_t$. | $\epsilon_{20}$. | $t_{25}$. |
|---|---|---|---|---|---|
| 2......... | 20·14 | 1022·59 | 80·27 | 80·32 | |
| | 24·88 | 1001·07 | 78·60 | | 78·55 |
| 3......... | 20·14 | 1021·82 | 80·21 | 80·26 | |
| | 24·88 | 999·49 | 78·47 | | 78·43 |
| 4......... | 20·14 | 1022·30 | 80·24 | 80·29 | |
| | 24·91 | 999·91 | 78·51 | | 78·47 |

The maximum discrepancy in the values for the d.c.'s is seen to be about 0·13 per cent., and the results give mean values and temperature coefficient as follows:—

$$\epsilon_{20}=80{\cdot}29\,;\quad \epsilon_{25}=78{\cdot}48\,;\quad \frac{d\epsilon}{d\theta}=-0{\cdot}362.$$

(i.) cylindrical condenser at approximately 20° C., 0·485,
(ii.) ,, ,, ,, ,, 25° C., 0·454,
(iii.) parallel plate ,, ,, ,, 20° C., 0·635,
(iv.) ,, ,, ,, ,, ,, 25° C., 0·605,

all readings having been taken at pulsatance (ii.), namely, $4{\cdot}221\times10^6$.

The results are arranged in a manner similar to those in Tables IV. (*a*) and IV. (*b*), and for each sample the values of the d.c. at the two standard temperatures are calculated from the values obtained at the two temperatures given in column 2.

TABLE V. (*b*).

Parallel Plate Condenser : Water.

$\omega=4\cdot221\times10^6$.

| Sample. no. | Temp. (° C.). | $D_u-D_{au}$. | $\epsilon_t$. | $\epsilon_{20}$. | $\epsilon_{25}$. |
|---|---|---|---|---|---|
| 1......... | 20·14 | 1072·69 | 80·24 | 80·29 | |
| | 24·89 | 1049·07 | 78·49 | | 78·45 |
| 2......... | 20·14 | 1073·82 | 80·32 | 80·37 | |
| | 24·89 | 1050·55 | 78·60 | | 78·56 |
| 3......... | 20·14 | 1072·52 | 80·23 | 80·28 | |
| | 24·89 | 1049·28 | 78·50 | | 78·46 |
| 4......... | 20·14 | 1073·54 | 80·30 | 80·35 | |
| | 24·92 | 1049·96 | 78·55 | | 78·52 |

The individual values do not differ by more than about 0·15 per cent., and the mean values are

$$\epsilon_{20}=80\cdot32\ ;\ \epsilon_{25}=78\cdot50\ ;\ \frac{d\epsilon}{d\theta}=-0\cdot365.$$

The agreement between the values given by the two condensers is seen to be better than one in two thousand.

Taking the means of the results obtained with the two condensers, the final results for water are

$$\epsilon_{20}=80\cdot31\ ;\ \epsilon_{25}=78\cdot49\ ;\ \frac{d\epsilon}{d\theta}=-0\cdot363.$$

### (iv.) *Alcohol-Water Mixtures.*

Some eleven mixtures, ranging from about 5 to 95 per cent. alcohol (by weight), were synthesized and their d.c.'s measured at approximately 20° and 25° C. In each instance the density of the mixture was determined using two pyknometers, and the two independent results so obtained never differed by more than one in four thousand. As a check on the accuracy of the synthesis, the concentration of each mixture was calculated by interpolation from the data of Dittmar and Fawsitt (4) for the density of alcohol-water mixtures at 20° C. For this purpose it is necessary to apply a small correction, since the value of the density of pure alcohol given by these authors is 0·7917, which is $0\cdot0003_7$ higher than the value found in the present work. Since the difference is so small, it can be assumed without appreciable error that the correction is a linear function of the concentration, the value of the correction being 0·0003$_7$ at 100 per cent. alcohol and zero at 0 per cent. alcohol, since the value assumed by Dittmar and Fawsitt for the density of water at 20° C. agrees with the standard value (0·99823) due to Thiesen, Scheel, and Diesselhorst.

Table VI. shows the composition of the mixtures. The "density" column gives the density obtained by experiment, reduced to 20° C.; the last two columns give the composition of the mixtures, expressed as percentage alcohol by weight, obtained from the weights of pure substances used in the synthesis, and by interpolation from the data of Dittmar and Fawsitt.

TABLE VI.

Composition of Mixtures.

| Mixture no. | Density (20° C.). | Composition: | |
|---|---|---|---|
| | | By synthesis. | By density. |
| | | Per cent. | Per cent. |
| 1........ | 0·9895$_1$ | 4·95 | 5·04 |
| 2........ | 0·9814$_8$ | 9·99 | 9·99 |
| 3........ | 0·9667$_4$ | 19·87 | 19·86 |
| 4........ | 0·9515$_1$ | 29·96 | 29·92 |
| 5........ | 0·9347$_5$ | 39·86 | 39·78 |
| 6........ | 0·9152$_1$ | 49·96 | 50·09 |
| 7........ | 0·8946$_9$ | 59·83 | 59·86 |
| 8........ | 0·8717$_1$ | 69·82 | 69·80 |
| 9........ | 0·8475$_1$ | 79·61 | 79·64 |
| 10........ | 0·8178$_4$ | 90·71 | 90·71 |
| 11........ | 0·8058$_4$ | 94·89 | 95·00 |

The two sets of values given for the composition of the mixtures are in good agreement for our present purpose; the biggest discrepancy is in the case of mixture no. 1, and the results given below show that, in this region, a change in composition from 4·95 to 5·04 per cent. corresponds to a change of 0·04 in the value of the d.c.; since the value of the d.c. is about 78, the change in question amounts to about one in two thousand.

The experimental results obtained with the cylindrical condenser are given in Table VII. (*a*) (p. 320), the arrangement of which is similar to

Tables V. (*a*) and (*b*). With the exception of the "*b*" reading with mixture no. 8, all experiments were carried out at a pulsatance of $4{\cdot}221\times10^6$, and the experimental results were calculated as for water, the B calibration being used. The value of the correction $e$ is given in the fourth column. The results for the "*b*" reading with mixture no. 8 were obtained at a pulsatance of $4{\cdot}765\times10^6$, and the values of the d.c. were calculated as in the case of methyl alcohol, using equations (3.1) and (3.2) of the present paper. The values of the d.c.'s at the two standard temperatures, given in the last two columns, are obtained by extrapolation from the results at the two temperatures given in column 2; on account of the difficulty of determining the temperature coefficients accurately, the values of this quantity, obtained experimentally, were plotted against concentration, and the temperature coefficient appropriate to any given concentration was obtained from the smoothed curve drawn through the points.

The corresponding results for the parallel plate condenser are given in Table VII. (*b*) (p. 321).

Comparing the results for $\epsilon_{20}$ and $\epsilon_{25}$ given by the two condensers, they are seen to be in good agreement, the maximum discrepancy between the two values being about 0·15 per cent. In addition, the results with the two sets of mixtures of the same concentration (nos. 6 *a* and 6 *b*, nos. 8 *a* and 8 *b*) are concordant.

The relationship between $\epsilon$ and concentration is found to be linear to a high degree of accuracy from a concentration of 20 per cent. to one of 80 per cent. alcohol; beyond these limits the curve connecting these variables shows definite curvature. The average value of the d.c., using the results obtained with the two condensers, can be represented by the following equations for concentrations between 20 and 80 per cent. :—

$$\left.\begin{aligned}\epsilon_{20}&=81{\cdot}15_6-0{\cdot}4656_3\,p,\\ \epsilon_{25}&=79{\cdot}18_9-0{\cdot}4573_9\,p,\end{aligned}\right\}\quad\ldots\ldots\quad(3.4)$$

where $p$ denotes the concentration; in connexion with the values of $p$ it was considered that the values interpolated from the results of Dittmar and Fawsitt were more accurate than the values obtained from the weights of pure substances used for the syntheses, and the former values were therefore used in deriving equations (3.4). It should be added that the differences between the value of the d.c.'s given by equations (3.4) and the experimental values never exceed 0·15 per cent.

The experimental results for water, alcohol, and alcohol-water mixtures are summarized in Table VIII. (p. 322). In finding the values of the d.c.'s corresponding to the concentrations given in the first column, the values between 20 and 80 per cent. concentration have been calculated from equations (3.4); the values outside these limits have been interpolated from large-scale graphs of d.c. against concentration. The values of the

### TABLE VII. (*a*).

### Cylindrical Condenser : Alcohol-Water Mixtures.

$\omega = 4{\cdot}221 \times 10^6$.

Temp. i.=20·14° C. ; Temp. ii.=24·88° C.

| Mixture no. | Temp. | $D_a - D_{au}$. | *e*. | $\epsilon_t$. | $\epsilon_{20}$. | $\epsilon_{25}$. |
|---|---|---|---|---|---|---|
| 1............ | i. | 994·34 | 0·455 | $78{\cdot}09_5$ | $78{\cdot}14_6$ | |
| | ii. | 972·20 | 0·435 | $76{\cdot}36_4$ | | $76{\cdot}31_3$ |
| 2............ | i. | 966·65 | 0·432 | $75{\cdot}95_8$ | $76{\cdot}00_9$ | |
| | ii. | 945·07 | 0·410 | $74{\cdot}27_4$ | | $74{\cdot}23_0$ |
| 3............ | i. | 911·81 | 0·380 | $71{\cdot}73_3$ | $71{\cdot}78_3$ | |
| | ii. | 890·08 | 0·360 | $70{\cdot}03_7$ | | $69{\cdot}99_4$ |
| 4............ | i. | 853·85 | 0·335 | $67{\cdot}25_8$ | $67{\cdot}30_0$ | |
| | ii. | 832·98 | 0·315 | $65{\cdot}63_0$ | | $65{\cdot}58_1$ |
| 5............ | i. | 793·99 | 0·290 | $62{\cdot}63_4$ | $62{\cdot}68_1$ | |
| | ii. | 773·91 | 0·274 | $61{\cdot}06_5$ | | $61{\cdot}02_5$ |
| 6 *a* .......... | i. | 731·57 | 0·240 | $57{\cdot}81_6$ | $57{\cdot}86_1$ | |
| | ii. | 712·46 | 0·227 | $56{\cdot}32_1$ | | $56{\cdot}28_3$ |
| 6 *b* .......... | i. | 731·88 | 0·240 | $57{\cdot}84_0$ | $57{\cdot}88_5$ | |
| | ii. | 712·72 | 0·227 | $56{\cdot}34_1$ | | $56{\cdot}30_3$ |
| 7............ | i. | 671·94 | 0·200 | $53{\cdot}20_5$ | $53{\cdot}24_7$ | |
| | ii. | 653·94 | 0·190 | $51{\cdot}79_6$ | | $51{\cdot}76_0$ |
| 8 *a* .......... | i. | 611·74 | 0·165 | $48{\cdot}54_5$ | $48{\cdot}58_4$ | |
| | ii. | 594·99 | 0·155 | $47{\cdot}23_4$ | | $47{\cdot}20_0$ |
| 8 *b* .......... | i. | 612·26 | 0·211 | $48{\cdot}54_0$ | $48{\cdot}57_9$ | |
| | ii. | 595·15 | 0·198 | $47{\cdot}20_4$ | | $47{\cdot}17_0$ |
| 9............ | i. | 553·20 | 0·132 | $44{\cdot}01_3$ | $44{\cdot}04_9$ | |
| | ii. | 537·49 | 0·125 | $42{\cdot}88_1$ | | $42{\cdot}74_5$ |
| 10............ | i. | 483·59 | 0·099 | $38{\cdot}61_7$ | $38{\cdot}64_9$ | |
| | ii. | 469·60 | 0·092 | $37{\cdot}52_1$ | | $37{\cdot}49_3$ |
| 11............ | i. | 455·69 | 0·086 | $36{\cdot}45_4$ | $36{\cdot}48_4$ | |
| | ii. | 442·69 | 0·081 | $35{\cdot}43_4$ | | $35{\cdot}40_4$ |

TABLE VII. (*b*).

Parallel Plate Condenser : Alcohol Water Mixtures.

$\omega = 4{\cdot}221 \times 10^6$.

Temp. i.=20·14° C. : Temp. ii.=24·89° C.

| Mixture no. | Temp. | $D_a - D_{au}$. | *e*. | $\epsilon_t$. | $\epsilon_{20}$. | $\epsilon_{25}$. |
|---|---|---|---|---|---|---|
| 1........... | i. | 1044·39 | 0·602 | $78{\cdot}16_4$ | $78{\cdot}21_5$ | |
| | ii. | 1021·24 | 0·572 | $76{\cdot}44_9$ | | $76{\cdot}40_1$ |
| 2........... | i. | 1016·09 | 0·567 | $76{\cdot}09_1$ | $76{\cdot}14_2$ | |
| | ii. | 992·87 | 0·540 | $74{\cdot}36_9$ | | $74{\cdot}32_9$ |
| 3........... | i. | 957·96 | 0·500 | $71{\cdot}83_0$ | $71{\cdot}88_0$ | |
| | ii. | 935·05 | 0·475 | $70{\cdot}13_0$ | | $70{\cdot}09_1$ |
| 4........... | i. | 896·16 | 0·438 | $67{\cdot}29_0$ | $67{\cdot}33_2$ | |
| | ii. | 874·24 | 0·415 | $65{\cdot}66_3$ | | $65{\cdot}61_8$ |
| 5........... | i. | 833·36 | 0·378 | $62{\cdot}67_4$ | $62{\cdot}72_1$ | |
| | ii. | 812·29 | 0·358 | $61{\cdot}10_8$ | | $61{\cdot}07_1$ |
| 6 *a* ......... | i. | 767·23 | 0·317 | $57{\cdot}81_1$ | $57{\cdot}85_6$ | |
| | ii. | 747·21 | 0·300 | $56{\cdot}32_2$ | | $56{\cdot}28_7$ |
| 6 *b* ......... | i. | 767·61 | 0·317 | $57{\cdot}83_9$ | $57{\cdot}88_4$ | |
| | ii. | 747·54 | 0·300 | $56{\cdot}34_7$ | | $56{\cdot}31_2$ |
| 7........... | i. | 705·01 | 0·267 | $53{\cdot}22_8$ | $53{\cdot}27_0$ | |
| | ii. | 686·44 | 0·250 | $51{\cdot}84_8$ | | $51{\cdot}81_5$ |
| 8 *a* ......... | i. | 641·47 | 0·217 | $48{\cdot}54_7$ | $48{\cdot}58_6$ | |
| | ii. | 623·96 | 0·205 | $47{\cdot}24_2$ | | $47{\cdot}21_1$ |
| 8 *b* ......... | i. | 642·14 | 0·277 | $48{\cdot}53_7$ | $48{\cdot}57_6$ | |
| | ii. | 624·18 | 0·260 | $47{\cdot}20_4$ | | $47{\cdot}17_3$ |
| 9........... | i. | 580·14 | 0·177 | $44{\cdot}02_0$ | $44{\cdot}05_6$ | |
| | ii. | 563·66 | 0·165 | $42{\cdot}79_4$ | | $42{\cdot}76_0$ |
| 10........... | i. | 507·35 | 0·132 | $38{\cdot}64_5$ | $38{\cdot}67_7$ | |
| | ii. | 492·57 | 0·122 | $37{\cdot}54_5$ | | $37{\cdot}52_0$ |
| 11........... | i. | 477·80 | 0·115 | $36{\cdot}46_2$ | $36{\cdot}49_2$ | |
| | ii. | 464·18 | 0·106 | $35{\cdot}44_7$ | | $35{\cdot}41_9$ |

temperature coefficient given in the last column have been taken from a smoothed curve of temperature coefficient plotted against concentration.

TABLE VIII.

| Concentration (per cent. MeOH by wt.). | $\epsilon_{20}$. | $\epsilon_{25}$. | $\frac{d\theta}{d\theta}$. |
|---|---|---|---|
| 0.............. | 80·31 | 78·49 | —0·363 |
| 5.............. | 78·21 | 76·41 | —0·362 |
| 10.............. | 76·07 | 74·24 | —0·362 |
| 20.............. | 71·84 | 70·04 | —0·357 |
| 30.............. | 67·19 | 65·47 | —0·344 |
| 40.............. | 62·53 | 60·89 | —0·328 |
| 50.............. | 57·88 | 56·32 | —0·311 |
| 60.............. | 53·22 | 51·75 | —0·295 |
| 70.............. | 48·56 | 47·17 | —0·279 |
| 80.............. | 43·91 | 42·60 | —0·260 |
| 90.............. | 38·99 | 37·85 | —0·228 |
| 95.............. | 36·42 | 35·36 | —0.212 |
| 100.............. | 33·58 | 32·61 | —0·195 |

## IV. *Discussion of the Results and Comparison with the Results of Previous Investigations.*

Considering first the agreement amongst themselves of the results given by a particular condenser, the maximum discrepancy nowhere exceeds 0·3 per cent., and the percentage accuracy of the mean is likely to be much better than this figure. As regards the results given by the cylindrical and parallel plate condensers, with the pure liquids, the discrepancy between the two independent results given by these condensers is less than 0·1 per cent., whilst for the mixtures the discrepancy is less than 0·15 per cent. In connexion with the mixtures, the agreement between the two independent determinations with mixtures nos. 6 and 8 is satisfactory. The good agreement between the results obtained with the two condensers points to the fact that there is unlikely to be a systematic error, and also that the lead inductance correction has been correctly applied. In connexion with the latter, it is interesting to compare the uncorrected values $\epsilon'$ of the d.c. (*vide* equation (3.3)) with the corrected values $\epsilon$ of equations (3.4). With water at 20° C. the mean values of $\epsilon'$ given by the cylindrical and parallel plate condensers are 80·78 and 80·96 respectively, the difference thus amounting to more than 0·2 per cent.; after applying the lead correction, the difference between the means is less than 0·05 per cent.

The results of previous determinations are summarized in Tables IX. and X. for methyl alcohol and water. In these tables the third and fourth columns give the temperature at which the d.c. was determined and the value so obtained. The value of the d.c. at 25° C. given in the sixth column has been calculated with the temperature coefficient found in the present work in those cases where no coefficient has been given by the author in question. The seventh column states whether the method employed was absolute (A) or comparative (C); the eighth column shows the method used, "Res." indicating a resonance method, "Br." a bridge method, and "S.W." a stationary wave method, such as the Lecher wire methods; the ninth column gives the frequency $n$ at which the determination was carried out; and the final column the value of the d.c. of benzene at the temperature given in the third column. The values given in this column are useful in estimating the accuracy of a particular determination, since they can be compared with the standard values of Hartshorn and Oliver (6); these values are given in the rows relating to the present work. The rows "I.C.T." refer to the values given in the 'International Critical Tables' (vol. vi. p. 83), and may be taken as the best values deduced from data available at the time of compilation (1925).

Inspection of the values of $\epsilon_{25}$ given in Tables IX. and X. shows that there are considerable differences in the values obtained by different observers, the values of $\epsilon_{25}$ varying from 30·0 to 34·0 in the case of pure alcohol and from 75·4 to 79·5 for water. In considering these discrepancies it is to be remembered that neglecting the lead inductance correction may introduce considerable errors in the final result, this error increasing with increasing frequency. The majority of the results given in the two tables were obtained by the use of frequencies higher than those used here; in addition, few of the authors appear to have considered the effect of lead inductance. It is important to notice that the lead inductance correction term $e$ (*vide* equation (3.4)) may be either positive or negative in sign. If the apparent d.c. $\epsilon'$ of the liquid under investigation is greater than the d.c. $\epsilon_s$ of the standardizing liquid, as in the present work, $e$ is positive and $\epsilon$ is less than $\epsilon'$. On the other hand, if $\epsilon'$ is less than $\epsilon_s$, as in the work of Åkerlöf, who uses water for standardization purposes, then $e$ is negative and $\epsilon$ will be greater than $\epsilon'$.

The value of the d.c. of water has been discussed by Lattey, Gatty, and Davies (22), and from this discussion and their own experiments they conclude that the most probable values are $\epsilon_{20}=80{\cdot}08$, $\epsilon_{25}=78{\cdot}25$, which differ from our values by about 0·3 per cent. It is interesting to compare our values with those found by Drake, Pierce, and Dow (17), and by Wyman (18), who show by their papers that their experimental procedure was carefully worked out with a view to eliminating the various

### TABLE IX.

Methyl Alcohol.

| Authors. | Date. | Temp. (° C.). | D.C. | $-\frac{d\theta}{d\epsilon}$. | $\epsilon_{25}$. | A or C | Method. | Freq. | D.C. of benzene. |
|---|---|---|---|---|---|---|---|---|---|
| I.C.T. ................ | 1925 | 20 | 33·7±1·0 | 0·18 | 32·8 | — | — | $10^2$–$10^6$ | 2·283 |
| Kyropoulos (7) .......... | 1927 | 20 | 33·79 | — | 32·82 | C | Res. | $8·6\times10^5$ | 2·284 |
| Astin (8) .............. | 1929 | 25 | 34·0 | — | 34·0 | A | Res. | $3\ \times10^6$ | 2·239 |
| Gundermann (9) ......... | 1930 | 21·5 | 31·2 | — | 30·5 | C | Res. | $2\ \times10^6$ | 2·265 |
| Ulich and Nespital (10) ... | 1932 | — | — | 0·17 | — | C | Res. | $3·8\times10^6$ | 2·282 |
| Farkas (11) ............ | 1932 | 18 | 31·4 | .. | 30·0 | A | S.W. | $4\ \times10^8$ | 2·6 |
| Åkerlöf (12) ............ | 1932 | 20 | 32·35 | 0·167 | 31·52 | C | Res. | $2\ \times10^6$ | — |
| le Fèvre (13)............ | 1938 | 20 | 32·35 | 0·17 | 31·50 | C | Res. | $1·2\times10^6$ | 2·2825 |
| Authors .............. | 1938 | 20<br>25 | 33·58<br>32·61 | 0·195<br>— | 32·61<br>32·61 | C<br>— | Res.<br>— | $6·7\times10^5$<br>— | 2·2825<br>2·2726 |

TABLE X.—Water.

| Authors. | Date. | Temp. (° C.). | D.C. | $-\frac{d\epsilon}{d\theta}$. | $\epsilon_{25}$. | A. or C. | Method. | Freq. | D.C. of benzene. |
|---|---|---|---|---|---|---|---|---|---|
| I.C.T. .................... | 1925 | 20 | 80 | 0·4 | 78 | — | — | $0–10^8$ | 2·283 |
| Deubner (14) ................ | 1927 | 17 | 80·94 | — | 78·03 | A | S.W. | $7·4\times10^7$ | — |
| Sack (15) ................... | 1927 | 18 | 80·85 | — | 78·30 | C | Br. | $2\ \times10^6$ | — |
| Kyropoulos (7) .............. | 1927 | 20 | 80·79 | — | 78·97 | C | Res. | $8·6\times10^5$ | 2·284 |
| Astin (8) .................. | 1929 | 25 | 79·5 | — | 79·5 | A | Res. | $3\ \times10^6$ | 2·239 |
| Novosilzew (16) ............ | 1929 | 17 | 81·04 | — | 78·13 | A | S.W. | $3\ \times10^7$ | — |
| Drake, Pierce, and Dow (17)... | 1930 | 25 | 78·57 | 0·368 | 78·57 | A | S.W. | $1·7\times10^7$ | — |
| Wyman (18) ................ | 1930 | 25 | 78·54 | 0·365 | 78·54 | A | Res. | $0·1–8\times10^7$ | — |
| Cuthbertson and Maas (19)..... | 1930 | 25 | 75·4 | 0·31 | 75·4 | A | Res. | $1·5\times10^6$ | — |
| Linton and Maas (20) ......... | 1931 | 25 | 79·2 | 0·347 | 79·2 | A | Res. | $1·5\times10^6$ | 2·272 |
| Graffunder and Heymann (21).. | 1931 | 25 | 79·45 | — | 79·45 | C | Res. | $6\ \times10^5$ | 2·282 |
| Lattey, Gatty, and Davies (22).. | 1931 | — | — | 0·363 | 78·25 | C | Res. | $1·5–4\times10^6$ | — |
| Authors .................. | 1938 | 20<br>25 | 80·31<br>78·49 | 0·363 | 78·49 | C | Res. | $6·7\times10^5$ | 2·2825<br>2·2762 |

possible errors. It should also be remembered that the methods used by these authors were absolute methods, and that the experimental methods are different from each other and from the method used here ; in addition, the frequencies used are different. The maximum discrepancy between the values obtained by these authors and in the present work is less than 0·1 per cent., and the magnitude of this discrepancy suggests that our values for the d.c. of water cannot be seriously in error, particularly when it is remembered that our results are derived from the values obtained with two different condensers of different replaceable air-capacitance, and for which the lead inductance correction is different.

TABLE XI.

$\epsilon_{20}$ for Methyl Alcohol–Water Mixtures.

| Composition (per cent. MeOH by weight). | Drude (23). (1897). | Harrington (25) (1916). | Errera (24) (1923). | Åkerlöf (12) (1932). | Present work (1938). |
|---|---|---|---|---|---|
| 0.......... | 81·5 | 78·0 | 80·3 | 80·37 | 80·31 |
| 10.......... | 76·5 | — | — | 75·84 | 76·07 |
| 20.......... | 71·7 | 69·3 | 68·9 | 71·02 | 71·84 |
| 30.......... | — | — | — | 66·01 | 67·19 |
| 40.......... | 62·0 | 60·4 | 60·7 | 61·24 | 62·53 |
| 50.......... | — | — | — | 56·53 | 57·88 |
| 60.......... | 51·3 | 51·6 | 51·8 | 51·53 | 53·22 |
| 70.......... | — | — | — | 46·46 | 48·56 |
| 80.......... | 41·8 | 42·7 | 42·6 | 41·46 | 43·91 |
| 90.......... | — | — | — | 36·80 | 38·99 |
| 100.......... | 33·2 | 33·4 | 33·4 | 32·35 | 33·58 |

In view of these facts, the discrepancies in the values given for the d.c. of methyl alcohol are disquieting. The only value within 1 per cent. of our value is that due to Kyropoulos (7); the remaining values differ by more than 3 per cent. from our values, although the values of le Fèvre (13) and Åkerlöf (12) are in excellent agreement with each other. It is difficult to see where our work can be in error ; from the chemical standpoint the alcohol used must have been pure in view of the value obtained for its density, whilst the arguments for the correctness of the experimental procedure and method of calculation of results have already been given. In all probability the discrepancies are due to the neglect of lead inductance correction, which must become very important at the frequencies used in most of the experiments in question.

Turning next to consider the results for the alcohol-water mixtures, Table XI. shows the results of various investigations for the d.c. at 20° C.

The results of Drude (23) and Errera (24) are taken from the I.C.T., where they have been reduced to correspond with $\epsilon_{20}=2{\cdot}283$ for benzene. The values of Åkerlöf (12) and Harrington (25) have been taken from their papers; the investigations of Harrington (25) were carried out with a Nernst bridge, using damped oscillations of frequency $10^6$. His method is absolute, and the data for the rounded values of the concentrations given in the table have been derived from a large-scale graph using the data given in his paper. The results of Drude (23), Errera (24), and Harrington (25) have been reduced to 20° C., with the temperature coefficients given in Table VIII.

It is difficult to reconcile the large discrepancies in the data given in this table. It should be added that the composition of the mixtures used here cannot be very much in error in view of the good agreement between the values of the composition as found by synthesis and by density (*vide* Table VI.).

In conclusion, the authors wish to express their thanks to Messrs. L. E. Sulston and D. Owen for their help in connexion with the construction of the apparatus and to Vice-Principal T. C. James for the loan of the refractometer.

## V. *References.*

(1) Davies, Phil. Mag. xxi. p. 1 (1936).
(2) Davies, Phil. Mag. xxi. p. 1008 (1936).
(3) Davies and Jones, Phil. Mag. xxviii. p. 289 (1939).
(4) Dittmar and Fawsitt, Trans. Roy. Soc. Edin. xxxiii. p. 509 (1888). Doroshewski and Rostdestwenski, *Journ. Russ. ph. ch. Gess.* xli. p. 980 (1909).
(5) Hartley and Barrett, J. C. S. p. 1072 (1911).
(6) Hartshorn and Oliver, Proc. Roy. Soc. cxxiii. p. 664 (1929).
(7) Kyropoulos, *Zeit für Phys.* xl. p. 507 (1927).
(8) Astin, Phys. Rev. xxxiv. p. 300 (1929).
(9) Gundermann, *Ann. der Phys.* vi. p. 545 (1930).
(10) Ulich and Nespital, *Zeit. f. phys. Chem.* xvi. B, p. 221 (1932).
(11) Farkas, *Zeits. Electrochem.* xxxviii. p. 654 (1932).
(12) Åkerlöf, J. A. C. S. liii. p. 4126 (1932).
(13) le Fèvre, Trans. Faraday Soc. xxxiv. p. 1127 (1938).
(14) Deubner, *Ann. der Phys.* lxxxiv. p. 448 (1927).
(15) Sack, *Phys. Zeit.* xxvii. p. 206 (1926); xxviii. p. 199 (1927).
(16) Novosilzew, *Ann. der Phys.* ii. p. 515 (1929).
(17) Drake, Pierce, and Dow, Phys. Rev. xxxv. p. 613 (1930).
(18) Wyman, Phys. Rev. xxxv. p. 623 (1930).
(19) Cuthbertson and Maas, J. A. C. S. lii. p. 483 (1930).
(20) Linton and Maas, J. A. C. S. liv. p. 1863 (1932).
(21) Graffunder and Heymann, *Zeit. f. Phys.* lxxii. p. 744 (1931).
(22) Lattey, Gatty, and Davies, Phil. Mag. xii. p. 1019 (1931).
(23) Drude, *Zeit. f. Phys. Chem.* xxiii. p. 267 (1897).
(24) Errera, *Kolloid Zett.* xxxii. p. 373 (1923).
(25) Harrington, Phys. Rev. viii. p. 581 (1916).

# XXVIII. *The Influence of the Cathode on the Sparking Potential of Heavy Hydrogen.*

By F. Llewellyn Jones, M.A., D.Phil.,
University College, Swansea *.

[Received June 20, 1939.]

## § 1. *Introduction.*

A comparison of the sparking potential of deuterium and hydrogen is of interest because differences between the electrical properties of the two isotopes are due simply to the greater mass of the deuterium atom, and therefore of the positive ion. While the inelastic losses and the collisional cross-sections are practically the same in the two gases, the elastic losses of energy in the collisions between the electrons and the molecules are less in deuterium than in hydrogen owing to the greater mass of the deuterium atom. Consequently, those properties determined by the elastic losses are different in the two gases.

Now the relative importance of the various factors which determine the mean energy of agitation of the electrons is itself determined by the ratio of the electric force Z to the pressure $\rho$. For instance, when $Z/\rho$ is low the mean energy is determined by the molecular cross-section and the elastic losses, but at high values of $Z/\rho$ the controlling factors are the molecular cross-section and the inelastic losses. Therefore, when $Z/\rho$ is low, as in the uniform positive column, the mean energies of the electrons are greater in deuterium than in hydrogen; and, in fact, Guntherschulze and Schultger † have found a difference of 16 per cent. in the mean energies in the two gases. On the other hand, when $Z/\rho$ is high, as at pressures near those corresponding to the minimum sparking potential, it is reasonable to conclude that, since factors like the molecular cross-section and the inelastic losses do not differ by any significant amount in the two isotopes, then the mean energies of the electrons are the same in the two gases. Hence it follows that the coefficient $\alpha$, of ionization of deuterium by electrons differs very little from that of hydrogen at high values of $Z/\rho$; in fact, measurements by Steenbeck ‡ of the force in the uniform positive column of hydrogen and deuterium show that there is no very great difference in $\alpha$ for the two gases even when $Z/p$ is low. Now at high pressures, when $Z/p$ is low, the sparking potential is mainly determined by $\alpha$, because changes in the coefficient of secondary ionization have then little effect on the sparking potential *. However, owing to the difference in their mass, the behaviour of the positive ions is very different in the two gases. This consideration is of particular interest in the explanation of the mechanism of the spark discharge. For it is reasonable to conclude that, at pressures near those corresponding to the minimum sparking potential, the factors which are determined by the motion of the electrons, such as the rate of emission of radiation, are the same in deuterium as in hydrogen. Consequently, if the photo-electric effect at the cathode, due to radiation emitted as a result of the collisions of the electrons and the gas molecules, is the predominating factor in the process of electron emission, then the minimum sparking potential of deuterium and hydrogen should be the same. On the other hand, if the secondary ionization process involves the velocities of the positive ions, then the minimum sparking potential of the two gases should be different, and higher for deuterium than for hydrogen.

---

* Communicated by the Author.

† A. Guntherschulze and H. Schultger, *Zeit. f. Phys.* civ. p. 395 (1937).

‡ M. Steenbeck, *Zeit. f. Phys.* ii. p. 379 (1936).

This paper describes experiments made, firstly, to investigate the effect of the cathode material on the sparking potential of deuterium in order to ascertain the importance of secondary emission from the cathode in the sparking mechanism ; and secondly, to compare the sparking potentials of deuterium and hydrogen in order to investigate the effect of the greater mass of the deuterium positive ion on the process of secondary emission.

## § 2. *Experimental Procedure.*

The experimental procedure and the discharge-tubes used were the same as those described in another paper on the sparking potential of hydrogen †. After those measurements the tubes were heated in electric furnaces at a temperature of 400° C. for several days, and continuously evacuated by means of a mercury diffusion pump and the usual liquid-air traps. Afterwards, the tubes were kept evacuated for some months, and this procedure was found to be very effective in removing gas layers from the electrode surfaces after their exposure to gas in the discharge-tubes. The electrodes were also treated after the admission of deuterium to the tubes by maintaining discharges of a few milliamperes between them. The deuterium was prepared by the electrolysis of a solution of pure barium oxide in heavy water, which was obtained 99·6 per cent. pure from Norsk Hydro-Elecktrisk Kvaelstofaktieselskab. A small voltmeter was constructed to contain about 25 c.c. of heavy water, and this was baked in order to drive off all moisture to avoid contamination by hydrogen. The pure barium oxide was prepared by heating a small quantity of pure barium carbonate, kept in a porcelain crucible, in an electric furnace at 1100° C., and afterwards transferring it to a desiccator to cool. The contents were then dropped into heavy water, and the solution filtered to remove unchanged carbonate. The deuterium was dried by storage over phosphorus pentoxide, and was admitted to the discharge-tubes through a tube immersed in liquid air. The sparking potentials were measured by a Ferranti sub-standard voltmeter.

---

* F. Llewellyn Jones, Phil. Mag. (in the press).

† F. Llewellyn Jones and J. P. Henderson, Phil. Mag. (in the press).

### § 3. *The Minimum Sparking Potential.*

The range of pressures near those corresponding to the minimum sparking potential was first investigated, and the results are given in fig. 1.

Fig. 1.

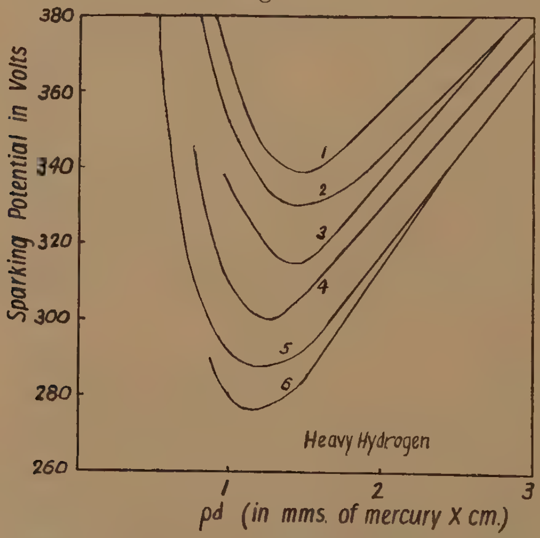

The minimum sparking potential of deuterium for different cathodes :— 1, Staybrite steel ; 2, copper ; 3, slightly oxidized Staybrite steel ; 4, nickel ; 5, pure aluminium ; 6, commercial aluminium.

As with hydrogen, it is seen that the minimum sparking potential V is strongly characteristic of the material of the cathode, and is lowered by slight oxidation of the cathode surface. Preliminary measurements showed that V depended on the history of the cathodes, as it was found that the values obtained after the tubes had been evacuated for some time were always higher than those obtained after even a short exposure to the gas at pressures of about 10 to 20 mm. of mercury. This result was obtained with different cathodes, and also with different specimens of gas. However, after exposure of the electrodes to gas, the higher values of V could be restored simply by keeping the tubes evacuated for about two days, and then measuring the sparking potential immediately after the admission of fresh gas. Further, the higher values of V could also be restored by maintaining a discharge of a few milliamperes between the electrodes for some minutes immediately before the measurement of the sparking potential. Owing to the thorough degassing of the tubes, and the general precautions taken, it was not considered that these variations in the values of the minimum sparking potential could be due to any impurities set free inside the tubes. Since, however, it was the previous presence of gas in the tubes at a moderate pressure which produced the fall in the sparking potential, it may be concluded that the presence of a layer of gas on the cathode surface was more probably the cause of the change. The highest reproducible values of the minimum sparking potential are given in the following table, and, with the possible exception of nickel, they are considered to be characteristic of the metal of the cathodes. In the measurements the electrodes were not exposed to the gas any longer than was necessary to make the measurement.

Minimum Sparking Potential in Volts.

| Cathode. | Deuterium. | | | Hydrogen. | | |
|---|---|---|---|---|---|---|
| | V. | $pd$. | $Z/p$. | V. | $pd$. | $Z/p$. |
| Commercial aluminium .... | 277 | 1·19 | 233 | 270 | 1·1 | 245 |
| Pure aluminium .......... | 288 | 1·24 | 232 | 279 | 1·2 | 232·5 |
| Nickel .................... | 300 | 1·28 | 234·4 | 288 | 1·25 | 230 |
| Oxidized Staybrite steel ... | 315 | 1·4 | 227 | 294 | 1·29 | 237 |
| Copper .................... | 330 | 1·44 | 230 | 319 | 1·38 | 230 |
| Staybrite steel ............ | 339 | 1·47 | 230 | 329 | 1·41 | 234 |

In the case of the nickel electrode, the variations of the sparking potential with the conditions of the measurement were greater than those found with the other electrodes, and the experiments indicated that nickel was very sensitive to the effect of gas on its surface. The work function of clean nickel is higher than that of copper or iron, so that the anomalous position of nickel in the table above may be due to the great difficulty of removing all traces of gas from its surface.

The table also gives the values of the product $pd$, where $d$ is the distance apart of the electrodes, corresponding to the minimum sparking potential for each cathode, and it can be seen that, within the experimental error, the ratio $Z/p$ is the same for all cathodes. At the minimum sparking potential it is not easy to determine $pd$ accurately, especially at the lower values, but a straight line drawn as near as possible through the six minima in fig. 1 has a slope of 232, which must then be taken to be the value of $Z/\rho$ at the minimum sparking potential of deuterium.

After continuous exposure to the gas, values of the minimum sparking potential were obtained which strongly varied with the cathode material and which were reproducible, but these were about 15 v. lower than those given above. They may be considered to be characteristic of the cathode material when covered with a thin gas layer, and the corresponding values of the ratio $Z/\rho$ lay between 225 and 240.

### § 4. *Results at Higher Pressures.*

The influence of the cathode on the sparking potential was examined by reversing the potential applied to each tube, and it was found that the resulting change in the potential depended on the gas pressure. For instance, with the tube containing the electrodes of commercial aluminium and oxidized Staybrite steel, the difference in the sparking potentials decreased rapidly at first, as the pressure increased above that which corresponded to the minimum sparking potential, and afterwards remained nearly constant at about 10 to 15 v. With the tube containing the electrodes of aluminium and nickel, the difference in V decreased steadily as the pressure was raised to 26 mm., at which point the sparking potentials were identical. With the copper and Staybrite steel electrodes the difference in the sparking potentials at first decreased, and then increased to about 26 v. at a pressure of 26 mm. It is of interest to compare the fractional change in the sparking potential due to a change of cathode near the minimum sparking potential with that which occurs at the higher pressure of 26 mm. With the commercial aluminium–oxidized Staybrite steel pair of electrodes, the fractional change in V was 9 per cent. at $\rho d = 1{\cdot}5$, but it was only 2 per cent. when $\rho d = 9$. With the pure aluminium–nickel pair, the changes were 3·3 per cent. at the lower pressure and zero at the higher pressure ; but with the copper–Staybrite steel pair, the change in V was 3 per cent. when $\rho d = 1{\cdot}5$, and was 4 per cent. when $\rho d = 9$.

Now, the measurements at the lower pressures indicated that the effect of exposure of the electrodes to the gas at pressures from 10 to 20 mm. was to reduce the sparking potential, and that this effect was very pronounced with nickel and, to a less extent, with copper. Consequently, it is possible that the rapid decrease in the difference $dV$ in the sparking potentials for the nickel and aluminium cathodes, and also the increase in $dV$ for the steel and copper cathodes, as the pressure increased to 26 mm., may partly be accounted for by the influence of the gas on the electrodes, because nickel and copper appear to be more affected than the others.

## § 5. *The Comparison of Light and Heavy Hydrogen.*

Although the sparking potential curves for hydrogen with the same sets of electrodes have been given in another paper *, nevertheless it was considered desirable to repeat the determinations after the measurements with deuterium. This was to see whether the electrode surfaces had undergone any permanent change, which would then invalidate the comparison of the sparking potential curves of the two gases. The discharge-tubes were not heated, but they were kept evacuated for several days and then washed out many times with pure hydrogen, which was prepared by the electrolysis of barium hydrate. With hydrogen in the tubes, the electrodes were further treated by maintaining discharges of a few milliamperes between them. The values of the sparking potential found were exactly the same as those given previously, and it was therefore concluded that the electrodes had not undergone any significant change. When the electrodes had been in continuous contact with the hydrogen for some time, the values of the minimum sparking potential obtained were within one volt of those given previously. However, as with deuterium, higher values of the minima were obtained after the discharge-tubes had been kept evacuated for some time before each measurement, to prevent the electrodes being long in contact with the gas. These values are given in the table (p. 331), where they may be compared with those found for deuterium under exactly similar conditions.

The full sparking curves for hydrogen, up to a pressure of 26 mm. with the steel and aluminium cathodes, are given in fig. 2. so that they can be directly compared with deuterium.

The curves show that when $pd=1{\cdot}4$ the sparking potential of deuterium is 3 per cent. higher than that of hydrogen †, but that when $pd=9$, deuterium has the lower sparking potential. Further, for a range of values of $Z/p$ from about 90 to 130, depending on the cathode material, the sparking potentials of deuterium and hydrogen are the same. With the steel cathode this range was from 88 to 120, while with aluminium the range was from 100 to 130. The curves show also that the general discussion of the variation of the sparking potential of hydrogen with the cathode material applies equally to deuterium ‡. However, in the absence of exact knowledge of the coefficient $\alpha$ for deuterium, no significance can be attached to the fact that deuterium has the lower sparking potential when $Z/p$ falls from 88 to 60, apart from the conclusion that in this range the coefficient $\alpha$ is higher in deuterium than in hydrogen. On the other hand, for low values of $pd$ where $Z/p$ exceeds 150, it is possible to arrive at definite conclusions about the secondary ionization coefficient, and therefore about the mechanism of the spark discharge.

---

* Llewellyn Jones and Henderson, *loc. cit.*

† A preliminary account of this appeared in ‘Nature,’ cxliii. p. 854 (1939)

‡ Llewellyn Jones, *loc. cit.*

Fig. 2.

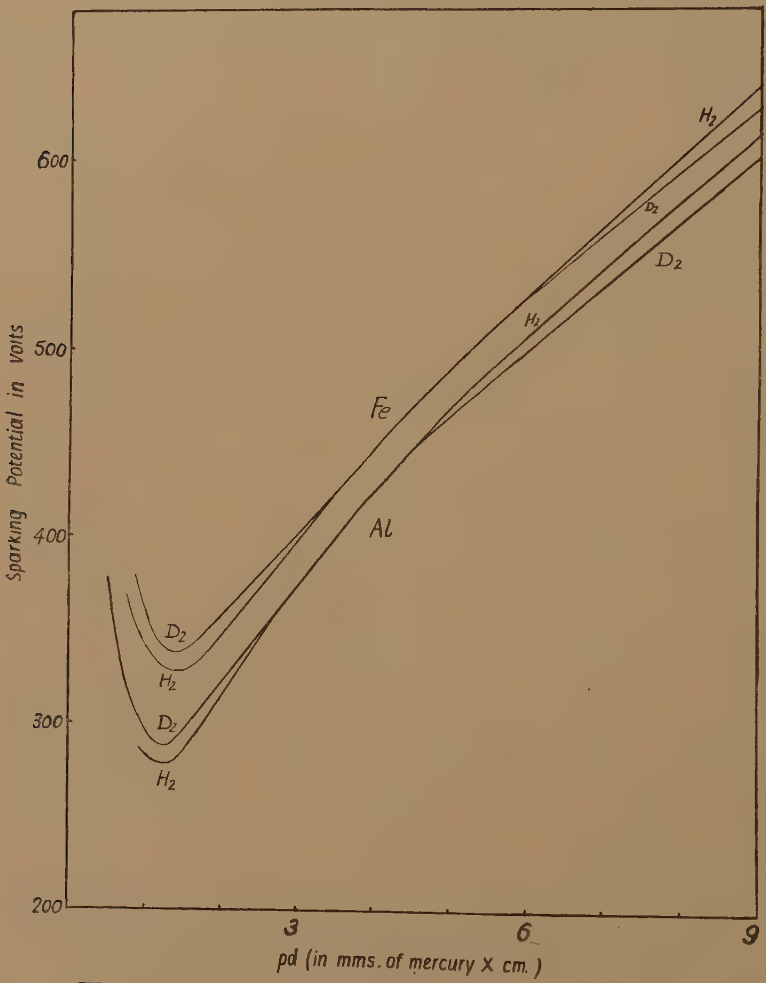

The sparking potential of light and heavy hydrogen.

## § 6. *The Second Townsend Coefficient.*

The considerations of § 1 show that a comparison of the values of the secondary ionization coefficient $\delta/\alpha$ in deuterium with those in hydrogen is of special interest, owing to the possibility of finding the relative importance of the two processes of secondary emission from the cathode. It has been shown above that if the secondary ionization is due simply to photo-electric emission, then $\delta/\alpha$ should be practically the same for the two gases, while on the other hand, if the ionization is due mainly to the action of the positive ions on the cathode, then large differences are to be expected between the values of $\delta/\alpha$ for deuterium and those for hydrogen.

The calculation of $\delta/\alpha$ from the value of the sparking potential by means of the equation

$$I-\delta/\alpha\,.\,(e^{\alpha d}-I)=0$$

Fig. 3.

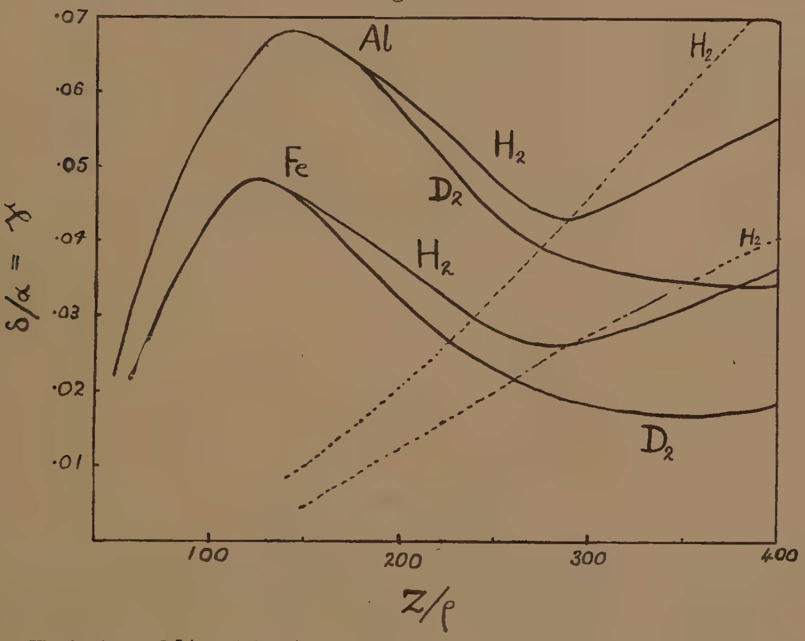

Variation of $\delta/\alpha$ with $Z/\rho$ in $H_2$ and $D_2$ for cathodes of Fe and Al.

depends on an accurate knowledge of $\alpha/\rho$ in terms of $Z/\rho$. Now values of $\alpha/\rho$ for hydrogen have recently been given by Hale *, and these differ markedly from those previously given by Ayres †, especially in the important range where $Z/\rho$ lies between 100 and 250. The coefficient $\delta/\alpha$ has been calculated from the curves in fig. 2, and the results for the steel and aluminium cathodes are given in fig. 3.

The values of $\delta/\alpha$ for deuterium and hydrogen, calculated with Hale's values of $\alpha/\rho$, are given by the full curves, while the dotted curves give for comparison the values of $\delta/\alpha$ in hydrogen calculated with the values

---

* D. H. Hale, Phys. Rev. lv. p. 815 (1939).

† T. L. R. Ayres, Phil. Mag. xlv. p. 353 (1923).

of $\alpha/p$ given by Ayres. The curves for the nickel and copper cathodes occupy intermediate positions, and are omitted. The full curves for hydrogen are in good agreement with the recent determinations of Hale, as they both show a maximum when $Z/p$ is about 140 ; but this was to be expected, as the corresponding sparking potential curves are very similar. These maxima in the values of $\delta/\alpha$, which are exhibited by all the electrodes, when $Z/p$ is less than about 200, may be taken to indicate that photo-electric emission is the predominating cathode process ; whereas when $Z/p$ exceeds about 250, both the full and dotted curves show an increase of $\delta/\alpha$ with $Z/p$, and this indicates the predominating influence of the action of the positive ions*. Moreover, strong evidence in support of this view is obtained by comparing the values of $\delta/\alpha$ for hydrogen with those for deuterium at the same values of $Z/p$.

In comparing the $(\delta/\alpha, Z/p)$ curves for deuterium and hydrogen, it is significant that for each cathode the range of $Z/p$, for which $\delta/\alpha$ is the same, is precisely that for which $\delta/\alpha$ has a maximum value. As $\delta/\alpha$ will be the same for deuterium and hydrogen only if it represents a photo-electric process, the view that the maxima in the curves indicate the predominating influence of photo-electric emission is thus confirmed. It is likewise significant that $\delta/\alpha$ for deuterium is much smaller than that for hydrogen just throughout that range of $Z/p$, where $\delta/\alpha$ increases with $Z/p$. This confirms the view that throughout this range the secondary ionization is due to the action of positive ions on the cathode. For, when $Z/p$ exceeds 200, the coefficient $\delta/\alpha$ for hydrogen is from 20 to 100 per cent. greater than that for deuterium, and such large differences cannot easily be accounted for if $\delta/\alpha$ represents a photo-electric process, because the only difference in the electrical properties of the two gases lies in the behaviour of the positive ions. This difference in the efficiency of secondary emission due to $H_2^+$ and $D_2^+$, which was calculated from the difference in the sparking potentials, is of the same order as that directly determined for high velocity positive ions and recently given by Healea †.

Since the potential energies of the positive ions of deuterium and of hydrogen are equal, the difference in $\gamma$ must therefore be attributed to the difference in the average velocities with which the ions strike the cathode. It would thus appear that the actual velocity of the ion, as distinct from its kinetic energy, is of importance in the mechanism of secondary emission.

## §7. *Summary.*

The sparking potential of deuterium between parallel electrodes was measured throughout a range of gas pressures from one to 26 mm. for six different cathodes. As with hydrogen, marked dependence on the cathode material was found, especially at the minimum sparking potential. For each electrode the minimum sparking potential of $D_2$ was about 3 per cent. greater than that of $H_2$, but at a pressure of 26 mm. the sparking potential of $D_2$ was 3 per cent. lower than that of $H_2$.

---

* F. Llewellyn Jones, *loc. cit.*

† M. Healea, Phys. Rev. lv. p. 984 (1939).

The second Townsend coefficient, $\delta/\alpha$, was calculated for $H_2$ and $D_2$ on the assumption that $\alpha$ was the same for both gases, and it was found that $\delta/\alpha$ was the same for $H_2$ and $D_2$ when $Z/\rho$ was from 100 to 150, but that when $Z/\rho$ exceeded 250, $\delta/\alpha$ for $H_2$ was from 20 to 100 per cent. greater than that for $D_2$.

It was therefore concluded that, when $Z/\rho=150$, photo-electric emission is the predominant cathode process; but that, when $Z/\rho$ exceeded 250, the secondary emission was due to the action of the positive ions. Further, it would appear that the actual velocity of the ions is of importance in the mechanism of secondary emission from the cathode.

In conclusion, I wish to express my best thanks to Professor E. J. Evans for extending the facilities of his laboratory, and for his kind interest.

Swansea.
19th June, 1939.

---

## *The Mechanism of the Spark Discharge in Hydrogen.*

By F. Llewellyn Jones, University College, Swansea.

Phil. Mag. xxviii. pp. 192–202 (August 1939).

### Addendum and Correction.

1. It is well known that atomic hydrogen has a profound effect on the photoelectric properties of many metals (R. Suhrmann, *Ergebnisse der Exakten Naturwissenschaften*, xiii. p. 148 (1934)). For example, a monatomic layer of hydrogen on the cathode surface can increase the photoelectric yield, while the addition of further layers leads to a decrease in the yield. Now the results described above indicate that the photoelectric effect plays a very important part in the spark mechanism in hydrogen even when $Z/\rho$ is as high as 150. Hence it follows that the effect of a spark in lowering the sparking potential of subsequent sparks may well be accounted for in hydrogen by the action of atomic hydrogen in increasing the photoelectric yield from the cathode.

2. The discussion of the action of positive ions within the range $27<Z/\rho<56$, given in the penultimate paragraph of a previous paper (Phil. Mag. xxviii. p. 201 (1939)) on the spark mechanism in $H_2$, contained a mis-statement in the last sentence owing to the omission of the words: " to the 4th power." The complete sentence should have been: " On the other hand, if the secondary emission from the cathode is proportional to the square of the energy, *i. e.*, to the 4th power of the velocity of the incident ions, instead of to their energy, then the total increase in $\gamma$, as $Z/\rho$ increases from 27 to 56, is about 9 or 10 times, which is just the increase required by the experimental results."

This discussion was based on the values of $\gamma$ derived from the values of $\alpha/\rho$ given by Ayres. However, the application of Hale's determinations of $\alpha/\rho$ to the calculation of $\gamma$ renders unnecessary any further discussion of the action of positive ions when $Z/\rho<100$, owing to the conclusion, reached above, that within this range the photoelectric effect is the predominant mechanism.

12th August, 1939.

## XXIX. *Harmonic Analysis by the Method of Central Differences.*

By D. C. Espley, M.Eng., M.I.E.E. (Communication from the Research Staff of the M.O. Valve Company, Limited, at the G.E.C . Research Laboratories, Wembley, England *.)

[Received November 1, 1938.]

### Summary.

A method for the treatment of non-linear characteristics is described. The analysis is not limited to any number of values of a tabulated function. To facilitate numerical calculation a table of constants is included, so that the direct evaluation of harmonics up to the fifth can be obtained from characteristics determined by a maximum of eleven points. Particular reference is made to distortion in thermionic valves, although the method is not limited to such cases.

### I. *Introduction.*

Most methods of harmonic analysis are suitable only for specific numbers of points on the non-linear characteristic. Even if the characteristic is available as a tabulated series of entries for equally spaced intervals of the argument, as is usual in the treatment of thermionic valves, the use of a large number of entries is often avoided owing to the laborious nature of the calculations. As a first step it appears logical to derive the equation for the characteristic, and in many cases this is expressed as a polynomial *. The present analysis uses this derivation as an intermediate step, and the actual numerical calculation of harmonic contents involves only a table of constants and the original entries.

The author has found the method to be wide in application as it is not limited to any number of points on the non-linear characteristic, or to any order of harmonic. The arithmetic is reduced to a minimum, and it will be found that in most cases the value of the harmonic is given as the sum of a number of terms which are rapidly convergent and so can be terminated at any point determined by the accuracy required. Most of the applications have been concerned with harmonic production in thermionic valves with resistive loads, and this basis has been adopted

* Communicated by C. C. Paterson.

in the following analysis, although the method is useful in the treatment of most non-linearity problems.

## 2. *Equation of the Load Line.*

It is assumed that the load characteristic is expressed as a power series *†

$$I=a_0'+a_1'k+a_2'k^2+\ldots\ldots a_s'k^s+\ldots\quad\quad(1)$$

in which $k=\dfrac{e_g}{\triangle e_g}$,

and the coefficients $a_0'$, $a_1'$, $a_2'$ ....... $a_s$ are obtainable directly in terms of points on this load characteristic; $e_g$ is the variable grid voltage measured from the working-point, and $\triangle e_g$ is the constant difference of this voltage as available from the valve static characteristic curves. The method adopted to obtain the polynomial coefficients makes use of a difference formula which is eminently suited to the analysis. The Newton-Stirling central difference formula ‡ was selected as being the most suitable, and probably the most reliable, as the maximum accuracy is obtainable in the middle of the range.

Suppose that for a number of equally spaced values of a variable we have tabulated the corresponding values of a function, then a difference table can be constructed from these quantities in the following manner :—

| Argument. | Entry. | | | | |
|---|---|---|---|---|---|
| $a-2\omega$ | $u_{-2}$ | | | | |
| | | $\delta u_{-3/2}$ | | | |
| $a-\omega$ | $u_{-1}$ | | $\delta^2 u_{-1}$ | $\delta^3 u_{-1/2}$ | |
| | | $\delta u_{-1/2}$ | | | |
| $a$ | $u_0$ | $(\mu\delta u_0)$ | $\delta^2 u_0$ | $(\mu\delta^3 u_0)$ | $\delta^4 u_0$ |
| | | $\delta u_{1/2}$ | | | |
| $a+\omega$ | $u_1$ | | $\delta^2 u_1$ | $\delta^3 u_{1/2}$ | |
| | | $\delta u_{3/2}$ | | | |
| $a+2\omega$ | $u_2$ | | | | |

The notation used is due to Sheppard § and will be employed throughout. The $u$ terms are the original entries to which a curve has to be fitted, and successive differences are taken and tabulated in the next column.

---

[*] D. C. Espley, "The Calculation of Harmonic Production in Thermionic Valves with Resistive Loads," Proc. I. R. E. xxi. pp. 1439–1446 (October 1933).

[†] D. C. Espley, "Harmonic Production and Cross Modulation in Thermionic Valves with Resistive Loads," Proc. I. R. E. xxii. pp. 781–790 (June 1934).

[‡] Whittaker and Robinson, 'Calculus of Observations,' Blackie and Son, London (1924).

[§] Proc. London Math. Soc. xxxi. p. 459 (1899).

Thus

$$u_{-1}-u_{-2}=\delta u_{-3/2},$$

and, in general,

$$u_n-u_{n-1}=\delta u_{\frac{2n-1}{2}}.$$

Also

$$\delta^r u_n-\delta^r u_{n-1}=\delta^{r+1} u_{\frac{2n-1}{2}}.$$

In the Newton-Stirling central difference formula it is also necessary to use mean differences which are found by taking the arithmetic mean of adjacent entries in the same column of differences. The mean differences are all designated by the symbol $\mu$.

Thus

$$\mu\delta u_0=\frac{\delta u_{1/2}+\delta u_{-1/2}}{2}$$

and

$$\mu\delta^r u_n=\frac{\delta^r u_{n+1/2}+\delta^r u_{n-1/2}}{2}.$$

The required expansion is then given in terms of these differences in the form :—

$$\begin{aligned} u_x=u_0+x\mu\delta u_0+\frac{x^2}{2\,!}\,\delta^2 u_0+\frac{x(x^2-1)}{3\,!}\,\mu\delta^3 u_0+\ldots\ldots \\ \ldots\ldots+\tfrac{1}{2}\{(x+r)_{2r}+(x+r-1)_{2r}\}\delta^{2r}u_0+\ldots\ldots \\ \ldots\ldots+(x+r)_{2r+1}\mu\delta^{2r+1}u_0+\ldots\ldots \quad . \quad . \quad . \quad . \quad . \quad . \quad (2) \end{aligned}$$

It should be noted that unit value of $x$ in our particular case will correspond to the unit interval $\triangle e_g$ in the static characteristics. Hence, if the characteristics are drawn at intervals of grid voltage of say 5 volts, putting $x=1$ will represent a movement along the $x$-axis corresponding to 5 volts. Expansion (2) may be put in a more convenient form by collecting terms in $x$; therefore

$$\begin{aligned} u_x=u_0 \\ +x\left[\mu\delta u_0-\frac{\mu\delta^3 u_0}{3\,!}+\frac{4\mu\delta^5 u_0}{5\,!}-\frac{36\mu\delta^7 u_0}{7\,!}+\frac{576\mu\delta^9 u_0}{9\,!}\ldots\ldots\right] \\ +x^2\left[\frac{\delta^2 u_0}{2\,!}-\frac{\delta^4 u_0}{4\,!}+\frac{4\delta^6 u_0}{6\,!}-\frac{36\delta^8 u_0}{8\,!}+\frac{576\delta^{10} u_0}{10\,!}-\ldots\ldots\right] \\ +x^3\left[\frac{\mu\delta^3 u_0}{3\,!}-\frac{5\mu\delta^5 u_0}{5\,!}+\frac{49\mu\delta^7 u_0}{7\,!}-\frac{820\mu\delta^9 u_0}{9\,!}+\ldots\ldots\right] \\ +x^4\left[\frac{\delta^4 u_0}{4\,!}-\frac{5\delta^6 u_0}{6\,!}+\frac{49\delta^8 u_0}{8\,!}-\frac{820\delta^{10} u_0}{10\,!}+\ldots\ldots\right] \end{aligned}$$

$$+x^5\left[\frac{\mu\delta^5u_0}{5\,!}-\frac{14\mu\delta^7u_0}{7\,!}+\frac{273\mu\delta^9u_0}{9\,!}-\ldots\ldots\right]$$

$$+x^6\left[\frac{\delta^6u_0}{6\,!}-\frac{14\delta^8u_0}{8\,!}+\frac{273\delta^{10}u_0}{10\,!}-\ldots\ldots\right]$$

$$+x^7\left[\frac{\mu\delta^7u_0}{7\,!}-\frac{30\mu\delta^9u_0}{9\,!}+\ldots\ldots\right]$$

$$+x^8\left[\frac{\delta^8u_0}{8\,!}-\frac{30\mu\delta^{10}u_0}{10\,!}+\ldots\ldots\right]$$

$$+x^9\left[\ldots\ldots\qquad\qquad\right]$$

$$+\ldots\ldots \qquad\qquad \ldots\ldots \quad (3)$$

The general terms are :—

$n$ odd

$$x^n\left[\frac{\mu\delta^nu_0}{n\,!}\ldots\ldots\frac{(-1)^{r-1}\mu\delta^{n+2r-2}u_0\,\Sigma_{r-1}\left(\frac{n+2r-3}{2}\right)^2}{(n+2r-2)\,!}\ldots\ldots\right],$$

$n$ even

$$x^n\left[\frac{\delta^nu_0}{n\,!}\ldots\ldots\frac{(-1)^{r-1}\delta^{n+2r-2}u_0\,\Sigma_{r-1}\left(\frac{n+2r-4}{2}\right)^2}{(n+2r-2)\,!}\ldots\ldots\right],$$

$$\ldots \quad (4)$$

where

$$\Sigma_{r-1}\left(\frac{n+2r-3}{2}\right)^2$$

represents the sum of the products, taken $(r-I)$ at a time, of the numbers

$$1^2,\ 2^2,\ 3^2\ldots\ldots\left(\frac{n+2r-3}{2}\right)^2.$$

In all cases

$$\Sigma_{r-1}\left(\frac{0}{2}\right)^2=1 \quad\text{or}\quad \Sigma_0\left(\frac{n-2}{2}\right)^2=1.$$

The coefficients of equations (1) and (3) are equal, assuming $k$ and $x$ are identical variables, and it follows that

$$\left.\begin{aligned}
a_0'&=u_0,\\
a_1'&=\mu\delta u_0-\frac{\mu\delta^3u_0}{3\,!}+\frac{4\mu\delta^5u_0}{5\,!}-\frac{36\mu\delta^7u_0}{7\,!}+\ldots\ldots,\\
a_2'&=\frac{\delta^2u_0}{2\,!}-\frac{\delta^4u_0}{4\,!}+\ldots\ldots,
\end{aligned}\right\}\ldots \quad (5)$$

and generally for odd and even coefficients respectively

$$\left.\begin{aligned} a_n' &= \frac{\mu\delta^n u_0}{n\,!} - \frac{\mu\delta^{n+2}\Sigma_1\left(\frac{n+1}{2}\right)^2}{(n+2)\,!} + \ldots\ldots, \\ a_n' &= \frac{\delta^n u_0}{n\,!} - \frac{\delta^{n+1}\Sigma_1\left(\frac{n}{2}\right)^2}{(n+2)\,!} + \ldots\ldots \end{aligned}\right\} \quad . \quad . \quad . \quad . \quad (6)$$

### 3. *Coefficients of Frequency Terms.*

All the frequency terms can be obtained from equation (1) by substitution of the sinusoidal variable $k \sin \omega t$ instead of $k$.

$$\begin{aligned} \mathrm{I}_a = a_0' + a_1'(k \sin \omega t) + a_2'(k \sin \omega t)^2 \\ + \ldots . \, a_{m-1}'(k \sin \omega t)^{m-1}. \quad . \quad . \quad . \quad (7) \end{aligned}$$

The power series is terminated at the $(m-1)th$ term, as it will be clear from the difference table that, for $m$ available values of the argument, the $m$th difference is zero, and hence from equation (6), $a_m'=0$. After expansion equation (7) can be reduced to

$$\begin{aligned} \mathrm{I}_a = & \left[a_0' + \frac{k^2a_2'}{2} + \frac{3k^4a_4'}{8} + \frac{10k^6a_6'}{32} + \frac{35k^8a_8'}{128} + \frac{126k^{10}a_{10}'}{512} + \ldots\ldots\right] \\ & + \sin \omega t\left[\frac{k\,a_1'}{1} + \frac{3k^3a_3'}{4} + \frac{10k^5a_5'}{16} + \frac{35k^7a_7'}{64} + \frac{126k^9a_9'}{256} + \ldots\ldots\right] \\ & - \cos 2\omega t\left[\frac{k^2a_2'}{2} + \frac{4k^4a_4'}{8} + \frac{15k^6a_6'}{32} + \frac{56k^8a_8'}{128} + \frac{210k^{10}a_{10}'}{512} + \ldots\ldots\right] \\ & - \sin 3\omega t\left[\frac{k^3a_3'}{4} + \frac{5k^5a_5'}{16} + \frac{21k^7a_7'}{64} + \frac{84k^9a_9'}{256} + \ldots\ldots\right] \\ & + \cos 4\omega t\left[\frac{k^4a_4'}{8} + \frac{6k^6a_6'}{32} + \frac{28k^8a_8'}{128} + \frac{120k^{10}a_{10}'}{512} + \ldots\ldots\right] \\ & + \sin 5\omega t\left[\frac{k^5a_5'}{16} + \frac{7k^7a_7'}{64} + \frac{36k^9a_9'}{256} + \ldots\ldots\right] \\ & + \ldots\ldots\ldots\ldots\ldots\ldots\ldots\ldots\ldots\ldots \quad (8) \end{aligned}$$

The general term ($r$th term of the $n$th order) is given by

$$\begin{matrix} \sin n\omega t \\ \\ \cos n\omega t \end{matrix}\left[\frac{\sin\left\{\frac{(2n+1)}{4}\pi\right\} \times (n+2r-2)\,!\,k^{n+2r-2}.\,a_{n+2r-2}'}{2^{n+2r-5/2}\quad(n+r-1)\,!\quad(r-1)\,!}\right]\begin{matrix} n \text{ odd} \\ \\ n \text{ even} \end{matrix}$$

$$. \quad . \quad . \quad (9)$$

The numerical coefficients in the series can be obtained directly from

Pascal's Triangle (Figurate Numbers) where the $p$th term of order $q$ is given by

$$\frac{(p+q-2)\,!}{(p-1)\,!\;(q-1)\,!}$$

$$\begin{array}{lccccccccc}
 & 1 & 1 & 1 & 1 & 1 & 1 & 1 & 1 & 1\ldots\ldots \\
\sin\omega t & 1 & 2 & 3 & 4 & 5 & 6 & 7 & 8\ldots. & \\
 & 1 & 3 & 6 & 10 & 15 & 21 & 28\ldots\ldots & & \\
 & 1 & 4 & 10 & 20 & 35 & 56\ldots\ldots & & & \\
 & 1 & 5 & 15 & 35 & 70\ldots\ldots & & & & \\
 & 1 & 6 & 21 & 56\ldots. & & & & & \\
 & \ldots\ldots & & & & & & & &
\end{array}$$

$$\begin{array}{lccc}
\sin n\omega t' & 1 & & \\
\cos n\omega t & & (n+2) & \\
 & & & \dfrac{(n+3)(n+4)}{2}
\end{array} \qquad \ldots \quad (10)$$

It will be seen that the coefficients of the series for the $n$th order frequency term occur along a diagonal line starting at the $(n+1)$*th* term in the first column.

It is now possible to express the values of the frequency terms in central differences by combining equations (5) and (8). Substituting the values of $a_0'$ $a_1'$ $a_2'$ etc. in equation (8) we obtain, by expansion, the following generalized results :—

*Coefficient of the Constant Term.*

$$\begin{aligned}
f(\omega_0)=u_0 & \\
&+\frac{\delta^2 u_0}{2\,!}\left[\frac{k^2}{2}\right] \\
&+\frac{\delta^4 u_0}{4\,!}\left[-\frac{k^2}{2}+\frac{3k^4}{8}\right] \\
&+\frac{\delta^6 u_0}{6\,!}\left[\frac{4k^2}{2}-\frac{15k^4}{8}+\frac{10k^6}{32}\right] \\
&+\frac{\delta^8 u_0}{8\,!}\left[-\frac{36k^2}{2}+\frac{147k^4}{8}-\frac{140k^6}{32}+\frac{35k^8}{128}\right]
\end{aligned}$$

$$+\frac{\delta^{10}u_0}{10\,!}\left[\frac{576k^2}{2}-\frac{2460k^4}{8}+\frac{2730k^6}{32}-\frac{1050k^8}{128}+\frac{126k^{10}}{512}\right]$$

$$+\ldots\ldots\ldots\ldots\ldots\ldots\ldots\ldots \qquad (11)$$

*Coefficient of the Fundamental* sin $\omega t$.

$$f(\omega_1)=\mu\delta u_0\,k$$

$$+\frac{\mu\delta^3u_0}{3\,!}\left[-k+\frac{3k^3}{4}\right]$$

$$+\frac{\mu\delta^5u_0}{5\,!}\left[4k-\frac{15k^3}{4}+\frac{10k^5}{16}\right]$$

$$+\frac{\mu\delta^7u_0}{7\,!}\left[-36k+\frac{147k^3}{4}-\frac{140k^5}{16}+\frac{35k^7}{64}\right]$$

$$+\frac{\mu\delta^9u_0}{9\,!}\left[576k-\frac{2460k^3}{4}+\frac{2730k^5}{16}-\frac{1050k^7}{64}+\frac{126k^9}{256}\right]$$

$$+\ldots\ldots\ldots\ldots\ldots\ldots\ldots\ldots \qquad (12)$$

*Coefficient of the Second Harmonic* cos $2\omega t$.

$$f(\omega_2)=\frac{\delta^2u_0}{2\,!}\left[-\frac{k^2}{2}\right]$$

$$+\frac{\delta^4u_0}{4\,!}\left[\frac{k^2}{2}-\frac{4k^4}{8}\right]$$

$$+\frac{\delta^6u_0}{6\,!}\left[-\frac{4k^2}{2}+\frac{20k^4}{8}-\frac{15k^6}{32}\right]$$

$$+\frac{\delta^8u_0}{8\,!}\left[\frac{36k^2}{2}-\frac{196k^4}{8}+\frac{210k^6}{32}-\frac{56k^8}{128}\right]$$

$$+\frac{\delta^{10}u_0}{10\,!}\left[-\frac{576k^2}{2}+\frac{3280k^4}{8}-\frac{4095k^6}{32}+\frac{1680k^8}{128}-\frac{210k^{10}}{512}\right]$$

$$+\ldots\ldots\ldots\ldots\ldots\ldots\ldots\ldots \qquad (13)$$

*Coefficient of the Third Harmonic* sin $3\omega t$.

$$f(\omega_3)=\frac{\mu\delta^3u_0}{3\,!}\left[-\frac{k^3}{4}\right]$$

$$+\frac{\mu\delta^5u_0}{5\,!}\left[\frac{5k^3}{4}-\frac{5k^5}{16}\right]$$

$$+\frac{\mu\delta^7u_0}{7\,!}\left[-\frac{49k^3}{4}+\frac{70k^5}{16}-\frac{21k^7}{64}\right]$$

$$+\frac{\mu\delta^9u_0}{9\,!}\left[+\frac{820k^3}{4}-\frac{1365k^5}{16}+\frac{630k^7}{64}-\frac{84k^9}{256}\right]$$

$$+\ldots\ldots\ldots\ldots\ldots\ldots\ldots\ldots \qquad (14)$$

*Coefficient of the Fourth Harmonic* cos $4\omega t$.

$$f(\omega_4)=\frac{\delta^4 u_0}{4\,!}\left[\frac{k^4}{8}\right]$$
$$+\frac{\delta^6 u_0}{6\,!}\left[-\frac{5k^4}{8}+\frac{6k^6}{32}\right]$$
$$+\frac{\delta^8 u_0}{8\,!}\left[\frac{49k^4}{8}-\frac{84k^6}{32}+\frac{28k^8}{128}\right]$$
$$+\frac{\delta^{10} u_0}{10\,!}\left[-\frac{820k^4}{8}+\frac{1638k^6}{32}-\frac{840k^8}{128}+\frac{120k^{10}}{512}\right]$$
$$+\ldots\ldots \qquad (15)$$

*Coefficient of the Fifth Harmonic* sin $5\omega t$.

$$f(\omega_5)=\frac{\mu\delta^5 u_0}{5\,!}\left[\frac{k^5}{16}\right]$$
$$+\frac{\mu\delta^7 u_0}{7\,!}\left[-\frac{14k^5}{16}+\frac{7k^7}{64}\right]$$
$$+\frac{\mu\delta^9 u_0}{9\,!}\left[\frac{273k^5}{16}-\frac{210k^7}{64}+\frac{36k^9}{256}\right]$$
$$+\ldots\ldots \qquad (16)$$

It is not thought worth while to include the coefficients of harmonics higher than the fifth, but further computation is quite straightforward, and sufficient of the analysis has been shown to indicate the procedure. In all cases it will be seen that the expansions have been terminated at $\delta^{10}u_0$ or $\mu\delta^9 u_0$. This implies that the expansions are adapted for any number of points, on the non-linear characteristic, up to and including 11 points. All the terms are automatically restricted if a smaller number of points is taken, owing to the vanishing of high order differences. It has already been stated that, in general, to fit $m$ points a curve of $(m-1)$th degree is necessary, but in all cases the $m$th difference of a polynomial of this degree is zero. For example, if nine points are taken on the characteristic the last differences which can occur are $\delta^8 u_0$ and $\mu\delta^7 u_0$, and all the differences beyond this are zero. The expansions for the coefficients of harmonics definitely stop at these differences, and thus the ninth and higher harmonics appear to have zero amplitude.

In practical applications of the analysis it is necessary to evaluate the limited series in $k$ which appear in equations (11)–(16). The author has found that the arithmetic is considerable even in normal cases, and to simplify the method Table I. has been prepared to show the values of terms by which the differences must be multiplied. Calculations are then quite straightforward for values of $k$ up to 5 at intervals of 0·5.

Intermediate values of $k$ are seldom necessary, but where they must be used it is better to substitute directly into the relevant equation as curves are not usually accurate enough.

Fig. 1.

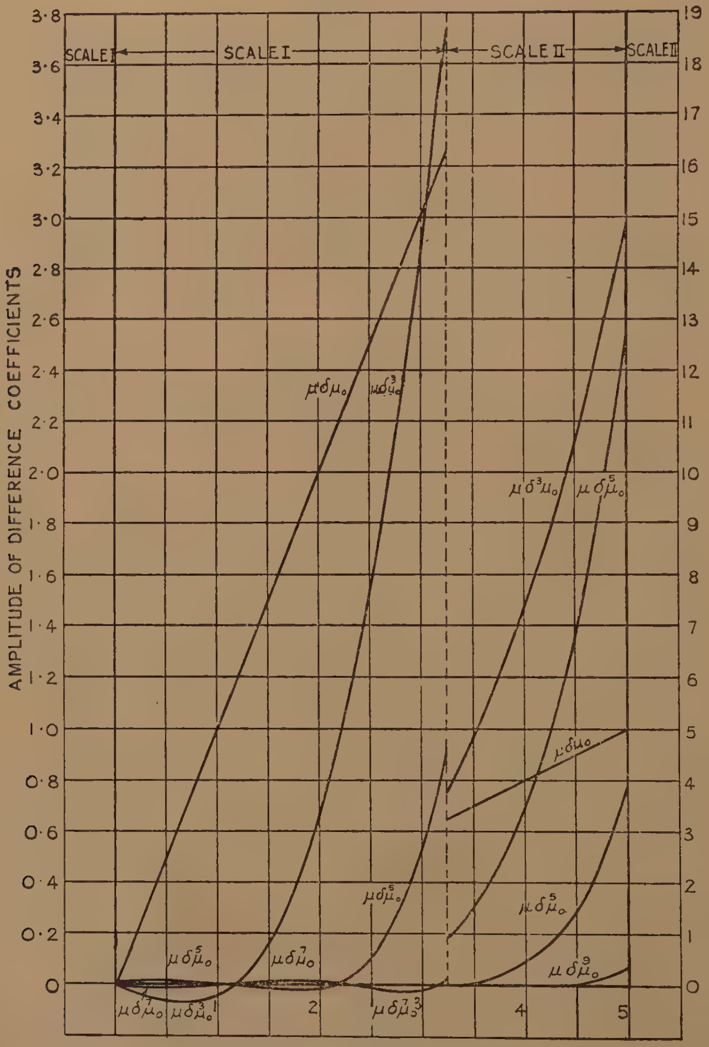

Amplitudes of Difference.
Coefficients for fundamental sin $\omega t$.

Fig. 1 shows the $k$ functions for the fundamental sin $\omega t$ (equation (12)).

The Difference Table can be constructed from the load line intercepts $I_1, I_2 \ldots\ldots I_m$, and by way of illustration we may take 5 points.

| Entry. | $\delta$. | $\delta^2$. | $\delta^3$. | $\delta^4$. |
|---|---|---|---|---|
| $I_1$ | | | | |
| | $(I_2-I_1)$ | | | |
| $I_2$ | | $(I_3-2I_2+I_1)$ | | |
| | $(I_3-I_2)$ | | $(I_4-3I_3+3I_2-I_1)$ | |
| $I_3$ | $\frac{1}{2}[I_4-I_2]$ | $(I_4-2I_3+I_2)$ | $\frac{1}{2}[I_5-2I_4+2I_2-I_1]$ | $(I_5-4I_4+6I_3-4I_2+I_1)$ |
| | $(I_4-I_3)$ | | $(I_5-3I_4+3I_3-I_2)$ | |
| $I_4$ | | $(I_5-2I_4+I_3)$ | | |
| | $(I_5-I_4)$ | | | |
| $I_5$ | | | | |

The central differences used in the analysis are

$$\mu\delta u_0=\tfrac{1}{2}[I_4-I_2],$$

$$\delta^2 u_0=I_4-2I_3+I_2,$$

$$\mu\delta^3 u_0=\tfrac{1}{2}[I_5-2I_4+2I_2-I_1],$$

$$\delta^4 u_0=I_5-4I_4+6I_3-4I_2+I_1.$$

The harmonics can be found by substitution in equations (11)–(15) to give results identical with those which appeared in a previous paper *.

For example, from equation (12), the value of the fundamental $\sin \omega t$ is

$$f(\omega_1)=\mu\delta u_0 k+\frac{\mu\delta^3 u_0}{3\,!}\left[-k+\frac{3k^3}{4}\right].$$

With 5 points available a peak amplitude $k=2$ covers the range over which the characteristic is tabulated. By substitution we obtain

$$f(\omega_1)=\tfrac{1}{3}[I_5+I_4-I_2-I_1].$$

Using this procedure it is possible to derive the coefficients of the harmonics for any number of entries $I_1, I_2 \ldots . I_m$ in the general form

$$f(\omega_x)=\frac{M_1I_1+M_2I_2+\ldots\ldots+M_mI_m}{S} \quad . \quad . \quad . \quad . \quad . \quad (17)$$

It can be proved that the following conditions must apply :—

(a) *Constant Term.*

$$M_1+M_2+M_3 \ldots\ldots+M_m=S \quad . \quad . \quad . \quad . \quad . \quad (18)$$

(b) *Frequency Terms.*

$$M_1+M_2+M_3 \ldots\ldots+M_m=0. \quad . \quad . \quad . \quad . \quad . \quad (19)$$

---

* *Loc. cit.* p. 1444.

### *Numerical Example.*

The following difference table is constructed from the load line (1000 ohms) intercepts for a triode valve. The characteristic curves are available at grid voltage intervals of 25 volts. Nine points were taken, and in the table mean central differences are bracketed. The working point is taken as $E_g = -100$ volts, and hence all grid voltage excursions are measured with respect to this point.

| $E_g$. | $I_a(mA)$. | $\delta$. | $\delta^2$. | $\delta^3$. | $\delta^4$. | $\delta^5$. | $\delta^6$. | $\delta^7$. | $\delta^8$. |
|---|---|---|---|---|---|---|---|---|---|
| −200 | 6·0 | | | | | | | | |
| | | 6·25 | | | | | | | |
| −175 | 12·25 | | 2·75 | | | | | | |
| | | 9·0 | | 5·0 | | | | | |
| −150 | 21·25 | | 7·75 | | −7·75 | | | | |
| | | 16·75 | | −2·5 | | 12·75 | | | |
| −125 | 38·0 | | 5·25 | | 5·25 | | −26·0 | | |
| | | 22·0 | | 2·75 | | −13·25 | | 46·25 | |
| −100 | 60·0 | (26·0) | 8·0 | (−1·25) | −8·0 | (− 3·125) | 20·25 | (18·125) | −56·25 |
| | | 30·0 | | −5·25 | | 7·0 | | −10·0 | |
| − 75 | 90·0 | | 2·75 | | −1·0 | | 10·25 | | |
| | | 32·75 | | −6·25 | | 17·25 | | | |
| − 50 | 122·75 | | −3·5 | | 16·5 | | | | |
| | | 29·25 | | 10·0 | | | | | |
| − 25 | 152·0 | | 6·5 | | | | | | |
| | | 35·75 | | | | | | | |
| 0 | 187·75 | | | | | | | | |

Suppose it is required to find the fundamental and second harmonic for a grid swing of 75 volts peak (*i. e.*, $e_g = 15 \sin \omega t$ and $k = \frac{75}{25} = 3$).

A typical calculation would appear as follows :—

(a) *Fundamental.*

$$(26{\cdot}0)\times(3{\cdot}0) = \phantom{-}78{\cdot}000$$
$$(-1{\cdot}25)\times(2{\cdot}875) = -\ 3{\cdot}594$$
$$(-3{\cdot}125)\times(0{\cdot}5219) = -\ 1{\cdot}631$$
$$(18{\cdot}125)\times(-0{\cdot}009124) = -\ 0{\cdot}165$$

therefore

*Peak milliamperes of Fundamental* $= 72{\cdot}610$.

(b) *Second Harmonic.*

$$8{\cdot}0\times(-2{\cdot}25) = -18{\cdot}000$$
$$-8{\cdot}0\times(-1{\cdot}5) = \phantom{-}12{\cdot}000$$

TABLE I.— Numerical Constants.

| | Coefficients. | k. | | | | | | | | | |
|---|---|---|---|---|---|---|---|---|---|---|---|
| | | 0·5. | 1·0. | 1·5. | 2·0. | 2·5. | 3·0. | 3·5. | 4·0. | 4·5. | 5·0. |
| Constant term. | $\delta^2 u_0 \left[\frac{k^2}{2}\right] \frac{1}{2\,!}$ | 0·06250 | 0·2500 | 0·5625 | 1·0000 | 1·5625 | 2·2500 | 3·0625 | 4·0000 | 5·06250 | 6·2500 |
| | $\delta^4 u_0 \left[-\frac{k^2}{2} + \frac{3k^4}{8}\right] \frac{1}{4\,!}$ | −0·004232 | −0·005208 | 0·03223 | 0·1667 | 0·4802 | 1·07810 | 2·0895 | 3·6667 | 5·9854 | 9·2448 |
| | $\delta^6 u_0 \left[\frac{4k^2}{2} - \frac{15k^4}{8} + \frac{10k^6}{32}\right] \frac{1}{6\,!}$ | 0·0005385 | 0·0006077 | −0·001990 | −0·002778 | 0·02160 | 0·1305 | 0·4411 | 1·1556 | 2·5924 | 5·2235 |
| | $\delta^8 u_0 \left[-\frac{36k^2}{2} + \frac{147k^4}{8} - \frac{140k^6}{32} + \frac{35k^8}{128}\right] \frac{1}{8\,!}$ | −0·00008479 | −0·00009242 | 0·0002405 | 0·0002976 | −0·001131 | −0·001708 | 0·01617 | 0·1095 | 0·4172 | 1·2273 |
| | $\delta^{10} u_0 \left[\frac{576k^2}{2} - \frac{2460k^4}{8} + \frac{2730k^6}{32} - \frac{1050k^8}{128} + \frac{126k^{10}}{512}\right] \frac{1}{10\,!}$ | 0·00001490 | 0·00001594 | −0·00003664 | −0·00004298 | 0·0001230 | 0·0001621 | −0·0007239 | −0·001164 | 0·01289 | 0·09560 |
| Fundamental sin *ωt*. | $\mu\delta u_0[k]$ | 0·5000 | 1·0000 | 1·5000 | 2·0000 | 2·5000 | 3·0000 | 3·5000 | 4·0000 | 4·5000 | 5·0000 |
| | $\mu\delta^3 u_0 \left[-k + \frac{3k^3}{4}\right] \frac{1}{3\,!}$ | −0·06771 | −0·04167 | 0·1719 | 0·6667 | 1·5365 | 2·8750 | 4·7758 | 7·3333 | 10·6410 | 14·7920 |
| | $\mu\delta^5 u_0 \left[4k - \frac{15k^3}{4} + \frac{10k^5}{16}\right] \frac{1}{5\,!}$ | 0·01292 | 0·007292 | −0·01592 | −0·01667 | 0·1037 | 0·5219 | 1·5124 | 3·4667 | 6·9132 | 12·5360 |
| | $\mu\delta^7 u_0 \left[-36k + \frac{147k^3}{4} - \frac{140k^5}{16} + \frac{35k^7}{64}\right] \frac{1}{7\,!}$ | −0·002713 | −0·001478 | 0·002565 | 0·002381 | −0·007239 | −0·009124 | 0·07390 | 0·4381 | 1·4833 | 3·9275 |
| | $\mu\delta^9 u_0 \left[576k - \frac{2460k^3}{4} + \frac{2730k^5}{16} - \frac{1050k^7}{64} + \frac{126k^9}{256}\right] \frac{1}{9\,!}$ | 0·0005962 | 0·0003180 | −0·0004887 | −0·0004299 | 0·0009843 | 0·001081 | −0·004137 | −0·005820 | 0·05727 | 0·3824 |
| Second harmonic cos 2*ωt*. | $\delta^2 u_0 \left[-\frac{k^2}{2}\right] \frac{1}{2!}$ | −0·06250 | −0·2500 | −0·5625 | −1·0000 | −1·5625 | −2·2500 | −3·0625 | −4·0000 | −5·0625 | −6·2500 |
| | $\delta^4 u_0 \left[\frac{k^2}{2} - \frac{4k^4}{8}\right] \frac{1}{4\,!}$ | 0·003906 | 0 | −0·05859 | −0·2500 | −0·6836 | −1·5000 | −2·8711 | −5·0000 | −8·1211 | −12·5000 |
| | $\delta^6 u_0 \left[-\frac{4k^2}{2} + \frac{20k^4}{8} - \frac{15k^6}{32}\right] \frac{1}{6\,!}$ | −0·0004876 | 0·00004340 | 0·003912 | 0·002777 | −0·04070 | −0·2184 | −0·7097 | −1·8200 | −4·0385 | −8·0718 |
| | $\delta^8 u_0 \left[\frac{36k^2}{2} - \frac{196k^4}{8} + \frac{210k^6}{32} - \frac{56k^8}{128}\right] \frac{1}{8\,!}$ | 0·00007613 | −0·000009300 | −0·0004958 | −0·0002976 | 0·002234 | 0·002260 | −0·03080 | −0·1928 | −0·7131 | −2·0645 |
| | $\delta^{10} u_0 \left[-\frac{576k^2}{2} + \frac{3280k^4}{8} - \frac{4095k^6}{32} + \frac{1680k^8}{128} - \frac{210k^{10}}{512}\right] \frac{1}{10\,!}$ | −0·00001332 | 0·000001859 | 0·00007790 | 0·00004354 | −0·0002511 | −0·0002143 | 0·001425 | 0·001728 | −0·02479 | −0·1733 |
| Third harmonic sin 3*ωt*. | $\mu\delta^3 u_0 \left[-\frac{k^3}{4}\right] \frac{1}{3\,!}$ | −0·005280 | −0·04167 | −0·1406 | −0·3333 | −0·6510 | −1·1250 | −1·7864 | −2·6667 | −3·7969 | −5·2080 |
| | $\mu\delta^5 u_0 \left[\frac{5k^3}{4} - \frac{5k^5}{16}\right] \frac{1}{5\,!}$ | 0·001221 | 0·007812 | 0·01538 | 0 | −0·09155 | −0·3515 | −0·9212 | −2·0000 | −3·8562 | −6·8359 |
| | $\mu\delta^7 u_0 \left[-\frac{49k^3}{4} + \frac{70k^5}{16} - \frac{21k^7}{64}\right] \frac{1}{7\,!}$ | −0·0002772 | −0·001628 | −0·002724 | 0 | 0·007057 | 0·002929 | −0·06716 | −0·3333 | −1·0524 | −2·6774 |
| | $\mu\delta^9 u_0 \left[\frac{820k^3}{4} - \frac{1365k^5}{16} + \frac{630k^7}{64} - \frac{84k^9}{256}\right] \frac{1}{9\,!}$ | 0·00006348 | 0·0003560 | 0·0005501 | 0·000005500 | −0·001024 | −0·0003476 | 0·004006 | 0·002822 | −0·05291 | −0·3108 |
| Fourth harmonic cos 4*ωt*. | $\delta^4 u_0 \left[\frac{k^4}{8}\right] \frac{1}{4\,!}$ | 0·0003255 | 0·005208 | 0·02637 | 0·08333 | 0·2035 | 0·4219 | 0·7816 | 1·3333 | 2·1357 | 3·2552 |
| | $\delta^6 u_0 \left[-\frac{5k^4}{8} + \frac{6k^6}{32}\right] \frac{1}{6\,!}$ | −0·00005018 | −0·0006076 | −0·001428 | 0·002777 | 0·02967 | 0·1195 | 0·3485 | 0·8444 | 1·8065 | 3·5265 |
| | $\delta^8 u_0 \left[\frac{49k^4}{8} - \frac{84k^6}{32} + \frac{28k^8}{128}\right] \frac{1}{8\,!}$ | 0·000008498 | 0·00009223 | 0·0001665 | −0·0003472 | −0·001682 | 0·0004390 | 0·02529 | 0·1277 | 0·4340 | 1·1970 |
| | $\delta^{10} u_0 \left[-\frac{820k^4}{8} + \frac{1638k^6}{32} - \frac{840k^8}{128} + \frac{120k^{10}}{512}\right] \frac{1}{10\,!}$ | −0·000001552 | 0·00001598 | −0·00002495 | 0·00005401 | 0·0001973 | −0·00005620 | −0·001225 | −0·0002471 | 0·02140 | 0·1271 |
| Fifth harmonic sin 5*ωt*. | $\mu\delta^5 u_0 \left[\frac{k^5}{16}\right] \frac{1}{5!}$ | 0·00001627 | 0·0005210 | 0·003955 | 0·01666 | 0·05080 | 0·1266 | 0·2736 | 0·5333 | 0·9611 | 1·6276 |
| | $\mu\delta^7 u_0 \left[-\frac{14k^5}{16} + \frac{7k^7}{64}\right] \frac{1}{7\,!}$ | −0·000005257 | −0·0001519 | −0·0009476 | −0·002777 | 0·003709 | 0·005273 | 0·04844 | 0·1777 | 0·4906 | 1·1529 |
| | $\mu\delta^9 u_0 \left[\frac{273k^5}{16} - \frac{210k^7}{64} + \frac{36k^9}{256}\right] \frac{1}{9\,!}$ | 0·000001399 | 0·00003836 | 0·0002175 | 0·0005456 | 0·0005511 | −0·002939 | −0·002939 | 0·001624 | 0·04212 | 0·1974 |

$$20{\cdot}25\times(-0{\cdot}2184)\ =-\ 4{\cdot}422$$
$$-56{\cdot}25\times(0{\cdot}00226)=-\ 0{\cdot}125$$

therefore

*Peak milliamperes of Second Harmonic*$=-10{\cdot}547$.

The various values of the differences will be recognized from the table and the factors (functions of $k$) have been obtained from Table I.

## 5. *Special Considerations.*

### (a) *Unequally Spaced Entries.*

When the values of the non-linear function are only available at unequally spaced values of the variable it is not possible to use the present form of difference table unless points are obtained from graphical data. In any case the method of Lagrange can be employed to derive the power series for $I_a$, and then the coefficients $a_0'\ a_1'\ a_2' \ldots\ldots a'_{m-1}$ can be substituted in equation (8).

### (b) *Smoothing of Data.*

Where experimental inaccuracies occur in the determination of the values of a function for a number of values of the variable, it is often necessary to perform some method of smoothing of the accumulated data. In the simplest possible case the values of the function are plotted against values of the variable, and a smooth curve is drawn to fit the points as well as possible. This procedure is obviously open to inaccuracies, and a much better approximation to the curve is obtained by some systematic method such as the one already described. It has been shown that by making use of all of the $m$ experimental values in general only a polynomial of degree $(m-1)$ can be made to fit these values, and the resultant curve actually passes through the points.

Suppose that a very large number of points have been taken on the load characteristic of a thermionic valve, then, due to accidental errors of observation, these points will not lie on a smooth curve. In general, therefore, the load characteristic should not be drawn through every point which has been plotted, but should be a curve drawn in the region of the points to give minimum error. The effect of irregular data is to produce an increasing inaccuracy as the order of the harmonic is increased. With $m$ points it does not follow that the resultant characteristic corresponds to a polynomial of degree $(m-1)$, but in general it can have some degree less than $(m-1)$.

Legendre's method of Least Squares or the method of Zero Sum [*] can be employed for smoothing, and then the Central Differences can be found from the graphical data.

---

[*] N. R. Campbell, "Fitting Observations to a Curve," Phil. Mag. (7) x. no. 66 (November 1930).

### (c) *Evaluation of Derivatives.*

In the analysis of the operation of thermionic valves it is often necessary to obtain the derivatives of a function from the equations containing the necessary variables *. Where the equation relates $I_a$ and $e_g$ we may require $\frac{\delta I_a}{\delta e_g}$ or derivatives of a higher order.

The polynomial is of the form (equation (2)).

$$I_a=f(e_g+x\Delta e_g)=u_0+x\mu\delta u_0+\frac{x^2}{2}\delta^2u_0$$

$$+\frac{x(x^2-1)}{3\,!}\mu\delta^3u_0+\ldots\ldots \quad . \quad . \quad . \quad (20)$$

This expansion can be rearranged in terms of $x$ (equation (3)), and by differentiating both sides and putting $x=0$ we obtain

$$f'(e_g)=\frac{1}{\Delta e_g}\left[\mu\delta u_0-\frac{\mu\delta^3u_0}{3\,!}+\frac{4\mu\delta^5u_0}{5\,!}-\frac{36\mu\delta^7u_0}{7\,!}+\frac{576\mu\delta^9u_0}{9\,!}\ldots\ldots\right],$$

$$f''(e_g)=\frac{2\,!}{\Delta e_g}\left[\frac{\delta^2u_0}{2\,!}-\frac{\delta^4u_0}{4\,!}+\frac{4\delta^6u_0}{6\,!}-\frac{36\delta^8u_0}{8\,!}+\frac{576\delta^{10}u_0}{10\,!}\ldots\ldots\right],$$

$$f'''(e_g)=\frac{3\,!}{\Delta e_g}\left[\frac{\mu\delta^3u_0}{3\,!}-\frac{5\mu\delta^5u_0}{5\,!}+\frac{49\mu\delta^7u_0}{7\,!}-\frac{820\mu\delta^9u_0}{9\,!}+\ldots\ldots\right],$$

$$f^{\mathrm{iv}}(e_g)=\frac{4\,!}{\Delta e_g}\left[\frac{\delta^4u_0}{4!}-\frac{5\delta^6u_0}{6!}+\frac{49\delta^8u_0}{8!}-\frac{820^{10}u_0}{10!}+\ldots\ldots\right].$$

$$f^{\mathrm{v}}(e_g)=\frac{5!}{\Delta e_g}\left[\frac{\mu\delta^5u_0}{5\,!}-\frac{14\mu\delta^7u_0}{7\,!}+\frac{273\mu\delta^9u_0}{9\,!}\ldots\ldots\right].$$

Higher derivatives can be written down by comparison with equation (3).

## 6. *Direct Measurement of First Order Differences.*

In the assessment of valve characteristics it is much more accurate to use a circuit arrangement which indicates the first order differences directly. This method avoids the main inaccuracies of point by point static measurement of the characteristics and provides what is probably the best form of smoothing. A low frequency voltage (say 10 cycles per second) of known amplitude is arranged to sweep the grid voltage base over the required range. A very small component of high frequency voltage (say 10,000 cycles per second) is added in series with the main sweep voltage, and the output of the H.F. component is measured across the load in the anode circuit of the valve. If a constant fraction of the sweep voltage is used to deflect a spot along the $x$-axis of a cathode ray oscillograph and the amplified H.F. component deflects the spot in the $y$ direction, then the diagram on the screen indicates the values of the first order of differences multiplied by an arbitrary factor. This factor is easily measured, once and for all, by an absolute voltage measurement of the H.F. component in the absence of the sweep voltage. The corresponding anode current is then known if the load resistance is known.

---

* F. B. Llewellyn, "Operation of Vacuum Tube Circuits," B. S. T. J. v. p. 433 (1926).

A simple high-pass filter, or equivalent, must be placed between the load and the plates of the oscillograph to remove the L.F. deflexion in the $y$ direction.

A suitable circuit is shown in fig. 2. The bias of the valve is adjusted to the desired working point $V_0$, and the sweep $V_1$ (L.F.) is given by the grid base over which the characteristic is required. The output voltage across $R_L$ is applied *via* the $R_1C_1$ and $R_2C_2$ networks to the $y$ plates of the oscillograph. $R_1C_1$ and $R_2C_2$ are adjusted so that the low frequency component is substantially removed, but only a very small loss is introduced at frequency $f_2$.

Fig. 2.

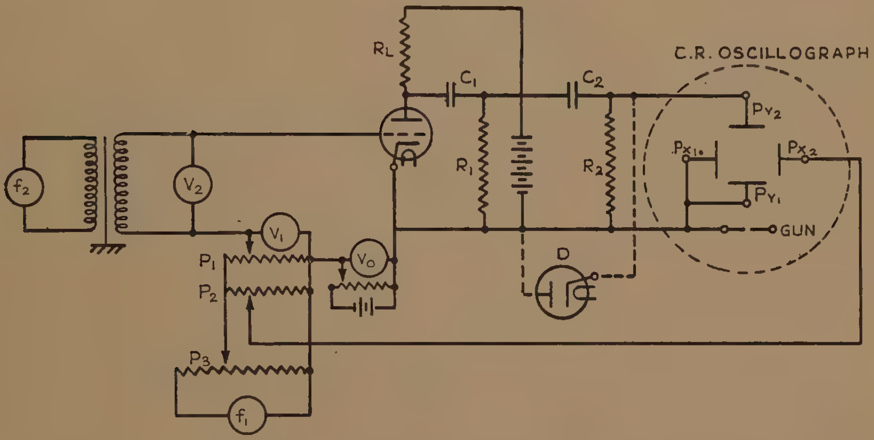

Dynamic characteristic measurement.

The necessary circuit elements depend on the frequencies used, but the approximate conditions are

$$R_1C_1 \doteqdot R_2C_2 \doteqdot \frac{1}{f_2} \ll \frac{1}{f_1}.$$

Sufficient output should be used from the $f_2$ oscillator so that a clear envelope is shown on the oscillograph. A typical envelope is shown in fig. 3, and the appropriate first differences are indicated for an example of five entries (*i. e.*, for first order differences). The factor K transfers the vertical ordinates into current values, and the method of measuring

K has been described. If it is desired to include more than five entries then the horizontal axis is simply divided into the appropriate number of parts. The horizontal axis can be adjusted to fit scale marks by control of potentiometer $p_2$.

The connexion of a diode D ensures that the voltage across the $y$ plates is unidirectional, and the screen diagram has a flat base and the upper part of the envelope has double the slope. It will be found that this form of diagram can be measured more easily from the straight line base.

Fig. 3.

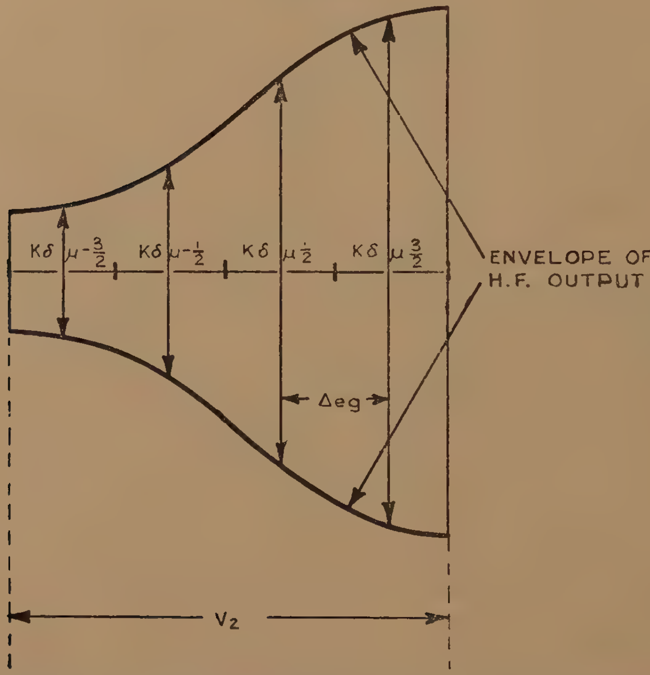

Envelope of first differences as shown by C.R. oscillograph.

The author desires to tender his acknowledgment to the Marconiphone Company Ltd. and the General Electric Company Ltd., on whose behalf the work was done which has led to this publication.

# XXX. *The Permeability of Metal Membranes to Diatomic Gases.*

By R. M. BARRER *.

[Received May 15, 1939.]

GAS flow through metals is accompanied by dissociation of the diffusing molecule, so that the rate is proportional to the square root of the pressure ($H_2$—Pd, Pt, Ni, Fe, Al ; $SO_2$—Cu ; $N_2$—Fe, Mo ; $O_2$—Ag ; CO—Fe, Ni). Closer examination of diffusion rate-pressure isotherms has shown that the $\sqrt{p}$ relationship is maintained up to pressures of 112 atmospheres for hydrogen-nickel systems, but that there are for many systems departures from the $\sqrt{p}$ law at very low pressures. The latter have been ascribed to adsorption on the surface of the metal (1), which at low pressures has not reached its saturation value ; and also alternatively to impurities in the metal (2). The obedience to the $\sqrt{p}$ law for hydrogen-nickel systems at high pressures has been the subject of two papers (3), (4). These papers sought to explain the dependence on pressure as a result of a number of phase boundary processes.

The purpose of this paper is to show that the processes proposed do not lead to a linear $\sqrt{p}$-permeation rate isotherm, at very high pressures, save under special conditions. The special conditions were in fact those employed by both the previous authors, by not completing the rate equations for a number of the mechanisms assumed. A possible reason for the continued validity of the $\sqrt{p}$ law for diffusion of hydrogen through nickel is then advanced, based on considerations of the previous paper.

## *Processes occurring in the Stationary State of Flow through a Metal.*

We consider a plate of metal, bounded by the planes $x=0$, $x=l$, the pressure at the boundary $x=0$ being $p$, while on the outgoing boundary $x=l$, zero pressure is maintained. The gas is diatomic, but is adsorbed, and diffuses, as atoms. The fractions of the surface covered on the ingoing and outgoing sides are $\theta_1$ and $\theta_2$, while the actual concentrations just inside the metal at the surfaces $x=0$ and $x=l$ are $u_0$ and $u_l$ respectively.

---

* Communicated by Eric K. Rideal.

As typical of the processes which can be supposed to occur one may write the following :—

(i.) A gas molecule strikes the surface, dissociates, and is adsorbed as atoms.

$$\text{Rate}=k_1.p.(1-\theta)^2.$$

(ii.) A pair of atoms combines, and evaporates as a molecule.

$$\text{Rate}=k_2\theta^2.$$

(iii.) An adsorbed atom passes into the interior of the metal.

$$\text{Rate}=k_3\theta\left(1-\frac{u}{u_s}\right),$$

where $u_s$ denotes the saturation concentration in the metal. This equation was incorrectly written by Wang (4) and by Smithells (5) as $k_3\theta$.

(iv.) An atom just inside the metal enters the surface.

$$\text{Rate}=k_4u.(1-\theta).$$

In his treatment Wang (4) added the following two processes :—

(v.) A molecule strikes the surface and dissociates, one atom staying on the surface and the other entering the metal.

$$\text{Rate}=k_5.p.(1-\theta)\left(1-\frac{u}{u_s}\right).$$

This rate equation was also wrongly written by Wang (4) as $k_5.p.(1-\theta)$. Wang thus neglected the effect of saturation of the metal.

(vi.) An atom inside the metal combines with an atom on the surface, and evaporates as a molecule.

$$\text{Rate}=k_6.u.(1-\theta).$$

In addition to the possible surface processes listed is the flow within the solid due to diffusion, which may be written as

$$\text{Rate}=\text{D}\frac{(u_0-u_l)}{l},$$

where D denotes the diffusion constant of Fick's law

$$\frac{\partial c}{\partial i}=\text{D}\frac{\partial^2 c}{\partial x^2}.$$

### *The Permeation Rate P.*

In the steady state one knows that the rate of accumulation of gas at any point in the solid is zero, and so one may sum the processes occurring at any interface, and equate the sum to zero. In this way the following set of equations was built up :—

$$P=k_1p.(1-\theta_1)^2-k_2\theta_1^2+k_5.p(1-\theta_1)\left(1-\frac{u_0}{u_s}\right)-k_6.\theta_1u_0. \quad . \quad . \quad (1)$$

$$P=k_3.\theta_1\left(1-\frac{u_0}{u_s}\right)-k_4u_0(1-\theta_1)+k_5p(1-\theta_1)\left(1-\frac{u_0}{u_s}\right)-k_6\theta_1u_0. \quad (2)$$

$$P=k_4u_l(1-\theta_2)-k_3\theta_2\left(1-\frac{u}{u_s}\right)+k_6\theta_2u_l. \quad . \quad . \quad . \quad . \quad . \quad . \quad . \quad . \quad . \quad (3)$$

$$P=k_2\theta_2^2+k_6\theta_1u_l. \quad . \quad . \quad . \quad . \quad . \quad . \quad . \quad . \quad . \quad . \quad . \quad . \quad . \quad . \quad . \quad . \quad (4)$$

$$P=\frac{D}{l}.(u_0-u_l). \quad . \quad . \quad . \quad . \quad . \quad . \quad . \quad . \quad . \quad . \quad . \quad . \quad . \quad . \quad . \quad . \quad (5)$$

These equations may be rearranged as follows :—

$$u_0\left[k_6\theta_1+k_5p\frac{(1-\theta_1)}{u_s}\right]=k_1p(1-\theta_1)^2-k_2\theta_1^2+k_5p(1-\theta_1)-P.. \quad . \quad (6)$$

$$u_0\left[\frac{k_3\theta_1}{u_s}+k_4(1-\theta_1)+k_5p\frac{(1-\theta_1)}{u_s}+k_6\theta_1\right]=k_3\theta_1+k_5p(1-\theta_1)-P. \quad (7)$$

$$u_l\left[k_6\theta_2+\frac{k_3\theta_2}{u_s}+k_4(1-\theta_2)\right]=k_3\theta_2+P. \quad . \quad . \quad . \quad . \quad . \quad . \quad . \quad . \quad . \quad (8)$$

$$u_l.k_6\theta_2=P-k_2\theta_2^2. \quad . \quad . \quad . \quad . \quad . \quad . \quad . \quad . \quad . \quad . \quad . \quad . \quad . \quad . \quad . \quad . \quad . \quad (9)$$

$$\frac{P.l}{D}=u_0-u_l. \quad . \quad . \quad . \quad . \quad . \quad . \quad . \quad . \quad . \quad . \quad . \quad . \quad . \quad . \quad . \quad . \quad . \quad . \quad (10)$$

It is now possible to eliminate $u_0$ and $u_l$ and to obtain three equations involving P, D, $\theta$, $u_s$, and the constants of the various reactions at the phase boundaries. For instance, from (10), (7), and (8) one obtains

$$P\left\{\frac{l}{D}+\frac{1}{\frac{k_3\theta_1}{u_s}+k_4(1-\theta_1)+k_5\frac{p(1-\theta_1)}{u_s}+k_6\theta_1}+\frac{1}{k_6\theta_2+\frac{k_3\theta_2}{u_s}+k_4(1-\theta_2)}\right\}$$

$$=\frac{k_3\theta_1+k_5p(1-\theta_1)}{\frac{k_3\theta_1}{u_s}+k_4(1-\theta_1)+k_5\frac{p(1-\theta_1)}{u_s}+k_6\theta_1}-\frac{k_3\theta_2}{k_6\theta_2+\frac{k_3\theta_2}{u_s}+k_4(1-\theta_2)}. \quad (11)$$

From (6) and (7) one finds

$$P\left[\frac{k_3\theta_1}{u_s}+k_4(1-\theta_1)\right]+k_2\theta_1^2\left[\frac{k_3k_6}{k_2}+k_6\theta_1+k_4(1-\theta_1)+\frac{k_3\theta_1}{u_s}+\frac{k_5p(1-\theta_1)}{u_s}\right]$$

$$=k_1p(1-\theta_1)^2\left[\frac{k_3\theta_1}{u_s}+k_4(1-\theta_1)+\frac{k_5p(1-\theta_1)}{u_s}+k_6k_1\theta_1+\frac{k_5k_4}{k_1}\right]. \quad (12)$$

From (8) and (9)

$$P\left[k_4(1-\theta_2)+\frac{k_3\theta_2}{u_s}\right]=k_2\theta_2^2\left[\frac{k_6k_3}{k_2}+k_4(1-\theta_2)+k_6\theta_2+\frac{k_3\theta_2}{u_s}\right]. \quad (13)$$

Similarly one could employ (11), (12), and (13) to eliminate $\theta_1$ and $\theta_2$, or any pair of constants, from the equation of flow. However, for the present purpose we wish simply to find whether P can tend to infinity as $p$ tends to infinity.

The permeation rate P, when the only phase boundary processes are those (i.) to (iv.) of p. 354 may be derived from (11), (12), and (13) by omitting terms with the multipliers $k_5$ or $k_6$.

### *The Permeation Rate as the Pressure tends to Infinity.*

As the pressure is made very great we can write

$$p\rightarrow\infty,$$
$$(1-\theta_1)\rightarrow 0,$$
$$\theta_1\rightarrow 1.$$

Equation (11) shows that the terms in $\theta_2$ and $(1-\theta_2)$ contributing to P never approach an infinite value whatever their value (between 0 and 1). The term $p(1-\theta_1)$ may approach $\infty$, 0, or a constant, and we may write down the limiting permeation rate, P, in each case, and then see that P is always finite [equations (11 *a*), (11 *b*), (11 *c*)].

(*a*) The limiting conditions are :—

$$p\rightarrow\infty,$$
$$(1-\theta_1)\rightarrow 0,$$
$$\theta_1\rightarrow 1,$$
$$p(1-\theta_1)\rightarrow\infty.$$

Here the limiting flow, P, is given by

$$\mathrm{P}\left[\frac{l}{\mathrm{D}}+\frac{1}{k_6\theta_2+\dfrac{k_3\theta_2}{u_s}+k_4(1-\theta_2)}\right]=1-\frac{k_3\theta_2}{k_6\theta_2+\dfrac{k_3\theta_2}{u_s}+k_4(1-\theta_2)}. \qquad (11a)$$

(*b*) The limiting conditions are :—

$$p\rightarrow\infty,$$
$$(1-\theta_1)\rightarrow 0,$$
$$\theta_1\rightarrow 1,$$
$$p(1-\theta_1)\rightarrow 0.$$

The limiting flow P is now given by

$$\mathrm{P}\left[\frac{l}{\mathrm{D}}+\frac{1}{\dfrac{k_3}{u_s}+k_6}+\frac{1}{k_6\theta_2+\dfrac{k_3\theta_2}{u_s}+k_4(1-\theta_2)}\right]$$
$$=\frac{k_3}{\dfrac{k_3}{u_s}+k_6}-\frac{k_3\theta_2}{k_6\theta_2+\dfrac{k_3\theta_2}{u_s}+k_4(1-\theta_2)}. \quad . \quad (11b)$$

(*c*) The limiting conditions are :—

$$p \rightarrow \infty,$$
$$(1-\theta_1) \rightarrow 0,$$
$$\theta_1 \rightarrow 1,$$
$$p(1-\theta_1) \rightarrow \text{constant}.$$

The limiting flow P is expressed as

$$\mathrm{P}\left[\frac{l}{\mathrm{D}}+\frac{1}{\frac{k_3}{u_s}+\frac{k_5 p(1-\theta_1)}{u_s}+k_6}+\frac{1}{k_6\theta_2+\frac{k_3\theta_2}{u_s}+k_4(1-\theta_2)}\right]$$
$$=\frac{k_3+k_5 p(1-\theta_1)}{\frac{k_3}{u_s}+k_5 p\frac{(1-\theta_1)}{u_s}+k_6}-\frac{k_3\theta_2}{k_6\theta_2+\frac{k_3\theta_2}{u_s}+k_4(1-\theta_2)} . \quad . \quad (11c)$$

Thus, since with the assumed limiting conditions (11 *a*), (11 *b*), and (11 *c*) contain only finite terms, P is always finite when $p$ approaches infinity. The previous and contrary findings of Wang were the result of omitting the terms $\left(1-\frac{u}{u_s}\right)$ in the rate equations for the processes (iii.) and (v.) of p. 354. Since, in fact, one may write

$$\mathrm{P}=\mathrm{D}\cdot\frac{u_0-u_l}{l},$$

one sees that the flow of gas through a metal *can never be infinite, whatever the pressure, and whatever mechanisms are assumed,* for $u_0$, the concentration just inside the metal at $x=0$, can never exceed its saturation value $u_s$, which experiment shows is finite.

### *A Reason for Persistence of the $\sqrt{p}$ Law of Flow at High Pressures.*

The results of previous calculations (6) indicated that concentration discontinuities (which are unexpectedly great) can exist at the faces $x=0$ and $x=l$. *In the non-equilibrium systems in which permeation is occurring the concentration $u_0$ may thus be nowhere near its saturation value $u_s$, at pressures where in equilibrium systems the metal would be saturated.* Thus the term $\left(1-\frac{u_0}{u_s}\right)$ may still be nearly unity even at high pressures, and if this is so the considerations of Wang or of Smithells and Ransley apply, the $\sqrt{p}$ relationship will be obeyed, and an explanation of this $\sqrt{p}$ law as observed by Smithells and Ransley (3) for hydrogen-nickel at 112 atmospheres is possible.

### *Summary.*

It is shown that the calculations of Wang, which indicate that the permeation rate through a metal plate can be infinite at infinite pressure, are due to incomplete rate equations for some of the phase boundary processes assumed by him. Using the completed rate equations, expressions for the permeation rate for the six-phase boundary processes assumed by Wang are then given, and it is shown that the permeation rate is always finite whatever the pressure.

The Fick law for the stationary state of flow is then used to show that, whatever phase boundary processes are assumed, the permeation rate can never under any conditions approach infinity.

An explanation of the persistence of linear permeation-rate $-\sqrt{p}$ isotherms up to 112 atmospheres is given from the findings of the previous paper, where it was shown that very great discontinuities in concentration may occur at the boundaries of the plate, and concentrations just inside the ingoing face of the metal may exist in non-equilibrium systems, which are very small compared with the saturation value of this concentration. Under these conditions, which may persist to high pressures, a $\sqrt{p}$ law is obeyed.

### *References.*

(1) C. Smithells and C. Ransley, Proc. Roy. Soc. cl. A, p. 172 (1935).
(2) C. Post and W. Ham, J. Chem. Phys. vi. p. 598 (1938).
(3) C. Smithells and C. Ransley, Proc. Roy. Soc. clvii. p. 292 (1936).
(4) J. S. Wang, Proc. Camb. Phil. Soc. xxxii. p. 653 (1936).
(5) C. Smithells, "Gases and Metals," Chapman and Hall, p. 105, process (i.) (1937).
(6) R. M. Barrer, Phil. Mag. (in the press).

# XXXI. *The Errors in the Numerical Solution of Differential Equations.*

By F. J. Turton, B.Sc., A.R.C.Sc.,
City and Guilds College *.

[Received February 24, 1939.]

The errors in the value Y of the dependent variable $y$ at $x=\mathrm{X}$, after a number of operations of "integrating ahead" from a differential equation, subject to initial conditions such as $y=\eta$ when $x=\xi$, $y'=\theta$ when $x=\xi$, etc., may be classified as

(1) due to uncertainty of $\eta$, $\xi$, X, etc.;

(2) due to intrinsic errors in the formulæ used in the step by step method;

(3) rounding off errors in (2) which can always be made small in comparison with the effect of the intrinsic errors, by carrying a sufficient number of additional figures, otherwise of no significance;

(4) random errors, which should be rejected as they arise by some system of checks.

### 1 (*a*). *Error in* Y *due to an Error in* $\eta$ *at* $\xi$.

Let the primitive be $f(x, y, k)=0$. Then if the constant be C for that member of the family through $(\xi, \eta)$,

$$f(\xi, \eta, \mathrm{C})=0, \quad \ldots \ldots \ldots \quad \text{(i.)}$$

and Y at X is found from

$$f(\mathrm{X}, \mathrm{Y}, \mathrm{C})=0. \quad \ldots \ldots \ldots \quad \text{(ii.)}$$

But if $\eta$ is incorrectly specified as $\eta+\delta\eta$, integration proceeds along a neighbouring member of the family, *i. e.*, with constant $\mathrm{C}+\delta\mathrm{C}$, such that

$$f(\xi, \eta+\delta\eta, \mathrm{C}+\delta\mathrm{C})=0, \quad \ldots \ldots \ldots \quad \text{(iii.)}$$

and Y at X is now incorrectly found as $\mathrm{Y}+\delta\mathrm{Y}$, where

$$f(\mathrm{X}, \mathrm{Y}+\delta\mathrm{Y}, \mathrm{C}+\delta\mathrm{C})=0. \quad \ldots \ldots \ldots \quad \text{(iv.)}$$

Expanding (iii.) and (iv.), and using (i.) and (ii.), we have

$$\delta\eta\,\frac{\partial f(\xi, \eta, \mathrm{C})}{\partial\eta}+\frac{\delta\eta^2}{2!}\,\frac{\partial^2 f(\xi, \eta, \mathrm{C})}{\partial\eta^2}+\ldots+\delta\mathrm{C}\,\frac{\partial f(\xi, \eta, \mathrm{C})}{\partial\mathrm{C}}+\frac{\delta\mathrm{C}^2}{2\,!}\,\frac{\partial^2 f(\xi, \eta, \mathrm{C})}{\partial\mathrm{C}^2}$$
$$+\ldots=0 \quad \ldots \quad \text{(v.)}$$

---

* Communicated by Dr. W. G. Bickley

and

$$\delta Y \frac{\partial f(X, Y, C)}{\partial Y} + \frac{\delta Y^2}{2\,!} \frac{\partial^2 f(X, Y, C)}{\partial Y^2} + \ldots + \delta C \frac{\partial f(X, Y, C)}{\partial C} + \frac{\delta C^2}{2\,!} \frac{\partial^2 f(X, Y, C)}{\partial C^2} + \ldots = 0 \quad . \quad . \quad . \quad \text{(vi.)}$$

Thus, to the first order,

$$\frac{\delta Y}{\delta \eta} \doteqdot \frac{\partial f(X, Y, C)}{\partial C} \times \frac{\partial f(\xi, \eta, C)}{\partial \eta} \Big/ \frac{\partial f(\xi, \eta, C)}{\partial C} \times \frac{\partial f(X, Y, C)}{\partial Y} . \qquad \text{(vii.)}$$

It is evident that there is no simple *à priori* way of calculating $\delta Y$ for a given $\delta \eta$; in particular, there is usually no correlation between the ratio of the errors $\delta Y$ and $\delta \eta$ at X and $\xi$ respectively, and the values Y and $\eta$ at X and $\xi$.

If $f(x, y, k)=0$ is the solution to a linear differential equation of the first order, it can be written in the form $y-F(x)-kG(x)=0$; all the second and higher partial derivatives in (v.) and (vi.) vanish, (vii.) is exact, the ratio $\delta Y/\delta \eta$ is equal to $G(X)/G(\xi)$ and is independent of $\delta \eta$, so that $\delta Y$ is directly proportional to $\delta \eta$. In this case, if $\eta$ lies between $\eta_1$ and $\eta_2$, and $\eta_1$ gives $Y_1$ at X and $\eta_2$ gives $Y_2$ at X, then Y at X must lie between $Y_1$ and $Y_2$ *.

If the differential equation is not linear, we must either ($\alpha$) establish that second order terms in (v.) and (vi.) are small enough to be negligible, so that, to the desired accuracy, $\delta Y$ *is* proportional to $\delta \eta$ †, by checking for values of $\eta$ between $\eta_1$ and $\eta_2$, in which case Y at X will lie between $Y_1$ and $Y_2$ corresponding to $\eta_1$ and $\eta_2$, as when linear; or ($\beta$), when ($\alpha$) fails, we must find $y$ at X for a sufficient number of values of $\eta$ between $\eta_1$ and $\eta_2$, to establish $y$ at X as a function of $\eta$ over the interval $\eta_1$ to $\eta_2$ (we may graph $y$ at X against $\eta$ for $\eta_1<\eta<\eta_2$); then Y at X will lie between the greatest and least value of $y$ in this interval.

(*b*) Let the primitive be $f_1(x, y, k_1, k_2)=0$, and denote

$$\frac{df_1(x, y, k_1, k_2)}{dx}=0 \text{ by } f_2(x, y, y', k_1, k_2)=0.$$

---

* It is misleading to speak of fractional or percentage errors in Y at X. Thus if $y'=y-1$ subject to $x=0$, $y=1$, $y=Ce^x+1$ where $C=0$; the solution is $y=1$, but if the initial $y$ is uncertain by $\alpha$, then Y at X is uncertain by $\alpha \,.\, e^X$, and this will certainly be important if the integration is carried far enough. The actual error and the fractional error in Y at X are each $\alpha \,.\, e^X$.

But if $y=Ce+\frac{1}{1+x^n}$ is the solution, with $x=0$, $y=1$ as before, $C=0$. The error in Y at X due to error $\alpha$ in $y$ at $x=0$ is $\alpha \,.\, e^X$ as before. But Y at X is less than $1/X^n$ and so the fractional error exceeds $X^n \,.\, \alpha \,.\, e^X$.

† When Y at X is being found from a succession of values of $\eta$ at the same $\xi$, this may be evident. The method of isoclinals may be used to see if it is probable.

If, when $x=\xi$, $y=\eta$, $y'=\theta$ and C and D be the constants for this member of the family, then

$$f_1(\xi, \eta, C, D)=0, \quad . \quad . \quad . \quad . \quad . \quad . \quad . \quad . \quad . \qquad (i.)$$

and

$$f_2(\xi, \eta, \theta, C, D)=0, \quad . \quad . \quad . \quad . \quad . \quad . \quad . \quad . \qquad (ii.)$$

and Y at X is found from

$$f_1(X, Y, C, D)=0. \quad . \quad . \quad . \quad . \quad . \quad . \quad . \quad . \quad . \qquad (iii.)$$

But if at $x=\xi$, $y$ is incorrectly taken as $\eta+\delta\eta$ and $y'$ as $\theta+\delta\theta$, integration proceeds along a neighbouring member of the family, for which, if the constants are $C+\delta C$, $D+\delta D$.

$$f_1(\xi, \eta+\delta\eta, C+\delta C, D+\delta D)=0, \quad . \quad . \quad . \quad . \quad . \quad . \quad . \qquad (iv.)$$

and

$$f_2(\xi, \eta+\delta\eta, \theta+\delta\theta, C+\delta C, D+\delta D)=0, \quad . \quad . \quad . \quad . \qquad (v.)$$

and Y at X is incorrectly found as $Y+\delta Y$ where

$$f_1(X, Y+\delta Y, C+\delta C, D+\delta D)=0. \quad . \quad . \quad . \quad . \quad . \quad . \qquad (vi.)$$

Expanding as in (*a*), we shall obtain a relation of the form

$$\delta Y \doteqdot A\delta\eta+B\delta\theta,$$

where A and B are independent of $\delta\eta$ and $\delta\theta$.

If the differential equation is linear, the solution can be put in the form $y=F(x)+k_1G(x)+k_2H(x)$. All the second and higher partial derivatives vanish and $\delta Y=A\delta\eta+B\delta\theta$. In this case, if $y$ at X be calculated from initial data $\eta_1\theta_1$, $\eta_1\theta_2$, $\eta_2\theta_1$ and also $\eta_2\theta_2$ (but this last may be obtained by adding the second and third and subtracting the first), then we can say that Y at X is between the greatest and least of the four values, when $\eta_1<\eta<\eta_2$ and $\theta_1<\theta<\theta_2$. If the differential equation is not linear, we must, as in (*a*), either show that the relation $\delta Y=A\delta\eta+B\delta\theta$ is true to the accuracy required, or when it is not, we must calculate $y$ at X for a sufficient number of values of $\eta$ between $\eta_1$ and $\eta_2$, and of $\theta$ between $\theta_1$ and $\theta_2$ (these being the bounds of the uncertain quantities $\eta$ and $\theta$) to establish $y$ as a function of $\eta$ and of $\theta$ within these intervals. Then Y at X will lie between the greatest and least value of $y$ so found.

(*c*) If the primitive be $f(x, y, k)=0$, and X is incorrectly taken as $X+\delta X$, $\xi$ as $\xi+\delta\xi$, $\eta$ as $\eta+\delta\eta$ we find, similarly, that

$$\delta Y \doteqdot L\,.\,\delta X+M\delta\eta+N\delta\xi,$$

where L, M, N are independent of $\delta X$, $\delta\eta$ and $\delta\xi$, and can discuss in a similar way the effect of uncertainty in $\xi$ and in X as well as in $\eta$.

### (2) *Cumulative Error due to the Errors intrinsic to the Method.*

In numerical integration by iteration (*e. g.*, of Simpson's rule) or by a formula for integrating ahead (Heun, Milne, etc.), $y$ is calculated at equal intervals $h$. The error at every "$h$" does not, however, directly affect Y at X. Thus in iterating Simpson's rule, $y_{2rh}$ is found from

$$y_{2rh}=y_{(2r-2)h}+\frac{h}{3}(y'_{2rh}+4y'_{(2r-1)h}+y'_{(2r-2)h}),$$

and thus $y_{2nh}$ contains consequential errors due directly to the intrinsic error

$$-\left(\frac{h^5}{90}y^{\text{v}}+\frac{h^6}{90}y\quad\ldots\right)\text{ at } x=0^*,\ 2h,\ \ldots(2n-2)h\,;$$

errors from $y$ at $h$, $3h$, etc., occur indirectly through $y_h{}'$, $y_{3h}{}'$, etc., but as these quantities are multiplied by $4h/3$ on insertion, their effect is comparatively small.

The consequential error at $X=2nh$, due to an error $\alpha_r$ at $x=2rh$, will be that which would arise if $\alpha_r$ were an error in the initial $y$ when integrating from the initial value $x=2rh$, and the total direct consequential error will be the sum of such errors. It is sometimes asserted that the total consequential error can be reliably estimated from the sum of the errors $\alpha_1 \ldots \alpha_n$ or by multiplying the largest of these by the number of them, $n$. It will be evident from (1) that such estimates are unreliable.

Thus, if the solution to the differential equation is

$$y=\text{F}(x)+k\text{G}(x),\quad\text{then}\quad\delta\text{Y}/\delta\eta=\text{G}(\text{X})/\text{G}(\xi)$$

and the total direct cumulative error, at $X=2nh$, will be (when iterating Simpson's rule)

$$\frac{\text{G}(\text{X})}{\text{G}(2h)}\alpha_1+\frac{\text{G}(\text{X})}{\text{G}(4h)}\alpha_2+\ldots+\frac{\text{G}(\text{X})}{\text{G}(\text{X}=2nh)}\alpha_n.$$

When $y'=py+a+bx+cx^2+dx^3+ex^4$, it is easy to show that the ratio of the total direct consequential error at $X=2nh$ (iterating Simpson's rule) to the sum of the errors $\alpha_1 \ldots a_n$, is approximately $p$X if $0<p<2$, is certainly greater than $p$X if $p>2$, and so increases indefinitely as X increases.

Again, with $y'=y+5x^4-x^5$, initially $x=0$, $y=1$, $h=\cdot 1$, the ratio of the total direct consequential error at $X=6$ (iterating Simpson's rule) to the sum $\alpha_1 \ldots \alpha_n$ up to $X=6$, exceeds 40; and further, the ratio of the total direct consequential error at $X=6$ to the product of the number of steps (30) and the largest of the $\alpha$'s (which is the last) exceeds 15.

In the absence of any reliable method of forecasting or finally estimating the error, the only alternative is to endeavour to have no error to the desired number of significant figures. This requires that at least two formulæ be used, in which the intrinsic errors are substantially different, to check each other (it will usually be impracticable to examine the intrinsic error at every step) ; and this check will eliminate random errors. But errors will, nevertheless, often accumulate to a unit in the "$p$"-th place before the check shows a discrepancy in that place, and so it will be desirable to carry an extra figure at least, to indicate the approach of a discrepancy in the values at the required place, when it will be necessary to reduce the interval. Rounding-off figures beyond this will be required. If the formula of Milne be used for integrating ahead (finding $y_4$ from $y_0, y_1', y_2'$ and $y_3'$), Simpson's rule may be used twice as a check : for $y_0, y_2, y_4$ and for $y_2, y_3, y_4$. In this method, a few addition decimal places add little to the labour. The values then obtained may be tested still further by long-range formulæ of a high order of accuracy, such as

---

* Assuming, as is usual, $x=0$ to be the initial value.

$$y_3=\frac{27}{11}(y_1-y_2)+y_0+\frac{3k}{11}(y_0'+9y_1'+9y_2'+y_3')-\frac{3}{1540}k^7y^{\mathrm{vii}}\ldots$$

$$y_4=\frac{32}{5}(y_1-y_3)+y_0+\frac{6k}{25}(y_0'+16y_1'+36y_2'+16y_3'+y_4')-\frac{1}{2625}k^9y^{\mathrm{ix}}\ldots$$

$k$ being $2h$, $3h$ or even more, and the passing of each such additional check greatly increases the probability that the values are correct.

A word may be added as to choice of interval. Except on rare occasions, $y_1$, $y_2$, and $y_3$, required to start Milne's method, will be found from power series, using Maclaurin's Theorem (or Picard's iterative method). The term in $h^5$ at $x=3h$, is $3^5h^5y^{\mathrm{v}}/5\,!$, which is practically six times the first error term in Milne's formula ; thus $h$ should be chosen so that the value of the term in $h^5$ in the power series, at $x=3h$, is substantially less than 3 in the place it is desired to have accurate ; if $y^{\mathrm{v}}$ is steadily increasing, very much less than 3, or it will be necessary to reduce the interval after a very few steps.

# XXXII. *A New Form of the Quantum Equation.*

By M. Fahmy, M.Sc., Egyptian University, Cairo*.

[Received January 19, 1939.]

In modern quantum theory the electron is described by means of an equation discovered by Dirac, which contains certain fundamental matrices described by $\alpha_x$, $\alpha_y$, $\alpha_z$, $\beta$. They have the following properties:

$$\alpha_x^2=1 \quad \alpha_x\alpha_y+\alpha_y\alpha_x=0,$$

and similar relations;

$$\beta^2=m_0{}^2c^2 \quad \alpha_x\beta+\beta\alpha_x=0.$$

$\beta$ is replaced by a matrix $\alpha_m$ where $\beta=m_0c\alpha_m$.

The above relations can be summarized in the form:

$$\alpha_r\alpha_s+\alpha_s\alpha_r=2\delta_{rs} \quad (r,\ s=x,\ y,\ z \text{ or } m). \quad . \quad . \quad . \quad . \quad (a)$$

The equation of the electron is written:

$$\left\{\frac{\mathrm{W}}{c}-\frac{e}{c}\phi+\alpha_x\left(\pi_x-\frac{e}{c}\mathrm{A}_x\right)+\alpha_y\left(\pi_y-\frac{e}{c}\mathrm{A}_y\right)+\alpha_z\left(\pi_z-\frac{e}{c}\mathrm{A}_z\right)+m_0c\alpha_m\right\}\psi=0,$$

where

$$\mathrm{W}=-\frac{h}{2\pi i}\frac{\partial}{\partial t}, \quad \pi_x=\frac{h}{2\pi i}\frac{\partial}{\partial x}, \quad \text{etc.}$$

The other quantities occurring here have their well-known meanings, and the equation may be written in the form:

$$\frac{h}{2\pi i}\frac{\partial\psi}{\partial t}=-\mathrm{H}\psi.$$

The expression

$$\mathrm{H}=e\phi-c\alpha_x\left(\pi_x-\frac{e}{c}\mathrm{A}_x\right)-c\alpha_y\left(\pi_y-\frac{e}{c}\mathrm{A}_y\right)-c\alpha_z\left(\pi_z-\frac{e}{c}\mathrm{A}_z\right)-m_0c^2\alpha_m$$

is the Hamiltonian operator, and plays an important part in matrix analysis, for it is used to define differentiation of operators with respect to time. The rule of differentiation of an operator $\xi$ is

$$\frac{d\xi}{dt}=\frac{2\pi i}{h}(\mathrm{H}\xi-\xi\mathrm{H}). \quad . \quad . \quad . \quad . \quad . \quad . \quad . \quad . \quad (b)$$

We suppose that $\xi$ does not contain $t$ explicitly.

---

* Communicated by H. T. Flint.

In particular, if $\xi$ is one of the fundamental matrices $\alpha_x$, we have

$$\alpha_x = \frac{2\pi i}{h}(\mathrm{H}\alpha_x - \alpha_x\mathrm{H}). \quad . \quad . \quad . \quad . \quad . \quad . \quad . \quad . \qquad (c)$$

It has been shown that the equation of the electron fits into the relativistic system of geometry and metrics, where it has a simple significance of a metrical character. Moreover, it can be derived by simple geometrical considerations. For the purpose of a geometric discussion, it is necessary to introduce the idea of a matrix length combined with the conception of a five-dimensional continuum on the pattern of that first introduced by Kaluza, and later developed to bring out the relation of the quantum theory and the theory of relativity *.

For this purpose, matrices described by $\gamma^\mu$, where $\mu$ has the value 1 to 5, are introduced and are shown to have a close relation to the Dirac matrices. In fact, when no gravitational field is present in atomic problems the $\gamma^m$, where $m$ has the values 1 to 3, are related to Dirac's $\alpha_x$, $\alpha_y$, $\alpha_z$. The five matrices, $\gamma^\mu$, are related to the coefficients $\gamma^{\mu\nu}$ of the continuum by means of the following equations, similar to those introduced by Tetrode for four dimensions :

$$\gamma^\mu\gamma^\nu + \gamma^\nu\gamma^\mu = 2\gamma^{\mu\nu}. \quad . \quad . \quad . \quad . \quad . \quad . \quad . \quad . \quad . \qquad (1)$$

According to Kaluza † the expression $\gamma^{mn} = g^{mn}$ when $m$ and $n$ have the values 1 to 4. In the case $\gamma^{m5}$ they are identified with the electromagnetic potential components $\phi^m$ by means of

$$\gamma^{m5} = -\alpha\phi^m, \quad . \quad . \quad . \quad . \quad . \quad . \quad . \quad . \qquad (2)$$

with

$$\alpha = \frac{e}{m_0 c^2}.$$

In this theory the $\gamma^\mu$, besides being matrices, have the property of contravariant vectors. The fifth of these does not appear explicitly in Dirac's theory, which, however, makes use of a matrix $\alpha_0$ which is perpendicular to $\gamma'$ $\gamma^2$ $\gamma^3$, and $\gamma^4$.

The relation between $\alpha_0$ and the fundamental matrices $\gamma^\mu$ is

$$\alpha_0 = \frac{\gamma_{\mu 5}}{\sqrt{\gamma_{55}}}\gamma^\mu, \quad . \quad . \quad . \quad . \quad . \quad . \quad . \quad . \quad . \qquad (3)$$

and $\alpha_0$ is related to $\alpha_m$.

The covariant components $\gamma_{m5}$ are equal to $\alpha\phi_m$ and $\gamma_{55} = 1$.

Thus

$$\alpha_0 = \alpha\phi_m\gamma^m + \gamma^5. \quad . \quad . \quad . \quad . \quad . \quad . \quad . \quad . \quad . \qquad (4)$$

It has also been shown that in all the known problems presented by the quantum theory $x^5$ appears as a cyclic coordinate in the factor

---

* Flint, Proc. Roy. Soc. A, cl. p. 421 (1935) ; Proc. Phys. Soc. l. p. 899 (1938).

† Kaluza, *S.B. Akad. Wiss.* p. 966 (1921).

$e^{\frac{2\pi i}{h} m_0 c x^5}$, so that the operator $\frac{\partial}{\partial x^5}$ is equivalent to multiplication by $\frac{2\pi i m_0 c}{h}$.

Thus, Dirac's equation can be written in the form

$$\gamma^\mu \frac{\partial \psi}{\partial x^\mu} = 0. \quad \ldots \ldots \ldots \quad (5)$$

It is to be noted that the electromagnetic potential components $A_x$, $A_y$, $A_z$ are now replaced by $\phi_1$, $\phi_2$, $\phi_3$. The derivation of the above equation indicates the importance of a matrix $K^\mu_\nu$, given by

$$K^\mu_\nu = \frac{\partial \gamma^\mu}{\partial x^\nu} + \Gamma^\mu_{\nu\lambda} \gamma^\lambda, \quad \ldots \ldots \ldots \quad (6)$$

where $\Gamma^\mu_{\nu\lambda}$ is the Christoffel index symbol, and it also indicates the existence of a law, which can be described as the quantum law, viz.,

$$K^\mu_\mu = 0. \quad \ldots \ldots \ldots \quad (7)$$

Further, it is shown that the relations (1) are satisfied if $K^\mu_\nu$ is of the form

$$K^\mu_\nu = \gamma^\mu \Gamma_\nu - \Gamma_\nu \gamma^\mu. \quad \ldots \ldots \ldots \quad (8)$$

We can regard

$$\frac{\partial \gamma^\mu}{\partial x^\nu} = \gamma^\mu \Gamma_\nu - \Gamma_\nu \gamma^\mu - \Gamma^\mu_{\nu\lambda} \gamma^\lambda \quad \ldots \ldots \quad (9)$$

as the definition of the differentiation of $\gamma^\mu$. But so far there is no suggestion of the form of $\Gamma_\nu$, which may be any covariant matrix.

It is our present purpose to suggest a value for this quantity.

We shall at present omit the term $\Gamma^\mu_{\nu\lambda}$, which does not appear in the usual quantum analysis.

This would be permissible in a four-dimensional analysis because in atomic problems there is no gravitational effect. But it must be remembered that in the analysis used here the $\Gamma^\mu_{\nu\lambda}$ depend also upon the electromagnetic potentials. Thus these coefficients cannot be simply neglected. We can, however, show that the additional terms in the above equations (9) are smaller than the others. For this reason we shall obtain a form for $\Gamma_\nu$, neglecting $\Gamma^\mu_{\nu\lambda}$.

The suggestion comes from a consideration of the definition of differentiation with respect to time, to which we have referred, viz.,

$$\frac{h}{2\pi i} \frac{\partial \psi}{\partial t} = -H\psi.$$

From equation (5) we obtain

$$\gamma^4 \frac{\partial \psi}{\partial x^4} = -\left[\gamma' \frac{\partial \psi}{\partial x'} + \gamma^2 \frac{\partial \psi}{\partial x^2} + \gamma^3 \frac{\partial \psi}{\partial x^3} + \gamma^5 \frac{\partial \psi}{\partial x^5}\right]. \quad \ldots \quad (10)$$

By means of equation (4), and remembering that

$$\frac{\partial\psi}{\partial x^5}=\frac{2\pi i m_0 c}{h}\psi \text{ and also } \alpha=\frac{e}{m_0 c^2},$$

equation (10) reduces to

$$\frac{h}{2\pi i}\gamma^4\frac{\partial\psi}{\partial x^4}=-\Big\{\gamma'\Big(\pi_1-\frac{e}{c}\phi_1\Big)+\gamma^2\Big(\pi_2-\frac{e}{c}\phi_2\Big)+\gamma^3\Big(\pi_3-\frac{e}{c}\phi_3\Big)$$
$$-\frac{e}{c}\gamma^4\phi_4+m_0 c\alpha_0\Big\}\psi. \quad . \quad . \quad . \quad . \quad . \quad . \quad . \quad (11)$$

$\pi_1$, $\pi_2$, $\pi_3$ are identical with $\pi_x$, $\pi_y$, $p_z$, occurring in Dirac's equation, $\phi_1$, $\phi_2$, $\phi_3$ replace $A_x$, $A_y$, $A_z$, and $\phi_4=i\phi$.

If we compare equation (11) with Dirac's equation, viz.:

$$\frac{h}{2\pi i}\frac{\partial\psi}{\partial t}=\Big\{c\alpha_x\Big(\pi_x-\frac{e}{c}A_x\Big)+\ldots+\ldots-e\phi+m_0 c^2\alpha_m\Big\}\psi, \quad . \quad (12)$$

we obtain the relation between the $\gamma$ matrices and the $\alpha$ matrices of equations (11) and (12) respectively. These equations are made identical term by term by multiplying the latter by $\gamma^4/ic$.

The following relations are then obtained:

$$\gamma'=i\gamma^4\alpha_x,\ \ \gamma^2=i\gamma^4\alpha_y,\ \ \gamma^3=i\gamma^4\alpha_y,\ \ \alpha_0=i\gamma^4\alpha_m. \quad . \quad . \quad . \quad (13)$$

Multiplying the relations (13) by $\gamma^4$, and putting $\gamma^4\gamma^4=\gamma^{44}$ in accordance with (1), these reduce to

$$\left.\begin{array}{ll}\alpha_x=\dfrac{\gamma^4\gamma'}{i\gamma^{44}}, & \alpha_y=\dfrac{\gamma^4\gamma^2}{i\gamma^{44}},\\[2ex] \alpha_z=\dfrac{\gamma^4\gamma^3}{i\gamma^{44}}, & \alpha_m=\dfrac{\gamma^4\alpha_0}{i\gamma^{44}}.\end{array}\right\} \quad . \quad . \quad . \quad . \quad . \quad . \quad . \quad (14)$$

The quantum equation (12) takes no account of the gravitational field, which is insignificant in the problems considered, so that the relations (14) denote that the quantities on the right-hand side reduce to the $\alpha$'s in the absence of gravitational effects.

It is necessary to show that the relations between the $\alpha$'s and those of equation (1) are compatible.

As an example, consider

$$\alpha_x\alpha_y+\alpha_y\alpha_x=2\delta_{xy}. \quad . \quad . \quad . \quad . \quad . \quad . \quad . \quad . \quad (15)$$

According to (14) this takes the form

$$\frac{1}{(i\gamma^{44})^2}(\gamma^4\gamma^1\gamma^4\gamma^2+\gamma^4\gamma^2\gamma^4\gamma^1). \quad . \quad . \quad . \quad . \quad . \quad . \quad . \quad (16)$$

When no gravitational field exists

$$\gamma^1\gamma^4+\gamma^4\gamma^1=2\gamma^{14}=2g^{14}=2\delta_{14}=0.$$

Thus $\gamma^4\gamma^1\gamma^4\gamma^2=-\gamma^4\gamma^4\gamma^1\gamma^2=-\gamma^{44}\gamma^1\gamma^2$, and we obtain instead of (15)

$$\frac{1}{\gamma^{44}}(\gamma^1\gamma^2+\gamma^2\gamma^1)=\frac{2\gamma^{12}}{\gamma^{44}}.$$

This reduces to zero since, in the absence of the field $\gamma^{44}=1$, $\gamma^{12}=g^{12}=0$. Thus (16) reduces to (15) in this case. The other relations between the $\alpha$'s can be verified in the same way.

A comparison of equation ($c$) and (9) indicates that $\Gamma_4$ and H are closely related, and that from a study of the form of H we may be able to derive the general matrix $\Gamma_n$.

Equation (12) can be written in the form

$$\frac{h}{2\pi i}\frac{\partial}{\partial x^4}=-\frac{\mathrm{H}}{ic}=-\frac{\gamma^4}{\gamma^{44}}\left(\gamma^1 u_x+\gamma^2 u_y+\gamma^3 u_z-\frac{e}{c}\gamma^4\phi_4+m_0 c\alpha_0\right),$$

where

$$u_x=\frac{h}{2\pi i}\frac{\partial}{\partial x^1}-\frac{e}{c}\phi_1, \text{ etc.}$$

We suggest that the right side of this equation be put equal to

$$-\frac{h}{2\pi i}\Gamma_4,$$

so that

$$\Gamma_4=\frac{2\pi}{hc}\mathrm{H}=\frac{2\pi i}{h}\frac{\gamma^4}{\gamma^{44}}\left\{\frac{h}{2\pi i}\gamma^1\frac{\partial}{\partial x^1}+\frac{h}{2\pi i}\gamma^3\frac{\partial}{\partial x^2}+\frac{h}{2\pi i}\gamma^3\frac{\partial}{\partial x^3}\right.$$
$$\left.-\frac{e}{c}\gamma^1\phi_1-\frac{e}{c}\gamma^2\phi_2-\frac{e}{c}\gamma^3\phi_3-\frac{e}{c}\gamma^4\phi_4+m_0 c\alpha_0\right\},$$

whence

$$\Gamma_4=-\frac{\gamma^4}{\gamma^{44}}\left(\gamma^1\frac{\partial}{\partial x^1}+\gamma^2\frac{\partial}{\partial x^2}+\gamma^3\frac{\partial}{\partial x^3}+\gamma^5\frac{\partial}{\partial x^5}\right),$$

and

$$\gamma^4\Gamma_4=-\Sigma\gamma^\nu\frac{\partial}{\partial x^\nu},$$

where $\nu$ is summed from 1 to 5, excluding the case $\nu=4$.

Thus in general we write

$$\gamma^\mu\Gamma_\mu=-\Sigma_\nu\gamma^\nu\frac{\partial}{\partial x^\nu}\qquad(\nu\neq\mu)\qquad(\mu\text{ not summed}).$$

$$\Gamma_\mu=\frac{-\gamma^\mu}{\gamma^{\mu\mu}}\Sigma_\nu\left(\gamma^\nu\frac{\partial}{\partial x^\nu}\right)\qquad\nu\neq\mu\qquad(\mu\text{ not summed}).$$

It follows that

$$\gamma^\mu\Gamma_\mu-\Gamma_\mu\gamma^\mu$$

when the summation is over $\mu$, for the values 1 to 5 is equal to

$$-\Sigma\gamma^\nu \frac{\partial}{\partial x^\nu} + \frac{\gamma^\mu}{\gamma^{\mu\mu}}\left(\Sigma\gamma^\nu \frac{\partial}{\partial x^\nu}\right)\gamma^\mu$$

$$= \frac{\gamma^\mu}{\gamma^{\mu\mu}}\gamma^\nu \frac{\partial\gamma^\nu}{\partial x^\nu} + \frac{\gamma^\mu\gamma^\nu\gamma^\mu}{\gamma^{\mu\mu}} \frac{\partial}{\partial x^\nu} - \gamma^\nu \frac{\partial}{\partial x^\nu} = 0 \text{ by equation (7).}$$

We sum for the values of $\mu$ from 1 to 5, but $\nu \neq \mu$ in any term. Thus

$$\frac{\gamma^\mu\gamma^\nu}{\gamma^{\mu\mu}} \frac{\partial\gamma^\mu}{\partial x^\nu} = \frac{1}{\gamma^{\mu\mu}}\left[\gamma^{\mu\mu}\gamma^\nu \frac{\partial}{\partial x^\nu} - \gamma^\mu\gamma^\nu\gamma^\mu \frac{\partial}{\partial x^\nu}\right]$$

$$= \frac{1}{\gamma^{\mu\mu}}[\gamma^\mu\gamma^\mu\gamma^\nu - \gamma^\mu\gamma^\nu\gamma^\mu] \frac{\partial}{\partial x^\nu}$$

$$= \frac{2\gamma^\mu S^{\mu\nu}}{\gamma^{\mu\mu}} \frac{\partial}{\partial x^\nu}.$$

Thus

$$\frac{\gamma^\mu}{\gamma^{\mu\mu}}\left[\gamma^\nu \frac{\partial\gamma^\mu}{\partial x^\nu} - 2S^{\mu\nu} \frac{\partial}{\partial x^\nu}\right] = 0. \quad . \quad . \quad . \quad . \quad . \quad . \quad (17)$$

Equation (17) is the form taken by the quantum law (7) for this choice of the form of $\Gamma_\mu$. The particular form of summation is to be noted. It takes place for all values of $\mu$, and for each value of $\mu$, $\nu$ is summed over $\nu=1$ to 5, excluding $\nu=\mu$. The quantum law is expressed as an operator equation.

In conclusion, I wish to thank Dr. H. T. Flint for a valuable discussion on this subject.

# XXXIII. *A Mobile Seismic Recording Unit.*

By F. M. G. Murphy, M.A., and S. T. Cope, Research and Development Department, Marconi Wireless Telegraph Company, Ltd., and J. H. Jones, D.Sc., Chief Geophysicist, Anglo-Iranian Oil Company, Ltd.*

[Received November 25, 1938.]

[Plates II.–IV.]

## *Introduction.*

The rapid growth in the number of proved oilfields is due largely to the high degree of efficiency which has been attained in modern geophysical surveys.

The outstanding successes which have been achieved by the seismic refraction and reflexion methods in different countries, and under different geological conditions, have established them as the two most powerful methods of applied geophysics. The refraction method was the first in the field, and much useful work has been, and still is being, accomplished by this method. The reflexion method is a later development, and it has the advantage that smaller charges of explosive can be used, on account of the shorter operating range. The detectors and recording apparatus which are described in this paper are suitable for both reflexion and refraction surveys, and have been successfully used for both.

In this paper, however, we shall confine our attention to the use of the apparatus for reflexion surveys, and we shall include a brief description of this particular method.

The seismic reflexion detectors are essentially short-period seismometers (periods ranging from 1/2 to 1/10 sec. or less), in which are incorporated some devices for converting the mechanical motion into electrical impulses. The detectors are connected by cable to a mobile central recording unit, where the electrical impulses are amplified and recorded on a single photographic strip.

Six detectors are normally used, and these are spaced at intervals of 150 feet, and at a mean distance of 2000 feet from the explosion point. The recording unit occupies the mid-position of the instrument spread, and telephonic communication, either by field telephone or short-wave radio, is established between the unit and the firing station. In addition,

---

* Communicated by the Authors.

there is a circuit (land line or radio) for transmitting the shot-instant to the central recording apparatus.

### *The Method of determining the Depth and Inclination of the Reflecting Layer.*

We shall only consider the case of a plane reflector which is inclined at a small angle to the horizontal. We shall assume that the reflecting plane has no inclination in the direction at right angles to the line of detectors and the shot-point.

Fig. 1.

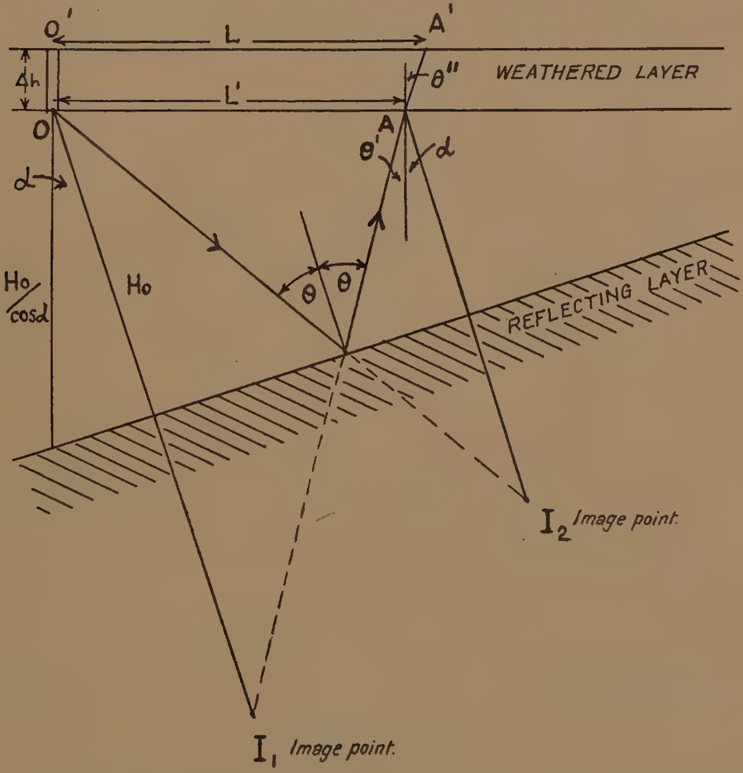
O'
L
A'
Δh
θ''
WEATHERED LAYER
L'
O
A
θ'
α
α
Ho/cosα
Ho
θ
θ
REFLECTING LAYER
I₂ Image point
I₁ Image point

Suppose that O in the diagram (fig. 1) represents the explosion-point, and that A′ represents the mid-point of the detector spread, so that O′A′ is about 2000 feet. The velocity of the compressional wave in the weathered layer * is $v_0$, $\theta'$ is the angle of incidence of the reflected ray on the lower boundary of the weathered layer, and $\theta''$ refers to the direction of travel within the layer. The angle of reflexion is $\theta$ and the inclination of the reflecting layer $\alpha$. If $\Delta L$ represents the detector spread and $\Delta T_1$ the difference in time of arrival of the reflected wave at No. 6 and No. 1 detectors, the ratio $\frac{\Delta L}{\Delta T_1}$ (usually referred to as the apparent velocity of the reflected wave along the direction O′A′) is given by

---

* A thin surface layer with very low elastic properties. The charge is fired below the bottom surface of this layer.

$$\frac{\Delta L}{\Delta T_1}=\frac{v_0}{\sin\theta''}=\frac{v}{\sin\theta'}=\frac{v}{\sin(\theta-\alpha)}, \quad \ldots\ldots \quad (1)$$

where $v$ is the velocity of the wave in the medium overlying the reflector.

We now suppose the charge to be fired at A, and that O′ is now the mid-point of the detector spread. The apparent velocity in the direction A′O′ is

$$\frac{\Delta L}{\Delta T_2}=\frac{v}{\sin(\theta+\alpha)}. \quad \ldots\ldots \quad (2)$$

From (1) and (2) we have the following relations :

$$\Delta T_1+\Delta T_2=\frac{2\Delta L}{v}\sin\theta\cos\alpha, \quad \ldots\ldots \quad (3)$$

$$\Delta T_2-\Delta T_1=\frac{2\Delta L}{v}\cos\theta\sin\alpha, \quad \ldots\ldots \quad (4)$$

from which we derive

$$\tan\alpha=\frac{\Delta T_2-\Delta T_1}{\Delta T_2+\Delta T_1}\tan\theta=\frac{b}{a}\tan\theta, \quad \ldots\ldots \quad (5)$$

where

$$a=\frac{\Delta T_2+\Delta T_1}{2} \quad \text{and} \quad b=\frac{\Delta T_2-\Delta T_1}{2}.$$

From the triangle $I_1OA$ we have

$$\frac{\cos\alpha}{I_1A}=\frac{\sin\theta}{OA}=\frac{\sin\theta}{L'}.$$

To a first approximation, since the angle $\theta''$ is usually very small, we can write $L'=L$, and then

$$\cos\alpha=\frac{v\,T\sin\theta}{L},$$

where T is the total time of travel from O to A. Substituting this value of $\cos\alpha$ in (3) we get

$$\sin\theta=\sqrt{\frac{La}{T\Delta L}}$$

and

$$\tan\theta=\sqrt{\frac{La}{T\Delta L-La}}. \quad \ldots\ldots \quad (6)$$

The inclination angle $\alpha$ can now be found by using relation (5), and the depth

$$H = H_0/\cos\alpha = \frac{L}{2}\{\cot\theta \pm \tan\alpha\}.$$

The quantities T, $a$, $b$ are determinable from the seismograms, so that the depth and inclination of the reflecting layer can be found.

In general we have to deal with an inclination of the reflecting plane in two directions, and the simple assumption of a uniform velocity in the overburden does not apply in practice. We need not, however, consider these complications in this paper.

Fig. 2.

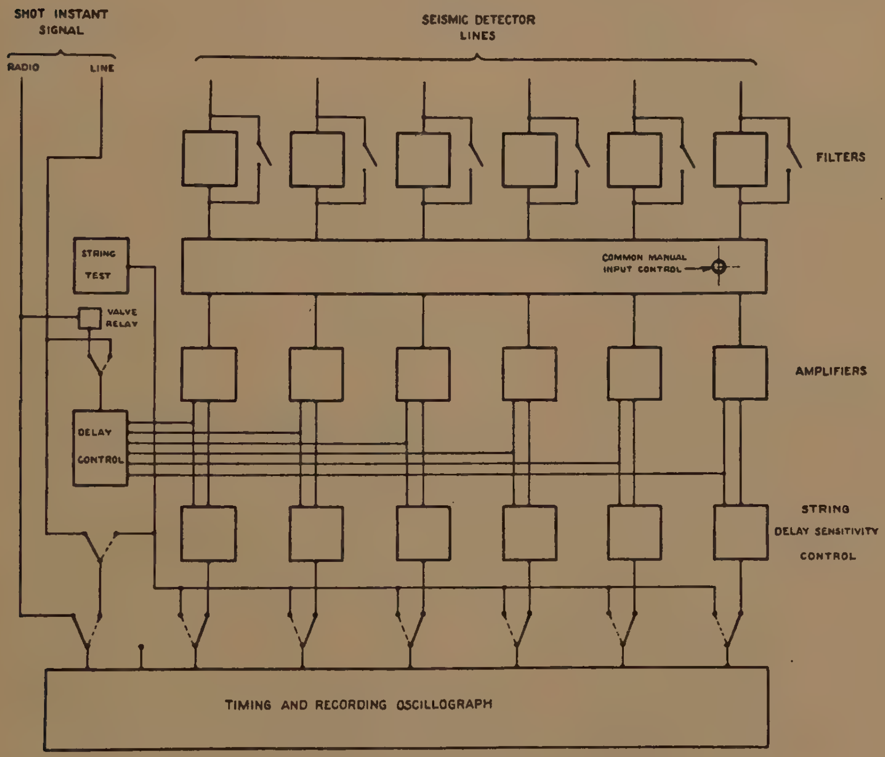
SHOT INSTANT SIGNAL
RADIO
LINE
SEISMIC DETECTOR LINES
FILTERS
STRING TEST
COMMON MANUAL INPUT CONTROL
VALVE RELAY
AMPLIFIERS
DELAY CONTROL
STRING DELAY SENSITIVITY CONTROL
TIMING AND RECORDING OSCILLOGRAPH

Block representation of the components.

## *General Description of System.*

The equipment evolved is shown in broad outline in fig. 2, where it will be seen that provision is made for six observation points. The impulses generated by the detector at each of these points are conveyed by lines to the main equipment and then pass to individual keys which control the insertion of a filter in each circuit. The signals are next subject to a common manual control which decreases their amplitude to some 10 per cent. or leaves it unaffected—a facility found useful in the field as a precaution against damage by very heavy disturbances. After this common control, the signals reach separate amplifiers, which include individual manual sensitivity controls. The amplified signals are subject to a further sensitivity control before finally reaching an oscillograph string, but this last control is not effective unless automatic sensitivity delay be in use.

The oscillograph provides eight strings and records their vibrations photographically on a time-scale marked by a fork-controlled interrupter. The complete set of strings may be removed as a unit, and the sensitivity of each string is adjustable on the oscillograph. To provide for this adjustment each string may be transferred by a key from its normal connexions to a test circuit.

Of the two idle strings, one is used to mark the shot-instant, which is signalled from the shot-point either by lines or radio equipment. For this purpose an auxiliary circuit carrying a small direct current is broken by the explosion, the interruption of the current providing the signal of the shot-instant. When lines are in use this current can be supplied from the main equipment and through this string. A seismic detector may be connected across the line to indicate the weathered layer velocity by providing a later signal on the same string.

When radio communication is used, it is necessary to use the interruption to operate a relay on the shot-point radio transmitter and apply the output of the radio receiver to the oscillograph string in the main equipment. For reasons of convenience, the shot-instant string can be transferred by a key operation between line and radio-receiver connexions.

The direct current interruption on the shot-instant line is also used to operate the automatic sensitivity control if this be in use. On connexion, the automatic gain delay both reduces the amplifiers' sensitivity to a low value and causes a high resistance to be inserted in the oscillograph circuit. When the shot interrupts the line current, the high resistance is removed and the amplifier sensitivity is gradually restored, so that the heavy initial disturbances are prevented from damaging the oscillograph strings.

The automatic sensitivity control can also be put into operation by the radio signal actuated by the explosion. The signal picked up by the receiver in the recording van is made to pass through a sensitive valve relay * connected to the automatic sensitivity control device, which is set in operation by the breaking of a local circuit in the recording van.

---

* The valve relay was supplied by the Cambridge Instrument Company.

## *Apparatus.*

### *Seismic Detectors.*

The preliminary research work on the most suitable type of electrical recording seismograph was carried out in the oilfields of Iran in 1934 and 1935. As a result of this work it was decided to design a detector with a natural period of half a second, with suitable oil damping, and incorporating the well-known magnet and coil device for registering the earth movements. Comparative tests made in Iran with this type of detector and a portable mechanical seismograph of rather longer period showed excellent agreement in the registration of the sharper movements, but the longer period mechanical instrument responded somewhat better to the slow surface waves. The detectors were made by the Cambridge Instrument Company, who are responsible for a number of features in the design.

### *Filters.*

It was a matter of doubt as to whether normal methods of filter design were applicable to seismic signals, since those methods are based on steady conditions. Field tests on a variety of designs showed that a filter might be shock excited and then continue in damped oscillation for an appreciable time, causing serious distortion of the signals. Since, however, the results obtained showed satisfactory agreement with previous laboratory tests, development could proceed until only final adjustment was necessary in the field. In this connexion it may be remarked that efficiency requires all the necessary damping to be provided by the connected apparatus, but this ideal may not be feasible if the frequency discrimination be concentrated and sharp.

The form of filter in use comprises a single section of band-pass characteristics, and this band may be chosen as around 20, 30, 40, or 50 c.p.s. by the adjustment of a single control, or the filter may be removed from the circuit by the operation of a key.

### *Amplifiers.*

The amplifier requirements were at first sufficiently similar to those of high performance types used for broadcast control purposes to present no special features beyond adaptation for the impedances of the seismic detectors and of the oscillograph strings. The circuit comprises three stages, resistance/capacity coupled with a choke coupled output transformer. Sensitivity control was provided by a potentiometer between the first and second valves, and this control was in twenty logarithmic steps.

This design was modified to cater for automatic sensitivity delay by inserting a screened grid valve of variable amplification factor in the first stage, so that the grid bias on this valve was provided both by the usual cathode resistance and by the charge on a condenser. Normally a large negative voltage is applied across this condenser, but, on the firing of the shot, this source of voltage is removed. The condenser charge then dissipates through the shunt resistance and, as this occurs, the amplifier becomes increasingly sensitive. It will be noted that the manual sensitivity control is not affected by this mechanism and that the speed at which the sensitivity increases automatically can be controlled by adjustment of the resistance through which the condenser discharges.

The amplifiers' gain is approximately 65 dB. and the maximum linear output power some 160 mW.

Fig. 3.

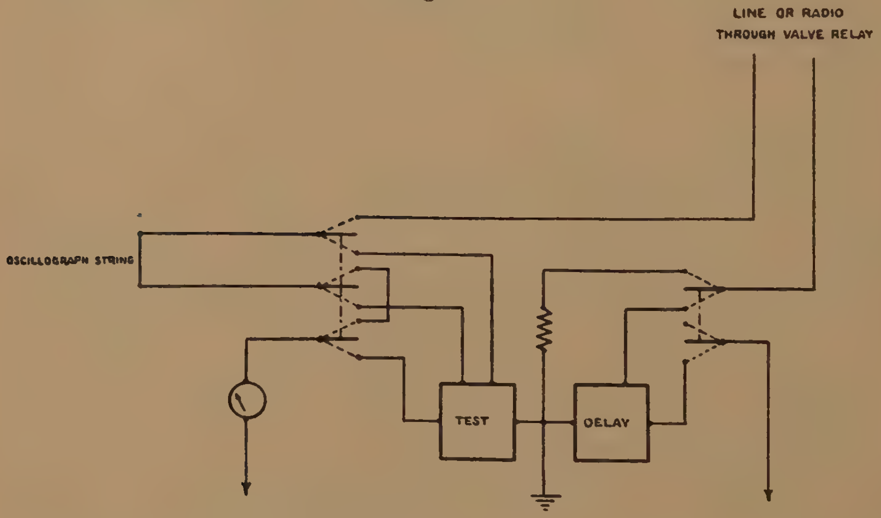

Shot string circuits.

*Camera and Recording Oscillograph.*

The oscillograph, which is of the Einthoven type, is provided with eight strings of diameter 15 $\mu$. Each string has a variable resistance in parallel so that the sensitivity can be quickly adjusted.

A phonic wheel controlled by a standard 100 c.p.s. fork interrupts a light beam and impresses a time-scale on the photographic paper, which is moved at a uniform rate by a clockwork motor. The rate of movement of the paper can be varied from about 10 to 30 cm. per second. This unit was provided by the Cambridge Instrument Company, Ossining, New York.

*Auxiliary Circuits.*

The shot string circuits are shown in fig. 3. It will be seen that both the radio and line connexions are through additional keys. Of these keys, one places the automatic sensitivity delay in service by connecting one line and battery * to the delay control or, when the device is not in use, earths the line through a resistance. The remaining key connects the string to line and battery on to the string-test circuit.

This string-test circuit, as shown to the right of fig. 4, is a potentiometer supply through a press key in parallel to all the string-test positions. It will be noted that a meter is included in this potentiometer circuit, but this inclusion is incidental to the shot line indication for which the instrument is normally used.

Fig. 4.

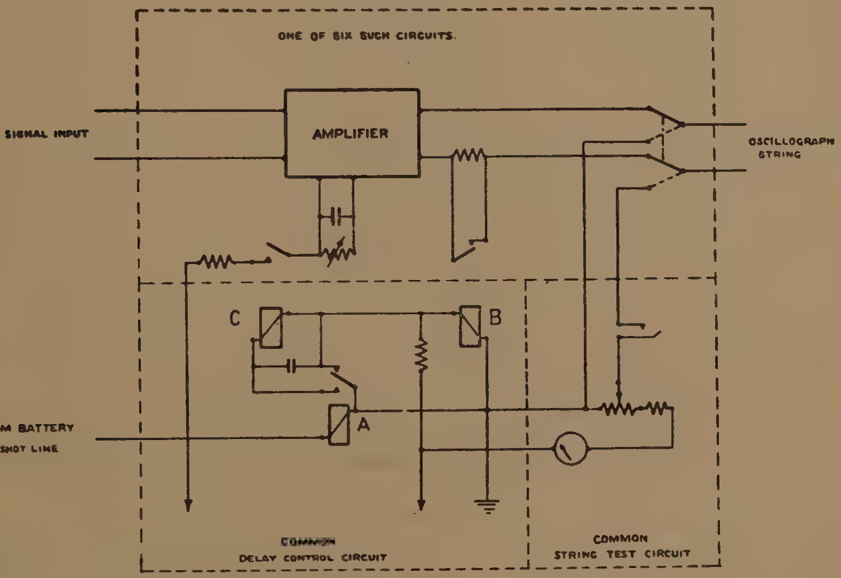
ONE OF SIX SUCH CIRCUITS.
SIGNAL INPUT
AMPLIFIER
OSCILLOGRAPH STRING
C
B
A
FROM BATTERY VIA SHOT LINE
COMMON DELAY CONTROL CIRCUIT
COMMON STRING TEST CIRCUIT

Delay and string test circuits.

The delay control is operated by the interruption of the shot line current through the relay A shown in fig. 4. The procedure is to place the charge of explosive in the hole and make all connexions before completing the shot line circuit to battery and earth. When this circuit is made, relay A operates and so causes relays B and C to operate. Relay B is provided with six pairs of contacts, each pair of which inserts a high resistance in an oscillograph string circuit when the relay is operated. Relay C operates to connect a large negative voltage through individual resistances to charge the respective amplifier time constant circuits.

* Or radio receiver and valve relay.

When the shot interrupts the line current *, relay A relapses and the other relays follow, so that the decay of the charges on the amplifier condenser-resistance circuits begins to increase the amplifier sensitivities and the string circuits become effective.

The sequence of these operations is important, for dangerously large impulses may be generated by the operation or relapse of relay C, were it not for the loss controlled by relay B. Hence the practical form of the circuit differs in detail from the simplified form shown in the figure so as to ensure protection of the strings while relay C is energized or released. It may be interesting to note that an early form of the circuit suffered from poor timing in this respect, although all adjustments seemed correct. The trouble was eventually traced as due to interaction between relay windings affecting the times of their operation and their freedom from contact bounce.

### *Supplies.*

The low voltage supplies for the amplifiers and the oscillograph could be furnished by accumulators through the usual switches and fuses, but the high voltage supplies for the amplifiers presented some difficulty. On the basis of providing this latter supply from low voltage batteries, the natural choice was between a motor-alternator and rectifiers or a motor-generator. The latter would require all the amplifier plate circuits to be connected together and so would involve each amplifier supply passing through de-coupling circuits to avoid interaction. These de-coupling circuits would be cumbersome on account of the low frequencies involved and might prove a source of very low frequency instability.

By choosing a motor-alternator, on the other hand, each amplifier was provided with its own rectifier and the possibility of interaction between amplifiers made remote. Further, the motor-alternator frequency could be chosen so as to be higher than that of the signals, so that the necessary smoothing of the rectified supply could be made compact and troublesome interference avoided. With such a system the chief risk of interference from the supplies arises if the motor-alternator output is modulated at low frequency, due to lack of balance etc. in the machine. Great care was taken therefore to procure dynamic balance, and, in addition, flexible mountings were used for the motor-alternator. Thermionic rectifiers were chosen for their small size, and the whole of the rectifier equipment was mounted on a small rack.

## *Assembly.*

All the apparatus mentioned in the foregoing paragraphs (apart from the geophones) is assembled on three sides of the interior of a 30 cwt.

---

* If radio is used, the shot-signal interrupts the current in the valve relay circuit.

van, as shown in the outline drawing, fig. 5. The rectifiers, amplifiers, and filters are assembled on racks; and the batteries and generator in

Fig. 5.

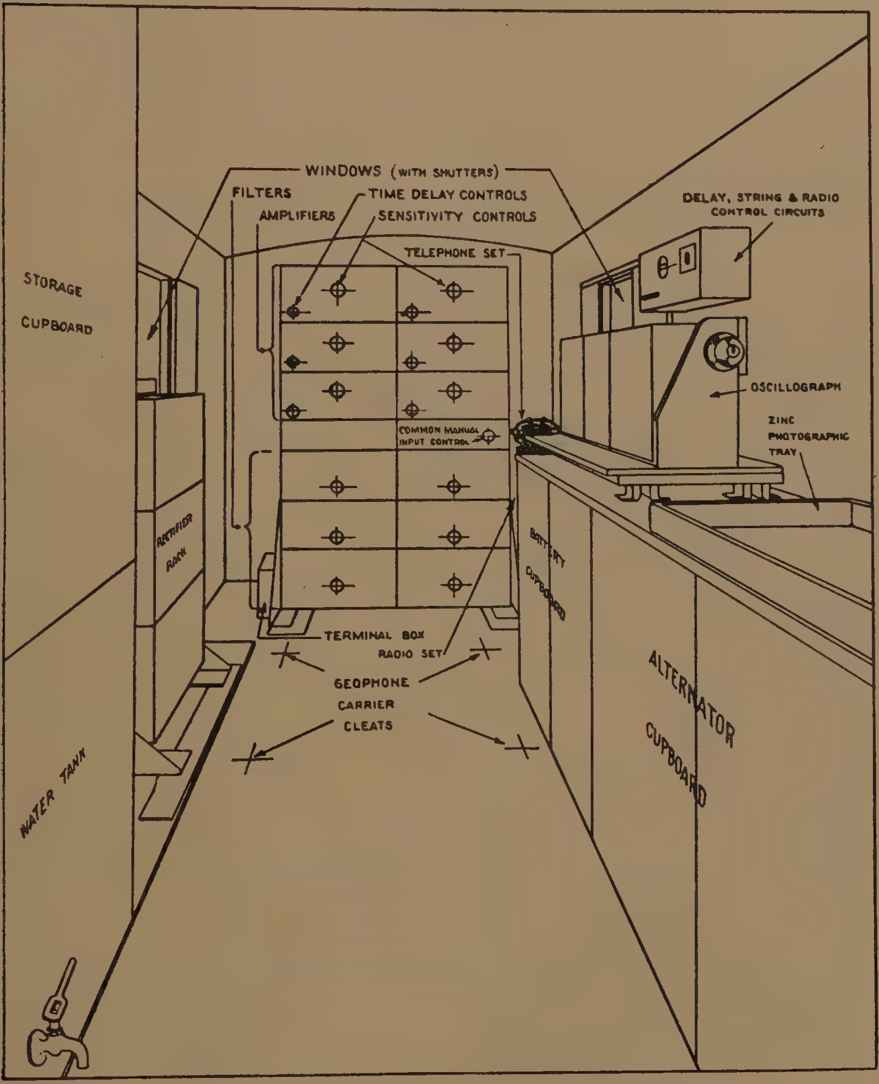
WINDOWS (WITH SHUTTERS)
FILTERS
TIME DELAY CONTROLS
AMPLIFIERS
SENSITIVITY CONTROLS
DELAY, STRING & RADIO CONTROL CIRCUITS
TELEPHONE SET
STORAGE CUPBOARD
OSCILLOGRAPH
COMMON MANUAL INPUT CONTROL
ZINC PHOTOGRAPHIC TRAY
RECTIFIER RACK
BATTERY CUPBOARD
TERMINAL BOX
RADIO SET
GEOPHONE CARRIER CLEATS
ALTERNATOR CUPBOARD
WATER TANK

Layout of seismographic equipment in van.

cupboards, to reduce noise from the generator and for the prevention of damage by battery acid. Although not shown in the figure, main switches for valve heating and generator starting mechanism, with indicating lamps, are fitted on the right-hand wall.

The type of layout adopted has resulted in ample space being available for operating the equipment, and when the window-shutters and the door are closed, the whole becomes a dark room for developing the oscillograph records. Suitable lighting is supplied from the van's normal lighting system.

In addition to the electrical equipment, a six-gallon water-tank, a large zinc tray for photographic purposes, and a storage cupboard are fitted on either side of the door which occupies half of the fourth side. To prevent damage during transit the various parts of the equipment are fitted on shock-absorbing mountings, while cleats are fixed to the floor for securing the geophone cases.

### *Field Tests.*

The mobile recording unit described in the preceding pages has been in use by the D'Arcy Exploration Company for a period of two years in oil exploration surveys in Eastern England.

It will be sufficient for the purpose of this communication to reproduce a few typical seismograms to illustrate some of the particular features of the unit. Thus Pl. II. shows a reflexion seismogram recorded with an instrument spread of 750 ft. at an average distance of 2000 ft. from the explosion. The charge of gelignite was $2\frac{1}{2}$ lb. at a depth of 36 ft. The automatic delay control was in operation, but the filters were not included in the circuit. A well-defined reflexion is shown at " *a* " and another from a deeper horizon at " *b*."

Pls. III. & IV. show seismograms recorded at the same positions with and without filters in circuit. The automatic delay device was not used with the first shot (Pl. III.). The charges of explosives were 5 and 10 lb. respectively at a depth of 50 ft. A reflexion is marked at " *a* " on both seismograms.

The unit has been used recently on an experimental seismic refraction survey in Lincolnshire, and excellent seismograms have been obtained at distances of five miles with a charge of 200 lb. of gelignite.

The writers wish to express their thanks to the Chairman and Directors of the Anglo-Iranian Oil Company, Limited, and to the Chairman and Directors of the Marconi Wireless Telegraph Company Limited for permission to publish this joint paper.

# XXXIV. *Two Notes on the Numerical Solution of Differential Equations.*

By F. J. Turton, B.Sc., A.R.C.Sc., City and Guilds College *.

[Received June 8, 1939.]

## (A) *Interpolation formulæ, not using finite differences, suitable for use when solving differential equations numerically by step-by-step methods at equal intervals.*

The following interpolation formulæ are suggested for use when values of $y$ and of its derivative $y'$ are available at equal intervals $h$ for $x$, as when solving differential equations numerically by the formulæ of Heun, Milne, etc. The value of $y$ at $x=rh$ is denoted by $y_r$ and the principal term of the error is given in brackets thus [ ]. The formulæ are also suitable for moderate extrapolation, say to $r=4/3$ or $3/2$.

(*a*) The formula of highest order of accuracy, using $y_0$, $y_0'$, $y_1$, and $y_1'$, is

$$\begin{aligned}y_r=&y_0(1-r)^2(1+2r)+y_1r^2(3-2r)+hy_0'r(1-r)^2-hy_1'r^2(1-r)\\&+[r^2(1-r)^2h^4y^{\text{iv}}/4\,!,\ \ngtr h^4y^{\text{iv}}/384 \text{ if } 0<r<1], \qquad (1.1)\end{aligned}$$

found by expanding $y_r$, $y_1$, and $y_1'$ in terms of $y_0$ and derivatives, and ascending powers of $h$, then choosing suitable multipliers so that, on addition, terms in $h^2y_0''$ and $h^3y_0'''$ vanish.

In particular,

$$y_{\frac{1}{2}}=(y_0+y_1)/2+h(y_0'-y_1')/8+[h^4y^{\text{iv}}/384], \qquad (1.2)$$

which is convenient when halving the interval.

These formulæ are suitable for use with Heun's formula for integrating ahead,

$$y_{n+3}=y_n+3h(y_n'+3y'_{n+2})/4+[3h^4y^{\text{iv}}/8], \qquad (2)$$

as the intrinsic error is substantially less than that of Heun's formula.

(*b*) The formula of highest order of accuracy, using $y_0$, $y_0'$, $y_1$, $y_1'$, $y_{-1}$ and $y'_{-1}$, is

$$\begin{aligned}y_r=&y_0(1-r^2)^2+y_1r^2(1+r)^2(4-3r)/4+y_{-1}r^2(1-r)^2(4+3r)/4+hy_0'r(1-r^2)^2\\&-hy_1'r^2(1+r)^2(1-r)/4+hy'_{-1}r^2(1-r)^2(1+r)/4\\&+[h^6y^{\text{vi}}r^2(1-r^2)^2/6\,!,\ \ngtr h^6y^{\text{vi}}/4860 \text{ if } 0<r<1], \qquad (3.1)\end{aligned}$$

found by an extension of the method indicated for finding (1.1). This is accurate enough for use with any of the usual step-by-step methods of integrating ahead.

---

* Communicated by Dr. W. G. Bickley.

In particular,

$$y_{\frac{1}{2}}=(11y_{-1}+72y_0+45y_1+3h(y'_{-1}+12y_0'-3y_1'))/128+[h^6y^{\text{vi}}/5120], \quad . \; (3.2)$$

which is accurate enough for halving the interval in such methods.

(*c*) If accuracy of order $h^5$ is sufficient an unlimited number of formulæ, using $y_0$, $y_0'$, $y_1$, $y'_1$, $y_{-1}$, and $y'_{-1}$, is available, some saving of labour being achieved, as compared with (3.1), at the expense of accuracy. Typical forms are

$$y_r=y_0(1-r^2)^2+y_1r^2(1+r)^2/4+y_{-1}r^2(1-r)(7+5r)/4+hy_0'r(1-r)(1+r)^2$$
$$+hy'_{-1}r^2(1-r^2)/2-[h^5y^{\text{v}}r^2(1+r)^2(1-r)/5\,!, \ngtr h^5y^{\text{v}}/270 \text{ if } 0<r<1], \quad (4.1)$$

$$y_r=y_{-1}r^2(2-r^2)+y_0(1-r^2)^2+hy'_{-1}r^2(1+r)(7-5r)/12$$
$$+hy_0'r(1+r)^2(3-2r)/3+hy_1'r^2(1+r)^2/12$$
$$-[h^5y^{\text{v}}r^2(1+r)^2(4-3r)/3\,.\,5\,!, \ngtr h^5y^{\text{v}}/90 \text{ if } 0<r<1]. \quad (4.2)$$

When halving the interval a convenient form is

$$y_{\frac{1}{2}}=(y_{-1}+9y_0+6y_1)/16+h(16y_0'-5y_1'+y''_{-1})/64+[h^5y^{\text{v}}/3840]. \quad . \; (4.3)$$

These are suitable when using Milne's formula for integrating ahead,

$$y_{n+4}=y_n+4h(2y'_{n+1}+2y'_{n+3}-y'_{n+2})/3+[14h^5y^{\text{v}}/45]. \quad . \; . \; (5)$$

(B) *New formulæ for starting the solution in step-by-step methods of integrating a differential equation numerically at equal intervals h for x.*

On occasion power series are inconvenient for obtaining the values necessary to start a systematic process in which a few early values of $y$ are required as well as $y_0$.

(i.) Milne has proposed a method of successive approximation, using the formula

$$y_1=y_0+h(5y_0'+8y_1'-y_2')/12+[h^4y^{\text{iv}}/24], \quad . \; . \; . \; (6.1)$$

together with Simpson's rule,

$$y_2=y_0+h(y_0'+4y_1'+y_2')/3-[h^5y^{\text{v}}/90], \quad . \; . \; . \; . \; (6.2)$$

trial values being substituted in the right-hand sides, leading in turn to better values.

If $h$ be put for $h/2$ in (1.2), we have

$$y_1=(y_0+y_2)/2+h(y_0'-y_2')/4+[h^4y^{\text{iv}}/24], \quad . \; . \; . \; . \; (6.3)$$

which may well be used with (6.2) in place of (6.1), giving simpler arithmetic with the same principal error term. Trial values inserted in (6.2) give a value for $y_2$; this in (6.3) gives a corrected $y_1$, and the process is repeated until successive values coincide; about three applications are usually sufficient to give results to as many places as the error terms justify. The method is suitable for determining the preliminary values to use with Heun's formula (2) for integrating ahead.

(ii.) For starting systematic applications of accuracy of order $h^5$ the method of (i.) would almost invariably necessitate the use of sub-intervals, and would even so suffer from a measure of uncertainty unless the relative magnitudes of $y^{\text{iv}}$ and $y^{\text{v}}$ were investigated.

The formulæ which follow give values of $y_1$, $y_2$, $y_3$, and $y_4$ with errors of the order of $h^5y^{\text{v}}/90$, and so are suitable for starting integration ahead by iterating Simpson's rule *.

Putting $h$ for $h/2$ in (4.3), and taking $x$ at 0, $2h$, and $4h$ instead of at $-2h$, 0, and $2h$, we have

$$y_3=(y_0+9y_2+6y_4)/16+h(y_0'+16y_2'-5y_4')/32+[h^5y^{\text{v}}/120]. \quad . \quad (7)$$

Also by Simpson's rule,

$$y_2=y_0+h(y_0'+4y_1'+y_2')/3-[h^5y^{\text{v}}/90], \quad . \quad . \quad . \quad . \quad (7.1)$$

$$y_3=y_1+h(y_1'+4y_2'+y_3')/3-[h^5y^{\text{v}}/90], \quad . \quad . \quad . \quad . \quad (7.2)$$

$$y_4=y_2+h(y_2'+4y_3'+y_4')/3-[h^5y^{\text{v}}/90], \quad . \quad . \quad . \quad . \quad (7.3)$$

and by analogy with (7),

$$y_1=(6y_0+9y_2+y_4)/16+h(5y_0'-16y_2'-y_4')/32-[h^5y^{\text{v}}/120]. \quad . \quad (7.4)$$

If trial values be assumed for $y_1$, $y_2$, $y_3$, and $y_4$, the equations (7.1) to (7.4) lead to corrected values for $y_2, y_3, y_4$, and $y_1$ in turn (using corrected values as they become available), the process being repeated until successive values agree. About four applications will usually suffice to give results as accurately as the error terms allow.

If the evaluation of $y'$ is laborious it is better to use (7.1), (7.3), (7.4), and (7), in which convergence is quicker, since the errors of the trial values of the $y$'s are not directly involved.

(iii.) For Milne's method (5) only $y_0$, $y_1$, $y_2$, and $y_3$ are essential. These can be found with ample accuracy by the following simpler method :—

$$y_2=y_0+h(y_0'+4y_1'+y_2')/3-[h^5y^{\text{v}}/90], \quad . \quad . \quad . \quad . \quad . \quad . \quad (8.1)$$

$$y_3=y_1+h(y_1'+4y_2'+y_3')/3-[h^5y^{\text{v}}/90], \quad . \quad . \quad . \quad . \quad . \quad . \quad (8.2)$$

$$y_1=(8y_0+y_3)/9+h(y_0'+2y_1'-y_2')/3-[h^5y^{\text{v}}/45], \quad . \quad . \quad (8.3)$$

putting in trial values, with corrected values as available, in the order given. About four applications are usually sufficient to give values as accurately as the error terms allow.

(iv.) It is suggested that the set (7.1) to (7.4) and/or the set (8.1) to (8.3) of these formulæ might well be used, when the preliminary values are found by series, as a routine check on such values, for there

---

* W. G. Bickley, Phil. Mag. (7) xiii. p. 1006 (1932).

is usually some uncertainty as to whether the terms not investigated are in fact negligible.

(v.) The following approximations usually give suitable trial values for the methods (i.), (ii.), or (iii.) :—

$$y_{\frac{1}{2}}=y_0+\tfrac{1}{2}hy_0',$$
$$y_1=y_0+hy_{\frac{1}{2}}',$$
$$y_2=y_0+2hy_1',$$
$$y_3=y_1+2hy_2',$$
$$y_4=y_2+2hy_3'.$$

## XXXV. *Notices respecting New Books.*

*Modern Developments in Fluid Dynamics.* Edited by S. GOLDSTEIN. (Oxford : Clarendon Press.) 2 vols. Price 50*s.* net.

ALL students of, and workers in, aerodynamics will welcome the publication of this authoritative account of the recent progress made in the study of the hydrodynamics of viscous fluids. The collaborators are all men of acknowledged position in the subject, and the editor is one of the most distinguished of the younger researchers in the subject.

While one of the great surprises of aerodynamics is the way in which the hydrodynamics of a perfect or non-viscous fluid has been reinstated as a subject of practical importance in aerofoil theory, it is, nevertheless, impossible to deal with the problems of the aeroplane, airship, etc., without introducing viscosity. The study of the boundary layer and of turbulence is fundamental to all problems of this kind, and even aerofoil theory based on the Kutta-Joukowski method has to be supplemented by the study of skin-friction, of the wake and of heat transfer.

The book is not a mathematical treatise, nor is it a purely physical account of the phenomena described. But, so far from falling between the two stools of mathematics and physics, it is a well thought-out combination of both points of view, with just enough of the mathematical theory to make the fundamentals clear, but without the mass of mathematical detail that often makes accounts of recent and current research so difficult to assimilate.

The book is profusely illustrated by means of photographs of fluid motion under various conditions, and applications to "experimental apparatus and methods of measurement" and other practical objects, like the Handley-Page slot and the Townend ring, are dealt with very adequately.

The editor and his collaborators are heartily to be congratulated on this notable publication.

S. B.

[*The Editors do not hold themselves responsible for the views expressed by their correspondents.*]

F. M. G. MURPHY, S. T. COPE,
& J. H. JONES.

Phil. Mag. Ser. 7. Vol. 28. Pl. II.

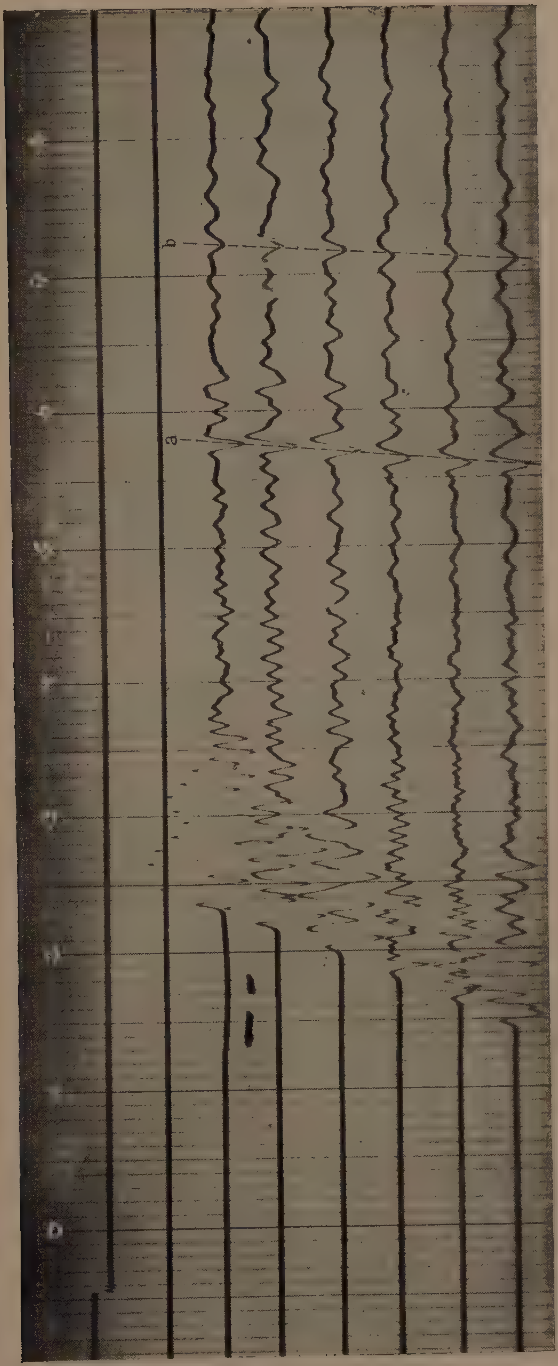

Reflexion Seismogram (i.).

F. M. G. MURPHY, S. T. COPE,
& J. H. JONES.

Phil. Mag. Ser. 7. Vol. 28. Pl. III.

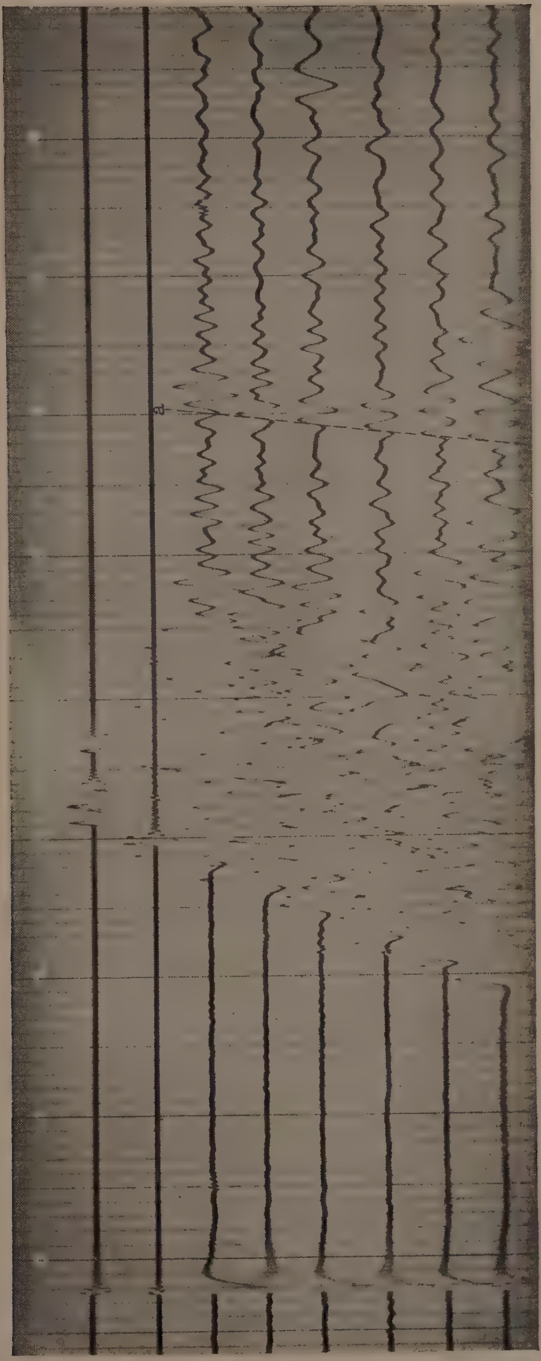

Reflexion Seismogram (ii.).

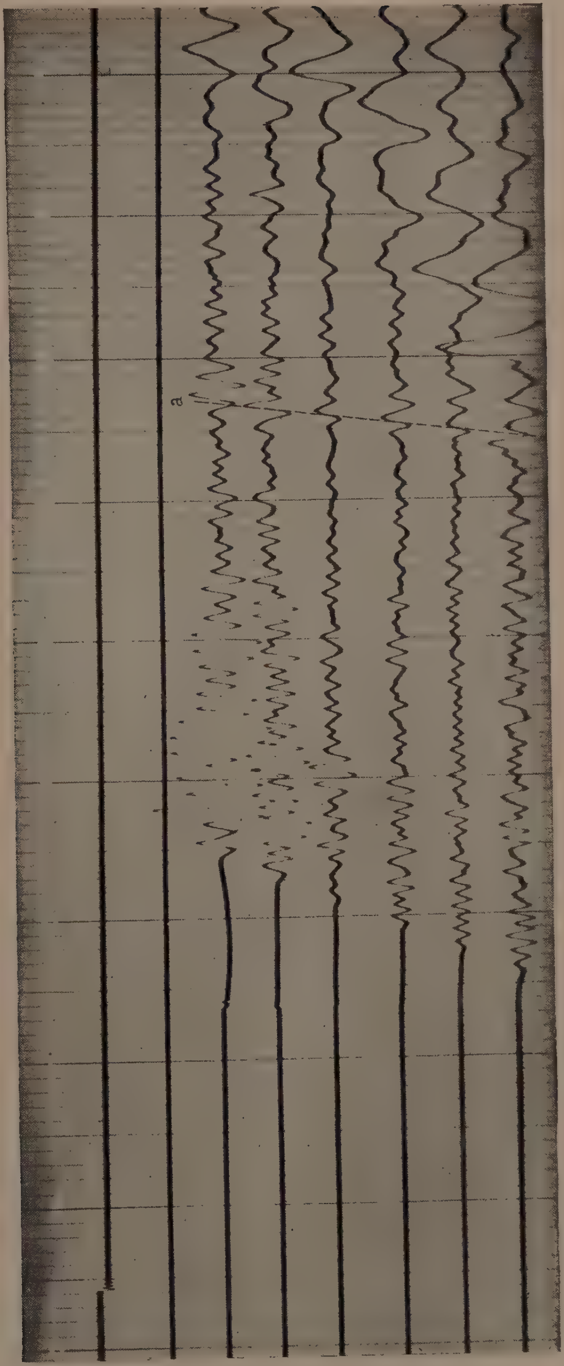

Reflexion Seismogram (iii.).

# XXXVI. *The Electron in Classical General Relativity Theory.*

By A. Lees, M.Sc., Ph.D., University College, Swansea *.

[Received December 12, 1938.]

## Summary.

The difficulties associated with the point electron in general relativity are avoided by ascribing to the electron a definite surface, for which a consistent scheme of stresses and electromagnetic properties is formulated. The external properties of the electron are preserved unchanged.

1. In general relativity theory the point electron is a singularity of both the electromagnetic field and the metric. It also encounters well-known physical objections. To avoid these difficulties we shall assume that each electron has a finite boundary in space-time, space-like sections of which are closed surfaces. The idea of considering the electron as a sphere, kept intact by suitable stresses, is not new, but what follows is believed to be the first formulation of such a stress system to be worked out fully for the case of general relativity.

We suppose space-time to extend through the interior of each electron. We shall simplify matters somewhat in this paper by assuming that there are no intersections of the boundaries with themselves or each other †. We adopt space-like variables $x^1$, $x^2$, $x^3$, and a time-like variable $x^4$, and introduce the metric tensor $g_{\mu\nu}$ and electromagnetic potential vector $\kappa_\mu$. At each boundary we require $g_{\mu\nu}$ and $\kappa_\mu$ to be continuous, but their normal derivatives may be discontinuous.

As our theory will treat all electrons similarly, in developing it we shall take the case of only one electron. We also adopt the following conventions. We require our coordinates to be such that $x^1$ has a constant value $(x^1)_0$ over the boundary, that the curves given by constant values of $x^2$, $x^3$, and $x^4$ cut the boundary orthogonally, and that the interval given by varying $x^1$ by a small constant amount from $(x^1)_0$ is constant all over the boundary. These conditions may always be satisfied, provided that the normal velocity of the electronic surface, relative to any coordinate frame, is less than that of light, and this is an obvious physical requirement.

---

* Communicated by Prof. H. T. H. Piaggio, M.A., D.Sc.

† It is still theoretically possible for one electron to enclose another completely.

The interval $ds$ being given by

$$ds^2 = g_{\mu\nu}\, dx^\mu\, dx^\nu, \qquad (1.1)$$

it may be seen that these conditions are expressible by the equations

$$x^1 = (x^1)_0 \qquad (1.2)$$

and

$$g_{1l} = 0,\ g_{11} = -k^2, \qquad (1.3)$$

applying to all points of the boundary. $k$ is a constant which we take as positive. In (1.3) we use, as hereafter, the convention that Latin (as distinct from Greek) suffixes take only the values 2, 3, and 4, and that repeated Latin suffixes are to be summed over only those values. It may be deduced from (1.3) that, on the boundary,

$$g^{1l} = 0,\ g^{11} = -k^{-2}. \qquad (1.4)$$

We shall use the term "free space-time" to denote all points of space-time exclusive of the boundary.

2. For any displacement along the boundary, $dx^1 = 0$, so (1.1) gives

$$ds^2 = g_{lm}\, dx^l\, dx^m.$$

Thus $g_{lm}$ gives the metric of the boundary with reference to $x^2$, $x^3$, and $x^4$. We call $g_{lm}$ a "boundary tensor," that is, one which refers only to the boundary and has only Latin suffixes. Similarly, from any ordinary tensor (the term including invariants and vectors), we obtain a boundary tensor by restricting its application to the boundary and changing its suffixes into Latin suffixes. Also it easily follows from (1.3) and (1.4) that, at the boundary, the raising or lowering of Latin suffixes is the same whether carried out by $g^{lm}$ and $g_{lm}$ or by $g^{\mu\nu}$ and $g_{\mu\nu}$, and that to raise or lower a suffix 1 we merely multiply by $g^{11}$ or $g_{11}$. Further, we may see that at the boundary $g^{lm}$ is given from $g_{lm}$ just as $g^{\mu\nu}$ is given from $g_{\mu\nu}$.

There are also, however, boundary quantities which are not derivable as above. Thus, we can form from $g_{lm}$ and its derivatives the Riemann-Christoffel tensor $B_{lmnp}$ for the boundary metric, corresponding to $\mathrm{B}_{\mu\nu\sigma\rho}$ for complete space-time, and just as*

$$\mathrm{B}_{\mu\nu\sigma}{}^{\sigma} = \mathrm{G}_{\mu\nu},\ \mathrm{G}^{\mu}_{\mu} = \mathrm{G}, \qquad (2.1)$$

we have

$$B_{lmn}{}^{n} = G_{lm},\ G^{l}_{l} = G,$$

$G$ being the Gaussian curvature of the boundary. Moreover, we can

---

[*] Eddington, 'The Mathematical Theory of Relativity,' § 37, pp. 81 and 82. (In $\mathrm{B}^{\epsilon}_{\mu\nu\sigma}$, $\epsilon$ is really the fourth suffix. Also $g^{\mu\nu}\mathrm{G}_{\mu\nu} = \mathrm{G}^{\mu}_{\mu}$.) In further references this treatise will be denoted by E.

differentiate any boundary tensor tensorially with respect to the boundary metric, just as similar processes are applied to ordinary tensors with respect to the complete metric.

3. We put

$$d\tau = dx^1 dx^2 dx^3 dx^4, \quad d\tau' = dx^2 dx^3 dx^4, \quad . \quad . \quad . \quad (3.1)$$

$d\tau$ and $d\tau'$ being elements of complete space-time and of the boundary respectively. Also we denote the determinants of $g_{\mu\nu}$ and $g_{lm}$ by $g$ and $g'$ respectively. From (1.3) we find that, on the boundary,

$$\sqrt{-g} = k\sqrt{g'}. \quad . \quad . \quad . \quad . \quad . \quad . \quad . \quad . \quad . \quad (3.2)$$

Then just as $\sqrt{-g}\,d\tau$ is an invariant *, so also is $\sqrt{g'}\,d\tau'$. For any quantity I, we refer to the integrals $\int \mathrm{I}\sqrt{-g}\,d\tau$ and $\int \mathrm{I}\sqrt{g'}\,d\tau'$, taken throughout any regions of space-time and the boundary, as space-time and boundary integrals of I. Also we refer to the integrals

$$\int \mathrm{I}\sqrt{-g}\,dx^1 dx^2 dx^3 \quad \text{and} \quad \int \mathrm{I}\sqrt{g'}\,dx^2 dx^3$$

($x^4$ being constant in each case), taken throughout any region of space and the electronic surface, simply as space and surface integrals of I. This agrees with common usage, and means that we regard

$$\sqrt{-g}\,dx^1 dx^2 dx^3 \quad \text{and} \quad \sqrt{g'}\,dx^2 dx^3$$

as elements of volume and surface area.

Let U be any function of the $g_{\mu\nu}$'s and $\kappa_\mu$'s and their first and second derivatives, involving the second derivatives linearly with algebraic coefficients. Let S be any region of the boundary, and consider $\int \mathrm{U}\sqrt{-g}\,d\tau$ taken throughout an infinitesimal region of space-time which just encloses S on either side. As the first derivatives of $g_{\mu\nu}$ and $\kappa_\mu$ may not be all continuous at the boundary, the value of the integral may be finite.

We may specify the region of space-time by letting $x^1$ vary between values just less and just greater than $(x^1)_0$, denoted, say, by $(x^1)_0 \pm 0$, whilst $x^2$, $x^3$, and $x^4$ are restricted to the continuum of sets of values which they have in S. With an obvious notation, we then have

$$\int \mathrm{U}\sqrt{-g}\,d\tau = \int_{\mathrm{S}} \left[\int_{(x^1)_0-0}^{(x^1)_0+0} \mathrm{U}\,dx^1\right] \sqrt{-g}\,dx^2 dx^3 dx^4. \quad . \quad . \quad (3.3)$$

Putting

$$[\mathrm{U}] = k\int_{(x^1)_0-0}^{(x^1)_0+0} \mathrm{U}\,dx^1, \quad . \quad . \quad . \quad . \quad . \quad . \quad . \quad . \quad . \quad (3.4)$$

it follows from equations (3.1) to (3.4) that

$$\int \mathrm{U}\sqrt{-g}\,d\tau = \int_{\mathrm{S}} [\mathrm{U}]\sqrt{g'}\,d\tau'. \quad . \quad . \quad . \quad . \quad (3.5)$$

---

* E, §49, pp. 109 and 110.

The meaning of [U], however, becomes clearer if in these equations we omit $dx^4$, keeping $x^4$ constant. Instead of (3.5), we then have

$$\int \mathrm{U}\sqrt{-g}\,dx^1\,dx^2\,dx^3 = \int_{\mathrm{S}} [\mathrm{U}]\sqrt{g'}\,dx^2\,dx^3,$$

S being now a region of the electronic surface. By what has been said, this equation means that [U] is the surface density of U.

If we now consider $\int \mathrm{U}\sqrt{-g}\,d\tau$ taken throughout all space-time, including the boundary, evidently we may put

$$\int \mathrm{U}\sqrt{-g}\,d\tau = \int_0 \mathrm{U}\sqrt{-g}\,d\tau + \int [\mathrm{U}]\sqrt{g'}\,d\tau', \quad . \quad . \quad . \quad (3.6)$$

in which the boundary integral is taken throughout the whole boundary and $\int_0$ denotes an integration throughout all *free* space-time.

We write

$$\mathrm{U} = \sum_{\mu,\nu=1}^{4} p_{\mu\nu} \frac{\partial^2 q_{\mu\nu}}{\partial x^\mu \partial x^\nu} + \ldots,$$

in which the $p_{\mu\nu}$'s and $q_{\mu\nu}$'s (which are not tensors) are algebraic functions of the $g_{\mu\nu}$'s and $\kappa_\mu$'s, and in which we omit terms not containing second derivatives. Then from (3.4) and the conditions of continuity at the boundary we easily find that

$$[\mathrm{U}] = kp_{11}\left\{ \left(\frac{\partial q_{11}}{\partial x^1}\right)_{x^1=(x^1)_0+0} - \left(\frac{\partial q_{11}}{\partial x^1}\right)_{x^1=(x^1)_0-0} \right\}.$$

From (1.1), (1.3), and (3.4) it may be seen that

$$[\mathrm{U}] = \int \mathrm{U}\sqrt{-ds},$$

the integration being along an infinitesimal line passing normally through the boundary at the point. From the invariant nature of this definition it follows that, if $t^{\alpha\beta\cdots}_{\mu\nu\cdots}$ be any tensor, $[t^{ab\cdots}_{lm\cdots}]$ is a boundary tensor.

4. We have now to formulate our scheme of differential equations. In this we shall be guided at first by physical considerations.

We intend to modify the orthodox theory only as regards the boundary. For free space-time, we therefore adopt the usual equations, namely * †,

$$(\mathrm{F}^{\mu\nu})_{\bar{\nu}} = 0, \quad . \quad . \quad . \quad . \quad . \quad . \quad . \quad . \quad (4.1)$$

in which ‡

$$\mathrm{F}_{\mu\nu} = \kappa_{\mu\bar{\nu}} - \kappa_{\nu\bar{\mu}} = \frac{\partial \kappa_\mu}{\partial x^\nu} - \frac{\partial \kappa_\nu}{\partial x^\mu}, \quad . \quad . \quad . \quad . \quad . \quad (4.2)$$

---

* E, p. 173, equation (73.74), putting $J^\mu = 0$ for empty space.

† We denote tensorial derivatives with regard to the complete metric, or the boundary metric, by placing bars respectively over or under the suffixes concerned. See also, *e. g.*, equation (7.7).

‡ E, p. 171, equation (73.3).

and *
$$G^{\nu}_{\mu}=-8\pi E^{\nu}_{\mu}, \qquad \qquad (4.3)$$

in which †
$$E^{\nu}_{\mu}=\tfrac{1}{4}g^{\nu}_{\mu}F^{\alpha\beta}F_{\alpha\beta}-F_{\mu\alpha}F^{\nu\alpha}. \qquad \qquad (4.4)$$

5. We come next to the boundary itself. Now, if our electron is to be a stable structure, evidently it should be of a definite size. The most obvious (if not the only) way to impose this condition is to require the Gaussian curvature $G$ of the boundary to have a definite value. We therefore put

$$G=G_0, \qquad \qquad (5.1)$$

$G_0$ being a constant to be determined later (equation (10.6)).

6. If we regard $x^4$ as time and $x^1$, $x^2$, $x^3$ as space variables, the electronic surface is stationary. We therefore assume that, as in the case of a charged surface in electrostatics, the electric field is normal to the surface at each point.

As the tangential electric field components are $F_{24}$ and $F_{34}$, this means that $F_{24}$ and $F_{34}$ must vanish. But coordinate transformations are possible among $x^2$, $x^3$, and $x^4$ without violating our conventions, and in any such transformation the new values of $F_{24}$ and $F_{34}$ may involve linearly the old values of $F_{24}$, $F_{34}$, and also $F_{23}$. Thus if $F_{24}$ and $F_{34}$ are still to vanish after any such transformation, $F_{23}$ must also vanish, that is, the magnetic field must be tangential to the surface. The conditions that $F_{24}$, $F_{34}$, and $F_{23}$ are to vanish are expressible as

$$F_{lm}=0 \qquad \qquad (6.1)$$

7. The stress-momentum-energy tensor $T^{\nu}_{\mu}$ is given by ‡

$$T^{\nu}_{\mu}=-\frac{1}{8\pi}(G^{\nu}_{\mu}-\tfrac{1}{2}g^{\nu}_{\mu}G). \qquad \qquad (7.1)$$

Also §
$$(G^{\nu}_{\mu}-\tfrac{1}{2}g^{\nu}_{\mu}G)_{\bar{\nu}}\equiv 0, \qquad \qquad (7.2)$$

hence
$$(T^{\nu}_{\mu})_{\bar{\nu}}=0 \qquad \qquad (7.3)$$

For free space-time (4.3) applies. Also on contracting (4.4) we have

$$E^{\mu}_{\mu}=0,$$

so on contracting (4.3) it follows, by (2.1), that

$$G=0. \qquad \qquad (7.4)$$

From (4.3), (7.1), and (7.4) we see that, in free space-time,

$$T^{\nu}_{\mu}=E^{\nu}_{\mu}. \qquad \qquad (7.5)$$

---

* E, p. 184, equation (77.7), the suffix $\nu$ being raised. ($G_{\mu\nu}$ and $E_{\mu\nu}$ are symmetrical.)

† E, p. 182, equation (77.2).

‡ E, p. 102, equation (46.6), the suffix $\nu$ being raised.

§ E, p. 115, equation (52).

As $g_l^1$ vanishes, it follows from (4.4) that

$$E_l^1 = -F_{l\alpha}F^{1\alpha}.$$

By (4.2) $F_{\mu\nu}$, and therefore $F^{\mu\nu}$, is antisymmetrical, so this gives

$$E_l^1 = -F_{lm}F^{1m},$$

and on using (6.1) and (7.5) this shows that, at the boundary,

$$T_l^1 = E_l^1 = 0. \quad . \quad . \quad . \quad . \quad . \quad . \quad . \quad . \quad (7.6)$$

Now (7.3) is an equation of conservation * for $T_\mu^4$, which therefore is conserved and has fluxes $T_\mu^1$, $T_\mu^2$, and $T_\mu^3$ in the directions of $x^1$, $x^2$, and $x^3$. The normal flux of $T_l^4$ at the electronic surface is therefore $T_l^1$, which vanishes by (7.6). It follows that the surface density $[T_l^4]$ of $T_l^4$ in the surface is conserved, and that its (tangential) fluxes in the directions of $x^2$ and $x^3$ are given by $[T_l^2]$ and $[T_l^3]$. We therefore infer that, analogously † to (7.3),

$$[T_l^m]_{\underline{m}} = 0. \quad . \quad . \quad . \quad . \quad . \quad . \quad . \quad . \quad (7.7)$$

The remaining components $[T_1^\nu]$ (or $[T_\mu^1]$) of $[T_\mu^\nu]$ give the surface densities of the stresses $p_{11}$, $p_{12}$, $p_{13}$, and of momentum normal to the surface. It is physically obvious, however, that these quantities can only be finite and cannot have surface densities. Thus the quantities $[T_1^\nu]$ must be identically equal to zero.

8. We now seek for an expression for $[T_l^m]$, satisfying (7.7) identically, in terms of variables which refer exclusively to the boundary. Our only such variables are $\kappa_l$ and $g_{lm}$. We should expect $\kappa_l$ to appear only in its curl $F_{lm}$, but by (6.1) $F_{lm}$ vanishes. Apparently, therefore, $\kappa_l$ will not appear so we have left only the $g_{lm}$'s.

It is convenient to start with $[T_{lm}]$ rather than $[T_l^m]$. There are six $[T_{lm}]$'s and six $g_{lm}$'s, but the $g_{lm}$'s have already satisfied (5.1). If $[T_{lm}]$ is to be unrestricted, its expression must therefore contain one more variable, $\xi$, say, in addition to the $g_{lm}$'s. Evidently $\xi$ will be a boundary invariant.

We assume that this expression is linear and homogeneous in $\xi$ and its derivatives, of the second degree, and linear in all second derivatives. Also, like $[T_{lm}]$ itself, it must be a symmetrical boundary tensor. The most general assumption satisfying these conditions is given by

$$[T_{lm}] = AG\xi_{lm} + B\xi g_{lm} + \frac{C}{2}(\xi_{\underline{l}\underline{m}} + \xi_{\underline{m}\underline{l}}) + D\xi_{\underline{n}}^{n} g_{lm}, \quad . \quad . \quad ; \quad (8.1)$$

in which A, B, C, D are constants to be determined. By (5.1), we need

---

* The physical arguments employed here are not completely rigorous in general relativity theory, but (7.7) may be verified analytically.

† See second footnote concerning equation (4.1).

not include a term in $\xi G g_{lm}$. Now the covariant derivative of an invariant is just its ordinary derivative *, so, similarly to (4.2),

$$\xi_{\underline{l}\underline{m}} - \xi_{\underline{m}\underline{l}} = \frac{\partial \xi_l}{\partial x^m} - \frac{\partial \xi_m}{\partial x^l} = \frac{\partial^2 \xi}{\partial x^m \, \partial x^l} - \frac{\partial^2 \xi}{\partial x^l \, \partial x^m} = 0. \quad . \quad . \quad . \quad (8.2)$$

Substituting from (8.2) in (8.1) and raising the suffix $m$, it becomes

$$[\mathrm{T}_l^m] = \mathrm{A}\xi G_l^m + \mathrm{B}\xi g_l^m + \mathrm{C}\xi_{\underline{l}}{}^{\underline{m}} + \mathrm{D}\xi_{\underline{n}}^{\underline{n}} g_l^m. \quad . \quad . \quad . \quad . \quad (8.3)$$

As the fundamental tensors (here $g_l^m$) behave as constants in covariant differentiation †, (8.3) gives

$$[\mathrm{T}_l^m]_{\underline{m}} = \mathrm{A}\xi_{\underline{m}} G_l^m + \mathrm{A}\xi (G_l^m)_{\underline{m}} + \mathrm{B}\xi_{\underline{m}} g_l^m + \mathrm{C}\xi_{\underline{l}}{}^{\underline{m}}{}_{\underline{m}} + \mathrm{D}(\xi_{\underline{n}}^{\underline{n}})_{\underline{m}} g_l^m. \quad . \quad . \quad (8.4)$$

The third and fifth terms on the right simplify to $\mathrm{B}\xi_{\underline{l}}$ and $\mathrm{D}(\xi_{\underline{m}}^{\underline{m}})_{\underline{l}}$ (changing $n$ into $m$). Further, corresponding to (7.2), we have

$$(G_l^m - \tfrac{1}{2} g_l^m G)_{\underline{m}} = 0.$$

By (5.1), and as $(g_l^m)_{\underline{m}}$ vanishes, this reduces to

$$(G_l^m)_{\underline{m}} = 0,$$

so (8.4) now becomes

$$[\mathrm{T}_l^m]_{\underline{m}} = \mathrm{A}\xi_{\underline{m}} G_l^m + \mathrm{B}\xi_{\underline{l}} + \mathrm{C}\xi_{\underline{l}}{}^{\underline{m}}{}_{\underline{m}} + \mathrm{D}(\xi_{\underline{m}}^{\underline{m}})_{\underline{l}}. \quad . \quad . \quad . \quad . \quad (8.5)$$

For any ordinary vector $v_\mu$, we have ‡

$$v_{\mu\overline{\nu}\overline{\sigma}} - v_{\mu\overline{\sigma}\overline{\nu}} = \mathrm{B}_{\mu\nu\sigma}{}^{\epsilon} v_\epsilon = \mathrm{B}_{\mu\nu\sigma\epsilon} v^\epsilon.$$

Raising the suffix $\mu$, and contracting $\mu$ and $\sigma$, this gives

$$v^{\mu}{}_{\overline{\mu}\overline{\nu}} - v^{\mu}{}_{\overline{\nu}\overline{\mu}} = \mathrm{B}^{\mu}{}_{\nu\mu\epsilon} v^\epsilon.$$

Now §

$$\mathrm{B}_{\mu\nu\sigma\epsilon} = -\mathrm{B}_{\epsilon\nu\sigma\mu},$$

hence, on raising $\mu$ and contracting $\mu$ and $\sigma$, it follows by (2.1) that

$$\mathrm{B}^{\mu}{}_{\nu\mu\epsilon} = -\mathrm{B}_{\epsilon\mu\nu}{}^{\mu} = -\mathrm{G}_{\epsilon\nu},$$

so our above equation becomes

$$v\,{}_{\overline{\nu}\overline{\mu}} - v^{\mu}{}_{\overline{\mu}\overline{\nu}} = -\mathrm{G}_{\epsilon\nu} v^\epsilon = -\mathrm{G}_\nu^\mu v_\mu.$$

The corresponding relation for the boundary vector $\xi_l$ is

$$\xi^{m}{}_{\underline{m}} - (\xi_{\underline{m}}^{m})_{\underline{l}} = -G_l^m \xi_{\underline{m}}.$$

From (8.2), on raising the suffix $m$ and taking the contracted covariant derivative, we have

$$\xi_{\underline{l}}{}^{m}{}_{\underline{m}} = \xi^{m}{}_{\underline{l}\underline{m}},$$

---

* E, p. 65, line 13.

† E, p. 63, lines 10 to 12.

‡ E, p. 72, equation (34.3). (In $\mathrm{B}^{\epsilon}_{\mu\nu\sigma}$, $\epsilon$ is really the fourth suffix.)

§ E, p. 72, lines 19 and 20.

so our previous equation may be written

$$\xi_{\underline{l}}{}^{\underline{m}}{}_{\underline{m}} - (\xi^{\underline{m}}_{\underline{m}})_{\underline{l}} = -G_l^m \xi_{\underline{m}}. \quad . \quad . \quad . \quad . \quad . \quad . \quad . \qquad (8.6)$$

We now substitute for $G_l^m \xi_{\underline{m}}$ from (8.6) in (8.5), giving

$$[\mathrm{T}_l^m]_{\underline{m}} = \mathrm{B}\xi_l + (\mathrm{C}-\mathrm{A})\xi_{\underline{l}}{}^{\underline{m}}{}_{\underline{m}} + (\mathrm{D}+\mathrm{A})(\xi^{\underline{m}}_{\underline{m}})_{\underline{l}}.$$

As this expression is to vanish identically, we must have

$$\mathrm{B}=0,\ \mathrm{C}=-\mathrm{D}=\mathrm{A}. \qquad . \quad . \quad . \quad . \quad . \quad . \qquad (8.7)$$

As $\xi$ may be multiplied by any constant factor, we may also put

$$\mathrm{A}=\frac{1}{8\pi}, \quad . \quad . \quad . \quad . \quad . \quad . \quad . \quad . \quad . \qquad (8.8)$$

and, by (8.7) and (8.8), the final form of (8.3) is

$$[\mathrm{T}_l^m] = \frac{1}{8\pi}(\xi G_l^m + \xi_{\underline{l}}{}^{\underline{m}} - \xi^{\underline{n}}_{\underline{n}} g_l^m), \quad . \quad . \quad . \quad . \quad . \qquad (8.9)$$

that is, by (7.1),

$$[\mathrm{G}_l^m - \tfrac{1}{2}g_l^m\mathrm{G}] = \xi^{\underline{n}}_{\underline{n}} g_l^m - \xi_{\underline{l}}{}^{\underline{m}} - \xi G_l^m. \quad . \quad . \quad . \quad . \quad . \quad . \qquad (8.10)$$

The stresses in the surface, given by (8.9), are those which maintain the electron as a stable structure *.

We take our complete set of equations to be given by (4.1), (4.3), (5.1), (6.1), and (8.10).

9. There remains the question as to whether this set of equations is mathematically complete and valid. This may be proved as follows, although considerations of space prevent more than a summary of the proof being given here.

Consider the variation principle

$$\delta\int(\mathrm{G}-4\pi\mathrm{F}^{\mu\nu}\mathrm{F}_{\mu\nu})\sqrt{-g}\,d\tau + \delta\dot{\int}\{\xi(G-G_0)-16\pi\sigma^l(\kappa_l-\mathrm{V}_{\underline{l}})\}\sqrt{g'}\,d\tau'=0. \quad (9.1)$$

The first integral is taken throughout all space-time, including the boundary in the sense of (3.6), and the second integral over the whole boundary. The first integral alone would give Eddington's variation principle †. $\sigma^l$ is a boundary vector and V a boundary invariant. It is evident that each integral is an invariant, hence the differential equations given by (9.1) will be a mathematically complete and valid set of equations in tensor form.

On carrying out the variation, using the ideas of § 3, we find after much

---

* Equation (5.1) may be deduced (apart from the value of $G_0$) from (7.7) and (8.9).

† E, p. 188, lines 2 to 5 up.

simplification that the resulting equations are given by (4.1), (4.3), (5.1), (8.10), and the equations

$$\kappa_l = V_l = \frac{\partial V}{\partial x^l} \quad . \quad . \quad . \quad . \quad . \quad . \quad . \quad . \quad . \qquad (9.2)$$

and

$$[(F^{l\nu})_{\bar{\nu}}] = \sigma^l. \quad . \quad . \quad . \quad . \quad . \quad . \quad . \quad . \quad . \qquad (9.3)$$

By (4.2), (6.1) is deducible from (9.2). Conversely, if (6.1) is true, we can find V so that (9.2) is true. We may therefore replace (9.2) by (6.1), and omit V from our set of variables. Moreover, (9.3) is the only equation involving $\sigma^l$. It therefore merely serves to give the value of $\sigma^l$, and so may be omitted, together with the variables $\sigma^l$. It may be noticed, however, that by (9.3) $\sigma^l$ gives the surface density of electric charge and current * in the electronic surface.

We conclude that our set of equations is equivalent to that given by (9.1), which establishes their complete validity.

By (4.1), the electric charge density $(F^{4\nu})_{\bar{\nu}}$ and its fluxes $(F^{1\nu})_{\bar{\nu}}$, $(F^{2\nu})_{\bar{\nu}}$, and $(F^{3\nu})_{\bar{\nu}}$ vanish throughout free space-time. It follows that the only charge present is that given by the surface density $\sigma^4$ on the electronic surface, and that its amount is a constant, $-4\pi\epsilon$, say. That is †,

$$\int \sigma^4 \sqrt{g'}\, dx^2\, dx^3 = -4\pi\epsilon, \quad . \quad . \quad . \quad . \quad . \quad . \quad . \qquad (9.4)$$

the integral being over the whole surface.

Our present account of the theory for the case of one electron is now complete. To extend it to the case of several electrons, we choose coordinates so that (1.2) and (1.3) apply to each boundary, and apply (5.1), (6.1), (8.10), and (9.4) to each boundary. We modify (9.1) to agree with this by including a boundary integral, of similar type to that in (9.1), for each electron.

10. We now investigate the nature of the static electron, by finding the form of a static, spherically symmetrical solution of our equations.

The most general such solution of (4.1) and (4.3) is given ‡, apart from coordinate transformations and irrelevant transformations of $\kappa_\mu$, by

$$ds^2 = -\gamma^{-1}\, dr^2 - r^2\, d\theta^2 - r^2 \sin^2\theta\, d\phi^2 + \gamma\, dt^2, \quad . \quad . \quad . \quad . \quad . \qquad (10.1)$$

with

$$\gamma = 1 - \frac{2m}{r} + \frac{4\pi\epsilon^2}{r^2}, \quad . \quad . \quad . \quad . \quad . \quad . \quad . \quad . \quad . \quad . \quad . \quad . \quad . \qquad (10.2)$$

and

$$\kappa_\mu = \left(0,\ 0,\ 0,\ -\frac{\epsilon}{r}\right)\ (x^1 = r,\ x^2 = \theta,\ x^3 = \phi,\ x^4 = t), \quad . \quad . \qquad (10.3)$$

---

* E, p. 173, equation (73.74).

† We call the charge $-4\pi\epsilon$, not $4\pi\epsilon$ as in E, p. 186, lines 7 and 8, where there appears to be an error in sign.

‡ E, § 78, pp. 185 and 186. See also previous footnote.

$m$ and $\epsilon$ being constants. These are identified as being respectively the electronic gravitational mass and $-\frac{1}{4\pi}$ times the electronic charge[*], the units being such that the gravitational constant, and the velocity of light for large values of $r$, are both unity. Thus $\epsilon$ in (10.2) and (10.3) agrees with (9.4).

Now, as $x^1$ is $r$, it follows from (1.2) that this solution will hold only for values of $r$ greater than the value $(x^1)_0$, or, as we shall now call it, $r_0$, which gives the electronic boundary, and with this provision the conventions of § 1 are easily seen to be satisfied. At $r=r_0$ there will be a discontinuity, and inside the electron $(r<r_0)$ the solution will be similar in form to that above, as it has to satisfy (4.1) and (4.3) as before, but the constants corresponding to $m$ and $\epsilon$ may now have different values. As there must be no singularity at the origin, it is evident that we must now replace $m$ and $\epsilon$ in (10.1), (10.2), and (10.3), by zero, giving, for the interior of the electron,

$$ds^2=-dr^2-r^2\,d\theta^2-r^2\sin^2\theta\,d\phi^2+dt^2, \quad \kappa_\mu=\left(0,\ 0,\ 0,\ -\frac{\epsilon}{r_0}\right). \qquad (10.4)$$

(We have added the constant $-\frac{\epsilon}{r_0}$ to the value of $\kappa_4$ in order to make $\kappa_\mu$ continuous at the boundary.) Thus inside the static electron space-time is flat and the electromagnetic field, given by (4.2), vanishes.

The condition of continuity of the $g_{\mu\nu}$'s at the boundary leads, by (10.1) and (10.4), to the equation

$$\gamma=1(r=r_0),$$

that is, by (10.2),

$$r_0=\frac{2\pi\epsilon^2}{m}, \quad . \quad . \quad . \quad . \quad . \quad . \quad . \quad . \quad . \qquad (10.5)$$

which is the radius usually ascribed to the spherical electron.

Our solution is now completely determined, and it may be verified that it satisfies also (6.1) and (8.10) (for which a calculation shows that $\xi=m$). As for (5.1), $G$ is now the Gaussian curvature of a sphere[†] of radius $r_0$, and so[‡] has the value $\frac{2}{r_0^2}$. Thus, by (10.5), (5.1) is satisfied if we put

$$G_0=\frac{2}{r_0^2}=\frac{m^2}{2\pi^2\epsilon^4}. \quad . \quad . \quad . \quad . \quad . \quad . \quad . \quad . \qquad (10.6)$$

---

[*] E, § 78, pp. 185 and 186. See also second previous footnote.

[†] This statement is exact, because the circumference is $2\pi r_0$.

[‡] E, p. 151, footnote.

Our equations are now all satisfied, and the exterior electromagnetic and gravitational fields of the electron remain unaltered by the system of stresses and electromagnetic properties which we have imposed upon it. Also our model for the electron involves two constants, $m$ and $\epsilon$, and these are fixed in value by (10.6) and the fact that the charge $-4\pi\epsilon$ is conserved and so may be given its known value.

There remains the problem of the motion of our electron, in an external electromagnetic field. This motion, however, evidently will depend only upon the general nature of the singularity represented by the electron in connexion with (4.1) and (4.3), and not upon the detailed structure of the electron which we have formulated*. The writer believes that the derivation of the equations of motion for the point electron from this basis has not yet been satisfactorily carried out. Nevertheless, in view of what has been said, this is not a matter to be considered here.

In conclusion, I wish to thank Professor H. T. H. Piaggio, of Nottingham, for many helpful suggestions in connexion with this paper.

Swansea.
2nd December, 1938.

---

* Equation (6.1) can be satisfied, for any given motion of the electron as a whole in any given external electromagnetic field, by giving the charge density on the surface a suitable distribution and motion.

# XXXVII. *A Note on the Solution of some Partial Differential Equations in the Finite Domain.*

By W. T. Howell *.

[Received November 28, 1938.]

In a large number of physical problems linear partial differential equations with constant coefficients are encountered. When a solution can be found to satisfy certain boundary conditions appropriate to the problem it is unique and complete.

In certain cases, however, the boundary is at infinity and we have to solve the differential equation subject to the initial conditions only. The solution obtained is not a complete solution, but it may often be adapted *mutatis mutandis* to fulfil the conditions imposed by finite boundaries. In other cases the construction of solutions to fit boundary conditions usually necessitates a different procedure.

Herein it is proposed to solve certain equations using the Laplace transform in combination with the operational method of Boole † and his contemporaries. The well-known problem of a vibrating string was solved by Jeffreys ‡ in a somewhat similar way. He used Heaviside's operational method where we shall use the Laplace transform.

The latter is more rigorous than the Heaviside procedure, and in view of the large number of transforms (operational forms) obtained by various writers in recent years it is simpler to apply. In the examples which follow some of the operational formulæ will be used in the solution of integral equations of the Laplace type.

Probably the best known partial differential equation which has been solved subject to given initial conditions is the wave-equation in one dimension, viz. :—

$$\frac{\partial^2 y}{\partial t^2}-c^2\frac{\partial^2 y}{\partial x^2}=0.$$

D'Alembert's solution such that $y=f(x)$, $\dfrac{\partial y}{\partial t}=\mathrm{F}(x)$ at $t=0$ is

$$y=\tfrac{1}{2}\{f(x+ct)+f(x-ct)\}+\frac{1}{2c}\int_{x-ct}^{x+ct}\mathrm{F}(x)dx.$$

---

* Communicated by the Author.

† Boole, 'Treatise on Differential Equations' (4th Edition, 1877). Davis, 'Theory of Linear Operators' (1937).

‡ Jeffreys, 'Operational Methods in Mathematical Physics' (1927).

### 1. *The Equation of Vertical Propagation of Wave-Motion in the Atmosphere.*

In the study of the vertical propagation of waves in the atmosphere we require to solve the differential equation

$$\frac{\partial^2 w}{\partial t^2}-c^2\frac{\partial^2 w}{\partial z^2}+a^2c^2w=0, \quad . \quad . \quad . \quad . \quad . \quad . \quad . \quad . \qquad (1)$$

subject to the initial conditions at $t=0$

$$w=f(z), \quad \frac{\partial w}{\partial t}=\mathrm{F}(z).$$

Multiply (1) by $pe^{-pt}$ and integrate from $t=0$ to $\infty$ *, thereby obtaining

$$p\int_0^\infty e^{-pt}\frac{\partial^2 w}{\partial t^2}\,dt-c^2p\int_0^\infty e^{-pt}\frac{\partial^2 w}{\partial z^2}\,dt+a^2c^2p\int_0^\infty e^{-pt}w\,dt=0. \quad . \quad . \qquad (2)$$

Taking the first member of (2) alone, we have

$$p\int_0^\infty e^{-pt}\,d\dot{w}=[p\dot{w}e^{-pt}]_0^\infty+p^2\int_0^\infty e^{-pt}\,dw \quad . \quad . \quad . \quad . \quad . \quad . \quad . \qquad (3)$$

$$=-p\mathrm{F}(z)+p^2[we^{-pt}]_0^\infty+p^3\int_0^\infty e^{-pt}w\,dt, \quad . \quad . \quad . \qquad (4)$$

$$=-p\mathrm{F}(z)-p^2f(z)+p^3\int_0^\infty e^{-pt}w\,dt, \quad . \quad . \quad . \quad . \quad . \qquad (5)$$

provided $\mathrm{F}(z)e^{-pt}\to 0$, $f(z)e^{-pt}\to 0$ when $t\to\infty$. Substituting from (5) into (2), we get

$$p\int_0^\infty e^{-pt}\left\{(p^2+a^2c^2)w-c^2\frac{\partial^2 w}{\partial z^2}\right\}dt=p\mathrm{F}(z)+p^2f(z). \quad . \quad . \qquad (6)$$

If $w$ is such that the order of differentiation and integration of the third term of the integral can be altered, then writing $\mathrm{D}=\frac{\partial}{\partial z}$ we obtain

$$\{p^2-c^2(\mathrm{D}^2-a^2)\}p\int_0^\infty e^{-pt}w\,dt=p\mathrm{F}(z)+p^2f(z). \quad . \quad . \quad . \qquad (7)$$

Thus if $b=c\sqrt{\mathrm{D}^2-a^2}$, (7) leads to the integral equation

$$p\int_0^\infty e^{-pt}w\,dt=\frac{p\mathrm{F}(z)+p^2f(z)}{(p-b)(p+b)}, \quad . \quad . \quad . \quad . \quad . \quad . \quad . \quad . \quad . \quad . \quad . \qquad (8)$$

$$=\frac{1}{2b}\left[\frac{p-b}{p}-\frac{p+b}{p}\right]\mathrm{F}(z)+\frac{1}{2}\left[\frac{p}{p-b}+\frac{p}{p+b}\right]f(z), \quad . \qquad (9)$$

---

* This procedure was first used by Bateman (Proc. Camb. Phil. Soc. xv. p. 423 (1910), and more recently by Doetsch (*Jahresberichte d. Deutsch. Math. Vereinigung*, xxxiii. (1925)), and van der Pol (Phil. Mag. vii. p. 1153 (1929)).

The solution of (9) is *

$$w=\frac{1}{2}[e^{bt}+e^{-bt}]f(z)+\frac{1}{2b}[e^{bt}-e^{-bt}]\mathrm{F}(z). \quad . \quad . \quad . \quad . \quad (10)$$

Using the formulæ †

$$\frac{e^{\pm ct\sqrt{\mathrm{D}^2-a^2}}}{\sqrt{\mathrm{D}^2-a^2}}=\int_{\mp ct}^{\infty} e^{-\mathrm{D}s}\,\mathrm{I}_0(a\sqrt{s^2-c^2t^2})\,ds, \quad . \quad . \quad . \quad . \quad (11)$$

$$e^{\pm ct\sqrt{\mathrm{D}^2-a^2}}=e^{\pm c\mathrm{D}t}\mp a\,ct\int_{\mp ct}^{\infty} e^{-\mathrm{D}s}\,\frac{\mathrm{I}_1(a\sqrt{s^2-c^2t^2})}{\sqrt{s^2-c^2t^2}}, \quad . \quad . \quad . \quad . \quad (12)$$

in connexion with (10) leads to

$$w=\frac{1}{2}\left[e^{c\mathrm{D}t}+e^{-c\mathrm{D}t}-a\,ct\int_{-ct}^{ct} e^{-\mathrm{D}s}f(z)\,\frac{\mathrm{I}_1(av)}{v}\,ds+\frac{1}{c}\int_{-ct}^{ct} e^{-\mathrm{D}s}\mathrm{F}(z)\mathrm{I}_0(av)\,ds\right], \quad (13)$$

where $v=\sqrt{s^2-c^2t^2}$.

Operating upon $f(z)$ and $\mathrm{F}(z)$ as indicated in (13), we obtain

$$w=\frac{1}{2}\left\{f(z+ct)+f(z-ct)-a\,ct\int_{-ct}^{ct}\frac{\mathrm{I}_1(av)}{z}f(z-s)\,ds\right.$$
$$\left.+\frac{1}{c}\int_{-ct}^{ct}\mathrm{I}_0(av)\mathrm{F}(z-s)\,ds\right\}. \quad . \quad . \quad (14)$$

## 2. *The Equation of Heat Conduction.*

Consider a uniform rod of infinite length with its sides thermally insulated and initially at a temperature $\mathrm{V}=f(x)$. The equation of heat conduction is

$$\frac{\partial \mathrm{V}}{\partial t}=h^2\,\frac{\partial^2 \mathrm{V}}{\partial x^2},$$

where $h$ is called the thermometric conductivity.

Proceeding as in § 1 we obtain the integral equation

$$p\int_0^{\infty} e^{-pt}\,\mathrm{V}\,dt=\frac{pf(x)}{p-h^2\mathrm{D}^2},$$

or

$$p\int_0^{\infty} e^{-pt}\,\mathrm{V}\,dt=\frac{1}{2}\left[\frac{p^{\frac{1}{2}}}{p^{\frac{1}{2}}-h\mathrm{D}}+\frac{p^{\frac{1}{2}}}{p^{\frac{1}{2}}+h\mathrm{D}}\right]f(x). \quad . \quad . \quad . \quad (1)$$

To solve (1) for $\mathrm{V}(t)$, we use the theorem ‡

if
$$\phi(p)=p\int_0^{\infty} e^{-ps}\,\mathrm{V}(s)\,ds, \quad . \quad . \quad . \quad . \quad . \quad . \quad . \quad . \quad (2)$$

---

* The solution of many integral equations of this type can be found immediately from a list of operational forms.

† McLachlan, Math. Gazette, xxii. p. 41 (1938).

‡ van der Pol and Niessen, Phil. Mag. xiii. p. 537 (1932).

the solution of the equation

$$\phi(p^{\frac{1}{2}})=p\int_0^\infty e^{-pt}\mathrm{V}(t)dt \quad . \quad . \quad . \quad . \quad . \quad . \quad . \quad . \qquad (3)$$

is

$$\mathrm{V}(t)=\frac{1}{\sqrt{\pi t}}\int_0^\infty e^{-\frac{s^2}{4t}}\mathrm{V}(s)\,ds. \quad . \quad . \quad . \quad . \quad . \quad . \qquad (4)$$

Thus by (1) and (2)

$$\mathrm{V}(s)=\tfrac{1}{2}[e^{hs\mathrm{D}}+e^{-hs\mathrm{D}}]f(x), \quad . \quad . \quad . \quad . \quad . \quad . \quad . \qquad (5)$$

so by (4)

$$\mathrm{V}(t)=\frac{1}{2\sqrt{\pi t}}\int_0^\infty e^{-\frac{s^2}{4t}}[e^{hs\mathrm{D}}+e^{-hs\mathrm{D}}]f(x)\,ds, \quad . \quad . \quad . \quad . \qquad (6)$$

$$=\frac{1}{2\sqrt{\pi t}}\int_0^\infty e^{-\frac{s^2}{4t}}[f(x+hs)+f(x-hs)]ds. \quad . \quad . \quad . \qquad (7)$$

### 3. *The Vibrations of an Infinite Elastic Bar.*

In the study of the transverse vibrations of an elastic bar of uniform section we have the differential equation

$$\frac{\partial^2 w}{\partial t^2}-c^2\frac{\partial^4 w}{\partial x^4}=0.$$

Suppose that at

$$t=0, \quad w=f(x), \quad \frac{\partial w}{\partial t}=\mathrm{F}(x),$$

then, proceeding as shown in §1, we obtain the integral equation

$$p\int_0^\infty e^{-pt}w\,dt=\frac{p^2f(x)+p\mathrm{F}(x)}{p^2-c^2\mathrm{D}^4}$$

$$=\frac{1}{2}\left\{\frac{p^{\frac{1}{2}}}{p^{\frac{1}{2}}-c^{\frac{1}{2}}\mathrm{D}}+\frac{p^{\frac{1}{2}}}{p^{\frac{1}{2}}+c^{\frac{1}{2}}\mathrm{D}}+\frac{p^{\frac{1}{2}}}{p^{\frac{1}{2}}-\iota c^{\frac{1}{2}}\mathrm{D}}+\frac{p^{\frac{1}{2}}}{p^{\frac{1}{2}}+\iota c^{\frac{1}{2}}\mathrm{D}}\right\}f(x)$$

$$+\frac{1}{2c}\left\{\left(\frac{p^{\frac{1}{2}}}{p^{\frac{1}{2}}-c^{\frac{1}{2}}\mathrm{D}}+\frac{p^{\frac{1}{2}}}{p^{\frac{1}{2}}+c^{\frac{1}{2}}\mathrm{D}}\right)\right.$$

$$\left.-\left(\frac{p^{\frac{1}{2}}}{p^{\frac{1}{2}}-\iota c^{\frac{1}{2}}\mathrm{D}}+\frac{p^{\frac{1}{2}}}{p^{\frac{1}{2}}+\iota c^{\frac{1}{2}}\mathrm{D}}\right)\right\}\frac{\mathrm{F}(x)}{\mathrm{D}^2}. \quad . \quad . \quad . \quad . \quad . \qquad (1)$$

Following the rule that operations involving negative powers of D must be carried out before those involving positive powers *, and using (1) and (2) of §2, we have at once

$$w=\frac{1}{2\sqrt{\pi t}}\int_{-\infty}^{\infty} e^{-\frac{s^2}{4t}}\{f(x+s\sqrt{c})+f(x+\iota s\sqrt{c})\}ds$$

$$+\frac{1}{2c\sqrt{\pi t}}\int_{-\infty}^{\infty} e^{-\frac{s^2}{4t}}\left\{\left[\int_0^x dx\int_0^x \mathrm{F}(x)\,dx\right]_{x=x+s\sqrt{c}}\right.$$

$$\left.-\left[\int_0^x dx\int_0^x \mathrm{F}(x)\,dx\right]_{x=x+\iota s\sqrt{c}}\right\}ds \quad . \quad . \quad . \quad . \quad . \quad . \quad 2)$$

4. The solution of

$$\left(\frac{\partial^n}{\partial x^n}\frac{\partial^2}{\partial t^2}-\sigma^2\frac{\partial^n}{\partial x^n}-\sigma^2\frac{\partial^{n-2}}{\partial x^{n-2}}\right)w=0.$$

Suppose, as before,

$$w=f(x), \quad \frac{\partial w}{\partial t}=\mathrm{F}(x)$$

when $t=0$. Proceeding as in §1, we obtain the integral equation

$$p\int_0^{\infty} e^{-pt}\,w\,dt=\frac{p^2 f(x)+p\mathrm{F}(x)}{\mathrm{D}^n p^2-\sigma^2\mathrm{D}^n-\sigma^2\mathrm{D}^{n-2}}$$

$$=\frac{1}{2}\left\{\frac{p}{p-\frac{\sigma\sqrt{\mathrm{D}^2+1}}{\mathrm{D}}}+\frac{p}{p+\frac{\sigma\sqrt{\mathrm{D}^2+1}}{\mathrm{D}}}\right\}\frac{f(x)}{\mathrm{D}^n}$$

$$+\frac{1}{2\sigma}\left\{\frac{p}{p-\frac{\sigma\sqrt{\mathrm{D}^2+1}}{\mathrm{D}}}-\frac{p}{p+\frac{\sigma\sqrt{\mathrm{D}^2+1}}{\mathrm{D}}}\right\}\frac{\mathrm{F}(x)}{\mathrm{D}^{n-1}\sqrt{\mathrm{D}^2+1}} \quad . \quad (1)$$

The solution of (1) is

$$w=\frac{1}{2}\left\{e^{\frac{t\sigma\sqrt{\mathrm{D}^2+1}}{\mathrm{D}}}+e^{-\frac{t\sigma\sqrt{\mathrm{D}^2+1}}{\mathrm{D}}}\right\}\frac{f(x)}{\mathrm{D}^n}$$

$$+\frac{1}{2\sigma}\left\{e^{\frac{\sigma t\sqrt{\mathrm{D}^2+1}}{\mathrm{D}}}-e^{-\frac{\sigma t\sqrt{\mathrm{D}^2+1}}{\mathrm{D}}}\right\}\frac{\mathrm{F}(x)}{\mathrm{D}^{n-1}\sqrt{\mathrm{D}^2+1}} \quad . \quad . \quad (2)$$

If we now make use of the identities

$$\frac{1}{\mathrm{D}^n}e^{-\frac{\sigma\sqrt{\mathrm{D}^2+1}}{\mathrm{D}}}=\int_0^{\infty} e^{-\mathrm{D}\xi}\left[\left(\frac{\xi}{\sigma}\right)^{\frac{n}{2}}\mathrm{J}_n(2\sqrt{\xi\sigma})\right.$$

$$\left.-\sigma\int_{\sigma}^{\infty}\left(\frac{\xi}{s}\right)^{\frac{n}{2}}\frac{\mathrm{J}_n(2\sqrt{\xi s})\mathrm{J}_1(\sqrt{s^2-\sigma^2})\,ds}{\sqrt{s^2-\sigma^2}}\right]d\xi, \quad . \quad . \quad (3)$$

---

* Jeffreys, *loc. cit.*

$$\frac{e^{-\frac{\sigma\sqrt{\mathrm{D}^2+1}}{\mathrm{D}}}}{\mathrm{D}^{n-1}\sqrt{\mathrm{D}^2+1}}=-\frac{\partial}{\partial\sigma}\int_0^\infty e^{-\mathrm{D}\xi}\Big[\Big(\frac{\xi}{\sigma}\Big)^{\frac{n}{2}}\mathrm{J}_n(2\sqrt{\xi\sigma})$$

$$-\sigma\int_\sigma^\infty\Big(\frac{\xi}{\sigma}\Big)^{\frac{n}{2}}\frac{\mathrm{J}_n(2\sqrt{\xi s})\mathrm{J}_1(\sqrt{s^2-\sigma^2})\,ds}{\sqrt{s^2-\sigma^2}}\Big]d\xi. \quad . \quad . \quad (4)$$

We find on operating on $f(x)$ and $\mathrm{F}(x)$

$$w=\frac{1}{2}\int_0^\infty f(x-\xi)\Big(\frac{\xi}{\sigma t}\Big)^{\frac{n}{2}}\{\mathrm{I}_n(2\sqrt{\xi\sigma t})+\mathrm{J}_n(2\sqrt{\xi\sigma t})\}\,d\xi$$

$$+\frac{\sigma t}{2}\int_0^\infty f(x-\xi)\Big\{\int_{\sigma t}^{-\sigma t}\Big(\frac{\xi}{s}\Big)^{\frac{n}{2}}\frac{\mathrm{J}_n(2\sqrt{\xi s})\mathrm{J}_1(\sqrt{s^2-\sigma^2t^2})\,ds}{\sqrt{s^2-\sigma^2t^2}}\Big\}\,d\xi$$

$$+\frac{\partial}{2\sigma^2\partial t}\int_0^\infty \mathrm{F}(x-\xi)\Big(\frac{\xi}{\sigma t}\Big)^{\frac{n}{2}}\{\mathrm{I}_n(2\sqrt{\xi\sigma t})+\mathrm{J}_n(2\sqrt{\xi\sigma t})\}\,d\xi$$

$$+\frac{t\partial}{2\sigma\partial t}\int_0^\infty \mathrm{F}(x-\xi)\Big\{\int_{\sigma t}^{-\sigma t}\Big(\frac{\xi}{s}\Big)^{\frac{n}{2}}\frac{\mathrm{J}_n(2\sqrt{\xi s})\mathrm{J}_1(\sqrt{s^2-\sigma^2t^2})\,ds}{\sqrt{s^2-\sigma^2t^2}}\Big\}\,d\xi. \quad (5)$$

5. The solution of

$$\Big(\frac{\partial^n}{\partial x^n}\frac{\partial^2}{\partial t^2}-\sigma^2\frac{\partial^{n-1}}{\partial x^{n-1}}\Big)w=0.$$

As a further example consider the differential equation

$$\mathrm{D}^{n-1}(\mathrm{D}p^2-\sigma^2)w=0$$

when

$$w=f(x),\quad \frac{\partial w}{\partial t}=\mathrm{F}(x),$$

when $t=0$.

Proceeding as before, we have to solve the following integral equation for $w$:

$$p\int_0^\infty e^{-pt}w\,dt=\frac{p^2f(x)+p\mathrm{F}(x)}{\mathrm{D}^n\Big(p^2-\frac{\sigma^2}{\mathrm{D}}\Big)}$$

$$=\frac{1}{2}\left\{\frac{p}{p-\frac{\sigma}{\mathrm{D}^{\frac{1}{2}}}}+\frac{p}{p+\frac{\sigma}{\mathrm{D}^{\frac{1}{2}}}}\right\}\frac{f(x)}{\mathrm{D}^n}$$

$$+\frac{1}{2\sigma}\left\{\frac{p}{p-\frac{\sigma}{\mathrm{D}^{\frac{1}{2}}}}-\frac{p}{p+\frac{\sigma}{\mathrm{D}^{\frac{1}{2}}}}\right\}\frac{\mathrm{F}(x)}{\mathrm{D}^{n-\frac{1}{2}}}, \quad . \quad . \quad . \quad (1)$$

so that

$$w=\left\{e^{\frac{\sigma}{\sqrt{\mathrm{D}}}}+e^{-\frac{\sigma}{\sqrt{\mathrm{D}}}}\right\}\frac{f(x)}{2\mathrm{D}^{n}}+\left\{e^{\frac{\sigma}{\sqrt{\mathrm{D}}}}-e^{-\frac{\sigma}{\sqrt{\mathrm{D}}}}\right\}\frac{\mathrm{F}(x)}{2\sigma\mathrm{D}^{n-\frac{1}{2}}}.$$

Now since*

$$\frac{e^{\frac{\sigma}{\sqrt{\mathrm{D}}}}}{\mathrm{D}^{\frac{\nu}{2}}}=\frac{1}{\sigma^{\frac{\nu}{2}}}\frac{1}{\sqrt{\pi x}}\int_{0}^{\infty}e^{-\frac{s^{2}}{4x}}\mathrm{I}_{\nu}(2\sqrt{\sigma s})s^{\frac{\nu}{2}}\,ds,$$

it follows that

$$\frac{e^{\frac{\sigma}{\sqrt{\mathrm{D}}}}}{\mathrm{D}^{\frac{\nu}{2}+1}}=\int_{0}^{\infty}e^{-\mathrm{D}\xi}\left\{\frac{1}{\sigma^{\frac{\nu}{2}}}\frac{1}{\sqrt{\pi\xi}}\int_{0}^{\infty}e^{-\frac{\eta^{2}}{4\xi}}\mathrm{I}_{\nu}(2\sqrt{\sigma\eta})\,\eta^{\frac{\nu}{2}}\,d\eta\right\}d\xi.$$

Hence

$$w=\frac{1}{2(\sigma t)^{n-1}}\int_{0}^{\infty}\int_{0}^{\infty}\frac{e^{-\frac{\eta^{2}}{4\xi}}}{\sqrt{\pi\xi}}f(x-\xi)\{\mathrm{I}_{2n-2}(2\sqrt{\sigma t\eta})+\mathrm{J}_{2n-2}(2\sqrt{\sigma t\eta})\}\eta^{n-1}\,d\eta\,d\xi$$

$$+\frac{1}{2\sigma(\sigma t)^{n-\frac{3}{2}}}\int_{0}^{\infty}\int_{0}^{\infty}\frac{e^{-\frac{\eta^{2}}{4\xi}}}{\sqrt{\pi\xi}}\mathrm{F}(x-\xi)\{\mathrm{I}_{2n-3}(2\sqrt{\sigma t\eta})+\mathrm{J}_{2n-3}(2\sqrt{\sigma t\eta})\}\eta^{n-\frac{3}{2}}\,d\eta\,d\xi.$$

## *Conclusion.*

It will have been seen that the operators acting on the functions representing the initial conditions are of the form $\phi(p)/\Phi(p)$, where $\phi(p)$ is usually some positive power of $p$ and $\Phi(p)$ is a polynomial in $p$. When the partial fraction rule is used we have

$$\frac{\phi(p)}{\Phi(p)}\cdot f(x)=\left\{\frac{\phi(0)}{\Phi(0)}+\Sigma_{\alpha}\frac{\phi(\alpha)}{\alpha\Phi'(\alpha)}e^{\alpha t}\right\}f(x),$$

where the $\alpha$'s are the roots, assumed distinct, of $\Phi(p)=0$. The $\alpha$'s are, of course, usually algebraic functions of D, and provided suitable integral (or otherwise) representations of the terms $e^{\alpha t}\phi(\alpha)/\alpha\Phi'(\alpha)$ exist and can be found the solution follows as exemplified in the foregoing.

## *Acknowledgments.*

I am grateful to Dr. N. W. McLachlan for generous advice in connexion with the presentation of this note, and to the Admiralty for permitting its publication.

---

* K. F. Niessen, Phil. Mag. xx. p. 977 (1935). The above modification of Niessen's result may be readily proved.

# XXXVIII. *Viscosity of Liquids at High Hydrostatic Pressures.*

By R. B. Dow, A.M., Ph.D., Department of Physics,
The Pennsylvania State College, State College, Pa.*

[Received October 20, 1938.]

## Introduction.

Viscosity is the one property of liquids that varies greatly with pressure, its increase for a rather viscous liquid like one of the chlorinated diphenyls(1) amounting to as much as 15-fold for an increase of pressure of 250 kg./cm.$^2$ at constant temperature of 30° C. Increase of temperature is effective similarly in reducing viscosity at high pressure; for example, at a temperature of 75° C. the percentage increase of the coefficient of viscosity for the same diphenyl amounts to only 29 for the same increase of pressure. Changes of this order of magnitude are measurable usually with a high degree of accuracy. Over a pressure range of several thousand atmospheres, however, difficulty of measurement arises through the necessity of constructing pressure-chambers of such size and design that they can withstand the extreme stresses brought about by change of pressure. If such chambers are to be of such mass that they can be manipulated conveniently under the conditions encountered in the laboratory the internal volume available for measuring devices becomes very limited. The available volume may be limited to approximately 25 cm.$^3$ if pressures of several thousand atmospheres are to be generated. High pressure viscometry, therefore, must be adapted to measurement in small volume, a restriction which necessitates considerable modification of standard instruments.

Measurement of viscosity of liquids at high pressure has not become commonplace even though the initial investigation of Röntgen was made in 1884. The early work, chiefly with pure liquids, is discussed by Hatschek(2). The lack of systematic study in this interesting field has been due undoubtedly to the difficulty of obtaining suitable high pressure equipment rather than to any intrinsic difficulty in designing viscometers. More recently the extensive work of Bridgman(3) on pure liquids at pressures higher than had been employed hitherto, the study of Hyde(4), and of Hersey and Shore(5) on lubricating oils have contributed decided advances in technique. Since the establishment of the high pressure laboratory of the department of Physics at The Pennsylvania State College in 1935 the author has been studying intensively the viscosity of pure liquids and of lubricating oils as principal items of a long-range programme of high pressure research.

---

* Communicated by the Authors.

During the past eight years it has been the privilege of the author to use the high pressure viscosity apparatus of Bridgman to study viscosity of liquids, and then to continue these studies with other viscometers upon the establishment of the laboratory at this college. It may therefore be of interest to review briefly the methods of high pressure viscometry, with reference to the various methods that have been used, or are being used at present by other investigators, as well as the recent investigations of the author. Consequently the first part of this communication will consider high pressure viscometry, the second part will contain data for the viscosity of $CS_2$—$CCl_4$ mixtures of liquids over a pressure range of 10,000 kg./cm.$^2$ at two temperatures, and, finally, the last part will summarize some of the theoretical aspects of viscosity of liquids at high pressures.

## I. HIGH PRESSURE VISCOMETRY.

### *Absolute Methods.*

The measurement of absolute viscosity of liquids at atmospheric pressure is made commonly by one of the following methods :—The capillary pipette method of Poiseuille, the falling sphere method of Stokes, or the rotating, concentric cylinder method of Margules and of Couette. Unfortunately no pure liquids have been investigated extensively over a wide range of pressure and temperature by any of these methods. There are several investigators, however, who have measured the absolute viscosity of oils at high pressures by applying these methods or modifications of them.

Hyde(4), using a modified capillary of the Poiseuille type, measured the viscosity of several mineral and fatty oils over a pressure range of several thousand atmospheres. Theoretically this method is capable of high precision, since capillary flow is well understood, the corrections can be determined readily, and further corrections due to pressure do not present serious difficulty. From the practical standpoint the method is not so satisfactory, chiefly on account of the difficulty of mounting capillary tubes in pressure chambers, the difficulty of obtaining continuous readings with good precision, and the questionable behaviour of glass capillaries at very high pressures. The reliability of glass instruments at high pressures has not been investigated extensively. While glass piezometers, properly annealed and seasoned, have been found by

Adams and his colleagues at the Geophysical Laboratory, Washington, D.C., to give precise results over a long period of time, there is evidence that glass chambers and tubes of thick wall are often cracked or deformed irreversibly at pressures exceeding a few thousand atmospheres. Metal capillaries, on the other hand, could be used undoubtedly with much success in this method. Comparison with some of Hyde's values of viscosity may be had through the work of Kleinschmidt(6), who tested several oils in Bridgman's viscometer(3). Using the same sperm-oil, Kleinschmidt's values were considerably greater, his coefficients of viscosity being 9·6 per cent. at 500 kg./cm.$^2$ and 11·5 per cent. at 1000 kg./cm.$^2$ more under the same conditions. For castor-oil, different samples, the relative viscosities of the two investigators are in better agreement. Table I. lists the relative viscosity of castor-oil as measured by various investigators at 40° C. at 1000 atmospheres. This compilation is taken from a summary by Hersey and Hopkins(8).

TABLE I.

Relative Viscosity of Castor-oil by different Observers.
Pressure 1000 atmospheres, temperature 40° C.

| Observer. | Coefficient of viscosity (centipoises). |
|---|---|
| Hersey and Shore .......... | 3·9 |
| Kleinschmidt ............. | 4·4 |
| Hyde ..................... | 4·3 |
| Suge ..................... | 3·9 |

Yoshio Suge(7) developed a modified Stokes' equation to compute the viscosity of several oils over a pressure range of 2000 kg./cm.$^2$ between the temperatures of 0° and 15° C. His apparatus employed the usual falling sphere, the distance of fall between the measuring electrodes being 30 cm. The time of fall was observed by means of a high frequency oscillatory device which operated by change of capacity between sphere and electrodes. Stokes' equation was modified to take account of the wall effect, the ratio of the diameter of the tube to that of the sphere being of the order of 3. The value of the coefficient of viscosity of castor-oil at 1000 atmospheres computed by Suge seems to be in agreement with other observers, within the precision indicated in Table I. It appears doubtful that his apparatus in its present form could be used for less viscous liquids.

More recently Dr. B. W. Thomas(9), in collaboration with Dr. W. R. Ham and the author, has developed a concentric cylinder viscometer for the purpose of testing lubricating oils under various experimental conditions. In order to test the validity of application of the Newtonian concept of a liquid (true viscosity) to ordinary lubricating oils over the experimental range in which they are fluid the apparatus was constructed so that different thicknesses of layer between the two cylinders and different angular velocities could be obtained. Since the immediate need was for a study of absolute viscosity of lubricating oils, the apparatus has not been developed, as yet, for use with less viscous liquids. Thus, while the ultimate precision and accuracy has not been achieved for this type of viscometer, its initial operation under high pressure conditions has been gratifying. The general details of design are shown in fig. 1.

The outer cylinder of the viscometer, of inner radius of 2·340 cm. and length of 10·00 cm., was rotated at a constant speed by a split-phase motor mounted in the bottom of the pressure-cylinder. The inner cylinder, of length 9·6 cm. and radius of 1·880 cm., was mounted on thrust ball-bearings and attached to a central post of a large threaded plug that closed the top of the pressure-chamber. Guard-rings of 1 cm. length were attached at each end, close to the inner cylinder. A helical, coiled spring mounted inside the inner cylinder opposed the displacement of the latter (*a*, fig. 1). The relationship between torque of the spring and angular displacement was obtained experimentally in the apparatus at atmospheric pressure. The angle of displacement was computed from the change of resistance of an alloy slide-wire (*b*, fig 1) that was mounted in such a fashion that connexions were made to the wire through an insulated sliding contact that had an external connexion through the insulated terminal at the top of the plug (e. g., *d*, fig. 1) and through the apparatus itself. The change of resistance was linear with displacement and was measured with a Wheatstone's bridge. The angular velocity of the outer cylinder was computed from the number of revolutions recorded by an external counter during a certain time interval. The counter circuit was operated by a simple type of contact interrupter attached to the shaft of the motor (*c*, fig. 1). Here also external connexions to the counter circuit were obtained by means of insulated single and double terminal plugs in the pressure-chamber (*d*, fig. 1).

The kinematic viscosity in stokes was computed from

$$=\frac{G}{4\pi h\,d\omega}\left(\frac{b^2-a^2}{a^2b^2}\right).$$

G is the torque of the spring, $h$ the length of the inner cylinder, $\omega$ the angular velocity of the rotating cylinder, $d$ density of the liquid, $b$ the inner radius of the outer cylinder, and $a$ the outer radius of the inner cylinder.

Typical results observed for a Pennsylvania extracted oil with this viscometer at various temperatures and pressures, as well as at different motor speeds and with outer cylinders of different radii, are shown in fig. 2.

Fig. 1.

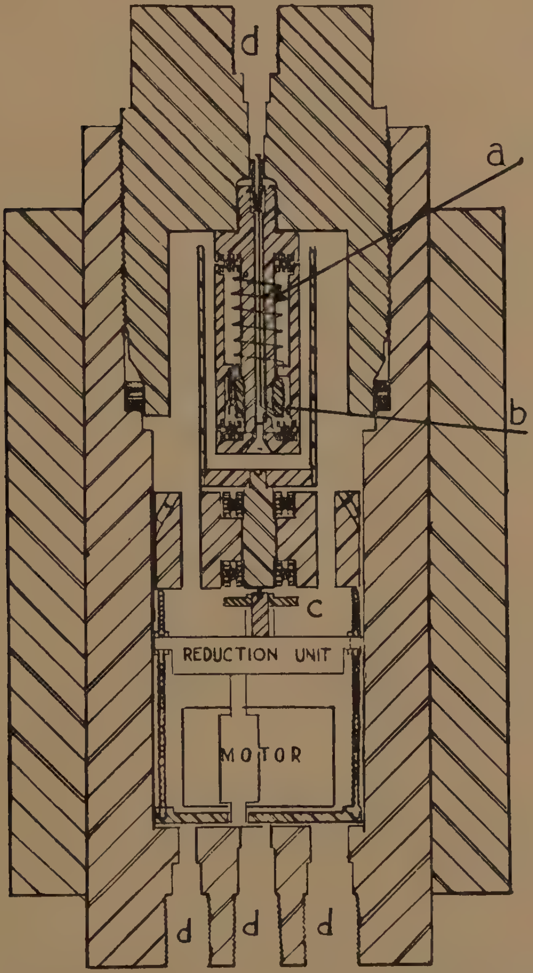

Concentric cylinder viscometer for high pressures.

The motor speeds are represented by M 1 (500 r.p.m.) and M 2 (100 r.p.m.) respectively, and the radii of the outer cylinders by C 1 (2·340 cm.) and C 2 (2·540 cm.) respectively. The results obtained with a relative viscometer (rolling-ball) are plotted in the same figure for the purpose of comparison. The pressure range was limited to about 3000 kg./cm.$^2$, the maximum pressure that could safely be used in the absolute viscometer due to the unusually large volume of the pressure-chamber.

The errors in G, $a$, and $b$ caused by pressure change were not important, since their variation with pressure was known from other investigations. The inaccuracy of $\omega$ could have amounted to several per cent., due to variation of motor speed and eccentricity of rotation of the outer cylinders. These effects were not observed to cause a serious error in the data, however, as can be judged from the precision represented in fig. 2. The most serious error appeared from the heat effect due to the motor. It will be noticed in fig. 1 that the test liquid fills the pressure-chamber, surrounding the reduction unit and motor as well as the cylinders. A thermostated bath outside the pressure-chamber helped materially in setting up a fairly constant transfer of heat from the apparatus to the bath after the former had been operated for a time sufficiently long at constant pressure to approach steady conditions. Yet this is not a satisfactory correction of the error, and future work will attempt to reduce this source of error. The friction of the bearings has not caused measurable error in the results obtained for viscous oils, but for less viscous liquids this effect would be a source of error. The estimated error of the viscometer, used under the conditions described, probably varied from 6 per cent. at the lowest pressures to 3 per cent. at the upper end of the pressure range.

On considering the results that have been obtained with absolute viscometers at high pressures it must be admitted that they, as a whole, were possibly in error by as much as 10 per cent., a figure which indicates that the precision has been correspondingly poor. At its present stage of development absolute viscometry at high pressures does not exceed in accuracy, precision, or convenience the results obtained by relative viscometry to be described in the following.

### *Relative Methods.*

The falling-weight viscometer of Bridgman(3) has proved to be one of the best that has been devised for high pressure measurement. The essentials of the method have been reviewed by Hatschek(2). The apparatus will be discussed further in a later part, Part II., in conjunction with the author's measurement of $CS_2-CCl_4$ mixtures. Bridgman(3) studied a wide range of pure liquids, and Dow(10) continued with mixtures of the same liquids. Kleinschmidt(6), as mentioned previously, studied the viscosity of several oils with this viscometer.

Bridgman checked the validity of his observations at atmospheric pressure by observing the ratios of his values to those obtained by other observers. Moreover, good agreement was obtained for the temperature coefficients at atmospheric pressure. No checks were possible over the pressure range, but there is no reason to suspect error in the method at high pressures.

Fig. 2.

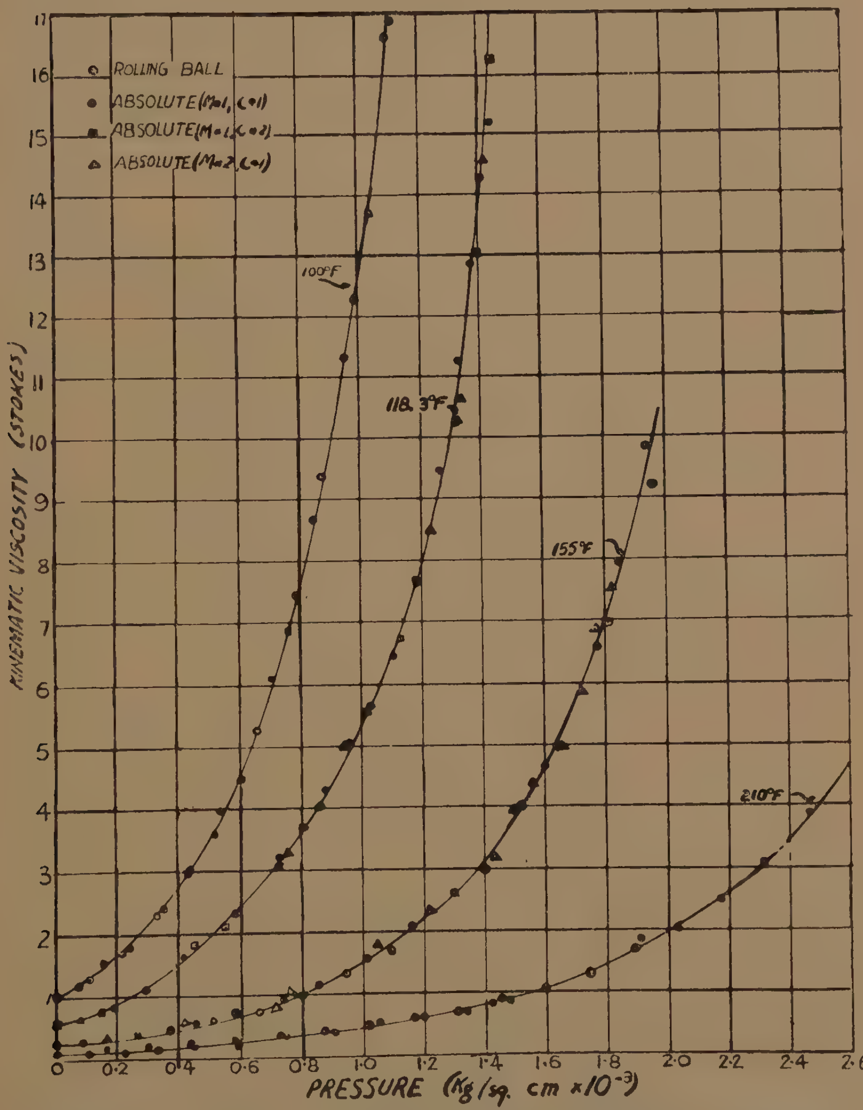

Viscosity of Pennsylvania extracted oil at high pressures; comparison of viscometers.

The rolling-ball method of Flowers(11) was applied to the measurement of viscosity of lubricants by Hersey and Shore(5). The method has been used extensively by the author and his students in studying the viscosity of oils (1), (12), (13) and pure liquids (14), (15). By this method the time of roll of a ball down an inclined path is measured at a constant pressure and temperature, and the viscosity computed from a calibration curve relating the time of roll to kinematic viscosity. The dimensional theory is reviewed by Barr(16). Fig. 3 is a typical calibration curve for an angle of inclination of the viscometer from the horizontal of about 15°. T is the corrected time of roll, $u$ is the kinematic viscosity, and S is a function of the density of the ball and of the liquid under test. The work of Heverly(15) in the writer's laboratory was for the purpose of showing the limitation of the rolling-ball method for short times of roll. For low roll times, region of non-linearity of the calibration curve, Heverly found that less than 10 per cent. of the roll time furnished a measure of the viscosity. It was possible, then, for a coefficient of viscosity of the order of 1 centipoise, or less, to be in error by as much as 10 to 20 per cent. on the basis of a possible error of ·01 or ·02 second in an observed roll time of the order of 1 or 2 seconds. Consequently the range of usefulness

Fig. 3.

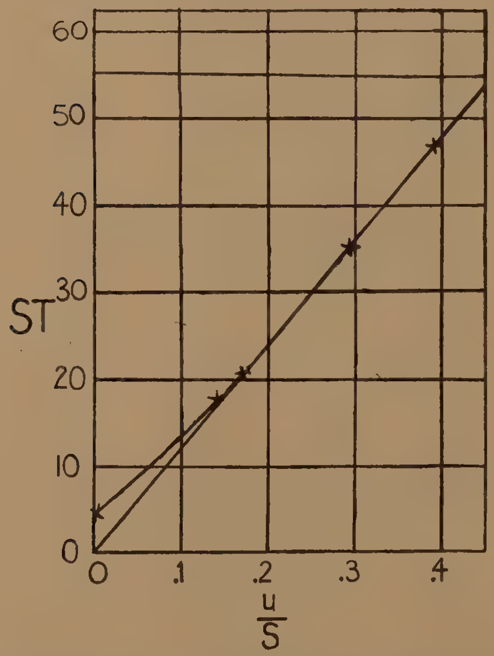

Calibration curve for rolling-ball viscometer.

of this instrument is limited to those liquids which allow a fairly long time of roll for small angles of tilt.

By Bridgman's method the time of fall is directly a measure of the coefficient of viscosity, whereas by the rolling-ball method only a fraction of the observed time is a measure of the coefficient. Bridgman's method thus appears to be capable of greater accuracy for less viscous liquids, since errors of time have a much less effect on the computed results. For ease of operation the rolling-ball apparatus is to be preferred to the falling-weight method. The latter assembly is of relatively small dimensions and requires considerable skill in assembling. Moreover, in operation the pressure generating apparatus must be rotated as well as the viscometer. The rolling-ball viscometer is essentially a simple cylinder of moderate size with a longitudinal hole that serves as a path of roll for a standard ball-bearing, and which is mounted on a horizontal axis that can be tilted without effort. The relatively larger dimensions of this viscometer allow about ten times greater volume of liquid and greater facility in assembling. For the highest pressures, of the order of 10,000 atmospheres, Bridgman's viscometer, due to the type of construction, must be used at present, since the rolling-ball instrument is limited to a pressure range of 6000 kg./cm.$^2$.

The relatively few corrections of these relative viscometers at high pressures and the greater convenience in operation make them preferable to the absolute instruments for routine measurement. Relative measurements with errors of a few per cent. are commonplace with the above viscometers, and a precision has been obtained which exceeds that possible with the absolute viscometers now in use.

## II. VISCOSITY OF CARBON DISULPHIDE—CARBON TETRACHLORIDE MIXTURES AT HIGH PRESSURES.

The author(10) has studied previously the viscosity of mixtures of liquids at high pressures, using the liquids that Bridgman investigated and his falling-weight viscometer. The results suggested that Bridgman's concept of interlocking of molecules and its resultant effect on viscosity at high pressures was a highly complicated phenomenon that was not susceptible to analysis by application of ordinary ideas about the nature of the liquid state. In the case of non-polar mixtures, consisting of liquids such as carbon disulphide, hexane, decane, etc., the interlocking or interlinking was thought to be somewhat simpler than in the case of highly polar liquids, since the logarithm of the coefficient of viscosity was additive linearly with the molar concentration over the ranges of pressure and temperature.

The present study was undertaken to investigate under similar conditions the viscosity effects in mixtures composed of non-polar liquids whose force-fields are quite different. Carbon disulphide and carbon tetrachloride were chosen as representative non-polar molecules possessing unlike characteristics in this respect. The liquids were of Eastman's best grade and were purified additionally by double distillation before mixing. The following six mixtures were prepared by mixing volumes that were measured by discharging between the fixed levels of calibrated, glass pipettes: 15, 30, 50, 60, 65, and 75 per cent. of $CS_2$ by volume at 30° C. The densities at the same temperature were measured by means of a standard pycnometer fitted with a ground-glass cap to prevent evaporation.

The pressure measurements were the same as described previously(10). It will be remembered that the viscometer of Bridgman is a relative one, the time of vertical fall of a small cylindrical weight being used as the measure of the relative coefficient of viscosity. Time of fall was found in opposite directions by rotating the pressure-chamber containing the viscometer through 180° after one fall was recorded, so that the weight could then fall back to its original position. The reader is referred to the original publication for further details of procedure and computation of errors.

The absolute viscosities of the mixtures at atmospheric pressure at 30° C. were measured independently by Mr. R. B. Healy, of the Petroleum Refining Laboratory of this college. The measurements were made with a glass capillary pipette under carefully controlled conditions.

The relative viscosities of the six mixtures were measured subsequently in the high pressure viscometer over a pressure range extending from atmospheric pressure to a pressure of 10,000 kg./cm.$^2$, the experiments being conducted at constant temperatures of 30° and 75° C. The measured quantities for a determination of viscosity were average time of fall in the two directions, pressure, and temperature. The time of fall, when corrected for various errors caused by pressure effects, was proportional to the absolute coefficient of viscosity. Knowing the absolute viscosity at atmospheric pressure, and the relative viscosities at higher constant pressures, the absolute coefficients were computed at the various pressures and temperatures of this investigation. The pressures were determined by measuring the change of electrical resistance of a manganin coil maintained at room-temperature and exposed to the liquid that transmitted the pressure.

The relation between pressure and resistance for this alloy is known to be linear. It is customary to determine the pressure coefficient of a coil by observing the resistance of it when a liquid freezes under compression at a known pressure and temperature. This is done most conveniently by pushing a piston into a steel cylinder containing a known liquid and the manganin coil. Freezing is recognized by the volume discontinuity which is read as a discontinuity in the piston displacement. The freezing of mercury at 7640 kg./cm.$^2$ at 0° C. was used to calibrate the coil used in this investigation. The error in this figure is probably within $\pm 10$ kg./cm.$^2$. The recorded temperatures are the corrected readings of a thermometer that was immersed entirely in a thermostated bath that completely surrounded the test-chamber.

Table II. contains density data of the components and six mixtures at atmospheric pressure at 30° C. Within the error of measurement, of the order of 1 per cent., the relation between density and concentration, expressed in terms of per cent. by volume of $CS_2$, appeared to follow a smooth curve that was practically linear.

TABLE II.

Density of $CS_2$—$CCl_4$ Mixtures at Atmospheric Pressure, 30° C.

| Liquid (volume per cent. $CS_2$). | Density (gm./cm.$^3$). |
|---|---|
| 0 | 1·555 |
| 15 | 1·509 |
| 30 | 1·462 |
| 50 | 1·399 |
| 60 | 1·368 |
| 65 | 1·350 |
| 75 | 1·320 |
| 100 | 1·241 |

Table III. shows the collected viscosity-pressure-temperature data for the component liquids and six mixtures. Those for the components were taken from Bridgman's$^{(3)}$ paper that the author had checked previously$^{(10)}$. It is believed that the possible error in these data may be of the order of 2 or 3 per cent., similar to that found previously.

The viscosity isobars at 30° C. are shown in fig. 4. Similar curves were obtained at 75° C. It is evident that viscosity is not a simple function of concentration of the component liquids. Plots of $\log_{10}\eta$, $\eta$ being the viscosity coefficient, against volume, weight, and molar per cent. respectively, did not simplify the characteristics of the curves to any extent.

Temperature variation of the coefficient of viscosity at high pressures is expressed in Table IV. as the ratio of the coefficient at 30° to that at 75° C. Initially the viscosity ratio decreased with increase of pressure for both components and mixtures. It is interesting to observe that the minimum value occurred at about 1500 kg./cm.$^2$ for all the mixtures except the 15 per cent. one. One would suspect this initial decrease to be due to a volume effect, since a uniform tendency to approach a common minimum would be hardly a characteristic of the molecules themselves. At higher pressures, *e. g.*, 7000 kg./cm.$^2$, it is noticeable that the ratio varies considerably with concentration. Viscosity seems to be less dependent on temperature when the volume effect becomes less important relatively.

TABLE III.

Viscosity-Pressure-Temperature Data for $CS_2$—$CCl_4$ Mixtures 30° C. ;
Coefficient of Viscosity in Centipoises.

| Pressure (kg./cm.$^2$). | Composition (volume per cent. $CS_2$). | | | | | | | |
|---|---|---|---|---|---|---|---|---|
| | 0*. | 15. | 30. | 50. | 60. | 65. | 75. | 100*. |
| 1 | ·830 | ·652 | ·541 | ·449 | ·419 | ·402 | ·382 | ·340 |
| 500 | 1·290 | ·874 | ·720 | ·585 | ·537 | ·510 | ·476 | ·419 |
| 1000 | 1·870 | 1·172 | ·906 | ·718 | ·650 | ·625 | ·580 | ·493 |
| 1500 | 2·539 | 1·545 | 1·105 | ·858 | ·770 | ·738 | ·693 | ·582 |
| 2000 | . . | 1·989 | 1·309 | 1·009 | ·913 | ·880 | ·816 | ·690 |
| 3000 | . . | 3·169 | 1·774 | 1·325 | 1·207 | 1·166 | 1·069 | ·881 |
| 4000 | . . | 4·662 | 2·552 | 1·745 | 1·554 | 1·471 | 1·348 | 1·100 |
| 5000 | . . | . . | . . | 2·315 | 1·978 | 1·817 | . . | 1·341 |
| 6000 | . . | . . | . . | 3·166 | 2·472 | 2·202 | . . | 1·609 |
| 7000 | . . | . . | . . | 4·337 | 3·063 | 2·641 | . . | 2·940 |
| 8000 | . . | . . | . . | . . | 3·759 | 3·168 | . . | 2·352 |
| 9000 | . . | . . | . . | . . | . . | 3·831 | . . | 3·892 |
| 10000 | . . | . . | . . | . . | . . | . . | . . | 3·483 |
| | 75° C. | | | | | | | |
| 1 | ·478 | ·413 | ·362 | ·304 | ·295 | ·285 | ·271 | ·255 |
| 500 | ·741 | ·609 | ·512 | ·425 | ·393 | ·378 | ·359 | ·319 |
| 1000 | 1·047 | ·819 | ·659 | ·540 | ·495 | ·472 | ·452 | ·383 |
| 1500 | 1·415 | 1·050 | ·806 | ·649 | ·591 | ·567 | ·533 | ·441 |
| 2000 | 1·852 | 1·317 | ·972 | ·759 | ·686 | ·661 | ·613 | ·516 |
| 3000 | 2·890 | 1·870 | 1·279 | ·990 | ·897 | ·859 | ·801 | ·652 |
| 4000 | . . | 2·420 | 1·617 | 1·248 | 1·138 | 1·060 | ·998 | ·803 |
| 5000 | . . | 2·991 | 1·966 | 1·497 | 1·374 | 1·272 | 1·190 | ·975 |
| 6000 | . . | . . | 2·323 | 1·765 | 1·628 | 1·487 | 1·386 | 1·143 |
| 7000 | . . | . . | . . | 2·052 | 1·890 | 1·706 | 1·592 | 1·360 |
| 8000 | . . | . . | . . | 2·341 | 2·158 | 1·925 | 1·809 | 1·596 |
| 9000 | . . | . . | . . | . . | . . | 2·151 | 2·022 | 1·881 |
| 10000 | . . | . . | . . | . . | . . | 2·370 | 2·250 | 2·185 |

* Bridgman's data (3).

These new data yield additional information about the concept of interlocking or interlinking of molcules under high pressure conditions. It has been suggested previously(10) that the observed effects in mixtures could be due to two factors or a combination of both : the degree of interlinking or interlocking may change with pressure if association or molecular aggregation varies with pressure ; also, the effect of interlocking must change alone with pressure, becoming stronger with increase of

Fig. 4.

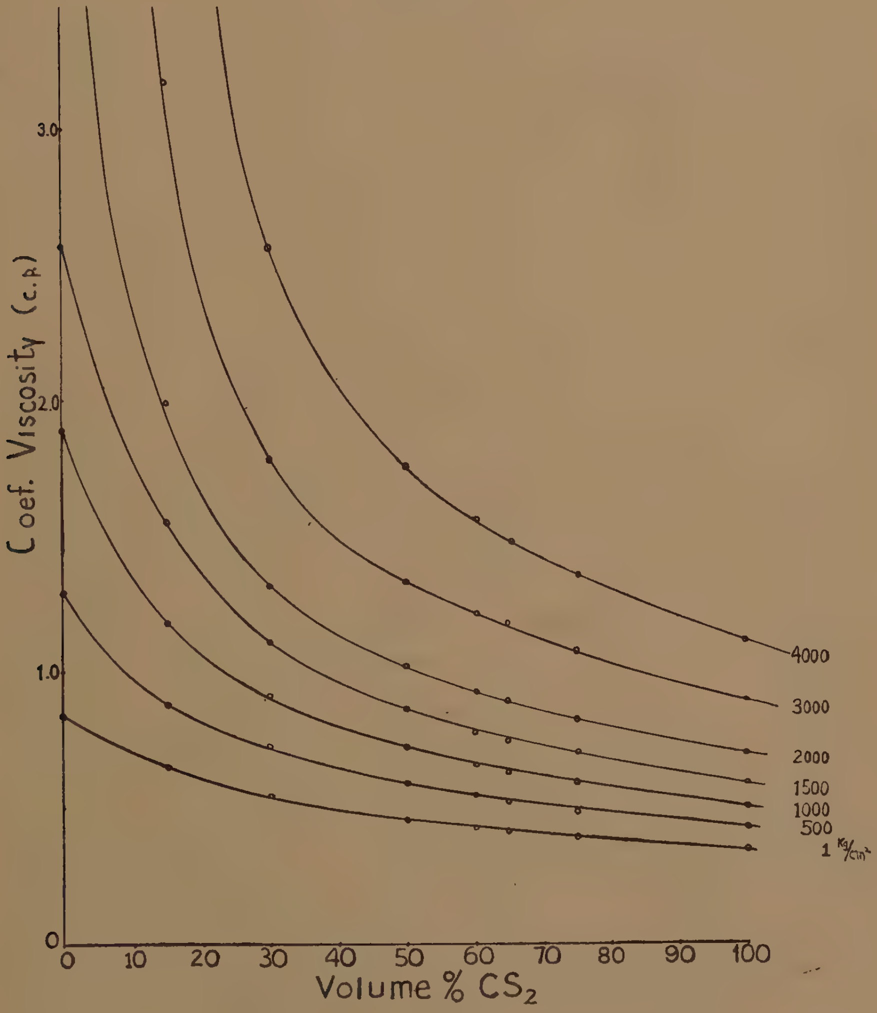

Viscosity isobars for $CS_2$–$CCl_4$ mixtures at 30° C.

pressure ; finally, one would expect both effects in highly polar liquids. The relatively simple results obtained for hexane-carbon disulphide and hexane-decane mixtures, as mentioned previously, were interpreted to mean that the increase of viscosity with pressure for these mixtures at constant temperature was due to the effect of interlocking alone. However, the essentially linear nature of the molecules involved would allow strong orientation effects at high pressures, the long axes of the molecules lining up in parallel fashion, so that a "bundle of sticks" type of arrangement would result. While the molecular aggregates in such a preferred orientation would begin to have structural characteristics at high pressures their basic structure would not be expected to undergo appreciable modification.

Table IV.

Temperature Variation of Viscosity, $\frac{\eta_{30}}{\eta_{75}}$, for $CS_2$—$CCl_4$ Mixtures.

| Pressure (kg./cm.$^2$). | Composition (volume per cent. $CS_2$). | | | | | | | |
|---|---|---|---|---|---|---|---|---|
| | 0. | 15. | 30. | 50. | 60. | 65. | 75. | 100. |
| 1 | 1·74 | 1·58 | 1·49 | 1·48 | 1·42 | 1·41 | 1·41 | 1·33 |
| 500 | 1·74 | 1·43 | 1·41 | 1·38 | 1·37 | 1·35 | 1·32 | 1·31 |
| 1000 | 1·79 | 1·43 | 1·37 | 1·33 | 1·31 | 1·32 | 1·28 | 1·29 |
| 1500 | 1·79 | 1·47 | 1·37 | 1·32 | 1·30 | 1·30 | 1·30 | 1·32 |
| 2000 | .. | 1·51 | 1·35 | 1·33 | 1·33 | 1·33 | 1·33 | 1·34 |
| 3000 | .. | 1·69 | 1·39 | 1·34 | 1·34 | 1·36 | 1·33 | 1·35 |
| 4000 | .. | 1·93 | 1·58 | 1·40 | 1·37 | 1·39 | 1·35 | 1·37 |
| 5000 | .. | .. | .. | 1·55 | 1·44 | 1·43 | .. | 1·38 |
| 6000 | .. | .. | .. | 1·79 | 1·52 | 1·48 | .. | 1·41 |
| 7000 | .. | .. | .. | 2·12 | 1·62 | 1·55 | .. | 1·43 |
| 8000 | .. | .. | .. | .. | 1·74 | 1·65 | .. | 1·47 |
| 9000 | .. | .. | .. | .. | .. | 1·78 | .. | 1·54 |
| 10000 | .. | .. | .. | .. | .. | .. | .. | 1·59 |

The preceding mixtures did not provide for an adequate examination of the possibility of change in the degree of interlocking or aggregation with pressure in liquids that are non-polar and of unlike molecules. In the sense of the above discussion the present mixtures do not yield information substantiating the hypothesis of change of degree of interlocking. The characteristic shape of the viscosity-concentration curve at atmospheric pressure at 30° continues at the higher pressures and temperature ; there are no abrupt changes in slope, such as the appearance of maxima or minima, to indicate that the degree of interlocking has suddenly changed with pressure or temperature. It would appear then that the degree of association depends on the kind and number of molecules involved, and associative characteristics at high pressures should be of the same degree as at atmospheric pressure, even though the effect itself must increase with pressure.

## III. THEORETICAL ASPECTS.

It is well known that when a liquid is compressed at constant temperature the work of compression is less than the heat of compression. Internal work is done against the attractive forces of the molecules, a result which gives a greater outflow of energy in the form of heat than is put in by the work of compression. The change of internal energy with pressure can be expressed in terms of the first law of thermodynamics as

$$\left(\frac{\partial E}{\partial p}\right)_t=\left(\frac{\partial Q}{\partial p}\right)_t+\left(\frac{\partial W}{\partial p}\right)_t \quad . \quad . \quad . \quad . \quad . \quad . \quad . \quad (1)$$

$$=-\left[t\left(\frac{\partial v}{\partial t}\right)_p+p\left(\frac{\partial v}{\partial p}\right)_t\right], \quad . \quad . \quad . \quad . \quad . \quad (2)$$

the quantities referring to 1 gram of substance.

As pressure is applied initially the first term of the equations predominates and the internal energy decreases. At high pressures, when the repulsive forces become greater than the attractive ones, the last term becomes important. The pressure at which the forces balance is given by equation (2) when $\left(\frac{\partial E}{\partial p}\right)_t=0$. Bridgman(17) has shown that the volume at normal temperatures at which the change of energy vanishes is less than the volume at 0° absolute at atmospheric pressure, a result to be expected if the molecules are compressible.

The effect of this increased complexity of force-fields in liquids at high pressures can be computed indirectly by considering the change of potential energy of the liquid with change of volume. This can be accomplished either by varying the temperature or the pressure, or both. At first sight one would expect that the potential energy-volume curve of a liquid would change with temperature and pressure in such a way that a decrease in energy due to lowering of temperature would be comparable to a decrease brought about by increase of pressure. But there is reason to believe that $\left(\frac{\partial V}{\partial v}\right)_p\neq\left(\frac{\partial V}{\partial v}\right)_t$. If the theorem of the virial is extended to apply to motion of charged particles in an electric field when constant pressure is applied, the equations of Schottky(18) are obtained:

$$dT=-\ dE+3d(pv), \quad . \quad . \quad . \quad . \quad . \quad . \quad . \quad (3)$$

$$dV=\ 2dE-3d(pv). \quad . \quad . \quad . \quad . \quad . \quad . \quad . \quad (4)$$

T and V are the average internal kinetic and potential energies respectively; E is the total energy of the system, including the electromagnetic as well as the kinetic and potential energy; $p$ is the pressure and $v$ the volume.

Bridgman[(19)] has put the equations into the following form for substitution of thermodynamic data:

$$dT=\left[4p\left(\frac{\partial v}{\partial t}\right)_p-C_p\right]dt+\left[3v+t\left(\frac{\partial v}{\partial t}\right)_p+4p\left(\frac{\partial v}{\partial p}\right)_t\right]dp, \quad . \quad (5)$$

$$dV=\left[2C_p-5p\left(\frac{\partial v}{\partial t}\right)_p\right]dt-\left[3v+2t\left(\frac{\partial v}{\partial t}\right)_p+5P\left(\frac{\partial v}{\partial p}\right)_t\right]dp.$$

Thus the change of potential energy with volume can be written

$$\left(\frac{\partial V}{\partial v}\right)_p=\frac{2C_p}{\left(\frac{\partial v}{\partial t}\right)_p}-5p, \quad . \quad . \quad . \quad . \quad . \quad . \quad . \quad (7)$$

$$\left(\frac{\partial V}{\partial v}\right)_t=-\left[\frac{3v+2t\left(\frac{\partial v}{\partial t}\right)_p}{\left(\frac{\partial v}{\partial p}\right)_t}\right]-5p. \quad . \quad . \quad . \quad . \quad . \quad (8)$$

Consider now the two coefficients at 1 kg./cm.$^2$ for $CS_2$ and $CCl_4$ at 0° C.:

| | $CS_2$. | $CCl_4$. |
|---|---|---|
| density | $=1{\cdot}292$ gm./cm.$^3$ | $1{\cdot}633$ |
| $C_p$ | $={\cdot}232$ cal./gm./C°. | ${\cdot}198$ |
| $\frac{1}{v}\left(\frac{\partial v}{\partial t}\right)_p$ | $=1{\cdot}14\times10^{-3}$ 1/C°. | $1{\cdot}49\times10^{-3}$ |
| $\frac{1}{v}\left(\frac{\partial v}{\partial p}\right)_t$ | $=66{\cdot}0\times10^{-6}$ cm.$^2$/kg. | $90{\cdot}7\times10^{-6}$ |
| $\left(\frac{\partial V}{\partial v}\right)_p$ | $=22\times10^3$ kg./cm.$^2$ | $\left(\frac{\partial V}{\partial v}\right)_p=19\times10^3$ |
| $\left(\frac{\partial V}{\partial v}\right)_t$ | $=55\times10^3$/ kg./cm.$^2$ | $\left(\frac{\partial V}{\partial v}\right)_t=42\times10^3$ |

The change of potential energy of both liquids for a given volume change is about twice as great when caused by change of pressure as when caused by change of temperature. This means in the final analysis that while E can be expressed as a function of pressure, volume, and temperature no general characteristic equation is known. At higher pressures, when the force fields of the molecules are further distorted by increase in the proximity of neighbouring molecules, the difficulty of visualizing a characteristic equation in terms of present concepts becomes so great as to be almost prohibitive.

The conclusion that the known characteristic equations or equations of state fail to represent the experimental facts when the potential energy varies appreciably with pressure and temperature is significant for theories of viscosity at high pressures. The recent theories of Andrade(20) and of Eyring and Ewell(21) express the coefficient of viscosity as a function of an activation energy which is computed in terms of thermodynamic quantities, but no fundamental distinction has been made between the effects of pressure and temperature on the activation energy or some similar concept of energy.

The energy of activation for flow of the latter theory is measured by the energy of vaporization that comprises the energies of directed bond structure as well as undirected bonds. But the energy of vaporization, being a measure of the potential energy of the molecules, must be likewise far from constant over the experimental range that has been studied.

The behaviour of the heat of vaporization, or any heat of change of state, may be visualized in another, although not independent, manner. Thermodynamically the variation of the energy of vaporization with pressure can be expressed as

$$\left(\frac{\partial Q}{\partial p}\right)_t = -t\left(\frac{\partial v}{\partial t}\right)_p . \qquad \ldots\ldots \quad (9)$$

The non-linear variation of the coefficient of thermal expansion with pressure is erratic for most liquids. It is about four or five times smaller at 5000 or 6000 atmospheres than at atmospheric pressure, and $\frac{\partial^2 v}{\partial t^2}$ reverses in sign usually at slightly lower pressures. It is well known that thermal expansion is a measure indirectly of complexity of force fields, a large expansion indicating a correspondingly large departure from a linear law of force. For a strictly linear law of force the restoring force is proportional to the displacement and the thermal expansion is zero.

Quite aside from the failure of equations of state there appears to be a part of the energy of viscous flow at high pressures that cannot be measured by thermodynamic quantities. This is the energy associated with weak bonds that are produced by pressure when interlocking occurs, and which are overcome when relative motion takes place within the liquid. While ultimately the origin of these bonds must be in the ordinary secondary or van der Waals' forces in a non-polar liquid that have been intensified by the closer approach of neighbouring molecules or aggregates at high pressure, they are somewhat different from the usual conception of secondary forces inasmuch as they can be thought of as highly directed forces in an oriented structure or between oriented structures, and, consequently, are functions of the size and shape of the molecules, *i. e.*, distribution of field as well as the magnitude of the electrical fields.

It is necessary that a fundamental distinction be made between the energy necessary to disperse a group of molecules, such as happens when a liquid vaporizes or evaporates, and the energy required to set up relative motion in the liquid whereby the interlocked molecules under pressure are displaced in translatory and rotary motion. When molecules are oriented in strongly interlinked or interlocked structures it is to be expected that this part of the energy of viscosity would be greater relatively than that due to intensified energy bonds which are present in the liquid at normal equilibrium conditions and which are thought of commonly as being functions of volume or " free space " in the liquid. The failure of any " volume function " to account for the observed viscosity in liquids and their mixtures at high pressures is due probably to the existence of this energy, which is not a function of volume but a function of the particular type of orientation and the resulting interlocking of molecules brought about by pressure.

To illustrate, consider the viscosity of benzene-pentane mixtures reported previously by the author(10). It was suggested that the interlocking in this mixture under pressure was of such a nature that the benzene molecules were oriented so that their planes tended to become parallel with the direction of flow. It seems clear that in this state the energy of flow must overcome bonds that are quite different in nature than those existing in the mixture at atmospheric pressure and which would be broken if the mixture was vaporized.

It has been thought by many investigators that the unit of viscous flow is not always the chemical molecule. The evidence for molecular association in Newtonian and non-Newtonian liquids is so abundant that any concept of interlocking as pictured here must grant the possibility that the unit of flow in certain cases may be a structure of many chemical molecules. However, there is no definite information on this point for pure liquids at present. If such structures exist at atmospheric pressure it is evident that energy bonds may be present that are quite different from those between single chemical molecules. As mentioned previously (p. 415) association, while complicating the degree of interlocking in any particular case, would not be expected to change in degree under pressure ; hence, whatever the unit of flow, there is no evidence that it varies with change of pressure.

The formation of weak structural bonds when orientation occurs in liquids is being recognized as increasingly important. Conant and Peterson(22), in their experiment on polymerization at high pressures, conclude that an essential part of the mechanism of the reaction must involve a definite orientation of molecules by the application of pressure. The action of a catalyst appeared to be more effective in producing long reaction chains when the molecular motion was less random and the molecules more orderly arranged in compact assemblages. Consequently the activation energy coming from the decomposition of the catalyst was more readily transferred from molecule to molecule of a uniformly oriented assembly. The energy transfer would supposedly take place along the direction of secondary bonds. Kienle(23), discussing polymerization, has stated fundamental postulates about molecular structure that are similar in many respects, although the valence forces are of another order of magnitude. Busse(24) has considered a sort of interlocking of kinky, flexible fibres, caused by secondary valence forces in colloidal substances like rubber, similar to the mechanism of interlocking considered here.

There are no theoretical methods available for determining the energy that depends on secondary bonds that are overcome in viscous flow. The partial success of present theories in yielding quantitative checks on viscosity of liquids over a moderate pressure range is limited to those liquids which do not have strong secondary bonds associated with orientation. For example, the viscosity of ether can be well represented by several theories over a range of 5000 or 6000 atmospheres, but for a liquid like eugenol or a chlorinated diphenyl, liquids in which there can be strong interlinking or interlocking, theory fails completely. In every case it is found that the computed viscosity at high pressure is less than the observed one, a result which suggests that some important factor has been neglected.

In conclusion, it seems inevitable that viscosity of liquids at high pressure must be considered as due to highly complicated individual mechanisms for every molecular species, about which no specific conclusions can be made. Individual differences of structure and force fields are so numerous that the number of possibilities of interlocking among molecules is almost without limit. Viscosity is a property that is sensitive to these differences of molecular structure ; statically determined energy conditions, on the other hand, may indicate many deceptive characteristics that appear to be common for many liquids. Even though the experimental data prohibit complete mathematical analysis, viscosity measurements at high pressures seem to be one of the best tools at hand for studying some aspects of molecular structure.

## *References.*

(1) Dow, R. B., Fenske, M. R., and Morgan, H. E., Ind. & Eng. Chem. xxix. p. 1078 (1937).
(2) Hatschek, E., 'The Viscosity of Liquids,' D. von Nostrand or Bell, Chap. VI.

(3) Bridgman, P. W., Proc. Amer. Acad. A. & S. lxi. p. 57 (1926).
(4) Hyde, J. H., Proc. Roy. Soc. A, xcvii. p. 240 (1920).
(5) Hersey, M. D., and Shore, H., Mech. Eng. l. p. 221 (1928).
(6) Kleinschmidt, R. V., Trans. A. S. M. E. APM 50–4 (1928).
(7) Suge, Y., General Disc. Lub., Inst. Mech. Eng. Group IV. p. 184 (1937).
(8) Hersey, M. D., and Hopkins, R. F., Jour. App. Physics, viii. p. 565 (1937).
(9) Thomas, B. W., Thesis, " An Absolute Viscometer for Lubricating Oils at High Pressure," The Pennsylvania State College (1938).
(10) Dow, R. B., ' Physics,' vi. p. 71 (1935).
(11) Flowers, A. E., Proc. Amer. Soc. Test. Mats. xiv. p. 565 (1914).
(12) Dow, R. B., J. App. Physics, viii. p. 367 (1937).
(13) Dibert, R. M., Thesis, " The Viscosity of Pennsylvania Oils at High Pressure," The Pennsylvania State College (1938).
(14) Morgan, H. E., Thesis, " The Effects of Pressure and Temperature on the Viscosity of Mono-substituted Toluenes," The Pennsylvania State College (1937).
(15) Heverly, J. R., Thesis, " A Study of Viscometry at High Pressure," The Pennsylvania State College (1938).
(16) Barr, G., ' A Monograph of Viscometry,' Oxford Press, p. 259 (1931).
(17) Bridgman, P. W., Reviews Mod. Physics, vii. p. 7 (1935).
(18) Schottky, W., *Phys. Zeits.* xxi. p. 232 (1920).
(19) Bridgman, P. W., reference (17), p. 3.
(20) Andrade, E. N., Phil. Mag. xvii. pp. 497, 698 (1934).
(21) Eyring, Henry, and Ewell, R. H., Jour. Chem. Physics, v. p. 726 (1937) ; Ewell, R. H., Jour. App. Physics, ix. p. 252 (1938).
(22) Conant, J. B., and Peterson, W. R., Jour. Amer. Chem. Soc. liv. p. 628 (1932).
(23) Kienle, R. H., Ind. Eng. Chem. xxii. p. 590 (1930) ; xxv. p. 971 (1933) ; J. Soc. Chem. Ind. lv. p. 228 T (1936).
(24) Busse, W. F., J. Phys. Chem. xxxvi. p. 2862 (1932).

## XXXIX. *Quantization under Two Centres of Forces.*—Part I. *The Hydrogen Molecular Ion.*

By S. K. Chakravarty, Calcutta (India) *.

[Received March 28, 1939.]

1. Several methods of wave-mechanics have been applied for the determination of the electronic energies of the $H_2{}^+$. The theory has been worked out in the old quantum theory by Pauli and Niessen. The energy of the ground state of the ion was first calculated by Burrau(1), but he could not obtain the eigenfunction. A perturbation method was used by Morse and Stuckelberg(2). The later works on the subject are those of Teller(3), Hylleraas(4), Jaffe(5), and others. One group is concerned mainly with an enquiry into the eigenvalue wherein the analytical character of the eigenfunction remains to be cleared. Others have solved the differential equations to obtain incorrect results. For the present, therefore, neither the eigenfunction nor the proper representation of eigenvalue is known.

The analysis in the present work has been given for the most general case of two unequally charged nuclei with one electron in their field, so that the electronic energies of homonuclear as well as heteronuclear molecules in all their different states can be calculated. The results have been applied to the calculations of the $1s\sigma$, $2s\sigma$, and $3d\sigma$ states of $H_2{}^+$.

2. Taking the unit of energy as that of the hydrogen atom in its lowest state, lengths in terms of the radius of the first Bohr orbit of the H atom and the unit of charge as equal to that of the electron, the electronic potential energy of the molecule, V, is given by

$$V=-\frac{Z_a}{r_a}-\frac{Z_b}{r_b}, \quad \ldots \ldots \ldots \ldots \quad (1)$$

where $Z_a$, $Z_b$ are the charges of the two fixed nuclei and $r_a$, $r_b$ the distances of the electron from the two nuclei. Considering the Schrödinger equation in elliptic coordinates $\xi$, $\eta$, $\phi$, where

$$\xi=\frac{r_a+r_b}{R}\,; \quad \eta=\frac{r_a-r_b}{R}\,;$$

---

* Communicated by the Author.

and $\phi$ the azimuth about the line of the nuclei and R the internuclear distance, and assuming the eigenfunction $\Psi$ in the form

$$\Psi \sim X(\xi)\gamma(\eta)\Phi(\phi), \quad . \quad . \quad . \quad . \quad . \quad . \quad . \quad . \quad . \quad (2)$$

we get
$$\frac{\partial^2\Phi}{\partial\phi^2}+m^2\Phi=0, \quad \text{which gives } \Phi=\frac{1}{\sqrt{2\pi}}\,.\,e^{im\phi}$$

$$\frac{\partial}{\partial\xi}\left\{(\xi^2-1)\frac{\partial X}{\partial\xi}\right\}-\frac{m^2X}{\xi^2-1}+[-\lambda^2\xi^2+B\xi-A]X=0 \quad . \quad . \quad (3)$$

for the range $1 \leqslant \xi < \infty$:

and
$$\frac{\partial}{\partial\eta}\left\{(1-\eta^2)\frac{\partial\gamma}{\partial\eta}\right\}-\frac{m^2\gamma}{1-\eta^2}+[\lambda^2\eta^2+D\eta+A]\gamma=0 \quad . \quad . \quad . \quad (4)$$

for the range $-1 \leqslant \eta \leqslant 1$;

where $\quad B=(Z_b+Z_a)R$; $D=(Z_b-Z_a)R$; $\lambda^2=-\tfrac{1}{4}E'R^2$,

A is the separation constant and E′ the electronic energy. The problem before us is to find the solutions of (3) and (4) subject to the conditions that X, $\gamma$ may remain finite, continuous, and uniform within the whole range $1 \leqslant \xi < \infty$; $-1 \leqslant \eta \leqslant +1$, respectively.

3. Consider equation (3), and put

$$X=e^{-\lambda\xi}(\xi^2-1)^{m/2}\,.\,y, \text{ and } x=\frac{\xi-1}{\xi+1}, \quad . \quad . \quad . \quad . \quad . \quad . \quad (5)$$

and then if we take $(1-x)^{\rho}Z$ for $y$, we get, after simplification,

$$x(1-x)^2\frac{\partial^2 z}{\partial x^2}-\{2(\rho+1)x(1-x)-(m+1)(1-x^2)+4\lambda x\}\frac{\partial z}{\partial x}$$
$$+\Big[\{\lambda\rho+\tfrac{1}{2}B-\lambda(m+1)\}\frac{4x}{1-x}+\rho(\rho+1)x-(m+1)\rho(1+x)$$
$$+m(m+1)-A-\lambda^2+B-2\lambda(m+1)\Big]Z=0, \quad . \quad . \quad . \quad . \quad (6)$$

where $0 \leqslant x < 1$.

If we take $\rho$ (which is as yet undefined) to be equal to $m+1-B/2\lambda$, then (5) is reduced to the form

$$x(1-x)^2\frac{\partial^2 z}{\partial x^2}-\{(m-2\rho-1)x^2+(2\lambda+\rho+1)\,.\,2x-(m+1)\}\frac{\partial Z}{\partial x}$$
$$+\{\rho(\rho-m)x-K\}Z=0, \quad . \quad . \quad . \quad . \quad (7)$$

where the domain of $x$ is $0 \leqslant x < 1$, and $p=B/2\lambda$, and

$$K=A+\lambda^2+(1-p)(m+1+2\lambda)+2m\lambda. \quad . \quad . \quad . \quad . \quad (7\,a)$$

Equation (7) has singularities at $x=0$ and $x=1$, so that for a solution in the vicinity of $x=0$ we assume

$$Z=x^{\rho'}\sum_{n=0}^{\infty} a_n x^n;$$

and substituting in (7), we get for the indicial equation

$$\rho'(\rho'+m)=0.$$

Hence the solution which is bounded at the origin is obtained when we take $\rho'=0$, provided $m$ is a positive quantity; so we assume

$$Z=\sum_{n=0}^{\infty} a_n x^n, \quad . \quad . \quad . \quad . \quad . \quad . \quad . \quad . \quad . \quad (8)$$

and substituting in (7), and equating the coefficients of $x^n$ on both sides, we get the recursion formula as

$$f_{n-1}a_{n-1}+g_n a_n+h_{n+1}a_{n+1}=0, \quad . \quad . \quad . \quad . \quad . \quad . \quad . \quad (9)$$

where $f_{n-1}=(n-p)(n+m-p),$

$$g_n=-\{2n(n+2\lambda+m+1-p)+K\},$$

$$h_{n+1}=(n+1)(n+m+1).$$

From (9) we have

$$h_{n+1}\frac{a_{n+1}}{a_n}=-g_n-f_{n-1}\frac{a_{n-1}}{a_n}$$

$$=-g_n+\frac{h_n f_{n-1}}{g_{n-1}-}\,\frac{h_{n-1}f_{n-2}}{g_{n-2}+\cdots}\,(-1)^{n-1}\frac{h_1 f_0}{g_0}. \quad . \quad . \quad . \quad . \quad (10)$$

Also, $$f_{n-1}\frac{a_{n-1}}{a_n}=-g_n-h_{n+1}\frac{a_{n+1}}{a_n}$$

$$=-g_n+\frac{h_{n+1}f_n}{g_{n+1}-}\,\frac{h_{n+2}f_{n+1}}{g_{n+2}+\cdots}. \quad . \quad . \quad . \quad . \quad . \quad . \quad (11)$$

But $$f_{n-1}\frac{a_{n-1}}{a_n}+g_n+h_{n+1}\frac{a_{n+1}}{a_n}=0;$$

$$\therefore \qquad g_n-L_{n+1}-H_{n-1}=0, \quad . \quad . \quad . \quad . \quad . \quad . \quad . \quad . \quad (12)$$

where $$L_{n+1}=\frac{h_{n+1}f_n}{g_{n+1}-}\,\frac{h_{n+2}f_{n+1}}{g_{n+2}+\cdots},$$

$$H_{n-1}=\frac{h_n f_{n-1}}{g_{n-1}-}\,\frac{h_{n-1}f_{n-2}}{g_{n-2}+\cdots}\,(-1)^n\frac{h_1 f_0}{g_0}.$$

Hence from (12) we have to a first approximation

$$g_n=0, \quad . \quad . \quad . \quad . \quad . \quad . \quad . \quad . \quad . \quad (13)$$

and to a second approximation, considering only the first convergents of $L_{n+1}$ and $H_{n+1}$, we get

$$g_n-\frac{h_{n+1}f_n}{g_{n+1}}-\frac{h_nf_{n-1}}{g_{n-1}}=0. \quad . \quad . \quad . \quad . \quad . \quad . \quad . \qquad (13\,a)$$

It is clear that the infinite continued fraction $L_{n+1}$ is convergent⁽⁶⁾. Moreover, it will be apparent from the calculated results that the first convergents of the continued fractions $L_{n+1}$ and $H_{n-1}$ are a sufficient approximation. From (13) we get

$$\left.\begin{aligned} &K=-2n(n+2\lambda+m+1-p)\,; \\ \therefore\quad &A=-2n(n+2\lambda+m+1-p)-\lambda^2-(1-p)(m+1+2\lambda)-2m\lambda. \end{aligned}\right\} \qquad (14)$$

Hence, substituting for K, its value as given by (14), wherever it occurs in the second-order terms in (13 *a*), *i. e.*, in $\dfrac{h_{n+1}f_n}{g_{n+1}}$ and $\dfrac{h_nf_{n-1}}{g_{n-1}}$, we have, on simplification,

$$\begin{aligned} A=&-2n(n+2\lambda+m+1-p)-\lambda^2-(1-p)(m+1+2\lambda)-2m\lambda \\ &+\left[\frac{(n+1)(n+m+1)(n+1-p)(n+m+1-p)}{2(2n+2\lambda+m+2-p)}\right. \\ &\left.\qquad-\frac{n(n+m)(n-p)(n+m-p)}{2(2n+2\lambda+m-p)}\right]. \quad . \quad . \quad (15) \end{aligned}$$

4. Consider equation (4). It is clear that if we make $\lambda=D=0$ the solution will be

$$\gamma=P_l^m(\eta),$$

with $A=l(l+1)$.

So let us assume that the solution of (4) is given by

$$\gamma=\sum_{l=m}^{\infty}C_lP_l^m(\eta).$$

Substituting in (4), and simplifying, we get

$$\sum_{l=m}^{\infty}C_l[\lambda^2\eta^2+D\eta+A-l(l+1)]P_l^m(\eta)=0. \quad . \quad . \quad . \quad . \quad . \qquad (16)$$

So that, substituting the values of $\eta P_l^m(\eta)$, $\eta^2P_l^m(\eta)$, and equating to zero the coefficient of $P_l^m(\eta)$, we get

$$p_{l-2}C_{l-2}+q_{l-1}C_{l-1}+(A-r_l)C_l+S_{l+1}C_{l+1}+T_{l+2}C_{l+2}=0, \quad . \quad . \qquad (17)$$

where

$$p_{l-2}=\frac{(l-m)(l-m-1)}{(2l-1)(2l-3)}\lambda^2\,;\quad q_{l-1}=\frac{l-m}{2l-1}D\,;$$

$$r_l=l(l+1)-\frac{2l^2-2m^2+2l-1}{(2l-1)(2l+3)}\lambda^2\,;$$

$$S_{l+1}=\frac{l+m+1}{2l+3}D\,;\quad T_{l+2}=\frac{(l+m+1)(l+m+2)}{(2l+3)(2l+5)}\lambda^2.$$

It should be noted that in (17) $l$ can have any positive integral value lying between $m$ and $\infty$. Thus we get an infinite number of linear equations involving the coefficients $C_{l-2}$, $C_{l-1}$, $C_l$, . . . etc., from which, in order that a non-trivial solution may exist, we get, by eliminating the coefficients $C_l$, $C_{l+1}$, $C_l$ . . ., an infinite determinantal equation which is bounded on the left and above and A can be obtained from it. The determinantal equation is

$$\left|\begin{array}{lllllllllll}
\cdot & \cdot & \cdot & \cdot & \cdot & \cdot & \cdot & \cdot & \cdot & \cdot & \cdot \\
0, & p_{l-4}, & q_{l-3}, & (A-r_{l-2}), & S_{l-1}, & T_l, & 0, & 0, & 0, & 0, & 0, \\
0, & 0, & p_{l-3}, & q_{l-2}, & (A-r_{l-1}), & S_l, & T_{l+1}, & 0, & 0, & 0, & 0, \\
0, & 0, & 0, & p_{l-2}, & q_{l-1}, & \underline{(A-r_l)}, & S_{l+1}, & T_{l+2}, & 0, & 0, & 0, \\
0, & 0, & 0, & 0, & p_{l-1}, & q_l, & (A-r_{l+1}), & S_{l+2}, & T_{l+3}, & 0, & 0, \\
0, & 0, & 0, & 0, & 0, & p_l, & q_{l+1}, & (A-r_{l+2}), & S_{l+3}, & T_{l+4}, & 0. \\
\cdot & \cdot & \cdot & \cdot & \cdot & \cdot & \cdot & \cdot & \cdot & \cdot & \cdot
\end{array}\right| = 0 \quad . \ . \ . \ (18)$$

The properties of such determinants were studied by Koch ⁽⁷⁾. This will be of the normal type if the doubly infinite series $\sum_{k=0}^{\infty}\sum_{i=0}^{\infty}|A_{ik}|$ converges, where $A_{ik}$ represents the element of the $i$th row and $k$th column and the principal diagonal term is of the form $(1+A_{jj})$. In the present case we see that if $A_{jj}=0$ then $A_{ik}\sim\frac{1}{l^2}$ for all values of $i$, $k$. Hence the determinant converges absolutely.

Expanding the determinant in the usual form ⁽⁸⁾ we get

$$(A-r_l)-\left\{\frac{S_l q_{l-1}}{(A-r_{l-1})}+\frac{S_{l+1}q_l}{(A-r_{l+1})}+\frac{T_{l+2}p_l}{(A-r_{l+2})}+\frac{T_l p_{l-2}}{(A-r_{l-2})}\cdot\right\}+\ldots=0.$$

So to a first approximation we have $A-r_l=0$,

$$i.\ e.,\qquad A=l(l+1)-\left\{\frac{(l-m+1)(l+m+1)}{(2l+1)(2l+3)}+\frac{(l-m)(l+m)}{(2l-1)(2l+1)}\right\}\lambda^2,$$

and to a second approximation

$$A=l(l+1)-\left\{\frac{(l-m+1)(l+m+1)}{(2l+1)(2l+3)}+\frac{(l-m)(l+m)}{(2l-1)(2l+1)}\right\}\lambda^2$$

$$+\left\{\frac{S_l q_{l-1}}{A-r_{l-1}}+\frac{S_{l+1}q_l}{A-r_{l+1}}+\frac{T_{l+2}p_l}{A-r_{l+2}}+\frac{T_l p_{l-2}}{A-r_{l-2}}\cdot\right\}, \quad . \quad (19)$$

where in the second-order terms we shall take for A its value as obtained in the first approximation, *i. e.*, on the right-hand side of (19) we shall take $r_l$ for A wherever it occurs.

Solving (19) we get a value of A as a function of $\lambda$, R and the quantum numbers $m$, $l$. Equating the two values of A as obtained from (15) and (19) we get an equation between $\lambda$, R and the quantum numbers $n$, $l$, $m$, viz. :—

$$
\begin{aligned}
l(l+1)-\left\{\frac{(l-m+1)(l+m+1)}{(2l+1)(2l+3)}+\frac{(l-m)(l+m)}{(2l-1)(2l+1)}\right\}\lambda^2+\lambda^2 \\
+\left(1-\frac{\mathrm{B}}{2\lambda}\right)(m+1+2\lambda)+2m\lambda+2n\left(n+2\lambda+m+1-\frac{\mathrm{B}}{2\lambda}\right) \\
+\left[\left\{\frac{\mathrm{S}_l q_{l-1}}{r_l-r_{l-1}}+\frac{\mathrm{S}_{l+1} q_l}{r_l-r_{l+1}}+\frac{\mathrm{T}_{l+2} p_l}{r_l-r_{l+2}}+\frac{\mathrm{T}_l p_{l-2}}{r_l-r_{l-2}}\right\}\right. \\
-\frac{(n+1)(n+m+1)\left(n+1-\frac{\mathrm{B}}{2\lambda}\right)\left(n+m+1-\frac{\mathrm{B}}{2\lambda}\right)}{2\left(2n+2\lambda+m+2-\frac{\mathrm{B}}{2\lambda}\right)} \\
\left.+\frac{n(n+m)\left(n-\frac{\mathrm{B}}{2\lambda}\right)\left(n+m-\frac{\mathrm{B}}{2\lambda}\right)}{2\left(2n+2\lambda+m-\frac{\mathrm{B}}{2\lambda}\right)}\right]=0, \quad . \quad . \quad . \quad (20)
\end{aligned}
$$

where $l \geqslant m$ and $m$ is a positive integer or zero, and also $n$ is a positive integer but can take any value lying between 0 and $\infty$. The algebraic solution of (20) is prohibitive, but we can solve it numerically for a particular state of the molecule and thus get $\lambda$ and hence E′ as a function of R. In the next section we shall discuss the case of $\mathrm{H}_2^+$ in its different states, and compare the results with those of other workers. In solving for $\lambda$ from (20) we shall follow the method of successive approximation.

The eigenfunction is given by :

$$\Psi=\mathrm{N}\mathrm{X}(\xi)\gamma(\eta)\Phi(\phi),$$

where N is the normalization constant and

$$\mathrm{X}(\xi)=e^{-\lambda\xi}(\xi^2-1)^{m/2}y, \quad y=(1-x)^\rho \mathrm{Z},$$

where $$\rho=m+1-\frac{\mathrm{B}}{2\lambda}, \quad x=\frac{\xi-1}{\xi+1}, \quad \text{and} \quad \mathrm{Z}=\sum_0^\infty a_n x^n,$$

in which the coefficients $a_n$, $a_{n+1}$, $a_{n+2}$ . . . are connected by the recursion relation (9). Also,

$$\gamma(\eta)=\sum_{l=m}^\infty \mathrm{C}_l \mathrm{P}_l^m(\eta),$$

where the coefficients $C_l$, $C_{l-1}$, $C_{l+1}\ldots$ are connected by the relation (17) and

$$\Phi=\frac{1}{\sqrt{2\pi}}\,.\,e^{im\phi}.$$

5. In the case of $H_2^+$ we have $B=2R$, $D=0$, so that with particular values of the quantum numbers which define the state of the molecule we get from (20) an equation in $\lambda$ and R from which we obtain values of $\lambda$ and hence of E′ for different values of R. Thus we get an idea of the E′—R curve which gives useful information in molecular spectra.

TABLE I.

(1$s\sigma$ state of $H_2^+$).

| —E′ / R | Chakravarty. | | Hylleraas. | Jaffe. | Morse and Stuckel-berg. | Gullemin and Zener(9). |
|---|---|---|---|---|---|---|
| | 1st app. | 2nd app. | | | | |
| 0·5 | 3·4629 | 3·4696 | 3·4698 | 3·4700 | 3·318 | . . |
| 1·0 | 2·8822 | 2·9035 | 2·9046 | 2·9035 | 2·750 | 2·903 |
| 1·5 | 2·4599 | 2·4972 | 2·4977 | . . | . . | . . |
| 2·0 | 2·1488 | 2·2044 | 2·2053 | 2·2052 | . . | 2·204 |
| 2·5 | 1·9112 | 1·9852 | 1·9878 | . . | . . | . . |
| 3·0 | 1·7234 | 1·8162 | 1·8218 | 1·8211 | 1·702 | 1·8207 |

Electronic energies of the 1$s\sigma$ state of $H_2^+$.

Consider the ground state (1$s\sigma$ state) of the molecule ion, so that we have $n=l=m=0$. In that case equation (20) is reduced to the form

$$\frac{2}{3}\lambda^2+2\lambda-(2R-1)-\frac{R}{\lambda}-\left[\frac{(4/45)\lambda^4}{6-(4/21)\lambda^2}+\frac{\left(1-\frac{R}{\lambda}\right)^2}{4+2\left(2\lambda-\frac{R}{\lambda}\right)}\right]=0, \qquad \ldots \quad (21)$$

where the terms in the parenthesis are the contributions of the second-order term. In Table I. we give the calculated values of E′ for different values of R and the corresponding values of other workers. The corrections introduced by the second-order terms are small, and so it can be assumed that the approximation up to a second-order will be sufficient to give a fairly accurate result. In the second-order terms in (21) the first one is the contribution of (19) and the second one that of (15). It can easily be shown that the values of the first one becomes larger than the second one as R increases, so there is no justification in neglecting the correction terms of (19) when that of (15) has been taken. This procedure was adopted by Jaffe⁽⁵⁾. In the $1s\sigma$ state the total correction for the second-order terms is small, so the error in the results of Jaffe is not perceptible, but for higher states the calculations on the basis of Jaffe's work will lead to incorrect results.

TABLE II.

($2s\sigma$ state of $H_2^+$).

| R <br> $-E=-(E'+2/R)$ | 0·5. | 1·0. | 3·0. | 4·0. | 6·0. | 8·0. | 10·0. |
|---|---|---|---|---|---|---|---|
| Chakravarty .. | −3·0326 | −1·1329 | 0·0591 | 0·0757 | 0·1613 | 0·1942 | 0·213 |
| Morse and Stuckelberg... | −3·090 | −1·178 | −0·024 | 0·072 | .. | .. | 0·200 |
| Lennard Jones.. | .. | .. | .. | .. | 0·209 | 0·257 | 0·270 |
| Belikov and Finkelstein(10). | .. | .. | .. | .. | 0·146 | 0·184 | 0·202 |

Potential energies of the $2s\sigma$ state of $H_2^+$.

Next consider the $2s\sigma$ state of the molecule, so that we have $m=l=0$, $n=1$. So that equation (20) is reduced to the form

$$\frac{2}{3}\lambda^2+\left(1-\frac{R}{\lambda}\right)(1+2\lambda)+2\left(2+2\lambda-\frac{R}{\lambda}\right)$$

$$+\left[-\frac{(4/45)\lambda^4}{6-(4/21)\lambda^2}-\frac{2\left(2-\frac{R}{\lambda}\right)^2}{\left(4+2\lambda-\frac{R}{\lambda}\right)}+\frac{\left(1-\frac{R}{\lambda}\right)^2}{2\left(2+2\lambda-\frac{R}{\lambda}\right)}\right]=0.$$

The results have been given in Table II. This state of the molecule is clearly unstable, as has been shown by other workers. It may be noted that the total potential energy of the molecule $E=E'+\frac{2}{R}$, where in terms of the units of the present paper $\frac{2}{R}$ represents the energy of repulsion.

Next consider the $3d\sigma$ state of the molecule, so that we have $m=n=0$, $l=2$, and equation (20) is reduced to the form

$$\frac{10}{21}\lambda^2+2\lambda+(7-2R)-\frac{R}{\lambda}$$
$$+\left[-\frac{(16/245)\lambda^4}{14+\frac{4}{231}\lambda^2}+\frac{(4/45)\lambda^4}{6-(4/21)\lambda^2}-\frac{\left(1-\frac{R}{\lambda}\right)^2}{4+2\left(2\lambda-\frac{R}{\lambda}\right)}\right]=0.$$

The results have been given in Table III. The results show that the $3d\sigma$ state of the molecule is a stable one.

TABLE III.

($3d\sigma$ state of $H_2^+$.)

| R<br>$-E=-(E'+2/R)$ | 5·0. | 6·0. | 7·0. | 8·0. | 9·0. |
|---|---|---|---|---|---|
| Chakravarty .. | 0·2186 | 0·3024 | 0·3056 | 0·2878 | 0·2377 |
| Teller ........ | .. | 0·288 | 0·330 | 0·346 | 0·350 |
| Belikov and Finkelstein (10). | .. | 0·390 | 0·362 | 0·360 | 0·352 |

Potential energies of the $3d\sigma$ state of $H_2^+$.

The results show a satisfactory agreement with those of the previous workers. The defects of the previous workers will be discussed in the next section.

6. Burrau(1) obtained the energies for the different values of R only for the ground state ($1s\sigma$) by a method of numerical integration in an unsatisfactory way, which presents some defects from the standpoint of analysis. These defects have been discussed by Wilson(15). Moreover, he could not obtain any form of eigenfunction. His method cannot be applied to get similar results for the excited states.

Wilson tried to solve the same problem and discussed the nature of the possible solutions of the equations (3) and (4). He observed that a solution giving the eigenfunction cannot be obtained. To avoid the difficulties in respect of the convergency of the solutions he assumed a solution in terms of a finite series. But such an assumption gave results in contradiction with experiment. He also tried to explain the experimental results with an eigenfunction which is not bounded at $\xi=1$. Such a representation of $\Psi$ can have no physical significance. His earlier statement, that the equations (3) and (4) cannot be solved in terms of an infinite series, is no longer tenable.

Morse and Stuckelberg have calculated the electronic energies of $H_2^+$ for the ground state as well as for some other excited states of the molecule. They have obtained the values of $\Psi$ from those for the two limiting values of R, viz., 0 and $\infty$, by a method of perturbation. Naturally their results were found to be unsatisfactory. The accuracy of approximation decreases as R recedes from its limiting values, *i. e.*, 0 and $\infty$, and at values near the usual value of $R_0$, where the value of E′ is most interesting, the accuracy is least.

Teller has also made the calculations for the different states using a variation method. He separated the wave-equation in elliptic coordinates. But in solving the $\xi$-equation (12) he takes

$$\Psi(\xi)=(\xi^2-1)^{\lambda/2}e^{-\sqrt{\gamma}\xi}f(\xi), \quad \text{and} \quad x=\xi-1,$$

and reduces (12) to the form

$$x(x+2)f''(x)+2[(\lambda+1)(x+1)-\sqrt{\gamma}(x^2+2x)]f'(x)$$
$$+[\lambda(\lambda+1)-\gamma+A+\{2\epsilon+\sqrt{\gamma}(2\lambda+2)\}(x+1)]f(x)=0.$$

Since $1\leqslant\xi<\infty$, we must have $0\leqslant x<\infty$, so that the above equation is to be solved so as to have a solution in the whole range, viz., $0\leqslant x<\infty$. But the above equation has a singularity at $x=-2$, and so the solution obtained as a power series is valid only in the range $0\leqslant x<2$, and thus cannot be accepted as the solution to give the eigenfunction. Consequently his results cannot be relied upon.

Hylleraas (4) made the calculations for the $1s\sigma$ state only. But in solving equation (7 *c*) he made a mistake similar to that made by Teller. In obtaining a solution of (12*c*) he takes in (14*b*) $y=\sum_{m+1}^{\infty} c_n Y_{n-1}$. But (12*c*) has singularities at $x=0$, $x=-4\sqrt{c}$, and $\infty$. So (14 *b*) will be a solution of (12 *c*) only within the range $0\leqslant x<4\sqrt{c}$. His representation of the eigenfunction is, therefore, wrong. Jaffe tried to prove that the solution of Hylleraas is divergent, and in a later paper Hylleraas (12) tried to explain the objections raised by Jaffe. He tried to show that the solution is not divergent, and the same point was discussed by Baber and Hasse (14), and by McCrea and Newing (13). But the main defect of Hylleraas's solution has not been discussed by any one of them. The solution of

(12 *c*) has been obtained in terms of an infinite series by the method of Forbenius in the vicinity of $x=0$, which clearly has a radius of convergence $4\sqrt{c}$. So the solution obtained can in no case be valid outside this range⁽¹¹⁾ whether the infinite series (14 *b*) is a power series or a series in terms of orthogonal polynomials. Peculiarly enough the energy values obtained by him are in fair agreement with the results of the present paper. It may be observed that if $\xi$ lies between 1 and 3, then the calculations of Teller and Hylleraas are correct. But there is no justification for such a restriction to the values of $\xi$.

Jaffe ⁽⁵⁾ solved the same problem only for the ground state; but whereas he made use of equation (16) to get the value of A, and calculated up to a higher order of approximation, he took the value of A obtained from the $\eta$-equation as given by (4 *a*) or (4 *b*), which are correct only up to the zeroeth order of approximation. Thus Jaffe neglected the correction terms in (4) and took those in the case of (3) to a much higher order. In fact if he took the value of A as obtained from the $\eta$-equation to a higher order his method would become impracticable. The correction terms in the $1s\sigma$ state being very small, the error is not perceptible. Moreover, he could not indicate any method for the calculations of the higher states.

Baber and Hasse⁽¹⁴⁾ tried to solve the same problem by the use of infinite continued fractions. But in obtaining the value of A they made use of the result of Hylleraas. So the defects are the same as that of Hylleraas.

Several other workers⁽¹⁶⁾ deduced certain related phenomena on the basis of the previous workers, mainly following the works of Hylleraas. It is therefore desirable that those works should be repeated by assuming the correct form of the eigenfunction and the eigenvalue.

My thanks are due to Dr. K. Basu, of our Department, for his suggestions during the working of this problem.

*Note added in proof.*—The dissociation energy of $H_2^+$ is equal to the negative energy of $H_2^+$ in the $1s\sigma$ state with fixed nuclei in the stable position, minus the vibrational zero point energy minus the Rydberg constant, so that

$$D(H_2^+)=16{\cdot}2955-0{\cdot}1399-13{\cdot}530$$
$$=2{\cdot}625e \quad e.v.,$$

which is in very fair agreement with the experimental value. Of the three states, viz., $1s\sigma$, $2s\sigma$, $3d\sigma$ calculated, the first and the third are stable while the second is unstable, as will be evident from the tables given. But for the discrete spectrum to be possible it is necessary that there should be transition between two stable states. But here the transition between the $1s\sigma$ and $3d\sigma$ states is not possible owing to $d \rightarrow s$ prohibition. This explains the absence of a discrete spectrum for $H_2^+$. Brassfield has observed the continuous spectrum of $H_2^+$ which is possible by a transition between a stable and an unstable state, viz., between $1s\sigma$ and $2s\sigma$, etc. The results can also be used in calculating the dissociation energy of the $H_2$ molecule. The method has been discussed by Richardson (17), and a reference to that will show that the calculated results are in fair agreement with those determined experimentally.

### *References.*

(1) O. Burrau, *Det Kgl. Danske Vid Selskab*, vii. nr. 14 (1927).
(2) P. M. Morse and E. C. G. Stuckelberg, Phys. Rev. xxxiii. p. 932 (1929).
(3) E. Teller, *Zeits. für Phys.* lxi. p. 458 (1930).
(4) E. A. Hylleraas, *Zeits. für Phys.* lxxi. p. 739 (1931).
(5) G. Jaffe, *Zeits. für Phys.* lxxxvii. p. 535 (1934).
(6) I. Todhunter, ‘Algebra,’ Art. 783.
(7) Von. Koch, *Acta Mathematica*, xv. p. 53 (1891) ; xvi. p. 217 (1892).
(8) S. K. Chakravarty, *Zeits. für Phys.* cix. p. 25 (1938).
(9) V. Gullemin and C. Zener, Proc. Nat. Acad. Sci. xv. p. 314 (1929).
(10) M. V. Belikov and B. N. Finkelstein, *Phys. Zeits. d. Sowjetunion*, xii. no. 3 (1937).
(11) E. T. Whittaker and G. N. Watson, ‘Modern Analysis,’ p. 199.
(12) E. A. Hylleraas, *Annales de l'Institute Henri Poincare*, vii. p. 121 (1937).
(13) W. H. McCrea and R. A. Newing, Proc. Lond. Math. Soc. xxxvii. p. 520 (1933).
(14) W. G. Baber and H. R. Hasse, Proc. Camb. Phil. Soc. xxxi. p. 564 (1938).
(15) A. H. Wilson, Proc. Roy. Soc. cxviii. pp. 617, 637 (1928).
(16) G. Steensholt, *Zeits. für Phys.* c. p. 547 (1936) ; E. Helling, *Zeits. für Phys.* civ. p. 694 (1937) ; N. Svartholm, *Zeits. für Phys.* cxi. p. 187 (1938).
(17) O. W. Richardson, Proc. Roy. Soc. clii. p. 503 (1935).

Department of Applied Mathematics,
Calcutta University,
Calcutta, India.

# XL. *The Electrical Double Layer at the Interface of Two Liquids.*

By E. J. W. Verwey and K. F. Niessen, Natuurkundig Laboratorium der N. V. Philips' Gloeilampenfabrieken, Eindhoven, Holland *.

[Received June 7, 1939.]

## Summary.

The potential function at the interface of two liquid phases about which a small amount of electrolyte is distributed is considered. The total potential drop D, due to the circumstance that one phase contains an excess of positive ions and the other an equal excess of negative ions, is divided up into two parts, occurring on both sides of the interface, the size of which is governed by $\alpha=\sqrt{\frac{n_2K_2}{n_1K_1}}$ ($n$=ionic concentrations, K= dielectric constants) and $\Delta=\frac{\epsilon D}{kT}$. Fig. 1 shows a typical potential curve, fig. 2 the corresponding charge curve, for small values of D. The largest part of the potential drop occurs in the phase where the product $nK$ has the smallest value. For the general case that $\alpha$ differs appreciably from one practically the whole potential drop occurs in one phase, provided D is not very large. This does not necessarily imply that the rates of decay of the charge density on both sides of the interface are very different. For larger values of D the partition of the potential drop about both phases becomes less unequal, and approaches equal parts on both sides for very large values of D (fig. 3, where $-z_1$ and $z_2$ are proportional to the partial potential drop in liquid 1 resp. 2).

### 1. *Introduction.*

The most simple case of an electrical double layer caused by a distribution equilibrium of potential determining ions ⁽¹⁾ is the case of two liquids in contact with each other. Except when at least one of the liquids is non-polar, and the solubility or electrolytic dissociation of electrolytes accordingly zero, every electrolyte added to the system, even in very small amounts, acts as a potential determining electrolyte. The electrolyte, apart from being generally distributed unequally about both phases, builds up an electrical double layer at the interface as a consequence of the generally unequal distribution coefficients of the positive and the negative ion (Nernst, van Laar (2)). Systems of this type have been investigated extensively by several authors, in accordance with their importance from a biological (3), colloid-chemical (4), and electrochemical (5) point of view.

---

* Communicated by the Authors.

In these systems we are dealing with a double layer with both layers falling into a solution phase, *i. e.*, according to the theory of Gouy (6) and Chapman (7) with a double layer which will have two "diffuse" layers.

The general properties of such a double layer have not been considered hitherto. In the present note we want to examine the distribution of the charges and the potential function in the neighbourhood of the interface. This problem has a bearing on a number of phenomena in which the electrical conditions at the interface play a part; as an example we mention the problem of the stability of emulsions *.

## 2. *Derivation of the General Potential Curve.*

We consider two liquid phases 1 and 2 in equilibrium with each other, with dielectric constants $K_1$ and $K_2$ and ionic concentrations $n_1$ and $n_2$ ions per cm.$^3$. For sake of simplicity all ions will be assumed to be monovalent. The $x$-axis is perpendicular to the interface; $x$ varies from $-\infty$ to 0 in phase 1; from 0 to $+\infty$ in phase 2. The interface is supposed to be a mathematical plane. Adsorption forces, and also the influence of finite dimensions of the ions, will be left out of the discussion (8). The solutions will therefore be considered to be diluted. The boundary potential drop (contact potential) between the uncharged liquids is probably not influenced by the presence of small amounts of electrolytes; the total potential drop is therefore a superposition of this boundary potential (due to oriented dipoles etc. and located in the immediate neighbourhood of the interface) and the double layer potential (due to free charges, *i. e.*, ions, and stretched out over a range of a great number of molecular dimensions, especially for diluted solutions). The potential curves (such as given in fig. 1) show therefore in reality a jump at the interface (say, $\chi$) shifting the whole potential curve in one phase a constant amount $\chi$ with respect to that in the other. For sake of convenience we take this constant boundary potential $\chi$ to be zero. We will measure the potential in phase 1 from the level $\phi_1$, in phase 2 from the level $\phi_2$ ($\phi_1$ and $\phi_2$ are the potentials in the bulk phases, $x=-\infty$ and $x=+\infty$; *cf.* fig. 1):

$$\psi_1(x)=\phi_1(x)-\phi_1\,;\quad \psi_2(x)=\phi_2(x)-\phi_2.$$

---

* E. J. W. Verwey, a paper to appear in the Transactions of the Faraday Society ("General Discussion on the Electric Double Layer," pp. 25–27 (Sept. 1939)). Also extension of the theory for the interaction of two double layers.

We start from the well-known differential equation of Gouy and Chapman, embracing the equilibrium of the electrical forces and the thermal agitation of the ions, which is obtained by applying Poisson's equation

$$4\pi\rho = -K\frac{d^2\psi}{dx^2}$$

Fig. 1.

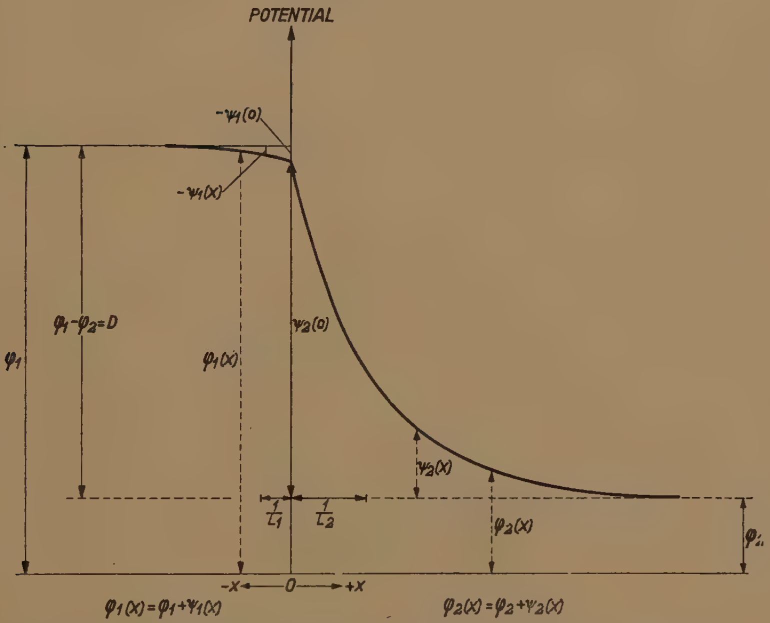

Potential distribution for small double layer potential values:

$$\sqrt{\frac{n_2K_2}{n_1K_1}} = \frac{1}{27};\ \sqrt{\frac{n_1K_2}{n_2K_1}} = 3.$$

At distances $\frac{1}{L_1}$ and $\frac{1}{L_2}$ from the interface the potentials $-\psi_1$ and $\psi_2$ have fallen off to $\frac{1}{e}$ of $-\psi_1(0)$ and $\psi_2(0)$.

and Boltzmann's theorem for the calculation of the space-charge

$$\rho(x)=\epsilon(n^+-n^-);\ n^+=n.\exp.\left(-\frac{\epsilon\psi}{kT}\right);\ n^-=n.\exp.\left(\frac{\epsilon\psi}{kT}\right):$$

$$\frac{d^2\psi}{dx^2}=\frac{4\pi\epsilon n}{K}\cdot\left\{e^{\frac{\epsilon\psi}{kT}}-e^{-\frac{\epsilon\psi}{kT}}\right\}, \quad . \quad . \quad . \quad . \quad . \quad (1\,a)$$

which we will simplify by writing

$$y=\frac{\epsilon\psi}{k\mathrm{T}},\quad \mathrm{L}=\sqrt{\frac{8\pi\epsilon^2 n}{\mathrm{K}k\mathrm{T}}},\quad \xi=x\mathrm{L}:$$

$$2\frac{d^2y}{d\xi^2}=e^y-e^{-y}. \qquad (1\,b)$$

A special solution, considering the limiting condition $\frac{dy}{d\xi}=0$ and $y=0$ for $\xi=\infty$ or $-\infty$, is

$$\frac{dy}{d\xi}=\pm(e^{\frac{y}{2}}-e^{-\frac{y}{2}}).$$

In phase 1 $\frac{d\psi}{dx}$ and $\psi$ have equal signs, in phase 2 the signs are mutually opposite, whence

$$\frac{dy_1}{d\xi_1}=e^{\frac{y_1}{2}}-e^{-\frac{y_1}{2}} \text{ and } \frac{dy_2}{d\xi_2}=e^{-\frac{y_2}{2}}-e^{\frac{y_2}{2}}. \qquad (2)$$

Equations (2), or similar forms, have been used for the case of a double layer at the interface of a solid and an electrolytic solution by several authors (6), (7), (8), (9). Before integrating a second time, in order to find expressions for $y_1(\xi_1)$ and $y_2(\xi_2)$, we will derive the equations giving the values of the potential drop in each of the phases as a function of the total potential drop. This partition of the double layer potential $\mathrm{D}=\phi_1-\phi_2$ about both phases is expressed by the quantities $y_1(0)$ and $y_2(0)$ $(\xi=0)$, which will be denoted by $z_1$ and $z_2$:

$$z_1=y_1(0)=\frac{\epsilon\psi_1(0)}{k\mathrm{T}},$$

$$z_2=y_2(0)=\frac{\epsilon\psi_2(0)}{k\mathrm{T}},$$

of which $z_1$ is negative in fig. 1.

In order to express $z_1$ and $z_2$ as physical constants of the system we consider the limiting conditions at the interface.

The first condition (since the boundary potential $\chi$ was taken to be zero) is $\phi_1(x)=\phi_2(x)$ for $x=0$, and introduces the double layer potential $\mathrm{D}=\phi_1-\phi_2$:

$$\phi_1(0)=\phi_2(0),\quad \phi_1-\phi_2=\mathrm{D}=-\psi_1(0)+\psi_2(0),$$

or

$$-z_1+z_2=\frac{\epsilon\mathrm{D}}{k\mathrm{T}}=\triangle. \qquad (3)$$

The second condition is that the double layer as a whole is electrically neutral:

$$\int_{-\infty}^{0}\rho_1(x)\,dx+\int_{0}^{\infty}\rho_2(x)\,dx=0, \text{ or}$$

$$-\frac{K_1}{4\pi}\int_{-\infty}^{0}\frac{d^2\psi_1}{dx^2}dx-\frac{K_2}{4\pi}\int_{0}^{\infty}\frac{d^2\psi_2}{dx^2}dx=0, \text{ or}$$

$$K_1\left(\frac{d\psi_1}{dx}\right)_0=K_2\left(\frac{d\psi_2}{dx}\right)_0, \text{ or}$$

$$K_1L_1\left(\frac{dy_1}{d\xi_1}\right)_0=K_2L_2\left(\frac{dy_2}{d\xi_2}\right)_0. \quad \ldots\ldots \quad (4)$$

These conditions, (3) and (4), give us together the desired equations for $z_1$ and $z_2$. The $\frac{dy}{d\xi}$ values for $x=0$ can be derived directly from eq. (2), whence

$$K_1L_1(e^{\frac{z_1}{2}}-e^{-\frac{z_1}{2}})=K_2L_2(e^{-\frac{z_2}{2}}-e^{\frac{z_2}{2}}). \quad \ldots\ldots \quad (5)$$

From (3) and (5) we can now solve the unknown constants $z_1$ and $z_2$; writing

$$\alpha=\frac{K_2L_2}{K_1L_1}=\sqrt{\frac{n_2K_2}{n_1K_1}},$$

we have
$$e^{\frac{z_1}{2}}-e^{-\frac{z_1}{2}}=\alpha(e^{-\frac{\Delta}{2}}.e^{-\frac{z_1}{2}}-e^{\frac{\Delta}{2}}e^{\frac{z_1}{2}}) \text{ or}$$

$$e^{z_1}=\frac{1+\alpha.e^{-\frac{\Delta}{2}}}{1+\alpha.e^{\frac{\Delta}{2}}} \text{ and } e^{z_2}=\frac{1+1/\alpha.e^{\frac{\Delta}{2}}}{1+1/\alpha.e^{-\frac{\Delta}{2}}}, \quad \ldots\ldots \quad (6)$$

or
$$-z_1=lg(1+\alpha e^{\frac{\Delta}{2}})-lg(1+\alpha e^{-\frac{\Delta}{2}})$$

$$z_2=lg\left(1+\frac{1}{\alpha}.e^{\frac{\Delta}{2}}\right)-lg\left(1+\frac{1}{\alpha}.e^{-\frac{\Delta}{2}}\right),$$

The partial potential drops in the phases 1 and 2 are now expressed into $\Delta$ and $\alpha$.

Furthermore, the complete potential function in both phases can be found by integrating equations (2) a second time; this integration yields

$$\frac{e^{\frac{y_1}{2}}-1}{e^{\frac{y}{2}}+1}=\gamma_1e^{\xi_1} \text{ and } \frac{e^{\frac{y_2}{2}}+1}{e^{\frac{y_2}{2}}-1}=\gamma_2e^{\xi_2},$$

where the integration constants $\gamma_1$ and $\gamma_2$ can be expressed into $z_1$ and $z_2$ (known from eq. (6)) by putting $\xi_1=0$ and $\xi_2=0$. The equations for $y_1$ and $y_2$ can be then brought into the following form:

$$\left.\begin{aligned} e^{\frac{y_1}{2}}&=\frac{1+\gamma_1e^{\xi_1}}{1-\gamma_1e^{\xi_1}} \text{ with } \gamma_1=\frac{e^{\frac{z_1}{2}}-1}{e^{\frac{z_1}{2}}+1},\\ e^{\frac{y_2}{2}}&=\frac{\gamma_2.e^{\xi_2}+1}{\gamma_2.e^{\xi_2}-1} \text{ with } \gamma_2=\frac{e^{\frac{z_2}{2}}+1}{e^{\frac{z_2}{2}}-1},\end{aligned}\right\} \quad \ldots\ldots \quad (7)$$

giving, together with eq. (6), the *general solution for the potential function in both phases* :

$$\psi_1(x)=\frac{kT}{\epsilon}\,y_1(L_1x) \text{ and } \psi_2(x)=\frac{kT}{\epsilon}\,y_2(L_2x), \quad . \quad . \quad . \quad . \quad (8)$$

where

$$\Delta=\frac{\epsilon D}{kT},\quad \xi=Lx,\quad L_1=\sqrt{\frac{8\pi n_1\epsilon^2}{K_1kT}},\quad L_2=\sqrt{\frac{8\pi n_2\epsilon^2}{K_2kT}},\quad \alpha=\sqrt{\frac{n_2K_2}{n_1K_1}}. \quad (9)$$

*Eq.* (6), (7), (8), *and* (9) *express* $\psi_1$ *and* $\psi_2$ *completely into* $n_1$, $n_2$, $K_1$, $K_2$. *and* D.

$-\psi_1(x)$ is the local potential drop in liquid 1 (reckoned from left to right in fig. 1) and $\psi_2(x)$ that in liquid 2.

### 3. *Discussion and Approximations in Special Cases.*

From the eq. (6) we directly read that $z_1$ and $z_2$ always have opposite signs, which means that the potential drops continually from the interior of one phase to the interior of the other. The fractions of the total potential drop occurring in one phase are governed by the factor

$$\alpha=\sqrt{\frac{n_2K_2}{n_1K_1}},$$

and it is readily seen that for $\alpha\lessgtr 1$ we have $-z_1\lessgtr z_2$.

We will consider eq. (6), giving $z_1$ and $z_2$ as functions of $\Delta$ and $\alpha$, in some more detail. Their properties depend greatly on the numerical values of $\Delta$ and $\alpha$.

As to the value of $\Delta$, we may state that absolute values of the double layer potential have only been determined in a few cases, viz., Hg/water and AgI/water (9) ; for systems as considered here we only know double layer potential values containing unknown constants. From the measurements of Beutner or Freundlich and Gyemant it may be concluded, however, that the absolute value of D is of the order of a few hundred millivolts or less, *i. e.*, $\left|\frac{\Delta}{2}\right|$ is often of the order 1 ($\Delta=2$ is at room-temperature, D=50 mv.). Hence we cannot cover eq. (6) by considering merely one of the extreme cases

$$\left|\frac{\Delta}{2}\right| \ll 1 \text{ or } \left|\frac{\Delta}{2}\right| \gg 1.$$

The factor $\alpha$ contains both $n$ and K of the phases. We will not consider non-equilibrium cases ; the systems dealt with in colloid chemistry are generally in equilibrium as to the mutual solubility of the solvents and the distribution equilibrium of the electrolytes about both phases. The two liquids of the system are therefore partly miscible or practically immiscible, and we must expect that the dielectric constants $K_1$ and $K_2$ will very rarely have about equal values. If $K_1 > K_2$ we must expect that generally both the solubility of the electrolyte and the grade of dissociation in phase 2 will be lower than in phase 1, *i. e.*, generally $n_1 \gg n_2$ and $\alpha \ll 1$. In the inverse case $K_1 < K_2$, of course, we will generally find that $\alpha \gg 1$.

In the following we will only consider separately the cases that $\alpha \sim 1$ and $\alpha \ll 1$. Since the third case, $\alpha \gg 1$, is not principally different from $\alpha \ll 1$, and can be transformed into the latter by interchanging the phases, the second case $\alpha \ll 1$ may be considered to cover the general case that $\alpha$ differs considerably from 1, realized in most of the practically occurring systems.

When the indices of the phases are chosen in such a way that $\alpha$ is always smaller than 1 the double layer potential D can be still positive or negative. In the following we will assume arbitrarily that D (and $\Delta$) is positive, and therefore $z_1$ negative and $z_2$ positive; the opposite case, however, leads to analogous equations.

The dependence of the parameters $-z_1$ and $z_2$ (proportional to the partial potential drops in the phases 1 and 2) on $\alpha$ and $\Delta$ will be given sufficiently by $-z_1$, since $-z_1 + z_2 = \Delta$. The general equation is

$$-z_1 = lg(1 + \alpha e^{\frac{\Delta}{2}}) - lg(1 + \alpha . e^{-\frac{\Delta}{2}}), \quad . \quad . \quad . \quad . \quad . \quad (10)$$

for which the following approximations can be given in the special cases given below:

$$\frac{\Delta}{2} \gg 1, \quad \alpha \sim 1, \quad -z_1 = \frac{\Delta}{2} + lg\, \alpha, \quad . \quad . \quad . \quad . \quad . \quad . \quad . \quad (10\,a)$$

$$\alpha \ll 1, \quad -z_1 = lg(1 + \alpha e^{\frac{\Delta}{2}}), \quad . \quad . \quad . \quad . \quad . \quad . \quad (10\,b)$$

$$\alpha e^{\frac{\Delta}{2}} \ll 1, \quad -z_1 = \alpha e^{\frac{\Delta}{2}}, \quad . \quad . \quad . \quad . \quad . \quad . \quad . \quad . \quad . \quad . \quad (10\,c)$$

$$\frac{\Delta}{2} \text{ arbitrary}, \quad \alpha e^{\frac{\Delta}{2}} \ll 1, \quad -z_1 = \alpha(e^{\frac{\Delta}{2}} - e^{-\frac{\Delta}{2}}), \quad . \quad . \quad . \quad . \quad . \quad . \quad (10\,d)$$

$$\frac{\Delta}{2} \ll 1, \quad \alpha \text{ arbitrary}, \quad -z_1 = \frac{\alpha}{1+\alpha}\Delta; \quad z_2 = \frac{1}{1+\alpha}\Delta. \quad . \quad . \quad (10\,e)$$

The general properties of eq. (10) can be examined very conveniently with the aid of these simplified relations.

It is interesting to consider also the simplified relations for the potential, *i. e.*, for $y_1$ and $y_2$. In some cases $z_2$ becomes practically identical with $\Delta$ (see, for instance, eq. (10 *e*) for $\alpha \ll 1$); the potential in one phase can therefore vary between the same limits as $\Delta$. We will consider the cases $z_2 \gg 1$, $z_2 \sim 1$, and $z_2 \ll 1$. The formulæ given above teach to which case a certain system of two phases belongs. The equations for $-y_1$ can be obtained from those for

$y_2$ by substituting $\xi_2$ and $z_2$ by $-\xi_1$ and $-z_1$; hence we only give approximations for $y_2$, where $z_2$ was chosen to be positive.

The general equation, expressed in $z_2$, is

$$e^{\frac{y_2}{2}}=\frac{(e^{\frac{z_2}{2}}+1)e^{\xi_2}+(e^{\frac{z_2}{2}}-1)}{(e^{\frac{z_2}{2}}+1)e^{\xi_2}-(e^{\frac{z_2}{2}}-1)}, \quad . \quad . \quad . \quad . \quad . \quad . \quad . \quad (11)$$

and we will examine this function especially for small, moderate, and large values of $\xi_2$. We have the following cases:

$$z_2 \geqslant 1;\ \xi_2 \geqslant 1, \quad y_2=4e^{-\xi_2}, \quad . \quad . \quad . \quad . \quad . \quad . \quad . \quad . \quad . \quad . \quad (11\,a)$$

$$\xi_2 \sim 1, \quad e^{\frac{y_2}{2}}=\frac{1+e^{-\xi_2}}{1-e^{-\xi_2}}, \quad . \quad . \quad . \quad . \quad . \quad . \quad . \quad . \quad (11\,b)$$

$$\xi_2 \leqslant 1, \quad y_2=-2lg\left(\frac{\xi_2}{2}+e^{-\frac{2}{2}}\right), \quad . \quad . \quad . \quad . \quad . \quad (11\,c)$$

limiting value $\xi_2 \rightarrow 0: y_2=z_2-e^{\frac{z_2}{2}}\cdot\xi_2$,

$$z_2 \sim 1;\ \xi_2 \geqslant 1, \quad y_2=4\frac{e^{\frac{z_2}{2}}-1}{e^{\frac{z_2}{2}}+1}e^{\xi_2}, \quad . \quad . \quad . \quad . \quad . \quad . \quad . \quad . \quad (11\,d)$$

$\xi_2 \sim 1$, general formula

$$\xi_2 \leqslant 1, \quad y_2=z_2-(e^{\frac{z_2}{2}}-e^{-\frac{z_2}{2}})\xi_2, \quad . \quad . \quad . \quad . \quad . \quad (11\,e)$$

$$z_2 \leqslant 1;\ \xi_2 \text{ arbitrary}, \quad y_2=z_2e^{-\xi_2}. \quad . \quad . \quad . \quad . \quad . \quad . \quad . \quad . \quad (11f)$$

### 4. *The Partition of the Potential Drop about both Phases.*

The most simple equations for $z_1$, $z_2$ (and $y_1$ and $y_2$) are obtained for the case that $\frac{\Delta}{2} \leqslant 1$ (eq. (10 $e$) and (11 $f$)). In the generally occurring case that $\alpha$ is very different from 1, in our case $\alpha \leqslant 1$, we see that also a very small fraction of the double layer potential falls into the phase 1, the phase with the largest value of $n$K, whereas practically the whole potential drop occurs in phase 2, where $n$K and therefore generally the dielectric constant is small.

The potential falls off with an exponential function of $x$ governed by $L_1$ and $L_2$. Since, for small values of $\Delta$, the equation for $\rho(x)=\epsilon(n^+-n^-)=$

$$n\epsilon\left\{\exp\left(-\frac{\epsilon\psi}{kT}\right)-\exp\left(\frac{\epsilon\psi}{kT}\right)\right\}$$

simplifies to

$$\rho(x)=-\frac{2n\epsilon^2}{kT}\cdot\psi(x),$$

the same holds for the decay of the charge at both sides of the interface.

The " thickness " of the diffuse layer (given by the distance where the charge density has fallen off to the $1/e$ part) in phase 2 is therefore

$$\frac{L_1}{L_2}=\sqrt{\frac{n_1K_2}{n_2K_1}}$$

times that in phase 1, and accordingly the density of the charge in the immediate neighbourhood of the interface is also

$$\sqrt{\frac{n_1K_2}{n_2K_1}}$$

times that in phase 2. We have seen that for $K_1>K_2$, mostly also $n_1>n_2$ (or even $n_1\gg n_2$),

$$\sqrt{\frac{n_2K_2}{n_1K_1}}=\alpha$$

Fig. 2.

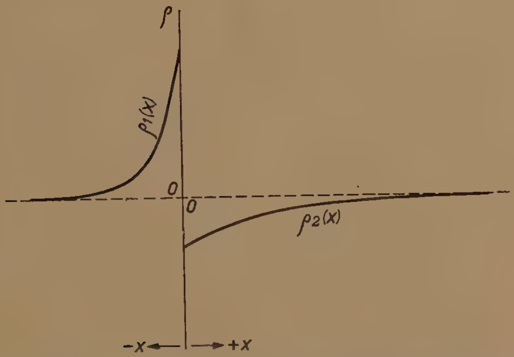

Distribution of the charges, corresponding to fig. 1.

may therefore be very small, although

$$\sqrt{\frac{n_1K_2}{n_2K_1}}$$

does not differ so much from unity. *A very unequal distribution of the potential drop about both phases therefore does not necessarily imply that the " thicknesses " of the diffuse layers are very different, nor the densities of the charge on both sides of the interface.* This may be illustrated by fig. 1 and fig. 2, showing the potential function (for small values of $\Delta$) and the charge distribution if we take

$$\frac{K_1}{K_2}=3^2=9,\quad \frac{n_1}{n_2}=3^4=81,$$

and accordingly

$$\alpha=3^{-3}=\frac{1}{27}\quad\text{and}\quad\frac{L_1}{L_2}=\sqrt{\frac{81}{9}}=3.$$

According to eq. (10 $e$) 1/28 of the double layer potential drop occurs in phase 1, 27/28 in phase 2. The rate of decay of the charge and of the potential in both phases does not differ so much ; the " thickness " of the diffuse layer in phase 2 is only three times that in phase 1.

For large values of $\Delta$ these conclusions are no longer true. Fig. 3 shows $-\frac{z_1}{\Delta}$, the fraction of the potential drop occurring in phase 1, as a function of $\Delta$ (eq. 10)), where $\alpha$ again has been taken 1/27. Although $\alpha$ is not extremely small eq. (10 $e$) is seen to hold very well for $\Delta \leq 1$, *i. e.*, $D > 25$ mv. For larger values of $\Delta$ the fraction $-\frac{z_1}{\Delta}$ increases, and for

Fig. 3.

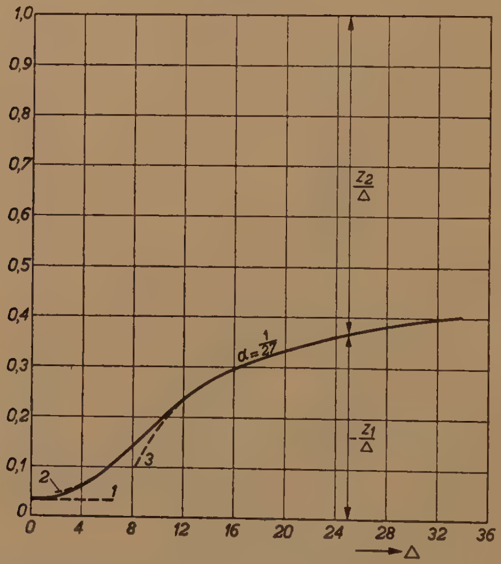

Fraction of the potential drop occurring in phase 1, with $\sqrt{\frac{n_2K_2}{n_1K_1}} = \frac{1}{27}$, for different values of the double layer potential $\left(\frac{-z_1}{\Delta} = \frac{-\psi_1(0)}{D}\ ;\ \Delta = \frac{\epsilon D}{kT}\right)$, according to eq. (10).

Curve 1 : $-z_1 = \frac{a}{1+a} \cdot \Delta = \frac{1}{28} \Delta.$

Curve 2 : $-z_1 = lg(1+a \, . \, e^{\frac{\Delta}{2}}) = lg\left(1 + \frac{1}{27} \cdot e^{\frac{\Delta}{2}}\right).$

Curve 3 : $-z_1 = \frac{\Delta}{2} + lg a$ or $-\frac{z_1}{\Delta} = \frac{1}{2} - \frac{lg\,27}{\Delta}.$

very large values of $\varDelta$ approaches $\frac{1}{2}$; as soon as $\varDelta$ exceeds the value 4 (*i. e.*, $D \geqq 100$ mv.) $-z_1$ is very well reproduced by the approximative equation (10 *b*).

*The very unequal partition of the potential drop about both phases for $\alpha$ differing appreciably from* 1, *found for small values of the double layer potential, appears to become less unequal for large values of $\varDelta$; for sufficiently large values of $\varDelta$ the potential drop tends to be divided equally about both phases.* These high values of D (of the order of 1 volt) are hardly ever realized; but $\varDelta$ values between 5 and 10 may be expected in many systems, and here the fraction of the potential drop occurring in the phase with the largest dielectric constant is already several times that for $\varDelta=1$.

Fig. 4.

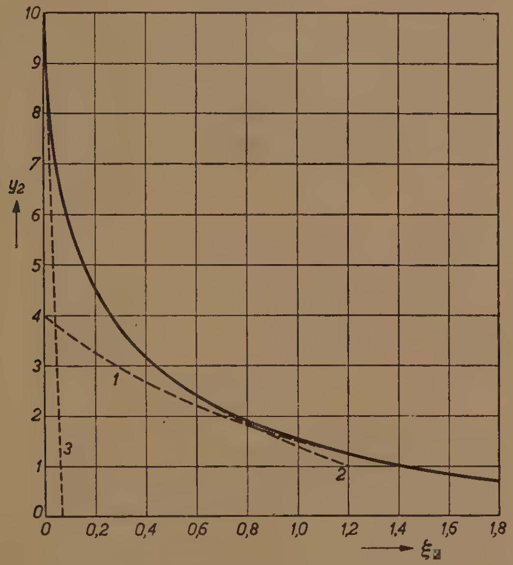

Potential function in one phase as a function of $\xi_2 = \varkappa L_2$, for $z_2 = 10$ or $\psi_2(0) = 250$ mv. (eq. 11).

Curve 1: $y_2 = 4e^{-\xi_2}$.

Curve 2: $y_2 = -2\,lg\left(\frac{\xi_2}{2} + e^{-\frac{z_2}{2}}\right) = -2\,lg\left(\frac{\xi_2}{2} + e^{-5}\right)$.

Curve 3: $y_2 = z_2 - e^{\frac{z_2}{2}}.\xi_2 = 10 - e^{+5}.\xi_2$.

Also the equations for $y_2$ are more complicated for large values of $z_2$. Fig. 4 shows the potential function in the case that $z_2 = 10(\psi_2(0) = 250$ mv.). We see that the curve for the general equation (7) is very well approached by eq. (11 *a*) as soon as $\xi_2$ exceeds the value 1, and by (11 *c*) for $\xi_2<0{\cdot}8$. For $\xi_2>1$ the potential function is therefore completely independent of the value of $z_2$ (*i. e.*, of the part of the curve for $\xi_2<1$), and again attains a simple exponential form.

## *References.*

(1) *Cf.* for instance E. J. W. Verwey, Chem. Rev. xvi. p. 369 (1935); 'Hydrophobic Colloids,' p. 58 (1937).

(2) *Cf.* for instance J. J. van Laar, 'Lehrbuch der theoretischen Elektrochemie,' pp. 117–128 (1910).

(3) R. Beutner, 'Die Erzeugung galvanischer Ströme im lebenden Gewebe' (1920).

(4) H. Freundlich and A. Gyemant, *Z. physikal. Chem.* c. p. 182 (1922).

(5) N. Bjerrum and E. Larsson, *ibid.* cxxvii. p. 358 (1927).

(6) G. Gouy, *J. de Physique* (4), ix. p. 457 (1910); *Ann. de Physique* (9), vii. p. 129 (1917).

(7) D. L. Chapman, Phil. Mag. (6) xxv. p. 475 (1913).

(8) O. Stern, *Z. Elektrochemie*, xxx. p. 508 (1924).

(9) E. J. W. Verwey, Chem. Rev. xvi. p. 363 (1935).

Eindhoven.
9th March, 1939.

# XLI. *The Periodic Flow of Heat in a Hollow Cylinder.*

By J. H. Awbery, B.A., B.Sc., Physics Department,
The National Physical Laboratory, Teddington, Middlesex *.

[Received August 12, 1939.]

## Abstract.

The problem of the flow of heat in a hollow cylinder, when the temperature of the inner wall is constrained to vary periodically, and the heat loss from the outer surface is proportional to its temperature excess over the surroundings, is investigated mathematically. The theory has applications to the heat phenomena in the cylinder of an engine, and would also be needed in determining the thermal diffusivity of a metal experimentally by measurements of temperature waves in a hollow rod.

The various Bessel functions occurring in the solution are complex numbers, though the expressions for such physical quantities as the amplitude and phase lag reduce to real numbers. The formulæ are written (in terms of the real and imaginary parts of the Bessel functions) so as to exhibit these quantities in a purely real form.

The thermal diffusivity of a metal, as a property governing the heat flow and temperature distribution in a non-steady state, must be measured in such a state. Many of the advantages of steady state measurements are retained, however, by using the quasi-steady state which results when the heat-flow and temperature are caused to fluctuate periodically. A similar periodic state of affairs occurs in the cylinder of the steam-engine, where there is a supply of heat once in each cycle, and on both accounts it has seemed worth while to calculate the temperature distribution in a hollow cylinder of which the inner wall is caused to vary sinusoidally in temperature.

In the case of the steam-engine cylinder, the curve of heat supply, though periodic, is not sinusoidal, but since any periodic curve can be built up from sinusoidal components, it suffices to consider one only of these components, having a period which we write as $2\pi/\alpha p$.

Although the temperature distribution will at first depend on the initial state of the cylinder, the temperature will eventually settle down

---

* Communicated by the Author.

everywhere to a periodic variation with the same period as the impressed distribution, and it is this quasi-steady state alone which we propose to investigate. The cylinder will be treated as indefinitely long, so that end effects do not occur, and the temperature $\theta$ will be a function only of $r$, the distance from the axis of the cylinder, and of $t$, the time.

Under these conditions, the temperature at $r$ and $t$ must be of the form $\theta=\theta_3+\mathrm{C}\log r+\theta e^{ip\alpha t}$, where $\theta$ is a function of $r$ only, and the real part is to be taken. This form allows for variations of phase and amplitude, but not period, from point to point of the cylinder.

Substituting this expression in the fundamental equation of heat-flow

$$\frac{\partial\theta}{\partial t}=\alpha\left(\frac{\partial^2\theta}{\partial r^2}+\frac{1}{r}\frac{\partial\theta}{\partial r}\right), \quad . \quad . \quad . \quad . \quad . \quad . \quad . \quad (1)$$

where $\alpha$ is the thermal diffusivity of the material of the cylinder, it leaves the constants $\theta_3$ and C arbitrary and yields a differential equation for $\theta$, of which the general solution is

$$\theta=\mathrm{AJ}_0(ri^{3/2}p^{1/2})+\mathrm{BN}_0(ri^{3/2}p^{1/2}). \quad . \quad . \quad . \quad . \quad . \quad . \quad (2)$$

Thus the solution of equation (1) is

$$\theta=\theta_3+\mathrm{C}\log r+[\mathrm{AJ}_0(ri^{3/2}p^{1/2})+\mathrm{BN}_0(ri^{3/2}p^{1/2})]e^{i} \quad , \quad . \quad . \quad (3)$$

where $\mathrm{N}_0$ is written for Neumann's function of the second kind, viz.:

$$\mathrm{N}_0(x)=-\frac{2}{\pi}\mathrm{K}_0(x)=-\frac{2}{\pi}\left[\mathrm{J}_0(x)\log x+\frac{x^2}{2^2}-(1+\tfrac{1}{2})\frac{x^4}{2^2.4^2}+\ldots\right].$$

We have now to adjust the constants in (3) to fit the boundary conditions, which, at the inner boundary $r=a$, will be taken as $\theta=\theta_2+\theta_1e^{ip\alpha t}$, and at the outer boundary $r=b$ as $-\kappa\partial\theta/\partial r=\mathrm{E}(\theta-\theta_0)$, where $\kappa$ is the thermal conductivity. Thus Newton's law is obeyed here, with a rate of heat loss E per unit area per unit temperature excess over the surroundings which are at temperature $\theta_0$.

These conditions lead to the equations

$$\theta_3+\mathrm{C}\log a=\theta_2$$
$$-\kappa\mathrm{C}/b=\mathrm{E}(\theta_3-\theta_0+\mathrm{C}\log b),$$

and to the pair

$$\mathrm{AJ}_0(ai^{3/2}p^{1/2})+\mathrm{BN}_0(aip^{3/2})=\theta_1 \quad . \quad . \quad . \quad . \quad . \quad (4)$$

$$\kappa i^{3/2}p^{1/2}[\mathrm{AJ}_1(bi^{3/2}p^{1/2})+\mathrm{BN}_1(bi^{3/2}p^{1/2})]=\mathrm{E}[\mathrm{AJ}_0(bi^{3/2}p^{1/2})+\mathrm{BN}_0(bi^{3/2}p^{1/2})], \quad . \quad . \quad . \quad (5)$$

whence

$$\mathrm{C}=\mathrm{E}(\theta_2-\theta_0)/(\mathrm{E}\log a/b-\kappa/b),$$
$$\theta_3=\frac{\mathrm{E}(\theta_0\log a-\theta_2\log b)-\kappa\theta_2/b}{\mathrm{E}\log(a/b)-\kappa/b},$$
$$\mathrm{A}=\theta_1[\mathrm{EN}_0(i^{3/2}p^{1/2}b)-\kappa i^{3/2}p^{1/2}\mathrm{N}_1(i^{3/2}p^{1/2}b)]/\mathrm{D},$$
$$\mathrm{B}=\theta_1[\kappa i^{3/2}p^{1/2}\mathrm{J}_1(i^{3/2}p^{1/2}b)-\mathrm{EJ}_0(i^{3/2}p^{1/2}b)]/\mathrm{D},$$

where

$$D=\kappa i^{3/2}p^{1/2}\{N_0(i^{3/2}p^{1/2}a)J_1(i^{3/2}p^{1/2}b)-J_0(i^{3/2}p^{1/2}a)N_1(i^{3/2}p^{1/2}b)\}$$
$$-E\{N_0(i^{3/2}p^{1/2}a)J_0(i^{3/2}p^{1/2}b)-J_0(i^{3/2}p^{1/2}a)N_0(i^{3/2}p^{1/2}b)\}.$$

Thus finally the temperature $\theta$ is given by (the real part of)

$$\frac{E(\theta_0 \log a-\theta_2 \log b)-\kappa\theta_2/b}{E \log a/b-\kappa/b}+\frac{E(\theta_2-\theta_0) \log r}{E \log a/b-\kappa/b}$$
$$+\theta_1 e^{ip\alpha t}[\{EN_0(i^{3/2}p^{1/2}b)-\kappa i^{3/2}p^{1/2}N_1(i^{3/2}p^{1/2}b)\}J_0(i^{3/2}p^{3/2}r)$$
$$+\{\kappa i^{3/2}p^{1/2}J_1(i^{3/2}p^{1/2}b)-EJ_0(i^{3/2}p^{1/2}b)\}N_0(i^{3/2}p^{1/2}r)]/D.$$

The coefficient of $e^{ip\alpha t}$ is of course complex, corresponding to the fact that the phase of the temperature wave varies with the radius. The expression given above is, however, quite suitable for numerical computation, since the various Bessel functions are given in the form $(x+iy)$ in tables in Jahnke and Emde's 'Funktionentafeln.' The actual quantities tabulated are $J_0(x\sqrt{i})$ $\sqrt{i}J_1(x\sqrt{i})$, $H_0^{(1)}(x\sqrt{i})$ and $\sqrt{i}H_1^{(1)}(x\sqrt{i})$, the first pair on pages 246 to 251 and the second pair (the Hankel functions) on pp. 252 to 257. The Neumann function is obtained from the Hankel function by the formula $N_r(z)=J_r(z)-H_r^{(1)}(z)$, and the functions of argument $ni^{3/2}$ are deduced from those of argument $ni^{1/2}$ by means of the following relations, which follow from the expansions of the Bessel functions in convergent series.

If $J_0(x\sqrt{i})=L+iM$ then $J_0(xi^{3/2})=L-iM$,
,, $N_0(x\sqrt{i})=N+iP$ ,, $N_0(xi^{3/2})=N-iP$,
,, $\sqrt{i}J_1(x\sqrt{i})=Q+iS$ ,, $\sqrt{i}J_1(xi^{3/2})=-S-iQ$,
,, $\sqrt{i}N_1(x\sqrt{i})=T+iW$ ,, $\sqrt{i}N_1(xi^{3/2})=-W-iT$.

In fact, using this notation, with $x=p^{1/2}r$ and denoting values for $r=b$ by primes ($'$) the coefficient of $\theta_1 e^{ip\alpha t}$ is found to be

$$\frac{F(r)+iG(r)}{F(a)+iG(a)},$$

where $F(r)=E(LN'-MP'-L'N+M'P)+Kp^{1/2}(MW'+NQ'-PS'-LT')$

and $G(r)=E(M'N+L'P-MN'-LP')+Kp^{1/2}(MT'+LW'-NS'-PQ')$.

### *Amplitude and Phase of Wave at Radius r.*

The amplitude and phase of the temperature wave, which are the quantities of most interest in practice, take simple forms in terms of the functions F and G, which, as has been shown, are immediately expressible in terms of tabulated quantities. The amplitude is in fact found to be

$$\theta_1\left[\frac{\{F(r)\}^2+\{G(r)\}^2}{\{F(a)\}^2+\{G(a)\}^2}\right]^{1/2},$$

and the phase angle $p$ is

$$\arctan\,[F(r)G(a)-F(a)G(r)]/[F(r)F(a)+G(r)G(a)].$$

In the figure the curves A to C show examples of the rate of falling-off of the amplitude in a material of conductivity and diffusivity 0·10, when

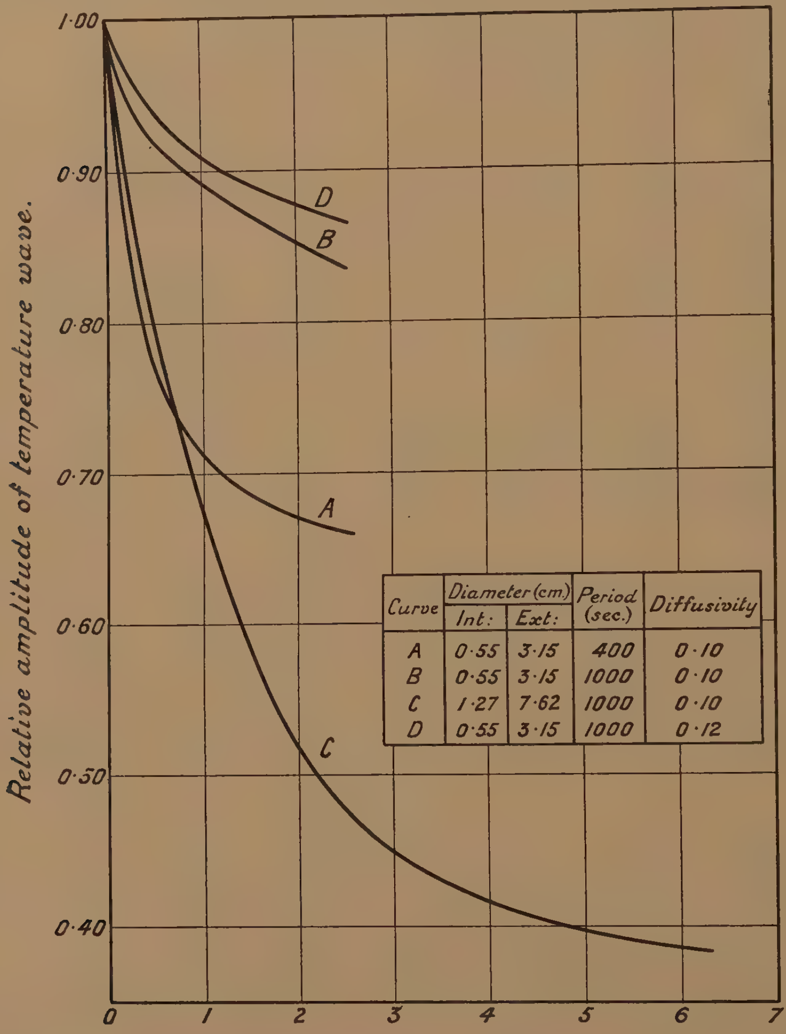

| Curve | Diameter (cm.) |  | Period (sec.) | Diffusivity |
|---|---|---|---|---|
|  | Int: | Ext: |  |  |
| A | 0·55 | 3·15 | 400 | 0·10 |
| B | 0·55 | 3·15 | 1000 | 0·10 |
| C | 1·27 | 7·62 | 1000 | 0·10 |
| D | 0·55 | 3·15 | 1000 | 0·12 |

Distance from inner wall of cylinder (cm.).

Amplitude of temperature waves in hollow cylinders.

E=0·00253, figures which would apply approximately to steel in air at 500° C. In curves A and B, the period of the wave is varied, whilst the size of the cylinder remains constant, whereas in curves B and C the period is in both cases 1000 secs., but one cylinder is larger than the other, as shown on the figure. The effect of a change in diffusivity is shown in curve D, where the dimensions and period are as in curve B, but the diffusivity is 20 per cent. greater.

### *Acknowledgment.*

I wish to thank Dr. C. G. Darwin for his most helpful interest in the problem and for suggesting considerable improvements in its presentation.

# XLII. *The Distortion of a Curved Tube due to Internal Pressure.*

By W. R. DEAN, M.A., Trinity College, Cambridge *.

[Received December 21, 1938.]

§ 1. THE writer is much indebted to Mr. G. S. Gough for suggesting the problem considered in the present paper and for providing references to the subject.

An approximation to the distribution of stress in a curved tube caused by a uniform internal hydrostatic pressure is already known, but the determination of the displacement presents more difficulty, since the method that gives correctly an approximation to the stress fails to produce a corresponding approximation to the displacement.

Some progress is made with the determination of the displacement in §§ 2–7 ; a method of successive approximation is used, and the work is carried far enough to find the part of the displacement that is of most interest physically. In § 9 the stress corresponding to this part of the displacement is compared with the known approximate result, and the two are shown to agree to the correct order of approximation. In § 10 it is shown that a simple process by which an approximation to the displacement can usually be found in such examples as the present, fails in this case, and it is suggested in § 11 that this failure is due to a relatively large (and approximately inextensional) displacement, the effect of which is to make the circular cross-section of the tube oval, the elongation being in the direction of the axis of symmetry of the tube.

§ 2. The volume of the tube is supposed formed by rotating the annulus shown in fig. 1 about the axis O$z$ so that C, the centre of the annulus, traces out a circle of radius R. The position of any particle P of the tube is defined by the coordinates $r$, $\theta$, $\phi$, and $u$, $v$, $w$ are the components with regard to these axes of the displacement $\mathbf{d}$ of P. A uniform hydrostatic pressure of intensity $p$ acts on the inner surface, $r=a$, of the tube ; there is no body force, and no applied surface force on the outer surface $r=b$.

It is clear from symmetry that $w=0$ and that $u$ and $v$ are independent of $\phi$ ; in this case the condition of equilibrium †,

$$(\lambda+2\mu)\ \text{grad div}\ \mathbf{d}-\mu\ \text{curl curl}\ \mathbf{d}=0,$$

---

* Communicated by the Author.

† A. E. H. Love, ‘ Mathematical Theory of Elasticity ’ (4th edition, 1934), §§ 19, 20, 21, 96.

reduces to the two equations

$$\frac{\lambda+2\mu}{\mu}\frac{\partial}{\partial r}\left\{\frac{\partial u}{\partial r}+\frac{u}{r}+\frac{1}{r}\frac{\partial v}{\partial \theta}+\frac{u\sin\theta+v\cos\theta}{\mathrm{R}+r\sin\theta}\right\}$$
$$-\frac{1}{r(\mathrm{R}+r\sin\theta)}\frac{\partial}{\partial\theta}\left\{(\mathrm{R}+r\sin\theta)\left(\frac{\partial v}{\partial r}+\frac{v}{r}-\frac{1}{r}\frac{\partial u}{\partial\theta}\right)\right\}=0, \quad . \quad (1)$$

$$\frac{\lambda+2\mu}{\mu r}\frac{\partial}{\partial \theta}\left\{\frac{\partial u}{\partial r}+\frac{u}{r}+\frac{1}{r}\frac{\partial v}{\partial \theta}+\frac{u\sin\theta+v\cos\theta}{\mathrm{R}+r\sin\theta}\right\}$$
$$+\frac{1}{\mathrm{R}+r\sin\theta}\frac{\partial}{\partial r}\left\{(\mathrm{R}+r\sin\theta)\left(\frac{\partial v}{\partial r}+\frac{v}{r}-\frac{1}{r}\frac{\partial u}{\partial\theta}\right)\right\}=0, \quad . \quad (2)$$

Fig. 1.

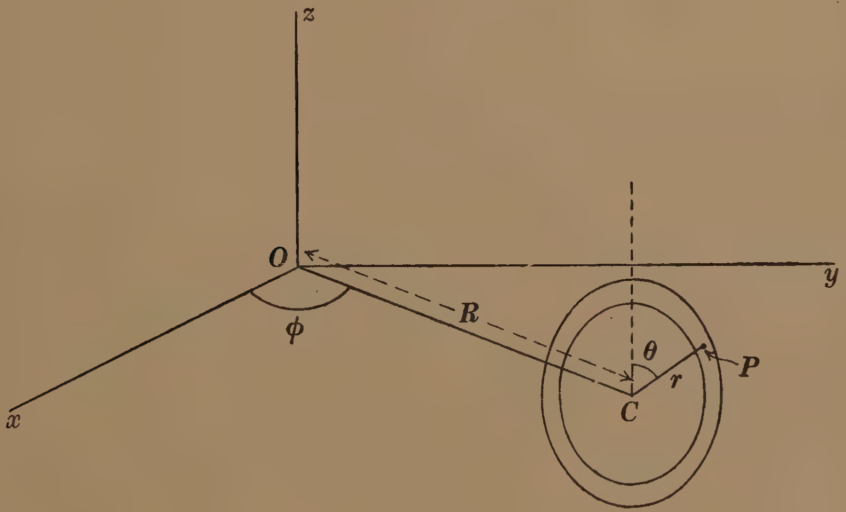

while the boundary conditions are

$$\lambda\left\{\frac{\partial u}{\partial r}+\frac{u}{r}+\frac{1}{r}\frac{\partial v}{\partial \theta}+\frac{u\sin\theta+v\cos\theta}{\mathrm{R}+r\sin\theta}\right\}+2\mu\frac{\partial u}{\partial r}=-p,\ r=a, \quad . \quad (3)$$
$$=0,\ r=b, \quad . \quad . \quad (4)$$

and

$$\frac{\partial v}{\partial r}-\frac{v}{r}+\frac{1}{r}\frac{\partial u}{\partial\theta}=0, \quad r=a,\ b. \quad . \quad . \quad . \quad . \quad . \quad . \quad . \quad (5)$$

§ 3. These equations are solved by the method of successive approximation, $u$ and $v$ being in effect expanded as power series in $b/\mathrm{R}$, but it will be seen from § 5 that if a direct attempt is made upon this it is impossible to find the second approximation. The difficulty is avoided if in equations (1) to (5) we write

$$u=u'+\sin\theta\left(K_1R+\frac{K_3}{R}+\frac{K_5}{R^3}+\ldots\right), \quad . \quad . \quad . \quad . \quad (6)$$

$$v=v'+\cos\theta\left(K_1R+\frac{K_3}{R}+\frac{K_5}{R^3}+\ldots\right), \quad . \quad . \quad . \quad . \quad (7)$$

where $K_1$, $K_3$, . . . are constants whose values can be determined subsequently. Next multiply equations (1) and (2) by $(R+r\sin\theta)^2$, equations (3) and (4) by $(R+r\sin\theta)$, write

$$u'=u_0+\frac{u_1}{R}+\frac{u_2}{R^2}+\ldots, \quad . \quad . \quad . \quad . \quad . \quad . \quad . \quad . \quad (8)$$

$$v'=v_0+\frac{v_1}{R}+\frac{v_2}{R^2}+\ldots, \quad . \quad . \quad . \quad . \quad . \quad . \quad . \quad . \quad (9)$$

and group the terms in each equation according to powers of R. We then have pairs of equations and conditions from which the pairs $u_0$, $v_0$ ; $u_1$, $v_1$ ; . . . . can be successively determined.

§ 4. If, after these changes, the terms in $R^2$ in (1) and (2) are equated to zero, we have the equations

$$\frac{\lambda+2\mu}{\mu}\frac{\partial}{\partial r}\left\{\frac{\partial u_0}{\partial r}+\frac{u_0}{r}+\frac{1}{r}\frac{\partial v_0}{\partial\theta}\right\}-\frac{1}{r}\frac{\partial}{\partial\theta}\left\{\frac{\partial v_0}{\partial r}+\frac{v_0}{r}-\frac{1}{r}\frac{\partial u_0}{\partial\theta}\right\}=0, \quad . \quad (10)$$

$$\frac{\lambda+2\mu}{\mu r}\frac{\partial}{\partial\theta}\left\{\frac{\partial u_0}{\partial r}+\frac{u_0}{r}+\frac{1}{r}\frac{\partial v_0}{\partial\theta}\right\}+\frac{\partial}{\partial r}\left\{\frac{\partial v_0}{\partial r}+\frac{v_0}{r}-\frac{1}{r}\frac{\partial u_0}{\partial\theta}\right\}=0, \quad . \quad (11)$$

together with, from equations (3), (4) and (5), the conditions

$$\frac{\lambda+2\mu}{\lambda}\frac{\partial u_0}{\partial r}+\frac{u_0}{r}+\frac{1}{r}\frac{\partial v_0}{\partial\theta}+K_1=-\frac{p}{\lambda}, \quad r=a, \quad . \quad . \quad . \quad (12)$$

$$=0, \quad r=b, \quad . \quad . \quad . \quad . \quad (13)$$

$$\frac{\partial v_0}{\partial r}-\frac{v_0}{r}+\frac{1}{r}\frac{\partial u_0}{\partial\theta}=0, \quad r=a,\ b. \quad . \quad . \quad . \quad (14)$$

It is readily verified that the solution of these equations is

$$u_0=\frac{A_0}{r}+B_0r, \quad v_0=0,$$

where

$$A_0=\frac{pb^2a^2}{2\mu(b^2-a^2)}, \quad B_0=\frac{1}{2(\lambda+\mu)}\left\{\frac{pa^2}{b^2-a^2}-\lambda K_1\right\}. \quad . \quad . \quad (15)$$

It is shown below that $K_1$ and $B_0$ must be equal. Hence

$$K_1=B_0=\frac{pa^2}{(3\lambda+2\mu)(b^2-a^2)}. \quad . \quad . \quad . \quad . \quad . \quad . \quad (16)$$

§5. The equations for $u_1$ and $v_1$, obtained similarly from (1) and (2), are

$$\begin{aligned}
&\frac{\lambda+2\mu}{\mu}\frac{\partial}{\partial r}\left\{\frac{\partial u_1}{\partial r}+\frac{u_1}{r}+\frac{1}{r}\frac{\partial v_1}{\partial \theta}\right\}-\frac{1}{r}\frac{\partial}{\partial \theta}\left\{\frac{\partial v_1}{\partial r}+\frac{v_1}{r}-\frac{1}{r}\frac{\partial u_1}{\partial \theta}\right\}\\
&\quad+2r\sin\theta\left[\frac{\lambda+2\mu}{\mu}\frac{\partial}{\partial r}\left\{\frac{\partial u_0}{\partial r}+\frac{u_0}{r}+\frac{1}{r}\frac{\partial v_0}{\partial \theta}\right\}\right.\\
&\quad\left.-\frac{1}{r}\frac{\partial}{\partial \theta}\left\{\frac{\partial v_0}{\partial r}+\frac{v_0}{r}-\frac{1}{r}\frac{\partial u_0}{\partial \theta}\right\}\right]+\frac{\lambda+2\mu}{\mu}\left\{\frac{\partial u_0}{\partial r}\sin\theta+\frac{\partial v_0}{\partial r}\cos\theta\right\}\\
&\quad-\cos\theta\left\{\frac{\partial v_0}{\partial r}+\frac{v_0}{r}-\frac{1}{r}\frac{\partial u_0}{\partial \theta}\right\}-\frac{\lambda+2\mu}{\mu}\mathrm{K}_1\sin\theta=0,
\end{aligned}$$

$$\begin{aligned}
&\frac{\lambda+2\mu}{\mu r}\frac{\partial}{\partial \theta}\left\{\frac{\partial u_1}{\partial r}+\frac{u_1}{r}+\frac{1}{r}\frac{\partial v_1}{\partial \theta}\right\}+\frac{\partial}{\partial r}\left\{\frac{\partial v_1}{\partial r}+\frac{v_1}{r}-\frac{1}{r}\frac{\partial u_1}{\partial \theta}\right\}\\
&\quad+2r\sin\theta\left[\frac{\lambda+2\mu}{\mu r}\frac{\partial}{\partial \theta}\left\{\frac{\partial u_0}{\partial r}+\frac{u_0}{r}+\frac{1}{r}\frac{\partial v_0}{\partial \theta}\right\}\right.\\
&\quad\left.+\frac{\partial}{\partial r}\left\{\frac{\partial v_0}{\partial r}+\frac{v_0}{r}-\frac{1}{r}\frac{\partial u_0}{\partial \theta}\right\}\right]+\frac{\lambda+2\mu}{\mu r}\frac{\partial}{\partial \theta}\{u_0\sin\theta+v_0\cos\theta\}\\
&\quad+\sin\theta\left\{\frac{\partial v_0}{\partial r}+\frac{v_0}{r}-\frac{1}{r}\frac{\partial u_0}{\partial \theta}\right\}-\frac{\lambda+2\mu}{\mu}\mathrm{K}_1\cos\theta=0.
\end{aligned}$$

Inserting the values of $u_0$, $v_0$, we have

$$\begin{aligned}
&\frac{\lambda+2\mu}{\mu}\frac{\partial}{\partial r}\left\{\frac{\partial u_1}{\partial r}+\frac{u_1}{r}+\frac{1}{r}\frac{\partial v_1}{\partial \theta}\right\}-\frac{1}{r}\frac{\partial}{\partial \theta}\left\{\frac{\partial v_1}{\partial r}+\frac{v_1}{r}-\frac{1}{r}\frac{\partial u_1}{\partial \theta}\right\}\\
&\qquad\qquad=-\frac{\lambda+2\mu}{\mu}\sin\theta\left\{\mathrm{B}_0-\mathrm{K}_1-\frac{\mathrm{A}_0}{r^2}\right\}, \quad . \quad . \quad . \quad (17)
\end{aligned}$$

$$\begin{aligned}
&\frac{\lambda+2\mu}{\mu r}\frac{\partial}{\partial \theta}\left\{\frac{\partial u_1}{\partial r}+\frac{u_1}{r}+\frac{1}{r}\frac{\partial v_1}{\partial \theta}\right\}+\frac{\partial}{\partial r}\left\{\frac{\partial v_1}{\partial r}+\frac{v_1}{r}-\frac{1}{r}\frac{\partial u_1}{\partial \theta}\right\}\\
&\qquad\qquad=-\frac{\lambda+2\mu}{\mu}\cos\theta\left\{\mathrm{B}_0-\mathrm{K}_1+\frac{\mathrm{A}_0}{r^2}\right\}. \quad . \quad . \quad . \quad (18)
\end{aligned}$$

The boundary conditions, from (3), (4) and (5), are

$$\begin{aligned}
&\frac{\lambda+2\mu}{\lambda}\frac{\partial u_1}{\partial r}+\frac{u_1}{r}+\frac{1}{r}\frac{\partial v_1}{\partial \theta}+u_0\sin\theta+v_0\cos\theta\\
&\qquad\qquad+r\sin\theta\left\{\frac{\lambda+2\mu}{\lambda}\frac{\partial u_0}{\partial r}+\frac{u_0}{r}+\frac{1}{r}\frac{\partial v_0}{\partial \theta}+\frac{p}{\lambda}\right\}=0, \quad r=a,
\end{aligned}$$

$$\begin{aligned}
&\frac{\lambda+2\mu}{\lambda}\frac{\partial u_1}{\partial r}+\frac{u_1}{r}+\frac{1}{r}\frac{\partial v_1}{\partial \theta}+u_0\sin\theta+v_0\cos\theta\\
&\qquad\qquad+r\sin\theta\left\{\frac{\lambda+2\mu}{\lambda}\frac{\partial u_0}{\partial r}+\frac{u_0}{r}+\frac{1}{r}\frac{\partial v_0}{\partial \theta}\right\}=0, \quad r=b,
\end{aligned}$$

$$\frac{\partial v_1}{\partial r}-\frac{v_1}{r}+\frac{1}{r}\frac{\partial u_1}{\partial \theta}=0, \quad r=a,\ b. \quad . \quad . \quad . \quad . \quad . \quad (19)$$

The first two of these conditions reduce, if the known expressions for $u_0$, $v_0$ are inserted, to

$$\frac{\lambda+2\mu}{\lambda}\frac{\partial u_1}{\partial r}+\frac{u_1}{r}+\frac{1}{r}\frac{\partial v_1}{\partial \theta}+r\sin\theta\left\{B_0-K_1+\frac{A_0}{r^2}\right\}=0, \quad r=a,\ b. \quad . \quad (20)$$

It now follows that the constant $K_1$, which is arbitrary so far, must have a definite value. For equations (17) to (20) are the equations of equilibrium, referred to plane polar coordinates $r$, $\theta$, of a straight circular cylinder; the cylinder is acted on by a force per unit volume of which the $r$, $\theta$ components, $f_r$, $f_\theta$, are given by

$$f_r=(\lambda+2\mu)\left(B_0-K_1-\frac{A_0}{r^2}\right)\sin\theta,$$

$$f_\theta=(\lambda+2\mu)\left(B_0-K_1+\frac{A_0}{r^2}\right)\cos\theta,$$

and by a pressure $p'$ which from equation (20) is such that

$$p'=\lambda\left(B_0-K_1+\frac{A_0}{r^2}\right)r\sin\theta, \quad r=a,\ b;$$

from equation (19) there is no shearing force on the surfaces $r=a$, $b$.

Now if there is to be a solution of these equations this system of external forces must be in statical equilibrium, and a necessary condition for this is

$$\int_0^{2\pi}d\theta\int_a^b(f_r\sin\theta+f_\theta\cos\theta)r\,dr+\int_0^{2\pi}(ap'_{r=a}-bp'_{r=b})\sin\theta\,d\theta=0,$$

which gives the relation

$$K_1=B_0. \quad . \quad . \quad . \quad . \quad . \quad . \quad . \quad . \quad . \quad (21)$$

The need for the transformation given by equations (6) and (7) is now clear; if it is not made, the second set of equations (for $u_1$, $v_1$) must be solved with the adjustable constant $K_1$ set equal to zero. This cannot be done, for the physical reason given above, or (from another point of view) because one of the four arbitrary constants contained in the complementary functions of (17) and (18) disappears in (19) and (20), with the result that only three constants are available to satisfy four conditions. The value of $K_1$ can alternatively be found as the condition that (19) and (20) can be satisfied by the solution of (17) and (18).

The part of the displacement depending on the constants $K_1$, $K_3$, . . . of equations (6) and (7) is a translation of the annulus shown in fig. 1 as a whole outwards from the axis Oz; this corresponds to an extension of the tube as a whole, that is, in effect, an increase in the radius R.

The equations for $u_1$, $v_1$ are now soluble, and give

$$\frac{4(\lambda+2\mu)u_1}{\sin\theta}=\frac{A_1}{r^2}+(\lambda-\mu)B_1r^2+A_0\left\{2\mu\log\frac{r}{a}-(2\lambda+3\mu)\right\}, \quad . \quad (22)$$

$$\frac{4(\lambda+2\mu)v_1}{\cos\theta}=-\frac{A_1}{r^2}+(3\lambda+5\mu)B_1r^2+A_0\left\{2\mu\log\frac{r}{a}+(2\lambda+3\mu)\right\}, \qquad (23)$$

where

$$\frac{A_1}{A_0}=\frac{(\lambda+\mu)b^2a^2}{(b^2+a^2)}, \quad \frac{B_1}{A_0}=\frac{1}{b^2+a^2}. \quad . \quad . \quad . \quad . \quad . \quad . \qquad (24)$$

It will be seen that the equations for $u_1$, $v_1$ will still be satisfied if a constant is added to the right-hand side of (22), provided that the same constant is added in (23); it is, in fact, this ambiguity that necessitates the transformation given in equations (6) and (7). This constant, however, need not be included; if it is, the only result is that the value of $K_3$ found below is altered by the corresponding amount.

§ 6. The equations and boundary conditions for $u_2$, $v_2$ will at first contain $u_0$, $v_0$, and $u_1$, $v_1$; inserting the values of these pairs of functions, we have the equations

$$\frac{\lambda+2\mu}{\mu}\frac{\partial}{\partial r}\left\{\frac{\partial u_2}{\partial r}+\frac{u_2}{r}+\frac{1}{r}\frac{\partial v_2}{\partial\theta}\right\}-\frac{1}{r}\frac{\partial}{\partial\theta}\left\{\frac{\partial v_2}{\partial r}+\frac{v_2}{r}-\frac{1}{r}\frac{\partial u_2}{\partial\theta}\right\}$$

$$=-\frac{\lambda A_0 r}{\mu(b^2+a^2)}+\frac{A_0\cos 2\theta}{2r}\left\{1-\frac{(\lambda+\mu)(b^2a^2+r^4)}{\mu(b^2+a^2)r^2}\right\},$$

$$\frac{\lambda+2\mu}{\mu r}\frac{\partial}{\partial\theta}\left\{\frac{\partial u_2}{\partial r}+\frac{u_2}{r}+\frac{1}{r}\frac{\partial v_2}{\partial\theta}\right\}+\frac{\partial}{\partial r}\left\{\frac{\partial v_2}{\partial r}+\frac{v_2}{r}-\frac{1}{r}\frac{\partial u_2}{\partial\theta}\right\}$$

$$=\frac{A_0\sin 2\theta}{\mu r}\left\{2\lambda+3\mu+\frac{\lambda+\mu}{2(b^2+a^2)}\left(r^2-\frac{b^2a^2}{r^2}\right)\right\},$$

with the boundary conditions

$$\frac{\lambda+2\mu}{\lambda}\frac{\partial u_2}{\partial r}+\frac{u_2}{r}+\frac{1}{r}\frac{\partial v_2}{\partial\theta}=-K_3+\tfrac{1}{2}A_0-\frac{A_0}{2(\lambda+2\mu)}\left\{\frac{(\lambda+\mu)r^2}{b^2+a^2}+\mu\log\frac{r}{a}\right\}$$

$$+\frac{A_0\cos 2\theta}{4(\lambda+2\mu)}\left\{\frac{(\lambda+\mu)b^2a^2}{(b^2+a^2)r^2}-\frac{(\lambda+3\mu)r^2}{b^2+a^2}-(4\lambda+7\mu)\right\}, \quad r=a, b,$$

$$\frac{\partial v_2}{\partial r}-\frac{v_2}{r}+\frac{1}{r}\frac{\partial u_2}{\partial\theta}=0, \quad r=a, b.$$

If

$$u_2=u_2'+u_2''\cos 2\theta, \quad v_2=v_2''\sin 2\theta, \quad . \quad . \quad . \quad . \quad . \qquad (25)$$

where $u_2'$, $u_2''$, $v_2''$ are independent of $\theta$, it can be shown that

$$u_2'=\frac{A_2}{r}+B_2r-\frac{\lambda A_0 r^3}{8(\lambda+2\mu)(b^2+a^2)}, \quad . \quad . \quad . \quad . \quad . \quad . \qquad (26)$$

where

$$\mathrm{A}_2=\frac{\lambda b^2a^2\mathrm{A}_0}{8(\lambda+2\mu)}\left\{\frac{1}{b^2+a^2}-\frac{2}{b^2-a^2}\log\frac{b}{a}\right\}, \quad . \quad . \quad . \quad . \quad . \quad . \quad . \quad . \quad (27)$$

$$\mathrm{B}_2=\frac{\lambda\mathrm{A}_0}{8(\lambda+\mu)(\lambda+2\mu)}\left\{2\lambda+5\mu-\frac{2\mu b^2}{b^2-a^2}\log\frac{b}{a}\right\}-\frac{\lambda\mathrm{K}_3}{2(\lambda+\mu)}, \quad . \quad (28)$$

and that

$$u_2''=-\frac{\mathrm{A}_0r}{8(\lambda+2\mu)}\left\{(3\lambda+4\mu)\log\frac{r}{a}+\frac{2(\lambda+\mu)r^2}{3(b^2+a^2)}\right\}$$
$$+\frac{\mathrm{C}_2}{r^3}-\frac{\lambda\mathrm{D}_2r^3}{3(\lambda+\mu)}-\frac{(\lambda+2\mu)\mathrm{E}_2}{(\lambda+\mu)r}+\mathrm{F}_2r, \quad . \quad . \quad . \quad (29)$$

$$v_2''=\frac{\mathrm{A}_0r}{8(\lambda+2\mu)}\left\{(3\lambda+4\mu)\log\frac{r}{a}+\frac{\lambda+\mu}{b^2+a^2}\left(\frac{b^2a^2}{r^2}+\frac{r^2}{3}\right)-\frac{5}{2}\lambda-4\mu\right\}$$
$$+\frac{\mathrm{C}_2}{r^3}+\frac{(2\lambda+3\mu)\mathrm{D}_2r^3}{3(\lambda+\mu)}+\frac{\mu\mathrm{E}_2}{(\lambda+\mu)r}-\mathrm{F}_2r, \quad . \quad . \quad . \quad (30)$$

where

$$8(\lambda+2\mu)\mathrm{C}_2=-\frac{\mathrm{A}_0b^4a^4}{(b^2-a^2)^2}\left\{\lambda+4\mu+\frac{(3\lambda+4\mu)(b^2+a^2)}{b^2-a^2}\log\frac{b}{a}\right\}, \quad . \quad . \quad . \quad (31)$$

$$8(\lambda+2\mu)\mathrm{D}_2=\mathrm{A}_0\left\{-\frac{2\lambda+3\mu}{b^2+a^2}+\frac{3(\lambda+4\mu)(b^2+a^2)}{2(b^2-a^2)^2}+\frac{6(3\lambda+4\mu)b^2a^2}{(b^2-a^2)^3}\log\frac{b}{a}\right\},$$
$$. \quad . \quad . \quad (32)$$

$$8(\lambda+2\mu)\mathrm{E}_2=-\mathrm{A}_0b^2a^2\left\{\frac{\mu}{b^2+a^2}+\frac{3(\lambda+4\mu)(b^2+a^2)}{2(b^2-a^2)^2}\right.$$
$$\left.+\frac{2(3\lambda+4\mu)(b^4+b^2a^2+a^4)}{(b^2-a^2)^3}\log\frac{b}{a}\right\}, \quad . \quad . \quad . \quad (33)$$

$$8(\lambda+2\mu)\mathrm{F}_2=\mathrm{A}_0\left\{\frac{2(\lambda+3\mu)(b^4+a^4)-\lambda b^2a^2}{(b^2-a^2)^2}\right.$$
$$\left.+\frac{(3\lambda+4\mu)(b^4+b^2a^2+4a^4)b^2}{(b^2-a^2)^3}\log\frac{b}{a}\right\}. \quad . \quad . \quad . \quad (34)$$

§ 7. The constant $\mathrm{K}_3$ is determined, as was $\mathrm{K}_1$ in § 5, from the condition that the equations for $u_3$, $v_3$ may be soluble ; these equations are

$$\frac{\lambda+2\mu}{\mu}\frac{\partial}{\partial r}\left\{\frac{\partial u_3}{\partial r}+\frac{u_3}{r}+\frac{1}{r}\frac{\partial v_3}{\partial\theta}\right\}-\frac{1}{r}\frac{\partial}{\partial\theta}\left\{\frac{\partial v_3}{\partial r}+\frac{v_3}{r}-\frac{1}{r}\frac{\partial u_3}{\partial\theta}\right\}$$
$$=\frac{\mathrm{A}_0\sin\theta}{16\mu}\left\{\frac{(21\lambda-5\mu)r^2}{b^2+a^2}-\frac{(\lambda+\mu)b^2a^2}{(b^2+a^2)r^2}-6\lambda\log\frac{r}{a}-\frac{1}{2}(39\lambda+64\mu)\right\}$$
$$+\frac{\lambda+2\mu}{\mu}\sin\theta\left\{\mathrm{K}_3-\mathrm{B}_2+\mathrm{F}_2+\frac{2\mathrm{A}_2+\mathrm{E}_2}{2r^2}-\frac{3\lambda+\mu}{2(\lambda+\mu)}\mathrm{D}_2r^2\right\}$$
$$+f_1(r)\sin 3\theta,$$

$$\frac{\lambda+2\mu}{\mu r}\frac{\partial}{\partial\theta}\left\{\frac{\partial u_3}{\partial r}+\frac{u_3}{r}+\frac{1}{r}\frac{\partial v_3}{\partial\theta}\right\}+\frac{\partial}{\partial r}\left\{\frac{\partial v_2}{\partial r}+\frac{v_3}{r}-\frac{1}{r}\frac{\partial u_3}{\partial\theta}\right\}$$

$$=\frac{\mathrm{A}_0\cos\theta}{16\mu}\left\{\frac{(7\lambda+9\mu)r^2}{b^2+a^2}+\frac{(\lambda+\mu)b^2a^2}{(b^2+a^2)r^2}-6\lambda\log\frac{r}{a}-\frac{1}{2}(27\lambda+40\mu)\right\}$$

$$+\frac{\lambda+2\mu}{\mu}\cos\theta\left\{\mathrm{K}_3-\mathrm{B}_2+\mathrm{F}_2-\frac{2\mathrm{A}_2+\mathrm{E}_2}{2r^2}-\frac{\lambda+3\mu}{2(\lambda+\mu)}\mathrm{D}_2r^2\right\}$$

$$+f_2(r)\cos 3\theta\,;$$

the boundary conditions are

$$\frac{\lambda+2\mu}{\lambda}\frac{\partial u_3}{\partial r}+\frac{u_3}{r}+\frac{1}{r}\frac{\partial v_3}{\partial\theta}$$

$$=\frac{\mathrm{A}_0 r\sin\theta}{16(\lambda+2\mu)}\left\{\frac{(7\lambda+\mu)r^2}{b^2+a^2}+\frac{(\lambda+\mu)b^2a^2}{(b^2+a^2)r^2}-6\lambda\log\frac{r}{a}-\frac{1}{2}(27\lambda+52\mu)\right\}$$

$$+r\sin\theta\left\{\mathrm{K}_3-\mathrm{B}_2+\mathrm{F}_2-\frac{\mathrm{A}_2}{r^2}-\frac{(\lambda+3\mu)\mathrm{E}_2}{2(\lambda+\mu)r^2}-\frac{1}{2}\mathrm{D}_2r^2\right\}$$

$$+f_3(r)\sin 3\theta,\qquad r=a,\ b,$$

$$\frac{\partial v_3}{\partial r}-\frac{v_3}{r}+\frac{1}{r}\frac{\partial u_3}{\partial\theta}=0,\quad r=a,\ b.$$

These are the equations of equilibrium of a straight circular cylinder under the action of given external body and surface forces; the condition, which determines $\mathrm{K}_3$, that the external force system must be in statical equilibrium does not depend on the functions $f_1(r)$, $f_2(r)$ and $f_3(r)$, which are not therefore given explicitly. It follows after some reduction that

$$\frac{\mathrm{K}_3}{\mathrm{A}_0}=\frac{1}{4(\lambda+2\mu)}\left\{\lambda+4\mu-\frac{2\mu b^2}{b^2-a^2}\log\frac{b}{a}\right\}. \qquad . \quad . \quad . \quad (35)$$

§ 8. It would be a laborious matter to proceed much further with the general case without some simplifying assumption, though in any given numerical case the work would be altogether lighter and the displacement could be found on the above lines to any degree of approximation likely to be required in practice. However, the calculation of the displacement has already been carried far enough to illustrate the points of physical interest.

We may first compare the displacement found here in the limiting case when R is large with the corresponding displacement of a straight circular cylinder. Suppose that the straight cylinder is acted upon by an internal pressure $p$, and also by a uniform tensile stress $\widehat{zz}$ applied to its end sections. Then * the cylinder has a longitudinal extension $e$ and a radial

---

* Love, *op. cit.*, § 100.

displacement $u$ given by

$$u=\frac{A}{r}+Br,$$

where

$$A=\frac{pb^2a^2}{2\mu(b^2-a^2)},\quad B=\frac{pa^2}{2(\lambda+\mu)(b^2-a^2)}-\frac{\lambda e}{2(\lambda+\mu)};$$

$$\widehat{zz}=\frac{\lambda pa^2}{(\lambda+\mu)(b^2-a^2)}+\frac{\mu(3\lambda+2\mu)}{\lambda+\mu}e.$$

When R is large the important part of the displacement of the curved cylinder is given by

$$u=K_1R\sin\theta+\frac{pa^2}{b^2-a^2}\left\{\frac{b^2}{2\mu r}+\frac{r}{3\lambda+2\mu}\right\},$$

$$v=K_1R\cos\theta,$$

where

$$K_1=\frac{pa^2}{(3\lambda+2\mu)(b^2-a^2)}.$$

The part of this displacement that depends on $K_1$ is, as explained above, a translation of the section as a whole outwards from the axis through the distance $K_1R$; this causes an extension of the length of the curved cylinder of amount $K_1$, thus $K_1$ corresponds to the extension $e$ of the straight cylinder. Now the curved cylinder is in tension in consequence of the internal pressure, for the pressure on the element of the cylinder contained between the $\phi$, $\phi+d\phi$ planes (fig. 1) has an outward component

$$p\,d\phi\int_0^{2\pi}a(R+a\sin\theta)\sin\theta\,d\theta,$$

or $\pi pa^2d\phi$, and this, since there are no shearing stresses of the kind required, must be balanced by a tensile stress $\widehat{\phi\phi}$; the average value of this tensile stress is

$$\frac{pa^2}{b^2-a^2},$$

and this corresponds to the tensile stress $\widehat{zz}$ of the straight cylinder. With this value of $\widehat{zz}$, $e$ is found from the above equation between $e$ and $\widehat{zz}$ to be

$$\frac{pa^2}{(3\lambda+2\mu)(b^2-a^2)},$$

so that $e$ and $K_1$ are the same. It easily follows that the radial displacements are the same in the two cases.

§ 9. An approximation to the distribution of stress in the tube is already known. The flexure of the surface being ignored, it has been shown * that the hoop tension, or $\widehat{\theta\theta}$ stress, is

$$\frac{pa}{2t}\,\frac{2\mathrm{R}+a\sin\theta}{\mathrm{R}+a\sin\theta}, \quad . \quad . \quad . \quad . \quad . \quad . \quad . \quad (36)$$

and that the tensile stress $\widehat{\phi\phi}$ is

$$\frac{pa}{2t}; \quad . \quad . \quad . \quad . \quad . \quad . \quad . \quad . \quad . \quad . \quad . \quad . \quad (37)$$

these are effectively mean values of the stresses taken throughout the thickness, $t$, of the wall of the tube.

The mean values of the stresses given by the above expression for the displacement agree with these values to the proper degree of approximation.

The extensional strains $e_{rr}$, $e_{\theta\theta}$, $e_{\phi\phi}$ are given by the equations †

$$e_{rr}=\frac{\partial u}{\partial r}, \quad e_{\theta\theta}=\frac{1}{r}\frac{\partial v}{\partial\theta}+\frac{u}{r}, \quad e_{\phi\phi}=\frac{u\sin\theta+v\cos\theta}{\mathrm{R}+r\sin\theta};$$

integrating throughout the thickness of the tube and retaining, on the assumption that $t/a$ is small, only the most important terms, we have the mean values

$$-\frac{3\lambda\mathrm{A}_0}{(3\lambda+2\mu)a^2}-\frac{(\lambda+2\mu)\mathrm{A}_0\cos 2\,\theta}{8(\lambda+\mu)\mathrm{R}^2},$$

$$\frac{(3\lambda+4\mu)\mathrm{A}_0}{(3\lambda+2\mu)a^2}-\frac{\mathrm{A}_0\sin\theta}{a\mathrm{R}}+\left\{\frac{\lambda}{8(\lambda+\mu)}-1\right\}\frac{\mathrm{A}_0\cos 2\theta}{\mathrm{R}^2},$$

$$\frac{2\mu\mathrm{A}_0}{(3\lambda+2\mu)a^2}+\frac{\mathrm{A}_0\sin\theta}{a\mathrm{R}}+\frac{\mathrm{A}_0\cos 2\theta}{\mathrm{R}^2};$$

and the mean values of the stresses are accordingly given by

$$\widehat{\theta\theta}=\frac{pa}{t}\left[1-\frac{a\sin\theta}{2\mathrm{R}}-\frac{a^2\cos 2\theta}{2\mathrm{R}^2}\right],$$

$$\widehat{\phi\phi}=\frac{pa}{2t}\left[1+\frac{a\sin\theta}{\mathrm{R}}+\left\{1-\frac{\lambda}{8(\lambda+\mu)}\right\}\frac{a^2\cos 2\theta}{\mathrm{R}^2}\right].$$

It will be seen that, whereas this expression for $\widehat{\theta\theta}$ agrees with (36) up to the term of order $a/\mathrm{R}$, there is not agreement to the same order between the expression for $\widehat{\phi\phi}$ and (37). The reason for this difference is to be found in the method by which (37) has been established. This has been done by considering the forces acting on the element of the tube that is

---

* A. Föppl, ‘ Vorlesungen über technische Mechanik ’ (9th edition, 1922), vol. iii. p. 331 ; R. V. Southwell, ‘ Theory of Elasticity ’ (1936), p. 255.

† Love, *op. cit.*, § 20.

obtained by rotating through 180° the part of the annulus (fig. 1) between the $\theta$ and $\theta+d\theta$ radii; this element is therefore generated by rotating an area approximately $ta\,d\theta$ through an arc of length approximately $\pi(R+a\sin\theta)$. Equal stresses $\widehat{\phi\phi}$ act on the two plane ends of the filament, while stresses $\widehat{r\theta}$ and $\widehat{\theta\theta}$ and the hydrostatic pressure $p$ act on the curved surfaces; $\widehat{\phi\phi}$ is found from the condition for the equilibrium of these forces. The areas of the curved surfaces of the filament depend on R, while the areas of the plane ends do not. It follows that if $\widehat{\phi\phi}$ is to be calculated in this way to the term of order $a/R$, the terms of order $a^2/R^2$ in $\widehat{r\theta}$ and $\widehat{\theta\theta}$ must be known, and these terms depend on the complicated expressions for the displacements $u_2/R^2$, $v_2/R^2$. As an additional check on the algebra it has been verified, by considering the equilibrium of the semi-circular filament more exactly, that the first two terms of the expression just given for $\widehat{\phi\phi}$ are correct.

§ 10. In such a case as the present a first approximation to the displacement can usually be found very simply by using a first approximation to the equations of the theory of thin shells *. The two equations for the equilibrium of an element of the surface of the tube can be written

$$\frac{\partial}{\partial\theta}\{(R+a\sin\theta)T_1\}-a\cos\theta T_2=0, \quad . \quad . \quad . \quad . \quad . \quad (38)$$

$$(R+a\sin\theta)T_1+a\sin\theta T_2=pa(R+a\sin\theta)\,; \quad . \quad . \quad . \quad (39)$$

in these equations $T_1$, $T_2$ are stress-resultants, that is, integrals throughout the thickness of the tube of the $\widehat{\theta\theta}$, $\widehat{\phi\phi}$ stresses. These equations are only first approximations to the equations of the theory of thin shells; they are obtained by ignoring the flexural terms, that is, terms formally of order $t^2/a^2$ compared with the terms retained. These equations are exactly satisfied by the mean stresses given above in equations (36), (37), that is, by writing

$$T_1=\frac{pa}{2}\,\frac{2R+a\sin\theta}{R+a\sin\theta}, \quad T_2=\frac{pa}{2}. \quad . \quad . \quad . \quad . \quad . \quad . \quad (40)$$

The relations between the stress-resultants $T_1$, $T_2$ and $u$, $v$, the displacements of points of the middle surface of the tube, are

$$T_1=\frac{Et}{1-\sigma^2}\left\{\frac{1}{a}\left(\frac{\partial v}{\partial\theta}+u\right)+\frac{\sigma(u\sin\theta+v\cos\theta)}{R+a\sin\theta}\right\}, \quad . \quad . \quad (41)$$

$$T_2=\frac{Et}{1-\sigma^2}\left\{\frac{\sigma}{a}\left(\frac{\partial v}{\partial\theta}+u\right)+\frac{u\sin\theta+v\cos\theta}{R+a\sin\theta}\right\}, \quad . \quad . \quad . \quad (42)$$

where E is Young's modulus and $\sigma$ Poisson's ratio.

It can now be shown that if the values set out in equation (40) are assigned to $T_1$ and $T_2$ it is not possible to find functions $u$, $v$ that will

---

* Love, *op. cit.*, chap. xxiv.

satisfy equations (41) and (42). This is shown most readily in the case $\sigma=0$; for then

$$\frac{\partial v}{\partial\theta}+u=\mathrm{C}\frac{2\mathrm{R}+a\sin\theta}{\mathrm{R}+a\sin\theta},\quad a(u\sin\theta+v\cos\theta)=\mathrm{C}(\mathrm{R}+a\sin\theta),$$

where C is a constant. If we now write

$$\mathrm{U}=u\sin\theta+v\cos\theta,\ \mathrm{V}=u\cos\theta-v\sin\theta,$$

so that U, V are Cartesian components of the displacement of a point of the middle surface,

$$a\mathrm{U}=\mathrm{C}(\mathrm{R}+a\sin\theta),$$

$$\frac{d\mathrm{U}}{d\theta}\cos\theta-\frac{d\mathrm{V}}{d\theta}\sin\theta=\mathrm{C}\frac{2\mathrm{R}+a\sin\theta}{\mathrm{R}+a\sin\theta},$$

whence

$$\frac{d\mathrm{V}}{d\theta}\sin\theta=\mathrm{C}\left\{\cos^2\theta-\frac{2\mathrm{R}+a\sin\theta}{\mathrm{R}+a\sin\theta}\right\}.$$

Since the expression on the right of the last equation does not vanish when $\sin\theta=0$, the equation cannot be satisfied by a finite value of V. It is not therefore possible to find a displacement $u$, $v$ that will satisfy the two differential equations obtained by substituting the expressions (41), (42) for $\mathrm{T}_1$, $\mathrm{T}_2$ in the two equations of equilibrium, and it has been verified (though it is clear physically) that this conclusion does not depend on the simplifying assumption that $\sigma=0$.

§ 11. The equations of equilibrium of the last paragraph are obtained from equations given in the theory of thin shells by ignoring the flexural terms. The full equations, which in this case would be of some complexity, would, of course, be compatible and would lead to a definite displacement.

The first approximation fails to find the displacement because of the part of the displacement depending on the terms $u_2''\cos 2\theta$, $v_2''\sin 2\theta$ of equation (25). If $t/a$ is assumed small, first approximations to the constants $\mathrm{C}_2$, $\mathrm{D}_2$, $\mathrm{E}_2$ and $\mathrm{F}_2$ of equations (31) to (34) are given by the simple relations

$$8t^2\mathrm{C}_2=-\mathrm{A}_0a^6,\ 8t^2\mathrm{D}_2=3\mathrm{A}_0,$$
$$8t^2\mathrm{E}_2=-3\mathrm{A}_0a^4,\ 8t^2\mathrm{F}_2=3\mathrm{A}_0a^2;$$

the corresponding part of the displacement of the tube is given by

$$u=\frac{(\lambda+2\mu)\mathrm{A}_0a^3}{2(\lambda+\mu)t^2\mathrm{R}^2}\cos 2\theta,\quad v=-\frac{(\lambda+2\mu)\mathrm{A}_0a^3}{4(\lambda+\mu)t^2\mathrm{R}^2}\sin 2\theta.\quad .\quad .\quad (43)$$

This part of the displacement therefore contains the factor $\mathrm{A}_0/t^2$, and it is the only part of the displacement (so far as the above calculations extend) that does. Compared with the rest of the displacement this part is formally of the order $a^2/t^2$, so that some of the flexural terms ignored in the equations of equilibrium (38), (39) will be of the same order as the terms kept in. So far as the calculation of the displacement is concerned the approximations made in reaching these simple equations are not valid; on the other hand, it has been seen that a correct approximation to the stress distribution can be obtained from them.

§ 12. Since the displacement (43) contains the factor $A_0/t^2$ it will be in thin tubes an important part of the displacement. In the displacement of the section of the tube as a whole owing to stretching the principal term is $K_1R$, that is, from equations (15) and (16),

$$\frac{2\mu A_0 R}{(3\lambda+2\mu)a^2},$$

approximately, while the mean value of the radial displacement $u_0$ is, to the same approximation,

$$\frac{(3\lambda+4\mu)A_0}{(3\lambda+2\mu)a};$$

Fig. 2.

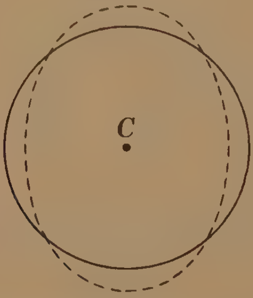

the ratios of the maximum value of $u$ in (43) to these displacements are

$$\frac{15a^5}{8t^2R^3}, \quad \frac{15\,a^4}{28t^2R^2},$$

respectively, if $\lambda$ is for simplicity assumed equal to $\mu$. In many ordinary cases (43) will give the largest part of the displacement. This displacement does not, however, cause correspondingly large extensional strains, as appears from the expressions for these strains in § 9, in which the thickness $t$ does not occur explicitly; it is approximately, therefore, an inextensional displacement.

The effect of a displacement of type (43) is, as shown in fig. 2, to make the circular section of the tube oval, the elongation being parallel to the axis, without extension of the line of the section.

It is clear physically, or follows from the theory of thin shells, that a continuation of the process of approximation of §§2–7 cannot lead to terms of relative order higher than the order $a^2/t^2$ of (43). All the most important parts of the displacement have therefore been calculated.

# XLIII. *The Latent Heats of Sublimation and Evaporation of certain Substances.*

By William Hume-Rothery, F.R.S.*

[Received August 18, 1939.]

## I.

At the triple point of a substance, the liquid, solid, and gaseous phases are in equilibrium, and the latent heat of sublimation of the solid ($\lambda_s$) is equal to the sum of the latent heats of evaporation of the liquid ($\lambda_l$) and of fusion of the solid ($f_s$). For normal metallic elements, and for the majority of other substances, the latent heat of fusion of the solid is a relatively small quantity, so that the ratio $\lambda_s/\lambda_l$ is nearly equal to unity. For some other substances the latent heat of fusion is relatively greater, and a survey of this type of substance has revealed some relations which we believe to be new, and which may be of considerable interest in connexion with the structure of liquids. These relations may be summarized by saying that *for many substances with relatively large latent heats of fusion, the values of the ratios $\lambda_s/\lambda_l$ at the triple points tend to approximate to the ratios of small whole numbers.* In the following sections we shall examine the evidence on which this conclusion is based, and shall describe some other relations which suggest that when a substance exists in different allotropic forms the latent heats of the different forms are simply related.

## II.

Most values of the latent heats of evaporation and sublimation are derived from an analysis of vapour-pressure curves, and as the same expressions are sometimes used with different meanings, their relations may be summarized briefly. For the process of vaporization, the Clausius-Clapeyron equation gives the relation

$$\frac{dp}{dT}=\frac{\lambda}{T\triangle V}, \quad \ldots \ldots \ldots \quad (1)$$

or

$$\frac{d\,ln\,p}{dT}=\frac{\lambda}{Tp\triangle V}, \quad \ldots \ldots \ldots \quad (1a)$$

---

* Communicated by the Author.

where $\lambda$ is the latent heat of vaporization (evaporation or sublimation), and $\triangle V$ the increase in volume on passing from the condensed to the gaseous state. If we assume the vapour to be a perfect gas, and ignore the volume of the solid or liquid, the above equation becomes

$$\frac{d\,ln\,p}{dT}=\frac{\lambda}{RT^2}. \qquad (2)$$

In this equation $\lambda$ is not a constant, but varies according to the difference $\triangle Cp$ between the specific heats of the condensed and gaseous phases, this difference being, in the general case, a function of temperature, although for some substances it is justifiable to consider $\triangle Cp$ constant for small temperature ranges. In some cases $\triangle Cp$ is either known, or can be estimated with reasonable accuracy, and for these substances we shall refer to the values for the solid and liquid at the triple point as $\lambda_s$ and $\lambda_l$ respectively, and we shall indicate the very few cases in which the data are sufficient to make allowance for the departure from the ideal gaseous state. This deviation from the ideal state is usually negligible when the pressure is small. For many substances data are not available for the temperature variations of $\triangle Cp$, but in a large number of cases it is found that the vapour pressure of a liquid or solid is in agreement over a surprisingly wide range with an empirical equation of the type

$$ln\,p=-\frac{a}{T}+b. \qquad (3)$$

It is important to recognize that the constant $a$ of equation (3) is not the same as the term $\lambda/R$ of equation (2), but is a combination of this term with the effects of the departure from the ideal gas laws, and of $\triangle Cp$. We shall use the symbols $a_s$ and $a_l$ for the values of $a$ in equation (3) when referring to the solid and liquid states respectively.

In cases where the vapour pressures near the triple point are given really accurately by equation (3), it is, of course, perfectly justifiable to use this equation to determine $d\,ln\,p/dT$, and then, when the assumption of a perfect gas is justified, to identify the constant $a$ of equation (3) with $\lambda/R$ in equation (2). Even where the assumption of a perfect gas is unjustified, it can readily be shown that if the vapour pressures of both liquid and solid phases near the triple point are given accurately by equation (3), the ratio $a_s/a_l$ will be very nearly equal to $\lambda_s/\lambda_l$. For if we combine equation (1), which always holds, with equation (3), we obtain

$$a=\lambda\frac{T}{p\triangle V}. \qquad (4)$$

At the triple point of a substance, $p$ and T are identical for both solid and liquid phases, whilst $\triangle V$ differs only by the small difference between the volumes of the liquid and solid. The ratio $a_s/a_l$ will therefore equal the ratio $\lambda_s/\lambda_l$ to a much higher degree of accuracy than $Ra_s$ and $Ra_l$ equal $\lambda_s$ and $\lambda_l$ respectively. In cases where the vapour-pressure data are expressed in the form of equation (3), it is essential for our purpose to verify that the constant $a$ refers to the observations near the triple point *, and is not merely a rough approximation over a wide range of points. In what follows we shall distinguish between the quantities $\lambda_s$ and $\lambda_l$, and $Ra_s$ and $Ra_l$, although, as shown above, their ratios may be directly compared at the triple point. Similar considerations apply when the vapour pressures of solid and liquid are given accurately by other empirical equations but where doubt exists as to the correction for gas imperfection, dissociation equilibria in the gaseous phase, etc. In such cases if we differentiate the equation to obtain $d\,ln\,p/d\mathrm{T}$ at the triple point for the solid and liquid, we can from equation (1 $a$) obtain the correct ratio $\lambda_s/\lambda_l$ except for the small difference in the volumes of the solid and liquid, since, at the triple point, $p$ and T in equation (1 $a$) are the same for both solid and liquid. Where accurate vapour-pressure curves are available for both phases near the triple point, the ratio $\lambda_s/\lambda_l$ can thus be obtained to a much higher accuracy than either $\lambda_s$ or $\lambda_l$. On the other hand, more care is necessary where the latent heat of sublimation of the solid is estimated by the addition of the directly measured latent heat of fusion to the latent heat of evaporation of the liquid as calculated from vapour-pressure data. Here the directly measured latent heat of fusion is the true value $(\lambda_s - \lambda_l)$, whilst the calculated value of $\lambda_l$ involves the assumptions made as regards the term $p\triangle\mathrm{V}$ in equation (1 $a$).

## III.

In the analysis of vapour-pressure curves errors of the order 1—2 per cent. must be expected for all but a minority of substances, so that errors of the order 2—4 per cent. may be expected for the ratio $\lambda_s/\lambda_l$, or $a_s/a_l$, in cases where the errors are in the opposite direction for the liquid and solid phases. In testing a whole-number hypothesis, it is, therefore, essential to avoid using such large whole numbers that the experimental error enables any value of $\lambda_s/\lambda_l$ to be expressed by a whole number ratio. Since there are eight groups in the Periodic Table, we have arbitrarily defined a small whole number as one not greater than 8, and the first column of Table I. shows all the possible ratios less than 4/1, which can be formed by numbers up to 8. The second column of the table shows these ratios expressed to three places of decimals, whilst the third column shows the difference between successive ratios expressed as a fraction of the smaller ratio. Thus the difference between the ratios 3/2=1·500 and 7/5=1·400 is 0·100, and this, expressed as a percentage of 1·400, is 7·14 per cent. From this it will be seen that with ratios less than 1·2, adjacent ratios are too close together for any satisfactory test to be made. With ratios greater than 1·2 the establishment of a whole number hypothesis may be possible, particularly if use is made of a method adopted by Stockdale (1) in a similar connexion. This consists in marking the observed values of the quantity under consideration—in this case $\lambda_s/\lambda_l$—on a scale, on which the positions of the whole number ratios are marked. In this way a distribution of points approximating to whole number ratios may be distinguished from a random distribution.

---

* A common mistake is to express the vapour-pressure data near the boiling-point of a liquid in the form of equation (3), and then to calculate the latent heat of evaporation, and to assume that this value applies near the melting-point.

TABLE I.

| Ratio. | Value. | Percentage difference from next ratio lower in Table. |
|---|---|---|
| 8/2=4/1 | 4·000 | 14·3 |
| 7/2 | 3·500 | 16·7 |
| 6/2=3/1 | 3·000 | 12·47 |
| 8/3 | 2·667 | 6·68 |
| 5/2 | 2·500 | 7·15 |
| 7/3 | 2·333 | 16·65 |
| 8/4=6/3=4/2=2/1 | 2·000 | 14·2 |
| 7/4 | 1·750 | 4·98 |
| 5/3 | 1·667 | 4·19 |
| 8/5 | 1·600 | 6·67 |
| 6/4=3/2 | 1·500 | 7·14 |
| 7/5 | 1·400 | 5·03 |
| 8/6=4/3 | 1·333 | 6·64 |
| 5/4 | 1·250 | 4·17 |
| 6/5 | 1·200 | 2·85 |
| 7/6 | 1·167 | 2·10 |
| 8/7 | 1·143 | |

## IV.

In order to avoid the danger of selecting subtances which fit our hypothesis, we have confined ourselves to those for which calculations have been made by Kelley (2) in his Bulletin on the " Free Energies of Vaporization and Vapour Pressures of Inorganic Substances." This author has surveyed the vapour-pressure data of inorganic and some organic substances, and presents the most probable values of the different constants in a series of equations, the form of which depends on the accuracy of the experimental data. Wherever possible we have consulted the original papers, and we have searched the British Chemical Abstracts for later work on all substances for which Kelley gives data for both solid and liquid phases. It is hoped that in this way a completely unbiased list of substances has been submitted for which $\lambda_s/\lambda_l > 1{\cdot}2$.

## V.

We may consider first the substances for which Kelley gives the variation of $\lambda_s$ and $\lambda_l$ with temperature, and in Table II. we have summarized the data for all cases in which $\lambda_s/\lambda_l > 1{\cdot}2$. The second and third columns of this table give the values of $\lambda_s$ and $\lambda_l$, calculated from Kelley's equations, for the temperature of the triple point, or the melting-point where the latter is not available *. The fourth column gives the values of $\lambda_s/\lambda_l$, and the next two columns give the percentage differences of these values from the nearest ratios in Table I. on either side. Thus the value 1·327 lies between the ratio $4/3 = 1{\cdot}333$ and $5/4 = 1{\cdot}250$, and differs from the former by $-0{\cdot}45$ per cent., and from the latter by $+6{\cdot}2$ per cent. In the last column of this and the succeeding tables, the following abbreviations are used to indicate the way in which Kelley's equations are derived :—

A. Both $\lambda_s$ and $\lambda_l$ (or $a_s$ and $a_l$ in later tables) are derived from the analysis of vapour-pressure curves obtained by the same experimenter.

$A_1A_2$. $\lambda_s$ and $\lambda_l$ (or $a_s$ and $a_l$) are from the data of different experimenters, or are from the averages of different experimenters.

B. $\lambda_l$ is obtained from the vapour-pressure curve of the liquid, and $\lambda_s$ by the addition of the directly determined latent heat of fusion.

It will be seen that the agreement with the hypothesis of small whole numbers is very striking. Of the sixteen substances contained in Table II., no fewer than nine give values of $\lambda_s/\lambda_l$ within 1 per cent. of a ratio of numbers less than 8.

In general the substances for which the data are most accurately known give good agreement with the whole number hypothesis. The substance investigated in greatest detail is nitrous oxide, for which Blue and Giauque ⁽³⁾ give directly measured values † of $\lambda_s$ and $\lambda_l$ as

---

* The values given are those calculated from the equations, but the last figures are, of course, not really significant.

† The boiling-point and melting-point of nitrous oxide are 184·59° and 182·26° K. respectively. Blue and Giauque's direct measurements gave $\lambda_l$ as 3958 as the boiling-point, and the value 3937 given above is obtained by using Kelley's value of $d\lambda_l/dT$ for the variations of $\lambda_l$ with T. The value for $\lambda_s$ is obtained by adding Blue and Giauque's value for the directly measured latent heat of fusion, 1563.

5500 and 3937 respectively, with $\lambda_s/\lambda_l=1{\cdot}397$. The close agreement with the value 1·400 (=7/5) is very striking. For nitrogen peroxide the data of Kelley have been superseded by a recent paper of Giauque and Kemp (18) who have investigated nitrogen peroxide in great detail. They present their vapour-pressure data for both solid and liquid in the form of empirical equations, and give data for estimating the degree of dissociation in the reaction $N_2O_4 \rightleftharpoons 2NO_2$. The data in Table II. are obtained by differentiating their equations, the degree of dissociation at the triple point being calculated as 0·8852. There is a slight discrepancy between the directly measured latent heat of fusion (3502), and the calculated value ($\lambda_s-\lambda_l=3443$), which is presumably due to the uncertainty in degree of dissociation and the lack of correction for gas imperfection. This does not affect the $\lambda_s/\lambda_l$ ratio, which equals 1·396, and the close agreement with the ratio 7/5=1·400 is again very striking. Other reliable data are those for the halogens and mercuric bromide.

Table II.

| Substance. | $\lambda_s$. | $\lambda_l$. | $\lambda_s/\lambda_l$. | % difference from nearest whole number ratio. | % difference from next whole number ratio. | Remarks and notes. |
|---|---|---|---|---|---|---|
| $NH_3$ .......... | 7511 | 6082 | 1·235 | 5/4−1·2 | 6/5+2·9 | $A_1A_2$. |
| $SbCl_3$ .......... | 15429 | 12406 | 1·244 | 5/4−0·48 | 6/5+3·7 | B. |
| $WF_6$ .......... | 8608 | 6810 | 1·264 | 5/4+1·1 | 4/3−5·2 | A. |
| Monoclinic S .. | 3454 | 2738 | 1·261 | 5/4+0·92 | 4/3−5·39 | B. (See p. 478.) |
| $HgBr_2$ .......... | 18818 | 14860 | 1·266 | 5/4+1·28 | 4/3−5·04 | $A_1A_2$. |
| $HgCl_2$ .......... | 18497 | 14350 | 1·289 | 5/4+3·12 | 4/3−3·31 | $A_1A_2$ |
| $HgI_2$ .......... | 19901 | 15396 | 1·293 | 4/3−3·01 | 5/4+3·44 | $A_1A_2$. |
| $Br_2$.......... | 10530 | 7946 | 1·325 | 4/3−0·6 | 5/4+6·0 | B. |
| $Cl_2$ .......... | 6576 | 4964 | 1·325 | 4/3−0·6 | 5/4+6·0 | B. |
| $I_2$ .......... | 14517 | 10864 | 1·336 | 4/3+0·23 | 7/5−4·6 | $A_1A_2$. |
| $Al_2Br_6$ .......... | 20317 | 14895 | 1·364 | 4/3+2·3 | 7/5−2·6 | B. (see p. 469). |
| $N_2O$ .......... | 5500 | 3937 | 1·397 | 7/5−0·2 | 4/3+4·8 | Calorimetric values. |
| $N_2O_4$ .......... | 12145 | 8702 | 1·396 | 7/5−0·3 | 4/3+4·7 | A. (See p. 470.) |
| $Al_2I_6$ .......... | 27912 | 19950 | 1·399 | 7/5−0·10 | 4/3+4·5 | B. |
| $Fe_2Cl_6$ .......... | 33082 | 12490 | 2·649 | 8/3−0·67 | 5/2+5·96 | A. |
| $Al_2Cl_6$ .......... | 26522 | 9562 | 2·774 | 8/3+4·01 | 3/1−7·53 | |

## VI.

In dealing with the substances for which Kelley ignores $\triangle Cp$, and gives the latent heats of sublimation or evaporation as constants independent of temperature, considerable care is necessary in using the data. In some cases reference to the original papers shows that the experimental points scatter so much from a single curve that the constant $a$ of equation (3) cannot really be determined accurately. We have separated these substances from the remainder, since, although Kelley's figures represent an impartial selection of the most probable values, they clearly do not here permit a critical test of a whole number hypothesis. For some other substances we find that equation (3) is really only an approximation, the actual points showing a slight but systematic deviation, which, in some cases, was noted by the original authors. For these substances we give the values of $\lambda_s$ and $\lambda_l$ obtained from the values of $d\ln p/dT$ at the triple point, using the calculations of the original authors wherever these are available. For simplicity these details are referred to in the appendix. In cases where Kelley has combined the results of different authors we have not altered his figures, since it is clearly preferable for the critical selection to have been made independently of an attempt to test a whole number hypothesis.

Table III.

| Substance. | $\lambda_s$. | $\lambda_l$. | $\lambda_s/\lambda_l$. | % difference from nearest whole number ratio. | % difference from next whole number ratio. | Remarks and notes. |
|---|---|---|---|---|---|---|
| $\alpha$ $SO_3$ | 12250 | 10190 | 1·202 | 6/5+0·17 | 5/4−3·8 | A. |
| $\beta$ $SO_3$ | 13080 | 10190 | 1·284 | 5/4+2·72 | 4/3−3·7 | A. |
| $SO_2$ | 8460 | 6400 | 1·322 | 4/3−0·83 | 5/4+5·8 | $A_1A_2$. |
| $(CN)_2$ | 7750 | 5846 | 1·326 | 4/3−0·53 | 5/4+6·1 | A. (See p. 479.) |
| HCN | 8940 | 6660 | 1·342 | 4/3+0·68 | 7/5−4·1 | $A_1A_2$. |
| $Se_6$ | 27920 | 20600 | 1·355 | 4/3+1·65 | 7/5−3·2 | B. |
| CNCl | 8971 | 6421 | 1·397 | 7/5−0·21 | 3/2+4·8 | A. (See p. 479.) |
| $AsF_5$ | 7625 | 5083 | 1·500 | 5/2 0 | See Table I. | A. (See p. 479.) |
| $Si_2F_6$ | 10400 | 6500 | 1·600 | 8/5 0 | See Table I. | A. |
| $\gamma$ $SO_3$ | 16500 | 10190 | 1·619 | 8/5+1·2 | 5/3−2·9 | A. |
| $Re_2O_7$ | 32910 | 18300 | 1·798 | 7/4+2·7 | 2/1−10·1 | A. (See p. 480.) |

Table III. shows the data for substances for which the results are consistent, and appear accurate. The agreement with whole number ratios is again very striking, no less than seven out of eleven substances giving values of $\lambda_s/\lambda_l$ or $a_s/a_l$ [*] which differ by less than 1 per cent. from a ratio of numbers up to 8. This is clearly very improbable on the basis of any random distribution of the values of $\lambda_s/\lambda_l$.

---

[*] It will be appreciated that where the deviation of the log P−1/T curves from a straight line is allowed for, the values given are $\lambda$ values, except for the departure from the ideal gas laws.

Table IV. shows the data for substances for which the possible errors appear to be much greater. This is included for completeness in order that the whole of Kelley's data may be surveyed. For three substances in this table $\lambda_s/\lambda_l$ differs by less than 1 per cent. from a ratio of numbers up to 8, but the data here have much less significance than those in Tables II. and III.

TABLE IV.

| Substance. | $Ra_s$ or $\lambda_s$. | $Ra_l$ or $\lambda_l$. | $\lambda_s/\lambda_l$. | % difference from nearest whole number ratio. | % difference from next nearest whole number ratio. |
|---|---|---|---|---|---|
| $H_2Te$ | 7320 | 5650 | 1·296 | 4/3—2·8 | 5/4+3·7 |
| $MoF_6$ | 8500 | 6000 | 1·417 | 7/5+1·2 | 3/2—5·5 |
| $B_{10}H_{14}$ | 19400 | 11600 | 1·672 | 5/3+0·30 | 7/4—4·5 |
| $P_4O_{10}$ | 36200 | 19700 | 1·838 | 7/4+5·02 | 2/1—8·1 |
| $Sb_4O_6$ | 44820 | 17820 | 2·515 | 5/2+0·6 | 8/3—5·7 |
| $OsO_4$ Yellow | 13510 | 9450 | 1·430 | 7/5+2·1 | 3/2—4·7 |
| $OsO_4$ White | 11790 | 9450 | 1·248 | 5/4—0·16 | 6/5+4·0 |

## VII.

Before discussing the meaning of their relations, we may consider briefly the data for some special substances in which different allotropic forms of the solid are found.

### (1) *Phosphorus.*

Of the allotropic forms of phosphorus the yellow variety resembles the liquid most closely, and for this modification the ratio $\lambda_s/\lambda_l<1{\cdot}2$. For the solid violet form Kelley gives $Ra_s=25{,}600$, and for liquid phosphorus $Ra_l=12{,}520$, the ratio of these being 2·045 : 1. For the violet form the vapour-pressure data are in agreement with equation (3), and Kelley's value of 25,600 is substantially the same as the value 25,839 given by Smits and Bokhorst (4). Kelley's value for the liquid is that for liquid white phosphorus at low temperatures (McCrae and V. Voorhis (5)) where the data obey equation (3). It is possibly of significance that the two quantities are almost in the ratio 2 : 1, but this ratio is not that at the triple point, since at the higher temperatures the log $P/\frac{1}{T}$ graph is a curve. The curvature was analysed by Smits and Bokhorst (*loc. cit.*), and their values at the triple point[*] were

$$\lambda_s=25{,}839 \text{ violet}, \qquad \lambda_l=10{,}221, \qquad \lambda_s/\lambda_l=2{\cdot}528.$$

---

[*] These values are from the gradients of the curves at the triple point, but as the pressure is high they are not necessarily the true $\lambda$ values, although their ratios (see p. 467) are almost the same as the ratio $\lambda_s/\lambda_l$.

The ratio is thus almost exactly 5/2, whilst if Kelley's value for the violet form is considered more probable, the agreement is even better, since

$$\frac{25,600}{10,221}=2\cdot505.$$

Data are not available for liquid phosphorus and black phosphorus at the melting-point of the latter, but for the black and yellow modifications Kelley gives $Ra_{s_{\text{black}}}=33,100$, and $Ra_{s_{\text{yellow}}}=13,135$, so that the ratio $\frac{\lambda_{s_{\text{black}}}}{\lambda_{s_{\text{yellow}}}}=2\cdot520$, is equal to 5/2 within the limits of experimental accuracy. The relation between the different modifications of phosphorus thus appear very significant.

### (2) *Arsenic.*

In view of the relations shown above for phosphorus, it is possibly significant that in the case of arsenic the ratio $a_s/a_l=3\cdot000$ according to the data of Horiba (6), whose equations of the type (3) give values for the solid and liquid as 33,600 and 11,200 respectively. The data for the liquid appear consistent, but for the solid the points show deviations near the melting-point, and the above values may not be those at the triple point.

### (3) *Phosphorus Pentoxide.*

The data referred to by Kelley have been superseded by those of Southard and Nelson (7), who confirm the conclusions of Hoeflake and Scheffer (8) in contradiction to those of Smits and Deinum (9). There are two solid forms for which the vapour pressures agree with equations of the type (3), and for these the latent heats of sublimation are calculated as 36,200 (high temperature form) and 22,800 (low temperature form) respectively. The ratio of these quantities is equal to 1·588, and thus agrees with the ratio 8/5 to within less than 1 per cent. The relation between the high temperature form and the liquid have been given in Table IV., and are, unfortunately, not of the highest accuracy.

### (4) *Arsenic Trioxide.*

This substance exists in three solid forms, of which two are well established. The high temperature monoclinic form melts at 586° K., and Kelley ignores the curvature of the $\log p \frac{1}{T}$ graph. This curvature was analysed by Smits and Beljaars (10), whose value for $\lambda_{s_{\text{monoclinic}}}$ is 23,676 at the triple point. For $\lambda_l$ these authors gave 14,734 as compared with the value 14,300 given by Kelley. We have plotted the points graphically, and obtain 14,635, in good agreement with Smits and Beljaars.

Using Smits and Beljaar's figures the ratio $\lambda_s/\lambda_l = 1{\cdot}607$ and thus differs from the ratio 8/5 by only 0·44 per cent.

The $\beta$ or orthorhombic form can also be obtained in (metastable) equilibrium with the liquid at 545·1° K., and gives a linear relation between log p and 1/T, from which Smits and Beljaars calculate $\lambda_{s_{\text{orthorhombic}}} = 29{,}833$. Using Smits and Beljaars's value for the liquid, the ratio $\lambda_{s_{\text{orthorhombic}}}/\lambda_l = 29{,}833/14{,}734 = 2{\cdot}025$ and thus differs from 2/1 by 1·25 per cent. The value given by Kelley for the orthorhombic form is 30,520, and from is obtained a combination of the values of Smits and Beljaars (*loc. cit.*) and of Rushton and Daniels (11), and this, of course, does not give such an exact agreement with the ratio 2/1, although even here the difference (3·5 per cent.) is not very great.

The third or $\gamma$ modification found by Smits and Beljaars yields a linear $\log p \Big/ \frac{1}{\mathrm{T}}$ graph from which they estimate $\lambda_s = 21{,}130$, so that the ratio

$$\frac{\lambda_s}{\lambda_l} = \frac{21130}{14734} = 1{\cdot}434,$$

which differs by 2·3 per cent. from the ratio 7/5.

The general impression gained from a study of these figures is clearly that the whole number relations are confirmed.

### (5) *Sulphur.*

The values for monoclinic sulphur given in Table IV. refer to the equilibrium form of liquid sulphur, and are calculated from the data of Lewis and Randal (12) quoted by Kelley. For rhombic sulphur $\lambda_s/\lambda_l < 1{\cdot}2$, and is thus not considered in these tables. It is perhaps significant that the latent heats of fusion of rhombic and monoclinic sulphur when melted to form pure liquid $S_\lambda$ are given by Lewis and Randall (*loc. cit.*) as 14·5 and 11·1 cal. per gram respectively with an error of ±2–3 per cent. The ratio $\frac{14{\cdot}5}{11{\cdot}1} = 1{\cdot}306$, and thus equals 4/3 within the limits of accuracy of the data.

These relations, together with those for $SO_3$ in Table III., clearly suggest that where substances exist in different allotropic forms, the latent heats of the different modifications are sometimes simply related.

## IX.

The ratios of $\lambda_s/\lambda_l$ given in the preceding sections are shown graphically in fig. 1. In this figure each value of $\lambda_s/\lambda_l$ is represented by a line of equal height, and where different substances have values of $\lambda_s/\lambda_l$ too nearly equal to be distinguished on this scale, the line is drawn a corresponding number of units long. The values from Table IV. are indicated by dotted lines in view of their less critical nature. The ratios of numbers up to 8 are marked underneath the scale, and it is at once apparent how the $\lambda_s/\lambda_l$ values are not distributed at random, but tend to approximate to the whole number ratios. The exception is the small group formed by $HgCl_2$, $HgI_2$, and $\beta SO_3$ for which $\lambda_s/\lambda_l = 1{\cdot}28 - 1{\cdot}29$, *i. e.*, almost midway between the two ratios 5/4 and 4/3. It will be appreciated that with the accuracy at present available there may really be agreement with either of these ratios, but a possible explanation of a genuine deviation from a simple ratio is given below.

Fig. 1.

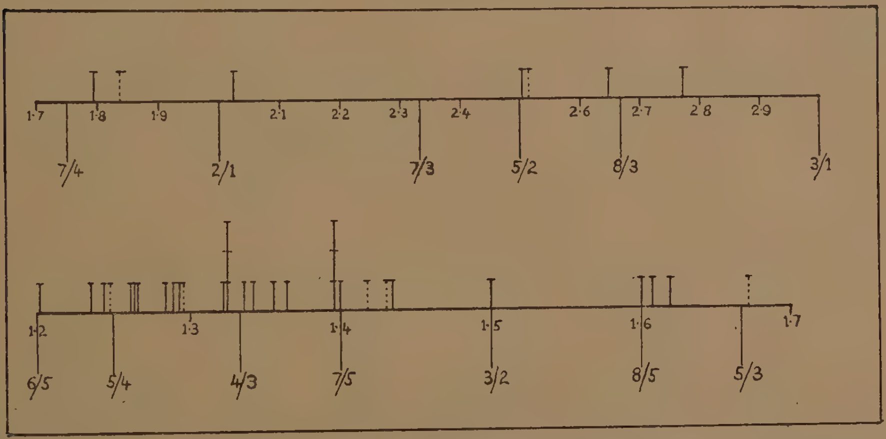

In the lower part of this figure the horizontal line is a scale from 1·2 to 1·7, and the positions of the values corresponding to whole-number ratios are marked below the scale. Each value of $\lambda_s/\lambda$ is indicated by a vertical line of uniform length drawn upward from the horizontal line. In cases where two or more substances have values of $\lambda_s/\lambda_l$ too nearly equal to be distinguished clearly, the line is drawn a corresponding number of units long. The upper part of the diagram shows a similar scale for the range 1·7 to 3·0. The dotted lines refer to substances in Table IV.

The meaning of these curious relations is at present unknown, but they may suggest that in the region of the triple points of the substances concerned, the liquid has a structure in which the atoms are held together by a definite number of bonds of the same nature as those concerned in the cohesion in a solid crystal. From this point of view simple whole number ratios might be expected in cases where the bonds in the solid and liquid were different in number but similar in nature, and where only a small influence was exerted by secondary factors such as differences in the angles between different bonds, or the existence of secondary bonds of a weaker nature. Some crystals have, for example, a molecular layer structure with comparatively large distances between the layers. In such cases, on sublimation, most of the energy change is that required to break the bonds (usually of the van der Waals type) between the molecules in each layer, and comparatively little energy is needed to break the bonds between the different layers. In such cases, if the liquid had a structure in which the bonds were of the same nature as those binding the molecules together in any one layer of the solid, we might expect the $\lambda_s/\lambda_l$ ratios to approximate to those of whole numbers, the divergence from the exact whole number ratio becoming greater as the forces between the layers became more important.

Reference to fig. 1 shows that of the various ratios concerned the ratio 4/3 is the most common. The following substances have $\lambda_s/\lambda_l$ ratios close to this value :—

| $\lambda_s/\lambda_l$ within 1 per cent. of 4/3 | $\lambda_s/\lambda_l$ within between 1 and 2·2 per cent. of 4/3. |
|---|---|
| — | CNCl |
| $I_2$ | $Al_2Br_6$ |
| $Br_2$ | $Se_6$ |
| $Cl_2$ | |
| HCN | |
| $SO_2$ | |
| $(CN)_2$ | |

Of these nine substances, $I_2$, $Br_2$, $Cl_2$, HCN, $(CN)_2$, and CNCl have molecules which are either linear or of the simple 0—0 type. $Al_2Br_6$ has a structure

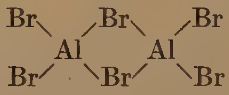

which is much longer than it is wide, whilst the molecule of $SO_2$ is of the bent

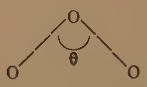

type, with the angle $\theta = 124°$ approximately. On the whole, therefore, the ratio $\lambda_s/\lambda_l = 4/3$ is favoured by a molecule resembling a thick rod.

The crystal structures of the halogens have been determined, and all contain $X_2$ molecules arranged in layers. It is, perhaps, significant that in the crystals of bromine and iodine each atom has one close neighbour corresponding to the covalent bond of the $Br_2$ or $I_2$ molecule, and two next nearest neighbours to which attraction is by the van der Waals forces. Each $Br_2$ or $I_2$ *molecule* is thus held in its layer by four van der Waals bonds, so that if in the liquid there were three such bonds per molecule, the $\lambda_s/\lambda_l=4/3$ ratio might be explained. For chlorine, however, the crystal structure is different, and such a simple relation would not suffice. This does not imply that an explanation on the above lines is incorrect, since the same factor which makes the $Cl_2$ molecules in the solid pack differently from $Br_2$ or $I_2$ molecules may also affect the packing of $Cl_2$ molecules in the liquid.

In this connexion the values for the mercuric halides may be of interest, since $HgCl_2$, $HgBr_2$, and $HgI_2$ all have linear X—Hg—X molecules, in which the mercuric ion * is much smaller than that of the halogen ions. The ion or atom of iodine is the largest in the halogen family, and hence the I—Hg—I molecule will have a shape most nearly resembling that of a diatomic halogen molecule, since the small mercuric ion will have relatively the least effect when the halogen ion is the largest. It will be seen in Table II. that for $HgI_2$, $\lambda_s/\lambda_l=1{\cdot}293$, this ratio being nearer to 4/3 than the ratios for $HgBr_2$ or $HgCl_2$. The crystal structure of the high temperature modification of $HgI_2$ has not apparently been determined, but since it is known to be isomorphous with, and to form solid solutions with $HgBr_2$, it has probably the same structure, which is different from that of $HgCl_2$, although both structures contain linear $HgX_2$ molecules. In neither structure is there such a well-defined single van der Waals distance of approach as in the crystals of the halogens, so that it is possible that the $\lambda_s/\lambda_l$ values for these halides are the result of secondary factors producing a genuine deviation from the ratio 4/3.

Sufficient data are not yet available to discuss the other whole-number ratios to which the $\lambda_s/\lambda_l$ values approximate, although it is perhaps significant that in Table II. both $NH_3$ and $SbCl_3$, which have tetrahedral molecules, have almost the same $\lambda_s/\lambda_l$ ratio. It is clear that the substances for which the $\lambda_s/\lambda_l$ ratios are large are those for which the change from the solid to the liquid is more drastic than the change from the liquid to the vapour state. When $\lambda_s/\lambda_l$ is greater than 2 the latent heat of fusion is greater than the latent heat of evaporation of the liquid. The substances dealt with above for which this is the case are $Fe_2Cl_6$, $Al_2Cl_6$, $Sb_4O_6$, P (black and violet modifications), and As. In ferric chloride and aluminium chloride this is probably due to the essentially ionic nature of the crystal and the co-valent nature of the molecules in the liquid and gas, which results in the change from solid to liquid being more drastic than that from liquid to gas. This, of course, does not explain the whole-number ratios, although these might be understood if the bonds in the solid and liquid were not purely ionic and co-valent, but correspond with different resonance bonds derived from the same two extreme states. In black phosphorus and arsenic the atoms are arranged in double layers, so that each has three close neighbours, the bond angles being approximately 90°. The vapours consist largely of $P_4$ and $As_4$ tetrahedral molecules, and the relatively small latent heat of evaporation suggests that the liquid also consists of these molecules, so that the change from liquid to gas is less drastic than from solid to liquid. This is in marked contrast to the behaviour of antimony and bismuth, which, in spite of having the same type of crystal structure as arsenic, have very stable liquids and relatively small latent heats of fusion. This difference is probably connected with the fact that molecules of $P_4$ and $As_4$ are much more stable than molecules of $Sb_4$ or $Bi_4$, and it is hoped to discuss this and similar relations in a later communication.

---

* The bond between the mercury and halogen atoms is usually regarded as ionic, but may be of a partly co-valent type.

The above tentative explanation of the approximation of the $\lambda_s/\lambda_l$ values to those of simple ratios also agrees with the fact that for the majority of normal metals $\lambda_s/\lambda_l$ is nearly unity, since the general conclusion is that the structure of a liquid metal at its melting-point tends to resemble that of the solid, in which case we should expect the change from solid to liquid to be much less drastic than that from liquid to gas. It seems possible, therefore, that a study of the $\lambda_s/\lambda_l$ ratios in conjunction with the crystal structures may throw light on the nature of the liquids.

## *Acknowledgements.*

The author must acknowledge his indebtedness to Professor C. N. Hinshelwood, F.R.S., for laboratory accommodation and many other facilities, which have helped the present work. Thanks are also due to Dr. F. Simon and Mr. H. M. Powell for much interesting discussion.

The Old Chemistry Department,
The University Museum,
Oxford.

## APPENDIX.

### *Table II.*

All the values in this table are calculated directly from the equations given in Kelley's review, except for sulphur, nitrous oxide, and nitrogen peroxide. For monoclinic sulphur Kelley refers to the text-book of Lewis and Randall, and we have used their results to calculate the latent heat of fusion of monoclinic sulphur to the equilibrium liquid. The value for $\lambda_l$ is taken from the more recent work of West and Menzies (13), who calculate $\lambda_l$ at intervals of 20°, and we have extrapolated their curve to the natural melting-point (114·6°). For nitrogen peroxide, and nitrous oxide as explained on p. 469–470, we have used the recent results of Giauque and Kemp (18), and Blue and Giauque (3).

*Table III.*

Data for the following substances are taken directly from Kelley's review :—$\alpha SO_3$, $\beta SO_3$, $\gamma SO_3$, $SO_2$, HCN, $Se_6$, and $Si_2F_6$. For all these, Kelley ignores the variations of $\lambda_s$ or $\lambda_l$ with temperature and uses a simple $\log p/\frac{1}{T}$ straight line. For selenium the dissociation of $Se_6$ molecules at the melting-point is negligible. For the substances detailed below reference to the original papers shows that a slight curvature of the $\log p/\frac{1}{T}$ line has been ignored, and Kelley's figures have been modified for the reasons described.

For $(CN)_2$, reference to the original paper of Perry and Bardwell (14) shows that the $\log P/\frac{1}{T}$ curve for the liquid is not really linear. These authors give an equation from which $\lambda_l$ at the triple point is calculated as 5846, in contrast to the value 5770 given by Kelley, who ignored the curvature. Perry and Bardwell's equation is in very good agreement with the data near the triple point. Kelley's value for the solid, 7770, is in good agreement with that of Perry and Bardwell (7750), the $\log p/\frac{1}{T}$ curve being linear.

For CNCl, the data given by Kelley were from very old work, and have been superseded by the work of Klemenc and Wagner (15). We have plotted these graphically in the usual $\log p/\frac{1}{T}$ way, and the figures given in Table III. are calculated from the slopes of the curves (which are nearly linear) at the triple point. A slight uncertainty exists because the lines do not intersect exactly at the triple point. The figures given in Table III. take the triple point into account, and if this were not done, the $\lambda_s/\lambda_l$ ratio would be very slightly higher.

For $AsF_5$, examination of the original data of Ruff, Braida, Bretschneider, Menzel, and Plant (16) showed that the $\log p/\frac{1}{T}$ curve was not exactly linear. The ratio $\lambda_s/\lambda_l=1·500$ was obtained by two workers who estimated the gradients at the triple point quite independently.

For $Re_2O_7$ the $\log p \Big/ \frac{1}{T}$ curve is again not exactly linear, and the original paper of Ogawa (17) gives the variation of $\lambda_s$ and $\lambda_l$ with temperature, and these results are used in Table III.

### *Table IV.*

The data in this table are taken directly from Kelley's review, and all are based on the assumption of a simple linear relation between log *p* and 1/T.

### *References.*

(1) Stockdale, Proc. Roy. Soc. [A], clii. p. 81 (1935).
(2) Kelley, U.S. Bureau of Mines, Bulletin No. 383.
(3) Blue and Giauque, J. Amer. Chem. Soc. lvii. p. 991 (1935).
(4) Smits and Bokhorst, *Z. phys. Chem.* xci. p. 249 (1916).
(5) McCrae and V. Voorhis, J. Amer. Chem. Soc. xliii. p. 547 (1921).
(6) Horiba, *Proc. Acad. Sci. Amsterdam*, xxv. p. 387 (1923).
(7) Southard and Nelson, J. Amer. Chem. Soc. lix. p. 911 (1937).
(8) Hoeflake and Scheffer, *Rec. Trav. Chim.* xlv. p. 191 (1926).
(9) Smits and Deinum, *Proc. Acad. Amsterdam* xxxiii. p. 514 (1930).
(10) Smits and Beljaars, *Proc. Acad. Amsterdam*, xxxiv. p. 1141 (1931).
(11) Rushton and Daniels, J. Amer. Chem. Soc. xlviii. p. 384 (1926).
(12) Lewis and Randall, 'Thermodynamics and the Free Energy of Chemical Substances,' 1923.
(13) West and Menzies, J. Phys. Chem. xxxiii. p. 1880 (1929).
(14) Perry and Bardwell, J. Amer. Chem. Soc. xlvii. p. 2629 (1925).
(15) Klemenc and Wagner, *Zeit. anorg. Chem.* ccxxxv. p. 427 (1937).
(16) Ruff, Braida, Bretschneider, Menzel, and Plant. *Zeit. anorg. Chem.* ccvi. p. 59 (1932).
(17) Ogawa, *Bull. Chem. Soc. Japan* vii. p. 265 (1932).
(18) Gianque and Kemp, J. Chem. Phys. vi. p. 40 (1938).

# XLIV. *The Magnitude of the Direct Stress in a Beam of Fixed Span.*

By R. J. Cornish, M.Sc., Assoc.M.Inst. C.E.*

[Received December 22, 1938.]

## (1) *Symbols.*

$b$ = breadth of beam.
$d$ = depth of beam.
$f_c$ = maximum concrete stress due to bending.
$f_s$ = maximum steel stress due to bending.
$l$ = span of beam.
$n = E_s/E_c$.
$r = f_s/f_c$.
$s$ = distance measured along neutral axis.
$u = \frac{l}{2}\sqrt{\frac{P}{EI}}$.
$v$ = distance of extreme fibre from neutral axis of beam.
$w$ = load per unit length of beam.
$x$, $y$ = coordinates of point on neutral axis.
$y_c$ = deflexion at centre of beam.
A = area of cross-section of beam.
E = Young's modulus.
$E_c$ = Young's modulus for concrete.
$E_s$ = Young's modulus for steel.
I = second moment of area of cross-section.
M = bending moment at any point of beam.
$M_{max.}$ = maximum bending moment in beam.
P = axial force at ends of beam, such that loaded span is kept equal to unloaded span.
W = concentrated load at centre of span.

## (2) *Introduction.*

When a beam, simply supported at two points, is deflected, the points of support must approach one another slightly, since the length of the neutral axis remains constant. If the beam has fixed "pin-jointed" ends or built-in ends, longitudinal movement is prevented, and a direct stress is developed in the beam. In the following paper general expressions for this stress are obtained in four representative cases and the probable maximum values of the stress are deduced for steel and reinforced concrete beams.

---

* Communicated by the Author.

### (3) *Derivation of General Expression.* (*Case I.*)

Fig. 1 illustrates a beam subject to a uniform continuous load $w$ per unit length. The beam is pin-jointed at the two ends A and B, and before loading the span AB is $l$. In order to maintain this span when the beam is loaded, outward horizontal forces P act at A and B.

Fig. 1.

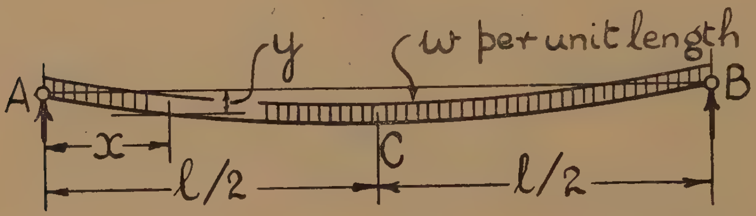

Then the bending moment at any point $(x, y)$ of the beam is given by

$$M=\tfrac{1}{2}wlx-\tfrac{1}{2}wx^2-Py.$$

Hence

$$EI\frac{d^2y}{dx^2}=-\tfrac{1}{2}wlx+\tfrac{1}{2}wx^2+Py. \quad \dots\dots \quad (1)$$

The solution of this equation is

$$y=\frac{wEI}{P^2}\left\{\frac{\cosh\left(1-\frac{2x}{l}\right)u}{\cosh u}-1\right\}+\frac{wx}{2P}(l-x), \quad \dots \quad (2)$$

where

$$u=\frac{l}{2}\sqrt{\frac{P}{EI}}. \quad \dots\dots \quad (3)$$

Since the slope of the beam at any point is small, we can write

$$\int ds=\int dx\left\{1+\frac{1}{2}\left(\frac{dy}{dx}\right)^2\right\}.$$

But

$$\int_{x=0}^{x=l} ds=l\left(1+\frac{P}{EA}\right) \text{ approximately,}$$

and

$$\int_0^l dx=l.$$

Hence

$$\frac{\mathrm{P}l}{\mathrm{EA}}=\int_0^l \frac{1}{2}\left(\frac{dy}{dx}\right)^2 dx, \quad \ldots \ldots \quad (4)$$

which gives

$$\frac{\mathrm{P}}{\mathrm{A}}=\frac{w^2l^6}{256\ \mathrm{EI}^2u^6}(\tanh^2 u+\frac{5}{u}\tanh u+\tfrac{2}{3}u^2-5). \quad \ldots \quad (5)$$

Tanh² $u$ and tanh $u$ may be replaced by their expansions in terms of $u$ (see Appendix), and equation (5) becomes

$$\frac{\mathrm{P}}{\mathrm{A}}=\frac{w^2l^6}{256\mathrm{EI}^2u^6}\left(\frac{34}{315}u^6-\frac{248}{2835}u^8+\ldots\right),$$

$$=\frac{17w^2l^6}{40{,}320\mathrm{EI}^2}\left(1-\frac{124}{153}u^2+\ldots\right). \quad \ldots \ldots \quad (6)$$

In practice $u$ appears to be always much less than 1 (its greatest value in the examples taken below is 0·02), and, therefore, $124u^2/153$ is negligible compared with 1.

In this beam

$$\mathrm{M}_{\mathrm{max.}}=\frac{wl^2}{8}-\mathrm{P}y_c,$$

$$=\frac{wl^2}{8} \text{ approximately.}$$

Thus equation (6) becomes

$$\frac{\mathrm{P}}{\mathrm{A}}=\frac{17}{630\mathrm{E}}\left\{\frac{\mathrm{M}_{\mathrm{max.}}l}{\mathrm{I}}\right\}^2. \quad \ldots \ldots \quad (7)$$

Alternatively, P/A can be expressed in terms of the ratio of the central deflexion $y_c$ to the span. From equation (2)

$$y_c=\frac{w\mathrm{EI}}{\mathrm{P}^2}(\operatorname{sech} u-1)+\frac{wl^2}{8\mathrm{P}},$$

$$=\frac{5wl^4}{384\mathrm{EI}}\left(1-\frac{61}{300}u^2+\ldots\right).$$

As before, the second term can be neglected, and the deflexion at the centre is seen to be approximately the same as for a simply supported beam. Then equation (6) can be written

$$\frac{\mathrm{P}}{\mathrm{A}}=\frac{2176\mathrm{E}}{875}\left\{\frac{y_c}{l}\right\}^2. \quad \ldots \ldots \quad (8)$$

### (4) *Other Cases.*

In the other cases considered, the proofs follow the same lines as in Case I., and will not be given in detail.

*Case II.* (see fig. 2).—Pin-jointed beam with central concentrated load.

Fig. 2.

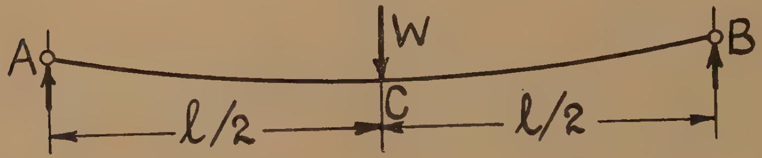

Between $x=0$ and $x=\frac{1}{2}l$,

$$y=-\frac{Wl}{4Pu}\cdot\frac{\sinh 2ux/l}{\cosh u}+\frac{Wx}{2P}.$$

Between $x=\frac{1}{2}l$ and $x=l$,

$$y=-\frac{Wl}{4Pu}\cdot\frac{\sinh 2u(l-x)/l}{\cosh u}+\frac{W(l-x)}{2P}.$$

$$\frac{P}{A}=\frac{W^2l^4}{256EI^2u^4}\left(3-\frac{3}{u}\tanh u-\tanh^2 u\right),$$

$$=\frac{W^2l^4}{960EI^2}\left(1-\frac{17}{42}u^2+\ldots\right),$$

$$=\frac{1}{60E}\left\{\frac{M_{\text{max.}}l}{I}\right\}^2, \qquad (9)$$

$$=\frac{12E}{5}\left\{\frac{y_c}{l}\right\}^2. \qquad (10)$$

*Case III.* (see fig. 3).—Beam, built in horizontally at both ends, with uniformly distributed load.

Fig. 3.

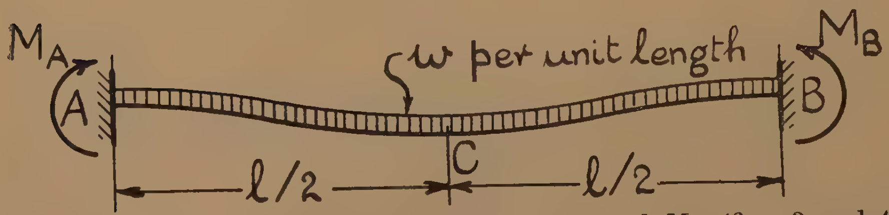

*Note.*—The arrows showing the directions of $M_A$ and $M_B$ (figs. 3 and 4) indicate the positive directions according to the sign convention adopted. The actual fixing moments in these cases are negative.

$$y=\frac{wl^2}{4Pu}\left\{\frac{\cosh\left(1-\frac{2x}{l}\right)u}{\sinh u}-\coth u\right\}+\frac{wx}{2P}(l-x).$$

$$M_A=M_B=\frac{wl^2}{4u^2}(1-u\coth u).$$

$$\frac{P}{A}=\frac{w^2l^6}{256EI^2u^6}\left(\frac{5}{3}+\frac{4}{u^2}-\frac{3}{u}\coth u-\coth^2 u\right),$$

$$=\frac{w^2l^6}{60480EI^2}\left(1-\frac{1}{5}u^2+\dots\right),$$

$$=\frac{1}{420E}\left\{\frac{M_{\max.}l}{I}\right\}^2, \qquad (11)$$

$$=\frac{256E}{105}\left\{\frac{y_c}{l}\right\}^2. \qquad (12)$$

*Case IV.* (see fig. 4).—Beam built in horizontally at both ends, with central concentrated load.

Fig. 4.

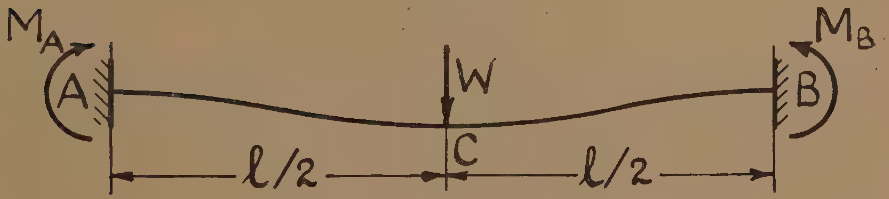

Between $x=0$ and $x=\frac{1}{2}l$:

$$y=\frac{Wl}{4Pu}\left\{\frac{\sinh\left(\frac{1}{2}-\frac{2x}{l}\right)u}{\cosh\frac{1}{2}u}-\tanh\tfrac{1}{2}u\right\}+\frac{Wx}{2P}.$$

Between $x=\frac{1}{2}l$ and $x=l$:

$$y=\frac{Wl}{4Pu}\left\{\frac{\sinh\left(-\frac{3}{2}+\frac{2x}{l}\right)u}{\cosh\frac{1}{2}u}-\tanh\tfrac{1}{2}u\right\}+\frac{W(l-x)}{2P}.$$

$$M_A=M_B=-\frac{Wl}{4u}\tanh\tfrac{1}{2}u.$$

$$\frac{P}{A}=\frac{W^2l^4}{256EI^2u^4}\left(3-\frac{6}{u}\tanh\frac{1}{2}u-\tanh^2\frac{1}{2}u\right),$$

$$=\frac{W^2l^4}{15360EI^2}\left(1-\frac{17}{84}u^2+\dots\right),$$

$$=\frac{1}{240E}\left\{\frac{M_{\max.}l}{I}\right\}^2, \qquad (13)$$

$$=\frac{12E}{5}\left\{\frac{y_c}{l}\right\}^2. \qquad (14)$$

### (5) *Steel Beams.*

British Standard Specification No. 449, 1937, requires that the ratio of the "calculated deflection of the beam" to the span shall be less than 1/325. Substitution of this value in equations (8), (10), (12), and (14) gives the following values of P/A in the various cases :—

I., 707 lb. per sq. in. ; II., 682 lb. per sq. in. ;
III., 692 lb. per sq. in. ; IV., 682 lb. per sq. in.

It should be pointed out that, except in Case I., the maximum B.S.S. deflexion is obtained only with values of $l/d$ greater than those usually met with in practice. If the maximum tensile stress is taken as 18,000 lb. per sq. in. and E as $30.10^6$ lb. per sq. in., the corresponding values of $l/d$ are :

I., 24·6 ; II., 30·8 ; III., 82·0 ; IV., 61·5.

### (6) *Reinforced Concrete Beams.*

The following assumptions have been made :—

(i.) The beam is singly reinforced, the concrete taking compression only (in Cases III. and IV. an actual beam would generally have double reinforcement).

(ii.) Both steel and concrete are stressed to the maximum. It follows then that $v$, the distance from the neutral axis to the extreme compression fibre, is equal to $nd/(r+n)$. [$d$ is here the effective depth to centre of reinforcement].

(iii.) On the analogy of the uniform beam, the second moment of area of the cross-section is defined by the equation

$$\mathrm{I}=\frac{\mathrm{M}_{\max.}v}{f_c}=\frac{\mathrm{M}_{\max.}}{f_c}\cdot\frac{nd}{r+n},$$

*i. e.,*

$$\frac{\mathrm{M}_{\max.}l}{\mathrm{I}}=\frac{(r+n)f_cl}{nd} \quad . \; . \; . \; . \; . \; . \; . \; . \; . \; . \quad (15)$$

(iv.) According to the Code of Practice for Reinforced Concrete (1933), reasonable maximum values for $f_s$ and $f_c$ are 20,000 lb. per sq. in. and 1250 lb. per sq. in. respectively, and $n$, the modular ratio, is $40{,}000/3\,f_c$.

Equation (15) then leads to the expression

$$\frac{1}{\mathrm{E}_c}\left\{\frac{\mathrm{M}_{\max.}l}{\mathrm{I}}\right\}^2=3{\cdot}47\left\{\frac{l}{d}\right\}^2.$$

(v.) If transverse bending is neglected, and the equations deduced above are considered applicable to slabs supported along two sides, $l/d$ may reach 30. In an ordinary beam it is unlikely to exceed 20.

The above assumptions are evidently far from exact, and it can only be claimed that they lead to results of the correct order. The maximum values of P/A, given by equations (7), (9), (11), and (13) respectively, in the various cases are as follows :—

Slabs : I., 84 lbs. per sq. in. ; II., 52 lb. per sq. in. ; III., 8 lb. per sq. in. ; IV., 13 lb. per sq. in.

Beams : I., 37 lb. per sq. in. ; II., 23 lb. per sq. in. ; III., 3·5 lb. per sq. in. ; IV., 6 lb. per sq. in.

### (7) *Summary.*

The direct stress in a beam of fixed span is examined for two types of loading combined with two types of end restraint. General equations are deduced for each case, and it is shown that, with beams of steel and reinforced concrete as at present designed, the direct stresses are small in comparison with those due to bending.

### (8) *Appendix.*

The expansions of hyperbolic functions used in the paper do not appear to be generally available to a sufficient number of terms ; they are given below :—

$$\tanh u = u - \frac{1}{3}u^3 + \frac{2}{15}u^5 - \frac{17}{315}u^7 + \frac{62}{2835}u^9 - \dots$$

$$\tanh^2 u = u^2 - \frac{2}{3}u^4 + \frac{17}{45}u^6 - \frac{62}{315}u^8 + \frac{1382}{14175}u^{10} - \dots$$

$$\coth u = \frac{1}{u} + \frac{1}{3}u - \frac{1}{45}u^3 + \frac{2}{945}u^5 - \frac{1}{4725}u^7 + \dots$$

$$\coth^2 u = \frac{1}{u^2} + \frac{2}{3} + \frac{1}{15}u^2 - \frac{2}{189}u^4 + \frac{1}{675}u^6 - \dots$$

# XLV. *Formulæ for Generalized Hypergeometric Functions as Particular Cases of more General Formulæ.*

By Professor T. M. MacRobert, University of Glasgow *.

[Received July 25, 1939.]

## § 1. *Introductory.*

In this paper it will be shown how certain known formulæ for Generalized Hypergeometric Functions can be derived as particular cases of formulæ of more general types. In section 2 two formulæ of Whipple's for nearly-poised series with unit argument are shown to be particular cases of a formula involving a double series with variable argument. In section 3 it is shown that Saalschütz's Theorem is a particular case of another formula of this type. In section 4 certain transformations of Saalschützian Series are derived from expressions for such series as multiple series; and in section 5 two known formulæ for terminating well-poised series are found to be degenerate cases of expressions for these series as multiple series.

## § 2. *Nearly-poised Series.*

In Whipple's formula (Proc. Lond. Math. Soc. ser. 2, xxvi. p. 267, 1926)

$$
{}_3F_2\left(\begin{matrix}\alpha,\ \beta,\ \gamma\ ;\ z\\ \alpha-\beta+1,\ \alpha-\gamma+1\end{matrix}\right)
=(1-z)^{-\alpha}{}_3F_2\left(\begin{matrix}\tfrac{1}{2}\alpha,\ \tfrac{1}{2}+\tfrac{1}{2}\alpha,\ 1+\alpha-\beta-\gamma\ ;\ \lambda\\ \alpha-\beta+1,\ \alpha-\gamma+1\end{matrix}\right), \quad . \ . \ . \quad (1)
$$

where $\lambda=-4z/(1-z)^2$, replace $z$ by $zt$, multiply by $t^{\delta-1}(1-t)^{\omega-\delta-1}$, where $R(\delta)>0$, $R(\omega-\delta)>0$, and integrate with regard to $t$ from 0 to 1. Then, if $z$ lies within the inner loop of the curve,

$$
16(x^2+y^2)=\{(x-1)^2+y^2\}^2,
$$

$$
{}_4F_3\left(\begin{matrix}\alpha,\ \beta,\ \gamma,\ \delta\ ;\ z\\ \alpha-\beta+1,\ \alpha-\gamma+1,\ \omega\end{matrix}\right)
=\sum_{n=0}^{\infty}\frac{(\tfrac{1}{2}\alpha\ ;\ n)(\tfrac{1}{2}+\tfrac{1}{2}\alpha\ ;\ n)(1+\alpha-\beta-\gamma\ ;\ n)(\delta\ ;\ n)}{n!\ (\alpha-\beta+1\ ;\ n)(\alpha-\gamma+1\ ;\ n)\ (\omega\ ;\ n)}(-4z)^n
$$

$$
\times F\left(\begin{matrix}\delta+n,\ \alpha+2n\ ;\ z\\ \omega+n\end{matrix}\right), \quad . \ . \ . \ . \ . \ . \ . \ . \quad (2)
$$

where the symbol $(k\ ;\ n)$ denotes the product

$$
k(k+1)(k+2)\ .\ .\ .\ (k+n-1).
$$

In the first place, put $\alpha=-m$, where $m$ is zero or a positive integer; then all the series in (2) are terminating. On putting $z=1$ and applying

---

* Communicated by the Author.

Gauss's Theorem it is found that

$${}_4F_3\left(\begin{matrix}-m,\ \beta,\ \gamma,\ \delta\ ;\ 1\\ 1-m-\beta,\ 1-m-\gamma,\ \omega\end{matrix}\right)$$
$$=\frac{(\omega-\delta\ ;\ m)}{(w\ ;\ m)}\,{}_5F_4\left[\begin{matrix}-\tfrac{1}{2}m,\ \tfrac{1}{2}-\tfrac{1}{2}m,\ 1-m-\beta-\gamma,\ \delta,\ 1-\omega-m\ ;\ 1\\ 1-m-\beta,\ 1-m-\gamma,\ \tfrac{1}{2}(1+\delta-\omega-m),\ \tfrac{1}{2}(2+\delta-\omega-m)\end{matrix}\right]. \quad . \quad . \quad . \quad (3)$$

Next, in (2) put $\delta=-m$, where $m$ is zero or a positive integer; the series again all terminate. Then, if $z=1$,

$${}_4F_3\left(\begin{matrix}\alpha,\ \beta,\ \gamma,\ -m\ ;\ 1\\ \alpha-\beta+1,\ \alpha-\gamma+1,\ \omega\end{matrix}\right)$$
$$=\frac{(\omega-\alpha\ ;\ m)}{(\omega\ ;\ m)}\,{}_5F_4\left[\begin{matrix}\tfrac{1}{2}\alpha,\ \tfrac{1}{2}+\tfrac{1}{2}\alpha,\ 1+\alpha-\beta-\gamma,\ 1+\alpha-\omega,\ -m\ ;\ 1\\ \alpha-\beta+1,\ \alpha-\gamma+1,\ \tfrac{1}{2}(1+\alpha-\omega-m),\ \tfrac{1}{2}(2+\alpha-\omega-m)\end{matrix}\right]. \quad . \quad . \quad . \quad (4)$$

Formulæ (3) and (4) were given by Whipple (Proc. Lond. Math. Soc. ser. 2, xxvi. pp. 266, 265, 1926). In both cases the functions on the right are Saalschützian.

### § 3. *Saalschütz's Theorem.*

The formula

$$\frac{\Gamma(1-\rho)\Gamma(\sigma-\rho+1)}{\Gamma(\alpha-\rho+1)\Gamma(\beta-\rho+1)\Gamma(\gamma-\rho+1)}\,{}_3F_2\left(\begin{matrix}\alpha,\ \beta,\ \gamma\ ;\ z\\ \rho,\ \sigma\end{matrix}\right)$$
$$+\frac{\Gamma(\rho-1)\Gamma(\sigma)}{\Gamma(\alpha)\Gamma(\beta)\Gamma(\gamma)}\,z^{1-\rho}\,{}_3F_2\left(\begin{matrix}\alpha-\rho+1,\ \beta-\rho+1,\ \gamma-\rho+1\ ;\ z\\ \sigma-\rho+1,\ 2-\rho\end{matrix}\right)$$
$$=\frac{\Gamma(\sigma-\rho+1)}{\Gamma(\gamma-\rho+1)\Gamma(\alpha+\beta-\rho+1)}\sum_{n=0}^{\infty}\frac{(\alpha\ ;\ n)(\beta\ ;\ n)(\gamma\ ;\ n)}{n\,!\,(\alpha+\beta-\rho+1\ ;\ n)\,(\sigma\ ;\ n)}$$
$$\times\,{}_3F_2\left(\begin{matrix}\alpha+n,\ \beta+n,\ \sigma-\gamma\ ;\ 1\\ \alpha+\beta-\rho+1+n,\ \sigma+n\end{matrix}\right)(1-z)^n, \quad . \quad . \quad . \quad . \quad . \quad . \quad (5)$$

where $R(\gamma-\rho+1)>0$, is a particular case of a more general formula (Proc. Roy. Soc. Edin. lix. p. 53, 1938).

If $\alpha=-m$, where $m$ is zero or a positive integer, the second term on the left of (5) vanishes identically. On putting $z=1$ the formula then reduces to

$${}_3F_2\left(\begin{matrix}-m,\ \beta,\ \gamma\ ;\ 1\\ \rho,\ \sigma\end{matrix}\right)=\frac{(\rho-\beta\ ;\ m)}{(\rho\ ;\ m)}\,{}_3F_2\left(\begin{matrix}-m,\ \beta,\ \sigma-\gamma\ ;\ 1\\ \beta-\rho+1-m,\ \sigma\end{matrix}\right) \quad . \quad . \quad (6)$$

Now let $\rho+\sigma=\beta+\gamma-m+1$, and the generalized hypergeometric function on the right of (6) reduces to

$$F\left(\begin{matrix}-m,\ \beta\ ;\ 1\\ \sigma\end{matrix}\right).$$

On applying Gauss's Theorem to this function, Saalschütz's Theorem,

$${}_3F_2\left(\begin{matrix}-m,\ \beta,\ \gamma\ ;\ 1\\ \rho,\ \sigma\end{matrix}\right)=\frac{(\rho-\beta\ ;\ m)(\sigma-\beta\ ;\ m)}{(\rho\ ;\ m)(\sigma\ ;\ m)}, \quad . \quad . \quad . \quad (7)$$

where $\rho+\sigma=\beta+\gamma-m+1$, is obtained.

It is possible to find quite a number of formulæ of the same type as (5) which give Saalschütz's Theorem as a particular case.

## § 4. *Saalschützian Series.*

In a previous paper (Proc. Roy. Soc. Edin. lix. p. 142, 1938) a generalization of Saalschütz's Theorem was obtained in which Saalschützian series are equated to multiple series. One example is

$$
{}_5F_4\left(\begin{matrix}\alpha,\ \beta,\ \gamma,\ \delta,\ -m\ ;\ 1\\ \rho,\ \sigma,\ \tau,\ \alpha+\beta+\gamma+\delta-\rho-\sigma-\tau+1-m\end{matrix}\right)
=\frac{(\rho+\sigma+\tau-\alpha-\beta-\gamma\ ;\ m)(\tau-\delta\ ;\ m)}{(\rho+\sigma+\tau-\alpha-\beta-\gamma-\delta\ ;\ m)(\tau\ ;\ m)}
$$

$$
\times\sum_{r=0}^{m}\frac{(\rho-\alpha\ ;\ r)(\rho-\beta\ ;\ r)(\gamma\ ;\ r)(\delta\ ;\ r)(-m\ ;\ r)}{r!\,(\rho+\sigma+\tau-\alpha-\beta-\gamma;\ r)\,(\delta-\tau+1-m;\ r)(\rho;\ r)(\sigma;\ r)}
$$

$$
\times{}_4F_3\left(\begin{matrix}\rho+\sigma-\alpha-\beta+r,\ \sigma-\gamma,\ \delta+r,\ r-m\ ;\ 1\\ \rho+\sigma+\tau-\alpha-\beta-\gamma+r,\ \delta-\tau+1+r-m,\ \sigma+r\end{matrix}\right)\ldots\quad . \qquad (8)
$$

Another example, which can be deduced from (8) by putting $\sigma$ equal to $\gamma$ and then writing $\gamma$ for $\delta$ and $\sigma$ for $\tau$, is

$$
{}_4F_3\left(\begin{matrix}\alpha,\ \beta,\ \gamma,\ -m\ ;\ 1\\ \rho,\ \sigma,\ \alpha+\beta+\gamma-\rho-\sigma+1-m\end{matrix}\right)=\frac{(\rho+\sigma-\alpha-\beta\ ;\ m)(\sigma-\gamma\ ;\ m)}{(\rho+\sigma-\alpha-\beta-\gamma\ ;\ m)(\sigma\ ;\ m)}
$$

$$
\times{}_4F_3\left(\begin{matrix}\gamma,\ \rho-\beta,\ \rho-\alpha,\ -m\ ;\ 1\\ \rho+\sigma-\alpha-\beta,\ \rho,\ \gamma-\sigma+1-m\end{matrix}\right),\quad .\ .\ .\ .\ . \qquad (9)
$$

a relation between two Saalschützian series which is due to Whipple (Proc. Lond. Math. Soc. ser. 2, xxv. p. 537 (1925)).

On applying (9) to the function on the right of (9), the further transformation

$$
{}_4F_3\left(\begin{matrix}\alpha,\ \beta,\ \gamma,\ -m\ ;\ 1\\ \rho,\ \sigma,\ \alpha+\beta+\gamma-\rho-\sigma+1-m\end{matrix}\right)
=\frac{(\rho+\sigma-\alpha-\beta\ ;\ m)(\rho+\sigma-\alpha-\gamma\ ;\ m)(\alpha\ ;\ m)}{(\rho+\sigma-\alpha-\beta-\gamma\ ;\ m)(\rho\ ;\ m)(\sigma\ ;\ m)}
$$

$$
\times{}_4F_3\left(\begin{matrix}\rho+\sigma-\alpha-\beta-\gamma,\ \rho-\alpha,\ \sigma-\alpha,\ -m\ ;\ 1\\ \rho+\sigma-\alpha-\beta,\ \rho+\sigma-\alpha-\gamma,\ 1-\alpha-m\end{matrix}\right)\quad .\ .\ . \qquad (10)
$$

is obtained. This formula was also given by Whipple (Journal Lond. Math. Soc. II. p. 87, 1926). A factor $(-1)^m$ is missing in Whipple's statement of the formula.

## § 5. *Formulæ for well-poised Terminating Series.*

In the paper referred to at the beginning of section 4 a general formula in which well-poised terminating series are equated to multiple series was obtained. In special cases the multiple series degenerate into generalized hypergeometric functions.

For example, we have

$$
{}_5F_4\left(\begin{matrix}\alpha,\ \beta,\ \gamma,\ \delta,\ -m\ ;\ 1, \\ \alpha-\beta+1,\ \alpha-\gamma+1,\ \alpha-\delta+1,\ \alpha+m+1\end{matrix}\right)
= \frac{(\alpha+1\ ;\ m)(\frac{1}{2}\alpha-\delta+1\ ;\ m)}{(\alpha-\delta+1\ ;\ m)(\frac{1}{2}\alpha+1\ ;\ m)}
$$

$$
\times \sum_{r=0}^{m} \frac{(\frac{1}{2}\alpha\ ;\ r)(\frac{1}{2}\alpha+\frac{1}{2}-\beta\ ;\ r)(\gamma\ ;\ r)(\delta\ ;\ r)(-m\ ;\ r)}{r\,!\,(\frac{1}{2}\alpha+\frac{1}{2}\ ;\ r)(\alpha-\beta+1\ ;\ r)(\alpha-\gamma+1\ ;\ r)(\delta-\frac{1}{2}\alpha-m\ ;\ r)}
$$

$$
\times {}_4F_3\left(\begin{matrix}\frac{1}{2}\alpha+r,\ \frac{1}{2}\alpha+\frac{1}{2}-\gamma,\ \delta+r,\ r-m\ ;\ 1 \\ \frac{1}{2}\alpha+\frac{1}{2}+r,\ \alpha-\gamma+1+r,\ \delta-\frac{1}{2}\alpha+r-m\end{matrix}\right). \quad . \quad . \quad . \quad (11)
$$

Now, by (8), the double series is equal to

$$
\frac{(\alpha-\gamma-\delta+1\ ;\ m)(1+\frac{1}{2}\alpha\ ;\ m)}{(\alpha-\gamma+1\ ;\ m)(\frac{1}{2}\alpha-\delta+1\ ;\ m)}
\times {}_5F_4\left(\begin{matrix}1+\frac{1}{2}\alpha-\beta,\ \frac{1}{2}+\frac{1}{2}\alpha,\ \gamma,\ \delta,\ -m\ ;\ 1 \\ \alpha-\beta+1,\ \frac{1}{2}+\frac{1}{2}\alpha,\ 1+\frac{1}{2}\alpha,\ \gamma+\delta-\alpha-m\end{matrix}\right).
$$

Hence

$$
{}_5F_4\left(\begin{matrix}\alpha,\ \beta,\ \gamma,\ \delta,\ -m\ ;\ 1 \\ \alpha-\beta+1,\ \alpha-\gamma+1,\ \alpha-\delta+1,\ \alpha+m+1\end{matrix}\right)
= \frac{(\alpha+1\ ;\ m)(\alpha-\gamma-\delta+1\ ;\ m)}{(\alpha-\gamma+1\ ;\ m)(\alpha-\delta+1\ ;\ m)}
$$

$$
\times {}_4F_3\left(\begin{matrix}1+\frac{1}{2}\alpha-\beta,\ \gamma,\ \delta,\ -m\ ;\ 1 \\ \alpha-\beta+1,\ 1+\frac{1}{2}\alpha,\ \gamma+\delta-\alpha-m\end{matrix}\right). \quad . \quad . \quad (12)
$$

On applying (10) to the last function it is found that

$$
{}_5F_4\left(\begin{matrix}\alpha,\ \beta,\ \gamma,\ \delta,\ -m\ ;\ 1 \\ \alpha-\beta+1,\ \alpha-\gamma+1,\ \alpha-\delta+1,\ \alpha+m+1\end{matrix}\right)
= \frac{(1+\alpha\ ;\ m)(1+\frac{1}{2}\alpha-\beta\ ;\ m)}{(1+\alpha-\beta\ ;\ m)(1+\frac{1}{2}\alpha\ ;\ m)}
$$

$$
\times {}_4F_3\left(\begin{matrix}1+\alpha-\gamma-\delta,\ \frac{1}{2}\alpha,\ \beta,\ -m\ ;\ 1 \\ 1+\alpha-\gamma,\ 1+\alpha-\delta,\ \beta-\frac{1}{2}\alpha-m\end{matrix}\right), \quad . \quad . \quad . \quad (13)
$$

a formula due to Bailey (Proc. Lond. Math. Soc. ser. 2, xxix. p. 505, 1928).

Again, if

$$
J \equiv {}_7F_6\left(\begin{matrix}\alpha,\ \beta,\ \gamma,\ \delta,\ 1+\frac{1}{2}\alpha,\ \epsilon,\ -m\ ;\ 1 \\ \alpha-\beta+1,\ \alpha-\gamma+1,\ \alpha-\delta+1,\ \frac{1}{2}\alpha,\ \alpha-\epsilon+1,\ \alpha+m+1\end{matrix}\right),
$$

$$
J = \frac{(\alpha+1\ ;\ m)(\frac{1}{2}\alpha-\epsilon+1\ ;\ m)}{(\alpha-\epsilon+1\ ;\ m)(\frac{1}{2}\alpha+1\ ;\ m)}
$$

$$
\times \sum_{p=0}^{m} \frac{(\frac{1}{2}\alpha+\frac{1}{2}-\beta\ ;\ p)(\gamma\ ;\ p)(\delta\ ;\ p)(1+\frac{1}{2}\alpha\ ;\ p)(\epsilon\ ;\ p)(-m\ ;\ p)}{p\,!\,(\frac{1}{2}\alpha+\frac{1}{2}\ ;\ p)(\alpha-\beta+1\ ;\ p)(\alpha-\gamma+1\ ;\ p)(\alpha-\delta+1\ ;\ p)(\epsilon-\frac{1}{2}\alpha-m\ ;\ p)}
$$

$$
\times \sum_{r=0}^{m-p} \frac{(\frac{1}{2}\alpha+\frac{1}{2}-\gamma\ ;\ r)(\delta+p\ ;\ r)(1+\frac{1}{2}\alpha+p\ ;\ r)(\epsilon+p\ ;\ r)(p-m\ ;\ r)}{r\,!\,(\frac{1}{2}\alpha+\frac{1}{2}+p\ ;\ r)(\alpha-\gamma+1+p\ ;\ r)(\alpha-\delta+1+p\ ;\ r)(\epsilon-\frac{1}{2}\alpha+p-m\ ;\ r)}
$$

$$\times \sum_{s=0}^{m-p-r} \frac{(\tfrac{1}{2}\alpha+\tfrac{1}{2}-\delta\,;\,s)(1+\tfrac{1}{2}\alpha+p+r\,;\,s)(\epsilon+p+r\,;\,s)(p+r-m\,;\,s)}{s\,!\,(\tfrac{1}{2}\alpha+\tfrac{1}{2}+p+r\,;\,s)(\alpha-\delta+1+p+r\,;\,s)(\epsilon-\tfrac{1}{2}\alpha+p+r-m\,;\,s)}$$

$$\times {}_3\mathrm{F}_2\left(\begin{matrix}-\tfrac{1}{2},\ \epsilon+p+r+s,\ p+r+s-m\,;\ 1\\ \tfrac{1}{2}\alpha+\tfrac{1}{2}+p+r+s,\ \epsilon-\tfrac{1}{2}\alpha+p+r+s-m\end{matrix}\right).$$

Now, by (7), the function in the last line is equal to

$$\frac{(\tfrac{1}{2}\alpha+\tfrac{1}{2}-\epsilon\,;\,m-p-r-s)(-\tfrac{1}{2}\alpha-m\,;\,m-p-r-s)}{(\tfrac{1}{2}\alpha+\tfrac{1}{2}+p+r+s\,;\,m-p-r-s)(\epsilon-\tfrac{1}{2}\alpha+p+r+s-m\,;\,m-p-r-s)}$$

$$=\frac{(\tfrac{1}{2}\alpha+1;\,m)(\epsilon-\tfrac{1}{2}\alpha+\tfrac{1}{2}-m;\,m)(\tfrac{1}{2}\alpha+\tfrac{1}{2};\,p+r+s)(\epsilon-\tfrac{1}{2}\alpha-m;\,p+r+s)}{(\tfrac{1}{2}\alpha+\tfrac{1}{2};\,m)(\epsilon-\tfrac{1}{2}\alpha-m;\,m)(\tfrac{1}{2}\alpha+1;\,p+r+s)(\epsilon-\tfrac{1}{2}\alpha+\tfrac{1}{2}-m;\,p+r+s)}.$$

Hence

$$\mathrm{J}=\frac{(\alpha+1\,;\,m)(\tfrac{1}{2}\alpha+\tfrac{1}{2}-\epsilon\,;\,m)}{(\alpha-\epsilon+1\,;\,m)(\tfrac{1}{2}\alpha+\tfrac{1}{2}\,;\,m)}$$

$$\times \sum_{p=0}^{m} \frac{(\tfrac{1}{2}\alpha+\tfrac{1}{2}-\beta\,;\,p)(\gamma\,;\,p)(\delta\,;\,p)(\epsilon\,;\,p)(-m\,;\,p)}{p\,!\,(\alpha-\beta+1\,;\,p)(\alpha-\gamma+1\,;\,p)(\alpha-\delta+1\,;\,p)(\epsilon-\tfrac{1}{2}\alpha+\tfrac{1}{2}-m\,;\,p)}$$

$$\times \sum_{r=0}^{m-p} \frac{(\tfrac{1}{2}\alpha+\tfrac{1}{2}-\gamma\,;\,r)(\delta+p\,;\,r)(\epsilon+p\,;\,r)(p-m\,;\,r)}{r\,!(\alpha-\gamma+1+p\,;\,r)(\alpha-\delta+1+p\,;\,r)(\epsilon-\tfrac{1}{2}\alpha+\tfrac{1}{2}+p-m\,;\,r)}$$

$$\times {}_3\mathrm{F}_2\left(\begin{matrix}\tfrac{1}{2}\alpha+\tfrac{1}{2}-\delta,\ \epsilon+p+r,\ p+r-m\,;\ 1\\ \alpha-\delta+1+p+r,\ \epsilon-\tfrac{1}{2}\alpha+\tfrac{1}{2}+p+r-m\end{matrix}\right).$$

Again, as before, the last function is equal to

$$\frac{(\tfrac{1}{2}\alpha+\tfrac{1}{2}\,;\,m)(\delta+\epsilon-\alpha-m\,;\,m)(\alpha-\delta+1\,;\,p+r)(\epsilon-\tfrac{1}{2}\alpha+\tfrac{1}{2}-m\,;\,p+r)}{(\alpha-\delta+1\,;\,m)(\epsilon-\tfrac{1}{2}\alpha+\tfrac{1}{2}-m\,;\,m)(\tfrac{1}{2}\alpha+\tfrac{1}{2}\,;\,p+r)(\delta+\epsilon-\alpha-m\,;\,p+r)}.$$

Therefore

$$\mathrm{J}=\frac{(\alpha+1\,;\,m)(\alpha-\delta-\epsilon+1\,;\,m)}{(\alpha-\delta+1\,;\,m)(\alpha-\epsilon+1\,;\,m)}$$

$$\times \sum_{p=0}^{m} \frac{(\tfrac{1}{2}\alpha+\tfrac{1}{2}-\beta\,;\,p)(\gamma\,;\,p)(\delta\,;\,p)(\epsilon\,;\,p)(-m\,;\,p)}{p\,!\,(\tfrac{1}{2}\alpha+\tfrac{1}{2}\,;\,p)(\alpha-\beta+1\,;\,p)(\alpha-\gamma+1\,;\,p)(\delta+\epsilon-\alpha-m\,;\,p)}$$

$$\times {}_4\mathrm{F}_3\left(\begin{matrix}\tfrac{1}{2}\alpha+\tfrac{1}{2}-\gamma,\ \delta+p,\ \epsilon+p,\ p-m\,;\ 1\\ \tfrac{1}{2}\alpha+\tfrac{1}{2}+p,\ \alpha-\gamma+1+p,\ \delta+\epsilon-\alpha+p-m\end{matrix}\right).$$

But, by (8), this double series is equal to

$$\frac{(\alpha-\gamma-\epsilon+1\,;\,m)(\alpha-\delta+1\,;\,m)}{(\alpha-\gamma+1\,;\,m)(\alpha-\delta-\epsilon+1\,;\,m)}$$

$$\times {}_5\mathrm{F}_4\left(\begin{matrix}1+\alpha-\beta-\delta,\ \tfrac{1}{2}+\tfrac{1}{2}\alpha,\ \gamma,\ \epsilon,\ -m\,;\ 1\\ 1+\alpha-\beta,\ \tfrac{1}{2}+\tfrac{1}{2}\alpha,\ \alpha-\delta+1,\ \gamma+\epsilon-\alpha-m\end{matrix}\right).$$

Hence

$$\mathrm{J}=\frac{(\alpha+1\,;\,m)(\alpha-\gamma-\epsilon+1\,;\,m)}{(\alpha-\gamma+1\,;\,m)(\alpha-\epsilon+1\,;\,m)}$$

$$\times {}_4\mathrm{F}_3\left(\begin{matrix}1+\alpha-\beta-\delta,\ \gamma,\ \epsilon,\ -m\,;\ 1\\ 1+\alpha-\beta,\ 1+\alpha-\delta,\ \gamma+\epsilon-\alpha-m\end{matrix}\right), \quad . \quad . \quad (14)$$

a formula which was given by Whipple (Proc. Lond. Math. Soc. ser. 2, xxiv. p. 253, 1924; Journal Lond. Math. Soc. I. pp. 138–145, 1926).

# XLVI. *Some Formulæ for the Product of two Whittaker Functions with Different Arguments.*

By W. T. Howell *.

[Received April 6, 1939.]

§ 1. Dr. C. S. Meijer (1) has given many integral representations for the product of two Whittaker Functions; one of Meijer's results has been simplified by Dr. W. N. Bailey (2) to the form

$$W_{k,\,m}(iz)W_{k,\,m}(-iz)=\frac{2z}{\Gamma(\frac{1}{2}+m-k)\Gamma(\frac{1}{2}-m-k)}\int_0^\infty \coth^{2k}\tfrac{1}{2}t K_{2m}(z\sinh t)\,dt,$$

where $z \neq 0$, $|\arg z| \leqslant \frac{\pi}{2}$ and $|R(m)|+R(k)<\frac{1}{2}$.

Meijer (3) subsequently gave a result of similar form for the product $W_{k,\,m}(z)M_{-k,\,m}(z)$. In this note I give corresponding formulæ for these products with different arguments.

The method I use is operational, the operators being the same as those used by Heaviside, in which, when

$$\phi(u)=u\int_0^\infty e^{-ut}f(t)\,dt,$$

$\phi(u)$ is called the operational representation or form of $f(t)$. The relation between $\phi(u)$ and $f(t)$ is usually written

$$\phi(u) \doteqdot f(t) \quad \text{or} \quad f(t) \doteqdot \phi(u),$$

while the dots are sometimes omitted. With these operators there is a one-to-one correspondence between any representation $\phi$ and its original $f$ and *vice versa*. I make use of what may be called the Parseval Theorem for these operators given by Goldstein (4), viz.,

If $\qquad \phi(u)=f(t)$

and $\qquad \psi(u)=g(t)$,

then $$\int_0^\infty \phi(u)\,g(u)\frac{du}{u}=\int_0^\infty f(t)\,\psi(t)\frac{dt}{t}. \qquad (1)$$

§ 2. I require the following known results:

$$2pK_\nu(2\sqrt{ap})K_\nu(2\sqrt{bp}) \doteqdot x^{-1}\exp-\left(\frac{a+b}{x}\right)K_\nu\left(\frac{2\sqrt{ab}}{x}\right), \qquad (2.1)$$

$$2pi^{-\nu}K_\nu(2\sqrt{ap})J_\nu(2\sqrt{bp}) \doteqdot x^{-1}\exp-\left(\frac{a-b}{x}\right)I_\nu\left(\frac{2i\sqrt{ab}}{x}\right), \qquad (2.2)$$

---

* Communicated by the Author.

for all $\nu$, $|\arg a| < \frac{\pi}{2}$, $|\arg b| < \frac{\pi}{2}$, $|\arg(a+b)| < \frac{\pi}{2}$,

$$\frac{1}{2}\Gamma(\tfrac{1}{2}+m-k)\Gamma(\tfrac{1}{2}-m-k)\mathrm{W}_{k,m}\left(\frac{a}{p}\right)e^{\frac{a}{2p}}p^{k+1}a^{-\frac{1}{2}} \doteqdot x^{-k-\frac{1}{2}}\mathrm{K}_{2m}(2\sqrt{ax}), \qquad (2.3$$

for all values of $\arg a$, and $\mathrm{R}(\frac{1}{2}+m-k)>0$.

$$\frac{\Gamma(\frac{1}{2}+k+m)}{\Gamma(2m+1)}e^{-\frac{a}{p}}p^{1-k}\mathrm{M}_{k,m}\left(\frac{a}{p}\right)a^{-\frac{1}{2}} \doteqdot x^{k-\frac{1}{2}}\mathrm{J}_{2m}(2\sqrt{ax}), \quad . \quad (2.4$$

for $\mathrm{R}(k+m)+\frac{1}{2}>0$.

$$2p^{l-\frac{1}{2}}\mathrm{K}_{2n}(2\sqrt{pb}) \doteqdot b^{-\frac{1}{2}}e^{-\frac{b}{2x}}x^{-l}\mathrm{W}_{l,n}\left(\frac{b}{x}\right). \quad . \quad . \quad . \quad (2.5)$$

The first two results are due to Macdonald[*], the third to Meijer, and the last to Goldstein[†].

From (2.3) and (2.5) on applying (1),

$$\frac{1}{2}\Gamma(\tfrac{1}{2}+m-k)\,\Gamma(\tfrac{1}{2}-m-k)\,x^{k-l}(ab)^{-\frac{1}{2}}e^{\frac{a-b}{2x}}\,\mathrm{W}_{k,m}\left(\frac{a}{x}\right)\mathrm{W}_{l,n}\left(\frac{b}{x}\right)$$

$$\doteqdot 2p\int_p^\infty \mathrm{K}_{2m}\{2\sqrt{a(t-p)}\}\mathrm{K}_{2n}\{2\sqrt{tb}\}\,(t-p)^{-k-\frac{1}{2}}t^{l-\frac{1}{2}}dt. \quad (2.6)$$

Similarly, from (2.4) and (2.5),

$$\frac{\Gamma(\frac{1}{2}+m-k)}{\Gamma(2m+1)}e^{-\frac{a+b}{2x}}(ab)^{-\frac{1}{2}}x^{-k-l}\mathrm{W}_{l,n}\left(\frac{b}{x}\right)\mathrm{M}_{k,m}\left(\frac{a}{x}\right)$$

$$\doteqdot 2p\int_p^\infty \mathrm{K}_{2n}(2\sqrt{tb})\,\mathrm{J}_{2m}\{2\sqrt{a(t-p)}\}\,(t-p)^{k-\frac{1}{2}}t^{l-\frac{1}{2}}d\,. \quad (2.7)$$

Making a change of variable $t=p\cosh^2\frac{u}{2}$, the left-hand side of (2.6) when $l=k$, $n=m$, and that of (2.7) when $k=-l$, $m=n$ become respectively

$$\doteqdot 2p\int_0^\infty \mathrm{K}_{2m}\left\{2\sqrt{bp\cosh^2\frac{u}{2}}\right\}\mathrm{K}_{2m}\left\{2\sqrt{ap\sinh^2\frac{u}{2}}\right\}\coth^{2k}\frac{u}{2}du, \quad (2.8)$$

and

$$\doteqdot 2p\int_0^\infty \mathrm{K}_{2n}\left\{2\sqrt{pb\cosh^2\frac{u}{2}}\right\}\mathrm{J}_{2m}\left\{2\sqrt{pa\sinh^2\frac{u}{2}}\right\}\coth^{2l}\frac{u}{2}du. \quad (2.9)$$

Using (2.1) and (2.2) in conjunction with (2.8) and (2.9) respectively, we get at once

$$\frac{1}{2}\Gamma(\tfrac{1}{2}+m-k)\Gamma(\tfrac{1}{2}-m-k)\,(ab)^{-\frac{1}{2}}e^{\frac{a-b}{2x}}\mathrm{W}_{k,m}\left(\frac{a}{x}\right)\mathrm{W}_{k,m}\left(\frac{b}{x}\right)$$

$$=\frac{1}{x}\int_0^\infty \exp -\frac{1}{x}\left(a\cosh^2\frac{u}{2}+b\sinh^2\frac{u}{2}\right)\mathrm{K}_{2m}\left(\frac{\sqrt{ab}}{x}\sinh u\right)\coth^{2k}\frac{u}{2}du,$$

---

[*] References are to be found in Watson, ‘Theory of Bessel Functions.’

[†] *Loc. cit.*

when $$R(\tfrac{1}{2}\pm m-k)>0,$$
and

$$\frac{\Gamma(\frac{1}{2}+n-l)}{\Gamma(2n+1)}e^{-\frac{a+b}{2x}}(ab)^{-\frac{1}{2}}W_{l,\,n}\left(\frac{b}{x}\right)M_{-l,\,n}\left(\frac{a}{x}\right)$$
$$=\frac{1}{x}\int_0^\infty \exp -\frac{1}{x}\left(b\cosh^2\frac{u}{2}-a\sinh^2\frac{u}{2}\right)J_{2n}\left(\frac{\sqrt{ab}}{x}\sinh u\right)\coth^{2l}\frac{u}{2}\,du,$$

when $$(R(n-l)+\tfrac{1}{2}>0,$$
or

$$e^{(a-b)\frac{x}{2}}W_{k,\,m}(ax)\,W_{k,\,m}(bx)$$
$$=\frac{2(ab)^{\frac{1}{2}}x}{\Gamma(\frac{1}{2}+m-k)\Gamma(\frac{1}{2}-m-k)}\int_0^\infty \exp -x\left(a\cosh^2\frac{u}{2}+b\sinh^2\frac{u}{2}\right)$$
$$\times K_{2m}(x\sqrt{ab}\sinh u)\coth^{2k}\frac{u}{2}\,du,$$
$$R(\tfrac{1}{2}\pm m-k)>0,$$
$$|\arg a|<\frac{\pi}{2};\quad |\arg b|<\frac{\pi}{2};\quad |\arg(a+b)|<\frac{\pi}{2},$$

and

$$e^{-(a+b)\frac{x}{2}}W_{l,\,n}(bx)\,M_{-l,\,n}(ax)$$
$$=\frac{\Gamma(2n+1)(ab)^{\frac{1}{2}}x}{\Gamma(\frac{1}{2}+n-l)}\int_0^\infty \exp x\left(a\sinh^2\frac{u}{2}-b\cosh^2\frac{u}{2}\right)$$
$$\times J_{2n}(x\sqrt{ab}\sinh u)\coth^{2l}\frac{u}{2}\,du,$$
$$R(n-l)+\tfrac{1}{2}>0;$$

$a$ and $b$ satisfying the above conditions.

Another formula easily obtained by the same methods is

$$\frac{\Gamma(\frac{1}{2}+m+k)\Gamma(\frac{1}{2}+m-k)}{[\Gamma(2m+1)]^2}(xy)^{-\frac{1}{2}}M_{k,\,m}(x)M_{-k,\,m}(y)$$
$$=\int_{-\infty}^{\infty} e^{2kt}\operatorname{sech} t\exp\left\{\frac{(x-y)}{2}\tanh t\right\}I_{2m}(\sqrt{xy}\operatorname{sech} t)\,dt$$

valid for $R(\frac{1}{2}+m\pm k)>0$, $R(m)>-\frac{1}{2}$.

I am obliged to D. S. R. Admiralty, for permission to publish this note.

## *References.*

(1) C. S. Meijer, Quart. J. of Math. (Oxford) vol. vi. pp. 241–9 (1935).
(2) W. N. Bailey, Quart.. J. of Math. (Oxford) vol. viii. p. 951 (1937).
(3) C. S. Meijer, *Proc. Kon· Akad. Wet.* vol. xl. p. 10 (1937).
(4) S. Goldstein, Proc. Math. Soc. Lond. ser. 2, vol. xxxiv. p. 104.

# XLVII. *Notices respecting New Books.*

*Modern Magnetism.* By Prof. L. F. Bates. [Pp. 339+ix.] (Cambridge University Press, 1939. Price 16*s.* net.)

As Prof. Bates points out, the conventional academic treatment of magnetism does not lay sufficient stress on the experimental aspect of the subject. This fault is undoubtedly remedied in Prof. Bates' book, which contains admirable digests of the fascinating experiments which serve as a basis for the imposing structure of the modern theory of magnetism. The task of giving, in brief compass, a clear account of a complicated experiment is one which calls for no little skill in exposition, and in this matter Prof. Bates must be deemed to have been completely successful.

But the book is far more than a mere collection of accounts of experiments. Experiments are means to an end; so should be accounts of experiments. And the end which Prof. Bates has in view is, presumably, that of giving to students of honours grade a clear account of the present state of modern magnetic theory, excluding any study of terrestrial magnetism.

In his development of this account, Prof. Bates is not afraid to begin at the beginning, laying down a series of definitions of the fundamental concepts of the science. He then devotes a chapter to magnetic-field production and measurements which contains a brief but valuable section on electromagnet design, and proceeds to discussions of susceptibility measurements on isotropic and on anisotropic bodies, of experiments on single particles, of nuclear spins, gyromagnetic effects, magnetic saturation and equations of state, of energy changes associated with reversible magnetisation, and of magneto-striction.

The book covers a wide field in a very thorough fashion. It reads easily and clearly, a virtue which, if an old epigram may be turned topsy-turvy, means much trouble spent on writing. The mathematics in the book is not difficult, and the student who obtains from it his first introduction to modern magnetism will have nothing to unlearn when he turns his attention to original sources.

The book deserves, and should be assured of, success.

*Introduction to Contemporary Physics.* By Karl K. Darrow. [Pp. 648+xii.] (London: Macmillan & Co., Ltd., 1939. Price 25*s.* 0*d.* net.)

Those whose privilege it was to survey contemporary physics in the pages of the first edition (1926) of Dr. Darrow's admirable book have waited more or less patiently for the appearance of a second edition which should tell the story as it appears to-day with the clarity, vigour and power of apt illustration which Dr. Darrow possesses in such high degree. Here it is; and the student who desires to take a rapid but accurate survey of some of the main developments in the physics of to-day could have no more trustworthy and pleasant guide than Dr. Darrow. The years since 1926 have seen astounding advances—the development of wave-mechanics; the discovery of new particles; electron diffraction; and a host of new transmutations. Withal, classical and applied physics have made notable advances during the last dozen years; and, comprehensive though the title 'Contemporary Physics' may be, it were too much to expect of Dr. Darrow that he should embark on their story. Even in that region which we may call modern, the author has had to adopt some principle of selections, and the chief topics he has chosen for elucidation may be briefly summed up as electrons, isotopes, atom-models, the correlation of waves and corpuscles, crystal-diffraction, ionization, excitation, spectrum analysis, wave-mechanics, magnetism, transmutations and nuclear instability.

A first-rate survey.

---

[*The Editors do not hold themselves responsible for the views expressed by their correspondents.*]

# XLVIII. *X-ray Study of some Meteoric Irons.*

By Prof. E. A. Owen, M.A., Sc.D., and B. D. Burns, M.Sc.,
University College of North Wales, Bangor *.

[Received August 2, 1939.]

[Plates V.–VII.]

## 1. *Introduction.*

In the course of a detailed study by X-ray analysis of the structure of artificially prepared iron-nickel alloys, it was discovered that it was extremely difficult to prepare alloys rich in iron, which were in a state of complete thermal equilibrium. Prolonged heat treatments were necessary, and certain precautions had to be taken in carrying out the heat treatments (5). In view of the difficulties experienced with these alloys, it was decided to make a study of the structure of meteoric iron in the hope that this material might furnish useful information concerning equilibrium conditions existing in iron-nickel alloys generally.

Meteoric irons may be divided into two main groups; those with nickel content below about 6 per cent., containing only one constituent (kamacite), and those of higher nickel content possessing a more complex structure of three separate constituents and in some of which are found characteristic patterns known as Widmanstätten figures. The three constituents are: (*a*) kamacite, which corresponds to the $\alpha$-phase in the pure iron-nickel alloys; (*b*) tænite, corresponding to the pure $\gamma$-phase; and (*c*) plessite, which may consist of a microscopic octahedral arrangement of kamacite and tænite or may be of a granular nature, showing no definite structure under the microscope.

The investigation might also shed some light on certain points in dispute concerning the constitution and structure of iron meteorites. Information would be welcomed concerning the constancy of the compositions of the two constituents, kamacite and tænite, in any given meteorite, and the variation, if any, in the composition of these constituents in various meteorites which show, for example, Widmanstätten patterns with kamacite bands of different widths. It is also of interest to know how far the natural alloys conform with existing knowledge derived from the study of artificial alloys of the same composition.

---

* Communicated by the Authors.

Table I.

| Name and date. | Museum and number. | Nickel content (weight per cent.). | Other information. |
|---|---|---|---|
| Bingera. | B.M. 1925.62 (N.S.W.). | 4·39 | Hexahedrite (granular) : Fe, 93·76 ; Ni, 4·39 ; Co, 0·67 ; P, 0·20 ; C, 0·14 ; insol., 0·55 ; Cu, trace. Sp. gr. 7·85. A. Liversidge, Proc. Roy. Soc. N.S.W. xvi. p. 35 (1883). |
| La Primitiva (1888). | B.M. 1906.21 (Chile). | 4·52 | Fe, 95·03 ; Ni, 4·52 Co, 0·65 ; C and P, trace. Sp. gr. 7·89. G. T. Prior, Min. Mag. xvii. p. 131 (1914). |
| Braunau (fell 1847). | H.M. 180 d. | 5·21 | Hexahedrite. |
| San Francisco (1868). | B.M. 43401 (Mexico). | 5·46 | Fe, 93·36 ; Ni, 5·46 ; Co, 0·87 ; Cu, 0·03 ; S, 0·15 ; P, 0·16 ; Cr, nil. Sp. gr. 7·77. E. Cohen, Meteoritenkunde, iii. p. 48 (1905). |
| Coahuila known (1837). | H.M. 132–24. | 6·07 | Hexahedrite (normal) ; many masses known. |
| Nedagolla (fell 1870). | H.M. 335 (Madras). | 6·20 | Nickel poor ataxite. |
| Seelasgen (before 1847). | B.M. 33928 (Brandenburg). | 6·23 | Coarsest octahedrite : Fe, 92·33 ; Ni, 6·23 ; Co, 0·67 ; Cu, 0·05 ; $SiO_2$, 0·03 ; C, 0·52 ; insol. 0·18. C. Rammelsberg, Ann. Phys. Chem. (Pogg) lxxiv. p. 443 (1849). |
| Murnpeowie (found 1909). | B.M. 1934.52. | 6·32 | Coarsest octahedrite : Fe, 93·88 ; Ni, 6·32 ; Co, 0·32 ; Cu, 0·002 ; Ge, 0·007 ; Pt, 0·07 ; S, 0·006 ; insol. 0·20. Sp. gr. 7·78. L. J. Spencer, Min. Mag. xxiv. p. 13 (1935). |
| Youndegin (found 1884). | B.M. 56150 (Australia). | 6·64 | Coarse octahedrite : Fe, 92·67 ; Ni, 6·46 ; Co, 0·55 ; Mg, 0·42 ; P, 0·24 ; C, 0·04 ; S, nil ; Cu, trace. Sp. gr. 7·85. L. Fletcher, Min. Mag. vii. p. 121 (1887) ; xii. p. 171 (1899) ; xv. p. 147 (1908). |
| Estherville (fell 1879). | B.M. 53764 (U.S.A.). | 7·10 | Mesosiderite : Fe, 92·00 ; Ni, 7·10 ; Co, 0·69 ; P, 0·11 ; Cu, trace. J. L. Smith, Am. Journ. Sci. xix. p. 459 (1880). |
| Henbury. | B.M. 1932.1529. | 7·26 | Medium octahedrite : Fe, 93·04 ; Ni, 7·26 ; Co, 0·22 ; Cu, 0·044 ; Pt, Cl, C, trace ; S, 0·06 ; Cr, P, nil ; insol. 0·06. Sp. gr. 7·69. L. J. Spencer and M. H. Hey, Min. Mag. xxiii. p. 387 (1933). |
| Henbury. | B.M. 1934.485. | 7·26 | Medium octahedrite, distorted. |

| | | | |
|---|---|---|---|
| Boogaldi (found 1900). | B.M. 1937.1271 (N.S.W.). | 8·05 | Fine octahedrite : Fe, 91·135 ; Ni, 8·052 ; Co, 0·483 ; Cu, 0·280 ; Au, Pt, As, trace ; insol. 0·040. Sp. gr. 7·85. A. Liversidge, Proc. Roy. Soc. N.S.W. xxxvi. p. 341 (1902). |
| Imilac (found 1822). | B.M. 33939 (Chile). | 8·60 | Pallasite : Fe, 90·40 ; Ni, 8·60 ; insol. 0·30. F. von Kobell and M. de Rivero, Korrespond. Blatt. Zoo. Min. Verein, Regensberg, p. 112 (1851). |
| Mantos Blancos (found 1876). | B.M. 53323 (Chile). | 8·83 | Fine octahedrite : Fe, 90·77 ; Ni, 8·83 ; Co, 0·55 ; Cu, P, trace. Sp. gr. 7·904. L. Fletcher, Min. Mag. viii. p. 257 (1889). |
| Narraburra (found 1855). | B.M. 1927.1269 (N.S.W.). | 9·74 | Finest octahedrite : Fe, 88·605 ; Ni, 9·741 ; Co, 0·474 ; P, 0·429 ; Cu, S, Au, trace. Sp. gr. 7·57. A. Liversidge, Proc. Roy. Soc. N.S.W. xxxvii. p. 234 (1904). |
| Castilia (fell 1874). | H.M. 357 *b*. | 10 | Mesosiderite. |
| Cowra (found 1888). | B.M. 68205, 68210 (N.S.W.). | 13·2 | Finest octahedrite ; (two analyses) : Fe, 85·31 ; 85·22 ; Ni, 13·18, 13·28 ; Co, 1·04, 1·00 ; Cu, 0·02, n.d. ; Sn, Mn, trace ; P, 0·22, 0·23 ; S, 0·01, n.d. ; C, 0·02, 0·03 ; Si, 0·01, n.d. Sp. gr. 7·805. J. C. H. Mingaye, Records of Geol. Survey of N.S.W. vii. p. 311 (1904). |
| Deep Springs (1846). | H.M. 175. | 13·44 | Nickel rich ataxite. |
| Cape Eisen (found 1793). | H.M. 29. | 15·67 | Nickel rich ataxite. |
| Kokomo (found 1862). | H.M. 269 *c*. | 15·76 | Nickel rich ataxite. |
| Smithland (found 1839). | H.M. 148 *b*. | 16·22 ? | Nickel rich ataxite. |
| Babb's Mill (found 1842). | H.M. 78 *d*. | 17·30 or 11·05 | Nickel rich ataxite (two irons known) : Troost's (17·30 per cent. Ni), Blake's (11·05 per cent. Ni). |
| Klondyke (found 1905). | B.M. 1919.43 (Yukon). | 18·2 | Nickel rich ataxite (material taken from Skookum Gulch mass) : Fe, 80·65 ; Ni, 18·20 ; Co, 0·91 ; Cu, nil ; Cr, 0·002 ; C, 0·015 ; P, 0·194 ; S, 0·002 ; Si, 0·003. R. A. A. Johnston, Mus. Bull. Geol. Survey Canada, No. 15 (Geol. Series, No. 26), i. (1915). |
| San Cristobal (found 1896). | B.M. 86763 (Chile). | 25·6 | Nickel rich ataxite : Fe, 73·72 ; Ni, 25·60 ; Co, 1·00 ; P, 0·18. Sp. gr. 7·86. E. Cohen, Sitzungsber, Preuss. Akad. Wiss. Berlin, p. 607 (1898). |

A great amount of work has been done on meteoric irons, but comparatively few X-ray investigations have been carried out on them. Amongst the more recent works are those of Young (1), Mehl and Barrett (2), and Derge and Kommel (3). There is also a useful summary of the present state of knowledge concerning iron-nickel alloys including meteoric irons to be found in a report written by Desch (4) to which is appended a comprehensive list of references.

## 2. *Material.*

Meteoric specimens were received from the museum of Harvard University and from the British Museum. The specimens covered a range of composition from 4·39 to 25·6 per cent. nickel by weight; the last figure represents the nickel content of the San Cristobal meteorite and is about the highest nickel content known in meteorites. Table I. contains particulars of all the specimens examined together with their distinguishing numbers in the respective museums from which they came.

In the second column of the Table, H.M. and B.M. refer respectively to Harvard Museum and British Museum. The nickel content of each specimen is given, but it is only in a limited number of cases that the full analysis is cited. In those cases it will be noted that they contain small amounts of impurities, but the combined content of iron and nickel does not fall below 98·35 per cent. The principal impurity in all the meteorites is cobalt, but they also contain small amounts of some of the elements copper, chromium, phosphorus, sulphur, and carbon. It was realized that the presence of these impurities would affect the parameter values and possibly prevent accurate correlation with observations made on pure iron-nickel alloys, but in spite of this some information concerning the equilibrium conditions of alloys in the range of composition covered by the meteorites might be obtained, since, according to the general belief, meteorites have been subjected to exceptional heat treatment.

No difficulty was anticipated with specimens containing only the α-phase, that is, specimens containing up to about 6·2 per cent. nickel by weight, and it was expected that the parameter values would correspond closely with those obtained with artificial alloys in this range of composition. This was found to be the case. With specimens containing the three components kamacite, tænite and plessite, it was impossible to predict what to expect in view of the lack of precise information concerning the behaviour of artificial alloys in this region. Further, if kamacite and tænite existed in separate zones apart from the corresponding components of plessite, it was not known whether the parameters of kamacite and the kamacitic component of plessite, and, similarly, the parameters of tænite and the tænitic component of plessite, were the same.

In determining the relative orientation of kamacite and tænite crystals in the Carlton and the Cañon Diablo meteorites, Young ⁽¹⁾ obtained parameter values for pure tænite and pure kamacite which showed so much variation that it was impossible to state with any degree of certainty whether there existed a difference between these values and the values of the parameters of the kamacitic and tænitic components of plessite in the meteorites. If, however, there are differences in the parameter values of these materials, a broadening of the spectral lines should be noticeable, provided this difference is sufficiently great. Differences of the order obtained by Young would be readily detected with the apparatus employed in the present investigation; for example, with the focusing camera the limit of accuracy of parameter measurements is within ±0·0003 Å., whereas Young obtained variations in the parameter values of the order of 0·01 Å.

### 3. *Heat Treatment.*

To avoid errors arising from lack of homogeneity of a specimen, samples were taken from different parts of it by filing with a dead smooth file, care being taken to perform the operation slowly in order to prevent excessive heating of the sample. In order to leave the original structures unimpaired the specimens were not annealed in lump form. The powder samples were, however, submitted in the first instance to certain annealing treatments. Afterwards observations were made on unannealed powders. These will be discussed after considering the results obtained with annealed samples.

Preliminary annealing treatments on powder samples were carried out with the Braunau meteorite, which contains 5·21 per cent. nickel by weight. According to the equilibrium diagram compiled by Merica *, this sample should consist of the pure $\alpha$-constituent, and it should be possible to raise it to a temperature slightly higher than 600° C. before it enters into the mixed phase region. The spectra obtained with a sample which had been annealed for 3 days at 500° C. and quenched, showed a number of lines not belonging to the $\alpha$-phase. To eliminate the possibility of contamination from the file, a sample was prepared by grinding the specimen on coarse glass paper and magnetically separating the alloy, but the lines persisted. Subsequent measurement proved that the lines were caused by the presence of traces of the $\gamma$-phase, so that the temperature of annealing was too high. On reducing the temperature to 420° C. or 350° C. and annealing at either of these temperatures for 3 days satisfactory results were obtained. Coahuila

* This was the equilibrium diagram consulted in the early stages of the investigation.

(6·07 per cent. Ni) and Nedagolla (6·2 per cent. Ni), in addition to Braunau (5.21 per cent. Ni), were subjected to this heat treatment.

It was decided to subject samples of meteorites which were expected to contain both the α- and the γ-phase, to a long period of annealing at a temperature which was considered low enough not to produce excessive disturbance of the crystal state existing in the meteorite. The samples were in the main subjected to heat treatment at 350° C. for periods of 5 weeks and 2 months respectively, and at the end of these periods were cooled over about 3 hours to room-temperature. This heat treatment removed the effect of cold work, and it was assumed also that it did not appreciably alter the structure. It was found later, however, that this assumption is untenable in the case of some of the meteorites.

## 4. *Apparatus.*

Two types of X-ray camera were used, the fibre camera and the focusing camera, both of which could be mounted in an evacuated enclosure and the specimen maintained, if necessary, at temperatures not exceeding 550° during the exposure. The X-ray tube was furnished with a target of copper, cobalt, nickel, manganese or vanadium ; each one of these targets was needed at some stage of the investigation.

## 5. *Measurement of X-ray Spectra.*

From the measurement of the lines in the spectra obtained with the focusing and fibre cameras, the lattice parameters of the constituents of the meteorites were determined. The results of the measurements on the spectra of all the meteorites examined are included in Table II. The table contains accurate values of the α-parameters, but the values of the γ-parameters, where they are given, are known to a much lower degree of accuracy, the lines of the γ-phase being diffuse at the larger angles, and, therefore, unsuitable for accurate measurement. The parameters given in the table are mainly those obtained after an annealing treatment of five weeks at 350° C. in a thermostatically controlled furnace. Different samples, in some cases as many as seven, were prepared from one specimen. The figures given in the table are the mean values of the parameters in each case.

The following short notes concerning the meteorites and the measurement of the spectra obtained after annealing at 350° C. supplement the information given in Table II.

(1) Bingera.—Two samples gave α-parameters agreeing within 0·0001 Å. Well-defined spectral lines were obtained belonging only to the α-phase. Gas was occluded by the material.

(2) La Primitiva.—The specimen was taken from the Angela mass. The two samples examined from different parts of the specimen yielded parameters in close agreement.

(3) Braunau.—Seven samples were examined after various heat treatments. The value included in the table is the mean of three values obtained after annealing at 350° C. for 7 days and cooling to room-temperature in 6 hours; two of the samples were prepared with a file, the parameters at 15° C. being 2·8624$_7$ Å. and 2·8625$_0$ Å. respectively; the third sample was prepared by grinding on glass paper and separating the alloy magnetically, the parameter was 2·8625$_4$ Å. The values of the parameter of artificial iron-nickel alloys of about the same com-

Table II.

| Name of meteorite. | Nickel content (weight per cent.). | Parameter (Å) at 15° C. | |
|---|---|---|---|
| | | $\alpha$-phase (kamacite). | $\gamma$-phase (tænite). |
| 1. Bingera | 4·39 | 2·8623$_3$ | — |
| 2. La Primitiva | 4·52 | 2·8621$_8$ | — |
| 3. Braunau | 5·21 | 2·8625$_0$ | — |
| 4. San Francisco | 5·46 | 2·8623$_2$ | — |
| 5. Coahuila | 6·07 | 2·8624$_8$ | — |
| 6. Nedagolla | 6·20 | 2·8625$_1$ | — |
| 7. Seelasgen | 6·23 | 2·8628$_2$ | — |
| 8. Murnpeowie | 6·32 | 2·8625$_2$ | — |
| 9. Youndegin | 6·46 | 2·8627$_6$ | — |
| 10. Estherville | 7·1 | 2·8628$_5$ | — |
| 11. Henbury | 7·26 | 2·8628$_7$ | — |
| 12. Boogaldi | 8·05 | 2·8627$_9$ | — |
| 13. Imilac | 8·6 | 2·8627$_5$ | — |
| 14. Mantos Blancos | 8·83 | 2·8628$_2$ | — |
| 15. Narraburra | 9·74 | 2·8629$_4$ | — |
| 16. Castilia | 10·0 | 2·8627$_5$ | 3·5800 |
| 17. Cowra | 13·18 | 2·8629$_6$ | 3·5786$_9$ |
| 18. Deep Springs | 13·44 | 2·8626$_7$ | 3·5834 |
| 19. Cape Eisen | 15·67 | 2·8629$_9$ | 3·5767$_7$ |
| 20. Kokomo | 15·76 | 2·8629$_8$ | 3·5793$_1$(Q.).<br>3·5807$_1$(S.C.). |
| 21. Babb's Mill | 17·30 | 2·8628$_1$ | 3·5825$_9$ |
| 22. Klondyke | 18·20 | 2·8627$_1$ | 3·5784$_2$ |
| 23. San Cristobal | 25·6 | 2·8626$_9$ | 3·5801$_3$ |
| 24. Smithland | 16·22 ? | 2·8628$_2$ | — |

(Q.... Quenched, S.C..... Slowly cooled.)

position measured previously at 15° C. were as follows: Jette and Foote, 5·07 per cent. Ni, 2·8626 Å.; Owen and Yates, 5·2 per cent. Ni, 2·8627 Å. These values are in fair agreement with the value now found for the meteorite.

(4) San Francisco del Mezquital.—Two samples from different parts of the specimen were examined. They were annealed at 350° C. for one month and furnace cooled *. The values of the $\alpha$-parameters were $2{\cdot}8623_4$ and $2{\cdot}8623_0$ Å. respectively. No trace of the $\gamma$ constituent (tænite) was found in the photographs.

(5) Coahuila.—Four samples of this hexahedrite yielded a mean parameter of $2{\cdot}8624_8$ Å. The individual results were as follows: annealed at 350° C. for 4 days, $2{\cdot}8623_7$; annealed at 350° C. for 5 weeks, $2{\cdot}8625_2$ and $2{\cdot}8623_7$; annealed at 420° C. for 3 days, $2{\cdot}8626_6$ Å. The variation in the parameter values is within the limits of experimental error, showing that the composition of the meteorite is uniform, as the samples were taken from different parts of the specimen. No trace of the $\gamma$-phase was found.

(6) Nedagolla.—Two samples taken from different parts of the specimen were annealed at 350° C. for 5 weeks. The parameters were $2{\cdot}8625_6$ and $2{\cdot}8624_7$ Å. The spectral lines were very sharp, only the pure body-centred cubic phase (kamacite) being present (see fig. 1 *d*) (Pl. V.).

(7) Seelasgen.—Two analyses are recorded for this meteorite, one giving 5·31 and the other 6·23 for the nickel content in weight per cent. The X-ray spectra showed that the specimen consisted mainly of the $\alpha$-phase with a slight trace of the $\gamma$-phase. Faint lines which did not correspond to the $\gamma$-phase or to oxides were present in the spectra; these were probably due to impurities. The presence of the $\gamma$-phase indicates that the analysis giving a nickel content of 6·23 is probably the more accurate. This is supported by the fact that etching discloses a coarse octahedral structure. The two samples examined yielded for the $\alpha$-parameter the values $2{\cdot}8627_9$ and $2{\cdot}8628_5$ Å. The $\gamma$-lines were too faint to measure with accuracy.

(8) Murnpeowie.—The specimen received for investigation was in the form of coarse filings which had to be ground in a mortar for X-ray examination. The X-ray spectrum gave no indication of the presence of the $\gamma$-phase, and the $\alpha$-lines were noticeably more diffuse than in the spectrum of Seelasgen. This may be due to the greater amount of cold work done on the sample in this case.

---

* Unless otherwise stated, the samples after the annealing operation were allowed to cool in the electric furnace after switching off the current. It took the furnace about 3½ hours to cool from 350° C. to room-temperature.

(9) Youndegin.—Two specimens of this meteorite were available and samples were prepared from each. The X-ray spectra showed only a trace of the $\gamma$-phase. The $\alpha$-phase parameters from two samples examined were $2{\cdot}8627_7$ and $2{\cdot}8627_4$ Å.

(10) Estherville.—To obtain a fairly pure sample of the metallic constituent in this mesosiderite, the filings were separated magnetically. X-ray spectrum analysis indicated a much greater proportion of the $\gamma$-phase than would be expected from a nickel content of 7·1. The two samples examined yielded for the $\alpha$-parameter the values $2{\cdot}8628_2$ and $2{\cdot}8628_8$ Å.

Fig. 2.

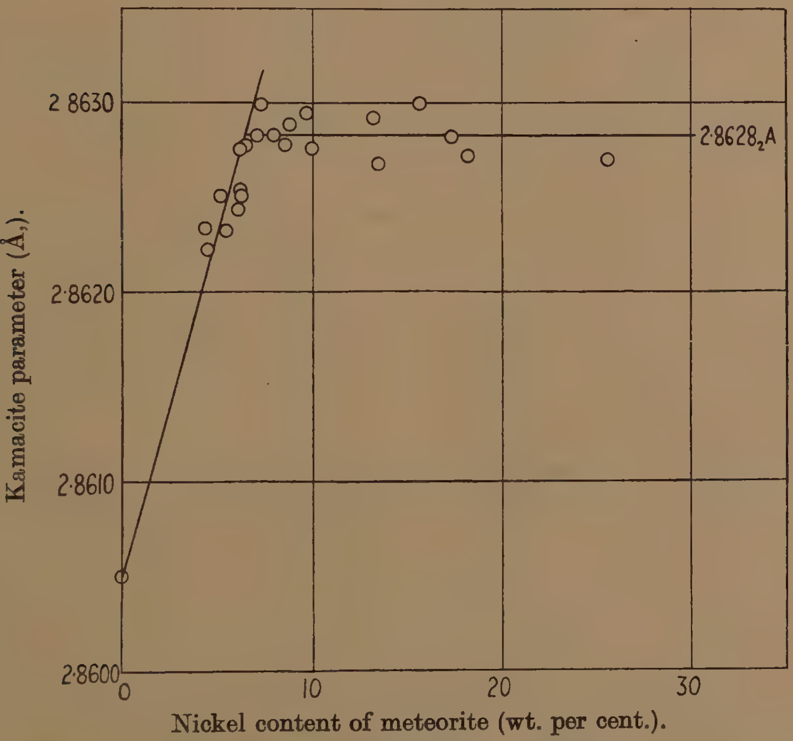

Parameters of the kamacite constituent of various meteorites annealed at 350° C. for 5 weeks and rapidly cooled.

(11) Henbury.—Two specimens of this meteorite were available, one being a small distorted piece and the other turnings from one of the larger masses of the fall. Only a trace of the $\gamma$-phase was to be observed in the X-ray spectra, and there were faint traces of extra lines

due to impurities. The α-phase from the turnings had the parameter value $2{\cdot}8629_8$ Å., and from the distorted lump the value $2{\cdot}8627_9$ Å. These figures agree within the limits of experimental error, but they show a greater difference than that found in general between two samples of the same meteorite.

(12) Boogaldi.—The samples examined after annealing at 350° C. for 3 weeks yielded well-defined spectral lines which gave the parameter values $2{\cdot}8628_0$ and $2{\cdot}8627_7$ for the α-phase. A small amount of γ-phase was also present, but its parameter could not be measured with accuracy.

(13) Imilac.—The metallic powder prepared from this pallasite was separated magnetically. The equilibrium attained after the usual heat treatment appeared inferior to that observed in Boogaldi and other meteorites of about the same nickel content. The values of the α-parameters were $2{\cdot}8627_7$ and $2{\cdot}8627_2$ Å.

(14) Mantos Blancos.—Good equilibrium was attained; a small amount of the γ-phase was present. The measured α-parameters were $2{\cdot}8628_8$ and $2{\cdot}8627_0$ Å.

(15) Narraburra.—This meteorite contains 9·74 per cent. nickel and, as would be expected, the lines from the γ-phase were stronger than in the spectra of the previous meteorites. The γ-parameter could, however, not be measured with accuracy. The two samples examined gave identical values for the α-parameter, namely, $2{\cdot}8629_4$ Å.

(16) Castilia.—In this mesosiderite the metal was apparently discontinuous and relatively sparse, consequently only small samples of the actual metal could be obtained. The sample was filed and the metallic powder was separated magnetically in stages until free from non-metallic powder. Two samples were prepared, one was annealed at 350° C. for 5 weeks and the other annealed at 350° C. for 8 weeks. The parameters at 15° C. were found to be $2{\cdot}8627_8$ and $2{\cdot}8627_1$ respectively. The spectra showed that a small amount of tænite was present. The kamacite was in a good state of equilibrium judging from the sharpness of the spectral lines, but the tænite lines were so diffuse that it was impossible to obtain precision films of the phase. Several attempts were made with vanadium, manganese, and molybdenum radiations. The lines in each case were not sufficiently well defined to measure with accuracy. The γ-phase parameter was, however, determined from measurements of spectral lines obtained with a fibre camera, but the accuracy of the determination was not as high as that obtained with the focusing camera.

The definition and the resolution of the α-phase (kamacite) lines in the spectra obtained with Castilia and with Braunau are almost equally good (see fig. 1 (Pl. V.)). Since the $\gamma$-phase is present it is likely that the third component, plessite, is also present. If this is so, from the well-defined lines in the spectrum of Castilia it may be inferred that the kamacitic component of plessite has the same parameter as pure kamacite.

(17) Cowra.—This meteorite is included amongst the "finest" octahedrites. It yielded well-defined spectral lines, the $\gamma$- as well as the $\alpha$-phase being prominent. The parameters of both phases could be measured. The two values of the $\alpha$-phase were $2{\cdot}8630_2$ and $2{\cdot}8629_1$ Å. and the mean $\gamma$-parameter, $3{\cdot}5786_9$ Å.

(18) Deep Springs.—This meteorite is peculiar in that it contained a quantity of gas which was evolved when the material was annealed. The spectra showed that, in addition to the lines corresponding to the $\alpha$- and $\gamma$-phases, a number of extra lines were present. Comparison of these extra lines with those obtained with samples which had been purposely oxidized, revealed the extra lines to be due to the oxides of the components. A rough spectral analysis of the occluded gases led to the conclusion that they were probably hydrogen and carbon monoxide.

Films taken with unannealed samples showed that the structure was the same as when the gas was removed, but the parameters of these unannealed specimens could not be determined because the spectral lines were too diffuse for exact measurement.

Three specimens were examined; two were annealed at 350° C. for 5 weeks and yielded for the $\alpha$-phase parameters $2{\cdot}8626_3$ and $2{\cdot}8627_1$, the third was annealed at 350° C. for 8 weeks and gave the parameter $2{\cdot}8626_7$ Å. The $\gamma$-parameter could not be measured to this accuracy as the lines were not well defined at the higher angles of reflexion. The mean value at 15° C. was found to be 3·5834 Å.

(19) Cape Eisen.—Three precision spectra after annealing the samples at 350° C., two for 5 and one for 8 weeks, yielded the parameters $2{\cdot}8630_0$, $2{\cdot}8629_8$, and $2{\cdot}8629_9$ Å. at 15° C. A spectrum of the sample which was annealed for 8 weeks showed that the $\alpha$-phase was in a good state of equilibrium, resolution of the K$\alpha$ doublets being noticed as far out as $\cos^2\theta=0{\cdot}22$, but the $\gamma$-phase still appeared to be in a distorted condition.

(20) Kokomo.—The nickel content of this meteorite is the same as that of Cape Eisen, and the three specimens examined gave three values of the $\alpha$-phase parameter agreeing well with each other, the mean value being identical with that of Cape Eisen. The $\gamma$-phase parameter was measured for two specimens; the first was annealed at 350° C. for 8 weeks and quenched and gave the value $3{\cdot}5793_1$, the second annealed at the same temperature for 11 weeks and slowly cooled gave $3{\cdot}5807_1$ Å. There is a marked difference between these two values; it is possible that they correspond to the state of the material at two different temperatures.

(21) Babb's Mill.—Two values of the composition of this meteorite were given as there are apparently two irons, one known as Troost's (17·30 per cent. Ni) and the other as Blake's (11·05 per cent. Ni). It was uncertain to which of these this particular specimen belonged. After 2 months' annealing at 350° C., good $\alpha$-phase lines were obtained, but the $\gamma$-phase lines, as with other meteorites, were not well defined. This lack of definition may be due to the fact that the crystals are of sub-microscopic size producing a broadening of the lines, or there may be slight variation in the $\gamma$-phase parameter in the meteorite. It would appear that the more probable nickel content in the specimen under examination is 17·3 per cent., because the amount of $\gamma$-phase present, judging from the intensity of the lines in the spectrum, far exceeded that in Castilia, the nickel content of which is 10 per cent.

(22) Klondyke.—The $\alpha$-phase appeared to be in good equilibrium. A careful examination of both spectrum and precision films failed to reveal any indication that a second $\alpha$-lattice existed with a slightly different parameter. The resolution was good, the K$\alpha$ lines being clearly resolved down to $\cos^2\theta=0{\cdot}22$. The $\gamma$-phase lines were again such that only approximate parameter values could be obtained.

(23) San Cristobal.—This contains a higher percentage of nickel (25·6) than any other meteorite examined. From the intensity of the lines in the spectrum it would appear that the specimen contains as much $\gamma$- as $\alpha$-phase. The sample examined was annealed at 350° C. for 4 weeks. Although the lines in the spectrum were rather diffuse, the precision doublets of the $\alpha$-phase were capable of accurate measurement. The accuracy of measurement of the $\gamma$-lines was much lower.

(24) Smithland.—Contrary to the analysis which accompanied this specimen stating that it contained 16·22 per cent. nickel, the X-ray spectra taken with samples from different parts of the specimen showed that the material consisted of almost pure $\alpha$-iron-nickel, a minute trace of the $\gamma$-phase being noticeable only after prolonged exposure. From this it was concluded that the analysis must be incorrect. The minute amount of $\gamma$-phase indicated a nickel content somewhere in the region of 8 to 9 per cent. Two samples, on which accurate measurements were made, gave $2{\cdot}8628_3$ and $2{\cdot}8628_1$ Å. for the $\alpha$-parameter, the first specimen having been annealed at 350° C. for 5 weeks and the second for 8 weeks and then quenched.

## 6. *Relation between Parameter and Nickel Content in Annealed Samples.*

### (a) *Kamacite.*

In fig. 2 are plotted the nickel content and the $\alpha$-parameters at 15° C. for all the meteorites examined. The parameter of pure iron at 15° C. is 2·8605 Å. As in artificial iron-nickel alloys, the solution of nickel in iron increases the lattice parameter until the nickel content reaches a value slightly greater than 6 per cent. For nickel contents greater than this the parameter remains tolerably constant. The mean value of the $\alpha$-parameter for meteorites annealed at 350° C. for about 2 months and containing more than 6·32 per cent. nickel by weight is $2{\cdot}8628_2$ Å., the maximum deviation from this figure being $\pm 1$ in 20,000. This slight variation in the value of the $\alpha$-parameter might well be accounted for by the impurities present in the meteroites.

Taking the values of the $\alpha$-parameter for the octahedrites only, the mean value is $2{\cdot}8629_1$ Å., which agrees within about 1 in 30,000 with the value $2{\cdot}8628_2$ Å. taken from the graph (fig. 2). The $\alpha$-parameter is therefore remarkably constant for the octahedrites.

From this and the fact that the $\alpha$-parameter is the same in samples taken from different parts of the meteoritic specimen, it may be concluded that there is no appreciable variation in the composition of this phase, either in any one meteorite or in different meteorites in the group of octahedrites examined.

Neither does there appear to be any measurable difference in the parameter of pure kamacite and the kamacitic component of plessite, but in some of the meteorites there may be a difference in their states of equilibrium, the former being in a better state of equilibrium than the latter, especially if plessite is in the granular form which shows no definite structure under the microscope.

The foregoing results lead also to the conclusion that the composition ot the pure $\alpha$-phase (kamacite) in octahedrites does not vary with the width of the kamacite bands.

### (b) *Tænite.*

The lines in the spectra of tænite were never found so well defined as those in the spectra of kamacite. The definition was such that accurate values of the parameter could not be made. It will be seen in Table II. that the $\gamma$-parameter values vary over a wide range in those meteorites which yielded spectra, the lines of which could be measured. There does not seem to be a definite relation between this parameter and the nickel content of the meteorite. The range of 0·0066 Å. between the highest and lowest parameter measured is much greater than the experimental error of measurement.

The question which naturally presents itself is why the $\gamma$-parameter should show so much variation compared with the $\alpha$-parameter. An answer may be offered in the light of the equilibrium diagram recently suggested for artificial iron-nickel alloys (5) on the assumption that the final states reached by the meteorites correspond to equilibrium states at different temperatures. This equilibrium diagram shows that between the temperatures of 300° C. and 400° C., for example, the change in the solubility of nickel in iron is only about 2 atomic per cent., whereas the change in the solubility of iron in nickel over the same range of temperature is not less than about 15 atomic per cent. Parameter measurements of the saturated $\alpha$- and $\gamma$-phases in artificial alloys show that the $\alpha$-parameter changes by 1 in 4000 between 300° C. and 400° C., but that the $\gamma$-parameter changes by 1 in 200, that is, the change in the $\gamma$-parameter is 20 times as great as the corresponding change in the $\alpha$-parameter.

From the parameter values given in Table II. it will be seen that the $\alpha$-parameter in the eight meteorites for which the $\gamma$-parameter was measured shows a variation of about 1 in 9500, but that the $\gamma$-parameter for the same group of meteorites varies by 1 in 540, that is, the change in the value of the $\gamma$-parameter is about 18 times as great as the corresponding change in the $\gamma$-parameter. This is the same order of relative change as that found in artificial alloys. This comparison is, of course, only approximate, but it does serve to show that if the phases in the meteorites have reached their final equilibrium values at different temperatures, the range of values of the $\alpha$- and $\gamma$-parameters actually found in the meteorites is about the same as that to be expected from the results of measurements made on artificial alloys, if the meteorites had been held at temperatures within the range between 300° C. and 400° C. for periods of time sufficiently long to have reached the state of equilibrium at these temperatures.

Hence the fact that the $\gamma$-parameter does not have a constant value in the different meteorites may only signify that the meteorites have been maintained at different temperatures for a long enough time to reach their equilibrium states before being rapidly cooled from those temperatures.

The indefiniteness of the $\gamma$-phase spectral lines points to another conclusion, namely, that if the meteorites had been allowed time to reach their equilibrium states at any temperature, the rate of cooling from this temperature was such that equilibrium conditions were not maintained at all intermediate stages ; neither could the cooling have been so rapid as to maintain completely the equilibrium state at the initial temperature. The falling temperature was therefore neither exceedingly slow nor exceedingly rapid after the final annealing treatment which the meteorite underwent before it reached the earth.

## 7. *Effect of Higher Temperatures on the Parameters of the Lattices.*

Further investigation was made on samples of the meteorites which had undergone periods of annealing at temperatures higher than 350° C.

A selection of the meteorites listed in Table II. was made for this purpose. One set of samples was annealed at 400° C. for 14 days, and another set was annealed at 500° C. for 2 days. The samples in both sets were cooled to room-temperature after these heat treatments at the rate of about 100° C. per hour. The parameters of the $\alpha$-phase in each specimen, determined from measurements of precision spectra, are collected in Table III.

TABLE III.

| Name of meteorite. | Nickel content (weight per cent.). | Parameter of $\alpha$-phase at 15° C. Specimen annealed at | | | Remarks. |
|---|---|---|---|---|---|
| | | 350° C. for 56 days. | 400° C. for 14 days. | 500° C. for 2 days. | |
| Bingera ......... | 4·39 | $2{\cdot}8623_3$ | $2{\cdot}8626_5$ | $2{\cdot}8626_8$ | Hexahedrite |
| Nedagolla ....... | 6·20 | $2{\cdot}8625_3$ | $2{\cdot}8625_8$ | $2{\cdot}8627_5$ | Ataxite. |
| Henbury ........ | 7·26 | $2{\cdot}8629_8$ | $2{\cdot}8629_6$ | $2{\cdot}8629_4$ | Medium octahedrite. |
| Boogaldi ........ | 8·05 | $2{\cdot}8628_2$ | $2{\cdot}8628_5$ | $2{\cdot}8629_4$ | Fine octahedrite. |
| Mantos Blancos .. | 8·83 | $2{\cdot}8628_8$ | $2{\cdot}8629_7$ | $2{\cdot}8629_7$ | Fine octahedrite. |
| Narraburra ...... | 9·74 | $2{\cdot}8629_4$ | $2{\cdot}8629_1$ | $2{\cdot}8628_3$ | Finest octahedrite. |
| Cowra ........... | 13·18 | $2{\cdot}8629_1$ | $2{\cdot}8630_2$ | $2{\cdot}8628_3$ | Finest octahedrite. |
| Cape Eisen ...... | 15·67 | $2{\cdot}8629_9$ | $2{\cdot}8631_3$ | $2{\cdot}8625_1$ | Ataxite. |
| Kokomo ......... | 15·76 | $2{\cdot}8629_8$ | $2{\cdot}8634_1$ | $2{\cdot}8626_9$ | Ataxite. |
| Babb's Mill....... | 17·30 | $2{\cdot}8628_1$ | $2{\cdot}8632_4$ | $2{\cdot}8620_6$ | Ataxite. |
| Klondyke ...... | 18·20 | $2{\cdot}8627_1$ | $2{\cdot}8630_4$ | $2{\cdot}8621_8$ | Ataxite. |
| San Cristobal .... | 25·6 | $2{\cdot}8626_9$ | $2{\cdot}8627_4$ | $2{\cdot}8627_2$ | Ataxite. |

The specimens examined may be divided into three classes: (1) Hexahedrites and ataxites, poor in nickel, comprising meteorites which contain only the $\alpha$-phase; (2) Octahedrites with nickel content between 7·26 and 13·18 per cent. by weight; (3) Ataxites, rich in nickel, containing between 15·67 and 25·6 per cent. nickel by weight.

The first group consists of the meteorites Bingera and Nedagolla. The maximum change in parameter as the temperature of annealing varies over the range from 350° C. to 500° C. is $0{\cdot}0003_5$ Å. This is just within the limits of error of measurement, so that within these limits it may be stated that the parameter is the same for the three temperatures of annealing. If the alloy remains in the α-region at all the temperatures, then no change in parameter would be expected. In the case of Bingera, the nickel content of which is 4·39 per cent., there is no doubt that the meteorite conforms to this condition judging from the behaviour of artificial alloys of this composition. The composition of Nedagolla, on the other hand, corresponds to the boundary composition of the α-phase in pure iron-nickel alloys at about 400° C. At 350° C. and 500° C. the composition is just within the duplex region $(\alpha+\gamma)$. The fact that there does not appear to be any change in the α-parameter at the differen temperatures shows that the boundary is nearly vertical between these temperatures which is consistent with the results obtained with artificial alloys.

The second group comprises the octahedrites which on etching show Widmanstatten structures. The range of variation of α-parameter in each meteorite over the range of temperature examined is about 0·0001 Å., and the total range of variation for all the five meteorites over the whole range of temperature is only 0·0002 Å., which signifies remarkable constancy of parameter. Temperatures of annealing up to 500° C. do not appear to have any effect on the parameter value during the periods of annealing chosen. The temperature of 500° C. was not exceeded, because it was found with artificial alloys that marked changes may occur in the structure at temperatures higher than about 580° C., and it was decided to keep well below this temperature for this investigation.

These observations show that kamacite in octahedrites is in a very stable state. But it was noticed in some of the spectra that the lines in the resolved doublet for which $Q^2=10$ were not as sharp as they might be if the whole material were in complete equilibrium (see Pl. V., fig. 1). Parts of the meteorite may be in good equilibrium, whereas others may not, these latter possibly comprising the granular plessite areas observed in octahedrites. Judging by the definition of the spectral lines, the γ-phase never appeared to be in as good a state of equilibrium as the α-phase. This is also true of artificial iron-nickel alloys within the same range of nickel content as the octahedrites which have been examined here. If the iron coming out of solution when the material is cooled forms particles of submicroscopic size it would account for this effect.

The third group consists of five ataxites ranging in nickel content from 15·67 to 25·6. The effect of heat treatment on these meteorites is quite marked; the α-parameter in all the specimens shows an increase at 400° C. over the value at 350° C., but the value at 500° C. is even smaller than that at 350° C. This effect is also found with pure artificial iron-nickel alloys. The parameters of alloys containing 16 and 23 atomic per cent. nickel are included in Table IV.

The material of the ataxites is therefore not in as stable a condition as the material of the octahedrites. On polishing and etching, the surface of these ataxites appears to be of a granular nature without any definite structural form when viewed under the microscope. The ataxites form an important group, as they provide information concerning the structure of meteorites which is not supplied by the other groups. Further consideration will be given to them later.

Table IV.

Parameter of the α-phase in artificial Iron-nickel Alloys.

| Composition (atoms per cent. Ni.). | Parameter of α-phase at 15° C. | | |
|---|---|---|---|
| | Specimen annealed at | | |
| | 350° C. for 89 days and quenched. | 400° C. for 6 days and quenched. | 500° C. for 2 days and quenched. |
| 15·98 | $2{\cdot}8633_7$ | $2{\cdot}8636_0$ | $2{\cdot}8624_5$ |
| 23·32 | $2{\cdot}8632_8$ | $2{\cdot}8633_9$ | $2{\cdot}8618_4$ |

### 8. *Spectra obtained with Unannealed Samples.*

Having obtained the results with the ataxites recorded in the last section it was decided to make a survey of the condition of the meteorites before they were submitted to any heat treatment. As was to be expected, the spectra obtained with the unannealed samples yielded lines which were very diffuse owing to the distortion caused by the cold work done in the filing operation when the samples were prepared.

Interesting results were obtained with some of these unannealed samples The hexahedrites (containing only the α-phase) gave identical spectra with those obtained with the same samples after annealing at 350° C. This was to be expected, as we are dealing here with unsaturated solutions of nickel in iron, and whatever the temperature of annealing, if it does not bring the alloy into the adjacent duplex region, the structure and also the parameter of the lattice of any given alloy will remain unaltered.

The octahedrites also showed no change so far as could be judged.

The α- and γ-phases were both present in the spectra obtained with samples in the unannealed as well as with those in the annealed state. The heat treatment had not produced any appreciable change.

The ataxites, rich in nickel, yielded results which differed from the other two classes. The ataxites examined were Cape Eisen, Kokomo, Babb's Mill, Klondyke, and San Cristobal; they contained between 15·7 and 25·6 per cent. nickel by weight. The first two, namely, Cape Eisen and Kokomo, yielded identical spectra whether they were annealed or not; both α- and γ-phases were present, the only difference being in the definition of the lines as compared with those in the spectra of the hexahedrites and octahedrites. Etchings of the materials showed that the materials were both homogeneous, and this was confirmed by the fact that samples from different parts of the specimens gave the same results.

The remaining three meteorites, namely, Babb's Mill (17·3 per cent. Ni), Klondyke (18·2 per cent. Ni), and San Cristobal (25·6 per cent. Ni) yielded spectra in the unannealed state which were different from those obtained after annealing at 350° C. In the unannealed state the α-structure, much distorted, appeared alone, whereas after annealing at 350° C. the α- and γ-phases were present together, the α-phase appearing fairly free from distortion.

These three meteorites will be considered in some detail.

(*a*) Babb's Mill.—Several samples taken from different parts of the specimen were examined in the unannealed state. The spectra were all similar. One of them is reproduced in fig. 3 *a* (Pl. VI.); it contains lines belonging to the distorted $\alpha_2$-structure, and there is no trace of lines belonging to the γ-phase.

One of these samples was afterwards annealed for 3 days at 250° C. There was not much change, but the lines were slightly better defined. Little further improvement in the definition of the lines was observed after 10 days' annealing at 250° C., but after 28 days at 250° C. the definition had distinctly improved (fig. 3 *b* (Pl. VI.)), line 10 now appearing as a broad line instead of a diffuse band, but no γ-lines appeared in the spectrum. More annealing at 250° C. produced further improvement of the lines, as is shown in fig. 3 *c* (Pl. VI.), which is the spectrum obtained after 56 days' annealing at this temperature. The γ-lines were still absent.

Fig. 3 *d* (Pl. VI.) shows the effect of annealing the original sample for 8 days at 300° C. In contrast to the spectra obtained after annealing at 250° C., the spectrum now contains γ as well as α-lines.

After 56 days' annealing at 350° C. all the lines in both the α- and the γ-spectra were well defined, line 10 of the α-phase appearing as a well-defined, resolved doublet. Line 8 was also almost resolved (fig. 3 *e* (Pl. VI.)).

The material thus appeared to be in a good state of equilibrium after this heat treatment.

(*b*) Klondyke.—Two samples from different parts of the meteorite were examined in the unannealed state. In each case only the distorted $\alpha_2$-structure was present (fig. 4 *a* (Pl. VI.)). An etched surface of this meteorite presented the same appearance as that obtained with the Babb's Mill meteorite.

After 3, 10 and 28 days' annealing at 250° C. only the distorted $\alpha_2$-structure was present, but the lines in the spectra showed progressive improvement in definition as the annealing period was increased. Fig. 4 *b* (Pl. VI.) shows the spectrum obtained with a sample which had been annealed for 28 days at 250° C. It consisted entirely of $\alpha$-lines.

On further annealing at 250° C. faint $\gamma$-lines are found to appear. Fig. 4 *c* (Pl. VI.) is the spectrum obtained after 56 days' annealing at 250° C. The $\alpha$-lines are fairly well defined, and faint $\gamma$-lines now accompany them in the spectrum.

When a sample of the Klondyke meteorite in the unannealed state and containing only the $\alpha_2$-structure was annealed for 8 days at 300° C., the $\gamma$-phase lines appeared, but they were faint compared with the $\alpha$-lines (fig. 4 *d* (Pl. VI.)). The $\alpha$-lines also showed improvement in definition after this heat treatment, line 10 appearing as a fairly well-defined band.

One month's annealing at 350° C. brought about a marked improvement, both the $\alpha$- and the $\gamma$-lines being well defined, and line 10 of the $\alpha$-spectrum being well resolved. The amount of the $\gamma$- relative to the $\alpha$-phase had also increased (fig. 4 *e* (Pl. VI.)).

(*c*) San Cristobal.—Four samples of this meteorite were examined in the unannealed condition. Two of these contained only $\alpha_2$-lines with no trace of the $\gamma$-phase (fig. 5 *a* (Pl. VII.)), and the other two showed a slight trace of the $\gamma$-phase.

After annealing for 28 days at 250° C., the spectrum shown in fig. 5 *b* (Pl. VII.) was obtained; the $\gamma$-lines are quite prominent and the $\alpha$-lines better defined. Both $\gamma$- and $\alpha$-lines were also present after 58 days' annealing at 250° C.

Eight days' annealing at 300° C. of the original sample in the spectrum of which no $\gamma$-lines appeared, yielded the film reproduced in fig. 5 *c* (Pl. VII.). The lines from the $\gamma$-constituent are as strong as those from the $\alpha$-constituent and the lines are fairly well defined, but line 10 of the $\alpha$-phase is not resolved.

A month's annealing of a sample of this meteorite at 350° C. produced a spectrum with well-defined lines of both $\alpha$- and $\gamma$-phases (fig. 5 *d* (Pl. VII.)) with line 10 of the $\alpha$-phase resolved.

The general behaviour of the three meteorites under the various heat treatments is the same, although there are significant differences in certain details. The results are exceedingly important, but before making any definite deductions from them it was necessary to investigate one possible explanation of the appearance of the $\alpha_2$.structure alone in the unannealed state. As is well known, the outer crust of a meteorite, owing to excessive heating when travelling through the atmosphere, consists of a zone exhibiting a granular structure, and this zone may vary in width in different meteorites from 1 to 10 mm. The specimen of the Babb's Mill meteorite available for examination was of a fair size, but those of the Klondyke and the San Cristobal meteorites were of small dimensions and, if taken from the outer regions of the meteorites, might consist only of material in the zone damaged by heating and would not therefore be a true representation of the inner structure of the meteorites. According to the results obtained with artificial iron-nickel alloys (5), a specimen quenched from high temperature should contain only the distorted $\alpha_2$-structure, and the behaviour of the three meteorites just examined might be explained on this ground if the samples were taken from the outer zones. It was essential, therefore, to obtain specimens which were definitely taken from the interior of the meteorites. Such specimens of the meteorites Klondyke and San Cristobal were obtained from the British Museum.

Fig. 6 *a* (Pl. VII.) shows a film obtained with an unannealed sample taken from the interior of the Klondyke meteorite. The material consists entirely of the distorted $\alpha_2$-structure; there is no trace of the $\gamma$-structure.

After 8 days' annealing at 300° C. the spectrum contained both $\alpha$ and $\gamma$-lines (fig. 6 *b* (Pl. VII.)), the $\alpha$-lines being somewhat diffuse but better defined than in the spectrum obtained with the unannealed sample. The behaviour of the sample under this heat treatment is exactly the same as that of the samples of the original specimen.

The new specimen of the San Cristobal meteorite consisted of millings taken from the interior. An unannealed sample yielded the spectrum shown in fig. 7 *a* (Pl. VII.). It contains both $\alpha$- and $\gamma$-lines; all the lines are diffuse, due no doubt to the excessive distortion produced by the milling process. After 14 days' annealing at 300° C. (fig. 7 *b* (Pl. VII.)), the lines at the lower angles of reflexion are quite sharp, and it appears, although it is difficult to say with certainty, that the amount of the $\gamma$-phase relative to the $\alpha$-phase has increased.

The new samples of San Cristobal differ from the original samples in that the $\gamma$-phase is present with the $\alpha$-phase and is more prominent in relation to the $\alpha$-phase in the new than in the old samples. But the $\alpha$-phase is much distorted in the unannealed state in both sets of samples and the $\gamma$-phase becomes more prominent with the annealing treatment at 300° C., and the definition of both the $\alpha$- and the $\gamma$-lines shows marked improvement.

From these results it is concluded that the specimens of the meteorites Babb's Mill and Klondyke submitted for examination consisted entirely of "martensite" (that is the distorted $\alpha_2$-structure) as distinct from plessite, which term is here strictly reserved for the duplex constituent found in meteorites, and that martensite is converted into plessite at comparatively low temperatures, for example, 8 days' annealing at 300° C. was sufficient to produce the change. The same statement can be made about the first specimen of San Cristobal that was examined, but the second specimen taken from the interior of the meteorite contained a duplex structure. Pfann (6) states that the San Cristobal meteorite consists mostly of tænite with patches of plessite, but from the X-ray spectra taken with samples of the meteorite in the present investigation it would perhaps be more correct to say that the meteorite consists of plessite and martensite.

## 9. *Summary of Results.*

### (i.) *Effect of Annealing at* 350° C.

The twenty-four meteorites investigated were annealed for periods of five or eight weeks at 350° C. and rapidly cooled. After this heat treatment the lines in the spectra were well defined, the $\alpha$-lines in general showing better definition than the $\gamma$-lines. Meteorites containing less than about 6·2 per cent. nickel by weight yielded spectra consisting of $\alpha$-lines alone, and meteorites above this nickel content, spectra containing both $\alpha$- and $\gamma$-lines. The $\alpha$-parameter could be accurately measured. It was found to increase in value with increasing nickel content up to about 6·2 per cent. nickel, and to remain approximately constant at the value $2{\cdot}8628_2$ Å. in meteorites of higher nickel content. The greatest deviation from this value was 1 in 20,000. In the group of octahedrites examined the greatest deviation from the mean value was 1 in 30,000. There is therefore very little variation in the composition of the $\alpha$-component in different meteorites the nickel content of which exceeds about 6·2 per cent.

From these X-ray measurements it may be concluded that the composition of kamacite in octahedrites is the same whatever the width of the kamacite bands in the Widmanstatten figures, and that the composition of the kamacitic component of plessite is the same, within the limits of measurement, as that of the kamacite bands.

The definition of the $\gamma$-lines was never as good as that of the $\alpha$-lines, and the variation in parameter value from one meteorite to another was quite pronounced. An attempt is made in the paper to explain this variation on the basis of the equilibrium diagram suggested for artificial iron-nickel alloys.

### (ii.) *Effect of Annealing at Higher Temperatures.*

With the heat treatments given at 350° C., 400° C., and 500° C. the octahedrites displayed remarkably constant $\alpha$-parameters, but the ataxites, rich in nickel, showed marked variation. The variation of parameter found in these meteorites was similar to that observed with artificial alloys of about the same composition and similarly heat treated.

### (iii.) *Unannealed Material.*

The spectra obtained with unannealed samples of hexahedrites, ataxites (poor in nickel), and octahedrites were similar to those obtained with annealed specimens of these meteorites, the only difference being that the lines were badly defined owing to the distortion caused by the cold work done in preparing the specimens.

Of the five ataxites (rich in nickel) that were examined two yielded spectra showing both the $\alpha$- and $\gamma$-phases as with the annealed samples, but with lines badly defined, and three, spectra containing only $\alpha$-lines, which were identified with the distorted $\alpha_2$-structure found in artificial alloys quenched from high temperature. These three ataxites were submitted to additional heat treatments at 250° C., 300° C., and 350° C. It was found that an annealing treatment of only 8 days at 300° C. sufficed in each case to break up the $\alpha_2$-structure into the $\alpha$- and $\gamma$-components—in other words, the martensite changes into plessite. An annealing treatment of 56 days at 250° C. brought about a similar change in one of the meteorites. From this it would appear that the equilibrium condition at these low temperatures is that in which the $\alpha$- and $\gamma$-phases exist together in equilibrium (plessite); material in the $\alpha_2$ state (martensite) is in a metastable condition.

It would appear from the results quoted in this paper that meteoric irons closely resemble the artificially prepared iron-nickel alloys in their reaction to different heat treatments. This being so, the two ataxites Babb's Mill and Klondyke, and possibly also San Cristobal, must have been rapidly cooled from elevated temperatures. The bearing of these results on the types of structure found in different meteoric irons will be discussed in another paper.

## 10. *Acknowledgements.*

The authors have pleasure in recording their thanks to Dr. Fletcher Watson, of Harvard College Observatory, Cambridge, Massachusetts, Professor Charles Palache, of the Department of Mineralogy, Harvard University, and the authorities of the British Museum for supplying

the meteorites. They would also like to express their indebtedness and gratitude to Dr. Max H. Hey of the British Museum for much valuable help and information concerning some of the meteorites.

### *References.*

(1) Young, Proc. Roy. Soc. A, cxii. p. 630 (1926).
(2) Mehl and Barrett, A. Inst. Min. and Met. Eng. Tech. Publ. no. 353 (1930).
(3) Derge and Kommel, Am. Journ. Sci. xxxv. p. 203 (1937).
(4) Desch, Iron and Steel Inst. Alloy Steels Report, Section 5 (1936).
(5) Owen and Sully, Phil. Mag. xxvii. p. 614 (1939).
(6) Pfann, *Inter. Zeits. f. Metallographie*, ix. p. 65 (1917).

# XLIX. *On a Hydraulic Problem involving Discharge into Tidal Water.*

By A. G. Walker, Ph.D., Department of Pure Mathematics,
University of Liverpool,
and
J. R. Daymond, M.Sc., Department of Civil Engineering,
University of Liverpool*.

[Received November 25, 1938.]

1. A problem of some interest in hydraulics is concerned with the outflow into tidal water from a tank which is at the same time receiving a constant inflow †. The problem is to examine the variation of the level in the tank, but it is found that this depends upon a first-order differential equation which cannot be solved in finite terms. A paper recently submitted by one of us ‡ gives a field of significant results derived by experiment from a model reproducing the conditions of the problem, but the object of the present paper is to discuss the problem theoretically.

The statement is as follows:—A cylindrical tank of area A receives water at a constant rate Q, and an outflow pipe leads from the tank to tidal water, the tide being assumed to take the form of a sine curve of amplitude 2R and period T. Adopting the usual formula for pipe flow, it will be assumed that the rate of outflow is $kh^{1/2}$, where $h$ is the head, *i.e.*, the height of the tank level above the tide, and $k$ is a constant depending upon the characteristics of the pipe. Since the tide may rise above the level in the tank, it will be assumed that the outflow pipe is equipped with a valve which prevents back-flow, so that the tank cannot be filled from the tide. It follows that we may regard the head $h$ for discharge as zero when the tank level is below the tide.

It will be shown that, whatever the initial level in the tank, the level will ultimately rise and fall periodically, reaching a maximum height H and a minimum height D. It is this "settled" state which is of practical importance, for the values of H and D determine the necessary

---

* Communicated by the Authors.

† An important practical application exists in engineering where it is required to design a drainage scheme involving discharge from a tank into tidal water, the tank receiving at the same time the contribution from a drainage area.

‡ J. R. Daymond, "On the Hydraulic Problem concerning the Design of Sewage Storage Tanks and Sea Outfalls." Submitted to the Institution of Civil Engineers.

and sufficient dimensions of the tank. The quantities H and D are found to depend upon R, T, $m$, $s$, where

$$m=Q/A, \qquad s=Q/k, \quad \dots\dots\dots \quad (1)$$

and for a given tide, *i. e.*, fixed R and T, the results can be represented by contour lines H=constant and D=constant in a "field" referred to $m$ and $s$ as coordinates. A field of results exists for each tide, and it will be found that a simple transformation relates any two fields, so that it is sufficient to consider the field for one tide only. In the experimental work all results were reduced to those for a *unit tide*, defined as having an amplitude of 2 feet and a period of one hour. From this field it is possible to determine at once, for any tide, any two of the four quantities H, D, $m$, $s$ when the other two are known, and the results are thus in a form suitable for practical application.

2. It is convenient to measure all heights above mean tide level, so that the height $\zeta$ of the tide at time $t$ is given by

$$\zeta=R\sin(2\pi t/T), \quad \dots\dots\dots \quad (2)$$

$t$ being measured from a suitable origin. If now $z$ is the height of the level in the tank at time $t$, then the head $h$ governing outflow is given by

$$\left.\begin{array}{ll} h=z-\zeta & \text{when } z>\zeta, \\ h=0 & \text{when } z\leqslant\zeta. \end{array}\right\} \quad \dots\dots\dots \quad (3)$$

In the interval of time $(t, t+dt)$ a quantity $Q\,dt$ of water flows into the tank, a quantity $kh^{1/2}dt$ flows out, and an amount $A\,dz$ is stored, where $dz$ is the increase in $z$ in this interval. We therefore have $A\,dz+kh^{1/2}dt=Q\,dt$, whence $z$ satisfies the first-order differential equation

$$\frac{1}{m}\frac{dz}{dt}+\frac{1}{s}h^{1/2}=1, \quad \dots\dots\dots \quad (4)$$

where $m$, $s$ are given by (1) and $h$ by (3) and (2).

The above equation, with the additional information that $z$ is continuous for all values of $t$, serves to define $z$ as a function of $t$ when its value is known at one instant. This is seen from the fact that $dz/dt$ exists and is unique when $z$ and $t$ are given values, so that there is one and only one solution passing through each point of the $(t, z)$ plane. It is useful to refer to each solution as a $z$-curve in the $(t, z)$ plane, and it follows from the above remark that no two such curves can intersect.

3. We shall now prove that for any given positive values of the constants $m$, $s$ equation (4) has one periodic solution which is approached asymptotically by each other solution as $t\to\infty$.

Let $z_1(t)$, $z_2(t)$ be two distinct solutions, with $z_1>z_2$ for one value of $t$.

Then $z_1 > z_2$ for all values of $t$, since the corresponding curves cannot intersect. From (4),

$$\frac{d}{dt}(z_1 - z_2) = -\frac{m}{s}(h_1^{1/2} - h_2^{1/2}), \quad . \quad . \quad . \quad . \quad . \quad . \quad . \quad (5)$$

where $h_1$ is given by $z_1$ and $h_2$ by $z_2$, and from (3) we see that $z_1 > z_2$ implies $h_1 \geqslant h_2$, whence, from (5), $\frac{d}{dt}(z_1 - z_2) \leqslant 0$. Thus $z_1 - z_2$ cannot increase, and must therefore tend to a limit as $t \to \infty$. Hence, as $t \to \infty$, $\frac{d}{dt}(z_1 - z_2) \to 0$, and therefore $h_1 \to h_2$ from (5), so that, from (3), either $z_1 \to z_2$, or $z_2 < z_1 \leqslant \zeta$ for all time after some instant. The latter case is impossible, since no solution $z(t)$ can remain less than $\zeta$, $dz/dt$ having a constant positive value $m$ when $z \leqslant \zeta$. Hence $z_1 \to z_2$, and the two solutions converge. It follows that all solutions converge to the same asymptote, which must itself evidently be a solution.

We can now see that this asymptote must be a periodic curve, for otherwise, from the form of (4), this same curve displaced through a period of the tide would be another asymptote, whereas we have proved that there is only one asymptote. Thus there is a periodic solution to equation (4), the period being that of the tide, and there cannot be more than one since all solutions converge. The existence of the periodic solution can also be demonstrated by taking two extreme solutions and showing that there must be an intermediate solution satisfying $z(t+T) = z(t)$ for one particular value of $t$, and hence for all values from the form of (4).

Since all solutions tend asymptotically to the periodic solution it follows that, whatever the initial level in the tank, the level will ultimately rise and fall periodically, the final behaviour being determined by the values of R, T, $m$, $s$.

4. We can now deduce the shape of the periodic $z$-curve. In figs. 1 ($a$) and 1 ($b$), let S be the tide curve given by $z = \zeta = R \sin(2\pi t/T)$ in the $(t, z)$ plane, and let M be the parallel curve given by $h = s^2$, *i. e.*, $z = \zeta + s^2$. Then, from equation (4), all points of a $z$-curve at which $z(t)$ is critical satisfy $h = s^2$, *i. e.*, lie on M. At any point below M, $h < s^2$ and $dz/dt > 0$, so that $z$ is increasing with $t$, and at any point above M, $h > s^2$ and $z$ is decreasing as $t$ increases. Hence in the full period between $\alpha$ and $\alpha'$, any maximum must lie on the branch $\alpha\beta$ of M and any minimum on the branch $\beta\alpha'$. It follows at once, since $z$ is continuous and since the periodic curve must have at least one maximum and one minimum in a full period, that the periodic $z$-curve has just one maximum an $\alpha\beta$ and one minimum on $\beta\alpha'$.

Between the two critical points there is just one inflexion. This can be seen by drawing the curve of all inflexions, given by $d^2z/dt^2=0$ from (4), *i. e.*,

$$h^{1/2}=s\left(1-\frac{1}{m}\frac{d\zeta}{dt}\right). \qquad (6)$$

If $m<2\pi R/T$, there are two points F, G on S at which $d\zeta/dt=m$, and from (6) the inflexion curve touches S at F and G, and does not exist between these points, since the positive square root of $h$ must be taken in (4). This case is shown in fig. 1 (*a*), where I is the inflexion curve. If $m \geqslant 2\pi R/T$, the inflexion curve lies wholly above S, as shown in fig. 1 (*b*). In both cases the inflexion curve lies above M between $\alpha$ and $\beta$, and from its shape it follows that the $z$-curve can have only one inflexion between these points.

Fig. 1 (*a*).

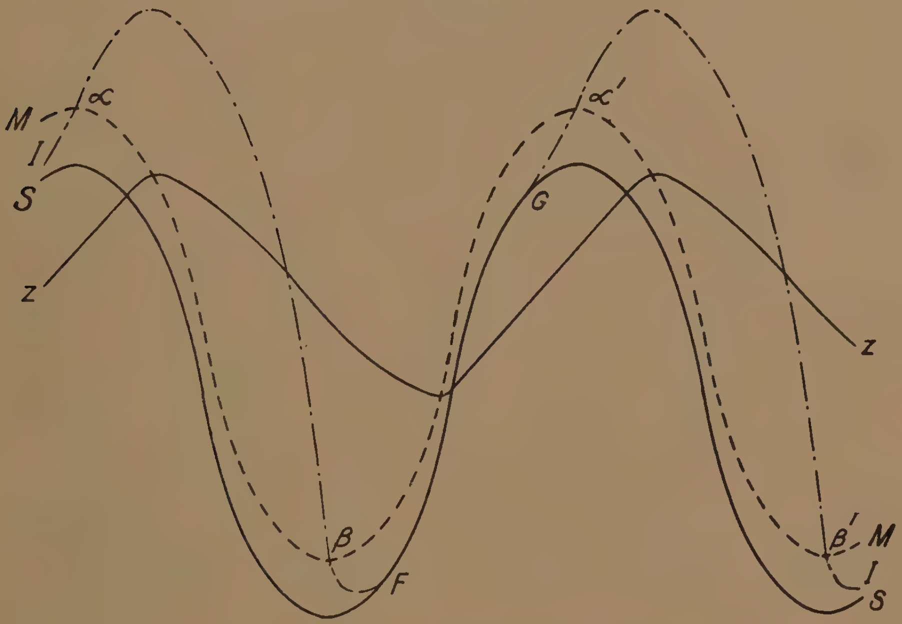

Between the minimum on $\beta\alpha'$ and the next maximum on $\alpha'\beta'$ there are two possibilities, since the $z$-curve may or may not cut the curve S. At any point of intersection, $h=0$ and the slope of the $z$-curve is $m$. The greatest slope of S is $2\pi R/T$, whence if $m \geqslant 2\pi R/T$ there is no point of intersection, and the $z$-curve lies wholly above S, as shown in fig. 1 (*b*). In this case there is another inflexion, between $\beta$ and $\alpha'$.

If $m<2\pi R/T$, the $z$-curve may again lie wholly above S, having an inflexion between G and $\alpha'$ in fig. 1 (*a*), or it may cut S between F and G. In the latter case the $z$-curve cuts S at slope $m$, and proceeds at this slope until it cuts S again, as shown in fig. 1 (*a*).

When the $z$-curve cuts S the valve on the outflow pipe comes into action, and there is no outflow for an interval of time during each full period of the tide. When the $z$-curve lies wholly above S there is outflow at all stages of the tide.

In all cases we see that the periodic $z$-curve has just one maximum, at height H say, and one minimum, at height D, and H and D are therefore determinate when R, T, $m$, $s$ are known. Keeping $s$ fixed we should expect, from the diagrams, to find that H increases and D decreases as $m$ increases. This does not appear to follow at once from the equation for $z$, but the result has been confirmed by experiment, as shown in the field of results in fig. 2.

Fig. 1 (*b*).

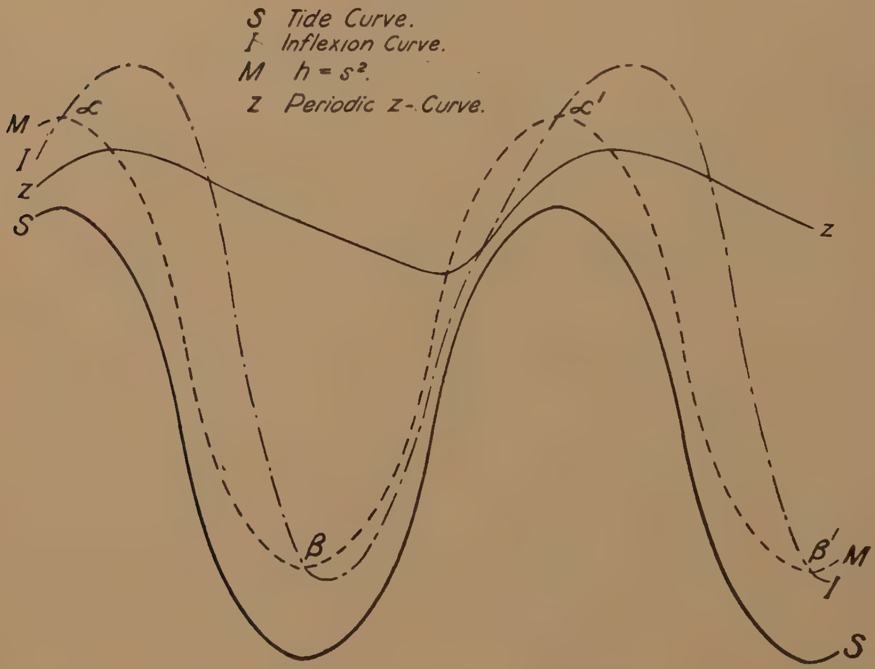

5. As mentioned before, the significant quantities are H and D, and the important problem is to find how H and D depend upon R, T, $m$, $s$. We can now show that it is sufficient to find how H and D depend upon $m$ and $s$ for one particular tide, *i. e.*, for particular values of R and T, and that results for any other tide can be deduced at once.

Suppose we know $H_1$ and $D_1$ for given constants $R_1$, $T_1$, $m_1$, $s_1$. Then $H_1$ and $D_1$ are given by the periodic solution of the equation

$$\frac{1}{m_1}\frac{dz}{dt}+\frac{1}{s_1}h_1^{1/2}=1, \qquad h_1=0 \text{ or } z-R_1\sin\frac{2\pi t}{T_1}. \quad . \quad . \quad . \quad (7)$$

If now we wish to consider the tide given by $R_2$ and $T_2$ we can transform from $z$, $t$ to new variables $z'$, $t'$, so that the equation takes the form (7) with $R_2$, $T_2$ in place of $R_1$, $T_1$. For on writing

$$t/T_1=t'/T_2, \qquad z/R_1=z'/R_2, \quad . \quad . \quad . \quad . \quad . \quad . \quad . \quad (8)$$

Fig. 2.

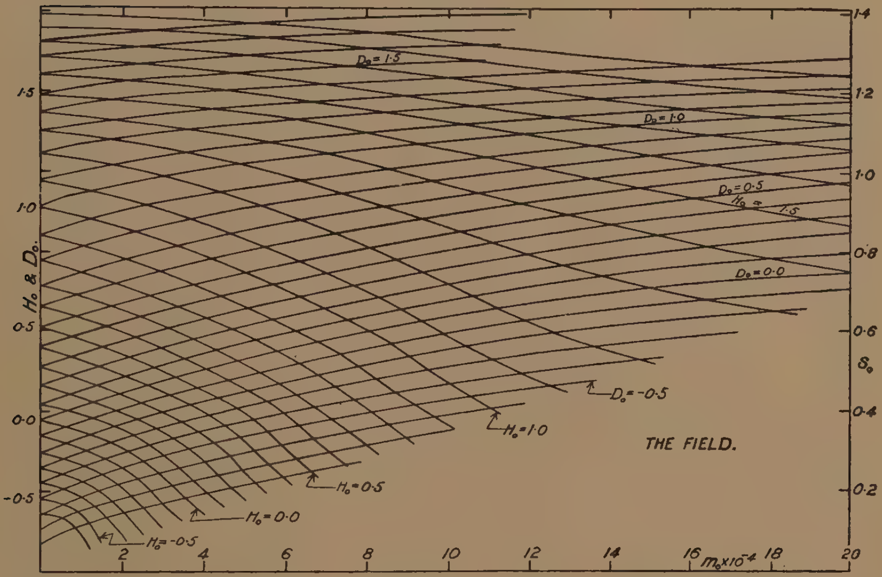

equation (7) becomes

$$\frac{1}{m_2}\frac{dz'}{dt'}+\frac{1}{s_2}h_2^{1/2}=1, \qquad h_2=0 \text{ or } z'-R_2\sin\frac{2\pi t'}{T_2},$$

where
$$m_2=\frac{R_2T_1}{R_1T_2}m_1, \qquad s_2=\left(\frac{R_2}{R_1}\right)^{1/2}s_1. \quad . \quad . \quad . \quad . \quad . \quad . \quad (9)$$

The transformation from $t$ to $t'$ is linear, and the transformation from $z$ to $z'$ does not involve $t$. It follows that the periodic solution in the $(t, z)$ plane transforms into the periodic solution in the $(t', z')$ plane and the critical points correspond. Hence, from (8), the maximum and minimum heights $H_2$ and $D_2$ given by $R_2$, $T_2$, $m_2$, $s_2$ satisfy

$$H_2/H_1=D_2/D_1=R_2/R_1. \quad . \quad . \quad . \quad . \quad . \quad . \quad . \quad (10)$$

Knowing therefore $R_1$, $T_1$, $H_1$, $D_1$, $m_1$, $s_1$, and $R_2$, $T_2$, we can find $m_2$, $s_2$ from (9) and $H_2$, $D_2$ from (10), and we have a solution for the second tide, as required. If we know the whole field of solutions for the first tide we can at once find the whole field for the second tide, and it is sufficient therefore to consider only one tide.

In the experimental work results were reduced to a *unit tide*, amplitude 2 feet and period one hour, and if therefore $m_0$, $s_0$, $H_0$, $D_0$ refer to the unit tide, the corresponding solution for any other tide R, T is given by

$$m=m_0 R/T, \quad s=s_0 R^{1/2}, \quad H=H_0 R, \quad D=D_0 R, \quad . \ . \quad (11)$$

where T is measured in hours and the other quantities in foot-second units. This transformation can be used in a number of ways. In the first place we can find, by experimental or approximate theoretical methods, a solution for any tide, and transform so that the results can be included in the field of results for the unit tide. On the other hand, the field of results for the unit tide can be applied to an actual example concerned with some given tide provided the tide has approximately the form of a sine curve. It is also possible to discuss the effect of a slow variation in the tide. This is important, since in practice a scheme must be designed to allow for the change in amplitude which occurs between spring and neap tides.

The field of results for the unit tide is given in fig. 2, where $m_0$ and $s_0$ are taken as coordinates. The two sets of curves, given by $H_0=\text{constant}$ and $D_0=\text{constant}$, are drawn on the same field, so that any two of $H_0$, $D_0$, $m_0$, $s_0$ can be found when the other two are given.

6. Certain information about the limits of the field can be obtained by direct integration. First consider the case when $m$ is small and $s$ finite. It then follows from equation (4) that $z$ is approximately constant, as would be expected, since in this case, from (1), the area of the tank is large, so that the inflow and outflow barely affect the level in the tank. With $z$ approximately constant, H and D will have this constant value, and the relation between H and $s$ can be found by considering the next approximate periodic solution of (4).

Taking $R=1$ and $T=2\pi$ for convenience, then from (11), $s=s_0$, and $H=H_0$ ($=D_0$ in the present case). Writing $z=H_0+mZ(t)$, then Z is finite, and substituting in (4), and neglecting powers of $m$, we see that Z satisfies the equations

$$\frac{dZ}{dt}=1-\frac{1}{s_0}(H_0-\sin t)^{1/2}, \quad \text{when } \sin t<H_0, \quad . \ . \ . \quad (12)$$

$$\frac{dz}{dt}=1, \qquad \text{when } \sin t \geqslant H_0. \quad . \ . \ . \quad (12')$$

There are now two cases to be considered:

I. $H_0<1$.

In this case the periodic $z$-curve is approximately parallel to the $t$-axis at height $H_0$, and therefore cuts the tide curve $z=\sin t$ in the full period $(-3\pi/2, \pi/2)$ at two points, given approximately by $t=-\alpha-\pi/2$ and $t=\alpha-\pi/2$, where $\alpha$ is defined by

$$\cos\alpha=-H_0,\quad 0\leqslant\alpha<\pi. \quad . \quad . \quad . \quad . \quad . \quad . \quad (13)$$

Since we are considering the periodic solution, $Z(t)$ must be periodic whence $\int_{t=-3\pi/2}^{\pi/2} dZ$ must vanish. Hence, from (12) and (12′),

$$\int_{-3\pi/2}^{-\alpha-\pi/2} dt+\int_{-\alpha-\pi/2}^{\alpha-\pi/2}\left(1-\frac{1}{s_0}(H_0-\sin t)^{1/2}\right)dt+\int_{\alpha-\pi/2}^{\pi/2} dt=0,$$

and we therefore have

$$s_0=\frac{1}{2\pi}\int_{-\alpha-\pi/2}^{\alpha-\pi/2}(H_0-\sin t)^{1/2}\,dt=\frac{1}{2\pi}\int_{-\alpha}^{\alpha}(H_0+\cos\theta)^{1/2}\,d$$

on writing $t=\theta-\pi/2$. This is seen to be equivalent to

$$s_0=\frac{1}{\pi}\int_0^{\alpha}(H_0+\cos\theta)^{1/2}\,d\theta, \quad . \quad . \quad . \quad . \quad . \quad . \quad (14)$$

giving $s_0$ in terms of $H_0$ when $-1\leqslant H_0<1$.

II. $H_0\geqslant 1$.

In this case the $z$-curve is again approximately parallel to the $t$-axis at height $H_0$, but does not now cut the tide curve, so that $Z$ is given by (12) for all values of $t$. As before, $Z(t)$ must be periodic, whence $\int_{3\pi/2}^{\pi/2} dZ=0$, and from (12) we have

$$s_0=\frac{1}{2\pi}\int_{-3\pi/2}^{\pi/2}(H_0-\sin t)^{1/2}\,dt.$$

Writing $t=\theta-\pi/2$, we find that $s_0$ is given in terms of $H_0$ by

$$s_0=\frac{1}{\pi}\int_0^{\pi}(H_0+\cos\theta)^{1/2}\,d\theta. \quad . \quad . \quad . \quad . \quad . \quad . \quad (15)$$

Equations (14) and (15) give $s_0$ in terms of $H_0$ for all values of $H_0$ in the limit $m\rightarrow 0$, and they give therefore the points where the curves $H_0=$ constant meet the $s_0$—axis in the field of results. Since $D_0$ is approximately $H_0$ when $m$ is small, the curves $D_0=$constant meet the $s_0$—axis at the same points.

The expressions for $s_0$ in (14) and (15) will be recognized as elliptic integrals, and we find that they can be expressed in terms of the complete elliptic functions E and K. Writing $H_0 = -\cos \alpha$ in (14), and making the substitution $\sin \theta/2 = \sin \phi \sin \alpha/2$, we get

$$s_0 = \frac{2\sqrt{2}}{\pi} \sin^2\frac{\alpha}{2} \int_0^{\pi/2} \left(1 - \sin^2\frac{\alpha}{2} \sin^2 \phi\right)^{-1/2} \cos^2 \phi \, d\phi$$

$$= \frac{2\sqrt{2}}{\pi} \int_0^{\pi/2} \left(1 - \sin^2\frac{\alpha}{2} \sin^2 \phi\right)^{1/2} d\phi$$

$$- \frac{2\sqrt{2}}{\pi} \cos^2\frac{\alpha}{2} \int_0^{\pi/2} \left(1 - \sin^2\frac{\alpha}{2} \sin^2 \phi\right)^{1/2} d\phi$$

$$= \frac{2\sqrt{2}}{\pi} \mathrm{E}\left(\sin\frac{\alpha}{2}\right) - \frac{2\sqrt{2}}{\pi} \cos^2\frac{\alpha}{2} \mathrm{K}\left(\sin\frac{\alpha}{2}\right). \quad \ldots\ldots\ldots \quad (16)$$

This, then, is the formula for $s_0$ when $H_0 < 1$. When $H_0 \geqslant 1$, we have, on making the substitution $\theta = 2\phi$ in (15),

$$s_0 = \frac{2}{\pi} (1+H_0)^{1/2} \int_0^{\pi/2} \left(1 - \frac{2}{1+H_0} \sin^2 \phi\right)^{1/2} d\phi$$

$$= \frac{2}{\pi} (1+H_0)^{1/2} . \mathrm{E}\left(\sqrt{\frac{2}{1+H_0}}\right). \quad \ldots\ldots\ldots \quad (17)$$

The functions $\mathrm{E}(\sin \theta)$, $\mathrm{K}(\sin \theta)$ are well known and have been tabulated for all values of $\theta$, so that it is possible to find $s_0$ for all values of $H_0$ from the above formulæ. Results found in this way have been compared with the experimental results, which were found to be remarkably accurate. A check of this kind is evidently very welcome, especially in hydraulics, where the probable errors are likely to be large.

7. Consider now what happens as $m$ increases. Here again there are two cases to be considered:

I. $H < R$.

When H has a given value less than R then there is an upper limit to the value of $m$, since $m$ is the slope of that part of the $z$-curve which is below the tide curve. If the line $z = H$ is drawn to cut the tide curve in the range (T/4, 3T/4) at P, and if Q in the range (—T/4, 0) is the point on the tide curve the tangent at which passes through P, then the slope of QP is the maximum value of $m$ for the given value of H; for it is seen from a figure that the periodic $z$-curve for any larger value of $m$ must have a maximum above the line $z = H$.

The maximum value of $m$ is reached only when the maximum of the $z$-curve is at P, whence $s = 0$, since $h = s^2$ at the critical points. From (4) we see that in this extreme case the $z$-curve is the line QP together with part of the tide-curve PQ′, where Q′ is found by displacing Q through a full period. From (1) this case arises when $k$ is very large, *i. e.*, when the diameter of the outfall pipe is large, in which case the level in the tank simply follows the tide until the valve comes into action.

This theoretical result is actually nullified in practice, for when the head is very small the discharge law $kh^{1/2}$ breaks down and the rate of flow is governed entirely by other factors not here taken into consideration. The region where this occurs, given by small values of $s_0$, is left blank in the field of results (fig. 2). We observe, however, that the curves $H_0$=constant tend to cut the $m_0$-axis when $H_0<1$.

II. $H \geqslant R$.

In this case the periodic $z$-curve can lie wholly above the tide curve, and $m$ can increase indefinitely. From equation (4) we see that when $m$ is very large the $z$-curve approximates to $z=\zeta+s^2$ given by raising the tide curve through a distance $s^2$. Hence as $m\rightarrow\infty$, $H\rightarrow R+s^2$ and $D\rightarrow -R+s^2$. It follows that on the field of results for the unit tide the curve $H_0$=constant for $H_0\geqslant 1$ has the line $s_0=(H_0-1)^{1/2}$ for an asymptote as $m\rightarrow\infty$, and the curve $D_0$=constant for any value of $D_0$ has the line $s_0=(D_0+1)^{1/2}$ for an asymptote.

The head for discharge is not here necessarily small, and the theoretical results can be used to check the experimental results, which were found to have the predicted tendency.

8. With a view to practical application in the design of a sea-outfall scheme it is important to note that any particular result taken from the field of results can be verified by two approximate theoretical methods. These methods are not, however, suitable for the derivation of the field, which is best done by experiment.

The first method is graphical, and the $z$-curve is here drawn step by step, the slope at any point being given by equation (4) simply in terms of the height $h$ above the tide curve. If $m_0$ and $s_0$ are given, then $H_0$ is read from the field, and this determines the position of the maximum on the $z$-curve, since the critical points are at height $s_0{}^2$ above the unit tide curve. Proceeding from this point the whole $z$-curve can be constructed from short segments of straight lines having the necessary slopes calculated from (4). The solution given by the field is then tested by observing whether the curve so drawn is periodic and whether the minimum is given correctly by $D_0$ read from the field.

The second method is algebraic, and depends upon approximating to the tide curve by means of segments of straight lines and arcs of parabolas. In this approximation the tide curve is given by $\zeta=f(t)$, where $f$ is linear or quadratic in $t$ and varies in form for different intervals. In each interval equation (4) gives

$$\frac{dh}{dt}+\frac{m}{s}h^{1/2}=m-\frac{df}{dt}=a+bt,$$

where $a$, $b$ are constants. Writing $h=(a+bt)^2u^2$, where $u$ is defined to have the sign of $a+bt$, then the equation for $u$ is

$$(a+bt)\frac{du}{dt}=\frac{1}{2u}-\frac{m}{2s}-bu, \quad \ldots \ldots \quad (18)$$

and this can be integrated at once. Starting with the maximum point, as in the graphical method, the above equation must be integrated in each interval and the various solutions fitted together to form a continuous curve. This curve will approximate to the $z$-curve, and the field solution can be tested as before.

9. It may be of interest to show that a simple and at the same time very close approximation to a sine curve can be constructed from straight lines and parabolas. The approximation to sin $t$ is given by $f(t)$ defined in the range $(0, \pi/2)$ as follows :—

$$\left.\begin{array}{ll} 0\leqslant t\leqslant \dfrac{\pi}{6}, & f(t)=\dfrac{3}{\pi}t\,; \\ \dfrac{\pi}{6}<t\leqslant\dfrac{\pi}{2}, & f(t)=1-\dfrac{9}{2\pi^2}\left(t-\dfrac{\pi}{2}\right) \end{array}\right\} \quad \ldots \ldots \quad (19)$$

Outside this range the form is reproduced as required for each range of $\pi/2$ to give the symmetry of sin $t$.

It is seen that $f(t)$ is continuous and is equal to sin $t$ when $t=n\pi/2$, $n\pi\pm\pi/6$ for all integral values of $n$. The segments of straight lines join the arcs of parabolas where $t=n\pi\pm\pi/6$, and we have that the derivative of $f(t)$ is continuous.

The closeness of this approximation is seen by forming the Fourier series for $f(t)$. We can write

$$f(t)=a_1\sin t+a_3\sin 3t+a_5\sin 5t+\ldots.$$

to hold for all values of $t$, and by the usual procedure we find, for odd values of $n$,

$$a_n=\frac{4}{\pi}\int_0^{\pi/2} f(t)\sin nt\,dt$$

$$=\frac{12}{\pi^2}\int_0^{\pi/6} t\sin nt\,dt+\frac{4}{\pi}\int_{\pi/6}^{\pi/2}\left(1-\frac{9}{2\pi^2}\left(t-\frac{\pi}{2}\right)^2\right)\sin nt\,dt,$$

whence $$a_n=\frac{36}{\pi^3n^3}\cos\frac{n\pi}{6}. \quad \ldots \ldots \quad (20)$$

We have, for integral values of N,

$n=12\mathrm{N}\pm1, \quad \cos n\pi/6=\sqrt{3}/2\,;$
$n=12\mathrm{N}\pm3, \quad \cos n\pi/6=0\,;$
$n=12\mathrm{N}\pm5, \quad \cos n\pi/6=-\sqrt{3}/2.$

Hence, for $n \neq 12N \pm 3$,

$$|a_n| = \frac{18\sqrt{3}}{\pi^3 n^3} = (1{\cdot}0055\ldots)\frac{1}{n^3},$$

and the Fourier series for $f(t)$ is

$$f(t) = 1{\cdot}0055\ldots\left(\sin t - \frac{1}{5^3}\sin 5t - \frac{1}{7^3}\sin 7t + \frac{1}{11^3}\sin 11t + \ldots\right). \quad (21)$$

10. This completes the theoretical discussion which may be considered of general interest. The application and the remaining properties of the field of results are concerned more with the engineering aspect of the hydraulic problem considered in the present paper, and these are to be found in another paper* on the subject. We may remark, in conclusion, that there are other similar problems, of importance in engineering, which may introduce points of mathematical interest. The outstanding case is the problem in connexion with a variable but periodic inflow to the tank, and it is probable that this can be discussed along the lines followed in the present paper.

---

* J. R. Daymond, *loc. cit.*

# L. *On the Dielectric Constant of Space containing Electrons.*

By S. R. Khastgir, D.Sc.(Edin.), Mem.I.R.E.,
and
K. Sirajuddin, M.Sc., Dacca University *.

[Received March 3, 1939.]

## 1. *Introduction.*

Some preliminary work † on the subject performed in this laboratory has already been reported. A more comprehensive ground is covered in the present investigation following a different method of measurement of the effective dielectric constant of an electronic medium for ultra-high radio-frequencies. Amongst the early workers on the subject, Bergmann and Düring ‡ conducted experiments with the experimental condenser in an atmosphere of electrons. Their results are in agreement with the simple theory which predicts a dielectric constant of such medium less than unity and steadily diminishing with increasing electron concentration. Sil §, on the other hand, observed a decrease, an increase, and also no change. Prasad and Verma || recently published some experimental results with medium radio-frequencies. Following the double-beat method they found the dielectric constant of an electronic medium inside a screen-grid valve always less than unity within the range of the concentrations and the wave-lengths employed in their investigations. They showed (1) that the dielectric constant decreased with increasing electron concentration, and (2) that it also decreased with increasing wave-length.

Usually the electronic medium under investigation is a high vacuum space in a thermionic valve filled with electrons from a heated filament under the influence of an electric field. Since the time of stay of the electrons in the inter-electrode space is only a small fraction of the period which corresponds to the radio-frequency of the alternating field, the contribution of the electrons towards the reduction of the dielectric

---

* Communicated by Dr. S. R. Khastgir.

† Ali Imam and Khastgir, Ind. Journ. Physics, xi. part 1, p. 37 (Feb. 1937).

‡ Bergmann and Düring, *Ann. der Physik*, v. p. 1041 (1929).

§ B. C. Sil, Phil. Mag. xvi. p. 1114 (1933).

|| Prasad and Verma, *Zeits. f. Phys.* Band 99, 7 & 8 heft. ; Band 107, 7 & 8 heft.

constant should therefore be correspondingly small. Benner * considered this effect of the finite time of transit of the electrons and deduced a correction factor to the Eccles-Larmor expression for the dielectric constant of a purely electronic medium. Recently Hollmann and Thoma † have given a different formula for the dielectric constant of such a medium. Accurate measurements were therefore felt necessary, and further investigations on the subject were accordingly undertaken. As before, the experiments were arranged in two sections :

I. Variation of the effective dielectric constant of the electronic medium in the inter-electrode space of a screen-grid valve with the frequency of the alternating field for definite electron concentrations.

II. Variation of the effective dielectric constant of the similar electronic medium with the thermionic current through the valve for a definite frequency of the alternating field.

## 2. *Experimental Arrangements.*

Essentially the method of measurement was to determine the capacity of the condenser formed by the anode and the control-grid of a Mullard P.M. 14 screen-grid valve, with the help of a Lecher wire system, once when the filament was cold and again when it was heated, the electrons emitted in the latter case having been drawn into the anode-grid space by the application of a suitable positive potential on the screen-grid.

The anode and the control-grid were connected to a pair of Lecher wires made of bare copper wire with a separation of about 9 cm. between the wires. Ultra-high frequency oscillation from a neighbouring oscillator was induced into the Lecher wire system. The bridge consisted of a stout copper wire with an air condenser of ·0003 $\mu$F conveniently mounted on an ebonite handle. The arrangements are shown in figs. 1 (*a*) and 1 (*b*). Suitable high positive voltages were applied to the anode and the screen-grid of the valve, the negative of the H.T. having been connected to the negative of the L.T. which fed the filament. The condenser K in the bridge prevented short-circuiting of the anode and the control-grid. The resonance was indicated by means of a sensitive valve-detector unit (consisting of an A.C.S$_2$ valve fed by D.C.) coupled to the Lecher wire system at the input end by means of two small condensers, *a a*, consisting of brass tubes insulated from the Lecher wires by glass sleeves. The valve-detector unit is shown in fig. 1 (*c*). Particular precaution was taken to avoid the effect of the neighbouring oscillator *directly* on the detector unit. To eliminate this direct effect, the detector unit was placed inside a shielded box mounted on a wooden frame at a certain height from the input end of the Lecher wire system.

---

* Benner, *Ann. d. Phys.* 5, iii. p. 993 (1929).

† Hollmann and Thoma, *Ann. d. Physik*, v. p. 32 (1938).

Fig. 1 (*a*).

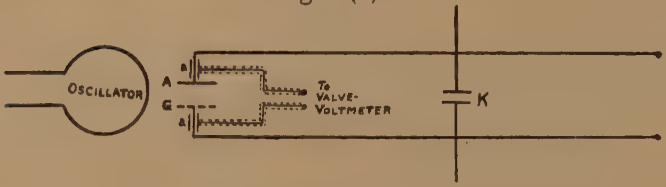
OSCILLATOR
A
G
a
a
To VALVE-VOLTMETER
K

Fig. 1 (*b*).

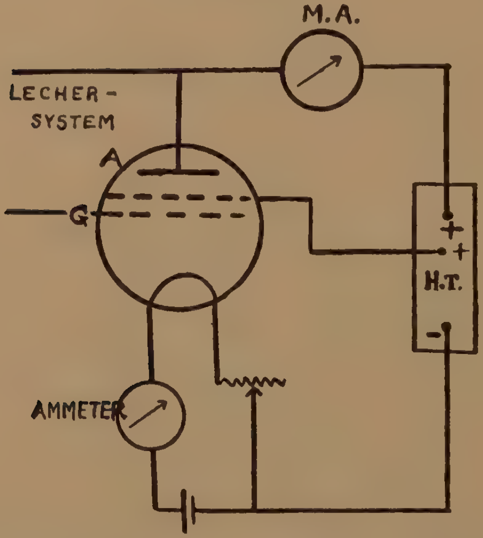
M.A.
LECHER-SYSTEM
A
G
+
+
H.T.
−
AMMETER

Anode-control grid used as terminal capacity of the Lecher system.

Fig. 1 (*c*).

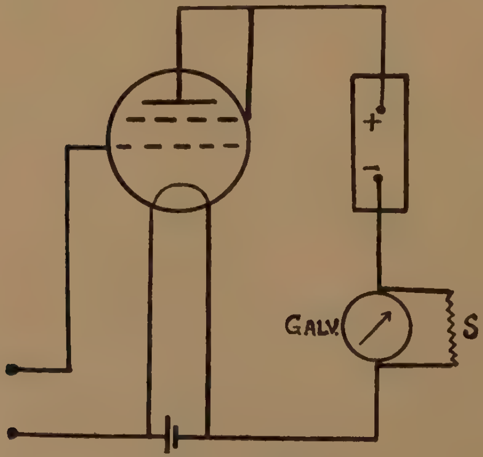

Valve voltmeter.

The connecting wires to the detector unit were enclosed in earthed casings of lead. That there was practically little or no direct effect of the oscillator on the detector unit was indicated by the symmetry of the resonance curve obtained when the readings of the galvanometer in the anode circuit of the valve detector unit were plotted against the scale readings. A small horizontal strip of metal with a mark was soldered in a convenient position to the copper bridge with the condenser K mounted on the ebonite handle. On sliding the bridge on the Lecher wires, this metal trip also ran parallel to and practically touching the wooden scale fixed alongside the Lecher wires. Much precision was obtained in this way in noting the position of the bridge for maximum voltage across the anode and the control-grid of the experimental valve. The positions of resonance were carefully determined first when the filament was off and next when the filament was on. The effective dielectric constant of the electronic medium in the anode-grid space of the valve was then calculated from these tuning positions according to the formula developed in the next section.

### 3. *Theory of the Method.*

The impedance of transmission line loaded with an impedance $Z_r$ at the far end is given by

$$Z=\frac{jZ_0 . \tan \beta l}{1+j\dfrac{Z_r}{Z_0} . \tan \beta l}-\frac{jZ_0 . Z_r . \cot \beta l}{Z_r-jZ_0 . \cot \beta l}, \quad . \quad . \quad . \quad . \quad . \quad . \quad (1)$$

where $l$=resonance length of the transmission line,

$\beta=\dfrac{2\pi}{\lambda}$=wave-length constant of the line

and $Z_0$=surge-impedance of the line.

If a condenser K is at the far end, $Z_r=\dfrac{1}{j\omega K}$, where $\omega$=angular frequency of the induced current. Thus it can be shown that

$$Z=\frac{jZ_0}{\omega KZ_0+\tan \beta l}[\omega KZ_0 \tan \beta l-1] \quad . \quad . \quad . \quad . \quad . \quad (2)$$

Considering now the anode-grid capacity $C_0$ at the input end of the Lecher wire system, the total impedance (neglecting the ohmic resistance of the Lecher wire) is given by

$$Z=\frac{jZ_0}{\omega KZ_0+\tan \beta l}[\omega KZ_0 \tan \beta l-1]-\frac{j}{\omega C_0} .$$

For current resonance, $Z=0$,

*i. e.*,
$$\frac{Z_0}{\omega KZ_0+\tan \beta l}[\omega KZ_0 \tan \beta l-1]=\frac{1}{\omega C_0} . \quad . \quad . \quad . \quad . \quad (3)$$

When the anode-grid space is filled with electrons (1) there will be a change in the dielectric constant of the medium, and (2) there will be a certain amount of leakage across the inter-electrode space. If we neglect the effect of the leak and consider the inter-electrode capacity to be a *perfect* condenser, the condition for current resonance will then be given by

$$\frac{Z_0}{\omega K Z_0 + \tan \beta l'}[\omega K Z_0 \tan \beta l' - 1] = \frac{1}{\omega C_0'} \quad . \quad . \quad . \quad . \quad (4)$$

where $C_0'$ is the changed value of the anode-grid capacity due to the change in the dielectric constant and $l'$ the changed resonance length when the inter-electrode space is filled with electrons. It should be remarked here that this condition of current resonance is identical with that for maximum voltage across the experimental condenser (*i. e.*, across the anode and the control-grid of the valve), provided the distribution of electrons is uniform in the inter-electrode space. The application of (3) and (4) to adjustments for voltage resonance is therefore subject to this limitation. The greatest advantage of voltage resonance adjustments is the *elimination* of the leakage or what is called the conductivity effect, for it is well known that the adjustment for voltage resonance is independent of the leak across the plates of the experimental condenser.

From (3) and (4) the effective dielectric constant of the electronic medium is easily obtained. The effective dielectric constant is thus given by

$$\epsilon = \frac{C_0'}{C_0} = \left[\frac{\omega K Z_0 + \tan \beta l'}{\omega K Z_0 + \tan \beta l}\right]\left\{\frac{\tan \beta l - \dfrac{1}{\omega K Z_0}}{\tan \beta l' - \dfrac{1}{\omega K Z_0}}\right\} \quad . \quad . \quad . \quad . \quad (5)$$

When $\omega K Z_0 \gg \tan \beta l$ or $\tan \beta l'$ the expression reduces itself to

$$\epsilon \approx \frac{\tan \beta l}{\tan \beta l'} \quad . \quad . \quad . \quad . \quad . \quad . \quad . \quad . \quad . \quad . \quad . \quad (6)$$

## 4. *Variation of the Effective Dielectric Constant of the Electronic Medium in the Inter-electrode Space of the Screen-grid Valve with the Frequency of the Alternating Field.*

(a) *Experimental Results.*—Figs. 2 and 3 illustrate the results of two sets of experiments where resonance lengths of the Lecher wire were determined for different wave-lengths of the ultra-high-frequency oscillations with and without the filament current which was kept at two definite values respectively. The anode and the screen-grid voltages were kept the same in each set of experiments. The shifts of the tuning position are shown in fig. 2 for different wave-lengths, and in fig. 3 the dielectric constant values are plotted against the square of the different wave-lengths. The dielectric constant was calculated from (5). The value

Fig. 2.

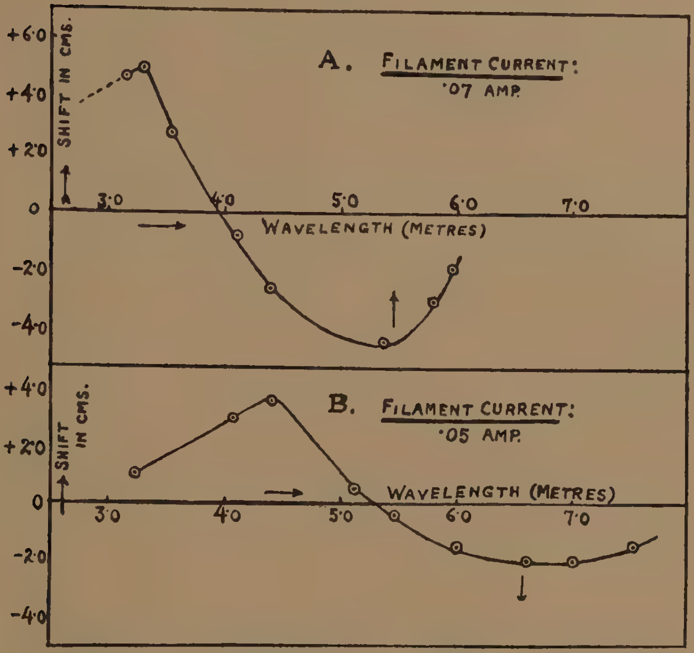

Shifts of the tuning position for different frequencies.

Fig. 3.

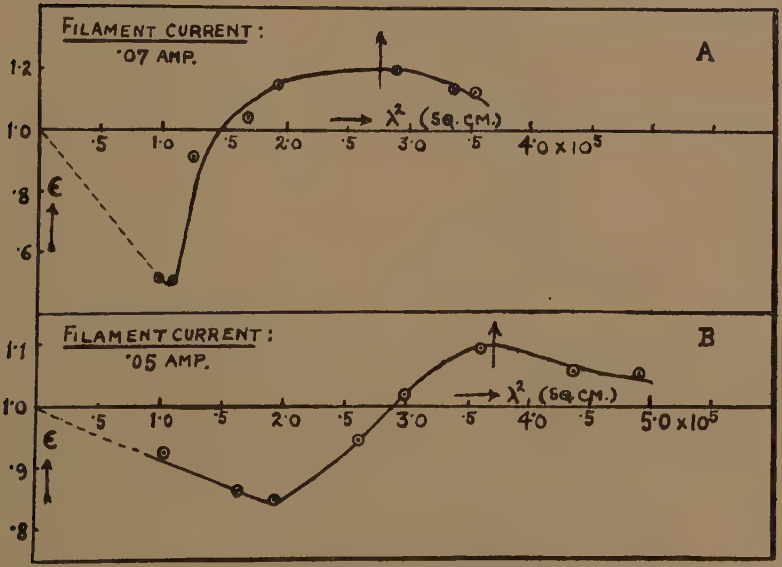

Values of the effective dielectric constant of the electronic medium for different frequencies.

of the surge-impedance of the Lecher system was found to be 598·8 ohms and the value of the capacity K in the bridge was $3\times10^{-4}\mu$F. The maximum range of wave-lengths was from 322 cm. to 754 cm., the corresponding range of angular frequency being $5{\cdot}855\times10^{8}$ to $2{\cdot}50\times10^{8}$.

It will be seen from figs. 2 (B) and 3 (B) that the dielectric constant of the medium decreased with the increase of wave-length up to a point beyond which there was a gradual rise in the value of the dielectric constant. This had been observed in our preliminary experiments where the method of measurements was different. Extending the range of wave-lengths in the present investigation it was, however, found that the value of the dielectric constant gradually increased and even became greater than unity with the increasing values of the wave-length. With still further increase of wave-length the dielectric constant, however, decreased again. It is worthy of notice that the maximum value of the dielectric constant was attained at a larger value of the wave-length for the smaller value of the current passing through the filament of the valve. Thus when the filament current was ·05 amp. the maximum value of the dielectric constant appeared at $\lambda=650$ cm., nearly, whereas when the filament current was ·07 amp. the corresponding wave-length was only about 550 cm.

The two sets of experiments with the two different values of the filament current were not, however, performed alternately :—in fact, one set was performed after the other set had been performed. The experiments were therefore repeated and observations of resonance lengths were taken alternately with the two different filament currents viz., ·06 and ·07 amperes. A similar result was obtained, viz., a shift of the peak towards the longer wave-length side with the smaller filament current.

(b) *Discussion and Conclusions.*—The different formulæ for the change in the dielectric constant of the electronic medium are written below :—

$$\text{Eccles-Larmor: } \Delta\epsilon=-\frac{4\pi Ne^2}{m\omega^2} \quad . \; . \; . \; . \; . \; . \; . \; . \; . \; . \; . \; . \; . \quad (7)$$

$$\text{Benner: } \Delta\epsilon=-\frac{4\pi Ne^2}{m\omega^2}\left(1-\frac{\sin\omega T}{\omega T}\right) \quad . \; . \; . \; . \; . \; . \; . \; . \; . \; . \; . \quad (8)$$

$$\text{Hollmann-Thoma: } \Delta\epsilon=\frac{2\pi Ne^2T^2}{m}\cdot\frac{\sin\frac{\omega T}{2}-\frac{\omega T}{2}\cos\frac{\omega T}{2}}{\left(\frac{\omega T}{2}\right)^3}.\cos\frac{\omega T}{2}, \quad . \quad (9)$$

where N=electronic concentration,
T=time of stay of the electrons from the filament in the inter-electrode space,
$\omega$=angular frequency of the field,

and $e$ and $m$ are the charge and mass of an electron.

The observed variation of the dielectric constant of the electronic medium inside the screen-grid valve with the frequency of the field shows only an approximate qualitative agreement with the Eccles-Larmor formula over a very limited range (*i. e.*, for the smaller wave-lengths). Benner's formula also cannot explain the experimental results, for a little inspection will show that, according to Benner, the dielectric constant should remain constant when the frequency only is changed. Hollmann and Thoma's formula, however, gives values of the dielectric constant greater or less than unity according to the value of $\omega$T. In fact, when the change of the dielectric constant calculated according to their formula is plotted against the different values of $\omega$T, a wavy curve of gradually decreasing amplitude is obtained about the zero value of the dielectric constant change. This curve has some similarity with our experimental curve, but there is no real agreement. Exact quantitative comparison is not possible, since the time of stay of the electrons from the filament in the inter-electrode space is not accurately known in our experiments. Accepting, however, the approximate estimate of T to be of the order of $10^{-9}$ sec., the value of $\omega$T in our experiments would range from about $\cdot 08\pi$ to about $\cdot 2\pi$. The variation of the dielectric constant observed within this range is in complete disagreement with Hollmann and Thoma's formula, for according to this formula, for values of $\omega$T less than $\pi$, the value of the dielectric constant would be greater than unity and would gradually increase with the decrease of $\omega$T approaching the limiting value, $\frac{2\pi \mathrm{N}e^2\mathrm{T}^2}{3m}$, when $\omega\mathrm{T}=0$. It is also significant that the position of each peak in Hollmann and Thoma's curve is independent of electron concentration, whereas our experiments clearly indicate that the frequency corresponding to the maximum value of the dielectric constant *does* depend on the electron concentration.

The experimental results, however, suggest a kind of resonance effect which affects our measurements of the effective dielectric constant of the electronic medium for various frequencies or wave-lengths. The gradual decrease of the dielectric constant with the increase of wave-length shows therefore a deviation as the resonance wave-length is approached, and the dielectric constant is found to increase with the increase of wave-length. Finally, however, at the resonance point the dielectric constant attains a maximum value which falls again as the wave-length is further increased. Tonks and Langmuir's * *plasma* electronic oscillation is not, however, possible inside a high vacuum screen-grid valve, nor does it seem possible to connect the observed anomalous dielectric constant with Gutton's † quasi-elastic resonance in the electronic medium inside the valve. We are, however, inclined to the view that the inductance of the short external connexion and the capacitance of the anode-grid condenser of the experimental valve make up an oscillatory circuit with a definite resonance frequency for a particular electron concentration in the valve. High frequency electronic oscillations in such an oscillatory circuit within the valve have been mentioned by Hund *, who holds that for the resonance of such oscillations the effective dielectric constant of the medium must be zero, so that when N is the electron concentration the resonance angular frequency is given by

---

* Tonks and Langmuir, Phys. Rev. (Feb. 1929).

† Gutton, *Ann. d. Phys.* xiii. p. 68 (1930).

$$\omega_0^2 = \frac{4\pi N e^2}{m}. \quad \dots\dots\dots \quad (10)$$

We have here, according to Hund, the equivalent case of a unit condenser $C = 1/4\pi$ shunted by an inductance $L = m/Ne^2$, since $\omega_0 = 1/\sqrt{LC}$, where L denotes the inductance of the external connexion and C the anode-grid capacity. Now writing $\lambda_0$ for the resonance wave-length we have from (10)

$$N\lambda_0^2 = \frac{\pi m c^2}{e^2} = \text{constant}\,\dagger.$$

According to this equation the resonance should take place at a larger value of the wave-length for the smaller electron concentration. This is what was actually observed in our experiments. We can therefore attribute a natural wave-length to the electrons in the valve. This is the same as the resonance wave-length of these electronic oscillations for a particular electron concentration. In our experiments the natural wave-lengths could be taken as 650 cm. and 550 cm. approximately when the filament current was ·05 ampere and ·07 ampere respectively.

## 5. *Variation of the Effective Dielectric Constant of the Electronic Medium in the Anode-Grid Space of the Thermionic Valve with the Thermionic Current for a Definite Frequency of the Field*

### *Experimental Results and Conclusions.*

Fig. 4 illustrates the results of a typical set of experiments carried out with alternating current of angular frequency $5{\cdot}714 \times 10^8$ ($\lambda = 3{\cdot}3$ metres). The screen-grid and the anode voltages were kept fixed and the anode current was varied by varying the filament current. The resonance lengths were determined with and without filament current for the definite frequency (or wave-length). The filament current ranged from 0·05 amp. to 0·07 amp., and the anode current under the conditions of the experiment ranged from 0·1 m.a. to 2·7 m.a. The calculated dielectric constant of the electronic medium from the observed shift of the tuning point was 0·48 for the maximum anode current. It will be seen that, on the whole, the dielectric constant of the electronic medium decreased linearly with the increase of the current. Such a linearity is expected on any theory. We shall, however, examine the different formulæ for the dielectric constant of the electronic medium in the light of our measurements.

---

* Hund, ‘ Phenomena in High-frequency Systems,’ 1st edition, p. 21 (1936).

† It should be noticed that this equation is the same as that for the plasma electronic resonance of Tonks and Langmuir.

Let us take Benner's formula. In our experiments $\omega = 5{\cdot}714 \times 10^8$ and, according to an approximate estimate, the time of stay of the electrons in the inter-electrode space of the valve can be taken as $0{\cdot}4 \times 10^{-9}$ sec.

Fig. 4.

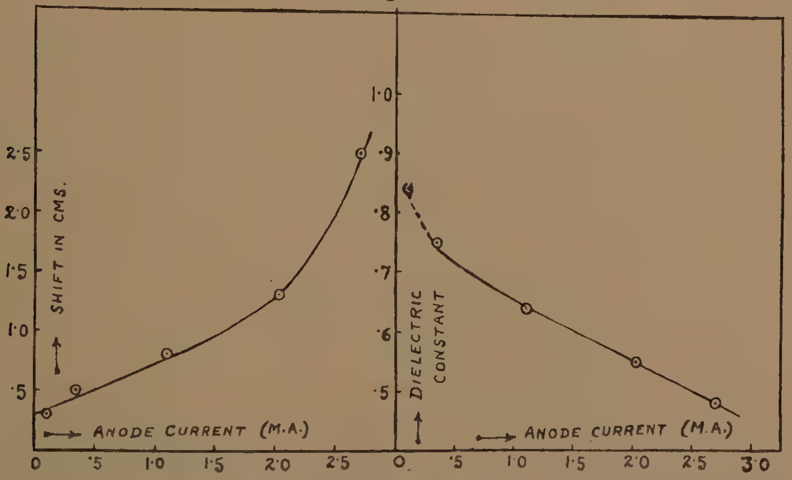

Variation of the effective dielectric constant of the electronic medium with thermionic current.

Considering now the value of the dielectric constant for the anode current equal to 2·7 m.a., *i. e.*, $\epsilon = 0{\cdot}48$, the number of electrons per c.c. as calculated from Benner's formula comes out to be $6{\cdot}4 \times 10^9$, which is decidedly a very high value.

Hollmann and Thoma's formula gives with these data a positive change of the dielectric constant equal to $7{\cdot}4 \times 10^{-10}$ N, so that the dielectric constant of the electronic medium should be greater than unity by this amount. This is contrary to the experimental value. It should be remembered that these calculations are based on an approximate estimate of T.

We shall now take the Lorentz expression for the dielectric constant and introduce a multiplying factor $\mu$ to obtain the effect of the finite time of stay of the electrons in the inter-electrode space of the valve. In interpreting our experimental results on the variation of the dielectric constant of the electronic medium with the frequency of oscillation, we have attributed a natural angular frequency $\omega_0$ (corresponding to a natural wave-length $\lambda_0$) to the electrons in the medium—a frequency which is the resonance frequency of the oscillatory circuit made up by the inductance of the external connexion and the anode-grid capacity of the valve. According to Lorentz the expression for the dielectric constant of the medium can be written as

$$\epsilon = n^2+\frac{c^2k^2}{\omega^2}=1+\frac{\alpha}{\alpha^2+\beta^2},$$

where $$\alpha = -\frac{m\omega^2}{4\pi\mathrm{N}e^2}-a+\frac{f}{4\pi\mathrm{N}e^2},$$

$$\beta = \frac{\omega . g}{4\pi\mathrm{N}e^2},$$

$f = m\omega_0{}^2$=restoring force per unit displacement,

$g$ = frictional constant,

$a$ = Lorentz term,

$n$ = refractive index,

$k$ = absorption index,

$\omega$ = angular frequency of the field,

N = electron concentration, and

$c$ = velocity of light.

Since the electronic medium inside the high vacuum valve can be regarded as frictionless, $\beta=0$, and on introducing the multiplying factor $\mu$, the dielectric constant of such medium is given by

$$\epsilon=1-\frac{4\pi\mathrm{N}\mu e^2}{m(\omega^2-\omega_0{}^2)+a(4\pi\mathrm{N}\mu e^2)} \quad . \; . \; . \; . \; . \; . \; . \quad (11)$$

Introducing the factor $\mu$ in relation (10), we get $\omega_0{}^2=\frac{4\pi\mathrm{N}\mu e^2}{m}$, and it is possible to calculate the value of $(\mathrm{N}.\mu)$ from this relation. In our experiments $\lambda_0=550$ cm. (when the filament current was 0·07 amp. and the anode current 2·7 m.a.), *i. e.* $\omega_0=3{\cdot}423\times10^8$ so that $(\mathrm{N}.\mu)$ comes out to be $3{\cdot}69\times10^7$. With this value of $(\mathrm{N}.\mu)$ and putting $\omega=5{\cdot}714\times10^8$ and $a=\frac{1}{3}$ in equation (11), we get the value of the dielectric constant of the electronic medium to be 0·53. The experimental value (see fig. 3 A) under the circumstances was 0·51. This is in good agreement with the value calculated according to Lorentz.

## 6. *Summary.*

Measurements of the effective dielectric constant of the electronic medium in the anode-grid space of a Mullard P.M. 14 valve were undertaken for various ultra-high frequencies and for various anode currents.

Working with a definite frequency, the dielectric constant of the electronic medium was found on the whole to decrease almost proportionately with the increase of the anode current.

When the wave-length was changed keeping the anode and screen-grid voltages and the filament current constant, the dielectric constant of the medium was found to decrease with the increase of wave-length up to a certain wave-length beyond which a gradual increase in the value of the dielectric constant was observed. This confirmed the experimental results which had previously been obtained by a different method. Extending the range of observations it was found that the dielectric constant gradually assumed values greater than unity, and after attaining a maximum value at a particular wave-length, decreased again with further increase of wave-length. It was also observed that the wave-length at which the dielectric constant of the electronic medium attained the maximum value was distinctly larger for the smaller electron concentration. These results are explained by supposing that the small inductance of the external connexion and the anode-grid capacitance of the experimental valve constitute an oscillatory circuit, so that the observed anomaly is expected to appear in the region of the resonance frequency of such oscillatory circuit. The condition of this resonance, according to Hund, is the same as that for the plasma electronic resonance of Tonks and Langmuir. The observed shift of the peak (in the dielectric constant-wave-length curve) towards the longer wave-length side with the smaller electron concentration can therefore be explained.

It is significant that neither Benner's nor Hollmann and Thoma's formula was found to agree with the experimental results. Attributing, however, a natural frequency to the electrons corresponding to the resonance frequency of the previously mentioned oscillatory circuit within the valve and introducing a multiplying factor to obtain the effect of the time of stay of the electrons in the inter-electrode space of the valve, it was found that the Lorentz expression for the dielectric constant for a frictionless medium would be consistent with our measurements.

Physics Department,
Dacca University.

# LI. *The Electric Glow between Carbon Electrodes.*

By F. H. Newman, D.Sc., F.Inst.P., Professor of Physics,
University College, Exeter *.

[Plate VIII.]

[Received August 5, 1939.]

Several types of cold-cathode arc in gases at low pressure have been described by the author in which the current is carried almost entirely by the gas between the electrodes, there being no indication of radiation from the vapour of the metal electrodes. In other words, the temperature of the latter is far below that associated with, and generally attributed to, the ordinary carbon and tungsten arcs which operate on the thermionic principle. Although such arcs show the usual characteristic, viz., a decreasing potential difference between the electrodes with an increasing current, it would be more appropriate to refer to them as glow discharges because the current is carried entirely by gaseous ions present in the tube.

The arc and glow discharges are closely related, the transition between the two depending upon several factors, viz., conditions of the gas pressure, the current passing through the discharge, the purity and form of the anode, and the values of the anode and cathode falls of potential. But the temperature of the electrodes in a glow discharge is far below that necessary to vaporize the metals to any appreciable extent.

In previous work † with graphite electrodes in gases at low pressure the author has described experiments in which radiation from the arc comes from the ionized residual gases in a tube, there being no thermionic effect at the graphite electrodes. The present paper describes further experiments on this type of glow.

The graphite employed was in the form of rods, 6·3 mm. diameter and of special purity for spectrographic purposes, the degree of purity being 99·98 per cent. Spectrographic analysis gave the following lines in the visible region from the impurities :—calcium, $\lambda$ 4226·7 ; sodium D lines, vanadium, $\lambda$ 4407·9; and lithium, $\lambda$ 6707·9. This pure graphite was selected because it was found in previous work that the existence of impurities on the cathode facilitated the striking of high-vacuum

---

* Communicated by the Author.

† Phil. Mag. xxiii. p. 181 (1937).

arcs. Although it has been suggested that such impurities may form the sharp points necessary for the high-field theory of the arc, there is the possibility that thermionic emission takes place from some of the impurities when the electrodes are bombarded by the ions, and it was desired to eliminate this effect as far as possible.

The glow tube was of pyrex, with tungsten rods sealed into the glass. Small holes bored along the graphite electrodes enabled the latter to be fixed to the tungsten, and this arrangement eliminated wax seals, which are always unsatisfactory where a considerable current is passing. A third tungsten wire electrode was inserted in the tube. The carbon electrodes were separated 3 mm., and if a steady potential difference of 100 volts was applied between them, and a "vacuum leak tester" brought near the third tungsten electrode, so that sparking occurred to the latter, a brilliant glow immediately started between the carbon electrodes. But the commencement of the glow depended upon the distance between the third electrode and the carbons. The leak tester simply supplies a high potential difference between the electrodes—the discharge passing through the gas and so to earth, and since this high potential difference is constant it is evident that the ions must possess a certain minimum energy when they bombard the electrodes in order that the glow shall commence. The gas pressure necessary for successful operation ranged from 5 to 0·01 mm. of mercury. With a current of 5 amperes the potential difference between the carbon electrodes was 40 volts—an external resistance regulating the current. The glow showed the usual arc characteristic of a falling potential difference with rising current.

If a direct current open arc is allowed to run for some time the characteristics which are first noted are that (*a*) the anode tip is cratered whilst the cathode end is pointed ; (*b*) most of the light comes from the brilliant anode crater and much less from the cathode tip ; (*c*) the discharge gives much less illumination. Observation shows that the ends of the electrodes are white-hot, and beads of metallic and other impurities are seen near the electrode ends. If the arc length is great and the current small the arc is seen to move round the anode while the negative end of the discharge remains stationary at the hot cathode spot.

In the present experiments none of these characteristics appeared, but the observations were confined to the first few seconds after the glow had been started. A photograph of the commencement of this glow is shown in Pl. VIII., nos. 1 and 2, the exposure being 1/15 sec. As will be seen there is no cathode bright spot and the electrodes are not incandescent. The luminous discharge does not pass between the ends of the two carbon electrodes, but tends to fill the whole of the space surrounding the ends. Some of the glow appears in front of the electrodes, and gives an impression that the ends of the carbons are white-hot, but such is not the case. In addition there are two distinct patches of luminosity in photograph 1, one of these patches surrounding the negative electrode at some distance from its end. None of the luminosity comes from the electrodes, and, as noted, it is in the form of a glow rather than the characteristic arc column. It was observed that the glow is initiated from one of the many bright spots which appear on the negative carbon when the starting electrical impulse is applied, and if these bright spots are not present the glow does not commence. Very little carbon vaporizes from the electrodes to the glass walls, but on examination after the glow had been obtained the negative carbon was "pitted" and covered with a film of amorphous carbon, whereas the positive electrode showed no signs of such an amorphous deposit. This pitting of the negative carbon is attributed to its bombardment by means of positive ions, and the bombardment effect would account for the minute bright sparks mentioned above. After the glow had existed for some time and was then extinguished it was difficult to restart, due apparently to the presence of the amorphous deposit. The latter covers the effective points—either specks of impurities or sharp carbon points—and prevents the positive ions from reaching them.

The radiation from the glow was photographed by means of a constant deviation spectrograph, and the result is shown in Pl. VIII., no. 3. There is little continuous spectrum, but the Swan bands of carbon are prominent, particularly those at λ 4381, 4737, 5165, and 5635. In addition the CN and CH bands are very marked. On the other hand, the Ångstrom bands of CO are faint. When, however, an electrical discharge from a coil, without self-inductance and secondary capacitance, was passed through the tube between the carbon electrodes the Ångstrom bands were very bright, those of CN, CH, and the Swan bands being extremely faint. This suggests that the excitation potential of the Ångstrom bands is higher than that required for these other bands, since the electrical discharge was sent through the tube immediately after the glow was extinguished, so that the gas pressure and the gas constituents were the same in the two cases. It is well known that the relative intensity of spectra depends more on the excitation potentials than on the percentage in which the components of a gas mixture are present. So with the electrical discharge, *i. e.*, a higher potential difference, we should expect those spectra of higher excitation potential to be produced at the expense of those of lower excitation potentials. On the other hand, the hydrogen lines were much stronger in the glow than in the electrical discharge. The residual gases present at the time of the glow were those to be normally found in any discharge-tube at low pressure, and since hydrogen is evolved in large quantities during the glow one would expect the hydrogen lines to be prominent in the radiation emitted during the electrical discharge. Generally the Swan spectrum is produced brilliantly when an electrical discharge is sent through CO, inductance and capacitance being included in the circuit and the gas pressure being a few mm. of mercury. If the latter is reduced the Ångstrom bands appear and eventually replace the Swan bands, particularly with uncondensed discharges. In the present experiments, however, the fact that the Swan bands are predominant in the glow, while the Ångstrom bands are faint but are enhanced in the electrical discharge, does indicate that the excitation potential of these Ångstrom bands is higher than that for the Swan, CN, and CH bands.

# LII. *The Magneto-Optical and Natural Dispersions of Isobutyl Butyrate and Ethylene Chloride.*

By W. J. G. BEYNON, B.Sc., Physics Department, University College of Swansea *.

[Received December 5, 1938.]

THE magneto-optical and natural dispersions of isobutyl butyrate and ethylene chloride in the visible and near ultra-violet spectrum have recently been examined in these laboratories. The results of the investigation are given in the present paper.

If the natural dispersion of a substance can be represented by a formula of the type

$$n^2-1=b_0+\frac{b_1}{\lambda^2-\lambda_1^2}, \quad \ldots \ldots \ldots \quad (1)$$

then, according to Larmor's theory of magnetic rotation, the formula

$$\phi\equiv n\delta\lambda^2=K_1\left[\frac{\lambda^2}{\lambda^2-\lambda_1^2}\right]^2 \quad \ldots \ldots \ldots \quad (2)$$

will represent the magneto-optical dispersion.

In the above formulæ $n$ is the refractive index for wave-length $\lambda$; $b_0$, $b_1$, $K_1$ are constants, and $\lambda_1$ is the wave-length of the controlling absorption band.

The constants $b_1$ and $K_1$ are related by the expression

$$\frac{e}{m}=-\frac{2\,K_1\,C^2}{b_1}, \quad \ldots \ldots \ldots \quad (3)$$

where $e/m$ is the ratio of the charge to the mass of the resonators and C is the velocity of light.

The significance of the constant $\lambda_1$ in simple formulæ of the above type has been referred to in a recent paper by Beynon and Evans(1). The use of the above simple formulæ, involving only one absorption band, is justified by the fact that the formulæ represent within experimental error the available experimental results. The substances considered in this paper may have more than one absorption band and probably the simple equations would have to be modified if rotations at much lower wave-lengths were available. Previous investigators in these laboratories have also been able to represent their results by simple formulæ involving only one absorption band, and in all probability these bands must be regarded as "single equivalent absorption bands," which produce on the natural and magneto-optical dispersions in the violet and near ultra-violet regions of the spectrum the same effect as that due to the actual system of bands of the substance under investigation.

---

* Communicated by Prof. E. J. Evans, D.Sc.

The methods employed in this investigation were similar to those described in earlier papers⁽²⁾. It may be mentioned that the liquids were purified by a process of fractional distillation, only the portion which distilled over at the accepted boiling-point being retained for use. The magnetic rotation at ultra-violet wave-lengths was measured for a 30 cm. column of liquid enclosed in a quartz tube placed along the axis of a large solenoid. The small rotations produced by the ends of the quartz tube were accurately determined in a set of preliminary experiments. The refractive index measurements in the visible spectrum were made visually, using a large prism spectrometer, and those in the ultra-violet by a photographic method. The two sets of measurements (visual and photographic) overlapped over a portion of the visible spectrum.

## EXPERIMENTAL RESULTS.

### *Natural Dispersion.*

TABLE I.

Visual Determinations.

| Wave-length in microns. | Refractive indices. | |
|---|---|---|
| | Isobutyl butyrate. at 15° C. | Ethylene chloride at 15° C. |
| ·6678 | $1·4035_8$ | $1·4443_7$ |
| ·5875 | $1·4060_3$ | $1·4472_6$ |
| ·5015 | $1·4100_6$ | $1·4519_3$ |
| ·4922 | $1·4106_0$ | $1·4526_0$ |
| ·4713 | $1·4120_6$ | $1·4543_4$ |
| ·4472 | $1·4137_8$ | $1·4565_7$ |

The temperature coefficient of refractive index of isobutyl butyrate in the visible spectrum is $\cdot 0004_9$ and the average temperature coefficient in the ultra-violet $\cdot 0005_0$. For ethylene chloride the corresponding coefficients are $\cdot 0005_6$ and $\cdot 0006_1$ respectively.

### *Magneto-Optical Dispersion.*

Verdet's constants at violet and ultra-violet wave-lengths for both isobutyl butyrate and ethylene chloride are given in Table III.

TABLE II.

Photographic Determinations.

| Isobutyl butyrate at 10·4° C. | | Ethylene chloride at 18·4° C. | |
|---|---|---|---|
| Wave-length (in microns). | Refractive index. | Wave-length (in microns). | Refractive index. |
| ·5782 | $1{\cdot}4085_0$ | ·5218 | $1{\cdot}4487_5$ |
| ·5293 | $1{\cdot}4107_1$ | ·5153 | $1{\cdot}4491_3$ |
| ·5218 | $1{\cdot}4111_9$ | ·4651 | $1{\cdot}4530_0$ |
| ·5106 | $1{\cdot}4118_6$ | ·4378 | $1{\cdot}4557_5$ |
| ·4675 | $1{\cdot}4146_0$ | ·4275 | $1{\cdot}4570_0$ |
| ·4540 | $1{\cdot}4154_6$ | ·4123 | $1{\cdot}4590_2$ |
| ·4275 | $1{\cdot}4179_5$ | ·4023 | $1{\cdot}4605_8$ |
| ·4063 | $1{\cdot}4202_5$ | ·3955 | $1{\cdot}4617_0$ |
| ·3825 | $1{\cdot}4233_2$ | ·3825 | $1{\cdot}4640_3$ |
| ·3654 | $1{\cdot}4259_9$ | ·3654 | $1{\cdot}4675_7$ |
| ·3602 | $1{\cdot}4268_8$ | ·3512 | $1{\cdot}4709_6$ |
| ·3534 | $1{\cdot}4280_1$ | ·3484 | $1{\cdot}4716_8$ |
| ·3337 | $1{\cdot}4322_4$ | ·3365 | $1{\cdot}4750_3$ |
| ·3274 | $1{\cdot}4337_5$ | ·3337 | $1{\cdot}4758_8$ |
| ·3142 | $1{\cdot}4372_3$ | ·3308 | $1{\cdot}4767_5$ |
| ·3064 | $1{\cdot}4396_8$ | ·3208 | $1{\cdot}4800_9$ |
| ·3012 | $1{\cdot}4411_9$ | ·3160 | $1{\cdot}4818_7$ |
| ·2961 | $1{\cdot}4430_2$ | ·3147 | $1{\cdot}4822_5$ |

### TABLE III.

| Isobutyl butyrate at 10·4° C. | | Ethylene chloride at 18·4° C. | |
|---|---|---|---|
| Wave-length (in microns). | Verdet's Constant (mins. per cm. gauss). | Wave-length (in microns). | Verdet's Constant (mins. per cm. gauss). |
| ·4582 | $\cdot 0211_2$ | ·4290 | $\cdot 0334_9$ |
| ·4493 | $\cdot 0222_5$ | ·4123 | $\cdot 0367_5$ |
| ·4310 | $\cdot 0244_8$ | ·4020 | $\cdot 0390_7$ |
| ·4148 | $\cdot 0266_9$ | ·3929 | $\cdot 0412_2$ |
| ·4008 | $\cdot 0289_2$ | ·3837 | $\cdot 0435_7$ |
| ·3841 | $\cdot 0318_1$ | ·3798 | $\cdot 0446_5$ |
| ·3764 | $\cdot 0333_7$ | ·3685 | $\cdot 0479_8$ |
| ·3702 | $\cdot 0347_3$ | ·3619 | $\cdot 0502_3$ |
| ·3660 | $\cdot 0355_7$ | ·3588 | $\cdot 0513_5$ |
| ·3611 | $\cdot 0367_4$ | ·3495 | $\cdot 0547_0$ |
| ·3568 | $\cdot 0378_1$ | ·3389 | $\cdot 0591_9$ |
| ·3529 | $\cdot 0389_4$ | ·3295 | $\cdot 0636_2$ |
| ·3485 | $\cdot 0400_5$ | ·3189 | $\cdot 0692_3$ |
| ·3405 | $\cdot 0422_4$ | ·3132 | $\cdot 0725_7$ |
| ·3268 | $\cdot 0467_1$ | ·3096 | $\cdot 0748_2$ |
| ·3203 | $\cdot 0489_5$ | | |

### *Magneto-Optical Dispersion Formulæ.*

In the case of each liquid the results have been considered in relation to the formula

$$\phi \equiv n\delta\lambda^2 = \mathrm{K}_1 \left[\frac{\lambda^2}{\lambda^2-\lambda_1{}^2}\right]^2.$$

Values of the function $\phi$ at two wave-lengths enable the constants $\mathrm{K}_1$ and $\lambda_1$ to be calculated. If the calculated values of these constants are independent of the wave-lengths chosen, then it may be inferred that the experimental results will fit a simple formula of the above type. For these calculations the wave-lengths and Verdet's Constants were obtained from Table III., and the corresponding refractive indices from large-scale graphs of Table II.

*Isobutyl Butyrate.*

The calculation of $\lambda_1$ and $K_1$ for different pairs of four separate wave-lengths is given below :—

| | Wave-length (in microns). | Refractive index. | Verdet's Constant. |
|---|---|---|---|
| (*a*) ......... | ·4493 | 1·4158 | $\cdot 0222_5$ |
| (*b*) ........ | ·3841 | 1·4229 | $\cdot 0318_1$ |
| (*c*) ........ | ·3611 | 1·4266 | $\cdot 0367_4$ |
| (*d*) ......... | ·3268 | 1·4340 | $\cdot 0467_1$ |

From (*a*) and (*b*) $\lambda_1 = \cdot 1112$ $K_1 = \cdot 005602_9$.
,, (*a*) ,, (*c*) $\lambda_1 = \cdot 1103$ $K_1 = \cdot 005614_3$.
,, (*a*) ,, (*d*) $\lambda_1 = \cdot 1106$ $K_1 = \cdot 005610_3$.
,, (*b*) ,, (*d*) $\lambda_1 = \cdot 1100$ $K_1 = \cdot 005624_1$.
,, (*c*) ,, (*d*) $\lambda_1 = \cdot 1108$ $K_1 = \cdot 005603_6$.

Thus the calculated values are fairly constant for different pairs of wave-lengths. The mean values of $\lambda_1$ and $K_1$ are respectively ·1106 and $\cdot 005611_0$.

Calculations similar to the above have been made for many different wave-lengths, and the final mean values obtained for $\lambda_1$ and $K_1$ are

$$\lambda_1 = \cdot 1106,$$

$$K_1 = \cdot 005616_5.$$

Thus the magneto-optical dispersion of isobutyl butyrate at 10·4° C. for the region of spectrum investigated (·4493 $\mu$ to ·3203 $\mu$) is

$$\phi \equiv n\delta\lambda^2 = \cdot 005616_5 \left[\frac{\lambda^2}{\lambda^2 - (\cdot 1106)^2}\right]^2 . \quad . \quad . \quad . \quad . \quad (4)$$

In Table IV. values of Verdet's Constant calculated from formula (4) are compared with the observed values at the respective wave-lengths.

The observed values of Verdet's Constant are considered to be accurate on the average to within one part in 300. Formula (4) thus represents the results to within experimental error.

The value of Verdet's Constant at the wave-length ·5893 $\mu$ calculated from formula (4) is $\cdot 0123_4$.

Perkin(3) made accurate determinations of Verdet's Constant at the wave-length of sodium light for many organic compounds. Measurements upon isobutyl butyrate are not included in Perkin's published results, but a value for this liquid can be deduced from the results of his observations on other butyrates. Perkin found that the addition of a $CH_2$ group produces an increase of 1·023 in the molecular rotation, and that in passing from a normal to an iso-ester the molecular rotation increases by approximately ·116. According to Perkin the molecular rotation of ethyl butyrate is 6·477. The molecular rotation of *n*-butyl butyrate will thus be 8·523 and of isobutyl butyrate 8·639. The specific rotation of isobutyl butyrate at 10·4° C. is then found to be ·9410. If we assume Verdet's Constant for water at the wave-length of sodium light to be ·0131, the value for isobutyl butyrate is $\cdot 0123_3$. This value is in very satisfactory agreement with that calculated from formula (4).

Table IV.

Calculated and Observed Values of Verdet's Constant for Isobutyl Butyrate.

| Wave-length (in microns). | Verdet's Constant calculated from formula (4). | Verdet's Constant observed. |
|---|---|---|
| ·4582 | $\cdot 0213_2$ | $\cdot 0211_2$ |
| ·4493 | $\cdot 0222_7$ | $\cdot 0222_5$ |
| ·4310 | $\cdot 0244_5$ | $\cdot 0244_8$ |
| ·4148 | $\cdot 0266_7$ | $\cdot 0266_9$ |
| ·4008 | $\cdot 0288_3$ | $\cdot 0289_2$ |
| ·3841 | $\cdot 0317_9$ | $\cdot 0318_1$ |
| ·3702 | $\cdot 0346_7$ | $\cdot 0347_3$ |
| ·3611 | $\cdot 0367_7$ | $\cdot 0367_4$ |
| ·3568 | $\cdot 0378_8$ | $\cdot 0378_1$ |
| ·3268 | $\cdot 0467_7$ | $\cdot 0467_1$ |
| ·3203 | $\cdot 0491_5$ | $\cdot 0489_5$ |

### *Ethylene Chloride.*

The magnetic rotation measurements for ethylene chloride are given in Table III. These observaitons have again been considered in relation to a formula of the type

$$\phi \equiv n\delta\lambda^2 = K_1 \left[\frac{\lambda^2}{\lambda^2-\lambda_1{}^2}\right]^2.$$

The following wave-lengths, with corresponding observed values of Verdet's Constant $\delta$ and refractive index $n$, were used to calculate $\lambda_1$ and $K_1$.

| | Wave-length (in microns). | Refractive index. | Verdet's Constant. |
|---|---|---|---|
| (*a*) ........... | ·4290 | 1·4568 | $\cdot 0334_9$ |
| (*b*) .......... | ·3798 | 1·4645 | $\cdot 0446_5$ |
| (*c*) .......... | ·3588 | 1·4692 | $\cdot 0513_5$ |
| (*d*) ........... | ·3295 | 1·4773 | $\cdot 0636_2$ |

From (*a*) and (*b*) $\lambda_1 = \cdot 1221$ $K_1 = \cdot 007580_7$.
„ (*a*) „ (*c*) $\lambda_1 = \cdot 1230$ $K_1 = \cdot 007563_7$.
„ (*a*) „ (*d*) $\lambda_1 = \cdot 1227$ $K_1 = \cdot 007570_3$.
„ (*b*) „ (*d*) $\lambda_1 = \cdot 1231$ $K_1 = \cdot 007554_5$.
„ (*c*) „ (*d*) $\lambda_1 = \cdot 1224$ $K_1 = \cdot 007583_7$.

The mean values of $\lambda_1$ and $K_1$ from these calculations are respectively ·1227 and $\cdot 007570_6$. Similar calculations have been made for many other wave-lengths, and the mean values of $\lambda_1$ and $K_1$ arising from these extended calculations are $\lambda_1 = \cdot 1227$ and $K_1 = \cdot 007569_1$.

The formula representing the magneto-optical dispersion of ethylene chloride at 18·4° C. is thus

$$\phi \equiv n\delta\lambda^2 = \cdot 007569_1 \left[\frac{\lambda^2}{\lambda^2 - (\cdot 1227)^2}\right]^2 . \quad . \quad . \quad . \quad . \quad . \quad . \quad (5)$$

Using values of the refractive index obtained from a large-scale graph of the results in Table II., Verdet's Constant at different wave-lengths has been calculated. These calculated values are compared with the observed values in Table V.

The general agreement within experimental error over the range of spectrum ·4290 $\mu$ to ·3096 $\mu$ is clear.

Perkin(3) gives 1·2569 for the specific rotation of ethylene chloride at 14·4° C. Assuming Verdet's Constant at the wave-length of sodium light to be ·0131, the value for ethylene chloride at this wave-length at the temperature 14·4° C. from Perkin's observations is $\cdot 0164_7$.

The value at 18·4° C. calculated from formula (5) is $\cdot 0164_8$. The agreement between the calculated and observed values at this wave-length well outside the range of the present observations is thus satisfactory.

### TABLE V.

### Calculated and Observed Values of Verdet's Constant for Ethylene Chloride.

| Wave-length (in microns). | Verdet's Constant calculated from formula (5). | Verdet's Constant observed. |
|---|---|---|
| ·4290 | $\cdot 0334_8$ | $\cdot 0334_9$ |
| ·4123 | $\cdot 0368_3$ | $\cdot 0367_5$ |
| ·4020 | $\cdot 0390_0$ | $\cdot 0390_7$ |
| ·3929 | $\cdot 0411_7$ | $\cdot 0412_2$ |
| ·3837 | $\cdot 0436_3$ | $\cdot 0435_7$ |
| ·3798 | $\cdot 0446_6$ | $\cdot 0446_5$ |
| ·3685 | $\cdot 0480_4$ | $\cdot 0479_8$ |
| ·3619 | $\cdot 0502_5$ | $\cdot 0502_3$ |
| ·3588 | $\cdot 0513_1$ | $\cdot 0513_5$ |
| ·3495 | $\cdot 0547_8$ | $\cdot 0547_0$ |
| ·3389 | $\cdot 0592_0$ | $\cdot 0591_9$ |
| ·3295 | $\cdot 0636_0$ | $\cdot 0636_2$ |
| ·3189 | $\cdot 0692_1$ | $\cdot 0692_3$ |
| ·3132 | $\cdot 0726_1$ | $\cdot 0725_7$ |
| ·3096 | $\cdot 0748_9$ | $\cdot 0748_2$ |

### *Formulæ for Natural Dispersion.*

In the case of both isobutyl butyrate and ethylene chloride it has been found possible to represent the magneto-optical dispersion by single-term formulæ. In the introduction to this paper it was indicated that the theory underlying these magneto-optical dispersion formulæ assumes that the natural dispersion of the liquids can be represented by a formula of the Ketteler-Helmholtz type involving the same absorption wave-length, *i. e.*, by a formula of the type

$$n^2-1=b_0+\frac{b_1}{\lambda^2-\lambda_1^2}.$$

Taking pairs of wave-lengths with corresponding refractive indices the constants $b_0$ and $b_1$ can readily be obtained. This calculation for each liquid is summarized below.

### *Isobutyl Butyrate.*

The absorption wave-length $\lambda_1$ for isobutyl butyrate was calculated to be $\cdot 1106\,\mu$.

The pairs of values of $\lambda$ and $n$ together with the calculated values of the constants $b_0$ and $b_1$ are given below.

| $\lambda$. | $n$. | $b_1$. | $b_0$. |
|---|---|---|---|
| ·5876 | $1{\cdot}4081_3$ | $\cdot 009697_2$ | ·95371 |
| ·4275 | $1{\cdot}4179_5$ | | |
| ·5876 | $1{\cdot}4081_3$ | $\cdot 009671_5$ | ·95380 |
| ·3274 | $1{\cdot}4337_5$ | | |
| ·4922 | $1{\cdot}4127_6$ | $\cdot 009662_8$ | ·95389 |
| ·3274 | $1{\cdot}4337_5$ | | |
| ·4675 | $1{\cdot}4146_0$ | $\cdot 009581_0$ | ·95565 |
| ·3337 | $1{\cdot}4322_4$ | | |
| ·5293 | $1{\cdot}4107_1$ | $\cdot 009605_6$ | ·95425 |
| ·3602 | $1{\cdot}4268_8$ | | |

The mean values of $b_0$ and $b_1$ from the above are ·95426 and $\cdot 009643_6$ respectively. The mean values for many further such calculations are

$$b_0 = \cdot 95409_0,$$

$$b_1 = \cdot 009642_1.$$

The formula for the natural dispersion of isobutyl butyrate at 10·4° C. is thus

$$n^2 - 1 = \cdot 95409 + \frac{\cdot 009642_1}{\lambda^2 - (\cdot 1106)^2} \quad . \quad . \quad . \quad . \quad . \quad . \quad (6)$$

Values of the refractive index $n$ calculated from this formula are compared with observed values in Table VI.

There is thus satisfactory agreement between observed and calculated values from $\cdot 6678\,\mu$ to $\cdot 3012\,\mu$.

TABLE VI.

Calculated and Observed Values for the Refractive Indices of Isobutyl Butyrate at 10·4° C.

| Wave-length (in microns). | Refractive index calculated from formula (6). | Refractive index. observed. |
|---|---|---|
| ·6678 | $1{\cdot}4058_2$ | $1{\cdot}4057_5$ |
| ·5876 | $1{\cdot}4082_0$ | $1{\cdot}4081_3$ |
| ·5293 | $1{\cdot}4107_0$ | $1{\cdot}4107_1$ |
| ·5016 | $1{\cdot}4122_2$ | $1{\cdot}4121_5$ |
| ·4922 | $1{\cdot}4128_0$ | $1{\cdot}4127_6$ |
| ·4675 | $1{\cdot}4145_1$ | $1{\cdot}4146_0$ |
| ·4275 | $1{\cdot}4179_7$ | $1{\cdot}4179_5$ |
| ·4063 | $1{\cdot}4202_2$ | $1{\cdot}4202_5$ |
| ·3825 | $1{\cdot}4233_8$ | $1{\cdot}4233_2$ |
| ·3602 | $1{\cdot}4269_3$ | $1{\cdot}4268_8$ |
| ·3534 | $1{\cdot}4281_7$ | $1{\cdot}4280_1$ |
| ·3337 | $1{\cdot}4322_5$ | $1{\cdot}4322_4$ |
| ·3274 | $1{\cdot}4337_5$ | $1{\cdot}4337_5$ |
| ·3012 | $1{\cdot}4411_6$ | $1{\cdot}4411_9$ |

*Ethylene Chloride.*

The value of $\lambda_1$ for ethylene chloride was calculated to be ·1227 $\mu$.

| $\lambda$. | $n$. | $b_1$. | $b_0$. |
|---|---|---|---|
| ·4378 | $1{\cdot}4557_5$ | $\cdot 01245_9$ | 1·04867 |
| ·3512 | $1{\cdot}4709_6$ | | |
| ·4275 | $1{\cdot}4570_0$ | $\cdot 01247_0$ | 1·04849 |
| ·3208 | $1{\cdot}4800_9$ | | |
| ·4275 | $1{\cdot}4570_0$ | $\cdot 01246_1$ | 1·04854 |
| ·3147 | $1{\cdot}4822_5$ | | |
| ·4123 | $1{\cdot}4590_2$ | $\cdot 01260_3$ | 1·04711 |
| ·3208 | $1{\cdot}4800_9$ | | |
| ·4123 | $1{\cdot}4590_2$ | $\cdot 01251_5$ | 1·04768 |
| ·3484 | $1{\cdot}4716_8$ | | |

The pairs of values of $\lambda$ and $n$ used to calculate the constants of the dispersion formula are given above, together with the corresponding values obtained for $b_0$ and $b_1$.

The mean values of $b_0$ and $b_1$ from the above are $1{\cdot}04809_8$ and $\cdot01250_2$ respectively. The mean values obtained from many further such calculations are

$$b_0 = 1{\cdot}04802_7,$$

$$b_1 = \cdot01255_1.$$

### TABLE VII.

Calculated and Observed Refractive Indices of Ethylene Chloride at 18·4° C.

| Wave-length (in microns). | Refractive index calculated from formula (7). | Refractive index observed. |
|---|---|---|
| ·4651 | $1{\cdot}4527_2$ | $1{\cdot}4530_0$ |
| ·4378 | $1{\cdot}4557_1$ | $1{\cdot}4557_5$ |
| ·4123 | $1{\cdot}4591_2$ | $1{\cdot}4590_2$ |
| ·4023 | $1{\cdot}4606_6$ | $1{\cdot}4605_8$ |
| ·3825 | $1{\cdot}4641_2$ | $1{\cdot}4640_3$ |
| ·3654 | $1{\cdot}4676_4$ | $1{\cdot}4675_7$ |
| ·3512 | $1{\cdot}4710_3$ | $1{\cdot}4709_6$ |
| ·3484 | $1{\cdot}4717_5$ | $1{\cdot}4716_8$ |
| ·3365 | $1{\cdot}4750_6$ | $1{\cdot}4750_3$ |
| ·3337 | $1{\cdot}4759_2$ | $1{\cdot}4758_8$ |
| ·3308 | $1{\cdot}4768_2$ | $1{\cdot}4767_5$ |
| ·3208 | $1{\cdot}4801_6$ | $1{\cdot}4800_9$ |
| ·3160 | $1{\cdot}4818_9$ | $1{\cdot}4818_7$ |
| ·3147 | $1{\cdot}4822_5$ | $1{\cdot}4822_5$ |

The formula for the natural dispersion of ethylene chloride at 18·4° C. is thus

$$n^2 - 1 = 1{\cdot}04802_7 + \frac{\cdot01255_1}{\lambda^2 - (\cdot1227)^2} \quad . \quad . \quad . \quad . \quad . \quad . \quad (7)$$

Values of the refractive index at wave-lengths ranging from ·46 $\mu$ to ·31 $\mu$ calculated from formula (7) are compared with the observed values in Table VII.

Formula (7) fits the observations over the range of spectrum $\cdot 4378\,\mu$ to $\cdot 3147\,\mu$ (this covers the range of wave-lengths of the magneto-optical measurements), but at longer wave-lengths it yields values which fall below the observed refractive indices. The application of formula (7) is thus confined to wave-lengths below $\cdot 465\,\mu$.

The process of extrapolating refractive indices to infinite wave-length was first carried out by Bruhl, and his value for the "molecular refraction" of ethylene chloride for a line of "infinite" wave-length is given in Watts's 'Dictionary of Applied Chemistry' as 34·12.

(Molecular refraction for any wave-length $\lambda$ is defined by $\frac{(n_\lambda - 1)M}{S}$, where $n_\lambda$ is the refractive index for wave-length $\lambda$, M is the molecular weight, and S the specific gravity.)

From formula (7) the refractive index for a line of "infinite" wave-length is given by $\sqrt{2{\cdot}04802_7}$. The specific gravity of ethylene chloride (at 20° C.) is 1·2521, and the molecular weight is 98·947.

Hence the calculated value of the molecular refraction is

$$\frac{(\sqrt{2{\cdot}04802_7} - 1) \times 98{\cdot}947}{1{\cdot}2521}$$

$$= 34{\cdot}06.$$

This value is approximately $\frac{1}{6}$ per cent. less than that given by Bruhl.

### *Calculation of e/m.*

The ratio of the charge to the mass of the resonators controlling the magneto-optical and natural dispersion is given by

$$\frac{e}{m} = -\frac{2K_1C^2}{b_1},$$

and can thus be calculated from the foregoing results.

For these calculations $K_1$ and $b_1$ must have the values corresponding to Verdet's Constant in radians per cm. gauss and the wave-length in cm.

The following are the values obtained for the two liquids isobutyl butyrate and ethylene chloride, after insertion of the constants $K_1$, $b_1$, and C :—

$$\text{Isobutyl butyrate } \frac{e}{m} = 1{\cdot}018 \times 10^7 \text{ e.m.u.}$$

$$\text{Ethylene chloride } \frac{e}{m} = 1{\cdot}028 \times 10^7 \text{ e.m.u.}$$

## SUMMARY AND DISCUSSION OF RESULTS.

1. (*a*) The magneto-optical dispersions of isobutyl butyrate and of ethylene chloride over the range of wave-lengths ·43 $\mu$ to ·31 $\mu$ can be represented by formulæ of the type

$$\phi \equiv n\delta\lambda^2 = \mathrm{K}_1 \left[\frac{\lambda^2}{\lambda^2 - \lambda_1{}^2}\right]^2,$$

where $n$ and $\delta$ are the values for wave-length $\lambda$ of the refractive index and Verdet's Constant, $\lambda_1$ the wave-length of the absorption band, and K is a constant for a given liquid at a particular temperature.

(*b*) The natural dispersion of isobutyl butyrate over the range of spectrum ·67 to ·30 $\mu$ and of ethylene chloride over the range ·44 to 30 $\mu$ can be represented by formulæ of the type

$$n^2 - 1 = b_0 + \frac{b_1}{\lambda^2 - \lambda_1{}^2},$$

where $b_0$ and $b_1$ are constants and $\lambda_1$ has the same value as in the corresponding equation for magneto-optical dispersion.

In the case of the refractive indices of ethylene chloride in the visible spectrum it was found that the formula yielded values below those actually observed. Hence for this liquid it would appear that if more accurate and extensive data were available the formulæ given in this paper would be found to be inapplicable.

The values of the constants $\lambda_1$, $\mathrm{K}_1$, $b_0$, and $b_1$ for the two liquids are given below :—

| | $\lambda_1$ (microns). | $\mathrm{K}_1$. | $b_0$. | $b_1$. |
|---|---|---|---|---|
| Isobutyl butyrate .. | ·1106 | ·005616$_5$ | ·95409 | ·009642 |
| Ethylene chloride .. | ·1227 | ·007569$_1$ | 1·04802$_7$ | ·01255$_1$ |

2. For each liquid the calculated values of Verdet's Constant for a wave-length in the visible spectrum well outside the range of the present investigation is in satisfactory agreement with that actually observed. From this result it is inferred that absorption bands in the infra-red have no appreciable effect on the magneto-optical and natural dispersions in the visible and ultra-violet regions of the spectrum.

3. The results for isobutyl butyrate may be compared with those

previously determined in this laboratory for butyric acid and other butyrates. These results are collected in the following table :—

| Liquid. | Molecular weight. | $\lambda_1$. | $K_1$. | $b_0$. | $b_1$. | Temp. °C. |
|---|---|---|---|---|---|---|
| Butyric acid ...... | 88 | ·1064 | ·005285 | ·9352 | ·009300 | 13·1 |
| Methyl butyrate... | 102 | ·1076 | $\cdot005113_6$ | $\cdot9081_6$ | ·009141 | 12·25 |
| Ethyl butyrate ... | 116 | ·1081 | ·005259 | ·9209 | ·009103 | 13·1 |
| Isopropyl butyrate. | 130 | ·1094 | ·005402 | $\cdot9263_7$ | ·009179 | 11·4 |
| Isobutyl butyrate.. | 144 | ·1106 | $\cdot005616_5$ | $\cdot9540_9$ | ·009642 | 10·4 |

Previous magneto-optical work has shown that in any homologous series the values of the constants $\lambda_1$, $K_1$, $b_1$, and $b_0$ generally increase progressively with molecular weight. It will be noted from the above table that the results for the normal and isobutyrates (the present liquid included) are consistent with that conclusion. The increase in $\lambda_1$ in passing from isopropyl butyrate to isobutyl butyrate is of the same order (·0012 $\mu$) as was previously observed for the transition from ethyl to isopropyl butyrate. The results of previous investigations have also shown that the values of $\lambda_1$ for corresponding normal and iso compounds are practically the same.

4. The values of $e/m$ calculated from the results are :—

Isobutyl butyrate $=1\cdot018\times10^7$ e.m.u.

Ethylene chloride $=1\cdot028\times10^7$ e.m.u.

The magnitudes of this ratio indicate that the resonators controlling the dispersion have an electronic nature, but the calculated values of $e/m$ are considerably lower than the accepted value for electrons ($1\cdot772\times10^7$ e.m.u.). Similar low values of $e/m$ have been obtained from magneto-optical work by other observers.

The author is indebted to Professor E. J. Evans, D.Sc., for facilitating this research and also for assistance in the experimental work involved.

### *References.*

(1) W. J. G. Beynon and E. J. Evans, Phil. Mag. (7) xxv. pp. 476–488 (March 1938).
(2) D. J. Stephens and E. J. Evans, Phil. Mag. iii. p. 546 *et seq.* (March 1927).
(3) Perkin, Journ. Chem. Soc. xlv. p. 528 (1884).

Physics Department,
University College, Swansea.
May 1938.

# LIII. *The Efficiency of Geiger-Müller Counters.*

By R. S. Shankland and C. H. Tindal,
Case School of Applied Science, Cleveland, Ohio *.

[Received November 25, 1938.]

The discharge of a Geiger-Müller counter results from the entry, into the space between the electrodes, of a primary or secondary ionizing particle which gains sufficient energy in the electric field of the device to cause multiple ionization. The initial ionizing agent may be a high speed charged particle which enters from outside ; it may also be a secondary particle liberated from the wall of the counter by the photoelectric or Compton processes, or for extreme energies by pair production. The efficiency of such secondary processes has been investigated by H. Yukawa and S. Sakata † by taking account of the absorption of the primary radiation in the walls of the counter, the range of secondaries in the wall, and their direction of emission within the counter. Whether such an ionizing particle moving within the counter will cause it to discharge depends on a number of factors including the applied voltage, counting rate, kind of gas and its pressure, and the electrical circuits used.

The present experiments were performed to determine the influence of voltage and counting rate on the efficiency of the Geiger-Müller counter, and to contribute to the knowledge of the phenomena of the counter discharge. The circuits used are shown in fig. 1. High voltage is supplied to the counter by a rectifier and voltage stabilizer circuit, and the counter discharges are amplified by three stages of resistance-capacitance amplification. The impulses are fed into a thyratron scale-of-sixteen circuit which operates a Cenco impulse recorder. The counter itself has a cathode cylinder of brass 6 centimetres long and 1 centimetre inside diameter with a 3 mil tungsten wire anode. The envelope is glass and contains dry air at a pressure of 9·5 centimetres of Hg at room-temperature. The experiments were performed in a constant temperature room, the temperature being 22° C. The counter has an operating range extending from 1300 to 1630 volts with a threshold at 1175 volts.

Observations are made of the residual discharge rate R, and of the rate N when the counter is stimulated with radium. The measurements are made with various voltages applied to the counter, and with radium at several distances. The radium is in the form of radium bromide having a "gamma radiation equivalent to that from 0·409 milligram of radium in radioactive equilibrium" *.

---

* Communicated by Prof. Dayton C. Miller.

† H. Yukawa and S. Sakata, Inst. of Phys. and Chem. Res., Tokyo, pp. 187–194 (1937).

The counting rates given by the Cenco recorder are corrected for the counts lost in the amplifying and recording circuits due to their finite recovery times. A. E. Ruark and F. E. Brammer † have pointed out that there are two limiting types of recorder. In the first the average recovery time depends on the counting rate and the corrections may be made to a close approximation with the equation developed by H. Volz ‡ and H. Todd §,

Fig. 1.

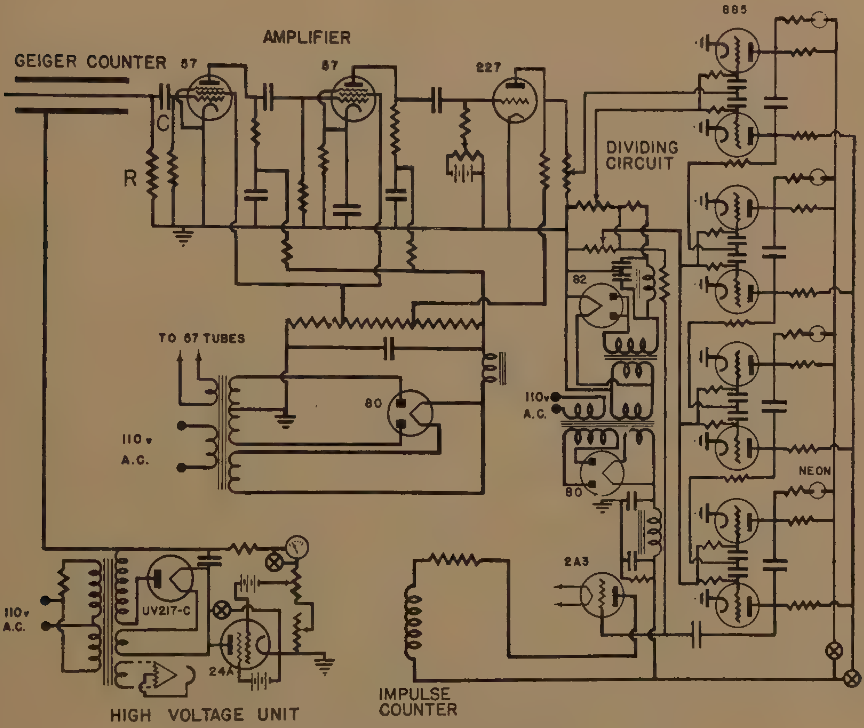
AMPLIFIER
GEIGER COUNTER
57
57
227
885
C
R
DIVIDING CIRCUIT
82
TO 57 TUBES
80
110v A.C.
110v A.C.
80
NEON
2A3
110v A.C.
UV217-C
24A
HIGH VOLTAGE UNIT
IMPULSE COUNTER

Circuit diagram of Geiger-Müller counter.

$$m = \mu e^{-\frac{\mu}{n_A}}, \quad . \; . \; . \; . \; . \; . \; . \; . \; . \quad (1)$$

---

[*] Report of U.S. Bureau of Standards, August 21, 1937.

[†] A. E. Ruark and F. E. Brammer, Phys. Rev. lii. pp. 322–324 (1937).

[‡] H. Volz, *Zeit. f. Phys.* xciii. pp. 539–542 (1935).

[§] H. Todd, Phil. Mag. xxiv. pp. 572–577 (1937).

where $m$ is the observed rate, $\mu$ is the true rate and $n_A = m_{\text{max.}} \cdot e$. The inverted form of this equation used for the corrections is

$$\mu = m \sum_{r=1}^{r=\infty} \frac{r^{r-1}}{r!} \left(\frac{m}{n_A}\right)^{r-1} \quad . \quad . \quad . \quad . \quad . \quad . \quad . \quad (2)$$

In the second type the recorder goes through its cycle of operations after being actuated independently of the arrival of any later impulse. The corrections for such a device are made by means of the relation

$$\mu = \frac{m}{1 - \dfrac{m}{n_R}} \quad . \quad . \quad . \quad . \quad . \quad . \quad . \quad . \quad . \quad (3)$$

Here $m$ and $\mu$ have the same meaning as above and $n_R$ is equal to the observed $m_{\text{max.}}$. In this type of recorder $n_R = m_{\text{max.}}$ may be conveniently found by observing the maximum number of evenly spaced pulses that the circuit will record.

In the present apparatus the thyratron scale-of-sixteen circuit has such a scaling ratio that the losses occurring in the mechanical ratchet of the Cenco recorder are completely negligible for the counting rates studied below *. The losses in this part of the apparatus are set by the recovery time of the first pair of thyratrons. The coupling circuit and the amplifier have an effective resolution time $\tau_A$ which depends on the circuit constants, the counting rate, and to a lesser degree, upon the voltage applied to the counter. The counter itself has a recovery time $\tau_c$ determined by the speed with which ions are swept to the electrodes after the discharge. In general $\tau_c < \tau_A$, since the counter must be free of ions before the voltage builds up to its operating value, otherwise a continuous corona discharge will result. A high value of R prevents this. The values of $n_R$ and $n_A = 1/\tau_A$ used in correcting the data are determined from the experiments with the highest counting rates. Then all other experimental points for slower rates are corrected using the same constants †. This procedure will give accurate corrected rates in all but the highest speed range. These corrected rates will be characteristic of the counter itself independent of the characteristics of the amplifying and recording system.

A set of data taken with the counter described above and corrected in this manner is shown in fig. 2. The abscissæ give the distances from the radium to the counter, and the ordinates are the corrected rates $\mu$ minus the residual rates R taken with the radium removed to a great distance. Each curve is for a different counter voltage as indicated by the key.

---

* L. Alaoglu and N. M. Smith, Phys. Rev. liii. p. 833 (1938).

† C. H. Tindal, Thesis, Case School of Applied Science (1938).

The dashed curve is the calculated variation with distance of the number of photons falling on the counter according to the inverse square law

Fig. 2.

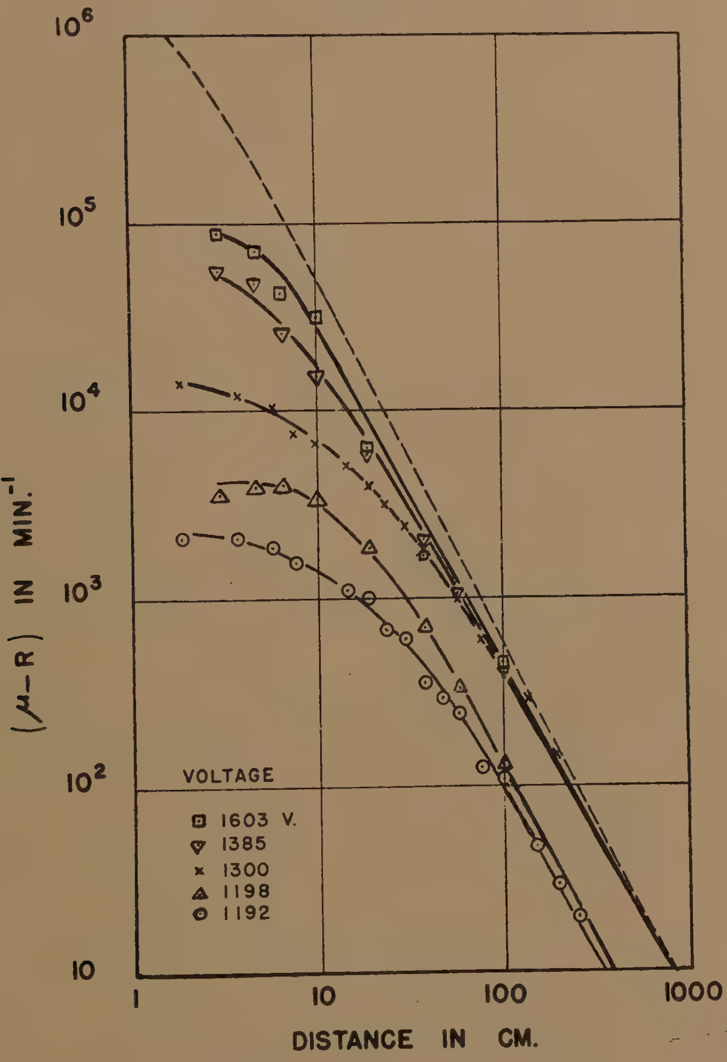

Effect of voltage on counting rate.

modified for the finite size of the counter and radioactive source. This curve has been adjusted vertically so that it forms the envelope of the experimental curves.

For the lower counting rates at each voltage the curves approach a slope of −2 on the log—log plotting, in agreement with the inverse square law. At higher counting rates, however, the curves fall off, showing a decreasing counter efficiency. Any uncertainties in the positions of points in fig. 2 due to the method of correction can only influence points above $10^4$ min.$^{-1}$, since for lower counting rates the corrections are quite small.

Fig. 3.

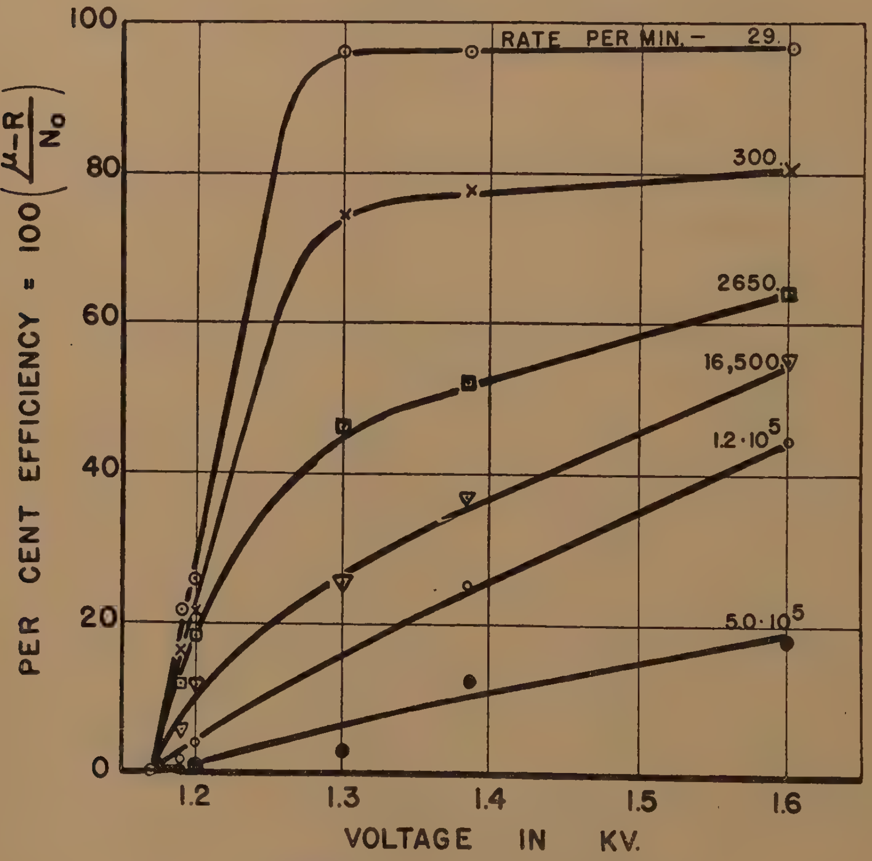

Efficiency of a Geiger-Müller counter.

Fig. 3 has been constructed from fig. 2 to give the counter efficiency as a function of applied voltage for six widely differing counting rates. The efficiency for all counting rates drops to zero at a threshold of 1175 volts. The threshold voltage produces an electric field in the counter which enables electrons to gain sufficient energy while traversing their mean free path to produce ionization by collision at the existing gas pressure *. The quantity of electricity carried across the counter during a discharge varies with the initial energy and direction of the ionizing agent and the conditions in the gas determining ionization and recombination. Just above the threshold only a few of the pulses will be large enough to actuate the recording system through the amplifier. As the voltage is raised above the threshold the size of the pulse increases, so that it is more likely to operate the recorder through the amplifier. For slow counting rates it is shown below (equation 4) that the size of the pulse is directly proportional to the overvoltage above threshold. This agrees with the efficiency curves for slow counting rates, which steadily rise until at about 125 volts above threshold all the pulses are large enough to be recorded. Assuming that the pulse sizes at the threshold are distributed according to the Maxwell-Boltzmann law, it can be shown, by graphical integration, that the number amplified by the overvoltage sufficiently to operate the amplifier follow a curve like that found for the 29 min.$^{-1}$ counting rate. For this slow counting rate the efficiency reaches a value of 96 per cent., in excellent agreement with the values obtained by the method of multiple coincidences used in cosmic ray experiments †.

At high counting rates the efficiency curves do not flatten out, but steadily increase with applied voltage. The counter operates properly only when the series resistance R is large enough to make the normal positive corona discharge intermittent. This resistance, however, increases the time-constant of the coupling circuit, so that for high counting rates the counter may not recover quickly enough to respond to the next ionizing particle. If $V_0$ is the threshold voltage, $V'$ the applied voltage, $t$ the time measured from the beginning of a pulse, and RC the time-constant, the voltage between the counter electrodes for the duration of the pulse is

$$V=(V'-V_0)(1-e^{-\frac{t}{RC}})+V_0.$$

If a second pulse begins after a time $\Delta t$, the voltage magnitude of this pulse is

$$\Delta V=(V'-V_0)(1-e^{-\frac{\Delta t}{RC}}).$$

For slow counting rates (large $\Delta t$) the size of the voltage pulse is

$$\Delta V=V'-V_0. \qquad (4)$$

---

[*] See experiments by C. L. Haines, Rev. Sci. Inst. vii. pp. 411–413 (1936).

[†] J. C. Street and R. H. Woodward, Phys. Rev. xlvi. p. 1029 (1934); D. K. Froman and J. C. Stearns, Can. Jl. Res. xvi. A, p. 36 (1938); V. C. Wilson, Phys. Rev. liii. p. 338 (1938).

This is in agreement with the statement made above and shows that the pulse size is independent of the counting rate when the latter is slow. It is also in agreement with fig. 3, which shows that the initial slopes of the efficiency-voltage curves for slow counting are independent of counting rate.

Fig. 4.

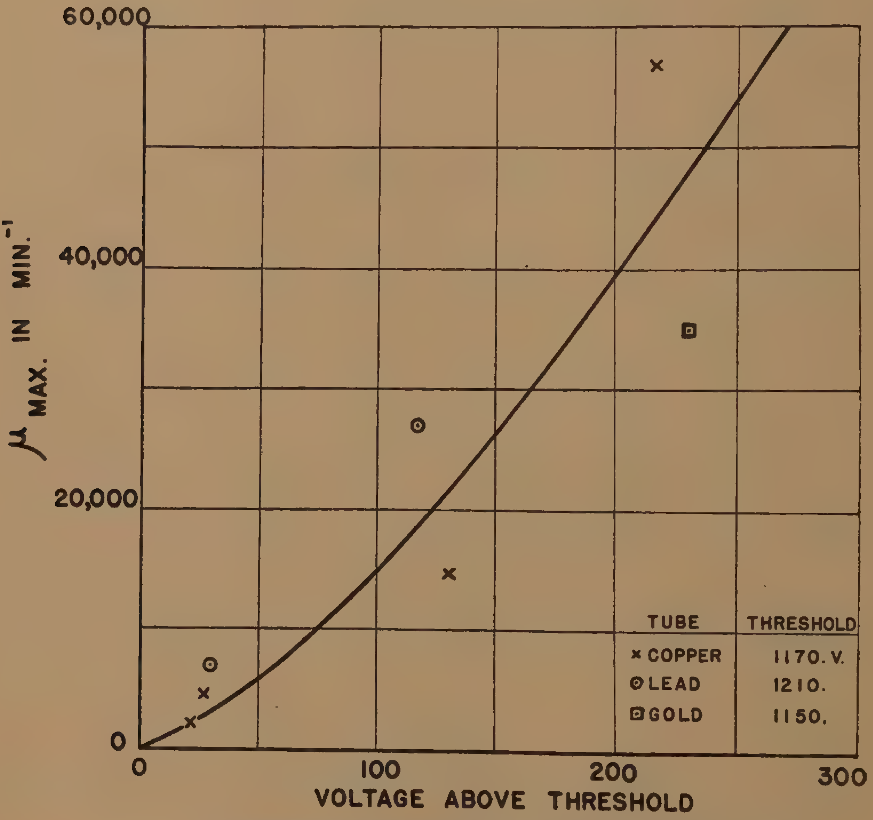

Maximum discharge rates of Geiger-Müller counters.

For fast counting rates, however (small $\Delta t$), we have

$$\Delta V=(V'-V_0)\frac{\Delta t}{RC}.$$

If we set the reciprocal of $\Delta t$ equal to the statistically averaged frequency of random discharges, then

$$\Delta V=\frac{V'-V_0}{\text{Rate}\times RC} \quad . \quad . \quad . \quad . \quad . \quad . \quad . \quad . \quad (5)$$

The shape of the efficiency-voltage curves for fast counting, therefore, will be straight lines with a slope inversely proportional to the counting rate. These curves will show saturation only at very high overvoltages sufficient to make all pulses $\Delta V$ large enough to be amplified. The two lower curves of fig. 3 are straight lines of this form and give approximate agreement with equation (5). A large overvoltage, therefore, not only gives larger pulses because of increased ionization, but also sharpens the pulses, so that they are more readily resolved into separate discharges.

The influence of the overvoltage $(V'-V_0)$ in sharpening the pulses and therefore permitting more rapid counting is also shown by fig. 4, which gives the maximum observed counting rates including residuals (both corrected for amplifier and recorder losses) as a function of overvoltage. This graph includes points from the counter already described and also data taken with counters having cathode cylinders of lead and gold, inside diameter one centimetre. The anodes are 3 mil tungsten wires. The lead counter contains dry air at a pressure of 11·1 centimetres of mercury, and the pressure in the gold counter is 10·5 centimetres of mercury. The threshold voltages are 1210 and 1150 respectively. Fig. 4 includes only points where the corrections to the counting rates are a small fraction of the value of $\mu_{\text{max.}}$. $\mu_{\text{max.}}$ is inversely proportional to the quantity $\Delta t$ used above as the statistical average of the time-intervals between random discharges. The points on the curve show a nearly linear dependence upon overvoltage as predicted by equation (5). The experimental points for high overvoltages, however, increase somewhat more rapidly than in direct proportion to the overvoltage. This is due to the increased speed with which the ions are swept out of the counter at high voltages (reduction of $\tau_c$). Accordingly, the average value of $\Delta t$ is smaller for the critical pulse size which can be amplified, and makes possible a larger value of $\mu_{\text{max.}}$.

The results given above explain some of the phenomena which occur during the discharge of a Geiger-Müller counter. The manner in which these affect the counter efficiency may be summarized as follows :—

1. The counter efficiency depends upon the constants R and C of the coupling circuit, and upon the counting rate and overvoltage as shown by equations (4) and (5) and by the experimental results shown in fig. 3.

2. In these experiments the discharges are initiated by photons which eject an ionizing secondary particle into the active volume of the counter. The efficiencies for low counting rates are in agreement with those found from cosmic ray studies.

3. For precise intensity measurements it is necessary to know the detailed efficiency data of the counter being used, as illustrated in fig. 3.

4. Fig. 3 also shows that experiments which use two or more counters to study "coincidences" will fail to record an important number of such events unless the counting rates are small.

The efficiency of a Geiger-Müller counter for either single or coincidence counting experiments will be considerably increased for high counting rates if a vacuum tube is used in place of the high resistance R to quench the counter discharge*.

---

* H. V. Neher and W. H. Pickering, Phys. Rev. liii. p. 316 (1938); T. H. Johnson. Rev. Sci. Inst. ix. p. 219 (1938).

# LIV. *The Influence of the Free End of a Rod on Heat Transfer.*

By Max Jakob, Research Foundation of Armour Institute
of Technology, Chicago, Illinois *.

[Received November 18, 1938.]

## Synopsis.

Simple equations of temperature and heat transfer are derived for the case in which the coefficient of heat transfer can be considered as constant over the whole surface of a rod, tube, or fin, which is heated or cooled at one end. An application to a thermometric arrangement shows that neglecting the end influence may cause considerable mistakes in temperature measurement.

### 1. *General Equations.*

One of the most frequent cases of heat transfer is that of a rod, held at constant temperature at one end, and heated or cooled uniformly over the surface. A straight tube or fin falls under the definition of "rod." The general equations of heat transfer for this case are well known, provided that the cross-section, the heat conductivity of the rod, the coefficient of heat transfer, and the temperature of the environment are invariable over the length, and that in any cross-section of the rod the heat flow can be considered as normal to the section inside the rod and normal to the circumference outside, as is practically the case with not too thick or short metal rods.

Harper and Brown, in a very thorough mathematical paper ⁽¹⁾, suggested that one might take into account the influence of the free end of a wide fin by imagining the fin length extended by one-half of the thickness $t$ (fig. 1) and then neglecting the heat transfer at the end in the distance $l+\frac{2}{t}$.

But it is not necessary to introduce a fictitious length $\left(l+\frac{t}{2}\right)$, if one assumes that the coefficient of heat transfer at the free end of the tube is the same as along the rod. For a rod (fig. 2) of cross-section area $f$, cross-section perimeter $p$, heat conductivity $k$, coefficient of heat transfer $h$

---

* Communicated by the Author.

—all these assumed to be constant over the length of the rod,—the equation for the temperature excess over that of the environment is

$$\theta=A(e^{-mx}-e^{mx})+\theta_0 e^{mx}, \quad . \quad . \quad . \quad . \quad . \quad . \quad . \quad (1)$$

where A is a constant and

$$m=\sqrt{\frac{h}{k}\frac{p}{f}}.$$

Fig. 1.

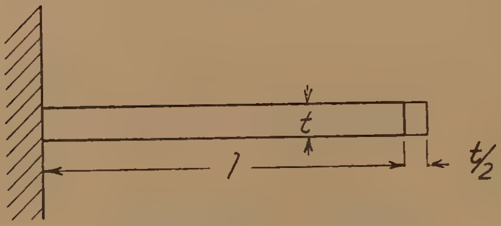

Fin with fictitious extension.

Fig. 2.

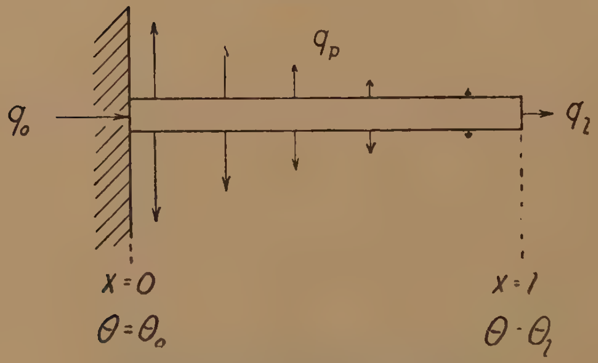

Heat-flow on the surface of a rod.

The heat flow entering the rod at $x=0$ is

$$q_0=-kf\left(\frac{d\theta}{dx}\right)_0=kfm(2A-\theta_0). \quad . \quad . \quad . \quad . \quad . \quad . \quad (2)$$

The heat given up along the rod is

$$q_p=\int_0^l hp\theta\, dx. \quad . \quad . \quad . \quad . \quad . \quad . \quad . \quad . \quad (3)$$

That given up at the end is

$$q_l=hf\theta_l. \quad . \quad . \quad . \quad . \quad . \quad . \quad . \quad . \quad . \quad . \quad (4)$$

From (2), (3), (4) and the equation of heat balance

$$q_0=q_p+q_l \qquad (5)$$

it follows

$$-kf\left(\frac{d\theta}{dx}\right)_0=\int_0^l hp\theta\,dx+hf\theta_l. \qquad (6)$$

By substitution of $\theta$ from (1) into (6) we obtain

$$A=\theta_0\,\frac{1}{1+\dfrac{km-h}{km+h}e^{-2ml}} \qquad (7)$$

Introducing this into (1) for $x=x$ and for $x=l$, and into (2), we find

$$\theta=\theta_0\left[\frac{1}{1+\dfrac{km-h}{km+h}e^{-2ml}}(e^{-mx}-e^{mx})+e^{mx}\right] \qquad (8)$$

$$\theta_l=\theta_0\left[\frac{1}{1+\dfrac{km-h}{km+h}e^{-2ml}}(e^{-ml}-e^{ml})+e^{ml}\right] \qquad (9)$$

$$q_0=kfm\theta_0\left(\frac{2}{1+\dfrac{km-h}{km+h}e^{-2ml}}-1\right) \qquad (10)$$

It can be shown easily that (9) and (10) never yield negative values of $\theta_l$ and $q_0$. $2lm$ can assume values between 0 and $+\infty$. In the first case $\theta_l$ becomes equal to $\theta_0$ and $q_0$ becomes zero, in the second case $\theta_l$ becomes zero and $q_0=kfm\theta_0$. For all other cases positive intermediate values will be obtained.

The equations (8), (9), and (10) may be compared with those obtained if one applies Harper and Brown's method to the general case of a rod. To this purpose one must imagine the rod to be extended so far that the total surface, assumed to give up heat, remains the same, *i. e.*, by a length $f/p$, corresponding to $t/2$ in fig. 1.

Whereas equation (1) remains unchanged, equation (6) is to be replaced by the boundary condition

$$\left(\frac{d\vartheta}{dx}\right)_{x=l+\frac{f}{p}}=0. \qquad (11)$$

In this case (1) and (2) lead to

$$A=\theta_0\,\frac{1}{1+e^{-2m\frac{f}{p}}e^{-2ml}} \qquad (12)$$

and to equations for $\theta$, $\theta_l$, and $q_0$ differing from (8), (9), (10) only by the one item, that $\frac{km-h}{km+h}$ has to be replaced by $e^{-2m\frac{f}{p}}$.

The difference, however, is small as can easily be demonstrated. Introducing the dimensionless group

$$n=\sqrt{\frac{h}{k}\frac{f}{p}}=\frac{h}{km}=m\frac{f}{p},$$

one obtains

$$\frac{km+h}{km-h}=\frac{\frac{km}{h}+1}{\frac{km}{h}-1}=\frac{1+n}{1-n}=1+2n+2n^2+2n^3+2n^4+\ldots \quad . \quad (13)$$

and

$$e^{2m\frac{f}{p}}=e^{2n}=1+\frac{2n}{1\,!}+\frac{(2n)^2}{2\,!}+\frac{(2n)^3}{3\,!}+\ldots=1+2n+2n^2+\frac{4}{3}n^3+\frac{2}{3}n^4+\ldots \quad . \quad . \quad . \quad (14)$$

Differences begin only in the 4th term of the series in equations (13) and (14). At all events, because the equations (8) to (10) are based on simpler assumptions and are a little simpler in application too, they seem to be preferable to Harper and Brown's equations.

### 2. *Application to a Thermometric Arrangement.*

Equation (8) may be applied to one of the most usual thermometric arrangements (fig. 3). It consists of a hollow metal block, *a*, which is supposed to be surrounded by a stirred liquid and to have the same temperature as this, and of a tube, *b*, intimately connected with the block, *a*, and having the same inside diameter as this. A thermocouple may be put into the hole, with the joint at the inner end. The temperature of this joint as compared with the temperature of the block *a* is required.

In a former publication (2) we derived the following equations for the temperature of the thermocouple, which was supposed to be replaced by a single wire, equivalent in heat exchange to the couple of wires :

$$\theta_{\mathrm{I}}=\theta_1 e^{-m_{\mathrm{I}}(x-x_1)} \quad . \quad . \quad . \quad . \quad . \quad . \quad . \quad . \quad (15)$$

$$\theta_{\mathrm{II}}=\mathrm{M}e^{m_{\mathrm{II}}x}+\mathrm{N}e^{-m_{\mathrm{II}}x}-\frac{m_{\mathrm{II}}^2}{m_b^2-m_{\mathrm{II}}^2}\theta_a e^{-m_b x} \quad . \quad . \quad . \quad . \quad (16)$$

$$\theta_{\mathrm{III}}=\theta_a-(\theta_a-\theta_0)e^{m_{\mathrm{III}}x} \quad . \quad . \quad . \quad . \quad . \quad . \quad . \quad . \quad (17)$$

The subscripts I, II, and III in these equations relate to the three branches I, II, III of the temperature curve of the wire, and the subscripts 0, 1, and 2 to the distances $x=0$, $x=x_1$, and $x=-x_2$, as indicated in fig. 3. Subscript *a* relates to the wall of block *a*, and *b* to the wall of the tube *b*. The four unknown constants $\theta_0$, $\theta_1$, M, and N are to be determined from the boundary conditions

$$\left.\begin{aligned}\theta_{\text{II}}&=\theta_{\text{III}}\\ \frac{d\theta_{\text{II}}}{dx}&=\frac{d\theta_{\text{III}}}{dx}\end{aligned}\right\}\text{ for } x=0. \qquad (18)$$

Fig. 3.

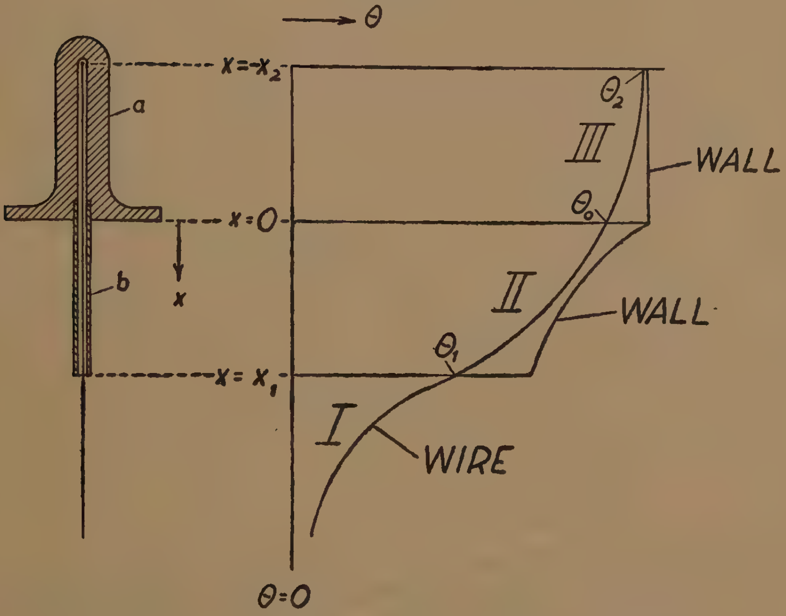

Thermometric arrangement with temperature distribution.

and

$$\left.\begin{aligned}\theta_{\text{I}}&=\theta_{\text{II}}\\ \frac{d\theta_{\text{I}}}{dx}&=\frac{d\theta_{\text{II}}}{dx}\end{aligned}\right\}\text{ for } x=x_1. \qquad (19)$$

In deriving equations (15) to (17) it had been supposed, however, that the wire can be considered as infinitely long in the negative direction of *x*, and the tube *b* as infinitely long in the positive direction. These simplifying assumptions were possible under the particular conditions of our former work (very thin and not so well conducting wires, narrow hole), but can lead to great mistakes with less favourable conditions, as will be seen from the numerical calculation at the last part of this paper.

But first the general solution without these restricting conditions may be derived.

Equation (15) remains unchanged; the condition involved in it, that the wire is infinite in the positive direction of $x$, is practically fulfilled.

For the branch II, the differential equation of the temperature is

$$\frac{d^2\theta_{\text{II}}}{dx^2} - m_{\text{II}}^2\theta_{\text{II}} = m_{\text{II}}^2[\mathrm{A}_b(e^{m_b x} - e^{-m_b x}) - \theta_a e^{m_b x}, \quad . \quad . \quad . \quad (20)$$

where

$$\mathrm{A}_b = \theta_a \frac{1}{1 + \dfrac{k_b m_b - h_b}{k_b m_b + h_b} e^{-2m_b x_1}} = \theta_a \frac{1}{1 + \dfrac{1 - n_b}{1 + n_b} e^{-2m_b x_1}} \quad . \quad . \quad . \quad (21)$$

corresponding to equations (7) and (13).

Integration of the differential equation (20) leads to

$$\theta_{\text{II}} = \mathrm{M}e^{m_{\text{II}} x} + \mathrm{N}e^{-m_{\text{II}} x} - \frac{m_{\text{II}}^2}{m_b^2 - m_{\text{II}}^2}[\mathrm{A}_b e^{-m_b x} - (\mathrm{A}_b - \theta_a)e^{m_b x}]. \quad . \quad (22)$$

In order to find $\theta_{\text{III}}$, we start from the general equation

$$\theta_{\text{III}} - \theta_a = \mathrm{A}_{\text{III}} e^{-m_{\text{III}}(x + x_2)} + \mathrm{B}_{\text{III}} e^{m_{\text{III}}(x + x_2)}, \quad . \quad . \quad . \quad . \quad (23)$$

with two unknown constants $\mathrm{A}_{\text{III}}$ and $\mathrm{B}_{\text{III}}$. These can be determined from the boundary conditions

$$\theta_{\text{III}} = \theta_0 \quad \text{for} \quad x = 0 \quad . \quad . \quad . \quad . \quad . \quad . \quad . \quad (24)$$

and

$$-k_{\text{III}} \frac{d\theta_{\text{III}}}{dx} = h_{\text{III}}(\theta_a - \theta_{\text{III}}) \text{ for } x = -x_2. \quad . \quad . \quad . \quad (25)$$

Thus one obtains

$$\theta_{\text{III}} = \theta_a - (\theta_a - \theta_0)\left(\frac{e^{m_{\text{III}} x}}{1 + \dfrac{1 - n_{\text{III}}}{1 + n_{\text{III}}} e^{-2m_{\text{III}} x_2}} + \frac{e^{-m_{\text{III}} x}}{1 + \dfrac{1 + n_{\text{III}}}{1 - n_{\text{III}}} e^{2m_{\text{III}} x_2}}\right). \quad (26)$$

The equations (15), (22), and (26) replace (15), (16), and (17). The boundary conditions (18) and (19), which remain unchanged, yield the following four equations:

$$\mathrm{M} + \mathrm{N} = \theta_0 + \frac{m_{\text{II}}^2}{m_b^2 - m_{\text{II}}^2}\theta_a. \quad . \quad . \quad . \quad . \quad . \quad . \quad . \quad . \quad . \quad . \quad . \quad . \quad (27)$$

$$\mathrm{M} - \mathrm{N} = (\theta_0 - \theta_a)\frac{m_{\text{III}}}{m_{\text{II}}} \frac{\dfrac{1 + n_{\text{III}}}{1 - n_{\text{III}}} e^{m_{\text{III}} x_2} - e^{-m_{\text{III}} x_2}}{\dfrac{1 + n_{\text{III}}}{1 - n_{\text{III}}} e^{m_{\text{III}} x_2} + e^{-m_{\text{III}} x_2}}$$

$$- \frac{m_b m_{\text{II}}}{m_b^2 - m_{\text{II}}^2}\theta_a\left(\frac{2}{1 + \dfrac{1 - n_b}{1 + n_b} e^{-2m_b x_1}} - 1\right). \quad (28)$$

$$\mathrm{M}e^{m_{\mathrm{II}}x_1}+\mathrm{N}e^{-m_{\mathrm{II}}x_1}=\frac{m_{\mathrm{II}}^2}{m_b^2-m_{\mathrm{I}}^2}[\mathrm{A}_b e^{-m_b x_1}-(\mathrm{A}_b-\theta_a)e^{m_b x_1}]-\theta_1. \quad . \quad . \quad (29)$$

$$\mathrm{M}e^{m_{\mathrm{II}}x_1}-\mathrm{N}e^{-m_{\mathrm{II}}x_1}=-\frac{m_b m_{\mathrm{II}}}{m_b^2-m_{\mathrm{II}}^2}[\mathrm{A}_b e^{-m_b x_1}+(\mathrm{A}_b-\theta_a)e^{m_b x_1}]+\frac{m_{\mathrm{I}}}{m_{\mathrm{II}}}\theta_1. \quad (30)$$

## 3. *Numerical Evaluation.*

Although in principle there is no difficulty in calculating the unknown constants $\theta_0$, $\theta_1$, M, and N from the above equations, it is very much simpler to introduce numerical values.

In fig. 3 let $x_1=5$ cm., $x_2=5$ cm., the inner diameter of the hole 0·3 cm., the outer diameter of the tube $b$, 0·6 cm. The tube $b$ is supposed to consist of copper, the thermocouple of a copper wire, and a constantan wire, each 0·05 cm. thick and held separated without special insulation. The temperature excess of the block $a$ above the air which surrounds $b$ and $c$ may be $\theta_a=75°$ C.

We imagine the two wires superseded by one of the same total circumference, *i. e.*, of 0·1 cm. thickness; since by this the cross-sectional area would be doubled, we assume the wire to have only half the mean thermal conductivity of copper and constantan, which would be about $\frac{0{\cdot}9+0{\cdot}1}{2}=0{\cdot}5$ cal./cm. sec. °C.; thus the conductivity of the substitute wire would be $k_{\mathrm{II}}=\frac{0{\cdot}5}{2}=0{\cdot}25$ cal./cm. sec. °C. By this transformation,

$$m_{\mathrm{II}}=\sqrt{\frac{h_{\mathrm{II}}\,p_{\mathrm{II}}}{k_{\mathrm{II}}\,f_{\mathrm{II}}}}$$

will be about the same as would be the mean value of $m_{\mathrm{II}}$ for the two wires. $h_{\mathrm{II}}$ can be calculated easily from the heat conductivity $k$ of the air surrounding the wire *, according to the equation

$$h_{\mathrm{II}}=\frac{k}{r_i\ln\frac{r_a}{r_i}}, \quad . \quad . \quad . \quad . \quad . \quad . \quad . \quad (31)$$

where $2r_i$ and $2r_a$ are the diameter of the wire, and the width of tube $b$, respectively. For our conditions, we find $h_{\mathrm{II}}=0{\cdot}0013$ cal./cm.$^2$ sec. °C., whereas according to data given in the literature for free convection on thin cylinders $h_{\mathrm{I}}=0{\cdot}0003$ only. That the heat transfer in a narrow tube is so much better is caused by the fact that the active temperature difference is concentrated to a much smaller distance in this case.

It may be mentioned that the small amount of heat given up by the tube $b$ to the wire has been neglected in deriving equation (22) for $\theta_{\mathrm{II}}$.

---

* The very small amount of radiation between the non-insulated wire and the wall has been neglected.

One can take, further, $h_{\mathrm{II}}=h_{\mathrm{III}}$ and $k_{\mathrm{I}}=k_{\mathrm{II}}=k_{\mathrm{III}}$, and for the copper tube $k_b=0{\cdot}9$ cal./cm. sec. °C. With these values we obtain $m_{\mathrm{I}}=0{\cdot}22$ cm.$^{-1}$, $m_{\mathrm{II}}=m_{\mathrm{III}}=0{\cdot}46$ cm.$^{-1}$, and $m_b=0{\cdot}05$ cm.$^{-1}$.

Substituting the above values in the equations (27) to (30), one finds $\theta_0=72{\cdot}0°$ C., $\theta_1=49{\cdot}5°$ C., and from equation (26) $\theta_2=74{\cdot}41°$ C. Therefore one would measure a temperature 0·6° C. too low by the thermometric arrangement described.

Putting $x_1=0$ one has the case without a protective tube $b$. This leads to $\theta_0=\theta_1=48{\cdot}3°$ C. and to $\theta_2=69{\cdot}76°$ C., a temperature too low by 5·2° C. This shows how wrong it would be to omit the protective tube $b$ in this case as often is done in thermoelectric measurements.

If one would have neglected the influence of the finite length, as has been done in equations (16) and (17), one would have found $\theta_0=72{\cdot}74°$ C., $\theta_1=43{\cdot}7°$ C., and $\theta_2=74{\cdot}77°$ C. with protective tube, and $\theta_0=\theta_1=50{\cdot}70°$ and $\theta_2=72{\cdot}57°$ C. without it, *i. e.*, much too favourable values. This, of course, comes from neglecting the fact that according to equation (25) only a very small amount of heat is transferred from block $a$ to the inside end of the wire, if this does not touch the block. Indeed it follows from this equation that the coefficient of heat transfer at the inner free end of the wire would have to be 0·113 or 0·115, in the cases with or without protective tube respectively, instead of the value $h_{\mathrm{III}}=0{\cdot}0013$ cal./cm.$^2$ sec. °C., if by the free end that heat energy should be picked up which is required for the heat balance according to equations (16) and (17).

Since filling the hole of block $a$ and tube $b$ by a liquid is not desirable with thermocouples, one would have to replace the copper wire by a less good conductor, *e. g.*, iron, and to choose wires thinner than 0·05 cm., or to take $x_1$ and $x_2$ longer, in order to reduce the error of temperature measurement revealed by the above calculations.

At all events, for exact thermometric measurements the probable error should be calculated by means of equations (26) to (30). These equations appear complicated, but are simple in numerical evaluation. Considering the most favourable effect of a protective tube, one must consider also whether this does not affect sensibly the temperature of the main body which has to be measured.

## *References.*

(1) D. R. Harper and P. W. Brown. Techn. Rep. no. 158 of the National Advisory Committee for Aeronautics, 1922, p. 677.
(2) M. Jakob, S. Erk, and H. Eck, *Physik Zeitschr* xxxvi. p. 73 (1935).

# LV. *Note on a Problem in the Conduction of Heat.*

By C. J. TRANTER, B.A.*

[Received December 9, 1938.]

ALTHOUGH problems in the conduction of heat from one medium to another of different material have been treated by various writers (and, in particular, by Carslaw † by his method of contour integrals), yet very little attention appears to have been given to those in which initial temperature discontinuities at the boundaries occur. It is the purpose of this note to show that a method essentially similar to that of Carslaw will deal with this type of problem.

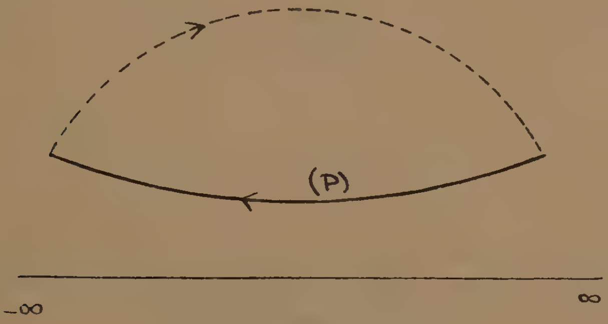

The path (P), in the $\alpha$-plane.

The solution to such problems seems to have considerable application to physical science. Actually, in point of fact, the problem arose from the case of a thermo-junction placed in a gas which suddenly expands, in which case there will be an initial temperature discontinuity at the boundary. Examples of this sort can be multiplied—a soldering-iron in contact with solder, a mercury thermometer in contact with the hand, the hot gaseous products in contact with the walls of a gun or engine cylinder. It is intended, however, to deal with more specific problems of this type at a later stage, and, in this note, the method is only illustrated by two examples in linear flow.

---

* Communicated by the Author.

† 'Introduction to the Mathematical Theory of the Conduction of Heat in Solids,' by H. S. Carslaw, 1921. Chap. xi.

The difference in the present method from that used by Carslaw is that one of the functions assumed for the temperature contains a term $\Phi e^{-k\alpha^2 t}$, where $\Phi$ is the initial temperature difference between the media, $k$ is the diffusivity of the medium at temperature $\Phi$, $t$ is time, and $\alpha$ is the complex variable. The assumed temperature functions are then made to satisfy the conditions obtaining at the surfaces of separation of the media, and the constants in them obtained in terms of $\Phi$. On integration along the path (P), shown in the figure, it will be found that functions have been obtained which satisfy all the conditions of the problem.

*Example I.—Two Semi-Infinite Solids of Different Materials in contact along the Plane $x=0$. Initial Temperature $\Phi$ for $x<0$, and Zero for $x>0$.*

It is assumed that, for the region $x<0$, the thermal conductivity, diffusivity, specific heat, density, and temperature are $K_1$, $k_1$, $c_1$, $\rho_1$, and $v_1$ respectively, while for the region $x>0$ the corresponding quantities are $K_2$, $k_2$, $c_2$, $\rho_2$, and $v_2$.

In this case $v_1$ and $v_2$ must satisfy the differential equations of conduction, viz.,

$$\frac{\partial v_1}{\partial t}=k_1\frac{\partial^2 v_1}{\partial x^2} \qquad (x<0), \quad \ldots \ldots \quad (1)$$

$$\frac{\partial v_2}{\partial t}=k_2\frac{\partial^2 v_2}{\partial x^2} \qquad (x>0). \quad \ldots \ldots \quad (2)$$

When $t=0$,

$$v_1=\Phi \qquad (x<0), \quad \ldots \ldots \quad (3)$$

$$v_2=0 \qquad (x>0). \quad \ldots \ldots \quad (4)$$

For all values of $t$,

$$\left.\begin{aligned} v_1&=v_2, \\ K_1\frac{\partial v_1}{\partial x}&=K_2\frac{\partial v_2}{\partial x}\,; \end{aligned}\right\} \text{ when } x=0. \quad \ldots \quad (5)$$

We assume for $v_1$ and $v_2$ the following expressions,

$$v_1=(A_1e^{-i\alpha x}+\Phi)e^{-k_1\alpha^2 t},$$

$$v_2=A_2e^{i\alpha\mu x-k_1\alpha^2 t},$$

where $\mu=\sqrt{\frac{k_1}{k_2}}$ and $A_1$, $A_2$ are constants.

These expressions satisfy equations (5), provided

$$A_1+\Phi=A_2,$$

$$-K_1A_1=K_2\mu A_2,$$

giving
$$A_1=-\sigma\Phi/(1+\sigma),$$
$$A_2=\Phi/(1+\sigma),$$
where
$$\sigma=K_2\mu/K_1.$$

Consider the integrals

$$\left.\begin{aligned} v_1&=\frac{\Phi}{i\pi}\int\left[1-\frac{\sigma}{1+\sigma}e^{-i\alpha x}\right]\frac{e^{-k_1\alpha^2t}}{\alpha}d\alpha,\\ v_2&=\frac{\Phi}{i\pi(1+\sigma)}\int e^{i\alpha\mu x}\frac{e^{-k_1\alpha^2t}}{\alpha}d\alpha,\end{aligned}\right\}\quad\ldots\ldots\quad(6)$$

taken along the path (P).

It is known that *

$$\frac{\Phi}{i\pi}\int\frac{e^{-k_1\alpha^2t}}{\alpha}d\alpha=\Phi,$$

and it is now clear that the integrals assumed for the temperatures satisfy the differential equations (1) and (2), while, from the manner in which they have been built up, they must satisfy the boundary conditions (5).

It can also be shown that *, provided $x>0$,

$$\frac{1}{i\pi}\int\frac{e^{i\alpha x}}{\alpha}d\alpha=0,$$

and so, when $t=0$,

$$v_1=\Phi,$$
$$v_2=0.$$

Hence the integrals (6) satisfy all the conditions of the problem.

These expressions can be put into a form suitable for numerical work in the following way:

$$\frac{1}{i\pi}\int e^{i\alpha x}\frac{e^{-k\alpha^2t}}{\alpha}d\alpha=1-\Theta\left(\frac{x}{2\sqrt{(kt)}}\right);$$

where
$$\Theta(x)=\frac{2}{\sqrt{\pi}}\int_0^x e^{-\xi^2}d\xi\ *.$$

Hence,

$$v_1=\frac{\Phi}{1+\sigma}\left[1-\sigma\Theta\left(\frac{x}{2\sqrt{(k_1t)}}\right)\right],$$
$$v_2=\frac{\Phi}{1+\sigma}\left[1-\Theta\left(\frac{\mu x}{2\sqrt{(k_1t)}}\right)\right],$$

where

$$\mu=\sqrt{\frac{k_1}{k_2}},\quad\text{and}\quad\sigma=\frac{K_2\mu}{K_1}=\sqrt{\frac{K_2c_2\rho_2}{K_1c_1\rho_1}}.$$

---

* Carslaw, *loc. cit.* p. 202.

*Example II.—Semi-Infinite Slab of thickness 2a, initially at Temperature Φ, placed in an Infinite Medium of Different Material, initially at Temperature Zero.*

With a similar notation, the differential equations and boundary conditions are

$$\frac{\partial v_1}{\partial t}=k_1\frac{\partial^2 v_1}{\partial x^2} \qquad (-a<x<a). \quad \ldots \ldots \quad (1)$$

$$\frac{\partial v_2}{\partial t}=k_2\frac{\partial^2 v_2}{\partial x^2} \qquad \begin{pmatrix} x>a \\ x<-a \end{pmatrix}. \quad \ldots \ldots \quad (2)$$

When $t=0$,

$$v_1=\Phi \qquad (-a<x<a), \quad \ldots \ldots \quad (3)$$

$$v_2=0 \qquad \begin{pmatrix} x>a \\ x<-a \end{pmatrix}. \quad \ldots \ldots \quad (4)$$

For all values of $t$,

$$\left.\begin{aligned} v_1&=v_2 \\ \mathrm{K}_1\frac{\partial v_1}{\partial x}&=\mathrm{K}_2\frac{\partial v_2}{\partial x} \end{aligned}\right\}, \text{ when } x=\pm a. \quad \ldots \ldots \quad (5)$$

Here we assume for $v_1$ and $v_2$

$$v_1=[\mathrm{A}_1(e^{i\alpha x}+e^{-i\alpha x})+\Phi]e^{-k_1\alpha^2 t} \qquad (-a<x<a),$$

$$v_2=\mathrm{A}_2 e^{i\alpha\mu x-k_1\alpha^2 t} \qquad (x>a),$$

$$v_2=\mathrm{A}_2 e^{-i\alpha\mu x-k_1\alpha^2 t} \qquad (x<-a).$$

These expressions satisfy equations (5), provided

$$\mathrm{A}_1(e^{i\alpha a}+e^{-i\alpha a})+\Phi=\mathrm{A}_2 e^{i\alpha\mu a},$$

$$\mathrm{K}_1\mathrm{A}_1(e^{i\alpha a}-e^{-i\alpha a})=\mathrm{K}_2\mu\mathrm{A}_2 e^{i\alpha\mu a},$$

giving

$$\mathrm{A}_1=\frac{-\sigma\Phi}{(1+\sigma)e^{-i\alpha a}-(1-\sigma)e^{i\alpha a}},$$

$$\mathrm{A}_2=\frac{e^{-i\alpha\mu a}(e^{-i\alpha a}-e^{i\alpha a})\Phi}{(1+\sigma)e^{-i\alpha a}-(1-\sigma)e^{i\alpha a}},$$

where

$$\sigma=\frac{\mathrm{K}_2\mu}{\mathrm{K}_1}.$$

Consider the following integrals

$$\left.\begin{aligned} v_1&=\frac{\Phi}{i\pi}\int\left[1-\frac{\sigma(e^{i\alpha x}+e^{-i\alpha x})}{(1+\sigma)e^{-i\alpha a}-(1-\sigma)e^{i\alpha a}}\right]\frac{e^{-k_1\alpha^2 t}}{\alpha}\,d\alpha, && (-a<x<a), \\ v_2&=\frac{\Phi}{i\pi}\int\frac{(e^{-i\alpha a}-e^{i\alpha a})e^{i\alpha\mu(x-a)}}{(1+\sigma)e^{-i\alpha a}-(1-\sigma)e^{i\alpha a}}\,\frac{e^{-ik_1\alpha^2 t}}{\alpha}\,d\alpha, && (x>a), \\ v_2&=\frac{\Phi}{i\pi}\int\frac{(e^{-i\alpha a}-e^{i\alpha a})e^{-i\alpha\mu(x+a)}}{(1+\sigma)e^{-i\alpha a}-(1-\sigma)e^{i\alpha a}}\,\frac{e^{-ik_1\alpha^2 t}}{\alpha}\,d\alpha, && (x<-a). \end{aligned}\right\}, \quad (6)$$

all the integrals being taken along the path (P).

As before, the expressions (6) satisfy the differential equations (1) and (2) and the boundary conditions (5).

The roots of the equation

$$(1+\sigma)e^{\ i\alpha a}-(1-\sigma)e^{i\alpha a}=0$$

are given by

$$\alpha=\frac{2n+1}{2a}\pi-\frac{i}{2a}\log_e\left(\frac{\sigma+1}{\sigma-1}\right),\quad \text{when } \sigma>1,$$

$$\alpha=\frac{n\pi}{\alpha}-\frac{i}{2a}\log_e\left(\frac{1+\sigma}{1-\sigma}\right),\qquad \text{when } 0<\sigma<1.$$

There are no poles of the integrands within the area bounded by the path (P) and the arc of a circle of infinite radius and with centre at the origin, shown dotted in the figure.

We can thus show that, when $t=0$,

$$v_1=\Phi,$$

$$v_2=0,$$

and the integrals (6) therefore satisfy all the conditions of the problem.

These results can be put into infinite series by expanding the integrands and expressing the resulting contour integrals in terms of Error Functions. The results are

$$v_1=\frac{\sigma\Phi}{1+\sigma}\sum_{n=0}^{\infty}y^n\left\{\Theta\left(\frac{2n+1a+x}{2\sqrt{(k_1t)}}\right)+\Theta\left(\frac{\overline{2n+1}a-x}{2\sqrt{(k_1t)}}\right)\right\},\quad (-a<x<a),$$

$$v_2=\frac{\Phi}{1+\sigma}\left[\Theta\left\{\frac{\mu(a-x)}{2\sqrt{(k_1t)}}\right\}+\frac{2\sigma}{1+\sigma}\sum_{n=0}^{\infty}y^n\Theta\left\{\frac{\mu(x-a)+(2n+1)a}{2\sqrt{(k_1t)}}\right\}\right],$$

$$(x>a),$$

$$v_2=\frac{\Phi}{1+\sigma}\left[\Theta\left\{\frac{\mu(a+x)}{2\sqrt{(k_1t)}}\right\}-\frac{2\sigma}{1+\sigma}\sum_{n=0}^{\infty}y^n\Theta\left\{\frac{\mu(x+a)-(2n+1)a}{2\sqrt{(k_1t)}}\right\}\right],$$

$$(x<-a),$$

where

$$\mu=\sqrt{\frac{k_1}{k_2}},\quad \sigma=\sqrt{\frac{K_2c_2\rho_2}{K_1c_1\rho_1}},\quad \text{and}\quad y=\frac{1-\sigma}{1+\sigma}.$$

Military College of Science,
Woolwich.

# LVI. *Note on the Relative Intensity of Spectrum Lines.*

By F. H. Newman, D.Sc., Professor of Physics,
University College, Exeter *.

[Received September 1, 1939.]

A review of the literature on the influence of components in a mixture on spectrum line intensities reveals considerable divergence of opinion with regard to the magnitude of this effect. Under suitable conditions one element may markedly affect the intensity of the emission spectrum lines of another element in a mixture containing the two. There is the classical example of the effect of mercury on the neon spectrum, the addition of a trace of mercury in a neon tube causing nearly complete elimination of the usual neon lines. In the case of alloys Negresco † states that the introduction of a third metal in an alloy totally changes the sensitivity of the spectrum lines of the other two elements, and quotes the case of a copper alloy containing 10 per cent. of manganese and 0·1 per cent. of aluminium. In the observed spectrum the aluminium lines are practically suppressed. Van Someren ‡ reports a similar effect with 10 per cent. of silicon in an aluminium alloy, both causing a lower intensity in the impurity lines. Similarly Duffendack, Wolfe, and Smith § found that with nickel and nickel-copper alloys containing barium there was an appreciable effect of copper on the relative intensity of the barium lines. On the other hand, Smith || concludes from his work that in general the presence of other impurities, other than the one under investigation, has no effect upon the intensity of the lines due to that particular element. In most cases this statement seems justified for small quantities—less than 1 per cent.—although the effects depend upon the method of excitation. Twyman and Hitchen ¶ also concluded that, although many complex factors may take part in the influence of one element on the line intensities of another, this effect is not so great,

---

* Communicated by the Author.

† ‘Researches expérimentales d’analyse spectral quantitative sur les allinges métalliques,’ p. 46 (1912).

‡ Journ. Inst. Metals, vol. lv. p. 273 (1934).

§ Journ. Ind. Eng. Chem. vol. v. p. 226 (1339).

|| Trans. Farad. Soc. vol. xxvi. p. 101 (1930).

¶ Proc. Roy. Soc. A, vol. cxxxiii. p. 72 (1931).

but that a direct examination of the unknown substance will give the concentration of the constituents to a first approximation.

Duffendack, Wiley, and Owens * divide the relative intensity effect of an element into two types. First there is what may be termed the solution characteristic, and second the effect which depends upon interactions in the vapour state with the arc or spark. Thus sodium, potassium, and magnesium suppress certain elements when compared with cadmium, while calcium enhances the intensities of the potassium and magnesium lines with respect to those of cadmium. Again, negative ions are known to have some effect on line intensities, *e. g.*, the chloride ion will increase the line intensity without changing the relative intensities, whereas sulphate and phosphate ions cause a decrease in intensities without an appreciable change in relative intensities. In some cases, such as the chlorides of the alkaline earth metals, a considerable amount of the element is excited as the calcium, strontium, or barium subhalide, to give the corresponding diatomic band spectra, and a portion of the same metal is excited, in the low temperature arc, as the oxide rather than the element.

The relative intensities of spectrum lines of the constituent gases in a mixture vary with the total gas pressure in the discharge-tube, even though the ratio of the partial pressures remains the same. There is, of course, the additional trouble of "clean up," *i. e.*, some gases are adsorbed on the walls as the discharge proceeds to a greater extent than others, and this effect changes the relative amounts of the constituents, but in addition there are very marked variations in the line intensities of certain gases resulting from changes in the amount of a second gas. Such an effect is particularly marked when helium, or another of the rare gases, is present. Hydrogen and oxygen specially cause a marked decrease in the intensities of the helium lines, and the relative intensities of the lines of other elements with respect to those of helium will vary with the amount of other gases present at the same time.

Wolfe and Duffendack † found that when a small amount of argon was introduced into helium the intensities of the argon lines remained remarkably constant even when considerable amounts of other gases were added to the mixture, such as hydrogen, nitrogen, oxygen, and carbon monoxide, each to a partial pressure of 2 mm. The intensity of the helium lines did not remain constant. Here again the effects vary with the pressures. For example, with argon at 0·08 mm. pressure and helium at 2 mm.

---

* Journ. Ind. Eng. Chem. vol. vii. p. 40 (1935).

† 'Proc. Sixth Summer Conference on Spectroscopy and its Applications,' p. 66 (1939).

the intensities of the argon lines varied with the amount of test gas present.

Summarizing these results, the relative intensities of spectrum lines of mixture components depend upon (*a*) the intrinsic characteristics of elements such as their ionization and resonance potentials, (*b*) their partial vapour pressures at different temperatures and the total vapour pressure, (*c*) the nature of the impressed electromotive force, its value and the current density, (*d*) the proportion of the constituents.

Some workers have suggested the possibility of establishing an ordered arrangement of elements much as in an electromotive series, in which the order follows the ionization potentials, with the indication that any element might have its lines depressed or enhanced by elements above or below it in the series. There appear to be numerous exceptions to this order.

Recently the author has examined the relative intensities of the spectrum lines of alkali amalgams, and in all cases the following general results have been obtained :—

(*a*) In the electrical discharge the emission lines of the alkali component show a marked relative increase in intensity—as the temperature of the amalgam is increased—compared with the mercury lines.

(*b*) At constant temperature, and with an uncondensed discharge, the alkali lines are relatively strong compared with those of mercury, but with the condensed discharge it is possible to suppress the alkali spectra, leaving only the mercury lines. This is true for all relative proportions of alkali and mercury in the amalgams.

Unfortunately very little is known about the relative vapour pressures of the components of alkali amalgams. Pedder and Barratt * have measured such partial pressures in the case of potassium amalgam, and the results are interesting. In the first place, whatever the percentage composition of the amalgam the total vapour pressure is always less than that of pure mercury at the same temperature. Thus at 300° C. the total vapour pressure of an amalgam containing 1·98 per cent. of potassium by weight is 179 mm., whereas the vapour pressure of pure mercury at this temperature is 248·5 mm. Again, at 387·5° C., with an amalgam containing 12·75 per cent. of potassium, the partial vapour pressure of mercury is 26·7 mm. and that of potassium 0·37 mm., whereas the vapour pressures of the pure metals at this temperature are, mercury 1280 mm., potassium 3·25 mm. Thus, although the partial pressure of the potassium increases with temperature, it decreases relatively with respect to the mercury vapour pressure. The effect of temperature on the relative intensity of the alkali lines thus appears to depend upon the total pressure and not upon the partial pressures.

---

* Journ. Chem. Soc. p. 537 (1933).

When we come to consider the effect of the condensed and uncondensed discharges upon the relative intensity of the lines it must be remembered that in the uncondensed discharge each break in the primary circuit gives a series of secondary discharges. The first of these has a peak potential very much greater than the succeeding ones, whereas in the case of a condensed discharge, *i. e.*, with a condenser in parallel with the secondary spark gap, one break of the primary circuit gives rise to a series of discharges, the first of which has the highest peak voltage—about equal to that of the first of the uncondensed type—but all the other discharges, although of somewhat lower peak voltage than the first, have much higher peak values than the corresponding ones in the uncondensed discharge.

It is generally assumed that the electrons moving through a gas or vapour never acquire a velocity greater than that corresponding to the ionization potential, V, of the gas or vapour. This would only be true if it were probable that a molecule would be ionized in most of the collisions where the velocity of the electron corresponds to V. But there is no evidence to show that this is the case, as the experiments by which the ionizing potential V is found only indicate that ions are produced in appreciable numbers which may be small compared with the total number of collisions with molecules of the gas in which the electrons are moving with the velocity corresponding to V. There is no reason to suppose that they do not attain velocities greater than that corresponding to V. Molecules may also be affected by previous collisions, so that they are finally ionized by an electron of lower energy than V.

After the electron has left the dark space of the electrical discharge the electric force is small, and when the electron loses energy by ionizing an atom or molecule there is little force acting on it to increase its energy. Under these conditions the energy may be sufficient to ionize atoms or molecules of low ionization potential in a vapour mixture. So that, in spite of the comparatively small number of alkali atoms present in the vapour from an amalgam, the small energy of the electrons and probably of positive ions is sufficient to ionize them at the expense of the mercury atoms. Thus with the condensed discharge each pulse in a secondary discharge is of higher peak value than in the uncondensed type, so that at each pulse the mercury atoms are ionized, and thus the mercury lines are predominant with the condensed discharge. These experiments indicate the important rôle of the value of ionization potentials in enhancing spectrum lines of component vapours.

# LVII. *Note on the Effective Wave-length to be used in calibrating a disappearing Filament Optical Pyrometer.*

By F. A. Cunnold, M.A., D.Phil.*

[Received September 18, 1939.]

The disappearing filament pyrometer is in general use both for accurate high temperature measurements and determinations of high temperature melting-points. Most of the published work, however, deals only with standard melting-point determinations and not with calibrations of instruments to give the relation between the current through the filament and the temperature of the source. During such a calibration of a disappearing filament pyrometer designed by Milford, Bracey, Cunnold, and Egerton (1) at the Clarendon Laboratory, Oxford, a certain amount of discussion ensued concerning the true value to be assigned to the effective wave-length throughout the calibration. This paper embodies an examination of this question which does not seem before to have been quite sufficiently elaborated (2), (3), (4).

The starting-point for the calibration was, as usual, the temperature of melting gold (1336° K.), and extrapolation from this point was effected by means of rotating sectors and a tungsten strip-lamp. The formula for the extrapolation was derived from Wien's law, *i. e.*,

$$E_\lambda . d\lambda = C_1 \lambda^{-5} \epsilon^{-\frac{c_2}{\lambda T}},$$

where $E_\lambda$ is the spectral energy of the radiation from a black body at temperature T for a wave-length $\lambda$ and $C_1$ and $c_2$ are constants.

Thus the ratio of the spectral energies ($E_1$ and $E_2$) at any wave-length $\lambda$ of the radiation from two black bodies at temperatures $T_1$ and $T_2$ is,

$$\frac{E_1}{E_2} = e^{\frac{c_2}{\lambda}\left[\frac{1}{T_2} - \frac{1}{T_1}\right]}$$

whence

$$\log\left(\frac{E_1}{E_2}\right) = \frac{c_2}{\lambda}\left[\frac{1}{T_2} - \frac{1}{T_1}\right]. \quad \ldots \ldots \quad (a)$$

This equation is derived assuming that pure monochromatic radiation is used, but in the case of the optical pyrometer a band of wave-lengths is transmitted by the instrument. In this case, therefore, in place of the spectral energies $E_1$ and $E_2$ the "total luminous flux" $H_1$ and $H_2$

---

* Communicated by Prof. A. C. Egerton, F.R.S.

perceived by the eye become effective, and the "effective" wave-length ($\lambda_e$) for the extrapolation between black body temperatures $T_1$ and $T_2$ is defined by the relation

$$\log\left(\frac{H_1}{H_2}\right)=\frac{c_2}{\lambda_e}\left[\frac{1}{T_2}-\frac{1}{T_1}\right], \quad \ldots\ldots\ldots \quad (b)$$

which is identical with the foregoing equation (*a*) except that $H_1$ and $H_2$ replace $E_1$ and $E_2$ and $\lambda_e$ replaces $\lambda$ (3).

The total luminous flux (H) is clearly the product, for each wave-length, of the radiated energy ($b_{\lambda T}$), the relative visibility of that radiation ($V_\lambda$) and the transmission factor ($t_\lambda$) of the optical system of the pyrometer integrated over the visible range.

Thus, $$H=\int_0^\infty b_{\lambda T}.V_\lambda.t_\lambda d\lambda\,.$$

In all that follows the integral $\int_0^\infty b_{\lambda T}.V_\lambda.t_\lambda d\lambda$ will be denoted by "I," and a suffix (1, 2, . . .) added to denote that it is evaluated for temperatures $T_1$, $T_2$, . . . . Further, if the product is obtained using the energy distribution ($b_{\lambda T}$) corresponding to a black body an index "°" will be added. Thus $I_2^\circ$ represents the value of the integral for a black body source at temperature $T_2$.

The above expressions (*a*) and (*b*) are derived considering only black body radiation. The radiation from the filament of a pyrometer lamp is not, however, black, but since the material is tungsten and the range of wave-lengths in use small it may be assumed to be "grey" (5), (6). The relative energy distribution is therefore the same as that of black body radiation, and thus the actual energy radiated at any wave-length bears a constant ratio to the corresponding black body energy.

Thus, $$E_\lambda.d\lambda=gC_1\lambda^{-5}e^{-\frac{c_2}{\lambda T}},$$

where the constant "*g*" is introduced into Wien's formula on account of the greyness of the radiation.

Consider the pyrometer sighted on a black body at a fixed temperature (T), first with a sector of transmission factor $\tau$ interposed and second without the sector. Let the filament be matched in both cases with the image of the black body, and let its apparent black body temperatures (or colour temperatures) be $T_1$ and $T_2$ respectively under these circumstances. If the corresponding brightness temperatures of the filament are $S_1$ and $S_2$ then, from (*b*),

$$\log\left(\frac{H_1}{H_2}\right)=\log\tau=\frac{c_2}{\lambda_e}\left[\frac{1}{S_2}-\frac{1}{S_1}\right],$$

where $\lambda_e$ is the unknown effective wave-length.

The conditions of matching are such that

$$\frac{1}{\tau}\,I_1=I_2,$$

since both are equal to the product of I° and the transmission factor of the optical system between the source and the plane of the pyrometer filament.

Since the radiation from the filament is grey,

$$I_1=g_1I^\circ_1 \quad\text{and}\quad I_2=g_2I^\circ_2.$$

The spectral distributions of the energies ($E_1$ and $E_2$) in the radiation from the filament in the two cases are given by

$$E_1.d\lambda=g_1C_1\lambda^{-5}e^{-\frac{c_2}{\lambda T_1}}$$

and

$$E_2d\lambda=g_2C_1\lambda^{-5}e^{-\frac{c_2}{\lambda T_2}},$$

whence

$$\frac{E_1}{E_2}=\frac{g_1}{g_2}e^{-\frac{c_2}{\lambda}\left[\frac{1}{T_2}-\frac{1}{T_1}\right]}, \quad \ldots\ldots \quad (c)$$

but for the effective wave-length $\lambda_e$

$$\frac{E_1}{E_2}=\frac{H_1}{H_2}=\frac{I_1}{I_2}=\frac{g_1I^\circ_1}{g_2I^\circ_2};$$

substituting this value of $E_1/E_2$ in equation (*c*) we find

$$\frac{I^\circ_1}{I^\circ_2}=e^{\frac{c_2}{\lambda_e}\left[\frac{1}{T_2}-\frac{1}{T_1}\right]},$$

whence

$$\lambda_e=\frac{c_2\left[\frac{1}{T_2}-\frac{1}{T_1}\right]}{\log\frac{I^\circ_1}{I^\circ_2}}.$$

This relation is the same as that derived by Foote (3) in considering the effective wave-length to be used when extrapolating between black body temperatures $T_1$ and $T_2$, assuming that the pyrometer filament is maintained at a constant temperature. In that case the true temperatures of the source $T_1$ and $T_2$ were to be used in the formula, but in the expression derived above the temperatures $T_1$ and $T_2$ are not the *true* temperatures of the filament but the *colour* temperatures.

Thus the effective wave-length $\lambda_e$ to be used in the extrapolation formula $\log\tau=\frac{c_2}{\lambda_e}\left[\frac{1}{S_2}-\frac{1}{S_1}\right]$ is that which is effective between the colour temperatures of the pyrometer filament; so that, when a pyrometer is calibrated in terms of the current through the filament, the effective wave-lengths to be used are obtained from the standard expressions, except that the colour temperatures of the filament must be the temperature values used.

Measurements of brightness temperatures of a source made with a pyrometer are then entirely independent of the optical properties of that source except in so far as the brightness temperature of the source controls the brightness, and hence the colour, temperature of the filament for matching. The brightness temperature of the source so found is measured in terms of that wave-length which is effective between the colour temperatures of the source and the filament.

In conclusion, I should like to thank Professor A. C. Egerton for his assistance and valuable comments during the preparation of this paper.

### *References.*

(1) Milford, Bracey, Cunnold, and Egerton, J. Sci. Inst. xii. p. 80 (1935).
(2) Hyde, Cady, and Forsythe, Astroph. J. xlii. p. 294 (1915).
(3) Foote, Bur. Stand. Bull. xii. p. 483 (1916).
(4) Ribaud, ‘Traité de Pyrometrie Optique’ (1931), chapter 12.
(5) Hyde, Astroph. J. xxxvi. p. 114 (1912).
(6) Ribaud, *loc. cit.* para. 90.

# LVIII. *Note on Synchronizing "Clocks" in a Moving System by a Connecting Spindle.*

By ALBERT EAGLE, B.Sc., A.R.C.Sc., Lecturer in Mathematics in the University of Manchester *.

[Received April 3, 1939.]

IN a recent short paper † I stated that two clocks in a system moving through the ether could be synchronized by connecting them by a spindle which was driven by a master clock at its mid-point, and that this would give the same result as would be obtained if they *could* be synchronized by means of signals sent from one to the other which travelled with an infinite velocity.

I unconsciously thought that any distortion of the spindle would necessarily, like the Lorentz-FitzGerald contraction, be proportional to $\omega^2/c^2$, where $\omega$ is the angular velocity of the spindle and $c$ is the velocity of light, and so any error thereby could be made as small as we pleased by the simple expedient of running the spindle as slow as we pleased and gearing up to the clock faces. I find, however, that there is an error of the first degree in $\omega$ which cannot be so eliminated, and which makes necessary a modification of the method of synchronism given in my previous paper.

For simplicity of consideration let the spindle be a thin-walled cylinder of radius $a$ rotating with an angular velocity $\omega$, and let it be travelling with a velocity $u$ in the direction of its length. The resultant velocity of the particles of this spindle is $(u^2+a^2\omega^2)^{\frac{1}{2}}$ in a direction $\alpha=\tan^{-1}a\omega/u$ with its axis. Assuming, to avoid mathematical complication, and because this case is the only one of any possible practical interest, that $(u^2+a^2\omega^2)^2/c^4$ is negligible, there is a Lorentz-FitzGerald contraction in the ratio of 1 to $1-\frac{1}{2}(u^2+a^2w^2)/c^2$ in the direction $\alpha$ with the axis of the spindle. This will cause the generating lines of the cylinder, originally parallel to the axis, to become inclined at a small angle $d\theta$, say, to the axis. A very simple diagram will show immediately that

$$\cot(\alpha+d\theta)=[1-\tfrac{1}{2}(u^2+a^2\omega^2)/c^2]\cot\alpha$$

exactly; whence

$$d\theta=\tfrac{1}{2}\sin\alpha\cos\alpha.(u^2+a^2\omega^2)/c^2=\tfrac{1}{2}ua\omega/c^2.$$

---

[*] Communicated by the Author.

[†] Phil. Mag. xxvi. p. 410 (Sept. 1938).

So that at a distance $l$ along the spindle a point on the circumference will be lagging behind by $\frac{1}{2}lua\omega/c^2$. As the rotational velocity of the circumference is $a\omega$ the error in time caused by neglecting this twist of the spindle will be $\frac{1}{2}lu/c^2$ in a distance $l$.

Now this error is just half the error caused when we synchronize the two clocks by sending light signals which travel with a speed relative to the spindle of $c-u$ in one direction and a speed of $c+u$ in the opposite direction *. Hence we deduce the following method of synchronizing two clocks at a distance $l$ apart. Set the two clock dials to give the same reading before starting the rotation of the spindle. Then send a signal from the first clock at a time $t_1$; let an observer at the second clock note the time of its arrival, and let the signal after reflexion at the second clock arrive back at the first at a time $t_2$. Then the time $\frac{1}{2}(t_1+t_2)$ will be less than the second clock's reading when the signal arrived by $\frac{1}{2}lu/c^2$, which at once reveals the velocity $u$ of the system through the ether. If now we advance the reading of the second clock by the amount $\frac{1}{2}lu/c^2$ we shall obviously have succeeded in synchronizing the clocks as signals travelling with an infinite velocity would synchronize them. Few will deny that this last method of synchronizing would give "true synchronism." If therefore it is only *theoretically* obtainable it must be accepted as our definition of "true synchronism."

The time interval given by $\triangle t=\frac{1}{2}lu/c^2$ is far too small to make the experiment practicable. If we had a spindle rotating so rapidly that we could detect a time diffeernce of only $10^{-7}$ secs. on its circumference, then a spindle length of 180 km. (112 miles) would be required just to detect a velocity of 100 km./sec. through the ether. But this note is only concerned with theoretical considerations, and the method described does theoretically seem capable of giving the velocity of a system through the ether, and so of theoretically determining whether or not there *is* a stationary medium through which material systems move.

*Note added Sept. 5th,* 1939.—The following considerations show very illuminatingly the conditions under which any interference experiment could, or could not, detect the earth's motion through the ether.

Let a single atom radiating waves of period $\tau$ be at rest in the ether and be infinitely near the centre of a perfectly reflecting spherical surface of radius $a$. The reflected rays will form an image of the source also infinitely near the centre; and the direct and reflected waves will fill the sphere with stationary waves, the distance between the nodal surfaces being $c/2\tau$, except near the centre of the sphere. The path length from source to image, $2a$, is equal to $2a/c\tau$ wave-lengths.

---

* *Loc. cit.* p. 412.

Now let a similar radiating atom be moving with a velocity $u$ through the ether. At what surface must the wave which leaves a point P at any time be reflected so as to be focused at a point Q distant $2au/c$ from P? Obviously the surface is a *prolate* ellipsoid with P and Q as foci and of polar semi-axis $a$ and equatorial semi-axes $a(1-u^2/c^2)^{\frac{1}{2}}$.

It is easily found that the surface which, moving with a velocity $u$, will coincide with this ellipsoid at the times at which the wave meets various parts of it is the *oblate* ellipsoid of polar semi-axis $a(1-u^2/c^2)$ and equatorial semi-axes of $a(1-u^2/c^2)^{\frac{1}{2}}$.

If the period of the vibrating atom were unaltered by its motion, clearly this latter ellipsoid will be occupied by as many ellipsoidal nodal surfaces as was the original sphere; and so no interference experiment could possibly detect the existence of the notion.

But a spherical body of radius $a$ does not, on the Lorentz-Larmor classical electromagnetic theory, transform into this ellipsoid, but into one of polar semi-axis $a(1-u^2/c^2)^{\frac{1}{2}}$ and of equatorial semi-axes $2a$. If we want to have the original number of nodal surfaces inside this ellipsoid we must increase the wave-length in the ratio $(1-u^2/c^2)^{\frac{1}{2}}$ to 1; that is, the period of the atom's vibration must be increased in this ratio. Now this is exactly the increase predicted by the Lorentz-Larmor theory, and which has been brilliantly confirmed by Ives and Stilwell for hydrogen canal rays *.

Hence I must differ from Professor Dingle † and, like Dr. H. E. Ives ‡, regard the Michelson-Morley and the Kennedy-Thorndike experiments together as confirming *both* the predictions of classical electromagnetic theory.

It is, in passing, difficult to see how an atom's motion could affect its period of vibrations unless as the result of some dynamical interaction between the atom and the medium through which it moved.

It seems a pity that physicists had so little confidence in the L.-L. theory that when Einstein announced his "principle" that no experiments could detect motion through the ether it was received by them as something new. It is, I believe, only *optical* experiments which must necessarily fail and not *mechanical* experiments (as with a long shaft).

Professor Dingle (*loc. cit.* p. 698) dissents from the idea that the nul result of the Kennedy-Thorndike experiment can depend upon the change of rate of "clocks" (using relativity language), as no *times* were measured in that experiment; but a change of period of the light source can obviously cause an effect by altering the wave-length of the light between the mirrors *.

---

* J. Opt. Soc. Amer. xxviii. pp. 215–226 (1938).

† Phil. Mag. p. 693 (June 1939).

‡ J. Opt. Soc. Amer. xxvii. p. 180 (1937).

Professor Dingle's assertion that " the aberration of light . . . reveals only the relative motion of the Earth and star " (*loc. cit.* p. 700) is extraordinary. Consider a double star in which the visible component possessed exactly the same vector velocity at every moment as the earth. A fluctuation of the star's position through 186,000,000 miles would be imperceptible at stellar distances (spectroscopic observations being excluded), yet this star would obviously show the same constant of aberration as all other stars though its relative velocity to the earth was always zero. The fact is, that aberration gives directly the shape, size, and manner of description of the earth's orbit in the luminiferous ether; and *therefore the actual velocity of the earth through the ether except for some unknown initial velocity* which can be regarded as the velocity of the solar system through the ether.

Professor Dingle seems to forget that astronomical and optical observations are not the only facts which require the existence of a medium independent of matter. The earth alone contains about $7 \times 10^{49}$ atoms for each of which the postulation of a relatively fixed medium in which their electrons and protons can move, and which is independent of these electrons and protons seems, on Wave Mechanics ideas, to be necessary.

When it is reflected what a simple idea a fixed medium (*i. e.*, a three dimensional lattice work) through which electrons and protons move is, as well as how indispensable it seems to be for nearly all astronomical, optical, and physical facts, it seems rather perverse to think that because we have so far failed to find the earth's velocity through it there can be no such medium.

---

* Prof. Dingle criticizes Dr. Ives's explanation as involving the idea that *every conceivable* form of " clock " must change its rate in the same degree due to its motion ; but Dr. Ives, in talking about " clocks " without specifying their nature, is only doing what Einstein has taught physicists to do.

# LIX. *The Effect of Variable Specific Heat of Gases on the Quantities involved in Heat Transmission between Liquids and Gases.*

By W. J. Walker *.

[Received March 4, 1939.]

*Note.*—The following communication is offered as a contribution to the general analysis of the effects of variable specific heats of gases on thermodynamic quantities, in this case quantities involved in heat transmission problems.

---

There are many practical instances in which the computation of the heat flow between gases and liquids is required. The effect of variable specific heat of gases on other quantities, such as internal combustion engine efficiences, discharge of gases through pipes, orifices, or nozzles, etc., is well known and can assume proportions of no little magnitude, yet no analysis appears to have been published hitherto indicating the precise quantitative effect of variable specific heat on heat transmission between liquids and gases. The following analysis was made for the purpose of computations relating to steam production by hot gases and also relating to the heat energy content in exhaust gases from internal combustion engines, and may prove of some utility to others engaged in similar work.

In determining these quantitative effects of variable specific heat of gases it has been found that, for all practical purposes, it is sufficient to assume a law of linear variation of specific heat with temperature. In this analysis, therefore, the following relation is assumed:—

$$C=B+ST=B(1+\lambda T),$$

where C is the specific heat of the gas under the flow conditions holding, and B, S, and $\lambda$ are constants.

The general nature of the problem discussed here is that of heat transmission between hot gases and liquids through the walls of circular tubes separating the two media. There are three particular cases involved:—

*Case* 1.—Hot gases cooling while liquid is evaporating at constant temperature.

*Case* 2.—Parallel flow of liquid and gases, both media changing in temperature.

---

* Communicated by the Author.

*Case* 3.—Counter flow of liquid and gases, both media changing in temperature.

The following symbols are used in the analysis :—

$T_h$ is the temperature of the hot gases.
$T_c$ is the temperature of the liquid.
$A=\pi DL$ is area of transmitting tube surface.
K is heat transmission coefficient in heat units per unit area per degree difference in mean temperature between liquid and gases.

### *Case 1.—Hot gases cooling while liquid is evaporating at constant temperature.*

Here
$$KdA(T_h-T_c)=-C_hW_h\,dT_h\,; \quad \ldots\ldots \quad (1)$$
$$\therefore \quad A=\frac{BW_h}{K}\int_{T_{h_2}}^{T_{h_1}}\frac{(1+\lambda T_h)T_h}{T_h-T_c}, \quad \ldots\ldots \quad (2)$$
from which
$$A=\frac{BW_h(1+\lambda T_c)}{K}\log\frac{T_{h_1}-T_c}{T_{h_2}-T_c}+\frac{\lambda BW_h}{K}\left[\frac{T_{h_1}-T_c}{T_{h_2}-T_c}\right] \quad \ldots \quad (3)$$
But, from (1),
$$KT_mA=BW_h\left[(T_{h_1}-T_{h_2})+\frac{\lambda}{2}(T_{h_1}^2+T_{h_2}^2)\right],$$
where $T_m$ is mean temperature difference between liquid and gases.
$$\therefore \quad T_m=\frac{(T_{h_1}-T_{h_2})\left\{1+\frac{\lambda}{2}(T_{h_1}+T_{h_2})\right\}}{(1+\lambda T_c)\log\left(\frac{T_{h_1}-T_c}{T_{h_2}-T_c}\right)+\lambda\left(\frac{T_{h_1}-T_c}{T_{h_2}-T_c}\right)} \quad \ldots\ldots \quad (4)$$

Equations (3) and (4) are precise relationships, but since $\lambda=0\cdot0003$ approximately for most of the combustion gas mixtures, the second term on the right-hand side of (3) is, for all practical purposes, negligible. Hence we may write
$$T_m=\frac{(T_{h_1}-T_c)-(T_{h_2}-T_c)}{\log\frac{T_{h_1}-T_c}{T_{h_2}-T_c}}\left\{1+\lambda\left[\left(\frac{T_{h_1}+T_{h_2}}{2}\right)-T_c\right]\right\} \quad \ldots \quad (5)$$
as a first and close approximation. This is Grashof's formula, with the approximate variable specific heat correction in double brackets.

A graphical determination of $T_{h2}$ can be made from (3), but it is sufficiently approximate again to write
$$T_{h_2}=T_c+(T_{h_1}-T_c)e^{-k_1L}, \quad \ldots\ldots \quad (6)$$
where
$$k_1=\frac{\pi KD}{BW_h}(1-\lambda T_c).$$

*Case* 2.—*Parallel flow of liquid and gases, both media changing in temperature.*

Here
$$K\,(T_h-T_c)\,dA=C_cW_c\,dT_c=-C_h\,W_h\,dT_h\,; \quad \ldots\ldots \quad (7)$$

$$\therefore\quad A=\frac{BW_h}{K}\int_{T_{h_2}}^{T_{h_1}}\frac{(1+\lambda T_h)dT_h}{T_h+T_c}\quad \ldots\ldots \quad (8)$$

From (7)
$$C_cW_c(T_c-T_{c1})=BW_h\left[(T_{h_1}-T_h)+\frac{\lambda}{2}(T_{h_1}^2-T_h^2)\right];$$

$$\therefore\quad T_c=T_{c_1}+\frac{BW_h}{C_cW_c}[(T_{h_1}-T_h)+(T_{h_1}^2-T^2)]\,;$$

$$\therefore\quad T_h-T_c=\alpha+\beta T_h+\gamma T_h^2,$$

where
$$\alpha=-\left(T_{c_1}+\frac{BW_h}{C_cW_c}T_{h_1}+\frac{\lambda}{2}\frac{BW_h}{C_cW_c}T_{h_1}^2\right),$$

$$\beta=1+\frac{BW_h}{C_cW_c},\quad \text{and}\quad \gamma=\frac{\lambda}{2}\frac{BW_h}{C_cW_c}.$$

From (8)
$$A=\frac{C_cW_c}{K}\left(1-\frac{1}{\sqrt{\beta^2-4\alpha\gamma}}\right)\log\frac{T_{h_1}-T_{c_1}}{T_{h_2}-T_{c_2}}+\frac{2C_cW_c}{K\sqrt{\beta^2-4\alpha\gamma}}$$
$$\times\left[\log\frac{2\gamma T_{h_1}+\beta+\sqrt{\beta^2-4\alpha\gamma}}{2\gamma T_{h_2}+\beta+\sqrt{\beta^2-4\alpha\gamma}}\right] \quad \ldots\ldots \quad (9)$$

The second term on the left-hand side of this equation is relatively small and negligible. We may write, therefore, to a first and close approximation

$$A=\frac{C_cW_c(\beta-1)}{K\beta}\left\{1-\frac{2\alpha\gamma}{\beta(\beta-1}\right\}\log\frac{T_{h_1}-T_{c_1}}{T_{\,2}-T_{h_2}}. \quad \ldots \quad (10)$$

Now
$$\frac{\beta}{\beta-1}=1+\frac{C_cW_c}{BW_h}=\frac{(T_{c_2}-T_{c_1})+(T_{h_1}-T_{h_2})+\lambda/2(T_{h1}^2-T_{h_2})}{T_{c_2}-T_{c_1}},$$

and since
$$KT_mA=C_cW_c(T_{c2}-T_{c1}),$$

$$\therefore\quad T_m=\frac{(T_{h_1}-T_{c_1})-(T_{h_2}-T_{c_2})}{\log\dfrac{T_{h_1}-T_{c_1}}{T_{h_2}-T_{c_2}}}$$
$$\times\left\{1+\frac{\lambda}{\beta}\left[\left(\frac{T_{h_1}+T_{h_2}}{2}\right)-T_{c_1}+T_{h_1}(\beta-1)\right]\right\} \quad \ldots \quad (11)$$

to a first and close approximation.

Again, a graphical determination of $T_{h2}$ can be made from (9), but to a first and close approximation we have

$$T_{h_2}=T_{c_2}+(T_{h_1}-T_{c_1})e^{-k_2L}, \quad \ldots\ldots \quad (12)$$

where
$$k_2=\frac{\pi DK\beta}{C_cW_c(\beta-1)}\left\{1+\frac{2\alpha\gamma}{\beta(\beta-1)}\right\}.$$

*Case 3.—Counter flow of liquid and gases, both media changing in temperature.*

The analysis for this case is similar to that for Case 2, the formulæ derived being the same, except that here

$$\alpha=\left(\frac{BW_h}{C_cW_c}T_{h_2}+\frac{\lambda}{2}\frac{BW_h}{C_cW_c}T_{h_2}^2-T_{c_1}\right),$$

$$\beta=1-\frac{BW_h}{C_cW_c}, \text{ and } \gamma=-\frac{\lambda}{2}\frac{BW_h}{C_cW_c}.$$

It should be noted that all the equations have been derived in a form similar to the standard forms used in constant specific heat analysis, correction factors being incorporated to indicate directly the effect of variable specific heat.

## LX. *Notices respecting New Books.*

*The Fundamentals of Electro-Magnetism.* By E. GEOFFREY CULLWICK, Head of Department of Electrical Engineering, University of Alberta. [Pp. 352+diag. 145.] (Cambridge University Press. Price 18*s*.)

IN his introduction the author says that " the usual education of the electrical engineering student has been specially designed to make it difficult for him to grasp the essential unity and coherence of his subject." It is, of course, no new thing for teachers of electrical engineering to write books on electromagnetism, but Professor Cullwick sets out to present the phenomena of electro-magnetism as a natural extension of electro-statics, and to rid us of the physical reality of lines of force and the even more artificial unit pole. Chapter I., therefore, deals with the electrostatic field, and introduces the electric current as a true stream of moving electric charges. Chapter II. introduces magnetic flux by the definition $e=-\frac{d\phi}{dt}$, and so deduces the law of magnetic force.

In Chapter III. the magnetic field is given as a property of moving charges, the conception being that the field moves with the system of currents to which it is ascribed; thus (*a*) " an observer moving across a magnetic field observes an electric field "; (*b*) " a charge moving relative to an observer causes that observer to experience a magnetic field." With this definition the author is immediately in difficulty with the case of a solenoid rotating about its axis, a difficulty which he does not shirk, but relegates to fourteen pages of appendix. There follows a short treatment of a law of force between individual moving charges. The remainder of Chapter III. deals with the calculation of air-core magnetic circuits, and Chapter IV. with ferro-magnetism.

Chapter V. deals with the electro-magnetic wave and the use of vector potential, leading, on p. 285, to the general expression for the electric field at a point in space as the mutual force between charges due to (1) their positions, (2) their velocities, (3) their accelerations.

The book has two most excellent features: firstly, the numerous examples of all kinds, many worked out very fully and covering a wide range both of easy and difficult problems; secondly, the fact that the author has shirked none of those difficult cases which have always proved stumbling blocks. On the other hand, having hoped for a text-book which would supersede all other, I must—and here I purposely write in the first person—express a sense of disappointment at the way in which the author presents his story. There is too much controversy for a book of instruction and too much elementary matter if the book is intended to argue a point of view; nor do I think it was wise to add the distinction of two sets of electro-magnetic units, whatever may be the merits of the new set over the classical tradition. Moreover, in two cases the theory seems to have led to incorrect conclusions, namely, on p. 139 as to the force on a cathode-ray, and on p. 277 as to the magnetic effect of a rotating solenoid. I doubt if Professor Cullwick's point of view will commend itself to physicists, but his book should certainly be read and will be found stimulating by all teachers of electrical engineering.

E. L. E. WHEATCROFT.

---

[*The Editors do not hold themselves responsible for the views expressed by their correspondents.*]

Fig. 1.

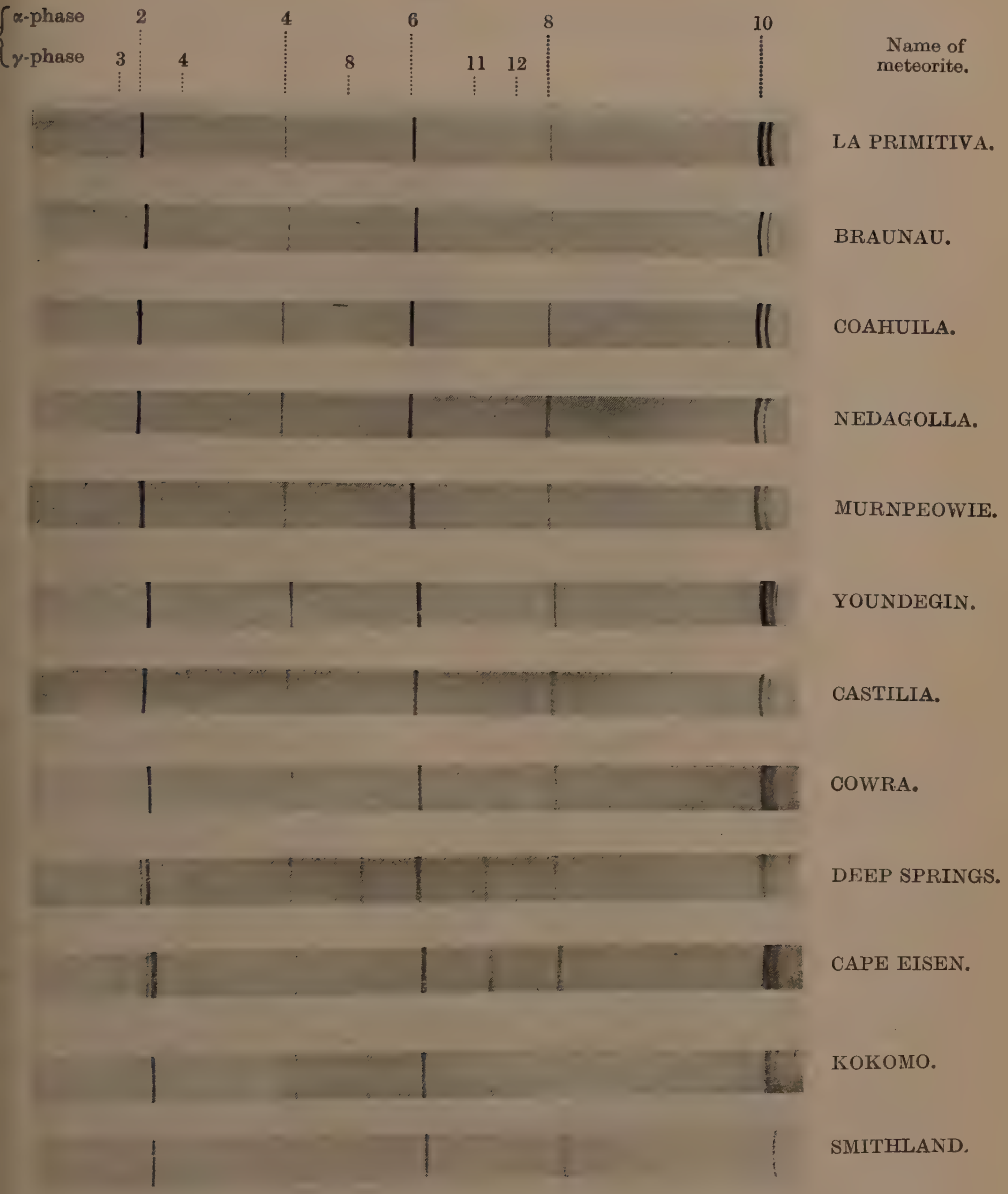
α-phase
γ-phase
2
4
6
8
10
3
4
8
11
12
Name of meteorite.
LA PRIMITIVA.
BRAUNAU.
COAHUILA.
NEDAGOLLA.
MURNPEOWIE.
YOUNDEGIN.
CASTILIA.
COWRA.
DEEP SPRINGS.
CAPE EISEN.
KOKOMO.
SMITHLAND.

Spectra obtained with meteorites annealed for 5 weeks at 350° C. and rapidly cooled.

FIG. 3.

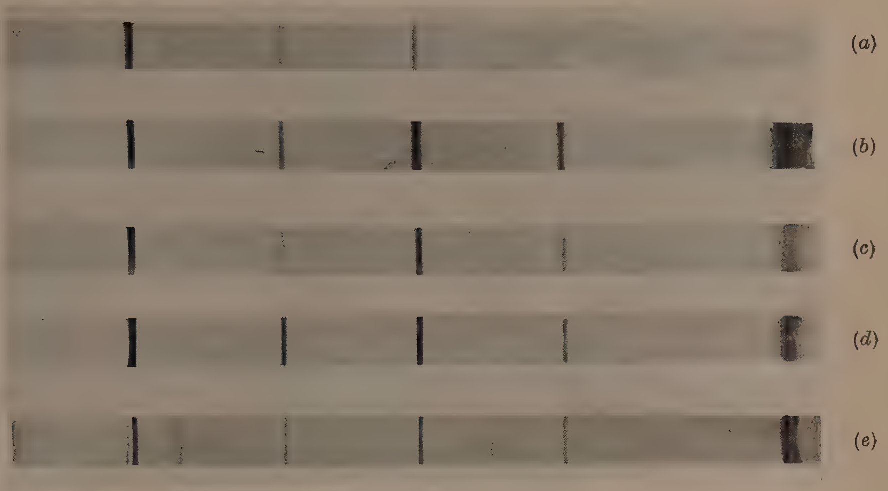

Babb's Mill meteorite.

(a) Unannealed.
(b) Annealed for 28 days at 250° C.
(c) Annealed for 56 days at 250° C.
(d) Annealed for 8 days at 300° C.
(e) Annealed for 56 days at 350° C.

FIG. 4.

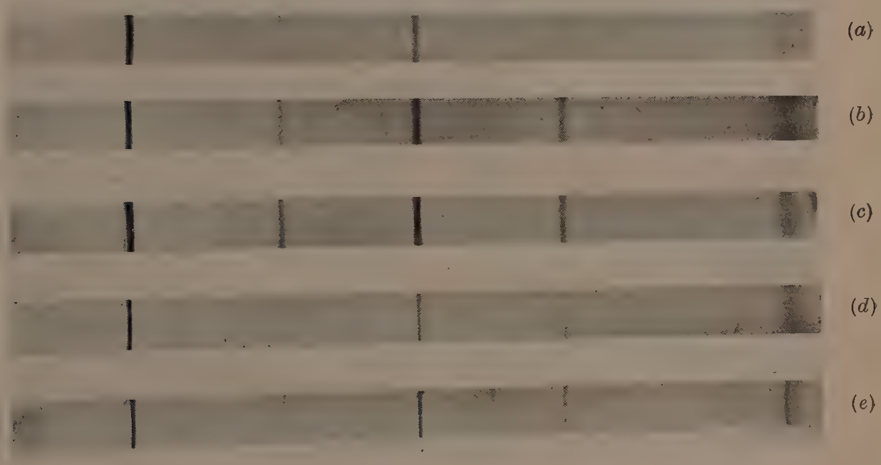

Klondyke meteorite.

(a) Unannealed.
(b) Annealed for 28 days at 250° C.
(c) Annealed for 56 days at 250° C.
(d) Annealed for 8 days at 300° C.
(e) Annealed for 28 days at 350° C.

Fig. 5.

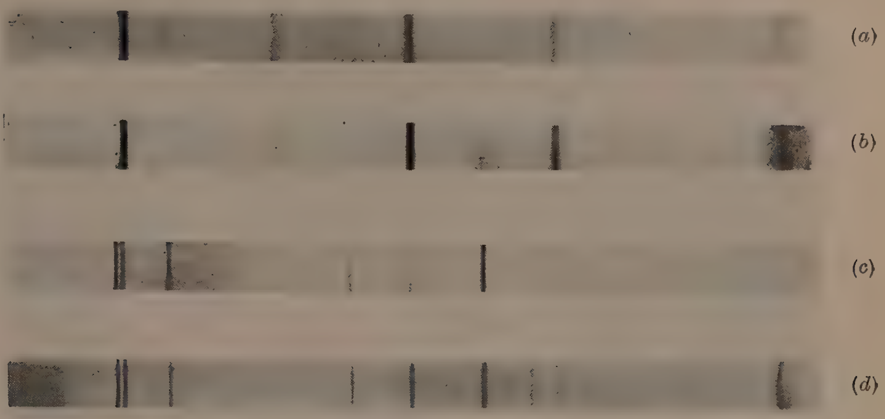

San Cristobal meteorite.

(a) Unannealed.
(b) Annealed for 28 days at 250° C.
(c) Annealed for 8 days at 300° C.
(d) Annealed for 28 days at 350° C.

Fig. 6.

Klondyke (specimen from interior of meteorite).

(a) Unannealed.
(b) Annealed for 8 days at 300° C.

Fig. 7.

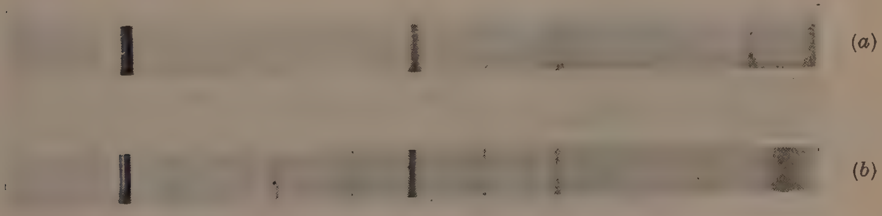

San Cristobal (specimen from interior of meteorite).

(a) Unannealed.
(b) Annealed for 14 days at 300° C.

Fig. 1.

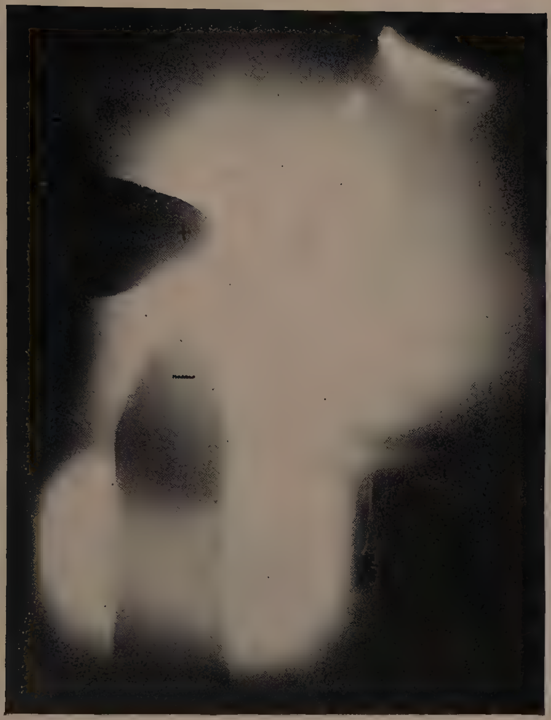

Fig. 2.

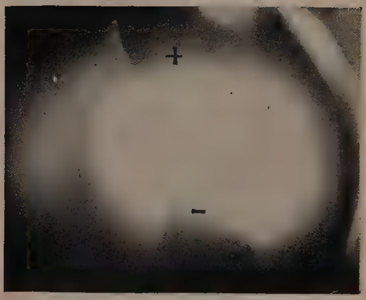

Fig. 3.

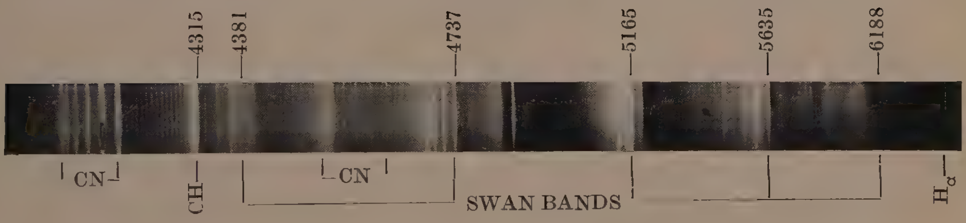

Fig. 4.

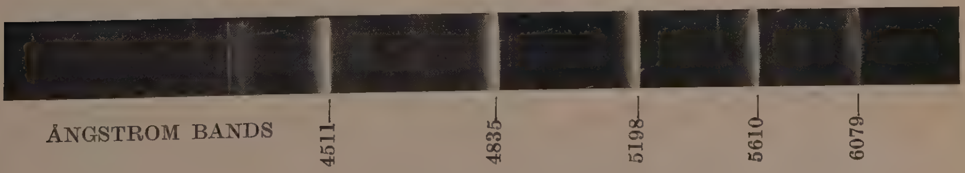

The carbon arc.

Figs. 1 & 2.—Initial stages of arc between carbon electrodes in a vacuum.
Fig. 3.—Spectrogram of radiation from arc.
Fig. 4.—Spectrogram of radiation from electric discharge under similar conditions.

# LXI. *The Magnetic Rotatory Dispersion and the Refractivity of Aqueous Solutions of Nickel Sulphate throughout the Range* 5780 Å. to 2482 Å; *especially the Magnetic Rotation in the* 3950 Å. *Absorption Band.*

By R. W. Roberts, D.Sc., and S. F. Adams, M.Sc.*

[Received February 28, 1939.]

## I. *Introduction.*

One of the interesting anomalies in the study of the Faraday effect of paramagnetic ions is that, whereas the rotations of the ions $Fe^{+++}$, $Fe^{++}$, and $Co^{++}$ are negative (1), (2), the rotation of the $Ni^{++}$ ion is positive, that is, in the same direction as the rotation produced by most diamagnetic substances. It is also known that the behaviour of the magnetic rotation of the $Co^{++}$ ion is distinctly anomalous in the neighbourhood of its absorption band at 5100 Å. (1), (3). But so far no corresponding measurements have been made for the $Ni^{++}$ ion in the immediate neighbourhood of its absorption bands.

In view of the apparent diamagnetic character of the rotation of the $Ni^{++}$ ion, it was thought that an extension of our previous work (1) on the magnetic rotation of nickel salts so as to include measurements in the violet absorption band would not be without interest.

We have made magnetic rotation measurements at 22·0° C. on two aqueous solutions of nickel sulphate throughout the range 5780 Å. to 2482 Å. and on six solutions for the line 3129 Å. In addition we have determined the dispersion of the refractivity of the solutions over the same range of wave-lengths for the purpose of interpreting the magnetic results.

## II. *The Solutions.*

The solutions were prepared from crystalline nickel sulphate of analytical reagent quality. Table I. gives the concentrations of the solutions in grammes, W, of the anhydrous salt per 100 grammes of solution, and the densities, $d$, of the solutions at the temperatures 18·0° C. and 22·0° C.

The concentrations of the solutions were deduced from the density-concentration data for nickel sulphate given in the International Critical Tables. For the interpolation, only the linear part of the $(d-1)/W$

---

* Communicated by the Authors.

against $(d-1)$ curve in the neighbourhood of the concentration of solution C was used. In the case of solutions A and B this necessitated dilution until the resulting concentrations were approximately the same as that of C.

Solutions D, E, F were derived from C by dilution ; their concentrations were determined from that of C and the weighings.

TABLE I.

W=Weight of Anhydrous Nickel Sulphate in 100 gm. of Solution.

| Solution. | W. | $d_4^{18\cdot 0}$. | $d_4^{22\cdot 0}$. |
|---|---|---|---|
| A ......... | 25·245 | 1·30970 | 1·30794 |
| B ......... | 18·707 | 1·21913 | 1·21774 |
| C ......... | 13·660 | 1·15329 | 1·15192 |
| D ......... | 7·310 | 1·07761 | 1·07646 |
| E ......... | 3·783 | 1·03870 | 1·03770 |
| F ......... | 1·917 | 1·01877 | 1·01849 |

## III. *Magnetic Rotation Measurements.*

Most of our measurements have been obtained by the photographic method of crossed nicols which has been investigated in detail by Bruhat and Pauthenier (4), and which we have previously found to be both accurate and free from systematic errors (5), (6). We shall refer to this method as method I.

For solution C we have carried out a second series of measurements, using the well-known method of the divided field. We shall refer to this as method II.

### *Method I.*

The details of this method have already been described. We shall confine our description to the alterations we have made.

Owing to the small effect expected in the neighbourhood of the absorption band, it was necessary to use very concentrated solutions. This in turn required the use of a high intensity mercury arc and the passage of a large flux of light through the optical system. To this end the quartz fluorite achromats of focal length 32 cm. previously used were replaced by ones of focal length 15 cm. To accommodate the beam a spectrograph (of greater aperture than that of our former spectrograph) was constructed in the laboratory.

The discarded quartz-fluorite achromats served as the collimator and telescope objectives of the new spectrograph. The mercury-vapour lamp used in our previous work was replaced by a more powerful model, which could be run at a current of 4 amp. on the 230-volt mains when suitably cooled by a small fan.

The constancy of the intensity of the arc was to a fair extent maintained, in spite of the variation of the mains voltage, with the aid of a photoelectric cell housed near the lamp and a rapidly adjustable resistance in series with the arc. This resistance was controlled by one of the observers, so that the galvanometer deflexion produced by the photoelectric current was, on the average, constant during the exposure.

Fig. 1 shows the essential parts of the apparatus. Light from the mercury-vapour lamp, used "end-on," passed out through the plane window W near the stop $S_1$ in the lamp-housing, and was focused by means of the lens $L_1$ on the stop $S_2$ at the focus of the quartz-fluorite achromat $L_2$, of 15 cm. focal length. After passing through the glycerine-cemented polariser P, the beam was limited by the stop $S_3$ and then passed through the slightly prismatic cell C supported in a definite position between the pole-pieces of a Du Bois electromagnet, the stop $S_4$, the glycerine-cemented analyser A, and the quartz-fluorite lens $L_3$ of 15 cm. focal length. At the focus of this lens was placed the slit $S_2'$ of the spectrograph. An image of the stop $S_4$ was focused by means of the lens $L_3$ on the collimating lens $S_4'$ of the spectrograph. To achieve this it was necessary to detach $L_3$ from the analyser circle.

Fig. 1.

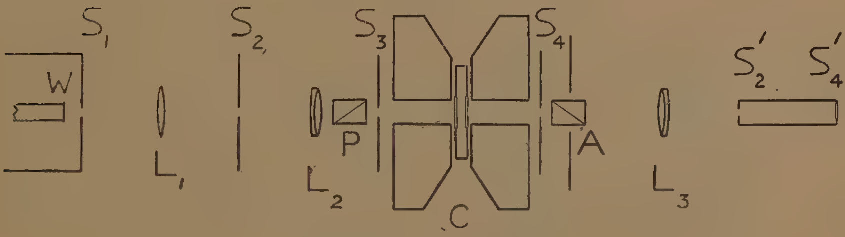

Diagram of apparatus.

Every care was taken that no undue amount of scattered light entered the spectrograph. The interior of the borings of the magnet was covered with matt-black paper. The resulting image produced in the spectrograph was carefully examined with the field excited, so that any spurious light superimposed on the main beam could be detected. Small tilts were given to both polariser and analyser to remove such spurious light. The cell containing the solution under test was sufficiently prismatic to prevent multiply reflected beams from passing through the narrow fixed slit of the spectrograph. The method of deducing the magnetic rotations from the photographic density measurements has already been described.

Table II. contains the results of our measurements expressed as Verdet constants. These are based on Rodger and Watson's value of 0·01308 min. per cm. Oersted for the Verdet constant of water at 22° C. for the mean wave-length 5893 Å., and the value 0·5162 for the ratio of the rotations of water for the wave-lengths 5893 Å. and 5461 Å. as found by Pierce and Roberts (6). Except for the line 2482·5 Å., the differences in the extinction settings of the analyser for the two directions of the current through the magnet agreed to a few hundredths of a degree for each wave-length. The mean value of the differences has been used in the deduction of the Verdet constant.

TABLE II.

Verdet Constants in min. per cm. Oersted at 22·0° C. for Solutions A and C and Water.

| λ in Å. | Solution. | | Water. |
|---|---|---|---|
| | A. | C. | |
| 5780 ..... | ·01661 | — | — |
| 5461 ..... | ·01872 | ·01704 | ·01538 |
| 4916 ..... | ·02378 | ·02151 | ·01942 |
| 4354·6 ... | ·03155 | ·02836 | ·02537 |
| 4046·6 .. | absorption | ·03374 | ·03003 |
| 3653·5 .. | ·04652 | ·04235 | ·03817 |
| 3341·4 ... | ·05855 | ·05295 | ·04740 |
| 3128·9 ... | ·06959 | ·06283 | ·05614 |
| 2803·4 ... | ·09462 | ·08477 | ·07526 |
| 2652·3 ... | ·11150 | ·09968 | ·08837 |
| 2482·5 ... | ·13710 | ·12216 | ·10766 |

The effective wave-lengths entered in the first column have been deduced with the aid of Lowry's tables (7) from observations on the natural rotation of a quartz end plate of thickness 1·92 cm.

### *Method II.*

It was our original intention to obtain numerous magnetic rotation readings throughout the violet absorption band using the wave-lengths of the iron arc. We adopted the usual method of observing rotations by the divided field method, and proceeded to find the azimuth of the analysing nicol which would yield equal intensities in the two halves of the field. This was obtained by interpolation from a graph in which the ratio of the densities of the two parts of the field was plotted against the analyser setting. The results obtained were not very satisfactory. As the solution C under test was rather strongly absorbing, it was necessary to use a current of about 11 amp. through the arc. This gave rise to a considerable amount of continuous radiation, which, with a spectroscope of small dispersion, is definitely harmful. After many trials with the iron arc we replaced it by the mercury arc. Much more satisfactory results were then obtained. These are given as Verdet constants in Table III.

Although this method has permitted us to obtain readings for wave-lengths in the absorption band, the results for other wave-lengths are not as accurate as those obtained by method I.

## IV. *Refractive Index Measurements.*

We have determined the refractive indices of our solutions and water by means of a modification of a method due to Fabry and Barot (8), which we have previously given and described (5). The accuracy of the determination of the refractive indices of the solutions is not as high as with water, as the temperature corrections were rather uncertain owing to the limited amount of the solutions available. The accuracy attained is, however, sufficient for the present purpose. As the method demands the use of a rather large prism, we have not been able to determine the refractive indices in the absorption band. The values of these indices have been obtained by extrapolation from the observed values of the indices outside the band.

TABLE III.

Verdet Constants in min. per cm. Oersted at 22·0° C. for Solution C (Method II).

| | | | | | |
|---|---|---|---|---|---|
| λ in Å....... | 5780 | 5461 | 4916 | 4358 | 4078 |
| V .......... | ·01503 | ·01702 | ·02153 | ·02824 | ·03323 |
| λ in Å....... | 4046·6 | 3906 | 3790 | 3653 | — |
| V .......... | ·03382 | ·03634 | ·03881 | ·04233 | — |

The results for the solutions A and C are given in Table IV.* From these values the molecular refractions of nickel sulphate have been calculated by means of the formula

---

* We intend to give the values of the refractive indices for water in a separate paper.

$$\frac{1}{d_4^{20}}\frac{n^2-1}{n^2+2}=\frac{1}{d_w^{20}}\left(1-\frac{W}{100}\right)\frac{n_w^2-1}{n_w^2+2}+\frac{W}{100}\frac{R}{M},$$

where

$n_w$ = refractive index of water at 20° C.
$n$ = „ „ solutions at 20·0° C.
R = molecular refraction of the anhydrous salt.
M = „ weight „ „ „

## Table IV.

Refractive Indices and Molecular Refractions at 20° C.

| λ in Å. | Refractive index. | | Molecular refraction. | | | |
|---|---|---|---|---|---|---|
| | A. | C. | A. | C. | Mean. | Calculated. |
| 5769·6 .... | 1·38721 | 1·36113 | 15·79 | 15·76 | 15·77$^5$ | 15·79$^5$ |
| 5460·72 ... | 1·38849 | 1·36229 | 15·83 | 15·80 | 15·81$^5$ | 15·82$^5$ |
| 4916·04 ... | 1·39129 | 1·36486 | 15·94 | 15·89 | 15·91$^5$ | 15·89$^5$ |
| 4358·3 .... | 1·39493 | 1·36850 | 15·98 | 15·99 | 15·98$^5$ | 16·00 |
| 3663·27 ... | absorption | 1·37578 | — | 16·21 | 16·21 | 16·21 |
| 3341·47 ... | 1·40817 | 1·38084 | 16·39 | 16·39 | 16·39 | 16·36 |
| 3131·70 ... | 1·41279 | 1·38516 | 16·50 | 16·49 | 16·49$^5$ | 16·49 |
| 2803·5 .... | 1·42291 | 1·39463 | 16·79 | 16·76 | 16·77$^5$ | 16·77 |
| 2652·07 ... | 1·42930 | 1·40066 | 16·96 | 16·93 | 16·94$^5$ | 16·95 |
| 2482·72 ... | 1·43846 | 1·40918 | 17·19 | 17·11 | 17·15 | 17·20 |

The values of R obtained from solutions A and C are given in the fourth and fifth columns of Table IV.

As the absorption bands of the solutions have not been located in the far ultra-violet, it is necessary to rely on hypothesis in order to account approximately for the dispersion. The most reasonable seems to be due to Heydweiller (9), who attributes a common frequency ($\nu_1$) to the loosely bound valency electrons and a second higher frequency ($\nu_2$) distributed among the remaining bound electrons in the molecule.

If the frequencies of the light are referred to a unit of time equal to $10^{-15}$ sec., then, according to Heydweiller, the refractivity R for frequency $\nu$ is given by

$$R=16{\cdot}280\ C_\nu,$$

where, in the case of nickel sulphate,

$$C_\nu = \frac{2}{\nu_1^2 - \nu^2} + \frac{74}{\nu_2^2 - \nu^2}.$$

We find from the mean value of the refractivities of solutions A and C

$$\nu_1^2 = 6{\cdot}364 \text{ and } \nu_2^2 = 115{\cdot}52.$$

The mean values of the refractivities of the two solutions and the values calculated from the above formula are given in the last two columns of Table IV. The agreement is satisfactory. The above values of $\nu_1$ and $\nu_2$ are approximately the same as the values obtained for a number of sulphates, so that these frequencies may be taken as characteristic of the $SO^{--}$ ion, the metal ion having little effect on the refractivity.

## V. *Absorption Data.* (Measurements by Dr. R. A. Morton.)

The absorption of a number of nickel salts in aqueous solution has been investigated by Houstoun and his co-workers $^{(10)}$. Their results show that there are absorption bands at ·405 $\mu$, ·690 $\mu$, and 1·21 $\mu$ in all the solutions of the nickel salts examined.

As our magnetic observations did not agree with the position of the violet absorption band given as ·405 $\mu$, Dr. R. A. Morton kindly investigated the absorption of our solution A. The results, relative to an absorption cell of thickness 1 mm., are given in fig. 2. The curve shows that the head of the absorption band in our solution is at ·395 $\mu$, about 100 Å. different from the position recorded by Houstoun. Incidentally it appears from the graph that the absorption band in the red has its maximum at ·720 $\mu$, and not at ·690 $\mu$ as stated above.

## VI. *The Analysis of the Observations.*

In order to obtain the contributions to the magnetic rotation of the solution due to the dissolved salt, it is necessary to take into account the contribution due to the water.

Neglecting interaction effects, theory shows that the difference

$$\Delta = \frac{n}{(n^2+2)^2}\frac{V}{d} - \frac{n_w}{(n_w^2+2)^2}\left(1 - \frac{W}{100}\right)\frac{V_w}{d_w},$$

where V and $V_w$ are the Verdet constants of the solution and water respectively, is a quantity characteristic of the salt. The quantity $\sigma = 900\ \Delta/W$ may be considered as an extension of the usual term specific rotation, and may therefore be called the "theoretical specific rotation." In the absence of interaction effects $\sigma$ should be constant. To test this in the case of nickel sulphate, we have determined the rotation of six solutions for the wave-length 3128·9 Å., which was transmitted well enough, even by the strongest solutions, to allow accurate measurements to be made. The results are given in Table V.

Fig. 2.

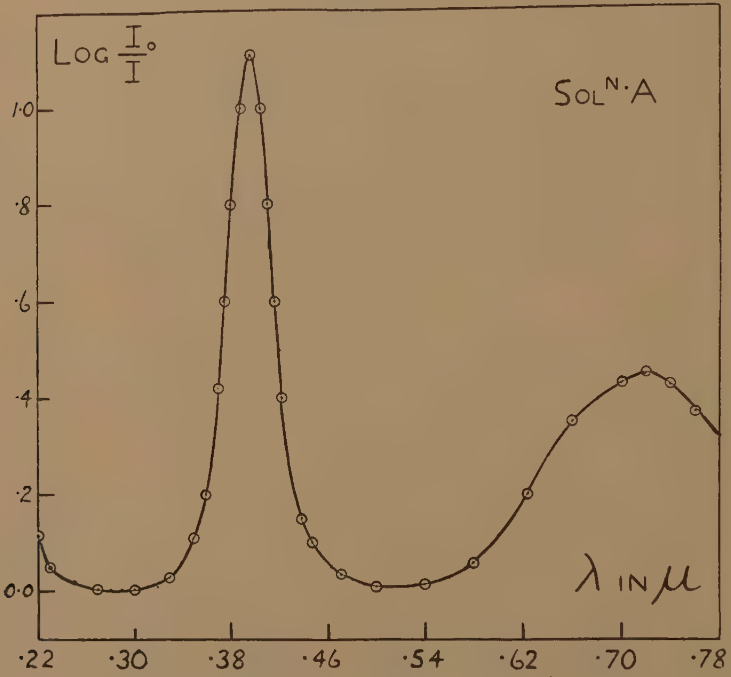

The absorption of nickel sulphate solution (A).

Table V.

Variation of $\Delta$ with W for λ 3128·9 Å.

| Solution. | V obs. | V calc. | $10^3 \times \frac{\text{V obs.}-\text{V calc.}}{\text{V obs.}}$ |
|---|---|---|---|
| A ....... | ·06959 | ·06962 | −0·4 |
| B ....... | ·06581 | ·06574 | +1·1 |
| C ....... | ·06283 | ·06288 | −0·8 |
| D ....... | ·05952 | ·05957 | −0·8 |
| E ....... | ·05793 | ·05788 | +0·9 |
| F ....... | ·05704 | ·05704 | 0·0 |

We find that the equation

$$\Delta=3{\cdot}3302\times10^{-5}\mathrm{W}-{\cdot}018305\times10^{-4}$$

represents the results to an accuracy of almost one in a thousand, as may be seen from the last column of Table V. It appears, therefore, that, for this wave-length at any rate, the interaction effects are not very great.

Table VI. gives the values of $\Delta/\mathrm{W}$ for the various wave-lengths for solutions A and C. It will be seen that these values are throughout greater for solution A than for solution C. It is probable that this increase in $\Delta/\mathrm{W}$ with increasing concentration, and the presence of the negative constant in the above formula, have their origin in the shift of the violet absorption band towards the red with increasing concentration.

TABLE VI.

Values of $\Delta/\mathrm{W}\times10^6$.

| λ in Å. | Solution. | | |
|---|---|---|---|
| | A. | C. | |
| | | Method I. | Method II. |
| 5780 ......... | 7·53 | — | 7·20 |
| 5461 ......... | 8·40 | 8·29 | 8·39 |
| 4916 ......... | 10·98 | 10·39 | 10·56 |
| 4358 ......... | — | — | 14·72 |
| 4354·6 ....... | 15·63 | 15·00 | — |
| 4078 ......... | — | — | 18·58 |
| 4046·6 ....... | — | 18·66 | 19·13 |
| 3906 ......... | — | — | 18·59 |
| 3790 ......... | — | — | 18·78 |
| 3653·5 ....... | 20·64 | 20·48 | 20·59 |
| 3341·4 ....... | 27·58 | 27·37 | — |
| 3128·9 ....... | 33·16 | 32·88 | — |
| 2803·4 ....... | 47·42 | 46·59 | — |
| 2652·3 ....... | 56·33 | 55·15 | — |
| 2482·5 ....... | 71·14 | 70·45 | — |

The values $\Delta/\mathrm{W}$ are plotted against the wave-length in fig. 3. The curve shows that the magnetic rotation in the neighbourhood of the violet absorption band is distinctly asymmetric.

To determine the rotation due to this band, it is necessary to take into account the effect on the rotation due to the ultra-violet absorption bands. As a first approximation, this effect can be represented by a term $A_1'\nu^2/(\nu_1'^2-\nu^2)^2$, where $A_1'$ is a constant and $\nu_1'$ is the effective frequency of the ultra-violet absorption bands. The values of $A_1'$ and $\nu_1'$ can be found from the observed values of $\Delta/W$ for wave-lengths far from

Fig. 3.

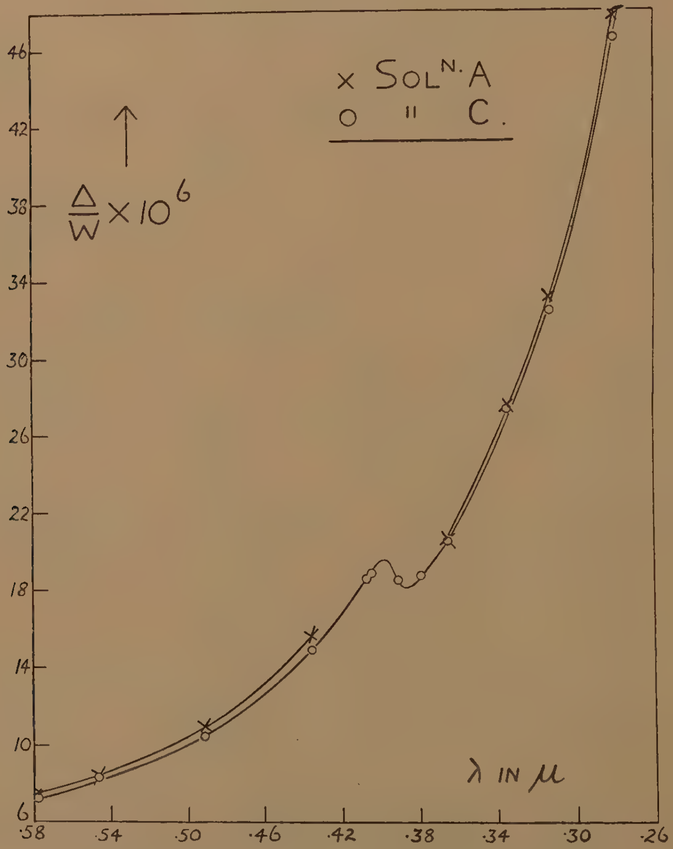

The dispersion of ($\Delta$/W) for nickel sulphate.

the 3950 Å. band, where the rotation contribution due to the band can be neglected to this approximation. If the difference,

$$\Delta/W-A_1'\nu^2/(\nu_1'^2-\nu^2)^2,$$

be plotted against the wave-length, a curve shaped like that in fig. 4 is obtained. As this is definitely asymmetric we are justified, in accordance with theory, in representing the effect of the 3950 Å. band, at wave-lengths far from the band, by a term $A_0\nu^2/(\nu_0{}^2-\nu^2)$, where $\nu_0$ is the frequency of this band.

We have, therefore, for such wave-lengths,

$$\frac{\Delta}{W}=\frac{A_0\nu^2}{\nu_0{}^2-\nu^2}+\frac{A_1\nu^2}{(\nu_1{}^2-\nu^2)^2}.$$

The constants $A_0$, $A_1$, and $\nu_1$ have been calculated from the values of $\Delta/W$ for the wave-lengths 5461, 3129 and 2482 Å. We find for

Solution A : $A_0=1{\cdot}39\times10^{-7}$, $A_1=5{\cdot}772\times10^{-4}$, $\nu_1{}^2=4{\cdot}897$.
Solution C : $A_0=1{\cdot}13\times10^{-7}$, $A_1=5{\cdot}706\times10^{-4}$, $\nu_1{}^2=4{\cdot}895$.

That the mean value of 4·896 for $\nu_1{}^2$ should be less than the dispersional value $\nu_1{}^2=6{\cdot}364$ is to be expected, as the magnetic value $\nu_1$ is only an effective one. In addition to the contribution to the rotation due to the $SO_4^{--}$ ion with its characteristic frequencies, given by $\nu_1{}^2=6{\cdot}364$ and $\nu_2{}^2=115{\cdot}52$, allowance has to be made for the contribution due to the absorption bands of the $Ni^{++}$ ion in the ultra-violet. The presence of one such band is quite noticeable by the rise of the absorption curve (fig. 2) in the neighbourhood of $\lambda={\cdot}22\,\mu$. The difference,

Fig. 4.

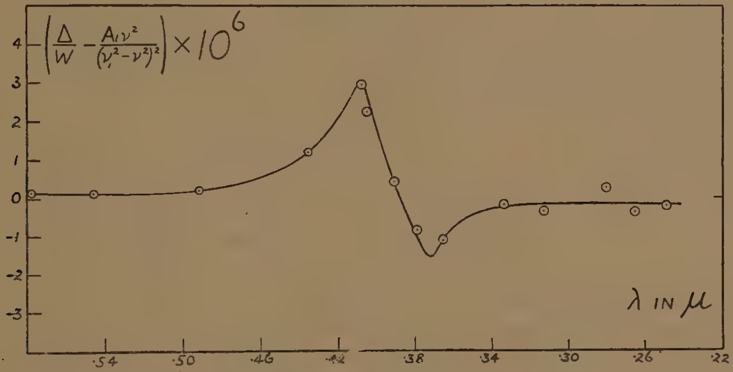

The dispersion of ($\Delta$/W) due to the absorption band of nickel sulphate at ·395 μ.

$$\frac{\Delta}{W}-\frac{A_1\nu^2}{(\nu_1{}^2-\nu^2)^2},$$

calculated for the remaining wave-lengths, will then represent the rotation due to the absorption band at 3950 Å. The mean of these differences for the two solutions is plotted against the wave-length in fig. 4.

This curve is very similar to that found for the rotation of the $Co^{++}$ ion at its 5100 Å. band. The existence of points below the axis on the short wave-length side of the band shows that a part of the rotation is certainly not of the purely diamagnetic type.

Now Ollivier and his co-workers (11) and Gorter (12) have found that the positive rotation of the $Ni^{++}$ ion in nickel chloride is almost independent of the temperature, whereas the negative rotations of the $Fe^{++}$ ion and other paramagnetic ions vary approximately inversely as the absolute temperature.

On the basis of these temperature measurements Gorter has put forward the view that the rotation of the nickel ion is partially of the paramagnetic temperature-independent type found by Van Vleck (13) and Serber (14). According to their theory such a rotation should exhibit an asymmetric behaviour in the neighbourhood of an absorption band. Our work confirms this theoretical prediction.

Although the cobalt ion shows a similar asymmetric effect at its 5100 Å. band to that of the nickel ion, we believe that its rotation is, in view of its negative value, of the temperature-dependent type. This assumption was made by one of us in discussing the magnetic rotation of the cobalt ion in cobalt sulphate.

We hope shortly to carry out experiments on the temperature variation of the magnetic rotation of salts containing the $Co^{++}$ ion to test this assumption.

The inequality of the heights of the maximum and the minimum of the curve of fig. 4, and the displacement of the point of zero rotation from the head of the absorption band at ·395 $\mu$ suggest that this curve results from a paramagnetic and a diamagnetic effect.

No further comparison of the experimental results with theory is possible, as a quantum mechanical theory of the rotation of ions of the iron group involving readily determinable atomic constants has not been given.

## *Summary.*

(1) The Verdet constants and refractivities of two solutions of nickel sulphate have been determined throughout the range 5780 Å. to 2482 Å.

(2) The " theoretical specific rotation " of nickel sulphate in six solutions has been found for wave-length 3128·9 Å., giving the relation between $\Delta$ and W as

$$\Delta = 3{\cdot}3302 \times 10^{-5}\,W - 0{\cdot}018305 \times 10^{-4}.$$

(3) The dispersion of $\Delta/W$ has been calculated, and from the results the contribution to the dispersion, due to the absorption band at ·395 $\mu$, has been estimated.

(4) The dispersion curve of the magnetic rotation in the neighbourhood of this band is asymmetric, in agreement with the theory of Van Vleck and Serber for the paramagnetic rotation independent of the temperature.

We owe our best thanks to Dr. R. A. Morton for his investigation of the absorption of one of our solutions.

## *References.*

(1) R. W. Roberts, J. H. Smith, and S. S. Richardson, Phil. Mag. xliv. p. 912 (1922) ; R. W. Roberts, *ibid.* xlix. p. 397 (1925), and ix. p. 361 (1930) ; C. E. Richards and R. W. Roberts, *ibid.* iii. p. 770 (1927).
(2) R. Cordonnier, *C. R.* ccv. p. 313 (1937).
(3) A. Cotton and M. Schérer, *C. R.* cxcv. pp. 915, 950 (1932) ; M. Schérer and R. Cordonnier, *C. R.* cxcvi. p. 1724 (1933).
(4) G. Bruhat and M. Pauthenier, *Rev. d'Opt.* vi. p. 163 (1927).
(5) R. W. Roberts, L. A. Wallace, and I. T. Pierce, Phil. Mag. xvii. p. 934 (1934).
(6) I. T. Pierce and R. W. Roberts, Phil. Mag. xxi. p. 164 (1936).
(7) T. M. Lowry, and W. R. C. Coode-Adams, Phil. Trans. A, ccxxvi. p. 391 (1927).
(8) C. Fabry and J. Barot, *Rev. d'Opt.* vii. p. 429 (1928).
(9) A. Heydweiller, *Phys. Zeits.* xxvi. p. 526 (1925).
(10) R. A. Houstoun, Proc. Roy. Soc. Edin. xxxi. p. 547 (1911).
(11) H. Ollivier, J. Pernet, and J. Lesne, *C. R.* cxciv. p. 2301 (1932).
(12) C. J. Gorter, *Phys. Zeits.* xxxiv. pp. 238 (1933).
(13) J. H. Van Vleck, 'Electric and Magnetic Susceptibilities,' pp. 369, 370 (1932).
(14) R. Serber, Phys. Rev. xli. p. 489 (1932).

George Holt Physics Laboratory Department,
The University of Liverpool.
Feb. 1939.

# LXII. *Crystal Structure of Cyclohexane at* —180° C.

By K. LONSDALE and H. SMITH, Davy Faraday Laboratory,
Royal Institution, London [†].

[Received September 26, 1939.]

[Plate IX.]

CYCLOHEXANE, $C_6H_{12}$, is liquid down to 6·5° C., and in order to obtain a clear X-ray photograph of the solid compound it is necessary (*a*) to maintain a small rod of the material at a uniform low temperature, (*b*) to use a powerful source of X-radiation, (*c*) to keep the specimen free from ice.

One of us (H. S.) has devised a method of making very fine cellophane tubes which are, for all practical purposes, transparent to iron and copper X-radiation. Cellophane cuttings are dissolved in a mixture of equal volumes of amyl acetate and acetone, until the resulting solution is fairly viscous. A piece of soft H.C. copper wire of the required diameter is dipped into this solution and hung up to harden for two days. When the cellophane-coated wire is quite dry the cellophane is scraped away from both ends with a razor blade, one end of the wire is fastened in a vice and the other end is pulled with a pair of strong pliers. The wire in stretching is reduced in diameter, so that the cellophane covering is left loose on the wire and can easily be slid off, cut into suitable lengths and sealed.

The liquid contained in such a thin cellophane tube is solidified and maintained at a temperature of —180° C. as follows :—an unsilvered double-walled Dewar vessel (obtainable from the National Glass Industry, 75 Lawrence Street, Tottenham, N. 15), 4 cm. diameter, 30 cm. long, with a lower outlet of about 3 mm. diameter, is fixed above the specimen to be photographed. A piece of Cupro nickel tube, 0·3 mm. bore, is wrapped round with black insulating tape until it is large enough to stopper the 3 mm. outlet of the Dewar vessel, and it is then caulked a little with a blunt tool to make quite sure that liquid air from the vessel can only flow through the 0·3 mm. tubular outlet. Starting with the flask quite dry, liquid oxygen is filtered in and the upper end of the flask is closed with a heavy, easy fitting rubber bung. The liquid oxygen now flows in a steady stream from the tube and can be arranged to impinge directly on to the cellophane tube containing the specimen to be photographed. Under these conditions no ice forms on the specimen, which remains at a uniform temperature of —180° C.

---

[†] Communicated by the Authors.

Using the 5 kw. tube at the Davy Faraday laboratory, a good powder photograph was obtained in 20 minutes with filtered CuKα radiation. The camera was of radius 5·7 cm. and the film showed lines corresponding to the following spacings :—

Table I.

| Å.U. | Int. | Å.U. | Int. | Å.U. | Int. | Å.U. | Int. |
|---|---|---|---|---|---|---|---|
| 7·18 | V.W. | 3·11 | W. | 1·87 | V.W. | *1·35$_5$ | W. |
| *5·86 | V.W. | *2·96 | M.S. | 1·80 | V.W. | *1·29 | V.W. |
| 5·31 | V.S. | *2·75 | M. | 1·74$_5$ | M. | 1·23$_5$ | V.W. |
| *4·77 | V.S. | *2·63 | S. | 1·69 | M.W. | *1·18 | V.W. |
| 4·44 | W. | *2·52 | V.W. | 1·63 | W. | 1·11 | V.W. |
| *4·22 | M.S. | 2·38 | V.W. | 1·57 | V.W. | 1·08 | V.W. |
| 4·02 | M.S. | *2·25 | W. | 1·55 | V.W. | 1·04 | W. |
| 3·74 | M.S. | 2·16 | M.S. | 1·49 | V.W. | 1·00$_5$ | W. |
| 3·49 | M.W. | *2·05 | M.W. | 1·43$_5$ | V.W. | | |
| 3·30 | S. | *1·96 | M. | 1·38$_5$ | W. | | |

O. Hassel and H. Kringstad (*Tids. Kemi Bergvesen*, x. pp. 128–130 (1930)), have made an X-ray examination of $C_6H_{12}$ frozen with solid $CO_2$—acetone mixture, that is, at about —80° C., using a Debye camera and iron radiation. They obtained the following lines :—

Table II.

| Å.U. | Int. | Å.U. | Int. | Å.U. | Int. | Å.U. | Int. |
|---|---|---|---|---|---|---|---|
| 5·67 | M.S. | 3·05 | W. | 2·24 | S. | 1·47 | W. |
| 4·76 | M.S. | 2·92 | | 2·13 | S. | 1·37 | M.S. |
| 4·21$_5$ | S. | 2·79$_5$ | W. | 2·07$_5$ | | 1·30 | W. |
| 3·90$_5$ | | 2·67 | M.S.—S. | 1·98 | W. | 1·26$_5$ | M.S. |
| 3·41 | M.S. | 2·56 | M.S. | 1·93 | W. | 1·19 | W. |
| | | 2·47 | | 1·53$_5$ | W. | | |

These can be ascribed to a cubic lattice, of side 8·41±0·02 Å.U., space-group probably $T_h^2$ or $O_h^4$, four molecules in the unit cell. The starred spacings in Table I. correspond moderately well in position to some of those found by Hassel and Kringstadt (allowance being made for the difference in temperature), but their intensities are not on the whole in agreement. Moreover, the reflexions still unaccounted for in Table I. include many of the strongest lines on the film ; these do not correspond to any cubic, hexagonal or tetragonal lattice, and it seems probable, therefore, that like many other simple chemical compounds, cyclohexane has a low temperature crystalline modification which is of a low class of symmetry. It is not certain whether all the observed reflections in Table I. are due to this lower symmetry form, or whether at the temperature of our experiment two crystalline modifications partially co-exist.

S. Katzoff (J. Chem. Physics, ii. p. 841 (1934)) has found that at 8° C. and at 65° C. X-ray photographs of liquid $C_6H_{12}$ show a strong band at about $d=5{\cdot}1$ Å.U., together with three weaker bands. This strong band might well correspond to a general broadening and merging of the 5·31, 4·77 Å.U. spacings found for the solid compound.

We are indebted to Sir William Bragg and to the Managers of the Royal Institution for research facilities in the Davy Faraday Laboratory.

## LXIII. *Radiation from a Point Charge revolving in a Circular Orbit.*

By Hillel Poritsky, Ph.D.*

[Received October 29, 1938.]

### 1. *Introduction.*

This paper constitutes essentially an exercise in classical electromagnetism. I became interested in the subject-matter about four years ago, as a result of a discussion with a colleague (Dr. J. J. Smith), who expressed the view that the usually accepted conclusion regarding radiation of energy from an accelerating electron may be a misapprehension based on the approximate methods of calculation usually employed . In offering for publication the following rigorous derivation of the field of a point charge moving with uniform velocity in a circular orbit, I was led by the belief that the results, as well as the steps leading to them, may have an intrinsic interest and value of their own. In particular they are closely related to the calculations of the natural frequency of electrical oscillations of a thin ring. Again, the fields considered in this paper resemble those investigated by Dr. N. S. Japolsky in a recent series of papers. Dr. Japolsky's objective is of a far more ambitious nature—to explain the de Broglie waves and the quantum theory on the basis of Maxwell's equations. A brief discussion of Dr. Japolsky's work is given and its relation to the fields of the present paper is indicated.

### 2. *Expression of Electromagnetic Fields in Terms of Scalar and Vector Potentials.*

It will be recalled that the electric and magnetic fields due to moving charges can be expressed in terms of a scalar potential $\phi$ and a vector potential **A** as follows :—

$$\left.\begin{aligned} \mathbf{E}&=-\nabla\phi-\frac{1}{c}\frac{\partial \mathbf{A}}{\partial t}, \\ \mathbf{H}&=\nabla\times\mathbf{A}, \end{aligned}\right\}, \quad . \quad . \quad . \quad . \quad . \quad . \quad . \quad (1)$$

where the potentials $\phi$, **A** themselves satisfy the " wave equations "

$$\left.\begin{aligned} \left(\nabla^2-\frac{1}{c^2}\frac{\partial^2}{\partial t^2}\right)\phi&=-4\pi\rho, \\ \left(\nabla^2-\frac{1}{c^2}\frac{\partial^2}{\partial t^2}\right)\mathbf{A}&=-\frac{4\pi\rho\mathbf{u}}{c}. \end{aligned}\right\}, \quad . \quad . \quad . \quad . \quad . \quad . \quad . \quad (2)$$

$\rho$ being the charge density, and $u$ the velocity of the charge.

---

* Communicated by the Author.

A fundamental difficulty that has to be very carefully attended to lies in the fact that both Maxwell's equation and the wave equations (2) resulting therefrom admit of *more than one* solution even after all the conditions at infinity have been imposed.

One solution, say of the first equation (2), is given by

$$\phi_r(\mathrm{P}, t)=\int \frac{\rho(\mathrm{P}', t-r/c)d\mathrm{P}'}{r(\mathrm{P}, \mathrm{P}')}, \quad . \quad . \quad . \quad . \quad . \quad . \quad . \quad (3)$$

where the integration is carried out over all the regions P′ which had charge in them at the " retarded " time $t-r/c$. The solution (3) can be further described by supposing that from each charge element $\rho d\mathrm{P}'$ situated at P′ at the time $t'$ there starts a spherical wavelet of scalar potential whose value vanishes except at the " wave front," where it is $\rho(\mathrm{P}', t')/r$. The potential at P is given by the sum of the potentials reaching P at the time in question.

Another solution of the first eq. (2), $\phi_a$, is obtained by an integral similar to (3), but with the " retarded " time $t-r/c$ replaced by the " advanced " time $t+r/c$. The general solution $\phi$ vanishing at infinity like

$$\text{const.}/r_0, \quad . \quad . \quad . \quad . \quad . \quad . \quad . \quad . \quad . \quad (4)$$

where $r_0$ is the distance from the origin, is given by " interpolating " between $\phi_r$ and $\phi_a$,

$$\phi=p\phi_r+(1-p)\phi_a, \quad . \quad . \quad . \quad . \quad . \quad . \quad . \quad . \quad (5)$$

where $p$ is any constant. It is customary to restrict oneself to retarded potentials only, since using the advanced potential would contradict common ideas of causality in that the present would turn out to depend not merely upon the past, but also upon the future. It would, indeed, contradict common experience in connexion with propagation of radiation from antennæ and electric discharge in tubes, etc. Thus, the advanced potential would make a wave start from infinity, converge to the antenna or discharge-tube just at the time the switch that starts the current or discharge is closed, and vanish then. Using (5) with $p=1/2$ would result in a similar wave reaching the antenna or discharge-tube, " turning itself inside out " in the wire or gaseous atoms in the same manner as a spherical wave passing through a focus, and speeding away again.

## 3. *Uniform Translation of a sinusoidally distributed Charge over the Plane $z=0$.*

We shall now consider the case in which time enters as a factor

$$e^{i\omega t}, \quad . \quad . \quad . \quad . \quad . \quad . \quad . \quad . \quad . \quad . \quad . \quad (6)$$

and shall further suppose that there is no charge anywhere except over the plane $z=0$, where there is a charge density

$$\sigma=\sigma_0 e^{i\omega t} \quad . \; . \; . \; . \; . \; . \; . \; . \; . \; . \quad (7)$$

per unit area. The first equation (2) is now replaced by (omitting the factor $e^{i\omega t}$)

$$\left(\nabla^2+\frac{\omega^2}{c^2}\right)\phi=0 \quad \text{for} \quad z\neq 0, \quad . \; . \; . \; . \; . \; . \quad (8)$$

$$\left.\frac{\partial\phi}{\partial z}\right|_{z=0+}-\left.\frac{\partial\phi}{\partial z}\right|_{z=0-}=-4\pi\sigma_0. \quad . \; . \; . \; . \; . \; . \; . \quad (9)$$

In view of symmetry about the plane $z=0$, we may confine ourselves to $z\geqq 0$, replacing (9) by

$$\left.\frac{\partial\phi}{\partial z}\right|_{z=0+}=-2\pi\sigma_0. \quad . \; . \; . \; . \; . \; . \; . \; . \quad (9')$$

Similar changes take place in the second eq. (2) with $\sigma u/c$ replacing $\sigma$. The charge density and its velocity are connected by means of the equation of continuity. For the case at hand this becomes

$$\frac{\partial\sigma}{\partial t}+\frac{\partial}{\partial x}(\sigma u_x)+\frac{\partial}{\partial y}(\sigma u_y)=0,$$

or, in view of the factor (6),

$$\sigma_0 i\omega+\frac{\partial}{\partial x}(\sigma_0 u_x)+\frac{\partial}{\partial y}(\sigma_0 u_y)=0. \quad . \; . \; . \; . \; . \; . \quad (10)$$

Equations (1) for the field are now replaced by (again omitting the factor $e^{i\omega t}$)

$$\mathbf{E}=-\nabla\phi-\frac{i\omega}{c}\mathbf{A}, \quad \mathbf{H}=\nabla\times\mathbf{A}. \quad . \; . \; . \; . \; . \; . \quad (11)$$

As a first example assume that $\phi$ is independent of $y$, while $x$ appears in $\phi$ as a factor

$$e^{i\alpha x}. \quad . \; . \; . \; . \; . \; . \; . \; . \; . \; . \; . \; . \quad (12)$$

Eq. (8) now becomes (omitting the factors (6), (12))

$$\frac{\partial^2\phi}{\partial z^2}+\left(\frac{\omega^2}{c^2}-\alpha^2\right)\phi=0,$$

and has as solutions

$$\exp\left[\pm\sqrt{\alpha^2-\frac{\omega^2}{c^2}}\,z\right].$$

Recalling the symmetry about the plane $z=0$, and restoring (6), (12) we have

$$\phi=\exp\left\{i(\omega t+\alpha x)\pm\sqrt{\alpha^2-\frac{\omega^2}{c^2}}\,|z|\right\}. \quad . \; . \; . \; . \quad (13)$$

Eq. (9′) yields

$$\sigma=\pm\frac{1}{2\pi}\sqrt{\alpha^2-\frac{\omega^2}{c^2}}\,e^{i(\omega t+\alpha x)}. \qquad \text{(14}$$

To interpret the above consider separately the cases

$$\alpha>\omega/c, \qquad (15)$$

$$\alpha<\omega/c. \qquad (15')$$

In the former case (15) the radicand in (13), (14) is real, and with a positive radical we are forced to pick the *lower signs* if the potential $\phi$ is not to become infinite at $z=\pm\infty$. In the latter case (15′) the radicand is negative. For definiteness, the radical will be taken positive imaginary. The two solutions (13) are then both finite for $z=\pm\infty$. Writing them in the form

$$\phi=\exp\left\{i\left[\alpha x+\omega t\pm\sqrt{\left(\frac{\omega}{c}\right)^2-\alpha^2}|z|\right]\right\}, \qquad (13')$$

$$\sigma=\mp\frac{2\pi}{i}\sqrt{\frac{\omega^2}{c^2}-\alpha^2}\,e^{i[\alpha x+\omega t]}, \qquad (14')$$

Fig. 1.

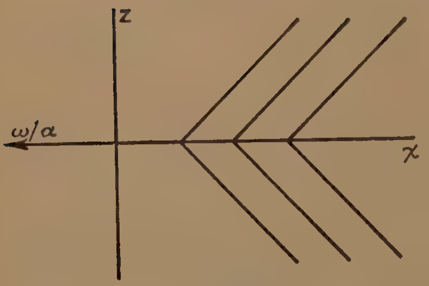

$$\phi=\exp\left[i\left(\alpha x-\sqrt{\left(\frac{\omega}{c}\right)^2-\alpha^2}|z|\right)\right],$$

Fig. 2.

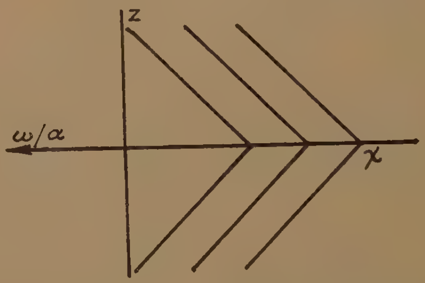

$$\phi=\exp\left[i\left(\alpha x+\sqrt{\left(\frac{\omega}{c}\right)^2-\alpha^2}|z|\right)\right].$$

and taking real (or imaginary parts) to interpret physically, we note that the charge distribution is sinusoidal in $x$ and moves in the direction of negative $x$ with velocity $\omega/\alpha>c$. The loci of constant $\phi$ are the broken straight lines of figs. 1, 2; they, too, move toward negative $x$ with velocity $\omega/\alpha$.

The first diagram shows the wave-pattern similar to one created by disturbances moving with a velocity greater than the speed of wave propagation, for instance that of a projectile moving with supersonic velocity. It will be recognized now, without resorting to (3) (which is indeed not convergent), that the lower sign in (13′) (14′) yields the physically real case of *retarded* potential, while the upper sign corresponds to the advanced potential and will be discarded.

Summarizing, we state that

$$\phi=\exp\left\{i(\omega t+\alpha x)-\sqrt{\alpha^2-\frac{\omega^2}{c^2}}\,|z|\right\}, \quad . \quad . \quad . \quad (13'')$$

yields the true scalar potential corresponding to the charge distribution

$$\sigma=\frac{1}{2\pi}\sqrt{\alpha^2-\frac{\omega^2}{c^2}}\,e^{i(\omega t+\alpha x)}, \quad . \quad . \quad . \quad . \quad . \quad (14'')$$

in either case (15) or (15′), provided that the radical be real and positive, or positive imaginary.

In case (15) the curves of constant $\phi$ (again taking, say, the real part) are as shown in fig. 3.

Fig. 3.

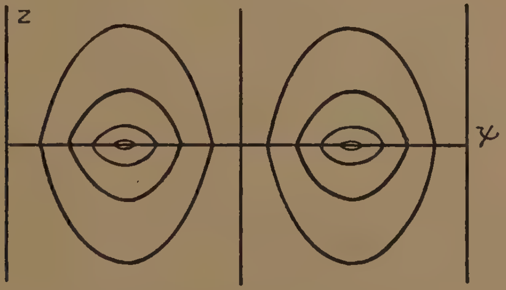

The velocity of motion of the sinusoidally distributed charge is now less than $c$. The values of $\phi$ decrease to 0 as $|z|$ becomes infinite, and there is now no distinction between the advanced and retarded solutions.

The (universally constant) velocity

$$\mathbf{u}=-\frac{\omega}{\alpha}\mathbf{i} \quad . \quad . \quad . \quad . \quad . \quad . \quad . \quad . \quad (16)$$

suggested above is compatible with (10). Adopting it we have

$$\frac{\rho u_x}{c}=-\frac{\omega}{c\alpha}\rho, \quad . \quad . \quad . \quad . \quad . \quad . \quad . \quad . \quad (17)$$

and hence conclude from (2) that

$$A_x=-\frac{\omega}{\alpha c}\phi. \quad . \quad . \quad . \quad . \quad . \quad . \quad . \quad . \quad (18)$$

In (17), (18), $p$, $\phi$ are given by (14″), (13″) respectively. The other components of **A** vanish.

Eq. (1) now yields

$$E_x=\frac{i}{\alpha}\left[\frac{\omega^2}{c^2}-\alpha^2\right]\exp\left\{i(\alpha x+\omega t)-\sqrt{\alpha^2-\left(\frac{\omega}{c}\right)^2}\,|z|\right\}. \quad . \quad (19)$$

Dividing the above by $\sqrt{\alpha^2-\left(\frac{\omega}{c}\right)^2}\Big/2\pi$, we summarize:

A charge density

$$\sigma=e^{i(\alpha x+\omega t)} \quad . \quad . \quad . \quad . \quad . \quad . \quad . \quad . \quad . \quad . \quad . \quad (20)$$

along $z=0$, moving in direction of negative $x$ with a speed $\omega/\alpha$ gives rise to a field described by

$$\left.\begin{aligned}
\phi&=\frac{2\pi}{\sqrt{\alpha^2-\left(\frac{\omega}{c}\right)^2}}\exp\left[i(\alpha x+\omega t)-\sqrt{\alpha^2-\left(\frac{\omega}{c}\right)^2}\,|z|\right],\\
A_x&=-\frac{2\pi\omega}{c\alpha\sqrt{\alpha^2-\left(\frac{\omega}{c}\right)^2}}\exp\left[i(\alpha x+\omega t)-\sqrt{\alpha^2-\left(\frac{\omega}{c}\right)^2}\,|z|\right],\\
E_x&=-\frac{2\pi i\sqrt{\alpha^2-\left(\frac{\omega}{c}\right)^2}}{\alpha}\exp\left[i(\alpha x+\omega t)-\sqrt{\alpha^2-\left(\frac{\omega}{c}\right)^2}\,|z|\right].
\end{aligned}\right\}. \quad (21)$$

When the speed of the charges is less than $c$ (case (15)) the force $E_x$ at $z=0$ is 90° out of phase with the current wave and no energy is radiated. When the speed of the charges is greater than $c$ (case (15′)), $E_x$ is 180° out of phase with the current and energy is constantly radiated.

The field determination may be completed by finding $E_z$, $H_y$. It is easily shown that for the case (15′) the field to each side of $z=0$ consists of a plane sinusoidal wave, the electric vector pointing along the lines of figs. 1, 2, while the direction of propagation is normal to them. For the retarded potential case portions of wave front continually originate at the charges (fig. 1), but for the advanced potential case they continually disappear at the charges (fig. 2). In case (15) the field to each side of $z=0$ is of the type encountered in the less dense mediumin case of *total reflexion* at a plane boundary.

## 4. *Rotation of Charges in the Plane $z=0$.*

By proper superposition of the solutions of the preceding section we shall now obtain the fields due to uniform rotation about the $z$-axis of charges in the plane $z=0$. To this end turn the charges and field described by (20) and the first eq. (21) through an angle $\theta'$ about the $z$-axis, multiply both by $e^{ik\theta'}\,d\theta'/2\pi$ ($k=0, \pm1, \pm2, \ldots$), and integrate over $\theta'$ from 0 to $2\pi$. The factor $e^{i\alpha x}$ is the only factor that will be affected in $\sigma$ and $\phi$, and it will be replaced by

$$\int_0^{2\pi} e^{i\alpha r\cos(\theta-\theta')}\,e^{ki\theta'}\,d\theta'/2\pi,$$

where $r^2$* $=x^2+y^2$, $\tan\theta=y/x$. Replacing $\theta-\theta'$ by $\theta''$ above, we obtain

$$-e^{ik\theta}\left[\int_0^{2\pi} e^{i\alpha r\cos\theta''}\,e^{-ki\theta}\,d\theta''/2\pi\right]=-e^{ik\theta}[(-i)^k \mathrm{J}_k(\alpha r)].$$

Eliminating the factor $-(-i)^k$ both in $\sigma$ and $\phi$, there follows :

The charge distribution

$$\sigma=e^{i(\omega t+k\theta)}\,\mathrm{J}_k(\alpha r) \quad . \;. \;. \;. \;. \;. \;. \;. \quad (23)$$

over $z=0$ gives rise to the scalar potential

$$\phi=\frac{2\pi}{\sqrt{\alpha^2-\left(\frac{\omega}{c}\right)^2}}\,e^{i(\omega t+k\theta)}\,\mathrm{J}_k(\alpha r)\exp\left\{-\sqrt{\alpha^2-\left(\frac{\omega}{c}\right)^2}\,|z|\right\}. \;. \;. \quad (24)$$

By utilizing the Bessel integral of a function $f(r)$ :

$$f(r)=\int_0^\infty \alpha \mathrm{F}(\alpha)\mathrm{J}_k(\alpha r)\,d\alpha,$$

where

$$\mathrm{F}(\alpha)=\int_0^\infty rf(r)\mathrm{J}_k(\alpha r)\,dr,$$

we may now obtain $\phi$ corresponding to the charge distribution

$$\sigma=e^{i(\omega t+k\theta)}\,f(r), \;. \;. \;. \;. \;. \;. \;. \;. \;. \;. \quad (25)$$

where $f(r)$ is an arbitrary function of $r$. To this end the right-hand member of (23), (24) are multiplied by $\alpha\mathrm{F}(\alpha)\,d\alpha$ and integrated with respect to $\alpha$. In particular, if $f(r)$ is made to approach the "unit impulse" at $r=a$, that is, if $f(r)$ is allowed to approach zero for $r\neq$ a while at $r=a$ it has a hump of unit area, then $\mathrm{F}(\alpha)$ is seen to approach $a\mathrm{J}_k(\alpha a)$. Thus there results

$$\phi=a2\pi e^{i(\omega t+k\theta)}\int_0^\infty \frac{\alpha \mathrm{J}_k(\alpha a)\mathrm{J}_k(\alpha r)}{\sqrt{\alpha^2-\left(\frac{\omega}{c}\right)^2}}\,e^{-\sqrt{\alpha^2-\left(\frac{\omega}{c}\right)^2}\,|z|}\,d\alpha, \;. \;. \quad (26)$$

as the scalar potential corresponding to the charge

$$e^{i(\omega t+k\theta)} \quad . \;. \;. \;. \;. \;. \;. \;. \;. \;. \quad (27)$$

---

* No confusion is likely to arise from the different meaning of $r$ employed in (3).

per unit length of the circle

$$r=a,\ z=0. \quad \ldots\ldots\ldots \quad (28)$$

The charge distributions (23), (25), (27) are consistent with a uniform angular rotation $-\omega/k$, of a charge varying with $\theta$ as $e^{ki\theta}$. To obtain **A** and **E** corresponding to such a rotation of the charge (27), we note that the current is tangent to (28), and in direction of increasing $\theta$ is equal to

$$\mathrm{I}=-\frac{a\omega}{k}e^{i(\omega t+k\theta)}. \quad \ldots\ldots\ldots \quad (29)$$

Resolving (29) in $x$- and $y$-directions, we obtain

$$\left.\begin{aligned}(\mathrm{I}_x, \mathrm{I}_y)&=-\frac{a\omega}{k}e^{i(\omega t+k\theta)}(-\sin\theta, +\cos\theta),\\ \text{or}\qquad \mathrm{I}_x&=\frac{a\omega}{k}\frac{(e^{(k+1)i\theta}-e^{(k-1)i\theta})}{2i}e^{i\omega t},\\ \mathrm{I}_y&=-\frac{a\omega}{k}\frac{e^{(k+1)i\theta}+e^{(k-1)i\theta}}{2}e^{i\omega t}.\end{aligned}\right\} \quad \ldots\ldots \quad (30)$$

For brevity write (26) in the form

$$\phi=e^{i(\omega t+k\theta)}[k], \quad \ldots\ldots\ldots \quad (26')$$

where $[k]$ is the value of $\phi$ for $t=0$, $\theta=0$ and is thus given by

$$[k]=2\pi a\int_0^\infty \frac{\alpha \mathrm{J}_k(\alpha a)\mathrm{J}_k(\alpha r)e^{-\sqrt{\alpha^2-\left(\frac{\omega}{c}\right)^2}z|}}{\sqrt{\alpha^2-\left(\frac{\omega}{c}\right)^2}}\,dx. \quad \ldots \quad (31)$$

Recalling that $\mathrm{A}_x$, $\mathrm{A}_y$ bear the same relation to $\mathrm{I}_x/c$, $\mathrm{I}_y/c$ that $\phi$ does to the charge distribution, and comparing (27), (30), one obtains

$$\left.\begin{aligned}\mathrm{A}_x&=\frac{a\omega}{kc}e^{i\omega t}\frac{e^{(k+1)i\theta}[k+1]-e^{(k-1)i\theta}[k-1]}{2i},\\ \mathrm{A}_y&=-\frac{a\omega}{kc}e^{i\omega t}\frac{e^{(k+1)i\theta}[k+1]+e^{(k-1)i\theta}[k-1]}{2}.\end{aligned}\right\} \quad \ldots\ldots \quad (32)$$

Hence $\mathrm{A}_\varphi$, the component of **A** in direction of increasing $\theta$, given by

$$\mathrm{A}_\theta=-\mathrm{A}_x\sin\theta+\mathrm{A}_y\cos\theta,$$

turns out to be

$$\mathrm{A}_\theta=-\frac{a\omega}{kc}e^{i(\omega t+k\theta)}\frac{[k+1]+[k-1]}{2}.$$

Applying (11), there results for $E_\theta$, the electric force in the direction of increasing $\theta$,

$$E_\theta = -\frac{\partial\phi}{r\,\partial\theta} - \frac{i\omega}{c}A_\theta = -\frac{ik}{r}\phi - \frac{i\omega}{c}A.$$

$$= ike^{i(\omega t+k\theta)}\left\{-\frac{[k]}{r} + \frac{a\omega^2}{2k^2c^2}([k+1]+[k-1])\right\}. \quad . \quad . \quad (33)$$

Along (28) this reduces to

$$E_\theta = 2\pi ike^{i(\omega t+k\theta)}\left[-\int_0^\infty \frac{\alpha J_k^2(\alpha a)}{\sqrt{\alpha^2-\left(\frac{\omega}{c}\right)^2}}d\alpha + \frac{1}{2}\left(\frac{\omega}{c}\right)^2\frac{a^2}{k^2}\int_0^\infty \frac{\alpha[J_{k+1}^2(\alpha a)+J_{k-1}^2(\alpha a)]}{\sqrt{\alpha^2-\left(\frac{\omega}{c}\right)^2}}d\alpha\right]. \quad . \quad . \quad (33')$$

By superposition of the fields (26), (32) for various $k$ there will be obtained in section 6 the field due to a revolving point charge.

### 5. *Radiation from the Fields of Sections* 3, 4.

As stated in Section 3, the fields of fig. 3 involve no net radiation, whereas those of fig. 1 do. The latter field may be described in $z<0$ as constituting a plane electromagnetic wave whose wave front makes an angle $\sin^{-1}(\alpha/c\omega)$ with the plane $z=0$. In $z<0$ the field may be obtained by positive reflexion of the field in $z<0$. The energy radiated is equal to the energy required to create new wave fronts in the gap left near $z=0$ as the plane waves speed away along their normals with velocity $c$. In fig. 2 the plane waves converge toward $z=0$ and disappear there, carrying energy toward the plane $z=0$.

Turning to the fields of Section 4, particularly those described by (26), (31), one notes from (33), (27), (29) that the component of tangential electric field *in phase* with the current is contributed by the part of the integral (33′) which arises from the values of $\alpha$ satisfying (15′), that is, from the field components resembling those of fig. 1. Replacing the limits 0, $\infty$ in (33′) by 0, $\omega/c$ and putting $\alpha a=\xi$, $\omega a/c=v$, there results

$$E_\theta\Big|_{\text{in phase}} = \frac{2\pi k}{a}e^{i(\omega t+k\theta)}\int_0^v\left\{\frac{v^2}{2k^2}[J_{k+1}^2(\xi)+J_{k-1}^2(\xi)]-J_k^2(\xi)\right\}\xi(v^2-\xi^2)^{-1/2}\,d\xi. \quad . \quad . \quad (34)$$

Now for $\xi<v$

$$\frac{v^2}{2k^2}[J_{k+1}^2(\xi)+J_{k-1}^2(\xi)]-J_k^2(\xi) > \frac{\xi^2}{2k^2}[J_{k+1}^2(\xi)+J_{k-1}^2(\xi)]-J_k^2(\xi) = \frac{k^2}{\xi^2}[J_k'(\xi)]^2. \quad . \quad . \quad (35)$$

The last equation is obtained by starting with the familiar relations

$$2J'_k(\xi)=J_{k-1}(\xi)-J_{k-1}(\xi),$$

$$2kJ_k(\xi)/\xi=J_{k-1}(\xi)+J_{k-1}(\xi),$$

squaring and adding both sides, dividing by $2k^2/x^2$, and transposing. In view of (35) it follows that the integrand of (34) is always positive. Since the current is given by (29) and corresponds to a rotation of the charge (27) in direction of negative $\theta$, it is seen that the field opposes the motion of the charge, thus resulting in positive radiation.

Introducing $\Omega$ for $\omega/k$, V for $\Omega a/c$, equations (27), (29), (33) become

$$e^{ik(\theta+\Omega t)}, \qquad \qquad (27')$$

$$I=-a\Omega e^{ik(\theta+\Omega t)}, \qquad \qquad (29')$$

$$E_\theta=\frac{\pi k}{a}e^{ik(\theta+\Omega t)}(I_k+iJ_k), \qquad \qquad (36)$$

where

$$I_k=\int_0^{kV}\{V^2[J^2_{k+1}(\xi)+J^2_{k-1}(\xi)]-2J^2_k(\xi)\}\xi(k^2V^2-\xi^2)^{-1/2}d\xi, \qquad (37)$$

and leads to the in-phase component of $E_\theta$, while $iJ_k$ yields the out-of-phase component of field, and is given by a similar integral with the limits $k$V and $\infty$, and the quantity $(k^2V^2-\xi^2)^{-1/2}$ positive imaginary.

In the above it has been assumed that $k$ is positive. For negative $k$ it is readily shown that (36) is replaced by

$$E_\theta=\frac{\pi|k|}{a}e^{ik(\theta+\Omega t)}(I_{|k|}-iJ_{|k|}). \qquad \qquad (38)$$

For $k=0$ (29′) becomes a uniform circular current and $E_\theta$ vanishes identically.

### 6. *Field of and Radiation from a Point Charge rotating around a Circle with Uniform Velocity.*

The results of the preceding sections allow the field due to the rotation of a charge distribution $f(\theta)$ per unit length of the circle (28) to be found. If $f(\theta)$ is real and

$$f(\theta)=\Sigma A_k e^{ik\theta}$$

is its Fourier series, the coefficients $A_k$, $A_{-k}$ are conjugate imaginaries. Introducing the rotation $-\Omega$, $f(\theta)$ is replaced by the charge

$$C=f(\theta+\Omega t)=\sum_{k=-\infty}^{+\infty}A_k e^{ik}(\theta+\Omega t). \qquad \qquad (39)$$

The tangential field is given by

$$E_\theta = \frac{2\pi}{a}\Sigma|k|A_k(I_{|k|} \pm iJ_{|k|})e^{ki(\theta+\Omega t)}, \quad . \quad . \quad . \quad . \quad . \quad (40)$$

and is likewise real. The rate of energy radiation is given by

$$W = -\int_0^{2\pi}[(-a\Omega)C]E_\theta a d\theta, \quad . \quad . \quad . \quad . \quad . \quad (41)$$

where the bracket represents the current per unit length of the circle (28). Substituting, there results

$$W = \Omega a 2\pi \int_0^{2\pi} (\Sigma A_k e^{ki(\theta+\Omega t)})[\Sigma|k|A_k(I_{|k|} \pm iJ_{|k|})e^{ki(\theta+\Omega t)}]\, d\theta$$

$$= 4\pi^2 a\Omega\Sigma|k|A_k A_{-k}(I_{|k|} \pm iJ_{|k|}).$$

Replacing $A_k A_{-k}$ by $|A_k|^2$, adding terms with equal numerical values of $k$, we obtain

$$W = 8\pi^2 a\Omega \sum_{k=1}^{\infty} k|A_k|^2 I_k. \quad . \quad . \quad . \quad . \quad . \quad . \quad . \quad (42)$$

In particular, if a charge $e$ is allowed to become concentrated at $\theta + \Omega t = 0$ the coefficients $A_k$ in (39) all approach $e/2\pi a$, and (42) becomes

$$W = \frac{2e^2\Omega}{a} \sum_{k=1,2,\ldots} k I_k,$$

or, more explicitly,

$$W = \frac{2e^2\Omega}{a} \sum_{k=1}^{\infty} k \int_0^{kV} \{V^2[J_{k-1}^2(\xi) + J_{k+1}^2(\xi)] - 2J_k^2(\xi)\} \frac{\xi}{\sqrt{k^2V^2 - \xi^2}} d\xi. \quad . \quad (43)$$

Expanding in powers of V, we obtain $V^3/2$ for the lowest power (this arises from the first term). Hence

$$W = \frac{2e^2\Omega}{a}\left(\frac{V^3}{2} + \ldots\right) = ce^2\frac{V^4}{a^2} + \ldots = e^2c^{-3}(A^2 + \ldots), \quad . \quad (44)$$

where A is the acceleration.

### 7. *An Alternative Procedure.*

One might object to the above procedure that no use was made of the original definition of the retarded potential as given by (3), and the derivations were based upon the diagrams of fig. 1 for a one-dimensional case for which the integrals (3) are only conditionally convergent. For this reason we shall outline an alternative procedure for calculating the potentials obtained in Section 4.

Applying (3) directly to the charge distribution (27) over the circle (28) there results, writing D in place of $r$,

$$\phi=ae^{i\omega t}\int_0^{2\pi}\frac{e^{ik\theta'}\,e^{-i\omega d/c}}{\mathrm{D}}\,d\theta'. \quad . \quad . \quad . \quad . \quad . \quad . \quad . \quad (45)$$

Since a rotation about the $z$-axis through an angle $\theta$ multiplies the charge by $e^{ik\theta}$, the same is also true of $\rho$, so that, introducing cylindrical coordinates $r$, $\theta$, $z$,

$$\phi(r,\theta,z)=ae^{i(\omega t+k\theta)}\,[k], \quad . \quad . \quad . \quad . \quad . \quad . \quad . \quad . \quad (46)$$

where, as in (26), (31), $[k]$ is the same as $\phi\,(r,0,z)$. Now recall the Sommerfeld integral *

$$\frac{\exp[-im(r^2+z^2)^{1/2}]}{(r^2+z^2)^{1/2}}=\int_0^{\infty}\frac{\mathrm{J}_0(\alpha r)\exp\,[-|z|\,(\alpha^2-m^2)^{1/2}]}{(\alpha^2-m^2)^{1/2}}\,\alpha d\alpha, \quad . \quad (47)$$

Fig. 4.

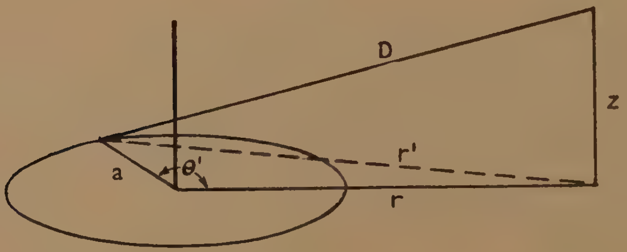

where $(\alpha^2-m^2)^{1/2}$ is positive imaginary for $\alpha<m$ and positive real for $\alpha>m$. Applying to (46), (45), we obtain, on interchanging the order of the integrations,

$$\phi=ae^{i(\omega t+k\theta)}\int_0^{\infty}\frac{\alpha e^{-z(\alpha^2-m^2)^{1/2}}}{(\alpha^2-m^2)^{1/2}}\int_\theta^{2\pi}\mathrm{J}_0(\alpha r')e^{ki\theta'}\,d\theta'\,d\alpha, \quad . \quad . \quad . \quad (48)$$

where (see fig. 4) $(r')^2=r^2+a^2-2\,ar\cos\theta'$, $m=\omega/c$.

Now, by multiplying both sides of Neumann's expansion

$$\mathrm{J}_0[(b^2+c^2-abc\cos\theta)^{1/2}]=\sum_{k=-\infty}^{+\infty}\mathrm{J}_k(b)\mathrm{J}_k(c)e^{ki\theta},$$

by $e^{ik\theta}$ and integrating over $\theta$, we see that the $\theta'$-integration in (48) evaluates to

$$2\pi\mathrm{J}_{-k}(\alpha r)\mathrm{J}_{-k}(\alpha a)=2\pi\mathrm{J}_k(\alpha r)\mathrm{J}_k(\alpha a).$$

The equivalence of (45), (46), and (26) has thus been proved.

---

* G. N. Watson, 'Bessel Functions,' p. 416.

Integrals similar to (45) may be obtained for **A**, **E**. In particular, for $E_\theta$ one obtains upon recalling (33).

$$E_\theta = ike^{i(\omega t+k\theta)}\int e^{ik\theta'}\left(-\frac{a}{r}+\frac{a^2\omega^2}{k^2c^2}\cos\theta'\right)e^{-i\omega D/c}D^{-1}\,d\theta', \quad . \quad . \quad (49)$$

$$D=(r^2+a^2-2ar\cos\theta+z^2)^{1/2}.$$

Along (28) D reduces to $2a\sin\theta'/2$. This vanishes at $\theta'=0$, $2\pi$ and results in an infinite real part of $E_\theta$; the imaginary part, however, is still finite, due to the simultaneous vanishing of the imaginary part of the numerator. Hence $E_\theta$ has a component out of phase with the current, which is infinite, though the in-phase component is finite. The same conclusion can be reached by examining the integrands in (33) for $a>\omega/c$, and utilizing asymptotic expressions for the Bessel functions for large arguments.

The present difficulty is due entirely to the *concentration* of charge along the circle (28). It has the same cause as (and is, in fact, equivalent to) the infinite inductance possessed by a current which is concentrated along a curve. The difficulty may be removed, say, by spreading the charge distribution and current over a band of finite height in the $z$-direction or over a torus whose centre line is the circle (28).

The integral (49) can be applied to a highly accurate calculation of the free electrical vibrations of a thin torus, by letting $\omega$ be complex (but with a positive imaginary part) and equating $E_\theta$ to zero for $z=0$, $r=a+\epsilon$, where $\epsilon$ is the radius of the torus and $a$ the radius of its circular axis. Lord Rayleigh * has discussed this procedure in detail. The period of oscillation is somewhat smaller than $2\pi a/k$, the time required to traverse one wave-length at the velocity of light. Thus for $k=1$ in the present notation

$$\frac{\omega a}{c}=1+\frac{\cdot 243+i\cdot 352}{\log(8a/\epsilon)}. \quad . \quad . \quad . \quad . \quad . \quad . \quad . \quad (50)$$

If $\epsilon/a$ is not very small, then a linear combination of the above field along with its derivatives with respect to $a$ and $z$ could be employed, and $E_\theta$ equated to zero at several points of the torus cross-section.

Another useful expression for the field is obtained by means of spherical harmonics. Introducing spherical coordinates R, $\lambda$, $\theta$ one obtains product solutions of the wave equation

$$e^{i\omega t}R^{-1/2}J_{\pm(n+1/2)}\left(\frac{\omega R}{c}\right)S_n(\lambda,\theta), \quad . \quad . \quad . \quad . \quad . \quad (51)$$

where $S_n$ is a spherical surface harmonic of degree $n$ †.

---

* Phil. Mag. xliii. p. 125 (1897); xliv. p. 199. 'Scientific Papers,' iv. pp. 276, 327; vi. p. 110, where references to Pocklington's work are also given.

† See for instance, H. Bateman, 'Partial Differential of Mathematical Physics,' pp. 386–388.

To expand (45) in terms of these functions start with the expansion

$$\frac{e^{-i\frac{\omega}{c}\mathrm{D}}}{\mathrm{D}} = -\frac{ic}{\omega \mathrm{R} a}\sum_{n=0}^{\infty}(2n+1)f_n\left(\frac{\omega \mathrm{R}}{c}\right)\mathrm{P}_n(\mu), \quad . \quad . \quad . \quad (52)$$

due to Macdonald * where

$$f_n(\vartheta \mathrm{R}) = \left\{ \begin{array}{l} \zeta_n(\vartheta a)\psi_n(\vartheta \mathrm{R}) \text{ for } \mathrm{R}<a, \\ \zeta_n(\vartheta \mathrm{R})\psi_n(\vartheta a) \text{ for } \mathrm{R}>a, \end{array} \right\}, \quad . \quad . \quad . \quad . \quad . \quad (53)$$

$$\left. \begin{array}{l} \psi_n(x) = \left(\frac{\pi x}{2}\right)^{1/2} \mathrm{J}_{n+1/2}(x), \\ \zeta_n(x) = \left(\frac{\pi x}{2}\right)^{1/2} [\mathrm{J}_{n+1/2}(x) + (-1)^n \mathrm{J}_{-n-1/2}(x)]. \end{array} \right\} \quad . \quad . \quad . \quad . \quad (54)$$

Expanding $\mathrm{P}_n(\mu)$ in terms of the surface harmonics $\mathrm{P}_{nm}(\cos\lambda)\cos m\theta$, substituting in (45) and carrying out the integrations there results

$$\phi = -\frac{2\pi ic}{\omega \mathrm{R}}e^{i(\omega t+k\theta)}\sum_{n=k}^{\infty}\frac{(n-k)!\,(2n+1)}{(n+k)!}\mathrm{P}_{nk}(0)\mathrm{P}_{nk}(\cos\lambda)f_n\left(\frac{\omega \mathrm{R}}{c}\right). \quad . . \quad (55)$$

Similar expansions are, of course, available for **A** and **E**. The advantage of the series over the integrals from a computational point of view is manifest.

### 7. *The Fields investigated by Dr. Japolsky* †.

Some of the fields considered above are closely related to the fields investigated by Dr. Japolsky. In this first paper the latter investigates solutions of the field equation called "rotating superfast cylindrical waves," which in the present notation are of the form

$$\mathrm{J}_k(\alpha r)\exp i\left(\omega t + k\theta + \sqrt{\left(\frac{\omega}{c}\right)^2 - \alpha^2} z\right);$$

this is obviously equivalent to (24) for $z>0$ when (15′) holds. The analysis of Section 4 shows that these fields may be formed by superposition of regular plane waves propagating normally with velocity $c$ and inclined to the axis $r=0$. The velocity with which the equiphase planes cut the axis $r=0$ is $c\Big/\sqrt{1-\left(\frac{\alpha c}{\omega}\right)^2}>c$ and turns out to be the phase velocity of (24) along this axis (hence the term "superfast").

In his second paper Dr. Japolsky comes even closer to (24) by substituting $|z|$ in place of $z$. This is done to avoid the field becoming infinite at $|z|=\infty$. He remarks (p. 426): "It will be easily seen that this substitution .... does not introduce any discontinuity in the e.m. field," but he is apparently not worried over the discontinuity in the normal derivatives at $z=0$, and does not mind the fact that Maxwell's equations no longer hold everywhere unless charges and currents are now introduced over $z=0$. He further replaces $z$ by $z+vt$ in the solutions so obtained, even though Maxwell's equations are not invariant under such a transformation *. On account of these difficulties I found Dr. Japolsky's papers hard reading.

---

* Bateman, *loc. cit.* p. 388, ex. 4.

† N. S. Japolsky, Phil. Mag. xix. p. 934 (1935); xx. pp. 417, 641 (1935).

General Electric Co.,
Schenectady, N.Y.

---

* In fact, he replaces $|z|$ by $|z|+vt$, thus imposing motion in *opposite* direction to each side of $z=0$.

# LXIV. *On Transverse Vibrations of Curved Membranes.*

By C. E. Weatherburn, M.A., D.Sc., Professor of Mathematics in the University of Western Australia *.

[Received February 6, 1939.]

Consider a flexible membrane in equilibrium in a state of tension, in the shape of a curved surface. We shall assume that the tension across a line in the membrane is at each point perpendicular to that line. Then from the equilibrium of an element of the membrane at P it follows that the magnitude T of the tension per unit length of the line is the same for all directions of the line through P. We have shown elsewhere † that if the impressed force on the membrane is everywhere normal to it (or zero), the tension is the same at all points; and if it is tangential to the membrane (or zero), the shape of the membrane is that of a minimal surface. We propose to investigate the differential equation of small transverse vibrations of such a membrane. By a transverse vibration we mean that the displacement of any particle is normal to the membrane, being expressible as $\xi\mathbf{n}$, where $\mathbf{n}$ is the unit vector normal to the surface at the point considered, and $\xi$ a small scalar point function on the surface, and a periodic function of the time. The differential invariants employed (gradient, divergence, curl, and Laplacian) are all two-parametric invariants relative to the surface ‡ of the membrane.

## 1. *Impressed Force Zero.*

Suppose first that there is no impressed force. Then T is constant, and the first curvature J of the surface is zero. The dilation $\theta$, due to the displacement $\xi\mathbf{n}$, is given by §

$$\theta=\text{div}\,(\xi\mathbf{n})=\xi\,\text{div}\,\mathbf{n}=-J\xi=0. \quad \ldots \ldots \quad (1)$$

The unit normal $\mathbf{n}'$ at the corresponding point of the deformed surface has the value ||

$$\mathbf{n}'=\mathbf{n}-\mathbf{n}\times\text{curl}\,(\xi\mathbf{n})=\mathbf{n}-\nabla\xi, \quad \ldots \ldots \ldots \quad (2)$$

---

* Communicated by the Author.

† *Cf.* p. 261 of a paper "On Differential Invariants in Geometry of Surfaces, with some Applications to Mathematical Physics," 'Quarterly Journal of Pure and Applied Mathematics,' l. pp. 230–269 (1925). This paper and the succeeding one, "On Small Deformation of Surfaces and of Thin Elastic Shells," will be indicated briefly by Q. J., with the page of reference.

‡ *Loc. cit.*, or the author's 'Differential Geometry,' vol. i. chap. xii. (Camb. Univ. Press, 1927). This book will be referred to briefly as D. G.

§ Q. J. p. 274.

|| Q. J. p. 275.

and the first curvature J′ the value *

$$\mathrm{J}'=\mathbf{n}\,.\,\nabla^2(\xi\mathbf{n})-2\overline{\nabla}\,.\,(\xi\mathbf{n}).$$

The first term in the second member is easily shown to be equal to $\nabla^2\xi+(2\mathrm{K}-\mathrm{J}^2)\xi$, where K is the Gaussian curvature of the surface of the membrane in equilibrium, while †

$$\overline{\nabla}\,.\,(\xi\mathbf{n})=\overline{\nabla}\xi\,.\,\mathbf{n}+\xi\overline{\nabla}\,.\,\mathbf{n}=(2\mathrm{K}-\mathrm{J}^2)\xi.$$

Consequently, since J is zero,

$$\mathrm{J}'=\nabla^2\xi-2\mathrm{K}\xi. \quad . \quad . \quad . \quad . \quad . \quad . \quad . \quad . \quad . \quad . \quad (3)$$

To evaluate the tensional force on an element of the membrane in the displaced position, consider first the force on the portion of the membrane bounded by a closed curve C, when the membrane is in the equilibrium position. This is given by $\int_{\mathrm{C}}\mathrm{T}\mathbf{m}\,ds$, where **m** is the unit surface vector in the direction of the outward normal to the curve at the point considered, and the line integral is taken round C. Now, since T is constant, this integral ‡ is equal to $\mathrm{T}\iint\mathrm{J}\mathbf{n}\,d\mathrm{S}$, where the surface integral is taken over the area enclosed by C. On an element of area $d\mathrm{S}$ the force is therefore simply $\mathrm{TJ}\mathbf{n}\,d\mathrm{S}$. For the deformed membrane the force on this element is similarly $\mathrm{T}'\mathrm{J}'\mathbf{n}'\,d\mathrm{S}'$, the primes being used to distinguish quantities relating to the deformed surface. Now in this expression $d\mathrm{S}'=d\mathrm{S}$, since the dilation is zero. Also J′ is a small quantity of the same order as $\xi$; and, therefore, since we retain only terms of this order, we may give T′ and **n**′ their equilibrium values T and **n**. The tensional force on the element is thus

$$\mathrm{T}(\nabla^2\xi-2\mathrm{K}\xi)\mathbf{n}\,d\mathrm{S}.$$

If $\rho$ is the surface-density of the membrane, the mass of the element is $\rho\,d\mathrm{S}$. Equating the force on the element to its mass-acceleration, we have the required differential equation of small vibrations,

$$\rho\frac{\partial^2\xi}{\partial t^2}=\mathrm{T}(\nabla^2\xi-2\mathrm{K}\xi). \quad . \quad . \quad . \quad . \quad . \quad . \quad . \quad (4)$$

In this equation $\nabla^2\xi$ is, of course, the Laplacian of $\xi$ with respect to the surface of the membrane in equilibrium. It is sometimes referred to as Beltrami's differential parameter of the second order §.

---

* Q. J. p. 281 (16).

† Q. J. pp. 277, 279.

‡ Q. J. p. 255 (47), or D. G. p. 240 (27).

§ *Cf.* Q. J. p. 239 (8), or D. G. p. 227 (8).

### 2. *Normal Impressed Force.*

The above result is independent of the elastic properties of the membrane because the surface is minimal. This, however, is not so in the more general case, which we shall now consider briefly. Let the impressed force be no longer zero, but everywhere normal to the membrane, and equal per unit area to the point-function R. For equilibrium T is still constant; but the first curvature J is now not zero, being connected with R and T by the equation *

$$\mathrm{JT}+\mathrm{R}=0. \quad . \quad . \quad . \quad . \quad . \quad . \quad . \quad . \quad . \quad (5)$$

For the normal displacement $\xi\mathbf{n}$ the dilation is given by

$$\theta=-\mathrm{J}\xi \quad . \quad . \quad . \quad . \quad . \quad . \quad . \quad . \quad . \quad (6)$$

and the first curvature J′ of the deformed membrane by †

$$\mathrm{J}'=\mathrm{J}+\mathbf{n}.\nabla^2(\xi\mathbf{n})-2\nabla.(\xi\mathbf{n}),$$

which simplifies to

$$\mathrm{J}'=\mathrm{J}+\nabla^2\xi-(2\mathrm{K}-\mathrm{J}^2)\xi. \quad . \quad . \quad . \quad . \quad . \quad . \quad (7)$$

We assume first that, in the displaced position of the membrane, the impressed force is still normal to it, and equal to R per unit area. Then, by the same reasoning as above, the force on the element $d$S after displacement is equal to $(\mathrm{T}'\mathrm{J}'+\mathrm{R})\mathbf{n}'d\mathrm{S}'$. We further assume the generalization of Hooke's law, that the small increase in the tension is proportional to the dilation, so that

$$\mathrm{T}'=\mathrm{T}+\lambda\theta=\mathrm{T}-\lambda\mathrm{J}\xi, \quad . \quad . \quad . \quad . \quad . \quad . \quad (8)$$

where $\lambda$ depends on the elastic properties of the membrane. Then, in virtue of (5),

$$\begin{aligned}\mathrm{T}'\mathrm{J}'+\mathrm{R}&=(\mathrm{T}-\lambda\mathrm{J}\xi)[\mathrm{J}+\nabla^2\xi-(2\mathrm{K}-\mathrm{J}^2)\xi]+\mathrm{R}\\&=\mathrm{T}[\nabla^2\xi-(2\mathrm{K}-\mathrm{J}^2)\xi]-\lambda\mathrm{J}^2\xi,\end{aligned}$$

since $\xi$ is small. Each term in this expression is a small quantity of the same order as $\xi$; and, as we retain only terms of this order, we may give to $\mathbf{n}'$ and $d$S′, in the above expression for the force on the element, their equilibrium values $\mathbf{n}$ and $d$S. Equating the value thus found for the force on the element to its mass-acceleration, we have the required differential equation of small vibrations of the membrane,

$$\rho\frac{\partial\,\xi}{\partial t^2}=\mathrm{T}[\nabla^2\xi-(2\mathrm{K}-\mathrm{J}^2)\xi]-\lambda\mathrm{J}^2\xi, \quad . \quad . \quad . \quad . \quad . \quad (9)$$

which reduces to (4) in the particular case for which $\mathrm{J}=0$.

If the normal force R varies during the vibration, and the increment due to the displacement $\xi\mathbf{n}$ is of the same order as $\xi$, this increment must be added to the second member of (9).

---

* Q. J. p. 261 (63).

† Q. J. p. 281 (16).

## LXV. *Scattering of Light in Bose-Einstein and Fermi-Dirac Gas.*

By B. N. Singh, M.Sc. University of Delhi *.

[Received December 19, 1938.]

It is well known, as has been shown by Einstein (1) and Smoluchowski (2), that the phenomenon of scattering of light by fluids is due to local variations in the density of the fluid *i. e.*, density fluctuations. In this paper we shall take account of the modifications introduced by quantum statistics in calculating the density fluctuations and hence the scattering for an ideal gas. The expression for density fluctuations involves the compressibility of the gas. In the first section the usual derivation of the scattering coefficient in terms of the compressibility is summarized. In the second section we determine the compressibility of the ideal gas obeying Bose-Einstein or Fermi-Dirac statistics. It is found that in non-degeneracy the effect of Bose-Einstein statistics is to increase the scattering coefficient over the value given by classical statistics. The effect of Fermi-Dirac statistics is to decrease this value. In degeneracy the scattering for the Bose-Einstein gas tends to infinity and for a Fermi-Dirac gas it tends to zero.

1. We shall give a brief derivation of the scattering coefficient in terms of compressibility, following the usual lines †.

Let us consider the substance in normal equilibrium to have $n_0$ particles in a volume $v_0$ at a pressure $p_0$. Let the volume occupied by this same number of particles at another instant be $v$. We can consider the process isothermal, as the rest of the substance occupies a very large volume. The maximum work which the assembly can do in returning to its normal equilibrium state is

$$\Sigma \Delta \mathrm{A}=\int_v^{v_0}(p-p_0)\,dv. \quad . \quad . \quad . \quad . \quad . \quad . \quad . \quad . \quad (1)$$

But according to Boltzmann's Principle

$$\mathrm{S}=k\log \mathrm{W}, \quad . \quad . \quad . \quad . \quad . \quad . \quad . \quad . \quad . \quad . \quad (2)$$

where S is the entropy of any assembly and W the probability of any specification of that assembly. Hence for an isothermal change

$$\mathrm{W}=\mathrm{C}e^{\frac{\Sigma \mathrm{A}}{k\mathrm{T}}}, \quad . \quad . \quad . \quad . \quad . \quad . \quad . \quad . \quad . \quad . \quad (3)$$

where C is a constant.

---

* Communicated by Dr. D. S. Kothari.

† Epstein, 'Textbook of Thermodynamics,' 1937.

The fraction of molecules of the assembly in which we find these $n_0$ molecules possessing a volume between $v$ and $v+dv$ is

$$W(v)\,dv = Ce^{-\frac{1}{kT}\int_v^{v_0}(p-p_0)\,dv}\,dv, \quad . \quad . \quad . \quad . \quad . \quad . \quad (4)$$

where C is determined by

$$\int W(v)\,dv = 1. \quad . \quad . \quad . \quad . \quad . \quad . \quad . \quad . \quad . \quad (5)$$

But

$$-\int_v^{v_0}(p-p_0)\,dv = \frac{(v-v_0)^2}{\underline{|2}}\frac{\partial p_0}{\partial v_0} + \frac{(v-v_0)^3}{\underline{|3}}\frac{\partial^2 p_0}{\partial {v_0}^2} + \ldots \quad . \quad . \quad (6)$$

So that, neglecting higher order terms and replacing $\frac{v-v_0}{v_0}$ by $\gamma$, we have

$$W(v)\,d_\gamma = C\,d\gamma\,e^{\frac{1}{kT}\cdot\frac{{v_0}^2\gamma^2}{\underline{|2}}\cdot\frac{\partial p_0}{\partial v_0}}, \quad . \quad . \quad . \quad . \quad . \quad . \quad . \quad (7)$$

and the mean square deviation of the parameter $r$ is given by

$$\overline{\gamma^2} = \int_{-\infty}^{+\infty}\gamma^2 W(\gamma)\,d\gamma, \quad . \quad . \quad . \quad . \quad . \quad . \quad . \quad . \quad (8)$$

$$= -\frac{kT}{{v_0}^2\frac{\partial p_0}{\partial v_0}}. \quad . \quad . \quad . \quad . \quad . \quad . \quad . \quad . \quad . \quad (9)$$

At this stage use is made of Rayleigh's well-known formula for scattering,

$$\frac{i}{I_0} = \frac{2\pi^2 {v_0}^2}{{\lambda_0}^4}\left(\frac{\mu-\mu_0}{\mu_0}\right)^2, \quad . \quad . \quad . \quad . \quad . \quad . \quad . \quad (10)$$

where $i$ is the intensity of scattered light at right angles to the incident beam of intensity $I_0$ and wave-length $\lambda_0$, and $v_0$ is the volume of the scattering element of refractive index $\mu$, surrounded by a medium of refractive index $\mu_0$. The difference between the refractive indices of the element and the surrounding medium is easily correlated with the condensation $\gamma$ by making use of the Lorentz-Mosotti law, according to which

$$\frac{\mu^2-1}{\mu^2+2} = \rho\,.\,\text{const.},$$

where $\rho$ is the density of the substance. From this we obtain, for small values of $\frac{\mu-\mu_0}{\mu_0}$,

$$\frac{\mu-\mu_0}{\mu_0} = \frac{({\mu_0}^2-1)({\mu_0}^2+2)}{6{\mu_0}^2}\gamma, \quad . \quad . \quad . \quad . \quad . \quad . \quad . \quad (11)$$

and, consequently, the intensity of light scattered at right angles is

$$\frac{\pi^2 v_0^2(\mu_0^2-1)^2(\mu_0^2+2)^2\gamma^2}{18\mu_0^4\lambda_0^4} . \quad . \quad . \quad . \quad . \quad . \quad . \quad . \qquad (12)$$

Now, since the inhomogeneities are distributed quite irregularly in the medium and there is no phase relationship between the light scattered by different elements, the total intensity of light scattered in any direction is the sum of the intensities scattered by each element in that direction. The number of scattering elements in unit volume is $1/v_0$, and the average of $\gamma^2$ is $\overline{\gamma^2}$ {equation (9)}. Therefore, the average intensity $i$ of the light scattered per unit volume at right angles to the incident beam of intensity I is given by

$$\frac{i}{\mathrm{I}} = -\alpha \frac{k\mathrm{T}}{v_0 \dfrac{\partial p_0}{\partial v_0}}, \quad . \quad . \quad . \quad . \quad . \quad . \quad . \quad . \qquad (13)$$

where
$$\alpha = \frac{\pi^2}{18\mu_0^4\lambda_0^4}(\mu_0^2-1)^2(\mu_0^2+2)^2. \quad . \quad . \quad . \quad . \quad . \qquad (14)$$

For a perfect gas, according to the classical statistics, the compressibility $\frac{1}{v}\frac{\partial v}{\partial p}$ is just $p$, but in the new mechanics this takes on different values. We calculate them in the following section.

2. In an ideal gas obeying Fermi-Dirac or Bose-Einstein statistics and taking account of the effect of relativity mechanics, the pressure is given by *

$$p = \frac{4\pi g k\mathrm{T}}{3}\left(\frac{k\mathrm{T}}{\mathrm{C}h}\right)^3 \int_0^\infty \frac{(u^2+2uy)^{3/2}}{\frac{1}{\mathrm{A}}e^u+\beta}\,du, \quad . \quad . \quad . \quad . \quad . \quad . \qquad (15)$$

where $c$ is the velocity of light, $h$ Planck's Constant, $m$ the mass of the particle and $g$ its weight factor. $y=\frac{mc^2}{k\mathrm{T}}$; $u=\frac{\epsilon}{k\mathrm{T}}$, where $\epsilon$ represents the kinetic energy of the particle and A is a constant independent of $u$. $\beta=+1$ for matter obeying Fermi-Dirac statistics and $\beta=-1$ for Bose-Einstein statistics.

From (15) we obtain

$$\begin{aligned}\frac{\partial p}{\partial v} &= \frac{\partial \mathrm{A}}{\partial v}\cdot\frac{\partial p}{\partial \mathrm{A}} \\ &= \frac{\partial \mathrm{A}}{\partial v}\cdot\frac{4\pi g k\mathrm{T}}{3}\left(\frac{k\mathrm{T}}{\mathrm{C}h}\right)^3 \int_0^\infty \frac{(u^2+2uy)^{3/2}}{\frac{1}{\mathrm{A}}e^u+\beta}\cdot\frac{e^u}{\mathrm{A}^2}\,du. \quad . \quad . \quad . \qquad (16)\end{aligned}$$

---

* For a complete list of formulæ relevant to this paper, see Kothari and Singh, *Zeit. für Astrophysik*, xv. p. 145 (1938).

The value of $\frac{\partial A}{\partial v}$ is obtained by making use of the relation

$$N=4\pi g v\left(\frac{kT}{Ch}\right)^3\int_0^\infty \frac{(u^2+2uy)^{1/2}(u+y)}{\frac{1}{A}e^u+\beta}\,du, \quad . \quad . \quad . \quad . \quad (17)$$

where N represents the total number of particles in the volume $v$. Differentiating with respect to $v$, we have

$$\frac{1}{A^2}\frac{\partial A}{\partial v}=-\frac{1}{v}\frac{\displaystyle\int_0^\infty \frac{(u^2+2uy)^{1/2}(u+y)}{\frac{1}{A}e^u+\beta}\,du}{\displaystyle\int_0^\infty \frac{(u^2+2uy)^{1/2}(u+y)e^u}{\left(\frac{1}{A}e^u+\beta\right)^2}\,du} \quad . \quad . \quad . \quad . \quad . \quad (18)$$

Hence, the compressibility

$$-\frac{1}{v}\frac{\partial v}{\partial p}=\frac{3}{4\pi g kT}\left(\frac{Ch}{kT}\right)^3\frac{\displaystyle\int_0^\infty \frac{(u^2+2uy)^{1/2}(u+y)}{\left(\frac{1}{A}e^u+\beta\right)^2}e^u\,du}{\displaystyle\int_0^\infty \frac{(u^2+2uy)^{1/2}(u+y)}{\frac{1}{A}e^u+\beta}\,du\int_0^\infty \frac{(u^2+2uy)^{3/2}e^u}{\left(\frac{1}{A}e^u+\beta\right)^2}\,du}. \quad (19)$$

But, as can be easily shown,

$$\int_0^\infty \frac{(u^2+2uy)^{3/2}e^u}{\left(\frac{1}{A}e^u+\beta\right)^2}\,du=3A\int_0^\infty \frac{(u^2+2uy)^{1/2}(u+y)}{\frac{1}{A}e^u+\beta}\,du, \quad . \quad . \quad (20)$$

and

$$\int_0^\infty \frac{(u^2+2uy)^{1/2}(u+y)}{\left(\frac{1}{A}e^u+\beta\right)^2}e^u\,du=A\int_0^\infty \frac{\frac{d}{du}(u^2+2uy)^{1/2}(u+y)}{\frac{1}{A}e^u+\beta}\,du, \quad . \quad (21)$$

and hence equation (19), giving the compressibility, reduces to

$$\chi\equiv-\frac{1}{v}\frac{\partial v}{\partial p}=\frac{1}{4\pi g kT}\left(\frac{Ch}{kT}\right)^3\frac{\displaystyle\int_0^\infty \frac{\frac{d}{du}(u^2+2uy)^{1/2}(u+y)}{\frac{1}{A}e^u+\beta}\,du}{\left[\displaystyle\int_0^\infty \frac{(u^2+2uy)^{1/2}(u+y)}{\frac{1}{A}e^u+\beta}\,du\right]^2} \quad . \quad . \quad (22)$$

Equation (22) represents the general formula of the paper. It is, however, difficult to evaluate the integrals for any arbitrary value of A, and we consider only the important limiting cases.

*Non-degenerate Case.*—We shall now calculate the compressibility in a non-degenerate case. Equation (22) gives the compressibility for an ideal gas obeying Bose-Einstein or Fermi-Dirac statistics, $\beta$ being given the proper value.

For a non-degenerate assembly $A \ll 1$, and the terms under the integral sign in (22) can be expanded in an infinite series. We shall further divide the non-degenerate case into two sub-cases, the non-relativistic case and the relativistic case. In the non-relativistic case the kinetic energy of the particle is very much less than its rest mass energy, *i. e.*, $y \gg 1$, and in the relativistic case the opposite is the case, *i. e.*, $y \ll 1$.

(*a*) Non-degenerate non-relativistic case ($A \sim A_0 \ll 1$, and $y \gg 1$)[*].

We have from (22), after a little reduction,

$$\chi = \frac{h^2}{kT . g(2\pi mkT)^{3/2} A} \left[ 1 - \beta^2 A^2 \left\{ \frac{1}{3^{3/2}} - \frac{5}{8} \right\} \ldots \right] . \quad . \quad . \quad (23)$$

But [†]

$$A = A_0 \left[ 1 - \frac{15}{8y} + \frac{\beta A_0}{2^{3/2}} \ldots \right] , \quad . \quad . \quad . \quad . \quad . \quad . \quad (24)$$

where

$$A_0 = \frac{nh^3}{g(2\pi mkT)^{3/2}} . \quad . \quad . \quad . \quad . \quad . \quad . \quad . \quad (25)$$

Hence, retaining terms of the first order in $A_0$, we have

$$\chi = \frac{1}{nkT \left[ 1 + \frac{\beta A_0}{2^{3/2}} - \frac{15}{8y} + \ldots \right]} , \quad . \quad . \quad . \quad . \quad . \quad (26)$$

and

$$\frac{i}{I} = \frac{\alpha}{n \left[ 1 + \frac{\beta A_0}{2^{3/2}} - \frac{15}{8y} + \ldots \right]} . \quad . \quad . \quad . \quad . \quad . \quad (27)$$

It is obvious from the above equation that for a gas obeying Fermi-Dirac statistics ($\beta = +1$) the value of the expression $i/I$ is less than $\alpha/n$, which is the value obtained for a *classical* gas (*i. e.*, gas obeying the law $pV = RT$). Opposite is the case when the gas obeys Bose-Einstein statistics ($\beta = -1$).

(*b*) Non-degenerate relativistic case ($A \sim A_0^R \ll 1$, $y \ll 1$)[‡]. As before, we expand the terms under the integral sign in equation (22), and neglecting $y$ in comparison with $u$, we have, after some simplification,

$$\chi = \frac{1}{8\pi gkT} \left( \frac{Ch}{kT} \right)^3 \frac{1}{A} \left[ 1 + \beta^2 A^2 \left( \frac{1}{3^2} + \frac{5}{2^6} \right) \ldots \right] . \quad . \quad . \quad . \quad (28)$$

[*] For a definition of $A_0$ see equation (25).

[†] Kothari and Singh, *loc. cit.*

[‡] For the definition of $A_0^R$ see equation (29).

But *

$$A=A_0^{\mathrm{R}}\left[1-y+\frac{\beta A_0^{\mathrm{R}}}{8}+\ldots\right],$$

where

$$A^{\mathrm{R}}=\frac{n}{8\pi g}\left(\frac{Ch}{kT}\right)^3 . \quad \ldots \ldots \ldots \quad (29)$$

Therefore, retaining terms of the first order in $A_0^{\mathrm{R}}$, we have

$$\chi=\frac{1}{nkT\left[1-y+\frac{\beta A_0^{\mathrm{R}}}{8}+\ldots\right]}, \quad \ldots \ldots \quad (30)$$

and

$$\frac{i}{I}=\frac{\alpha}{n\left[1-y+\frac{\beta A_0^{\mathrm{R}}}{8}+\ldots\right]} . \quad \ldots \ldots \quad (31)$$

We notice in this case, too, that for a gas obeying Fermi-Dirac statistics ($\beta=+1$) the scattering is less than that deduced for a *classical* gas, whereas for a gas obeying Bose-Einstein statistics it is greater.

*Degenerate Case.*—We shall now calculate the scattering in degenerate matter which obeys Fermi-Dirac statistics ($\beta=+1$ and $A\gg 1$). We shall make use of Sommerfeld's formula, according to which

$$\int_0^\infty \frac{\frac{d}{du}\phi(u)}{\frac{1}{A}e^u+1}\,du=\phi(u_0)+2\{c_2\phi''(u_0)+\ldots\}, \quad \ldots \ldots \quad (32)$$

where $u_0=\log A$, and $c_2=\pi^2/12$.

Equation (22) takes the form

$$\chi=\frac{9}{4\pi gkT}\left(\frac{Ch}{kT}\right)^3 \frac{\displaystyle\int_0^\infty \frac{\frac{d}{du}(u^2+2uy)^{1/2}(u+y)}{\frac{1}{A}e^n+1}\,du}{\left[\displaystyle\int_0^\infty \frac{\frac{d}{du}(u^2+2uy)^{3/2}}{\frac{1}{A}e^u+1}\,du\right]^2} . \quad \ldots \ldots \quad (33)$$

(*a*) In the non-relativistic case $y\gg 1$, and we have

$$u_0=A_0^{2/3}\left(\frac{3\pi^{1/2}}{4}\right)^{2/3}\left[1-\frac{\pi^{4/3}2^{2/3}}{3^{7/3}A_0^{4/3}}\ldots\right], \quad \ldots \ldots \quad (34)$$

$$\chi=\frac{1}{nkTA_0^{2/3}\left(\frac{\pi}{6}\right)^{1/3}\left[1+\frac{\pi^{4/3}2^{2/3}}{3^{7/3}A_0^{4/3}}\ldots\right]}, \quad \ldots \ldots \quad (35)$$

---

* Kothari and Singh, *loc. cit.*

and hence

$$\frac{i}{\mathrm{I}}=\frac{\alpha}{n\mathrm{A}_0{}^{2/3}\left(\frac{\pi}{6}\right)^{1/3}\left[1+\frac{\pi^{4/3}2^{2/3}}{3^{7/3}\mathrm{A}_0{}^{4/3}}\cdots\right]} . \quad . \quad . \quad . \quad . \qquad (36)$$

(*b*) Relativistic degeneracy :—

In this case $y \ll 1$ and equation (33) becomes

$$\chi=\frac{9}{4\pi gk\mathrm{T}}\cdot\frac{1}{u_0{}^4}\cdot\frac{1}{\left[1+\frac{\pi^2}{u_0{}^2}\cdots\right]^2\left[1+\frac{\pi^2}{3u_0{}^2}\cdots\right]} . \quad . \quad . \qquad (37)$$

In this case $u_0=\log \mathrm{A}$

$$=\frac{\mathrm{C}h}{k\mathrm{T}}\left(\frac{3n}{4\pi g}\right)^{1/3}\left[1-\frac{\pi^2}{2^{2/3}3^{5/3}(\mathrm{A}_0^{\mathrm{R}})^{2/3}}\cdots\right] . \quad . \quad . \quad . \quad . \quad . \qquad (38)$$

$$=(6\mathrm{A}_0^{\mathrm{R}})^{1/3}\left[1-\frac{\pi^2}{2^{2/3}3^{5/3}(\mathrm{A}_0^{\mathrm{R}})^{2/3}}\cdots\right], \quad . \quad . \quad . \quad . \quad . \quad . \qquad (39)$$

and therefore

$$\chi=\frac{3}{nk\mathrm{T}6^{1/3}(\mathrm{A}_0{}^{\mathrm{R}})^{1/3}}\cdot\frac{1}{\left[1+\frac{\pi^2}{(\mathrm{A}_0^{\mathrm{R}})^{2/3}3^{5/3}2^{2/3}}\cdots\right]}, \quad . \quad . \quad . \qquad (40)$$

and

$$\frac{i}{\mathrm{I}}=\frac{\alpha}{n\left(\frac{4}{3}\right)^{2/3}(\mathrm{A}_0^{\mathrm{R}})^{1/3}}\cdot\frac{1}{\left[1+\frac{\pi^2}{(\mathrm{A}_0^{\mathrm{R}})^{2/3}3^{5/3}2^{2/3}}\cdots\right]} . \quad . \quad . \quad . \qquad (41)$$

It is obvious from equations (36) and (41) that the scattering in both the cases of relativistic and non-relativistic degeneracy in a gas obeying Fermi-Dirac statistics is less than the scattering for a *classical* perfect gas.

For a gas obeying Bose-Einstein statistics degeneracy occurs as A→1. It can be shown from equation (22), by putting $\beta=-1$ and $\mathrm{A}=1$, that the scattering tends to infinity for this case.

F. London (3) has recently suggested that the peculiar behaviour of liquid Helium II is possibly connected with the " condensation phenomena " of a degenerate Bose-Einstein gas. In view of the above it may be of interest to investigate experimentally the scattering of helium near the λ-point, and to see if any discontinuity appears at this point.

My best thanks are due to Dr. D. S. Kothari for his kind interest in the work.

## *References.*

(1) Einstein, *Ann. der Phys.* xxxiii. p. 1275 (1910).
(2) Smoluchowski, *Ann. der Phys.* xxv. p. 205 (1908).
(3) London, ' Nature,' cxli. p. 644 (1938). Tisza, ' Nature,' cxli. p. 913 (1938).

Physics Department,
University of Delhi.

# LXVI. *Changes in the Internal Resistance of Selenium Barrier-layer Cells caused by Exposure to Light.*

By Arne Eld Sandström, D.Sc.*

[Received January 29, 1939.]

Whilst engaged upon measurements on barrier-layer cells the author observed † some considerable changes of their internal resistance and, therefore, an investigation was carried out into the effects of illumination on the resistance of photo-elements. The measurements revealed the fact that, if a barrier-layer cell, which for some time has been stored in darkness, is exposed to light, the value of its barrier-layer resistance decreases by an amount about ten times the errors of measurement. If, thereafter, the element is once again stored in darkness its resistance increases slowly.

For this investigation the author had access to three selenium barrier-layer cells. One of these was found to be non-rectifying, the barrier-layer of this element being insufficiently developed. The other two elements were of different make, one being a Lange " ocular-cell " and the other one a " Pressler "-cell, but both of the Falkenthal type. The elements were alternately exposed to the light from a small electrical bulb, to soft X-rays of the wave-length region 3·5 to 20 Å.U., and to hard X-rays of the wave-length region 0·3 to 1·0 Å.U. mainly giving the K-series of silver. In the first case the element was mounted on an optical bench in front of the electrical bulb receiving approximately 0·5 lumen per cm.$^2$ For the exposure of the elements to soft X-rays the author used an optical bench for high vacuum which has already been described in a previous paper ‡. In the case of hard X-rays the element was placed in front of a technical X-ray tube with a silver anti-cathode. As regards both soft and hard X-rays, filters were used to limit the wave-length range of the radiation. Unfortunately, it was impossible to measure the relative intensities of three radiations which have such vastly different wave-length ranges as those which were used for the present investigation. In all cases the illuminated area of the photo-element was 2 cm.$^2$

---

* Communicated by Prof. Axel E. Lindh.

† A. E. Sandström, Phil. Mag. xxvi. p. 906 (1938).

‡ A. E. Sandström, *l. c.*

A volt-ampere method was applied for measuring the resistance. The frontal electrode was earthed and the voltage was put on the rear one. At first the voltage was varied between −0·8 and +0·8 volt. The corresponding resistances were plotted against the voltage in a diagram (fig. 1). As usual, the resistance for the voltage 0 was taken as the value of the barrier resistance of the element. As the resistance commences to increase immediately the illumination of the photo-element ends, the measurements have to be made in as short a time as possible so that the points of the resistance characteristic can be considered coherent. Therefore, it is usually inconvenient to determine such a long range of the characteristics as has been done in fig. 1 *a*. Mostly the author measured the resistances corresponding to voltages between −0·1 and +0·1 volt only. These values give the straight part of the characteristic, and it is possible to find the intersection-point with the ordinate axis with a precision of about 2 per cent., as is easily found from the examples given in fig. 1 *b*. Usually the author contrived not to spend more than five to eight minutes on each series of measurements, but even during such a short time the resistance of an element just

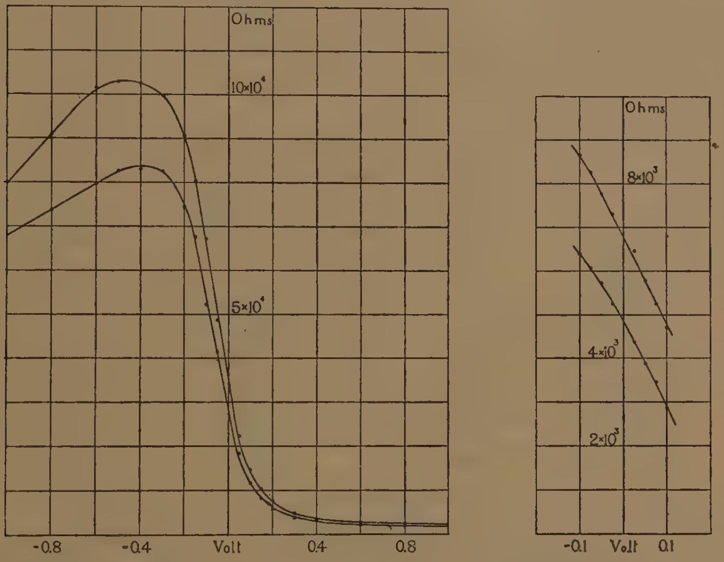
Fig. 1 *a*.

Fig. 1 *b*.

Resistance characteristics of a photo-element before (upper curve), and after (lower curve), exposure to soft X-rays; (*a*) the "Pressler"-element, (*b*) the "Lange" element.

exposed to light will increase by quite a considerable amount, as will be gathered from the curves in figs. 3 and 4.

The upper curve in fig. 1 *a* represents the resistance characteristic of the Pressler-cell before the exposure, and the lower curve the resistance characteristic after the exposure. The values in the table indicate beyond doubt that the ratio of the resistance after to that before exposure is constant irrespective of the voltage.

Unfortunately, it is impossible to measure the resistance for higher voltages without the risk of destroying the element. Therefore, we do not know if the ratio really is constant for higher positive voltages or if the two curves in fig. 1 *a* converge to one and the same point.

As already mentioned, the resistance of an element just exposed to light increases rather rapidly, and, therefore, it is difficult to obtain the foregoing decrease of the internal resistance as a function of the time of exposure. If the element is exposed to light for some moments and then kept in darkness during a series of measurements, which perhaps will take five or six minutes, its resistance will have increased before there is time for further exposures. Under these circumstances the curves in fig. 2 must be considered as only approximately correct. They suffice, however, to show that the change of barrier resistance is of the same character in the case of soft or hard X-rays as in the case of visible light. It is also evident that the resistances of both elements examined decrease in the same way. After an exposure of 5 to 10 minutes the resistance does not change so rapidly as in the beginning, and we may assume that the changes are not big enough to be of any practical importance.

Ratio of the Resistance R after the Exposure to that before, $R_0$.

| Voltage. | $R/R_0$. | Voltage. | $R/R_0$. |
|---|---|---|---|
| —0·8 | 0·80 | +0·1 | 0·80 |
| —0·7 | 0·79 | +0·2 | 0·77 |
| —0·6 | 0·79 | +0·3 | 0·81 |
| —0·5 | 0·82 | +0·4 | 0·83 |
| —0·4 | 0·82 | +0·5 | 0·79 |
| —0·3 | 0·82 | +0·6 | 0·78 |
| —0·2 | 0·81 | +0·7 | 0·79 |
| —0·1 | 0·82 | +0·8 | 0·79 |

As regards the increase of the internal resistance after an exposure while the photo-element is stored in darkness, all the results are graphically recorded in figs. 3 and 4. As in this case the resistance changes more slowly it is possible to determine more accurately the various points, even for moments shortly after the exposure. At first, if we regard the diagrams for the element with the lower resistance, we find that the curve is undoubtedly the same after exposure to light of the most different wave-length ranges.

To ascertain whether the curve really was the same in all cases the following scheme was adopted. With due regard to the fact that the average resistance of the element was different in each case, the points of the four series of measurements were plotted in a diagram and the corresponding curve drawn on paper. This curve was successively corrected until it fitted all four cases, and from the curve a wooden template was then made. All the four curves in fig. 3 were then drawn with this template. Obviously no point lies farther away from the curve than is to be expected from the errors of measurement. During a prolonged series of observations, as in the case of "soft X-rays," small abrupt changes may cause some points to lie too far away from the curve. These abrupt changes really limit the series of measurements, and only

Fig. 2.

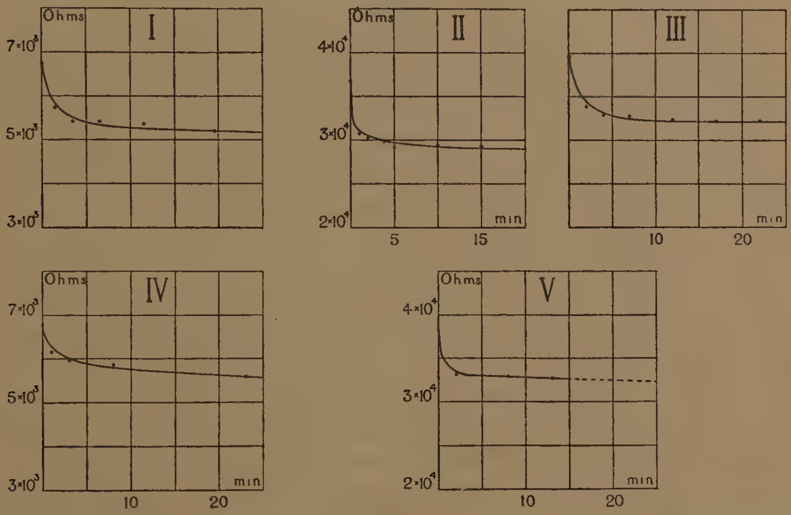

Decrease of the barrier resistance of the photo-elements after exposure to light.

I. The "Lange"-element and soft X-rays.
II. The "Pressler"-element and visible light.
III. The "Pressler"-element and soft X-rays.
IV. The "Lange"-element and hard X-rays.
V. The "The "Pressler"-element and hard X-rays.

once was the author fortunate enough to obtain an unbroken series of observations for 255 hours. Certainly these changes, which must be of another character than those subject to the present investigation, also caused the difference in the "average" resistance of the elements on different occasions. The diagrams I. and II. in fig. 3 both relate to the decrease in resistance after exposure to visible light. The two curves are displaced 500 ohms with respect to each other, without any change in their shape being caused by this fact.

The scale of ordinates of the diagrams of the element with the higher internal resistance has been chosen one-fifth of that of the other element, since the resistance of the former is about five times that of the latter.

Fig. 3.

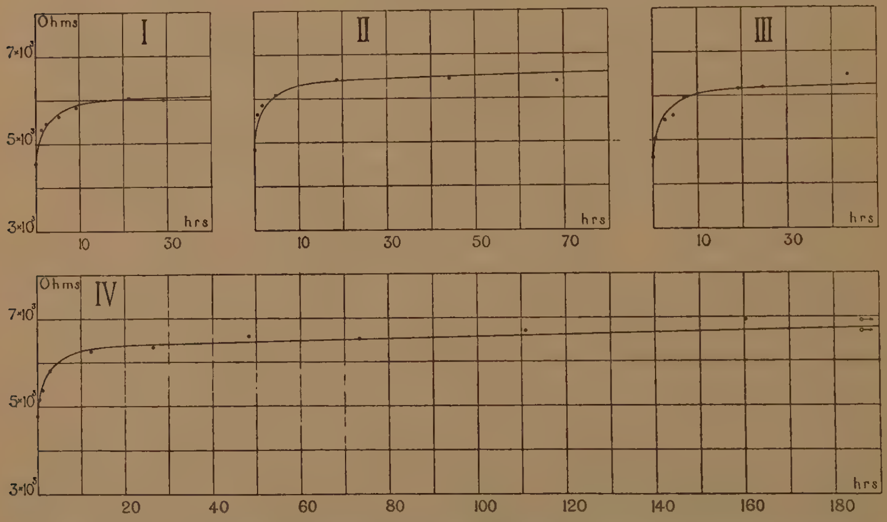

Increase of the barrier resistance of the "Lange"-element after exposure to
I. and II. Visible light.
III. Hard X-rays.
IV. Soft X-rays.

For want of space only a part of the latter curve is reproduced. Of the two points marked with arrows that with the lower value corresponds to 207, and the other one to 255 hours rest after the exposure.

The two diagrams are drawn with the same template as those of the "Lange"-element. It is interesting to see how closely they fit the points of measurements. The curves in fig. 4 suffice to show that the increase of resistance of this element (the "Pressler"-cell) after exposure to light follows the same function as that of the other element (the "Lange"-cell).

It remains to try to locate these changes of resistance in a selenium barrier-layer element. For this purpose the author carried out some measurements on the non-rectifying cell. It turned out that this cell has the same resistance before and after an exposure, which fact seems to indicate that the changes occur in the barrier-layer itself. This conclusion is not necessarily contradicted by the fact that the ratio of the resistance after to that before an exposure is constant for increasing positive voltages, as far as can be judged by the values in the table. For high positive voltages the curves in fig. 1 *a* ought to give the resistance of the selenium layer only, and therefore, they ought really to converge to one and the same point if the changes of resistance are located in the barrier-layer itself. In practice this would mean that the functions corresponding to the curves in fig. 1 *a* would assume the same constant value. To ascertain this, however, it would evidently be necessary to apply such high voltages that the element would be in danger of being destroyed.

Fig. 4.

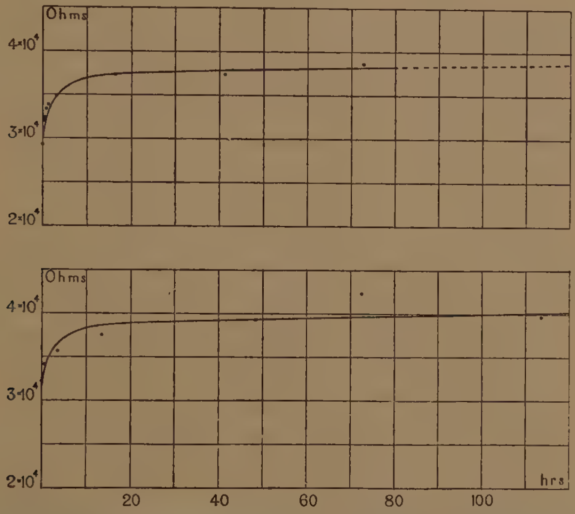

Increase of the barrier resistance of the "Pressler"-element after exposure to visible light (upper curve) and soft X-rays (lower curve).

As already mentioned, only two selenium barrier-layer cells were availalbe for this investigation, the non-rectifying one not being included. But as they have come from different manufacturers and were bought at an interval of two years it does not seem probable that the observed phenomena are characteristic of these two elements only. Naturally the changes of the barrier-layer resistance may be the cause of errors in measuring intensities with selenium barrier-layer photo-elements and, therefore, these phenomena had better be taken into consideration in all arrangements where barrier-layer photo-elements are expected to give currents more or less accurately proportional to the intensity of the incident light.

Uppsala, Physics Laboratory
of the University.

# LXVII. *Torsional Vibration in Heavy Shafts.*

By W. A. Tuplin, M.Sc.*

[Received December 21, 1938.]

In previous communications † the writer has made reference to certain aspects of torsional vibration in systems whose elastic elements were regarded as massless. In practice many systems approximate very closely to the condition implied by this assumption, but there are cases in which it would not be justified. The present communication derives methods of calculation applicable to torsionally vibrating systems in which the moments of inertia of the elastic elements (considered to be shafts) are comparable with those of the rotors and must therefore be taken into account.

## *Torque Variation in Heavy Shaft.*

Let P and Q be sections perpendicular to the axis of a shaft of uniform circular section. Let P and Q be distant $x$ and $x+\delta x$ respectively from an arbitrary section.

Let

$C=$modulus of rigidity of the material of the shaft.

$z=$density of the material of the shaft.

$J=$second moment of area of section of shaft about its axis.

$\mu=$instantaneous torque about shaft axis exerted on the part of the shaft between sections P and Q by the part of the shaft on the left of P, and transmitted across P.

$\mu+\delta\mu=$corresponding torque at section Q.

$\theta=$instantaneous angular displacement at section P from an arbitrary angular position.

$n=2\pi\times$natural frequency of torsional vibration.

$p=2\pi\times$frequency of external harmonic torque.

$$c=n\sqrt{\frac{z}{C}} \quad \text{or} \quad p\sqrt{\frac{z}{C}}.$$

---

* Communicated by the Author.

† Phil. Mag. ser. 7, xxi. p. 1097 (June 1936), and xxvi. p. 729 (November 1938).

Then the moment of inertia of the part of the shaft between P and Q is $zJ\delta x$.

Equating the total torque exerted on the part of the shaft between P and Q to the product of the moment of inertia and the angular acceleration,

$$(\mu+\delta\mu)-\mu=zJ\delta x\frac{\partial^2\theta}{\partial t^2},$$

or, in the limit,

$$\frac{\partial\mu}{\partial x}=zJ\frac{\partial^2\theta}{\partial t^2}. \quad . \quad . \quad . \quad . \quad . \quad . \quad . \quad . \quad . \quad (1)$$

If the angular displacement at section Q is $\theta+\delta\theta$, the angle of twist between P and Q is $\delta\theta$, and from the simple theory applying to torsion of shafts

$$\mu=CJ\frac{\partial\theta}{\partial x}. \quad . \quad . \quad . \quad . \quad . \quad . \quad . \quad . \quad . \quad (2)$$

Differentiating (2) with respect to $x$, and making use of (1), we have

$$\frac{\partial^2\theta}{\partial t^2}=\frac{C}{z}\frac{\partial^2\theta}{\partial x^2}, \quad . \quad . \quad . \quad . \quad . \quad . \quad . \quad . \quad . \quad (3)$$

to which the solution is

$$\theta=a\sin(cx+nt)+b\cos(cx+nt), \quad . \quad . \quad . \quad . \quad . \quad . \quad (4)$$

where $a$, $b$, $c$, and $n$ are constants to be determined.

By double differentiation of (4), first with respect to $t$ and then with respect to $x$, it is found that

$$n^2=c^2\frac{C}{z} \quad . \quad . \quad . \quad . \quad . \quad . \quad . \quad . \quad . \quad (5)$$

or

$$n=\pm c\sqrt{\frac{C}{z}}. \quad . \quad . \quad . \quad . \quad . \quad . \quad . \quad . \quad . \quad (6)$$

Considering this in conjunction with (4), it is seen that the value of $\theta$ remains unaltered when $t$ is increased by $t_1$ if at the same time $x$ is reduced by

$$\frac{n}{c}t_1=\pm\left(\sqrt{\frac{C}{z}}\right)t_1.$$

Hence the variations of $\theta$ with $x$ and $t$ take the form of waves, of velocity $\sqrt{\frac{C}{z}}$, which is a constant for the material of the shaft. The double sign before $\sqrt{\frac{C}{z}}$ indicates that the waves travel in each direction, and since neither direction has a distinction from the other both signs must appear in (4), which thus becomes

$$\begin{aligned}\theta &= a[\sin(cx+nt)+\sin(cx-nt)]+b[\cos(cx+nt)+\cos(cx-nt)]\\ &= 2a\sin cx\cos nt+2b\cos cx\cos nt\\ &= (\mathrm{A}\sin cx+\mathrm{B}\cos cx)\cos nt, \qquad (7)\end{aligned}$$

where $\mathrm{A}=2a$ and $\mathrm{B}=2b$.

The amplitude of $\theta$ at any section is thus

$$\lambda=\mathrm{A}\sin cx+\mathrm{B}\cos cx. \qquad (8)$$

From (2) and (7)

$$\mu=c\mathrm{CJ}(\mathrm{A}\cos cx-\mathrm{B}\sin cx)\cos nt,$$

and the amplitude of $\mu$ at any section is thus

$$m=c\mathrm{CJ}(\mathrm{A}\cos cx-\mathrm{B}\sin cx). \qquad (9)$$

The values of A, B, and $c$ are determined from the end conditions of the shaft.

Since $\mathrm{A}\sin cx+\mathrm{B}\cos cx=\sqrt{(\mathrm{A}^2+\mathrm{B}^2)}\sin(cx+\alpha)$, where $\tan\alpha=\mathrm{B}/\mathrm{A}$, $\lambda$ cannot exceed $\sqrt{(\mathrm{A}^2+\mathrm{B}^2)}$ at any section, and similarly $m$ cannot exceed $c\mathrm{CJ}\sqrt{(\mathrm{A}^2+\mathrm{B}^2)}$.

## *Uniform Shaft alone.*

Since the torques at the free end sections of a shaft must be zero we have, from (9), writing $x=0$, $\mathrm{A}=0$, and writing $x=l$ either $\mathrm{B}=0$ or $\sin cl=0$. If $\mathrm{B}=0$, $\lambda$ and $m$ are zero throughout the shaft. Taking $\sin cl=0$, we have

$$c=0,\ \pm\frac{\pi}{l},\ \pm\frac{2\pi}{l},\ \text{etc., or }\ \frac{s\pi}{l},$$

where $s$ is an integer. The value $c=0$ makes $\lambda$ and $m$ zero throughout. The other values, in conjunction with (6), give

$$n=\frac{s\pi}{l}\sqrt{\frac{\mathrm{C}}{z}},$$

and from this the natural frequencies of torsional vibration of the shaft are found to be

$$\frac{n}{2\pi}=\frac{1}{2}\frac{s}{l}\sqrt{\frac{\mathrm{C}}{z}}. \qquad (10)$$

The natural frequencies thus depend on the length of the shaft but not on its diameter.

Substituting for A, $c$, and $n$ in (7),

$$\theta=\mathrm{B}\cos\frac{s\pi x}{l}\cos\frac{s\pi}{l}\sqrt{\left(\frac{\mathrm{C}}{z}\right)}t. \qquad (11)$$

From (2) $$\mu = -B\frac{s\pi}{l}\sin\frac{s\pi x}{l}\cos\frac{s\pi}{l}\sqrt{\left(\frac{C}{z}\right)}t. \quad \cdots\cdots \quad (12)$$

In (11) and (12) $s$ may have any integral value and B is a constant dependent on the total vibration energy. For any particular value of $x$ the amplitudes $\lambda$ and $m$ are found from (11) and (12) by writing $t=0$. The variation of these amplitudes over the length of the shaft are shown in fig. 1 for values $s=1$, 2, and 3, corresponding to the three lowest natural frequencies.

Fig. 1.

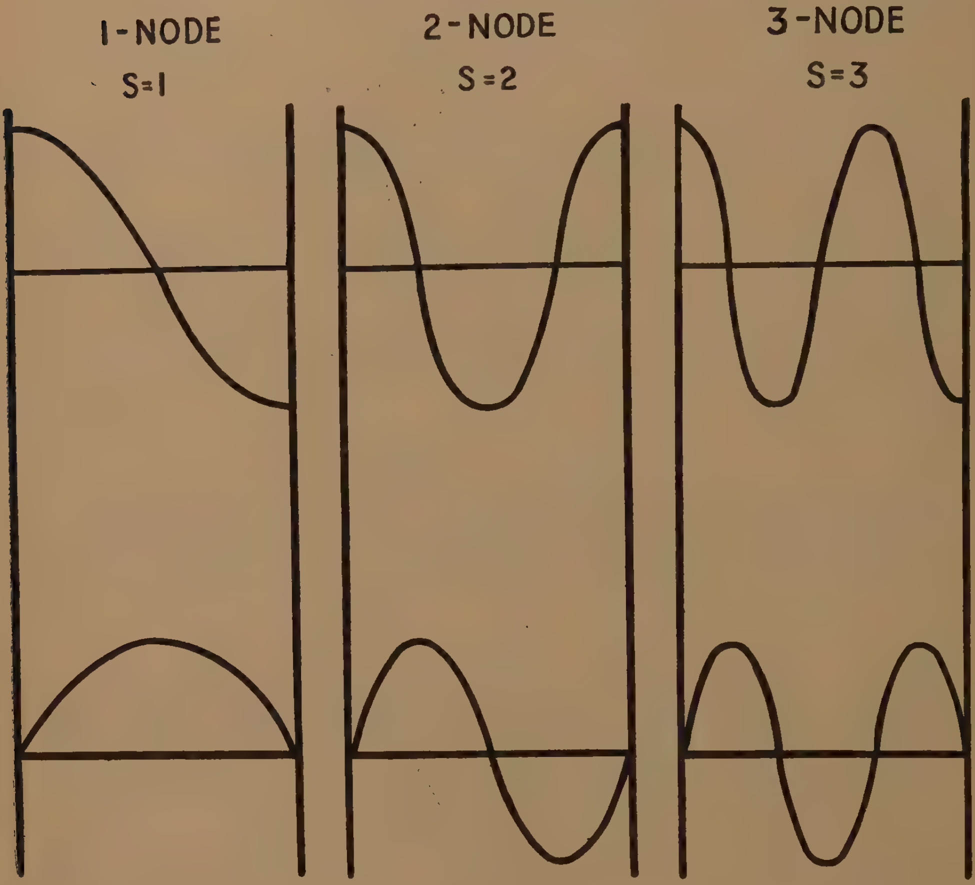

The upper curves are called the "normal elastic curves" for these vibration-forms and represent amplitudes of angular displacement. The lower curves represent amplitudes of torque.

### *Rotors connected by Shafts of uniform section.*

The arrangement shown in fig. 2 represents the general case of a "straight-line" system in which the shaft connecting any pair of adjacent rotors is of uniform section different from that of other shafts. Each rotor is subjected to an external torque whose magnitude is represented by F cos $pt$, where F varies from rotor to rotor but $p$ is the same throughout.

In the steady state of forced vibration the torque at any point in the system is represented by an expression of the form $\mu$ cos $pt$, and the angular displacement by $\theta$ cos $pt$, i. e., torque and displacement have each the same frequency and phase as the external torques.

Numbering shafts and rotors from left to right, the $r$th shaft in the system is that shown in fig. 3.

Fig. 2.

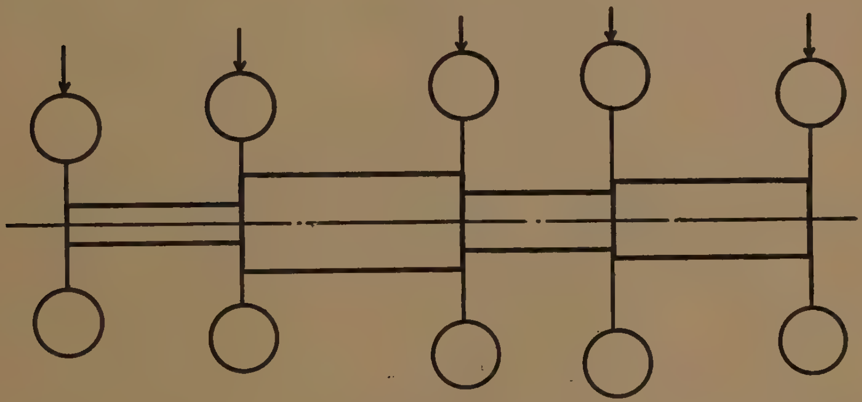

The amplitudes of angular displacement ($\lambda_r$) and of torque ($m_r$) at any point in shaft $r$ distant $x$ from rotor $r$ are given by (8) and (9); thus

$$\lambda_r = A_r \sin cx + B_r \cos cx, \quad \text{. . . . . . . .} \quad (13)$$

$$m_r = cCJ_r(A_r \cos cx - B_r \sin cx). \quad \text{. . . . . .} \quad (14)$$

The constant $c$ is equal to $p\sqrt{\frac{z}{C}}$ (see (6)), and it is the same for all shafts, since the material is assumed to be the same throughout, $z$ and C therefore being common to all shafts.

Now using ${}_1\lambda_r$ to represent the amplitude of angular displacement at the left-hand end of shaft $r$, and ${}_2\lambda_r$ that at the right-hand end, we have

$$ {}_2\lambda_r = A_r \sin cl_r + B_r \cos cl_r$$

and
$$ {}_1\lambda_{r+1} = A_{r+1} \sin 0 + B_{r+1} \cos 0 = B_{r+1}.$$

But ${}_2\lambda_r$ and ${}_1\lambda_{r+1}$ are equal, since each represents the angular displacement at rotor $(r+1)$. Hence

$$B_{r+1}=A_r \sin cl_r+B_r \cos cl_r. \quad \text{. . . . . . (15)}$$

Rotor $r+1$ is subjected to the external torque $F_{r+1}$ and to the torques at the adjacent ends of shafts $r$ and $(r+1)$. Using the same convention as for $\lambda$, these are ${}_2m_r$ and ${}_1m_{r+1}$.

Fig. 3.

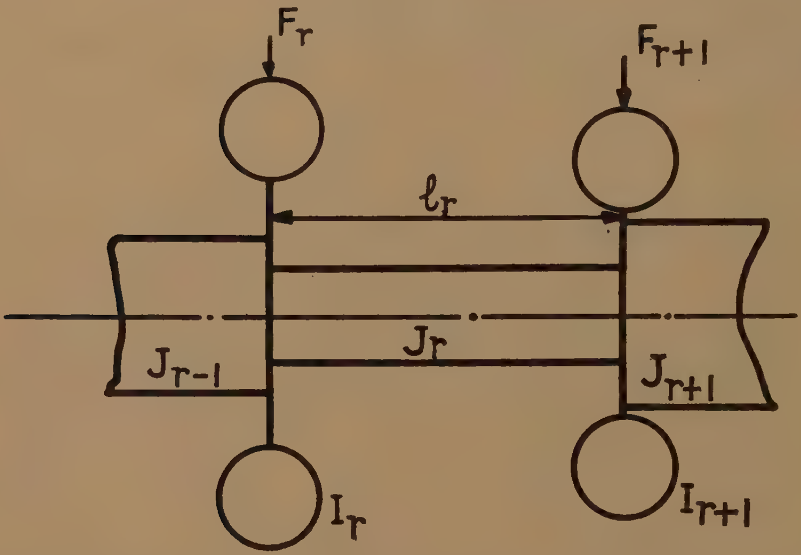

Now adopting the convention of sign which causes ${}_1m_{r+1}$ to act on rotor $(r+1)$ in the same direction as does $F_{r+1}$, we have

$$(F_{r+1}+{}_1m_{r+1}-{}_2m_r)\cos pt=I_{r+1}\frac{\partial^2\theta_{r+1}}{\partial t^2}=I_{r+1}\frac{d^2\lambda_{r+1}}{dt^2}\cos pt$$

$$=-p^2I_{r+1}\lambda_{r+1}\cos pt,$$

and therefore $$F_{r+1}+{}_1m_{r+1}-{}_2m_r=-p^2I_{r+1}\lambda_{r+1}. \quad \text{. . . . (16)}$$

Now from (14), writing $x=0$,

$${}_1m_{r+1}=cCJ_{r+1}A_{r+1}.$$

From (14), writing $x=l_r$,

$${}_2m_r=cCJ_r(A_r\cos cl_r-B_r\sin cl_r).$$

From (13), writing $x=0$,

$${}_1\lambda_{r+1}=B_{r+1}.$$

Hence (16) becomes

$$cCJ_{r+1}A_{r+1}=cCJ_r(A_r\cos cl_r-B_r\sin cl_r)-p^2I_{r+1}B_{r+1}-F_{r+1}, \quad . \quad (17)$$

whence

$$A_{r+1}=\frac{J_r}{J_{r+1}}(A_r\cos cl_r-B_r\sin cl_r)-\frac{p^2I_{r+1}}{cCJ_{r+1}}\left(B_{r+1}+\frac{F_{r+1}}{p^2I_{r+1}}\right),$$

or

$$A_{r+1}=L_r(A_r\cos cl_r-B_r\sin cl_r)-G_{r+1}\left(B_{r+1}+\frac{F_{r+1}}{p^2I_{r+1}}\right), \quad . \quad . \quad (18)$$

where
$$L_r=J_r/J_{r+1},$$
$$G_r=\frac{p^2I_{r+1}}{cCJ_{r+1}}=\frac{c}{z}\frac{I_{r+1}}{J_{r+1}} \quad \left(\text{since } p^2=c^2\frac{C}{z}\right).$$

Equations (15) and (18) permit the A and B for any shaft to be determined from those of the preceding shaft. To commence such operations we have $L_0=0$ since $J_0=0$ (there being no shaft on the left of rotor 1), and therefore

$$A_1=-G_1\left(B_1+\frac{F_1}{p^2I_1}\right). \quad . \quad . \quad . \quad . \quad . \quad . \quad . \quad (19)$$

This gives $A_1$ in terms of $B_1$, which, in the first instance, is unknown. Then by repeated use of (15) and (18) the values of the A's and B's are determined in terms of $B_1$ for all shafts up to the extreme right-hand one (the Rth).

Now, since there is no shaft on the right of rotor (R+1), $J_{R+1}=0$, and from (17), writing $r=R$,

$$cCJ_R(A_R\cos cl_R-B_R\sin cl_R)-p^2I_{R+1}B_{R+1}-F_{R+1}=0,$$

and this is equivalent to $A_{R+1}=0$ if in determining $A_{R+1}$ by means of (18) the symbol $J_{R+1}$ is given any finite value, say unity.

The equation $A_{R+1}=0$ enables $B_1$ to be determined, and the angular displacement and torque are then known for every instant and every point in the system.

In the special case of $I_1=\infty$ there is no angular displacement at the left-hand end of shaft 1. Hence $B_1=0$, and $\lambda_1=A_1\sin cx$, and $m_1=cCJ_1A_1\cos cx$. The calculations then proceed as before, but in terms of $A_1$ instead of $B_1$.

## *External Torques differing in Phase.*

If the external torques are of different phases and are represented by the general expression $F\cos(pt+\beta)$ each of them can be divided into two parts,

$$(F\sin\beta)\cos pt+(F\cos\beta)\sin pt.$$

The calculation of forced vibrations is then performed in two similar operations, the first using $F \sin \beta$ instead of F, and giving shaft torques of the form $\mu_1 \cos pt$, and the second using $F \cos \beta$ instead of F, and giving shaft torques of the form $\mu_2 \sin pt$. The torque at any shaft section is then obtained by vector addition, and is represented by an expression of the form $\sqrt{(\mu_1^2+\mu_2^2)} \sin (pt+\gamma)$.

### *External Torques differing in Frequency.*

If the external torques have different frequencies the calculation of forced vibrations must be repeated for each frequency, and the resulting torques added together.

### *Resonance.*

The quantity $A_{R+1}$ is of the form $B_1M(c)+\Sigma Ff(c)$, where $f(c)$ is a function of $c$ and of certain dimensions of the system associated with the point of application of the external torque F. The quantity $M(c)$ is a function of the dimensions of the system and of $c$.

Now since

$$A_{R+1}=0, \quad B_1=-\frac{\Sigma Ff(c)}{M(c)}, \quad . \quad . \quad . \quad . \quad . \quad . \quad (20)$$

and if $M(c)=0$ and $\Sigma Ff(c) \neq 0$ $B_1$ becomes infinite, and with it torques and angular displacements throughout the system (except for certain sections). This is the condition of resonance.

### *Natural Frequencies.*

To investigate the condition of free vibration the foregoing procedure is followed with an assumed value for $c$ and with all F's equal to zero. The condition $A_{R+1}=0$ then becomes $B_1M(c)=0$. If $B_1=0$, torques and angular displacements are everywhere zero and the system is therefore not vibrating. The condition for free vibration is therefore

$$M(c)=0. \quad . \quad . \quad . \quad . \quad . \quad . \quad . \quad . \quad . \quad . \quad (21)$$

This is called the "frequency equation" because it gives the values of $c$ (and therefore of $n$) corresponding to the frequencies of natural vibration of the system.

Comparison with (20) shows that resonance occurs when the frequency of any external harmonic torque is equal to a natural frequency of the system.

In general the algebraic form of $M(c)$ is complicated, and the most convenient way of finding a solution to equation (21) for a particular system is to assume a numerical value for $c$, to write $B_1=1$, and to work through the system by repeated use of (15) and (18) with numerical values for L's and G's until the value of $A_{R+1}$ is obtained. A value of $c$ corresponds to a natural frequency if it leads to $A_{R+1}=0$; such values of $c$ are found by repeated trial.

In special cases, some of which are considered below, the frequency equation may be expressed in a simple manner.

*Case* 1.—The system comprises two shafts, length $l_1$ and $l_2$, and second moments of area equal to $J_1$ and $J_2$, with no rotor.

Here $$G_1=G_2=G_3=0.$$

From (19), $$A_1=0.$$

From (15), writing $B_1=1$, $$B_2=\cos cl_1.$$

From (18) $$A_2=L_1(-\sin cl_1).$$

From (18), $A_3=L_2(L_1(-\sin cl_1)\cos cl_2-\cos cl_1 \sin cl_2)$.

Now $$L_2=J_2/J_3=\infty\text{ , since } J_3=0.$$

Also $A_3=0$, and therefore,

$$J_1 \sin cl_1 \cos cl_2+J_2 \cos cl_1 \sin cl_2=0, \quad . \quad . \quad . \quad . \quad (22)$$

and this is the frequency equation.

If $l_1=l_2$ $$(J_1+J_2)\sin cl_1 \cos cl_1=0,$$

and therefore either $\sin cl_1=0$, giving $c=s\dfrac{\pi}{l_1}$,

or $\cos cl_1=0$, giving $c=(\frac{1}{2}+s)\dfrac{\pi}{l_1}$.

The lowest frequency, obtained by writing $s=0$ in the second of these, corresponds to $c=\dfrac{\pi}{2l_1}$, and it is therefore the same as the lowest frequency of a uniform shaft of the same total length $(2l_1)$ as the original shaft.

Dividing (22) throughout by $J_2 \cos cl_1 \cos cl_2$ and writing $J_1/J_2=L_1$,

we have $$L_1 \tan cl_1+\tan cl_2=0.$$

If $l_2=rl_1$, where $r$ is an integer, $\tan cl_1$ is a factor of the left-hand side of the equation, and therefore a series of solutions is given by

$$\tan cl_1=0,$$

*i.e.*, $$c=\frac{\pi}{l_1},\ \frac{2\pi}{l_1},\ \frac{3\pi}{l_1},\text{ etc.,}$$

and this applies irrespective of the value of $L_1$.

*Case* 2.—The system comprises three shafts, lengths $l_1$, $l_2$, and $l_3$, second moments of area equal to $J_1$, $J_2$, and $J_3$, and no rotor.

The procedure is identical with that for Case 1, so far as it goes. After a further step it is found that

$$A_4=L_3\left\{\begin{array}{l}-L_2[L_1\sin cl_1\cos cl_2+\cos cl_1\sin cl_2]\cos cl_3\\ \qquad+[L_1\sin cl_1\sin cl_2-\cos cl_1\cos cl_2]\sin cl_3,\end{array}\right\}$$

and since $A_4=0$ and $L_3\neq0$, the frequency equation becomes, after multiplication throughout by $J_3\sec cl_1\sec cl_2\sec cl_3$,

$$J_1\tan cl_1+J_2\tan cl_2+J_3\tan cl_3-\frac{J_1J_3}{J_2}\tan cl_1\tan cl_2\tan cl_3=0. \quad (23)$$

*Case 3.—Uniform Shaft with Rotor at each end.*

The determination of the frequency equation proceeds thus:

$$G_1=\frac{c}{z}\frac{I_1}{J_1}.$$

From (19), $$A_1=-\frac{c}{z}\frac{I_1}{J_1}B_1.$$

From (15), $$B_2=A_1\sin cl_1+B_1\cos cl_1=-B_1\left(\frac{c}{z}\frac{I_1}{J_1}\sin cl_1-\cos cl_1\right).$$

From (18), $$A_2=\frac{J_1}{J_2}(A_1\cos cl_1-B_1\sin cl_1)-\frac{c}{z}\frac{I_2}{J_2}B_2.$$

Multiplying throughout by $J_2$, and writing $A_2=0$, we have

$$-\frac{c}{z}I_1\cos cl_1-J_1\sin cl_1+\frac{c}{z}I_2\left(\frac{c}{z}\frac{I_1}{J_1}\sin cl_1-\cos cl_1\right)=0,$$

and after writing $$\frac{c}{z}\frac{I_1}{J_1}=\frac{cI_1l_1}{zJ_1l_1}=cl_1\frac{I_1}{I_0},$$

where $I_0$ is the moment of inertia of the shaft about its axis, we have as the frequency equation

$$\tan cl_1=\frac{cl_1I_0(I_1+I_2)}{(cl_1)^2I_1I_2-I_0^2}.$$

*Numerical Example.*

The operations involved in calculating $A_{R+1}$ are conveniently carried out in tabular form, and as an example figures are given for a system having these characteristics:

$$I_1=I_2=I_3=I_4=10, \qquad J_1=J_2=J_3=1,$$
$$l_1=l_2=l_3=2, \qquad C=1000, \qquad z=0\cdot5,$$
$$\sqrt{\frac{C}{z}}=44\cdot7.$$

Hence
$$n = 44{\cdot}7\,c,$$

$$G_1 = G_2 = G_3 = \frac{c}{0{\cdot}5} \times \frac{10}{1} = 20c.$$

From (19), $A_1 = -G_1 B_1 = -20\,c$ (assuming $B_1 = 1$).

Table I. shows the method of calculating $A_4$ for an assumed value of $c$. In this example $c = 0{\cdot}118$, and the small value ($-0{\cdot}002$) of $A_4$ compared with those of other A's shows that there is a natural frequency corresponding to that value of $c$.

TABLE I.

$c = 0{\cdot}118$. ($n = 44{\cdot}7 \times 0{\cdot}118 = 5{\cdot}27$.)

| $r$. | 0. | 1. | 2. | 3. |
|---|---|---|---|---|
| $cl_r$ | — | 0·236 | 0·236 | 0·236 |
| $\sin cl_r$ | — | 0·2338 | 0·2338 | 0·2338 |
| $\cos cl_r$ | — | 0·9723 | 0·9723 | 0·9723 |
| $A_r \sin cl_r$ | — | −0·561 | −0·817 | −0·586 |
| $B_r \cos cl_r$ | — | 0·9723 | 0·400 | −0·405 |
| $B_{r+1}$ | 1 | 0·4113 | −0·417 | −0·991 |
| $G_{r+1}$ | 2·36 | 2·36 | 2·36 | 2·36* |
| $A_r \cos cl_r$ | — | −2·295 | −3·400 | −2·440 |
| $-B_r \sin cl_r$ | — | −0·234 | −0·094 | 0·098 |
| $A_r \cos cl_r - B_r \sin cl_r$ | — | −2·529 | −3·494 | −2·342 |
| $L_r = J_r/J_{r+1}$ | — | 1 | 1 | 1* |
| $L_r(A_r \cos cl_r - B_r \sin cl_r)$ | — | −2·529 | −3·494 | −2·342 |
| $-G_{r+1}B_{r+1}$ | −2·36 | −0·970 | 0·985 | 2·340 |
| $A_{r+1}$ | −2·36 | −3·499 | −2·509 | −0·002 |

Table II. is given as an example of calculation of amplitudes of forced vibration. The system is the one described above, and the amplitudes of the external torques applied at the rotors are $F_1 = F_2 = F_3 = F_4 = 100$. Each external torque is represented by $100 \cos 8{\cdot}95t$.

Therefore
$$c = \frac{8{\cdot}95}{44{\cdot}7} = 0{\cdot}2,$$

$$G_1 = G_2 = G_3 = G_4 = \frac{0{\cdot}2}{0{\cdot}5} \times \frac{10}{1} = 4,$$

$$A_1 = -4\left(B_1 + \frac{100}{8{\cdot}95^2 \times 10}\right) = -0{\cdot}5 - 4B_1.$$

---

* Here $J_{R+1} = J_4$ is assumed equal to unity.

Under each value of $r$ in the table there are two columns. The value of any of the expressions in the extreme left-hand column for any particular value of $r$ is the corresponding quantity in the first of the columns under that value of $r$ plus $B_1$ times the quantity in the second of the columns,

*e. g.*, $A_2 \cos cl_2 = -0{\cdot}1673 - 1{\cdot}384\, B_1$.

Since $A_4 = 0$, then $0{\cdot}2589 + 2{\cdot}491\, B_1 = 0$,

whence $B_1 = -0{\cdot}104$.

Table II.

$p = 8{\cdot}95$. $c = 8{\cdot}95/44{\cdot}7 = 0{\cdot}2$.

| $r$. | 1. | | 2. | | 3. | |
|---|---|---|---|---|---|---|
| $cl_r$ | 0·4 | — | 0·4 | — | 0·4 | — |
| $\sin cl_r$ | 0·3894 | — | 0·3894 | — | 0·3894 | — |
| $\cos cl_r$ | 0·9211 | — | 0·9211 | — | 0·9211 | — |
| $A_r$ | −0·5 | −4 | −0·1818 | −1·5024 | 0·4084 | 3·578 |
| $B_r$ | 0 | 1 | −0·1947 | −0·6439 | −0·2499 | −1·178 |
| $A_r \sin cl_r$ | −0·1947 | −1·565 | −0·0707 | −0·585 | 0·1586 | 1·390 |
| $B_r \cos cl_r$ | 0 | 0·9211 | −0·1792 | −0·593 | −0·23 | −1·084 |
| $B_{r+1}$ | −0·1947 | −0·6439 | −0·2499 | −1·178 | −0·0714 | 0·316 |
| $F_{r+1}/p^2 I_{r+1}$ | 0·125 | — | 0·125 | — | 0·125 | — |
| $B_{r+1} + F_{r+1}/p^2 I_{r+1}$ | −0·0697 | −0·6439 | −0·125 | −1·178 | 0·0536 | 0·316 |
| $G_{r+1} = \frac{c}{z} I_{r+1} / J_{r+1}$ | 4 | — | 4 | — | 4* | — |
| $A_r \cos cl_r$ | −0·4606 | −3·689 | −0·1673 | −1·384 | 0·376 | 3·295 |
| $-B_r \sin cl_r$ | 0 | −0·3894 | 0·0757 | 0·250 | 0·0973 | 0·458 |
| $A_r \cos cl_r - B_r \sin cl_r$ | −0·4606 | −4·078 | −0·0916 | −1·134 | 0·4733 | 3·753 |
| $L_r$ | 1 | — | 1 | — | 1* | — |
| $L_r(A_r \cos cl_r - B_r \sin cl_r)$ | −0·4606 | −4·078 | −0·0916 | −1·134 | 0·4733 | 3·753 |
| $-G_{r+1}(B_{r+1} + F_{r+1}/p^2 I_{r+1})$ | 0·2788 | 2·5756 | 0·5 | 4·712 | −0·2144 | −1·262 |
| $A_{r+1}$ | −0·1818 | −1·5024 | 0·4084 | 3·578 | 0·2589 | 2·491 |

Then, as a check, the calculation is repeated with this value of $B_1$, only single columns being required. This calculation starts with $A_1 = -0{\cdot}5 - 4(-0{\cdot}104) = -0{\cdot}084$.

### *Branched Systems.*

The methods described above need extension to render them capable of dealing with the "branched system" typified in fig. 4. Here a number of straight-line systems have a common rotor at their right-hand ends. For the purposes of analysis the junction rotor is imagined to be divided equally between the shafts which are attached to it. Also the external torque applied to the junction rotor is imagined to be divided equally between the separate rotors which are regarded as replacing the junction rotor. Then the dynamic conditions which correspond to the joining of the branches are:

---

* Here $J_{R+1} = J_4$ is assumed equal to unity.

(*a*) the total external torque on the right-hand side of all the branches is zero,

(*b*) the right-hand rotors of all branches have a common angular displacement.

The manner of dividing the junction rotor and its external torque is arbitrary, and equal division is adopted as a convenient working rule.

Fig. 4.

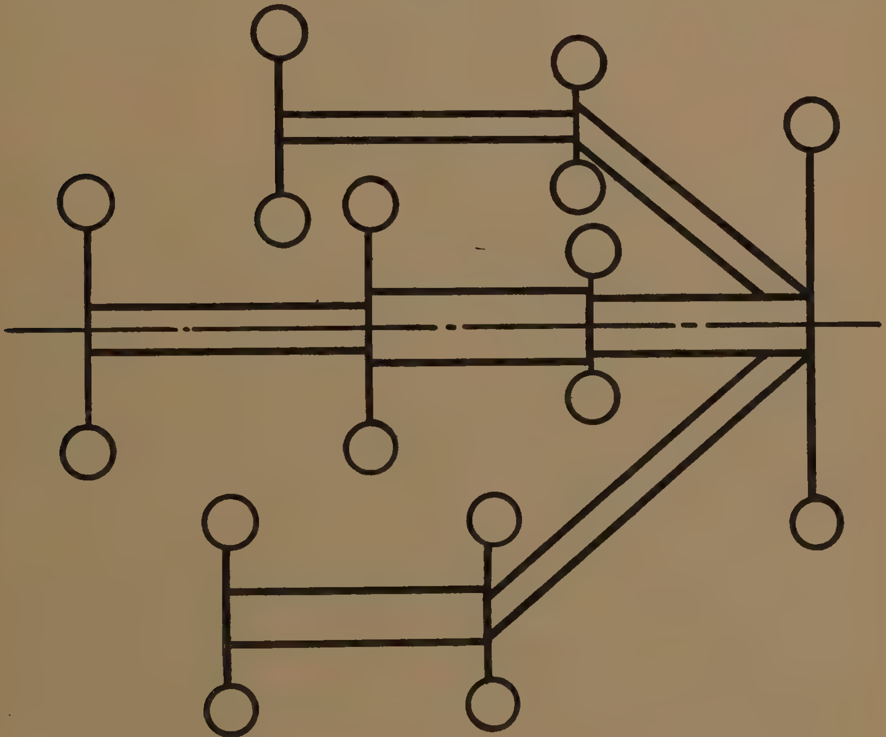

## *Forced Vibrations in Branched Systems.*

Considering any branch, possessing R shafts, the external torque $cCJ_{R+1}A_{R+1}$ on the right-hand side may be determined by the method already described in connexion with straight-line systems. The expression for it is of the form

$$B_1M(c)+\Sigma Ff(c), \qquad (24)$$

where $B_1$ has yet to be determined. Since the sum of such torques for all the branches is zero,

$$\Sigma[B_1 M(c)+\Sigma F f(c)]=0, \quad \ldots \ldots \quad (25)$$

where the outer summation sign refers to the branches and the inner one to the shafts within a branch.

In any branch the angular displacement of the right-hand rotor is represented by $B_{R+1}$, and the expression for this is of the form

$$B_{R+1}=B_1 N(c)+\Sigma F\phi(c), \quad \ldots \ldots \quad (26)$$

where $N(c)$ is a function of $c$ and of the dimensions of the branch, and $\phi(c)$ is a function of $c$ and of certain dimensions of the system associated with the point of application of the external torque F. Since $B_{R+1}$ is common to all branches, the value of $B_1$ for any branch is given by

$$B_1=\frac{B_{R+1}-\Sigma F\phi(c)}{N(c)}, \quad \ldots \ldots \quad (27)$$

and therefore (25) becomes

$$\Sigma\left(\frac{B_{R+1}-\Sigma F\phi(c)}{N(c)}M(c)+\Sigma F f(c)\right)=0, \quad \ldots \ldots \quad (28)$$

whence
$$B_{R+1}=\frac{\Sigma\left[\frac{M(c)}{N(c)}\Sigma F\phi(c)-\Sigma F f(c)\right]}{\Sigma\frac{M(c)}{N(c)}}. \quad \ldots \ldots \quad (29)$$

This gives $B_{R+1}$ in terms of the external torques and of $c\left(=P\sqrt{\frac{z}{C}}\right)$. Equation (27) then gives $B_1$ for each branch, and repeated use of (15) and (18) gives torques and angular displacements at all rotors. A final check on the calculations is afforded by (25).

## *Resonance in Branched Systems.*

Unless the numerator of the fraction in (29) be zero the condition $\Sigma\frac{M(c)}{N(c)}=0$ makes $B_{R+1}$ infinite, and with it torques and angular displacements at most points in the system. This is the condition of resonance.

## *Natural Frequencies of Branched Systems.*

If there are no external torques applied to the system equation (28) becomes, after writing all F's equal to zero, and dividing by $B_{R+1}$ which is assumed not to be zero,

$$\Sigma\frac{M(c)}{N(c)}=0. \quad \ldots \ldots \quad (30)$$

This is the frequency equation, and comparison with (29) shows that resonance occurs when the frequency of any external torque is equal to a natural frequency of the system.

As in dealing with straight-line systems, the most convenient way of finding solutions to (30) is to assume a value for $c$ and, working along the shafts from left to right, to determine numerical values for $M(c)$ and $N(c)$ for all the branches. Values of $c$ which satisfy (30) are found by successive approximation and repeated trial.

### *Endless Systems.*

If the extreme right-hand rotor in a straight-line system is connected directly to the extreme left-hand rotor by a shaft external to the system the result is an "endless system," as typified in fig. 5. The principle of the method of analysing such a system is to regard the "closing" shaft as a means of applying external torques at two points in the straight-line system. The relation between these two torques is determined by the characteristics of the closing shaft.

Fig. 5.

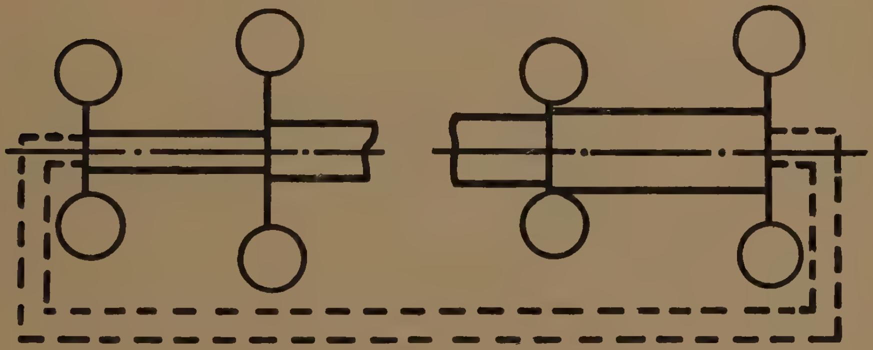

### *Forced Vibrations in Endless Systems.*

Let the number of shafts be R, and let external torques $F_1$, $F_2$, etc. be applied to rotors 1, 2, etc. Let the torque exerted by shaft R on rotor 1 be $m$. Then, from (19),

$$A_1 = -G_1\left(B_1 + \frac{m+F_1}{p^2 I_1}\right).$$

By repeated use of (15) and (18) the A's and B's for all shafts may be found in terms of $B_1$ and $m$.

Now $$m = cCJ_R(A_R \cos cl_R - B_R \sin cl_R),$$

and this is found to be of the form

$$m = B_1M(c) + mP(c) + \Sigma Ff(c). \quad \ldots \ldots \quad (31)$$

Here $f(c)$ is a function of $c$ and of certain dimensions of the system associated with the point of application of the external torque F. The quantities $M(c)$ and $P(c)$ are functions of the dimensions of the system and of $c$. Each of them is expressible as a numerical value when $c$ is known.

Also $$B_1 = A_R \sin cl_R + B_R \cos cl_R$$

$$= B_1M'(c) + mP'(c) + \Sigma Ff'(c). \quad \ldots \ldots \quad (32)$$

Here $M'(c)$, $P'(c)$, and $f'(c)$ are also functions of the system expressible as numerical values when $c$ is known. From (31) and (32),

$$B_1M(c) + m(P(c) - 1) + \Sigma Ff(c) = 0,$$

and $$B_1(M'(c) - 1) + mP'(c) + \Sigma Ff'(c) = 0,$$

whence $$B_1 = \frac{(P(c)-1)\Sigma Ff'(c) - P'(c)\Sigma Ff(c)}{M(c)P'(c) - (P(c)-1)(M'(c)-1)}, \quad \ldots \quad (33)$$

and $$m = \frac{-M(c)\Sigma Ff'(c) + (M'(c)-1)\Sigma Ff(c)}{M(c)P'(c) - (P(c)-1)(M'(c)-1)}. \quad \ldots \quad (34)$$

Equations (33) and (34) give numerical values for $B_1$ and $m$, and by using them in a repetition of the previous calculation the A's and B's for all shafts are found. Equation (31) provides a check on the working.

If the denominator of the fractions in (33) and (34) is zero, the condition of resonance occurs and, in general, torques and angular displacements become infinite.

### *Natural Frequencies of Endless Systems.*

If there are no external torques applied to the system all the F's are zero, and, from (33) and (34), $m$ and $B_1$ (and with them all torques and angular displacements) are zero, *i. e.*, the system is not vibrating, unless the denominator of (33) and (34) is also zero. The condition for natural vibrations is therefore

$$M(c)P'(c) - (P(c)-1)(M'(c)-1) = 0, \quad \ldots \ldots \quad (35)$$

and this is the frequency equation.

### *Network Systems.*

A number of rotors connected by shafts arranged in any manner whatever may be described as a "network system." The general procedure in analyzing such systems is to begin by selecting from the network a straight-line system which includes all the rotors. (In general, there is more than one way of doing this.) The shafts not included in the straight-line system then become elements which apply external torques to certain rotors in it, just as does the closing shaft in an endless system. The principle of the method of analysis is shown by the following description of the procedure used in determining the effect of a link-shaft.

Let the amplitudes of the torques applied by the link-shafts to rotors in the straight-line system be $q_1$, $q_2$, etc. Let the shaft which links rotors $r$ and $s$ in the straight-line system be denoted by $rs$;

then $$\lambda_{rs}=\mathrm{A}_{rs}\sin cx+\mathrm{B}_{rs}\cos cx,$$

and $$m_{rs}=c\mathrm{CJ}_{rs}(\mathrm{A}_{rs}\cos cx-\mathrm{B}_{rs}\sin cx),$$

where $x$ refers to the distance of a section of shaft $rs$ from rotor $r$. Now the amplitude $\mathrm{B}_r$ of angular displacement at rotor $r$ is the same as that at the section $x=0$ in the link-shaft.

Hence $$\mathrm{B}_r=\mathrm{B}_{rs}. \qquad (36)$$

Similarly $$\mathrm{B}_s=\mathrm{A}_{rs}\sin cl_{rs}+\mathrm{B}_{rs}\cos cl_{rs},$$
$$=\mathrm{A}_{rs}\sin cl_{rs}+\mathrm{B}_r\cos cl_{rs}. \qquad (37)$$

Also the external torque exerted on the straight-line system at rotor $r$ is the same as that at the section $x=0$ in the linking shaft.

Hence $$q_r=c\mathrm{CJ}_{rs}\mathrm{A}_{rs}. \qquad (38)$$

Similarly $$q_s=-c\mathrm{CJ}_{rs}(\mathrm{A}_{rs}\cos cl_{rs}-\mathrm{B}_{rs}\sin cl_{rs})$$
$$=-c\mathrm{CJ}_{rs}(\mathrm{A}_{rs}\cos cl_{rs}-\mathrm{B}_r\sin cl_{rs}). \qquad (39)$$

(The negative sign is used in (39) because a torque of the same sign throughout shaft $rs$ exerts opposite torques on rotors $r$ and $s$.)

In working through the straight-line system the external torque $\mathrm{F}_r$ is increased by $c\mathrm{CJ}_{rs}\mathrm{A}_{rs}$ (from (38)), where $\mathrm{A}_{rs}$ is as yet undetermined. At a later stage, by use of (15), the value of $\mathrm{B}_s$ is determined from $\mathrm{A}_{s-1}$ and $\mathrm{B}_{s-1}$ and its expression involves $\mathrm{A}_{rs}$. Then, by virtue of (37), $\mathrm{A}_{rs}$ may be determined.

In proceeding further the external torque $\mathrm{F}_s$ is increased by $q_s$, expressible in terms of $\mathrm{B}_r$ by virtue of (39).

Each of these quantities is in the form of a numerical value added to a multiple of $\mathrm{B}_1$, which is eventually determined from $\mathrm{A}_{\mathrm{R}+1}=0$, as in the case of a straight-line system.

To determine natural frequencies the same procedure is followed, using $\mathrm{B}_1=1$ and an assumed value for $c$. It is necessary to find by repeated trial values of $c$ which make $\mathrm{A}_{\mathrm{R}+1}$ equal to zero, and these correspond to natural frequencies of the system.

Network systems of greater complexity are dealt with in a similar manner, but the determination of the A's for the link-shafts may involve the solution of a greater number of simultaneous equations.

# LXVIII. *The Electric Strength of Gases, measured by Corona Discharge.*

By Emer. Prof. W. M. THORNTON, D.Sc., D.Eng.*

[Received July 20, 1939.]

1. THE glow or corona that appears suddenly in gases on the surface of a wire that is maintained at a high rising potential is a form of incomplete spark discharge. The maximum electric gradient $Gm$ at which it occurs on the surface of a small wire may be much higher than that at which a spark passes between plane surfaces. It is a function of the latter, the density of the gas and the radius $r$ of the wire, that is expressed by the relation $Gm=kG_0\rho\{1+B(r\rho)^{-\frac{1}{2}}\}$, where $G_0$ is the sparking potential gradient, $\rho$ the density of the gas, taken as unity at 0° C. and 760 mm. pressure, $k$ and B constants. In the case of a wire surrounded by a cylinder of radius $a$, $Gm=V/r \log \frac{a}{r}$, where V is the potential difference between the wire and the cylinder at which corona begins. It may then be measured by observing the peak starting voltage for several values of $r$ and $\rho$. The results, when set down with $(r\rho)^{-\frac{1}{2}}$ as abscissa, lie on a straight inclined line cutting the vertical axis at a value $Gm_0=kG_0$. This gradient, $Gm_0$, is that which would cause a glow to appear on the surface of a wire of large radius in a gas at 0° C. and 760 mm. pressure. The smaller the diameter of the wire the higher is the corona starting gradient $Gm$ on its surface. The sparking field $G_0$ is itself not constant, but is, in air, a logarithmic function of the spacing between the parallel surfaces by which it is measured (1). For the present purpose it is not necessary to know $G_0$, but when $k$ is known for any assumed sparking distance in air $G_0$ in a uniform field can be found at the same spacing for other gases by corona measurements.

2. Working in the author's laboratory, with a sine wave alternating current supply at a frequency of 50, Mr. J. D. Stephenson measured the corona strengths of a number of gases, and to compare them took the mean free path of the gas, as did Röntgen in the case of spark discharge. He found the product $G_0L$, where $G_0$ in his case was taken as 0·8 $Gm_0$, to be the same for many of the gases examined, and, further, that the gases fell into two groups in one of which $G_0L$, where L was here the electron mean free path, was twice that of the other: 0·85 volts for

---

* Communicated by the Author.

the paraffins, 1·71 for gases such as hydrogen and oxygen (2). This observation provides a clue to the ionizing energy relations in corona discharge for the product $G_0Le$, where $e$ is the electron charge, $1{\cdot}59.10^{-20}$ E.M.U. is the energy added to the electron by the field $G_0$ in its travel along the path L between collisions with molecules. L is here, as usual, taken to be $4\sqrt{2}$ the gas kinetic mean free path. The gas pressure in this work was as nearly as possible atmospheric, though some change of pressure had to be made to widen the range of the product $r\rho$. This is more convenient in practice than changing the radius of the wire, though this was also done.

The electrical gradient in corona is the most intense that can be applied to a gas, having regard to the number of molecules in the field, and it is the only form of discharge that can be maintained at this gradient at normal pressures and temperatures. The conditions of ionization in corona are at the limit of energy of electron collision with molecules that is possible at these gas pressures. The electrical state of the gas within the luminous region is complex. There are electrons and positive ions, a recombination of ions, a photoelectric effect, and, in addition, ultra-violet, thermal and short wave radiations have all been observed. When the field is alternating there is a vigorous pulsating wind due to the action of the field on the molecular ions. It is probably because of the strong sustained electric field to which the molecules and electrons are subjected in this form of discharge that it has been possible to observe the separation of gases into groups.

These measurements of corona starting voltage were made in the first instance to find the cause of the differences in the cooling effect of the pulsating wind induced by an alternating field in various gases when surrounding a wire heated to redness by an electric current (3). The voltage at which this effect begins, which may cool the wire to blackness, is very sharply defined, and marks the commencement of ionization by collision in the gas at the surface of the wire that is already ionized by the thermionic emission. At this point, and because of the cooling wind, the resistance of the wire changes suddenly, and this, and the subsequent change as the voltage is raised, has been used to measure high alternating and unidirectional fields. In the present work the wire was cold and the effect was observed by noting in darkness the sudden appearance or disappearance of the glow. The voltage readings were taken when it appeared; on lowering the voltage there was a marked lag before the glow vanished.

3. Proceeding in this way with apparatus of improved design former values of $Gm_0$ were confirmed, within the limits of experimental error, about 1 per cent. in general, and are given, with those for many other

gases, in the table and in fig. 1, the abscissæ of which are, as before; the reciprocals of the electron mean free paths and the ordinates the values of $Gm_0$, the corona peak starting voltage, calculated from $V_0/r \log \frac{a}{r}$, where $V_0$ is taken as 1·414 of the potential difference. This

Fig. 1.

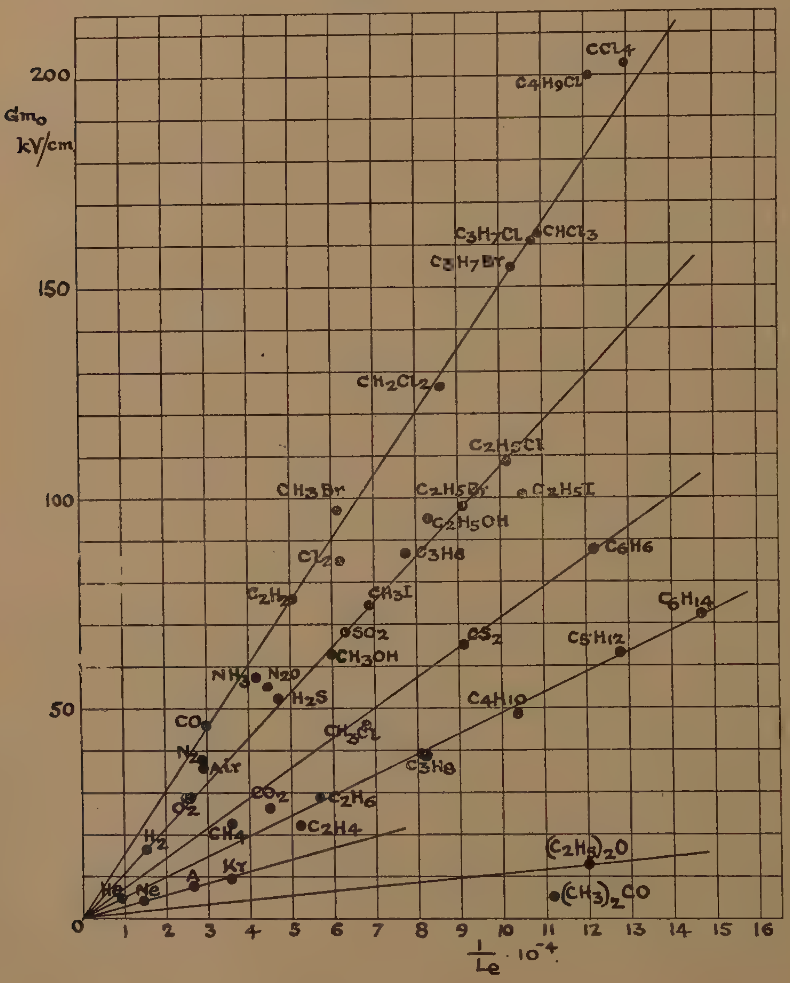

was read from a Weston substandard voltmeter on the primary side of a transformer of which the ratio of transformation was known at all voltages.

The tabulated values of the mean free paths of gases leave much to be desired. Most of them are calculated from the viscosity $\eta$, using the formula

Electric Strength of Gases in an Alternating Field of Force in Peak Kilovolts per centimetre at 760 mm. and 0° C. and at 50 Periods per second.

| Gas. | Maximum corona starting gradient $Gm_0$. | Gas kinetic mean free path. | Reciprocal of electron M.F.P. |
|---|---|---|---|
| | | cm. | |
| Air | 35·5 | $6·03 \times 10^{-6}$ | $2·93 \times 10^{4}$ |
| $H_2$ | 15·5 | 11·20 | 1·58 |
| He | 4·0 | 18·0 | 0·98 |
| Ne | 4·5 | 12·1 | 1·46 |
| A | 7·2 | 6·36 | 2·78 |
| Kr | 9·5 | 4·86 | 3·64 |
| $O_2$ | 29·1 | 6·43 | 2·74 |
| $N_2$ | 38·0 | 5·95 | 2·96 |
| $Cl_2$ | 85·0 | 2·75 | 6·41 |
| CO | 45·5 | 5·91 | 2·98 |
| $CO_2$ | 26·2 | 3·94 | 4·48 |
| $NH_3$ | 56·7 | 4·18 | 4·24 |
| $N_2O$ | 55·3 | 3·94 | 4·48 |
| $H_2S$ | 52·1 | 3·76 | 4·69 |
| $SO_2$ | 67·2 | 2·74 | 6·45 |
| $CS_2$ | 64·2 | 1·93 | 9·17 |
| $CH_4$ | 22·3 | 4·83 | 3·66 |
| $C_2H_6$ | 26·2 | 2·89 | 5·64 |
| $C_3H_8$ | 37·2 | 2·14 | 8·26 |
| $C_4H_{10}$ | 47·7 | 1·71 | 10·35 |
| $C_5H_{12}$ | 63·1 | 1·39 | 12·73 |
| $C_6H_{14}$ | 72·0 | 1·20 | 14·72 |
| $C_2H_2$ | 75·2 | 3·51 | 5·03 |
| $C_2H_4$ | 21·3 | 3·37 | 5·24 |
| $C_3H_6$ | 87·2 | 2·27 | 7·79 |
| $C_6H_6$ | 86·7 | 1·45 | 12·20 |
| $CH_2Cl_2$ | 126·0 | 1·87 | 8·63 |
| $CHCl_3$ | 162·0 | 1·62 | 10·92 |
| $CCl_4$ | 204·0 | 1·37 | 12·90 |
| $CH_3Cl$ | 45·6 | 2·59 | 6·82 |
| $C_2H_5Cl$ | 109·0 | 1·74 | 10·16 |
| $C_3H_7Cl$ | 160·9 | 1·64 | 10·75 |
| $C_4H_9Cl$ | 200·0 | 1·53 | 12·05 |
| $C_5H_{11}Cl$ | 264·0 | 1·25 | 14·1 |
| $CH_3Br$ | 97·0 | 2·89 | 6·12 |
| $C_2H_5Br$ | 98·0 | 1·93 | 9·2 |
| $C_3H_7Br$ | 155·0 | 1·73 | 10·2 |
| $CH_3I$ | 75·0 | 2·60 | 6·81 |
| $C_2H_5I$ | 101·8 | 1·66 | 10·65 |
| $CH_3OH$ | 62·5 | 2·90 | 6·09 |
| $C_2H_5OH$ | 97·0 | 2·10 | 8·41 |
| $(C_2H_5)_2O$ | 15·3 | 1·47 | 12·02 |
| $(CH_3)_2CO$ | 5·4 | 1·56 | 11·33 |
| $C_2H_4Cl_2$ | 240·0 | — | — |

$L=2{\cdot}027\eta/(p\rho)^{\frac{1}{2}}$. The viscosity of a gas is itself difficult to determine with accuracy, and it is necessary to apply Chapman's amendment of the formula in order to bring the values found from viscosity into line with measurements made by other methods. This has been done by Mr. A. E. Schuil, who has collected the available data (4), and I am indebted to him for the new values used here. The final result is to make the values of the product $Gm_0L$ (not $G_0L$), found by dividing the ordinates by the abscissa in fig. 1, 1·5 volts for the upper line, 1·08 for the hydrogen-oxygen line, 0·71 for the $CS_2$-benzene line, 0·486 for the paraffins, 0·286 for the monatomic gases. When these are multiplied by the electron charge the energies of the groups become respectively 2·38, 1·72, 1·13, 0·79, and 0·45, $10^{-12}$ erg. These energies are of the same order, $10^{-12}$ erg, as those of quanta in the visible spectrum. The results do not appear to have any direct relation to the ionizing potentials of the gases as tabulated, nor do they depend in any simple manner on the arrangement of the electrons about the nucleus. The cause of the identity of energy in the groups and of the separation of gases into groups has still to be found. The wave theory of collisions between molecules and the relatively slow electrons in the corona field does not indicate that there should be such groups. A comparison between diffraction patterns of gases for fast electrons shows that there are characteristic differences in the molecular fields, between $CCl_4$ and benzene for example, that might possibly be the cause.

Since, however, the corona starting gradients in each group are proportional to the cross-sectional area of its molecules it can be inferred, from the existence of groups, that when molecules that have the same electric strength differ in area they do so in well-marked and fairly regular steps, similar to those that exist in the electron orbits of their atoms. Whether these differences can be observed by electron diffraction patterns is beyond the present enquiry. All that is attempted here is to give the results obtained and to point out some of their more evident relations.

4. Chlorine proved to be a difficult gas in which to observe corona; with bromine it was impossible to obtain reliable readings. In the latter there appeared to be dissociation in the intense field at the moment corona started. The figure given, 85 kilovolts per cm., is the most probable value for chlorine. It has in corona an electric strength several times that of air and is the strongest gaseous element that it has been possible to measure. Hydrogen, on the other hand, is the weakest active element. For this reason and the fact that several substitution compounds of chlorine for hydrogen with low boiling-points were available, measurements were made on the chlorides of the paraffins up to pentane. When an

atom of chlorine is substituted for one of hydrogen in methane, $CH_4$, the starting corona gradient of which is 22·3 kv./cm., that of the resulting compound $CH_3Cl$, methyl chloride, is 45·6. Methylene dichloride, $CH_2Cl_2$, has a much greater strength, 126 kv./cm.; chloroform, $CHCl_3$, has 162, and carbon tetrachloride, $CCl_4$, 204 kv./cm. In every case the substitution of chlorine increases the electric strength of the gas. Dichlorethane, $C_2H_4Cl_2$, whose mean free path is not known, has an electric strength of 240, an abnormally high value, comparable with that of amylchloride, $C_5H_{11}Cl$, 264 kv./cm. Ethylene dichloride, $C_2H_2Cl_2$, has 144, greater than $CH_2Cl_2$ by 18 kv./cm. The average rise in the

Fig. 2.

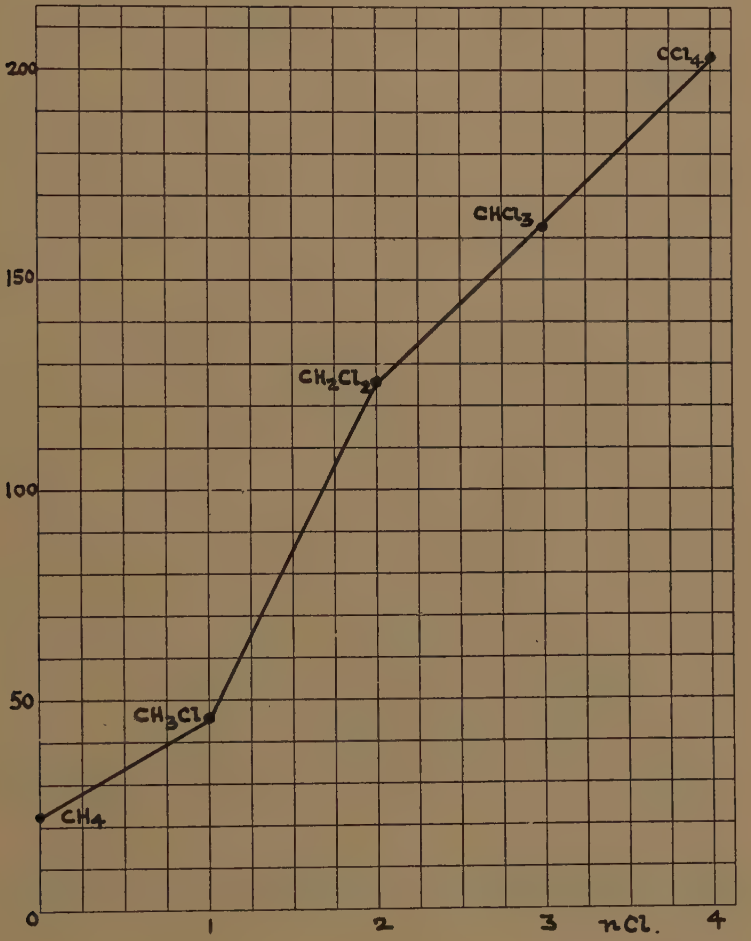

paraffin series due to the addition of one $CH_2$ group is 12 kv. Hydrogen in general, though not always, lowers the strength of a molecule. Acetylene, $C_2H_2$, has 75·2, ethylene, $C_2H_4$, 21·3 kv./cm.

When $Gm_0$ is set down as in fig. 2 against the number of chlorine atoms in the substitution compounds from methane the step is the same, 40 kv./cm., for the higher gases on the line, but there is a disproportion in the first two steps. The tetrahedral shape of the methane molecule would lead to the view that the substitution of one atom of chlorine gives a molecule electrically symmetrical about one axis, but that that of two atoms produces asymmetry. This may be the reason for the small first step of 27 kv. and the next, larger one, of 80 kv., that shears the curve upwards.

Fig. 3.

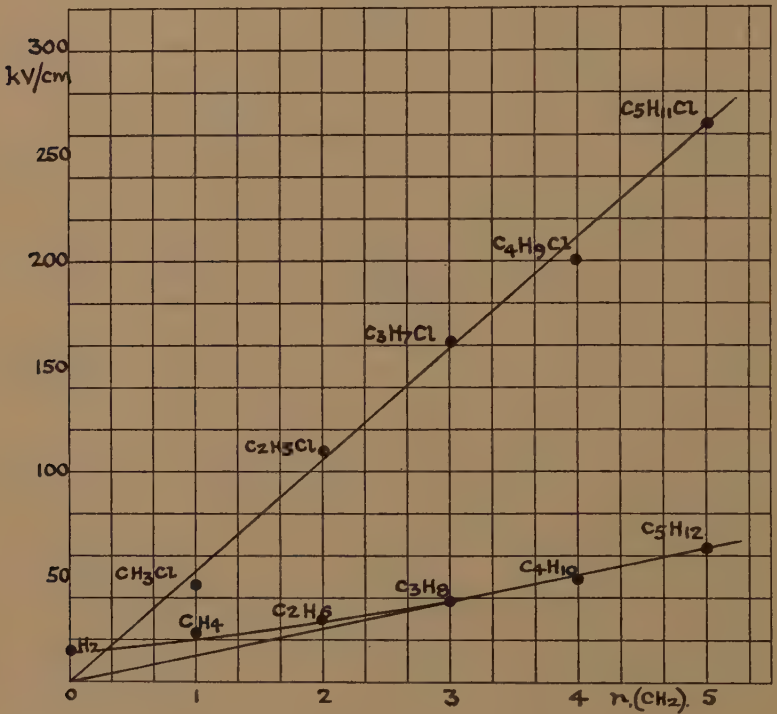

When again, as in fig. 3, the abscissa is taken as the number of $CH_2$ groups in the compounds formed by the substitution of one chlorine atom for hydrogen in each of the paraffins up to pentane, the line passes through the origin with a mean increase of 51 kv./cm. for each step in the series. The mean free paths of the two gases $C_3H_7Cl$ and $C_4H_9Cl$ are due to Steudel ⁽⁵⁾, whose results are known to be somewhat high.

Expressed, as in fig. 3, in relation to the $CH_2$ groups the electric strengths of these gases are consistent with the others.

5. The linear relations between the gases in fig. 1 show that the intensity of ionization that leads to corona discharge is proportional in any one group of gases only to the effective areas of the molecules, for the gas kinetic mean free path is inversely proportional to the effective cross-sectional area, which could in fact be substituted for $1/L_e$ as abscissa in fig. 1.

Fig. 4.

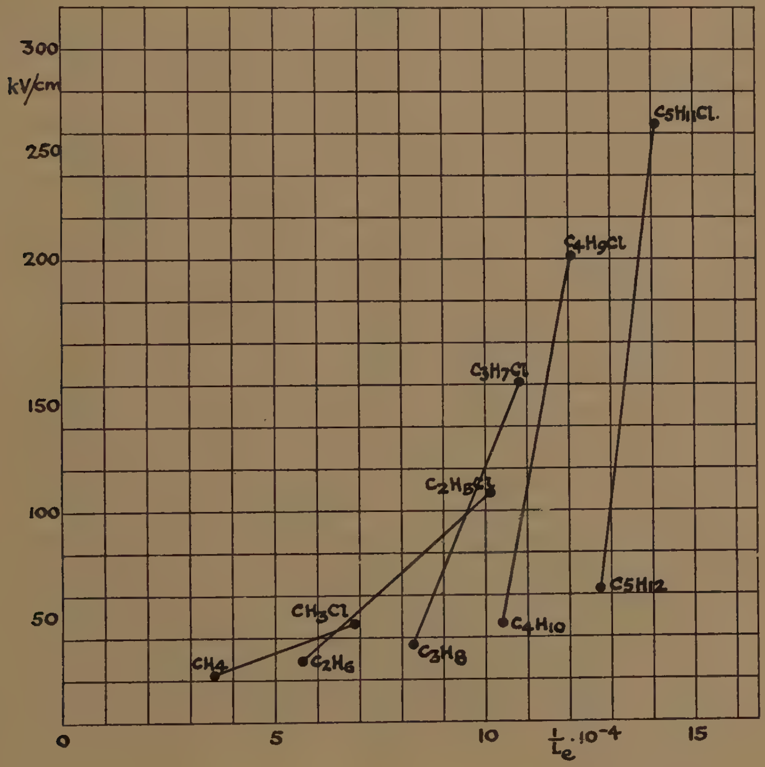

The difference between the ordinates of the two lines in fig. 3 is the rise of electric strength due to the substitution of a chlorine atom for hydrogen at one end of the paraffin molecule, and since $Gm_0$ is proportional to the area it would appear that the effect of placing the one chlorine atom there is to increase the apparent or electric area in the ratio 51/12 of the slopes of the lines, or nearly four times. It doubles in effect the diameter, at least of the longer molecules in the paraffin series, as a target for the relatively slow alternating electron stream.

The lower line in fig. 3 is drawn through the origin. It is the slope of the paraffins above butane. The transition of electric strength from that of hydrogen, through methane, ethane, and propane, to this line is evident. It was thought at first that the proportionally higher values of the lower paraffins might be due to impurities, though these must have been small, but they appear to be the normal result of the arrangement of atoms in the molecules.

Fig. 5.

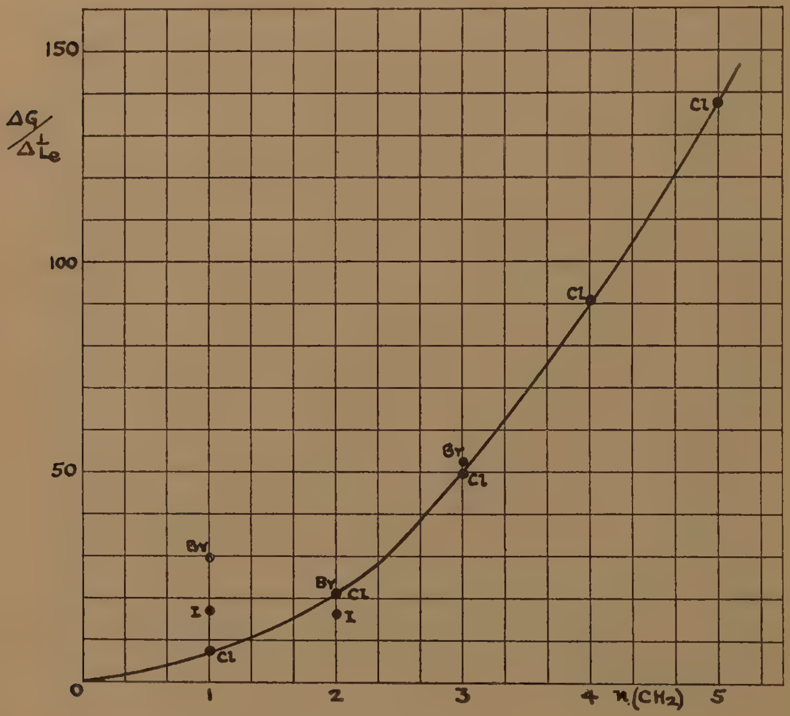

Fig. 4 shows the relations between the electric strength and 1/L or the cross-sectional areas of these molecules. Although the actual strength is, as shown in fig. 3, proportional to the number of $CH_2$ groups in the molecule, its rate of rise with increase of area is not uniform, but grows rapidly, as shown in fig. 5. The great electric strength given to the higher paraffins by chlorination is most probably due to the electric structure of the molecules themselves rather than to their manner of aggregation in liquids or solids. The curve of fig. 5, of which the ordinates are $\triangle Gm_0/\triangle 1/L_e$ from fig. 1*, and the abscissæ are the number *n* of the $CH_2$ groups in the series, is a parabola, and, after the abnormal positions of $CH_3Br$ and $CH_3I$, fits the bromine substitution compounds as well as those of chlorine. The one normal case of the iodine compounds, $C_2H_5I$, is also near this curve. Methyl bromide, $CH_3Br$, proved to be a very difficult gas to measure; the scattering of the observations was wide. In the attempt to obtain consistent results with this gas some 130 determinations were made, and the final result, 97 kv./cm., was obtained by applying statistical methods. The curve of fig. 5 should be a parabola for gases in which G and the change of effective molecular areas are both proportional to *n*. The high values of methyl bromide and iodide are probably due to dissociation of the compounds into the element and ethane, though, as shown by fig. 1, these gases occupy places on group lines. In each case there was some change of colour of the gas after the discharge had passed.

Fig. 6 is drawn in order to follow the change of $1/L_e$, or the effective molecular area, in its relation to the number of $CH_2$ groups in the molecule. The effective areas of the paraffins are shown to be closely proportional to the number of groups *n*. Brüche's maximum value of cross-sectional areas, expressed as the ratio $cm.^2 cm.^3$, found by Ramsauer's method for electrons with velocities $2{\cdot}6\sqrt{\text{volts}}$, at 1 mm. pressure and 0° C., are shown by the dotted line. They are in gradients much lower than those in corona discharge ⁽⁶⁾.

The starting points of the lines giving the results of the substitution of a halogen element for hydrogen are the compounds HCl, HBr, and HI. The lines connecting the values of the higher points in the series should converge towards the paraffins line. The actual change is not uniform. There is in each case a fluctuation about a mean converging line, but this is not sufficient to disturb greatly the upper parts of the lines. From this figure the most probable value of $1/L_e$ for $C_4H_9Cl$ is just over 12 and for $C_5H_{11}Cl$ just over 14. Taking a value for the former of 12·05 places the compound on the curve of fig. 5, and with 14·15 $C_5H_{11}Cl$ lies on the curve. The mean free path of the latter has not been determined experimentally, and Steudel's value for the former is probably high, so that $1/L_e$ is low. It is one of the most striking points in the substitution of chlorine for one hydrogen atom that its effect rises in a succession of steps with the place of the paraffins in the series. From $CH_4$ to $CH_3Cl$ there is a step of one group, from $C_2H_6$ to $C_2H_5Cl$ of two, from $C_3H_8$ to $C_3H_7Cl$ of three groups. From $C_4H_{10}$ to $C_4H_9Cl$ there are probably three, and from $C_5H_{12}$ to $C_5H_{11}Cl$ four energy steps.

---

* *E.g.*

$$Gm_0\,(C_3H_7Cl+C_3H_8)\Big/\frac{1}{L_e}\,(C_3H_7Cl-C_3H_8)$$
$$(160{\cdot}9-37{\cdot}2)/(10{\cdot}75-8{\cdot}26)=49{\cdot}7.$$

6. The other results may be summarized as follows:—Nitrogen, nitrous oxide, and ammonia are all near to, though rather less than, the upper, 1·5 volts, line of fig. 1. Hydrogen sulphide and sulphur dioxide are in the 1·08 volt group, carbon disulphide is on the 0·71 volt line.

Fig. 6.

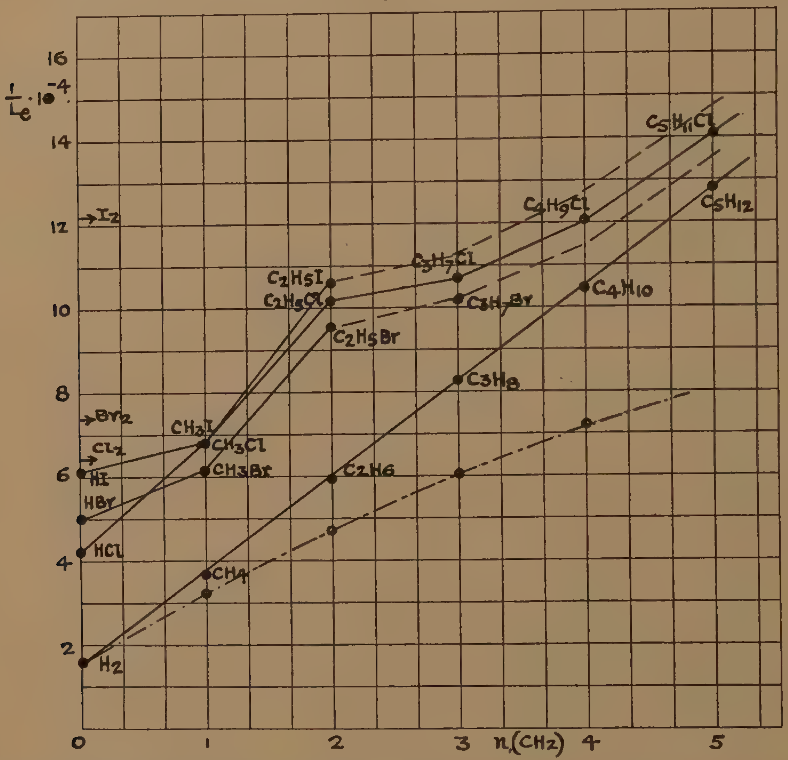

Unsaturated hydrocarbons are, in general, though not always, stronger than saturated, as shown below.

| | | $Gm_0$=kv./cm. | $\frac{1}{L_e}$ $10^{-4}$. | $Gm_0L$ volts. |
|---|---|---|---|---|
| Acetylene ...... | $C_2H_2$ | 75·2 | 5·03 | 1·54 |
| Ethylene ...... | $C_2H_4$ | 21·3 | 5·24 | 0·40 |
| Ethane ......... | $C_2H_6$ | 26·2 | 6·12 | 0·47 |
| Propylene ...... | $C_3H_6$ | 87·2 | 7·99 | 1·06 |
| Propane ........ | $C_3H_8$ | 37·2 | 8·26 | 0·40 |

Certain other compounds were examined, since their mean free paths were known and their vapour pressures were suitable. Benzene, $C_6H_6$, was found to be very sensitive to impurities. The least trace of wax or a small air leak lowered its starting voltage. The result given, 88 kv./cm., is the most probable value from many determinations. It lies in the 0·71 volt group. Ether, $(C_2H_5)_2O$, is a relatively poor insulator with 13·2 kv./cm., lower than hydrogen, and acetone, $(CH_3)_2CO$, with 5 kv./cm., can scarcely be regarded as an insulating vapour. Helium at 4 kv. lies on the paraffins line. Neon, argon, and krypton form a sub-group ranging from 4·5 to 9·5 kv./cm., the lowest group of the gaseous elements.

Measurements are being made on other gases for which the mean free paths are not as yet known. The number of gaseous elements and compounds for which this constant is known with fair accuracy does not exceed fifty, that is of gases or vapours to which a strong electric field can be applied with the gas approaching atmospheric pressure.

Measurements of the electric strength of gases have been made by observing the potential sparking gradient between small spheres, and, provided that the ratio of the gap to the diameter of the spheres is small, results may be obtained that agree within 5 to 10 per cent. between themselves; but it is difficult to correlate the results of different observers. The electric strengths of gases at atmospheric pressure when measured under constant conditions by the sparking potentials in uniform fields of force might, if they were available, follow the same order as in corona discharge and show the same division into groups, each having a characteristic energy of ionizing collision; but the maximum gradient $Gm$ in corona measurements is higher than that at which a spark passes; in air it may be as much as five times greater when fine wires are used.

There is at the present time much work being done on the fundamental theory of insulating materials. Since a gas is the simplest form of insulator, the results now given may provide material for further work on this subject.

The author is indebted to the Electrical Research Association, whose help and interest made the work possible, and to Dr. J. D. Stephenson, Mr. A. E. Schuil, B.Sc., and Mr. W. Ridley, M.Sc., who made many of the measurements and reduced them.

## *Summary.*

When the electrical potential of a wire surrounded by a gas at or near atmospheric pressure is slowly raised a glow or corona appears on the wire as if the surface became suddenly luminous. This is the first stage of spark discharge in the gas that is prevented from developing

farther by the rapid divergence of the field. The electric gradient at which it occurs is much higher than that at which a spark passes in a uniform field of force, but the latter can be derived from measurements of the corona starting voltage, the radius of the wire, and the density of the gas. In the present work the electric strength of some fifty gases has been found in this way. When set down against the reciprocal of the electron mean free path the gases are found to fall into several groups which lie on straight lines converging to the origin. In each of these the product of the electric strength and the free path is constant. This is interpreted to mean that the energy of ionization by collision that starts spark discharge is constant in each group of gases. Since the free path is inversely proportional to the cross-sectional area of the molecules it follows that the molecular areas of gases that have the same electric strengths in the several groups differ by finite and nearly equal steps. The electric strengths of gases having the same molecular area change only by such steps. Chlorine has the greatest strength of the elements examined, the monatomic gases the least. The paraffin series is most uniform ; its chlorine substitution compounds show a regular change and reach remarkably high values.

## *References.*

(1) *Vide* ‘The Theory of Dielectrics,’ by A. Schwaiger, pl. i. p. 465.
(2) J. D. Stephenson, Phil. Mag. vol. xv. fig. 3, p. 257 (1933).
(3) Journ. Inst. Elec. Eng. vol. lxix. no. 412 (April 1931).
(4) Phil. Mag. xxviii. p. 679 (1939).
(5) *Ann. der Physik*. vol. xvi. p. 369 (1882).
(6) *Ann. der Physik*. vol. iv. p. 387 (1930).

# LXIX. *A Note on the Viscosity of Gases and Molecular Mean Free Path.*

By A. E. Schuil, B.Sc.*

[Received July 20, 1939.]

The electric strength of a gas in a uniform field, derived from measurements of corona starting voltage on wires, has been found to be directly proportional to the cross-sectional area of its molecules, that is, to the reciprocal of its mean free path. The gases examined fell into groups in each of which the product of the electric strength G and the mean free path L is constant, and the value of this varies from one group to another in finite and nearly equal steps. Measurements of the electric strength can be made within about one per cent., but the tabulated values of the mean free path are much less certain. For the purpose of the above work it became necessary to compare the most recent determinations of mean free path, taking into account in particular Sutherland's modification of Maxwell's theory and Chapman's later views and to recalculate them in some cases.

The various models that have been used all lead to the same form of equation for the viscosity of a gas, viz., $\eta = \mathrm{C} \,.\, \rho \mathrm{L} v$, where $\rho$ is the density, $v$ the mean molecular velocity, L the mean free path, and C a constant. They only differ in the value given to the constant. Thus when the molecules are considered as inert spheres C is 0·33 (1). Viscosity is independent of pressure (5), (6), but not in general proportional to any power of temperature (1), (2), (3), (4). Sutherland (7), by considering attraction between molecules, increased the effective diameter $\sigma$ by a factor

$$\left\{ 1 + \frac{2}{v^2} \int_{\sigma}^{\infty} \mathrm{F}(\rho) d\rho \right\}^{\frac{1}{2}},$$

where $\mathrm{F}(\rho)$ is a characteristic function of the gas, and $v$ the relative velocity between two molecules, which is proportional to $\mathrm{T}^{\frac{1}{2}}$. This was slightly modified by Reinganum (8). Trautz (9), from a very comprehensive series of researches, shows that without exception $\frac{d \log \eta}{d \log \mathrm{T}} = 1$, at the critical temperature. Boltzmann's (10) value for the constant was 0·35 (see also Tait (11)), and Jeans (3), by postulating that a molecule retains some of its original momentum after collision, showed that a more

---

* Communicated by W. M. Thornton, D.Sc., D.Eng.

## Table I.—Viscosity Data for Inorganic Substances.

| | Viscosity ($\eta \times 10^7$) at various temperatures, C. | | | | | | | $\eta_0 \times 10^7$. | Sutherland's. C. | Remarks. | References. |
|---|---|---|---|---|---|---|---|---|---|---|---|
| | 0°. | 20. | 50. | 100. | 150. | 200. | 250. | | | | |
| Air | 1708 | 1807 | — | 2171 | — | 2569 | 2751 | — | 112 | Obeys Sutherland's law. | 20, 21, 24, 26, 27, 28, 29, 31, 32, 36, 51, 52. |
| Ammonia | [916] | 982 | 1092 | 1278 | 1463 | 1645 | 1813 | 1380 | 503 | C constant from 20–300° C. | 37, 42, 46. |
| Argon | [2114] | 2217 | — | 2695 | — | 3223 | 3444 | 1209 | 142 | C constant up to 800° C. | 14, 15, 31, 32, 34, 42. |
| Bromine | [1464] | (19) 1526 | (25) 1528 | (94) 1921 | — | (190) 2369 | — | 2958 | 533 | C increases with temp. Value 533 holds above 460°. | 17, 47. |
| Carbon monoxide | 1659 | 1763 | 1864 | 2083 | 2276 | 2463 | 2632 | 878 | 101·2 | Obeys Sutherland's law. | 28, 31, 33, 42. |
| Carbon dioxide | [1375] | (26·9) 1493 | (76·9) 1725 | — | (126·9) 2160 | (226·9) 2354 | (276·9) 2556 | 1510 | 254 | C constant above 300° C. when its value is 213. | 22, 34, 35, 42. |
| Carbon disulphide | [886] | — | — | (114·3) 1303 | (152·5) 1434 | (190·2) 1561 | (267·3) 1830 | — | 499·5 | — | 50. |
| Chlorine | [1227] | 1312 | (55·1) 1470 | (99·4) 1651 | (145·4) 1845 | (199·5) 2081 | 2244 | 1839 | 330 | C=350 from 100–250°. | 16, 38. |
| Cyanogen | 928 | (17) 987 | — | 1271 | — | — | — | — | 330 | — | 19. |
| Helium | 1885 | 1941 | — | 2281 | — | 2672 | 2853 | 97·1 | 80 | — | 32, 42. |
| Hydrogen | 835 | 876 | 937 | 1032 | 1126 | 1212 | 1297 | 153 | 84·4 | $\eta \alpha (T)^{0·675}$ | 26, 27, 28, 29, 31, 32, 33, 34, 36, 51. |
| Hydrogen sulphide | 1166 | (17) 1241 | — | 1587 | — | — | — | — | 331 | — | 22. |
| Hydrogen bromide | [1697] | (18·7) 1819 | — | (100·2) 2344 | — | — | — | 2305 | 357 | — | — |
| Hydrogen chloride | [1313] | (21) 1434 | (54·0) 1600 | (99) 1832 | (154·0) 2093 | 2303 | 2530 | 1581 | 362 | — | 27, 52. |
| Hydrogen iodide | [1726] | (20·5) 1857 | — | (96·6) 2310 | (149·4) 2631 | (198·6) 2922 | (251) 3228 | 2640 | 331 | C=355 between 100–200° C. | 38, 52 |
| Iodine | [1228] | — | — | (102·2) 1785 | — | (232·2) 2319 | (319·2) 2561 | 3615 | 568 | — | 18, 46 |
| Krypton | 2327 | (15) 2460 | — | — | — | — | — | 1780 | 188 | — | 14, 15. |
| Neon | [2962] | 3111 | — | 3646 | (184·5) 4177 | 4248 | 4532 | 705 | 56 | — | 14, 15, 23, 32, 42. |
| Nitrogen | [1652] | (16·1) 1728 | (51·6) 1880 | 2084 | (151·9) 2287 | 2461 | 2629 | 835 | 104 | C constant up to 830° C. | 28, 33, 34. |
| Nitrous oxide | 1381 | (26·9) 1488 | (76·9) 1723 | (126·9) 1943 | (176·9) 2158 | (226·9) 2355 | (276·9) 2555 | 1536 | 260 | — | 35. |
| Nitric oxide | 1777 | 1876 | 2036 | 2272 | 2474 | 2682 | 2870 | 1208 | 128 | — | 13, 41, 42, 44. |
| Oxygen | [1911] | (14·8) 1985 | (127·7) 2568 | — | — | (227) 3017 | (277) 3220 | 1154 | 125 | C constant up to 830° C. | 13, 33, 34. |
| Sulphur dioxide | 1158 | 1266 | (40) 1352 | 1612 | (120) 1716 | 2038 | — | 1884 | 416 | — | 38, 49, 51. |
| Water | 861 | 937 | — | 1255 | 1445 | 1635 | 1827 | — | 650 | $\eta$ indep. of press. up to 93 atm. | 5, 46. |
| Xenon | 2107 | (16·5) 2250 | — | (99·4) 2871 | — | — | — | 2249 | 252 | — | 42. |

## TABLE I. (*cont.*).—Viscosity Data for Organic Substances.

| | Viscosity ($\eta \times 10^7$) at various temperatures. | | | | | | | $\eta_c \times 10^7$. | C. | Remarks. | References. |
|---|---|---|---|---|---|---|---|---|---|---|---|
| | 0°C. | 20. | 50. | 100. | 150. | 200. | 250. | | | | |
| Methane, $CH_4$ .... | [1022] | 1087 | 1182 | 1331 | 1471 | 1603 | 1725 | 726 | 164 | — | 22, 36, 42. |
| Methyl alcohol, $CH_3OH$. | [865] | — | — | (111·3)<br>1259 | (153·9)<br>1408 | (188·8)<br>1527 | 1725 | — | 487 | — | 49. |
| Methyl chloride, $CH_3Cl$. | [981] | 1061 | 1175 | 1357 | — | (219·4)<br>1769 | — | 1512 | 454 | — | 46, 49. |
| Methylene chloride, $CH_2Cl_2$. | [910] | (22·1)<br>991 | — | 1267 | — | (219·1)<br>1667 | — | 1752 | 395 | C computed graphically. | 42. |
| Chloroform, $CHCl_3$ | [929] | 1001 | — | 1267 | (161·3)<br>1491 | (189·1)<br>1579 | 1776 | 1780 | 373 | — | 42, 46, 49. |
| Carbon tetrachloride, $CCl_4$. | [898] | — | — | (127·9)<br>1334 | (169·3)<br>1463 | 1562 | (282·2)<br>1808 | 1750 | 365 | — | 42, 49. |
| Methyl bromide, $CH_3Br$. | [1229] | 1327 | 1457 | (120)<br>1797 | — | — | – | 2115 | 402 | C computed graphically. | 13, 42, 49. |
| Methyl ether $(CH_3)_2O$. | [846] | (19·5)<br>909 | (60)<br>1044 | 1167 | (120)<br>1228 | — | — | 1255 | 426 | — | 42, 49. |
| Ethane, $C_2H_6$ ..... | [851] | 909 | 998 | 1142 | 1278 | 1408 | 1525 | 935 | 252 | — | 36, 42, 49. |
| Ethyl alcohol, $C_2H_5OH$. | [752] | — | — | (130·2)<br>1173 | (170·7)<br>1293 | (191·8)<br>1355 | (251·7)<br>1519 | — | 407 | — | 49. |
| Ethyl chloride, $C_2H_5Cl$. | 937 | — | — | — | — | — | — | — | 411 | C computed from $T_C$. | 13. |
| Ethylene, $C_2H_4$.... | [944] | 1008 | 1103 | 1256 | 1403 | 1541 | 1666 | 962 | 241 | — | 29, 33, 37, 42, 49. |
| Acetone $(CH_3)_2CO$ . | [660] | — | — | (119)<br>991 | (159·5)<br>1101 | (190·4)<br>1186 | (247·7)<br>1334 | — | 541 | — | 49. |
| Acetylene, $C_2H_2$ ... | [955] | 1020 | 1113 | 1254 | (120)<br>1318 | — | — | 1073 | 215 | — | 49. |
| Propane $C_3H_8$ .... | [746] | 801 | 880 | 1008 | 1132 | 1253 | 1362 | 990 | 278 | — | 35, 36. |
| *n*-Propyl alcohol, $C_3H_7OH$. | [682] | — | — | (121·7)<br>1025 | (149)<br>1102 | (209·7)<br>1267 | (243·2)<br>1350 | — | 515·6 | — | 49. |
| Iso-Propyl alcohol, $C_3H_7OH$. | [698] | — | — | (119·2)<br>1028 | (149·2)<br>1112 | (198·4)<br>1248 | (251·0)<br>1382 | — | 459·9 | — | 49. |
| Propylene, $C_3H_6$. | [775] | 835 | (60)<br>959 | 1071 | (120)<br>1122 | — | — | 1045 | 362 | — | 42, 49. |
| Ether $(C_2H_5)_2O$.... | [679] | — | — | 955 | (159·4)<br>1079 | (217·7)<br>1222 | (251·0)<br>1300 | — | 404 | — | 13, 49. |
| *n*-Butane, $C_4H$ .... | [686] | 739 | (40)<br>787 | 947 | (120·0)<br>998 | — | — | — | 358 | — | 49. |
| Iso-Butane, $C_4H_{10}$ • | [692] | 744 | (40)<br>792 | 947 | (120)<br>995 | — | — | — | 330 | — | 49. |
| *n*-Pentane, $C_5H_{12}$ .. | [621] | — | — | (121·6)<br>911 | (158·9)<br>995 | (219·1)<br>1126 | (249·5)<br>1191 | — | 383 | — | 49. |
| Benzene, $C_6H_6$ .... | [677] | (14·2)<br>738 | 918 | (131·3)<br>1031 | (161·3)<br>1110 | (194·6)<br>1198 | (252·5)<br>1343 | 1423 | 447·5 | — | 49. |
| *n*-Hexane ........ | [586] | — | — | (120·7)<br>866 | (160·8)<br>958 | (188·9)<br>1021 | (248·0)<br>1144 | — | 436·1 | — | 49. |

Values in square brackets computed by the author. Where viscosities were not measured at the temperature shown at the heads of the columns, the temperature is given in small brackets. $n_c$ is the viscosity at the critical temperature.

probable value is 0·461. Finally, Chapman (12) gave the most rigorous treatment of the subject and arrived at a value 0·49. This last figure has been used in calculating Table II. The relation is then $\eta = 0{\cdot}49\ \rho v L$, or taking for $v$ the value

$$\left(\frac{8p}{\pi\rho}\right)^{-\frac{1}{2}},\ L = 1{\cdot}28\eta(pd)^{-\frac{1}{2}}.$$

### Table II.

### Mean Free Paths and Molecular Diameters for Inorganic Substances.

| | $l_0 \times 10^6$. | $\sigma_\eta \times 10^8$. | $\sigma_b \times 10^8$. |
|---|---|---|---|
| Air | 6·03 | — | — |
| Ammonia | 4·18 | 2·64 | 3·05 |
| Argon | 6·36 | 2·94 | 2·86 |
| Bromine | 2·33 | 3·28 | 3·05 |
| Carbon monoxide | 5·91 | 3·20 | 3·09 |
| Carbon dioxide | 3·94 | 3·44 | 3·40 |
| Carbon disulphide | 1·93 | 3·90 | 3·93 |
| Chlorine | 2·75 | 3·69 | 3·30 |
| Cyanogen | 2·32 | 4·03 | 3·78 |
| Helium | 18·0 | 2·08 | 2·30 |
| Hydrogen | 11·2 | 2·40 | 2·32 |
| Hydrogen bromide | 3·57 | 3·18 | 3·28 |
| Hydrogen chloride | 4·12 | 2·92 | 3·12 |
| Hydrogen iodide | 2·89 | 3·45 | 3·47 |
| Hydrogen sulphide | 3·76 | 3·16 | 3·24 |
| Iodine | 1·45 | 4·32 | — |
| Krypton | 4·86 | 3·19 | 3·14 |
| Neon | 12·1 | 2·62 | 2·39 |
| Nitrogen | 5·95 | 3·18 | 3·53 |
| Nitrous oxide | 3·94 | 3·13 | 3·28 |
| Nitric oxide | 7·85 | 2·69 | 2·83 |
| Oxygen | 6·43 | 2·97 | 2·93 |
| Phosphine | 3·38 | 3·45 | — |
| Sulphur dioxide | 2·74 | 3·81 | 3·55 |
| Water | 3·84 | 2·53 | 2·76 |
| Xenon | 3·49 | 3·52 | 3·42 |

Thus for argon, taking a density of 1·78098 ms./litre at normal temperature and pressure,

$$L = \frac{1{\cdot}28 \times 2114 \times 10^{-7}}{(1{\cdot}0132\,.\,10^6 \times 1{\cdot}7809\,.\,10^{-3})^{\frac{1}{2}}} = 6{\cdot}36\,.\,10^{-6}\ \text{cm}.$$

The values of the molecular diameter $\sigma_n$, calculated from viscosity, and of $\sigma_b$, from van der Waals's constant "$b$," are also given in Table II. The latter are probably only reliable to within about 30 per cent.

Table II. (*continued*).

Mean Free Paths and Molecular Diameters for Organic Substances.

| | $l_0 \times 10^6$. | $\sigma_\eta \times 10^8$. | $\sigma_b \times 10^8$. |
|---|---|---|---|
| Methane | 4·83 | 3·28 | 3·23 |
| Methyl alcohol | 2·90 | 3·21 | 3·75 |
| Methyl chloride | 2·59 | 3·47 | 3·71 |
| Methylene dichloride | 1·87 | 4·27 | — |
| Chloroform | 1·62 | 4·65 | 4·32 |
| Carbon tetrachloride | 1·37 | 5·09 | 4·64 |
| Methyl bromide | 2·89 | 3·42 | — |
| Methyl ether | 2·37 | 3·70 | 3·96 |
| Ethane | 2·89 | 3·87 | 3·70 |
| Ethyl alcohol | 2·10 | 3·99 | 4·05 |
| Ethyl chloride | 1·74 | 4·37 | 4·16 |
| Ethylene | 3·37 | 3·62 | 3·54 |
| Acetone | 1·56 | 4·23 | 4·19 |
| Acetylene | 3·51 | 3·99 | 3·44 |
| Propane | 2·14 | 4·38 | 4·04 |
| *n*-Propyl alcohol | 1·66 | 4·21 | 4·42 |
| Iso-Propyl alcohol | 1·71 | 4·26 | 4·26 |
| Ether | 1·47 | 4·77 | 4·73 |
| *n*-Butane | 1·71 | 4·59 | 4·59 |
| Iso-Butane | 1·73 | 4·66 | 4·48 |
| Pentane | 1·39 | 5·0 | 4·86 |
| Benzene | 1·45 | 4·66 | 4·56 |
| *n*-Hexane | 1·20 | 5·18 | 5·18 |
| Cyclo-hexane | 1·35 | 5·19 | 4·83 |

The author is indebted to the Electrical Research Association who made this study possible, and to Professor Thornton for his constant advice and guidance.

## *Bibliography.*

(1) E. H. Kennard, 'Kinetic Theory of Gases.'
(2) L. B. Loeb, 'Kinetic Theory of Gases.'
(3) J. H. Jeans, 'Dynamical Theory of Gases.'
(4) J. P. Kuenen, "Die Eigenschaften der Gase," *Handbuch der Allgemeinen Chemie*, Band III.
(5) W. Schugajew, *Phys. Zeits. der Soviet Union*, v. p. 659 (1934).
(6) J. H. Boyd, Phys. Rev. xxxv. p. 1284 (1930).
(7) W. Sutherland, Phil. Mag. xxxvi. p. 507 (1893).
(8) Reinganum, *Physik. Zeit.* ii. p. 242 (1900).

(9) M. Trautz. *Ann. d. Phys.* x. 2, p. 190 (1931).

(10) L. Boltzmann, *Sitzb. Akad. Wiss. Wien.* lxiv. p. 824 (1892).

(11) P. G. Tait, "Scientific Papers," Trans. Roy. Soc. Edin. xxxiii. (1887).

(12) S. Chapman, Phil. Trans. Roy. Soc. A, ccxi. p. 433 (1922); A, 216, p. 279 (1915); A 217, p. 115 (1916); Proc. Roy. Soc. A, 93, p. 19 (1916).

(13) H. Vogel, *Ann. der Physik*, xliii. p. 1235 (1914).

(14) A. O. Rankine, Proc. Roy. Soc. lxxxiii. pp. 265 & 516 (1910).

(15) A. O. Rankine, Proc. Roy. Soc. lxxxiv. p. 181 (1911).

(16) A. O. Rankine, Proc. Roy. Soc. lxxxvi. p. 162 (1912).

(17) A. O. Rankine, Proc. Roy. Soc. lxxxviii. p. 575 (1913).

(18) A. O. Rankine, Proc. Roy. Soc. xci. p. 201 (1915).

(19) A. O. Rankine & C. J. Smith, Proc. Roy. Soc. xcix. pp. 331–336 (1921).

(20) A. O. Rankine, Proc. Roy. Soc. cxi. p. 219 (1926).

(21) A. O. Rankine & R. S. Edwards, Proc. Roy. Soc. cxvii. p. 245 (1927).

(22) A. O. Rankine & C. J. Smith, Phil. Mag. xlii. p. 615 (1921).

(23) R. S. Edwards, Proc. Roy. Soc. cxix. p. 578 (1928).

(24) F. A. Williams, Proc. Roy. Soc. cx. p. 141 (1926).

(25) A. G. Nasini, Proc. Roy. Soc. cxxiii. p. 692 (1929).

(26) M. Trautz & W. Weizel, *Ann. der Phys.* lxxviii. p. 305 (1925).

(27) M. Trautz & A. Narath, *Ann. der Phys.* lxxix. p. 637 (1926).

(28) M. Trautz & P. B. Baumann, *Ann. der Phys.* ii. 6, p. 733 (1929).

(29) M. Trautz & F. W. Stauf, *Ann. der Phys.* ii. 6, p. 737 (1929).

(30) M. Trautz & K. F. Kipphan, *Ann. der Phys.* ii. 6, p. 743 (1929).

(31) M. Trautz & W. Ludewigs, *Ann. der Phys.* iii. 3, p. 409 (1929).

(32) M. Trautz & H. Binkele, *Ann. der Phys.* v. 5, p. 561 (1930).

(33) M. Trautz & A. Melster, *Ann. der Phys.* vii. 4, p. 409 (1930).

(34) M. Trautz & R. Zink, *Ann. der Phys.* vii. 4, p. 427 (1930).

(35) M. Trautz & F. Kurz, *Ann. der Phys.* ix. 8, p. 981 (1931).

(36) M. Trautz & K. G. Sorg, *Ann. der Phys.* x. 1, p. 81 (1931).

(37) M. Trautz & R. Heberling, *Ann. der Phys.* x. 2, p. 155 (1931).

(38) M. Trautz & Winterkorn, *Ann. der Phys.* x. 4, p. 511 (1931).

(39) M. Trautz & Winterkorn, *Ann. der Phys.* x. 3, p. 263 (1931).

(40) M. Trautz & Winterkorn, *Ann. der Phys.* xi. 2, p. 190 (1931).

(41) M. Trautz & Gabriel, *Ann. der Phys.* xi. 5, p. 606 (1931).

(42) M. Trautz, *Ann. der Phys.* xv. 2, p. 198 (1932).

(43) M. Trautz, *Ann. der Phys.* xvi. 7, p. 751 (1933).

(44) M. Trautz & A. Freytag, *Ann. der Phys.* xx. 2, p. 135 (1934).

(45) M. Trautz & H. Zimmermann, *Ann. der Phys.* xxii. 2, p. 189 (1935).

(46) Braune & Lincke, *Zeits. f. Phys. Chem.* cxlviii A, p. 195 (1930).

(47) Braune, Basch & Wentzel, *Zeits f. Phys. Chem.* cxxxvii. p. 176 (1938).

(48) H. E. Binkele, *Ann. der Physik*, xv. 6, p. 729 (1932).

(49) Titani, Chem. Soc. Jap. Bull. iv. p. 277 (1930); v. p. 98 (1930); p. 255 (1933).

(50) Sutherland & Maass, Canad. Journ. of Research, vi. p. 428 (1932).

(51) Stewart & Maass, Canad. Journ. of Research, vi. p. 453 (1932).

(52) Partington, *Phys. Zeits.* xxxiv. p. 289 (1933).

(53) Hare & Mack, J. Am. C. S. p. 4272 (1932).

(54) Maleven & Mack, J. Am. C. S. p. 888 (1932).

# LXX. *The Surface Tension of Water and Heavy Water.*

By A. H. Cockett and Allan Ferguson *.

[Received November 13, 1939.]

## *Introductory.*

A number of determinations of the surface tension of heavy water have been made, with inconsistent results. Thus, Selwood and Frost (1) give 67·8 dyne/cm. for the surface tension of heavy water at 20° C., as compared with 72·8 dyne/cm. for the surface tension of pure water at the same temperature. On the other hand, Flood and Tronstad (2) find that the surface tension of deuterium oxide of 99 per cent. purity is greater than that of pure water by an amount which barely exceeds the accuracy ($\pm 0{\cdot}15$ dyne/cm.) of measurement.

Through the kindness of Imperial Chemical Industries, Ltd., we have been supplied with a specimen of deuterium oxide of 99·2 per cent. purity, and it seemed desirable to make a determination of the surface tension of the specimen at different temperatures and to compare the resulting values with those of the surface tension of distilled water over the same temperature range.

## *Method.*

Without appreciable loss of precision it is possible to made a determination of a surface tension and of its temperature variation using no more than a few cubic millimetres of liquid. The method consists in measuring the pressure required to force a thread of liquid along a horizontal capillary into such a position that the meniscus at the open end is accurately plane. When this condition holds it easily follows that, small corrections neglected, the surface tension $\gamma$ is given by

$$\gamma=\tfrac{1}{2}rh\rho g,$$

where $r$ is the radius of the capillary, $\rho$ the density and $h$ the head of the *manometer liquid*. It will be seen that the density of the liquid under test does not enter into the problem, and the only outstanding matter of importance is—how far is one justified in using the simple formula which neglects the possible gravitational distortion of the meniscus ?

The distortion of the meniscus in a horizontal capillary is not a promising subject for analysis, but the matter may easily be tested by comparing, in effect, the values of a surface tension obtained from experiments carried out, first in a vertical capillary for which first and second order corrections may be calculated, and then in a horizontal capillary.

---

* Communicated by the Authors.

This has been done (3), and experiment clearly shows that it is safe, under ordinary conditions, to use the simple formula for tubes one millimetre and less in diameter.

### *Details of Experimental Method.*

In the experiments to be described, the capillary tube and liquid were located in a simple furnace consisting of a brass tube about 10 cm. long and 3 cm. in diameter, overwound with nichrome wire. The ends were closed by means of corks bored to accept the capillary tube. The furnace had been designed for use in the measurement of the surface tensions of liquid crystals at temperatures ranging from 100° C. to 200° C., but it could easily be maintained at any temperature between 20° C and 75° C. The temperature-gradient along the tube at the point where the meniscus was arranged to lie was found to be 0·1° C. per cm., the temperatures either side of this point diminishing at this rate. Care was taken in all the experiments to see that the meniscus was accurately located at this point. The temperature difference through the walls of the capillary tube in the neighbourhood of the meniscus was measured at three temperatures by means of a differential thermocouple :—

| Room temp. | Temp. of furnace. | Temp. difference. |
|---|---|---|
| °C. | °C. | °C. |
| 22 | 37·5 | ±0·00 |
| 22 | 55·0 | −0·05 |
| 22 | 62·5 | −0·07 |

It was therefore quite safe to take the temperature of the liquid as given by the temperature of a thermocouple junction placed in contact with the capillary tube at the point occupied by the meniscus.

Fig. 1 shows the disposition of the furnace and the tube.

It will be seen that the capillary tube is so arranged that it projects from both ends of the furnace. This was done in order to make it possible to use a longer thread of liquid than would have been possible if the whole of it were to be kept inside, as it was found that when working at the higher temperatures a short thread of liquid evaporated before the completion of the observations. The end B of the capillary is connected to the manometer and to a simple arrangement for pressure adjustment. The thread of liquid, which extends from A to C, is forced along the tube until the meniscus at A is accurately plane. There is, therefore, no pressure-difference across this meniscus; it is across the curved meniscus at C that the measured pressure-difference exists.

The planeness of the meniscus was judged either by illuminating it by means of a small lamp and watching the meniscus through a pocket lens (4), or, later, by putting an aperture crossed by a fine hair in front of the end A of the tube, and observing the distortion of the image of the hair seen in the meniscus and in the end of the tube.

Fig. 1.

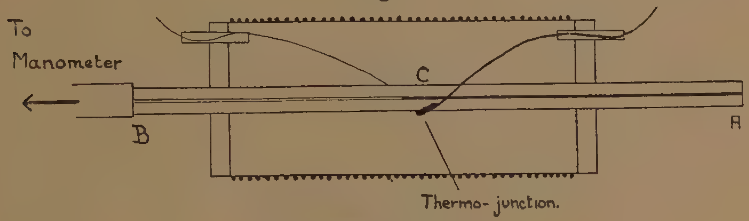

Furnace and tube.

The general disposition of the apparatus is shown in fig. 2, which is self-explanatory.

Fig. 2.

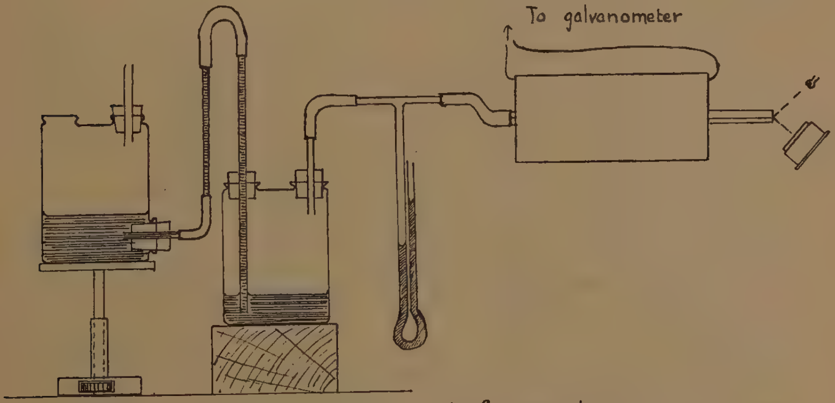

General arrangement of apparatus.

It shows the manometer, in which the liquid used is aniline, and the simple arrangement employed to force the thread of liquid along the tube to its standard position of equilibrium.

The density of the aniline, measured after redistilling prior to use, was 1·0227 (1·023) grams/c.c. at 17·5° C.

All temperature measurements were made by means of a chromel-alumel thermocouple which was connected to a sensitive galvanometer of high resistance. One junction of the thermocouple was kept permanently in melting ice, and temperatures were read in terms of the galvanometer deflexions which had been calibrated by comparison with a standard thermometer with N.P.L. certificate. A deflexion of one centimetre (at one metre) was equivalent to a temperature difference of 1·60 degrees Centigrade.

### TABLE I.

Diameter of tube .................... 0·0631 cm.(d)

Hence, surface tension is given by

$$\gamma = \frac{gdh\rho}{4},$$
$$= 1{\cdot}580\,h.$$

*Water.*

| Temp. °C. | $h$ (cm.). | Surface tension. |
|---|---|---|
| 18·5 | 4·590 | 72·65 |
| ,, | 4·603 | 72·85 |
| ,, | 4·604 | 72·87 |
| 30·1 | 4·497 | 71·17 |
| ,, | 4·495 | 71·19 |
| ,, | 4·501 | 71·23 |
| 33·2 | 4·490 | 71·06 |
| ,, | 4·481 | 70·92 |
| ,, | 4·484 | 70·97 |
| 36·6 | 4·430 | 70·11 |
| ,, | 4·436 | 70·20 |
| ,, | 4·434 | 70·17 |
| 38·4 | 4·426 | 70·05 |
| ,, | 4·429 | 70·09 |
| 43·6 | 4·384 | 69·38 |
| ,, | 4·389 | 69·46 |
| 50·0 | 4·306 | 68·15 |
| ,, | 4·301 | 68·08 |
| ,, | 4·307 | 68·17 |

*Heavy water.*

| Temp. °C. | $h$ (cm.). | Surface tension. |
|---|---|---|
| 17·6 | 4·560 | 72·17 |
| ,, | 4·544 | 71·91 |
| ,, | 4·562 | 72·20 |
| ,, | 4·562 | 72·20 |
| 22·2 | 4·491 | 71·08 |
| ,, | 4·507 | 71·33 |
| ,, | 4·510 | 71·38 |
| 22·7 | 4·498 | 71·20 |
| ,, | 4·496 | 71·16 |
| 24·6 | 4·498 | 71·20 |
| ,, | 4·479 | 70·89 |
| ,, | 4·471 | 70·76 |
| 26·5 | 4·479 | 70·89 |
| ,, | 4·480 | 70·90 |
| ,, | 4·480 | 70·90 |
| 35·6 | 4·385 | 69·40 |
| ,, | 4·389 | 69·60 |
| ,, | 4·381 | 69.34 |
| ,, | 4·371 | 69·18 |
| ,, | 4·374 | 69·22 |
| 39·5 | 4·323 | 68·42 |
| ,, | 4·327 | 68·48 |
| ,, | 4·320 | 68·37 |
| ,, | 4·334 | 68·59 |

The capillary tubes were all carefully selected, and cleaned with nitric acid, caustic potash, and chromic acid, then rinsed in distilled water.

In some instances the tube was tested for uniformity of bore by means of a mercury thread, and if any tendency to conicality were apparent, measurements of the mean diameter were taken at each end of the tube, and the diameter hence estimated at the point where the meniscus was placed. In other instances the tube was cut through at this point when an experiment was complete, and the diameter measured directly. In every instance the effect of such slight ellipticity as was present was allowed for by taking the mean of readings at right angles to each other. The diameters of all the tubes used were between 0·05 and 0·08 cm.

All length measurements, of pressure head and of tube diameter, were made on a travelling microscope of high quality, provided with verniers reading to 0·001 cm.

With each tube used several groups of experiments were made, each group covering the available temperature range. At each temperature several settings of the meniscus were made. The figures obtained in one such group of experiments with water and with heavy water are shown in Table I., these being typical of the results obtained.

## *Surface Tension of Water.*

The values obtained for the surface tension of ordinary water are closely represented by the equation

$$\gamma_t = 75{\cdot}23 - 0{\cdot}06667\, t^{1{\cdot}2},$$

the value of 73·51 dyne/cm. at 15° C. being in very close agreement with the generally accepted value.

The full results are contained in Table II.

TABLE II.

| Temp. °C. | $\gamma$, dyne/cm. | T. °C. | $\gamma$, dyne/cm. |
|---|---|---|---|
| 17·3 | 72·84 | 38·1 | 70·32 |
| 18·5 | 72·69 | 38·4 | 70·07 |
| 18·7 | 73·00 | 39·9 | 69·52 |
| 19·1 | 72·84 | 42·0 | 69·24 |
| 20·4 | 72·75 | 43·6 | 69·42 |
| 21·5 | 72·56 | 44·6 | 68·86 |
| 24·4 | 72·56 | 45·8 | 68·66 |
| 25·5 | 71·94 | 48·4 | 68·19 |
| 28·6 | 71·86 | 50·0 | 68·13 |
| 30·1 | 71·20 | 52·3 | 67·65 |
| 31·9 | 70·98 | 60·2 | 65·93 |
| 33·2 | 70·98 | 61·3 | 66·19 |
| 34·5 | 70·35 | 65·7 | 65·39 |
| 34·6 | 70·07 | 73·1 | 63·60 |
| 36·6 | 70·16 | | |

### *Surface Tension of Heavy Water.*

As was remarked in the introductory paragraph, the heavy water was a specimen of 99·2 per cent. purity given to us by the Imperial Chemical Industries, Ltd. The specimen, about 5 gm. in mass, was kept in a sealed container, and a thread of the requisite length was drawn into the tube before the commencement of each run.

Table III. below shows the experimental values of the surface tension of heavy water.

Table III.

*Surface Tension of Heavy Water. Experimental Values.*

| T. °C. | $\gamma$, dyne/cm. | T. | $\gamma$. | T. | $\gamma$. | T. | $\gamma$. | T. | $\gamma$. |
|---|---|---|---|---|---|---|---|---|---|
| 12·1 | 72·88 | 22·7 | 71·26 | 32·2 | 69·74 | 43·1 | 67·42 | 55·0 | 65·63 |
| 12·8 | 72·81 | 23·5 | 71·18 | 32·6 | 69·88 | 44·9 | 67·21 | 56·0 | 64·79 |
| 14·6 | 72·75 | 24·0 | 70·98 | 33·6 | 69·70 | 45·0 | 67·22 | 56·2 | 65·96 |
| 15·2 | 72·40 | 24·6 | 71·05 | 33·8 | 69·16 | 45·4 | 67·16 | 56·2 | 65·49 |
| 16·3 | 72·09 | 24·8 | 71·38 | 34·1 | 69·49 | 46·2 | 66·77 | 56·9 | 64·73 |
| 16·8 | 71·96 | 25·6 | 70·76 | 35·0 | 69·51 | 46·8 | 66·92 | 58·2 | 65·16 |
| 17·0 | 72·03 | 26·1 | 70·48 | 35·6 | 69·35 | 47·1 | 66·46 | 58·7 | 65·07 |
| 17·1 | 71·66 | 26·2 | 70·80 | 35·7 | 68·64 | 48·0 | 67·38 | 61·9 | 64·54 |
| 17·3 | 72·40 | 26·5 | 70·90 | 36·8 | 68·91 | 48·1 | 67·04 | 62·6 | 64·47 |
| 17·6 | 71·68 | 27·3 | 70·87 | 38·1 | 68·47 | 48·5 | 66·65 | 62·8 | 64·95 |
| 17·6 | 72·12 | 27·4 | 70·42 | 38·4 | 68·54 | 48·8 | 66·74 | 63·5 | 63·88 |
| 18·0 | 72·05 | 28·0 | 70·57 | 38·6 | 68·76 | 50·2 | 66·05 | 64·5 | 63·99 |
| 18·9 | 72·08 | 30·1 | 70·17 | 39·0 | 68·90 | 50·8 | 66·18 | 65·5 | 64·53 |
| 19·9 | 72·14 | 30·6 | 69·65 | 39·5 | 68·46 | 51·0 | 67·03 | 65·5 | 64·46 |
| 20·1 | 71·97 | 31·1 | 69·70 | 39·5 | 68·42 | 51·9 | 66·43 | 69·0 | 63·37 |
| 20·2 | 71·50 | 31·2 | 70·05 | 40·4 | 68·05 | 52·0 | 65·95 | 73·5 | 62·66 |
| 21·8 | 71·30 | 31·3 | 70·04 | 41·1 | 67·81 | 52·8 | 66·11 | 75·6 | 61·42 |
| 22·2 | 71·26 | 31·4 | 70·24 | 42·0 | 67·89 | 54·0 | 65·92 | | |

It is advisable, perhaps, to point out that we make a distinction between ordinary distilled water and hydrogen monoxide, as we do between heavy water of 99·2 per cent. purity and deuterium monoxide.

### *The Algebraic Representation of the Results.*

The results, both for heavy and for ordinary water, show very slight scatter when exhibited graphically, and fig. 3 below shows the irregularities of the individual determinations, separate determinations of the surface tension of heavy water being marked by crosses, of ordinary water by points.

The results may be summed up in equations of the form

$$\gamma = A - Bt^{n},$$

where, for ordinary water,

$$A = 75{\cdot}23,\ B = 0{\cdot}06667,\ n = 1{\cdot}20,$$

Fig. 3.

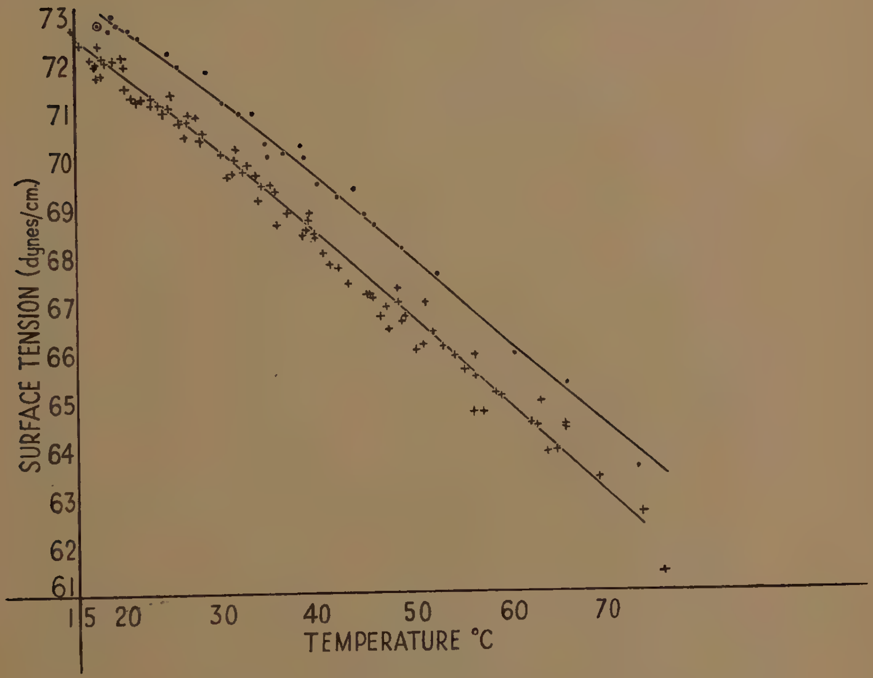

Surface tension—Temperature curves.

and for heavy water

$$A = 74{\cdot}64,\ B = 0{\cdot}1082,\ n = 1{\cdot}10.$$

Table IV. gives the values of surface tensions calculated from these formulæ.

It is unlikely that this formula will bear extrapolation over any wide range, but it represents the experimental results with considerable accuracy over the range 10°–75° C., and may be depended upon over the range 0°–80° C. (*cf.* Table V. The second decimal figure is not to be regarded as significant).

If we calculate a critical temperature by finding the value of T for which the surface tension vanishes we find, for ordinary water,

$$T_c = 350° \text{ C.}$$

and for heavy water $T_c = 382°$ C.

The experimental value for ordinary water is 374° C., and the departure of this value from what may be termed the metacritical value calculated from the formula is a measure of the change in the molecular complexity of the liquid between ordinary temperatures and the critical value.

TABLE IV.

*Calculated Values of Surface Tensions.*

| Temperature | Ordinary water. | Heavy water. |
|---|---|---|
| 0 | 75·23 | 74·64 |
| 5 | 74·79 | 74·00 |
| 10 | 74·18 | 73·28 |
| 15 | 73·51 | 72·52 |
| 20 | 72·80 | 71·72 |
| 25 | 72·06 | 70·91 |
| 30 | 71·28 | 70·08 |
| 35 | 70·48 | 69·24 |
| 40 | 69·65 | 68·38 |
| 45 | 68·81 | 67·51 |
| 50 | 67·94 | 66·64 |
| 55 | 67·06 | 65·75 |
| 60 | 66·16 | 64·86 |
| 65 | 65·24 | 63·96 |
| 70 | 64·31 | 63·05 |
| 75 | 63·36 | 62·14 |

The experiments show that heavy water, like ordinary water, is associated at ordinary temperatures. If we apply Eötvos's rule (6) *i. e.*,

$$\frac{d}{dt}\left[\gamma\left(\frac{M}{\rho}\right)^{2/3}\right] = -2{\cdot}1,$$

where $\gamma$=surface tension, M=molecular weight and $\rho$=density of the liquid, $t$=temperature, to calculate the effective molecular weight $M_e$ we find for ordinary water between 5° and 40° C., the mean value of $M_e/M = 3{\cdot}4$, while for heavy water (using density at 20° C.=1·1079, and variation of density given by Lewis and Macdonald (7)) the same quantity over this temperature range is 2·8 ; thus it appears that heavy water is less associated than is ordinary water.

Roughly speaking, the relation between the surface tensions of ordinary and of heavy water over this range may be summed up in the statement that the surface tension of heavy water at any temperature is approximately equal to that of ordinary water at (T+7·5)° C.

### Table V.

*Showing Agreement between Observed and Calculated Surface Tensions.*

| A. Heavy water. | | | |
|---|---|---|---|
| T. °C. | $\gamma$ obs. | $\gamma$ calc. | Diff. |
| 12·1 | 72·88 | 72·96 | −0·08 |
| 15·2 | 72·40 | 72·48 | −0·08 |
| 20·1 | 71·97 | 71·70 | +0·27 |
| 24·0 | 71·50 | 71·07 | −0·02 |
| 30·1 | 70·17 | 70·06 | +0·11 |
| 35·0 | 69·51 | 69·24 | +0·27 |
| 39·5 | 68·44 | 68·47 | −0·03 |
| 45·0 | 67·22 | 67·51 | −0·29 |
| 50·8 | 66·18 | 66·50 | −0·32 |
| 55·0 | 65·63 | 65·75 | −0·12 |
| 61·9 | 64·54 | 65·52 | +0·02 |
| 64·5 | 63·99 | 64·05 | −0·06 |
| 69·0 | 63·37 | 63·24 | +0·13 |
| 73·5 | 62·66 | 62·42 | +0·24 |

| B. Ordinary water. | | | |
|---|---|---|---|
| T. °C. | $\gamma$ obs. | $\gamma$ calc. | Diff. |
| 17·3 | 72·84 | 73·19 | −0·35 |
| 20·4 | 72·75 | 72·74 | +0·01 |
| 25·5 | 71·94 | 71·98 | −0·04 |
| 28·6 | 71·86 | 71·50 | +0·36 |
| 30·1 | 71·20 | 71·27 | −0·07 |
| 34·5 | 70·35 | 70·56 | −0·21 |
| 38·4 | 70·07 | 69·92 | +0·15 |
| 44·6 | 68·86 | 68·88 | −0·02 |
| 50·0 | 68·13 | 67·94 | +0·19 |
| 60·2 | 65·93 | 66·11 | −0·18 |
| 65·7 | 65·39 | 65·11 | +0·28 |
| 73·1 | 63·60 | 63·99 | −0·39 |

These experiments were made possible by the generosity of Imperial Chemical Industries, Ltd., who supplied us with a specimen of heavy water. We desire to thank them, and Professor H. R. Robinson, who has given every facility for the experimental work.

### *References.*

(1) Jour. Amer. Chem. Soc. lv. p. 4335 (1933).
(2) *Zeit. f. phys. chem.* clxxv. Abt. A, p. 347 (1936).
(3) Proc. Phys. Soc. xliv. p. 511 (1932).
(4) Proc. Phys. Soc. xliv. p. 511 (1932).
(6) *Wied. Ann.* xxvii. p. 448.
(7) Jour. Amer. Chem. Soc. lv. p. 3057 (1933).

Queen Mary College.
August 1939.

## LXXI. *An Alternative Explanation of Relativity Phenomena.*

By Albert Eagle, B.Sc., A.R.C. Sc., Lecturer in Mathematics
in the University of Manchester *.

[Received April 3, 1939.]

The following paper gives a brief alternative explanation of the three minute, but certainly very important, phenomena which are generally considered as convincing verification of the truth of Einstein's 'General Theory of Relativity.'

The phenomena are (i.) the deflexion of light passing near the sun; (ii.) the shift towards the red of the spectrum lines of the solar spectrum, and (iii.) the rotation of the orbit of the planet Mercury.

Undoubtedly the first effect is the most fundamental one, and may be the cause of the other two. We will consider the three effects in turn.

### I. *The Velocity of Light in a Gravitational Field.*

The discovery of the deviation of rays of light passing near the sun at the 1919 solar eclipse, which showed convincingly that light travelled more *slowly* in a gravitational field, was the first observational detection of any connexion between electromagnetic and gravitational phenomena. It was the discovery of an important point of incompleteness in the Lorentz-Larmor electromagnetic theory, which naturally took the velocity of light as constant throughout all space, as nothing to the contrary had up to that time been detected.

Let us assume that the velocity of light *may* alter in a gravitational field. The simplest assumption is that the change in velocity will be proportional to the *potential* of the gravitational field. Now this potential is proportional to the square of the velocity $v_\infty$, say, with which a particle falling from infinity would arrive at any point in the field. So if we denote by V and $V_0$ the velocity of light at any point in a gravitational field and outside its influence, respectively, we must have a relation of the form

$$V=V_0(1-\lambda v_\infty^2/V_0^2), \quad . \quad . \quad . \quad . \quad . \quad . \quad . \quad . \quad (1)$$

where $\lambda$ is some pure number.

The actual amount of the deflexion which would be produced by this law is easily calculated. Consider the case of a narrow beam of light of width $b$ passing by the sun at a minimum distance $a$ from the sun's centre. The velocity of light at a point at a distance $x$ along the beam from the point of nearest approach must be given by

---

* Communicated by the Author.

$$V=V_0\left(1-\frac{k}{\sqrt{(a^2+x^2)}}\right), \quad . \; . \; . \; . \; . \; . \; . \; . \quad (2)$$

where $k$ is some constant, since the last term is proportional to the gravitational potential at $x$. The difference, $\Delta V$, in the velocity of light on the two sides of the beam is at once given by differentiating (2) with respect to $a$ and replacing the differential $da$ by $b$. Hence

$$\Delta V=\frac{V_0 kab}{(a^2+x^2)^{3/2}}.$$

If $\rho$ is the radius of curvature of the beam at any point, obviously

$$\frac{\rho+b}{\rho}=\frac{V+\Delta V}{V}; \quad \text{or} \quad \frac{b}{\rho}=\frac{\Delta V}{V}\doteq\frac{\Delta V}{V_0}.$$

But if $y$ is the transverse deflexion at $x$ we have

$$\frac{1}{\rho}=\frac{d^2y}{dx^2}; \quad \text{so} \quad \frac{d^2y}{dx^2}=\frac{\Delta V}{bV_0}=\frac{ka}{(a^2+x^2)^{3/2}}.$$

Hence the total deviation from $x=-\infty$ to $x=+\infty$ undergone by the beam is

$$\left(\frac{dy}{dx}\right)_{\infty}-\left(\frac{dy}{dx}\right)_{-\infty}=\int_{-\infty}^{\infty}\frac{d^2y}{dx^2}dx=ka\int_{-\infty}^{\infty}\frac{dx}{(a^2+x^2)^{3/2}}=\frac{2k}{a}.$$

Observationally, the deflexion when $a$ is equal to the sun's radius is 1·7 seconds of arc, which is $\frac{1}{120{,}000}$ of a radian. So $\frac{k}{a}=\frac{1}{240{,}000}$. But, by (2) the velocity of light at the sun's surface is given by $V=V_0(1-k/a)$, and so is reduced by one part in 240,000.

Now the velocity of a particle falling from infinity to the sun's surface is about 612 km./sec., giving $\frac{v_\infty^2}{V_0}=\frac{1}{240{,}000}$; whence we instantly see from (1) that $\lambda=1$ exactly.

Hence (1) becomes

$$V=V_0(1-v_\infty^2/V_0^2), \quad . \; . \; . \; . \; . \; . \; . \; . \quad (3)$$

or, what is the same thing, since in all the gravitational fields we know $v_\infty^4/V_0^4$ is negligible,

$$V^2=V_0^2-2v_\infty^2, \quad . \; . \; . \; . \; . \; . \; . \; . \; . \; . \quad (4)$$

an extremely simple equation for the change of velocity of the velocity of light in a gravitational field.

## II. *The Shift of Spectrum Lines in a Gravitational Field.*

The shift of the spectrum lines cannot be so definitely worked out as the previous problem as the result will depend on *how* a gravitational field affects the ether; *i. e.*, whether it alters the electrical elasticity or the magnetic elasticity of the ether. If K and $\mu$ are the specific inductive capacity and magnetic permeability of the ether respectively (both measured in the same set of units, e.s. or e.m.), it is well known that $V^2K\mu=1$. As, by (3), V decreases by $v_\infty^2/V^2$ parts in unity in a gravitational field, the product $K\mu$ must increase by $2v_\infty^2/V^2$ parts in unity. Three possibilities seem to me more likely than any others. These are: (i.) $\mu$ remains constant; (ii.) K remains constant; and (iii.) K and $\mu$ both increase in the same ratio, namely, by $v_\infty^2/V^2$ parts in unity.

Consider an electron describing a circular atomic orbit of radius $a$ with an angular velocity $n$. The force of attraction to the nucleus will vary as 1/K, while the mass of the electron will be proportional to $\mu$. Hence we have, on equating the centrifugal force to the attractive force, $\mu mn^2a=e^2/Ka^2$, in which we have inserted $\mu$ and K to show the dependence of the orbit on $\mu$ and K. Having done this, $m$ must be treated as an unalterable constant.

Differentiating logarithmically, we see that small variations in $\mu$, $n$, $a$, K are connected by

$$\frac{d\mu}{\mu}+\frac{dK}{K}+\frac{2dn}{n}+\frac{3da}{a}=0. \qquad (5)$$

We have also the condition that the angular momentum of the orbit, which is $\mu mna^2$, must remain constant. Hence

$$\frac{d\mu}{\mu}+\frac{dn}{n}+\frac{2da}{a}=0. \qquad (6)$$

Eliminating $da/a$ between (5) and (6), we have

$$\frac{dn}{n}=\frac{d\mu}{\mu}-\frac{2dK}{K}.$$

We have also seen that $\frac{d\mu}{\mu}+\frac{dK}{K}=\frac{2v_\infty^2}{V^2}$ in all cases. Hence in the alternative (i.), when $d\mu=0$, we have

$$\frac{dn}{n}=-\frac{4v_\infty^2}{V^2}. \qquad (7)$$

In the alternative (ii.), when $dK=0$, we have

$$\frac{dn}{n}=+\frac{2v_\infty^2}{V^2}; \qquad (8)$$

while in the case of alternative (iii.), when $d\mu/\mu=d\mathrm{K}/\mathrm{K}=v_\infty^2/\mathrm{V}^2$, we have

$$\frac{dn}{n}=-\frac{v_\infty^2}{\mathrm{V}^2} \quad . \quad . \quad . \quad . \quad . \quad . \quad . \quad . \quad . \quad . \quad (9)$$

In the case of the sun, where $\frac{v_\infty^2}{\mathrm{V}^2}=\frac{1}{240{,}000}$, alternative (i.) would give an increase of wave-length of 1 part in 60,000 parts; alternative (ii.) would give a *decrease* of 1 part in 120,000 parts, while alternative (iii.) would give an increase of 1 part in 240,000 parts. The shift predicted by Einstein's theory is 1 part in 480,000 parts. We can easily obtain this shift if we take $d\mu/\mu=3d\mathrm{K}/\mathrm{K}=3v_\infty^2/2\mathrm{V}^2$. But this choice of $d\mu/\mu=3d\mathrm{K}/\mathrm{K}$ is so deliberately artificial, and so devoid of any known justification, that it must be considered theoretically valueless.

The alternatives (i.) and (ii.) are certainly flatly ruled out by observational evidence. There remains only alternative (iii.) to be considered, that the actual shift may really be double Einstein's predicted amount.

Actually it is found that different spectrum lines show great irregularities compared with the small Einstein shift; but for light from near the centre of the sun's disc the irregularities seem to have a centre of gravity at about Einstein's shift ,while light from the sun's limb certainly indicates a probable shift of about twice Einstein's amount. No explanation of this apparently excessive shift has or can be given.

I suggest that the true shift of spectrum lines in a gravitational field *is* really double Einstein's amount; and that the smaller shift indicated by light from the centre of the sun's disc is because the shift to the red is partly masked by a shift to the violet due to the emitting gases having a velocity upwards from the sun's surface. A vertical velocity of only 0·6 km./sec. would reduce my predicted shift to Einstein's value. There may very well be vertical circulation currents in which only the ascending material is engaged in emission. An irregular electron bombardment from below would necessarily cause such vertical motion both in bulk and in every individual atom struck.

It should be noted that alternative (iii.), which we favour, makes $da/a=0$ by (6) and (9); and so there is no change in the *size* of the atomic orbits. Had this result been otherwise, all solid bodies would necessarily undergo an alteration in size in a gravitational field which would have had the effect of making three-dimensional space appear as if it were "non-Euclidean." We must also note, for later reference, that this same alternative, with the relation $\mathrm{K}\mu\mathrm{V}^2=1$ and equation (1), give

$$\mathrm{K}=\mathrm{K}_0(1+v_\infty^2/\mathrm{V}^2) \quad \text{and} \quad \mu=\mu_0(1+v_\infty^2/\mathrm{V}^2) \quad . \quad . \quad . \quad . \quad (10)$$

for the values of K and $\mu$ at any point in a gravitational field.

### III. *The Rotation of the Apse Line of Mercury's Orbit.*

This rotation, over and above that due to other known causes (the perturbations from the other planets), amounts to about 43 seconds of arc a century. That is about 0·104 seconds of arc per revolution of the planet. As there are 1,296,000 seconds of arc in one revolution, the planet must make $1+\frac{1}{12,500,000}$ revolutions between one perihelion position and the next. Now the mean velocity, $u_m$, of Mercury in its orbit is about 48·2 km./sec., so that $\frac{u_m^2}{V^2}=\frac{1}{39,000,000}$; hence the rotation of the apse line is $3u_m^2/V^2$ revs. per revolution of the planet within observational errors.

Our task is now to find the modification of the law of gravitation which will give this result. Since to every action there is a reaction, and since, as we have seen, a gravitational field affects the properties of the ether, it is most likely that the affected ether will affect the constant of gravitation in its turn. The simplest supposition is to suppose that the constant of gravitation, G, at any point varies as some power of the velocity of light at that point, say as $V^{-\lambda}$, where $\lambda$ is to be determined.

The expression of the law of gravitation will naturally take a different form according as to whether we write the force between two masses M and $m$ as $GM_0m_0/r^2$, or as $GMm/r^2$, where the zero suffixes indicate the masses when at rest, and without suffixes, the masses as in motion. It will be more in accordance with modern physics if we adopt the latter expression. So we will take the force, $F_m$, which a large mass M exerts on an infinitesimal mass $m$ to be

$$F_m=\frac{GMm}{r^2}\left(\frac{V}{V_0}\right)^{-\lambda}.$$

Since, by (3), $V/V_0=1-v_\infty^2/V^2$, and since $v_\infty^2=2GM/r$, we have

$$F_m=\frac{GMm}{r^2}\left(1+\frac{2\lambda GM}{V^2r}\right). \quad . \quad . \quad . \quad . \quad . \quad . \quad . \quad . \qquad (11)$$

If the mass $m$ describes a circular orbit of radius $a$ with an angular velocity $n$ and M, we have, on balancing against the centrifugal force,

$$mn^2a=\frac{GMm}{a^2}\left(1+\frac{2\lambda GM}{V^2a}\right); \quad . \quad . \quad . \quad . \quad . \quad . \quad . \qquad (12)$$

so that $GM \doteqdot n^2a^3$, which may be substituted in the small term. Then, on dividing (11) by (12) to eliminate G, we have

$$F_m=\frac{mn^2a^3}{r^2}\left\{1+\frac{2\lambda n^2a^3}{V^2}\left(\frac{1}{r}-\frac{1}{a}\right)\right\}. \quad . \quad . \quad . \quad . \quad . \quad . \qquad (13)$$

For a nearly circular orbit let $r$, $\theta$ be the coordinates at any time. We will write $r=a+x$ and $\theta=nt+\chi$, where $x$ and $\chi$ are small quantities whose squares and products are to be neglected. Then, since $r^{-2} \doteqdot a^{-2}(1-2x/a)$ etc., (13) gives

$$F_m=mn^2a\left(1-\frac{2x}{a}-\frac{2\lambda n^2ax}{V^2}\right). \quad . \quad . \quad . \quad . \quad . \quad . \quad (14)$$

The linear momentum of a mass $m$, moving with a velocity $u$, is $mu$, where $m=m_0(1+\frac{1}{2}u^2/V^2)$. Its moment of momentum about the origin is $mup=mr^2\dot\theta$. Now for a circular orbit $u^2=n^2a^2$. For a nearly circular one we shall have, therefore, $u^2=n^2a^2-2n^2ax$, this being the energy equation for small changes in $r$. This is sufficiently accurate to substitute for $u^2$ in the small $u^2/V^2$ term. Hence the moment of momentum about the origin becomes

$$m_0\left\{1+\frac{n^2(a^2-2ax)}{2V^2}\right\}(a+x)^2.(n+\dot\chi).$$

This is constant. Keeping only first-order small quantities in this equation, we see that

$$a^2\dot\chi+2nax-n^3a^3xV^{-2}=0\,;$$

or

$$2an\dot\chi=-4n^2x+2n^4a^2xV^{-2}. \quad . \quad . \quad . \quad . \quad . \quad . \quad . \quad (15)$$

Now the components of momentum in the radial and transverse directions are $m\dot r$ and $mr\dot\theta$ respectively. Hence the rate of change of momentum in the radial direction is

$$\frac{d}{dt}(m\dot r)-\dot\theta(mr\dot\theta)=m\ddot r+\dot m\dot r-mr\dot\theta^2.$$

Now $\dot m$ is proportional to $\dot x$, and $\dot r=\dot x$, so that $\dot m\dot r$ is a negligible second-order term. Hence this rate of change is

$$m(\ddot r-r\dot\theta^2)=m[\ddot x-(a+x)(n+\dot\chi)^2]=m(\ddot x-n^2a-n^2x-2an\dot\chi).$$

Eliminating $\dot\chi$ by (15), this becomes

$$m[\ddot x-n^2a+(4-1)n^2x-2n^4a^2xV^{-2}].$$

Equating this to $-F_m$ from (14), we have, on division by $m$,

$$\ddot x+(3-2)n^2x-2(1+\lambda)n^4a^2xV^{-2}=0,$$

or

$$\ddot x+n^2[1-2(1+\lambda)n^2a^2V^{-2}]x=0,$$

the ordinary equation of simple harmonic motion. As $n^2a^2V^{-2}$ is very small, the solution is

$$x=A\cos\{[1-(1+\lambda)n^2a^2V^{-2}](nt+\alpha)\},$$

showing that $x$ goes through its period in the time

$$\frac{2\pi}{n}[1+(1+\lambda)n^2a^2V^{-2}],$$

very approximately; or, as $2\pi/n$ is the period of revolution of the planet, the planet requires $1+(1+\lambda)n^2a^2V^{-2}$ revolutions to pass from one perihelion position to the next. As the observed result is $1+3n^2a^2V^{-2}$ revolutions, we see that $1+\lambda=3$ or $\lambda=2$. Hence

$$F_m=\frac{GMm}{r^2}\left(\frac{V}{V_0}\right)^{-2}.$$

On alternative (iii.), this gives by (10),

$$F_m=\frac{GMm}{r^2}\left(\frac{\mu}{\mu_0}\right)^2=\frac{GMm}{r^2}\left(1+\frac{2v_\infty^2}{V^2}\right).$$

Now $m\mu/\mu_0$ is the true value of $m$ at its actual position; we will denote it by $m_m$; also $M\mu/\mu_0$ is the true value of M when it is in the potential of $m$; we will denote it by $M_m$; whence we see that the force which M exerts on $m$ is given by

$$F_m=\frac{GM_m m_m}{r^2}. \quad \ldots \ldots \ldots \ldots \quad (16)$$

Conversely the force which $m$ exerts on M must be given by

$$F_M=\frac{GM_M m_M}{r^2}.$$

The fact that these forces are not equal and opposite is no evidence that they cannot be correct, since forces on the masses can arise directly from the medium itself, as is well known in the case of a moving and radiating isolated sun whose own radiation exerts a retarding force on its motion.

Re-writing (16) by the help of (10), we have, on neglecting the products of small terms,

$$F_m=\frac{GM_0m_0}{r^2}\left(1+\frac{U^2+u^2}{2V^2}+\frac{2v_{\infty m}^2}{V^2}\right), \quad \ldots \ldots \quad (17)$$

where U and $u$ are the velocities of M and $m$ respectively, and $M_0$ and $m_0$ are the values of the masses when at rest away from any gravitational field (even their own!); and $v_{\infty m}$ is the velocity of free fall from infinity into $m$'s position. If the ratio $m/M$ is infinitesimal $v_{\infty m}^2=2GM/r$; but if not, let $m$ be a homogeneous sphere of radius $a$. Then the gravitational potential at $m$'s surface will exceed $GM/r$ by $Gm/a$, and at $m$'s centre will exceed $GM/r$ by $3Gm/2a$. A simple integration will show that the *mean* gravitational potential throughout $m$'s mass is

$$\frac{GM}{r}+\frac{6}{5}\frac{GM}{a}.$$

It is this which is equal to $\frac{1}{2}v_{\infty m}^2$.

Hence the expression for $F_m$ in (17) becomes

$$F_m = \frac{GM_0m_0}{r^2}\left(1+\frac{U^2+u^2}{2V^2}+\frac{4GM}{r}+\frac{24}{5}\frac{Gm}{a}\right). \quad . \quad . \quad . \quad (18)$$

If the mass M is similarly a homogeneous sphere of radius $b$ we have, for $F_M$, the force of attraction which $m$ exerts on M,

$$F_M = \frac{GM_0m_0}{r^2}\left(1+\frac{U^2+u^2}{2V^2}+\frac{4Gm}{r}+\frac{24}{5}\frac{GM}{b}\right).$$

It is obvious that as mass alters with velocity and, as we have seen (very probably), with the potential of the gravitational field in which it is situated, that Newton's law of gravitation $F=GMm/r^2$, which ignores such changes, cannot be a final statement of the law. It has, in fact, no precise meaning till the values to be taken for the masses in this equation have been defined. It is surely remarkable that we find that no more modification of Newton's law is required than that we take M and $m$ as the masses they possess at their actual velocities, and as if they were both situated in the gravitational field at $m$ if we want the force which M exerts on $m$.

Thus we have seen that the three minute astronomical phenomena which are often regarded as proof of the existence of some "space-time-continuum" and of "curved space" can be explained in a perfectly rational manner by only a slight development of pre-Relativity electromagnetic theory.

It cannot be contended that we have done nothing but put forward *ad hoc* ideas invented to give the same results as Einstein's theory, since we have had the courage to declare from our work that Einstein's predicted shift of the spectrum lines in a gravitational field is, in all probability, wrong, the actual shift, which the observations decidedly seem to confirm, being double Einstein's amount.

While the ether was regarded as having identical properties throughout all space it was just possible to think that there might be no such medium at all; but it is hardly possible to doubt the existence of a medium whose properties, as we have seen, vary from point to point with the gravitational field there.

## LXXII. *Notices respecting New Books.*

*The Geometry of Determinantal Loci.* By T. G. Room, Professor of Mathematics in the University of Sydney; sometime Fellow of St. John's College, Cambridge; and Lecturer in Mathematics in the University of Cambridge. [500 pages approx.] (Cambridge University Press. Price 42*s*. net.)

There comes a time in the development of every big subject, which has merited the attention of investigators the world over, when someone must arise and undertake the labour of presenting it as a coherent whole, with the unessentials pruned away and the relationship of the various portions to one another clearly exhibited. This very necessary task has been undertaken and excellently executed in the present handsome volume by Professor T. G. Room for the case of those loci in Synthetic Geometry which are dominated by algebraic equations, determinantal in form. There exists a school of Synthetic Geometers who, fascinated by the vigour and clarity of purely synthetic methods, rule out practically entirely the use of algebra in establishing their results. Artistically, the appeal of the stark severity of these synthetic methods is at once easily comprehensible and defensible, and Synthetic Geometry owes a great debt of gratitude to those practitioners who rigorously rule out all algebraic aids, inasmuch as a synthetic proof reveals throughout its steps the inner wheels working in a manner which is not possible in the case of a proof resting upon—to quote the words of an eminent geometer—an algebraic accident. Be that as it may, Professor Room makes his own position clear at the outset. "Synthetic and algebraic methods are used impartially," he says, and he cites Professor H. F. Baker as having followed the same lines in his treatises on Geometry.

The subject-matter covers a wide territory. Chapter I. deals with "some fundamental ideas in Projective Geometry"; Chapter II. with "projectively generated manifolds, definitions and elementary properties"; Chapter III. with "birationally related and degenerate determinantal loci"; Chapter IV. with "the pairing-theorems and the theorem of the double-N"; Chapter V. with "the key-manifolds"; Chapter VI. with "determinantal primals"; Chapter VII. with "the freedom of a projectively generated manifold."

This concludes Part I. of the treatise, which deals with "manifolds defined by matrices of general form." Part II. deals with "manifolds defined by matrices of special forms."

Chapter VIII. treats of "the key-manifolds of the types defined by symmetrical determinants: the Veroneseans of quadrics"; Chapter IX. of "primals represented by symmetrical determinants"; Chapter X. of "manifolds defined by Skew symmetrical determinants: Grassmannians of lines"; Chapter XI. of "normal rational scrolls"; Chapter XII. of "representations of spaces by points"; Chapter XIII. of "some association and other incidence theorems."

Parts I. and II. are occupied in the main with theorems of a very general character. The author begins with such fundamental entities as the conic, the quadric, the cubic surface, the twisted cubic, etc., all of which are capable of being easily represented by equations determinantal in form. From these equations are deducible immediately methods of generating these geometrical entities by means of correspondences between members of pencils of lines, sheaves of planes, etc. The relationship between such modes of generation and the mapping of rational surfaces, etc., on planes is then exhibited, particular stress being laid upon such examples as the double-six, where the point-to-point relationship between the points of a cubic surface and the points of a plane breaks down. All such results are immediately generalized to space of $n$-dimensions, and further developments obtained. On the whole, one will look in vain in these chapters for the detailed "personal" properties of such entities as the cubic curves, cubic surfaces, rational normal curve in space of four dimensions, etc. They are merely cited throughout these sections of the book in order to clarify and bring to earth the immensely general properties whose establishment forms the main substance of these portions of the treatise.

We pass now to Part III., which is much less general in character, and for that reason will be for many types of geometer the most interesting part of the volume. Its general theme is "determinantal quartic primals in space of four dimensions."

Chapter XIV. occupies itself with "the Bordiga sextic surface in four dimensions"; Chapter XV. with "primals represented by the vanishing of a general determinant of order 4"; Chapter XVI. with "some special quartic determinantal primals in four dimensions." For geometers who prefer definite surfaces to general theory, these chapters will be found particularly interesting. Modern primals, such as those of Todd, Edge, Segre and Lüroth, are discussed. Double-twenties of planes; systems of lines; trisecants, etc. etc., flit across the pages. The representation of lines and planes finds a place.

The book concludes with three appendixes on "Veroneseans and Grassmannians"; "the characteristic numbers of certain determinantal manifolds"; and "the freedoms of manifolds" respectively.

In a treatise so large and containing so many good things it is difficult to particularize in any great detail. The del Pezzo surfaces are interesting in themselves and have many useful contacts with other geometrical entities. The fact that any plane curve can be represented by a symmetrical determinant has been developed from Hesse's work on a plane quartic by Grace and Dixon. The Veronese Surface makes its appearance frequently. The work of White on certain types of surfaces affords much interesting material. Everywhere "incidence properties" find an honoured place, as would be expected by anyone who is familiar with the author's work and knows his special leanings towards theorems of that type.

The book must have taken much time to write, and much care must have been expended upon its preparation. The author is to be congratulated on the finished product.

The Cambridge University Press have done their part with their usual attention to detail and general finish.

W. P. M.

*Hearing: Its Psychology and Physiology.* By Dr. S. S. Stevens and Dr. H. Davis. (New York: John Wiley and Sons. London: Chapman and Hall. Price 22*s*. 6*d*. net.)

This is a remarkably well-balanced book, which may be read with pleasure and profit by all physicists interested in acoustics. On the physiological side, the descriptions of the auditory processes and mechanisms are clear and well drawn, detailed enough to satisfy the needs of those interested in physiology, and yet not so overloaded with detail as to confuse the physicists.

On the psychological side, scores of problems are discussed which are of fundamental interest to the specialist in acoustics. In particular the chapters which deal with the sensitivity of the ear, pitch, loudness and other attributes of tones, auditory localization, masking, fatigue and persistence, provide a wealth of well-documented material for discussion. The description of the "sone-scale" will be read with special interest by those who do (and by those who do not) assert the possibility of making quantitative estimates of a sensory event such as a loudness.

The book is well produced, contains a valuable bibliography and glossary, and may be unreservedly recommended.

---

[*The Editors do not hold themselves responsible for the views expressed by their correspondents.*]

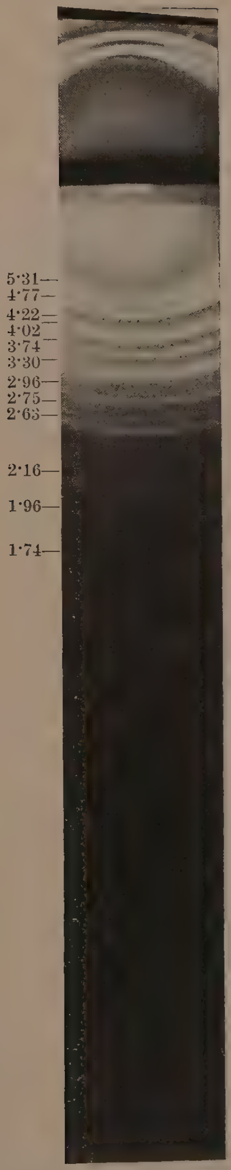
5·31
4·77
4·22
4·02
3·74
3·30
2·96
2·75
2·63
2·16
1·96
1·74

Cyclohexane at —180° C.

# INDEX TO VOL. XXVIII.

ADAMS (S. F.) and Roberts (R. W.), the magnetic rotatory dispersion and the refractivity of aqueous solutions of nickel sulphate throughout the range 5780 Å. to 2482 Å.; especially the magnetic rotation in the 3950 Å. absorption band, 601.

Alternative explanation of relativity phenomena, 694.

Arms of a spiral nebula, 118.

Astronomical consequences of relativistic two-body problem, 227.

Awbery (J. H.), the periodic flow of heat in a hollow cylinder, 447.

Banerji (A. C.) and Bhatnagar (P. L.), the arms of a spiral nebula, 118.

Barrer (R. M.), gas flow in solids, 148.

——, the permeability of metal membranes to diatomic gases, 353.

Bate (A. E.), the surface tension and angle of contact of mercury *in vacuo*, 252.

Bending of thick plates under certain specified conditions of support, 73.

Beynon (W. J. G.), the magneto-optical and natural dispersions of isobutyl butyrate and ethylene chloride, 548.

Bhatnagar (P. L.) and Banerji (A. C.), the arms of a spiral nebula, 118.

Books new :—N. Rashevsky, Mathematical Biophysics, 127; G. Stead, Notes on Practical Physics, 127; Encyclopædia Britannica Book of the Year 1939, 128; R. C. Evans, Crystal Chemistry, 256; S. Goldstein, Modern Developments in Fluid Dynamics, 384; L. F. Bates, Modern Magnetism, 496; K. K. Darrow, Introduction to Contemporary Physics, 496; E. G. Cullwick, The Fundamentals of Electromagnetism, 600; T. G. Room, The Geometry of Determinantal Loci, 702; S. S. Stevens and H. Davis, Hearing: Its Psychology and Physiology, 703.

Boutry (G. A.) and Gillod (P.), studies in photoelectric photometry. A photoemissive cell specially designed for high precision measurements, 163.

Burns (B. D.) and Owen (E. A.), X-ray study of some meteoric irons, 497.

Calibrating a disappearing filament optical pyrometer, note on the effective wave-length to be used in, 588.

Chakravarty (S. K.), quantization under two centres of force.—Part I. The hydrogen molecular ion, 423.

Changes in the internal resistance of selenium barrier-layer cells caused by exposure to light, 642.

Chapman (S.) and Hammad (A.), the primary and secondary scattering of sunlight in a plane-stratified atmosphere of uniform composition, 99.

Cockett (A. H.) and Ferguson (A.), the surface tension of water and heavy water, 685.

Conduction of heat, note on a problem in the, 579.

Cope (S. T.), Murphy (F. M. G.), and Jones (J. H.), a mobile seismic recording unit, 370.

Cornish (R. J.), the magnitude of the direct stress in a beam of fixed span, 481.

Crowther (J. A.), Liebmann (H.), and Jones (R.), further observations on the action of X-rays on the electrophoretic mobility of colloid particles, 64.

Crystal structure of cyclohexane at —180° C., 614.

Crystalline nickel sulphate in the near ultra-violet, optical activity and magneto-optical activity of, 241.

Cunnold (F. A.), note on the effective wave-length to be used in calibrating a disappearing filament optical pyrometer, 588.

Cyclohexane at —180° C., crystal structure of, 614.

Daunt (J. G.), the threshold and equilibrium curves of supraconductors, 24.

Davies (R. M.) and Jones (T. Tyssul) on the determination of the dielectric constants of liquids at radio frequencies.—Part III. Methyl alcohol, water, and alcohol water mixtures: theoretical, 289; Part IV. Methyl alcohol, water, and alcohol water mixtures: experimental, 307.

Daymond (J. R.) and Walker (A. G.), on a hydraulic problem involving discharge into tidal water, 520.

Dean (W. R.), the distortion of curved tube due to internal pressure, 452.

Density and compressibility of solid hydrogen and deuterium at 4·2° K., 129.

Dielectric constant of space containing electrons, on the, 532.

—— constants of liquids at radio frequencies, on the determinations of the.—Part III. Methyl alcohol, water, and alcohol water mixtures: theoretical, 289; Part IV. Methyl alcohol, water, and alcohol water mixtures: experimental, 307.

Distortion of a curved tube due to internal pressure, 452.

Dow (R. B.), viscosity of liquids at high hydrostatic pressures, 403.

Eagle (A.), an alternative explanation of relativity phenomena, 694.

——, note on synchronizing "clocks" in a moving system by a connecting spindle, 592.

Effect of variable specific heat of gases on the quantities involved in heat transmission between liquids and gases, 596.

Efficiency of Geiger-Müller counters, 562.

Electric glow between carbon electrodes, 544.

—— strength of gases, measured by corona discharge, 666.

Electrical double layer at the interface of two liquids, 435.

Electron distribution in electron-optically focused electron beams, 81.

—— in classical general relativity theory, 385.

Electrophoretic mobility of colloid particles, further observation on the action of X-rays on, 64.

Errors in the numerical solution of differential equations, 359.

Espley (D. C.), harmonic analysis by the method of central differences, 338.

Fahmy (M.), a new form of the quantum equation, 364.

Ferguson (A.) and Cockett (A. H.), the surface tension of water and heavy water, 685.

Fermi-Dirac gas, the thermodynamic functions of a, 257.

Formulæ for generalized hypergeometric functions as particular cases of more general formulæ, 488.

Further observations on the action of X-rays on the electrophoretic mobility of colloid particles, 64.

Gas flow in solids, 148.
Geiger-Müller counters, the efficiency of, 562.
Generalization of the polynomial $F_n(x)$, 209.
Gill (E. W. B.), a short wave generator, 203.
Gillod (P.) and Boutry (G. A.), studies in photoelectric photometry. A photoemissive cell specially designed for high precision measurements, 163.
Grisdale (G. L.) and MacGregor-Morris (J. T.), the thermal method of measuring losses in sheet dielectrics at radio frequencies and high electrical stresses, 34.
Hammond (A.) and Chapman (S.), the primary and secondary scattering of sunlight in a plane-stratified atmosphere of uniform composition, 99.
Harmonic analysis by the method of central differences, 338.
Heat transmission between liquids and gases, the effect of variable specific heat of gases on the quantities involved in, 596.
Henderson (J. P.) and Jones (F. Llewellyn), the influence of the cathode on the sparking potential of hydrogen, 185.
Howell (W. T.), a note on Laguerre polynomials, 287.
——, the solution of some partial differential equations in the finite domain, 396.
——, some formulæ for the product of two Whittaker functions with different arguments, 493.
Hume-Rothery (W. ), the latent heats of sublimation and evaporation of certain substances, 465.
Hydraulic problem involving discharge into tidal water, on a, 520.
Ignition of inflammable gases by hot moving particles, 1.
Influence of the cathode on the sparking potential of hydrogen, 185.
—— of heavy hydrogen, 328.
Influence of the free end of a rod on heat transfer, 571.
Ionization by collision of positive ions, 111.
Jacob (L.), electron distribution in electron-optically focused electron beams, 81.
Jakob (M.), the influence of the free end of a rod on heat transfer, 571.
Jones (F. Llewellyn), the influence of the cathode on the sparking potential of heavy hydrogen, 328.
——, the mechanism of the spark discharge in hydrogen, 192.
—— and Henderson (J. P.), the influence of the cathode on the sparking potential of hydrogen, 185.
Jones (J. H.), Murphy (F. M. G.), and Cope (S. T.), a mobile seismic recording unit, 370.
Jones (R.), Crowther (J. A.), and Liebmann (H.), further observations on the action of X-rays on the electrophoretic mobility of colloid particles, 64.
Jones (T. Tyssul) and Davies (R. M.) on the determination of the dielectric constants of liquids at radio frequencies.—Part III. Methyl alcohol, water, and alcohol water mixtures: theoretical, 289; Part IV. Methyl alcohol, water, and alcohol water mixtures: experimental, 307.
Khastgir (S. R.) and Sirajuddin (K.) on the dielectric constant of space containing electrons, 532.
Laguerre polynomials, a note on, 287.
Latent heats of sublimation and evaporation of certain substances, 465.
Lees (A.), the electron in classical general relativity theory, 385.
Liebmann (H.), Jones (R.), and Crowther (J. A.), further observations on the action of X-rays on the electrophoretic mobility of colloid particles, 64.

Lonsdale (K.) and Smith (H.), crystal structure of cyclohexane at −180° C., 614.

MacGregor-Morris (J. T.) and Grisdale (G. L.), the thermal method of measuring losses in sheet dielectrics at radio frequencies and high electrical stresses, 34.

MacRobert (T. M.), formulæ for generalized hypergeometric functions as particular cases of more general formulæ, 488.

Magnetic rotatory dispersion and the refractivity of aqueous solutions of nickel sulphate throughout the range 5780 Å. to 2482 Å.; especially the magnetic rotation in the 3950 Å. absorption band, 601.

Magneto-optical and natural dispersions of isobutyl butyrate and ethylene chloride, 548.

Magnitude of the direct stress in a beam of fixed span, 481.

Marro (M.), two-way speech by wireless, 248.

Mechanism of the spark discharge in hydrogen, 192.

Megaw (H. D.), the density and compressibility of solid hydrogen and deuterium at 4·2° K., 129.

Mobile seismic recording unit, 370.

Morrow (J.), the bending of thick plates under certain specified conditions of support, 73.

Murphy (F. M. G.), Cope (S. T.), and Jones (J. H.), a mobile seismic recording unit, 370.

New form of the quantum equation, 364.

Newman (F. H.), note on the relative intensity of spectrum lines, 584.

——, the electric glow between carbon electrodes, 544.

Niessen (K. F.) and Verwey (E. J. W.), the electrical double layer at the interface of two liquids, 435.

Note on a problem in the conduction of heat, 579.

—— —— Laguerre polynomials, 287.

Note on synchronizing "clocks" in a moving system by a connecting spindle, 592.

—— —— the effective wave-length to be used in calibrating a disappearing filament optical pyrometer, 588.

—— —— the relative intensity of spectrum lines, 584.

—— —— the solution of some partial differential equations in the finite domain, 396.

—— —— the viscosity of gases and molecular mean free path, 679.

Numerical solution of differential equations, the errors of, 359.

——, two notes on, 381.

On the determination of the dielectric constants of liquids at radio frequencies.—Part III. Methyl alcohol, water, and alcohol water mixtures: theoretical, 289; Part IV. Methyl alcohol, water, and alcohol water mixtures: experimental, 307.

Optical activity and magneto-optical activity of crystalline nickel-sulphate in the near ultra-violet, 241.

Owen (E. A.) and Burns (B. D.), X-ray study of some meteoric irons, 497.

Partial differential equations in the finite domain, a note on the solution of some, 396.

Pasternack (S.), a generalization of the polynomial $F_n(x)$, 209.

Paterson (S.), the ignition of inflammable gases by hot moving particles, 1.

Periodic flow of heat in a hollow cylinder, 447.

Permeability of metal membranes to diatomic gases, 353.

Photoelectric photometry, studies in. A photoemissive cell specially designed for high precision work, 163.

Point charge revolving in a circular orbit, radiation from a, 617.

Polynomial $F_n(x)$, a generalization of, 209.
Poritsky (H.), radiation from a point charge revolving in a circular orbit, 617.
Primary and secondary scattering of sunlight in a plane-stratified atmosphere of uniform composition, 99.
Quantization under two centres of forces.—Part I. The hydrogen molecular ion, 423.
Quantum equation, a new form of the, 364.
Radiation from a point charge revolving in a circular orbit, 617.
Ray (Manohar) on turbulent liquid motion outside a circular boundary, 231.
Relativistic two-body problem, astronomical consequences of, 227.
Relativity phenomena, an alternative explanation of, 694.
Roberts (R. W.) and Adams (S. F.), the magnetic rotatory dispersion and the refractivity of aqueous solutions of nickel sulphate throughout the range 5780 Å. to 2482 Å.: especially the magnetic rotation in the 3950 Å. absorption band, 601.
Rudwick (P.) and Slack (F. G.), optical activity and magneto-optical activity of crystalline nickel sulphate in the near ultra-violet, 241.
Sandström (A. E.), changes in the internal resistance of selenium barrier-layer cells caused by exposure to light, 642.
Scattering of light in Bose-Einstein and Fermi-Dirac gas, 635.
Schuil (A. E.), a note on the viscosity of gases and molecular mean free path, 679.
Selenium barrier layer cells, changes in the internal resistance of, caused by exposure to light, 642.
Shankland (R. S.) and Tindal (C. H.), the efficiency of Geiger-Müller counters, 562.
Sheet dielectrics, the thermal method of measuring losses in, at radio frequencies and high electrical stresses, 34.
Short wave generator, 203.
Singh (B. N.), scattering of light in Bose-Einstein and Fermi-Dirac gas, 635.
Sirajuddin (K.) and Khastgir (S. R.) on the dielectric constant of space containing electrons, 532.
Slack (F. G.) and Rudwick (P.), optical activity and magneto-optical activity of crystalline nickel sulphate in the near ultra-violet, 241.
Smith (H.) and Lonsdale (K.), crystal structure of cyclohexane at −180° C., 614.
Solids, gas flow in, 148.
Some formulæ for the product of two Whittaker functions with different arguments, 493.
Spark discharge in hydrogen, the mechanism of the, 192.
Sparking potential of heavy hydrogen, the influence of the cathode on the, 328.
—— —— of hydrogen, influence of the cathode on the, 185.
Spectrum lines, note on the relative intensity of, 584.
Spiral nebula, the arms of, 118.
Stoner (E. C.), the thermodynamic functions of a Fermi-Dirac gas, 257.
Studies in photoelectric photometry. A photoemissive cell specially designed for high precision measurements, 163.
Sulaiman (S.), the astronomical consequences of relativistic two-body problem, 227.
Supraconductors, the threshold and equilibrium curves of, 24.
Surface-tension and angle of contact of mercury *in vacuo*, 252.
—— of water and heavy water, 685.
Thermal method of measuring losses in sheet dielectrics at radio frequencies and high electrical stresses, 34.

Thermodynamic functions of a Fermi-Dirac gas, 257.
Thornton (W. M.), the electric strength of gases measured by corona discharge, 666.
Threshold and equilibrium curves of supraconductors, 24.
Tindal (C. H.) and Shankland (R. S.), the efficiency of Geiger-Müller counters, 562.
Torsional vibration in heavy shafts, 649.
Townsend (J. S.), ionization by collisions of positive ions, 111.
Transverse vibrations of curved membranes, 632.
Tranter (C. J.), note on a problem in the conduction of heat, 579.
Tuplin (W. A.), torsional vibration in heavy shafts, 649.
Turbulent liquid motion outside a circular boundary, 231.
Turton (F. J.), the errors in the numerical solution of differential equations, 359.
——, two notes on the numerical solution of differential equations, 381.
Two-way speech by wireless, 248.
Verwey (E. J. W.) and Niessen (K. F.), the electrical double layer at the interface of two liquids, 435.
Viscosity of gases and molecular mean free path, note on, 679.
—— —— liquids at high hydrostatic pressures, 403.
Walker (W. J.), the effect of variable specific heat of gases on the quantities involved in heat transmission between liquids and gases, 596.
—— and Daymond (J. R.) on a hydraulic problem involving discharge into tidal water, 520.
Weatherburn (C. E.) on transverse vibrations of curved membranes, 632.
Whittaker functions with different arguments, some formulæ for the product of two, 493.
Wireless, two-way speech by, 248.
X-ray study of some meteoric irons, 497.
X-rays, on the action of, on the electrophoretic mobility of colloid particles, 64.

END OF THE TWENTY-EIGHTH VOLUME.

---

PRINTED BY TAYLOR AND FRANCIS. LTD., RED LION COURT, FLEET STREET, E.C.4.

Wool Research